SSI-20

Program Guide

20th International Conference on Solid State Ionics

June 14-19, 2015

KEYSTONE RESORT
& CONFERENCE CENTER
KEYSTONE, COLORADO, USA

WELCOME TO THE CONFERENCE!

On behalf of the Conference Chairs and Committee Members, it is with great pleasure that I welcome you to the **20th International Conference on Solid State Ionics (SSI-20)**. With the Rocky Mountains as our backdrop, we expect you'll find an excellent and engaging technical program and an exciting place to explore in your free time.

We are confident this Conference will provide essential information on the breadth and depth of current solid state ionics research worldwide. Below are some highlights we believe will be of interest to you.

Sangtae Kim, University of California, Davis

CONFERENCE HIGHLIGHTS

THE SSI-20 PROGRAM

Scientists from around the world will converge in Keystone, Colorado this week to share ideas, present technical information and contribute to the advancement of solid state ionics. Featuring over **625 oral/poster presentations**, SSI-20 will offer a strong program of plenary, keynote, invited and contributed talks, poster sessions, and tutorials covering topics from fuel cells and electrolyzers, to proton-conducting oxides—confirming the great diversity of science that is enabled by solid state ionics.

TUTORIALS

Start the Conference off on Sunday afternoon with **four tutorial sessions** designed to complement the technica program. Attendance to these sessions is not included in the Conference registration fee. You may purchase entrance to the tutorials for $100 at the Registration Desk located in the Main Lobby. Featured topics are *Advanced Methods in Electrochemical Impedance Spectroscopy*; *Defect Chemistry in Solid State Ionics*; *Battery Materials and Electrochemistry*; and *Atomistic Modeling in Solid State Ionics*. For more details, see page 3.

WELCOME RECEPTION

Conference attendees are invited to the Welcome Reception on Sunday evening from 5:00 pm - 7:00 pm in Shavano Terrace. Before a full day of technical sessions, this is a great time to **enjoy light snacks and refreshments**, meet with old colleagues, make new connections and share information.

PLENARY SESSIONS

Don't miss the five Plenary Sessions held Monday - Friday mornings. **Shu Yamaguchi**, University of Tokyo, starts the week off on Monday with his talk, *Bulk and Surface Oxide Protonics for Energy Conversion Devices: Role of Percolation and Grotthus Mechanism in Oxide Protonics*. Next, **Sossina M. Haile**, Northwestern University, shares *Insights into Proton Transport in Superprotonic Solid Acids*. On Wednesday, *Electrode Kinetics in the Solid State* is presented by **Juergen Janek** of Justus Liebig University Giessen. Then Thursday, **Joachim Heberle**, Free University of Berlin, gives his presentation, *On the Mechanism of Cation Translocation across Channelrhodopsin*. A special Plenary Session featuring **John B. Goodenough,** University of Texas at Austin, rounds out the Conference Friday morning with *Alternative Strategies for Electrical Energy Storage*.

POSTER SESSIONS/RECEPTIONS

Poster authors will be available for **in-depth discussions on Monday and Tuesday** in Red Cloud Peak. These popular sessions are open to all Conference attendees. During the Monday afternoon session, complimentary lunch and refreshments will be served. The Tuesday evening session will include light snacks and refreshments.

ISSI YOUNG SCIENTIST AWARD

To recognize the outstanding contributions made by young scientists to the field of solid state ionics, the International Society of Solid-State Ionics established the ISSI Young Scientist Award. This year, **six young scientists** have been selected as finalists. On Tuesday, don't miss the award finalists' talks from 1:30 pm - 3:00 pm in Quandary Peak I/II.

ISSI ELECTION

All SSI-20 attendees are encouraged to attended the SSI Election on Wednesday morning in Shavano Peak. The new ISSI Vice President and Board of Directors' members will be elected.

CONFERENCE BANQUET

Make time for this year's Conference Banquet on Wednesday evening at Soda Ridge Stables. **One Conference Banquet ticket is included in your registration fee**. Additional tickets may be purchased for $80 per person at the Registration Desk located in the Main Lobby. This event takes place outside, so please plan and dress for the weather accordingly. Transportation will be provided to and from the Conference Banquet.

TABLE OF CONTENTS

COMMITTEES

CHIEF ORGANIZER

Sangtae Kim, University of California, Davis

CO-ORGANIZERS

William Chueh, Stanford University

Joachim Maier ***(ISSI President)***, Max Planck Institute for Solid State Research

Ryan O'Hayre, Colorado School of Mines

LOCAL ORGANIZING COMMITTEE

Scott Barnett, Northwestern University

Shannon Boettcher, University of Oregon

Yi Cui, Stanford University

David Ginley, National Renewable Energy Laboratory

Sossina Haile, Northwestern University

Andrew Herring, Colorado School of Mines

Joshua Hertz, University of Delaware

Fritz Prinz, Stanford University

John Turner, National Renewable Energy Laboratory

Bilge Yildiz, Massachusetts Institute of Technology

INTERNATIONAL ADVISORY BOARD

Henny Bouwmeester, University of Twente

Gyeong Man Choi, Pohang University of Science and Technology

Juergen Fleig, Vienna University of Technology

Klaus Funke, Westfälische Wilhelms–Universität Münster

Ludwig Gauckler, ETH Zürich

Clare Grey, University of Cambridge

John Irvine, University of St. Andrews

Tatsumi Ishihara, Kyushu University

Saiful Islam, University of Bath

Ellen Ivers–Tiffee, Karlsruhe Institute of Technology

Tatsuya Kawada, Tohoku University

John A. Kilner, Imperial College London

Hong Li, Chinese Academy of Science

Manfred Martin, RWTH Aachen University

Hiroshige Matsumoto, Kyushu University

Truls Norby, University of Oslo

Ilan Riess, Israel Institute of Technology

Werner Sitte, Univeristy of Leoben

Shu Yamaguchi, University of Tokyo

Han–Ill Yoo, Seoul National University

PROGRAM COMMITTEE

A. SOLID OXIDE FUEL CELLS AND ELECTROLYZERS

Rotraut Merkle, Max Planck Institute

Werner Sitte, Univeristy of Leoben

B. POLYMER ELECTROLYTE FUEL CELLS AND ELECTROLYZERS

Vito Di Noto, University of Padova

Andew Herring, Colorado School of Mines

Tom Zawodzinski, University of Tennessee

C. ELECTRODES AND SOLID ELECTROLYTES FOR BATTERIES

Scott Barnett, Northwestern University

William Chueh, Stanford University

Juergen Janek, Justus-Liebig University, Giessen

Shirley Meng, University of California

D. FUNDAMENTALS OF TRANSPORT AND REACTIVITY AND NANOIONICS

Giuliano Gregori, Max Planck Institute

Joshua Hertz, University of Delaware

Sangtae Kim, University of California, Davis

Bilge Yildiz, Massachusetts Institute of Technology

E. TRANSPARENT CONDUCTING OXIDES

Joseph Berry, National Renewable Energy Laboratory

David Ginley, National Renewable Energy Laboratory

David Paine, Brown University

F. SOLID STATE PHOTOELECTROCHEMISTRY

Shannon Boettcher, University of Oregon

G. SWITCHING AND SENSING PHENOMENA

Jennifer Rupp, ETH Zürich

Shu Yamaguchi, University of Tokyo

H. HIGH TEMPERATURE ROUTES FOR SOLAR FUELS

Tim Davenport, California Institute of Technology

Sossina Haile, Northwestern University

Ryan O'Hayre, Colorado School of Mines

I. ION TRANSPORT IN HYBRID ORGANIC-INORGANIC SOLIDS

Hema Karunadasa, Stanford University

David Cahen, Weizmann Institute of Science

J. PERMEATION MEMBRANES

Robert Kee, Colorado School of Mines

Jonathan Lane, Praxair

Jose Serra, Polytechnic University of Valencia

K. PROTON-CONDUCTING OXIDES

Hiroshige Matsumoto, Kyushu University

Truls Norby, University of Oslo

MEETING INFORMATION

KEYSTONE CONFERENCE CENTER FLOORPLAN

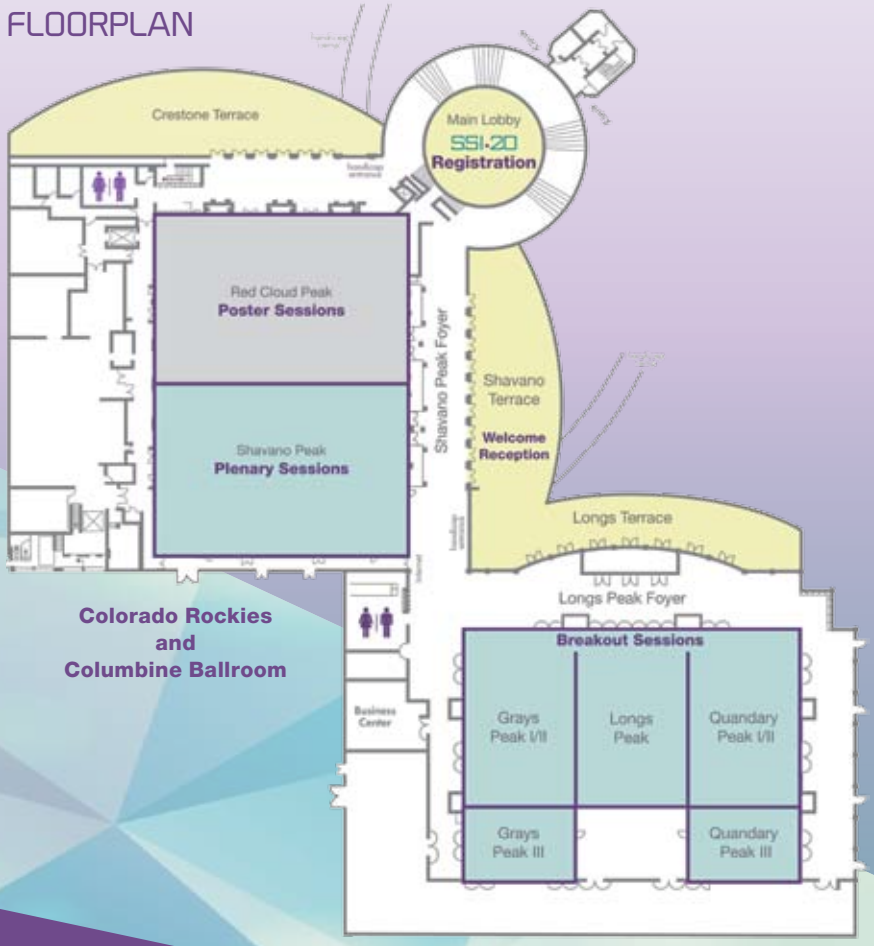

TECHNICAL SESSIONS

A. Solid Oxide Fuel Cells and Electrolyzers

B. Polymer Electrolyte Fuel Cells and Electrolyzers

C. Electrodes and Solid Electrolytes for Batteries

D. Fundamentals of Transport and Reactivity and Nanoionics

E. Transparent Conducting Oxides

F. Solid State Photoelectrochemistry

G. Switching and Sensing Phenomena

H. High Temperature Routes for Solar Fuels

I. Ion Transport in Hybrid Organic-Inorganic Solids

J. Permeation Membranes

K. Proton-Conducting Oxides

TUTORIALS

SUNDAY | GREYS PEAK I/II

Attendance of SSI-20 tutorial sessions is not included in the Conference registration fee. You may purchase entrance to the tutorials for $100.00 at the Registration Desk located in the Main Lobby.

1:00 pm - 1:45 pm Advanced Methods in Electrochemical Impedance Spectroscopy
Bernard Boukamp, University of Twente

1:45 pm - 2:30 pm Defect Chemistry in Solid State Ionics
Truls Norby, University of Oslo

2:30 pm - 2:50 pm *Break, Longs Peak Foyer*

2:50 pm - 3:35 pm Battery Materials and Electrochemistry
Wei Lai, Michigan State University

3:35 pm - 4:20 pm Atomistic Modeling in Solid State Ionics
Dario Marrocchelli, Massachusetts Institute of Technology

DAILY SCHEDULE

SUNDAY

Registration ..... 12:00 pm – 7:00 pm
Main Lobby

Tutorial: Advanced Methods in Electrochemical Impedance Spectroscopy ..... 1:00 pm – 1:45 pm
Greys Peak I/II

Tutorial: Defect Chemistry in Solid State Ionics ..... 1:45 pm – 2:30 pm
Greys Peak I/II

Break ..... 2:30 pm – 2:50 pm
Longs Peak Foyer

Tutorial: Battery Materials and Electrochemistry .... 2:50 pm – 3:35 pm
Greys Peak I/II

Tutorial: Atomistic Modeling in Solid State Ionics ... 3:35 pm – 4:20 pm
Greys Peak I/II

Welcome Reception ..... 5:00 pm – 7:00 pm
Shavano Terrace

MONDAY

Registration ..... 8:00 am – 5:30 pm
Main Lobby

Poster Authors Set–up ..... 9:00 am – 11:30 am
Red Cloud Peak

L1: **Plenary** ..... 9:15 am – 10:10 am
Shavano Peak

Break ..... 10:10 am – 10:30 am
Shavano Foyer

A1: **SOFC—Cathodes I** ..... 10:10 am – 12:00 pm
Longs Peak

C1 **Rational Design of Battery Materials** ..... 10:10 am – 12:00 pm
Shavano Peak

D1 **Fundamentals of Transport and Reactivity and Nanoionics I** ..... 10:10 am – 12:00 pm
Grays Peak I/II

E1: **TCO—Defects, Materials** ..... 10:10 am – 12:00 pm
Quandary Peak I/II

F/H1: **Solid State Photoelectrochemistry/ High Temperature Routes to Solar Fuels I** ..... 10:10 am – 12:00 pm
Gray Peak III

Poster Session I—General Viewing and Lunch ..... 12:00 pm – 2:30 pm
Red Cloud Peak

A3: **SOFC—Cathodes II** ..... 2:30 pm – 5:30 pm
Longs Peak

C3 **Solid Electrolyte I** ..... 2:30 pm – 5:10 pm
Shavano Peak

C4 **Interfaces in Batteries** ..... 2:30 pm – 5:10 pm
Quandary Peak I/II

D3: **Fundamentals of Transport and Reactivity and Nanoionics II** ..... 2:30 pm – 5:30 pm
Grays Peak I/II

F/H3: **Solid State Photoelectrochemistry/High Temperature Routes to Solar Fuels II** ..... 2:30 pm – 5:20 pm
Grays Peak III

TUESDAY

Registration ..... 8:00 am – 7:30 pm
Main Lobby

Poster Authors Set–up ..... 9:00 am – 5:00 pm
Red Cloud Peak

L2: **Plenary** ..... 9:15 am – 10:10 am
Shavano Peak

Break ..... 10:10 am – 10:30 am
Shavano Foyer

A4: **SOFC—Cathodes III** ..... 10:10 am – 12:00 pm
Longs Peak

C5: **Metal–Air Batteries** ..... 10:10 am – 12:00 pm
Shavano Peak

D4: **Fundamentals of Transport and Reactivity and Nanoionics III** ..... 10:10 am – 12:00 pm
Grays Peak I/II

E3: **TCO—Materials, Processing, and Structures** ..... 10:10 am – 12:00 pm
Quandary Peak I/II

G1: **Switching and Sensing Phenomena I** ..... 10:10 am – 12:00 pm
Grays Peak III

Lunch (on your own) ..... 12:00 pm – 1:30 pm

ISSI Young Scientist Awards ..... 1:30 pm – 3:00 pm
Quandary Peak I/II

B1: **PEMFC/DMFC I** ..... 1:30 pm – 3:10 pm
Grays Peak III

C6: **Solid Electrolyte II** ..... 1:30pm – 5:10 pm
Shavano Peak

D5: **Fundamentals of Transport and Reactivity and Nanoionics IV** ..... 1:30p pm – 5:10 pm
Grays Peak I/II

K2: **Protonic Oxides I** ..... 1:30 pm – 3:00 pm
Longs Peak

Break ..... 3:10 pm – 3:30 pm
Longs Peak Foyer

A5: **SOFC—Electrolytes I** ..... 3:10 pm – 5:30 pm
Longs Peak

C7: **Characterization of Nanoscale and Local Structures I** ..... 3:10 pm – 5:10 pm
Quandary Peak I/II

G2: **Switching and Sensing Phenomena II** ..... 3:10 pm – 5:50 pm
Grays Peak III

Poster Session II—General Viewing ..... 5:20 pm – 7:20 pm
Red Cloud Peak

CONFERENCE BANQUET

Make time for this year's Conference Banquet on Wednesday evening at Soda Ridge Stables. **One Conference Banquet ticket is included in your registration fee.** Additional tickets may be purchased for $80 per person at the Registration Desk located in the Main Lobby. This event takes place outside, so please plan and dress for the weather accordingly. Transportation will be provided to and from the Conference Banquet.

WEDNESDAY

Registration.....8:00 am – 12:00 pm
Main Lobby

SSI Election.....8:00 am – 9:00 am
Shavano Peak

L3: **Plenary**.....9:15 am – 10:10 am
Shavano Peak

Break.....10:10 am – 10:30 am
Shavano Foyer

A7: **SOFC**.....10:10 am – 12:00 pm
Longs Peak

B3: **PEMFC/DMFC II**.....10:10 am – 12:00 pm
Quandary Peak I/II

C9: **Characterization of Nanoscale and Local Structures II**.....10:10 am – 11:50 am
Shavano Peak

I2: **Ion Transport in Hybrid Perovskites**.....10:10 am – 12:00 pm
Grays Peak I/II

J3: **Permeation Membranes I**.....10:10 am – 12:00 pm
Grays Peak III

Lunch and Optional Excursion (on your own).....12:00 pm – 5:00 pm

Conference Banquet.....5:00 pm – 7:00 pm
Soda Ridge Stables

THURSDAY

Registration.....8:00 am – 5:30 pm
Mail Lobby

L4: **Plenary**.....9:15 am – 10:10 am
Shavano Peak

Break.....10:10 am – 10:30 am
Shavano Foyer

A8: **SOEC**.....10:10 am – 12:00 pm
Longs Peak

C10: **Fundamentals of LIB Electrodes I**.....10:10 am – 12:00 pm
Shavano Peak

D7: **Fundamentals of Transport and Reactivity and Nanoionics** V.....10:10 am – 12:00 pm
Grays Peak I/II

J4: **Permeation Membranes II**.....10:10 am – 12:00 pm
Grays Peak III

K4: **Protonic Oxides II**.....10:10 am – 12:00 pm
Quandary Peak I/II

Lunch (on your own).....12:00 pm – 1:30 pm

A9: **SOFC—Electrolytes II, Anodes**.....1:30 pm – 5:30 pm
Longs Peak

B4: **PEMFC/DMFC III**.....1:30 pm – 3:10 pm
Grays Peak III

C11: **Beyond Lithium**.....1:30 pm – 4:50 pm
Shavano Peak

D8: **Fundamentals of Transport and Reactivity and Nanoionics VI**.....1:30 pm – 5:10 pm
Grays Peak I/II

K5: **Protonic Oxides III**.....1:30 pm – 5:10 pm
Quandary Peak I/II

Break.....3:10 pm – 3:30 pm
Longs Peak Foyer

J5: **Permeation Membranes III**.....3:10 pm – 5:30 pm
Grays Peak III

FRIDAY

Registration.....8:00 am – 12:30 pm
Mail Lobby

L4: **Plenary**.....9:15 am – 10:10 am
Shavano Peak

Break.....10:10 am – 10:30 am
Shavano Foyer

A10: **SOFC—Cathodes IV**.....10:10 am – 11:50 am
Longs Peak

C12: **Fundamentals of LIB Electrodes II**.....10:10 am – 12:00 pm
Shavano Peak

D9: **Fundamentals of Transport and Reactivity and Nanoionics VII**.....10:10 am – 12:00 pm
Grays Peak I/II

I3: **Ion Transport in Organic–Inogranic Hybrid Solids**.....10:10 am – 12:00 pm
Quandary Peak I/II

K6: **Protonic Oxides V**.....10:10 am – 11:50 am
Grays Peak III

CONFERENCE PROCEEDINGS

COST

Attendees who registered for this Conference at the full-price, regular rate, will receive one copy of the SSI-20 Proceedings. Student, retired and unemployed attendees, as well as those who wish to purchase additional copies, may do so at the Registration Desk located in the Main Lobby. The cost of Conference Proceedings is $70.

SUBMISSION INSTRUCTIONS

A special issue of the journal *Solid State Ionics* will be published with peer-reviewed papers from the 20th International Conference on Solid State Ionics.

- Submit your manuscript by July 17 at **ees.elsevier.com/ssi/default.asp**
- Be sure to select **SI: SOSI_SSI20** at the article type
- Adhere to the following page limits:
  - Plenary talks: no limit
  - Keynote and invited talks: 6 journal pages
  - Regular talks and posters: 4 journal pages

PLENARY SPEAKERS

9:15 AM – 10:10 AM · SHAVANO PEAK

MONDAY

Shu Yamaguchi
University of Tokyo

Bulk and Surface Oxide Protonics for Energy Conversion Devices: Role of Percolation and Grotthus Mechanism in Oxide Protonics

Shu Yamaguchi is professor at the department of materials engineering, School of Engineering, The University of Tokyo, Japan. He is a graduate from Tokyo Institute of Technology, earning his Dr. Eng. in metallurgy on thermodynamic activity measurements in sodium silicate and phosphate melts using Na beta–alumina as a solid electrolyte in 1983. His expertise in solid state chemistry has initiated from the research on tracer diffusivity measurements of 18O in $Fe_{1-x}O$ and Co_{1-x} O using SIMS in 1980. He is engaged in the interdisciplinary area between chemical thermodynamics and solid state chemistry, such as the electronic structure in oxide protonics materials, atomic switch, surface protonics, etc.

TUESDAY

Sossina M. Haile
Northwestern University

Insights into Proton Transport in Superprotonic Solid Acids

Sossina M. Haile is the Walter P. Murphy Professor of Materials Science and Engineering at Northwestern University. She earned her PhD degree in materials science and engineering from the Massachusetts Institute of Technology in 1992. As part of her studies, Haile spent two years at the Max Plank Institute for Solid State Research, Stuttgart, Germany, first as a Fulbright Fellow, then as a Humboldt Fellow.

She has published more than 150 articles and holds 15 patents on these and other topics. Haile is the recipient of many prestigious awards including an American Competitiveness and Innovation (ACI) Fellowship in 2008 from the National Science Foundation in recognition of "her timely and transformative research in the energy field and her dedication to inclusive mentoring, education and outreach across many levels," the 2012 International Prize in Ceramics from the World Academy of Ceramics, and the 2010 Chemical Pioneers Award of the Chemical Heritage Foundation. Haile was named by *Newsweek* magazine in its 2007 end-of-the-year issue as one of twelve people to watch in 2008.

WEDNESDAY

Juergen Janek
Justus-Liebig University, Giessen

Electrode Kinetics in the Solid State

Juergen Janek received his PhD in chemistry from the University of Hannover. He finished his Habilitation and became assistant professor at the University of Hannover in 1997. After a short period in Kiel in 1999, he accepted a position as chair of physical chemistry at Justus-Liebig University, Giessen and became director of the Institute of Physical Chemistry. In 2004 he was invited to Seoul National University and Tohoku University as a visiting professor, and in 2008 he became a visiting professor at Aix Marseille University. Since 2011, he has served as scientific director of BELLA (Batteries and Electrochemistry Laboratory), a joint lab of BASF SE and Karlsruhe Institute of Technology, and member of the International Network for Batteries and Electrochemisty of BASF SE. Janek holds several patents and is author of about 200 peer–reviewed papers in a wide range of journals.

THURSDAY

Joachim Heberle
Free University of Berlin

On the Mechanism of Cation Translocation across Channelrhodopsin

Joachim Heberle has a scientific background at the interface between biology, chemistry and physics. He studied chemistry at the Universities of Stuttgart and Wuerzburg. He moved to Berlin to defend his PhD thesis in biophysics at the Free University of Berlin (1991) followed by a postdoc at the Hahn–Meitner Institute Berlin (1991–1993). He served as group leader at the Research Center Juelich (1993–2005) and received the Habilitation in Biophysical Chemistry from the University of Duesseldorf (1998).

During his time as a postdoc, he was a visiting scientist at the Universities of Tucson and Gothenburg. In 2005, he became the professorial chair for biophysical chemistry at Bielefeld University. In 2009, he accepted the offer from the physics department of the Free University of Berlin and has been a full professor in biophysics since then. Heberle served as a member of the study section of chemistry of the German Research Foundation and is currently a member of the Excellence Council of his host university.

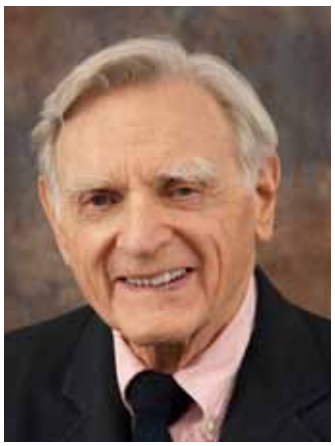

FRIDAY

John B. Goodenough
University of Texas at Austin

SPECIAL PLENARY SPEAKER

Alternative Strategies for Electrical Energy Storage

After receiving his PhD degree in physics in 1952, John B. Goodenough was a group leader at the MIT Lincoln Laboratory where he helped to develop the ferrimagnetic spinels used in the first Ram memory of the digital computer. In the course of this work, he identified structural transitions caused by cooperative orbital ordering and he developed the rules for the sign of the interatomic spin–spin magnetic interactions. In the subsequent decade, Goodenough explored the magnetic and transport properties of transition–metal compounds, including the transition from localized to itinerant electron behavior where strong electron–lattice interactions give rise to static or dynamic charge–density waves. These studies were summarized in his two books *Magnetism and the Chemical Bond* and *Les oxydes des métaux de transition*, translated from his long review titled *Metallic Oxides*.

With the first oil crisis in the early 1970s, Goodenough turned to the study of energy materials. Called in 1976 to head the Inorganic Chemistry Laboratory of the University of Oxford, UK, he developed in England the layered $Li_{1-x}CoO_2$ for the cathode of a rechargeable Li–ion battery; it was used in the battery of the first cell telephone marketed by the SONY Corporation that launched the wireless revolution. Goodenough subsequently identified two other transition–metal oxide structures, spinel and ordered olivine, as potential cathodes material that are also used as cathodes in commercial Li–ion batteries. In 1986, Goodenough took the Virginia H. Cockrell Centennial Chair of Engineering at the University of Texas at Austin where he has returned to his fundamental studies of transition–metal oxides and their use as electrodes of Li–ion batteries and the solid–oxide fuel cell.

THANK YOU!

The SSI-20 Conference has been funded, in part, by the generous contributions of these organizations.

Platinum Sponsor

CoorsTek
Amazing Solutions®

www.coorstek.com

Conference Support

Travel support for attendees has been provided by the U.S. Army Research Office under Grant W911NF-15-1-0122. Co-sponsorship by for-profit companies does not constitute endorsement or recommendation of products by the U.S. Government or the Army Research Office.

www.arl.army.mil/

ORAL PRESENTATIONS AT-A-GLANCE

MONDAY

Shavano Peak	Longs Peak	Grays Peak I/II	Quandary Peak I/II	Grays Peak III
Welcome and Introductions 9:15 am - 9:25 am				
Plenary Speaker L1.01 - Shu Yamaguchi 9:25 am - 10:10 am				
BREAK 10:10 am - 10:30 am				
C: Electrodes and Solid Electrolytes for Batteries	**A: Solid Oxide Fuel Cells and Electrolyzers**	**D: Fundamentals of Transport and Reactivity and Nanoionics**	**E: Transparent Conducting Oxides**	**F/H: Solid State Photoelectrochemistry/ High Temperature Routes to Solar Fuels**
C1: Rational Design of Battery Materials	**A1: SOFC—Cathodes I**	**D1: Fundamentals of Transport and Reactivity and Nanoionics I**	**E1: FTCO I—Defects, Materials**	**F/H1: Solid State Photoelectrochemistry/ High Temperature Routes to Solar Fuels I**
** C1.01 - Yi Cui 10:30 am - 11:00 am	** A1.01 - Bilge Yildiz 10:30 am - 11:00 am	** D1.01 - Harry Tuller 10:30 am - 11:00 am	** E1.01 - Stephan Lany 10:30 am - 11:00 am	** F/H 1.01 - Ellen Stechel 10:30 am - 11:00 am
C1.02 - Saiful Islam 11:00 am - 11:20 am	A1.02 - Andrea Cavallaro 11:00 am - 11:20 am	D1.02 - David McComb 11:00 am - 11:20 am	E1.02 - Cleva Ow-Yang 11:00 am - 11:20 am	F/H1.02 - Antoine Emery 11:00 am - 11:20 am
C1.03 - Yifei Mo 11:20 am - 11:40 am	A1.03 - Hiroki Muroyama 11:20 am - 11: 40 am	D1.03 - Jose Santiso 11:20 am - 11:40 am	E1.03 - Piero Mazzolini 11:20 am - 11:40 am	* F/H1.03 - Christian Sattler 11:20 am - 11:40 am
C1.04 - Ruijuan Xiao 11:40 am - 12:00 pm	* A1.04 - Koji Amezawa 11:40 am - 12:00 pm	D1.04 - Matthias Elm 11:40 am - 12:00 pm	E1.04 - Yang Song 11:40 am - 12:00 pm	F/H1.04 - Yoshihiro Yamazaki 11:40 am - 12:00 pm
POSTER SESSION RED CLOUD PEAK 12:00 pm - 2:30 pm				
C: Electrodes and Solid Electrolytes for Batteries	**A: Solid Oxide Fuel Cells and Electrolyzers**	**D: Fundamentals of Transport and Reactivity and Nanoionics**	**C: Electrodes and Solid Electrolytes for Batteries**	**F/H: Solid State Photoelectrochemistry/ High Temperature Routes to Solar Fuels**
C3: Solid Electrolyte I	**A3: SOFC—Cathodes II**	**D3: Fundamentals of Transport and Reactivity and Nanoionics II**	**C4: Interfaces in Batteries**	**F/H3: Solid State Photoelectrochemistry/ High Temperature Routes to Solar Fuels II**
* C3.01 - Wei Lai 2:30 pm - 2:50 pm	* A3.01 - David Mueller 2:30 pm - 2:50 pm	* D3.01 - Klaus Funke 2:30 pm - 2:50 pm	* C4.01 - Yue Qi 2:30 pm - 2:50 pm	* F/H3.01 - Jonathan Scheffe 2:30 pm - 2:50 pm
C3.02 - William Manalastas 2:50 pm - 3:10 pm	A3.02 - Florent Tonus 2:50 pm - 3:10 pm	D3.02 - Osamu Kamishima 2:50 pm - 3:10 pm	C4.02 - Arnulf Latz 2:50 pm - 3:10 pm	F/H3.02 - Gregory Jackson 2:50 pm - 3:10 pm
C3.03 - Rowena Brugge 3:10 pm - 3:30 pm	A3.03 - Ghislain Rupp 3:10 pm - 3:30 pm	D3.03 - Kaustubh Bhat 3:10 pm - 3:30 pm	C4.03 - Taro Hitosugi 3:10 pm - 3:30 pm	** F/H3.03 - Ian Sharp 3:10 pm - 3:40 pm
C3.04 - Michal Struzik 3:30 pm - 3:50 pm	A3.04 - Mathew Niania 3:30 pm - 3:50 pm	D3.04 - Alexander Rettie 3:30 pm - 3:50 pm	C4.04 - Lijun Fu 3:30 pm - 3:50 pm	** F/H3.04 - Gordana Dukovic 3:40 pm - 4:10 pm
C3.05 - Matthew Klenk 3:50 pm - 4:10 pm	A3.05 - David Halat 3:50 pm - 4:10 pm	D3.05 - Ilia Valov 3:50 pm - 4:10 pm	C4.05 - Rene Hausbrand 3:50 pm - 4:10 pm	** F/H3.05 - Kevin Sivula 4:10 pm - 4:40 pm
C3.06 - Tsuyoshi Ohnishi 4:10 pm - 4:30 pm	* A3.06 - Stephen Skinner 4:10 pm - 4:30 pm	D3.06 - Xuedong Bai 4:10 pm - 4:30 pm	C4.06 - Hirotoshi Yamada 4:10 pm - 4:30 pm	F/H3.06 - Liming Zhang 4:40 pm - 5:00 pm
C3.07 - Chih-Long Tsai 4:30 pm - 4:50 pm	A3.07 - Chuancheng Duan 4:30 pm - 4:50 pm	D3.07 - Cristina Tealdi 4:30 pm - 4:50 pm	C4.07 - Yusuke Ito 4:30 pm - 4:50 pm	F/H3.07 - Giuliano Gregori 5:00 pm - 5:20 pm
C3.08 - Miaofang Chi 4:50 pm - 5:10 pm	A3.08 - Liangdong Fan 4:50 pm - 5:10 pm	D3.08 - Julia Langer 4:50 pm - 5:10 pm	C4.08 - Lei Cheng 4:50 pm - 5:10 pm	
	A3.09 - Giuseppe Brunello 5:10 pm - 5:30 pm	D3.09 - Subramanian Sankaranarayanan 5:10 pm - 5:30 pm		

* Invited **Keynote

TUESDAY

Shavano Peak	Longs Peak	Grays Peak I/II	Quandary Peak I/II	Grays Peak III
Welcome and Introductions 9:15 am - 9:25 am				
Plenary Speaker L2.01 - Sossina Haile 9:25 am - 10:10 am				
BREAK 10:10 am - 10:30 am				
C: Electrodes and Solid Electrolytes for Batteries	**A: Solid Oxide Fuel Cells and Electrolyzers**	**D: Fundamentals of Transport and Reactivity and Nanoionics**	**E: Transparent Conducting Oxides**	**G: Switching and Sensing Phenomena**
C5: Metal-Air Batteries	**A4 SOFC—Cathodes III**	**D4: Fundamentals of Transport and Reactivity and Nanoionics III**	**E3: TCO 2—Materials, Processing, and Structures**	**G1: Switching and Sensing Phenomena I**
** C5.01 - Linda Nazar 10:30 am - 11:00 am	** A4.01 - Henny Bouwmeester 10:30 am - 11:00 am	** D4.01 - Rotraut Merkle 10:30 am - 11:00 am	** E3.01 - Hideo Hosono 10:30 am - 11:00 am	** G1.01 - Manfred Martin 10:30 am - 11:00 am
* C5.02 - Arumugam Manthiram 11:00 am - 11:20 am	A4.02 - Alexander Tomkiewicz 11:00 am - 11:20 am	D4.02 - John Druce 11:00 am - 11:20 am	E3.02 - Shu-Yi Tsai 11:00 am - 11:20 am	* G1.02 - Dario Marrocchelli 11:00 am - 11:20 am
* C5.03 - Hong Li 11:20 am - 11:40 am	A4.03 - Andreas Nenning 11:20 am - 11: 40 am	D4.03 - Maxim Ananyev 11:20 am - 11:40 am	E3.03 - Jitendra Kumar 11:20 am - 11:40 am	G1.03 - Dima Kalaev 11:20 am - 11:40 am
C5.04 - Stefan Adams 11:40 am - 12:00 pm	* A4.04 - Edith Bucher 11:40 am - 12:00 pm	D4.04 - Eugene Kotomin 11:40 am - 12:00 pm	E3.04 - Gesa Beck 11:40 am - 12:00 pm	G1.04 - Nahum Maso 11:40 am - 12:00 pm
LUNCH 12:00 pm - 1:30 pm				
C: Electrodes and Solid Electrolytes for Batteries	**K: Proton-Conducting Oxides**	**D: Fundamentals of Transport and Reactivity and Nanoionics**	**M1: ISSI Young Scientist Award**	**B: Polymer Electrolyte Fuel Cells and Electrolyzers**
C6: Solid Electrolyte II	**K2: Protonic Oxides I**	**D5: Fundamentals of Transport and Reactivity and Nanoionics IV**		**B1: PEMFC/DMGC I**
* C6.01 - Diana Golodnitsky 1:30 pm - 1:50 pm	**K2.01 - Clare Grey 1:30 pm - 2:00 pm	* D5.01 - Hans Wiemhoefer 1:30 pm - 1:50 pm	M1.01 - To Be Determined 1:30 pm - 1:45 pm	* B1.01 - Joseph Dura 1:30 pm - 1:50 pm
C6.02 - Martin Wilkening 1:50 pm - 2:10 pm	K2.02 - Itaru Oikawa 2:00 pm - 2:20 pm	D5.02 - Kerstin Neuhaus 1:50 pm - 2:10 pm	M1.02 - To Be Determined 1:45 pm - 2:00 pm	B1.02 - Vito Di Noto 1:50 pm - 2:10 pm
C6.03 - Marie Guin 2:10 pm - 2:30 pm	* K2.03 - Jong-Ho Lee 2:20 pm - 2:40 pm	* D5.03 - Igor Lubomirsky 2:10 pm - 2:30 pm	M1.03 - To Be Determined 2:00 pm - 2:15 pm	B1.03 - Michael Marino 2:10 pm - 2:30 pm
C6.04 - Qianli Ma 2:30 pm - 2:50 pm	K2.04 - Kwati Leonard 2:40 pm - 3:00 pm	D5.04 - Jianmin Shi 2:30 pm - 2:50 pm	M1.04 - To Be Determined 2:15 pm - 2:30 pm	B1.04 - Tara Pandey 2:30 pm - 2:50 pm
C6.05 - Yue Deng 2:50 pm - 3:10 pm		* D5.05 - Tatsuya Kawada 2:50 pm - 3:10 pm	M1.05 - To Be Determined 2:30 pm - 2:45 pm	* B1.05 - Robert Moore 2:50 pm - 3:10 pm
			M1.06 - To Be Determined 2:45 pm - 3:00 pm	
BREAK 3:10 pm - 3:30 pm				
C: Electrodes and Solid Electrolytes for Batteries	**A: Solid Oxide Fuel Cells and Electrolyzers**	**D: Fundamentals of Transport and Reactivity and Nanoionics**	**C: Electrodes and Solid Electrolytes for Batteries**	**G: Switching and Sensing Phenomena**
C6: Solid Electrolyte II	**A5: SOFC — Electrolytes**	**D5: Fundamentals of Transport and Reactivity and Nanoionics IV**	**C7: Characterization of Nanoscale and Local Structures I**	**G2: Switching and Sensing Phenomena II**
C6.06 - Ruigang Zhang 3:30 pm - 3:50 pm	* A5.01 - Koichi Eguchi 3:30 pm - 3:50 pm	* D5.06 - Jennifer Rupp 3:30 pm - 3:50 pm	C7.01 - Ruimin Qiao 3:30 pm - 3:50 pm	* G2.01 - Kazuya Terabe 3:30 pm - 3:50 pm
C6.07 - Fabien Lalere 3:50 pm - 4:10 pm	A5.02 - David Kiercks 3:50 pm - 4:10 pm	D5.07 - Alex Morata 3:50 pm - 4:10 pm	C7.02 - Janina Molenda 3:50 pm - 4:10 pm	* G2.02 - Daniele Ielmini 3:50 pm - 4:10 pm
C6.08 - Philipp Braun 4:10 pm - 4:30 pm	A5.03 - Nan Yang 4:10 pm - 4:30 pm	D5.08 - Yeliz Unutulmazsoy 4:10 pm - 4:30 pm	C7.03 - Matthew McDowell 4:10 pm - 4:30 pm	* G2.03 - Monica Burriel 4:10 pm - 4:30 pm
C6.09 - Dominik Weber 4:30 pm - 4:50 pm	A5.04 - Jiwoong Bae 4:30 pm - 4:50 pm	D5.09 - John Irvine 4:30 pm - 4:50 pm	C7.04 - Xuefeng Wang 4:30 pm - 4:50 pm	G2.04 - Anja Wedig 4:30 pm - 4:50 pm
C6.10 - Yo Kobayashi 4:50 pm - 5:10 pm	A5.05 - Julius Koettgen 4:50 pm - 5:10 pm	D5.10 - David Mebane 4:50 pm - 5:10 pm	C7.05 - Nils Ohmer 4:50 pm - 5:10 pm	G2.05 - Sebastian Schweiger 4:50 pm - 5:10 pm
	A5.06 - Wojciech Wrobel 5:10 pm - 5:30 pm		C7.06 - William Gent 5:10 pm - 5:30 pm	G2.06 - Fernando Garzon 5:10 pm - 5:30 pm
				G2.07 - Xin Guo 5:30 pm - 5:50 pm

* Invited **Keynote

ORAL PRESENTATIONS AT-A-GLANCE

WEDNESDAY

Shavano Peak	Longs Peak	Grays Peak I/II	Quandary Peak I/II	Grays Peak III
ISSI Election 8:00 am - 9:00 am				
Welcome and Introductions 9:15 am - 9:25 am				
Plenary Speaker L3.01 - Juergen Janek 9:25 am - 10:10 am				
BREAK 10:10 am - 10:30 am				
C: Electrodes and Solid Electrolytes for Batteries	**A: Solid Oxide Fuel Cells and Electrolyszers**	**I: Ion Transport in Hybrid Organic-Inorganic Solids**	**B: Polymer Electrolyte Fuel Cells and Electrolyzers**	**J: Permeation Membranes**
C9: Characterization of Nanoscale and Local Structures II	**A7: SOFC**	**I2: Ion Transport in Hybrid Perovskites**	**B3: PEMFC/DMFC II**	**J3: Permeation Membranes I**
C9.01 - Thomas Leichtweiss 10:30 am - 10:50 am	** A7.01 - Eric Wachsman 10:30 am - 11:00 am	** I2.01 - Jinsong Huang 10:30 am - 11:00 am	** B3.01 - Stephen Paddison 10:30 am - 11:00 am	** J3.01 - Michael Carolan 10:30 am - 11:00 am
C9.02 - Sabrina Sartori 10:50 am - 11:10 am	A7.02 - Carlos Bernuy-Lopez 11:00 am - 11:20 am	I2.02 - Daniel Slotcabage 11:00 am - 11:20 am	B3.02 - Andrew Herring 11:00 am - 11:20 am	J3.02 - Hailei Zhao 11:00 am - 11:20 am
C9.03 - Naoaki Kuwata 11:10 am - 11:30 am	A7.03 - Gyeong Man Choi 11:20 am - 11: 40 am	I2.03 - Abraham Saldivar Valdes 11:20 am - 11:40 am	B3.03 - Matthew Liberatore 11:20 am - 11:40 am	* J3.03 - Christian Niedrig 11:20 am - 11:40 am
C9.04 - Steven DeCaluwe 11:30 am - 11:50 am	A7.04 - Francesco Ciucci 11:40 am - 12:00 pm	I2.04 - Francesca Maria Toma 11:40 am - 12:00 pm	B3.04 - Ye Liu 11:40 am - 12:00 pm	J3.04 - Jitendra Kumar 11:40 am - 12:00 pm

* Invited **Keynote

TRAVEL RESOURCES

COLORADO MOUNTAIN EXPRESS

1-800-525-6363 • www.mrs.org/ssi-20-travel-resources

The Colorado Mountain Express offers **daily shuttle service** between the Denver International Airport and Keystone Resort from 9:30 am - 9:30 pm. It also offers private shuttle, chauffeured travel and scheduled shuttle service. Visit **www.coloradomountainexpress.com/schedules** for a schedule of shuttle destinations and times.

Reduced Rates

$ 54 – Shared Shuttle Van (10-12 passengers)

$ 312 – Charter Van Private (10 passengers)

$350 – Premier SUV Private (5 Passengers)

** Rate includes three bags per person ($50 for additional bags).*

GETTING AROUND THE RESORT

Keystone Resort offers its own transportation system for guests to and from lodging locations, the Conference Center and local restaurants. Shuttles operate 6:00 am – 12 midnight daily. Shuttles pick up at stops throughout the Resort on 20-minute intervals.

PARKING

Self-parking is complimentary throughout the Keystone Resort property.

INTERNET ACCESS

Conference attendees will have **complimentary wireless internet access** in their sleeping room and throughout the meeting space at Keystone Resort and Conference Center.

THURSDAY

Shavano Peak	Longs Peak	Grays Peak I/II	Quandary Peak I/II	Grays Peak III
Welcome and Introductions 9:15 am - 9:25 am				
Plenary Speaker L4.01 - Joachim Heberle 9:25 am - 10:10 am				
BREAK 10:10 am - 10:30 am				
C: Electrodes and Solid Electrolytes for Batteries	**A: Solid Oxide Fuel Cells and Electrolyszers**	**D: Fundamentals of Transport and Reactivity and Nanoionics**	**K: Proton-Conducting Oxides**	**J: Permeation Membranes**
C10: Fundamentals of LIB Electrodes I	**A8: SOEC**	**D7: Fundamentals of Transport and Reactivity and Nanoionics V**	**K4: Protonic Oxides II**	**J4: Permeation Membranes II**
** C10.01 - Stanley Whittingham 10:30 am - 11:00 am	** A8.01 - Peter Hendriksen 10:30 am - 11:00 am	** D7.01 - Han-Ill Yoo 10:30 am - 11:00 am	** K4.01 - Marie-Laure Fontaine 10:30 am - 11:00 am	** J4.01 - Wolff-Ragnar Keibach 10:30 am - 11:00 am
* C10.02 - Jordi Cabana 11:00 am - 11:20 am	A8.02 - Alexander Opitz 11:00 am - 11:20 am	D7.02 - Edmund Mills 11:00 am - 11:20 am	K4.02 - Neal Sullivan 11:00 am - 11:20 am	J4.02 - Yu Zhang 11:00 am - 11:20 am
C10.03 - Yiyang Li 11:20 am - 11:40 am	A8.03 - Einar Vollestad 11:20 am - 11: 40 am	D7.03 - Konrad Swierczek 11:20 am - 11:40 am	K4.03 - Laura Navarette 11:20 am - 11:40 am	J4.03 - Madhumidha Ramasamy 11:20 am - 11:40 am
C10.04 - Frederic Blanc 11:40 am - 12:00 pm	A8.04 - Chi Chen 11:40 am - 12:00 pm	D7.04 - Kazuaki Toyoura 11:40 am - 12:00 pm	K4.04 - Michael Stoukides 11:40 am - 12:00 pm	J4.04 - Jong Joo Hoon 11:40 am - 12:00 pm
LUNCH 12:00 pm - 1:30 pm				
C: Electrodes and Solid Electrolytes for Batteries	**A: Solid Oxide Fuel Cells and Electrolyszers**	**D: Fundamentals of Transport and Reactivity and Nanoionics**	**K: Proton-Conducting Oxides**	**B: Polymer Electrolyte Fuel Cells and Electrolyzers**
C11: Beyond Lithium	**A9: SOFC—Electrolytes II, Anodes**	**D8: Fundamentals of Transport and Reactivity and Nanoionics VI**	**K5: Protonic Oxides II**	**B4: PEMFC/DMFC III I**
* C11.01 - Yan Yu 1:30 pm - 1:50 pm	* A9.01 - Tatsumi Ishihara 1:30 pm - 1:50 pm	* D8.01 - Roger De Souza 1:30 pm - 1:50 pm	K5.01 - Hanlin Xie 1:30 pm - 1:50 pm	* B4.01 - Cristina Iojoiu 1:30 pm - 1:50 pm
C11.02 - Yong-Sheng Hu 1:50 pm - 2:10 pm	A9.02 - Hailei Zhao 1:50 pm - 2:10 pm	D8.02 - Russell Maier 1:50 pm - 2:10 pm	K5.02 - Jianhua Tong 1:50 pm - 2:10 pm	B4.02 - Kun-lin Liu 1:50 pm - 2:10 pm
C11.03 - Rengarajan Shanmugam 2:10 pm - 2:30 pm	A9.03 - Alevtina Smirnova 2:10 pm - 2:30 pm	D8.03 - Wolfgang Preis 2:10 pm - 2:50 pm	K5.03 - Tor Grande 2:10 pm - 2:30 pm	B4.03 - Ilya Zharov 2:10 pm - 2:30 pm
C11.04 - Satoshi Kajiyama 2:30 pm - 2:50 pm	A9.04 - Jong-Sook Lee 2:30 pm - 2:50 pm	D8.04 - Jean-Marc Bassat 2:30 pm - 2:50 pm	K5.04 - Steven McIntosh 2:30 pm - 2:50 pm	B4.04 - Shannon Boettcher 2:30 pm - 2:50 pm
C11.05 - Timothy Arthur 2:50 pm - 3:10 pm	A9.05 - Nicola Perry 2:50 pm - 3:10 pm	D8.05 - Lixin Sun 2:50 pm - 3:10 pm	K5.05 - Mariya Ivanova 2:50 pm - 3:10 pm	B4.05 - Korakot Sombatmankhong 2:50 pm - 3:10 pm
BREAK 3:10 pm - 3:30 pm				
C: Electrodes and Solid Electrolytes for Batteries	**A: Solid Oxide Fuel Cells and Electrolyszers**	**D: Fundamentals of Transport and Reactivity and Nanoionics**	**K: Proton-Conducting Oxides**	**J: Permeation Membranes**
C11: Beyond Lithium	**A9: SOFC—Electrolytes II, Anodes**	**D8: Fundamentals of Transport and Reactivity and Nanoionics VI**	**K5: Protonic Oxides III**	**J5: Permeation Membranes III**
C11.06 - Ryan Bayliss 3:30 pm - 3:50 pm	* A9.06 - WooChul Jung 3:30 pm - 3:50 pm	* D8.06 - Truls Norby 3:30 pm - 3:50 pm	K5.06 - Francesco Bozza 3:30 pm - 3:50 pm	* J5.01 - Ian Metcalfe 3:30 pm - 3:50 pm
C11.07 - Yuki Orikasa 3:50 pm - 4:10 pm	A9.07 - Mirai Takeda 3:50 pm - 4:10 pm	D8.07 - Tor Bjorheim 3:50 pm - 4:10 pm	K5.07 - Erik Jedvik 3:50 pm - 4:10 pm	J5.02 - Hitoshi Takamura 3:50 pm - 4:10 pm
C11.08 - Premkumar Senguttuvan 4:10 pm - 4:30 pm	A9.08 - Xavier Flandre 4:10 pm - 4:30 pm	D8.08 - Sangtae Kim 4:10 pm - 4:30 pm	K5.08 - Anders Lindman 4:10 pm - 4:30 pm	J5.03 - Enrique Ruiz-Trejo 4:10 pm - 4:30 pm
C11.09 - Austin Sendek 4:30 pm - 4:50 pm	A9.09 - Jun Jiang 4:30 pm - 4:50 pm	D8.09 - Mehmet Ali Gulgun 4:30 pm - 4:50 pm	K5.09 - Daniel Clark 4:30 pm - 4:50 pm	J5.04 - Maria Balaguer 4:30 pm - 4:50 pm
	A9.10 - Dino Klotz 4:50 pm - 5:10 pm	D8.10 - Helena Tellez 4:50 pm - 5:10 pm	K5.10 - Anna Magraso 4:50 pm - 5:10 pm	J5.05 - Sonia Escolastico 4:50 pm - 5:10 pm
	A9.11 - Javier Macias 5:10 pm - 5:30 pm			J5.06 - Jonathan Polfus 5:10 pm - 5:30 pm

* Invited **Keynote

ORAL PRESENTATIONS AT-A-GLANCE

FRIDAY

Shavano Peak	Longs Peak	Grays Peak I/II	Quandary Peak I/II	Grays Peak III
Welcome and Introductions 9:15 am - 9:25 am				
Special Plenary Speaker L5.01 - John Goodenough 9:25 am - 10:10 am				
BREAK 10:10 am - 10:30 am				
C Electrodes and Solid Electrolytes for Batteries	**A: Solid Oxide Fuel Cells and Electrolyszers**	**D: Fundamentals of Transport and Reactivity and Nanoionics**	**K: Proton-Conducting Oxides**	**I: Ion Transport in Hybrid Organic-Inorganic Solids**
C12: Fundamentals of LIB Electrodes II	**A10: SOFC—Cathodes IV**	**D9: Fundamentals of Transport and Reactivity and Nanoionics VII**	**K6: Protonic Oxides V**	**I3: Ion Transport in Organic-Inorganic Hybrid Solids**
** C12.01 - Miran Gaberscek 10:30 am - 11:00 am	* A10.01 - Ranran Peng 10:30 am - 10:50 am	** D9.01 - Maria Forsyth 10:30 am - 10:00 am	* K6.01 - Genki Kobayashi 10:30 am - 10:50 am	** I3.01 - Satoshi Horike 10:30 am - 10:55 am
C12.02 - Feng Lin 11:00 am - 11:20 am	A10.02 - Rose-Noelle Vannier 10:50 am - 11:00 am	* D9.02 - Bettina Lotsch 11:00 am - 11:20 am	K6.02 - Yuji Okuyama 10:50 am - 11:10 am	** I3.02 - George Shimizu 10:55 am - 11:20 am
C12.03 - Zhaoxiang Wang 11:20 am - 11:40 am	A10.03 - Katherine Bagarinao 11:10 am - 11:30 am	D9.03 - Takashi Nakamura 11:20 am - 11:40 am	K6.03 - Takahisa Omata 11:10 am - 11:30 am	I3.03 - Rajendra Singh 11:20 am - 11:40 am
C12.04 - Jung-Hyun Kim 11:40 am - 12:00 pm	A10.04 - Saim Saher 11:30 am - 11:50 am	D9.04 - Yaoqing Zhang 11:40 am - 12:00 pm	K6.04 - Hiroshige Matsumoto 11:30 am - 11:50 am	I3.04 - Xiaohui Song 11:40 am - 12:00 pm

* Invited **Keynote

MONDAY POSTER SESSIONS AT-A-GLANCE

POSTER AUTHORS SET-UP

Monday 9:00 am - 11:30 am
Tuesday 9:00 am - 5:00 pm

GENERAL VIEWING

Red Cloud Peak

Monday 12:00 pm - 2:30 pm
Tuesday 5:20 pm - 7:20 pm

A: Solid Oxide Fuel Cells and Electrolyzers
B: Polymer Electrolyte Fuel Cells and Electrolyzers
C: Electrodes and Solid Electrolytes for Batteries
D: Fundamentals of Transport and Reactivity and Nanoionics
E: Transparent Conducting Oxides
F/H: Solid State Photoelectrochemistry/High Temperature Routes for Solar Fuels
G: Switching and Sensing Phenomena
I: Ion Transport in Hybrid Organic-Inorganic Solids
J: Permeation Membranes
K: Proton-Conducting Oxides

POSTER WINNERS will be announced at the SSI-20 Conference Banquet on Wednesday evening and will be treated to an exclusive celebration dinner on Thursday night sponsored by CoorsTek.

PAPER #	PRESENTER
A2.01	Maija Kuklja
A2.02	Steffen Grieshammer
A2.04	Marco Arrigoni
A2.05	Jason Kim
A2.06	Ji-Su Kim
A2.07	Ryan Jacobs
A2.08	Xingfeng He
A2.09	Shany Hershkovitz
A2.10	Eiki Niwa
A2.11	Aleksey Yaremchenko
A2.12	Chang Sub Kim
A2.13	Vladimir Sereda
A2.14	Dmitry Tsvetkov
A2.15	Vasileios Kyriakou
A2.16	Steven McIntosh
A2.17	Yihan Ling
A2.18	Monica Sandoval
A2.19	Jason Nicholas
A2.20	Elena Pikalova
A2.21	Alevtina Smirnova
A2.22	Gyeong Man Choi
A2.23	Samir Boulfrad
A2.24	Theodore Burye
A2.25	Elena Pikalova
A2.26	Shengli An
A2.27	Keiji Yashiro
A2.28	Michael Machala
A2.29	Liangdong Fan
A2.30	Heike Stoermer
A2.31	Tobias Huber
A2.32	Ryan Bayliss
A2.33	Zhongliang Zhan
A2.34	Bo Yu
A2.35	Jinxia Wang
A2.36	Michael Stoukides
A2.37	Robson Grosso
A2.38	Xiaomei Liu
A2.39	Xiaomei Liu
A2.40	Prabhakar Singh
A2.41	Emily Fraik
A2.42	Efstratios Stavrakakis
A2.43	Anna Shlyakhtina
A2.44	Sunghwan Lee
A2.45	Anna Borowska-Centkowska
A2.46	Eui-Chol Shin
A2.47	Denis Osinkin

PAPER #	PRESENTER
A2.48	Eric Straley
A2.49	Mattia Saccoccio
A2.50	Taehyun Park
A2.51	Zulma Moreno
A2.52	Pravin Kumar
A2.53	Takuya Hashimoto
A2.54	Sergey Pikalov
A2.55	Jean-Marc Bassat
A2.56	Enrique Ruiz-Trejo
C2.01	Andreas Dunst
C2.02	Marcin Molenda
C2.03	Neelesh Rai
C2.04	Kikuko Hayamizu
C2.05	Jennifer Rupp
C2.06	Fuminori Mizuno
C2.07	Timothy Arthur
C2.08	Selvasekarapandian Subramanian
C2.09	Selvasekarapandian Subramanian
C2.10	Sandra Lobe
C2.11	Atsutaka Kato
C2.12	Miriam Botros
C2.13	Jong-Sook Lee
C2.14	Chia-Chin Chen
C2.15	Lin Gu
C2.16	Muhammad Hasanuzzaman
C2.17	Tomonari Takeuchi
C2.18	Miriam Kunze
C2.19	Rengarajan Shanmugam
C2.20	Josh Thomas
C2.21	Sumaletha Narayanan
C2.22	Toyoki Okumura
C2.23	Ruzica Djenadic
C2.24	Fangfang Chen
C2.25	Takuya Matsuyama
C2.26	Xinzhi Chen
C2.27	Xingyu Chen
C2.28	A K Thakur
C2.29	A K Thakur
C2.30	Su-Hyun Moon
C2.31	Su-Hyun Moon
C2.32	Linqin Mu
C2.33	Prasanna Kadirvelayutham
C2.34	Yuhki Yui
C2.35	Wagiyo Honggowiranto
C2.36	Anna Milewska
C2.37	Diana Golodnitsky

PAPER #	PRESENTER
C2.38	Kaiqi Xu
C2.39	Akito Takasaki
C2.40	Lukasz Kondracki
C2.41	Akihisa Aimi
C2.42	Ryoji Inada
C2.43	Rotraut Merkle
C2.44	Namrata Tripathi
C2.45	Sven Uhlenbruck
C2.46	Durgaprasad Ramteke
C2.47	Fudong Han
C2.48	Kazunori Nishio
C2.49	Evvy Kartini
C2.50	Wojciech Zajac
C2.51	Feng Zhao
C2.52	Feng Zhao
C2.53	Nguyen Phuc
C2.54	Takashi Hakari
C2.55	Yong Nam Jo
C2.56	Yasuaki Matsuda
C2.57	Nils Wagner
C2.58	Yang Hu
C2.59	Alice Cassel
C2.60	Ilya Zharov
C2.61	Kun-lin Liu
C2.62	Rayavarapu Prasada Rao
C2.63	Virginie Viallet
C2.64	M.V. Reddy
C2.65	Kuldeep Mishra
D2.01	Nicola Perry
D2.02	Teruyoshi Awano
D2.03	Romain Perriot
D2.04	Ann Deml
D2.05	Marcin Krynski
D2.06	Fumihiko Kosaka
D2.07	Giuliano Gregori
D2.08	Maxwell Marple
D2.09	Stefan Adams
D2.10	William Bowman
D2.11	Yuxi Ma
D2.12	Stuart Cook
D2.13	Francesco Ciucci
D2.14	Jakyu Chun
D2.16	Jonathan Polfus
D2.17	Vadim Eremin
D2.18	Igor Lubomirsky
D2.19	Chi Chen

PAPER #	PRESENTER
D2.20	Maxim Ananyev
D2.21	Marit Getz
D2.22	Yogita Oza
E2.01	Yoshiyuki Abe
E2.02	Avneesh Mishra
E2.03	Till Froemling
E2.04	Stefan Nikodemski
F/H2.01	Alexander Bork
F/H2.02	Timothy Davenport
F/H2.03	Debora Barcellos
F/H2.04	Blair Connelly
F/H2.05	Shannon Boettcher
F/H2.06	Pengli Yan
F/H2.07	Dang-Thanh Nguyen
F/H2.08	Dang-Thanh Nguyen
F/H2.09	Madhur Boloor
F/H2.10	Eui-Chol Shin
F/H2.11	Eui-Chol Shin
F/H2.12	Stefan Adams
J1.01	Yoshitaka Aoki
J1.02	Rayane Vale
J1.03	Seon Rho
J1.04	Despoina Papargyriou
J1.05	Chi Ho Wong
J1.06	Sapna Gupta
J1.07	Jean-Marc Bassat
J1.08	Marie-Laure Fontaine
J1.09	Sonia Escolastico
J1.10	Matthias Meffert
K1.01	Sarmad Saeed
K1.02	Huyra Araujo
K1.03	Grant Hudish
K1.04	Genki Imai
K1.05	Tomohiro Ishiyama
K1.06	Akihide Kuwabara
K1.07	Joon-Hyung Lee
K1.08	Shogo Miyoshi
K1.09	Yoshihiro Yamazaki
K1.10	Elcio Pires
K1.11	Alexander Benes
K1.12	Ragnar Strandbakke
K1.13	Kevin Albrecht
K1.14	Tor Bjorheim
K1.15	Takuya Yamaguchi
K1.16	Al-Moatasem El-Sayed
K1.17	Tor Bjorheim

TUESDAY POSTER SESSIONS AT-A-GLANCE

PAPER #	PRESENTER
A6.01	Monica Sandoval
A6.02	Kalpana Singh
A6.03	Elena Pikalova
A6.04	Hanping Ding
A6.05	Sonia Escolastico
A6.06	Sanghoon Ji
A6.07	Fumitada Iguchi
A6.08	Mattia Saccoccio
A6.09	Takaaki Sakai
A6.10	Gesa Beck
A6.11	Enrique Ruiz-Trejo
A6.12	Wenqiang Zhang
A6.13	Sergey Pikalov
A6.14	Dmitry Tsvetkov
A6.15	Zulma Moreno
A6.17	Ragnar Kiebach
A6.18	Jeffrey De Vero
A6.19	Alexander Opitz
A6.20	Jae Jin Kim
A6.21	Samuel Cooper
A6.22	Zohar Drach
A6.23	Martin Perz
A6.24	Jun-Young Park
A6.25	Na Ni
A6.26	Mabel Lew
A6.27	Marcin Malys
A6.28	Liudmila Kolchina
A6.29	Samir Boulfrad
A6.30	Ibtissam Kehal
A6.31	Yuan Ji
A6.32	Tianmin He
A6.33	Fang Wang
A6.34	Xiaomei Liu
A6.35	Kuan-Zong Fung
A6.37	Eui-Chol Shin
A6.38	Andreas Nenning
A6.39	Tzvia Radlauer
A6.40	Nahum Maso
A6.41	Ghislain Rupp
A6.43	Lyudmyla Stackpool
A6.44	Hung-Cuong Pham
A6.45	Yoshihisa Ishikawa
A6.46	Denis Osinkin
A6.47	Kun Zheng
A6.48	Matthias Gerstl
A6.49	Aleksey Yaremchenko
A6.50	Kang Yan
A6.51	Javier Macias
A6.52	Yoonseok Choi
A6.53	Vasileios Kyriakou
B2.01	Andrew Motz
B2.02	Shogo Nagaya
B2.03	Hadi Tavassol
B2.04	Young-Jun Sohn

PAPER #	PRESENTER
B2.05	Minjin Kim
B2.06	Ken Akizuki
B2.07	Kun-lin Liu
C8.01	Rao Huang
C8.02	Kuan-Zong Fung
C8.03	Ryosuke Okamoto
C8.04	Przemyslaw Michalski
C8.05	Dale Teeters
C8.06	Masahiro Tatsumisago
C8.07	Aude Hubaud
C8.08	Jack Vaughey
C8.09	Dmitry Malyshkin
C8.10	Hanxing Liu
C8.11	Marcin Molenda
C8.12	Raymond Blanga
C8.13	Takanori Kobayashi
C8.14	Takahiro Yoshinari
C8.15	M.V. Reddy
C8.16	Tatsuya Nakamura
C8.17	Wojciech Zajac
C8.18	Wojciech Zajac
C8.19	Naokai Kuwata
C8.20	Kosuke Ishizu
C8.21	Hirokazu Kitaura
C8.22	Yoshihiro Oka
C8.23	Xiangwei Wu
C8.24	Xiangwei Wu
C8.25	Zhaoyin Wen
C8.26	Zhaoyin Wen
C8.27	Zhaoyin Wen
C8.28	Oscar Hernandez-Daguer
C8.29	Kota Suzuki
C8.30	Yoshiki Iwai
C8.31	Ryan Bayliss
C8.32	Haruka Itabashi
C8.33	Masaaki Hirayama
C8.34	Gwangseok Oh
C8.35	Zhiyong Yu
C8.36	David McComb
C8.37	Eui-Chol Shin
C8.38	Jin-Myoung Lim
C8.39	Jan Nowinski
C8.40	Alon Oz
C8.41	Koichi Kino
C8.42	Shin-ichi Nishimura
C8.43	Xiaoli Xi
C8.44	Kazufumi Otani
C8.45	Xiaodi Ren
C8.46	Yan Yu
C8.47	Yan Yu
C8.48	Janina Molenda
C8.49	Duho Kim
C8.50	Lu Wang
C8.51	Yingbin Lin

PAPER #	PRESENTER
C8.52	Anna Milewska
C8.53	Masao Yonemura
C8.54	Satoshi Hori
C8.55	Wojciech Zajac
C8.56	Thomas Hupfer
C8.57	Danielle Proffit
C8.58	Prashant Dabas
C8.59	Justin Whiteley
C8.60	Hailei Zhao
C8.61	Alexey Levchenko
C8.62	Toshinori Okura
C8.63	Shogo Komagata
C8.64	Nellie Khasanova
C8.65	Andrzej Kulka
C8.66	Nataly Rosero Navarro
C8.67	Naohiro Horiuchi
C8.68	Makoto Moriya
C8.69	Tetsuro Kobayashi
C8.70	Yang Lei
C8.71	Dominika Baster
C8.72	Dominika Baster
C8.73	A Thakur
C8.74	Awalendra Thakur
C8.75	Awalendra Thakur
D6.01	Wenyi Tan
D6.02	Bernhard Stanje
D6.03	Alicja Klimkowicz
D6.04	Yoshinobu Adachi
D6.05	Yusuke Okamoto
D6.06	Kuan-Ting Wu
D6.07	Sindre Stub
D6.08	Matthias Kleine-Boymann
D6.09	Tanmoy Paul
D6.10	Celeste van den Bosch
D6.11	Steven Harvey
D6.12	Stefan Nikodemski
D6.13	George Harrington
D6.14	Scott Lewis
D6.15	Tomasz Pietrzak
D6.16	Melissa Novy
D6.18	Yachao Chen
D6.19	NoWoo Kwak
D6.20	Elisa Gilardi
D6.21	Jens Zosel
D6.22	Amy Morrissey
D6.23	Junji Hyodo
D6.24	Fangfang Wang
D6.25	Stephen Skinner
D6.26	Peter Hendriksen
D6.27	Erik Burton
D6.28	Truls Norby
D6.29	Zixuan Guan
D6.30	Haruyuki Takahashi
D6.31	Chirranjeevi Balaji Gopal

PAPER #	PRESENTER
D6.32	Cortney Kreller
D6.33	William Bowman
D6.34	Ian Metcalfe
G3.01	Kiran Adepalli
G3.02	Qiyang Lu
G3.03	David Gao
G3.04	Markus Kubicek
G3.05	Seung-Yun Lee
G3.06	Geyu Lu
G3.07	Geyu Lu
G3.08	Matthias Schelter
G3.09	Dongwook Kim
G3.10	Ho Won Jang
I1.01	Saki Ito
I1.02	Matin Roshanzamir Modaberi
I1.03	Govind Prajapati
J2.01	Jitendra Kumar
J2.02	Jason Fish
J2.03	Chiharu Kura
J2.04	Di He
J2.05	Seon Rho
J2.06	Bernhard Tjaden
J2.07	Zonghao Shen
J2.08	Zac Dehaney-Steven
J2.09	Maria Balaguer
J2.10	Lana-Simone Unger
J2.11	Tsubasa Sato
J2.12	Matthias Meffert
J2.13	Mtabazi Sahini
K3.01	Joon-Hyung Lee
K3.02	Efstratios Stavrakakis
K3.03	Jong-Sook Lee
K3.04	Sandrine Ricote
K3.05	Shay Robinson
K3.06	Wade Rosensteel
K3.07	Konrad Swierczek
K3.08	Mateusz Tarach
K3.09	Ji Haeng Yu
K3.10	Hailei Zhao
K3.11	Marie-Laure Fontaine
K3.12	Fumitada Iguchi
K3.13	Denis Osinkin
K3.14	Nahum Maso
K3.15	Toshiaki Yamaguchi
K3.16	Andreas Falkenstein
K3.17	Cheng Li
K3.18	Su-Hyun Moon
K3.19	Einar Vollestad
K3.20	Rotraut Merkle
K3.21	Cristina Tealdi
K3.22	Goeran Wahnstroem

INVITED SPEAKERS

NAME	PAPER #	SESSION TITLE	DAY	TIME	LOCATION
Amezawa, Koji	A1.04	Quantitative Evaluation of Effective Reaction Area in Solid Oxide Fuel Cell Cathodes	Monday	11:40 am	Longs Peak
Bucher, Edith	A4.04	Phase Decomposition and Secondary Phase Formation in the Chromium and Silicon Poisoned IT-SOFC Cathode Materials $La_{0.6}Sr_{0.4}CoO_{3-\partial}$ and $La2NiO_{4+\partial}$	Tuesday	11:40 am	Longs Peak
Burriel, Monica	G2.03	La0.8Sr0.2(Mn,Co)O3 Perovskite Oxides as Resistive Switches: Influence of B-Site Substitution on the Resistive Switching Properties	Tuesday	4:10 pm	Grays Peak III
Cabana, Jordi	C10.02	Parameters Influencing Reversible Intercalation of Cations in Spinel Oxides	Thursday	11:00 am	Shavano Peak
De Souza, Roger	D8.01	The Transport Properties of Dislocations in the Perovskite-Oxide SrTiO	Thursday	1:30 pm	Grays Peak I/II
Dura, Joseph	B1.01	Nanoscaled Structure of Nafion at Interfaces	Tuesday	1:30 pm	Grays Peak III
Eguchi, Koichi	A5.01	Formation of $SrZrO_3$ in Perovskite Cathode /Ceria Interlayer /Zirconia Electrolyte during Operation of Solid Oxide Fuel Cells	Tuesday	3:30 pm	Longs Peak
Funke, Klaus	D3.01	Low-Temperature Alpha Silver Iodide Confined in Glass: Structure and Dynamics	Monday	2:30 pm	Grays Peak I/II
Garbayo, Inigo	D5.06	Electro-Chemo-Mechanics in Solid State Materials: Let`s Design the Structural-Defect Twists	Tuesday	3:30 pm	Grays Peak I/II
Golodnitsky, Diana	C6.01	Confined-in-Ceramic Solid Polymer Electrolyte for Microbattery Application	Tuesday	1:30 pm	Shavano Peak
Ielmini, Daniele	G2.02	Ionic Switching Devices: Operation Principle and Application in Computing	Tuesday	3:50 pm	Grays Peak III
Iojoiu, Cristina	B4.01	Nano-Structured Aromatic Ionomers for PEMFC	Thursday	1:30 pm	Grays Peak III
Ishihara, Tatsumi	A9.01	Oxide Ion Conductivity in Doped $LnBaInO_4$(Ln=La, Nd)	Thursday	1:30 pm	Longs Peak
Jung, WooChul	A9.06	Sintering-Resistant Metal Nanoparticles for High Temperature Electrocatalysis	Thursday	3:30 pm	Longs Peak
Kawada, Tatsuya	D5.05	Effect of Chemomechanical Coupling on Defect Equilibrium and Transport in Solid State Ionic Devices	Tuesday	2:50 pm	Grays Peak I/II
Kobayashi, Genki	K6.01	Hydride Conduction in Oxyhydrides	Friday	10:30 am	Quandary Peak I/II
Lai, Wei	C3.01	Structure and Dynamics of Lithium Garnet Oxides Studied by Neutron Scattering and Molecular Dynamics Simulation	Monday	2:30 pm	Shavano Peak
Lee, Jong-Ho	K2.03	Variation of Kinetic Parameters, Chemical Diffusivity and Surface Exchange Coefficient of $Ba(Zr_{0.84}Y_{0.15}Cu_{0.01})O_{3-\delta}$ during the Conductivity Relaxation Experiments	Tuesday	2:20 pm	Longs Peak
Li, Hong	C5.03	Ionic Transport Issue in Solid Lithium Air Batteries	Tuesday	11:20 am	Shavano Peak
Lotsch, Bettina	D9.02	Structure and Lithium Ion Dynamics of the Tetragonal LGPS-Type Superionic Conductors $Li_{11-x}M_{2-x}P_{1+x}S_{12}$ with M = Si, Ge, Sn	Friday	11:10 am	Grays Peak I/II
Manthiram, Arumugam	C5.02	Hybrid Lithium-Air Batteries: Inexpensive Catalysts and Novel Cell Designs	Tuesday	11:00 am	Shavano Peak
Marrocchelli, Dario	G1.02	Dislocations in $SrTiO_3$: Easy to Reduce but not so Fast for Oxygen Transport	Tuesday	11:00 am	Grays Peak III
Metcalfe, Ian	J5.01	Ceramic Permeation Membranes and Membrane Reactors	Thursday	3:30 pm	Grays Peak III
Moore, Robert	B1.05	Thermoreversible Gels—A New Route to Create Blocky Ionomer Membranes via Non-Random Functionalization	Tuesday	2:50 pm	Grays Peak III
Mueller, David	A3.01	Perovskite Oxides as Materials for Energy Conversion: Towards a Fundamental Understanding of Surface Properties by Operando Spectroscopic Methods	Monday	2:30 pm	Longs Peak
Norby, Truls	D8.06	Space Charge Layers and Their Role in Properties of Interfaces in Solid State Ionics	Thursday	3:30 pm	Grays Peak I/II
Peng, Ranran	A10.01	A Novel R-P Structure Cathode with High Performance for Intermediate Temperature Solid Oxide Fuel Cells	Friday	10:30 am	Longs Peak
Qi, Yue	C4.01	Predicting Lithium Transport in Solid Electrolyte Interphases	Monday	2:30 pm	Quandary Peak I/II
Sattler, Christian	F/H1.03	Fuel Production from Concentrated Solar Radiation	Monday	11:20 am	Grays Peak III
Scheffe, Jonathan	F/H3.01	Characterization of La-Mn Perovskites and Doped Ceria for Thermochemical H_2O and CO_2 Splitting Applications	Monday	2:30 pm	Grays Peak III
Skinner, Stephen	A3.06	Acceptor Doped $CeNbO_4$ as a Potential Mixed Proton Conducting Electrode	Monday	4:10 pm	Longs Peak
Terabe, Kazuya	G2.01	Various Functional Nano-Ionic Devices Achieved by Controlling Hetero-Interface Characteristics using Local Ion Migration	Tuesday	3:30 pm	Grays Peak III
Unger, Lana-Simone	J3.03	Influence of Yttrium Doping on $Ba_{0.5}Sr_{0.5}Co_{0.8}Fe_{0.2}O_{3-}$	Wednesday	11:20 am	Grays Peak III
Wiemhoefer, Hans	D5.01	An Extended Analysis of Dopant Strategies to Control Mixed Ion and Electron Transport in Ceria Based Oxide Solutions	Tuesday	1:30 pm	Grays Peak I/II
Yu, Yan	C11.01	Room-Temperature Sodium-Ion Batteries: Improving the Rate Capability Using Porous Carbon Networks	Thursday	1:30 pm	Shavano Peak

KEYNOTE SPEAKERS

NAME	PAPER #	SESSION TITLE	DAY	TIME	LOCATION
Bouwmeeste, Henny	A4.01	Measuring Oxygen Surface Exchange Kinetics on Mixed–Conducting Composites by Electrical Conductivity Relaxation	Tuesday	10:30 am	Longs Peak
Carolan, Michael	J3.01	Advances in ITM Technology for Oxygen and Syngas Production	Wednesday	10:30 am	Grays Peak III
Cui, Yi	C1.01	Lithium Sulfur Batteries: Fundamental Understanding and Materials Design	Monday	10:30 am	Shavano Peak
Dukovic, Gordana	F/H3.04	Excited State Dynamics in Oxynitride Nanocrystals and Implications for Solar Fuel Generation	Monday	3:40 pm	Grays Peak III
Fontaine, Marie–Laure	K4.01	Development of Proton Conducting Electrolyser Cells	Thursday	10:30 am	Quandary Peak I/II
Forsyth, Maira	D9.01	Molecular Insights Into Structure and Dynamics of Organic Ionic Plastic Crystal Electrolytes	Friday	10:40 am	Grays Peak I/II
Gaberscek, Miran	C12.01	Powerful Electrical Model Explaining the Operation of Insertion Batteries	Friday	10:30 am	Shavano Peak
Grey, Clare	K2.01	Protonic Conduction in Perovskites: NMR and DFT Studies of Yttrium–Doped $BaZrO_3$ and Related Perovskites	Tuesday	1:30 pm	Longs Peak
Hendriksen,Peter	A8.01	Prospects and Challenges of Solid Oxide Electrolysis	Thursday	10:30 am	Longs Peak
Horike, Satoshi	I3.01	Discovery of Molecular Disorders in Coordination Frameworks for Solid State Ionics	Friday	10:30 am	Grays Peak III
Hosono, Hideo	E3.01	Material Design of Novel Transparent Oxide Conductors/Semiconductors	Tuesday	10:30 am	Quandary Peak I/II
Huang, Jinsong	I2.01	Electromigration of Ions in Hybrid Perovskites for Switchable Photovoltaic, Memristors and Synapses	Wednesday	10:30 am	Grays Peak I/II
Lany, Stephan	E1.01	Defect Theory for Transparent Conducting Oxides	Monday	10:30 am	Quandary Peak I/II
Martin, Manfred	G1.01	Bulk Mixed Ion Electron Conduction in Highly Disordered Oxides Causes Memristive Behavior	Tuesday	10:30 am	Grays Peak III
Merkle, Rotraut	D4.01	Cathode Materials for Proton Conducting SOFC: Bulk Defect Chemistry and Mechanism of Oxygen Reduction Reaction	Tuesday	10:30 am	Grays Peak I/II
Nazar, Linda	C5.01	Aprotic Sodium (And Li)–Oxygen Batteries	Tuesday	10:30 am	Shavano Peak
Paddison, Stephen	B3.01	Structural Aspects of PFSA Ionomers as Determined by STEM and Simulations	Wednesday	10:30 am	Quandary Peak I/II
Sharp, Ian	F/H3.03	Engineering Materials and Interfaces for Efficient and Stable Photocatalytic Water Splitting	Monday	3:10 pm	Grays Peak III
Shimizu, George	I3.02	Designing Proton Conducting MOFs	Friday	10:55 am	Grays Peak III
Sivula, Kevin	F/H3.05	Charge Carrier Transport and Catalysis on Solution–Processed Photoelectrodes for Solar Water Splitting	Monday	4:10 pm	Grays Peak III
Stechel, Ellen	F/H1.01	Concentrating Solar Thermochemical Fuels: Key Materials Issues for Commercial Viability and Scalability	Monday	10:30 am	Grays Peak III
Tuller, Harry	D1.01	Oxygen Nonstoichiometry in Thin Films and Nanoparticles: Measurement, Control and Implications for Energy and Memory Related Devices	Monday	10:30 am	Grays Peak I/II
Wachsman, Eric	A7.01	SOFC Cathode Oxygen Reduction Reaction Mechanisms under Real World Conditions	Wednesday	10:30 am	Longs Peak
Whittingham, Stanley	C10.01	The Ultimate Limits of Intercalation Reactions for Battery Electrodes	Thursday	10:30 am	Shavano Peak
Yildiz, Bilge	A1.01	Oxygen Reduction Kinetics on Perovskite Oxides: Effects of Dissimilar Interfaces and Surfaces	Monday	10:30 am	Longs Peak
Yoo, Han–III	D7.01	Oxygen Thermotranspor in Mixed Conductor Oxides	Thursday	10:30 am	Grays Peak I/II

SSI·20

Oral Presentations

ORAL PRESENTATIONS

MONDAY June 15, 2015

PLENARY

SESSION L1: Plenary I
Chair: Joachim Maier
Monday Morning, June 15, 2015
Keystone Resorts, Shavano Peak

9:15 AM INTRODUCTION

9:25 AM L1.01
Bulk and Surface Oxide Protonics for Energy Conversion Devices: Role of Percolation and Grotthus Mechanism in Oxide Protonics Shu Yamaguchi; Department of Materials Engineering School of Engineering, The University of Tokyo, Tokyo, Japan.

A: Solid Oxide Fuel Cells and Electrolyzers

* Invited Speaker
** Keynote Speaker

SESSION A1: SOFC—Cathodes I
A: Solid Oxide Fuel Cells and Electrolyzers
Chair: William Chueh
Monday Morning, June 15, 2015
Keystone Resorts, Longs Peak

10:10 AM BREAK

10:30 AM **A1.01
Oxygen Reduction Kinetics on Perovskite Oxides: Effects of Dissimilar Interfaces and Surfaces Bilge Yildiz; Massachusetts Institute of Technology, Cambridge, Massachusetts, United States.

11:00 AM A1.02
Chemical Composition Study of the LSC-113/LSC-214 Surface and its Effect on the ORR Enhancement Andrea Cavallaro, John Kilner and Stephen Skinner; Materials, Imperial College London, London, United Kingdom.

11:20 AM A1.03
Effect of Heterointerface on Oxygen Reduction Kinetics of (Sm,Sr) CoO_3-Based Electrodes Hiroki Muroyama, Hideyuki Kanazawa, Takeou Okanishi, Toshiaki Matsui and Koichi Eguchi; Kyoto University, Kyoto, Japan.

11:40 AM *A1.04
Quantitative Evaluation of Effective Reaction Area in Solid Oxide Fuel Cell Cathodes Koji Amezawa[1], Yoshinobu Fujimaki[2], Takashi Nakamura[1], Katherine D. Bagarinao[3], Katsuhiko Yamaji[3], Kiyofumi Nitta[4], Yasuko Terada[4], Keiji Yashiro[5], Fumitada Iguchi[2], Hiroo Yugami[2] and Tatsuya Kawada[5]; [1]IMRAM, Tohoku University, Sendai, Japan; [2]Graduate School of Engineering, Tohoku University, Sendai, Japan; [3]AIST, Tsukuba, Japan; [4]JASRI, Sayo, Japan; [5]Graduate School of Environmental Studies, Tohoku University, Sendai, Japan.

SESSION A3: SOFC—Cathodes II
A: Solid Oxide Fuel Cells and Electrolyzers
Chairs: Ryan O'Hayre and Harry Tuller
Monday Afternoon, June 15, 2015
Keystone Resorts, Longs Peak

2:30 PM *A3.01
Perovskite Oxides as Materials for Energy Conversion: Towards a Fundamental Understanding of Surface Properties by *Operando* Spectroscopic Methods David N. Mueller[2, 1], Michael L. Machala[2], Zixuan Guan[2], Hendrik Bluhm[3] and William C. Chueh[2, 4]; [1]Peter Gruenberg Institute (PGI-6), Research Center Juelich, Juelich, Germany; [2]Department of Materials Science & Engineering, Stanford University, Stanford, California, United States; [3]Chemical Sciences Division, Lawrence Berkeley National Laboratory, Berkeley, California, United States;[4]Stanford Institute for Materials and Energy Sciences, SLAC National Accelerator Laboratory, Menlo Park, California, United States.

2:50 PM A3.02
***In Situ* X-Ray Synchrotron Spectroscopy Study of IT-SOFC Stability under Operating Conditions** Florent Tonus and Stephen J. Skinner; Materials, Imperial College London, London, United Kingdom.

3:10 PM A3.03
Surface Chemistry of $La_{0.6}Sr_{0.4}CoO_{3-\delta}$ Thin Films and Its Impact on the Oxygen Surface Exchange Resistance Ghislain M. Rupp[1], Helena Tellez[2], John Druce[2], Andreas Limbeck[3], Tatsumi Ishihara[2], John Kilner[4, 2] and Juergen Fleig[1]; [1]Institute of Chemical Technologies and Analytics - Electrochemistry, Vienna University of Technology, Vienna, Austria;[2]International Institute for Carbon-Neutral Energy Research, Kyushu University, Fukuoka, Japan; [3]Institute of Chemical Technologies and Analytics - Instrumental Analytical Chemistry, Vienna University of Technology, Vienna, Austria; [4]Department of Materials, Imperial College London, London, United Kingdom.

3:30 PM A3.04
Surface Analysis of SOFC Cathode Degradation Using Low Energy Ion Scattering and *In-Operando* Atmospheres Mathew Niania[1], Samuel Cooper[1], Helena Tellez[2], John Druce[2], Stephen Skinner[1], Tatsumi Ishihara[2] and John Kilner[1, 2]; [1]Materials, Imperial College London, London, United Kingdom; [2]I2CNER, Kyushu University, Fukuoka, Japan.

3:50 PM A3.05
Oxide-Ion Dynamics in the MIEC SOFC Cathode Material $La_2NiO_{4+\delta}$ by Experimental and Computational Solid-State ^{17}O NMR Spectroscopy David M. Halat[1], Riza Dervisoglu[2], Gunwoo Kim[1] and Clare P. Grey[1, 2]; [1]Department of Chemistry, University of Cambridge, Cambridge, United Kingdom; [2]Department of Chemistry, Stony Brook University, Stony Brook, New York, United States.

4:10 PM *A3.06
Acceptor Doped $CeNbO_4$ as a Potential Mixed Proton Conducting Electrode Stephen Skinner and Cassandra Harris; Imperial College London, London, United Kingdom.

4:30 PM A3.07
A Cost-Effective Approach for Next Generation High-Performance Fuel-Flexible Protonic Ceramic Fuel Cell Chuancheng Duan, Jianhua Tong, Meng Shang and Ryan O'Hayre; Colorado School of Mines, Golden, Colorado, United States.

4:50 PM A3.08
A New Ternary Protonic/Oxygen Ionic/Electronic Conducting Cathode for Proton Conducting Solid Oxide Fuel Cell Liangdong Fan and Pei-Chen Su; School of Mechanical and Aerospace Engineering, Nanyang Technological University, Singapore, Singapore.

5:10 PM A3.09
Nano-CT Enabled, Bayesian Model-Based Analysis of Impedance Data for a Porous, Lanthanum Strontium Manganate Cell Giuseppe F. Brunello[1], Billy Epting[2], Shawn Litster[2], Paul A. Salvador[3], Harry O. Finklea[4], David S. Mebane[1] and Juwana De Silva[4]; [1]Mechanical and Aerospace Engineering, West Virginia University, Atlanta, Georgia, United States;[2]Department of Mechanical Engineering, Carnegie Mellon University, Pittsburgh, Pennsylvania, United States; [3]Department of Materials Science and Engineering, Carnegie Mellon University, Pittsburgh, Pennsylvania, United States; [4]Department of Chemistry, West Virginia University, Morgantown, West Virginia, United States.

C: Electrodes and Solid Electrolytes for Batteries

SESSION C1: Rational Design of Battery Materials
C: Electrodes and Solid Electrolytes for Batteries
Chair: Arumugam Manthiram
Monday Morning, June 15, 2015
Keystone Resorts, Shavano Peak

10:10 AM BREAK

10:30 AM **C1.01
Lithium Sulfur Batteries: Fundamental Understanding and Materials Design Yi Cui; Department of Materials Science and Engineering, Stanford University. Stanford Institute for Materials and Energy Sciences, SLAC National Accelerator Laboratory, Stanford, California, United States.

11:00 AM C1.02
Atomic-Scale Insights into Lithium and Sodium Battery Materials: Intercalation, Diffusion and Surfaces Saiful Islam; Chemistry, University of Bath, Bath, United Kingdom.

11:20 AM C1.03
Accelerated Computation Materials Design of Solid-Electrolyte Materials in All-Solid-State Li-Ion Batteries Yifei Mo; Materials Science and Engineering, University of Maryland, College Park, College Park, Maryland, United States.

11:40 AM C1.04
Fast Design and Optimization of Solid State Electrolytes for Lithium Rechargeable Batteries Guided by the Combination of Bond-Valence Method and Density Functional Theory Ruijuan Xiao, Hong Li and Liquan Chen; Institute of Physics, Chinese Academy of Sciences, Beijing, China.

SESSION C3: Solid Electrolyte I
C: Electrodes and Solid Electrolytes for Batteries
Chair: Diana Golodnitsky
Monday Afternoon, June 15, 2015
Keystone Resorts, Shavano Peak

2:30 PM *C3.01
Structure and Dynamics of Lithium Garnet Oxides Studied by Neutron Scattering and Molecular Dynamics Simulation Wei Lai[1], Yuxing Wang[1], Matthew Klenk[1] and Katharine Page[2]; [1]Michigan State University, East Lansing, Michigan, United States; [2]Oak Ridge National Lab, Oak Ridge, Tennessee, United States.

2:50 PM C3.02
A Full Study of a Garnet Ceramic Electrolyte: From Atomistic Simulation to Actual Application in Rechargeable Lithium-Metal Batteries William Manalastas[1], Randy Jalem[2, 3], Frederic Aguesse[1], Lucienne Buannic[1], Juan Miguel Lopez del Amo[1], Carlos Bernuy-Lopez[1], Gurpreet Singh[1], Ainara Aguadero[4], Anna Llordes[1], Masanobu Nakayama[3] and John Kilner[4,1]; [1]Solid State Electrolytes Group, CIC Energigune, Miñano, Spain; [2]Unit of Element Strategy Initiative for Catalysts and Batteries, Kyoto University, Kyoto, Japan; [3]Department of Materials Science and Engineering, Nagoya Institute of Technology, Nagoya, Japan; [4]Department of Materials, Imperial College, London, United Kingdom.

3:10 PM C3.03
Revealing Lithium Conduction Pathways in Lithium-Rich Garnets Using Aliovalent Dopants Rowena H. Brugge, Ainara Aguadero and John Kilner; Imperial College London, London, United Kingdom.

3:30 PM C3.04
Charge Transport Properties in the Li-Garnet $Li_{7-x}La_3Zr_{2-x}Te_xO_{12}$ System Michal Struzik, Reto Pfenninger and Jennifer L. Rupp; Department of Materials, ETH Zurich, Zurich, Switzerland.

3:50 PM C3.05
Investigating the Effects of Al Doping on the Local and Average Structure of Al-LLZ Using Atomistic Simulations Matthew Klenk and Wei Lai; Chemical Engineering and Material Science, Michigan State University, East Lansing, Michigan, United States.

4:10 PM C3.06
Influence of La Ordering in $Li_{3x}La_{2/3-x}TiO_3$ Epitaxial Films on Li-Ion Conduction Tsuyoshi Ohnishi, Kazutaka Mitsuishi, Kazunori Nishio and Kazunori Takada; National Institute for Materials Science, Tsukuba, Japan.

4:30 PM C3.07
Lithium Dendrite Growth in Hot Pressed Ta-Substituted $Li_7La_3Zr_2O_{12}$ Chih-Long Tsai[1], Vinodchandran Chandrasekharan Nair[2], Astrid Besmehn[3], Sven Uhlenbruck[1], Hans G. Gehrke[1], Thorsten Reppert[1], Paul Heitjans[2] and Olivier Guillon[1]; [1]Institut fuer Energie- und Klimaforschung: Werkstoffsynthese und Herstellungverfahren (IEK-1) , Forschungszentrum Juelich GmbH, Juelich, Germany; [2]Institut für Physikalische Chemie und Elektrochemie, Leibniz Universität Hannover , Hannover, Germany; [3]ZEA-3, Forschungszentrum Juelich GmbH, Juelich, Germany.

4:50 PM C3.08
Excellent Stability of a Solid Electrolyte upon Li^+/H^+ Exchange: A Discovery Resulting from Successfully Suppressing Electron Beam Damage Cheng Ma[1], Chengdu Liang[1], Jeffrey Sakamoto[2], Karren More[1] and Miaofang Chi[1]; [1]Center for Nanophase Materials Sciences, Oak Ridge National Laboratory, Oak Ridge, Tennessee, United States; [2]Department of Chemical Engineering and Materials Science, Michigan State University, East Lansing, Michigan, United States.

C: Electrodes and Solid Electrolytes for Batteries

SESSION C4: Interfaces in Batteries
C: Electrodes and Solid Electrolytes for Batteries
Chair: M. Stanley Whittingham
Monday Afternoon, June 15, 2015
Keystone Resorts, Quandary Peak I/II

2:30 PM *C4.01
Predicting Lithium Transport in Solid Electrolyte Interphases Yue Qi; Department of Chemical Engineering and Materials Science, Michigan State University, Lansing, Michigan, United States.

2:50 PM C4.02
Theory of Space Charge Layers in Lithium All-Solid-State Batteries Arnulf Latz[1, 2, 3], Stefanie Braun[1, 2] and Chihiro Yada[4]; [1]German Aerospace center , Stuttgart, Germany;[2]Helmholtz Institute Ulm for Electrochemical Energy Storage, Ulm, Germany; [3]Institute for Electrochemistry, University of Ulm, Ulm, Germany; [4]Toyota Motor Europe NV/SA, Zaventem, Belgium.

3:10 PM C4.03
Negligible "Negative Space-Charge Layer Effects" at LiPON/ $LiCoO_2$ Interfaces of Thin-Film Batteries Taro Hitosugi, Masakazu Haruta, Ryota Shimizu and Susumu Shiraki; Tohoku University, Sendai, Japan.

3:30 PM C4.04
Lithium and Hydrogen Storage at Abrupt Junctions Lijun Fu, Chia-Chin Chen and Joachim Maier; Max Planck Institute for Solid State Research, Stuttgart, Germany.

3:50 PM C4.05
Double Layer Formation and Energy Level Alignment at Li-Ion Electrode-Electrolyte Interfaces: Impact on Charge Transfer and Electrode Potential Rene Hausbrand, Andre Schwoebel, Wolfram Jaegermann, Mathias Fingerle and Ruben Precht; Institute of Materials Science, Darmstadt University of Technology, Darmstadt, Germany.

4:10 PM C4.06
Reduced Grain-Boundary Resistance of Oxide-Type Lithium Ion Conductors by Surface Coating Hirotoshi Yamada[1], Daisuke Tsunoe[2] and Shota Shiraishi[1]; [1]Graduate School of Engineering, Nagasaki University, Nagasaki, Japan; [2]Faculty of Engineering, Nagasaki University, Nagasaki, Japan.

4:30 PM C4.07
Investigation of Electrode-Electrolyte Interface in Bulk-Type All-Solid-State Lithium Batteries Using $LiCoO_2$ Particles Coated with Sulfide Solid Electrolyte Thin Films Yusuke Ito[1], Atsushi Sakuda[1], Takamasa Ohtomo[2], Akitoshi Hayashi[1] and Masahiro Tatsumisago[1]; [1]Department of Applied Chemistry, Osaka Prefecture University, Sakai, Japan; [2]Battery Research Division, Toyota Motor Corporation, Shizuoka, Japan.

4:50 PM C4.08
Probing Interfaces of Garnet Solid Electrolytes in Lithium Batteries Lei Cheng[1, 2], Guoying Chen[2] and Marca Doeff[2]; [1]Material Science and Engineering, University of California, Berkeley, Berkeley, California, United States; [2]Environmental Energy Technological Division, Lawrence Berkeley National Laboratory, Berkeley, California, United States.

D: Fundamentals of Transport and Reactivity and Nanoionics

SESSION D1: Fundamentals of Transport and Reactivity and Nanoionics I
D: Fundamentals of Transport and Reactivity and Nanoionics
Chair: Joachim Maier
Monday Morning, June 15, 2015
Keystone Resorts, Grays Peak I/II

10:10 AM BREAK

10:30 AM **D1.01
Oxygen Nonstoichiometry in Thin Films and Nanoparticles: Measurement, Control and Implications for Energy and Memory Related Devices Harry L. Tuller; Department of Materials Science and Engineering, MIT, Cambridge, Massachusetts, United States.

11:00 AM D1.02
Investigating Thin YSZ Perovskite Films Using Analytical Electron Microscopy Melissa Neish[2], Frank Scheltens[1], Robert E. Williams[1], Leslie J. Allen[2] and David W. McComb[1];[1]Materials Science and Engineering, The Ohio State University, Columbus, Ohio, United States; [2]School of Physics, University of Melbourne, Melbourne, Victoria, Australia.

11:20 AM D1.03
Cation Surface Segregation and Composition Depth Profile Variations in Thin Films Of SOFC Cathode Materials Analysed by Low Energy Ion Scattering Jose Santiso[1], Helena Tellez-Lozano[2], Araceli Gutierrez-Llorente[3], James Zapata[1], Roberto Moreno[1], Jaume Roqueta[1], Nuria Bagues[1], Anna Magraso[1], Jose M. Caicedo[1], John Druce[2], John A. Kilner[2] and Tatsumi Ishihara[2]; [1]ICN2 Institut Catala de Nanociencia i Nanotecnologia, Barcelona, Spain; [2]Hydrogen Production, I2CNER, International Institute for Carbon Neutral Energy Research, Fukuoka, Japan; [3]Universidad Rey Juan Carlos, Madrid, Spain.

11:40 AM D1.04
The Influence of Water on the Ionic Conductivity in Ordered Mesoporous YSZ Thin Films Matthias T. Elm[1, 2], Jonas D. Hofmann[1], Christian Suchomski[1, 3], Jueürgen Janek[1] and Torsten Brezesinski[3]; [1]Institute of Physical Chemistry, Justus-Liebig University Giessen, Giessen, Germany; [2]Institute of Experimental Physics I, Justus-Liebig University Giessen, Giessen, Germany; [3]Institute of Nanotechnology, Karlsruhe Institute of Technology, Eggenstein-Leopoldshafen, Germany.

SESSION D3: Fundamentals of Transport and Reactivity and Nanoionics II
D: Fundamentals of Transport and Reactivity and Nanoionics
Chair: Hans-Dieter Wiemhoefer
Monday Afternoon, June 15, 2015
Keystone Resorts, Grays Peak I/II

2:30 PM *D3.01
Low-Temperature Alpha Silver Iodide Confined in Glass: Structure and Dynamics Klaus Funke[1], Radha Banhatti[1], Pawel Grabowski[2], Jan Nowinski[2], Wojtek Wrobel[2], Robert Dinnebier[3] and Oxana Magdysyuk[3]; [1]Institute of Physical Chemistry, University of Muenster, Muenster, Germany; [2]Faculty of Physics, Warsaw University of Technology, Warsaw, Poland; [3]Max Planck Institut für Festkörperforschung, Stuttgart, Germany.

2:50 PM D3.02
Frequency - Dependent Conductivity and Anomalous Diffusion in Ag β-alumina Osamu Kamishima[1], Junichi Kawamura[2] and Yoshiki Iwai[2]; [1]Faculty of Science and Engineering, Setsunan University, Neyagawa, Japan; [2]Institute of Multidisciplinary Research for Advanced Materials, Tohoku University, Sendai, Japan.

3:10 PM D3.03
Investigation of the Effect of Pressure and the Concentration of Charge Carriers on the Ionic Transport in Sodium Scandium Phosphate $Na_3Sc_2(PO_4)_3$ Kaustubh Bhat[1], Marie Guin[2], Stefan Bluegel[1] and Hans Lustfeld[1]; [1]Peter Grünberg Institute (PGI-1)/Institute for Advanced Simulation (IAS-1), Forschungszentrum Jülich GmbH, Jülich, Germany; [2]Institute of Energy and Climate Research (IEK-1), Forschungszentrum Jülich GmbH, Jülich, Germany.

3:30 PM D3.04
Electronic Transport of Metal Oxide Single Crystals for Solar Water Splitting: Bismuth Vanadate and Iron Oxide Alexander J. Rettie[1], William Chemelewski[2], Jeffrey Lindemuth[3], John McCloy[4], Luke Marshall[5], David Eisenberg[6], Jianshi Zhou[2], David Emin[7] and Buddie Mullins[1, 4, 8]; [1]Chemical Engineering, University of Texas at Austin, Austin, Texas, United States; [2]Materials Science and Engineering, University of Texas at Austin, Austin, Texas, United States; [3]LakeShore Cryotronics, Westerville, Ohio, United States; [4]Materials Science and Engineering, Washington State University, Pullman, Washington, United States; [5]Chemical Engineering, Northeastern University, Boston, Massachusetts, United States; [6]Van't Hoff Institute for Molecular Sciences, University of Amsterdam, Amsterdam, Netherlands; [7]Physics and Astronomy, University of New Mexico, Albuquerque, New Mexico, United States;[8]Chemistry, University of Texas at Austin, Austin, Texas, United States.

3:50 PM D3.05
Redox Reactions and Transport at Room Temperature in Nanoionic Systems Based on Macroscopic Insulators Ilia Valov; Electronic Materials, Research Centre Juelich, Juelich, Germany.

4:10 PM D3.06
Atomistic Mechanism of Lithiation of Nanomaterials as Li-Ion Battery Anodes Studied by *In Situ* TEM Xuedong Bai; Institute of Physics, Chinese Academy of Sciences, Beijing, China.

4:30 PM D3.07
The Effects of Lattice Strain and Cationic Disorder on the Li-Ion Diffusion in $LiFePO_4$ Cristina Tealdi[1, 2] and Piercarlo Mustarelli[1, 2]; [1]Department of Chemistry, University of Pavia , Pavia, Italy; [2]UdR Pavia, INSTM, Pavia, Italy.

4:50 PM D3.08
Elucidating Li Ion Dynamics and Diffusion Pathways in Li_2SnO_3 – A Comparative $^{6,7}Li$ NMR Study Julia Langer[1, 2], Patrick Bottke[1, 2] and Martin Wilkening[1, 2, 3]; [1]Institute for Chemistry and Technology of Materials, Graz University of Technology, Graz, Austria; [2]DFG Research Unit 1277, Graz University of Technology, Graz, Austria; [3]Graz University of Technology, Christian Doppler Laboratory for Lithium Batteries, Graz, Austria.

5:10 PM D3.09
Lithium Segregation Induces Localized Order-Disorder Transitions Amorphous TiO_2 Nanoparticles Subramanian Sankaranarayanan[1, 2]; [1]Center for Nanoscale Materials, Argonne National Laboratory, Argonne, Illinois, United States; [2]Computation Institute, University of Chicago, Chicago, Illinois, United States.

E: Transparent Conducting Oxides

SESSION E1: TCO I—Defects, Materials
E: Transparent Conducting Oxides
Chair: David Paine
Monday Morning, June 15, 2015
Keystone Resorts, Quandary Peak I/II

10:10 AM BREAK

10:30 AM **E1.01
Defect Theory for Transparent Conducting Oxides Stephan Lany; National Renewable Energy Laboratory, Golden, Colorado, United States.

11:00 AM E1.02
Tuning Charge Collection Efficiency at the Transparent Conductive Electrode in Polymer Photovoltaics with Solution-Processed LiF Cleva W. Ow-Yang[1, 2], Hasan Kurt[1], Junjun Jia[3] and Yuzo Shigesato[3]; [1]Materials Science and NanoEngineering, Sabanci University, Istanbul, Turkey; [2]Nanotechnology Research and Application Center, Sabanci University, Istanbul, Turkey; [3]Graduate School of Science and Engineering, Aoyama Gakuin University, Sagamihara/Kanagawa, Japan.

11:20 AM E1.03
Tuning of Electrical and Optical Properties of Polycrystalline TiO_2-Based Transparent Conducting Films Piero Mazzolini[1, 2], Giuliano Gregori[3], Valeria Russo[1], Daniel Chrastina[4], Rafael O. Ferragut[4], Carlo S. Casari[1, 2] and Andrea Li Bassi[1, 2]; [1]Energy, Politecnico di Milano, Milano, Italy; [2]CNST @PoliMI, Istituto Italiano di Tecnologia, Milano, Italy; [3]Physical Chemistry of Solids, Max Planck Institute for Solid State Research, Stuttgart, Germany; [4]L-NESS, physics department, Politecnico di Milano, Como, Italy.

11:40 AM E1.04
Indium-Zinc-Oxide TFTs Using *In Situ* Converted Al_2O_3/HfO_2 Gate Stack Yang Song[1], Stylianos Siontas[2], Alexander Zaslavsky[1, 2], David Paine[2] and Alexander Katsman[3]; [1]Physics, Brown University, Providence, Rhode Island, United States; [2]School of Engineering, Brown University, Providence, Rhode Island, United States; [3]Dept. of Materials Science and Engineering, Technion, Haifa, Israel.

F/H: Solid State Photoelectrochemistry/High Temperature Routes to Solar Fuels

SESSION F/H1: Solid State Photoelectrochemistry/High Temperature Routes to Solar Fuels I
F/H: Solid State Photoelectrochemistry/High Temperature Routes to Solar Fuels
Chair: Tim Davenport
Monday Morning, June 15, 2015
Keystone Resorts, Grays Peak III

10:10 AM BREAK

10:30 AM **F/H1.01
Concentrating Solar Thermochemical Fuels: Key Materials Issues for Commercial Viability and Scalability Ellen B. Stechel[1] and James E. Miller[2]; [1]LightWorks, Arizona State University, Tempe, Arizona, United States; [2]Sandia National Laboratories, Albuquerque, New Mexico, United States.

11:00 AM F/H1.02
Discovery of Novel Perovskites for Solar Thermochemical Water Splitting from High-Throughput First-Principles Calculations Antoine A. Emery and Chris Wolverton; Materials Science and Engineering, Northwestern University, Evanston, Illinois, United States.

11:20 AM *F/H1.03
Fuel Production from Concentrated Solar Radiation Christian Sattler and Martin Roeb; Solar Chemical Engineering, German Aerospace Center - DLR, Cologne, Germany.

11:40 AM F/H1.04
Decisive Thermodynamic Factor of Perovskite Catalysts for Thermochemical Water Splitting Yoshihiro Yamazaki[1, 2], Chih-Kai Yang[3] and Sossina M. Haile[3]; [1]Inamori Frontier Research Center, Kyushu University, Fukuoka, Japan; [2]Japan Science and Technology Agency, Kawaguchi, Japan; [3]California Institute of Technology, Pasadena, California, United States.

SESSION F/H3: Solid State Photoelectrochemistry/High Temperature Routes to Solar Fuels II
F/H: Solid State Photoelectrochemistry/High Temperature Routes to Solar Fuels
Chairs: Shannon Boettcher and Tim Davenport
Monday Afternoon, June 15, 2015
Keystone Resorts, Grays Peak III

2:30 PM *F/H3.01
Characterization of La-Mn Perovskites and Doped Ceria for Thermochemical H_2O and CO_2 Splitting Applications Jonathan Scheffe[1], Thomas Cooper[2], Michael Takacs[2] and Aldo Steinfeld[2]; [1]Mechanical and Aerospace Engineering, University of Florida, Gainesville, Florida, United States; [2]Department of Mechanical and Process Engineering, ETH Zurich, Zurich, Switzerland.

2:50 PM F/H3.02
Perovskites from Earth-Abundant Elements for Thermochemical Energy Storage Rounak Kharait[1], Luca Imponenti[1], Michael Sanders[2], Jianhua Tong[2], Ryan O'Hayre[2] and Gregory S. Jackson[1]; [1]Mechanical Engineering, Colorado School of Mines, Golden, Colorado, United States; [2]George S. Ansell Dept. of Metallurgical and Materials Engineering, Colorado School of Mines, Golden, Colorado, United States.

3:10 PM **F/H3.03
Engineering Materials and Interfaces for Efficient and Stable Photocatalytic Water Splitting Jinhui Yang, Jason K. Cooper, Francesca M. Toma and Ian D. Sharp; Lawrence Berkeley National Laboratory, Berkeley, California, United States.

3:40 PM **F/H3.04
Excited State Dynamics in Oxynitride Nanocrystals and Implications for Solar Fuel Generation Gordana Dukovic; Chemistry and Biochemistry, University of Colorado Boulder, Boulder, Colorado, United States.

4:10 PM **F/H3.05
Charge Carrier Transport and Catalysis on Solution-Processed Photoelectrodes for Solar Water Splitting Kevin Sivula; Laboratory for Molecular Engineering of Optoelectronic Nanomaterials, Institute of Chemical Science and Engineering, École Polytechnique Fédérale de Lausanne, Lausanne, Switzerland.

4:40 PM F/H3.06
Enhanced Photoactivity in Mo:$BiVO_4$ by Thermally Activating Small Polaron Hopping Liming Zhang, Xiaofei Ye, Madhur Boloor, Andrey Poletayev, Nicholas Melosh and William Chueh; Materials Science & Engineering, Stanford University, Stanford, California, United States.

5:00 PM F/H3.07
Mixed Conductivity as the Origin of Capacitive and Hysteretic Anomalies in Organo-Lead Halide Perovskites Giuliano Gregori[1], Tae-Youl Yang[1], Norman Pellet[2], Michael Graetzel[2] and Joachim Maier[1]; [1]Max Planck Institute for Solid State Research, Stuttgart, Germany; [2]Swiss Federal Institute of Technology, Lausanne, Switzerland.

ORAL PRESENTATIONS

TUESDAY June 16, 2015

PLENARY

SESSION L2: Plenary II
Chair: Harry Tuller
Tuesday Morning, June 16, 2015
Keystone Resorts, Shavano Peak

9:15 AM INTRODUCTION

9:25 AM L2.01
Insights into Proton Transport in Superprotonic Solid Acids Sossina M. Haile; Department of Materials Science and Engineering, Northwestern University, Evanston , Illinois, United States.

A: Solid Oxide Fuel Cells and Electrolyzers

* Invited Speaker
** Keynote Speaker

SESSION A4: SOFC—Cathodes III
A: Solid Oxide Fuel Cells and Electrolyzers
Chair: Harry Tuller
Tuesday Morning, June 16, 2015
Keystone Resorts, Longs Peak

10:10 AM BREAK

10:30 AM **A4.01
Measuring Oxygen Surface Exchange Kinetics on Mixed-Conducting Composites by Electrical Conductivity Relaxation Bobing Hu[2], Yunlong Wang[2], Zhuoying Zhu[2], Changrong Xia[2] and Henny J. Bouwmeester[1, 2]; [1]Department of Science and Technology, University of Twente, Enschede, Netherlands; [2]Department of Materials Science and Engineering, AS Key Laboratory of Materials for Energy Conversion, University of Science and Technology of China, Hefei, China.

11:00 AM A4.02
On the Link between Oxygen Surface Exchange and Bulk Oxygen Anion Transport in SOFC Cathode Material Alexander C. Tomkiewicz[1], Mazin A. Tamimi[1], Ashfia Huq[2] and Steven McIntosh[1]; [1]Chemical Engineering, Lehigh University, Bethlehem, Pennsylvania, United States; [2]Neutron Sciences, Oak Ridge National Laboratory, Oak Ridge, Tennessee, United States.

11:20 AM A4.03
Fast Tracer and Slow Electrical Kinetics of ^{18}O Exchange on Mixed Conducting Surfaces: A Combined Tracer and Impedance Study Andreas Nenning, Edvinas Navickas, Sandra Kogler, Katharina Langer-Hansel, Alexander K. Opitz and Jueürgen Fleig; Institute of Chemical Technologies and Analytics, Vienna University of Technology, Vienna, Austria.

11:40 AM *A4.04
Phase Decomposition and Secondary Phase Formation in the Chromium and Silicon Poisoned IT-SOFC Cathode Materials $La_{0.6}Sr_{0.4}CoO_{3-\delta}$ and $La_2NiO_{4+\delta}$ Edith Bucher[1], Nina Schroedl[1], Christian Gspan[2], Andreas Egger[1], Christian Ganser[3], Christian Teichert[3], Ferdinand Hofer[2] and Werner Sitte[1]; [1]Chair of Physical Chemistry, Montanuniversitaet Leoben, Leoben, Austria; [2]Institute for Electron Microscopy and Nanoanalysis (FELMI), Graz University of Technology & Graz Center for Electron Microscopy (ZFE), Austrian Cooperative Research (ACR), Graz, Austria; [3]Institute of Physics, Montanuniversitaet Leoben, Leoben, Austria.

SESSION A5: SOFC—Electrolytes I
A: Solid Oxide Fuel Cells and Electrolyzers
Chair: Koji Amezawa
Tuesday Afternoon, June 16, 2015
Keystone Resorts, Longs Peak

3:10 PM BREAK

3:30 PM *A5.01
Formation of $SrZrO_3$ in Perovskite Cathode /Ceria Interlayer / Zirconia Electrolyte during Operation of Solid Oxide Fuel Cells Koichi Eguchi, Toshiaki Matsui, Hiroki Muroyama, Masahiro Komoto, Kyosuke Kishida and Haruyuki Inui; Graduate School of Engineering, Kyoto University, Kyoto, Japan.

3:50 PM A5.02
Three-Dimensional Quantification of Composition and Space Charge Potential at Doped Ceria Grain Boundaries using Atom Probe Tomography David R. Diercks[1], Jianhua Tong[1], Huayang Zhu[2], Robert Kee[2], Juan C. Nino[3], Ryan O'Hayre[1] and Brian P. Gorman[1]; [1]Metallurgical and Materials Engineering, Colorado School of Mines, Golden, Colorado, United States; [2]Mechanical Engineering, Colorado School of Mines, Golden, Colorado, United States; [3]Materials Science and Engineering, University of Florida, Gainesville, Florida, United States.

4:10 PM A5.03
Nanoscale Electrochemical Investigation on SDC Thin Films for µ-SOFCs Applications Nan Yang[1, 2], Vittorio Foglietti[1], Antonello Tebano[1], Giuseppe Balestrino[1], Carmela Arruta[1], Stephen Jesse[3] and Sergei Kalinin[3]; [1]CNR-SPIN&University of Rome Tor Vergata, Rome, Italy; [2]UniCusano Online University, Rome, Italy; [3]Oak Ridge National Laboratory, Oak Ridge, Tennessee, United States.

4:30 PM A5.04
Dopant Segregation Effect on Ionic Conductivity of Nanocrystalline Gadolinium-Doped Ceria Thin Film Jiwoong Bae, Yonghyun Lim and Young-Beom Kim; Mechanical Convergence Engineering, Hanyang University, Seoul, Korea (the Republic of).

4:50 PM A5.05
A First-Principles Approach to the Attempt Frequency of Oxygen Ion Jumps in Doped Ceria Julius Koettgen, Tobias Zacherle, Steffen Grieshammer and Manfred Martin; Institute of Physical Chemistry, RWTH Aachen University, Aachen, Germany.

5:10 PM A5.06
Rare Earth Doped Bismuth Lead System Wojciech Wrobel[1], Anna Borowska-Centkowska[1], Marzena Leszczynska-Redek[1], Marcin Malys[1], Marcin Krynski[1], Franciszek Krok[1] and Isaac Abrahams[2]; [1]Faculty of Physics, Warsaw University of Technology, Warsaw, Poland; [2]Materials Research Institute, Queen Mary University of London, London, United Kingdom.

B: Polymer Electrolyte Fuel Cells and Electrolyzers

SESSION B1: PEMFC/DMFC I
B: Polymer Electrolyte Fuel Cells and Electrolyzers
Chair: Andrew Herring
Tuesday Afternoon, June 16, 2015
Keystone Resorts, Grays Peak III

1:30 PM *B1.01
Nanoscaled Structure of Nafion at Interfaces Joseph Dura[1], Steven DeCaluwe[2] and Paul Kienzle[1]; [1]NCNR, National Institute of Standards and Technology, Gaithersburg, Maryland, United States; [2]Mechanical Engineering, Colorado School of Mines, Golden, Colorado, United States.

1:50 PM B1.02
Interplay between Relaxations and Structure in Anion-Exchange Membranes (AEMs) Vito Di Noto[1, 2], Graeme Nawn[1], Keti Vezzu[1, 3], Federico Bertasi[1, 2], Enrico Negro[1, 2], Sandra Lavina[1, 2], Ashley Maes[4], Andrew Herring[4], Sedef Piril Ertem[5] and Bryan Coughlin[5]; [1]Chemical Sciences, University of Padova, Padova, Italy; [2]Consorzio Interuniversitario Nazionale per la Scienza e la Tecnologia dei Materiali, Padova, Italy; [3]Veneto Nanotech S.C.p.a., Padova, Italy; [4]Colorado School of Mines, Golden, Colorado, United States; [5]Department of Polymer Science and Engineering, University of Massachusetts, Amherst, Amherst, Massachusetts, United States.

2:10 PM B1.03
Anion Exchange Membranes for Fuel Cells and Flow Batteries: Quaternary Ammonium Group Stability and Transport Properties of a Model Membrane Michael G. Marino, Giorgi Titvinidze and Klaus-Dieter Kreuer; Maier, Max Planck Institute for Solid State Research, Stuttgart, Germany.

2:30 PM B1.04
Chemically Stable and Highly Conductive Alkaline Poly(phenylene oxide) Poly(vinyl benzyl trimethyl ammonium) Di-Block Membrane for Fuel Cell Applications Tara P. Pandey, Matthew W. Liberatore and Andrew M. Herring; Chemical and Biological Engineering, Colorado School of Mines, Golden, Colorado, United States.

2:50 PM *B1.05
Thermoreversible Gels – A New Route to Create Blocky Ionomer Membranes via Non-Random Functionalization Samantha Talley, Greg Fahs, Xijing Yuan, Sonya Benson and Robert Moore; Department of Chemistry, Virginia Tech, Blacksburg, Virginia, United States.

C: Electrodes and Solid Electrolytes for Batteries

SESSION C5: Metal-Air Batteries
C: Electrodes and Solid Electrolytes for Batteries
Chair: Yue Qi
Tuesday Morning, June 16, 2015
Keystone Resorts, Shavano Peak

10:10 AM BREAK

10:30 AM **C5.01
Aprotic Sodium (And Li)-Oxygen Batteries Chun Xia, Robert Black, Russel Fernandes, Dipan Kundu, Brian Adams and Linda Nazar; Department of Chemistry, University of Waterloo, Waterloo, Ontario, Canada.

11:00 AM *C5.02
Hybrid Lithium-Air Batteries: Inexpensive Catalysts and Novel Cell Designs Arumugam Manthiram, Longjun Li and Siyang Liu; Materials Science and Engineering, University of Texas at Austin, Austin, Texas, United States.

11:20 AM *C5.03
Ionic Transport Issue in Solid Lithium Air Batteries Hao Zheng[1], Dongdong Xiao[2], Jiayue Peng[1], Jie Huang[1], Degang Xie[3], Xin Li[4], Penghan Lu[3], Yuecun Wang[3], Hangyu Xu[1], Xianlong Wei[4], Qing Chen[4], Zhiwei Shan[3], Lin Gu[2] and Hong Li[1]; [1]Renewable Energy Laboratory, Institute of Physics, Chinese Academy of Sciences, Beijing, China; [2]Laboratory for Advanced Materials, Institute of Physics, Beijing, China; [3]State Key Laboratory for Mechanical Behavior of Materials, Xi'an Jiaotong University, Xi'an, China; [4]Key Laboratory for the Physics and Chemistry of Nanodevices, Peking University, Beijing, China.

11:40 AM C5.04
Inorganic-Organic Composite Membranes for Aqueous Li-Air Batteries Dorsasadat Safanama, Zhen Feng Yow, Hu Yan, Daniel H. Chua and Stefan Adams; Materials Science & Eng., National University of Singapore, Singapore, Singapore.

SESSION C6: Solid Electrolyte II
C: Electrodes and Solid Electrolytes for Batteries
Chair: Yan Yu
Tuesday Afternoon, June 16, 2015
Keystone Resorts, Shavano Peak

1:30 PM *C6.01
Confined-in-Ceramic Solid Polymer Electrolyte for Microbattery Application Diana Golodnitsky[1], Raymond Blanga[1], Yevgeny Rakita[2] and Amir Natan[2]; [1]School of Chemistry, Tel Aviv University, Tel Aviv, Israel; [2]Engineering Department, Tel Aviv University, Tel Aviv, Israel.

1:50 PM C6.02
Extremely Mobile Ions in Solid Electrolytes as Seen by NMR Martin Wilkening; Institute for Chemistry and Technology of Materials, Graz University of Technology, Graz, Austria.

2:10 PM C6.03
High Ionic Conductivity in the System $Na_{3+x}Sc_2(SiO_4)_x(PO_4)_{3-x}$ Marie Guin[1], Kaustubh Bhat[2], Frank Tietz[1] and Olivier Guillon[1, 3]; [1]Forschungszentrum Jülich GmbH, Institute of Energy and Climate Research (IEK-1), Jülich, Germany; [2]Forschungszentrum Jülich GmbH, Peter-Grünberg-Institute (PGI-1), Jülich, Germany; [3]Jülich Aachen Research Alliance, JARA-Energy, Aachen, Germany.

2:30 PM C6.04
Very High Li-Ion Conductivity in $Li_{1.5}Al_{0.5}Ti_{1.5}(PO_4)_3$ Prepared by a Novel Sol-Gel Method Qianli Ma[1, 2], Chih-Long Tsai[1, 2], Qi Xu[1, 2], Frank Tietz[1, 2] and Olivier Guillon[1, 2];[1]Forschungszentrum Jülich, Jülich, Germany; [2]Jülich Aachen Research Alliance, JARA-Energy, Jülich, Germany.

2:50 PM C6.05
Structural and Fast-Ion Conduction Properties of Solid Electrolytes within the Li_4SiO_4- Li_3PO_4 System Yue Deng[1], Chris Eames[2], Jean-Noël Chotard[1], Christian Masquelier[1] and Saiful Islam[2]; [1]Laboratoire de Réactivité et Chimie des Solides, Université de Picardie Jules Verne, Amiens, France; [2]Department of Chemistry, University of Bath, Bath, United Kingdom.

3:10 PM BREAK

3:30 PM C6.06
Investigation of Electrolyte-Electrolyte Interface in All-Solid-State Metal-Metal Battery Ruigang Zhang[1], Timothy S. Arthur[1], Donovan N. Leonard[2], Miaofang Chi[2] and Fuminori Mizuno[1]; [1]Toyota Technical Center, Ann Arbor, Michigan, United States; [2]Oak Ridge National Lab, Oak Ridge, Tennessee, United States.

3:50 PM C6.07
An All-Solid State NASICON Sodium Battery Operating at 200°C Fabien Lalere[1, 2], Jean-Bernard Leriche[1, 2], Mattieu Courty[1, 2], Sylvain Boulineau[1, 2], Virginie Viallet[1, 2], Christian Masquelier[1, 2] and Vincent Seznec[1, 2]; [1]Laboratoire de Réactivité et Chimie des Solides, Amiens, France; [2]Réseau de Stockage Electrochimique de l'Energie, Amiens, France.

4:10 PM C6.08
Assessment of Solid Electrolytes for All-Solid-State Lithium Batteries Philipp Braun, Moses Ender, Joerg Illig and Ellen Ivers-Tiffee; Institute for Applied Materials (IAM-WET), Karlsruhe Institute of Technology (KIT), Karlsruhe, Germany.

4:30 PM C6.09
Solid Electrolytes in Batteries Dominik A. Weber[1], Stefan Berendts[2], Joachim Sann[1], Martin Busche[1], Sebastian Wenzel[1] and Juergen Janek[1]; [1]Physikalisch-Chemisches Institut, Justus-Liebig-Universität Gießen, Gießen, Germany; [2]Institut für Chemie, Technische Universität Berlin, Berlin, Germany.

4:50 PM C6.10
Safety Assessment of All-Solid-State Lithium-Ion Polymer Battery Using Forced Destruction System Yo Kobayashi, Kumi Shono, Takeshi Kobayashi and Hajime Miyashiro; Central Research Institute of Electric Power Industry, Tokyo, Japan.

C: Electrodes and Solid Electrolytes for Batteries

SESSION C7: Characterization of Nanoscale and Local Structures I
C: Electrodes and Solid Electrolytes for Batteries
Chair: Wei Lai
Tuesday Afternoon, June 16, 2015
Keystone Resorts, Quandary Peak I/II

3:30 PM C7.01
Soft X-Ray Absorption Spectroscopy Studies on $LiNi_{0.5}Mn_{1.5}O_4$ Spinel Ruimin Qiao[1], Jung-Hyun Kim[2], Nicholas P. Pieczonka[3], Andrew Wray[4] and Wanli Yang[1]; [1]Advanced Light Source, Lawrence Berkeley National Lab, Berkeley, California, United States; [2]Chemical & Materials Systems Laboratory, General Motors Global R&D Center, Warren, Michigan, United States; [3]Optimal CAE Inc, Plymouth, Michigan, United States; [4]Department of Physics, New York University, New York, New York, United States.

3:50 PM C7.02
Electronic Origin of the Step-Like Character of the Discharge Curve for Na_xCoO_{2-y} Cathode Janina Molenda; AGH University of Science and Technology, Krakow, Poland.

4:10 PM C7.03
In Situ TEM of Lithiation-Induced Displacement Reactions in Individual Copper Sulfide Nanocrystals Matthew McDowell[1] and Yi Cui[2]; [1]Chemistry and Chemical Engineering, California Institute of Technology, Pasadena, California, United States; [2]Materials Science and Engineering, Stanford University, Stanford, California, United States.

4:30 PM C7.04
Atomic-Scale Recognition of Structure and Intercalation Mechanism of MoS_2 and Ti_3C_2X Xuefeng Wang, Xi Shen, Yurui Gao, Zhaoxiang Wang, Richeng Yu and Liquan Chen; Institute of Physics, Chinese Academy of Sciences, Beijing, China.

4:50 PM C7.05
Phase Evolution in Single-Crystalline $LiFePo_4$ in a Micrometer-Sized Battery Followed by *In Situ* Scanning Transmission X-Ray Microscopy Nils Ohmer[1], Bernhard Fenk[1], Dominik Samuelis[1], Chia-Chin Chen[1], Joachim Maier[1], Markus Weigand[2], Eberhard Goering[2] and Gisela Schuetz[2]; [1]Max Planck Institute for Solid State Research, Stuttgart, Germany;[2]Max Planck Institute for Intelligent Systems, Stuttgart, Germany.

5:10 PM C7.06
Investigating Transient and Persistent Chemical Heterogeneity in $Li[Ni_{1/3}Co_{1/3}Mn_{1/3}]O_2$ Secondary Particles Using Transmission X-Ray Microscopy William Gent[1], Yiyang Li[1], Johanna Weker[2], Anna Wise[2], David Mueller[1] and William Chueh[1]; [1]Stanford University, Stanford, California, United States; [2]SLAC National Laboratory, Stanford, California, United States.

D: Fundamentals of Transport and Reactivity and Nanoionics

SESSION D4: Fundamentals of Transport and Reactivity and Nanoionics III
D: Fundamentals of Transport and Reactivity and Nanoionics
Chair: John Irvine
Tuesday Morning, June 16, 2015
Keystone Resorts, Grays Peak I/II

10:10 AM BREAK

10:30 AM **D4.01
Cathode Materials for Proton Conducting SOFC: Bulk Defect Chemistry and Mechanism of Oxygen Reduction Reaction Rotraut Merkle, Daniel Poetzsch and Joachim Maier; MPI for Solid State Research, Stuttgart, Germany.

11:00 AM D4.02
Oxygen Exchange and Transport in Mixed Conducting Dual Phase Composites John Druce[1], Helena Tellez[1], Tatsumi Ishihara[1] and John A. Kilner[1, 2]; [1]I2CNER, Kyushu University, Fukuoka, Japan; [2]Department of Materials, Imperial College London, London, United Kingdom.

11:20 AM D4.03
A Concept of Three Exchange Types in Oxygen Isotope Exchange Kinetic Analysis for Solid Oxide Materials Maxim Ananyev[1, 2]; [1]Laboratory of the Electrochemical Materials Science, Institute of High Temperature Electrochemistry, Ural Branch of Russian Academy of Sciences, Yekaterinburg, Russian Federation; [2]Institute of Chemical Technology, Ural Federal University, Yekaterinburg, Russian Federation.

11:40 AM D4.04
First Principles Calculations of Formation and Migration of Oxygen Vacancies in the Bulk and on Surface of Complex Perovskites for Solid Oxide Fuel Cell Cathodes Eugene Kotomin[1], Yuri Mastrikov[2], Rotraut Merkle[1], Maija Kuklja[3] and Joachim Maier[1]; [1]Dept.Phys.Chem., Max-Planck-Institute FKF, Stuttgart, Germany; [2]Institute for Solid State Physics, Riga, Latvia; [3]University of Maryland, College Park , Maryland, United States.

SESSION D5: Fundamentals of Transport and Reactivity and Nanoionics IV
D: Fundamentals of Transport and Reactivity and Nanoionics
Chairs: Rotraut Merkle and Truls Norby
Tuesday Afternoon, June 16, 2015
Keystone Resorts, Grays Peak I/II

1:30 PM *D5.01
An Extended Analysis of Dopant Strategies to Control Mixed Ion and Electron Transport in Ceria Based Oxide Solutions Jens-Peter Eufinger[2], Maximilian Daniels[1], Stefan Berendts[3], Kerstin Neuhaus[1], Sebastian Eickholt[1], Gregor Ulbrich[3], Aditya Maheshwari[1], Annika Buchheit[1], Juergen Janek[2], Martin Lerch[3] and Hans D. Wiemhoefer[1]; [1]Institute of Inorganic and Analytical Chemistry, Univ. Münster, Münster, Germany; [2]Physikalisch-Chemisches Institut, Univ. Giessen, Giessen, Germany; [3]Institute of Chemistry, Techn. Univ. Berlin, Berlin, Germany.

1:50 PM D5.02
Room Temperature Polarization Phenomena in Doped Ceria Kerstin Neuhaus[1], Gregor Ulbrich[2], Martin Lerch[2] and Hans-Dieter Wiemhöfer[1]; [1]Institute for Inorganic and Analytical Chemistry, University of Münster, Münster, Germany; [2]Institut für Chemie, Technische Universität Berlin, Berlin, Germany.

2:10 PM *D5.03
Microscopic Origin of Electrostriction in Gd-Doped Ceria and Prospects for Practical Applications in MEMS Roman Korobko[1], Eran Mishuk[1], Nimrod Yavo[1], Alyssa Lerner[2], Yuanyuan Li[2], Wachtel Wachtel[1], Anatoly Frenkel[2] and Igor Lubomirsky[1]; [1]Materials and Interfaces, Weizmann Institute of Science, Rehovot, Israel; [2]Physics Department, Yeshiva University, New York, New York, United States.

2:30 PM D5.04
An *In Situ* Optical Spectroscopic Study of Thermodynamics and Redox Kinetics of $Ce_{0.08}Y_{0.2}Zr_{0.72}O_{2-\delta}$ Jianmin Shi[1], Martin Lerch[2], Juergen Janek[3] and Klaus D. Becker[1];[1]Technische Universität Braunschweig, Braunschweig, Germany; [2]Technische Universität Berlin, Berlin, Germany; [3]Justus Liebig University Giessen, Giessen, Germany.

2:50 PM *D5.05
Effect of Chemomechanical Coupling on Defect Equilibrium and Transport in Solid State Ionic Devices Tatsuya Kawada, Yuta Kimura, Yuki Gonoi, Keiji Yashiro, Shin-ichi Hashimoto and Koji Amezawa; Tohoku University, Sendai, Japan.

3:10 PM BREAK

3:30 PM *D5.06
Electro-Chemo-Mechanics in Solid State Materials: Let`s Design the Structural-Defect Twists Jennifer L. Rupp; Electrochemical Materials, ETH Zurich, Zurich, Switzerland.

3:50 PM D5.07
Engineering Mixed Ionic Electronic Conduction in $La_{0.8}Sr_{0.2}MnO_{3+\delta}$ Nanostructures through Fast Grain Boundary Oxygen Diffusivity Aruppukottai Muruga Saranya[1], Dolors Pla[1], Alex Morata[1], Andrea Cavallaro[2], Jesus Canales-Vazquez[3], John A Kilner[2], Monica Burriel[1, 2] and Albert Tarancon[1]; [1]Catalonia Institute for Energy Research (IREC), Barcelona, Spain; [2]Imperial College London, London, United Kingdom; [3]Universidad Castilla la Mancha, Albacete, Spain.

4:10 PM D5.08
Oxidation Kinetics of Thin Metal Films & Diffusion in NiO Yeliz Unutulmazsoy, Rotraut Merkle, Joachim Maier and Jochen Mannhart; Max Planck Institute for Solid State Research, Stuttgart, Germany.

4:30 PM D5.09
H^- Ionic Conduction in Alkaline Hydrides John T. Irvine[1], George Carins[1], Maarten Verbaeken[1] and Martin Owen Jones[2]; [1]School of Chemistry, University of St Andrews, St Andrews, United Kingdom; [2]STFC, Didcot, United Kingdom.

4:50 PM D5.10
Modeling a Surface-Mediated Spinodal in Doped Mixed Conducting Perovskites David S. Mebane; Mechanical and Aerospace Engineering, West Virginia University, Morgantown, West Virginia, United States.

E: Transparent Conducting Oxides

SESSION E3: TCO 2—Materials, Processing, and Structures
E: Transparent Conducting Oxides
Chair: David Ginley
Tuesday Morning, June 16, 2015
Keystone Resorts, Quandary Peak I/II

10:10 AM BREAK

10:30 AM **E3.01
Material Design of Novel Transparent Oxide Conductors/ Semiconductors Hideo Hosono; Tokyo Institute of Technology, Yokohama, Japan.

11:00 AM E3.02
Effect of Phase Transition on Electronic Defects of Ni-Co Oxide and Its Application on Optoelectronics Shu-Yi Tsai[3, 1], Kuan-Zong Fung[1, 3], H.-Y. Bor[2] and C.-N. Wei[2]; [1]Materials Science and Engineering, National Cheng Kung University, Tainan City, Taiwan; [2]Chung-Shan Institute of Science and Technology(CSIST), Taoyuan County, Taiwan; [3]Research Center for Energy Technology and Strategy, National Cheng Kung University, Tainan City, Taiwan.

11:20 AM E3.03
Effect of Precursor Solvent on the Nature of Spin Coated 1at%Ga-ZnO Transparent Conducting Films Amit K. Srivastava and Jitendra Kumar; Materials Science, I I T Kanpur, Kanpur, India.

11:40 AM E3.04
Transparent and Conductive Coatings with Nanoparticulate Magnetic Additives Gesa Beck[1], Stephan Barcikowski[2], Bilal Goekce[2], Maja Jelic[1] and Martin Kirsch[3]; [1]Physics, Chair of Resource Strategies, Augsburg, Germany; [2]Technical Chemistry I , University of Duisburg-Essen and Center for Nanointegration Duisburg-Essen (CENIDE) , Essen, Germany; [3]Fa. Kirsch Kunststofftechnik GmbH, Ebersbach, Germany.

G: Switching and Sensing Phenomena

SESSION G1: Switching and Sensing Phenomena I
G: Switching and Sensing Phenomena
Chairs: Jennifer Rupp and Shu Yamaguchi
Tuesday Morning, June 16, 2015
Keystone Resorts, Grays Peak III

10:10 AM BREAK

10:30 AM **G1.01
Bulk Mixed Ion Electron Conduction in Highly Disordered Oxides Causes Memristive Behavior Manfred Martin[1, 2]; [1]Institute of Physical Chemistry, RWTH Aachen University, Aachen, Germany; [2]Department of Materials Science and Engineering, Seoul National University, Seoul, Korea (the Republic of).

11:00 AM *G1.02
Dislocations in $SrTiO_3$: Easy to Reduce but not so Fast for Oxygen Transport Dario Marrocchelli, Lixin Sun and Bilge Yildiz; Nuclear Science & Engineering, Massachusetts Institute of technology, Cambridge, Massachusetts, United States.

11:20 AM G1.03
Electroforming in Valence Change Memories Based on Mixed Ionic Electronic Conductors Dima Kalaev[1], Eilam Yalon[2] and Ilan Riess[1]; [1]Physics, Israel Institute of Technology, Haifa, Israel; [2]Microelectronics Research Center, Technion – Israel Institute of Technology, Haifa, Israel.

11:40 AM G1.04
Field-Enhanced Bulk Conductivity and Resistive-Switching in Ca-Doped $BiFeO_3$ Ceramics Nahum Maso[1, 2] and Anthony R. West[2]; [1]Chemistry, University of Oslo, Oslo, Norway;[2]Materials Science and Engineering, University of Sheffield, Sheffield, United Kingdom.

SESSION G2: Switching and Sensing Phenomena II
G: Switching and Sensing Phenomena
Chairs: Jennifer Rupp and Shu Yamaguchi
Tuesday Afternoon, June 16, 2015
Keystone Resorts, Grays Peak III

3:10 PM BREAK

3:30 PM *G2.01
Various Functional Nano-Ionic Devices Achieved by Controlling Hetero-Interface Characteristics using Local Ion Migration Kazuya Terabe, Takashi Tsuchiya and Masakazu Aono; MANA, National Institute for Materials Science, Tsukuba, Japan.

3:50 PM *G2.02
Ionic Switching Devices: Operation Principle and Application in Computing Daniele Ielmini; Politecnico di Milano, Milano, Italy.

4:10 PM *G2.03
$La_{0.8}Sr_{0.2}(Mn,Co)O_3$ Perovskite Oxides as Resistive Switches: Influence of B-Site Substitution on the Resistive Switching Properties Monica Burriel[1, 2], Rafael Schmitt [3], Aruppukottai Muruga Saranya[2], Alex Morata[2], Aitor Hornes[2], Sebastian Schweiger[3], Michel Bourdard[1], Jennifer L. M. Rupp[3] and Albert Tarancon[2]; [1] Laboratoire des Matériaux et du Génie Physique (LMGP), Grenoble, France; [2]Catalonia Institute for Energy Research-IREC, Barcelona, Spain; [3]ETH Zurich, Zurich, Switzerland.

4:30 PM G2.04
STM Investigations of Resistive Switching on Binary Metal Oxides and Chalcogenides Anja Wedig[1], Marco Moors[1], Tsuyoshi Hasegawa[2], Masakazu Aono[2], Rainer Waser[1, 3] and Ilia Valov[1, 3]; [1]Electronic Materials, Juelich Research Center, Juelich, Germany; [2]International Center for Materials Nanoarchitectonics, National Institute for Materials Science, Tsukuba, Japan; [3]Institute for Materials in Electrical Engineering II, RWTH Aachen University, Aachen, Germany.

4:50 PM G2.05
Strained Heterolayers as Resistive Switching Oxide: Materials and Devices Sebastian Schweiger, Reto Pfenninger and Jennifer L. Rupp; Materials, ETH Zurich, Zurich, Switzerland.

5:10 PM G2.06
Sensing Nitrogen Oxides and Ammonia with Porous Electrolyte Devices Fernando Garzon[1], Eric Brosha[2], Cortney Kreller[2] and Rangachary (Mukund) Mukundan[2]; [1]Chemical and Biological Engineering, University of New Mexico, Albuquerque, New Mexico, United States; [2]Materials Physics and Applications, Los Alamos National Laboratory, Los Alamos, New Mexico, United States.

5:30 PM G2.07
Single Crystalline $SrTiO_3$ as a Memristive Model System: Roles of Oxygen Vacancies and Schottky Barrier, and Neural Function Mimicking Xin Guo; Materials Science and Engineering, Huazhong University of Science and Technology, Wuhan, China.

K: Proton-Conducting Oxides

SESSION K2: Protonic Oxides I
K: Proton-Conducting Oxides
Chairs: Truls Norby and Yoshihiro Yamazaki
Tuesday Afternoon, June 16, 2015
Keystone Resorts, Longs Peak

1:30 PM **K2.01
Protonic Conduction in Perovskites: NMR and DFT Studies of Yttrium-Doped $BaZrO_3$ and Related Perovskites Luke Sperrin[1], Riza Dervisoglu[1], Lucienne Buannic[1], Frederic Blanc[2] and Clare Grey[1]; [1]Department of Chemistry, University of Cambridge, Cambridge, United Kingdom; [2]Department of Chemistry, University of Liverpool, Liverpool, United Kingdom.

2:00 PM K2.02
Local Structural Analysis of Sc-Doped $BaZrO_3$ Using Electric-Field Gradient at Sc Site Itaru Oikawa and Hitoshi Takamura; Department of Materials Science, Tohoku University, Sendai, Japan.

2:20 PM *K2.03
Variation of Kinetic Parameters, Chemical Diffusivity and Surface Exchange Coefficient of $Ba(Zr_{0.84}Y_{0.15}Cu_{0.01})O_{3-\delta}$ during the Conductivity Relaxation Experiments Jong-Ho Lee, Sung Min Choi, Moon-Bong Choi, Jongsup Hong, Hyoungchul Kim, Kyung Joong Yoon, Ji-Won Son and Byung-Kook Kim; High-Temperature Energy Materials Research Center, Korea Institute of Science and Technology, Seoul, Korea (the Republic of).

2:40 PM K2.04
The Influence of Dopant Levels on the Hydration Properties of SZCY and BZCY Proton Conducting Ceramics for Hydrogen Production Kwati Leonard[1], Yuji Okuyama[4], Young-Sung Lee[1] and Hiroshige Matsumoto[1, 2, 3]; [1]International Institute for Carbon-Neutral Energy Research (I2CNER-WPI), Kyushu University, Fukuoka, Japan; [2]INAMORI Frontier Research Center (IFRC), Kyushu University, Fukuoka , Japan; [3]Next Generation Fuel cell Research Center (NEXT-FC), Kyushu University, Fukuoka, Japan; [4] Organization for the Promotion of Tenure Track, University of Miyazaki, Miyazaki, Japan.

3rd ISSI Young Scientist Award

SESSION: 3rd ISSI Young Scientist Award
ISSI Young Scientist
Tuesday Afternoon, June 16, 2015
Keystone Resorts, Quandary Peak I/II

To recognize the outstanding contributions made by young scientists to the field of solid state ionics, the International Society of Solid-State Ionics established the ISSI Young Scientist Award. This year, six young scientists will be awarded. Don’t miss the award recipients’ talks from 1:30pm - 3:10pm in Quandary Peak I/II.

ORAL PRESENTATIONS

WEDNESDAY June 17, 2015

ISSI ELECTION

Keystone Resorts, Shavano Peak
8:00 AM - 9:00 AM

All SSI-20 attendees are encouraged to attended the ISSI Election. The new ISSI Vice President and Board of Directors' members will be elected.

PLENARY

SESSION L3: Plenary III
Chair: Klaus Funke
Wednesday Morning, June 17, 2015
Keystone Resorts, Shavano Peak

9:15 AM INTRODUCTION

9:25 AM L3.01
Electrode Kinetics in the Solid State Juergen Janek; Institute of Physical Chemistry, Justus-Liebig University, Giessen, Germany.

A: Solid Oxide Fuel Cells and Electrolyzers

* Invited Speaker
** Keynote Speaker

SESSION A7: SOFC
A: Solid Oxide Fuel Cells and Electrolyzers
Chair: Stephen Skinner
Wednesday Morning, June 17, 2015
Keystone Resorts, Longs Peak

10:10 AM BREAK

10:30 AM **A7.01
SOFC Cathode Oxygen Reduction Reaction Mechanisms under Real World Conditions Eric D. Wachsman, Y. L. Huang, C. Pellegrinelli, J. A. Taillon and L. G. Salamanca-Riba; University of Maryland Energy Research Center, University of Maryland, College Park, Maryland, United States.

11:00 AM A7.02
Correlation Between Cation Ordering and Oxygen Vacancies in Layered Double Perovskite Cathodes Carlos Bernuy-Lopez, Mari-Ann Einarsrud and Tor Grande; NTNU, Trondheim, Norway.

11:20 AM A7.03
Fabrication and Performance of Stainless Steel-Supported SOFC Kun Joong Kim, Byung Hyun Park, Sun Jae Kim and Gyeong Man Choi; Mat. Sci. & Eng., POSTECH, Pohang, Korea (the Republic of).

11:40 AM A7.04
Cobalt-Free Polycrystalline $Ba_{0.95}La_{0.05}FeO_{3-\delta}$ Thin Films as Cathodes for Intermediate-Temperature Solid Oxide Fuel Cells Francesco Ciucci[1, 2], Chi Chen[1] and Dengjie Chen[1];[1]Mechanical and Aerospace Engineering, The Hong Kong University of Science and Technology, Kowloon, Hong Kong; [2]Chemical and Biomolecular Engineering, The Hong Kong University of Science and Technology, Kowloon, Hong Kong.

B: Polymer Electrolyte Fuel Cells and Electrolyzers

SESSION B3: PEMFC/DMFC II
B: Polymer Electrolyte Fuel Cells and Electrolyzers
Chair: Thomas Zawodzinski
Wednesday Morning, June 17, 2015
Keystone Resorts, Quandary Peak I/II

10:10 AM BREAK

10:30 AM **B3.01
Structural Aspects of PFSA Ionomers as Determined by STEM and Simulations Stephen J. Paddison; Chemical & Biomolecular Engineering, University of Tennessee, Knoxville, Tennessee, United States.

11:00 AM B3.02
Anion Transport in Polymer Electrolytes Andrew Herring, Ashley Maes, Himanshu Sarode, Ye Liu and Tara Pandey; Chemical and Biological Engineering, Colorado School of Mines, Golden, Colorado, United States.

11:20 AM B3.03
Effect of Hydration on Mechanical Properties of Anion Exchange Membranes Benjamin Caire, Melissa Vandiver, Andrew Herring and Matthew W. Liberatore; Chemical and Biological Engineering, Colorado School of Mines, Golden, Colorado, United States.

11:40 AM B3.04
Fundamental Understanding of Water Contribution for Ion Mobility in Anion Exchange Membranes Applied in Alkaline Fuel Cells Ye Liu[1], Bingzi Zhang[2], Söenke Seifert[3], Yuan Yang[4], Yushan Yan[2], Matthew Liberatore[1] and Andrew Herring[1]; [1]Chemical Engineering, Colorado School of Mines, Golden, Colorado, United States; [2]Chemical Engineering, University of Delaware, Newark, Delaware, United States; [3]Argonne National Laboratory, Argonne, Illinois, United States; [4]Chemistry, Colorado School of Mines, Golden, Colorado, United States.

C: Electrodes and Solid Electrolytes for Batteries

SESSION C9: Characterization of Nanoscale and Local Structures II
C: Electrodes and Solid Electrolytes for Batteries
Chair: Miran Gaberscek
Wednesday Morning, June 17, 2015
Keystone Resorts, Shavano Peak

10:10 AM BREAK

10:30 AM C9.01
A Simple *In Situ* Approach to Study the Solid Electrolyte / Lithium Interphase by Photoelectron Spectroscopy Thomas Leichtweiss, Sebastian Wenzel, Dominik Krueger, Achim Kronenberger, Joachim Sann and Juergen Janek; Institute of Physical Chemistry, Justus-Liebig-University Giessen, Giessen, Germany.

10:50 AM C9.02
***Operando* SAXS/WAXS Measurements of Amorphous and Nano-Crystalline Anodes for Na-Ion Batteries** Sabrina Sartori; Department of Physics, University of Oslo, Oslo, Norway.

11:10 AM C9.03
***In Situ* Raman Spectroscopy of Thin-Film Battery Li/Li_3PO_4/$LiMn_2O_4$ Using a Transparent Electrode** Naoakai Kuwata[1], Tatsunori Okawa[1], Yasutaka Matsuda[1], Osamu Kamishima[2]and Junichi Kawamura[1]; [1]IMRAM, Tohoku University, Sendai, Japan; [2]Faculty of Science and Engineering, Setsunan University, Neyagawa, Japan.

11:30 AM C9.04
Pore Collapse and Regrowth in Silicon Electrodes for Rechargeable Batteries Steven C. DeCaluwe[2, 1, 4], Bal-Mukund Dar[3], Joseph A. Dura[2] and Howard Wang[3, 4, 5]; [1]NIST Center for Neutron Research, Gaithersburg, Maryland, United States; [2]Mechanical Engineering, Colorado School of Mines, Golden, Colorado, United States; [3]Institute for Materials Research and Dept. of Mechanical Engineering, State University of New York, Binghamton, New York, United States; [4]Materials Science and Engineering, University of Maryland, College Park, Maryland, United States; [5]Material Measurement Laboratory, National Institute of Standards and Technology, Gaithersburg, Maryland, United States.

I: Ion Transport in Hybrid Organic-Inorganic Solids

SESSION I2: Ion Transport in Hybrid Perovskites
I: Ion Transport in Hybrid Organic-Inorganic Solids
Chair: Hemamala Karunadasa
Wednesday Morning, June 17, 2015
Keystone Resorts, Grays Peak I/II

10:10 AM BREAK

10:30 AM **I2.01
Electromigration of Ions in Hybrid Perovskites for Switchable Photovoltaic, Memristors and Synapses Jinsong Huang; Department of Mechanical and Materials Engineering, University of Nebraska, Lincoln, Lincoln, Nebraska, United States.

11:00 AM I2.02
Photo-Induced Instability in Mixed Halide Perovskite Absorbers Daniel Slotcavage[1], Eric Hoke[1], Emma Dohner[2], Andrea Bowring[1], Hemamala Karunadasa[2] and Michael McGehee[1];[1]Materials Science & Engineering, Stanford University, Stanford, California, United States; [2]Chemistry, Stanford University, Stanford, California, United States.

11:20 AM I2.03
Ionic Conductivity in 3-D Organic-Inorganic Mixed Halide Perovskites Abraham Saldivar Valdes and Hemamala Karunadasa; Chemistry, Stanford University, Stanford, California, United States.

11:40 AM I2.04
Uniform Perovskite Layers for Low Hysteresis Planar Heterojunction Solar Cells Yanbo Li[1, 2], Ian D. Sharp[2] and Francesca Maria Toma[1, 2]; [1]Lawrence Berkeley National Lab, Berkeley, California, United States; [2]Joint Center for Artificial Photosynthesis, Berkeley, California, United States.

J: Permeation Membranes

SESSION J3: Permeation Membranes I
J: Permeation Membranes
Chairs: Jonathan Lane and Martin Sogaard
Wednesday Morning, June 17, 2015
Keystone Resorts, Grays Peak III

10:10 AM BREAK

10:30 AM **J3.01
Advances in ITM Technology for Oxygen and Syngas Production Michael F. Carolan[1], Lori L. Anderson[1], Phillip A. Armstrong[1], Robert R. Broekhuis[1], Charles M. Woods[1], Mark Hutcheon[1], Charles A. Lewinsohn[2], Jack Chen[2] and Dale Taylor[2]; [1]Air Products and Chemicals, Inc., Allentown, Pennsylvania, United States; [2]Ceramatec, Inc. , Salt Lake City, Utah, United States.

11:00 AM J3.02
Lattice Structure and Oxygen Permeability of In-Doped $BaFeO_{3-\delta}$ Perovskite-Type Oxides Yao Lu[1], Hailei Zhao[1], Xing Cheng[1], Kun Zheng[2] and Konrad Swierczek[2]; [1]University of Science and Technology Beijing, Beijing, China; [2]AGH University of Science and Technology, Krakow, Poland.

11:20 AM *J3.03
Influence of Yttrium Doping on $Ba_{0.5}Sr_{0.5}Co_{0.8}Fe_{0.2}O_{3-\delta}$ Lana-Simone Unger[1], Stefan Baumann[2], Christian Niedrig[1], Wolfgang Menesklou[1], Stefan Wagner[1], Wilhelm A. Meulenberg[2]and Ellen Ivers-Tiffee[1]; [1]Institute for Applied Materials (IAM-WET), Karlsruhe Institute of Technology (KIT), Karlsruhe, Germany; [2]Institute of Energy and Climate Research IEK-1 Materials Synthesis and Processing, Forschungszentrum Jülich GmbH, Jülich, Germany.

11:40 AM J3.04
Stability and Oxygen Permeability of Sol-Gel Derived $SrCo_{0.8}Fe_{0.2}O_{3-\delta}$ Based Compound Membranes Vijay K. Kashyap and Jitendra Kumar; Materials Science, I I T Kanpur, Kanpur, India.

ORAL PRESENTATIONS

THURSDAY June 18, 2015

PLENARY

SESSION L4: Plenary IV
Chair: Maria Forsyth
Thursday Morning, June 18, 2015
Keystone Resorts, Shavano Peak

9:15 AM INTRODUCTION

9:25 AM L4.01
On the Mechanism of Cation Translocation across Channelrhodopsin Joachim Heberle; Experimental Molecular Biophysics, Freie Universität Berlin, Berlin, Germany.

A: Solid Oxide Fuel Cells and Electrolyzers

* Invited Speaker
** Keynote Speaker

SESSION A8: SOEC
A: Solid Oxide Fuel Cells and Electrolyzers
Chair: Steven McIntosh
Thursday Morning, June 18, 2015
Keystone Resorts, Longs Peak

10:10 AM BREAK

10:30 AM **A8.01
Prospects and Challenges of Solid Oxide Electrolysis Peter V. Hendriksen[1], Ming Chen[1], Ragnar Kiebach[1], Xiufu Sun[1], Karsten Agersted[1], Yi-Lin Liu[1], Sebastian Molin[1], Sune D. Ebbesen[1], Christopher Graves[1], Anne Hauch[1], Karen Brodersen[1], Mogens B. Mogensen[1], Johan Hjelm[1], Soren H. Jensen[1], Christodoulos Chatzichristodoulou[1] and Brian V. Mathiesen[2];[1]Department of Energy Conversion and Storage, Technical University of Denmark, Roskilde, Denmark; [2]Department of Development and Planning, Aalborg University, Copenhagen SV, Denmark.

11:00 AM A8.02
Surface and Bulk Properties of Polarized Mixed Conducting LSF Electrodes: An in-situ Study in H_2/H_2O and O_2 by Simultaneous near-Ambient Pressure XPS and Impedance Spectroscopy Alexander K. Opitz[1], Andreas Nenning[1], Sandra Kogler[1], Christoph Rameshan[2], Raffael Rameshan[3, 4], Raoul Blume[4, 5], Michael Haevecker[4, 5], Axel Knop-Gericke[4], Guenther Rupprechter[2], Bernhard Kloetzer[3] and Juergen Fleig[1]; [1]Insititute of Chemical Technologies and Analytics, Vienna University of Technology, Vienna, Austria; [2]Institute of Materials Chemistry, Vienna University of Technology, Vienna, Austria; [3]Institute of Physical Chemistry, University of Innsbruck, Innsbruck, Austria; [4]Department of Inorganic Chemistry, Fritz Haber Institute of the Max Planck Society, Berlin, Germany; [5]Catalysis for Energy, Group E-GKAT, Helmholtz-Zentrum Berlin fuer Materialien und Energie GmbH, Berlin, Germany.

11:20 AM A8.03
Infiltrated Double Perovskite Electrodes for Proton Conducting Steam Electrolysers Einar Vollestad, Ragnar Strandbakke and Truls Norby; Department of Chemistry, University of Oslo, Oslo, Norway.

11:40 AM A8.04
Compositional Engineering of Perovskite Oxides for Highly Efficient Oxygen Reduction Reactions Chi Chen[1], Dengjie Chen[1], Zongping Shao[2] and Francesco Ciucci[1]; [1]Mechanical and Aerospace Engineering, Hong Kong University of Science and Technology, Kowloon, Hong Kong; [2]Nanjing Tech University, Nanjing, China.

SESSION A9: SOFC—Electrolytes II, Anodes
A: Solid Oxide Fuel Cells and Electrolyzers
Chairs: John Irvine and Manfred Martin
Thursday Afternoon, June 18, 2015
Keystone Resorts, Longs Peak

1:30 PM *A9.01
Oxide Ion Conductivity in Doped $LnBaInO_4$(Ln=La, Nd) Tatsumi Ishihara[1], Yu Yan[2], Takaaki Sakai[2] and Shintaro Ida[2]; [1]International Institute for Carbon Neutral Energy Research, Kyushu University, Fukuoka, Japan; [2]Department of Applied Chemistry, Faculty of Engineering, Kyushu University, Fukuoka, Japan.

1:50 PM A9.02
Double Perovskite Oxide $Sr_2FeMo_{2/3}Mg_{1/3}O_6$ as Redox Stable Anode Material for Solid Oxide Fuel Cells Zhihong Du, Hailei Zhao, Yang Zhang and Mengya Fang; University of Science and Technology Beijing, Beijing, China.

2:10 PM A9.03
Structural and Transport Properties of Doped LAMOX - Electrolytes for IT SOFC Svetlana Pavlova[1], Yuliya Bespalko[1], Vladislav Sadykov[1], Vladimir Pelipenko[1], Nikita Eremeev[1], Tamara Krieger[1], Yurii Chesalov[1], Ekaterina Sadovskaya[1], Artem Ulihin[2], Nikolai Uvarov[2] and Alevtina Smirnova[3]; [1]Boreskov Institute of Catalysis SB RAS, Novosibirsk, Russian Federation; [2]Institute of Solid State Chemistry SB RAS, Novosivirsk, Russian Federation; [3]South Dakota School of Mines and Technology, Rapid City, South Dakota, United States.

2:30 PM A9.04
Ubiquitous Current Constriction Impedance in Oxide Ion Conductors Described by Capacitance Spectroscopy Young-Hun Kim[1], Su-Hyun Moon[1], Dong-Chun Cho[1], Eui-Chol Shin[1], Ji Haeng Yu[3], Jong-Ho Lee[2] and Jong-Sook Lee[1]; [1]Materials Science and Engineering, Chonnam National University, Gwangju, Korea (the Republic of); [2]Korea Institute of Science and Technology, Seoul, Korea (the Republic of); [3]Korea Institute of Energy Research, Daejeon, Korea (the Republic of).

2:50 PM A9.05
Factors Impacting Chemical Expansion in Perovskite Oxides Nicola H. Perry[1, 2], Dario Marrocchelli[3], Harry L. Tuller[2, 1] and Sean R. Bishop[2, 1]; [1]I2CNER, Kyushu University, Nishi-ku, Fukuoka, Japan; [2]Materials Science and Engineering, MIT, Cambridge, Massachusetts, United States; [3]Nuclear Science and Engineering, MIT, Cambridge, Massachusetts, United States.

3:10 PM BREAK

3:30 PM *A9.06
Sintering-Resistant Metal Nanoparticles for High Temperature Electrocatalysis Yoonseok Choi, Siwon Lee and WooChul Jung; DMSE, KAIST, Daejeon, Korea (the Republic of).

3:50 PM A9.07
Evaluation of Degradation Behavior of Ni-YSZ Using Electrochemical Capacitance Mirai Takeda[1], Keiji Yashiro[1], Shinichi Hashimoto[2] and Tatsuya Kawada[1]; [1]Graduate School of Environment Studies, Tohoku University , Sendai, Japan; [2]Graduate School of Engineering, Tohoku University , Sendai, Japan.

4:10 PM A9.08
Ca_2MnAlO_5 and $La_4Ti_2O_{10}$ Derivatives as Potential SOFC's Anodes Xavier Flandre, Ibtissam Kehal, Christian Eroume, Aurelie Rolle, Edouard Capoen, Axel Loefberg and Rose-Noelle Vannier; Solid State Chemistry, Unit of Catalysis and Solid state Chemistry, Villeneuve d'Ascq, France.

4:30 PM A9.09
Thin Film Carbide Anodes for Solid Oxide Fuel Cells Jun Jiang, Xiaofei Guan and Shriram Ramanathan; School of Engineering and Applied Sciences, Harvard University, Cambridge, Massachusetts, United States.

4:00 PM A9.10
Nanoscaled Ni/YSZ Anodes for Solid Oxide Fuel Cells: Processing and Characterization Dino Klotz[1], Julian T. Szasz[1], Heike Stoermer[2], Dagmar Gerthsen[2] and Ellen Ivers-Tiffee[1];[1]Institute for Applied Materials (IAM-WET), Karlsruhe Institute of Technology (KIT), Karlsruhe, Germany; [2]Laboratorium für Elektronenmikroskopie (LEM), Karlsruhe Institute of Technology (KIT), Karlsruhe, Germany.

5:10 PM A9.11
Redox Stability and Electrical Properties of $Sr_{1-x}Y_xV_{1-y}Nb_yO_3$ for Prospective SOFC Anodes Javier Macias, Aleksey Yaremchenko and Jorge Frade; Department of Materials and Ceramic Engineering, University of Aveiro, Aveiro, Portugal.

B: Polymer Electrolyte Fuel Cells and Electrolyzers

SESSION B4: PEMFC/DMFC III
B: Polymer Electrolyte Fuel Cells and Electrolyzers
Chair: Vito Di Noto
Thursday Afternoon, June 18, 2015
Keystone Resorts, Grays Peak III

1:30 PM *B4.01
Nano-Structured Aromatic Ionomers for PEMFC Cristina Iojoiu[1, 2], Huu Dat Nguyen[2, 1], Olesia Danyliv[1, 2] and Sandrine Lyonnard[3]; [1]LEPMI, CNRS, Saint Martin d'Hères, France;[2]Grenoble University, Saint Martin D'Hères , France; [3]INAC SPrAM, CEA Grenoble, Grenoble, France.

1:50 PM B4.02
Nafion/Zirconium Sulfonylphosphonate Composite Membranes for DMFC and PEMFC Kun-lin Liu[1], Chia-Chin Hsu[1], Cheng-Wei Pai[1], Ying-Ling Liu[2] and Chi-Yang Chao[2];[1]Materials Science and Engineering, National Taiwan University, Taipei, Taiwan; [2]Department of Chemical Engineering, National Tsing Hua University, Taipei, Taiwan.

2:10 PM B4.03
Preparation and Properties of DMFC Membranes from Polymer-Brush Nanoparticles Ilya Zharov[1, 2] and Shelley D. Minteer[1, 2]; [1]Chemistry, University of Utah, Salt Lake City, Utah, United States; [2]Materials Science and Engineering, University of Utah, Salt Lake City, Utah, United States.

2:30 PM B4.04
Activity Trends and Design Principles for Multi-Transition-Metal (Oxy)hydroxide Oxygen Evolution Catalysts Shannon W. Boettcher; Chemistry, University of Oregon, Eugene, Oregon, United States.

2:50 PM B4.05
Synthesis and Characterization of Pd-Ni-Sn Electrocatalyst for Use in Direct Ethanol Fuel Cells Sompoch Jongsomjit[1], Paweena Prapainainar[2, 3, 4] and Korakot Sombatmankhong[5];[1]Interdisciplina ry Graduate Program in Advanced and Sustainable Environmental Engineering (International Program),Faculty of Engineering, Kasetsart University , Ladyao, Jatujak, Thailand; [2]Department of Chemical Engineering, Faculty of Engineering, Kasetsart University, Ladyao, Jatujak, Thailand; [3]National Center of Excellence for Petroleum, Petrochemicals and Advance Material, Kasetsart University, Ladyao, Jatujak, Thailand; [4]Department of Chemistry and NANOTEC Center for Nanoscale Materials Design for Green Nanotechnology, Kasetsart University, Ladyao, Jatujak, Thailand; [5]National Metal and Materials Technology Center, Thanon Phahonyothin, Tambon Khlong Nueng, Amphoe Khlong Luang, Thailand.

C: Electrodes and Solid Electrolytes for Batteries

SESSION C10: Fundamentals of LIB Electrodes I
C: Electrodes and Solid Electrolytes for Batteries
Chair: William Chueh
Thursday Morning, June 18, 2015
Keystone Resorts, Shavano Peak

10:10 AM BREAK

10:30 AM **C10.01
The Ultimate Limits of Intercalation Reactions for Battery Electrodes Stanley Whittingham; NECCES, SUNY, Binghamton, New York, United States.

11:00 AM *C10.02
Parameters Influencing Reversible Intercalation of Cations in Spinel Oxides Jordi Cabana; Chemistry, University of Illinois at Chicago, Chicago, Illinois, United States.

11:20 AM C10.03
Revealing the Origins of Lithiation Heterogeneities in $LiFePO_4$ Using Nanoscale Chemical Imaging Yiyang Li[1], William E. Gent[1], Jongwoo Lim[1], Johanna Nelson Weker[2], Norman Jin[1], Sophie Meyer[1], Daniel A. Cogswell[3], Tolek Tyliszczak[4] and William C. Chueh[1]; [1]Stanford University, Stanford, California, United States; [2]SLAC National Accelerator Center, Menlo Park, California, United States; [3]Samsung Advanced Institute of Technology-America, Cambridge, Massachusetts, United States; [4]Berkeley National Laboratory, Berkeley, California, United States.

11:40 AM C10.04
Computational Identification and Experimental Realisation of Lithium Vacancy Introduction into the Olivine $LiMgPO_4$ Leopoldo Enciso-Maldonado[1], Matthew S. Dyer[1], Michael D. Jones[1], Ming Li[1], Michael J. Pitcher[1], Mona K. Omir[1], John B. Claridge[1], Frederic Blanc[1, 2] and Matthew J. Rosseinsky[1]; [1]Department of Chemistry, University of Liverpool, Liverpool, United Kingdom; [2]Stephenson Institute for Renewable Energy, University of Liverpool, Liverpool, United Kingdom.

SESSION C11: Beyond Lithium
C: Electrodes and Solid Electrolytes for Batteries
Chair: Scott Barnett
Thursday Afternoon, June 18, 2015
Keystone Resorts, Shavano Peak

1:30 PM *C11.01
Room-Temperature Sodium-Ion Batteries: Improving the Rate Capability Using Porous Carbon Networks Yan Yu, Joachiam Maier and Changbao Zhu; Max Planck Institute for Solid State Research, Stuttgart, Germany.

1:50 PM C11.02
Recent Progress for Room-Temperature Stationary Sodium-Ion Batteries Yong-Sheng Hu; Key Laboratory for Renewable Energy, Institute of Physics, Chinese Academy of Sciences, Beijing, China.

2:10 PM C11.03
Structural Study of $Na_{2/3}[Ni_{1/3}Ti_{2/3}]O_2$ Using Neutron Diffraction and Atomistic Simulations for Na-Ion Batteries Rengarajan Shanmugam and Wei Lai; CHEMS, Michigan State University, East Lansing, Michigan, United States.

2:30 PM C11.04
Electrochemical Properties for MXene $Ti_3C_2T_x$ as Negative Electrode in a Non-Aqueous Sodium-Ion Electrolyte Satoshi Kajiyama, Hiroki Iinuma, Masashi Okubo and Atsuo Yamada; Department of Chemical System Engineering, School of Engineering, The University of Tokyo, Tokyo, Japan.

2:50 PM C11.05
Amorphous Cathodes for Magnesium Batteries Timothy S. Arthur, Keiko Kato, Fuminori Mizuno and Jason Germain; Materials Research, Toyota Research Institute of North America, Ann Arbor, Michigan, United States.

3:10 PM BREAK

3:30 PM C11.06
Magnesium Ion Intercalation into a Spinel like *λ*-Manganese Oxide Ryan D. Bayliss[1], Chunjoong Kim[1], Tanghong Yi[1], Abdullah Adil[1], Patrick J. Phillips[2], Baris Key[3], Young-Sang Yu[4], Tiffany L. Kinnibrugh[5], Karena W. Chapman[5], Peter J. Chupas[5], Robert K. Klie[2] and Jordi Cabana[1]; [1]Department of Chemistry, University of Illinois at Chicago, Chicago, Illinois, United States; [2]Department of Physics, University of Illinois at Chicago, Chicago, Illinois, United States; [3]Chemical Sciences and Engineering Division, Argonne National Laboratory, Argonne, Illinois, United States; [4]Advanced Light Source, Lawrence Berkeley National Laboratory, Berkeley, California, United States; [5]Advanced Photon Source, Argonne National Laboratory, Argonne, Illinois, United States.

3:50 PM C11.07
Rechargeable Magnesium Battery Using Polyanion Compounds Cathode and Triglyme Electrolyte Yuki Orikasa, Titus Masese, Yukinori Koyama, Takuya Mori, Masashi Hattori, Kentaro Yamamoto, Cedric Tassel, Yoji Kobayashi, Takeshi Abe, Hiroshi Kageyama and Yoshiharu Uchimoto; Kyoto University, Kyoto, Japan.

4:10 PM C11.08
Reversible Intercalation of Multivalent Ions into Nanostrctured Vanadium Oxide Cathodes Premkumar Senguttuvan and Christopher S Johnson; Chemical Sciences and Engineering, Argonne National Laboratory, Argonne, Illinois, United States.

4:30 PM C11.09
Data-Driven Models of Ion Conduction for Rapid Screening of New Generation Conductors Using Statistical Methods Austin Sendek[1], Qian Yang[3], Yi Cui[2] and Evan Reed[2]; [1]Applied Physics, Stanford University, Stanford, California, United States; [2]Materials Science, Stanford University, Stanford, California, United States; [3]Institute for Computational and Mathematical Engineering, Stanford University, Stanford, California, United States.

D: Fundamentals of Transport and Reactivity and Nanoionics

SESSION D7: Fundamentals of Transport and Reactivity and Nanoionics V
D: Fundamentals of Transport and Reactivity and Nanoionics
Chair: Jennifer Rupp
Thursday Morning, June 18, 2015
Keystone Resorts, Grays Peak I/II

10:10 AM BREAK

10:30 AM **D7.01
Oxygen Thermotransport in Mixed Conductor Oxides Han-Ill Yoo; Materials Science and Engineering, Seoul National University, Seoul, Korea (the Republic of).

11:00 AM D7.02
Reduction of the Grain Boundary Resistance in Yttria Stabilized Zirconia Thin Films: Incorporation of Mg^{2+} from the Substrate Edmund M. Mills[1], Matthias Kleine-Boymann[2], Juergen Janek[2], Hao Yang[1], Nigel Browning[3], Yayoi Takamura[1] and Sangtae Kim[1]; [1]CHMS, UC Davis, Davis, California, United States; [2]Institute of Physical Chemistry, Justus-Liebig University Geissen, Geissen, Germany; [3]Pacific Northwest National Laboratory, Richland, Washington, United States.

11:20 AM D7.03
Determination of Transport Coefficients *D* and *K* in Materials Having Mixed Ionic-Electronic Conductivity Kun Zheng[1], Konrad Swierczek[1], Alicja Klimkowicz[1, 2] and Grzegorz Brus[1]; [1]Faculty of Energy and Fuels, AGH University of Science and Technology, Kraków, Poland; [2]Department of Engineering Science and Mechanics, Shibaura Institute of Technology, Tokyo, Japan.

11:40 AM D7.04
Oxide-Ion Conduction with Strong Correlation in Apatite-Type Lanthanum Silicate Kazuaki Toyoura[1], Kouta Imaizumi[1], Atsutomo Nakamura[1] and Katsuyuki Matsunaga[1, 2];[1]Nagoya University, Nagoya, Japan; [2]Japan Fine Ceramics Center, Nagoya, Japan.

SESSION D8: Fundamentals of Transport and Reactivity and Nanoionics VI
D: Fundamentals of Transport and Reactivity and Nanoionics
Chairs: Roger De Souza and Han-Ill Yoo
Thursday Afternoon, June 18, 2015
Keystone Resorts, Grays Peak I/II

1:30 PM *D8.01
The Transport Properties of Dislocations in the Perovskite-Oxide SrTiO Roger A. De Souza; Institute of Physical Chemistry, RWTH Aachen University, Aachen, Germany.

1:50 PM D8.02
Driving Forces Related to Acceptor-Oxygen Vacancy Defect Complex Formation in Perovskite Oxides Russell Maier; NIST, Gaithersburg, Maryland, United States.

2:10 PM D8.03
Conductivity Relaxation Experiments on Donor Doped Barium Titanate Ceramics: Effect of Microstructure Wolfgang Preis and Werner Sitte; Chair of Physical Chemistry, Montanuniversitaet Leoben, Leoben, Austria.

2:30 PM D8.04
Oxygen Diffusion/Exchange Processes in Two-Dimensional $Ln_2NiO_{4+\delta}$ (Ln=La, Pr, and Nd) Single Crystals: IEDP/LEIS Measurements Jean-Marc Bassat[2], Helena Tellez[1], Monica Burriel[3], Remi Castaing[2, 3], W. Paulus[4], P. Veber[2], Tatsumi Ishihara[1] and John Kilner[1, 3]; [1]Hydrogen Production Division, International Institute for Carbon-Neutral Energy Research, Fukuoka, Japan; [2]Institut de Chimie de la Matière Condensée de Bordeaux, Pessac, France; [3]Department of Materials, Imperial College London, London, United Kingdom; [4]Institut Charles Gerhardt, Montpellier, France.

2:50 PM D8.05
Influence of Dislocations on Electrical and Chemical Properties in Metal Oxides Lixin Sun[1], Dario Marrocchelli[1] and Bilge Yildiz[1, 2]; [1]Department of Nuclear Science and Engineering, Massachusetts Institute of Technology, Cambridge, Massachusetts, United States; [2]Department of Material Science and Engineering, Massachusetts Institute of Technology, Cambridge, Massachusetts, United States.

3:10 PM BREAK

3:30 PM *D8.06
Space Charge Layers and Their Role in Properties of Interfaces in Solid State Ionics Truls Norby; Department of Chemistry, University of Oslo, Oslo, Norway.

3:50 PM D8.07
Defect Chemistry of CeO_2 Surfaces from First Principles and Space Charge Theory Tor S. Bjorheim[1], Eugene Kotomin[2] and Joachim Maier[2]; [1]FASE, Department of Chemistry, University of Oslo, Oslo, Norway; [2]Max Planck Institute for Solid State Research, Stuttgart, Germany.

4:10 PM D8.08
On Determining the Built-In Potential at Grain Boundaries in Ion-Conducting Oxides Sangtae Kim[1], Seong K. Kim[1], Sergey Khodorov[2] and Igor Lubomirsky[2]; [1]University of California, Davis, Davis, California, United States; [2]Weizmann Institute of Science, Rehovot, Israel.

4:30 PM D8.09
Solid Oxide-Molten Carbonate Nanocomposite Fuel Cells II: Surface Charge Effects Mehmet Ali Gulgun[1, 2], Yelda Yorulmaz[1], Hazal Batili[1], Cinar Oncel[1], Shalima Shawuti[3] and Miran Ceh[4]; [1]FENS, Sabanci University, Istanbul, Turkey; [2]Nanotechnology Application Center, Sabanci University, Istanbul, Turkey; [3]Physics Dept, Istanbul University, Istanbul, Turkey;[4]Department for Nanostructured Materials, Josef Stefan Institute, Ljubljana, Slovenia.

4:50 PM D8.10
Accurate Measurement of Fast Grain Boundary Ionic Diffusion by ToF-SIMS Depth Profiling with Selective Attenuation of Specific Secondary Ions (SASI) Helena Tellez[1], John Druce[1], Tatsumi Ishihara[1, 2] and John Kilner[3, 1]; [1]Hydrogen Production Division, International Institute for Carbon-Neutral Energy Research, Fukuoka, Japan; [2]Department of Applied Chemistry, Kyushu University, Fukuoka, Japan; [3]Department of Materials, Imperial College London, London, United Kingdom.

J: Permeation Membranes

SESSION J4: Permeation Membranes II
J: Permeation Membranes
Chairs: Henny Bouwmeester and Robert Kee
Thursday Morning, June 18, 2015
Keystone Resorts, Grays Peak III

10:10 AM BREAK

10:30 AM **J4.01
Dual Phase Membranes for Oxygen Separation Martin Sogaard, Jonas Gurauskis, Andreas Kaiser, Peter V. Hendriksen and Wolff-Ragnar Kiebach; Department of Energy Conversion and Storage, Technical University of Denmark, Roskilde, Denmark.

11:00 AM J4.02
Phase Inversion Tape Casting and Oxygen Permeation Properties of $Zr_{0.84}Y_{0.16}O_{1.92}$-$La_{0.8}Sr_{0.2}Cr_{0.5}Fe_{0.5}O_{3-\delta}$ Dual-Phase Composite Membranes with Asymmetric Structure Yu Zhang, Ronghua Yuan, Jianfeng Gao and Chusheng Chen; University of Science and Technology of China, Hefei, China.

11:20 AM J4.03
Microstructural Influence on Oxygen Transport of $Ce_{0.8}Gd_{0.2}O_{2-\delta}$ - $FeCo_2O_4$ Dual Phase Membrane Madhumidha Ramasamy[1], Stefan Baumann[1], Falk Schulze-Kueppers[1], Maria Balaguer[1], Wilhelm A. Meulenberg[1], Justinas Palisaitis[2], Joachim Mayer[2], Ramesh Bhave[3], Daejin Kim[3] and Martin Bram[1]; [1]Institute of Energy and Climate Research, Forschungszentrum Juelich GmbH, Juelich, Germany; [2]Ernst Ruska-Centre (ER-C) for Microscopy and Spectroscopy with Electrons, Juelich, Germany; [3]Chemical Sciences Division, Oak Ridge National Laboratory, Oak Ridge, Tennessee, United States.

11:40 AM J4.04
Dramatically Enhanced Oxygen Permeation Fluxes in Fluorite-Rich Dual-Phase Membrane by Surface Modification Jong Hoon Joo, Kyong Sik Yun, Chung-Yul Yoo and Ji Haeng Yu; Korea Institute of Energy Research, Daejeon, Korea (the Republic of).

SESSION J5: Permeation Membranes III
J: Permeation Membranes
Chairs: Truls Norby and Jose Serra
Thursday Afternoon, June 18, 2015
Keystone Resorts, Grays Peak III

3:10 PM BREAK

3:30 PM *J5.01
Ceramic Permeation Membranes and Membrane Reactors Ian S. Metcalfe; Chemical Engineering, Newcastle University, Newcastle upon Tyne, United Kingdom.

3:50 PM J5.02
Defect Chemistry and Oxygen Transport Properties of Bi-Sr-Fe-Based Perovskite-Type Oxides Doohyun Baek, Itaru Oikawa, Atsunori Kamegawa and Hitoshi Takamura; Department of Materials Science, Tohoku University, Sendai, Japan.

4:10 PM J5.03
Low Metal Content Silver/Doped Ceria Composites for Oxygen Separation and Methane Partial Oxidation Enrique Ruiz-Trejo[1], Paul Boldrin[1], Jawwad Darr[2], Alan Atkinson[3] and Nigel P. Brandon[1]; [1]Earth Science and Engineering, Imperial College London, London, United Kingdom; [2]Chemistry, University College London, London, United Kingdom; [3]Materials, Imperial College London, London, United Kingdom.

4:30 PM J5.04
Characterization of Dual Phase $BaCe_{1-x}Eu_xO_{3-\delta}$:$Ce_{1-y}Y_yO_{2-\delta}$ (x=0-0.2; y=0-0.2) Ceramic Composite for Membrane Application in H_2-Separation Maria Balaguer[1], Mariya E. Ivanova[1], Sonia Escolastico[2], Justinas Palisaitis[3], Yoo Jung Sohn[1], Jose M. Serra[2], Wilhelm A. Meulenberg[1], Olivier Guillon[1] and Joachim Mayer[3]; [1]Institute for Energy and Climate Research Materials Synthesis and Processing (IEK-1), Forschungszentrum Jülich GmbH, Jülich, Germany; [2]Instituto de Tecnologia Quimica , Valencia, Spain; [3]Ernst Ruska Center, Jülich, Germany.

4:50 PM J5.05
Hydrogen Permeation through CO_2-Stable Dual Phase Ceramic Membranes Sonia Escolastico, Cecilia Solis and Jose M. Serra; Instituto de Tecnología Química (UPV-CSIC), Valencia, Spain.

5:10 PM J5.06
Chemical Stability of Cercer H_2 Membranes in the Lanthanum Tungstate–Lanthanum Chromite System Jonathan M. Polfus, Zuoan Li, Martin F. Sunding, Wen Xing, Marie-Laure Fontaine, Partow P. Henriksen and Rune Bredesen; Materials and Chemistry, SINTEF, Oslo, Norway.

K: Proton-Conducting Oxides

SESSION K4: Protonic Oxides II
K: Proton-Conducting Oxides
Chairs: Marie-Laure Fontaine and Jose Serra
Thursday Morning, June 18, 2015
Keystone Resorts, Quandary Peak I/II

10:10 AM BREAK

10:30 AM **K4.01
Development of Proton Conducting Electrolyser Cells Marie-Laure Fontaine, Jonathan Polfus, Wen Xing, Rune Bredesen and Christelle Denonville; Materials and Chemistry, SINTEF, Oslo, Norway.

11:00 AM K4.02
Exploring BCZY Proton-Conducting Ceramics for Use in Electrolysis Michael Dippon[3], Sean Babiniec[1], Hanping Ding[1], Sandrine Ricote[1] and Neal P. Sullivan[2]; [1]Mechanical Engineering, Colorado School of Mines, Golden, Colorado, United States; [3]Institute of Materials for Electrical and Electronic Engineering, Karlsruhe Institute of Technology, Karlsruhe, Germany.

11:20 AM K4.03
CsH_2PO_4-Based Fuel Cells and Electrolyzers Laura Navarrete and Jose M. Serra; ITQ (UPV-CSIC), Valencia, Spain.

11:40 AM K4.04
Electrochemical Synthesis of Ammonia under Atmospheric Pressure Using a $BaCe_{0.2}Zr_{0.7}Y_{0.1}O_{2.9}$ Electrolyte Michael Stoukides[1, 2], Eirini Vasileiou[1, 2], Vasileios Kyriakou[1, 2], Ioannis Garagounis[1, 2], Anastasios Vourros[1, 2], Anthony Manerbino[3] and Grover Coors[3]; [1]Chemical Engineering, Aristotle University of Thessaloniki, Thessaloniki, Greece; [2]Chemical Process and Energy Resources Institute, Centre for Research and Technology Hellas, Thessaloniki, Greece; [3]CoorsTekInc, Golden, Colorado, United States.

SESSION K5: Protonic Oxides III
K: Proton-Conducting Oxides
Chairs: Tor Grande, Jong-Ho Lee, Anna Magraso and Hiroshige Matsumoto
Thursday Afternoon, June 18, 2015
Keystone Resorts, Quandary Peak I/II

1:30 PM K5.01
Preparation and Electrochemical Characterization of Yttrium-Doped Barium Zirconate Thin Films by Chemical Solution Deposition Hanlin Xie, Mridula Biswas, Yong Li and Pei-Chen Su; School of Mechanical and Aerospace Engineering, Nanyang Technological University, Singapore, Singapore.

1:50 PM K5.02
A Novel High-Performance Triple Conducting Oxide Cathode for Protonic Ceramic Fuel Cell Jianhua Tong, Meng Shang, Chuancheng Duan, David Shnaider and Ryan O'Hayre; MME, Colorado School of Mines, Golden, Colorado, United States.

2:10 PM K5.03
All-Oxide Composite Cathode Materials Prepared by *In Situ* Oxidation Driven Decomposition Tor Grande, Mari-Ann Einarsrud and Guttorm Syvertsen-Wiig; Materials Science and Engineering, Norwegian University of Science and Technology, Trondheim, Norway.

2:30 PM K5.04
Catalytic Properties of Proton Conducting Oxides in Cermet Electrodes and as Ceramic Supports for Dehydrogenation Catalysts Hyun H. Shin and Steven McIntosh; Chemical Engineering, Lehigh University, Bethlehem, Pennsylvania, United States.

2:50 PM K5.05
Chemical Stability and Membrane-Catalyst Compatibility of Selected Proton Conducting Materials Potentially Applicable in Hydrogen Membrane Reactors Mariya E. Ivanova[1], Desiree van Holt[1, 2], Emanuel Forster[3], Maria Balaguer[1], Wendelin Deibert[1], Wilhelm A. Meulenberg[1], Michael Mueller[3] and Olivier Guillon[1]; [1]Institute for Energy and Climate Research Materials Synthesis and Processing (IEK-1), Forschungszentrum Jülich GmbH, Jülich, Germany; [2] Institute of Energy and Climate Research Fundamental Electrochemistry (IEK-9), Forschungszentrum Jülich GmbH, Jülich, Germany; [3]Institute for Energy and Climate Research (IEK) IEK-2: Material Structure and Properties, Forschungszentrum Jülich GmbH, Jülich, Germany.

3:10 PM BREAK

3:30 PM K5.06
Y-doped Barium Zirconate prepared by Flame Spray Synthesis as Electrolyte for Intermediate Temperature Proton Conducting Fuel Cells Francesco Bozza and Thomas Graule; Laboratory for High Performance Ceramics, EMPA, Dübendorf, Switzerland.

3:50 PM K5.07
Size and Shape of Oxygen Vacancies and Protons in Acceptor-Doped Barium Zirconate Erik Jedvik, Anders Lindman and Goeran Wahnstroem; Applied Physics, Chalmers University of Technology, Göteborg, Sweden.

4:10 PM K5.08
Proper Theoretical Description of Oxidation of Acceptor-Doped Perovskites Anders Lindman, Paul Erhart and Göran Wahnström; Applied Physics, Chalmers University of Technology, Gothenburg, Sweden.

4:30 PM K5.09
Understanding Blocking Grain Boundaries within Proton Conducting Ceramics Using Atom Probe Tomography Daniel Clark[1], Dave Diercks[1], Huayang Zhu[2], Robert Kee[2], Sandrine Ricote[2], Brian Gorman[1] and Ryan O'Hayre[1]; [1]Metallurgical and Materials Engineering, Colorado School of Mines, Golden, Colorado, United States; [2]Mechanical Engineering, Colorado School of Mines, Golden, Colorado, United States.

4:50 PM K5.10
On the Impact of Strain on the Proton Conductivity of Barium Zirconate Thin Films Anna Magraso[1, 3], Jonathan Polfus[2] and Jose Santiso[1]; [1]ICN2, Bellaterra, Spain; [2]SINTEF, Oslo, Norway; [3]Dep. Chemistry, University of Oslo, Oslo, Norway.

ORAL PRESENTATIONS

FRIDAY June 19, 2015

PLENARY

SESSION L5: Special Plenary
Chair: M. Stanley Whittingham
Friday Morning, June 19, 2015
Keystone Resorts, Shavano Peak

9:15 AM INTRODUCTION

9:25 AM L5.01
Alternative Strategies for Electrical Energy Storage John Goodenough; University of Texas at Austin, Austin, Texas, United States.

A: Solid Oxide Fuel Cells and Electrolyzers

* Invited Speaker
** Keynote Speaker

SESSION A10: SOFC—Cathodes IV
A: Solid Oxide Fuel Cells and Electrolyzers
Chair: Werner Sitte
Friday Morning, June 19, 2015
Keystone Resorts, Longs Peak

10:10 AM BREAK

10:30 AM *A10.01
A Novel R-P Structure Cathode with High Performance for Intermediate Temperature Solid Oxide Fuel Cells Ranran Peng, Zhiquan Wang, Daoming Huan, Wenqiang Yang and Yalin Lu; University of Science and Technology of China, Hefei, China.

10:50 AM A10.02
Optimization of the Electrochemical Performances of $Ca_3Co_4O_{9+\delta}$ as Air Electrode for Solid Oxide Cell Aurelie Rolle[1], Xavier Flandre[2], Hussein A. Abbas Mohamed[1], Da Huo[2], Giuliano Mignardi[2], Sylvie Daviero-Minaud[2], Edouard Capoen[3], Marie-Helene Chambrier[4], Elisabeth Djurado[5], Amelie Salauen[5], Monica Burriel[5] and Rose-Noelle Vannier[1]; [1]UCCS, ENSCL, Villeneuve d'Ascq, France; [2]UCCS, Université Lille1, Villeneuve d'Ascq, France; [3]UCCS, CNRS, Villeneuve d'Ascq, France; [4]UCCS, Université Jean Perrin, Villeneuve d'Ascq, France; [5]LEPMI, Grenoble-INP - UdS - UJF, Saint Martin d'Hères, France.

11:10 AM A10.03
Effect of $La_{0.6}Sr_{0.4}Co_{0.2}Fe_{0.8}O_{3-\delta}$ Microstructure on Oxygen Surface Exchange Kinetics Katherine D. Bagarinao, Haruo Kishimoto, Katsuhiko Yamaji and Teruhisa Horita; National Institute of Advanced Industrial Science and Technology, Tsukuba, Japan.

11:30 AM A10.04
Oxygen Surface Exchange Kinetics of Praseodymium Nickelates Saim Saher[1], Jean-Marc Bassat[2] and Henny J. Bouwmeester[1]; [1]MESA+ Institute for Nanotechnology, Faculty of Science and Technology, University of Twente, Enschede, Netherlands; [2]Institut de Chimie de la Matière Condensée de Bordeaux (ICMCB-CNRS), Université Bordeaux I, Pessac-Cedex, France.

C: Electrodes and Solid Electrolytes for Batteries

SESSION C12: Fundamentals of LIB Electrodes II
C: Electrodes and Solid Electrolytes for Batteries
Chair: Jordi Cabana
Friday Morning, June 19, 2015
Keystone Resorts, Shavano Peak

10:10 AM BREAK

10:30 AM **C12.01
Powerful Electrical Model Explaining the Operation of Insertion Batteries Miran Gaberscek; National Institute of Chemistry, Ljubljana, Slovenia.

11:00 AM C12.02
Layered Cathode Materials Prepared by Spray Pyrolysis for High-Energy Lithium-Ion Batteries Feng Lin[1], Yuyi Li[1], Dennis Nordlund[2], Tsu-Chien Weng[2], Huolin Xin[3], Yijin Liu[2]and Marca Doeff[1]; [1]Lawrence Berkeley National Lab, Berkeley, California, United States; [2]SLAC, Menlo Park, California, United States; [3]BNL, Upton, New York, United States.

11:20 AM C12.03
Stabilizing the Structure of Li-Rich Oxide Cathode Materials Zhaoxiang Wang[1], Yurui Gao[1], Xin Feng[1], Jun Ma[1], Yong-ning Zhou[2], Lin Gu[1], Qingyu Kong[3], Xiao-qing Yang[2] and Liquan Chen[1]; [1]Institute of Physics, Chinese Academy of Sciences, Beijing, China; [2]Brookhaven National Laboratory, Upton, New York, United States; [3]Argonne National Laboratory, Argonne, California, United States.

11:40 AM C12.04
Integrated Nano-Domains of Disordered and Ordered Spinel Phases in $LiNi_{0.5}Mn_{1.5}O_4$ for Li-Ion Batteries Jung-Hyun Kim[1], Ashfia Huq[2], Craig A. Bridges[2], Miaofang Chi[2], Nicholas P. Pieczonka[3], Arumugam Manthiram[4] and Bob R. Powell[1]; [1]Chemical and Materials Systems Laboratory, General Motors R&D Center, Warren, Michigan, United States; [2]Oak Ridge National Laboratory, Oak Ridge , Tennessee, United States; [3]Optimal CAE., Plymouth, Michigan, United States; [4]Materials Science and Engineering Program, The University of Texas at Austin, Austin, Texas, United States.

D: Fundamentals of Transport and Reactivity and Nanoionics

SESSION D9: Fundamentals of Transport and Reactivity and Nanoionics VII
D: Fundamentals of Transport and Reactivity and Nanoionics
Chair: Igor Lubomirsky
Friday Morning, June 19, 2015
Keystone Resorts, Grays Peak I/II

10:10 AM BREAK

10:30 AM **D9.01
Molecular Insights Into Structure and Dynamics of Organic Ionic Plastic Crystal Electrolytes Maria Forsyth[1, 2]; [1]Institute for Frontier Materials, Deakin University, Burwood, Victoria, Australia; [2]ARC Center of Excellence for Electromaterials Science, Burwood , Victoria, Australia.

11:00 AM *D9.02
Structure and Lithium Ion Dynamics of the Tetragonal LGPS-Type Superionic Conductors $Li_{11-x}M_{2-x}P_{1+x}S_{12}$ with M = Si, Ge, Sn Alexander Kuhn[1], Sascha Harm[1, 2] and Bettina V. Lotsch[1, 2]; [1]Chemistry , Max Planck Institute for Solid State Research, Stuttgart, Germany; [2]Chemistry, University of Munich (LMU), Munich, Germany.

11:20 AM D9.03
Correlation Between the Electronic Structure and the Interstitial Oxygen Formation in Layered Perovskite Oxides Takashi Nakamura[1], Yihan Ling[1], Ryo Oike[1], Yusuke Tamenori[2]and Koji Amezawa[1]; [1]IMRAM, Tohoku University, Sendai, Japan; [2]JASRI, Sayo-gun, Japan.

11:40 AM D9.04
Vacancy Engineering for New Compounds and Low Temperature Oxide Ion Conduction Yaoqing Zhang; Tokyo Institute of Technology, Yokohama, Japan.

I: Ion Transport in Hybrid Organic-Inorganic Solids

SESSION I3: Ion Transport in Organic-Inorganic Hybrid Solids
I: Ion Transport in Hybrid Organic-Inorganic Solids
Chair: Abraham Saldivar Valdes
Friday Morning, June 19, 2015
Keystone Resorts, Grays Peak III

10:10 AM BREAK

10:30 AM **I3.01
Discovery of Molecular Disorders in Coordination Frameworks for Solid State Ionics Satoshi Horike; Kyoto University, Kyoto, Japan.

10:55 AM **I3.02
Designing Proton Conducting MOFs George Shimizu; Chemistry, University of Calgary, Calgary, Alberta, Canada.

11:20 AM I3.03
Effect of Ionic Liquid 1-Butyl-3-Methylimidazolium Methylsulfate on (Polyethylene Oxide, PEO + Sodium Methyl Sulfate Salt, Nams) Polymer Electrolyte Membrane Rajendra K. Singh; Physics, Banaras Hindu University, Varanasi, India.

11:40 AM I3.04
On the Origin and Underappreciated Effects of Ion Doping in Silica Xiaohui Song and Hongyu Chen; Chemistry and Biological Chemistry, Nanyang Technological University, Singapore, Singapore.

K: Proton-Conducting Oxides

SESSION K6: Protonic Oxides V
K: Proton-Conducting Oxides
Chairs: Tor Bjorheim and Jong-Sook Lee
Friday Morning, June 19, 2015
Keystone Resorts, Quandary Peak I/II

10:10 AM BREAK

10:30 AM *K6.01
Hydride Conduction in Oxyhydrides Genki Kobayashi[1, 2]; [1]Research Center of Integrative Molecular Systems, Institute for Molecular Science, Okazaki, Japan; [2]Precursory Research for Embryonic Science and Technology, Japan Science and Technology Agency, Kawaguchi, Japan.

10:50 AM K6.02
Development of Hydrogen Sensor Using Proton Conductor with Redox Protonation Yuji Okuyama[1], Shinya Nagamine[2], Akira Nakajima[3], Fusako Takahashi[4], Koji Kimata[4], Tomoko Oshima[4], Go Sakai[5] and Naoki Matsunaga[5]; [1]Organaization for Promotion of Tenure Track, University of Miyazaki, Miyazaki, Japan; [2]Department of Applied Chemistry, Faculty of Engineering, University of Miyazaki, Miyazaki, Japan; [3]Frontier Science Research Center, University of Miyazaki, Miyazaki, Japan; [4]Functional Materials R&D Center, TYK Corp., Tajimi, Japan; [5]Department of Environmental Robotics, Faculty of Engineering, University of Miyazaki, Miyazaki, Japan.

11:10 AM K6.03
Impact of the Electrochemical Proton-Carrier Injection on the Structure of $NaO_{1/2}$-WO_3-$NbO_{5/2}$-$LaO_{3/2}$-$PO_{5/2}$ Glass Takahisa Omata[1], Tomohiro Ishiyama[2], Junji Nishii[3], Toshiharu Yamashita[4], Hiroshi Kawazoe[4], Naoaki Kuwata[5] and Junichi Kawamura[5]; [1]Graduate School of Engineering, Osaka University, Suita, Japan; [2]National Institute of Advanced Industrial Science and Technology (AIST), Tsukuba, Japan; [3]Research Institute for Electronic Science, Hokkaido University, Sapporo, Japan; [4]Kawazoe Frontier Technologies Corp., Yokohama, Japan; [5]Tohoku University, Sendai, Japan.

11:30 AM K6.04
Surface-Proton Conductivity of Titanium Phosphate Nanoparticles in Water Hiroshige Matsumoto, Osamu Fujiwara, Kwati Leonard and Young-Sung Lee; International Institute for Carbon-Neutral Energy, Kyushu University, Fukuoka, Japan.

SSI-20

Poster Presentations

POSTER PRESENTATIONS

MONDAY June 15, 2015

SESSION A2: Poster Session I
A: Solid Oxide Fuel Cells and Electrolyzers
Monday Afternoon, June 15, 2015
12:00 PM
Keystone Resorts, Red Cloud Peak

A2.01
Structural Stability of Complex Perovskites for Solid Oxide Fuel Cells from First Principles Calculations Maija M. Kuklja[1], Eugene A. Kotomin[2, 3], David Fuks[4], Yuri A. Mastrikov[2]and Joachim Maier[3]; [1]Materials Science and Engineering Department, University of Maryland College Park, College Park, Maryland, United States; [2]Institute for Solid State Physics, University of Latvia, Riga, Latvia; [3]Max Planck Institute for Solid State Research, Stuttgart, Germany; [4]Dept Materials Engineering, Ben Gurion University of the Negev, Beer Sheva, Israel.

A2.02
Long Term Degradation Effects in Doped Ceria from First Principles Steffen Grieshammer[1, 2, 3], Benjamin O. Grope[1, 2, 3], Julius Koettgen[1, 2, 3] and Manfred Martin[1, 2, 3]; [1]Institute of Physical Chemistry I, RWTH Aachen University, Aachen, Germany; [2]JARA-ENERGY, Aachen, Germany; [3]JARA-HPC, Aachen, Germany.

A2.03 WITHDRAWN

A2.04
First Principles Thermodynamics of Oxygen Vacancies in Ultrathin Films of $BaZrO_3$ Marco Arrigoni[1], Eugene A. Kotomin[1], Joachim Maier[1] and Tor S. Bjorheim[2]; [1]Physical Chemistry of Solids, Max Planck Institute for Solid State Research, Stuttgart, Germany; [2]Department of Chemistry, University of Oslo, Oslo, Norway.

A2.05
Optimum Zr Configurations in $Ce_{1-x}Zr_xO_2$ ($x \in [0,1]$) Solid Solution Using Genetic Algorithm and Density Functional Theory Jason Kim[2], Shin-Won Hwang[1], Ji-Su Kim[1], Byung-Kook Kim[3] and Yeong-Cheol Kim[1]; [1]School of Energy, Materials, and Chemical Engineering, KoreaTech, Cheonan, Korea (the Republic of); [2]School of Electrical and Computer Engineering, UNIST, Ulsan, Korea (the Republic of); [3]High Temperature Energy Materials Center, Korea Institute of Science and Technology, Seoul, Korea (the Republic of).

A2.06
Theoretical Study of Oxygen Vacancy Formation in $Ce_{0.75}Zr_{0.25}O_2$ Solid Solution Using Density Functional Theory Ji-Su Kim[1], Shin-Won Hwang[1], Jason Kim[2], Byung-Kook Kim[3]and Yeong-Cheol Kim[1]; [1]School of Energy, Materials, and Chemical Engineering, KoreaTech, Cheonan, Korea (the Republic of); [2]School of Electrical and Computer Engineering, UNIST, Ulsan, Korea (the Republic of); [3]High Temperature Energy Materials Center, Korea Institute of Science and Technology, Seoul, Korea (the Republic of).

A2.07
High-Throughput Density Functional Theory Screening of Perovskite Compounds for High Oxygen Surface-Exchange for Solid Oxide Fuel Cell Cathodes Ryan Jacobs[1], Dane Morgan[1, 3] and John Booske[2]; [1]Materials Science Program, University of Wisconsin- Madison, Madison, Wisconsin, United States; [2]Electrical and Computer Engineering, University of Wisconsin- Madison, Madison, Wisconsin, United States; [3]Materials Science and Engineering, University of Wisconsin-Madison, Madison, Wisconsin, United States.

A2.08
Accelerated Materials Design of $Na_{0.5}Bi_{0.5}TiO_3$ Oxygen Ionic Conductors Based on First Principles Calculations Xingfeng He and Yifei Mo; Department of Materials Science and Engineering, University of Maryland, College Park, College Park, Maryland, United States.

A2.09
Evaluation of the Chemical Expansion Coefficient Using Modulated Dilatometry Shany Hershkovitz, Lea Halimi and Yoed Tsur; Chemical Engineering, Techion IIT-Israel Institute of Technology, Haifa, Israel.

A2.10
The Effect of Oxygen Nonstoichiometry on Thermal Expansion and Conduction Mechanism of $LaNi_{1-x}Fe_xO_{3-\delta}$ Eiki Niwa and Takuya Hashimoto; Department of Physics, Nihon University, Setagaya-ku, Japan.

A2.11
Oxygen Nonstoichiometry, Electrical Properties and Thermochemical Expansion of Strontium-Rich $Nd_{2-X}Sr_xNiO_{4\pm D}$ Mixed Conductors Ekaterina Kravchenko[1, 2], Kiryl Zakharchuk[1], Jekabs Grins[3], Gunnar Svensson[3], Vladimir Pankov[2] and Aleksey Yaremchenko[1]; [1]CICECO, Department of Materials and Ceramic Engineering, University of Aveiro, Aveiro, Portugal; [2]Department of Chemistry, Belarusian State University, Minsk, Belarus; [3]Department of Materials and Environmental Chemistry, Stockholm University, Stockholm, Sweden.

A2.12
Oxygen Nonstoichiometry and Defect Chemistry of Perovskite-Structured $SrSn_{1-x}Fe_xO_{3-x/2+\delta}$ Chang Sub Kim[1], Sean R. Bishop[1, 2], Nicola H. Perry[1, 2], Jae Jin Kim[1] and Harry L. Tuller[1, 2]; [1]Department of Materials Science and Engineering & Skoltech Center for Electrochemical Energy Storage, MIT, Cambridge, Massachusetts, United States; [2]International Institute for Carbon Neutral Energy Research (WPI-I2CNER), Kyushu University, Fukuoka, Japan.

A2.13
Defect Structure and Related Properties of $SrTi_{1-x}Fe_xO_{3-d}$ Vladimir Sereda, Dmitry Tsvetkov, Ivan Ivanov and Andrey Zuev; Department of Physical Chemistry, Ural Federal University, Ekaterinburg, Russian Federation.

A2.14
Oxygen Content, Thermodynamic Stability and Electrical Properties of $YBaCo_{4-x}Zn_xO_{7-\delta}$ Dmitry S. Tsvetkov, Nadezhda S. Tsvetkova and A. Y. Zuev; Department of Chemistry, Ural Federal University, Ekaterinburg, Russian Federation.

A2.15
Iso-Octane Internal Reforming in a Solid Oxide Cell Reactor Abdullah Al-Musa[2], Mohamed Al-Saleh[2], Ayman Al-Zahrani[2], Vasileios Kyriakou[3, 4], George Marnellos[1, 4] and Nikolaos Kaklidis[1]; [1]Department of Mechanical Engineering, University of Western Macedonia, Kozani, Greece; [2]Water & Energy Research Institute, King Abdulaziz City for Science & Technology, Riyadh, Saudi Arabia; [3]Department of Chemical Engineering, Aristotle University of Thessaloniki, Thessaloniki, Greece; [4]Chemical Process & Energy Resources Institute, Centre for Research & Technology Hellas, Thessaloniki, Greece.

A2.16
Insights into Oxygen Anion Transprt in Layered Oxides via *In-Situ* Powder Neutron Diffraction Steven McIntosh[1], Alexander C. Tomkiewicz[1], Mazin A. Tamimi[1] and Ashfia Huq[2];[1]Chemical & Biomolecular Engineering, Lehigh University, Bethlehem, Pennsylvania, United States; [2]Neutron Sciences, Oak Ridge National Laboratory, Oak Ridge, Tennessee, United States.

A2.17
Oxygen Nonstoichiometry and Defect Equilibrium in the Ruddlesden–Popper Type Oxides $La_xSr_{3-x}Fe_2O_{7-\delta}$ (x=0, 0.25 and 0.5) Yihan Ling, Fang Wang, Yusuke Okamoto, Takashi Nakamura and Koji Amezawa; Institute of Multidisciplinary Research for Advanced Materials, Tohoku University, Sendai, Japan.

A2.18
Synthesis and Preliminary Characterization of $Sr_{2-x}La_xMnO_{4\pm\delta}$ ($0.25 \leq x \leq 0.6$) Series as Symmetric SOFC Electrode Monica V. Sandoval[1, 2], Freddy L. Duran[1, 2], Caroline Pirovano[2], Edouard Capoen[2], Rose Noelle Vannier[2], Pascal Roussel[2] and Gilles H. Gauthier[1]; [1]Grupo INTERFASE, Universidad Industrial de Santander, Bucaramnaga, Colombia; [2]Unité de Catalyse et de Chimie du Solide, Université Lille 1, Lille, France.

A2.19
The Impact of Precursor Gel Desiccation, Ceria Oxide Pre-Infiltration, and Solution Composition on Tailoring Lanthanum Strontium Cobalt Iron Oxide Nano-Particle Size Theodore E. Burye, Hongjie Tang and Jason Nicholas; Chemical Engineering and Materials Science, Michigan State University, East Lansing, Michigan, United States.

A2.20
Influence of Synthesis Method on the Electrochemical Properties of Bilayer Electrodes Based on $La_2NiO_{4+\delta}$ and $LaNi_{0.6}Fe_{0.4}O_{3-\delta}$ Elena Pikalova[3, 1], Nina Bogdanovich[3], Alexander Kolchugin[3], Alexander Pankratov[3] and Dimitry Bronin[3, 2]; [1]Department of Environmental Economics, Ural Federal University, Ekaterinburg, Russian Federation; [2]Institute of Natural Sciences, Ural Federal University, Ekaterinburg, Russian Federation; [3]Institute of High Temperature Electrochemistry, Ekaterinburg, Russian Federation.

A2.21
Oxygen Mobility in Microwave Sintered Praseodymium Nickelates-Cobaltites and Their Nanocomposites with Yittria-Doped Ceria Vladislav A. Sadykov[1, 2], Nikita F. Eremeev[1], Vasiliy A. Bolotov[1], Yuriy Y. Tanashov[1], Yulia E. Fedorova[1, 3], Daiana G. Amanbayeva[1, 4], Aleksey S. Bobin[1], Ekaterina M. Sadovskaya[1], Vitaliy S. Muzykantov[1], Vladimir V. Pelipenko[1], Anton I. Lukashevich[1], Tamara A. Krieger[1], Arkadiy V. Ishchenko[1, 2] and Alevtina L. Smirnova[5]; [1]Boreskov Institute of Catalysis, Novosibirsk, Russian Federation;[2]Novosibirsk State University, Novosibirsk, Russian Federation; [3]Novosibirsk State Pedagogical University, Novosibirsk, Russian Federation; [4]Novosibirsk State Technical University, Novosibirsk, Russian Federation; [5]South Dakota School of Mines & Technology, Rapid City, South Dakota, United States.

A2.22
Electrochemical Performance of La and Ni Co-Doped $SrTiO_3$ Anode of Solid Oxide Fuel Cell Byung Hyun Park and Gyeong Man Choi; Mat. Sci. & Eng., POSTECH, Pohang, Korea (the Republic of).

A2.23
Functionally Graded Electrodes Using Centrifuge Deposition for Solid Oxide Fuel and Electrolysis Cells Shahid P. Shafi , Ioannis Bantounas, Udo Schwingenschloegl, Enrico Traversa and Samir Boulfrad; Physical Sciences and Engineering, King Abdullah University of Science and Technology (KAUST), Thuwal, Saudi Arabia.

A2.24
The Impact of Surfactant Choice on Infiltrate Size-Tailored Nano-Composite Solid Oxide Fuel Cell Cathodes Theodore E. Burye and Jason D. Nicholas; Chemical Eng and Material Science, Michigan State University, East Lansing, Michigan, United States.

A2.25
Preparation of Thin Films by the Method of Electrophoretic Deposition of Nanopowders on the Cathode Substrate Elena Kalinina[1], Elena Pikalova[2, 3], Anastasia Men'shikova[3] and Irina Nikolaenko[4, 3]; [1]Institute of Electrophysics of the Ural Branch of the Russian Academy of Sciences, Ekaterinburg, Russian Federation; [2]Institute of High Temperature Electrochemistry, UB RAS, Ekaterinburg, Russian Federation; [3]Ural Federal University, Ekaterinburg, Russian Federation; [4]Institute of Solid State Chemistry, UB RAS , Ekaterinburg, Russian Federation.

A2.26
The Electrochemical Reduction Mechanism of $Sm_{0.35}Ba_{0.15}Sr_{0.5}Co_{0.8}Fe_{0.2}O_{3-\delta}$ and Graded Composite Cathode Jianquan Gao, Shengli An, Fen Zhou and Xiwen Song; School of Materials and Metallurgy, Inner Mongolia University of Science and Technology, Baotou, China.

A2.27
Oxygen Exchange Kinetics of Doped Lanthanum Cobaltite System Keiji Yashiro[2], Hiroki Sato[1], Mie Sasaki[1], Takashi Nakamura[3], Shinichi Hashimoto[1], Koji Amezawa[3] and Tatsuya Kawada[1]; [2]GSES, Tohoku University, Sendai, Japan; [3]IMRAM, Tohoku University, Sendai, Japan.

A2.28
Surface Modification of $La_{0.6}Sr_{0.4}Co_{0.2}Fe_{0.8}O_{3-\delta}$ by Nanometer-Thick Mixed Conducting Oxide Films Michael L. Machala, Burcu Oeguet, David N. Mueller and William C. Chueh; Stanford University, Stanford, California, United States.

A2.29
Microstructural Effect to Thermal Stability and Cathode Performance by Nanoscale ZrO_2 Capping in Platinum Based-Solid Oxide Fuel Cells Kang-Yu Liu[1], Liangdong Fan[1], Chen-Chiang Yu[2] and Pei-Chen Su[1]; [1]School of Mechanical and Aerospace Engineering, Nanyang Technological University, Singapore, Singapore; [2]Interdisciplinary Graduate School, Nanyang Technological University, Singapore, Singapore.

A2.30
Microstructure and Functionality of Cathode/Electrolyte Interfaces in SOFCs Virginia Wilde[1], Heike Stoermer[1], Julian Szasz[2], Florian Wankmueller[2], Ellen Ivers-Tiffee[2] and Dagmar Gerthsen[1]; [1]Laboratory for Electron Microscopy (LEM), Karlsruhe Institute of Technology (KIT), Karlsruhe, Germany; [2]Institute of Materials for Electric and Electronic Engineering (IWE), Karlsruhe Institute of Technology (KIT), Karlsruhe, Germany.

A2.31
Bias Enhanced Fast Oxygen Exchange and Diffusion Kinetics of Grain Boundaries in LSM Thin Films Tobias M. Huber[1, 2, 3], Edvinas Navickas[4], Daio Takeshi[1], George F. Harrington[1, 2, 3], Nicola H. Perry[3, 5], Ghislain Rupp[4], Walid Hetaba[6], Michael Stoeger-Pollach[6], Harry L. Tuller[2, 5], Bilge Yildiz[3, 2], Kazunari Sasaki[5] and Juergen Fleig[4]; [1]Mechanical Engineering, Kyushu University, Fukuoka, Japan; [2]Materials Science and Engineering, Massachusetts Institute of Technology, Cambridge, Massachusetts, United States; [3]Department of Nuclear Science & Engineering, Massachusetts Institute of Technology, Cambridge, Massachusetts, United States; [4]Institute of Chemical Technologies and Analytics, Research Division Electrochemistry, Vienna University of Technology, Vienna, Austria; [5]International Center for Carbon Neutral Energy Research (I2CNER), Kyushu University, Fukuoka, Japan; [6]University Service Centre for Transmission Electron Microscopy, Vienna University of Technology, Vienna, Austria.

A2.32
Variable Temperature Multinuclear Solid State NMR Study of "Sr0.55Na0.45SiO2.775" Ryan D. Bayliss[1], Frederic Blanc[2, 3], John Corley[2], John A. Kilner[4, 5] and Stephen Skinner[4];[1]Department of Chemistry, University of Illinois at Chicago, Chicago, Illinois, United States; [2]Department of Chemistry, University of Liverpool, Liverpool, United Kingdom; [3]Stephenson Institute for Renewable Energy, University of Liverpool, Liverpool, United Kingdom; [4]Department of Materials, Imperial College London, London, United Kingdom; [5]International Institute for Carbon-Neutral Energy Research (I2CNER), Nishi-Ku, Japan.

A2.33
Nanostructured Electrodes for Metal-Supported Solid Oxide Fuel Cells Zhongliang Zhan, Yucun Zhou, Hao Wu, Ting Luo and Ting-Lian Wen; CAS Key Laboratory of Materials for Energy Conversion, Shanghai Institute of Ceramics, Shanghai, China.

A2.34
Kinetics of Surface Activation and Oxygen Transfer Acceleration Induced by A_2BO_4/ABO_3 Hetero-Interface for SOEC Application Bo Yu, Wenqiang Zhangwq and Jingming Xu; Tsinghua University, Beijing, China.

A2.35
Effect of Sintering Temperature on Properties of 8YSZ Prepared by SPS Jinxia Wang, Zhiqun Ding and Hongxia Zhao; School of Electronic and Information Engineering, Ningbo University of Technology, Ningbo, China.

A2.36

Methanol Synthesis at Atmospheric Pressure in Co-Ionic Electrochemical Membrane Reactors Anastasios Vourros[1, 4], Vasileios Kyriakou[4, 1], Ioannis Garagounis[1, 4], Michalis Konsolakis[2], Zisis Ioakimides[3, 4], George Marnellos[3, 4] and Michael Stoukides[1, 4]; [1]Chemical Engineering, Aristotle University of Thessaloniki, Thessaloniki, Greece; [2]School of Production Engineering and Management, Technical University of Crete, Chania, Greece; [3]Department of Mechanical Engineering, University of Western Macedonia, Kozani, Greece;[4]Chemical Process and Energy Resources Institute, Centre for Research and Technology Hellas, Thessaloniki, Greece.

A2.37

Structural and Electrical Properties of Spark Plasma Sintered Scandia- and Dysprosia-Stabilized Zirconia Robson L. Grosso[1], Ana J. Tertuliano[2], Izabel F. Machado[2] and Eliana N. Muccillo[1]; [1]Energy and Nuclear Research Institute (IPEN), Sao Paulo, Brazil; [2]Polytechnique School, Sao Paulo, Brazil.

A2.38

Electrical Properties of GDC-BCY Composite Electrolytes for Intermediate Temperature Solid Oxide Fuel Cell Xiaomei Liu, Hailin Bi, Haopeng Wang, Shenglong Yu, Fei Han, Lili Zhu, Jialing Sun and Li Pei; Key Laboratory of Physics and Technology for Advanced Batteries, Physics Department, Jilin University, Changchun, China.

A2.39

$Ni_{1-x}Cu_x$-SDC Anodes for Intermediate Temperature Solid Oxide Fuel Cell Lili Zhu[1, 2], Xiaomei Liu[1], Jialing Sun[1], Fei Han[1], Hailin Bi[1], Haopeng Wang[1], Shenglong Yu[1] and Li Pei[1]; [1] Key Laboratory of Physics and Technology for Advanced Batteries, Physics Department , Jilin University, Changchun, China; [2]Beihua University, Jilin, China.

A2.40

Electrical Conductivity of YSZ-SDC Composite Solid Electrolyte Synthesized via Glycine-Nitrate Method Prabhakar Singh; Department of Physics, Indian Institute of Technology (BHU) Varanasi, Varanasi, India.

A2.41

Wet Chemical Synthesis of $(DyO_{1.5})_x(WO_3)_y$ $(BiO_{1.5})_{1-x-y}$ and Application in Bilayer Low Temperature SOFCs Ashley L. Ruth[2], Emily A. Fraik[2], Daniel D. Taylor[1], Hee Sung Yoon[2] and Eric D. Wachsman[2]; [1]Chemistry, University of Maryland, College Park, Maryland, United States; [2]Energy Research Center, University of Maryland, College Park, Maryland, United States.

A2.42

Electrochemical Promotion of CO Oxidation on Pt/YSZ- Interaction between Multiple Promoting Species Danai Poulidi and Efstratios Stavrakakis; Chemistry and Chemical Engineering, Queen's University Belfast, Belfast, United Kingdom.

A2.43

Electrochemical Behavior of the Pyrochlore- and Fluorite-Like Solid Solutions in the Pr_2O_3-ZrO_2 System: Part II J.C. C. Jabrantes[1, 2], E. Gomes[1], Anna V. Shlyakhtina[3], Alexander N. Shchegolikhin[4] and Lidia G. Shcherbakova[3]; [1]UIDM, ESTG, Instituto Politécnico de Viana do Castelo, Viana do Castelo, Portugal; [2]Aveiro Institute of Materials – CICECO (DEMAC), University of Aveiro, Aveiro, Portugal; [3]Kinetics and Catalysis, Semenov Institute of Chemical Physics, Russian Academy of Sciences, Moscow, Russian Federation; [4]Emanuel Institute of Biochemical Physics, Russian Academy of Sciences, Moscow, Russian Federation.

A2.44

Thin Flim Oxy-Apatites for Solid Oxide Fuel Cell Sunghwan Lee and Shriram Ramanathan; School of Engineering and Applied Sciences, Harvard University, Cambridge, Massachusetts, United States.

A2.45

Structural Stability and Conductivity of the $Bi_3Y_{1-x}W_xO_{6+3x/2}$ System Anna Borowska-Centkowska[1], Wojciech Wrobel[1], Marcin Malys[1], Isaac Abrahams[2] and Franciszek Krok[1];[1]Faculty of Physics Warsaw University of Technology, Warsaw, Poland; [2]Materials Research Institute, Queen Mary University of London, London, United Kingdom.

A2.46

High Humidity Effects in Reversible Solid Oxide Cells and in Ni-YSZ Symmetric Cells Eui-Chol Shin[1], Pyung-An Ahn[1], Hyun-Ho Seo[1], Dang-Thanh Nguyen[1], Sun-Dong Kim[2], Sang-Kuk Woo[2], Ji Haeng Yu[2] and Jong-Sook Lee[1]; [1]Materials Science and Engineering, Chonnam National University, Gwang-Ju, Korea (the Republic of); [2]Korea Institute of Energy Research , Daejeon, Korea (the Republic of).

A2.47

High-Performance Anode-Supported Solid Oxide Fuel Cell with Impregnated Electrodes Denis Osinkin[1], Nina Bogdanovich[1], Sergey Beresnev[1] and Viktor Zhuravlev[2]; [1]Laboratory of SOFC, Institution of High Temperature Electrochemistry, Yekaterinburg, Russian Federation; [2]Institute of Solid State Chemistry, Yekaterinburg, Russian Federation.

A2.48

Extending the Simple Infiltrated Microstructure Polarization Loss Estimation (SIMPLE) Model to Infiltrated Solid Oxide Fuel Cell (SOFC) Anodes Eric Straley and Jason D. Nicholas; Chemical Engineering and Material Science, Michigan State University, East Lansing, Michigan, United States.

A2.49

A High Performance Anode Material for Solid Oxide Fuel Cells: Ni Exsolution on A-Site Deficient $La_{0.4}Sr_{0.4}Sc_{0.9}Ni_{0.1}O_{3-\delta}$ Mattia Saccoccio[1], Yang Gao[1], Dengjie Chen[1], Chi Chen[1] and Francesco Ciucci[1, 2]; [1]Department of Mechanical and Aerospace Engineering, The Hong Kong University of Science and Technology, Clear Water Bay, Hong Kong;[2]Department of Chemical and Biomolecular Engineering, The Hong Kong University of Science and Technology, Clear Water Bay, Hong Kong.

A2.50

Fabrication of Co/Fe-Doped Ni/$BaZr_{0.8}Y_{0.2}O_{3-\delta}$ Anode for Methane-Fueled PCFC Taehyun Park[2, 1], Chuancheng Duan[2], Jianhua Tong[2], Suk Won Cha[1] and Ryan O'Hayre[2];[1]Mechanical and Aerospace Engineering, Seoul National University, Gwanak-gu, Korea (the Republic of); [2]Metallurgical and Materials Engineering, Colorado School of Mines, Golden, Colorado, United States.

A2.51

Synthesis and Preliminary Study of Pure and Zr-Substituted $YMnO_3$ Compounds as Solid Oxide Fuel Cells Electrode Zulma L. Moreno[1, 3], Alberto Caneiro[3], Pascal Roussel[2] and Gilles H. Gauthier[1]; [1]Grupo INTERFASE, Universidad Industrial de Santander, Bucaramanga, Colombia; [2]Université Lille 1, Université Lille Nord de France, Lille, France; [3]Comisión Nacional de Energía Atómica, Centro Atómico de Bariloche, San Carlos de Bariloche, Argentina.

A2.52

Structural and Electrical Properties of Ceria (Ce^{3+}) Doped Double Perovskite System $Sr_2NiMoO_{6-\delta}$ Pravin Kumar, Nitish Kumar Singh and Prabhakar Singh; Physics, Indian Institute of Technology (BHU) , Varanasi, India.

A2.53

Chemical Stability of Double-Perovskite Anode Material Sr_2MgMoO_6 for Solid Oxide Fuel Cells Masahiro Kinoshita[1], Kyota Hara[2], Tomohiro Onozawa[2], Kiyoto Shin-mura[1], Yu Otani[1], Eiki Niwa[3], Takuya Hashimoto[3] and Kazuya Sasaki[1, 2]; [1]Course of Mechanical Engineering, Graduate School of Engineering, Tokai University, Hiratsuka, Japan; [2]Department of Prime Mover Engineering, School of Engineering, Tokai University, Hiratsuka, Japan; [3]Department of Physics, College of Humanities and Sciences, Nihon University, Setagaya-ku, Japan.

A2.54

Novel Ni and Ni Alloy/γ-Al_2O_3 Anode Materials for Direct Carbon SOFCs Sergey Pikalov[2], Evgeny Selivanov[2], Olga Russkikh[1], Elena Filonova[1], Valery Polukhin[2] and Irina Nikolaenko[3]; [1]Institute of Natural Sciences, Ural Federal University, Ekaterinburg, Russian Federation; [2]Institute of Metallurgy, UB RAS, Ekaterinburg, Russian Federation; [3]Institute of Solid State Chemistry, UB RAS, Ekaterinburg, Russian Federation.

A2.55
Novel Double-Layer La_2NiO_{4+d} Cathodes: Screen Printing vs. Electrostatic Spray Deposition R. K. Sharma[1, 2], M. Burriel[3], L. Dessemond[1, 2], Jean-Marc Bassat[4] and E. Djurado[1, 2];[1]LEPMI, Univ. Grenoble Alpes, Grenoble, France; [2]LEPMI, CNRS, Grenoble, France; [3]Catalonia Institute for Energy Research (IREC), Barcelona, Spain; [4]ICMCB-CNRS, Pessac , France.

A2.56
Patterned Electrodes for the Study of CO/CO2 Electrolysis Vladislav Duboviks[1], Enrique Ruiz-Trejo[1], Farid Tariq[1], Paul Boldrin[1], Robert C. Maher[2], Gregory J. Offer[3], Gabriel Castillo[4], Javier Rodriguez Vazquez de Aldana[4], Masashi Kishimoto[1], Leslie F. Cohen[2] and Nigel P. Brandon[1]; [1]Earth Science and Engineering, Imperial College London, London, United Kingdom; [2]Physics, Imperial College London, London, United Kingdom; [3]Mechanical Engineering, Imperial College London, London, United Kingdom; [4]Ciencias, Universidad de Salamanca, Salamanca, Spain.

SESSION C2: Poster Session I
C: Electrodes and Solid Electrolytes for Batteries
Monday Afternoon, June 15, 2015
12:00 PM
Keystone Resorts, Red Cloud Peak

C2.01
Fast Li Self-Diffusion in Amorphous Li-Si Electrochemically Prepared from Semiconductor Grade, Monocrystalline Silicon — Insights from Spin-Locking Nuclear Magnetic Relaxometry Andreas Dunst, Michael Sternad, Viktor Epp and Martin Wilkening; Christian-Doppler Laboratory for Lithium Batteries, Institute for Chemistry and Technology of Materials, Graz University of Technology, Graz, Austria.

C2.02
Solubility Behavior of Nanograined Li_2MnSiO_4 Cathode Material in Liquid Electrolytes Marcin Molenda, Michal Swietoslawski and Roman Dziembaj; Faculty of Chemistry, Jagiellonian University, Krakow, Poland.

C2.03
Studies on PVA Based Nanocomposite Polymer Gel Electrolyte Membranes for High Performance Proton Conducting Batteries S. L. Agrawal[1] and Neelesh Rai[2]; [1]Department of Physics, APS University, Rewa , India; [2]Department of Physics, AKS University, Satna, India.

C2.04
Lithium in Diffusion Measurements on a Garnet-Type Solid Conductor $Li_{6.6}La_3Zr_{1.6}Ta_{0.4}O_{12}$ (LLZO-Ta) by Pulsed-Gradient Spin-Echo NMR Method Kikuko Hayamizu[1], Yasuaki Matsuda[2], Masaki Matsui[2], Yasuo Takeda[2] and Nobuyuki Imanishi[2]; [1]Institute of Applied Physics, University of Tsukuba, Tsukuba, Japan; [2]Department of Chemistry for Materials, Mie-University, Tsu, Mie, Japan.

C2.05
All Solid State Li-Garnet-Based Batteries: From Materials Development to Thin Film Microstructures Jennifer L. Rupp[1], Semih Ayfon[1], Inigo Garbayo[1], Reto Pfenninger[1], Michael Rawlence[2, 1] and Michal Struzik[1]; [1]Electrochemical Materials, ETH Zurich, Zurich, Switzerland; [2]Laboratory for Thin Films and Photovoltaics, EMPA, Dübendorf, Switzerland.

C2.06
Proof-of-Concept of All-Solid-State Metal-Metal Battery Fuminori Mizuno[1], Ruigang Zhang[1], Timothy S. Arthur[1], Donovan N. Leonard[2], Miaofang Chi[2] and Jeff Sakamoto[3];[1]Materials Research Department, Toyota Research Institute of North America, Ann Arbor, Michigan, United States; [2]Oak Ridge National Laboratory, Oak Ridge, Tennessee, United States;[3]Mechanical Engineering, University of Michigan, Ann Arbor, Michigan, United States.

C2.07
The $Li_{(m)}$ / Li_3PS_4 Interface for Solid-State Batteries Timothy S. Arthur[1], Ruigang Zhang[1], Regina Garcia[2], Jeff Sakamoto[2] and Fuminori Mizuno[1]; [1]Materials Research, Toyota Research Institute of North America, Ann Arbor, Michigan, United States; [2]University of Michigan, Ann Arbor, Michigan, United States.

C2.08
Li-Ion Conducting Polymer Electrolytes Based on Biopolymer, Agar Agar Selvasekarapandian Subramanian[1], Vinitha Thiyagarajan Upaassana[1], Sindhuja Manohar[1], Monisha Sampath[1] and Arun A[2]; [1]Physics, Materials Research Centre, Coimbatore, India; [2]Chemistry, Government Arts College, Thiruvannamalai, India.

C2.09
A Comparative Study of Impact in Conductivity of $LiNiPO_4$ on Doping Europium and Samarium in Lithium and Nickel Sites Prepared Using Modified Pechini and Polymeric Precursor Method Selvasekarapandian Subramanian[1, 2], Goutam Anbunathan V N[2], Kalpana M[2], Senthil Kumar P[3], Vinoth Pandi D[4], Sakunthala A[3] and Gunasekaran K[2]; [1]Physics, Materials Research Centre, Coimbatore, India; [2]Department of Nano Science and Technology, Tamilnadu Agricultural University, Coimbatore, India; [3]Department of Physics, Karunya University, Coimbatore, India; [4]Department of Physics, Coimbatore Institute of Technology, Coimbatore, India.

C2.10
Sputter Deposited $Li_7La_3Zr_2O_{12}$ as Electrolyte for Thin Film Cells Sandra Lobe[1], Christian Dellen[1], Hans-Gregor Gehrke[1], Chih-Long Tsai[1], Martin Finsterbusch[1], Sven Uhlenbruck[1]and Olivier Guillon[1, 2]; [1]Institute of Energy and Climate Research (IEK-1) , Forschungszentrum Jülich, Jülich, Germany; [2]Institut für Gesteinshüttenkunde, Rheinisch-Westfälische Technische Hochschule (RWTH) Aachen, Aachen, Germany.

C2.11
Evaluation of Mechanical Properties of Li_2S-P_2S_5-LiI Glass Electrolytes for All-Solid-State Lithium Batteries Atsutaka Kato[1], Atsushi Sakuda[2], Akitoshi Hayashi[1] and Masahiro Tatsumisago[1]; [1]Applied Chemistry, Osaka Prefecture University, Sakai, Japan; [2]Research Institute for Ubiquitous Energy Devices, National Institute of Advanced Industrial Science and Technology (AIST), Ikada, Japan.

C2.12
Aluminum-Doped $Li_7La_3Zr_2O_{12}$ - A Promising Candidate as a Solid Electrolyte for Lithium-Ion Batteries Miriam Botros[1], Ruzica Djenadic[1, 2, 3] and Horst Hahn[1, 2, 3]; [1]Joint Research Laboratory Nanomaterials, Technical University Darmstadtand and Karlsruhe Institute of Technology, Darmstadt, Germany; [2]Institute for Nanotechnology, Karlsruhe Institute of Technology, Eggenstein-Leopoldshafen, Germany; [3]Helmholtz Institute Ulm, Ulm, Germany.

C2.13
Microstructure-Electrical Property Relationship in Polycrystalline Sodium β"-Alumina by New Impedance Modelling Approach Jee-Hoon Kim[1], Dong-Chun Cho[1], Su-Hyun Moon[1], Eui-Chol Shin[1], Sansudae Lim[2], Sooseok Kim[2], Keedeok Yang[2], Jinhyung Beom[2] and Jong-Sook Lee[1]; [1]Materials Science and Engineering, Chonnam National University, Gwangju, Korea (the Republic of); [2]FineTech Co., Ltd., Daejeon, Korea (the Republic of).

C2.14
Non-Stoichiometry of Composites: Thermodynamic Analysis of Dissociative Storage at Interfaces Chia-Chin Chen, Lijun Fu and Joachim Maier; Max Planck Institute for Solid State Research, Stuttgart, Germany.

C2.15
Rechargeable Batteries and Condensed Matter Physics Lin Gu; Institute of Physics, Chinese Academy of Sciences, Beijing, China.

C2.16
Diatomaceous Earth and Algae Based Aqueous Binders Make Environmentally Friendly High-Performance Anodes for Lithium-Ion Batteries Muhammad Hasanuzzaman and Fride Vullum-Bruer; Materials Science and Engineering, Norwegian University of Science and Technology, NTNU, Trondheim, Norway.

C2.17
Preparation of Li_2S-$FePS_3$ Composite Positive Electrode Materials and Their Electrochemical Properties Tomonari Takeuchi[1], Hiroyuki Kageyama[1], Masahiro Ogawa[2], Koji Nakanishi[3], Toshiaki Ohta[2], Atsushi Sakuda[1], Hikari Sakaebe[1], Hironori Kobayashi[1] and Zempachi Ogumi[3]; [1]National Institute of Advanced Industrial Science and Technology, Ikeda, Japan; [2]Ritsumeikan University, Kusatsu, Japan; [3]Kyoto University, Kyoto, Japan.

C2.18
Highly Conductive Glass-Ceramic Electrolytes for Advanced Lithium Batteries Miriam Kunze, Meike Schneider, Maria-Luisa Reich, Wolfgang Schmidbauer and Andreas Roters; SCHOTT AG, Mainz, Germany.

C2.19
Investigation of O3-$Na_{0.9}[Ni_{0.45}Ti_{0.55}]O_2$ Using Electroanalytical Techniques and Ex-Situ XRD for Na-Ion Batteries Rengarajan Shanmugam and Wei Lai; CHEMS, Michigan State University, East Lansing, Michigan, United States.

C2.20
Evidence for a >1 Electron Reaction in Li_2FeSiO_4: An *in situ* Mössbauer Spectroscopy Study Anti Liivat[1], Josh Thomas[1], Jianghuai Guo[2] and Yong Yang[2]; [1]Chemistry, Uppsala University, Uppsala, Sweden; [2]Chemistry, Xiamen University , Xiamen, China.

C2.21
Optimization of Ionic Conductivity in Garnet-Type Solid State Electrolytes for Lithium Ion Batteries Sumaletha Narayanan, Xia Tong and Venkataraman Thangadurai; Department of Chemistry, University of Calgary, Calgary, Alberta, Canada.

C2.22
Electrochemical Properties of All-Solid-State Lithium-Ion Batteries Using Li_2CO_3-Li_3BO_3 Electrolyte Toyoki Okumura, Tomonari Takeuchi, Masahiro Shikano and Hironori Kobayashi; Advanced Battery Research Group, National Institute of Advanced Industrial and Technology (AIST), Ikeda, Japan.

C2.23
Spinel-Based Solid Electrolyte for Lithium-Ion Battery Application Ruzica Djenadic[1, 2, 3], Miriam Botros[3], Chritoph Loho[3] and Horst Hahn[2, 3, 1]; [1]Helmholtz Institute Ulm, Ulm, Germany; [2]Institute of Nanotechnology, Karlsruhe Institute of Technology, Eggenstein-Leopoldshafen, Germany; [3]Joint Research Laboratory Nanomaterials – Technical University Darmstadt & Karlsruhe Institute of Technology, Darmstadt, Germany.

C2.24
Transport of Alkali Ions in an Organic Ionic Plastic Crystal Fangfang Chen and Maria Forsyth; Institute for Frontier Materials, Deakin University, Burwood, Victoria, Australia.

C2.25
Electrochemical Properties and Structural Evaluation of Amorphous MoS_3 Positive Electrode Active Materials in All-Solid-State Lithium Secondary Batteries Takuya Matsuyama[1], Minako Deguchi[1], Akitoshi Hayashi[1], Masahiro Tatsumisago[1], Tomoatsu Ozaki[2] and Shigeo Mori[3]; [1]Department of Applied Chemistry, Osaka Prefecture University, Sakai, Japan; [2]Technology Research Institute of Osaka Prefecture, Izumi, Japan; [3]Department of Materials Science, Osaka Prefecture University, Sakai, Japan.

C2.26
Comparing Electrochemical Performance of Silicate Cathodes and Chevrel Phase Mo_6S_8 in the Analogous Rechargeable Mg-Ion Battery System Xinzhi Chen[1], Lu Wang[1], Sidsel M. Hanetho[2], Paul I. Dahl[2] and Fride Vullum-Bruer[1]; [1]Department of Materials Science and Engineering, Norwegian University of Science and Technology, Trondheim, Norway;[2]Department of Sustainable Energy Technology, SINTEF Materials and Chemistry, Trondheim, Norway.

C2.27
Computer Aided Design of Polyanionic Electrolytes: A Molecular Dynamic Study Xingyu Chen; Institute of Frontier Materials, Deakin University, Melbourne, Victoria, Australia.

C2.28
Enhancement of Ionic Conductivity of Battery Electrolytes Using Nanoconfined Polymer Electrolyte, Ionic Liquids and Ionic Liquid/ Polymer Electrolyte Blends Indumini Jayasekara and Dale Teeters; Chemistry and Biochemistry, The University of Tulsa, Tulsa, Oklahoma, United States.

C2.29
Investigation of the Unique Crystalline Orientation of a Nanostructured Lithium Cobalt Oxide Thin Film Cathodes for Lithium Ion Batteries Mark Poyner and Dale Teeters; Chemistry and Biochemistry, The University of Tulsa, Tulsa, Oklahoma, United States.

C2.30
Electrical Characterization of $Na_3Sc_2(PO_4)_3$:Eu2+ Su-Hyun Moon, Yun-Hwa Kim, Dong-Chun Cho, Eui-Chol Shin, Won-Bin Im and Jong-Sook Lee; School of Materials Science and Engineering, Chonnam National University, Gwangju, Korea (the Republic of).

C2.31
Dispersive Frequency Response in Low Temperature Silver Iodide by Immittance Spectroscopy Su-Hyun Moon, Young-Hun Kim, Dong-Chun Cho, Eui-Chol Shin and Jong-Sook Lee; School of Materials Science and Engineering, Chonnam National University, Gwangju, Korea (the Republic of).

C2.32
Novel Copper-Based Layered Oxide Cathode for Room-Temperature Sodium-Ion Batteries Linqin Mu, Yong-Sheng Hu, Shuyin Xu, Yunming Li and Liquan Chen; Chinese Academy of Sciences, Institution Of Physics, Beijing, China.

C2.33
The Degradation Mechanism of Nickel-Rich Cathode Active Materials with Vinylene Carbonate in An Electrolyte for Lithium Ion Batteries at Various Temperatures Su Jung Do,Prasanna Kadirvelayutham, Yong Nam Jo, Robert Ilango Pushparaj and Chang Woo Lee; Kyung Hee University, Yongin-si, Korea (the Republic of).

C2.34
Electrochemical Properties of Sn-Co Electrode with Various Kinds of Binder Materials for Sodium Ion Batteries Yuhki Yui, Masahiko Hayashi, Katsuya Hayashi and Jiro Nakamura; NTT, Atsugi, Japan.

C2.35
Synthesis of Chatode Materials $LiFePO_4$ by Hydrothermal and Ultrasonic Method Wagiyo Honggowiranto and Evvy Kartini; Advanced Materials, National Nuclear Energy Agency, Tangerang Selatan, Indonesia.

C2.36
Characterization of Structural and Transport Properties of $LiMn_{1.7}Cu_{0.3}O_4$ Lukasz Kondracki, Anna G. Milewska and Janina Molenda; AGH University of Science and Technology, Kraków, Poland.

C2.37
Comparative Analysis of Structure-Property Relationship of Nanosilicon Anodes for Lithium-Ion Batteries Diana Golodnitsky, Emanuel Peled, Fernando Patolsky, Kathrin Freedman, Meital Goor, Keren Goldstein, Guy Davidi and Dan Schneier; School of Chemistry, Tel Aviv University, Tel Aviv, Israel.

C2.38
A Na^+ Superionic Conductor Based on NASICON and Its Application in All-Solid-State Sodium Batteries Zhizhen Zhang, Kaiqi Xu, Yong-Sheng Hu and Liquan Chen; Institute of Physics Chinese Academy of Sciences, Beijing, China.

C2.39
Impedance Measurement for Ti-Zr-Ni Alloy Electrodes Produced by Mechanical Alloying and Subsequent Annealing Akito Takasaki[1], Youhei Ariga[1], Wojciech Zajac[2] and Konrad Swierczek[2]; [1]Engineering Science and Mechanics, Shibaura Institute of Technology, Tokyo, Japan; [2]Faculty of Energy and Fuels, AGH University of Science and Technology, Krakow, Poland.

C2.40
Structural Evaluation of Delithiated $Li_xMn_{1.5}Ni_{0.5-y}Cu_yO_4$ Spinels Lukasz Kondracki, Anna Milewska, Artur Bogacki, Slawomir Lalik and Janina Molenda; AGH University of Science and Technology, Kraków, Poland.

C2.41
Synthesis, Structure and Ionic Conductivities of Novel Li-Ion Conductor $A_3Li_xTa_{6-x}Zr_xSi_4O_{26}$ (A = Ba, Sr) Akihisa Aimi[1], Yoshiyuki Inaguma[1], Miki Kubota[1], Daisuke Mori[1], Tetsuhiro Katsumata[2], Minoru Ikeda[3] and Takahisa Ohno[3, 4]; [1]Chemistry, Gakushuin University, Toshima-ku, Japan; [2]Chemistry, Tokai University, Hiratsuka-shi, Japan; [3]National Institute for Materials Science, Tsukuba-shi, Japan; [4]Global Research Center for Environment and Energy based Nanomaterials Science, Tsukuba-shi, Japan.

C2.42
Properties of Lithium-Stuffed Garnet-Type Oxide Solid Electrolyte Thick Film Fabricated by Aerosol Deposition Method Ryoji Inada, Takayuki Okada, Keiji Tsuritani, Kota Wagatsuma, Tomohiro Tojo and Yoji Sakurai; Department of Electrical and Electronic Information Engineering, Toyohashi University of Technology, Toyohashi, Japan.

C2.43
Defect Chemistry and Transport in Alkali Superoxides Oliver Gerbig, Rotraut Merkle and Joachim Maier; MPI for Solid State Research, Stuttgart, Germany.

C2.44
Dielectric and Transport Properties Study of Clay Based Solid Polymer Electrolyte Namrata Tripathi[1], Awalendra K. Thakur[3], Archana Shukla[2] and David T. Marx[1]; [1]Physics, Illinois State University, Normal, USA, Normal, Illinois, United States; [2]Physics, Indian Institute of Technology Bombay, Maharastra, Mumbai, India; [3]Physics, Indian Institute of Technology Patna, Bihar, Patna, India.

C2.45
The Effect of Cathode Microstructure on the Performance of All Solid-State Li Battery Sven Uhlenbruck, Chih-Long Tsai, Christian Dellen, Qianli Ma, Sandra Lobe and Olivier Guillon; Institute of Energy and Climate Research, Forschungszentrum Jülich GmbH, Jülich, Germany.

C2.46
Conductivity and Scaling Behavior of Nd^{3+} Ions Containing Lithium Borate Glasses Durgaprasad D. Ramteke[1, 2], Hendrik C. Swart[1] and Rupesh S. Gedam[2]; [1]Department of Physics, University of Free State , Bloemfontein , South Africa; [2]Department of Applied Physics, Visvesvaraya National Institute of Technology, Nagpur, India.

C2.47
A Battery Made from a Single Material Fudong Han[1], Tao Gao[1], Yujie Zhu[1], Karen J. Gaskell[2] and Chunsheng Wang[1]; [1]Department of Chemical and Biomolecular Engineering, University of Maryland, College Park, Maryland, United States; [2]Department of Chemistry and Biochemistry, University of Maryland, College Park, Maryland, United States.

C2.48
High Rate Growth by Pulsed Laser Deposition and Characterization of Epitaxial $LiCoO_2$ Films Kazunori Nishio[1], Tsuyoshi Ohnishi[1, 2, 3], Minoru Osada[3], Narumi Ohta[1, 2], Ken Watanabe[2] and Kazunori Takada[1, 2, 3]; [1]Global Research Center for Environment and Energy based on Nanomaterials Science, National Institute for Materials Science, Tsukuba, Japan;[2]Environment and Energy Materials Division, National Institute for Materials Science, Tsukuba, Japan; [3]International Center for Materials Nanoarchitectronics , National Institute for Materials Science, Tsukuba, Japan.

C2.49
Assembly and Electrochemical Properties of $LiFePO_4$/C Pouch Cell Evvy Kartini and Wagiyo Honggowiranto; Science and Technology Center for Advanced Materials, National Nuclear Energy Agency, South Tangerang, Indonesia.

C2.50
Towards Control over Redox Behavior and Ionic Conductivity in $LiTi_2(PO_4)_3$ Fast Lithium-Ion Conductor Wojciech Zajac[1], Mateusz Tarach[1] and Anita Trenczek-Zajac[2]; [1]Faculty of Energy and Fuels, AGH University of Science and Technology, Krakow, Poland; [2]Faculty of Materials Science and Ceramics, AGH University of Science and Technology, Krakow, Poland.

C2.51
Advanced Planar Lithium-Sulfur Batteries Based on Solid Ceramic Li-Ion Conducting Separators Feng Zhao and John Bi; Ceramatec, Inc. , Salt Lake City, Utah, United States.

C2.52
Development of NaSICON-Type Lithium Ion Conductors Feng Zhao and John Bi; Ceramatec, Inc. , Salt Lake City, Utah, United States.

C2.53
Preparation of Li_2S–P_2S_5 Solid Electrolytes Using Organic Solvents as Synthetic Media Nguyen H. Phuc, Kei Morikawa, Mitsuhiro Totani, Hiroyuki Muto and Atsunori Matsuda; Electrical and Electronic Information Engineering, Toyohashi University of Technology, Toyohashi, Japan.

C2.54
Mechanochemical Preparation of Lithium Sulfide-Lithium Iodide Solid Solutions as Active Materials for All-Solid-State Lithium Secondary Batteries Takashi Hakari, Akitoshi Hayashi and Masahiro Tatsumisago; Department of Applied Chemistry , Osaka Prefecture University, Sakai-shi, Japan.

C2.55
A Study on the Effects of Mechanical Alloys as Anodes on Corrosion and Hydrogen Evolution Reaction in Zinc-Air System Yong Nam Jo, Prasanna Kadirvelayutham, Su Jung Do, Subburaj Thiruvengadam and Chang Woo Lee; Kyung Hee University, Yongin-si, Korea (the Republic of).

C2.56
Synthesis and Electrochemical Property of Garnet-Type Lithium-Ion Conductor $Li_{7-x-y}Al_yLa_3Zr_{2-x}Ta_xO_{12}$ Yasuaki Matsuda[1], Yuya Itami[1], Masaki Matsui[1, 2], Yasuo Takeda[1] and Nobuyuki Imanishi[1]; [1]Chemistry, Mie University, Tsu, Japan; [2]PRESTO, Japan Science and Technology Agency, Honcho, Kawaguchi, Japan.

C2.57
On V Substitution in Li_2MnSiO_4/C as Potential Positive Electrode for Li-Ion Batteries Nils Wagner, Ann-Mari Svensson and Fride Vullum-Bruer; Material Science and Engineering, Norwegian University of Science and Technology, Trondheim, Norway.

C2.58
Electrical Conductivity Characterization of $LiAlO_2$ Thin Films Prepared by ALD Yang Hu, Amund Ruud, Ville Miikkulainen, Truls Norby, Ola Nilsen and Helmer Fjellvag; Centre for Materials Science and Nanotechnology, Department of Chemistry, University of Oslo, Oslo, Norway.

C2.59
Solid Electrolytes for Lithium-Sulfur Batteries Alice Cassel[1, 2, 3], Benoit Fleutot[1, 2, 3], Christine Surcin[1, 2, 3], Virginie Viallet[1, 2, 3] and Mathieu Morcrette[1, 2, 3]; [1]Laboratoire de Réactivité et Chimie des Solides, Amiens, France; [2]Réseau sur le Stockage Electrochimique de l'Energie, Amiens, France; [3]Alistore-ERI, Amiens, France.

C2.60
Preparation and Properties of Lithium Conducting Membranes from Polymer-Brush Nanoparticles Ilya Zharov[1, 2]; [1]Chemistry, University of Utah, Salt Lake City, Utah, United States; [2]Materials Science and Engineering, University of Utah, Salt Lake City, Utah, United States.

C2.61
Separators Based on Novel Triblock Polyelectrolyte for Lithium Battery: Improving Performance and Safety Kun-lin Liu and Chi-Yang Chao; Materials Science and Engineering, National Taiwan University, Taipei, Taiwan.

C2.62
Rechargeable Lithium Semi-Flow Battery Using $Li_7P_3S_{11}$ Rayavarapu Prasada Rao, Jia Ming Yuen and Stefan Adams; Materials Science & Eng., National University of Singapore, Singapore, Singapore.

C2.63
$Li_{10}SnP_2S_{12}$, an Electrolyte and Negative Electrode Material for Solid State Li-Ion Batteries? Ilyas Tarhouchi[3, 2], Virginie Viallet[1, 2], Philippe Vinatier[3, 2] and Michel Menetrier[3, 2];[1]LRCS - UMR CNRS 7314, Amiens, France; [2]Réseau sur le Stockage Electrochimique de l'Energie (RS2E), FR CNRS 3459, Amiens, France; [3]ICMCB - CNRS, Pessac, France.

C2.64
Preparation and Electrochemical Studies on Fe-Doped $LiVPO_4F$ Cathode M.V. Reddy[1, 2], Rayavarapu Prasada Rao[1], Stefan Adams[1] and B.V.R. Chowdari[2]; [1]Materials Science & Eng., National University of Singapore, Singapore, Singapore; [2]Dep. of Physics, National University of Singapore, Singapore, Singapore.

C2.65
Effect of Polysorbate Plasticizer on the Structural and Ion Conduction Properties of the Polyethylene oxide/NH_4PH_6 Solid Polymer Electrolyte Kuldeep Mishra[2], Saurabh S. Pundir[1] and D. K. Rai[1]; [1]Department of Physics & Materials Science & Engineering, Jaypee Institute of Information Technology University, Noida , Noida, India; [2]Department of Physics & Materials Science, Jaypee University, Anoopshahr, Bulandshahr, India.

SESSION D2: Poster Session: Fundamentals of Transport and Reactivity and Nanoionics I
D: Fundamentals of Transport and Reactivity and Nanoionics
Monday Afternoon, June 15, 2015
12:00 PM
Keystone Resorts, Red Cloud Peak

D2.01
***In Situ* Optical Absorption Studies of Defect Equilibria and Kinetics: Application to $Sr(Ti,Fe)O_{3-\alpha}$ Thin Films** Nicola H. Perry[1, 2], Jaejin Kim[2] and Harry L. Tuller[2, 1]; [1]I2CNER, Kyushu University, Nishi-ku, Fukuoka, Japan; [2]Materials Science and Engineering, MIT, Cambridge, Massachusetts, United States.

D2.02
Millimeter Wave Spectroscopy and Molecular Dynamics Simulation of Ionic Liquids Teruyoshi Awano[1], Arimitsu Shikoda[1] and Toshiharu Takahashi[2]; [1]Tohoku Gakuin University , Tagajo, Japan; [2]Research Reactor Institute, Kyoto University, Kumatori, Japan.

D2.03
Structural vs. Intrinsic Carriers: Contrasting Effects of Cation Disorder on Ionic Conductivity in Pyrochlores Romain Perriot and Blas P. Uberuaga; Materials Science and Technology Division, Los Alamos National Laboratory, Los Alamos, New Mexico, United States.

D2.04
Intrinsic Material Properties Dictating the Formation Energetics of Oxygen Vacancies in Wide Gap Oxides Ann Deml[1, 2], Aaron Holder[2], Ryan O'Hayre[1], Charles Musgrave[3] and Vladan Stevanovic[1, 2]; [1]Colorado School of Mines, Golden, Colorado, United States; [2]National Renewable Energy Laboratory, Golden, Colorado, United States; [3]University of Colorado Boulder, Boulder, Colorado, United States.

D2.05
***Ab Initio* Studies on Bismuth Oxide Based Solid Electrolytes** Marcin Krynski[1], Franciszek Krok[1], Isaac Abrahams[2], Wojeciech Wrobel[1], Jozef Dygas[1] and Piotr Spiewak[3]; [1]Physics, Warsaw University of Technology, Warszawa, Poland; [2]Centre for Materials Research, School of Biological and Chemical Sciences, Queen Mary, London, United Kingdom; [3]Materials Engineering, Warsaw University of Technology, Warszawa, Poland.

D2.06
Role of Oxide Ion Transport on Promoting Iron Oxide Redox Reaction with Oxide Ion Conductors as Supports for Energy Storage and Conversion Fumihiko Kosaka[1], Hiroyuki Hatano[2], Yoshito Oshima[1] and Junichiro Otomo[1]; [1]The University of Tokyo, Kashiwa City, Japan; [2]Chuo University, Bunkyo-Ku, Japan.

D2.07
Ionic and Electronic Energy Level Diagrams for the CaF_2/BaF_2 Heterojunction Giuliano Gregori and Joachim Maier; Max Planck Institute for Solid State Research, Stuttgart, Germany.

D2.08
Glass Formation and Fast Ag Ion Conduction in the System Ag_2Se-Ga_2Se_3-$GeSe_2$ Maxwell A. Marple[1], Derrick Kaseman[1], Bruce Aitken[2], Sangtae Kim[1] and Sabyasachi Sen[1];[1]Chemical Engineering and Materials Science, University of California Davis, Davis, California, United States; [2]Corning Inc, Corning, New York, United States.

D2.09
Fast-Ion Conductor Design for Grid-Scale Batteries Stefan Adams, Haomin Chen, Lee L. Wong and Rayavarapu Prasada Rao; Materials Science & Eng., National University of Singapore, Singapore, Singapore.

D2.10
Grain Boundaries Across Length Scales; Correlating Orientation Imaging and Nanospectroscopy William J. Bowman[1], Amith Darbal[2], Madeleine Kelly[3], Gregory S. Rohrer[3], Cruz A. Hernandez[1], Kimberly McGuinness[1] and Peter A. Crozier[1]; [1]Materials Science and Engineering, Arizona State University, Tempe, Arizona, United States; [2]AppFive LLC, Tempe, Arizona, United States; [3]Materials Research Science and Engineering Center, Carnegie Mellon University, Pittsburgh, Pennsylvania, United States.

D2.11
Determining the Effect of Gas Phase Concentration Polarization on Porous Thick Film Oxygen Surface Exchange Coefficients Determined via the Curvature Relaxation Technique Yuxi Ma and Jason D. Nicholas; Chemical Engineering and Material Science, Michigan State University, East Lansing, Michigan, United States.

D2.12
The Direct Measurement of Ionic Piezoresistance Stuart N. Cook, Jae Jin Kim and Harry L. Tuller; Massachusetts Institute of Technology, Cambridge, Massachusetts, United States.

D2.13
Statistical Methods for Solid State Electrochemistry with Applications to Impedance Spectroscopy and Conductivity Relaxation Francesco Ciucci[1, 2]; [1]Mechanical and Aerospace Engineering, The Hong Kong University of Science and Technology, Kowloon, Hong Kong; [2]Chemical and Biomolecular Engineering, The Hong Kong University of Science and Technology, Kowloon, Hong Kong.

D2.14
Kinetic Unmixing and Decomposition in Ternary Oxides under Electric Field Jakyu Chun[1], Manfred Martin[2] and Han-Ill Yoo[1]; [1]Department of Materials Science and Engineering, Seoul National University, Seoul, Korea (the Republic of); [2]Institute of Physical Chemistry, RWTH Aachen University, Aachen, Germany.

D2.15 Moved to C11.09

D2.16
Influence of Space-Charge on the Surface Defect Chemistry of $BaZrO_3$ Jonathan M. Polfus[1], Tor S. Bjørheim[2], Mehdi Pishahang[1], Truls Norby[2] and Rune Bredesen[1]; [1]Materials and Chemistry, SINTEF, Oslo, Norway; [2]Department of Chemistry, University of Oslo, Oslo, Norway.

D2.17
A Novel Oxygen Pressure Relaxation Technique and Isotope Exchange on $SmBaCo_2O_{6-\delta}$ Vadim Eremin[1], Maxim Ananyev[1, 2] and Edhem Kurumchin[1]; [1]Laboratory of the Electrochemical Materials Science, Institute of High Temperature Electrochemistry, UB RAS, Yekaterinburg, Russia, Yekaterinburg, Russian Federation; [2]Institute of Chemical Technology, Ural Federal University, Yekaterinburg, Russian Federation.

D2.18
Giant Electrostriction in Doped Bi_2O_3 Ceramics Nimrod Yavo[1], Alaric Smith[2], Roman Korobko[1], Peter R. Slater[2] and Igor Lubomirsky[1]; [1]Materials and Interfaces, Weizmann Institute of Science, Rehovot, Israel; [2]School of Chemistry, University of Birmingham, Birmingham, United Kingdom.

D2.19
A Molecular Dynamics Study of Oxygen Ion Diffusion in A-Site Ordered Perovskite $PrBaCo_2O_{5.5}$: Data Mining the Oxygen Trajectories Chi Chen and Francesco Ciucci; Mechanical and Aerospace Engineering, Hong Kong University of Science and Technology, Kowloon, Hong Kong.

D2.20
A Novel Model for Gas Phase Analysis of Oxygen Isotope Exchange in Ceramic Materials with Different Diffusion Pathways Lev Putilov[1] and Maxim Ananyev[1, 2]; [1]Laboratory of the Electrochemical Materials Science, Institute of High Temperature Electrochemistry, Ural Branch of Russian Academy of Sciences, Yekaterinburg, Russian Federation; [2]Institute of Chemical Technology, Ural Federal University, Yekaterinburg, Russian Federation.

D2.21
DFT and Hybrid Calculations on the Stability of Shear Planes and Point Defects in WO_3 Marit N. Getz, Tor S. Bjorheim and Truls Norby; Department of Chemistry, University of Oslo, Oslo, Norway.

D2.22
Lithium Ion Mobility in Sulphonate-Based Ionomer Systems Containing Quaternary Ammonium Co-Cations Yogita Oza, Luke A. O'Dell and Maria Forsyth; Institute for Frontier Materials, Deakin University ARC Centre of Excellence for Electromaterials Science (ACES), Victoria, New South Wales, Australia.

SESSION E2: Poster Session
E: Transparent Conducting Oxides
Monday Afternoon, June 15, 2015
12:00 PM
Keystone Resorts, Red Cloud Peak

E2.01
Textured Transparent Conductive Oxide Electrode having Bilayer Structure of ITiO/GAZO Prepared by D.C. Magnetron Sputtering Yoshiyuki Abe and Kazuhide Hayashi; Ichikawa Research Laboratories, Sumitomo Metal Mining Co., Ltd., Ichikawa-city, Japan.

E2.02
Effect of Different Size Silver Nano Particles on Frequency and Temperature Dependent Parameters of Discotic Liquid Crystals for Solar Cell Applications Avneesh Mishra; Centre of Material Sciences, University of Allahabad, Allahabad, India.

E2.03
On the Application of ZnO Varistor Material in Piezotronics Till Froemling[1], Raschid Baraki[1], Nikola Novak[1], Michael Hofstaetter[2], Peter Supancic[2] and Juergen Roedel[1]; [1]Materials Science, Technische Universtät Darmstadt, Darmstadt, Germany; [2]ISFK, Montanuniversität Leoben, Leoben, Germany.

E2.04
Atomic Layer Deposition of Nanoscale Seed Layers for Enhanced Performance of Transparent Conducting Oxide Thin Films on Glass Stefan B. Nikodemski[1], Ryan O'Hayre[1], Arrelaine Dameron[2], David Ginley[2], John Perkins[2] and Joseph Berry[2]; [1]Metallurgical and Materials Engineering, Colorado School of Mines, Golden, Colorado, United States; [2]National Renewable Energy Laboratory, Golden, Colorado, United States.

SESSION F/H2: Poster Session: Solid State Photelectrochemistry/ High Temperature Routes to Solar Fuels
F/H: Solid State Photoelectrochemistry/High Temperature Routes to Solar Fuels
Monday Afternoon, June 15, 2015
12:00 PM
Keystone Resorts, Red Cloud Peak

F/H2.01
Material Design Criteria for Solar-to-Fuel Perovskites: Lower Temperature-Operation Range with Strontium and Cobalt Doped Lanthanum Chromates Alexander H. Bork, Markus Kubicek, Michal Struzik and Jennifer Rupp; Materials - Electrochemical Materials, ETH Zürich, Zürich, Switzerland.

F/H2.02
Thermodynamics of Praseodymium-Doped Ceria for Thermochemical Water Splitting Timothy C. Davenport[1], Webster Guan[1] and Sossina M. Haile[2]; [1]California Institute of Technology, Pasadena, California, United States; [2]Northwestern University, Evanston, Illinois, United States.

F/H2.03
Investigation on Nonstoichiometric Perovskite Oxides of $Sr_{1-x}La_xMn_{1-y}Al_yO_{3-\delta}$ for Solar Thermochemical Hydrogen Production Debora Barcellos[1], Jianhua Tong[1], Michael Sanders[1], Anthony McDaniel[2] and Ryan O'Hayre[1]; [1]Metallurgical & Materials Engineering, Colorado School of Mines, Golden, Colorado, United States; [2]Sandia National Laboratories, Livermore, California, United States.

F/H2.04
Polarization Enhanced Transport of Hot Carriers in Liquid/InGaN Semiconductor Junctions Blair C. Connelly, Anand V. Sampath, Ryan W. Enck, Chad S. Gallinat, Stephen B. Kelley, Nathaniel T. Woodward, Grace D. Metcalfe, David R. Baker, Cynthia A. Lundgren, Hongen Shen, Meredith L. Reed and Michael Wraback; US Army Research Laboratory, Adelphi, Maryland, United States.

F/H2.05
Electrocatalyst-Semiconductor Interfaces in Water Splitting Photoelectrodes Shannon W. Boettcher; Chemistry, University of Oregon, Eugene, Oregon, United States.

F/H2.06
Photoelectrochemical Water Splitting Promoted with a Disordered Surface Layer Created by Electrochemical Reduction Pengli Yan[1, 2], Yang Gan[1] and Can Li[2]; [1]Harbin Institute of Technology, Harbin, China; [2]Dalian Institute of Chemical Physics, Chinese Academy of Sciences, Dalian, China.

F/H2.07
Comprehensive Photoelectric Characterization of Dye-Sensitized Solar Cells Dang-Thanh Nguyen[1], Seok-Jae Kim[3], Eui-Chol Shin[1], Soon-Hyung Kang[2], Eun-Mi Han[3] and Jong-Sook Lee[1]; [1]School of Materials Science and Engineering, Chonnam National University, Gwangju, Korea (the Republic of); [2]Department of Chemistry Education, Chonnam National University, Gwangju, Korea (the Republic of); [3]School of Applied Chemical Engineering, Chonnam National University, Gwangju, Korea (the Republic of).

F/H2.08
Impedance Spectroscopy of Various ZnO Photoelectrodes Prepared by Solution Method Dang-Thanh Nguyen, Dong-Chun Cho, Eui-Chol Shin and Jong-Sook Lee; School of Materials Science and Engineering, Chonnam National University, Gwangju, Korea (the Republic of).

F/H2.09
Transport Properties of the Heterojunction Formed between a Fe/Y-Codoped $BaZrO_3$ Mixed Conductor and a Ti-Doped Fe_2O_3 Light Absorber for an Elevated-Temperature Solid-State Photoelectrochemical Cell Madhur Boloor, Xiaofei Ye, Liming Zhang, Nicholas A. Melosh and William C. Chueh; Materials Science and Engineering, Stanford University, Fremont, California, United States.

F/H2.10
Polarity and Doping Effects on the Photoelectrochemial Performance of ZnO Single Crystalline Anode by In-Depth Impedance Spectroscopy Eui-Chol Shin[1], Dang-Thanh Nguyen[1], Joachim Maier[2] and Jong-Sook Lee[1]; [1]Materials Science and Engineering, Chonnam National University, Gwang-Ju, Korea (the Republic of); [2]Max Planck Institute for Solid State Research, Stuttgart, Germany.

F/H2.11
Impedance Spectroscopy on Fe_2O_3 Films Prepared by Anodization for Photoelectrochemical Applications Eui-Chol Shin[1], Dong-Chun Cho[1], Dang-Thanh Nguyen[1], Soon-Hyung Kang[2], Hui-Kyung Park[1], Jaeyeong Heo[1] and Jong-Sook Lee[1]; [1]Materials Science and Engineering, Chonnam National University, Gwang-Ju, Korea (the Republic of); [2]Chemistry Education, Chonnam National University, Gwang-ju, Korea (the Republic of).

F/H2.12
Cation-Control of Aggregation in the Conjugated Polyelectrolyte TFB Meilin Li and Stefan Adams; Materials Science & Eng., National University of Singapore, Singapore, Singapore.

SESSION J1: Poster Session I
J: Permeation Membranes
Monday Afternoon, June 15, 2015
12:00 PM
Keystone Resorts, Red Cloud Peak

J1.01
Hydrogen Membranes Based on Group-IV Metal Nitrides Yoshitaka Aoki[1, 2], Chiharu Kura[1], Etsushi Tsuji[1] and Hiroki Habazaki[1]; [1]Faculty of Engineering, Hokkaido University, Sapporo, Japan; [2]JST-PRESTO, Kawaguchi, Japan.

J1.02
Synthesis and Characterization of Chitosan/Sulfonated Poly(terephthalate) Polyelectrolyte Complexes and Study of Its Effects on Water Vapor Flux in Commercial Polycarbonate Membranes Rayane d. Vale; Chemistry, Universidade Federal de São Carlos, São Carlos, Brazil.

J1.03
The Effect of Compatibilizer in sPEEK/PVdF/UAN Composite Membrane for Vanadium Redox Flow Battery Seon G. Rho[1] and Ho Y. Jung[2]; [1]School of Applied Chemical Engineering, Chonnam National University, Gwangju, Korea (the Republic of); [2]Department of Environment & Energy Engineering, Chonnam National University, Gwangju, Korea (the Republic of).

J1.04
Nickel Nanocatalyst Exsolution on Modified $La_{0.75}Sr_{0.25}Cr_{0.5}Mn_{0.5}O_3$ and $La_{0.75}Sr_{0.25}Cr_{0.5}Fe_{0.5}O_3$ Perovskites for the Fuel Oxidation Layer of Oxygen Transport Membranes Despoina Papargyriou and John T. Irvine; School of Chemistry, University of St Andrews, St Andrews, United Kingdom.

J1.05
Surface Characterization of Dual-Phase Oxygen Transport Membrane by Low Energy Ion Scattering (LEIS) Chi Ho Wong, Stephen Skinner and John Kilner; Materials, Imperial College London, London, United Kingdom.

J1.06
A and B Site Co-Doped Lanthanum Chromite Perovskite – Doped Zirconia Fluorite Composites for Oxygen Transport Membrane Systems Sapna Gupta[1, 2] and Prabhakar Singh[1, 2];[1]Materials Science and Engineering, University of Connecticut, Storrs, Connecticut, United States; [2]Center for Clean Energy Engineering, University of Connecticut, Storrs, Connecticut, United States.

J1.07
Influence of the Oxygen Partial Pressure on the Oxygen Diffusion and Surface Exchange Coefficients in Mixed Conductors Jean-Marc Bassat; ICMCB-CNRS, Pessac , France.

J1.08
Scaling of Oxygen Transport Membranes Marie-Laure Fontaine[1], Christelle Denonville[1], Adam Stevenson[2], Christian His[2], Emmanuel Mercier[2], Caroline Tardivat[2], Xing Wen[1], Jonathan Polfus[1], Ove Paulsen[1], Paul Inge Dahl[1], Partow Henriksen[1] and Rune Bredesen[1]; [1]Materials and Chemistry, SINTEF, Oslo, Norway; [2]Saint Gobaine CREE, Cavaillon, France.

J1.09
Freeze-Casting Technique for the Manufacture of Hierarchical Porous Planar and Tubular Support for Gas Separation Ceramic Membranes Cyril Gaudillere, Julio Garcia-Fayos, Jose M. Serra and Sonia Escolastico; ITQ (UPV-CSIC), Valencia, Spain.

J1.10
Cation-Site Determination in $(Ba_{0.5}Sr_{0.5})(Co_{0.8}Fe_{0.2})O_{3-d}$ by Exploiting Channelling Effects in Transmission Electron Microscopy Matthias Meffert, Heike Stoermer and Dagmar Gerthsen; Laboratory for Electron Microscopy (LEM), Karlsruhe Institute of Technology (KIT), Karlsruhe, Germany.

SESSION K1: Poster Session I
K: Proton-Conducting Oxides
Monday Afternoon, June 15, 2015
12:00 PM
Keystone Resorts, Red Cloud Peak

K1.01
Defect Chemistry of $LaCrO_3$ from First Principles Calculations Sarmad W. Saeed, Tor S. Bjorheim, Reidar Haugsrud and Truls Norby; Department of Chemistry, University of Oslo, Oslo, Norway.

K1.02
Investigation of Sinterability of $BaCe_{0,9}Y_{0,1}O_{3-\delta}$ at Several Schedules Profiles Huyra E. Araujo[3, 2] and Dulcina M. Souza[1, 3]; [1]Materials Engineering Department, Federal University of Sao Carlos, Sao Carlos, Brazil; [2]Federal Institute of Education, Science and Technology, Piracicaba, Brazil; [3]PPGCEM-UFSCar, Sao Carlos, Brazil.

K1.03
Lattice Expansion upon Hydration of Doped Barium Cerate/Zirconate (BZY/BCZY) Proton Conducting Ceramics as Measured by High Temperature X-Ray Diffraction (HTXRD) Grant A. Hudish[1], Sandrine Ricote[2], Anthony Manerbino[1], W. G. Coors[1] and Neal P. Sullivan[2]; [1]R&D, CoorsTek, Golden, Colorado, United States; [2]Department of Mechanical Engineering, Colorado School of Mines, Golden, Colorado, United States.

K1.04
Proton Dissolution in $BaZr_{1-x}Y_xO_{3-\delta}$ Genki Imai[1], Takashi Nakamura[2] and Koji Amezawa[2]; [1]Graduate School of Engineering, Tohoku University, Sendai, Japan; [2]Institute of Multidisciplinary Research for Advanced Materials, Tohoku University, Sendai, Japan.

K1.05
Incorporation and Dissociation Behavior of Protons in $BaZrO_3$-Based Perovskite-Type Proton Conductors Tomohiro Ishiyama[1, 3], Haruo Kishimoto[1, 3], Katherine D. Bagarinao[1, 3], Katsuhiko Yamaji[1, 3], Toshiaki Yamaguchi[2, 3] and Yoshinobu Fujishiro[2, 3]; [1]Energy Technology Research Institute, National Institute of Advanced Industrial Science and Technology, Tsukuba, Japan; [2]Advanced Manufacturing Research Institute, National Institute of Advanced Industrial Science and Technology, Nagoya, Japan; [3]CREST, Japan Science and Technology Agency (JST), Saitama, Japan.

K1.06
First Principles Calculations of Carrier Trapping in Proton Conductive Acceptor-Doped $BaZrO_3$ Akihide Kuwabara, Craig A. Fisher and Hiroki Moriwake; Japan Fine Ceramics Center, Nagoya, Japan.

K1.07
Densification and Microstructural Evolution in NiO-Added $BaZr_{0.8}Y_{0.2}O_{3-\delta}$ Ceramics Young-Woo Ryu, Joon-Hyung Lee, Young-Woo Heo and Jeong-Joo Kim; School of Materials Science & Engineering, Kyungpook National University, Daegu, Korea (the Republic of).

K1.08
Dopant Concentration Dependence of Electrical Transport in Y-Doped $BaZrO_3$ Shogo Miyoshi, Ayano Ebara and Shu Yamaguchi; Department of Materials Engineering, The University of Tokyo, Tokyo, Japan.

K1.09
Proton Trapping: A Key to Control Proton Transport in Oxides Yoshihiro Yamazaki[1, 4], Yuji Okuyama[2], Jason Potticary[3], Kentaro Yamamoto[1] and Sossina M. Haile[3]; [1]Inamori Frontier Research Center, Kyushu University, Fukuoka, Japan; [2]Miyazaki University, Miyazaki, Japan; [3]California Institute of Technology, Pasadena, Colorado, United States; [4]Japan Science and Technology Agency, Kawaguchi, Japan.

K1.10
The Effect of Yttrium Source on the Microstructure and Hygroscopic Behavior of $BaCe_{0.8}Y_{0.2}O_{3-\delta}$ Using ZnO as Sintering Aid Elcio L. Pires; Materials Engineering, Federal University of São Carlos, São Carlos, Brazil.

K1.11
Y-doped $BaZrO_3$ Thin Films for Water Electrolysis at Intermediate Temperatures Deposited by Aerosol Assisted Chemical Vapor Deposition Alexander Benes[2], Oliver Clemens[2,1], Wolfram Jaegermann[3] and Horst Hahn[2, 1]; [1]Institute for Nanotechnology, Karlsruhe Institute of Technology (KIT), Karlsruhe, Germany; [2]Joint Research Laboratory Nanomaterials, Technical University of Darmstadt and Karlsruhe Institute of Technology (KIT), Darmstadt, Germany; [3]Surface Science Group, Technical University of Darmstadt, Darmstadt, Germany.

K1.12
Investigation of $Ba_{1-x}Gd_{0.8}La_{0.2+x}Co_2O_{6-\delta}$ (X = 0 - 0.5) as Oxygen Electrode Material for Proton Conducting Fuel Cells and Electrolyzer Cells Ragnar Strandbakke, Einar Vollestad and Truls Norby; Department of Chemistry, University of Oslo, Oslo, Norway.

K1.13
Channel-Level Modeling of Protonic Ceramic Fuel Cells and Model Calibration Kevin J. Albrecht[1], Chuancheng Duan[2], Robert J. Braun[1] and Ryan P. O'Hayre[2]; [1]Mechanical Engineering, Colorado School of Mines, Golden, Colorado, United States; [2]Materials Science, Colorado School of Mines, Golden, Colorado, United States.

K1.14
Defect Entropies of $BaZrO_3$ from First Principles Phonon Calculations Tor S. Bjorheim[1], Eugene Kotomin[2] and Joachim Maier[2]; [1]FASE, Department of Chemistry, University of Oslo, Oslo, Norway; [2]Max Planck Institute for Solid State Research, Stuttgart, Germany.

K1.15
Effect of Al_2O_3 and Y_2O_3 Addition on Proton Conductivity of Electrochemically Proton Injected Phosphate Glasses Takuya Yamaguchi[1], Kanji Sakuragi[1], Takahisa Omata[1], Tomohiro Ishiyama[2], Junji Nishii[3], Toshiharu Yamashita[4], Hiroshi Kawazoe[4], Naoaki Kuwata[5] and Junichi Kawamura[5]; [1]Graduate School of Engineering, Osaka University, Suita, Japan;[2]National Institute of Advanced Industrial Science and Technology (AIST), Tsukuba, Japan; [3]Research Institute for Electronic Science, Hokkaido University, Sapporo, Japan; [4]Kawazoe Frontier Technologies Corp., Yokohama, Japan; [5]Tohoku University, Sendai, Japan.

K1.16
Hydrogen Induced Rupture of Si-O Bonds in Amorphous Silicon Dioxide Al-Moatasem El-Sayed[1, 2], Matthew Watkins[1, 2], Tibor Grasser[3], Valery Afanas'ev[4] and Alexander Shluger[1,2]; [1]Department of Physics and Astronomy, University College London, London, United Kingdom; [2]London Centre for Nanotechnology, London, United Kingdom; [3]Institute for Microelectronics, Technische Universitat Wien, Vienna, Austria; [4]Department of Physics, University of Leuven, Leuven, Belgium.

K1.17
Defect Associations as a Potential Cause for Limiting Proton Concentrations in Acceptor Doped Oxides Andreas Loken, Tor S. Bjorheim and Reidar Haugsrud; Department of Chemistry, University of Oslo, Oslo, Norway.

POSTER PRESENTATIONS

TUESDAY June 16, 2015

SESSION A6: Poster Session II
A: Solid Oxide Fuel Cells and Electrolyzers
Tuesday Afternoon, June 16, 2015
5:20 PM
Keystone Resorts, Red Cloud Peak

A6.01
Thermal Stability and Compatibility with SOFC/PCFC Electrolyte of $La_4BaCu_5O_{13+\delta}$ and $La_{6.4}Sr_{1.6}Cu_8O_{20\pm\delta}$ Perovskite Monica V. Sandoval[1, 2], Giovanny Martinez[1], Santiago Vasquez-Cuadriello[3], Mario A. Macias[1], Leopoldo Suescun[3], Pascal Roussel[2] and Gilles H. Gauthier[1]; [1]Grupo INTERFASE, Universidad Industrial de Santander, Bucaramanga, Colombia;[2]Unité de Catalyse et de Chimie du Solide, Université Lille 1, Lille, France; [3]Facultad de Química - Cryssmat-Lab/DETEMA , Universidad de la República, Montevideo, Uruguay.

A6.02
Electrochemical Studies of $GdPrBaCo_2O_{5+\delta}$ and $GdPrBaCoFeO_{5+\delta}$ Cathodes for Oxide Ion and Proton Conducting Solid Oxide Fuel Cells Kalpana Singh, Ashok Baral and Venkataraman Thangadurai; Department of Chemistry, University of Calgary, Calgary, Alberta, Canada.

A6.03
Development of the Composite Electrodes for the New $CaZr_{0.95}Sc_{0.05}O_{3-\delta}$ Proton-Conducting Electrolyte Elena Pikalova[1, 2], Nina Bogdanovich[1], Alexander Kolchugin[1], Dimitry Bronin[1, 3], Anton Kuz'min[1] and Azat Khasanov[3]; [1]Institute of High Temperature Electrochemistry UB RAS, Ekaterinburg, Russian Federation; [2]Department of Environmental Economics, Ural Federal University, Ekaterinburg, Russian Federation; [3]Institute of Natural Sciences, Department of Chemistry, Ural Federal University, Ekaterinburg, Russian Federation.

A6.04
A Layered Perovskite Oxide $PrBaCo_2O_{5+\delta}$ as Cathode for Highly Stable $BaCe_{0.1}Zr_{0.8}Y_{0.1}O_{3-\delta}$ Based Protonic Ceramic Fuel Cells (PCFCs) Hanping Ding and Neal P. Sullivan; Mechanical Engineering, Colorado School of Mines, Golden, Colorado, United States.

A6.05
Steam Electrode Development for BCZY Based High Temperature Protonic Electrolysers Nuria Bausa, Cecilia Solís, Sonia Escolastico and Jose M. Serra; Instituto de Tecnología Química (UPV-CSIC), Valencia, Spain.

A6.06
Atomic Layer Deposition of Dense Nano-Thin Platinum Films for Low-Temperature Solid Oxide Fuel Cells Sanghoon Ji[1], Taehyun Park[2], Gu Young Cho[2], Waqas H. Tanveer[2], Wonjong Yu[2] and Suk Won Cha[2]; [1]Graduate School of Convergence Science and Technology, Seoul National University, Seoul, Korea (the Republic of); [2]Department of Mechanical Engineering, Seoul National University, Seoul, Korea (the Republic of).

A6.07
Development of Low Temperature Operating Micro-SOFC System for Mobile Electronic Devices Shoya Murayama, Fumitada Iguchi, Makoto Shimizu and Hiroo Yugami; Graduate School of Engineering, Tohoku University, Sendai, Japan.

A6.08
$Ba_{0.95}La_{0.05}FeO_{3-\delta}$-Graphene as a Low-Cost and Synergistic Catalyst for Oxygen Evolution Reaction Mattia Saccoccio[1], Hong Zhao[1], Chi Chen[1], Dengjie Chen[1], Jian Wang[1], Yang Gao[1], Hei Ting Wan[1] and Francesco Ciucci[1, 2]; [1]Department of Mechanical and Aerospace Engineering, The Hong Kong University of Science and Technology, Clear Water Bay, Hong Kong; [2]Department of Chemical and Biomolecular Engineering, The Hong Kong University of Science and Technology, Clear Water Bay, Hong Kong.

A6.09
Investigation of Low Temperature Operation of Fe-Air Battery Using YSZ Electrolyte Takaaki Sakai[1, 2], Masako Ogushi[2], Atsushi Inoishi[3], Shintaro Ida[2] and Tatsumi Ishihara[2];[1]Center for Molecular Systems, Kyushu University, Fukuoka, Japan; [2]Department of Applied Chemistry, Faculty of Engineering, Kyushu University , Fukuoka, Japan; [3]Research and Education Center for Advanced Energy Materials, Devices, and Systems, Kyushu University, Fukuoka, Japan.

A6.10
Improving the Material Efficiency or Substitution of Platinum in the System Pt/YSZ Gesa Beck[1] and Christoph Bachmann[2]; [1]Physics, Chair of Resource Strategies, Augsburg, Germany; [2]Institute of Physical Chemistry, Justus-Liebig-University, Giessen, Germany.

A6.11
Conductivity and Structure of Sub-Micrometric $SrTiO_3$ -YSZ Composites Enrique Ruiz-Trejo[1], Nikolaos Bonanos[2], Karl Thyden[2] and Mogens Mogensen[2]; [1]Earth Science and Engineering, Imperial College London, London, United Kingdom; [2]Department of Energy Conversion and Storage, Technical University of Denmark, Roskilde, Denmark.

A6.12
Microstructure and Electrochemical Properties of CeO2-Based Cathodes for SOEC Application Wenqiang Zhang, Bo Yu and Jingming Xu; Tsinghua University, Beijing, China.

A6.13
Structural, Electrical and Electrochemical Properties of Calcium-Doped Lanthanum Nickelate Alexandr Kolchugin[1], Elena Pikalova[1, 3], Nina Bogdanovich[1], Dimitry Bronin[1], Sergey Pikalov[2] and Irina Nikolaenko[4]; [1]Institute of High Temperature Electrochemistry UB RAS, Ekaterinburg, Russian Federation; [2]Institute of Metallurgy UB RAS, Ekaterinburg, Russian Federation; [3]Department of Environmental Economics, Ural Federal University, Ekaterinburg, Russian Federation; [4]Institute of Solid State Chemistry UB RAS, Ekaterinburg, Russian Federation.

A6.14
Defect Structure and Related Properties of $YBaCo_2O_{6-\delta}$ Dmitry S. Tsvetkov, Anton L. Sednev, Ivan L. Ivanov, Dmitry A. Malyshkin and Andrey Y. Zuev; Department of Chemistry, Ural Federal University, Ekaterinburg, Russian Federation.

A6.15
Synthesis and Study of the Ordered Double Perovskite $NdBaMn_2O_{5+d}$ to be Used as Symmetric SOFC Electrode Material Gilles H. Gauthier[2], Konrad Swierczek[1], Pascal Roussel[3], Oscar L. Pineda[2, 1] and Zulma L. Moreno[2]; [1]AGH University of Science and Technology, Cracow, Poland; [2]Grupo INTERFASE, Universidad Industrial de Santander, Bucaramanga, Colombia; [3]Université Lille 1, Université Lille Nord de France, Lille, France.

A6.16 Withdrawn

A6.17
TOF-SIMS Characterization of Impurity Enrichment and Redistribution in Solid Oxide Electrolysis Cells during Operation Ragnar Kiebach, Kion Norrman, Ming Chen and Peter V. Hendriksen; DTU, Roskilde, Denmark.

A6.18
Role of Gadolinia-Doped Ceria Interlayer Microstructure and Orientation on the Cation Diffusion Behavior in LSCF/GDC/YSZ Model Heterostructures Jeffrey C. De Vero[1], Katherine D. Bagarinao[1], Do-Hyung Cho[1], Haruo Kishimoto[1], Katsuhiko Yamaji[1], Teruhisa Horita[1] and Harumi Yokokawa[1, 2]; [1]National Institute of Advanced Industrial Science and Technology, Tsukuba, Japan; [2]Institute of Industrial Science, University of Tokyo, Tokyo, Japan.

A6.19
The Utility of Model Electrodes for the Separation of Current Pathways in Solid State Electrochemistry Alexander K. Opitz, Markus Kubicek, Stefanie Taibl, Tobias Huber, Gerald Holzlechner, Herbert Hutter and Juergen Fleig; Institute of Chemical Technologies and Analytics, Vienna University of Technology, Vienna, Austria.

A6.20
Rapid Measurement of Chemical Diffusion in Oxide Thin Films by Color Front Motion Tracking Jae Jin Kim[1], Stuart N. Cook[1], Di Chen[1], Sean R. Bishop[1] and Harry L. Tuller[1, 2];[1]Materials Science and Engineering, Massachusetts Institute of Technology, Cambridge, Massachusetts, United States; [2]International Institute for Carbon-Neutral Energy Research (WPI-I2CNER), Kyushu University, Fukuoka, Japan.

A6.21
TraceX: Isotope Exchange Data Analysis, Back-Diffusion Simulation and Profile Fitting Samuel J. Cooper, Mathew Niania and John A. Kilner; Department of Materials, Imperial College London, London, United Kingdom.

A6.22
Impedance Spectroscopy Analysis Inspired by Evolutionary Programming as a Diagnostic Tool for SOEC Zohar Drach, Shany Hershkovitz, Sioma Baltianski and Yoed Tsur; Chemical Engineering, Technion Israel Institute of Technology, Haifa, Israel.

A6.23
Long-Term Degradation of $La_{0.6}Sr_{0.4}Co_{0.2}Fe_{0.8}O_{3-\delta}$ IT-SOFC Cathodes due to Silicon Poisoning Martin Perz[1], Edith Bucher[1], Christian Gspan[2, 3], Joerg Waldhaeusl[1], Ferdinand Hofer[2, 3] and Werner Sitte[1]; [1]Chair of Physical Chemistry, Montanuniversitaet Leoben, Leoben, Austria; [2]Institute for Electron Microscopy and Nanoanalysis (FELMI), Graz University of Technology, Graz, Austria; [3]Graz Center for Electron Microscopy (ZFE), Austrian Cooperative Research (ACR), Graz, Austria.

A6.24
Degradation Mechanisms of Cathode Materials for Intermediate Temperature-Solid Oxide Fuel Cells Soo-Yeon Jo, Ka-Young Park and Jun-Young Park; Department of Nanotechnology and Advanced Materials Engineering, Sejong University, Seoul, Korea (the Republic of).

A6.25
Transmission Electron Microscopy Study of Cr Poisoning of LSCF Cathodes Na Ni and Stephen Skinner; Materials, Imperial College London, London, United Kingdom.

A6.26
Effects of Chemical and Interfacial Strain on the Transport and Mechanical Properties of $PrCoO_3$ Mabel Lew, Stevin Pramana, Andrea Cavallaro, Ji Wu and Stephen Skinner; Materials, Imperial College London, Kingston, United Kingdom.

A6.27
Electrical Properties of LSM-$Bi_3Y_{0.9}W_{0.1}O_{6.15}$ Composite Solid Membranes Marcin Malys[1], Wojciech Wrobel[1], Marcin Dudz[1], Marzena Leszczynska-Redek[1], Anna Borowska-Cenkowska[1], Maciej Wojcik[1], Kuan-Zong Fung[2], Isaac Abrahams[3] and Franciszek Krok[1]; [1]Faculty of Physics, Warsaw University of Technology, Warszawa, Poland; [2]Material Science and Engineering, National Cheng Kung University, Tainan, Taiwan; [3]Materials Research Institute, Queen Mary University of London, London, United Kingdom.

A6.28
Optimization of Pr_2CuO_4-$Ce_{0.9}Gd_{0.1}O_{1.95}$ Composite Cathode for SOFC Application Liudmila Kolchina[1], Nikolay Lyskov[2] and Galina Mazo[1]; [1]Chemistry Department, Lomonosov Moscow State University, Moscow, Russian Federation; [2]Institute of Problems of Chemical Physics RAS, Chernogolovka, Russian Federation.

A6.29
Optimized PBCO-PCO-CGO Cathode for IT-SOFC Samir Boulfrad[1], Stevin Pramana[2], Mabel Lew[2], Udo Schwingenschloegl[1], Enrico Traversa[1] and Stephen Skinner[2]; [1]Physical Sciences and Engineering, King Abdullah University of Science and Technology (KAUST), Thuwal, Saudi Arabia; [2]Department of Materials , Imperial College London, London, United Kingdom.

A6.30
Optimization of $Ba_2Co_9O_{14}$ as an Innovative SOFC's Cathode Material Ibtissam Kehal, Marie-Helene Chambrier, Aurelie Rolle, Sylvie Daviero-Minaud, Rose-Noelle Vannier and Xavier Flandre; Unité de Catalyse et de Chimie du Solide, Université Lille, Villeneuve d'Ascq, France.

A6.31
Electrochemical Characterization of B-Site Cation-Excess $Pr_2Ni_{0.75}Cu_{0.25}Ga_{0.05}O_{4+\delta}$ Cathode for IT-SOFCs Yuan Ji and Xiangwei Meng; Jilin University, Changchun, China.

A6.32
$SrCo_{1-x}Mo_xO_{3-\delta}$ Pervoskites as Cathode Materials for $LaGaO_3$-Based Intermediate-Temperature Solid Oxide Fuel Cells Rui Wang, Fangjun Jin and Tianmin He; College of Physics, Jilin University, Changchun, China.

A6.33
Tailoring of the Chemical Stability of (Ba,Sr)(Co,Fe)O_3-Based Perovskite Mixed Conductors Fang Wang[1], Koki Igarashi[2], Takashi Nakamura[1], Keiji Yashiro[3], Junichiro Mizusaki[1]and Koji Amezawa[1]; [1]Institute of Multidisciplinary Research for Advanced Materials, Tohoku University, Sendai, Japan; [2]Graduate School of Engineering, Tohoku University, Sendai, Japan; [3]Graduate School of Environmental Studies, Tohoku University, Sendai, Japan.

A6.34
$NdBa_{1-x}Co_2O_{5+\delta}$ as Cathode Materials for Intermediate Temperature Solid Oxide Fuel Cell Jialing Sun[1, 2], Xiaomei Liu[1], Lili Zhu[1], Fei Han[1], Hailin Bi[1], Haopeng Wang[1], Shenglong Yu[1] and Li Pei[1]; [1]Key Laboratory of Physics and Technology for Advanced Batteries,Physics Department, Jilin University, Changchun, China; [2]Beihua University, Jilin, China.

A6.35
Effect of Thermal Reduction on Electrical Properties of Protecting Oxides for SOFC Interconnect Applications Kuan-Zong Fung[1, 3], Shu-Yi Tsai[1] and Chung-Ta Ni[2]; [1]Materials Science and Engineering, National Cheng Kung University, Tainan City, Taiwan; [3]Research Center for Energy Technology and Strategy, National Cheng Kung University, Tainan City, Taiwan.

A6.36 moved A9.07

A6.37
Deconvolution of Four Transmission-Line-Model Impedances in Ni-YSZ/YSZ/LSM Solid Oxide Cells and Mechanistic Insights Eui-Chol Shin, Jianjun Ma, Pyung-An Ahn, Hyun-Ho Seo, Dang-Thanh Nguyen and Jong-Sook Lee; Materials Science and Engineering, Chonnam National University, Gwang-Ju, Korea (the Republic of).

A6.38
The Electrolyte Spreading Resistance - More than a Resistive Offset Andreas Nenning, Michael Doppler and Juergen Fleig; Institute of Chemical Technologies and Analytics, Vienna University of Technology, Vienna, Austria.

A6.39
Electrical Characterization of the Active Cathode Area in Solid Oxide Fuel Cells Tzvia Radlauer[1], Sioma Baltianski[2], Ilan Riess[3] and Yoed Tsur[2]; [1]Energy Engineering, Technion, Haifa, Israel; [2]Chemical Engineering, Technion, Haifa, Israel; [3]Physics, Technion, Haifa, Israel.

A6.40
Electronic Conductivity in Yttria-Stabilised Zirconia under a Small *dc* Bias Nahum Maso[1, 2] and Anthony R. West[2]; [1]Chemistry, University of Oslo, Oslo, Norway; [2]Materials Science and Engineering, The University of Sheffield, Sheffield, United Kingdom.

A6.41
Impedance Study on LSGM Single Crystals Ghislain M. Rupp[1], Michal Glowacki[2] and Juergen Fleig[1]; [1]Institute of Chemical Technologies and Analytics - Electrochemistry, Vienna University of Technology, Vienna, Austria; [2]Institute of Physics, Polish Academy of Sciences, Warsaw, Poland.

A6.42 WITHDRAWN

A6.43
Synthesis and Study of Solid Electrolytes $Nd_{5-X}Ln_XMo_3O_{16}$ (Ln = Sm, Eu, Gd) Lyudmyla I. Stackpool[1], Konstantin Chebyshev[2] and Lyudmila Pasechnik[2]; [1]Chemistry and Geology, Minnesota State University, Mankato, Mankato, Minnesota, United States; [2]Department of Inorganic Chemistry, Donetsk National University, Donetsk, Ukraine.

A6.44
Modification of Surface Oxide of Porous Fe-Cr-Al Alloy by Coating and Heat-Treatment for the Application of Metal Supported SOFCs Hung-Cuong Pham[1], Shunsuke Taniguchi[2,3,4], Yuko Inoue[4], Jyh-Tyng Chou[5], Toru Izumi[6], Koji Matsuoka[6] and Kazunari Sasaki[1, 2, 7]; [1]Hydrogen Energy Systems, Kyushu University, Fukuoka, Japan; [2]International Research Center for Hydrogen Energy, Kyushu University, Fukuoka, Japan; [3]Center for Co-evolutional Social Systems, Kyushu University, Fukuoka, Japan; [4]Next-Generation Fuel Cell Research Center (NEXT-FC), Kyushu University, Fukuoka, Japan; [5]Kurume National College of Technology, Fukuoka, Japan; [6]JX Nippon Oil and Energy Corporation, Yokohama, Japan;[7]International Inst, for Carbon Neutral Energy Research (WPI-I2CNER), Kyushu University, Fukuoka, Japan.

A6.45
Crystal Structure of $R_{10}Mo_6O_{33}$ (R = Nd, Pr) from 3 K to 973 K by Neutron Powder Diffraction Yoshihisa Ishikawa[1, 2], Sergey A. Danilkin[3], Maxim Avdeev[3], Valentina I. Voronkova[4] and Takashi Sakuma[2]; [1]Institute of Materials Structure Science, High Energy Accelerator Research Organization, Tokai, Japan; [2]Institute of Applied Beam Science, Ibaraki University, Mito, Japan; [3]Bragg Institute, Australian Nuclear Science and Technology Organization, Kirrawee, New South Wales, Australia; [4]Moscow State University, Leninskie Gory, Russian Federation.

A6.46
Long-Time Testing of Ni-YSZ Substrates under Operating Conditions Denis Osinkin[1], Dimitry Bronin[1, 2], Robert Steinberger-Wilckens[3], L.G.J. de Haart[4] and Josef Mertens[4];[1]Laboratory of SOFC, Institution of High Temperature Electrochemistry, Yekaterinburg, Russian Federation; [2]Ural Federal University, Yekaterinburg,, Russian Federation; [3]University of Birmingham, Birmingham, United Kingdom; [4]Institute of Energy and Climate Research, Fundamental Electrochemistry (IEK-9) Forschungszentrum Jülich GmbH, Jülich, Germany.

A6.47
Carbon Deposition and Sulfur Poisoning in Mo-Containing Anode Materials for SOFCs Studied in CO and CH_4 Fuels Kun Zheng and Konrad Swierczek; AGH University of Science and Technology, Faculty of Energy and Fuels, Kraków, Poland.

A6.48
Model-Composite Electrodes as a Tool to Evaluate Alternative SOFC Anode Materials and Their Sulphur Poisoning Behaviour Matthias Gerstl[2], Michael Doppler[1], Marco Brandner[3], Martin Bram[4], Juergen Fleig[1] and Alexander K. Opitz[1]; [1]Electrochemistry, Vienna University of Technology, Wien, Austria; [2]Electrochemistry, Vienna University of Technology, Vienna, Austria; [3]Innovation Services, Plansee SE, Reutte, Austria; [4]Institute of Energy and Climate Research, Forschungszentrum Juelich GmbH, Juelich, Germany.

A6.49
Electrical Conductivity and Redox Behavior of Donor and Acceptor Co-Substituted $SrTiO_3$ as Fuel Electrode Material Aleksey Yaremchenko, Javier Macias and Jorge Frade; CICECO, Department of Materials and Ceramic Engineering, University of Aveiro, Aveiro, Portugal.

A6.50
Chemical Compatibility of Doped Yttrium Chromite and Ceria Composite Anode with YSZ Electrolyte Kang Yan[1], Haruo Kishimoto[1], Katherine D. Bagarinao[1], Katsuhiko Yamaji[1], Teruhisa Horita[1] and Harumi Yokokawa[1, 2]; [1]National Institute of Advanced Industrial Science and Technology, Tsukaba, Japan; [2]the University of Tokyo, Tokyo, Japan.

A6.51
In Search for Alternative Ceramic Components for SOFC Anodes: $SrVO_3$-$SrTiO_3$ Solid Solutions Javier Macias, Aleksey Yaremchenko and Jorge Frade; Department of Materials and Ceramic Engineering, University of Aveiro, Aveiro, Portugal.

A6.52
Electrochemically Modified, Robust Solid Oxide Fuel Cell Anode for Direct-Hydrocarbon Utilization Yoonseok Choi and WooChul Jung; Materials Science and Engineering, Korea Advanced Institute of Science and Technology, Daejeon, Korea (the Republic of).

A6.53
Effect of Fuel Thermal Pretreatment on the Electrochemical Performance of a Direct Lignite Coal Fuel Cell Nikolaos Kaklidis[1], Vasileios Kyriakou[3, 2], George Marnellos[1, 2], Ana Arenillas[4] and Michalis Konsolakis[5]; [1]Department of Mechanical Engineering, University of Western Macedonia, Kozani, Greece; [2]Chemical Process & Energy Resources Institute, Centre for Research & Technology Hellas, Thessaloniki, Greece; [3]Department of Chemical Engineering, Aristotle University of Thessaloniki, Thessaloniki, Greece; [4]Instituto Nacional del Carbon, Oviedo, Spain; [5]School of Production Engineering and Management, Technical University of Crete, Chania, Greece.

SESSION B2: Poster Session: PEMFC/DMFC
B: Polymer Electrolyte Fuel Cells and Electrolyzers
Tuesday Afternoon, June 16, 2015
5:20 PM
Keystone Resorts, Red Cloud Peak

B2.01
Synthesis and Characterization of Water Stable, Silicotungstic Acid Functionalized Perfluorocyclobutyl Polymer Electrolyte Andrew R. Motz, Mei-Chen Kuo and Andrew M. Herring; Chemical and Biological Engineering , Colorado School of Mines, Lakewood, Colorado, United States.

B2.02
Synthesis and Properties of Poly(phenylene)-Poly(ether ketone) Block Copolymer Electrolytes (V)-Investigation of Chemical Composition Shogo Nagaya, Masahiro Fujita, Yuko Takeoka and Rikukawa Masahiro; Sophia University, Tokyo, Japan.

B2.03
Activity of Nanographitic Structures toward Oxygen Reactions in the Solid State CsH_2PO_4 Electrochemical System Hadi Tavassol[2, 1] and Sossina M. Haile[2, 1]; [1]Material Science, California Institute of Technology, Pasadena, California, United States; [2]Material Science, Northwestern University, Evanston, Illinois, United States.

B2.04
Characterization of PBI Based High Temperature PEMFC Using Methanol Reformed Gas Properties Sung-Kwan Ryu[3], Seung-Gon Kim[1], Minjin Kim[1, 2] and Young-Jun Sohn[1, 2];[1]Korea Institute of Energy Research, Daejeon, Korea (the Republic of); [2]University of Science and Technology, Daejeon, Korea (the Republic of); [3]Chemical Engineering, Yonsei University, Seoul, Korea (the Republic of).

B2.05
Optimization of the Lifetime for Polybenzimidazole Based High Temperature PEM Fuel Cell Stacks Minjin Kim, Young-Jun Shon and Seung-Gon Kim; Fuel Cell Research Center, Korea Institute of Energy Research, Daejeon, Korea (the Republic of).

B2.06
Application of Block Copolymers Having Aliphatic Side Chains to Cathode Ionomer (II) - Properties Related to Gas Transport Ken Akizuki[2, 3], Atsushi Ohma[3], Toyoaki Matsuura[1], Masahiro Yoshizawa-Fujita[1], Yuko Takeoka[1] and Masahiro Rikukawa[1]; [1]Department of Materials and Life Sciences, Faculty of Science and Technology, Sophia University, Tokyo, Japan;[2]Department of Materials and Life Sciences, Sophia University, Tokyo, Japan; [3]Nissan Research Center, Nissan Motor Co., Ltd., Kanagawa, Japan.

B2.07
Zirconium Phosphate-Grafted-Sulfoanted Polystyrene/Nafion Composite Membranes for Direct Methanol Fuel Cell Kun-lin Liu, Chi-Yang Chao and Cheng-Wei Pai; Materials Science and Engineering, National Taiwan University, Taipei, Taiwan.

SESSION C8: Poster Session II
C: Electrodes and Solid Electrolytes for Batteries
Tuesday Afternoon, June 16, 2015
5:20 PM
Keystone Resorts, Red Cloud Peak

C8.01
Structural and Electronic Properties of Na2MnPO4F as a Cathode Material for Na-Ion Batteries Yin Zheng, Rao Huang, Yuhua Wen and Zizhong Zhu; Xiamen University, Xiamen, China.

C8.02
Investigation of Capacity Fading of Li-Rich Layer-Structured Cathode Materials Kuan-Zong Fung[2, 1], Shu-Yi Tsai[1, 2], Chung-Ta Ni[1, 2] and Wei-Zhi Lin[1, 2]; [1]Materials Science and Engineering, National Cheng Kung University, Tainan City, Taiwan; [2]Research Center for Energy Technology and Strategy, National Cheng Kung University, Tainan City, Taiwan.

C8.03
Improvement of Cycling Performance of $LiMn_{1.5}Ni_{0.5}O_4$ Cathodes by Surface Treatment with Trimethyl Phosphite Vapor Ryosuke Okamoto[1], Kazuhiko Okubo[1], Mitsukuni Kondo[2] and Yoshiyuki Abe[1]; [1]Ichikawa Research Laboratories, Sumitomo Metal Mining Co., Ltd., Ichikawa-City, Japan; [2]Battery Research Laboratories, Sumitomo Metal Mining Co., Ltd., Niihama-city, Japan.

C8.04
Synthesis of Nanostructured $Li_3M_2(PO_4)_2F_3$ Glass-Ceramics (M = V, Fe, Ti) Tomasz K. Pietrzak, Przemyslaw P. Michalski, Agata Dorau, Anna Kaleta, Agnieszka Starobrat, Jakub Plachta, Marek Wasiucionek and Jerzy E. Garbarczyk; Physics, Warsaw University of Technology, Warszawa, Poland.

C8.05
Lithium/Polymer Electrolyte Interface Stabilization by In Situ and Ex Situ Formation of Protective Surface Layers Nassus Brown and Dale Teeters; Chemistry and Biochemistry, The University of Tulsa, Tulsa, Oklahoma, United States.

C8.06
Development of Na_3PS_4-Based Sulfide Electrolytes for All-Solid-State Batteries Masahiro Tatsumisago[1] and Akitoshi Hayashi[1, 2]; [1]Department of Applied Chemistry, Osaka Prefecture University, Sakai, Osaka, Japan; [2]ESICB, Kyoto Univ., Kyoto, Japan.

C8.07
Development of Solid Electrolyte Membranes Aude A. Hubaud[1], David Schroeder[2, 1], Brian Ingram[1] and John Vaughey[1]; [1]Argonne National Laboratory, Argonne, Illinois, United States; [2]Northern Illinois University, Dekalb, Illinois, United States.

C8.08
Reactions at Silicon Electrode Surfaces Fulya Dogan[1], Aude Hubaud[1], Zhenzhen Yang[1], Danielle Proffit[1], David Schroeder[2] and Jack Vaughey[1]; [1]Chemical Sciences and Engineering, Argonne National Laboratory, Lemont, Illinois, United States; [2]College of Engineering and Engineering Technology, Northern Illinois University, DeKalb, Illinois, United States.

C8.09
Oxygen Nonstoichiometry and Charge Transfer in the Double Perovskites $Gd_{1-x}La_xBaCo_2O_{6-\delta}$ (x=0-1) Dmitry Malyshkin, Dmitry Tsvetkov, Evgeny Sterkhov, Ivan Ivanov and Andrey Zuev; Ural Federal University, Ekaterinburg, Russian Federation.

C8.10
Synthesis and Electrochemical Performance of Carbon-Coated $0.8Li_2MnO_3$-$0.2LiCoO_2$ Cathode Material for Lithium Ion Batteries Zhuang Wang, Zhiyong Yu, Wenji Li, Mengyun Lu and Hanxing Liu; School of Materials Science and Engineering, Wuhan University of Technology, Wuhan, China.

C8.11
Advanced, Nanostructured $LiMn_2O_{4-y}S_y$ Cathode Materials Exhibiting an Outstanding Capacity and Rate Capability Marcin Molenda, Monika Bakierska and Roman Dziembaj; Faculty of Chemistry, Jagiellonian University, Krakow, Poland.

C8.12
Study of the Mechanism of Electrophoretic Deposition of Composite Lithium-Ion-Conducting Membranes Raymond Blanga and Diana Golodnitsky; Chemistry, Tel Aviv University, Biniamina, Israel.

C8.13
***Operando* X-Ray Absorption Study on Charge-Discharge Mechanism of Li_2MnO_3 and Li_2RuO_3 Lithium-Rich Cathode** Takanori Kobayashi, Koji Nakanishi, Takuya Mori, Kentaro Yamamoto, Titus Masese, Yuki Orikasa and Yoshiharu Uchimoto; Kyoto University, Kyoto-shi, Japan.

C8.14
Phase Transition Mechanism of $LiFePO_4$-$FePO_4$ Using a Thin-Film Model Electrode Takahiro Yoshinari, Kentaro Yamamoto, Eri Kato, Mori Takuya, Titus Masese, Yuki Orikasa and Yoshiharu Uchimoto; Kyoto University, Kyoto, Japan.

C8.15
Molten Salt Method of Preparation and Electrochemical Characterisation of MnO_2 M.V. Reddy, Yun Hong Lee and Stefan Adams; Materials Science & Eng., National University of Singapore, Singapore, Singapore.

C8.16
Electrochemical and Magnetic Properties of $LiMn_{1.5}Ni_{0.5}O_4$ Spinel Oxide Reiko Hanafusa, Kazuki Kotani, Kousuke Ishidzu, Yoshihiro Oka and Tatsuya Nakamura; Dept. of Electrical Engineering , University of Hyogo, Himeji, Japan.

C8.17
Influence of Synthesis Conditions on Crystal Structure and Electrochemical Properties of Spinel $Li_4Ti_5O_{12}$ Used as Anode Material for Li-Batteries Anna Drobniak, Danuta Olszewska and Wojciech Zajac; AGH University of Science and Technology, Krakow, Poland.

C8.18
$Li_4Ti_5O_{12}$ Doped with Copper as Anode Material for Li-Batteries Anna Drobniak, Danuta Olszewska and Wojciech Zajac; AGH University of Science and Technology, Krakow, Poland.

C8.19
Acoustic Emission Study of SnO Anode for Lithium-Ion Batteries Naoakai Kuwata[1], Shutaro Kato[1], Junichi Kawamura[1], Kazuhisa Sato[1, 2] and Junichiro Mizusaki[1]; [1]IMRAM, Tohoku University, Sendai, Japan; [2]Graduate School of Engineering, Tohoku University, Sendai, Japan.

C8.20
Lattice Volume Change of $Li[Ni_xCo_yMn_z]O_2$ Cathodes during Charge/ Discharge Reaction and Their Cycle Performance Kosuke Ishizu, Yoshihiro Oka and Tatsuya Nakamura; University of Hyogo, Himeji, Japan.

C8.21
Investigation of All-Solid-State Li-O_2 Batteries Hirokazu Kitaura and Haoshen Zhou; Energy Technology Research Institute, National Institute of Advanced Industrial Science and Technology, Tsukuba, Japan.

C8.22
Electrochemical Properties of $LiNi_{1/3}Co_{1/3}Mn_{1/3}$ Electrodes Prepared with Water-Based Slurry Dispersed Conducting Additive by Using Plasma Treatment Yoshihiro Oka, Tomoya Sasaki, Hideyoshi Matsumoto and Tatsuya Nakamura; University of Hyogo, Himeji, Japan.

C8.23
Fabrication of High-Purity LATP Powders and Ceramic Pellet by a Wet Chemistry Process Xiangwei Wu, Cai Liu, Meifen Wu and Zhaoyin Wen; CAS Key Laboratory of Materials for Energy Conversion, Shanghai Institute of Ceramics, Chinese Academy of Sciences, Shanghai, China.

C8.24
Reduced Free-Standing Co_3O_4 Electrode for Li-Oxygen Battery Chen Shen, Zhaoyin Wen, Fan Wang and Xiangwei Wu; CAS Key Laboratory of Materials for Energy Conversion, Shanghai Institute of Ceramics, Chinese Academy of Sciences, Shanghai, China.

C8.25
Lithium Storage in Tin Oxide@Carbon by Carbonizing Polydopamine Coating Peng Peng, Zhaoyin Wen, Yu Liu and Jun Jin; CAS Key Laboratory of Materials for Energy Conversion, Shanghai Institute of Ceramics, Chinese Academy of Sciences, Shanghai, China.

C8.26
Electrode and Interface Design for Rechargeable Lithium Sulfur Batteries Zhaoyin Wen, Guoqiang Ma, Jun Jin, Xiangwei Wu, Qingsong Wang and Meifen Wu; CAS Key Laboratory of Materials for Energy Conversion, Shanghai Institute of Ceramics, Chinese Academy of Sciences, Shanghai, China.

C8.27
Rechargeable Na–O_2 Batteries with a Covalently Coupled Three-Dimensional Graphene/ Mn_3O_4 Hybrids as an Oxygen Cathode Catalyst Sanpei Zhang, Zhaoyin Wen and Xiangwei Wu; CAS Key Laboratory of Materials for Energy Conversion, Shanghai Institute of Ceramics, Chinese Academy of Sciences, Shanghai, China.

C8.28
Defect Interaction and Solid Electrolyte Transition in $K_3H(SeO_4)_2$ Oscar S. Hernandez-Daguer[2, 1], Diego Pena-Lara[3] and Ruben A. Vargas-Zapata[3]; [1]Department of Physics, Universidad del Atlántico, Barranquilla, Colombia; [2]Department of Physics, University of Puerto Rico., Mayaguez, Puerto Rico, United States; [3]Department of Physics, Universidad del Valle, Cali, Colombia.

C8.29
Synthesis, Structure and Electrochemical Properties of Lithium Solid Electrolyte: The Li-P-S-O System Kota Suzuki[1], Satoshi Hori[1], Masamitsu Sakuma[1], Tetsuya Nakazawa[1], Miki Kubota[2], Masaaki Hirayama[1], Masao Yonemura[2] and Ryoji Kanno[1]; [1]Electronic Chemistry, Tokyo Institute of Technology, Yokohama, Japan; [2]High Energy Accelerator Research Organization, Tokai, Japan.

C8.30
High Sensitivity Detection of Mn Ion Dissolution by *In Situ* 1H MRI Yoshiki Iwai, Masato Ohzu, Naoaki Kuwata and Junichi Kawamura; Institute of Multidisciplinary Research for Advanced Materials, Tohoku University, Sendai, Japan.

C8.31
Li Ion Conductivity in a Cation Deficient Scheelite Ryan D. Bayliss[1], Stuart N. Cook[2] and Jordi Cabana[1]; [1]Department of Chemistry, University of Illinois at Chicago, Chicago, Illinois, United States; [2]Department of Materials Science and Engineering, Massachusetts Institute of Technology, Boston, Massachusetts, United States.

C8.32
High Volt Stability of Lithium Borate Thin-Film as Solid Electrolyte for All-Solid-State Thin-Film Battery Haruka Itabashi, Naoaki Kuwata and Junichi Kawamura; IMRAM, Tohoku University, Sendai, Japan.

C8.33
Highly Reversible Capacity at the Surface of a Lithium-Rich Manganese Oxide Li_2MnO_3 Masaaki Hirayama[1], Sou Taminato[1], Kota Suzuki[1], Ryoji Kanno[1] and Masao Yonemura[2];[1]Tokyo Institute of Technology, Yokohama, Japan; [2]KEK, Tokai, Japan.

C8.34
Fabrication and Electrochemical Properties of All-Solid-State Batteries with 5V $LiNi_{0.5}Mn_{1.5}O_4$ Cathode and $Li_{10}GeP_2S_{12}$ Solid Electrolyte Gwangseok Oh, Masaaki Hirayama, Ohmin Kwon, Kota Suzuki and Ryoji Kanno; Electronic Chemistry, Tokyo Institute of Technology, Yokohama, Japan.

C8.35
Electrochemical Performance of Li_2MnO_3 Cathode Material by Fluorine Substitution Sha Wu, Zhiyong Yu, Hanxing Liu, Wenji Li and Mengyun Lu; School of Materials Science and Engineering, Wuhan University of Technology, Wuhan, China.

C8.36
EELS Investigations of Aging Mechanisms in $LiFePO_4$ Cathodes after Extended Electrochemical Cycling Samartha Channagiri[1], Nicholas Warner[2], Frank Scheltens[1], Marcello Canova[2], Yann Guezennec[2] and David W. McComb[1]; [1]Materials Science and Engineering, The Ohio State University, Columbus, Ohio, United States; [2]Center for Automotive Research, The Ohio State University, Columbus, Ohio, United States.

C8.37
Mixed Conduction Transmission Line Impedance Model for Olivine Structured Cathode Material Eui-Chol Shin[1], Jihyeon Gim[1], Jinju Song[1], Sung-Won Kang[1], Docheon Ahn[2], Jaekook Kim[1] and Jong-Sook Lee[1]; [1]Materials Science and Engineering, Chonnam National University, Gwang-Ju, Korea (the Republic of); [2]Pohang Accelerator Laboratory, Pohang, Korea (the Republic of).

C8.38
In Depth First-Principles Study with Experiment on Origins and Mechanism of Phase Transformation of Mn^{4+}-Related Bulk Li_2MnO_3 Jin-Myoung Lim[1], Duho Kim[1], Young-Geun Lim[2], Min-Sik Park[2], Young-Jun Kim[2], Kyeongjae Cho[3] and Maenghyo Cho[1]; [1]Seoul National University, Seoul, Korea (the Republic of); [2]Korea Electronics Technology Institute, Seongnam, Korea (the Republic of); [3]The University of Texas at Dallas, Richardson, Texas, United States.

C8.39
The High-Capacity Effect in the All-Glass Composites Conducting Electrons and Silver Ions Wioleta Slubowska, Jan L. Nowinski, Jerzy E. Garbarczyk and Marek Wasiucionek; Faculty of Physics, Warsaw University of Technology, Warsaw, Poland.

C8.40
Electrochemical Impedance Spectroscopy of Supercapacitors: Analysis Using Evolutionary Programming Alon Oz, Shany Hershkovitz, Emanuelle Goren, Sioma Baltianski and Yoed Tsur; Technion - Israel Institute of Technology, Haifa, Israel.

C8.41

Two-Dimensional Imaging of Charge/Discharge by the Bragg Edges Analysis of the Electrode Materials for the Pulsed Neutron-Beam Transmission Spectra of a Li-Ion Battery Koichi Kino[1], Masao Yonemura[2], Yoshihisa Ishikawa[2] and Takashi Kamiyama[2, 3]; [1]Faculty of Engineering, Hokkaido University, Sapporo, Japan; [2]Institute of Materials Structure Science, High Energy Accelerator Research Organization, Tokai, Japan; [3]The Graduate University for Advanced Studies (Sokendai), Tokai, Japan.

C8.42

Alluaudite Sodium Iron Sulfate $Na_{2+2x}Fe_{2-x}(SO_4)_3$ for High Energy Density Sodium-Ion Battery Shin-ichi Nishimura[1, 2], Prabeer Barpanda[3, 1], Gosuke Oyama[1] and Atsuo Yamada[1,2]; [1]Department of Chemical System Engineering, The University of Tokyo, Bunkyo-ku, Japan; [2]ESICB, Kyoto University, Kyoto, Japan; [3]Indian Institute of Science, Bangalore, India.

C8.43

Structure and Electrochemical Performance of $LiCoO_2$ Cathode Materials Xiaoli Xi; Beijing University of Technology, Beijing, China.

C8.44

Origin of High Rate Performance of $LiFePO_4$ Investigated by Time-Resolved X-Ray Diffraction Kazufumi Otani[1], Toshiyuki Munesada[1], Takuya Mori[1], Kentaro Yamamoto[1], Titus N. Masese[1], Yuki Orikasa[1], Koji Ohara[2], Katsutoshi Fukuda[2], Yukinori Koyama[2], Toshiyuki Nohira[3], Rika Hagiwara[4], Zempachi Ogumi[2] and Yoshiharu Uchimoto[1]; [1]Graduate School of Human and Environmental Studies, Kyoto University, Kyoto, Japan; [2]Office of Society-Academia Collaboration for Innovation, Kyoto University, Uji, Japan; [3]Institute of Advanced Energy, Kyoto University, Uji, Japan; [4]Graduate School of Energy Sciences, Kyoto University, Kyoto, Japan.

C8.45

A Cation-Selective Separator as the Oxygen-Barrier for Non-Aqueous Metal-Air Batteries Xiaodi Ren[1], Mingzhe Yu[1], Mitchell E. Steindler[2], Qiang Zhao[1] and Yiying Wu[1];[1]Chemistry and Biochemistry, Ohio State University, Columbus, Ohio, United States; [2]Chemical and Biomolecular Engineering, Ohio State University, Columbus, Ohio, United States.

C8.46

How to Get a Conversion Reaction Reversible? Lithium Storage in Electroactive Metal Sulphide Nanodots Yan Yu[1, 2], Changbao Zhu[2] and Joachiam Maier[2]; [1]Department of Materials Science and Engineering, University of Science and Technology of China, Hefei, China; [2]Max-Planck-Institute for Solid State Research, Stuttgart, Germany.

C8.47

Constructing 3D Porous and Carbon-Coated Electrode Materials for High Performances Li-Ion Batteries Yan Yu[1, 2], Jun Liu[2] and Joachiam Maier[2]; [1]Department of Materials Science and Engineering, University of Science and Technology of China, Hefei, China; [2]Max Planck Institute for Solid State Research, Stuttgart, Germany.

C8.48

Synthesis and Characterization of $Li(Li_yFe_zV_{1-y-z})O_{2-\delta}$ – Anode Material for Li-Ion Batteries Bartlomiej Gedziorowski and Janina Molenda; AGH University of Science and Technology, Krakow, Poland.

C8.49

Unusual Surface Redox Behaviors of Li_2MnO_3: First-Principles Prediction and Experimental Validation Duho Kim[1], Jin-Myoung Lim[1], Young-Geun Lim[2], Min-Sik Park[2], Young-Jun Kim[2], Kyeongjae Cho[3] and Maenghyo Cho[1]; [1]School of Mechanical Aerospace Engineering, Seoul National University, Seoul, Korea (the Republic of); [2]Advanced Batteries Research Center, Korea Electronics Technology Institute, Seongnam, Korea (the Republic of); [3]Department of Materials Science and Engineering, University of Texas at Dallas, Dallas, Texas, United States.

C8.50

Ultrasonic-Assisted Synthesis of Nanostructured Transition Metal Oxides as Cathode Materials for Mg-Ion Batteries Lu Wang[1], Xinzhi Chen[1], Sidsel M. Hanetho[2] and Fride Vullum-Bruer[1]; [1]Department of Materials Science and Engineering, Norwegian University of Science and Technology, Trondheim, Norway; [2]SINTEF Materials and Chemistry, Trondheim, Norway.

C8.51

Synthesis and Electrochemical Performance of $Li_4Ti_5O_{12}$ Modified with Carbon Nanotubes Yingbin Lin and Zhigao Huang; Physics and Energy College, Fujian Normal University, Fuzhou City, China.

C8.52

Structural, Electrical and Electrochemical Properties of the $Na_{2/3}Ni_{1/3}Mn_{2/3-x}Ti_xO_{2-\delta}$ ($0 \le x \le 1/3$) Cathode Materials Anna G. Milewska and Janina Molenda; AGH Academy of Science and Technology, Krakow, Poland.

C8.53

Dynamics Study of Lithium Ion Diffusion in Super Lithium Ion Conductors, $Li_{10}GeP_2S_{12}$ (LGPS) Masao Yonemura[1], Takashi Kamiyama[1, 2], Ohmin Kwon[3], Satoshi Hori[3], Masaaki Hirayama[3], Ryoji Kanno[3], Kazuhiro Mori[4], Kaoru Shibata[5], Takeshi Yamada[6] and Yukinobu Kawakita[5]; [1]Institute of Materials Structure Science (IMSS), High Energy Accelerator Research Organization (KEK), Tokai, Japan; [2]The Graduate University for Advanced Studies (Sokendai), Tokai, Japan; [3]Department of Electronic Chemistry, Interdisciplinary Graduate School of Science and Engineering, Tokyo Institute of Technology, Yokohama, Japan; [4]Research Reactor Institute, Kyoto University, Kumatori, Japan; [5]Materials and Life Science Division, J-PARC Center, JAEA, Tokai, Japan; [6]Neutron R&D Division, CROSS-Tokai, Tokai, Japan.

C8.54

Lithium Superionic Conductors with $Li_{10}GeP_2S_{12}$-type Structure in the Li_4MS_4 – Li_3PS_4 System (M = Si, Ge, Sn): Synthesis, Conduction Mechanism and Phase Relationships Satoshi Hori[1], Ohmin Kwon[1], Kota Suzuki[1], Masaaki Hirayama[1], Masao Yonemura[2], Takashi Kamiyama[2, 3] and Ryoji Kanno[1]; [1]Electrochemistry, Tokyo Institute of Technology, Yokohama, Japan; [2]High Energy Accelerator Research Organization, Institute of Materials Structure Science, Ibaraki, Japan; [3]The Graduate University for Advanced Studies (Sokendai), Ibaraki, Japan.

C8.55

Effect of Zn-Doping on Densification of $Li_7La_3Zr_2O_{12}$ Emil Hanc, Wojciech Zajac, Angelika Orzeszek and Janina Molenda; Faculty of Energy and Fuels, AGH University of Science and Technology, Cracow, Poland.

C8.56

Evolution of Microstructure and Its Relation to Ionic Conductivity in $Li_{1+x}Al_xTi_{2-x}(PO_4)_3$ Thomas Hupfer[1], Claudia Bucharsky[1], Günter Schell[1], Anatoliy Senyshyn[2], Mykhailo Monchak[2, 3] and Michael J. Hoffmann[1]; [1]IAM-KWT, KIT, Karlsruhe, Germany; [2]FRM II, SPODI, TU Munich, Garching, Germany; [3]IAM-ESS, KIT, Karlsruhe, Germany.

C8.57

New Intercalation Cathodes for Calcium Ion Batteries Danielle Proffit[1], Albert Lipson[1], Baofei Pan[1], Brian Ingram[1], Miao Liu[2], Anubhav Jain[2], Kristin Persson[2] and Jack Vaughey[1];[1]Chemical Sciences and Engineering, Joint Center for Energy Storage Research, Argonne National Laboratory, Lemont, Illinois, United States; [2]Electrochemical Technologies Group, Joint Center for Energy Storage Research, Lawrence Berkeley National Laboratory, Berkeley, California, United States.

C8.58

Mixed Glass Former Effect in $50Li_2O$-$50[xNb_2O_5$-$(1-x)P_2O_5]$ Glasses Prashant Dabas and K. Hariharan; Physics, Indian Institute of Technology Madras, Chennai, India.

C8.59

Tin Networked Electrode Providing Enhanced Volumetric Capacity and Pressureless Operation for All-Solid-State Li-Ion Batteries Justin M. Whiteley[1], Ji Woo Kim[1], Chan Soon Kang[2], Jong Soo Cho[1], Kyu Hwan Oh[2] and Se-Hee Lee[1]; [1]Mechanical Engineering, University of Colorado, Boulder, Boulder, Colorado, United States; [2]Materials Science and Engineering, Seoul National University, Seoul, Korea (the Republic of).

C8.60
Synthesis and Electrochemical Properties of SiO_x/C Amorphous Composite as Anode Material for Lithium Ion Batteries Pengpeng Lv, Hailei Zhao, Chunhui Gao and Zhaolin Li; University of Science and Technology Beijing, Beijing, China.

C8.61
Impedance Investigation of the Processes on SiC/Li^+-Electrolyte Interface Ekaterina Antonova[2], Elizaveta Evschik[1], Alexey Levchenko[1], Viktor Berestenko[1] and Yury Dobrovolsky[1];[1]IPCP RAS, Chernogolovka, Russian Federation; [2]IHTE UB RAS, Ekaterinburg, Russian Federation.

C8.62
Synthesis and Na^+ Conduction Properties of Rare Earth-Free NASICON-Type Solid Electrolyte Toshinori Okura[1], Naoya Yoshida[1] and Kimihiro Yamashita[2]; [1]Kogakuin University, Hachioji, Japan; [2]Tokyo Medical and Dental University, Chiyoda, Japan.

C8.63
Interfacial Modification of All-Oxide-Solid-State Battery with Low Surface Energy Solid Electrolyte Shogo Komagata, Shingo Ohta and Takahiko Asaoka; Toyota Central R&D Labs. Inc., Nagakute, Japan.

C8.64
Fluoride-Phosphates as Positive Electrode Materials for Metal-Ion Batteries Nellie Khasanova, Stanislav Fedotov, Oleg Drozhzhin and Evgeny Antipov; Chemistry Department, Lomonosov Moscow State University, Moscow, Russian Federation.

C8.65
Evaluations of Iron Based Cathode Materials for Li-Ion Batteries--Case of $LiFe_{1-y}M_yPO_4$, Nanometric $LiFePO_4$ and $LiFeO_2$ Andrzej J. Kulka, Wojciech Zajac, Konrad Swierczek, Katarzyna Walczak and Janina Molenda; AGH-University of Science and Technology, Cracow, Poland.

C8.66
Effect of Glass Additives on Relative Density and Li-Ion Conductivity of $Li_{7-x}La_3Zr_{2-x}Nb_xO_{12}$ Solid Electrolyte Nataly C. Rosero Navarro, Taira Yamashita, Akira Miura, Mikio Higuchi and Kiyoharu Tadanaga; Hokkaido University, Sapporo, Japan.

C8.67
Sodium Ion Conducting Ceramics with $Na_3YSi_4O_{12}$-Type Structure Synthesized by a Polymerized Complex Method Naohiro Horiuchi[1], Kaede Ryu[2], Naoya Yoshida[2], Toshinori Okura[2] and Kimihiro Yamashita[1]; [1]Institute of Biomaterial & Bioengineering, Tokyo Medical and Dental University, Tokyo, Japan; [2]Kogakuin University, Hachioji-shi, Japan.

C8.68
Development of Salty-Gel Electrolytes Composed of Metal Salt and Small Amount of Organic Solvent as a New Concept for Organic Solid Electrolytes Makoto Moriya[1, 2, 3], Shohei Nabeno[3], Yutaro Hanawa[3], Wataru Sakamoto[3] and Toshinobu Yogo[3]; [1]Graduate School of Science, Shizuoka University, Shizuoka, Japan; [2]JST PRESTO, Kawaguchi, Japan; [3]EcoTopia Science Institution, Nagoya University, Nagoya, Japan.

C8.69
Investigation of Negative Electrode for All-Solid-State Lithium Ion Battery using Garnet-Type Oxide Electrolyte Tetsuro Kobayashi, Shingo Ohta and Takahiko Asaoka; Toyota Central R&D Labs.,Inc., Nagakute, Japan.

C8.70
Low Temperature Synthesis of Yb Doped $SrCeO_3$ Electrolyte Thin Film for Hydrogen Separation Yang Lei, Chao Zhang, Di He, Shuai Li, Xiaopeng Liu and Lijun Jiang; Department of Energy Materials and Technology, General Research Institute for Non-Ferrous Metals, Beijing, China.

C8.71
Improved of Electrochemical Performances of Manganese-Substituted $Na_{0.7}Co_{1-y}Mn_yO_2$ - Cathode Material for Rechargeable Sodium-Ion Batteries Dominika Baster, Filip Hartman, Lukasz Kondracki, Andrzej Kulka, Wojciech Zajac and Janina Molenda; AGH University of Science and Technology, Krakow, Poland.

C8.72
Earth-Abundant Cathode Materials for Sodium-Ion Batteries P2-$Na_{2/3}Fe_{1-y}Mn_yO_2$ Dominika Baster, Piotr Trzaska and Janina Molenda; AGH University of Science and Technology, Krakow, Poland.

C8.73
Low Temperature Conductivity Response in Polymer Blend Electrolyte Avirup Das[2], A K. Thakur[1] and K Kumar[2]; [1]Physics, Indian Institute of Technology Patna, Patna, India;[2]Physics, Indian Institute of Technology Kharagpur, Kharagpur, India.

C8.74
Supercapacitor Response of Tin Sulfide Electrodes Pradip Leuaa, Ajay D. Thakur and Awalendra K. Thakur; Physics, IIT Patna, Patna, India.

C8.75
Spinel $LiCrTiO_4$ as a LIB Anode : A Density Functional Theory Approach Biswajit Mondal and Awalendra K. Thakur; Physics, IIT Patna, Patna, India.

SESSION D6: Poster Session: Fundamentals of Transport and Reactivity and Nanoionics II
D: Fundamentals of Transport and Reactivity and Nanoionics
Tuesday Afternoon, June 16, 2015
5:20 PM
Keystone Resorts, Red Cloud Peak

D6.01
The Role of Ceria in Electro-Reduction of Nitrogen Oxide Based on Solid State Cell Reactor at Intermediate-Temperature Wenyi Tan[1, 2], Fei Chen[1], Lei Gong[1], Yunfei Bu[2], Yang Song[2] and Qin Zhong[2]; [1]Nanjing Institute of Technology, Nanjing, China; [2]School of Chemical Engineering, Nanjing University of Science & Technology, Nanjing, China.

D6.02
Li-Ion Dynamics Along the Inner Surfaces of Layer-Structured 2H-Li_xNbS_2 Bernhard Stanje[1], Viktor Epp[1], Suliman Nakhal[2], Martin Lerch[2] and Martin Wilkening[1]; [1]Institute for Chemistry and Technology of Materials, Technical University of Graz, Graz, Austria; [2]Institut für Chemie, Technische Universität Berlin, Berlin, Germany.

D6.03
Catalytic Activity and Oxygen Storage Properties of Doped $Ba_{1-x}Sr_xY_{1-y}Ln_yMn_2O_{5+\delta}$ (Ln - lanthanides) for Application in Three-Way Catalytic Converters Alicja Klimkowicz[2,1], Konrad Swierczek[2], Tomasz Rzasa[2], Akito Takasaki[1] and Bogdan Dabrowski[3]; [1]Department of Engineering Science and Mechanics, Shibaura Institute of Technology, Tokyo, Japan;[2]Faculty of Energy and Fuels, AGH University of Science and Technology, Krakow, Poland; [3]Department of Physics, Northern Illinois University, DeKalb, Illinois, United States.

D6.04
Electrical Conductivity, Oxygen Diffusion Coefficient and Surface Exchange Coefficient of $La_4Co_3O_{10}$ by Electrical Conductivity Relaxation Technique Yoshinobu Adachi, Naoyuki Hatada and Tetsuya Uda; Materials Science and Engineering, Kyoto University, Kyoto, Japan.

D6.05
Influence of Cation Nonstoichiometry to Oxygen Nonstoichiometry in Mixed Ionic and Electronic Conducting Perovskite Oxides Yusuke Okamoto[1], Akihide Kuwabara[2], Takashi Nakamura[3], Tatsuya Kawada[1] and Koji Amezawa[3]; [1]Graduate Study of Environmental Studies, Tohoku University, Sendai, Japan; [2]Japan Fine Ceramics Center, Atsuta, Japan; [3]IMRAM, Tohoku University, Sendai, Japan.

D6.06
Structure, Transport and Stability of Layered Ruddlesden-Popper $La_{n+1}Ni_nO_{3n+1}$ (n = 1, 2 and 3) Epitaxial Films Kuan-Ting Wu[1, 2], Monica Burriel[5, 2], Fan Yang[3], David McComb[3], John Kilner[2, 4] and Stephen Skinner[2]; [1]Department of Applied Chemistry, Kyushu University, Fukuoka, Japan; [2]Department of Materials, Imperial College London, London, United Kingdom; [3]Department of Materials Science and Engineering, Ohio State University, Columbus, Ohio, United States; [4]International Institute for Carbon-Neutral Energy Research (wpi-I2CNER), Fukuoka, Japan; [5]Laboratoire des Matériaux et du Génie Physique (LMGP), Grenoble, France.

D6.07
Low Temperature Protonic Transport in Nanocrystalline Porous Oxides Sindre O. Stub[1], Per M. Rorvik[2], Reidar Haugsrud[1] and Truls Norby[1]; [1]Centre for Materials Science and Nanotechnology, Department of Chemistry, University of Oslo, Oslo, Norway; [2]Sector for Sustainable Energy Technology, SINTEF Materials and Chemistry, Oslo, Norway.

D6.08
The Influence of Aging and Humidity on Transport Properties of Ceria Thin Films at Low Temperatures Matthias Kleine-Boymann, Matthias Elm, Raika W. Oppermann and Juergen Janek; Institute of Physical Chemistry, Justus-Liebig University, Giessen, Germany.

D6.09
Correlation between Mobile Oxygen Ion Distances and Characteristic Length Scales for $La_{2-x}Er_xMo_2O_9$ Type Oxide Ion Conductor Tanmoy Paul and Aswini Ghosh; Solid State Physics, Indian Association for the Cultivation of Science, Kolkata, India.

D6.10
Tuning the Defect Structure of $La_{0.5}Sr_{0.5}Co_{0.5}Mn_{0.5}O_{3-\delta}$ for Optimized Redox Behavior under Polarisation Conditions Celeste A. van den Bosch, George F. Harrington, Stephen J. Skinner and Ainara Aguadero; Department of Materials, Imperial College London, London, United Kingdom.

D6.11
Defect Chemistry and Diffusion in $Cu_2ZnSnSe_4$ and Cu_2ZnSnS_4 Thin Films Steven Harvey, Glenn Teeter and Ingrid Repins; National Renewable Energy Laboratory, Golden, Colorado, United States.

D6.12
Ionic Conductivity Modification in Nanoscale Proton-Conducting Oxide Heterostructures Prepared by Pulsed Laser Deposition Stefan B. Nikodemski[1], Daniel Clark[1], Jianhua Tong[1], Ryan O'Hayre[1], Philip Parilla[2], David Ginley[2] and Joseph Berry[2]; [1]Metallurgical and Materials Engineering, Colorado School of Mines, Golden, Colorado, United States; [2]National Renewable Energy Laboratory, Golden, Colorado, United States.

D6.13
Investigating the Origins of Modified Transport Properties of YSZ in Confined Systems George Harrington[1, 2, 3], Andrea Cavallaro[3], Tobias M. Huber[1, 2], Harry L. Tuller [2, 4], Bilge Yildiz[5, 2], Kazunari Sasaki[6, 1], David W. McComb[7, 3], Stephen J. Skinner[3] and John A. Kilner[3]; [1]Next-Generation Fuel Cell Research Centre, Kyushu University, Fukuoka, Japan;[2]Department of Materials, Massachusetts Institute of Technology, Cambridge, Massachusetts, United States; [3]Department of Materials, Imperial College London, London, United Kingdom;[4]International Institute for Carbon Neutral Energy Research, Kyushu University, Fukuoka, Japan; [5]Lab. for Electrochemical Interfaces, Massachusetts Institute of Technology, Cambridge, Massachusetts, United States; [6]Department of Mechanical Engineering, Kyushu University, Fukuoka, Japan; [7]Department of Materials Science and Engineering, The Ohio State University, Columbus, Ohio, United States.

D6.14
Understanding Proton Conductivity within Porous Organic Cage Networks Scott Lewis, Ming Liu, Linjiang Chen, Iain Aldous, Marc Little, Samantha Chong, Laurence Hardwick and Andrew I. Cooper; Chemistry, University of Liverpool, Liverpool, United Kingdom.

D6.15
Highly-Conductive Nanomaterials Based on Li_2O–FeO–V_2O_5–P_2O_5 Glasses Tomasz K. Pietrzak, Jerzy E. Garbarczyk, Marek Wasiucionek, Jan L. Nowinski and Przemyslaw P. Michalski; Physics, Warsaw University of Technology, Warszawa, Poland.

D6.16
The Mixed Alkali Effect in $(Li_{1-x}A_x)_2Si_2O_5$ (A = K, Rb) Glasses Melissa Novy, Sabyasachi Sen and Sangtae Kim; Materials Science and Engineering, UC Davis, Davis, California, United States.

D6.17 moved to D7.02

D6.18
Ionic Conductivity of β-eucryptite Doped with Mg Yachao Chen and Ivar E. Reimanis; Colorado School of Mines, Golden, Colorado, United States.

D6.19
Analysis of Grain Boundary Conductivity of Ionic Oxides at Elevated Temperature: Doped CeO_2 and Bi_2O_3 – a Case Study NoWoo Kwak and WooChul Jung; Material Science & Engineering, Korea Advanced Institute of Science and Technology (KAIST), Daejeon, Korea (the Republic of).

D6.20
Interfacial Ionic Conductivity in Epitaxial $Y_2Zr_2O_7$ Thin Films Elisa Gilardi[1], Giuliano Gregori[1], Yi Wang[2], Wilfried Sigle[2], Peter A. van Aken[2] and Joachim Maier[1]; [1]Physical Chemistry of Solids, Max Planck Institute for Solid State Research, Stuttgart, Germany; [2]Stuttgart Center for Electron Microscopy, Max Planck Institute for Intelligent System, Stuttgart, Germany.

D6.21
Nanocomposite Ceramics Based on $Ce_{0.9}Gd_{0.1}O_{1.95}$ and MgO Jens Zosel[1], Vladimir Vashook[1], Evgeni Sperling[2], Kristina Ahlborn[1], Frank Gerlach[1], Wolfgang Fichtner[1], Matthias Schelter[1], Ulrich Guth[1, 2] and Michael Mertig[1]; [1]Kurt-Schwabe-Institut für Mess- und Sensortechnik e.V. Meinsberg, Waldheim, Germany; [2]Chemistry, Dresden University of Technology, Dresden, Germany.

D6.22
Reduction Stages of Ni-doped Polycrystalline YSZ Amy Morrissey[1], James R. O'Brien[2], Jianhua Tong[1] and Ivar E. Reimanis[1]; [1]Colorado School of Mines, Golden, Colorado, United States; [2]Off Grid Research, San Diego, California, United States.

D6.23
Electrical and Oxide Ionic Conductivity in Metal Disparsed Pr_2NiO_4-Based Oxides Junji Hyodo[1, 2], Shintaro Ida[1, 2] and Tatsumi Ishihara[1, 2]; [1]Applied Chemistry, Kyushu University, Fukuoka, Japan; [2]International Institute for Carbon Neutral Energy Research (I2CNER), Fukuoka, Japan.

D6.24
Encroachment of Titanium Oxide on Ni Surface for Ni/TiO_2 under Reducing Atmosphere Fangfang Wang[1, 2], Haruo Kishimoto[1, 2], Katherine D. Bagarinao [1, 2], Katsuhiko Yamaji[1, 2], Teruhisa Horita[1, 2] and Harumi Yokokawa[3]; [1]National Institute of Advanced Industrial Science and Technology, Tsukuba, Japan; [2]CREST, JST, Kawaguchi, Japan; [3]The University of Tokyo, Tokyo, Japan.

D6.25
Ionic Transport Properties of $NdBaInO_4$ Stephen Skinner, Yuning Zhou and Manyu Chen; Imperial College London, London, United Kingdom.

D6.26
Oxygen Transport Properties of Ca/W-Substituted Lanthanum Nickelate Peter V. Hendriksen and Simona Ovtar; Department of Energy Conversion and Storage, Technical University of Denmark, Roskilde, Denmark.

D6.27
Characterization of Solid Lithium Ceramic and Glass-Ceramic Nano-Thin Film Electrolytes Prepared by RF Magnetron Sputtering Erik Burton and Dale Teeters; Chemistry and Biochemistry, University of Tulsa, Tulsa, Oklahoma, United States.

D6.28
Characterisation of Electrochemical Transport Parameters in Multi-Ion Systems Truls Norby, Ragnar Strandbakke, Anna Evans and Shay A. Robinson; Department of Chemistry, University of Oslo, Oslo, Norway.

D6.29
Dependence of Surface Defect Chemistry on Sr Concentration in $La_{1-x}Sr_xFeO_{3-\delta}$ Zixuan Guan; Applied Physics, Stanford University, Stanford, California, United States.

D6.30
Glass Transition in Superprotonic Phase of Inorganic Solid Acid Haruyuki Takahashi, Yoshitaka Suzuki and Takashi Sakuma; Graduate School of Science and Engineering, Ibaraki University, Hitachi, Japan.

D6.31
Unraveling the Origin of Surface Capacitance in Mixed Ion Electron Conducting Oxides Chirranjeevi Balaji Gopal, Albert Z. Feng and William Chueh; Materials Science and Engineering, Stanford University, Menlo Park, California, United States.

D6.32
Disorder and Ionic Transport in Pyrochlore/Defect Fluorite Oxides Cortney Kreller[1], James Valdez[2], Terry Holesinger[1], Yongqiang Wang[2] and Blas Uberuaga[2]; [1]Materials Physics and Applications, Los Alamos National Laboratory, Los Alamos, New Mexico, United States; [2]Materials Science in Radiation and Dynamics Extremes, Los Alamos National Laboratory, Los Alamos, New Mexico, United States.

D6.33
Correlating Conductivity and Composition of $Ca_xCe_{1-x}O_{2-\delta}$ Grain Boundaries via Aberration-Corrected Transmission Electron Microscopy William J. Bowman, Kimberly McGuinness, Cruz A. Hernandez and Peter A. Crozier; Materials Science and Engineering, Arizona State University, Tempe, Arizona, United States.

D6.34
Dynamic Pulse Isotopic Exchange for Assessing Oxygen Transport Kinetics Prasna S. Ray, Brian Ray, Guangru Zhang, Evangelos I. Papaioannou and Ian S. Metcalfe; Chemical Engineering and Advanced Materials, Newcastle University, Newcastle-upon-Tyne, United Kingdom.

SESSION G3: Poster Session
G: Switching and Sensing Phenomena
Tuesday Afternoon, June 16, 2015
5:20 PM
Keystone Resorts, Red Cloud Peak

G3.01
Resistive Switching in $SrRuO_3$ Probed by Scanning Tunneling Microscopy Kiran K. Adepalli[1, 2], Marco Moors[3], Qiyang Lu[1], Rainer Waser[3], Harry Tuller[1], Ilia Valov[3] and Bilge Yildiz[2]; [1]Materials Science and Engineering, Massachusetts Institute of Technology, Cambridge, Massachusetts, United States; [2]Nuclear Science and Engineering, Massachusetts Institute of Technology, Cambridge, Massachusetts, United States; [3]Peter Grünberg Institute, Forschungszentrum Jülich, Jülich , Germany.

G3.02
Topotactic Phase Transition in $SrCoO_x$ Controlled by Electrochemical Potential Qiyang Lu[1] and Bilge Yildiz[1, 2]; [1]Department of Materials Science and Engineering, Massachusetts Institute of Technology, Cambridge, Massachusetts, United States; [2]Department of Nuclear Science and Engineering, Massachusetts Institute of Technology, Cambridge, Massachusetts, United States.

G3.03
Atomistic Modelling of the Formation of Conducting Filaments in Resistive RAM Cells David Z. Gao, Samuel R. Bradley, Manveer Munde and Alexander L. Shluger; Physics and Astronomy, University College London, London, United Kingdom.

G3.04
Controllable Resistive ON- and OFF-States by Two Switching Mechanisms in Epitaxial Strontium Titanate-Based Resistive Switches Markus Kubicek, Rafael Schmitt, Felix Messerschmitt and Jennifer Rupp; Department of Materials, ETH Zurich, Zurich, Switzerland.

G3.05
Enhanced Stability of Ag-SbTe Chalcogenide Solid Electrolyte by Nitrogen Doping Young Sam Park[2] and Seung-Yun Lee[1]; [1]Department of Applied Materials Engineering, Hanbat National University, Daejeon, Korea (the Republic of); [2]ETRI, Daejeon, Korea (the Republic of).

G3.06
YSZ-based NO_2 Sensor Utilizing Hierarchical In_2O_3 Electrode Fangmeng Liu[1, 2], Yehui Guan[1, 2], Ruize Sun[1, 2], Xishuang Liang[1, 2], Peng Sun[1, 2], Yuan Gao[1, 2] and Geyu Lu[1, 2];[1]College of Electronic Science and Engineering, Jilin University, Changchun, China; [2]State Key Laboratory on Integrated Optoelectronics, Jilin University, Changchun, China.

G3.07
Mixed Potential Type Acetone Sensor Using Stabilized Zirconia And $M_3V_2O_8$ (M: Zn, Co, Ni and Mg) Sensing Electrode Fangmeng Liu [1, 2], Yehui Guan[1, 2], Ruize Sun[1, 2], Xishuang Liang [1, 2], Peng Sun[1, 2], Fengmin Liu [1, 2] and Geyu Lu[1, 2]; [1]College of Electronic Science and Engineering, Jilin University, Changchun, China; [2]State Key Laboratory on Integrated Optoelectronics, Jilin University, Changchun, China.

G3.08
Electrolyte Related Parameters of Coulometric Solid State Devices Jens Zosel, Matthias Schelter, Vladimir Vashook, Ulrich Guth and Michael Mertig; Kurt-Schwabe-Institut für Mess- und Sensortechnik e.V. Meinsberg, Waldheim, Germany.

G3.09
Enhanced Ambient-Dependent Photoresponse of $LaAlO_3$/$SrTiO_3$ Heterointerface via Catalytic Pd Nanoparticles Haeri Kim[1, 2], Ngai Yui Chan[3], Ji-yan Dai[3] and Dongwook Kim[1];[1]Physics, Ewha Womans University, Lexington, Kentucky, United States; [2]Clean Energy Research Center, Korea Institute of Science and Technology (KIST), Seoul, Korea (the Republic of); [3]The Hong Kong Polytechnic University, Hong Kong, Hong Kong.

G3.10
Hybrid Organic-Inorganic Perovksite Thin Films for Nonvolatile Memory and Broadband Photodetector Koo Tak Hong[1], Jaeho Choi[1], Ki Chang Kwon[1], Sunghak Park[1], Sooyoung Kim[2], Ki Tae Nam[1] and Ho Won Jang[1]; [1]Materials Science & Engineering, Seoul National University, Seoul, Korea (the Republic of); [2]School of Chemical Engineering and Materials Science, Chung-Ang University, Seoul, Korea (the Republic of).

SESSION I1: Poster Session
I: Ion Transport in Hybrid Organic-Inorganic Solids
Tuesday Afternoon, June 16, 2015
5:20 PM
Keystone Resorts, Red Cloud Peak

I1.01
Hydration and Proton Transfer in DNA-M (M=H, Li, Na) Saki Ito, Hitoki Semizo and Yasumitsu Matsuo; Department of Science and Engineering, Setsunan University, Osaka, Japan.

I1.02
Synthesis and Characterization of Bis (acetylacetonato κ-O, O') [zinc (II)/cobalt (II)] Hybrid Organic-Inorganic Complexes as Solid Metal Organic Precursor Reza Rooydell,Matin Roshanzamir Modaberi, Sanjaya Brahma and Chuan-Pu Liu; MSE Material and Science Engineering, National Cheng Kong University, Tainan, Taiwan.

I1.03
Nanocomposite Polymer Electrolyte Membranes Based on PVA-PVP Blend Polymer: An Evidence of Ion Diffusion through Open and Closed Polymer Network Govind K. Prajapati[1], Prem N. Gupta[2] and Ravindra Dhar[1]; [1]Center of Material Sciences, Institute of Interdisciplinary Center, University of Allahabad, Allahabad, India; [2]Department of Physics, Faculty of Science, Banaras Hindu University, Varanasi, Varanasi, India.

SESSION J2: Poster Session II
J: Permeation Membranes
Tuesday Afternoon, June 16, 2015
5:20 PM
Keystone Resorts, Red Cloud Peak

J2.01
Oxygen Permeation Characteristics of Strontium Cobaltite Membranes Shivendra K. Jaiswal[2] and Jitendra Kumar[1]; [1]Materials Science, I I T Kanpur, Kanpur, India; [2]Physics, NIT Patna, Patna, India.

J2.02
Investigation of Ceramic Composite Membranes for Hydrogen Gas Separation Jason Fish[1, 2], Sandrine Ricote[3], Ryan O'Hayre[1] and Nikolaos Bonanos[2]; [1]Metallurgical and Materials Engineering, Colorado School of Mines, Golden, Colorado, United States; [2]Energy Conversion and Storage, Technical University of Denmark, Roskilde, Denmark; [3]Mechanical Engineering, Colorado School of Mines, Golden, Colorado, United States.

J2.03
Hydrogen Permeability of TiN_x Thin Films Prepared by RF Reactive Sputtering Chiharu Kura[1], Yoshitaka Aoki[1, 2], Etsushi Tsuji[1, 2] and Hiroki Habazaki[1, 2]; [1]Graduate School of Chemical Sciences and Engineering, Hokkaido University, Sapporo, Japan; [2]Graduate School of Engineering, Hokkaido University, Sapporo, Japan.

J2.04
Influence of Crystal Orientation on the Deuterium Permeation of Cr_2O_3 Coatings Deposited by MOCVD Di He, Shuai Li, Xiaopeng Liu, Yang Lei, Chao Zhang, Shumao Wang and Lijun Jiang; Department of Energy Materials and Technology, General Research Institute for Nonferrous Metals, Beijing, China.

J2.05
The Composite Membrane Based on Sulfonated Graphene Oxide/ Sulfonated Poly(Ether Ether Ketone) for Unitized Regenerative Fuel Cells Seon G. Rho[1] and Ho Y. Jung[2];[1]School of Applied Chemical Engineering, Chonnam National University, Gwangju, Korea (the Republic of); [2]Department of Environment & Energy Engineering, Chonnam National University, Gwangju, Korea (the Republic of).

J2.06
The Application of 3D Imaging Techniques, Simulation and Diffusion Experiments to Explore Transport Properties in Porous OTM Support Materials Bernhard Tjaden[1], Zac Dehaney-Steven[2], Philip Withers[3], Robert Bradley[3], Jonathan Lane[4], Dan J. Brett[1] and Paul R. Shearing[1]; [1]Chemical Engineering, UCL, London, United Kingdom; [2]School of Chemistry, University of St Andrews, St Andrews, United Kingdom; [3]School of Materials, The University of Manchester, Manchester, United Kingdom; [4]Praxair, Inc, Tonawanda, New York, United States.

J2.07
LSCr-ScSZ Composites as Dense Separation Layers in Oxygen Transport Membranes Zonghao Shen, Stephen J. Skinner and John A. Kilner; Materials, Imperial College London, London, United Kingdom.

J2.08
Rapid Oxygen Transport Membrane Evaluation at St Andrews Zac Dehaney-Steven, Despoina Papargyriou and John Irvine; School of Chemistry, University of St Andrews, St Andrews, United Kingdom.

J2.09
Dual Phase Composite Materials as Oxygen Suppliers under Harsh CO_2 and SO_2-Containing Environments Julio Garcia-Fayos[1], Maria Balaguer[1, 2] and Jose M. Serra[1]; [1]ITQ (UPV-CSIC), Valencia, Spain; [2]IEK-1, Forschungszentrum Jülich, Jülich, Germany.

J2.10
Oxygen Transport in $(Ba_{0.5}Sr_{0.5})(Co_{0.8}Fe_{0.2})_{1-x}Y_xO_{3-\delta}$ (x = 0.01…0.1) Determined by ECR Measurements Lana-Simone Unger, Christian Niedrig, Wolfgang Menesklou, Stefan Wagner and Ellen Ivers-Tiffee; Institute for Applied Materials (IAM-WET), Karlsruhe Institute of Technology (KIT) , Karlsruhe, Germany.

J2.11
Chemical State and Electrical Conducting Property of $Ba_{2-x}La_xFe_2O_{5+\delta}$ Tsubasa Sato[1], Takashi Okiba[1], Katsumi Shozugawa[2], Motoyuki Matsuo[2], Fumito Fujishiro[3], Eiki Niwa[1] and Takuya Hashimoto[3]; [1]College of Humanities and Sciences, Nihon University, Setagaya-ku, Japan; [2]College of Arts and Sciences, The University of Tokyo, Meguro-ku, Japan; [3]Kochi University, Faculty of Science, Akebono-cho, Japan.

J2.12
Study of Y-doped $(Ba_{0.5}Sr_{0.5})(Co_{0.8}Fe_{0.2})O_{3-d}$ by Analytical Transmission Electron Microscopy Matthias Meffert[1], Lana S. Unger[2], Heike Stoermer[1], Christian Niedrig[2], Stefan F. Wagner[2], Ellen Ivers-Tiffee[2] and Dagmar Gerthsen[1]; [1]Laboratory for Electron Microscopy (LEM), Karlsruhe Institute of Technology (KIT), Karlsruhe, Germany; [2]Institute of Materials for Electrical and Electronic Engineering (IWE), Karlsruhe Institute of Technology (KIT), Karlsruhe, Germany.

J2.13
Oxygen Non-Stoichiometry and Thermo-Chemical Expansion of Ba0.5Sr0.5Co0.8Fe0.2O3-δ Studied by High Temperature X-Ray Diffraction and Thermogravimetry Mtabazi G. Sahini[1], Julian R. Tolchard[2], Kjell Wiik[1] and Tor Grande[1]; [1]Materials Science and Engineering, Norwegian University of Science and Technology (NTNU), Trondheim, Norway; [2]SINTEF Materialer og kjemi, Trondheim, Norway.

SESSION K3: Poster Session II
K: Proton-Conducting Oxides
Tuesday Afternoon, June 16, 2015
5:20 PM
Keystone Resorts, Red Cloud Peak

K3.01
Effect of Ba Nonstoichiometry in $Ba_x(Zr_{0.8}Y_{0.2})O_{3-\delta}$ on Population of 5-Coordinated Y Joon-Hyung Lee[1], Young-Woo Heo[1], Jeong-Joo Kim[1], Zhehong Gan[2] and Oc Hee Han[3];[1]School of Materials Science & Engineering, Kyungpook National University, Daegu, Korea (the Republic of); [2]National High Magnetic Field Laboratory, Tallahassee, Florida, United States; [3]Korea Basic Science Institute, Western Seoul Center, Seoul, Korea (the Republic of).

K3.02
Studies of Y-Doped Ba (Ce, Zr) O_3 for Electrochemical Promotion Applications Efstratios Stavrakakis and Danai Poulidi; Chemistry and Chemical Engineering, Queen's University Belfast, Belfast, United Kingdom.

K3.03
Moving Boundary Diffusion Mechanism for Non-Monotonic Conductivity Relaxation of Proton Conducting Perovskites Gye-Rok Kim[1], Hyun-Ho Seo[1], Jung-Mo Jo[1], Eui-Chol Shin[1], Ji Haeng Yu[2] and Jong-Sook Lee[1]; [1]Materials Science and Engineering, Chonnam National University, Gwangju, Korea (the Republic of); [2]Korea Institute of Energy Research, Daejeon, Korea (the Republic of).

K3.04
The Influence of NiO Sintering Additive on the Stability and Conductivity of $BaCe_{0.9-x}Zr_xY_{0.1}O_{3-d}$ Proton-Conducting Ceramics Sandrine Ricote[1], Anthony Manerbino[2], David Martinefski[2], W. Grover Coors[2] and Neal P. Sullivan[1]; [1]Department of Mechanical Engineering, Colorado School Of Mines, Golden, Colorado, United States; [2]CoorsTek Inc., Golden, Colorado, United States.

K3.05
Development of Cu-Based Anodes for BZCY72 Proton Ceramic Membrane Reactors Shay A. Robinson[1], Christian Kjøølseth[2], W. Grover Coors[2] and Truls Norby[1]; [1]Chemistry, University of Oslo, Oslo, Norway; [2]Protia AS, Oslo, Norway

K3.06
Hydrogen Permeation Degradation due to Yttrium Migration in Dense $BaCe_{0.8}Y_{0.2}O_{3-\delta}$-$Ce_{0.8}Y_{0.2}O_{2-\delta}$ Composite-Ceramic Membranes Wade A. Rosensteel, Sandrine Ricote and Neal P. Sullivan; Mechanical Engineering - Colorado Fuel Cell Center, Colorado School of Mines, Golden, Colorado, United States.

K3.07
Correlation between Structural and Transport Properties of Proton-Conducting $Ba_{1-x}Ln_x(Zr,In,Sn)O_{3-\delta}$ (Ln - lanthanides) Oxide Konrad Swierczek[1], Xin Liu[2], Alicja Klimkowicz[1, 3], Wojciech Zajac[1] and Bogdan Dabrowski[4]; [1]Faculty of Energy and Fuels, AGH University of Science and Technology, Kraków, Poland; [2]School of Materials Science and Engineering, University of Science and Technology Beijing , Beijing, China; [3]Department of Engineering Science and Mechanics, Shibaura Institute of Technology, Tokyo, Japan;[4]Department of Physics, Northern Illinois University, DeKalb , Illinois, United States.

K3.08
Studies of Chemical Stability of Dense $BaCe_{0.6-x}Zr_{0.2}Y_{0.2}M_xO_{3-\delta}$ (M-transition metal) Protonic Conductors Mateusz Tarach, T. Jerominek, M. Szymula and Wojciech Zajac; AGH University of Science and Technology, Faculty of Energy and Fuels, Department of Hydrogen Energy, Krakow, Poland.

K3.09
Enhanced Chemical Stability and Sinterability of Refined Proton-Conducting Perovskite: Case Study of $BaCe_{0.5}Zr_{0.3}Y_{0.2}O_{3-\delta}$ Ji Haeng Yu[1], Muhammad Hakim[2], Chung-Yul Yoo[1]and Jong Hoon Joo[1]; [1]Advanced Materials and Devices Lab., Korea Institute of Energy Research, Daejeon, Korea (the Republic of); [2]Advanced Energy Technology, University of Science and Technology, Daejeon, Korea (the Republic of).

K3.10
Effect of Titanium Doping on Structural Stability and Electrical Properties of Proton-Conducting Solid Electrolyte $BaCe_{0.8}Sm_{0.2}O_{3-\delta}$ Hailei Zhao, Chunyang Yang, Zhihong Du, Yongna Shen and Chunli Yan; University of Science and Technology Beijing, Beijing, China.

K3.11
Up-Scaling of Metallic Nanoparticle Production by Electrical Discharge for Use in Catalytic Membrane Reactor Christelle Denonville[1], Jicheng Feng[2], Marie-Laure Fontaine[1], Harald Fjeld[3], Amin A. Azar[1] and Andreas Schmidt-Ott[2]; [1]SINTEF Materials and Chemistry, Oslo, Norway; [2]Delft University of Technology, Delft, Netherlands; [3]PROTIA AS, Oslo, Norway.

K3.12
Proton Conductors Based on Lanthanum Scandate for an Electrolyte of Intermediate Temperature Operating SOFCs Takuya Yamane[1], Fumitada Iguchi[1], Hisahi Kato[2], Takahiro Ouchi[2], Makoto Shimizu[1] and Hiroo Yugami[1]; [1]Graduate School of Engineering, Tohoku University, Sendai, Japan; [2]Tohoku Electric Power Co., Inc., Sendai, Japan.

K3.13
Ni - $BaCe_{0.89}Gd_{0.1}Cu_{0.01}O_3$ as Perspective Anode Material for Proton-Conducting SOFC Denis Osinkin[1], Nina Bogdanovich[1], Elena Pikalova[1, 2] and Dimitry Bronin[1, 2]; [1]Laboratory of SOFC, Institution of High Temperature Electrochemistry, Yekaterinburg, Russian Federation; [2]Ural Federal University, Yekaterinburg, Russian Federation.

K3.15
Development of Anode-Supported Electrochemical Cell Based on Proton-Conductive $Ba(CeZr)O_3$ Electrolyte Toshiaki Yamaguchi, Hiroyuki Shimiada, Haruo Kishimoto and Yoshinobu Fujishiro; National Institute of Advanced Industrial Science and Technology, Nagoya, Japan.

K3.14
Electrical Properties of Nonstoichiometric $Ba_xZr_{0.85}Y_{0.15}O_{2.925}$ Ceramics Prepared by Solid State Reactive Sintering Nahum Maso[1], Jonathan . Polfus[2], Marie-Laure Fontaine[2] and Truls E. Norby[1]; [1]Chemistry, University of Oslo, Oslo, Norway; [2]SINTEF Materials and Chemistry, Oslo, Norway.

K3.16
Transport Kinetics of the Mixed Conductor Lanthanum Tungstate Andreas Falkenstein[1, 2] and Manfred Martin[1, 2]; [1]Institute of Physical Chemistry I, RWTH Aachen University, Aachen, Germany; [2]JARA-ENERGY, Aachen, Germany.

K3.17
Surface Segregation in Sr Doped $LaNbO_4$: Implications for Proton Transport Cheng Li and Stephen J. Skinner; Department of Materials, Imperial College London, London, United Kingdom.

K3.18
Impedance Spectroscopy on Proton Conducting Oxides $La_{1-x}A_xNbO_4$ (x=Sr,Ca) Su-Hyun Moon, Dieu Nguyen, Dong-Chun Cho, Young-Hun Kim, Eui-Chol Shin, John G. Fisher and Jong-Sook Lee; School of Materials Science and Engineering, Chonnam National University, Gwangju, Korea (the Republic of).

K3.19
Cation Diffusion in Proton Conducting Lanthanum Tungstate Einar Vollestad and Reidar Haugsrud; Department of Chemistry, University of Oslo, Oslo, Norway.

K3.20
Thermodynamics and Stoichiometry Relaxation Kinetics in Materials with Three Carriers: Analytic Relations and Numerical Simulations Daniel Poetzsch, Rotraut Merkle and Joachim Maier; MPI for Solid State Research, Stuttgart, Germany.

K3.21
Nanoscale Stabilization of Scheelite-Type Structure in $La_{0.99}Ca_{0.01}NbO_4$ Thin Films Cristina Tealdi[1, 2], Eliana Quartarone[1, 2], Piercarlo Mustarelli[1, 2] and Lorenzo Malavasi[1, 2];[1]Department of Chemistry, University of Pavia , Pavia, Italy; [2]UdR Pavia, INSTM, Pavia, Italy.

K3.22
Modeling of Defect Segregation and Space-Charge Formation in Proton-Conducting Oxides Edit E. Helgee, Anders Lindman and Goeran Wahnstroem; Applied Physics, Chalmers University of Technology, Gothenburg, Sweden.

SSI-20

Abstracts

A: Solid Oxide Fuel Cells and Electrolyzers

* Invited Speaker
** Keynote Speaker

SESSION A1: SOFC—Cathodes I
A: Solid Oxide Fuel Cells and Electrolyzers
Chair: William Chueh
Monday Morning, June 15, 2015
Keystone Resorts, Longs Peak

10:30 AM **A1.01
Oxygen Reduction Kinetics on Perovskite Oxides: Effects of Dissimilar Interfaces and Surfaces Bilge Yildiz; Massachusetts Institute of Technology, Cambridge, Massachusetts, United States.

In this talk, I will present our studies on how to improve the kinetics of oxygen reduction reactions on perovskite oxide electrocatalysts. Two related themes are of focus; improving the stability of the surface chemistry, and tuning the electron transfer kinetics at dissimilar interfaces. On the first, I will present that elastic and electrostatic interactions of the dopants within the lattice are key drivers to the detrimental segregation and phase separation of dopants at the surface. Based on this understanding, I will show that we can tune the surface charge on perovskite oxides with heterogeneous doping, and improve the chemical and electrochemical stability of the surfaces. On the second theme, I will present that, if well understood and controlled, dissimilar oxide interfaces can provide a new way to enable high-performance solid-oxide fuel cells. The hetero-interfaces between the perovskite and ruddlesden-popper type cobaltites are a prime, though so-far unique example for this capability. The underlying mechanisms must be understood quantitatively, so that we can go beyond an isolated and empirically found interface or surface structures to rationally designing dissimilar oxide interfaces with superior properties. Towards this goal, we used a novel combination of *in-situ* scanning tunneling spectroscopy, high energy x-ray photoelectron spectroscopy and density functional theory calculations. I will present our results on the local electronic structure, defect chemistry and surface chemistry at nanometer resolution in model hetero-structured thin films in the form of multilayers and vertically aligned nanostructures. These recent results are encouraging for an improved understanding of oxide hetero-interfaces and surfaces at elevated temperatures, and could enable the discovery of new interfaces with fast oxygen transport and oxygen reduction kinetics.

11:00 AM A1.02
Chemical Composition Study of the LSC-113/LSC-214 Surface and its Effect on the ORR Enhancement Andrea Cavallaro, John Kilner and Stephen Skinner; Materials, Imperial College London, London, United Kingdom.

Introduction
The reduction of the operating temperature of SOFC devices to an intermediate temperature (500-700 °C), to reduce cost and increase the mechanical stability of the cell, has mainly been limited by the performance of the cathode materials at these temperatures. In recent years many research efforts have been focused on studying how to accelerate the kinetics of the oxygen reduction reaction of the cathode materials. Sase et al. in 2008 found that the segregation at the LSC-113 perovskite surface of a small amount of LSC-214 led to an increase of the oxygen reduction activity of several orders of magnitude [1]. Despite the efforts of other groups [2-8] to investigate the origin of the oxygen reduction enhancement, this effect is still not fully understood. In this study the effect of the surface chemical composition, analyzed by Low Energy Ion Scattering (LEIS), on the oxygen surface exchange coefficient of the LSC-113 has been examined by the isotope exchange depth profiling technique.

Results and discussion
LSC thin films of the perovskite phase (LSC-113) with the composition of $La_{0.8}Sr_{0.2}CoO_{3-d}$ and $La_{0.6}Sr_{0.4}CoO_{3-d}$, and the Ruddlesden-Popper phase $(La_{0.5}Sr_{0.5})CoO_4$ (LSC214) have been prepared by pulsed laser deposition (PLD). Films of each composition have been prepared with a thickness of 200nm. After preparation the samples have been isotopically exchanged in an ^{18}O enriched atmosphere with the purpose of determine their diffusion (D^*) and surface exchange (k) properties by TOF-SIMS depth profiling analysis.
Samples of LSC-113 with both stoichiometries have been decorated with 1nm of LSC-214 by PLD and exchanged in ^{18}O. TOF-SIMS depth profiling comparison between LSC-113 samples (both stoichiometries) and samples with the same composition but decorated with 1 nm of Ruddlesden-Popper phase shows an increase in the oxygen surface activity for the decorated ones.
After the TOF-SIMS analysis the same samples have been analyzed by LEIS to investigate their chemical surface composition. LEIS is a very powerful technique that is sensitive only to the uppermost atomic layer. Normally no matrix effect is expected and then the quantification of the different surface atomic species is direct.
A depth profile analysis has been obtained alternating the primary ion source He^+ (3keV) with a secondary sputtering ion gun of Ar^+ (0.5 keV). LEIS surface spectra analysis of the exchanged samples show, for the ones decorated with 1nm of LSC-214, an excess of Sr at the top surface. A relation between the Sr concentration in the uppermost surface of the LSC-113/LSC-214 and the higher surface exchange coefficient at the heterointerface has been disclosed.

References:
[1] Sase M. et al., Solid State Ionics 2008, 178, 1843
[2] Crumling E.J. et al. J.Phys.Chem.Lett. 2010, 1, 3,149
[3] Nikolai Tsvetkov et al., J. Mater. Chem. A, 2014, 2, 14690–14695
[4] Keiji Yashiro et al., Electrochemical and Solid-State Letters, 12 _9_ B135-B137 _2009_
[5] Gerardo Jose la O' et al., Angew. Chem. Int. Ed. 2010, 49, 5344 –5347
[6] Jan Hayd et al., Journal of The Electrochemical Society, 160 (4) F351-F359 (2013)
[7] Wen Ma et al., J. Mater. Chem. A, 2015, 3, 207–219, 217
[8] Dongkyu Lee et al., J. Mater. Chem. A, 2015, 3, 2144–2157

11:20 AM A1.03
Effect of Heterointerface on Oxygen Reduction Kinetics of (Sm,Sr)CoO_3-Based Electrodes Hiroki Muroyama, Hideyuki Kanazawa, Takeou Okanishi, Toshiaki Matsui and Koichi Eguchi; Kyoto University, Kyoto, Japan.

Recently, many researches have devoted to reduce the operating temperature of solid oxide fuel cells (SOFCs). Mixed ionic-electronic conductors (MIECs) are the most promising material for cathode in intermediate-temperature SOFCs. The oxygen exchange reaction on the electrode surface is a key process for the oxygen reduction over MIEC electrodes. For $(La,Sr)CoO_3$-based electrode, it was reported that this reaction process was facilitated at the $(La,Sr)CoO_3$/$(La,Sr)_2CoO_4$ heterointerface. In this study, therefore, we focused on $(Sm,Sr)CoO_3$ perovskite oxide, which exhibits higher cathode performance than $(La,Sr)CoO_3$. The composite of $(Sm,Sr)CoO_3$–$(Sm,Sr)_2CoO_4$ was fabricated and the effect of heterointerface in this composite on the cathode performance was investigated.

The oxide materials of $Sm_{0.5}Sr_{0.5}CoO_3$ (SSC113), $SmSrCoO_4$ (SSC214), and SSC113–SSC214 composites (SSC comp., SSC113:SSC214 = 80:20, 50:50, 30:70 wt.%) were synthesized by Pechini method. A single cell was fabricated for the evaluation of their performance. Gadolinium-doped ceria (GDC) was selected as an electrolyte. The synthesized oxide materials and SSC113–GDC composite were employed as working and counter electrodes, respectively. Impedance spectra of working electrode were obtained at 550–800 ºC in 79% N_2−21% O_2.
The interfacial conductivity of the SSC comp. (80:20 wt.%) was the highest among all oxide materials investigated. This result indicated that the formation of heterointerface in the composite was effective for the enhancement of cathode performance. Then, the amount of heterointerface

in the composites was estimated from the SEM image. The SSC comp. (50:50 wt.%) and SSC comp. (30:70 wt.%) possessed larger amount of heterointerface than the SSC comp. (80:20 wt.%). This result did not correspond to the order of interfacial conductivity. Accordingly, the cathode performance of SSC comp. was affected by the content ratio of SSC113 as well as the formation of heterointerface in the sample.

11:40 AM *A1.04

Quantitative Evaluation of Effective Reaction Area in Solid Oxide Fuel Cell Cathodes Koji Amezawa[1], Yoshinobu Fujimaki[2], Takashi Nakamura[1], Katherine D. Bagarinao[3], Katsuhiko Yamaji[3], Kiyofumi Nitta[4], Yasuko Terada[4], Keiji Yashiro[5], Fumitada Iguchi[2], Hiroo Yugami[2] and Tatsuya Kawada[5]; [1]IMRAM, Tohoku University, Sendai, Japan; [2]Graduate School of Engineering, Tohoku University, Sendai, Japan; [3]AIST, Tsukuba, Japan; [4]JASRI, Sayo, Japan; [5]Graduate School of Environmental Studies, Tohoku University, Sendai, Japan.

Recent years, solid oxide fuel cells (SOFCs) attract much attention as energy conversion devices with high efficiency. For further enhancement of the performance, oxygen reduction kinetics at cathodes should be understood and improved. When a mixed ionic-electronic conducting oxides, such as (La,Sr)CoO_3 and (La,Sr)(Co,Fe)O_3, is used as an SOFC cathode, electrochemical oxygen reduction can occur not only at the electrode/electrolyte/gas interface (triple phase boundary) but also at the electrode surface/gas. Thus, in mixed conducting oxide cathodes, it is considered the reaction sites are not limited to the triple phase boundaries but distribute to a certain distance from the electrode/electrolyte interface. It is believed that the effective reaction area is determined by the ratio between the resistances of the surface reaction at the oxide surface and of the oxide ion diffusion in the oxide bulk. However, to the best of our knowledge, no one has confirmed this hypothesis with experimental observation.

In this work, we proposed patterned thin film electrodes, which is suitable for direct observation of the effective reaction area in SOFC cathodes. With the proposed electrodes, we performed *operando* micro X-ray absorption spectroscopy (XAS) or $^{18}O/^{16}O$ isotope exchange measurements in addition to conventional electrochemical measurements including electrochemical impedance spectroscopy (EIS). $La_{0.6}Sr_{0.4}CoO_{3-d}$ was chosen as a model mixed conducting oxide, and the effective reaction area for electrochemical oxygen reduction in this oxide electrode was experimentally evaluated in a quantitative way.

SESSION A2: Poster Session I
A: Solid Oxide Fuel Cells and Electrolyzers
Monday Afternoon, June 15, 2015
12:00 PM
Keystone Resorts, Red Cloud Peak

A2.01

Structural Stability of Complex Perovskites for Solid Oxide Fuel Cells from First Principles Calculations Maija M. Kuklja[1], Eugene A. Kotomin[2, 3], David Fuks[4], Yuri A. Mastrikov[2]and Joachim Maier[3]; [1]Materials Science and Engineering Department, University of Maryland College Park, College Park, Maryland, United States; [2]Institute for Solid State Physics, University of Latvia, Riga, Latvia; [3]Max Planck Institute for Solid State Research, Stuttgart, Germany; [4]Dept Materials Engineering, Ben Gurion University of the Negev, Beer Sheva, Israel.

Among advanced materials for clean energy, non-stoichiometric $Ba_xSr_{1-x}Co_{1-y}Fe_yO_{3-\delta}$ (BSCF) and $La_xSr_{1-x}Co_{1-y}Fe_yO_{3-\delta}$ (LSCF) are considered as promising materials for cathodes in solid oxide fuel cells (SOFC) and oxygen permeation membranes [1-3]. BSCF exhibits the best oxygen exchange performance among similar materials, mixed ionic and electronic conductivity, high oxygen vacancy concentration, and low oxygen diffusion activation barrier, which largely define the oxygen reduction kinetics. However, it tends to decompose at low temperatures into a mixture of cubic and hexagonal perovskite phases, which strongly affects its practical applications.

To understand the mechanism(s) of this unwanted process, the first principles quantum mechanical calculations of BSCF and LSCF crystals with different non-stoichiometry were performed and possible decomposition scenarios were studied. It is shown [3,4] that formation energies of oxygen vacancies in the cubic and hexagonal phases of BSCF differ considerably and also behave in quite different ways depending on non-stoichiometry; in fact, it is the oxygen non-stoichiometry that makes the cubic phase more stable than the hexagonal phase. In comparison, LSCF is shown to be much more stable with respect to both the phase transformation and phase decomposition. First principles calculations were performed also for a series of related perovskite solid solutions with a detailed thermodynamic analysis of the conditions under which a cubic phases are stable [5], in good agreement with experimental data.

[1] J. A. Kilner et al, Ann. Rev. Mater. Res. 44, 365 (2014).
[2] M. Kuklja, et al, Phys. Chem. Chem. Phys. **15**, 5443 (2013).
[3] Yu. Mastrikov et al, Phys. Chem. Chem. Phys. **15**, 911 (2013).
[4] M.M. Kukla et al, J Phys Chem C 116, 18605 (2012).
[5] D. Fuks et al. J. Mater. Chem. A **1**, 14320 (2013)

A2.02

Long Term Degradation Effects in Doped Ceria from First Principles Steffen Grieshammer[1, 2, 3], Benjamin O. Grope[1, 2, 3], Julius Koettgen[1, 2, 3] and Manfred Martin[1, 2, 3]; [1]Institute of Physical Chemistry I, RWTH Aachen University, Aachen, Germany; [2]JARA-ENERGY, Aachen, Germany; [3]JARA-HPC, Aachen, Germany.

The properties of rare earth doped ceria have been investigated for many years due to its high oxygen ion conductivity and potential application in solid oxide fuel cells. Theoretical as well as experimental approaches are both vital in understanding the underlying mechanisms in order to provide tailor-made materials specified for individual technical requirements. The ionic conductivity of doped ceria has been thoroughly investigated applying ab initio calculations and Kinetic Monte Carlo simulations. However, information about the impact of the cation distribution on the conductivity is yet missing.

We therefore investigate the dopant distribution and its influence on the oxygen ion conductivity of rare earth doped ceria by combining density functional theory and Monte Carlo simulations. The interaction of defects and the energy barriers for oxygen ion migration are described by a pair interaction model where the corresponding energies of association and migration are calculated by means of DFT+*U* including finite size corrections. Coordination numbers obtained by applying the Metropolis Monte Carlo algorithm show remarkable agreement with experimental data.

We utilize different simulated cation lattices for Kinetic Monte Carlo simulations to predict the oxygen ion conductivity. Compared to randomly generated lattices a decrease of the conductivity in the equilibrated lattices can be observed due to local ordering of dopant ions. We interpret this observation as a long term degradation effect in the electrolyte under operation conditions of a solid oxide fuel cell.

A2.03 WITHDRAWN

A2.04

First Principles Thermodynamics of Oxygen Vacancies in Ultrathin Films of $BaZrO_3$ Marco Arrigoni[1], Eugene A. Kotomin[1], Joachim Maier[1] and Tor S. Bjorheim[2]; [1]Physical Chemistry of Solids, Max Planck Institute for Solid State Research, Stuttgart, Germany; [2]Department of Chemistry, University of Oslo, Oslo, Norway.

$BaZrO_3$ membranes have attracted considerable attention for potential applications in electrochemical devices such as solid oxides fuel cells (SOFCs), sensors and hydrogen pumps, due to high solid state proton conductivity and good chemical stability. Doping with trivalent cations (usually Y^{3+}) results in the formation of charge-compensating oxygen vacancies, which upon subsequent exposure to humid atmospheres, leads to incorporation of protons by dissociative absorption of $H_2O(g)$. Although the doubly positively charged oxygen vacancies dominate in acceptor doped oxides, vacancies with two trapped electrons (color *F*-centers) are created under strongly reducing conditions. In addition, these two charge states (+2 and 0) represent limiting cases for oxygen vacancies in partly ionic and partly covalent ABO_3 type perovskites. Understanding the vacancy formation, migration and segregation to the surfaces/interfaces is important for numerous applications including SOFC. In this contribution, we explore possible effects of thin film confinement on the structural, thermodynamic and electronic properties of oxygen vacancies in $BaZrO_3$.

We apply two complementary first principles methods (the linear combination of atomic orbitals (LCAO) and the plane-wave method within the projector augmented waves (PAW) approach), employing the hybrid HF-DFT PBE0 functional and different DFT functionals, to develop a more accurate and complete approach for investigation of structural, electronic and vibrational properties of oxygen vacancies in variable charge states in ultrathin films of $BaZrO_3$. We considered non-stoichiometric symmetrical (001) terminated slabs, with 3 to 9 atomic layers; corresponding to a free standing film up to ca. 2 nm thick. We explore the defect formation energy and charge density redistribution in different film thicknesses, in order to predict the differences between surface, sub-surface and bulk defects, and thus the defect's segregation properties. Particular emphasis is laid on the vibrational contributions to the Gibbs formation energy and the confinement effects for charge carriers in thin perovskite films in general.

A2.05

Optimum Zr Configurations in $Ce_{1-x}Zr_xO_2$ (x∈[0,1]) Solid Solution Using Genetic Algorithm and Density Functional Theory Jason Kim[2], Shin-Won Hwang[1], Ji-Su Kim[1], Byung-Kook Kim[3] and Yeong-Cheol Kim[1]; [1]School of Energy, Materials, and Chemical Engineering, KoreaTech, Cheonan, Korea (the Republic of); [2]School of Electrical and Computer Engineering, UNIST, Ulsan, Korea (the Republic of); [3]High Temperature Energy Materials Center, Korea Institute of Science and Technology, Seoul, Korea (the Republic of).

CeO_2 has been known for excellent oxygen storage capacity (OSC) and the addition of Zr improves the OSC further. The added Zr atoms into CeO_2 reside on Ce sites with many different configurations. The number of configurations increases very fast with the Zr concentration. It is ${}_{32}C_8$ (~ 10 million) in case of a supercell containing 32 Ce atoms and 64 O atoms, and replacing a quarter of Ce atoms with Zr atoms. We could drastically reduce the number of configurations by converting the coordinate data of the Zr atoms into the distance data among the Zr atoms. This conversion reduces the number of configurations from 10 million to 600. Genetic algorithm was employed to further reduce the number of configurations. We obtained optimum Zr configurations in the $Ce_{1-x}Zr_xO_2$ (x∈[0,1]) solid solution using density functional theory, in addition to genetic algorithm.

A2.06

Theoretical Study of Oxygen Vacancy Formation in $Ce_{0.75}Zr_{0.25}O_2$ Solid Solution Using Density Functional Theory Ji-Su Kim[1], Shin-Won Hwang[1], Jason Kim[2], Byung-Kook Kim[3]and Yeong-Cheol Kim[1]; [1]School of Energy, Materials, and Chemical Engineering, KoreaTech, Cheonan, Korea (the Republic of); [2]School of Electrical and Computer Engineering, UNIST, Ulsan, Korea (the Republic of); [3]High Temperature Energy Materials Center, Korea Institute of Science and Technology, Seoul, Korea (the Republic of).

$Ce_{0.75}Zr_{0.25}O_2$ (CZO) solid solution has been widely used in solid oxide fuel cells and solid oxide electrolyzer cells due to its high oxygen release and storage capacity (OSC) and high ionic conductivity. To understand high OSC and ionic conductivity, many researchers have worked on the oxygen vacancy (V_O) formation and its migration in CZO using density functional theory (DFT). However, the reported supercell structures of CZO solid solutions were energetically unfavorable [1] or too small to describe V_O formation [2]. The V_O formation should be described carefully based on an optimum solid solution of CZO. We investigated the V_O formation in CZO solid solution using DFT. In order to find an optimum solid solution of the 2x2x2 CZO super cell, a genetic algorithm was introduced. The calculated formation enthalpy of the CZO solid solution was lower than that of the CZO compound by 1.04 eV. The V_O formation energy was calculated from the optimum CZO solid solution. They were varied with neighboring metal (Ce or Zr) tetrahedral clusters; the metal tetrahedral clusters are composed of Ce-Ce-Ce-Ce, Ce-Ce-Ce-Zr, Ce-Ce-Zr-Zr, and Ce-Zr-Zr-Zr. The V_O formation energies of the CZO solid solution were increased in order of Ce-Zr-Zr-Zr, Ce-Ce-Zr-Zr, Ce-Ce-Ce-Zr, and Ce-Ce-Ce-Ce. Based on the vacancy formation energy, the concentration of V_O as a function of temperature was calculated at 0.2 atm of O_2 partial pressure. We found that the V_O concentration in the solid solution was 6 orders of magnitude higher than that of the CZO compound at 1000 K and 0.2 atm of O_2 partial pressure.

[1] H.-F. Wang, H.Y Li, X.-Q. Gong, Y.-L. Guo, G.-Z. Lu, and P. Hu, Phys. Chem. Chem. Phys. 14, 16521 (2012).
[2] H.-T. Chen and J.-G chang, J. Chem. Phys. 132 214702 (2010).

A2.07

High-Throughput Density Functional Theory Screening of Perovskite Compounds for High Oxygen Surface-Exchange for Solid Oxide Fuel Cell Cathodes Ryan Jacobs[1], Dane Morgan[1, 3] and John Booske[2]; [1]Materials Science Program, University of Wisconsin- Madison, Madison, Wisconsin, United States; [2]Electrical and Computer Engineering, University of Wisconsin- Madison, Madison, Wisconsin, United States; [3]Materials Science and Engineering, University of Wisconsin-Madison, Madison, Wisconsin, United States.

We employed high-throughput Density Functional Theory (DFT) methods using the Materials Simulation Toolkit (MAST)[1] software and the Python Materials Genome (Pymatgen)[2] software to search a broad composition space for high activity, thermodynamically stable perovskite (chemical formula $A_{1-x}A'_xB_{1-x}B'_xO_3$) compounds for application as cathodes in solid oxide fuel cells (SOFCs). The perovskite A-site composition space contains the alkaline earth and rare earth elements A:{Ca, Sr, Ba, La, Pr, Nd, Sm, Gd, Dy, Ho} while the B-site composition space consists of the 3d transition metals B:{Sc, Ti, V, Cr, Mn, Fe, Co, Ni} and, in the case of $(Ba,Sr)(Co,Fe)O_3$–based materials, the 4d and 5d transition metal elements B:{Zr, Nb, Mo, Ru, Rh, Pd, Hf, Ta, W, Re, Os, Ir, Pt, Au}. Recent computational work has demonstrated there exists a linear relationship between the calculated O p-band center and experimental surface exchange coefficient (k^*) values for numerous perovskites, and O p-band center is thus a useful descriptor for k^* and the strongly correlated overall oxygen reduction reaction (ORR) activity for perovskite materials.[3] For the approximately 1,300 perovskites considered in this work, we screened each material for two properties: predicted ORR activity and thermodynamic stability under SOFC operating conditions. The ORR activity is screened using the k^* - p-band correlation first described in Ref. [3]. The stability of each material is analyzed using the multicomponent grand-potential phase diagram analysis tool from Pymatgen, assuming a system open to both O and H to account for stability under environments of specific pO_2 and pH_2O. Overall, we found there are numerous materials that are both thermodynamically stable and have predicted k^* values as good or better than top performing materials like $(La,Sr)(Co,Fe)O_3$ and $(Ba,Sr)(Co,Fe)O_3$.

References:
[1] Angsten, T., et. al. New Journal of Physics (2014)
[2] Ong, S. P., et. al. Computational Materials Science (2013)
[3] Lee, Y. L., et. al. Energy and Environmental Science (2011)

A2.08

Accelerated Materials Design of $Na_{0.5}Bi_{0.5}TiO_3$ Oxygen Ionic Conductors Based on First Principles Calculations Xingfeng He and Yifei Mo; Department of Materials Science and Engineering, University of Maryland, College Park, College Park, Maryland, United States.

Over the past decades, significant research efforts have been dedicated to seeking fast oxygen ion conductor materials, which have important technological applications in electrochemical devices such as solid oxide fuel cells, oxygen separation membranes and sensors. Recently, sodium bismuth titanate, $Na_{0.5}Bi_{0.5}TiO_3$ (NBT), was reported as a new family of fast oxygen ionic conductor. This first principles computation study aims to understand the O diffusion mechanisms in the NBT material and to design this material with enhanced oxygen ionic conductivity. Using the NBT materials as an example, we demonstrate the computation capability to evaluate the phase stability, chemical stability, and ionic diffusion of the ionic conductor materials. We identify the intrinsic limiting factors in increasing the ionic conductivity of the NBT materials, and predict new doping strategies to achieve significant increase in oxygen ionic conductivity. Our results provide new avenues for the future design of the NBT materials and demonstrate the accelerated design of new ionic conductor materials based on first principles techniques. The materials design workflow demonstrated in this study is not limited to oxygen ionic conductor materials, and can be easily transferred to any (e.g. Li^+, Na^+) ionic conductor materials.

A2.09

Evaluation of the Chemical Expansion Coefficient Using Modulated Dilatometry Shany Hershkovitz, Lea Halimi and Yoed Tsur; Chemical Engineering, Techion IIT-Israel Institute of Technology, Haifa, Israel.

Understanding and evaluating the correlation between the thermal, chemical and mechanical properties of ceramic materials is both an industrial and scientific challenge. For instance, the reliability of SOFC stacks needs to be addressed since they exhibit failures caused by thermal and chemical cycling. The structure of SOFC, where the various components are held together at intimate contact, results in development of stress between and in some cases within the materials upon heating or cooling. This stems from (a) the difference in thermal expansion coefficient (CTE) and (b) chemical strain. The latter can be a result of either chemical cycling including operational error or as part of the total CTE.

Modulated Dilatometry is used in this research for isolating the chemical expansion coefficient (CTE_C) from the total expansion CTE. Gd doped Ceria (CGO) is chosen here as a case study for two main reasons: 1. CGO is one of the most promising electrolyte materials for intermediate temperatures SOFC due to its high ionic conductivity at relatively low temperature; 2. CGO exhibits “chemical stain effect” whereas the elastic energy is converted to chemical energy of point defects. Accurate calculation of the CTE and CTE_C can assist in comprehending of the defect model of this system and its behavior at different real world conditions.

A2.10

The Effect of Oxygen Nonstoichiometry on Thermal Expansion and Conduction Mechanism of $LaNi_{1-x}Fe_xO_{3-\delta}$ Eiki Niwa and Takuya Hashimoto; Department of Physics, Nihon University, Setagaya-ku, Japan.

As an electrode material for solid oxide fuel cells, SOFC, thermal expansion coefficient, TEC, is important information since mismatch of TEC between electrolyte and electrode is one of the causes of mechanical destruction of SOFC. Dependence of TEC of $LaNi_{0.6}Fe_{0.4}O_{3-\delta}$, LNF64, which is candidate material for SOFC cathode, on oxygen partial pressures, $P(O_2)$ has been investigated by dilatometry and compared with that of $La_{0.6}Sr_{0.4}Co_{0.2}Fe_{0.8}O_{3-\delta}$, LSCF6428. TEC of LNF64 is $P(O_2)$ independent, for example 1.26×10^{-5} K^{-1} at 500 °C under $P(O_2)$ between 10^{-4} bar and 1 bar, which can be attributed to little dependence of δ of about 0.10 on temperature and $P(O_2)$. The almost constant δ, which results in little variation of average valence of B-site by delocalization of electron between Fe ion and Ni ion, is also an origin of $P(O_2)$ independent activation energy of hopping conduction of LNF64. On the contrary, TEC of LSCF6428 increases with decreasing $P(O_2)$ due to variation of oxygen nonstoichiometry, δ, accompanied by variation of valence of Co ion. TEC of LSCF6428 at 500 °C under $P(O_2)$ of 1 bar and 10^{-4} bar are 1.56×10^{-5} K^{-1} and 1.80×10^{-5} K^{-1}, respectively. Since TEC of 8 mol % yttria stabilized zirconia, 8YSZ, is 1.01×10^{-5} K^{-1} at 500 °C under $P(O_2)$ between 1 bar and 10^{-4} atm, it can be concluded that the mechanical stress generated by change of temperature and/or $P(O_2)$ between LNF64 and 8YSZ is smaller than that between LSCF6428 and 8YSZ.

A2.11

Oxygen Nonstoichiometry, Electrical Properties and Thermochemical Expansion of Strontium-Rich $Nd_{2-x}Sr_xNiO_{4\pm D}$ Mixed Conductors Ekaterina Kravchenko[1, 2], Kiryl Zakharchuk[1], Jekabs Grins[3], Gunnar Svensson[3], Vladimir Pankov[2] and Aleksey Yaremchenko[1]; [1]CICECO, Department of Materials and Ceramic Engineering, University of Aveiro, Aveiro, Portugal; [2]Department of Chemistry, Belarusian State University, Minsk, Belarus; [3]Department of Materials and Environmental Chemistry, Stockholm University, Stockholm, Sweden.

Perovskite-related nickelates with layered Ruddlesden-Popper (RP) structure and general formula $Ln_{1+n}Ni_nO_{3n+1}$ (n = 1-3) combine redox stability with oxygen stoichiometry changes, yielding enhanced mixed transport and electrocatalytic properties. These unique features are promising for applications as oxygen electrodes with good electrochemical performance in reversible SOFC/SOEC (solid oxide fuel/electrolysis cell) systems. The present work was focused on the assessment of neodymium-strontium nickelates with n = 1 RP structure as prospective reversible oxygen electrodes. $Nd_{2-x}Sr_xNiO_{4\pm d}$ (x = 1.0-1.6) ceramic samples were prepared by Pechini method with repeated annealings at 650-1000°C, and sintered at 1150-1200°C for 15h under oxygen atmosphere. Variable-temperature XRD studies confirmed that all studied compositions retain tetragonal RP structure in the temperature range 25-1000°C and $p(O_2)$ = 0.21-1.00 atm. The characterization of ceramic materials included microstructural studies, controlled-atmosphere dilatometry and thermogravimetry, and measurements of electrical conductivity as function of temperature and oxygen partial pressure. The absolute values of oxygen nonstoichiometry were determined from the mass changes on total reduction to Nd_2O_3, SrO and metallic Ni.

The results demonstrated that, contrary to parent oxygen-overstoichiometric Ln_2NiO_{4+d} (Ln = La, Pr, Nd) compounds, strontium-rich $Nd_{2-x}Sr_xNiO_{4-d}$ exhibit oxygen deficiency under oxidizing conditions in high-temperature range with d increasing from 0.04 for x = 1.0 to 0.42 for x = 1.6 at 950°C. Electrical conductivity shows metallic-like behavior at 600-1000°C and decreases on reducing $p(O_2)$. At 800°C, the values of conductivity in air vary in the range 75-290 S/cm, with the maximum observed for x = 1.2. Thermochemical expansion and electrical properties of the studied materials were correlated with defect chemistry, oxygen nonstoichiometry and structural parameters.

A2.12

Oxygen Nonstoichiometry and Defect Chemistry of Perovskite-Structured $SrSn_{1-x}Fe_xO_{3-x/2+\delta}$ Chang Sub Kim[1], Sean R. Bishop[1, 2], Nicola H. Perry[1, 2], Jae Jin Kim[1] and Harry L. Tuller[1, 2]; [1]Department of Materials Science and Engineering & Skoltech Center for Electrochemical Energy Storage, MIT, Cambridge, Massachusetts, United States; [2]International Institute for Carbon Neutral Energy Research (WPI-I2CNER), Kyushu University, Fukuoka, Japan.

There is great interest in identifying alternate solid oxide fuel cell (SOFC) cathode materials capable of operating at reduced temperatures. The mixed ionic and electronic conducting (MIEC) perovskite-structured $SrTi_{1-x}Fe_xO_{3-x/2+\delta}$ (STF) was identified as a promising candidate for solid oxide fuel cell cathodes given rapid oxygen surface exchange kinetics. The exchange kinetics were correlated with the minority electron charge density in STF, which in turn depends on its defect chemistry and band structure [1]. In this study, we examine the oxygen nonstoichiometry and defect chemistry of the related $SrSn_{1-x}Fe_xO_{3-x/2+\delta}$ (SSF) system by means of thermogravimetry as a function of oxygen partial pressure at 973-1272 K. Higher reducibility is observed compared to corresponding compositions in $SrTi_{1-x}Fe_xO_{3-x/2+\delta}$ system. The bulk electrical conductivity is measured in parallel to examine how changes in defect chemistry and electronic band structure associated with the substitution of Ti by Sn impact carrier density and ultimately electrode performance.

[1] W. Jung and H. L. Tuller, *A New Model Describing Solid Oxide Fuel Cell Cathode Kinetics: Model Thin Film $SrTi_{1-x}FexO_{3-\delta}$ Mixed Conducting Oxides – a Case Study,* Advanced Energy Materials, 1, 1184-1191 (2011).

A2.13

Defect Structure and Related Properties of $SrTi_{1-x}Fe_xO_{3-d}$ Vladimir Sereda, Dmitry Tsvetkov, Ivan Ivanov and Andrey Zuev; Department of Physical Chemistry, Ural Federal University, Ekaterinburg, Russian Federation.

Various perovskite-type oxides with general formula ABO_3 are commonly regarded as promising materials for different high-temperature electrochemical devices. The possibility of doping enables precise tailoring of the physical properties of these materials, vastly expanding their applicability ranges. Thus, doped with Fe strontium titanates $SrTi_{1-x}Fe_xO_{3-d}$ combine the high stability of $SrTiO_3$ with the elevated mixed ionic-electronic conductivity of $SrFeO_3$. That is why they have received great attention over the past few decades as materials for solid oxide fuel cell (SOFC) cathodes, oxygen separation membranes and oxygen sensors. So far, the important properties of $SrTi_{1-x}Fe_xO_{3-d}$ such as oxygen nonstoichiometry, chemical expansion, total conductivity and Seebeck

coefficient were studied in the relatively narrow range of temperature and oxygen partial pressure (pO_2). Therefore, the main purposes of the work were (i) to study these properties in wide range of pO_2 and temperature and (ii) to find the relationship between them and the defect structure of $SrTi_{1-x}Fe_xO_{3-d}$.

Powder samples of $SrTi_{1-x}Fe_xO_{3-d}$ were synthesized using the standard ceramic and spray-pyrolysis techniques. XRD analysis of the samples obtained accordingly showed no indication for the presence of a second phase. Oxygen nonstoichiometry of $SrTi_{1-x}Fe_xO_{3-d}$ was measured using the coulometric titration method in the ranges of temperature and log(pO_2, atm) $750 \leq T \leq 1050$°C and $-18 \leq \log(pO_2) \leq -0.7$, respectively. Total conductivity and Seebeck coefficient of $SrTi_{1-x}Fe_xO_{3-d}$ as functions of T and pO_2 were measured simultaneously using the standard 4-probe DC technique. Chemical expansion was measured using the original dilatometric setup. The experimental results obtained were discussed on the basis of the defect structure model proposed for $SrTi_{1-x}Fe_xO_{3-d}$. This work was supported by Russian Fund for Basic Research, grant No 15-03-07446.

A2.14

Oxygen Content, Thermodynamic Stability and Electrical Properties of $YBaCo_{4-x}Zn_xO_{7-\delta}$ Dmitry S. Tsvetkov, Nadezhda S. Tsvetkova and A. Y. Zuev; Department of Chemistry, Ural Federal University, Ekaterinburg, Russian Federation.

Complex oxides $LnBaCo_4O_{7-d}$ (Ln=Y and rare-earth cations), a new class of geometrically frustrated magnets, have already attracted great attention in the recent years due to their unusual physical properties.
However, the main disadvantage of $LnBaCo_4O_7$ materials is instability of their hexagonal crystal structure in the intermediate temperature range 873-1050 K. One possibility to increase the stability of $LnBaCo_4O_7$ materials is to be substitution of zinc for cobalt. Therefore, the priority purposes of the present work were (i) to determine the solubility limit for Zn in $YBaCo_{4-x}Zn_xO_{7-d}$, (ii) to study the thermodynamic stability of corresponding solid solutions, (iii) to measure their oxygen nonstoichiometry, overall conductivity and thermo-EMF as a function of oxygen partial pressure (*pO2*) and temperature.

Powder samples of the nominal composition $YBaCo_{4-x}Zn_xO_{7-d}$ (x=0-3) were prepared by means of glycerol – nitrate method using Y_2O_3, $BaCO_3$, ZnO and Co as starting materials. All materials used had a purity of 99.99%. The powders obtained were finally calcined at 1100 °C for 12 h in air. The phase composition of the powder sample prepared accordingly was studied at room temperature by means of X-ray diffraction (XRD) with Equinox 3000 diffractometer (Inel, France) using Fe K_α radiation. Oxygen nonstoichiometry, d, of $YBaCo_{4-x}Zn_xO_{7-d}$ (x=0-3) was measured by means of thermogravimetric (TG) technique and coulometric titration. Total conductivity and Seebeck coefficient were measured simultaneously by 4-probe dc-method.

Zn doping was shown to increase thermodynamic stability of the oxides $YBaCo_{4-x}Zn_xO_{7-d}$ (x=0-3) at high *pO2*. However, it was shown that $YBaCo_{4-x}Zn_xO_{7-d}$ (x=0-3) oxides possess narrow range of homogeneity with respect to oxygen. Both total conductivity increase with *pO2* and positive sign of thermo-EMF indicate in favor of electron holes as predominant charge carriers in $YBaCo_{4-x}Zn_xO_{7-d}$ (x=0-3).

This work was supported by the Russian Foundation for Basic Research (grant No. 13-03-01031).

A2.15

Iso-Octane Internal Reforming in a Solid Oxide Cell Reactor Abdullah Al-Musa[2], Mohamed Al-Saleh[2], Ayman Al-Zahrani[2], Vasileios Kyriakou[3, 4], George Marnellos[1, 4] and Nikolaos Kaklidis[1]; [1]Department of Mechanical Engineering, University of Western Macedonia, Kozani, Greece; [2]Water & Energy Research Institute, King Abdulaziz City for Science & Technology, Riyadh, Saudi Arabia; [3]Department of Chemical Engineering, Aristotle University of Thessaloniki, Thessaloniki, Greece; [4]Chemical Process & Energy Resources Institute, Centre for Research & Technology Hellas, Thessaloniki, Greece.

Introduction:
The increasing energy demands are mainly compensated by fossil fuels employing thermodynamic limited heat cycle configurations. This "business as usual" scenario is leading to natural sources depletion and significant environmental implications, which is in contrast with the strategies for a sustainable future imposed by international organizations. Fuel cells are considered as a promising energy conversion technology, capable to satisfy the needs of high efficiency and low environmental footprint [1]. Although H_2 is the ideal fuel for fuel cells, several obstacles related to its limited availability, the absence of relevant infrastructure and the difficulties associated with its storage and transport retard their market roll out [2]. In the meantime, the use of conventional fuels with established infrastructure, like gasoline, could be an alternative solution to accelerate the commercialization of fuel cells. SOFCs due to their high operating temperature, can be potentially operated directly on conventional hydrocarbon fuels [2].

To this end, electro-catalytic active and conductive composites, exhibiting tolerance toward cabon poisoning, should be developed. Recently, the substitution of Ni cermets, that are suffering from deactivation when exposed to hydrocarbon fuels, by Cu-based composites has been succesfully demonstrated [2].

In the present work, iso-octane and steam is cofed in a solid oxide reactor of the type $Cu\text{-}CeO_2$/YSZ/Pt. The impact of temperature, feed composition and overpotential on products' distribution and electro-catalytic activity is examined. Furthermore the as prepared cell was also electrochemically characterized employing typical fuel cell measurements and AC impedance spectroscopy.

Experimental:
The electrochemical experiments were performed in an YSZ tube, closed flat at its bottom end. Metallic Pt was employed as cathode, while the anode was consisted of a Cu/CeO_2 mixed oxide composite. The measurements were carried out in the temperature range of 750-850°C at atmospheric pressure. The cell voltage and developed electrical current were monitored by means of digital multi-meters and the external resistive load was controlled by a resistance box (Time Electronics 1051). The electrochemical impedance spectra were acquired under open circuit conditions in the frequency range from 0.01 Hz to 1 MHz, using the IVIUM technologies electrochemical workstation and the corresponding software (IVIUMSOFT) for data processing.

Results and Discussion
$Cu\text{-}CeO_2$ composites exhibited high (electro-)catalytic activity and stability toward iso-octane steam reforming to syngas and electro-oxidation of all combustible species that are present at the anode chamber. Fuel cell experiments showed that the achieved power densities were substantially increased with temperature and i-C_8H_{18}/H_2O feed molar ratios. AC impedance studies revealed contributions both from charge and mass transfer processes. The increase in cell temperature led to reduced cell and interfacial resistances. The effect of feed composition was clearer in the portion of the interfacial resistance associated to diffusion limitations.

Conclusions:
The obtained results show that i-C_8H_{18} is efficiently reformed by H_2O to syngas over Cu/CeO_2 composites. Under open circuit conditions, the distribution of products is also influenced by the associated i-C_8H_{18} thermal/catalytic decomposition reactions, while electro-oxidation of combustible species is prevailing during anodic polarization. Under fuel cell operation, the electrochemical performance of $Cu\text{-}CeO_2$ was investigated by voltage-current density-power density and AC impedance measurements. The achieved power output was enhanced at higher cell temperatures and C/H_2O ratios.

References:
[1] Singhal SC, Kendall K, High Temperature Solid Oxide Fuel Cells: Fundamentals, Design and Applications, Elsevier Advanced Technology, 2003.
[2] Gorte RJ, Vohs JM, McIntosh S. Solid State Ionics 2004;175(1-4):1-6

A2.16

Insights into Oxygen Anion Transprt in Layered Oxides via *In-Situ* Powder Neutron Diffraction Steven McIntosh[1], Alexander C. Tomkiewicz[1], Mazin A. Tamimi[1] and Ashfia Huq[2];[1]Chemical & Biomolecular Engineering, Lehigh University, Bethlehem, Pennsylvania, United States; [2]Neutron Sciences, Oak Ridge National Laboratory, Oak Ridge, Tennessee, United States.

The promise of direct and efficient conversion of chemical to electrical energy makes fuel cell development an area of great technological interest. Solid Oxide Fuel Cells (SOFCs) are one of the most promising technologies to meet this goal. A significant barrier to progress is a lack of experimental techniques that can probe the properties of these materials under high temperate working conditions in both oxidizing and reducing gas environments.

Neutron diffraction is one technique that can achieve this goal to reveal information relating to phase transition, order-disorder phenomenon, and the presence of anionic and cationic vacancies in crystalline oxides. Most powerfully, all of this information is collected in a single experiment over a wide variety of operating conditions. Analysis of these results enables visualization of transport pathways in ionic conductors, guiding future material development. This visualization is achieved through analysis of both occupancy (providing vacancy concentration) and the anisotropic atomic displacement (providing magnitude and direction of motion) of the oxygen sites in the structure. For layered oxides this reveals preferential vacancy localization and associated preferred transport pathways. This presentation will discuss results from a recently developed in-situ neutron diffraction cell developed for the POWGEN beam line at the Spallation Neutron Source, Oak Ridge National Laboratory. Results will be presented for a variety of materials to demonstrate the versatility of this technique.

A2.17

Oxygen Nonstoichiometry and Defect Equilibrium in the Ruddlesden–Popper Type Oxides $La_xSr_{3-x}Fe_2O_{7-\delta}$ (x=0, 0.25 and 0.5) Yihan Ling, Fang Wang, Yusuke Okamoto, Takashi Nakamura and Koji Amezawa; Institute of Multidisciplinary Research for Advanced Materials, Tohoku University, Sendai, Japan.

The Ruddlesden-Popper type oxide $Sr_3Fe_2O_{7-\delta}$ belongs to the space group *I4/mmm* with tetragonal symmetry, and consists of same elements as the typical perovskite $SrFeO_{3-\delta}$. It possesses several oxygen-ion sites, O1, O2, and O3. Oxygen vacancies preferentially exist in O1 and O3 sites, and the redistribution of oxygen vacancies occurs between these sites by the substitution for Sr. In this work, we evaluated the variation of oxygen nonstoichiometry in $La_xSr_{3-x}Fe_2O_{7-\delta}$ (x = 0, 0.25 and 0.5) by means of high temperature gravimetry and coulometric titration. The measurements were carried out in the temperature range between 773 and 1073 K and the $P(O_2)$ range between 10^{-35} and 1 bar. The $P(O_2)$ dependencies of the oxygen nonstoichiometry exhibited typical plateaus at δ~1.0 for $Sr_3Fe_2O_{7-\delta}$, δ~0.875 for $La_{0.25}Sr_{2.75}Fe_2O_{7-\delta}$ and δ~0.75 for $La_{0.5}Sr_{2.5}Fe_2O_{7-\delta}$ where the average oxidation state of iron is 3+. Besides, the decomposition $P(O_2)$ was extended by doping La, indicating the phase stability was improved under low $P(O_2)$. The relationship between δ and $P(O_2)$ were analyzed by assuming defect equilibrium models, and can be well explained with an idea solution approximation.

A2.18

Synthesis and Preliminary Characterization of $Sr_{2-x}La_xMnO_{4\pm\delta}$ ($0.25 \leq x \leq 0.6$) Series as Symmetric SOFC Electrode Monica V. Sandoval[1, 2], Freddy L. Duran[1, 2], Caroline Pirovano[2], Edouard Capoen[2], Rose Noelle Vannier[2], Pascal Roussel[2] and Gilles H. Gauthier[1]; [1]Grupo INTERFASE, Universidad Industrial de Santander, Bucaramnaga, Colombia; [2]Unité de Catalyse et de Chimie du Solide, Université Lille 1, Lille, France.

The symmetric SOFC is a promising and cost effective evolution of classical SOFC, in which the same electrode material can operate simultaneously as an anode and a cathode [1-2]. Unfortunately, the development of such technology suffers from the lack of material able to fulfill the numerous requirements of such dual electrode. The present work deals with a preliminary study concerning the preparation, redox stability and electrical conductivity measurements of Ruddlesden-Popper (RP) manganites of general formula $Sr_{2-x}La_xMnO_{4\pm\delta}$ (x=0.25-0.6).

The materials were prepared through solid state reaction in air up to 1300°C for 12h and X-Ray Powder Diffraction showed that the whole range compositions can be obtained as single phased materials (S.G. *I4/mmm*), in agreement with literature [3].

The thermal stability in diluted hydrogen of all compounds was checked at a temperature of 850°C, and proved their stability in typical anodic conditions. A Rietveld refinement procedure was carried out using XRD data and confirm that the structure remains stable after reduction. The oxygen loss and changes in the oxidation state of Mn were determined by TGA and iodometric titration, respectively.

The thermal and redox behavior of the materials was further studied by HT-XRD in air and diluted hydrogen up to 800°C and the evolution of cell parameters as a function of temperature demonstrated that the RP manganites are completely stable to redox cycles (Fig. 1). Thermal expansion coefficients are in the 12.4-12.9 $x10^{-6} K^{-1}$ range in air and ~13.7 $x10^{-6} K^{-1}$ in hydrogen, very close to the values reported for conventional electrolytes. Acceptable electrical conductivity values of the materials have been obtained in both anode and cathode conditions, showing a p-type behavior with Ea= 0.18(2) eV in air and Ea= 0.32(3) eV in diluted hydrogen for x=0.5, characteristic of a small polaron mechanism.

Acknowledgments: This work was developed with the financial support from UIS/VIE, COLCIENCIAS, CNRS, Région Nord Pas-de-Calais, MENESR.

References: [1] J.T.S. Irvine *et al.* J. Mater. Chem. 16 (2006) 1603, [2] J.C. Ruiz-Morales *et al.* Electrochim. Acta 52 (2006) 278,[3] C, Munning, *et al.* Solid State Ionics 177 (2006) 1849.

A2.19

The Impact of Precursor Gel Desiccation, Ceria Oxide Pre-Infiltration, and Solution Composition on Tailoring Lanthanum Strontium Cobalt Iron Oxide Nano-Particle Size Theodore E. Burye, Hongjie Tang and Jason Nicholas; Chemical Engineering and Materials Science, Michigan State University, East Lansing, Michigan, United States.

Recently, infiltrated SOFC cathodes have received a great deal of attention in the literature.[1-3] Unfortunately, it has been difficult to control the average size of infiltrate nano-particles produced by conventional infiltration techniques. For instance, the average size of $Sm_{0.5}Sr_{0.5}CoO_{3-\delta}$ infiltrate particle on doped ceria backbones have ranged from 40 to 100 nm for studies utilizing identical firing conditions, heating rates, and nominally identical compositions.[4-6] Therefore, the objective of the present work was to determine if average infiltrate particle sizes could be influenced by nitrate gel desiccation and/or cerium oxide nano-particle pre-infiltration.

Here, desiccated cathodes were produced by screen printing and firing $Gd_{0.1}Ce_{0.9}O_{1.95}$ (GDC) colloidal inks on dense GDC electrolytes, infiltrating GDC backbones with $La_{0.6}Sr_{0.4}Co_xFe_{1-x}O_{3-\delta}$ ($0 \leq x \leq 1$) precursor nitrate solutions, desiccating the infiltrated cells, and firing the cells at 700°C. Ceria pre-infiltrated cells were produced by screen printing and firing $Gd_{0.1}Ce_{0.9}O_{1.95}$ (GDC) colloidal inks onto dense GDC electrolytes, infiltrating GDC backbones with precursor GDC precursor nitrate solutions, firing the cells at 700°C, infiltrating $La_{0.6}Sr_{0.4}Co_xFe_{1-x}O_{3-\delta}$ ($0 \leq x \leq 1$) precursor nitrate solutions, and firing the cells again at 700°C. Electrochemical impedance spectroscopy measurements up to 500 hours in length were used to measure the cathode polarization resistance (R_p), and scanning electron microscopy was used to determine average infiltrate particle size.

For all tested infiltrate compositions, both desiccation and pre-infiltration were found to lower R_p. Further, the observed performance improvements were found to scale with the infiltrate particle size and were not due to changes in infiltrate phase purity, gas concentration polarization, or electronic conductivity.[7] In all cases, the average infiltrate particle size was found to scale with the infiltrate oxide formation temperature. Long term electrical performance testing revealed that desiccated cells achieved degradation rates of < 1.3% per 1000 hours.

Reference
1. J. M. Vohs and R. J. Gorte, *Advanced Materials*, **21**, 943 (2009).
2. S. P. Jiang, *Materials Science and Engineering A*, **418**, 199 (2006).
3. D. Ding, X. Li, S. Y. Lai, K. Gerdes and M. Liu, *Energy Environ. Sci.*, **7**, 552 (2014).
4. J. D. Nicholas and S. A. Barnett, *Journal of the Electrochemical Society*, **157**, B536 (2010).
5. J. D. Nicholas, L. Wang, A. V. Call and S. A. Barnett, *Phys. Chem. Chem. Phys.*, **14**, 15379 (2012).
6. H. Zhang, F. Zhao, F. L. Chen and C. R. Xia, *Solid State Ionics*, **192**, 591 (2011).
7. T. E. Burye and J. D. Nicholas, *Journal of Power Sources*, **276**, 54 (2015).

A2.20

Influence of Synthesis Method on the Electrochemical Properties of Bilayer Electrodes Based on $La_2NiO_{4+\delta}$ and $LaNi_{0.6}Fe_{0.4}O_{3-\delta}$ Elena Pikalova[3, 1], Nina Bogdanovich[3], Alexander Kolchugin[3], Alexander Pankratov[3] and Dimitry Bronin[3, 2]; [1]Department of Environmental Economics, Ural Federal University, Ekaterinburg, Russian Federation; [2]Institute of Natural Sciences, Ural Federal University, Ekaterinburg, Russian Federation; [3]Institute of High Temperature Electrochemistry, Ekaterinburg, Russian Federation.

The development of a cathode stable against CO_2 present in the atmosphere still remains a challenge. Over the past ten years Sr- and Ba-free layered perovskite $La_2NiO_{4+\delta}$ (LNO) has been the subject of careful research in connection with its potential use as a cathode in electrochemical devices. The interest is based on its mixed ionic-electronic conductivity nature and good compatibility in a coefficient of thermal expansion with a wide row of solid state electrolytes; however its performance as a cathode is limited by a low level of electronic conductivity. In this work, with the sake to improve electrochemical activity, bilayer electrodes based on LNO were fabricated with $LaNi_{0.6}Fe_{0.4}O_3$ (LNF) collector, which possesses a high level of electronic conductivity. The LNO powders were synthesized by various methods: a two-step solid-state reaction (S), Pechini (P) and nitrate combustion (C). LNF was prepared by solid-state reaction and Pechini method. The electrolyte of $Ce_{0.8}Sm_{0.2}O_{1.9}$ (SDC) composition was synthesized via one-step ceramic technology. The cathode slurries were prepared by mixing in a planetary mill the powdered components with ethyl alcohol and butyral resin binder. Some cathodes examined in this work were manufactured with admixtures of CuO for better sintering. The measurements were performed by a impedance spectroscopy method on the electrochemical cells with symmetrically arranged electrodes. Electrodes were made in the form of one- or bilayer coatings with functional (LNO) and with/without collector (LNF) layers with total amount of the electrode mass per unit surface area of the SDC electrolyte equal to 45-75 mg/cm^2. The influence of method of synthesis of powders, sintering temperature of the electrode layers and their various combinations on the polarization and serial resistances of the electrodes was investigated. Usage of LNF collector significantly decreases serial resistance due to better current distribution along the electrode surface. The lowest ASR value (0.23 Ω cm^2 at 700^{o}C) was found for the bilayer electrode with LNO functional layer prepared by nitrate combustion method with LNF collector made by Pechini method. The research was partly supported by the Russian Foundation for Basic Research and the Sverdlovsk Region Government (grants 14-03-00414, 13-03-96098).

A2.21

Oxygen Mobility in Microwave Sintered Praseodymium Nickelates-Cobaltites and Their Nanocomposites with Yittria-Doped Ceria Vladislav A. Sadykov[1, 2], Nikita F. Eremeev[1], Vasiliy A. Bolotov[1], Yuriy Y. Tanashov[1], Yulia E. Fedorova[1, 3], Daiana G. Amanbayeva[1, 4], Aleksey S. Bobin[1], Ekaterina M. Sadovskaya[1], Vitaliy S. Muzykantov[1], Vladimir V. Pelipenko[1], Anton I. Lukashevich[1], Tamara A. Krieger[1], Arkadiy V. Ishchenko[1, 2] and Alevtina L. Smirnova[5]; [1]Boreskov Institute of Catalysis, Novosibirsk, Russian Federation;[2]Novosibirsk State University, Novosibirsk, Russian Federation; [3]Novosibirsk State Pedagogical University, Novosibirsk, Russian Federation; [4]Novosibirsk State Technical University, Novosibirsk, Russian Federation; [5]South Dakota School of Mines & Technology, Rapid City, South Dakota, United States.

$PrNi_{1-x}Co_xO_{3-\delta}$ – $Ce_{0.9}Y_{0.1}O_{2-\delta}$ composites are promising as IT SOFC cathodes provided their sintering conditions are optimized. In this work effect of microwave sintering (MS) on properties of such materials is studied.

Perovskite (P) $PrNi_{0.5}Co_{0.5}O_{3-\delta}$ (PNC) and fluorite (F) $Ce_{0.9}Y_{0.1}O_2$ (YDC) oxides were synthesized by Pechini route. PNC – YDC composites were prepared by ultrasonic dispersion of the oxides mixture in isopropanol. Pellets made from powders were sintered at 870 – 1100 °C using specially designed microwave set-up. Phase composition was determined by X-ray diffraction, microstructure and elemental composition – by TEM with EDX. Oxygen mobility and reactivity were estimated by O_2 TPD (up to 800 ^{o}C) and oxygen isotope heteroexchange with $^{18}O_2$ and $C^{18}O_2$ in static and flow reactors.
MS provides dense materials (porosity < 10 %) even at the lowest temperatures. PNC is single-phase perovskite with minor admixtures of Pr_6O_{11} or $Pr_4Co_3O_{10}$. Composites are comprised of P+F phases with some Pr_6O_{11} admixture, strong elements redistribution between P and F domains occurs.

The total amount of oxygen desorbed is up to 20 monolayers for PNC (T_{max} ~ 800 ^{o}C) and 70 monolayers for PNC – YDC (T_{max} ~ 500 °C), being ~ 1.5 times higher as compared to conventionally sintered (CS) samples. This is due to a higher disordering of P and F domains as well as their boundaries for MS samples.

The oxygen isotope exchange is characterized by R^2 mechanism with the surface exchange constant k_{ex} ~ 10^{-6} cm/s at 700 °C for both PNC and PNC – YDC, being close to CS samples. The oxygen diffusion coefficient D_O for highly mobile oxygen in nanocomposite is ~10^{-8} cm^2/s at 700 °C, which is also close to that for the best CS samples made at higher temperatures. Hence, MS at lower temperatures provides even better functional characteristics of PNC- YDC nanocomposite cathodes.

A2.22

Electrochemical Performance of La and Ni Co-Doped $SrTiO_3$ Anode of Solid Oxide Fuel Cell Byung Hyun Park and Gyeong Man Choi; Mat. Sci. & Eng., POSTECH, Pohang, Korea (the Republic of).

Conventional Ni-cermet anodes show good performance in H_2 but have problems for stability aspects: carbon coking, sulphur poisoning, Ni coarsening, or redox stability. Perovskite oxides are attracting increasing interest in application as an alternative anode. Electro-catalytic nanoparticles can be produced in oxide anodes by ex-solution method, i.e., by incorporating Ni, Ru or Pd into a perovskite oxide phase in air, followed by the reduction in H_2 atmosphere. The Ni ex-solution in $La_{0.2}Sr_{0.8}Ti_{0.9}Ni_{0.1}O_{3-\delta}$ (LSTN) was determined in our previous work. In this study, the electrochemical performances of electrolyte (ScSZ, scandia-stabilized zirconia)-supported cells with LSTN-based anodes were compared at 800^{o}C in H_2 and CH_4 fuel. We varied the temperature (1100, 1250 °C) and atmosphere (air, H_2) of LSTN anode firing to control the degree of Ni ex-solution and microstructure. We have also used $Gd_{0.2}Ce_{0.8}O_2$ (GDC) as both an anode interlayer and a composite phase of LSTN anode. Impedance spectra and power measurement of the cells have shown the stable and improved performance of LSTN anode fired at 1250 °C in H_2 when GDC was composited with LSTN and used as an anode interlayer in both hydrogen and methane fuels.

A2.23

Functionally Graded Electrodes Using Centrifuge Deposition for Solid Oxide Fuel and Electrolysis Cells Shahid P. Shafi , Ioannis Bantounas, Udo Schwingenschloegl, Enrico Traversa and Samir Boulfrad; Physical Sciences and Engineering, King Abdullah University of Science and Technology (KAUST), Thuwal, Saudi Arabia.

Optimized electrode microstructure of solid oxide fuel/electrolysis cells is a key to improve their performance and lifetime. Electrode requirements are well documented. The main microstructural challenge is the optimization of the 3D distribution of the three phases involved (ionic-conducting, catalyst/electronic-conducting and gas) in order to get the maximum contact area (triple phase boundaries – TPB) while each phase presents a continuous percolated network.

Many simulation works have pointed out the benefits of functionally graded electrodes, reducing both the activation and concentration overpotentials and improving the cell performance by up to 70%. Graded electrodes are structures with a gradient of composition and porosity. The electrode is highly porous and fully constituted of the electronic conducting/catalyst phase. The ionic conducting phase is then introduced and its amount gradually increases towards the electrolyte where it becomes 100%. Simultaneously, the porosity decreases gradually towards 0% at the electrolyte. The fabrication of graded electrodes with techniques such as tape-casting and screen-printing requires subsequent deposition of layers with different composition, resulting in stairs like cross sectional composition.

In this work, centrifuge deposition is used to fabricate a continuous gradient of LSM and YSZ/LSM electrodes. A liquid suspension of the powders is speedily rotated. The centrifuge force makes the solid particles deposit on a substrate placed at the end of the container. Since LSM and YSZ present close density values, the nature of the deposition is mainly dictated by the particle size distribution. Larger particles would, in average, reach the substrate first, followed by smaller ones. While the optimization of the process is in progress, our preliminary results demonstrate a continuous porosity gradient from 5% near the electrolyte to 60% by the edge of the electrode. Symmetrical cell electrochemical characterization is in progress using impedance spectroscopy.

A2.24

The Impact of Surfactant Choice on Infiltrate Size-Tailored Nano-Composite Solid Oxide Fuel Cell Cathodes Theodore E. Burye and Jason D. Nicholas; Chemical Eng and Material Science, Michigan State University, East Lansing, Michigan, United States.

Recently, precursor nitrate solution desiccation [1] and ceria nano-particle pre-infiltration [2-4] have been shown to reduce the average size of mixed ionic electronic conducting solid oxide fuel cell infiltrate particles. The objective of the present work was to evaluate how two common [5-8] solution surfactant additions, Triton X-100 (TX) and Citric Acid (CA), independently impact the microstructure, phase purity, and performance of infiltrated nano-composite cathodes made using precursor gel desiccation or ceria nano-particle pre-infiltration.
Desiccated symmetrical cathodes were infiltrated using CA or TX containing $La_{0.6}Sr_{0.4}Co_{0.8}Fe_{0.2}O_3$ (LSCF) precursor solutions, desiccated with $CaCl_2$ for 10 hrs, and then fired at 700°C to form LSCF oxide nano-particles. Cathodes with identical $Gd_{0.1}Ce_{0.9}O_{1.95}$ (GDC) scaffolds containing pre-infiltrated GDC nano-particles were infiltrated with CA or TX containing LSCF precursor solutions, and fired at 700°C. In all cases, up to 6 infiltrations were performed to achieve a LSCF loading level of 12.0 vol%. Cells were characterized through AC electrochemical impedance spectroscopy and scanning electron microscopy. 500 hr, open-circuit, polarization resistance (R_p) degradation measurements were also conducted.

LSCF oxide nano-particles were phase pure when the infiltrate was produced from CA-containing precursor solutions, but secondary phase impurities were present when the infiltrate was produced from TX-containing precursor solutions. Both CA and TX were found to lower R_p when used with desiccation or pre-infiltration, but TX had a much larger impact, lowering R_p to 0.1 Ωcm² at 550°C and reducing the average infiltrate particle size from 50 to 22 nm. For both TA and CA-containing solutions, the observed performance improvements were found to scale directly with the infiltrate particle size and were not due to changes in gas concentration polarization, infiltrate phase purity, or electronic conductivity. Cells made with TX and CA had nearly identical R_p degradation with a 1.3%/1000 hr degradation rate achieved.

Reference:
[1] Burye, T. E. & Nicholas, J. D. Improving $La_{0.6}Sr_{0.4}Co_{0.8}Fe_{0.2}O_{3-\delta}$ Infiltrated Solid Oxide Fuel Cell Cathode Performance through Precursor Solution Desiccation. *J. Power Sources*276, 54-61 (2015).
[2] Burye, T. E. & Nicholas, J. D. The Impact of Nano-Ceria Pre-Infiltration on $La_{0.6}Sr_{0.4}Co_{0.8}Fe_{0.2}O_{3-d}$Infiltrated Solid Oxide Fuel Cell Cathodes *J. Electrochem. Soc.* Submitted (2015).
[3] Burye, T. E. & Nicholas, J. D. The Impact of Infiltrate Composition on Solid Oxide Fuel Cell Cathodes Produced Using Precursor Solution Desiccation or Nano-Ceria Pre-Infiltration. *J. Electrochem. Soc.* Submitted (2015).
[4] Zhan, Z. L. *et al.* A Solid Oxide Cell Yielding High Power Density below 600ºC. *RSC Adv.* 2, 4075-4078 (2012).
[5] Nicholas, J. D. & Barnett, S. A. Measurements and Modeling of $Sm_{0.5}Sr_{0.5}CoO_{3-d}$-$Ce_{0.9}Gd_{0.1}O_{1.95}$ SOFC Cathodes Produced Using Infiltrate Solution Additives. *J. Electrochem. Soc.*157, B536-B541 (2010).
[6] Sholklapper, T. Z., Kurokawa, H., Jacobson, C. P., Visco, S. J. & De Jonghe, L. C. Nanostructured Solid Oxide Fuel Cell Electrodes. *Nano Letters* 7, 2136-2141 (2007).
[7] Sholklapper, T. Z., Radmilovic, V., Jacobson, C. P., Visco, S. J. & De Jonghe, L. C. Nanocomposite Ag-LSM solid oxide fuel cell electrodes. *J. Power Sources* 175, 206-210 (2008).
[8] Samson, A., Sogaard, M., Knibbe, R. & Bonanos, N. High Performance Cathodes for Solid Oxide Fuel Cells Prepared by Infiltration of $La_{0.6}Sr_{0.4}CoO_{3-d}$ into Gd-Doped Ceria. *J. Electrochem. Soc.* 158, B650-B659 (2011).

A2.25 Withdrawn

A2.26

The Electrochemical Reduction Mechanism of $Sm_{0.35}Ba_{0.15}Sr_{0.5}Co_{0.8}Fe_{0.2}O_{3-\delta}$ and Graded Composite Cathode Jianquan Gao, Shengli An, Fen Zhou and Xiwen Song; School of Materials and Metallurgy, Inner Mongolia University of Science and Technology, Baotou, China.

The low barium-containing $Sm_{0.35}Ba_{0.15}Sr_{0.5}Co_{0.8}Fe_{0.2}O_{3-\delta}$ (SBSCF) perovskite oxide was synthesized and evaluated as the cathode for an intermediate temperature solid oxide fuel cell on a samarium-doped ceria(SDC) electrolyte. The SBSCF-SDC graded composite cathodes in 50:50 and 70:30 weight ratio were fabricated and investigated to optimize the cathode microstructure and further to minimize the cathode interfacial polarization resistance. The interfacial polarization resistance of the graded composite cathodes was obtained only 0.064Ω cm^2at 650 ºC. The electrochemical reaction mechanism of graded composite cathodes has found to be similar to that of SBSCF cathode. However, both oxygen ion incorporation and charge transfer steps are greatly accelerated for the graded composite cathode, Anode-supported single cells with the SBSCF and SBSCF-SDC graded composite cathodes have achieved a maximum peak power density of 650 mW cm^{-2} and 800 mW cm^{-2} at 600 ºC respectively, These results suggest that graded composite configuration is very promising for developing IT-SOFC cathode with low Rp values.

A2.27

Oxygen Exchange Kinetics of Doped Lanthanum Cobaltite System Keiji Yashiro[2], Hiroki Sato[1], Mie Sasaki[1], Takashi Nakamura[3], Shinichi Hashimoto[1], Koji Amezawa[3] and Tatsuya Kawada[1]; [2]GSES, Tohoku University, Sendai, Japan; [3]IMRAM, Tohoku University, Sendai, Japan.

A series of Sr doped $LaCoO_3$ (LSC) is one of the promising candidates for cathode of solid oxide fuel cells. It has been reported LSC has high catalytic activity for oxygen reduction reaction due to extension of reaction zone to two phase boundary by mixed ionic electronic conduction. Determination of rate determining step (RDS) is indispensable to improve the cathode performance. In the case of LSC thin film electrode, surface reaction was reported to be the RDS. However, the RDS of porous LSC electrode might be different from that of thin film. Therefore, in this study, surface reaction rate was measured under different surface conditions such as thin film, bulk, and powder. For thin film and bulk specimens, oxygen isotope diffusion profiles were analyzed by secondary ion mass spectrometry. Whereas, for powder specimen, pulse isotope exchange was conducted to determine surface exchange coefficients. The results indicate that surface exchange coefficients of bulk and powder were different depending on heat treatment prior to the measurement.

A2.28

Surface Modification of $La_{0.6}Sr_{0.4}Co_{0.2}Fe_{0.8}O_{3-\delta}$ by Nanometer-Thick Mixed Conducting Oxide Films Michael L. Machala, Burcu Oeguet, David N. Mueller and William C. Chueh; Stanford University, Stanford, California, United States.

The oxygen evolution and reduction reactions are ubiquitous in many energy conversion processes. Of particular interest are reactions that take place over the solid/gas interface of perovskite-structured (ABO_3) mixed ionic and electronic conductors (MIECs). In conjunction with a solid electrolyte, devices using MIEC electrocatalysts —such as solid oxide fuel cells and electrolyzers—can operate at elevated temperatures (500-800°C), leading to faster kinetics of oxygen exchange reactions.

To further enhance device performance, heterostructured electrocatalysts have been employed through extrinsic decoration of MIEC oxide surfaces with dissimilar materials. Here, we study dense, thin film $La_{0.6}Sr_{0.4}Co_{0.2}Fe_{0.8}O_{3-\delta}$ (LSCF) electrodes grown by pulsed-laser deposition. LSCF is a promising MIEC scaffold with high electronic and ionic conductivity but a moderate and unstable oxygen reaction rate. We deposited nanometer-thick layers of MIEC oxides on top of thin-film LSCF electrodes and investigated their effect on electrochemical activity and stability. Crystal structure and chemical composition at the nanoscale was also investigated by high-resolution transmission electron microscopy. The precise role of the nanometer-thick surface coating in modifying and stabilizing the oxygen exchange reactions will be discussed.

A2.29

Microstructural Effect to Thermal Stability and Cathode Performance by Nanoscale ZrO_2 Capping in Platinum Based-Solid Oxide Fuel Cells Kang-Yu Liu[1], Liangdong Fan[1], Chen-Chiang Yu[2] and Pei-Chen Su[1]; [1]School of Mechanical and Aerospace Engineering, Nanyang Technological University, Singapore, Singapore; [2]Interdisciplinary Graduate School, Nanyang Technological University, Singapore, Singapore.

Thermally-driven agglomeration of platinum electrode heavily induced the loss of effective triple phase boundary (TPB) densities as temperature increases and irreversibly deteriorates fuel cell performances. This work demonstrates the capping of a nanoscale zirconia on a nano-porous platinum cathode, which has effectively improved the chronically poor thermal stability of such porous metal electrode and at the same time obtained an unexpected cathode performance enhancement. An approximately 1.6 nm of zirconia capping deposited on platinum by atomic layer deposition (ALD) serves as a mechanical barrier to prevent the rapid thermally-driven agglomeration of platinum nanoparticles. The oxygen-rich zirconia nanoparticles deposited on platinum surface may possibly decreased the oxygen adsorption-desorption resistance and rendered the unexpected drop in cathode polarization resistance. The behavior of cathode enhancement is dependent on zirconia capping by using ALD with thickness below 10nm. The nanometer-thin zirconia capping may lead to different microstructural effects on the cathode enhancement. These results point out the explicit phenomenon of improving both thermal stability and cathode polarization by decorating a nanoscale zirconia on metal electrode. It might be a trigger point of exploring wider usage of other metal electrode in solid oxide fuel cells. Further confirmation on the microstructural effect of the nanoscale zirconia on platinum and the rate limited step of the cathode polarization are undergoing to clarify the fundamental mechanism for the unexpected cathode performance enhancement observed in this work.

A2.30

Microstructure and Functionality of Cathode/Electrolyte Interfaces in SOFCs Virginia Wilde[1], Heike Stoermer[1], Julian Szasz[2], Florian Wankmueller[2], Ellen Ivers-Tiffee[2] and Dagmar Gerthsen[1]; [1]Laboratory for Electron Microscopy (LEM), Karlsruhe Institute of Technology (KIT), Karlsruhe, Germany; [2]Institute of Materials for Electric and Electronic Engineering (IWE), Karlsruhe Institute of Technology (KIT), Karlsruhe, Germany.

Future solid oxide fuel cells (SOFC) with long lifetime and high efficiency at low operating temperatures require a thorough selection of materials for the different SOFC components cathode, electrolyte and anode. $La_{1-x}S_xCo_{1-y}Fe_yO_{3-d}$ (LSCF) is a high performance cathode material, however, when directly applied to Yttria-stabilized Zirconia (YSZ) electrolyte, a Strontiumzirconate (SZO) blocking layer is formed. One option to prevent SZO formation is the insertion of a dense Gd-doped Ceria (GDC) layer between LSCF and YSZ. Yet, to achieve highly functional GDC interlayers, sophisticated processing is essential. The present study combines electrochemical characterization of LSCF-GDC-YSZ interfaces with detailed microstructural characterization at the nanoscale using conventional and analytical (scanning) transmission electron microscopy ((S)TEM). Symmetric cell samples were fabricated by screen-printing a 5 µm thick GDC layer on both sides of YSZ substrates, followed by sintering at different temperatures from 1100 °C to 1400 °C. The LSCF was also screen-printed and sintering at 1080°C was applied to all LSCF layers irrespective of the GDC sintering temperature. The study shows that the nature of the GDC barrier layer depends strongly on the GDC sintering temperature and controls the area specific resistance of the cathode. Detailed TEM investigations give new insights into material interactions at the YSZ/GDC and GDC/LSCF interfaces for different GDC sintering temperatures. The study focuses particularly on the effect of GDC sintering temperature on SZO formation and cation interdiffusion. The origin of secondary phase formation between LSCF, GDC and YSZ and the effects of the microstructural development on electrochemical SOFC performance is discussed.

A2.31

Bias Enhanced Fast Oxygen Exchange and Diffusion Kinetics of Grain Boundaries in LSM Thin Films Tobias M. Huber[1, 2, 3], Edvinas Navickas[4], Daio Takeshi[1], George F. Harrington[1, 2, 3], Nicola H. Perry[3, 5], Ghislain Rupp[4], Walid Hetaba[6], Michael Stoeger-Pollach[6], Harry L. Tuller[2, 5], Bilge Yildiz[3, 2], Kazunari Sasaki[5] and Juergen Fleig[4]; [1]Mechanical Engineering, Kyushu University, Fukuoka, Japan; [2]Materials Science and Engineering, Massachusetts Institute of Technology, Cambridge, Massachusetts, United States; [3]Department of Nuclear Science & Engineering, Massachusetts Institute of Technology, Cambridge, Massachusetts, United States; [4]Institute of Chemical Technologies and Analytics, Research Division Electrochemistry, Vienna University of Technology, Vienna, Austria; [5]International Center for Carbon Neutral Energy Research (I2CNER), Kyushu University, Fukuoka, Japan; [6]University Service Centre for Transmission Electron Microscopy, Vienna University of Technology, Vienna, Austria.

Introduction

The kinetics of the oxygen reduction reaction on solid oxide electrolytes and electrodes has been widely investigated in recent years. Although it is one of the best studied reactions in solid state ionics, several questions remain including the actual site of the oxygen reduction reaction (ORR). Sr-doped lanthanum manganite (LSM) is the most commonly used cathode material in solid oxide fuel cells (SOFC). Recently attention has been focused on ORR on LSM thin films via the grain boundary dependent path [1]. An improved understanding of the role of grain boundaries in perovskite materials may lead to improved electrode kinetics. In this work the ORR was investigated on pulsed laser deposited (PLD) LSM thin films. Voltage-driven ^{18}O tracer incorporation [2] was investigated by time of flight secondary ion mass spectrometry (ToF-SIMS) and analyzed with a 3D finite element model. The micro structure of the thin films was analyzed by transmission electron microscopy (TEM) and scanning tunneling microscopy (STM).

^{18}O incorporation/exchange experiments

Geometrically well defined and dense, columnarly grown thin film electrodes with well-defined microstructure on YSZ (100) single crystals were annealed with and without polarization in ^{18}O tracer gas atmosphere. After ^{18}O incorporation, the electrodes were quenched and analyzed by ToF-SIMS to obtain depth profiles of the ^{18}O incorporation. Numerical analysis of the profiles allowed a quantification of the surface oxygen incorporation kinetics and diffusion coefficients. This method allows one to distinguish between oxygen transport and oxygen incorporation at grains and grain boundaries. Microelectrodes were additionally electrochemically characterized by impedance spectroscopy at different temperatures and with varying microstructures.

Grain boundary diffusion and surface exchange values obtained from the measurements were approximately two to three orders of magnitude larger than those of the grains [1]. By applying cathodic bias surface exchange is enhanced and diffusion coefficients are increased as a function of depth, according to the gradient of chemical potential. Due to the voltage, and thereby depth dependent increase in transport properties of grains and grain boundaries, an apparent uphill diffusion appears in the depth profiles. This behavior is also computable with the 3D finite element model.

References

[1] E. Navickas, T. M. Huber, et al, Phys. Chem. Chem. Phys. DOI: 10.1039/C4CP05421K.
[2] T. Horita, et al, Solid State Ionics, 2000, 127, 55–65.

A2.32

Variable Temperature Multinuclear Solid State NMR Study of "Sr0.55Na0.45SiO2.775" Ryan D. Bayliss[1], Frederic Blanc[2, 3], John Corley[2], John A. Kilner[4, 5] and Stephen Skinner[4];[1]Department of Chemistry, University of Illinois at Chicago, Chicago, Illinois, United States; [2]Department of Chemistry, University of Liverpool, Liverpool, United Kingdom; [3]Stephenson Institute for Renewable Energy, University of Liverpool, Liverpool, United Kingdom; [4]Department of Materials, Imperial College London, London, United Kingdom; [5]International Institute for Carbon-Neutral Energy Research (I2CNER), Nishi-Ku, Japan.

Monoclinic Na or K substituted strontium silicates SrSiO3 and germanates SrGeO3 (e.g. Sr1-xAxSi1-yGeyO3-0.5x) have recently been reported1–4 and attracted much attention in the literature due to the proposed exceptional oxide ion conductivity at relatively low temperature (i.e. 1.79 x 10-2 S cm-1 at 550 °C for Sr0.55Na0.45SiO2.775). The conductivity was proposed to originate from oxygen vacancy defects resulting from the aliovalent substitution of Sr with alkali metals. This doping strategy is unusual due to the known fast ion conduction of alkali metals and hence has raised questions regarding the real nature of the charge carriers in these materials, and more generally about the structure.

Revaluation of these materials by neutron powder diffraction, chemical ion mapping and time-of-flight secondary ion mass spectrometry revealed an inhomogeneous chemical composition and that the materials Sr1-xNa/KxSi1-yGeyO3-0.5x are not single phase,5,6 with the absence of a secondary phase in the diffraction suggesting that the secondary phase is amorphous. The nature of this amorphous phase is still unclear and was postulated to be a glass with composition K2O:SiO2 or Na2O:SiO25,6 or Na2Si2O57 based on known glass chemistry and 29Si solid state NMR spectroscopy.7 Most importantly, oxygen ion diffusivity measurements have shown very low levels of oxide ion conductivity in these composites, demonstrating that the total conductivity in these materials is likely not due to oxygen ion migration.5,6

Here we present more recent results using multinuclear solid state NMR spectroscopy data collected on the nominal Na doped strontium silicate composition Sr0.55Na0.45SiO2.775, highlighting the presence of a multiphasic material. 23Na has been studied through variable temperature measurements giving elemental specific insight into Na mobility. Moreover, a better understanding into the amorphous glassy phase has been obtained from multinuclear NMR data collection.8

(1) Singh, P.; Goodenough, J. B. Energy Environ. Sci. 2012, 5, 9626. (2) Singh, P.; Goodenough, J. B. J. Am. Chem. Soc. 2013, 135, 10149–54. (3) Martinez-Coronado, R.; Singh, P.; Alonso-Alonso, J.; Goodenough, J. B. J. Mater. Chem. A 2014, 2, 4355. (4) Wei, T.; Singh, P.; Gong, Y.; Goodenough, J. B.; Huang, Y.; Huang, K. Energy Environ. Sci. 2014, 7, 1680. (5) Bayliss, R. D.; Cook, S. N.; Fearn, S.; Kilner, J. A.; Greaves, C.; Skinner, S. J. Energy Environ. Sci. 2014, 7, 2999. (6) Bayliss, R. D.; Cook, S. N.; Scanlon, D. O.; Fearn, S.; Cabana, J.; Greaves, C.; Kilner, J. A.; Skinner, S. J. J. Mater. Chem. A 2014, 2, 17919–17924. (7) Evans, I. R.; Evans, J. S. O.; Davies, H. G.; Haworth, A. R.; Tate, M. L. Chem. Mater. 2014, 26, 5187–5189. (8) Corley, J; Kilner, J. A.; Skinner, S. J.; Bayliss, R. D.; Blanc, F. in preparation (2015).

A2.33

Nanostructured Electrodes for Metal-Supported Solid Oxide Fuel Cells Zhongliang Zhan, Yucun Zhou, Hao Wu, Ting Luo and Ting-Lian Wen; CAS Key Laboratory of Materials for Energy Conversion, Shanghai Institute of Ceramics, Shanghai, China.

Solid oxide fuel cells (SOFCs) have great potentials for stationary and portable generation of electric energy using the existing hydrocarbon fuel infrastructure. Key obstacles to preclude their practical applications include high costs, low reliability and low durability. Here we report some of our recent progresses in nano-scale electrode catalysts for metal-supported SOFCs using the liquid phase impregnation technique. Such cells were based upon a tri-layer structure - porous 430L | dense YSZ | porous YSZ. Redox-stable catalysts such as $SrFe_{0.75}Mo_{0.25}O_{3-d}$and $La_{0.6}Sr_{0.4}Fe_{0.9}Sc_{0.1}O_{3-d}$ were simutaneously impregnated into the porous 430L and YSZ layers and acted as the anode and cathode catalysts, respectively. These metal-supported fuel cells exhibited power densities of 0.4-0.8 W cm^{-2} at 700-800°C when operating on humidified hydrogen fuels and ambient air oxidants. Use of altervative anode catalysts such as Ni-doped ceria yielded enhanced power densities, e.g., 1.2 W cm^{-2} at 800°C.

A2.34

Kinetics of Surface Activation and Oxygen Transfer Acceleration Induced by A_2BO_4/ABO_3 Hetero-Interface for SOEC Application Bo Yu, Wenqiang Zhangwq and Jingming Xu; Tsinghua University, Beijing, China.

Flexible nuclear power for clean fuels and peak electricity production by co-electrolysis of CO_2 and H_2O/fuel cell technology (HTEFC), which can extend the novel uses of nuclear plant to decrease CO_2 emission, enable large-scale energy storage and load-following capability, is the cutting-edge research frontier around the world. While technically feasible and carries the above-mentioned advantages in concert with nuclear energy, operation in electrolytic mode and high working temperature have thus far been challenged by accelerated materials degradation and high cost. The low activity and durability of oxygen electrodes are primarily responsible for the loss in efficiency. The slow Oxygen reduction reaction (ORR) and Oxygen evolution reaction (OER) kinetics at the oxygen electrode become one of the major barriers to the implementation of A_2BO_4.

In this paper, our research focus on the A_2BO_4/ABO_3 hetero-interface materials, which aims at accelerating the charge transfer and oxygen defects exchange kinetics of A_2BO_4 due to electronic activation induced by high electron carrier density of ABO_3 intervention. The perovskite oxides ($ABO_{3-\delta}$), such as $Ba_{0.5}Sr_{0.5}Co_{0.8}Fe_{0.2}O_{3-\delta}$ (BSCF-113), $La_{0.6}Sr_{0.4}Co_{0.2}Fe_{0.8}O_{3-\delta}$ (LSCF-113) and the Ruddlesden–Popper structure oxides ($A_2BO_{4+\delta}$) $Nd_{1.5}Sr_{0.5}CoO_{4+\delta}$ (NSC-214) were successfully prepared by the citric acid–nitrate combustion method. The X-ray diffraction (XRD) and scanning electron microscopy (SEM) were used to determine the crystallinities and structure of the samples. Electrolyte supported symmetric cells with various electrodes were studied by electrochemical impedance spectroscopy (EIS).Furthermore, the possible origin of the local electronic activation near the perovskite A_2BO_4/ABO_3 hetero-interface was presented. And the relations of hetero-interface structure to its reactivity with various oxygen pressure were discussed.

A2.35

Effect of Sintering Temperature on Properties of 8YSZ Prepared by SPS Jinxia Wang, Zhiqun Ding and Hongxia Zhao; School of Electronic and Information Engineering, Ningbo University of Technology, Ningbo, China.

Eight mol% yttria-stabilized zirconia (8YSZ) electrolytes were prepared by spark-plasma sintering (SPS) method. X-ray diffraction results showed that all the samples were found to crystallize in a single-phase cubic structure after sintering at 1050 °C to 1350 °C temperature ranges in 50 °C intervals. SEM micrographs showed that all the samples were quite dense and without significant pores. The grain sizes of the samples increased gradually with increasing sintering temperature and reached a *plateau* at 1250 °C. The grain sizes were calculated by the XRD data to be less than 100 nm. However, SEM results showed that grain sizes in the samples quickly become greater with increasing sintering temperature above 1250 °C. The ionic conductivities of the samples evaluated by AC impedance

spectra increased with increasing sintering temperature. The sample sintered at 1050 °C showed the lowest ionic conductivity. The relationship between the ionic conductivity, sintering temperature and grain size are expatiated in detail.

A2.36

Methanol Synthesis at Atmospheric Pressure in Co-Ionic Electrochemical Membrane Reactors Anastasios Vourros[1,4], Vasileios Kyriakou[4,1], Ioannis Garagounis[1,4], Michalis Konsolakis[2], Zisis Ioakimides[3,4], George Marnellos[3,4] and Michael Stoukides[1,4]; [1]Chemical Engineering, Aristotle University of Thessaloniki, Thessaloniki, Greece; [2]School of Production Engineering and Management, Technical University of Crete, Chania, Greece; [3]Department of Mechanical Engineering, University of Western Macedonia, Kozani, Greece;[4]Chemical Process and Energy Resources Institute, Centre for Research and Technology Hellas, Thessaloniki, Greece.

Introduction

The hydrogenation of CO_2 to fuels and useful chemical products is one of the most important challenges in heterogeneous catalysis. The development of effective catalytic systems in CO_2hydrogenation could contribute effectively both to environmental protection and to the production of added value chemicals such as methanol [1]. Currently, palladium-based catalysts supported on various metal oxides are the most effective materials for this application. To attain industrially acceptable conversions, the reaction must be carried out at elevated pressures (> 100 bar) [2].

The purpose of this study is the electrochemical production of methanol from carbon dioxide and water, in a co-ionic conducting solid electrolyte cell at atmospheric pressure (Figure 1). A success in this direction will have a significant financial benefit, given the abundance of the raw materials and the moderate reaction conditions. The production of CH_3OH from CO_2 and $H_2$was studied over Cu, Co and Pd catalysts/electrodes supported on ceria and zinc oxides.

Experimental

The catalytic experiments were conducted in a quartz reactor, using a H_2/CO_2 ratio equal to 9/1 and a total flow rate of 100 cm^3/min. The optimum catalyst was applied as an electrode in a solid electrolyte membrane reactor. Preliminary studies in relation to the effect of several operation parameters (temperature, anode and cathode feed gas composition) on methanol efficiency at open and closed (potensiostatic mode) circuit conditions, were carried out.

Results and Discussion

The cobalt catalysts presented higher selectivity toward methane production, reaching efficiencies up to 98% at temperatures near 400 °C. In contrast, the copper catalysts showed higher selectivity toward methanol production, but at lower temperatures. Finally, the palladium catalysts exhibited the greatest methanol yield, equal to 7% at 225 °C.

Acknowledgements

We gratefully acknowledge financial support of this research by the European Union and the General Secretariat of Research and Technology of Greece (13CAPITA-13-8A), within the project "CO_2 and H_2O toward methanol synthesis at atmospheric pressure in co-ionic electrochemical membrane reactors", ERA-NET, 7th FP.

References

[1] Wang W., Wang S., Ma X., Gong J., Recent advances in catalytic hydrogenation of carbon dioxide, *Chem. Soc. Rev*. 40 (2011) 3703
[2] Jadhav S.G., Vaidya P.D., Bhanage B.M., Joshi J.B., Catalytic carbon dioxide hydrogenation to methanol: A review of resent studies, *Chem. Eng. Research and Design*, 92 (2014), p. 2557

A2.37

Structural and Electrical Properties of Spark Plasma Sintered Scandia- and Dysprosia-Stabilized Zirconia Robson L. Grosso[1], Ana J. Tertuliano[2], Izabel F. Machado[2] and Eliana N. Muccillo[1]; [1]Energy and Nuclear Research Institute (IPEN), Sao Paulo, Brazil; [2]Polytechnique School, Sao Paulo, Brazil.

The effects of spark plasma sintering on structure, densification and ionic conductivity of 10 mol% Sc_2O_3–1 mol% Dy_2O_3–stabilized ZrO_2 (10Sc1DySZ) were investigated. Nanopowders of 10Sc1DySZ were synthesized by the coprecipitation method and consolidated by spark plasma sintering with varying dwell temperature and time. Solid electrolytes with relative density higher than 95% were obtained after sintering at 1100 °C. This sintering temperature is much lower than those typically reported for scandia-stabilized zirconia sintered by the conventional method. X-ray diffraction results evidence the full stabilization of the cubic structure in scandia- and dysprosia-stabilized zirconia at room temperature. The ionic conductivity was determined by impedance spectroscopy. The activation energy value obtained by the Arrhenius plots in the 500-800ºC range amounts 0.72 eV.

A2.38

Electrical Properties of GDC-BCY Composite Electrolytes for Intermediate Temperature Solid Oxide Fuel Cell Xiaomei Liu, Hailin Bi, Haopeng Wang, Shenglong Yu, Fei Han, Lili Zhu, Jialing Sun and Li Pei; Key Laboratory of Physics and Technology for Advanced Batteries, Physics Department, Jilin University, Changchun, China.

The electrolyte material $Ce_{0.9}Gd_{0.1}O_{1.95}$(GDC) powders are synthesized by glycine-nitrate processes and $BaCe_{0.83}Y_{0.17}O_{3-\delta}$(BCY) powders are synthesized by solegel processes, respectively. Then GDC-BCY composite electrolytes are prepared by mixing GDC and BCY. The GDC and BCY powders are mixed in the weight ratio of 99:1, 98:2 , 97:3 and 95:5 and named as GB99, GB98, GB97 and GB95 respectively. X-ray diffraction patterns indicate that GDC-BCY specimens show the pure perovskite phase from the BCY and the cubic fluorite phase from the GDC. Scanning electron microscope microstructures indicate that the grain size increases with increase in BCY content. The electrical properties of GDC and GDC-BCY composites are investigated. Impedance spectroscopy measurements reveal that the grain boundary resistance can be significantly reduced by adding BCY to SDC. Among all of the samples, GB98 exhibits the lowest total resistance. Single cells based on GDC-BCY electrolytes are fabricated using $Ni_{0.9}Cu_{0.1}O_x$/SDC as anode and $BaCo_{0.7}Fe_{0.2}Nb_{0.1}O_{3-\delta}$ as cathode. Among these electrolytes, the maximum power density reaches as high as 204mWcm^2 for the fuel cell based on SB99 composite electrolyte at 600℃. We can indicate that a certain extent doping some BCY to GDC can increase the open-circuit voltage of the fuel cell and, there was obvious enhancement of the fuel cells performance.

Acknowledgements

This work was supported by the National Natural Science Foundation of China (no. 51272087, 50872041) and the National Foundation for Fostering Talent in Basic Science of China (no. J1103202).

A2.39

$Ni_{1-x}Cu_x$-SDC Anodes for Intermediate Temperature Solid Oxide Fuel Cell Lili Zhu[1,2], Xiaomei Liu[1], Jialing Sun[1], Fei Han[1], Hailin Bi[1], Haopeng Wang[1], Shenglong Yu[1] and Li Pei[1]; [1] Key Laboratory of Physics and Technology for Advanced Batteries, Physics Department , Jilin University, Changchun, China; [2]Beihua University, Jilin, China.

Ni based materials, such as Ni-$Ce_{0.85}Sm_{0.15}O_{1.925}$ (Ni-SDC)cermets are the most commonly used anodes for the oxidation of H_2 with Intermediate Temperature Solid Oxide Fuel Cells (IT-SOFCs). One promising approach under investigation is partial substitution of Ni with other electronic conductors to optimize the physical catalytic activity of metallic component in the anode. In the present work, the samples $Ni_{1-x}Cu_x$-SDC(x=0, 0.05, 0.10, 0.15) were prepared by glycine–nitrate process. The XRD of $Ni_{1-x}Cu_x$-SDC exhibited a well-cubic fluorite structure and a good Ni-Cu alloy phase after tested in H_2 at 700℃ for 2h, no new phase was formed. The anodes were prepared with the same process so that the same microstructures were expected. The differences between the anode performances are thus mainly caused by the metal composite. It was observed that the polarization resistance decreased first and then increased with increasing Cu content, obtaining a minimum at x=0.10 Cu. At a Cu content of x=0, the polarization resistance was 1.02 and was reduced to 0.50 when the Cu content increased to x=0.10. The initial decrease of the polarization resistance was attributed to the increase of electronic conductivity with Cu. However, when Cu content was x=0.15, the

polarization resistance increased again. It could be attributed to the relatively lower catalytic activity of Cu than that of Ni. It is clear that the $Ni_{0.90}Cu_{0.10}$–SDC cell shows the highest power density and yields improved performance compared with the Ni–SDC cell. The encouraging results suggested that $Ni_{0.90}Cu_{0.10}$-SDC was a very promising anode material for IT-SOFCs.

Acknowledgement
This work was supported by the National Natural Science Foundation of China (no. 51272087, 50872041)

A2.40
Electrical Conductivity of YSZ-SDC Composite Solid Electrolyte Synthesized via Glycine-Nitrate Method Prabhakar Singh; Department of Physics, Indian Institute of Technology (BHU) Varanasi, Varanasi, India.

Solid oxide fuel cells (SOFCs) are considered to have great potential for highly efficient stationary power generation. Yttria-stabilized zirconia (YSZ) is a common solid electrolyte for SOFCs because of its reasonably high electrical conductivity and high ionic transference number in both oxidizing and reducing atmospheres. Samarium doped ceria (SDC) has also been considered as an alternative electrolyte material to YSZ for intermediate temperature SOFC because of its high conductivity at relatively low temperatures. Due to improved ionic conductivity of YSZ at high temperature (~ 800 °C) and good conductivity of SDC in the intermediate temperature range (600 – 800 °C), the electrical properties of YSZ-SDC composites were investigated. Composite oxides containing YSZ and SDC with weight ratio 9.5:0.5, 9:1 and 8.5:1.5 were synthesized via glycine-nitrate route. XRD pattern of the systems revealed the formation of composite phases. Biphasic electrolyte microstructures were observed, in which SDC grains are dispersed in YSZ matrix. Relative density of the compositions was found to more than 94% to the theoretical density. It was observed that the interface provides a channel for ionic transport, leading to an impressive ionic conductivity. As SDC weight ratio increases the electrical conductivity was found to increase. It showed that when the composition was 85 wt.% YSZ and 10 wt.% SDC, the electrolyte has higher electrical conductivity as compared to YSZ in the temperature range 500–700 °C. At further higher weight ratios (above 8.5:1.5), a few secondary phases were observed leading to decrease in the conductivity. The electrode polarization (in impedance studies) was also found to be reduced significantly by using the SDC in the composite electrolyte. Thus, the composite system may be useful for improving the ionic conductivity of the composite electrolytes.

A2.41
Wet Chemical Synthesis of $(DyO_{1.5})_x(WO_3)_y$ $(BiO_{1.5})_{1-x-y}$ and Application in Bilayer Low Temperature SOFCs Ashley L. Ruth[2], Emily A. Fraik[2], Daniel D. Taylor[1], Hee Sung Yoon[2] and Eric D. Wachsman[2]; [1]Chemistry, University of Maryland, College Park, Maryland, United States; [2]Energy Research Center, University of Maryland, College Park, Maryland, United States.

Stabilized bismuth oxides are known to be among the highest ionic conductivity solid oxide fuel cell (SOFC) electrolyte materials below 700 °C, making them a probable solution for reducing the operating temperature of SOFCs. A high ionic conductivity $(DyO_{1.5})_x(WO_3)_y(BiO_{1.5})_{1-x-y}$ (DWSB) material was synthesized using solid state and wet chemical methods and compared with the well studied $(BiO_{1.5})_{1.6}(ErO_{1.5})_{0.4}$ (ESB). Upon calcination of the wet chemical precursors, nano-sized $(DyO_{1.5})_x(WO_3)_y(BiO_{1.5})_{1-x-y}$ powder with the appropriate fluorite phase was generated. The conductivity of DWSB symmetric cells exhibited a significant change in activation energy between 550 °C and 500 °C while the ESB demonstrated a more subtle transition at 600 °C. The phase stability of DWSB at 500 °C was investigated using neutron diffraction of aged and unaged DWSB. The highest conductivity in DWSB was achieved using the wet chemical synthesis over the solid state route and the wet chemical powder was selected for bilayer SOFC button cell incorporation. DWSB and ESB powders were deposited onto sintered 10 mol% gadolinia doped ceria (GDC)/NiO-GDC functional layer/NiO-GDC anode substrates with a nano-composite $La_{0.8}Sr_{0.2}MnO_{3-\delta}$ (LSM)-ESB cathode and achieved 0.91 W/cm^2 and 0.60 W/cm^2 under flowing H_2 with 3% H_2O at 650 °C, respectively. The total ASR was decreased by using the higher conductivity DWSB, achieving 0.16 Ωcm^2 versus 0.28 Ωcm^2 for ESB.

A2.42
Electrochemical Promotion of CO Oxidation on Pt/YSZ- Interaction between Multiple Promoting Species Danai Poulidi and Efstratios Stavrakakis; Chemistry and Chemical Engineering, Queen's University Belfast, Belfast, United Kingdom.

Electrochemical Promotion of Catalysis (EPOC) is a phenomenon where the application of small currents or potentials causes significant activity and selectivity modification of catalysts supported on ionic or mixed ionic-electronic conductors [1]. Various studies indicate that EPOC is due to electrochemically controlled migration (spillover or backspillover) of promoting species from the conducting support to the catalyst surface and vice versa [1].

The present study addresses electrochemical promotion of CO oxidation on Pt/YSZ pre—covered with sodium. In relevant investigations [2], it has been found that the pre-existing sodium surface species can affect the overall promotional behaviour of the catalyst system. Initial experiments included reaction kinetics under open circuit conditions at 350°C and atmospheric pressure. The results showed that the catalytic rate has positive order with respect to low P_{O2} and zero order to higher P_{O2}. Regarding to CO effect on the catalytic rate, the reaction has positive order in low P_{co} and negative order in higher P_{co}. Chemically supplied low (approx. 0.2%) sodium coverage on the catalyst promotes the reaction while higher sodium coverage induces a poisoning effect. Further work will investigate this hypothesis accompanied with induction of electrochemical promotion in the catalytic system.

The aim of this project is to investigate further and understand the complexity of the interaction between multiple promoters on electropromoted catalytic systems and develop a model that will allow the prediction of the promotional behaviour of more complex reactions and catalyst systems.

[1] C.G. Vayenas, S. Bebelis, C. Pliangos, S. Brosda, D. Tsiplakides, Electrochemical Activation of Catalysis: Promotion Electrochemical Promotion and Metal-Support Interactions, Kluwer Academic/Plenum Publishers, New York, 2001.
[2] N. Ibrahim, D. Poulidi, I. Metcalfe, J.Catal. 303 (2013) 100-109.

A2.43
Electrochemical Behavior of the Pyrochlore- and Fluorite-Like Solid Solutions in the Pr_2O_3-ZrO_2 System: Part II J.C. C. Jabrantes[1, 2], E. Gomes[1], Anna V. Shlyakhtina[3], Alexander N. Shchegolikhin[4] and Lidia G. Shcherbakova[3]; [1]UIDM, ESTG, Instituto Politécnico de Viana do Castelo, Viana do Castelo, Portugal; [2]Aveiro Institute of Materials – CICECO (DEMAC), University of Aveiro, Aveiro, Portugal; [3]Kinetics and Catalysis, Semenov Institute of Chemical Physics, Russian Academy of Sciences, Moscow, Russian Federation; [4]Emanuel Institute of Biochemical Physics, Russian Academy of Sciences, Moscow, Russian Federation.

Praseodymium zirconium solid solutions has been studied as an oxygen storage material, a potential cathode material for medium-temperature solid oxide fuel cells (SOFCs), and a material for sensors, catalysis, thermal barrier coatings, and medical applications. The rare-earth ions having multiple valences are likely to exhibit electronic as well as ionic conductivities. Coprecipitation method was used to prepare $Pr_{2\pm x}Zr_{2\pm x}O_{7\pm\delta}$ solid solutions solutions containing 18, 26.6, 30, 33.3, 35.5, 54, and 60 mol % Pr_2O_3. Linear TEC of the $Pr_3ZrO_{6.5}$ (60% Pr_2O_3) fluorite material has nonlinear behavior. It is important to separate out the chemical expansion contribution from pure thermal contribution. In nonstoichiometric PrZrO ceramics chemical expansion contribution is related to the interaction of the solids with gas atmosphere (Pr3+/Pr4+ active electrochemical couple). Electrochemical impedance spectroscopy was used to obtain electrical conductivity measurements as a function of temperature and oxygen partial pressure. It was observed an increase of the ionic conductivity for both Pr- and Zr-rich pyrochlore compositions. Oxygen vacancies are dominant for Pr-rich compositions, while interstitial oxygen are responsible for the ionic conductivity of Zr-rich compositions. In addition, p-type electronic conductivity was also founded for Pr-rich compositions. Defect chemistry analysis was used to interpret the experimental results.

This work was supported by the Russian Foundation for Basic Research (grant no. 13-03-00680). by the Presidium of the Russian Academy of Sciences (program Synthesis of Inorganic Substances with Controlled Properties and Fabrication of Related Functional Materials, grant no. 17/2015).

A2.44

Thin Flim Oxy-Apatites for Solid Oxide Fuel Cell Sunghwan Lee and Shriram Ramanathan; School of Engineering and Applied Sciences, Harvard University, Cambridge, Massachusetts, United States.

Apatite-phase oxides based on rare-earth silicates ($A_{10-x}(SiO_4)_6O_{2\pm x}$, A=rare earth cation)[1,2] are of interest for potential use as electrolytes or electrodes in solid oxide fuel cell (SOFC) applications for high ionic conductivity at lower temperature. The crystal structure enables a wide choice for ion substitution and compositional variation, and also the ability to tune ionic and electronic transference by altering the stoichiometry of the cation sub-lattice. However, thus far experimental efforts on this new class of materials have been limited to bulk forms and their structural characteristics, and thin-film forms and electrical measurement studies are rarely available in the literature.

In this presentation, we will report on successful synthesis of cerium-based apatites with various cation dopants. The formation of homogeneous apatite phases were identified by X-ray diffraction (XRD) and X-ray photoemission spectroscopy (XPS) analyses with electron microscopy. *In-situ* conductivity measurements as a function of oxygen partial pressure were made at temperatures ranging from 500-800 °C. During *in-situ* measurements, the onset of apatite phase formation, which were correlated with structural and chemical changes observed in XRD and XPS studies, and ionic conduction behavior were clearly observed. The studies present a new way to grow apatites by inter-diffusion in superlattices or alloy mixtures.

A2.45

Structural Stability and Conductivity of the $Bi_3Y_{1-x}W_xO_{6+3x/2}$ System Anna Borowska-Centkowska[1], Wojciech Wrobel[1], Marcin Malys[1], Isaac Abrahams[2] and Franciszek Krok[1];[1]Faculty of Physics Warsaw University of Technology, Warsaw, Poland; [2]Materials Research Institute, Queen Mary University of London, London, United Kingdom.

Introduction

Due to their instability, bismuth oxide based systems have long been thought to be unsuitable for fuel cell applications. However, it has recently been shown that using suitable device construction these materials can indeed be used for such applications [1] and that through careful co-doping of bismuth oxide leads to materials with enhanced stability. The yttrium substituted system Bi_2O_3-Y_2O_3 is found to exhibit high conductivity, but shows some phase instability during long term experiments at temperatures around 650°C [2]. However, in similar system co-doping with W^{6+} has been shown to eliminate this instability [3].
In this study the aging effect on crystal structure and electrical conductivity in the pseudo-binary system B_3YO_6-$Bi_3WO_{7.5}$ of general formula $Bi_3Y_{1-x}W_xO_{6+3x/2}$ in compositional range $0.0 \leq x \leq 0.2$ is presented.

Experimental

Samples of general composition $Bi_3Y_{1-x}W_xO_{6+3x/2}$ (x = 0.0, 0.05, 0.1. 0.15 and 0.2) were prepared by conventional solid state reaction. Structural studies were carried out using X-ray and neutron powder diffraction. Additionally, total scattering analysis using reverse Monte Carlo (RMC) modeling was used to analyse the short-range ion pair correlations. Electrical conductivity was characterised using a.c. impedance spectroscopy. Isothermal X-ray and impedance measurements were carried out at 650 °C. Neutron powder diffraction studies were carried out before and after annealing of the samples at 650 °C.

Results and Discussion

The Bi_3YO_6 composition is found to exhibit high conductivity, but shows some phase instability during long term experiments at temperature around 650 °C. However, di-substitution of Bi_2O_3 can lead to enhanced stability, using tungsten as a second dopant.

Room temperature X-ray and neutron powder diffraction studies revealed that for the examined compositions: x = 0.0, 0.05, 0.1, 0.15 and 0.2 of general formula $Bi_3Y_{1-x}W_xO_{6+3x/2}$, cubic fluorite type structure is maintained and stable over heating and cooling cycle. Long term structural and conductivity studies of cubic phase compositions of $Bi_3Y_{1-x}W_xO_{6+3x/2}$ system show that for the x = 0.1 composition the fluorite type structure is stable over 1000 hours of annealing at temperature 650 °C. Interestingly, the annealed material with lower level of substitution (x= 0.05) as well as the compositions with higher level of substitution of Y^{3+} by W^{6+} (x = 0.15 and 0.2) revealed a mixture of phases. For example for the x = 0.2 composition a second phase appears already after first five hours.

Rietveld analysis using X-ray and neutron powder diffraction data revealed significant changes in the cubic lattice parameter during long term annealing experiment for the $Bi_3Y_{0.9}W_{0.1}O_{6.15}$ composition, which can be associated with redistribution of oxide ions in the fluorite phase.

References

[1] E.D. Wachsman, K.T. Lee, *Science*, 334 (2011) 935.
[2] A. Joshi, S. Kulkarni, J. Nachlas, J. Diamond, N. Weber, *Journal of Mater. Science* 25 (1990) 1237.
[3] S-H. Jung, E.D. Wachsman, N. Jiang, *Journal of American Ceram. Soc.* 93 [5] (2010) 1384.

A2.46

High Humidity Effects in Reversible Solid Oxide Cells and in Ni-YSZ Symmetric Cells Eui-Chol Shin[1], Pyung-An Ahn[1], Hyun-Ho Seo[1], Dang-Thanh Nguyen[1], Sun-Dong Kim[2], Sang-Kuk Woo[2], Ji Haeng Yu[2] and Jong-Sook Lee[1]; [1]Materials Science and Engineering, Chonnam National University, Gwang-Ju, Korea (the Republic of); [2]Korea Institute of Energy Research , Daejeon, Korea (the Republic of).

The impedance behavior of the archetypal Ni-YSZ/YSZ/LSM solid oxide cells was investigated in reversible operation at different humidity condition up to 90%. The major electrode polarizations of the full cell at 850◦C are identified with the electrochemical polarization of the LSM-YSZ electrode modeled by three-parameter transmission line model and the gas concentration impedance of the Ni-YSZ electrode modeled by an ideal Gerischer element. The gas concentration polarization increases with the dehumidification by the electrolysis, which is thus reduced by the increased ambient humidity. According to the non-faradaic chemical reaction controlled mechanism for the electrochemical reaction suggested by Mizusaki, diffusion-reaction parameter for LSM electrode was estimated from the transmission line model analysis. Surface diffusivity is shown to enhance strongly with oxygen activity induced by electrolysis, which can be partly ascribed to the decreased surface adsorption capacitance as well as increased mobility. Surface reaction rate increase essentially reflects the decreased adsorption capacitance. The kinetics becomes more limited by the surface adsorption reactions but overall diffusion-limited, which is represented by the Gerischer-like response. Less pronounced performance deterioration in SOFC operation may be ascribed to the mixed conduction contribution. Electrolyte-supported symmetric Ni-YSZ cermet electrodes of ca. 23μm were prepared by screen printing and the impedance was measured as a function of humidity from 2% to 90% balanced in H2 at fixed total flow rate of 50 sccm. Ni-felt of 1 mm thickness and a few ten mm thin Pt paste were used for current collectors, respectively. Ni-felt current collectors exhibit Gerischer-like gas concentration impedance, similarly observed in the cermet-supported solid oxide cells as above, while in the case of Pt collector the gas concentration polarization was negligible. Application of diffusion-reaction transmission line model for the electrochemical polarization was possible with capacitors replaced by CPEs with fixed α=0.5 for both cases. Both D and k appear to increases with humidity. Less pronounced humidity dependence and lower utilization length for Ni-felt collector compared to thin Pt collector can be attributed to the gas concentration impedance imposed by the Ni-felt.

A2.47

High-Performance Anode-Supported Solid Oxide Fuel Cell with Impregnated Electrodes Denis Osinkin[1], Nina Bogdanovich[1], Sergey Beresnev[1] and Viktor Zhuravlev[2]; [1]Laboratory of SOFC, Institution of High Temperature Electrochemistry, Yekaterinburg, Russian Federation; [2]Institute of Solid State Chemistry, Yekaterinburg, Russian Federation.

The aim of this study is to show the possibility of the produce the high-performance single solid oxide fuel cells by simple ways.

Composite powders 61%NiO + 39%$Zr_{0.84}Y_{0.16}O_{1.92}$ (NiO-YSZ) and 56%NiO + 44%$Zr_{0.83}Sc_{0.16}Ce_{0.01}O_{1.92}$ (NiO-CeSSZ) were prepared by two-steps and one-step combustion synthesis, respectively. The supported NiO-YSZ layer was prepared in the shape of a disc by isostatic pressing at 150 MPa cm^{-2} and sintered at 1400 °C for 2 hours in air. The NiO-CeSSZ functional layer, thickness about 20 µm, was applied by brush painting onto one side of the sintered NiO-YSZ disk. When the functional layer dried the first layer of commercial $Zr_{0.84}Sc_{0.16}O_{1.92}$(SSZ) electrolyte powder was applied by painting onto the functional layer. After fired the second SSZ layer was applied onto the first SSZ layer and then sintered at 1360 °C with isothermal exposure for 5 hours in air. The total thickness of the SSZ electrolyte was approximately 30 µm. The self-made Pt + 3%YSZ cathode was applied onto SSZ electrolyte and sintered at 1100 °C for 1 hour.

Power density and I-U curves of the initial fuel cell and after impregnated of cathode and anode by praseodymium and cerium nitrate, respectively, were measurement at different temperatures. At wet hydrogen (air) supply to the anode (cathode) and 900 °C the maximum of power density of the initial cell was 0.35 W cm^{-2}. After the electrodes had been impregnated this value increased by seven times and was approximately 2.4 W cm^{-2} at 0.6 V. It was suggested that after the electrodes impregnation the polarization resistance of the fuel cell was determined by the gas diffusion in the supported anode.

A2.48

Extending the Simple Infiltrated Microstructure Polarization Loss Estimation (SIMPLE) Model to Infiltrated Solid Oxide Fuel Cell (SOFC) Anodes Eric Straley and Jason D. Nicholas; Chemical Engineering and Material Science, Michigan State University, East Lansing, Michigan, United States.

Recently, infiltrated Solid Oxide Fuel Cell (SOFC) cathodes have received a great deal of attention in the literature [1-3]. Advances in infiltrated cathode design have been assisted by models such as the Simple Infiltrated Microstructure Polarization Loss Estimation (SIMPLE) model, which predicts infiltrated cathode performance using intrinsic materials properties (i.e. the infiltrate surface exchange resistance and scaffold ionic conductivity) and electrode microstructural parameters (i.e. the cathode thickness, infiltrate surface area, scaffold column width, and pre-infiltrated cathode porosity) [4]. Unfortunately, no models, to date, have been shown to effectively predict the performance of infiltrated nano-composite anodes (NCAs). Therefore, the objective of the present work was to compare the polarization resistance, Rp, of $La_{0.75}Sr_{0.25}Cr_{0.5}Mn_{0.5}O_{2.8}$ (LSCrM) infiltrated $(Y_2O_3)_{0.08}(ZrO_2)_{0.92}$ (8YSZ) anodes to SIMPLE model predictions of these anodes.

To achieve this, LSCrM infiltrated 8YSZ NCAs were fabricated by screen printing porous 8YSZ scaffolds on both sides of dense 8YSZ electrolytes, infiltrating the scaffolds with LSCrM nitrate precursor solutions, and thermally decomposing the nitrate solutions through firing at 800°C in air for 1 hour. Porous $La_{0.3}Sr_{0.7}TiO_3$ current collectors and gold grids where then screen printed onto each NCA. The 400-700°C Rp values in 4% H_2 (balance Ar) were then determined using controlled atmosphere electrochemical impedance spectroscopy (EIS). Focused Ion Beam – Scanning Electron Microscope (FIB-SEM) experiments on EIS-tested samples and non-infiltrated scaffolds were then used to determine the cathode thickness, the infiltrate surface area, the scaffold column width, and the pre-infiltrated cathode porosity. These microstructural parameters, the 8YSZ ionic conductivity [5], and the LSCrM intrinsic oxygen surface resistance [6] were then used to produce SIMPLE model NCA Rp predictions. A comparison between the measured and predicted Rp values revealed the accuracy of applying the SIMPLE model to infiltrated anodes containing a mixed ionic electronic conducting (MIEC) infiltrate on an ionic conducting (IC) scaffold.

References:

Vohs, J. M. and Gorte R. J. "*High-Performance SOFC Cathodes Prepared by Infiltration*" Advanced Materials **21** (9): 943-956 (2009).

Jiang, S. P. "*Nanoscale and Nano-structured Electrodes of Solid Oxide Fuel Cells by Infiltration: Advances and Challenges*" International Journal of Hydrogen Energy **37** (1): 449-470 (2012).

Ding, D., et al. "*Enhancing SOFC Cathode Performance by Surface Modification through Infiltration*" Energy and Environmental Science **7**: 552-575 (2014).

Nicholas, J. D. et al."*Use of the Simple Infiltrated Microstructure Polarization Loss Estimation (SIMPLE) Model to Describe the Performance of Nano-Composite Solid Oxide Fuel Cell Cathodes*" Physical Chemistry Chemical Physics **14** (44): 15379 (2012).

Steele, B. C. H. and Heinzel, A. (2001). "*Materials for Fuel-Cell Technologies*" Nature **414** (6861): 345-352.

Raj, E. S. et al. "*Oxygen Diffusion and Surface Exchange Studies on* $(La_{0.75}Sr_{0.25})_{0.95}Cr_{0.5}Mn_{0.5}O_{3-d}$" Solid State Ionics **177** (19-25): 1747-1752 (2006).

A2.49

A High Performance Anode Material for Solid Oxide Fuel Cells: Ni Exsolution on A-Site Deficient $La_{0.4}Sr_{0.4}Sc_{0.9}Ni_{0.1}O_{3-\delta}$ Mattia Saccoccio[1], Yang Gao[1], Dengjie Chen[1], Chi Chen[1] and Francesco Ciucci[1, 2]; [1]Department of Mechanical and Aerospace Engineering, The Hong Kong University of Science and Technology, Clear Water Bay, Hong Kong;[2]Department of Chemical and Biomolecular Engineering, The Hong Kong University of Science and Technology, Clear Water Bay, Hong Kong.

Solid oxide fuel cells (SOFCs) are among the most efficient systems to convert chemical energy directly into electricity. While perovskite-type materials have been used as SOFC anodes to overcome many of these challenges, their catalytic activity is typically poor. In this work we report the synthesis of a novel Sc-based A-site deficient perovskite $La_{0.4}Sr_{0.4}Sc_{0.9}Ni_{0.1}O_{3-\delta}$(LSSN) as an anode material for solid oxide fuel cells. Recently, exsolution of catalytic nanoparticles on the surface of perovskites has drawn great research interest because of the potential enhancement in electrochemical activity. LSSN is reduced in hydrogen at 900 °C for 15 hours to form a highly active and stable anode. Spherical Ni nanoparticles (~60 nm in diameter) with well-defined boundaries are exsolved on the surface after reduction. In comparison to previously reported perovskite materials and Ni/YSZ, the reduced LSSN (rLSSN) shows high electrochemical catalytic activity in symmetric cell configurations, with the area specific resistances as low as 0.13 Ω cm^2 (rLSSN) and 1.3 Ω cm^2 (LSSN) at 700 °C and 20% H_2 + 80% N_2.

A2.50

Fabrication of Co/Fe-Doped Ni/$BaZr_{0.8}Y_{0.2}O_{3-\delta}$ Anode for Methane-Fueled PCFC Taehyun Park[2, 1], Chuancheng Duan[2], Jianhua Tong[2], Suk Won Cha[1] and Ryan O'Hayre[2];[1]Mechanical and Aerospace Engineering, Seoul National University, Gwanak-gu, Korea (the Republic of); [2]Metallurgical and Materials Engineering, Colorado School of Mines, Golden, Colorado, United States.

Protonic ceramic fuel cells (PCFCs) are being increasingly examined for operation on non-hydrogen fuels such as methane. However, because steam is primarily generated at the cathode in a PCFC, these cells can suffer from significant carbon-coking and sulfur poisoning issues. This research examines the inclusion of Co and Fe nanoparticles to a Ni/$BaZr_{0.8}Y_{0.2}O_{3-\delta}$ cermet anode in order to mitigate carbon coking and sulfur poisoning while maintaining or improving the electrochemical performance of the PCFC. Co and Fe are chosen to impart carbon coking resistance and to improve methane decomposition, respectively. A series of PCFC single cells with varying amounts of Co and Fe loading are prepared via the sol-gel method. Anode compositions are analyzed using X-ray diffractometry and anode morphologies are investigated via scanning electron microscopy. Cell performance is investigated as a function of the Co and Fe content.

A2.51

Synthesis and Preliminary Study of Pure and Zr-Substituted $YMnO_3$ Compounds as Solid Oxide Fuel Cells Electrode Zulma L. Moreno[1, 3], Alberto Caneiro[3], Pascal Roussel[2] and Gilles H. Gauthier[1]; [1]Grupo INTERFASE, Universidad Industrial de Santander, Bucaramanga, Colombia; [2]Université Lille 1, Université Lille Nord de France, Lille, France; [3]Comisión Nacional de Energía Atómica, Centro Atómico de Bariloche, San Carlos de Bariloche, Argentina.

Manganites of the $Y_{1-x}Zr_xMnO_3$ series ($0 \leq x \leq 0.30$) have been studied with the aim of using them as SOFC electrode materials. These compounds adopt a layered structure of hexagonal symmetry (S.G. $P6_3cm$) in which manganese cations are located in trigonal bi-pyramidal coordination of oxygen atoms, different from the classical perovskite. The materials synthesis has been carried out by solid state reaction and X-ray Diffraction technique revealed that pure phases can be obtained until x~0.10. For $x \geq 0.10$, an additional YSZ phase is formed, similar to the common SOFC electrolyte material.

High-Temperature XRD (HT-XRD) in air followed by structural refinement allows calculating a volumetric TEC value b=30.39 x 10^{-6} K^{-1} for $YMnO_3$, closed to the b value of 31-33 x $10^{-6}K^{-1}$ generally found for 8YSZ [1]. In a similar way as between YSZ and the La/Sr manganites (b ~ 33-36 x 10^{-6} K^{-1} [2]), it should not normally induce any thermal expansion mismatch between the electrode and electrolyte. Using HT-XRD and thermogravimetric analysis in reducing atmosphere, pure and Zr-substituted $YMnO_3$ were proved to be unstable in diluted dry H_2 for T>600ºC, what precludes their use as SOFC anode material.

Nevertheless, reactivity studies at high temperature (T=1300ºC) between $Y_{1-x}Zr_xMnO_3$ (x=0, 0.05 and 0.1) and 8YSZ show a good chemical compatibility with no formation of electrically insulating phase, but a crossed diffusion of Y^{3+}/ Mn^{3+} and Zr^{4+} at the interface between both materials.

Acknowledgments: This work was developed with the financial support from UIS/VIE (project #1333), CNEA, FEDER, CNRS, Région Nord Pas-de-Calais, MENESR, LNLS, Laboratorio de Rayos X (UIS).
References: [1] F. Tietz *et al*. in Proceedings of the 5th European Conference on Advanced Materials and Processes and Applications (Euromat '97), 2, (1997) 271. [2] Kendall K, Minh NQ and Singhal SC. *High Temperature Solid Oxide Fuel Cells: Fundamentals, Design and Applications*. Oxford: Elsevier; (2003).

A2.52

Structural and Electrical Properties of Ceria (Ce^{3+}) Doped Double Perovskite System $Sr_2NiMoO_{6-\delta}$ Pravin Kumar, Nitish Kumar Singh and Prabhakar Singh; Physics, Indian Institute of Technology (BHU) , Varanasi, India.

Solid oxide fuel cells (SOFCs) are suitable candidates in revolution of green energy technology. It has long term stability and better fuel flexibility. In the development of SOFCs, double perovskite materials may play an important role as electrode material due to their enhanced electrical properties.
In the present work, double perovskite $Sr_{1.95}Ce_{0.05}NiMoO_{6-\delta}$ (SCNM) was prepared by auto-combustion synthesis route. The thermal study was carried out using simultaneous differential scanning calorimetry and thermal gravimetry. These studies showed completion of reaction at about 900 ˚C. The phase formation was studied by the powder X-ray diffraction. This indicated the formation of $SrNiMoO_6$ major phase with minor phase of $SrMoO_4$. The Rietveld refinement showed the tetragonal crystal structure with space group I4/m for major phase $SrNiMoO_6$. Micro-structural studies revealed the formation of uniform grains with the average grain size of 2 mm. The thermal expansion coefficient (TEC) measurement of the studied sample revealed that it is compatible to the TEC of standard electrolytes. The electrical conductivity was studied using impedance spectroscopy in the temperature range 200 ˚C - 600 ˚C. The electrical conductivity was found to show thermally activated behavior with activation energy 0.98.eV.

A2.53

Chemical Stability of Double-Perovskite Anode Material Sr_2MgMoO_6 for Solid Oxide Fuel Cells Masahiro Kinoshita[1], Kyota Hara[2], Tomohiro Onozawa[2], Kiyoto Shin-mura[1], Yu Otani[1], Eiki Niwa[3], Takuya Hashimoto[3] and Kazuya Sasaki[1, 2]; [1]Course of Mechanical Engineering, Graduate School of Engineering, Tokai University, Hiratsuka, Japan; [2]Department of Prime Mover Engineering, School of Engineering, Tokai University, Hiratsuka, Japan; [3]Department of Physics, College of Humanities and Sciences, Nihon University, Setagaya-ku, Japan.

Solid oxide fuel cells (SOFCs) can, in principle, use hydrocarbon fuels having high energy density without external reforming. Then, SOFCs are promising as power sources for many potential mobile applications. Performance of the internal reforming SOFCs is governed by anode electrode material. Conventional Ni-cermet anodes used in SOFCs, however, have several potential issues typified by poor redox stability, low sulfur tolerance, and propensity to coking, in the direct use of hydrocarbon fuels. In recent years, many efforts have been devoted to the development of ceramic anodes for direct utilization of hydrocarbon fuels, and have reported that some oxide ceramics based on double perovskites exhibit the ability to directly operate on hydrocarbon fuels. Among them, Sr_2MgMoO_6 (SMM) has attracted much attention as a promising anode material for hydrocarbon-fueled SOFCs, because of its high tolerance to carbon deposition and sulfur poisoning. SMM exhibits high performance by the addition of Pt or ceria because Pt and ceria are catalytically active for the oxidation of H_2 and CH_4. For their high performance, SMM must be compatible with the electrolyte material and the additives. In this study, the compatibility under the electrode preparation process and actual working condition of the SOFCs is evaluated. Mixtures of the powders of SMM, yttria-stabilized zirconia (YSZ), scandia-stabilized zirconia, strontium- and magnesium-doped lanthanum gallate, and gadoria-doped ceria were fired in pure-H_2, 5%-H_2, 1%-H_2, or air. Crystal phase stability was analyzed by X-ray diffraction at room temperature. Second phase formation temperature was revealed by high temperature X-ray diffraction. As a result, for example, it was revealed that SMM reacts with YSZ at the high temperature around 1000 ºC in air, though they maintained compatibility at below 900 ºC. Limitations in electrode preparation conditions and operating conditions for the realization of high performance SMM electrodes were also investigated.

A2.54

Novel Ni and Ni Alloy/γ-Al_2O_3 Anode Materials for Direct Carbon SOFCs Sergey Pikalov[2], Evgeny Selivanov[2], Olga Russkikh[1], Elena Filonova[1], Valery Polukhin[2] and Irina Nikolaenko[3]; [1]Institute of Natural Sciences, Ural Federal University, Ekaterinburg, Russian Federation; [2]Institute of Metallurgy, UB RAS, Ekaterinburg, Russian Federation; [3]Institute of Solid State Chemistry, UB RAS, Ekaterinburg, Russian Federation.

The advantage of direct hydrocarbon solid oxide fuel cells (SOFCs) over the other reformers-based fuel cells is their ability to increase the total efficiency by excluding external fuel processing. Ni-YSZ cermets, widely used as SOFC anodes, possess high electrical conductivity and excellent electrochemical activity. However, when using methane as a fuel, because of high catalytic activity of sintered nickel towards hydrocarbon cracking reaction, coke is easily formed over anode surface rapidly decreasing the fuel cell performance. Most recently, the concept of applying γ-Al_2O_3 supported nickel catalysts over a conventional nickel cermet was proposed for operating on methane fuel. In this work Ni and Ni-Al alloys were utilized as the components of the composite anodes on the base of Al_2O_3 fabricated by the air plasma spraying (APS) method in a shape of porous tubes which are proposed to be used as supported catalytically active anode layer for direct methane oxidation. As the feedstock powders for the production of the composite anode materials (50 wt.% of Ni or Ni alloy and 50 wt.% ceramic component), flowable Ni powder of 20-80 μm fraction (98% purity, Norilsk Nickel, Russia) or Ni-Al (Al-plated Ni with Al content of 5% and 15%, Tulachermet, Russia) and α-$A1_2O_3$ (99% purity,

Rusal, Russia) of regular spherical shape with a mean particle size of 50 µm and a flowing rate of no less than 60 g/min were used. The powders were mixed in planetary mill and samples of tube shape were formed by APS method on a metal pin 9 mm in diameter with a pre-coated anti-adhesive layer. The thickness of fabricated porous anode tubes was 400-600 µm. The surface morphology was studied by a scanning electron microscope JEOL JSM 6390LA combined with JED-2300 energy dispersive x-ray analyser.

XRD study of the samples was done using a DMAX-2500 with Ni-filtered CuKα radiation in the range of $15° \leq 2\theta \leq 85°$. It was found that in as-prepared samples Ni stays mainly in metal state with trace amount of NiO and Al_2O_3 in γ-phase state. Doping Ni alloy with low amount of Al (5 %) leads to an appearance of spinel which after decomposition and reduction in hydrogen favours more uniform Ni distribution in ceramic matrix and prevents a coarsening of Ni particles. It leads to an increasing of conductivity and better thermal properties of cermets. The total conductivity of $Ni_{95}Al_5$-Al_2O_3 cermet in hydrogen was 1134 S/cm at 900°C (in comparison with 127 S/cm for Ni-YSZ prepared by the same procedure) with the CTE value 10.5×10^{-6} K^{-1} in range 25-900°C.
The catalytic properties of Ni- and $Ni_{95}Al_5$-Al_2O_3 in methane oxidation by atmospheric oxygen were investigated in the flow-circulation apparatus Bi-CATrEXP combined with external chromatographic analyser. The study has revealed a complete oxidation of methane in gas mixture (1 vol. % of CH_4 and 4 vol.% of O_2 in Ar carrier gas) with carbon dioxide and water as reaction products; carbon monoxide impurity in the final mixture were not found.

A2.55

Novel Double-Layer La_2NiO_{4+d} Cathodes: Screen Printing vs. Electrostatic Spray Deposition R. K. Sharma[1, 2], M. Burriel[3], L. Dessemond[1, 2], Jean-Marc Bassat[4] and E. Djurado[1, 2];[1]LEPMI, Univ. Grenoble Alpes, Grenoble, France; [2]LEPMI, CNRS, Grenoble, France; [3]Catalonia Institute for Energy Research (IREC), Barcelona, Spain; [4]ICMCB-CNRS, Pessac , France.

The main objective of current research in Solid Oxide Fuel Cells (SOFCs) is to reduce the operating temperature down to intermediate temperatures (IT, 500-700°C) without compromising the performances of the device. However the reduction of the operating temperature leads to a significant decrease of the electrode performance and therefore the choice of suitable cathode materials becomes more critical and important. Recently, rare earth nickelate oxides with K_2NiF_4 structure have attracted considerable attention as IT-SOFC cathode materials because of their high electronic and ionic conductivity and similar thermal expansion coefficient (TEC) to the most commonly used solid electrolyte, $Ce_{0.9}Gd_{0.1}O_{2-\delta}$ (CGO). Both the composition and the microstructural design of the cathode film play a significant role in obtaining optimal performances [1]. In this work, La_2NiO_{4+d} (LNO) cathodes have been prepared on CGO electrolytes by Electrostatic Spray Deposition (ESD) and screen-printing (SP). Their electrochemical properties have been studied as a function of the cathode micro-structural design.

Experiments
Predetermined amounts of nitrate metal salts, citric acid, water and ethanol were used to prepare the precursor solution. The LNO films were deposited on CGO substrates by ESD in air after the optimization of the process parameters such as deposition time, flow rate, substrate temperature and nozzle to substrate distance [1]. The same precursor solution has been used for the preparation of LNO powder by auto-combustion. Both, as prepared films and powders were subsequently calcined in air at 950°C for 6 h. KD2921-based slurry was prepared with LNO powder. A total of 3 cathodes in symmetrical mode have been prepared: ESD single layer, SP single layer and ESD + SP (double layer) and sintered at 1050°C/2h + 1100°C/30 min. Impedance spectroscopy was carried out in air from 500 to 700°C at OCP using an autolab potentiostat-galvanostat in the frequency range 0.05 to 10 kHz.

Results and Discussion
XRD patterns of the LNO film and powder confirm the formation of single phase La_2NiO_{4+d} with orthorhombic symmetry (Fmmm). SEM micrographs of the surface and cross section of each electrode prepared by ESD and double layer (ESD + SP) are shown in Fig. 1(a)-(d). A 3D coral type highly porous microstructure with sub-micron sized grains and uniformly distributed micro-pores has been observed throughout the cathode. The SP layer is partially penetrating the ESD layer (Fig 1d).

Fig. 1. SEM images of the $La_2NiO_{4+\delta}$ films, (a),(b) surface and cross section of ESD; (c),(d) surface and cross section (ESD + SP)

Fig. 2. Arrhenius plot of La_2NiO_{4+d} cathode; ESD vs. SP.
The Arrhenius plot of the polarization resistance R_p is shown in Fig. 2. The expected thermal dependence of R_p is evidenced and the R_p values decrease when the architecture of the cathode is optimized. For example, the R_p values for ESD (good cathode/electrolyte interface), SP (good current collecting layer, CCL) and double layer (good interface as well as good current collecting) are equal to 1.26, 0.58 and 0.08 Ω.cm² respectively at 700°C [2]. This significant decrease of R_p is due to the use of a CCL which homogenizes the distribution of the current lines through the cathode functional layer. The recorded R_p value (0.08 Ω.cm² at 700°C) is far lower than the ones previously reported in the literature for $La_2NiO_{4+\delta}$ cathode, i.e. 1.0 (SP) [3] and 0.3 Ω.cm² (SP) [4] at 700°C respectively. This indicates that such architecturally designed LNO cathode is novel and promising as IT-SOFC cathode.

References
[1] D. Marinha et al., Current Inorganic Chemistry 3, 2 (2013).
[2] R.K. Sharma et al., Advanced Functional Materials, in redaction.
[3] R. Sayers et al., Solid State Ionics 192, 531 (2011).
[4] V. Vibhu et al., ECS Trans. 57 (1), 2093 (2013).

A2.56

Patterned Electrodes for the Study of CO/CO_2 Electrolysis Vladislav Duboviks[1], Enrique Ruiz-Trejo[1], Farid Tariq[1], Paul Boldrin[1], Robert C. Maher[2], Gregory J. Offer[3], Gabriel Castillo[4], Javier Rodriguez Vazquez de Aldana[4], Masashi Kishimoto[1], Leslie F. Cohen[2] and Nigel P. Brandon[1]; [1]Earth Science and Engineering, Imperial College London, London, United Kingdom; [2]Physics, Imperial College London, London, United Kingdom; [3]Mechanical Engineering, Imperial College London, London, United Kingdom; [4]Ciencias, Universidad de Salamanca, Salamanca, Spain.

A series of patterned electrodes were manufactured by machining a grid of trenches with a femto-second laser on a CGO or YSZ disc followed by nickel sputtering and electrodeposition. The trenches were 100µm wide, 100µm deep and were equidistantly spaced by 300µm in both directions resulting in a total geometric TPB of 4.44m leading to well-defined triple phase boundary after the nickel deposit. These electrodes were used to study carbon deposition under CO/CO2 electrolysis at 600 °C by Raman mapping. The charge-transfer reaction occurring on the TPB in electrolysis mode was shown to facilitate carbon deposition. Charge-transfer current density in the electrochemically active region of our electrodes was modelled indicating that most of the electrochemical reactions occur less than 5µm away from the electrolyte-electrode interface. Our results confirmed previous observations of superior resistance of Ni/CGO to coking in comparison to Ni/YSZ. Deposition of carbon at the interface between nickel and the electrolyte was also detected and we discuss the possible origin of this deposit using the 3-D reconstruction of the electrode microstructure by X-Ray tomography.

SESSION A3: SOFC—Cathodes II
A: Solid Oxide Fuel Cells and Electrolyzers
Chairs: Ryan O'Hayre and Harry Tuller
Monday Afternoon, June 15, 2015
Keystone Resorts, Longs Peak

2:30 PM *A3.01

Perovskite Oxides as Materials for Energy Conversion: Towards a Fundamental Understanding of Surface Properties by *Operando* Spectroscopic Methods David N. Mueller[2, 1], Michael L. Machala[2], Zixuan Guan[2], Hendrik Bluhm[3] and William C. Chueh[2, 4]; [1]Peter Gruenberg Institute (PGI-6), Research Center Juelich, Juelich, Germany; [2]Department of Materials Science & Engineering, Stanford University, Stanford, California, United States; [3]Chemical Sciences Division, Lawrence Berkeley National Laboratory, Berkeley, California, United States;[4]Stanford Institute for Materials and Energy Sciences, SLAC National Accelerator Laboratory, Menlo Park, California, United States.

Oxides of the perovskite structure with the general formula ABO_3 are versatile materials owing to their chemical flexibility, accommodating a huge portion of the periodic table as constituents. This allows the tailoring of the chemical composition to attain specific properties harvestable in a wide range of applications, such as electrodes for solid state electrochemical cells or oxygen separation membranes, where the ability of the oxide to rapidly exchange oxygen with the surrounding atmosphere is utilized.

In this work, critical surface properties that give rise to high catalytic activities with regard to oxygen exchange in $(La,AE)(Co,Fe)O_{3-d}$ (with AE = alkaline earth) thin film model systems will be examined. Surface-sensitive *in operando* X-ray spectroscopy measurements link the surface electronic properties and composition to the catalytic activity, and investigate surface reorganization processes upon exposure to high temperatures, gas atmospheres and electrochemical polarization.
The holistic picture of the interplay between electronic structure and compositional as well as phase changes may allow a deeper understanding of processes on an atomistic scale and guide design of perovskite materials for improved performance and stability.

2:50 PM A3.02
***In Situ* X-Ray Synchrotron Spectroscopy Study of IT-SOFC Stability under Operating Conditions** Florent Tonus and Stephen J. Skinner; Materials, Imperial College London, London, United Kingdom.

In order to reduce the greenhouse effect, research on fuel cells and particularly on SOFCs has been extensively developed as the only produced waste is water. One of the main issues with SOFCs lies in the high operating temperature (800 ºC) that causes rapid aging of the elements of the cell, implying cation migration from one element of the cell to another, causing the formation of a passive phase at the interface or undesirable electronic conductivity in the electrolyte. Previous research has been undertaken *in-situ* in an attempt to understand the degradation processes of the cell, investigating the interaction between the different functional components. However most of these studies were undertaken in conditions far from operating conditions, and on high temperature SOFC materials when the future of SOFCs lies in lower operating temperature materials in order to decrease aging effects.

In this work, we study *in-situ* in operating conditions by synchrotron X-ray spectroscopy the interaction between 2 promising IT-SOFC materials, $La_{0.6}Sr_{0.4}Co_{0.2}Fe_{0.8}O_3$(LSCF) and $Ce_{0.9}Gd_{0.1}O_{2-d}$ (CGO). A symmetrical cell of LSCF/CGO/LSCF was heated up to 600 ºC under air and a potential of ±0.5 V and ±1.5 V was applied to the cell. On the surface (down to a few mm), the chemical composition of the 2 phases was measured across the interface by XRF and XANES. Its evolution was observed over time applying different potentials. The results show a stability of CGO during the experiment, and whilst LSCF was stable under low voltages (±0.5 V), a migration of La and Co into the electrolyte could be observed at higher voltages (±1.5 V) while Fe remained stable.

3:10 PM A3.03
Surface Chemistry of $La_{0.6}Sr_{0.4}CoO_{3-\delta}$ Thin Films and Its Impact on the Oxygen Surface Exchange Resistance Ghislain M. Rupp[1], Helena Tellez[2], John Druce[2], Andreas Limbeck[3], Tatsumi Ishihara[2], John Kilner[4, 2] and Juergen Fleig[1]; [1]Institute of Chemical Technologies and Analytics - Electrochemistry, Vienna University of Technology, Vienna, Austria;[2]International Institute for Carbon-Neutral Energy Research, Kyushu University, Fukuoka, Japan; [3]Institute of Chemical Technologies and Analytics - Instrumental Analytical Chemistry, Vienna University of Technology, Vienna, Austria; [4]Department of Materials, Imperial College London, London, United Kingdom.

Sr doped $LaCoO_3$ is a very attractive cathode material for intermediate temperature solid oxide fuel cells. Very low oxygen surface exchange resistances have been reported, particularly for thin films. However, degradation of the very fast electrochemical kinetics is found already at temperatures as low as 500°C. This is largely caused by chemical or structural changes of the surface. In this study, we used Low-Energy Ion Scattering Spectrometry (LEIS) and on-line Inductively Coupled Plasma Mass Spectrometry (ICP-MS) as surface sensitive methods to analyze the true cation composition of the near surface layers of dense $La_{0.6}Sr_{0.4}CoO_{3-\delta}$ (LSC) thin film model electrodes. Together with Electrochemical Impedance Spectroscopy (EIS) experiments it was thus possible to correlate changes of the cation composition of the LSC surface and variations in the electrochemical oxygen exchange kinetics.
The measurements revealed that freshly prepared LSC thin films, deposited by pulsed layer deposition at 600°C on yttria-stabilized zirconia (100) electrolytes, already show a Sr-rich termination layer (80% surface coverage). This Sr-rich surface layer is removed when treating the sample in ultrapure H_2O and it forms again, when annealing the sample at temperatures above ca. 550°C for 1 h. This suggests that a Sr-termination of the LSC lattice is thermodynamically favored and that Sr in the LSC thin films has a very high mobility. Impedance experiments on as-prepared samples and samples treated in ultrapure water showed the detrimental effect of this Sr-rich and Co-poor layer. An empirical correlation between accessible Co-atoms at the surface and oxygen incorporation kinetics was found. Interestingly, further annealing at 600°C in synthetic air did not lead to further significant accumulation of Sr at the surface. Nevertheless, the surface exchange resistance continuously increased. Hence, Sr segregation is not the only mechanism that may cause degradation of the electrochemical kinetics of LSC.

3:30 PM A3.04
Surface Analysis of SOFC Cathode Degradation Using Low Energy Ion Scattering and *In-Operando* Atmospheres Mathew Niania[1], Samuel Cooper[1], Helena Tellez[2], John Druce[2], Stephen Skinner[1], Tatsumi Ishihara[2] and John Kilner[1, 2]; [1]Materials, Imperial College London, London, United Kingdom; [2]I2CNER, Kyushu University, Fukuoka, Japan.

Solid Oxide Fuel Cell (SOFC) cathode materials rely on the catalytic processes at their surfaces to reduce and incorporate molecular oxygen. For many common cathode materials surface passivation occurs through 'A site' segregation at common operating temperatures [1]. These processes have a negative effect upon the oxygen reduction rates and therefore overall cell performance. Quantifying the true extent these segregation effects have on the exchange properties has not been fully explored but it is clear that the properties of the surface are essential.

A well-studied method for measuring equilibrium exchange kinetics and diffusion properties of oxygen in an oxide material is the Isotopic Exchange Depth Profiling (IEDP) technique. Diffusion profiles are introduced, analysed using Secondary Ion Mass Spectrometry (SIMS) and fit using the Crank-Nickleson solutions to the diffusion equation to determine exchange coefficient and diffusivity properties. In order to decouple the effect of gas phase impurities have on the exchange kinetics high purity (99.999%) gases are typically used (^{16}O and isotopically labelled ^{18}O). However, all of SOFC systems aim to use atmospheric air as their cathode gas stream which contains a number of different gases which have been shown to affect cell performance negatively [2,3].

In this work a novel extension to the IEDP method, known as 'Back Diffusion', has been developed to allow kinetic and diffusivity properties to be measured accurately in any atmosphere. In order to characterise the surface fully, both chemical and morphological changes have been followed over a range of annealing times and temperatures using highly sensitive surface analysis techniques. Low Energy Ion Scattering (LEIS) has allowed chemical analysis with a depth resolution of a single atomic layer and Atomic Force Microscopy (AFM) has provided high resolution topographical data of said surfaces. Combining these analytical techniques it has been possible to compare surface evolution of SOFC cathode materials with their reaction kinetics in significantly greater detail and report the difference pure and impure environments have on these materials.

[1] M. Kubicek, A. Limbeck, T. Fromling, H. Hutter, and J. Fleig, "Relationship between cation segregation and the electrochemical oxygen reduction kinetics of $La_{0.6}Sr_{0.4}Co_{0.2}Fe_{0.8}O_{3-\delta}$thin film electrodes" Journal of The Electrochemical Society, vol. 158, no. 6, pp. B727–B734, 2011.

[2] Bucher, E., Gspan, C., Hofer, F., & Sitte, W. (2013). Sulphur poisoning of the SOFC cathode material $La_{0.6}Sr_{0.4}CoO_{3-\delta}$. *Solid State Ionics*, *238*, 15–23. doi:10.1016/j.ssi.2013.03.007

[3] Bucher, E., Sitte, W., Klauser, F., & Bertel, E. (2012). Impact of humid atmospheres on oxygen exchange properties, surface-near elemental composition, and surface morphology of $La_{0.6}Sr_{0.4}CoO_{3-\delta}$. *Solid State Ionics*, *208*, 43–51. doi:10.1016/j.ssi.2011.12.005

3:50 PM A3.05
Oxide-Ion Dynamics in the MIEC SOFC Cathode Material $La_2NiO_{4+\delta}$ by Experimental and Computational Solid-State ^{17}O NMR Spectroscopy David M. Halat[1], Riza Dervisoglu[2], Gunwoo Kim[1] and Clare P. Grey[1, 2]; [1]Department of Chemistry, University of Cambridge, Cambridge, United Kingdom; [2]Department of Chemistry, Stony Brook University, Stony Brook, New York, United States.

Mixed ionic-electronic conductors (MIECs) show promise as next-generation solid oxide fuel cell (SOFC) cathode materials with improved performance at intermediate temperatures (500-800°C) as compared to materials lacking oxide-ion conductivity. The complex interplay of electronic and ionic conductivity in these strongly correlated systems often derives from the mutual influence of transition metal cation mixed valency and oxygen nonstoichiometry. Among MIECs tested as SOFC cathodes, the Ruddlesden-Popper phase $La_2NiO_{4+\delta}$ exhibits rapid oxygen transport at low temperatures, attributed to loosely bound interstitial oxides ($0 < \delta < 0.3$). Key to understanding the high oxide-ion conductivity in $La_2NiO_{4+\delta}$ is experimental confirmation of hypothesized interstitial- and vacancy-mediated mechanisms at the atomic level.

In this study, solid-state ^{17}O MAS-NMR spectroscopy of $La_2NiO_{4+\delta}$ at temperatures up to 800°C is supported by a theoretical methodology equipped with results from periodic hybrid DFT calculations. Three distinct ^{17}O resonances are observed and assigned to equatorial, axial, and interstitial oxygen environments in $La_2NiO_{4+\delta}$. Moreover, with high-resolution MAT-PASS experiments, the axial feature splits into several resonances, consistent with local structural distortions due to nearby interstitials. Loss of the interstitial oxygen feature in the NMR spectra upon heating to ~150°C is attributed to onset of exchange of interstitial and axial oxygen sites. Structural rearrangements due to interstitial motion also manifest as linewidth changes in the axial and equatorial resonances. At operational SOFC temperatures (600-800°C), interstitialcy and vacancy mechanisms of oxide-ion conduction are tentatively confirmed for the first time, showing that interstitial-axial exchange continues to dominate transport at the highest temperatures. Slow vacancy diffusion (equatorial-axial exchange) is surmised to limit the overall three-dimensional ionic conduction. This work is among the first examples of dynamics in a paramagnetic oxide-ion conductor studied by ^{17}O solid-state NMR.

4:10 PM *A3.06
Acceptor Doped $CeNbO_4$ as a Potential Mixed Proton Conducting Electrode Stephen Skinner and Cassandra Harris; Imperial College London, London, United Kingdom.

Rare earth orthoniobates of general composition $LnNbO_4$ (Ln = La, Nd, Gd, Tb) have been identified as effective proton conducting electrolytes, with Haugsrud [1] highlighting that substitution of Ca or Sr for Ln increased the protonic transport in these phases. Additionally the Ce analogue has been shown to be a mixed conductor [2-3], with Ce^{3+} species oxidising, resulting in incorporation of interstitial oxygen species, with a reported ionic transport number of ~0.5 at T > 800ºC. Further studies on these orthoniobate systems have considered aliovalent substitution of La/Ce or Nb with 4+ or 6+ cations in an effort to stabilise the oxide ion conducting phase. From these studies we have identified modulated superstructures in which the conduction is via interstital oxide ions [4,5]. Whilst these studies have focussed on the potential for oxide ion conduction few studies have explored the potential of the $CeNbO_{4+/-d}$ phases to perform as mixed proton-electron conductors. In this work we report our findings on the $Ce_{1-x}Sr_xNbO_{4+/-d}$ phases, focusing on the stability of the materials under conditions relevant to operation of a proton conducting solid oxide fuel cell, and discuss the conductivity of these materials in both wet and dry atmospheres. The effect of varying the Sr content and its effect on the defect compensation mechanism will be discussed.

[1] R. Haugsrud & T. Norby, Nat. Mater. 5 193 2006
[2] R.J. Packer & S.J. Skinner, Adv. Mater. 22 1613 2010
[3] R.J. Packer, S.J. Skinner, A.A. Yaremchenko, et al, J. Mater. Chem., 16 3503 2006
[4] C. Li, R.D. Bayliss & S. J. Skinner, Solid State Ionics, 262 530 2014
[5] M.A. Laguna-Bercero, R. Bayliss & S.J. Skinner, Solid State Ionics, 262 298 2014

4:30 PM A3.07
A Cost-Effective Approach for Next Generation High-Performance Fuel-Flexible Protonic Ceramic Fuel Cell Chuancheng Duan, Jianhua Tong, Meng Shang and Ryan O'Hayre; Colorado School of Mines, Golden, Colorado, United States.

The fabrication of typical ceramic-based fuel cells, such solid oxide fuel cells (SOFCs) or protonic ceramic fuel cells (PCFCs) is a complex, expensive, and time-intensive process nvolving multiple powder synthesis, calcination, grinding, coating, and firing steps. Here, we present a novel approach to fabricate the complete sandwich structure of a PCFC (porous anode, dense electrolyte, and porous cathode bone) directly from raw precursor oxides or carbonates in a single firing step. Our novel approach, which leverages the recently discovered solid-state eactive sintering process, greatly simplifies ceramic fuel cell fabrication and lowers costs, while also yielding cells with superior performance. We show that proper choice of the solid-state reactive sintering additives enables conversion of the precursor oxides to the desired phase-pure perovskite compositions and promotes full densification of the electrolyte layer while ensuring that the anode and cathode structures remain highly porous. We demonstrate the approach with a PCFC consisting of a porous cermet anode, a dense protonic conductor electrolyte, and a porous composite cathode which obtains excellent power density under both H2/air (> 250 mW/cm^2 at 00 ºC) and CH4/Air (> 200 mW/cm^2 at 600 ºC) with stable performance for >1000 hours.

4:50 PM A3.08
A New Ternary Protonic/Oxygen Ionic/Electronic Conducting Cathode for Proton Conducting Solid Oxide Fuel Cell Liangdong Fan and Pei-Chen Su; School of Mechanical and Aerospace Engineering, Nanyang Technological University, Singapore, Singapore.

Proton conducting electrolyte represents one of the approaches to lower down the operating temperature of current high temperature (700-1000 ºC) solid oxide fuel cell (SOFC) to reduce the system investment and enhance the durability. However, cathode materials for proton conducting solid oxide fuel cells (H-SOFC) are critically required because the cathode reaction is much complicate compared with that of the normal oxygen ionic conducting SOFC (O-SOFC), additional water generation capability is required. Current cathode materials of H-SOFC are derived from the O-SOFC, i.e. the mixed oxygen ionic and electronic conducting materials, such as LSCF and BSCF. But the electrochemical performances of those oxide cathodes are much inferior than operating at the O-SOFC condition due to the limited triple phase boundaries. The application of ternary protonic/oxygen ionic/electronic (H+/O2-/e-) conducting would effectively overcome such issue. Thus, in this work, a novel/series of simple oxide(s), lithiated transition metal (Ni, Co, Mn, Fe and Cu) oxide with unique layer structure is first proposed as the cathode for H-SOFC. A simple solid state reaction is employed for preparation of target oxides. The lithium doping/intercalation can improve the electrical conductivity and oxygen reduction activity. More importantly, they show the proton conducting capability in the humidified atmosphere as verified by the electrochemical impedance spectroscopy measurements. Combining of the excellent oxygen reduction kinetic and the proton conducting properties, single cell used the above ternary conducting oxide cathode and proton conducting electrolyte show promising power output at the low temperatures. Peak power density over than 350 $mW\ cm^{-2}$ has been achieved at 650 ºC, which is much higher than most published cathode materials with similar cell configuration.

5:10 PM A3.09
Nano-CT Enabled, Bayesian Model-Based Analysis of Impedance Data for a Porous, Lanthanum Strontium Manganate Cell Giuseppe F. Brunello[1], Billy Epting[2], Shawn Litster[2], Paul A. Salvador[3], Harry O. Finklea[4], David S. Mebane[1] and Juwana De Silva[4]; [1]Mechanical and Aerospace Engineering, West Virginia University, Atlanta, Georgia, United States;[2]Department of Mechanical Engineering, Carnegie Mellon University, Pittsburgh, Pennsylvania, United States; [3]Department of Materials Science and Engineering, Carnegie Mellon University, Pittsburgh, Pennsylvania, United States; [4]Department of Chemistry, West Virginia University, Morgantown, West Virginia, United States.

Despite the longstanding popularity of strontium-doped lanthanum manganite (LSM) as an electrode for solid oxide fuel cells, questions

remain about the relative importance of each of the available electrochemical pathways. Surface diffusion of oxygen and direct incorporation into the electrolyte at the triple phase boundary is believed to be favored over diffusion in the bulk due to LSM's low ionic conductivity. However, most experiments investigating the relative importance f the two pathways utilize thin film or patterned electrodes, which may be susceptible to small size effects.

To avoid size effects, this ongoing study applies an electrochemical continuum model to a porous, symmetric LSM-yttria stablized zirconia cell. The microstructural geometry was precisely characterized using nanotomography (nano-CT), and the electrochemical behavior using impedance spectroscopy at open circuit. The continuum model includes thermodynamic nd linearized kinetic models of the bulk defect chemistry, surface reactions, and transport as ell as the triple phase boundary and electrode-electrolyte interface reactions. The periodic steady-state solution is obtained in frequency space. Model-based analysis of the experimental data was performed using Bayesian calibration. The joint posterior probability distribution for the unknown model parameters can be used to rigorously assess hypotheses regarding the oxygen reduction mechanism on LSM.

SESSION A4: SOFC—Cathodes III
A: Solid Oxide Fuel Cells and Electrolyzers
Chair: Harry Tuller
Tuesday Morning, June 16, 2015
Keystone Resorts, Longs Peak

10:30 AM **A4.01
Measuring Oxygen Surface Exchange Kinetics on Mixed-Conducting Composites by Electrical Conductivity Relaxation Bobing Hu[2], Yunlong Wang[2], Zhuoying Zhu[2], Changrong Xia[2] and Henny J. Bouwmeester[1, 2]; [1]Department of Science and Technology, University of Twente, Enschede, Netherlands; [2]Department of Materials Science and Engineering, AS Key Laboratory of Materials for Energy Conversion, University of Science and Technology of China, Hefei, China.

The oxygen surface exchange kinetics of mixed-conducting $Sr_2Fe_{1.5}Mo_{0.5}O_{6-\delta}$ – $Sm_{0.2}Ce_{0.8}O_{2-\delta}$ (SFM-SDC) dual-phase composites has been investigated, at 750 °C, using electrical conductivity relaxation (ECR). Measurements were conducted to assess the role of triple phase boundaries (TPB) on oxygen surface exchange under oxidizing and reducing conditions. Whilst SDC is a well-known electrolyte with promise for use in SOFCs operating at moderate temperatures, the double perovskite SFM has potential for use both as cathode and as anode because of its excellent chemical stability in oxidizing and reducing environments [1,2]. Gas mixtures of O_2/N_2, H_2/H_2O and CO/CO_2 were used to control step changes in the pO_2 ranges 0.01 – 1 atm and 10^{-24} – 10^{-20} atm. Oxygen re-equilibration under the experimental conditions is controlled by the surface exchange kinetics. A model is developed which allows deconvolution of the effective time constant of the relaxation process in terms of the intrinsic contributions of both constituent phases in the composites to oxygen surface exchange, and the synergetic contributions caused by the presence of heterogeneous interfaces. The rate of oxygen incorporation under oxidizing conditions is found to increase profoundly with increasing the phase volume fraction of SDC in the composites. Already at SDC phase volume fraction of 0.105, the oxygen uptake via the synergistic TPB route, following a step-wise increase in the ambient pO_2, comprises more than 75% of the overall uptake of oxygen by the composite. On the contrary, only a modest, or even negligible (under H_2/H_2O atmosphere) influence of the TPB boundaries on oxygen release kinetics is found under reducing conditions. The oxygen release kinetics under H_2/H_2O atmosphere merely is a weighted average of the intrinsic contributions of SFM and SDC phases.

[1] G. Xiao, F. Chen, Front. Energy Res. 2 (2014)
[2] Q. Liu, X. Dong, G. Xiao, F. Zhao, F. Chen, Adv. Mater. 22 (2010) 5478

11:00 AM A4.02
On the Link between Oxygen Surface Exchange and Bulk Oxygen Anion Transport in SOFC Cathode Material Alexander C. Tomkiewicz[1], Mazin A. Tamimi[1], Ashfia Huq[2] and Steven McIntosh[1]; [1]Chemical Engineering, Lehigh University, Bethlehem, Pennsylvania, United States; [2]Neutron Sciences, Oak Ridge National Laboratory, Oak Ridge, Tennessee, United States.

A link between the surface oxygen exchange rate and bulk ion diffusivity of mixed ionic-electronic conductors has been hypothesized in the literature. However, most of data available in the literature is derived from experiments that simultaneously measure both properties. This stems from the complexity of measuring these properties under realistic in-situ conditions. We have recently focused on implementing new experimental approaches to independently characterize these properties for SOFC cathode materials.

The bulk ionic transport is characterized by *in-situ* powder neutron diffraction; a powerful technique that enables the simultaneous determination of the position, occupancy, and anisotropic average displacement of the atoms in the unit cell. In contrast to X-ray diffraction, neutron diffraction is sensitive to the oxygen within the material, allowing identification of the ionic transport pathways in the material through analysis of site occupancy and average displacement magnitude and anisotropy of the various oxygen sites within these materials. In this case measurements were performed at temperatures ranging from 765K to 1070K with a pO_2 from 10^{-3} to 10^{-1} atm.

The surface oxygen exchange is measured by pulsed isotopic exchange and complemented by surface composition analysis via high sensitivity-low energy ion scattering (HS-LEIS) and X-ray photoelectron spectroscopy (XPS). This data is then utilized to interpret the electrochemical performance, in terms of the impedance spectra, of the materials as SOFC electrodes.

We will present a summary of recent work on a number of materials, and provide a potential explanation for the observed link between surface and bulk properties based on the potential rate-determining steps for oxygen incorporation.

11:20 AM A4.03
Fast Tracer and Slow Electrical Kinetics of ^{18}O Exchange on Mixed Conducting Surfaces: A Combined Tracer and Impedance Study Andreas Nenning, Edvinas Navickas, Sandra Kogler, Katharina Langer-Hansel, Alexander K. Opitz and Juergen Fleig; Institute of Chemical Technologies and Analytics, Vienna University of Technology, Vienna, Austria.

Electrochemical impedance spectroscopy and oxygen tracer exchange with subsequent depth profiling are usually used as complementary tools for measuring the oxygen exchange activity of SOFC electrode materials. Tracer exchange experiments usually take place in dry oxidizing atmospheres. There, the derived electrical (k^q) and tracer (k^*) exchange coefficients are in good agreement. This agreement is not mandatory: If the tracer exchange reaction does not involve a bulk electron transfer, the two coefficients should differ significantly. For many years, such mechanisms have remained speculative. In this contribution we provide for the first time experimental evidence that mechanistically different electrical and tracer exchange reactions are more the rule than the exception when employing $H_2{}^{18}O$ as the oxygen tracer source.

Oxygen-deficient perovskite-type ($SrTi_{0.3}Fe_{0.7}O_{3-\delta}$, $La_{0.6}Sr_{0.4}FeO_{3-\delta}$) and fluorite-type ($Ce_{0.8}Gd_{0.2}O_{2-\delta}$, $Zr_{0.81}Y_{0.19}O_{2-\delta}$) thin films were exposed to dry and humidified oxidizing as well as reducing atmospheres containing either $^{18}O_2$ or $H_2{}^{18}O$ as tracer source. For comparison k^q was simultaneously measured by electrocheimcal impedance spectroscopy.

Good agreement of k^* and k^q was found in dry $^{18}O_2$ atmosphere. The situation is different in humid atmosphere. The water adsorbs by formation of surface hydroxyl groups. This dissociative adsorption and desorption of water is already assumed to be fast on ceria surfaces. Furthermore, the fast adsorption and desorption of water acts as an oxygen exchange mechanism that does not involve an electron transfer and its rate is roughly 2 orders of magnitude higher than the electrical one.

These results are of high relevance for oxidizing tracer exchange experiments as they highlight the importance of having absolutely water-free atmosphere during a tracer exchange experiment. In reducing atmosphere, valuable mechanistic information can be gained: The rate of water adsorption and dissociation is high, and either the charge transfer from a surface transition-metal to a surface hydroxyl or the formation of H_2 from two hydroxyl groups is rate-limiting.

11:40 AM *A4.04

Phase Decomposition and Secondary Phase Formation in the Chromium and Silicon Poisoned IT-SOFC Cathode Materials $La_{0.6}Sr_{0.4}CoO_{3-\delta}$ and $La_2NiO_{4+\delta}$ Edith Bucher[1], Nina Schroedl[1], Christian Gspan[2], Andreas Egger[1], Christian Ganser[3], Christian Teichert[3], Ferdinand Hofer[2] and Werner Sitte[1]; [1]Chair of Physical Chemistry, Montanuniversitaet Leoben, Leoben, Austria; [2]Institute for Electron Microscopy and Nanoanalysis (FELMI), Graz University of Technology & Graz Center for Electron Microscopy (ZFE), Austrian Cooperative Research (ACR), Graz, Austria; [3]Institute of Physics, Montanuniversitaet Leoben, Leoben, Austria.

Chromium and silicon poisoning have been identified as important degradation mechanisms limiting the life-time of intermediate temperature solid oxide fuel cell (IT-SOFC) cathodes. In recent studies, the effects of combined Cr and Si poisoning on the long-term stability of the IT-SOFC cathode materials $La_{0.6}Sr_{0.4}CoO_{3-\delta}$ and $La_2NiO_{4+\delta}$ were investigated using the DC-conductivity relaxation method [1]. Over a period of 3500 h at 700°C both materials exhibited a significant decrease in the kinetic parameters for oxygen exchange. In order to obtain a deeper insight into the degradation mechanisms, post-test analyses were performed. Analytical transmission electron microscopy revealed phase decomposition of the original, oxygen exchange-active materials and the formation of secondary phases (binary and ternary oxides, chromates, silicates) which exhibit low to negligible activity for oxygen exchange and poor electrical conductivity. Atomic force microscopy was used to determine the three-dimensional shape including interplanar facet angles of the crystallites covering the surface of degraded $La_{0.6}Sr_{0.4}CoO_{3-\delta}$. A good agreement with the theoretical angles obtained from crystal structure data of $SrCrO_4$ (monazite-type) was found.

References

[1] N. Schrödl, E. Bucher, A. Egger, P. Kreiml, C. Teichert, T. Höschen, W. Sitte, *Solid State Ionics* (2015) under review.

SESSION A5: SOFC—Electrolytes I
A: Solid Oxide Fuel Cells and Electrolyzers
Chair: Koji Amezawa
Tuesday Afternoon, June 16, 2015
Keystone Resorts, Longs Peak

3:30 PM *A5.01

Formation of $SrZrO_3$ in Perovskite Cathode /Ceria Interlayer / Zirconia Electrolyte during Operation of Solid Oxide Fuel Cells Koichi Eguchi, Toshiaki Matsui, Hiroki Muroyama, Masahiro Komoto, Kyosuke Kishida and Haruyuki Inui; Graduate School of Engineering, Kyoto University, Kyoto, Japan.

Lanthanum strontium cobalt ferrite (LSCF) is one of the promising candidates for the cathode of solid oxide fuel cells (SOFCs) because of relatively high mixed ionic-electronic conductivity. Generally, a doped ceria is used as an interlayer to prevent the reaction between LSCF cathode and yttria-stabilized zirconia (YSZ) electrolyte, which results in the formation of insulating $SrZrO_3$ layer at the cathode/electrolyte interface. At this stage, however, it is difficult to totally prevent this unfavorable reaction, and the formation mechanism of insulating layer has not been elucidated yet. In this study, the miscrostructural change at the LSCF/SDC/YSZ interface upon discharge was quantified by using a focused ion beam–scanning electron microscope (FIB-SEM). The influences of current passage and heat treatment conditions on microstructural change were also studied.

The electrolyte-supported cells were fabricated using a disk of YSZ. The Ni–YSZ cermet anode with a volume ratio of 50/50 was prepared from NiO and YSZ powder. The slurry of NiO–YSZ was screen-printed onto the electrolyte and subsequently fired at 1400ºC for 5 h in air. The slurry of $Ce_{0.8}Sm_{0.2}O_{1.9}$ (SDC) was screen-printed on the other face of electrolyte, and then fired at 1250ºC for 10 h in air. After that, LSCF cathode at a composition of $La_{0.6}Sr_{0.4}Co_{0.2}Fe_{0.8}O_3$ was applied; the slurry was screen printed and subsequently fired at 1150ºC for 5 h in air. The reference electrode of platinum wire was attached to surround the side edge of the YSZ disk and fixed by a platinum paste. The gaseous mixtures of O_2–N_2 and 3% H_2O–97% H_2were supplied to the cathode and anode of the single cell, respectively. Electrochemical measurements were conducted at 1000ºC. The microstructure of LSCF/SDC/YSZ system was quantitatively analyzed by using an FIB–SEM equipped with an energy dispersive X-ray spectrometer (EDX). The 3D microstructure of LSCF/SDC/YSZ system was virtually reconstructed in a computational field.

In the time courses of cathode overpotential and ohmic loss during discharge for 400 h, both resistive components decreased from the beginning of discharge up to *ca*. 100 h. This decrease in overvoltage is ascribed to the current passage effect; the improved binding between LSCF and SDC is one of the reasons. Over 100 hours of operation, however, the resistances were turned into an increase, indicating the deterioration progress.

The volume fraction of each phase in LSCF/SDC/YSZ system before and after discharge for 400 h; the reconstructed structure was virtually-sliced along the distance from the YSZ/SDC interface, and then the volume fraction of each component in the small rectangular pieces were plotted. Even before discharge, the formation of $SrZrO_3$ phase was detected at the SDC/YSZ interface. This indicates that this insulating phase was formed due to the elemental diffusion during the sintering-bonding step of LSCF and SDC layers. The formation of $SrZrO_3$ was limited in the SDC phase as the precipitated secondary phase near the YSZ/SDC interface either before or after discharge. After discharge operation, the volume of the $SrZrO_3$ phase has increased six-fold. The formation area of $SrZrO_3$ phase was expanded from the SDC/YSZ interface to the bulk SDC. It is noted that the pore fraction decreased accompanied with the formation of the $SrZrO_3$ phase. This means that the secondary phase was formed by filling the pores which is originally contained in the SDC layer after sintering. Thus, it can be considered that strontium was diffused from LSCF cathode side through SDC layer, and then reacted with zirconium in the vicinity of SDC/YSZ interface.

This work was partially supported by New Energy & Technology Development Organization (NEDO), Japan.

3:50 PM A5.02

Three-Dimensional Quantification of Composition and Space Charge Potential at Doped Ceria Grain Boundaries using Atom Probe Tomography David R. Diercks[1], Jianhua Tong[1], Huayang Zhu[2], Robert Kee[2], Juan C. Nino[3], Ryan O'Hayre[1] and Brian P. Gorman[1]; [1]Metallurgical and Materials Engineering, Colorado School of Mines, Golden, Colorado, United States; [2]Mechanical Engineering, Colorado School of Mines, Golden, Colorado, United States; [3]Materials Science and Engineering, University of Florida, Gainesville, Florida, United States.

Despite comprising a small volume fraction of the material, grain boundaries (GBs) are frequently the limiting factor in the electrical conductivity and optical and mechanical properties of polycrystalline oxide ceramics. In particular, oxygen ion conductivities at GBs have been observed to be lower by a factor of one hundred or more than the bulk material in many technologically-relevant oxide-ion conductors. Past research has supported the theory that accumulation of oxygen vacancies at GBs induces a static internal voltage that can affect the transport of charged species. While the origin of oxygen vacancy accumulation is still not completely understood, there appears to be a strong correlation between the grain boundary structure and composition and space charge accumulation. Unfortunately, quantitative measurement of the oxygen stoichiometry with sufficiently high spatial resolution has been elusive.

In this work, atom probe tomography (APT) is shown to quantitatively measure changes in the cation - oxygen stoichiometry with sub-nm spatial resolution. This is demonstrated through three-dimensional compositional

measurement of all species across GBs for two different doping levels of Nd in ceria: $Ce_{0.9}Nd_{0.1}O_{2-\delta}$ and $Ce_{0.7}Nd_{0.3}O_{2-\delta}$. Oxygen vacancy and Nd segregation to the GB regions are observed to different extents for these two materials, with the greater segregation occurring in the 10 cation % doped material. From these measurements, we obtain three-dimensional quantification of the local charge density, which is then used to determine the local potentials in the GB regions. Such space charge voltages determined through direct atomic-scale APT measurements are found to correlate well with impedance spectroscopy measurements when taking into account changes in the Ce valence state at the GB. The techniques employed here are directly applicable to other ionic conductors and open up avenues to refine space-charge theory while also improving device performance and modeling.

4:10 PM A5.03
Nanoscale Electrochemical Investigation on SDC Thin Films for µ-SOFCs Applications Nan Yang[1, 2], Vittorio Foglietti[1], Antonello Tebano[1], Giuseppe Balestrino[1], Carmela Arruta[1], Stephen Jesse[3] and Sergei Kalinin[3]; [1]CNR-SPIN&University of Rome Tor Vergata, Rome, Italy; [2]UniCusano Online University, Rome, Italy; [3]Oak Ridge National Laboratory, Oak Ridge, Tennessee, United States.

The growing demand for miniaturized systems for energy conversion and storage has prompted extensive research aimed at fabricating electrochemical devices, such as solid oxide fuel cells for portable applications (µ-SOFCs). This goal requires reducing the operating temperature by producing components as thin films. Nowadays, there is a huge gap between macroscopic device-level electrochemical techniques and microscopic electrochemical techniques to study atomic-level diffusion and transport process.

Recently, a new scanning probe microscopy technique, named electrochemical strain microscopy (ESM) has been developed in order to study the structure and physical properties on the microscopic level. After applying the dc bias to the tip, the oxygen vacancies and protons injection or annihilation can occur, depending on the working conditions and the material properties. The subsequent oxygen ion or proton movement results in localized strain under the tip, which can be detected through dynamic surface displacement.[1] This technique can be very useful to investigate the electrochemical activity at the nano-scale in ionic or proton conductors.

In this presentation, I will discuss several examples of high-resolution studies of pure and Sm-doped CeO_2 epitaxial thin films surfaces which allowed to understand water interaction and conductivity mechanisms on the nanoscale. In particular I will show:

(1) The effect of the different doping concentrations on $Sm_{1-x}Ce_xO_{2-a}$ in terms of different transport mechanism and different type of charge carriers [2].
(2) The role of granularity and porosity on the oxygen ion or proton conduction 20% Sm doped CeO_2 nanocrystalline films [3].
(3) The bias dependent mechanisms of irreversible cathodic and anodic processes on a pure CeO_2 film.[4]

[1] A. Kumar et al. Nature Chemistry, 2011, 3,707.
[2] Nan Yang et al. ACS Nano DOI: 10.1021/nn505345c (2014)
[3] S. Doria, Nan Yang, et al. Appl. Phys. Lett. 103, 171605 (2013)
[4] Nan Yang et al. Nanotechnology 25, 075701 (2014).

4:30 PM A5.04
Dopant Segregation Effect on Ionic Conductivity of Nanocrystalline Gadolinium-Doped Ceria Thin Film Jiwoong Bae, Yonghyun Lim and Young-Beom Kim; Mechanical Convergence Engineering, Hanyang University, Seoul, Korea (the Republic of).

Solid state ionic conductors have been studied to understand and enhance ionic conduction especially for solid oxide fuel cells (SOFCs) where ohmic resistance through solid state electrolyte is crucial on cell performance. However, due to its restriction of high operating temperature, system durability, material selectivity, and cost have been critical obstacles for its commercialization. Therefore, acceptor-doped ceria has been attracted many attentions because of its fast ionic conduction and high surface exchange coefficient even at low temperature regime (< 500ºC).

In previous literature, the ionic conduction of grain boundary is hindered by space charge layer, and therefore decreases by several orders of magnitude in conductivity compared to bulk conduction [1]. This blocking effect is known to stem from dopant segregation in grain boundary area or grain boundary core which generates positive charge core, and thus space charge layer along with grain boundary [2-3]. Therefore, the dopant distribution in nanocrystalline material is important to understand ionic conduction since it has extremely high grain boundary density.

In this study, we investigated dopant distribution effect on ionic conductivity of nanocrystalline gadolinium-doped ceria (GDC) thin film through scanning transmission electron microscopy (STEM) along with energy dispersive X-ray spectroscopy (EDX) and electron energy loss spectroscopy (EELS). Dopant distribution is systematically controlled by post-annealing process at moderate temperature (< 1100ºC) on RF sputtered GDC thin film, and subsequently, the ionic conductivity is measured by electrochemical impedance spectroscopy (EIS) analysis.

[1] X. Guo, W. Sigle, J. Maier, “Blocking grain boundaries in yttria-doped and undoped ceria ceramics of high purity”, J. Am. Ceram. Soc. 86 (2003) 77-87.
[2] Y. Lei, Y. Ito, N. D. Browning, “Segregation effects at grain boundaries in fluorite-structured ceramics”, J. Am. Ceram. Soc. 85 (2002) 2359-63.
[3] S. Kim, J. Maier, “On the conductivity mechanism of nanocrystalline ceria”, J. Electrochem. Soc. 149 (2002) J73-83.

4:50 PM A5.05
A First-Principles Approach to the Attempt Frequency of Oxygen Ion Jumps in Doped Ceria Julius Koettgen, Tobias Zacherle, Steffen Grieshammer and Manfred Martin; Institute of Physical Chemistry, RWTH Aachen University, Aachen, Germany.

The rate of oxygen ion jumps in a solid oxide depends not only on the activation energy but also on the pre-exponential factor of diffusion. In order to allow a fully ab initio prediction of the oxygen ion conductivity in pure and samarium doped ceria we calculated the attempt frequency for an oxygen ion jump from first-principles using DFT+U, NEB, phonon calculations and the transition state theory. The equivalence of the Eyring and the Vineyard method is shown without restriction to the Gamma point. Convergence checks of the phonon mesh show that the common reduction to the Gamma point is not sufficient to calculate the attempt frequency. The pre-exponential factor is unaffected for doping with a single Sm ion at the migration edge while a Sm-Sm edge exhibits a significantly larger attempt frequency. The attempt frequencies for the constant volume and constant pressure case in harmonic and quasi-harmonic approximation are in agreement with literature approximations and experiments.

5:10 PM A5.06
Rare Earth Doped Bismuth Lead System Wojciech Wrobel[1], Anna Borowska-Centkowska[1], Marzena Leszczynska-Redek[1], Marcin Malys[1], Marcin Krynski[1], Franciszek Krok[1] and Isaac Abrahams[2]; [1]Faculty of Physics, Warsaw University of Technology, Warsaw, Poland; [2]Materials Research Institute, Queen Mary University of London, London, United Kingdom.

In this study structural and electrical properties of bismuth lead oxide doped with different rare earth metal cation dopants will be presented. Studied compounds of general formula $Bi_{3-x}Pb_xMeO_{6-x/2}$ (*Me* = Y, Yb, Er) exhibit very high conductivities, comparable to that of pure Bi_2O_3 at high temperatures. In the binary Bi_2O_3 – PbO system, despite the close similarity of the Bi^{3+} and Pb^{2+} cations, in terms of their stereochemistries (dominated by the $6s^2$ lone pair) and polarizabilties, lead substitution for bismuth does not lead to the appearance of the δ-Bi_2O_3type phase at low temperatures [1]. However, in studied ternary systems, Bi_2O_3-Me_2O_3-PbO (*Me* = Y, Yb, Er), preservation of the δ-type phase to room temperature is observed [3].

Local surrounding of metal cations and their influence on the conductivity in the studied compounds will be discussed. For this purpose structural studies were carried out using X-ray and neutron powder diffraction as well as the total scattering analysis using Reverse Monte Carlo modelling.

These results are compared to those from density functional theory (DFT) simulations to yield a comprehensive picture of the vacancy distribution and conduction mechanism in these compounds. Electrical conductivity was characterised by a.c. impedance spectroscopy and the ionic transference numbers were measured using concentration cell by the modified e.m.f. method.

Some of the bismuth based compounds at intermediate temperatures as well as under reducing atmospheres are known to show instabilities, which might be related with the oxidation/reduction processes [3]. The above processed will be discussed with respect to the vacancy/oxide ion distribution. In order to study oxidation – reduction effects the X-ray diffraction and impedance spectroscopy experiments were done in the controlled oxygen partial pressure atmospheres.

[1] R.M. Biefeld, S.S. White, *J. Am. Ceram. Soc.*, 64 (1981) 182.
[2] M. Omari, M. Drache, P. Conflant, J.C. Boivin, *Solid. State Ionics*, 40/41 (1990) 929.
[3] A. Borowska-Centkowska, X. Liu, M. Holdynski, M. Malys, S. Hull, F. Krok, W. Wrobel, I. Abrahams, *Solid State Ionics* 254(2014) 59-64.

SESSION A6: Poster Session II
A: Solid Oxide Fuel Cells and Electrolyzers
Tuesday Afternoon, June 16, 2015
5:20 PM
Keystone Resorts, Red Cloud Peak

A6.01

Thermal Stability and Compatibility with SOFC/PCFC Electrolyte of $La_4BaCu_5O_{13+\delta}$ and $La_{6.4}Sr_{1.6}Cu_8O_{20\pm\delta}$ Perovskite Monica V. Sandoval[1, 2], Giovanny Martinez[1], Santiago Vasquez-Cuadriello[3], Mario A. Macias[1], Leopoldo Suescun[3], Pascal Roussel[2] and Gilles H. Gauthier[1]; [1]Grupo INTERFASE, Universidad Industrial de Santander, Bucaramanga, Colombia;[2]Unité de Catalyse et de Chimie du Solide, Université Lille 1, Lille, France; [3]Facultad de Química - Cryssmat-Lab/DETEMA , Universidad de la República, Montevideo, Uruguay.

The development of new cathode materials remains an issue for the development of low temperature Solid Oxide Fuel Cells (SOFC), a promising alternative for future highly efficient energy sources [1]. In this work, we present a preliminary study based on thermal stability and compatibility with classical SOFC electrolyte materials of two ordered oxygen-deficient perovskites, $La_4BaCu_5O_{13+\delta}$ (LBCu) and $La_{6.4}Sr_{1.6}Cu_8O_{20\pm\delta}$ (LSCu). Pure phase materials were obtained by EDTA assisted gel combustion method, confirming the aforedescribed structure of both compounds, of respective tetragonal *P*4/*m* and *P*4/*mbm* space groups and refined cell parameters *a*=8.64459(4)Å / *c*=3.85998(3) Å and *a*=10.8500(13)Å / *c*=3.8595(5)Å, respectively [2-3]. X-ray thermodiffraction experiments have been carried out in air to examine the structural and thermomechanical behaviour of both materials in cathodic conditions (**Figure 1**). Additionally, the samples were subjected to thermogravimetric analysis, using consecutive heating/cooling cycles from room temperature to 800°C.

LBCu and LSCu present strongly anisotropic expansion coefficients with apparent TEC values of 17.3 $x10^{-6}$ K^{-1} and 12.1 $x10^{-6}$ K^{-1}, respectively, relatively far for the Ba-containing compound from conventional electrolytes values, *e.g.* 10-11 $x10^{-6}$ K^{-1} or 12-13 $x10^{-6}$ K^{-1} for 8YSZ* or 10GDC* electrolytes, respectively. The high temperature chemical reactivity of the materials with the usual electrolytes was investigated at 1000°C for 3h. After thermal treatment in air, LBCu and LSCu show high chemical reactivity with both YSZ and GDC electrolytes. However, the reactivity with Ba containing electrolytes, *i.e.* BCG* and BZY*, were far less, especially in the case of LBCu, resulting in a promising candidate for SOFC or PCFC cathode.

Acknowledgments: This work was developed with the financial support from UIS/VIE, COLCIENCIAS, UdelaR, FEDER, CNRS, Région Nord Pas-de-Calais, MENESR, LNLS.

References: [1] Singhal, S. C. Solid State Ionics. 135 (2000) 305. [2] P.S. Anderson, *et al.* J. Solid State Chem. 170 (2003) 1. [3] L. Er-Rakho, *et al.* J. Solid State Chem. 73 (1988) 514.

A6.02

Electrochemical Studies of $GdPrBaCo_2O_{5+\delta}$ and $GdPrBaCoFeO_{5+\delta}$ Cathodes for Oxide Ion and Proton Conducting Solid Oxide Fuel Cells Kalpana Singh, Ashok Baral and Venkataraman Thangadurai; Department of Chemistry, University of Calgary, Calgary, Alberta, Canada.

This work presents the synthesis and characterization of layered structured $GdPrBaCo_2O_{5+\delta}$ and $GdPrBaCoFeO_{5+\delta}$ cathodes for solid oxide fuel cells (SOFCs). The single phase layered structured materials $GdPrBaCo_2O_{5+\delta}$ and $GdPrBaCoFeO_{5+\delta}$ were prepared by solid state reaction method successfully, after calcining the precursor powder at 900 °C (10 h). Reactivity of these materials with the oxygen ion and proton conducting solid electrolytes ($Zr_{0.92}Y_{0.08}O_{2-\delta}$ (8YSZ) and $Ba_{0.5}Sr_{0.5}Ce_{0.6}Zr_{0.2}Gd_{0.1}Y_{0.1}O_{3-\delta}$ (BSCZGY), respectively) were studied by in-situ and ex-situ XRD diffraction studies. The DC conductivities of the samples are found to remain similar in both ambient air condition and in wet air. Electrochemical performance of the cathodes were studied by symmetrical cell measurements. Area specific resistance (ASR) of the cell with $GdPrBaCo_2O_{5+\delta}$ as cathode and 8YSZ as electrolyte is found to be about 0.87 Ω cm^2 at 906 °C. The ASR value (in logarithmic scale) is found to vary linearly with temperature and the activation energy for the overall cathode process is found to be 1.6 eV. Performances of the cathodes and oxygen surface exchange properties using $Ce_{0.8}Gd_{0.2}O_{2-\delta}$ (GDC) buffer layer and by making composite with GDC are thoroughly discussed, for both the YSZ and BSCZGY electrolyte systems. Performance of the O-SOFC and H-SOFC cells with 8YSZ and BSCZGY as electrolytes, nickel based anode composites (Ni-8YSZ and Ni-BSCZGY) and the present cathodes are studied thoroughly.

A6.03

Development of the Composite Electrodes for the New $CaZr_{0.95}Sc_{0.05}O_{3-\delta}$ Proton-Conducting Electrolyte Elena Pikalova[1, 2], Nina Bogdanovich[1], Alexander Kolchugin[1], Dimitry Bronin[1, 3], Anton Kuz'min[1] and Azat Khasanov[3]; [1]Institute of High Temperature Electrochemistry UB RAS, Ekaterinburg, Russian Federation; [2]Department of Environmental Economics, Ural Federal University, Ekaterinburg, Russian Federation; [3]Institute of Natural Sciences, Department of Chemistry, Ural Federal University, Ekaterinburg, Russian Federation.

Substituted $CaZrO_3$ is of great interest for its application in fuel cells, as the doping of Zr^{4+} ions by trivalent cations, for example Sc^{3+}, results in formation of defects in the oxygen sublattice causing a high level of oxygen–ionic and protonic conductivity. At present there is little data presented in literature connected with the fabrication and investigation of the electrode materials in contact the $CaZr_{0.95}Sc_{0.05}O_{3-\delta}$ electrolyte. As far as its value of the thermal expansion coefficient is low and closed to those for YSZ electrolyte (10.03 and 10.30 × 10^{-6} K^{-1} in dry and wet air, respectively) in this work for the first experiments the traditional electrode materials used for YSZ such the composites based on manganite and ferrite-cobaltite of lanthanum-strontium (LSM and LSFC) were chosen. Additionally, the composites based on the layered perovskites $La_{1.7}Ca(Sr)_{0.3}NiO_4$ were investigated (LCNO and LSNO). As a ceramic component of composite electrode the solid state electrolytes $Zr_{0.9}Sc_{0.1}O_{1.9}$ (SSZ), $Ce_{0.8}Sm_{0.2}O_{1.9}$ (SDC) and $BaCe_{0.89}Gd_{0.1}Cu_{0.01}O_3$ (BCGdCu) were taken.

The electrodes for electrochemical characterization were fabricated symmetrically on the 1 mm thick electrolyte substrate with area of approximately 0.25-0.36 cm^2. The electrochemical measurements were carried out by the method of impedance spectroscopy. The best from the electrodes investigated is (50 wt.% LSFC +50 wt.%SDC)+0.5%CuO, which may be replaced with Co-free 50 wt.%LSNO+50 wt.% SDC and 50 wt.%LCNO+50 wt.% SDC electrodes. ASR values for these electrodes at 800°C are 1.36, 1.42 and 1.78 Ωcm^2, respectively. The analysis of the data received have shown that the main problems of the way of the improvement of the operational behavior of electrodes in contact with proton conducting $CaZr_{0.95}Sc_{0.05}O_{3-\delta}$ electrolyte are interaction of these materials and matching of the content and thickness of collector layer which would permit to keep electrode integrity during sintering and operation.

A6.04

A Layered Perovskite Oxide $PrBaCo_2O_{5+\delta}$ as Cathode for Highly Stable $BaCe_{0.1}Zr_{0.8}Y_{0.1}O_{3-\delta}$ Based Protonic Ceramic Fuel Cells (PCFCs) Hanping Ding and Neal P. Sullivan; Mechanical Engineering, Colorado School of Mines, Golden, Colorado, United States.

The development of proper cathode materials for highly stable protonic ceramic fuel cells (PCFCs) still remains challenge. While the traditional barium zirconates (BaZrO3) proton conductors exhibit excellent chemical stability over a wide fuel cell operation range, the proton conductivity is relatively low, particularly operating at low-temperature range of 500-700 oC, which limits the further development of PCFCs due to high electrolyte resistance. Meanwhile, the electrode polarization resistance is another critical factor that can dominate the total cell resistance due to the sluggish oxygen reduction reaction in cathode. Therefore, a cathode material with fast oxygen surface exchange and diffusion coefficient and a BaZrO3 based electrolyte with low grain boundary resistance should be combined to improve the cell performance of PCFCs. In this work, we investigated a layered perovskite of PrBaCo2O5+δ (PBCO) as cathode for BaCe0.1Zr0.8Y0.1O3-δ (BCZY18) based PCFCs at low temperatures (500-700 oC). The PBCO oxide was synthesized by modified Pechini combustion method and calcined at 1000 oC to obtain the pure phase. The anode/electrolyte assembly was prepared by solid state reactive sintering method at 1450 oC. The dense BCZY18 membrane was successfully prepared with assistance of little sintering additive. The results of electrochemical measurements show that the electrolyte and electrode polarization resistances were both decreased significantly, resulting in reasonable cell performance at this operation temperature range. It has been demonstrated that PBCO is a proper cathode material with layered perovskite structure for development of PCFCs.

A6.05

Steam Electrode Development for BCZY Based High Temperature Protonic Electrolysers Nuria Bausa, Cecilia Solís, Sonia Escolastico and Jose M. Serra; Instituto de Tecnología Química (UPV-CSIC), Valencia, Spain.

The use of high temperature electrolyzers (HTE) of steam offers high efficiency of conversion of renewable and peak electricity to H_2. In solid oxide electrolyzers (SOECs), that use oxide ion conducting electrolytes and operate at around 800 °C, the hydrogen is produced on the steam feed side. However, in proton conducting electrolyzers (PCECs) a high temperature proton conducting electrolyte is used instead and protons are pumped and form dry H_2, leaving O_2 on the steam side. These PCECs can produce pressurized dry H_2 directly.

$BaCe_{0.2}Zr_{0.7}Y_{0.1}O_{3-d}$ (BCZY27) was selected as electrolyte material for the high temperature protonic electrolyzer, thus this study is focused on the study of suitable anodes for this electrolyte.
The compatibility of different proposed phases with the BCZY was tested upon a heat treatment together with the electrolyte and under high temperature and high steam pressure conditions (700 ºC, 1.5 bars of steam in air and 2 bars of total pressure). First selected candidates were $La_{0.8}Sr_{0.2}MnO_3$ (LSM), $Ba_{0.5}Sr_{0.5}Co_{0.8}Fe_{0.2}O_3$ (BSCF) and $La_{0.6}Sr_{0.4}Co_{0.2}Fe_{0.8}O_3$ (LSCF). Afterwards, the anodes were prepared as composites by mixing one of these phases with the BCZY27 electrolyte.

Composite anodes were tested by impedance spectroscopy on BCZY27 electrolytes as symmetrical cells as a function of the temperature (800-500 ºC) under air with 1.5 bar of steam, with a total pressure of 2 bars. First screening was performed by using 50-50 vol.% of each phase and LSCF based anode showed the best properties. Then the performance of the LSCF/BCZY27 composite was improved by (1) changing the ratio of the different phases and (2) improving its microstructure.

Finally, a deep study by changing the measurement conditions (mainly steam, pO_2 and total pressures) was carried out in order to analyze and understand the different processes that take place in the anode under realistic operation conditions.

A6.06

Atomic Layer Deposition of Dense Nano-Thin Platinum Films for Low-Temperature Solid Oxide Fuel Cells Sanghoon Ji[1], Taehyun Park[2], Gu Young Cho[2], Waqas H. Tanveer[2], Wonjong Yu[2] and Suk Won Cha[2]; [1]Graduate School of Convergence Science and Technology, Seoul National University, Seoul, Korea (the Republic of); [2]Department of Mechanical Engineering, Seoul National University, Seoul, Korea (the Republic of).

A dense but nano-thin platinum (Pt) film for use as an electrode catalyst for LT-SOFCs was fabricated by ALD and micro-structurally and electrochemically characterized. The purity of the ALD Pt film was controlled by changing the O_2 pulsing time. The ALD Pt thin film was annealed in an air atmosphere, replicating the operating conditions of the cathode, which was micro-structurally characterized. Considering that the fuel diffusion and thermal stability simultaneously have to be guaranteed, the authors limited the thickness of ALD Pt electrode catalysts to approximately 25 nm, which is close to the minimum thickness required to form a dense microstructure. To investigate the electrochemical properties, the ALD Pt thin film was used as a cathode electrode catalyst in LT-SOFCs supported by anodic aluminumoxide with a sputtered porous palladium current collecting layer. The initial cell performance was evaluated as a function of the operating temperature, and electrochemical impedance spectroscopy results were analyzed in terms of the dwell time.

A6.07

Development of Low Temperature Operating Micro-SOFC System for Mobile Electronic Devices Shoya Murayama, Fumitada Iguchi, Makoto Shimizu and Hiroo Yugami; Graduate School of Engineering, Tohoku University, Sendai, Japan.

Micro-SOFCs, which cell volume is minimized using micro electro mechanical systems (MEMS) technologies and use liquid fuels, will be promising candidate as new power sources for mobile electronic devices because such micro-SOFCs shows higher power and energy densities than conventional Li-ion batteries. Actually, “State of the art” of micro-SOFC shows maximum power density over 1 Wcm^{-1} at 500 oC. However, micro-SOFC systems, which can work independently in mobile electronic devices requires various accessory such as fuel and air pumps, electronics. Moreover, thermal insulation structure must be equipped in micro-SOFC systems to prevent harmful damage to other electronics in mobile devices due to high temperature and heat loss to archive thermally self-sustained operation. Such thermal insulation structure is required to archive high thermal resistance as small as possible, and conventional thermal insulators based on glass wool could not be satisfied the requirement. Therefore, we focused on the development of packages for micro-SOFC systems, which equipped with the thermal insulation structure, and stored micro-SOFC itself.

In this study, packages were designed by thermal analysis based on thermodynamics. Thermal analysis revealed that packages with vacuum thermal insulation structure and gas-liquid heat exchanger, which collect waste heat from exhaust gas and prevent heating of the package’s surface, could be archive self-sustained operation with the surface temperature lower than 85 ºC, which was maximum operating temperature of electronic elements.

In accordance with the design, thermal insulation package with gas-liquid heat exchanger was fabricated (75 cm^3), and stored micro-SOFCs (Pt-Pd | 15 mol% Y-doped $BaZrO_3$ | Pt-Pd) with micro-heater for self-start up to be a micro-SOFC system. This system could operate at 300 ºC by heating of micro-heater and maximum power density was ca. 1.2 $mWcm^{-2}$.

A6.08

$Ba_{0.95}La_{0.05}FeO_{3-\delta}$-Graphene as a Low-Cost and Synergistic Catalyst for Oxygen Evolution Reaction Mattia Saccoccio[1], Hong Zhao[1], Chi Chen[1], Dengjie Chen[1], Jian Wang[1], Yang Gao[1], Hei Ting Wan[1] and Francesco Ciucci[1, 2]; [1]Department of Mechanical and Aerospace Engineering, The Hong Kong University of Science and Technology, Clear Water Bay, Hong Kong; [2]Department of Chemical and Biomolecular Engineering, The Hong Kong University of Science and Technology, Clear Water Bay, Hong Kong.

Oxygen evolution reaction (OER) is critical to many important energy conversion and storage processes. However the kinetics of OER is typically sluggish and conventional OER catalysts are scarce and expensive. Hence, inexpensive and effective catalysts that accelerate the OER kinetics and reduce the overpotential are urgently needed. In this poster, we report graphene-supported perovskite $Ba_{0.95}La_{0.05}FeO_{3-\delta}$ (BLF-graphene) as a highly active OER catalyst. Electrochemical results showed that the BLF-graphene hybrid exhibited a high current density (~23 mA/cm^2 at 0.60 V vs. MMO) and a more negative onset potential (~0.43 V vs. MMO). Furthermore, the hybrid showed a small Tafel slope (77 mV/decade) and good long-term stability. The remarkable OER performance is mainly attributed to the synergistic effect between BLF and graphene.

A6.09

Investigation of Low Temperature Operation of Fe-Air Battery Using YSZ Electrolyte Takaaki Sakai[1, 2], Masako Ogushi[2], Atsushi Inoishi[3], Shintaro Ida[2] and Tatsumi Ishihara[2];[1]Center for Molecular Systems, Kyushu University, Fukuoka, Japan; [2]Department of Applied Chemistry, Faculty of Engineering, Kyushu University , Fukuoka, Japan; [3]Research and Education Center for Advanced Energy Materials, Devices, and Systems, Kyushu University, Fukuoka, Japan.

Recently, the development of rechargeable battery with higher energy density has been desired due to the energy storage for renewable energies. As the rechargeable battery, metal-air batteries have attracted much attention owing to its high energy density. Thus far, the Fe-air battery using O^{2-} ion conductor has been proposed by several groups. The configuration of the Fe-air battery is as follows; The O^{2-} ion conductor is used as the electrolyte. For air electrode and fuel electrode, commercially available platinum electrode is generally used. Fe is filled in the fuel electrode side with H_2/H_2O redox mediator. The reaction in the discharging operation is as follows.

$1/2O_2 + 2e^- \rightarrow O^{2-}$ eq. (1), $H_2+1/2O^{2-} \rightarrow H_2O+2e^-$ eq. (2), $4H_2O+3Fe \rightarrow Fe_3O_4+4H_2$ eq. (3).

O_2 at air electrode changes into O^{2-} ion (eq. 1). The O^{2-} ion migrates to fuel electrode through electrolyte, and the O^{2-} ion reacts with H_2 at fuel electrode (eq. 2). After that, H_2O is regenerated as H_2 by oxidizing Fe into Fe_3O_4 at the fuel electrode side (eq. 3). In this manner, the continuous power generation can be obtained until Fe is completely oxidized. The target temperature of this battery is around 350^{o}C since its practical use is same as Na-S battery. So far, it was found that the Fe-air battery using $LaGaO_3$ electrolyte can be operated at 500^{o}C. From a perspective of the cost performance, the use of YSZ as electrolyte is preferable. However, its operation temperature was around 1000^{o}C so far. The decrease in the operation temperature directly leads to the increase in electrode reaction resistance. Thus the choice of the electrode material becomes important. In this work, the authors chose the Ni-Fe bimetal and $Ba_{0.6}La_{0.4}CoO_{3-d}$ for the respective electrodes, and attempted to operate the Fe-air battery using YSZ electrolyte at 600^{o}C.

A6.10

Improving the Material Efficiency or Substitution of Platinum in the System Pt/YSZ Gesa Beck[1] and Christoph Bachmann[2]; [1]Physics, Chair of Resource Strategies, Augsburg, Germany; [2]Institute of Physical Chemistry, Justus-Liebig-University, Giessen, Germany.

Platinum has several outstanding properties and is, therefore, used in a lot of applications. One important example is the use of platinum in the solid state electrode Pt|YSZ (as oxygen sensor, elecrocatalyst or as model system for SOFCs). In the last years the demand and the price of platinum has greatly increased. Since it has also very limited sources and is mined in only a few countries platinum is rated as critical. Accordingly, there are research activities to reduce the demand of platinum by substitution or more efficient use in its applications or to introduce effective recycling methods and systems. In the here presented work we studied different microstructures of platinum films in the Pt|YSZ electrode during thermal treatment and during polarisation to find a best efficient microstructure of platinum. In addition, we used other metals in the metal|YSZ electrode (silver, palladium, copper and iron) to study their behaviour during annealing and polarisation. Accordingly, we found that platinum films with many twin boundaries are very efficient in the electrode Pt|YSZ electrode. From the microstructural point of view an appropriate substitute could not be found up to now.

A6.11

Conductivity and Structure of Sub-Micrometric $SrTiO_3$ -YSZ Composites Enrique Ruiz-Trejo[1], Nikolaos Bonanos[2], Karl Thyden[2] and Mogens Mogensen[2]; [1]Earth Science and Engineering, Imperial College London, London, United Kingdom; [2]Department of Energy Conversion and Storage, Technical University of Denmark, Roskilde, Denmark.

Sub-micrometric composites of $SrTiO_3$-YSZ (1:1 volume) and single-phase samples of $SrTiO_3$ were prepared by high temperature consolidation of precursors obtained by precipitation with sodium hydroxide. The structure development and morphology of the precursors were studied by XRD and SEM. $SrTiO_3$ can be formed at temperatures as low as 400°C while the perovskite and fluorite phases in the composites are clearly formed at 600°C with no signs of reaction up to 1100°C. Composites with sub-micrometric grain sizes can be prepared successfully without reaction between the components, although a change in the cell parameter of the $SrTiO_3$ is attributed to the presence of sodium.

The consolidated composites were studied by impedance spectroscopy between 200-400°C and at a fixed T of 600°C with a scan in the partial pressure of oxygen. The composites did not exhibit high levels of ionic conductivity in the grain boundary or the bulk. The conductivity of Na-free composites shows lower levels of conductivity than pure YSZ while samples with sodium showed increased conductivity. The conductivity of single phase $SrTiO_3$ exhibited an enhancement attributed to p-type conductivity although contributions from protons cannot be disregarded.

A6.12

Microstructure and Electrochemical Properties of CeO2-Based Cathodes for SOEC Application Wenqiang Zhang, Bo Yu and Jingming Xu; Tsinghua University, Beijing, China.

High temperature co-electrolysis (HTCE) technology has become a new research focus in world's energy field, which can produce synthesis gas by dissociation of CO_2 and H_2O using a solid oxide electrolysis cell (OEC). The polarization loss, operational stability and interfacial behavior of SOEC cathode are the key issues for the development of HTCE technology.

In this paper, several high performance CeO_2 based catalysts were introduced into the cathode/electrolyte interface of the SOECs, and their catalytic performance for high temperature reverse water-gas shift (RWGS) reaction were investigated in detail. By material selection and interfacial structure control, the composite cathode materials with higher performance for HTCE were developed successfully. The X-ray diffraction (XRD) and scanning electron microscopy (SEM) were used to determine the crystallinities and structure of the samples. Cathode supported cells with different CeO2 based cathodes were studied by electrochemical impedance spectroscopy (EIS).The results showed that the electrode polarization loss in the HTCE process were smaller than that of the conventional Ni-YSZ cathode. Based on the above results, the mechanisms of HTCE's electrochemical reaction were investigated by the material characterization coupled with electrochemical measurements.

A6.13

Structural, Electrical and Electrochemical Properties of Calcium-Doped Lanthanum Nickelate Alexandr Kolchugin[1], Elena Pikalova[1, 3], Nina Bogdanovich[1], Dimitry Bronin[1], Sergey Pikalov[2] and Irina Nikolaenko[4]; [1]Institute of High Temperature Electrochemistry UB RAS, Ekaterinburg, Russian Federation; [2]Institute of Metallurgy UB RAS, Ekaterinburg, Russian Federation; [3]Department of Environmental Economics, Ural Federal University, Ekaterinburg, Russian Federation; [4]Institute of Solid State Chemistry UB RAS, Ekaterinburg, Russian Federation.

$La_2NiO_{4+\delta}$ (LNO) mixed conductor with a bilayer perovskite structure type K_2NiF_4, characterized by higher values of the surface oxygen exchange k compared to nickelates of other rare earth elements, and high values of the diffusion coefficient D* due to interstitial oxygen ions. The coefficient of thermal expansion (CTE) of LNO allows one to successfully apply it in the intermediate temperature SOFC combined with solid electrolytes based on CeO_2 and $BaCeO_3$ with closed CTE values. The $La_{2-x}Ca_xNiO_{4+\delta}$ (LCNO) powders were synthesized by a two-step solid-state reaction method. Structural properties were investigated by a X-Ray

diffraction method (XRD), High temperature XRD methods with using diffractometers DMAX-2500 RIGAKU and DRON 2.0. The surface morphology and chemical content of ceramic samples were characterized by scanning electron microscope JEOL JSM 6390LA combined with JED-2300 energy dispersive X-ray analyzer. The results of XRD analysis reveal for all the samples an appearance of tetragonal structure (I4/mmm). The decrease in *a* parameter with an increase of Ca can be explained in terms of the changes in nickel oxidation state from +2 to +3. For electrical conductivity and dilatometric the LCNO compact samples were prepared of bar shape by pressing under specific pressure ~80MPa with following sintering at temperatures 1350°C and 1450°C. CTE of the samples in the air was analyzed by automated complex - Zirconia-318-Tesatronic-TT60. CTE of materials depends nonlinearly on the calcium content to x=0.3 increases. The measurements of electrical conductivity were performed by a direct current four-probe method in air. The increase of Ca content increases LCNO conductivity of samples having similar density (from 50 to 100 S/cm at 900°C, depending on the composition). The cathode slurries were prepared by mixing in a planetary mill the powdered components with ethyl alcohol and polyvinylbutyral binder and were formed on $Ce_{0.8}Sm_{0.2}O_{1.9}$ (SDC) electrolyte at 1100-1400°C. The electrochemical measurements were carried out by the method of impedance spectroscopy on the samples with symmetrically arranged electrodes. With an increase in Ca content from x=0 to 0.4 polarization conductivity of electrodes decreases noticeably (from 12 to 0.8 S/cm^{2}at 900°C). The electrochemical characteristics of the electrodes is significantly improved by the organization on them of $LaNi_{0.6}Fe_{0.4}O_3$ (LNF) collector layer. The Polarization conductivity of the LCNO electrodes with x=0.3 Ca content is 2.4 and 0.4 S/cm^2 at 900°C with and without collector LNF layers.

A6.14

Defect Structure and Related Properties of $YBaCo_2O_{6-\delta}$ Dmitry S. Tsvetkov, Anton L. Sednev, Ivan L. Ivanov, Dmitry A. Malyshkin and Andrey Y. Zuev; Department of Chemistry, Ural Federal University, Ekaterinburg, Russian Federation.

Double perovskites $REBaCo_2O_{6-d}$, where RE is a rare-earth element, have received great attention as potential cathode materials for SOFCs due to high mixed ionic–electronic conductivity and fast oxygen transport. Among these oxides only $YBaCo_2O_{6-d}$ has a thermal expansion coefficient, CTE, close to that for standard electrolyte materials. However, the important properties of $YBaCo_2O_{6-\delta}$ such as oxygen nonstoichiometry, total conductivity and Seebeck coefficient have not been studied so far.

Powder sample of $YBaCo_2O_{6-\delta}$ was prepared using glycerol–nitrate technique. Phase composition of the as-synthesized powder sample was controlled by X-ray powder diffraction.

Oxygen nonstoichiometry of the double perovskite $YBaCo_2O_{6-\delta}$ was measured as a function of oxygen partial pressure (*pO2*) and temperature (*T*) using two independent techniques: thermogravimetry and solid state coulometric titration. Oxygen content in $YBaCo_2O_{6-\delta}$ as a function of *T* and *pO2* was found to change in a relatively narrow range as compared to similar double perovskites like, for example, $GdBaCo_2O_{6-\delta}$. Total conductivity and Seebeck coefficient of $YBaCo_2O_{6-\delta}$ were measured as a function of *T* and *pO2* by four probe dc-method. A significant drop in the total conductivity of $YBaCo_2O_{6-\delta}$was found below the certain value of *pO2* at given *T* suggesting the thermodynamic stability limit of this double perovskite with respect to pO_2 decrease. It was shown that both total conductivity and Seebeck coefficient of $YBaCo_2O_{6-\delta}$ are almost independent of pO_2 within the range of its thermodynamic stability due to weak pO_2 dependence of the oxygen content. Positive value of Seebeck coefficient and decrease of the $YBaCo_2O_{6-d}$ conductivity with lowering *pO2* indicate in favor of holes as dominating charge carriers. The experimental results obtained were discussed on the basis of the defect structure model proposed for $YBaCo_2O_{6-\delta}$.

A6.15

Synthesis and Study of the Ordered Double Perovskite $NdBaMn_2O_{5+d}$ to be Used as Symmetric SOFC Electrode Material Gilles H. Gauthier[2], Konrad Swierczek[1], Pascal Roussel[3], Oscar L. Pineda[2, 1] and Zulma L. Moreno[2]; [1]AGH University of Science and Technology, Cracow, Poland; [2]Grupo INTERFASE, Universidad Industrial de Santander, Bucaramanga, Colombia; [3]Université Lille 1, Université Lille Nord de France, Lille, France.

The symmetric SOFC is an interesting concept, in which the same electrode material can operate simultaneously as an anode and a cathode [1-2]. Recently, double perovskite-type compounds $LnBa(Co,Mn)_2O_{5+d}$ (Ln = lanthanide) have been considered as SOFC cathodes, in which the main interesting feature, on the structural point of view, is the Ln/Ba ordering stabilizing oxygen vacancies in the lanthanide plane [3]. Whereas high Co-containing compositions are not sufficiently stable in reducing conditions, the pure manganite gives very interesting performance as an SOFC anode [4].

In our work, the $NdBaMn_2O_{5+d}$ compound is studied for symmetric SOFC electrode. The ordered material synthesis has been performed by solid-state reaction in reducing atmosphere at 1100°C for 12 h; the material crystallizes in the tetragonal system with space group *P4/mmm*.

Thermogravimetric coupled with HT-XRD analysis in air and diluted H_2 shows the material is completely oxidized to $NdBaMn_2O_6$ (*Pmmm*) around 300°C and subsequently reduced to its initial state, with possible intermediate $NdBaMn_2O_{5.5}$ composition (not observed by XRD). In both cases, Nd/Ba ordering is preserved, in a similar way as for recently studied $PrBaMn_2O_{5+d}$ [1].

At 1300°C in air, conditions that simulate the electrode sintering process, a loss of ordering is evidenced by the absence of the (*001*) reflection in the respective diffractogram but the vacancy ordering and tetragonal symmetry is still recovered at 850°C in reducing atmosphere. While the material reacts strongly with YSZ at 1300°C, no redhibitory chemical affinity with GDC was observed at high temperature. At this first stage of investigation, we can confirm that $NdBaMn_2O_{5+d}$ could be a possible electrode material for symmetric SOFC.

Acknowledgments: This work was developed with the financial support from UIS/VIE, AGH University of Science and Technology, FEDER, CNRS, Région Nord Pas-de-Calais, MENESR, LNLS, Laboratorio de Rayos X (UIS).

References: [1] J.T.S. Irvine et al. J. Mater. Chem. 16 (2006) 1603, [2] J.C. Ruiz-Morales et al. Electrochim. Acta 52 (2006) 278, [3] Broux *et al.* J. Materials Chem. A, 2, (2014) 17015-17023, [4] Kim Guntae *et al.* Nature Materials 14 (2014) 205-209.

A6.16 Withdrawn

A6.17

TOF-SIMS Characterization of Impurity Enrichment and Redistribution in Solid Oxide Electrolysis Cells during Operation Ragnar Kiebach, Kion Norrman, Ming Chen and Peter V. Hendriksen; DTU, Roskilde, Denmark.

In order to operate solid oxide electrolysis cells (SOECs) with high performance and achieve sufficient long-term stability, degradation factors must be identified. Among many degradation factors, impurities (e.g. Si, Cr and alkaline earth elements) in the raw materials, components and in the gases can affect the performance and long-term stability. To detect such impurities, even in low concentration of less than 1000 ppm, time-of-flight secondary ion mass spectrometry (TOF-SIMS) is a power full tool.

Here we present TOF-SIMS analyses of SOECs before and after testing under different operation conditions. The investigated cells consist of an yttria stabilized zirconia (YSZ) electrolyte, a lanthanum strontium cobalt ferrite LSCF/CGO anode and a Ni/YSZ cathode. SIMS analysis of the cross sections of the cells a) before testing, b) after single cell testing and c) after operated in a SOEC stack were performed to distinguish between impurities agglomerating before and during operation.

Several elements (e.g. Na, Cr and Si) were successfully determined and enrichment and migration of these elements during operation is reported. The enrichment of impurities in the active Ni/YSZ cathode was found to be well correlated with the steam flow direction, which could be a result of steam concentration and distance to the Si-containing glass. The influence of impurity deposition on the degradation of Ni/YSZ cathodes is further discussed.

A6.18

Role of Gadolinia-Doped Ceria Interlayer Microstructure and Orientation on the Cation Diffusion Behavior in LSCF/GDC/YSZ Model Heterostructures Jeffrey C. De Vero[1], Katherine D. Bagarinao[1], Do-Hyung Cho[1], Haruo Kishimoto[1], Katsuhiko Yamaji[1], Teruhisa Horita[1] and Harumi Yokokawa[1, 2]; [1]National Institute of Advanced Industrial Science and Technology, Tsukuba, Japan; [2]Institute of Industrial Science, University of Tokyo, Tokyo, Japan.

The stability of gadolinia-doped ceria (GDC) as a diffusion barrier between porous $La_{0.6}Sr_{0.4}Co_{0.2}Fe_{0.8}O_{3-\delta}$ (LSCF) cathode and polycrystalline yttria-stabilized zirconia YSZ electrolyte plays a key role in understanding cation diffusion towards improved performance of LSCF cathodes at the required operating temperatures. However, GDC interlayer microstructure in porous LSCF/GDC/poly-YSZ heterostructure is complicated by the extreme reactivity of LSCF to YSZ, and the electrochemical reaction conditions. For this purpose, ~1.0 µm–thick GDC interlayers were prepared by pulsed laser deposition on single crystal YSZ substrates with termination planes (100) and (111), which were subsequently pre-annealed at 1300°**C** for 5h, and finally deposited with ~ 0.35 µm–thick dense LSCF layers. The samples were then annealed between 800°**C** and 1000°**C** starting from 168 hours up to 731 hours. We found that the resulting microstructure and crack density in LSCF/GDC/YSZ heterostructures after annealing depended strongly on the GDC interlayer orientation. Sr and Zr surface diffusions along the cracks or crack–walls of GDC interlayer were found to be relatively fast in LSCF/GDC/YSZ(100) compared to LSCF/GDC/YSZ(111), which exhibited significantly different crack densities. We also made systematic comparison with dense LSCF films on GDC/polycrystalline YSZ substrates to elucidate the possible contribution of grain boundaries as well as the influence of density of microcracks in GDC interlayer on cation diffusion. This result highlights the importance of GDC interlayer microstructure in understanding cation diffusion in LSCF/GDC/YSZ heterostructures.

A6.19

The Utility of Model Electrodes for the Separation of Current Pathways in Solid State Electrochemistry Alexander K. Opitz, Markus Kubicek, Stefanie Taibl, Tobias Huber, Gerald Holzlechner, Herbert Hutter and Juergen Fleig; Institute of Chemical Technologies and Analytics, Vienna University of Technology, Vienna, Austria.

Micro-patterned thin film electrodes offer a powerful tool for the separation and investigation of different reaction pathways and rate determining reaction steps on electrodes in solid state electrochemistry, since they allow well-defined electrode geometries and direct access of the electrochemically active zones to surface analytical tools. In this work, the usefulness of model-type electrodes is exemplified by platinum electrodes on yttria stabilized zirconia (Pt|YSZ) as well as mixed conducting electrode materials such as (La,Sr)MnO_3, (La,Sr)$FeO_{3-\delta}$, and (La,Sr)$CoO_{3-\delta}$.

On Pt electrodes two different parallel reaction pathways were identified under equilibrium conditions in air: A diffusion limited path along Pt grain boundaries dominating at lower temperatures, and an electrode surface path with oxygen incorporation at the three phase boundary at higher temperatures. An additional electrolyte surface path with electron transfer via the YSZ electrolyte can be activated by applying a strong cathodic polarization. The electrochemically active zone of this electrolyte surface path was visualized by ^{18}O tracer incorporation experiments in combination with time-of-flight secondary ion mass spectrometry (ToF-SIMS) analysis.

This tracer incorporation technique also enabled a separation of surface and bulk path on $La_{0.8}Sr_{0.2}MnO_{3-\delta}$ (LSM) electrodes by applying different cathodic overpotentials. On the mixed conducting electrode materials $La_{0.6}Sr_{0.4}CoO_{3-\delta}$ (LSC) and $La_{0.6}Sr_{0.4}FeO_{3-\delta}$ (LSF) the limitations of the tracer method are demonstrated. Due to the low polarization resistance of LSC electrodes the ^{18}O incorporation is determined by the current distribution in the electrolyte (i.e. the primary current distribution) and thus the electrochemically active zone of LSC cannot be visualized. The effect of changes of the electrode's electronic conductivity caused by cathodic polarization is demonstrated for LSF.

A6.20

Rapid Measurement of Chemical Diffusion in Oxide Thin Films by Color Front Motion Tracking Jae Jin Kim[1], Stuart N. Cook[1], Di Chen[1], Sean R. Bishop[1] and Harry L. Tuller[1, 2];[1]Materials Science and Engineering, Massachusetts Institute of Technology, Cambridge, Massachusetts, United States; [2]International Institute for Carbon-Neutral Energy Research (WPI-I2CNER), Kyushu University, Fukuoka, Japan.

The direct quantification of ionic conductivity in mixed ionic-electronic conductors (MIECs) is of tremendous importance in developing novel materials for applications such as solid oxide fuel/electrolysis cell (SOFC/SOEC) electrodes. In MIECs the level of ionic conduction is typically significantly lower than that of the electronic contribution and its measurement is therefore more complex. Perhaps the most common technique is the quantification of the oxygen kinetics, i.e. the diffusion coefficient, which can be related to ionic conduction by the Nernst-Einstein relationship. This is typically performed by relaxation or isotopic tracer measurement techniques.

In order to measure the oxygen migration kinetics via relaxation, the material of interest must have a measurable property that depends on the oxygen defect concentration, for example electronic conductivity or lattice parameter, and a means of rapidly changing this concentration, such as temperature or oxygen partial pressure. The technique must therefore be tailored to individual materials. An additional complicating factor lies in the inherent convolution of the surface exchange and diffusion coefficients, that needs to be resolved in subsequent fitting of the relaxation curve.

Oxygen isotope tracer measurement allows the clear deconvolution of these two fitting parameters using quenched in diffusion profiles, however it is time consuming, utilizes expensive equipment and is typically a destructive technique.

In this work we demonstrate a novel technique to overcome the limitations of these methods by taking advantage of the previously demonstrated redox-state dependent color change in Pr doped ceria (PCO). This color change arises from the Pr (3+/4+) transition and can therefore serve as a means of quantifying the equilibrium Pr oxidation state and, in turn, the oxygen stoichiometry. Upon subjecting a thin film of PCO to a rapid change in pO_2, the change in oxygen stoichiometry is limited by the kinetics of oxygen surface exchange and diffusion. In order to track this diffusion over reasonable timescales, we limit the region exposed to the atmosphere using a blocking surface layer, so that the oxygen must diffuse laterally through the film. The diffusion profiles can therefore be optically recorded, in-situ, as the motion of a color front and evaluated by fitting to appropriate solutions to the diffusion equation to enable extraction of the oxygen surface exchange and chemical diffusion coefficients.

The results for PCO films over a range of partial pressures and temperatures are reported and contrasted with those determined by other methods. The potential application of this technique to other materials systems is also discussed, taking into account both its strengths and limitations.

A6.21

TraceX: Isotope Exchange Data Analysis, Back-Diffusion Simulation and Profile Fitting Samuel J. Cooper, Mathew Niania and John A. Kilner; Department of Materials, Imperial College London, London, United Kingdom.

Isotopic exchange has been well established as a technique to determine the diffusivity and surface exchange coefficients of ceramic materials for over two decades. The mass specific image data obtained, often through Time-Of-Flight Secondary Ion Mass Spectrometry (TOF-SIMS), requires some data analysis before a meaningful depth profile can be extracted. Factors such as sample alignment, correct surface location and the exclusion of porous regions must all be determined before a profile is generated [1].

The following work describes a new graphical user interface (GUI), based in the widely used MATLAB® environment, that offers image data analysis and curve fitting, as well as generating *back-diffusion* profiles through a finite difference simulation.

Firstly, accurate sample alignment can be difficult and will cause an apparent increase in diffusivity if uncorrected. TraceX implements a simple alignment detection algorithm that searches for the angle (to within ±0.1°) at which the total counts gradient is at a maximum. This method also determines the location of the surface. In addition, certain regions, such as surface scratches and internal pores, are identified and excluded from profile calculations. This masking is typically determined by comparing the counts in each voxel to the global mean.

TraceX then allows the users to perform curve fitting based on the *fminsearch* algorithm, which implements an unconstrained non-linear optimisation to minimise the value of R^2. In addition to the conventional Crank [2] solution to diffusion with surface exchange, TraceX can calculate a *back-diffusion* profile using a finite difference approach, which offers insights into the effect of impurities in the exchange gas.

It is hoped that through better data analysis, more consistency in the interpretation of isotopic exchange will be achieve within the SSI community.

[1] R.J. Chater, in: Department of Materials, Imperial College London, 2014.
[2] J. Crank, The Mathematics of Diffusion, 1975.

A6.22

Impedance Spectroscopy Analysis Inspired by Evolutionary Programming as a Diagnostic Tool for SOEC Zohar Drach, Shany Hershkovitz, Sioma Baltianski and Yoed Tsur; Chemical Engineering, Technion Israel Institute of Technology, Haifa, Israel.

Solid oxide fuel cell (SOFC) and solid oxide electrolysis cell (SOEC) are promising electrochemical devices which are based on a solid oxide electrolyte that operates at relatively high temperatures (500-1000 oC). Impedance spectroscopy (IS) is an effective tool for the analysis of SOFC and SOEC performance. The challenge using this characterization tool lies within the analysis method. Impedance spectroscopy genetic programming (ISGP) is a novel analysis technique for impedance spectroscopy measurements that has been developed in our group. The ISGP combines evolutionary programming techniques for finding the best fitting distribution functions of relaxation times (DFRT). This approach leads toward a better analysis of impedance spectroscopy results. The outcome of our analysis is an analytic function, comprised of known mathematical peaks (e.g. Gaussian, Lorentzian, etc.) that can be assigned to the different processes taking place in the tested cell.In this work the operation and degradation of anode supported SOFC operated as SOEC were examined using IS measurements and analyzed using ISGP. The aim of this work is to find a DFRT model which reflects the physical processes occurring during the SOEC operation. Our primary model suggests several peaks; each corresponds to a different physical processes occurring during cell operation.

A6.23

Long-Term Degradation of $La_{0.6}Sr_{0.4}Co_{0.2}Fe_{0.8}O_{3-\delta}$ IT-SOFC Cathodes due to Silicon Poisoning Martin Perz[1], Edith Bucher[1], Christian Gspan[2, 3], Joerg Waldhaeusl[1], Ferdinand Hofer[2, 3] and Werner Sitte[1]; [1]Chair of Physical Chemistry, Montanuniversitaet Leoben, Leoben, Austria; [2]Institute for Electron Microscopy and Nanoanalysis (FELMI), Graz University of Technology, Graz, Austria; [3]Graz Center for Electron Microscopy (ZFE), Austrian Cooperative Research (ACR), Graz, Austria.

The impact of silicon - which is frequently found as an impurity in raw powders or originates from glass seals and thermal insulation in the solid oxide fuel cell (SOFC) stack - on the long-term stability of $La_{0.6}Sr_{0.4}Co_{0.2}Fe_{0.8}O_{3-d}$ (LSCF) cathodes was investigated by electrochemical impedance spectroscopy with symmetric cells of LSCF on $Gd_{0.1}Ce_{0.9}O_{1.95-d}$. At 700°C the area specific resistance (ASR) of the fresh LSCF cathode was 0.6 W cm². During 1000 h an increase in the cathode ASR by a factor of 5, which may be attributed to changes in the surface elemental composition, was observed. Subsequently, a 10 nm thick silicon layer was sputtered onto the LSCF cathode. Under these conditions a strong degradation occurred during additional 1000 h at 700°C. Post-test analyses by scanning electron microscopy (SEM) and transmission electron microscopy (TEM) revealed the formation of a nanocrystalline 25-50 nm thick silicon-rich layer on the surface of the LSCF cathode and a decomposition of the perovskite phase into La-Sr-silicate and Co-Fe-oxide. The present results indicate that even small contaminations with silicon can result in a strong decrease in the oxygen exchange activity of LSCF and similar cathode materials.

A6.24

Degradation Mechanisms of Cathode Materials for Intermediate Temperature-Solid Oxide Fuel Cells Soo-Yeon Jo, Ka-Young Park and Jun-Young Park; Department of Nanotechnology and Advanced Materials Engineering, Sejong University, Seoul, Korea (the Republic of).

Degradation Mechanisms of Cathode Materials for Intermediate Temperature-Solid Oxide Fuel Cells

Soo-Yeon Jo, Ka-Young Park and Jun-Young Park*

Green Energy Research Institute, Department of Nanotechnology and Advanced Materials Engineering, Sejong University, 209 Neungdong-ro, Gwangjin-gu, Seoul, 143-747, Republic of Korea

Solid oxide fuel cells (SOFCs) have a number of advantages as clean and renewable power generation electrochemical devices including high efficiency, high power density, environmental friendliness, fuel flexibility, and no use of metal catalysts. In order to make commercialization SOFCs in the near future, however, the long-term durability of SOFCs with high performance still needs to be improved at the intermediate temperature. Toward this goal, primarily, it is necessary to understand the major degradation mechanisms of SOFC components after the long-term durability tests in various operating conditions. However, researches for improving the durability are still in the early stages, compared to other efforts to reduce operating temperature of SOFCs by using the advanced materials and ceramic processing. In particular, highly durable cathode materials with better performances are one of vital works, because the cathode overpotential affects the SOFC performance at the intermediate temperature.

Until now, the classical SOFC cathode material is strontium doped lanthanum manganite (LSM). However, LSM shows the high overpotential at the intermediate temperature operation of SOFCs. Moreover, the chemical reactions of LSM with yttria-stabilized zirconia (YSZ) electrolytes cause severe performance degradations during the hot-temperature SOFC operation, such as the formation of insulating phases of $La_2Zr_2O_7$ and $SrZrO_3$. In addition, the LSM materials are also more likely to decompose at the high humidified air condition due to the strong reaction of SrO with H_2O.

To overcome these drawbacks, we investigate double perovskite structured materials as the candidate cathode, because they have excellent electrochemical properties with the high stability. In this work, degradation mechanisms of Ni-ceria cermets based anode-supported SOFCs with various double perovskite cathode materials are studied under a number of failure mode testing and analysis modes. Nd-doped ceria (NDC) electrolytes are prepared by the glycine-nitrate combustion method. The durability testing double perovskite structured cathode materials is performed under the constant current mode by the periodical on/off supply of hydrogen and air in the anode and cathode side, respectively. After the durability testing of SOFCs, electrochemical analysis and physicochemical analysis such as EIS, SEM, TEM, and XRD are carried out to find main degradation mechanisms of cells.

1. Lowering the temperature of solid oxide fuel cells, E. D. Wachsman, and K. T. Lee, *Science*, **334**, 935 (2011).
2. Durability test of SOFC cathodes, M. J. Jørgensen, P. Holtappels and C. C. Appel, *Applied Electrochemistry*, **30**, 411 (2000).
3. Chemical compatibility of the $LaFeO_3$ base perovskites $(La_{0.6}Sr_{0.4})_zFe_{0.8}M_{0.2}O_{3-\delta}$ (z = 1, 0.9; M = Cr, Mn, Co, Ni) with yttria stabilized zirconia, L. Kindermann, D. Das, H. Nickel, and K. Hilpert, *Solid state ionics*, **89**, 215 (1996).
4. Fundamental mechanisms limiting solid oxide fuel cell durability, H. Yokokawa, H. Tu, B. Iwanschitz and A. Mai, *J. Power sources*, **182**, 400 (2008).

* Corresponding authors: jyoung@sejong.ac.kr (J.-Y. Park)

A6.25

Transmission Electron Microscopy Study of Cr Poisoning of LSCF Cathodes Na Ni and Stephen Skinner; Materials, Imperial College London, London, United Kingdom.

(La,Sr)(Co,Fe)O3-δ (LSCF) perovskite oxides have been considered to be a promising cathode material for solid oxide fuel cells (SOFCs) operating in the intermediate temperature range due to their significantly higher electrochemical activity for the O2 reduction reaction and higher oxygen ion conductivity than the conventional (La,Sr)MnO3 (LSM) cathode [1,2]. Metallic materials have become a preferential choice for the interconnect due to their excellent physical and chemical properties. However the presence of chromium in all commonly used metallic alloys has been found to cause poisoning of the cathode under operating conditions leading to rapid electrochemical performance degradation of the cathodes including LSCF [3–5].

Development of a Cr tolerant cathode material for increased long-term durability of SOFCs relies on a fundamental understanding of the mechanism of the chromium deposition and poisoning of the cathode materials. Extensive research on the chromium deposition and poisoning processes on SOFC cathodes has been carried out but careful microstructural studies especially on the nanometer to atomic scale are very limited. This is however a subject that can give valuable information on the detailed process of Cr incorporation and evolution in the cathode materials, providing an important insight for the mechanistic understanding of the Cr poisoning.

In this work, the effect of Cr poisoning at 900 ˚C in air on the electrochemical behavior of LSCF/CGO/LSCF symmetrical cells was assessed by impedance spectroscopy, and the change in nano/microstructure and chemistry between cells with and without Cr poisoning were studied in parallel by advanced transmission electron microscopy (TEM). Application of the electron energy loss spectroscopy (EELS) provided more reliable results for the chemical analysis than EDX, as the latter suffers from the overlap of La and Cr peaks and poorer spatial resolution due to various artefacts.

Our results show that Cr is incorporated in LSCF in more complicated ways than a simple formation of $SrCrO_x$ as suggested by previous studies. Cr was found to segregate in Sr rich phases that also contain other elements such as Fe and Co. In addition, Cr was incorporated in the LSCF perovskite structure and repelled sometimes the other B site elements from the lattice. As a result, Cr rich phases take the form of various compositions such as $(La,Sr)(Fe,Co,Cr)O_x$, $(La,Sr)(Fe,Cr)O_x$ and $(La,Sr)CrO_x$. It is interesting to note that Cr appears to repel more readily Co than Fe. The Cr poisoning also promotes the formation of Co and Co-Fe rich phases that may contribute to the deficiency of Co in the LSCF grains. It can be seen that the area adjacent to the Fe-Co rich particles contains Cr and are deficient in Co with a composition close to that of $(La,Sr)(Cr,Fe)O_x$. Careful examination of Cr incorporation was also extended to LSCF grain boundaries with both structural and chemical analysis. The high-resolution microscopy results and their implications are discussed in relation to the degraded electrochemical properties of the LSCF cathode and the Cr poisoning mechanisms.

[1] S. Jiang, Solid State Ionics 146 (2002) 1.
[2] A. Esquirol, N.P. Brandon, J.A. Kilner, M. Mogensen, J. Electrochem. Soc. 151 (2004) A1847.
[3] M.C. Tucker, H. Kurokawa, C.P. Jacobson, L.C. De Jonghe, S.J. Visco, J. Power Sources 160 (2006) 130.
[4] L. Zhao, J. Drennan, C. Kong, S. Amarasinghe, S.P. Jiang, ECS Trans. 57 (2013) 599.
[5] S.P. Jiang, X. Chen, Int. J. Hydrogen Energy 39 (2014) 505.

A6.26

Effects of Chemical and Interfacial Strain on the Transport and Mechanical Properties of $PrCoO_3$ Mabel Lew, Stevin Pramana, Andrea Cavallaro, Ji Wu and Stephen Skinner; Materials, Imperial College London, Kingston, United Kingdom.

Defect chemistry has long been utilised to tailor the properties of functional materials. In the field of solid oxide fuel cell cathode materials, A-site dopants such as Sr, Ca and Ba are often introduced to optimise electrical properties of promising perovskite and Ruddlesden-Popper materials through the creation of additional charge carriers. However, this is not an isolated effect. Recently, there has been interest in the local strain structures that result from doping, and their effect on mechanical properties (Bishop et al.), such as chemical expansion coefficient, which is a consideration when pairing potential cathode materials to existing electrolytes. Another form of defect chemistry that is of increasing interest in SOFC materials research is interfacial strain. Multilayers of $SrTiO_3$/YSZ have been fabricated with an enhancement of eight orders of magnitude in the ionic conductivity of YSZ, which have been attributed to interfacial strain effects (Garcia-Barriocanal et al.). This concept is also being applied to cathode materials (Kubicek et al.).

A clearer understanding of the electrochemomechanics of defect chemistry is required to take full advantage of its application. Therefore, the objective of this study is to compare the effects of two different forms of defect chemistry: interfacial strain against chemical strain. Specifically, the effects of the two strains on transport and mechanical properties will be compared.

For this work, single phase $PrCoO_3$ samples of varying metal cation stoichiometries were synthesized using the sol-gel method and pelletized in order to produce bulk samples with a range of A site vacancy concentrations (along with their charge compensating defect). Thin films of stoichiometric $PrCoO_3$, with different interfacial strains arising from the lattice mismatch between the film and substrate, were also fabricated by pulsed laser deposition onto a YSZ (8mol%) substrate with a $Ce_{0.9}Gd_{0.1}O_2$ buffer layer.

A6.27

Electrical Properties of LSM-$Bi_3Y_{0.9}W_{0.1}O_{6.15}$ Composite Solid Membranes Marcin Malys[1], Wojciech Wrobel[1], Marcin Dudz[1], Marzena Leszczynska-Redek[1], Anna Borowska-Cenkowska[1], Maciej Wojcik[1], Kuan-Zong Fung[2], Isaac Abrahams[3] and Franciszek Krok[1]; [1]Faculty of Physics, Warsaw University of Technology, Warszawa, Poland; [2]Material Science and Engineering, National Cheng Kung University, Tainan, Taiwan; [3]Materials Research Institute, Queen Mary University of London, London, United Kingdom.

Introduction

$(La,Sr)MnO_3$ perovskite (LSM) is regarded as one of the most promising cathode material for the use in high temperature SOFC due to its high thermal and chemical stability, relatively good compatibility with electrolytes based on yttria-stabilised zirconia YSZ. Improvement of performance of cathode based on LSM, which is mostly electronic conductor, can be obtained by forming a composite cathode through addition of oxygen-ion conducting second phase. Recently much work was carried out on development of LSM/YSZ or LSM/GDC (gadolinium-doped ceria) composite cathodes suitable for SOFC systems.

The aim of this study is to investigate a composite cathodic system, consisting of LSM and bismuth based oxide material; $Bi_3Y_{0.9}W_{0.1}O_{6.15}$ was selected due to relatively high long term stability of electrical conductivity. It is also important that both components of composite cathode, LSM and $Bi_3Y_{0.9}W_{0.1}O_{6.15}$, have similar thermal expansion coefficients. Significant decrease of interfacial resistance of the composite system is expected in comparison to that of LSM material.

Experimental

Powders of component materials were mixed in different molar ratios (LSM : $Bi_3Y_{0.9}W_{0.1}O_{6.15}$) from 5:1 to 1:5, then formed into disc membranes, pressed and sintered. Structure of obtained composites were investigated by HT-XRD, SEM and DTA methods. Electrical conductivity of composites was examined by a.c. impedance spectroscopy, while ionic and electronic contribution to the total conductivity (transference numbers) were measured using modified e.m.f. method with oxygen concentration cell.

Results and Discussion

Analysis of XRD and DTA measurements indicated that there was no chemical reaction between component phases of composites in temperature range from room temperature to 850ºC. It has been shown that total conductivity of composite systems decreased with the increasing rate of $Bi_3Y_{0.9}W_{0.1}O_{6.15}$, in particular in the systems with dominant share of

these ionic component. Applicability of the classical percolation model was examined. The results of transference number studies shows, that for the systems with molar ratio equal 1:1, and above this ratio, the electronic conductivity is dominating, whereas ionic conductivity is dominating for the systems with molar ratio below 1:2.

A6.28

Optimization of Pr_2CuO_4-$Ce_{0.9}Gd_{0.1}O_{1.95}$ Composite Cathode for SOFC Application Liudmila Kolchina[1], Nikolay Lyskov[2] and Galina Mazo[1]; [1]Chemistry Department, Lomonosov Moscow State University, Moscow, Russian Federation; [2]Institute of Problems of Chemical Physics RAS, Chernogolovka, Russian Federation.

The present work is intended to the electrochemical characterization of Pr_2CuO_4-$Ce_{0.9}Gd_{0.1}O_{1.95}$ (PCO-GDC) composites supported on $Ce_{0.9}Gd_{0.1}O_{1.95}$ (GDC) electrolyte as promising cathode materials for intermediate temperature solid oxide fuel cells (IT-SOFCs) operating at 600-750°C.

The electrochemical properties of PCO-GDC*x* (*x* = 20, 33, 50 wt. %) composites were systematically studied. Phase composition, microstructure and electrochemical properties were investigated by X-ray powder diffraction, scanning electron microscopy, four-probe DC conductivity measurements and AC impedance spectroscopy, respectively. The oxygen reduction on porous PCO-GDC electrode applied on GDC electrolyte was studied in an electrode/electrolyte/electrode symmetrical cell by AC impedance spectroscopy at OCV conditions in the temperature range of 670-730 °C and at the oxygen partial pressures of 10^{-2}-0.21 atm. Analysis of the dependences of the normalized conductivity against volume fraction at different temperatures has shown that conductivity of PCO-GDC*x* composites can be described by the percolation theory. The percolation threshold is 38 vol. % of PCO.

The PCO/GDC/PCO electrochemical cells with different electrode thickness were prepared for optimization of area specific resistance (*ASR*) of an electrode/electrolyte interface. The lowest*ASR* value (0.57 Ω•cm^2 at 700°C) was achieved at the electrode thickness of 20 μm. Such electrode thickness was used for comparison of electrochemical characteristics of pure PCO and PCO-GDC*x* composites.

Results of electrochemical study of the electrode/electrolyte interface reveal that both GDC addition and electrode morphology have strong influence on *ASR*. The *ASR* value is reduced to a minimum at 33 wt. % GDC at temperatures below 700 °C (the lowest *ASR* value is equal to 0.41 Ω•cm^2 at 700 °C in air). Further temperature rise (T > 700 °C) leads to the shift of the *ASR*minimum to 20 wt. % GDC. The variation of the PCO-GDC composition, which exhibited the lowest polarization resistance, is attributed to the change of the rate-determining step of oxygen reduction reaction. The data obtained allow considering the PCO-GDC33 composite as a promising cathode material for IT-SOFCs.

This work was supported by Skolkovo Institute of Science and Technology, Russian Foundation for Basic Research (grant nos. 14-08-01260) and MSU-development Program up to 2020.

A6.29

Optimized PBCO-PCO-CGO Cathode for IT-SOFC Samir Boulfrad[1], Stevin Pramana[2], Mabel Lew[2], Udo Schwingenschloegl[1], Enrico Traversa[1] and Stephen Skinner[2]; [1]Physical Sciences and Engineering, King Abdullah University of Science and Technology (KAUST), Thuwal, Saudi Arabia; [2]Department of Materials , Imperial College London, London, United Kingdom.

Lowering the working temperature of solid oxide fuel cells (SOFCs), to the range of 600 – 700°C, is a major track in solid-state electrochemical energy conversion research. The potential benefit of such an advance is well known and described in the literature. However, this requires all components of the cell, electrodes and electrolyte, to operate efficiently at intermediate – low temperatures, where the kinetics of the thermally activated processes involved are expected to be much slower.

At the cathode level, several materials have been investigated to replace the state-of-the-art $La_{1-x}Sr_xMnO_{3-\delta}$ (LSM). Despite its high thermal expansion coefficient (TEC), the double perovkite $PrBaCo_2O_{5+\delta}$ (PBCO) is being considered as a promising cathode material for intermediate temperatures because of its high electronic conductivity and good oxygen surface exchange coefficient. Another material of potentially high interest is $PrCoO_3$ (PCO). This material was developed in the late nineteen sixties but was judged to be inconvenient because of its high thermomechanical mismatch and reactivity with zirconia based electrolytes. However, lately, it has been regaining interest as demonstrated in some recent publications.

In this work, a composite PBCO-CGO (gadolinia doped ceria) has been developed as a base cathodic framework. Powders of both PBCO and PCO were milled, using a high energy ball mill, down to nanometric size (<100nm). Suspensions were prepared using each of the oxide nanoparticles in order to infiltrate the PBCO-CGO porous structure. Symmetrical cell electrochemical characterization is in progress, results will be presented and discussed as a function of the PBCO/CGO ratio as well as the content level of PBCO and PCO nanoparticles.

A6.30

Optimization of $Ba_2Co_9O_{14}$ as an Innovative SOFC's Cathode Material Ibtissam Kehal, Marie-Helene Chambrier, Aurelie Rolle, Sylvie Daviero-Minaud, Rose-Noelle Vannier and Xavier Flandre; Unité de Catalyse et de Chimie du Solide, Université Lille, Villeneuve d'Ascq, France.

The $Ba_2Co_9O_{14}$ cobaltite (BCO) exhibits very interesting proprieties, which makes it a potential cathode material for solid oxide fuel cells (SOFC). It is the first member of the $Ba_{n+1}Co_nO_{3n+3}$ (Co_8O_8) series. Its structure consists of blocks of assembly [Ba_2CoO_6] between layers of [Co_8O_8] [1,2]. With an electrical conductivity of 100-240 s.cm^{-1} between 450 and 650°C, it was tested as electrode in composite with ceria gadolinium oxide (CGO) on a (CGO) electrolyte. A study was made by complex impedance spectroscopy after optimization of screen printing deposition conditions. The impact of the addition of an interlayer of BCO at the interface between the electrode and the electrolyte was also studied. An Area Specific Resistance of only 0.08 Ω.cm^2 was obtained at 700°C on a symmetrical cell with CGO as electrolyte material and a dense layer of BCO between electrode of 50% wt CGO + 50%wt BCO and electrolyte. Results obtained by impedance spectroscopy were modeled by an equivalent circuit using the Zview software. Several parameters were studied: thickness, grain size, composition and the addition of a dense layer between the electrolyte and the electrode with the aim to optimize the cell performances and to go further in the understanding of the mechanism involved. Their influence on the electrochemical performance of the symmetric cell will be presented.

[1] S. Junliang, Y. Min, L. Guobao, Y. Tao, L. Fuhui, W. Yingxia, X. Ming, L. Jianhua, *Inorganic Materials* **2006**, *45*, 9151.
[2] G. Ehora, S. Daviero-Minaud, M. Colmont, G. André, O. Mentré, *Chemistry of Materials* **2007**, *19*, 2180.

A6.31

Electrochemical Characterization of B-Site Cation-Excess $Pr_2Ni_{0.75}Cu_{0.25}Ga_{0.05}O_{4+\delta}$ Cathode for IT-SOFCs Yuan Ji and Xiangwei Meng; Jilin University, Changchun, China.

A B-site cation-excess K_2NiF_4-type structure oxide, $Pr_2Ni_{0.75}Cu_{0.25}Ga_{0.05}O_{4+\delta}$ (PNCG) is investigated as a cathode for intermediate-temperature solid oxide fuel cells (IT-SOFCs). XRD results show that PNCG cathode is chemically compatible with the electrolyte $Gd_{0.2}Ce_{0.8}O_{1.9}$ (GDC) at 900 °C for 5 h. The PLNCG material exhibits a semiconductor to metal transition around 425 °C. The thermal expansion coefficient (TEC) of the PNCG sample is 12.72×10^{-6} K^{-1} between 30 and 850 °C in air. The R_p of PNCG cathode on GDC electrolyte is 0.105, 0.197 and 0.300 Ω cm^2 at 800, 750, 700 °C, respectively. A maximum power density of 371 mW cm^{-2} is obtained at 800 °C for single-cell with 300 μm thick GDC electrolyte and PNCG cathode. The results of this study demonstrate that PNCG can be a promising cathode material for IT-SOFCs.

A6.32

$SrCo_{1-x}Mo_xO_{3-\delta}$ Pervoskites as Cathode Materials for $LaGaO_3$-Based Intermediate-Temperature Solid Oxide Fuel Cells Rui Wang, Fangjun Jin and Tianmin He; College of Physics, Jilin University, Changchun, China.

Perovskite oxides $SrCo_{1-x}Mo_xO_{3-\delta}$ (SCM, x = 0.05-0.2) were synthesized by a combined EDTA-citrate complexing method and assessed as potential cathode materials for intermediate-temperature solid oxide fuel cells (IT–SOFCs) based on $La_{0.9}Sr_{0.1}Ga_{0.8}Mg_{0.2}O_{3-\delta}$ (LSGM) electrolyte. The SCM materials with x = 0.05 and 0.1 sintered at 1000 °C for 10 h were well crystallized in a single-phase tetragonal structure at room temperature; they exhibited a good chemical compatibility with the LSGM electrolytes at 950 °C for 10 h. Several additional diffraction peaks were observed in the XRD patterns for the x = 0.15 and 0.2 samples. The Mo doping for Co efficiently inhibits the structural phase-transition in SCM materials. The best electrical conductivity for the x = 0.05 and 0.1 samples were 286 and 170 S cm^{-1} at around 400 °C, respectively. The area specific resistances of the x = 0.05 and 0.1 cathodes on the LSGM electrolyte were 0.020 and 0.026 Ω cm^2 at 800 °C, respectively. The maximum power densities of the single-cell on a 300 μm–thick LSGM electrolyte reached 795 and 687 mW cm^{-2} at 800 °C for the x = 0.05 and 0.1 cathodes, respectively. These results indicated that the SCM perovskites are promising cathode materials for application in IT-SOFCs.

A6.33

Tailoring of the Chemical Stability of $(Ba,Sr)(Co,Fe)O_3$-Based Perovskite Mixed Conductors Fang Wang[1], Koki Igarashi[2], Takashi Nakamura[1], Keiji Yashiro[3], Junichiro Mizusaki[1]and Koji Amezawa[1]; [1]Institute of Multidisciplinary Research for Advanced Materials, Tohoku University, Sendai, Japan; [2]Graduate School of Engineering, Tohoku University, Sendai, Japan; [3]Graduate School of Environmental Studies, Tohoku University, Sendai, Japan.

$Ba_{0.5}Sr_{0.5}Co_{0.8}Fe_{0.2}O_{3-\delta}$ (BSCF) has been extensively studied as cathode materials for intermediate temperature solid oxide fuel cells (IT-SOFC) due to its high catalytic activity for the reduction of oxygen gas [1]. However, the poor chemical instability BSCF limits its practical application [2]. In our previous work [3], we established the chemical stability diagram of BSCF in a wide range of $p(O_2)$ and temperature by the crystal structure and the oxygen nonstoichiometry analysis. It demonstrated the cubic BSCF was instable in IT-SOFC working conditions. The results also suggest the stability of cubic BSCF is mainly governed by the oxidation or reduction of trivalent Co ions.
Many research groups attempt to optimize the stability of BSCF by B-site doping. However, the fundamental understandings of the chemical stability and factors that influence the chemical stability were still insufficient. In this work, we try to stabilize the cubic BSCF by doping high valence cations Sb or Nb to the B-site. The chemical stability of the cubic BSCF doped with Sb (BSCF-Sb) or Nb (BSCF-Nb) under both oxidative and reductive conditions was investigated by studying the oxygen nonstoichiometry, the crystal structure and the oxidation state of the containing cations in various $p(O_2)$ and temperatures by coulometric titration, iodometric titration, *in situ* high-temperature X-ray diffraction, and soft-X-ray absorption spectroscopy (S-XAS). From results of the oxygen nonstoichiometry and the crystal structure, we established the chemical stability map of BSCF-Sb and BSCF-Nb with oxidative and reductive stable boundaries. The Co valence change by B-site doping and the effect on the chemical stability of the doped BSCF were also discussed.

[1] Z. P. Shao *et. al.*, *Nature*, 2004, **431**, 170.
[2] D. N. Mueller, *et. al.*, *PCCP*, 2010, **12**, 10320.
[3] F. Wang *et. al.*, *PCCP*, 2014, **16**, 7307.

A6.34

$NdBa_{1-x}Co_2O_{5+\delta}$ as Cathode Materials for Intermediate Temperature Solid Oxide Fuel Cell Jialing Sun[1, 2], Xiaomei Liu[1], Lili Zhu[1], Fei Han[1], Hailin Bi[1], Haopeng Wang[1], Shenglong Yu[1] and Li Pei[1]; [1]Key Laboratory of Physics and Technology for Advanced Batteries,Physics Department, Jilin University, Changchun, China; [2]Beihua University, Jilin, China.

The layered perovskites with $LnBaCo_2O_5$ formula have attracted much interest as possible cathode materials for Intermediate Temperature Solid Oxide Fuel Cell （IT-SOFC）, owing to their unusually rapid oxygen-transport properties at low temperature. The $LnBaCo_2O_5$ cathodes with an intermediate size lanthanide ion such as Nd may be preferred, considering the trade-off between electrochemical performance. Introduction of A-site cationic deficiency is another feasible way of improving electrochemical performance of perovskite oxides. $NdBa_{1-x}Co_2O_{5+\delta}$ （NBCO x=0.00,0.02,0.04，0.06） oxides are synthesized via an EDTA-citrate sol-gel procss and evaluated as cathode materials for IT-SOFC.The X-ray diffraction pattern of NBCO indicate that all the samples can be indexed with a tetragonal P4/mmm space group with lattice parameters of a=b=0.3903Å≈a_p and c=0.7627Å≈2a_p (a_p: the cell parameter of the primitive perovskite). The increase of Ba-deficiency concent causes a significantly decrease in the interfacial polarization resistances (R_p) .In the NBCO system, the content of the Ba-deficiency may generate more oxygen vacancies and therefore advantage for the oxygen surface exchange and oxygen ionic bulk transport and helps improve the catalytic activities for oxygen reduction reaction, thus resulting in low polarization resistance of the cathodes. A further increase in deficiency content to a value higher than 0.04 results in a higher interfacial polarization resistances. It is becasure that the oxygen vacancies at a high concentration would be trapped by forming clusters, which results in lowering of the oxygen ionic diffusivity. Among all these compositions, the $NdBa_{0.96}Co_2O_{5+\delta}$ cathode shows the lowest R_p value of 0.27Ωcm² at 750℃. The full cell performances improve with increasing Ba-deficiency content up to 0.04 in the NBCO oxides.

Acknowledgement
This work was supported by the National Natural Science Foundation of China (no. 51272087, 50872041)

A6.35

Effect of Thermal Reduction on Electrical Properties of Protecting Oxides for SOFC Interconnect Applications Kuan-Zong Fung[1, 3], Shu-Yi Tsai[1] and Chung-Ta Ni[2]; [1]Materials Science and Engineering, National Cheng Kung University, Tainan City, Taiwan; [3]Research Center for Energy Technology and Strategy, National Cheng Kung University, Tainan City, Taiwan.

Thermal reduction has played important role on the electrical property of several oxides used for energy applications. Furthermore, the phase transformation may be also caused by thermal reduction of functional oxides. In our study, plasma sprayed (Mn,Co)3O4 (MCO) spinel coating with spinel structure are used to form protective layer for metallic interconnects of solid oxide fuel cells. However, the temperature during thermal spraying may be high enough to change the crystal structure and conductivity of protective oxides. The structure change is caused by the removal of oxygen ions at higher temperature. More importantly, the transformation of MCO Spinel to a NaCl-type structure also reduces its conductivity by several orders of magnitude. With the understanding of mechanism of phase transformation, it is believed that the proper heat treatment is an adequate method to obtain desired properties for protective oxide. Therefore, the crystal structure of materials with different functionality may change during the processing or operation. With better understanding and control of thermal reduction and/or phase transformation, better performance of these energy devices may be accomplished.

A6.36 moved A9.07

A6.37

Deconvolution of Four Transmission-Line-Model Impedances in Ni-YSZ/YSZ/LSM Solid Oxide Cells and Mechanistic Insights Eui-Chol Shin, Jianjun Ma, Pyung-An Ahn, Hyun-Ho Seo, Dang-Thanh Nguyen and Jong-Sook Lee; Materials Science and Engineering, Chonnam National University, Gwang-Ju, Korea (the Republic of).

Four impedance components with the two respectively from the cathode and anode have been successfully deconvoluted for the temperature range between 800°C and 600°C of cermet-supported Ni-YSZ/YSZ/LSM-YSZ solid oxide fuel cells with 5μm thin YSZ electrolyte layers with different

porosities in Ni-YSZ support. Gas concentration impedance of Ni-YSZ cermets, smaller for higher porosity, described by Gerischer model is largely responsible for the performance under light load condition. The contribution of lower frequency responding gas concentration impedance of LSM-YSZ occurs becomes substantial at high temperature. Bisquert transmission line model or finite-length Gerischer model in three-parameter ideal form was applied for both Ni-YSZ and LSM-YSZ electrode reactions. Application of non-faradaic chemical reaction mechanism provides the activation energies 0.38 and 0.58eV, for surface hydrogen diffusion and the dissociation surface reaction in Ni-YSZ electrodes, where the adsorption capacitance activated by 0.4~0.5eV is taken into consideration. For LSM-YSZ electrode response, mobility and absolute reaction rate of surface oxygen were found activated with 0.85 and 1.25eV, respectively. Surface reaction is more strongly activated than the surface diffusion and thus utilization length slightly increases with decreasing temperature around 50%. The typical utilization length explains Gerischer-like electrode reaction impedance. While mobility and thus the diffusivity parameter is governed by YSZ network, the reaction rate and adsorption capacitance are considered characteristic of the electrode materials. Unprecedentedly, multiple kinetic parameters of straightforward physical mechanism are simultaneous determined by impedance spectroscopy.

A6.38

The Electrolyte Spreading Resistance - More than a Resistive Offset Andreas Nenning, Michael Doppler and Juergen Fleig; Institute of Chemical Technologies and Analytics, Vienna University of Technology, Vienna, Austria.

Thin film microelectrodes are frequently used to investigate fundamental properties of mixed conducting or metallic SOFC electrode materials. When a sufficiently large counter electrode is used, the polarization resistance is given by the sum of electrolyte and working electrode resistance and the counter electrode resistance is negligible.
Usually, the electrolyte spreading resistance is regarded as a resistive offset in the impedance spectra of microelectrodes, which is determined in the high-frequency regime. In contrast to this interpretation, numerical simulations and impedance measurements of triple-phase active (Ni and Pt) and mixed conducting ($La_{0.6}Sr_{0.4}CoO_{3-\delta}$ and $Ce_{0.8}Gd_{0.2}O_{2-\delta}$) electrodes reveal that the electrolyte resistance depends on the frequency and electrode type.

In the high-frequency limit the electrode is short-circuited via its capacitance and the spreading resistance depends only on electrode diameter and electrolyte conductivity. In DC conditions the current density distribution of the electrode is dominated by the electrochemical properties of the electrode. On triple-phase active electrodes the current enters the electrolyte only in a very narrow region at the electrode border. Surface active electrodes have homogeneous current density beneath the electrode in DC conditions. The real (DC) resistive contributions of the electrolyte are therefore significantly larger than the (high frequency) spreading resistance. When the electrode arc is significantly larger than the electrolyte resistance, these contributions have a minor impact on the DC polarization resistance. Nevertheless the frequency dependence of the electrolyte current paths causes impedance features that are usually assigned to electrode processes. These can range from weakly pronounced high-frequency shoulders shoulders to even well-separated, distorted semicircles. A modified spreading-resistance formula that accounts for the effect of a finite substrate and finally suggestions that help to identify or avoid the discussed impedance features are presented.

A6.39

Electrical Characterization of the Active Cathode Area in Solid Oxide Fuel Cells Tzvia Radlauer[1], Sioma Baltianski[2], Ilan Riess[3] and Yoed Tsur[2]; [1]Energy Engineering, Technion, Haifa, Israel; [2]Chemical Engineering, Technion, Haifa, Israel; [3]Physics, Technion, Haifa, Israel.

The performance of SOFCs is limited by the cathodic reaction, which requires adsorption and dissociation of oxygen molecules on the cathode surface and diffusion of the adsorbed atomic or ionic oxygen to the active electrode area, where it is caught by an oxygen vacancy in the electrolyte together with electrons (if required). When the cathode is a poor ionic conductor (while the electrolyte is by definition a poor electronic conductor), the active electrode area is limited to the triple phase boundary (TPB) between the gas, electrode and solid oxide electrolyte phases. Various mathematical models have been proposed to describe the TPB [1-3]. Experimentally, the width has been followed with isotope exchange[4,5]. In our work, we measured the resistance between parallel Au cathode stripes applied to a solid electrolyte (SE). This reflects mixed conductivity in the SE, and possible electron transfer and oxygen reduction and oxidization at the Au electrode stripes. We here report on that resistance vs. the current through the SOFC element. An interdigitated gold electrode arrangement was fabricated on an Yttria-stabilized Zirconia (YSZ) solid electrolyte in order to generate and follow changes in local stoichiometry. Impedance spectroscopy (IS) and cyclic voltammetry (CV) measurements were performed at intermediate temperatures (250-350°C). A three electrode arrangement allowed biasing the gold electrode with respect to a counter electrode on the opposite side of the YSZ crystal. In the three-electrode arrangement, the effect of both anodic and cathodic biases on the interdigitated electrodes is reported.

References:

[1] A.M. Gokhale, S. Zhang, M. Liu, J. Power Sources, 194 (2009) 303
[2] X. Deng, A. Petric, J. Power Sources, 140 (2005) 297
[3] R. O'Hayre, D.M. Barnett, F.B. Prinz, J.Electrochem.Soc., 152(2005) A439.
[4] H. Kishimoto, N. Sakai, K. Yamaji, T. Horita, M.E. Brito, H. Yokokawa, K. Amezawa, Y. Uchimoto, Solid State Ionics, 179 (2008) 347-354
[5] J. Fleig, A. Schintlmeister, A.K. Opitz, H. Hutter, Scripta Mater. 65 (2011) 7

A6.40

Electronic Conductivity in Yttria-Stabilised Zirconia under a Small *dc* Bias Nahum Maso[1, 2] and Anthony R. West[2]; [1]Chemistry, University of Oslo, Oslo, Norway; [2]Materials Science and Engineering, The University of Sheffield, Sheffield, United Kingdom.

Yttria-stabilised zirconia, YSZ, is the oxide ion conducting electrolyte of choice in many solid oxide fuel cells, because of its resistance to reduction at the fuel electrode. Here, we demonstrate that electronic conduction is introduced into YSZ under the action of a small *dc* bias at high temperatures in air. A reversible decrease in sample grain and grain boundary resistances occurs with increasing bias in the range 1 to 15 V and the Warburg impedance at the sample-electrode-air interface collapses. Similar conductivity changes are seen with acceptor-doped dielectrics and are attributed to the ionisation of underbonded oxide ions in the crystal structure, with O^- ions acting as the location of the holes and the source of p-type conduction; the ionized electrons are trapped by changes to the equilibria among oxygen species at the sample surface. A similar mechanism may explain the onset of electronic conductivity in YSZ.

We thank EPSRC and RCN (219731) for financial support

A6.41

Impedance Study on LSGM Single Crystals Ghislain M. Rupp[1], Michal Glowacki[2] and Juergen Fleig[1]; [1]Institute of Chemical Technologies and Analytics - Electrochemistry, Vienna University of Technology, Vienna, Austria; [2]Institute of Physics, Polish Academy of Sciences, Warsaw, Poland.

The materials family of $La_{1-x}Sr_xGa_{1-y}Mg_yO_{3-\delta}$ (LSGM) has received considerable interest in the past two decades because of its high ionic conductivity and its acceptably low electronic transference number. Hence, it is regarded as a promising electrolyte candidate for intermediate solid oxide fuel cells and alternative to yttria-stabilized zirconia (YSZ) electrolytes. However, almost exclusively polycrystalline LSGM has been investigated so far, in contrast to YSZ where many studies are available also on single crystals.

In this work we studied the defect chemistry and charge carrier transport properties of $La_{0.95}Sr_{0.05}Ga_{0.95}Mg_{0.05}O_{3-\delta}$ single crystals grown by Czochralski technique. Slabs of 500 µm thickness were prepared with a surface area of 25 mm² perpendicular to the (100) growth direction and both surfaces were epi-polished. An oxygen-blocking electrode of 200 nm $La_{0.8}Sr_{0.2}MnO_{3-\delta}$ and 400 nm Pt was deposited on both sides of the electrolyte for electrochemical impedance spectroscopy investigations. At

elevated temperatures, above 500°C, impedance spectra with a high frequency intercept and an almost ideal Warburg element were obtained. Quantitative fitting of a single spectrum based on the model of Ref. [1], thus yielded the electronic conductivity, ionic conductivity and ionic mobility, the ambipolar diffusion coefficient and the concentration of electronic charge carriers (including trapped electrons) of LSGM. Temperature dependent measurements were used to calculate the activation energy for electronic and ionic transport. Oxygen partial pressure dependent measurements revealed that the p-type conductivity is precisely proportional to $p_{O2}^{1/4}$ in the range of 10^{-4} to 1 bar oxygen partial pressure at all measured temperatures and the ionic transference number approaches 1 for low oxygen partial pressures and low temperatures.

[1] W. Lai and S. M. Haile, *J. Am. Ceram. Soc.*, 2005, **88**, 2979-2997

A6.42 WITHDRAWN

A6.43

Synthesis and Study of Solid Electrolytes $Nd_{5-x}Ln_xMo_3O_{16}$ (Ln = Sm, Eu, Gd) Lyudmyla I. Stackpool[1], Konstantin Chebyshev[2] and Lyudmila Pasechnik[2]; [1]Chemistry and Geology, Minnesota State University, Mankato, Mankato, Minnesota, United States; [2]Department of Inorganic Chemistry, Donetsk National University, Donetsk, Ukraine.

Ion transport in solids is an interesting functional property of a whole group of solid electrolytes or superionics. Size and polarizability of the ions within the structure have great influence on the transport properties. The research on these effects is an important aspect in the study of superionics.

Neodymium molybdate $Nd_5Mo_3O_{16}$ with fluorite structure has high conductivity where its oxygen component reaches 90% at 700°C. A change in the electrical conductivity of $Nd_5Mo_3O_{16}$was expected as the result of a substitution of rare-earth elements for neodymium. Therefore, in this paper the systems $Nd_{5-x}Ln_xMo_3O_{16}$, where Ln = Sm, Eu, Gd have been studied. The synthesis was carried out at a final temperature of 1050 °C with calcination for 20 hours.

According to the XRD, the substitution limits in systems $Nd_{5-x}Ln_xMo_3O_{16}$ were found within the ranges $0 \le x \le 2$ for Sm, $0 \le x \le 1$ for Eu, and $0 \le x \le 0.7$ for Gd. The increase of the additive leads to the appearance of monoclinic phase with the structure Ln_2MoO_6. Decrease in unit cell parameter as the content of lanthanide increases and shear bands of characteristic vibrations of molybdate anions in the infrared spectra toward higher wavenumbers up to 6 cm^{-1}, confirm the entry of rare-earth elements into the molybdate structure.

The crystal structure refinement shows that the lanthanide with a smaller size than neodymium, occupies the Nd (2) position. This explains that the interatomic distances Nd (1) - O and Mo – O remain virtually unchanged. The decrease in O (1) - O (1) distance increases the electrostatic repulsion, reduces the stability of the structure, and affects its conductivity. Conductivity for the limiting composition of the solid solutions is approximately three times as much as it is in $Nd_5Mo_3O_{16}$ and their activation energy of the conductivity is somewhat reduced.

A6.44

Modification of Surface Oxide of Porous Fe-Cr-Al Alloy by Coating and Heat-Treatment for the Application of Metal Supported SOFCs Hung-Cuong Pham[1], Shunsuke Taniguchi[2,3,4], Yuko Inoue[4], Jyh-Tyng Chou[5], Toru Izumi[6], Koji Matsuoka[6] and Kazunari Sasaki[1,2,7]; [1]Hydrogen Energy Systems, Kyushu University, Fukuoka, Japan; [2]International Research Center for Hydrogen Energy, Kyushu University, Fukuoka, Japan; [3]Center for Co-evolutional Social Systems, Kyushu University, Fukuoka, Japan; [4]Next-Generation Fuel Cell Research Center (NEXT-FC), Kyushu University, Fukuoka, Japan; [5]Kurume National College of Technology, Fukuoka, Japan; [6]JX Nippon Oil and Energy Corporation, Yokohama, Japan;[7]International Inst, for Carbon Neutral Energy Research (WPI-I2CNER), Kyushu University, Fukuoka, Japan.

Fe-Cr-Al alloy was investigated for the porous support material of metal supported SOFCs on the cathode side. We found that surface oxide layer of the porous Fe-Cr-Al alloy shows low electrical resistance when the porous alloy was coated with $La_{0.6}Sr_{0.4}Co_{0.2}Fe_{0.8}O_3$ (LSCF) first, and then heat-treated at 700 °C in air. Small amount of Sr included in the Al_2O_3-rich surface oxide layer may change microstructure and contribute to electronic conduction. In this study, we investigated effect of coating materials using $La_{0.8}Sr_{0.2}MnO_3$ (LSM), $LaNi_{0.6}Fe_{0.4}O_3$ (LNF), $Pr_{0.8}Sr_{0.2}MnO_3$ (PrSM), $Ba_{0.5}Sr_{0.5}Co_{0.8}Fe_{0.2}O_3$ (BSCF), $Nd_{0.8}Sr_{0.2}MnO_3$ (NdSM), $La_{0.8}Ca_{0.2}CrO_3$(LCC), or $Li_{0.025}Ni_{0.975}O$ (LNO). Relatively low contact resistances were obtained in all cases when these materials were coated on the porous alloy first, and then heat-treated at 700 °C in air. Morphology and crystal structure of the surface oxide layer of the alloy was analyzed by STEM-EDS and TEM in detail to clarify the cause of low electrical resistance.

A6.45

Crystal Structure of $R_{10}Mo_6O_{33}$ (R = Nd, Pr) from 3 K to 973 K by Neutron Powder Diffraction Yoshihisa Ishikawa[1,2], Sergey A. Danilkin[3], Maxim Avdeev[3], Valentina I. Voronkova[4] and Takashi Sakuma[2]; [1]Institute of Materials Structure Science, High Energy Accelerator Research Organization, Tokai, Japan; [2]Institute of Applied Beam Science, Ibaraki University, Mito, Japan; [3]Bragg Institute, Australian Nuclear Science and Technology Organization, Kirrawee, New South Wales, Australia; [4]Moscow State University, Leninskie Gory, Russian Federation.

Oxygen ion conductor is expected practical application for solid electrolytes and cathodes, which is included in solid oxide fuel cells (SOFCs). Since it is known that the oxygen conductivity is dependent on crystal structure such as fluorite, perovskite, and pyrochlore, it is effective to elucidate the accurate crystal structure by using X-ray and neutron diffraction. Recently, Voronkova reported the phase diagram in rare-earth molybdenum oxides. In its paper, Nd-Mo-O system has been revealed the high conductivity about 10^{-2} S/cm at 1073 K. In addition, it is suggested the structural phase transition at 923 K from temperature dependency of the bulk conductivity. As a viewpoint of crystal structure study, Martinez-Lope reported the crystal structure of $Pr_5Mo_3O_{16}$ is the fluorite-like structure by Rietveld analysis from neutron powder diffraction. Moreover, Alekseeva investigated the accurate crystal structure of $Nd_5Mo_3O_{16}$under low temperature by single crystal synchrotron X-ray diffraction. In its literature, it has been point out the splitting of Nd atom from deformation electron density distribution. In this study, to reveal the role between the rare-earth and oxygen atoms, we investigated the accurate crystal structure of $Nd_{10}Mo_6O_{33}$ and $Pr_{10}Mo_6O_{33}$ which are excess oxygen content compound by neutron powder diffraction from 3 K to 973 K. Neutron diffraction experiments were carried out using high-resolution neutron powder diffractometer ECHIDNA, which is installed at ANSTO. The wavelength was 1.60 Å, and samples were mounted on cryo-furnaces. Crystal structure analysis were performed by using Z-Rietveld and Jana2006 as the structural model described in the fluorite-like structure (space group P*n-3n*). In this presentation, we introduce and discuss the detailed structure parameters in whole temperature ranges.

A6.46

Long-Time Testing of Ni-YSZ Substrates under Operating Conditions Denis Osinkin[1], Dimitry Bronin[1,2], Robert Steinberger-Wilckens[3], L.G.J. de Haart[4] and Josef Mertens[4];[1]Laboratory of SOFC, Institution of High Temperature Electrochemistry, Yekaterinburg, Russian Federation; [2]Ural Federal University, Yekaterinburg,, Russian Federation; [3]University of Birmingham, Birmingham, United Kingdom; [4]Institute of Energy and Climate Research, Fundamental Electrochemistry (IEK-9) Forschungszentrum Jülich GmbH, Jülich, Germany.

Solid Oxide Fuel Cell anode Ni-YSZ substrates experience significant changes in their properties under SOFC anode operating conditions. These changes can be induced by solid state diffusion and by evaporation/condensation/volatilization mechanisms related to the Ni phase in the cermet. The inevitable consequences of the above mentioned processes are degradation due to Ni-phase coarsening, decrease in Ni phase content due to $Ni(OH)_2$ formation and volatilization. The present study is devoted to the characterization and description of the Ni-cermet degradation.

The long-time electrical conductivity measurements of the Ni-cermet anode substrates (Forschungszentrum Jülich GmbH) were performed by a four-probe DC method at temperatures of 700 and 800°C with the composition of the gas mixture of 80% of water and 20% of hydrogen. At such experimental conditions a strong degradation and changes as well in electrical properties as in microstructure were expected. The total gas flow rate was 5 l/h (1 and 4 l/h for hydrogen and water, respectively)

The dependence for 800ºC is described by the sum of two decaying exponential functions One decay exponent was used for the data description at 700°C. From the results of the fitting can be assumed that the degradation is higher at higher temperature. At 800°C the infinite relative resistance value (time $\rightarrow \infty$) is about 23-29% higher than the initial value and only about 1-2% higher in case of 700°C. Comparing relaxation times τ, the observed rate of degradation processes is also higher at higher temperature. One can assume from these data that the degradation is, most probably, a thermally activated process(es). In order to further clarify the possible nature of the degradation process(es) in the substrates it is necessary to examine the Ni-cermet microstructure at initial state and the time evolution of microstructure during the course of degradation.

A6.47

Carbon Deposition and Sulfur Poisoning in Mo-Containing Anode Materials for SOFCs Studied in CO and CH_4 Fuels Kun Zheng and Konrad Swierczek; AGH University of Science and Technology, Faculty of Energy and Fuels, Kraków, Poland.

Development of SOFCs fueled by non-hydrogen fuels or syngas is of high importance, as usage of such fuels, e.g. methane, can significantly reduce costs, and therefore, can accelerate commercialization of SOFC technology [1-4]. For cells running on non-hydrogen fuels, on the commonly used Ni-YSZ cermet anode, carbon deposition can occur, which considerably decreases performance and causes problems with stability. Sulfur poisoning on the anode is also detrimental, as the considered fuels usually contain sulfur impurity. Recently, $A_2MMoO_{6-\delta}$(A: Sr, Ba; M: 3d metals) perovskite-type oxides were considered as candidate anode materials for cells fueled with such fuels [1-4]. However, tolerance mechanism of carbon deposition and sulfur poisoning in these materials is still under intense research [1, 2].

In this study, Mo-containing $Sr_2Fe_{1.5-x}Mn_xMo_{0.5}O_{6-\delta}$ perovskites were proposed as novel electrode materials for symmetrical SOFCs (i.e., cells, in which identical materials are applied on anode and cathode). In such constructed cells, deposited carbon and adsorbed sulfur can be potentially removed by switching of the working mode between anode and cathode. Physicochemical and electrochemical properties of the proposed anode materials were systematically investigated, and carbon deposition, as well as sulfur poisoning tolerance were studied in CO, CH_4 gases and H_2S-containing atmospheres. Elucidation of poisoning mechanisms in $Sr_2Fe_{1.5-x}Mn_xMo_{0.5}O_6$-based anodes is also given.

The project was funded by the National Science Centre Poland (NCN) on the basis of the decision number DEC-2011/03/N/ST5/04785, and supported under the ETIUDA doctoral scholarship on the basis of the decision number DEC-2013/08/T/ST5/00100.

1. X. Ge, S. Chan, Q. Liu, Q. Sun, Adv. Energy Mater. 2 (2012) 1156.
2. Y.H. Huang, R.I. Dass, Z.L. Xing, J.B. Goodenough, Science 312 (2006) 254.
3. K. Zheng, K. Świerczek, J. Eur. Ceram. Soc. 34 (2014) 4273.
4. K. Zheng, K. Świerczek, W. Zając, A. Klimkowicz, Solid State Ionics 257 (2014) 9.

A6.48

Model-Composite Electrodes as a Tool to Evaluate Alternative SOFC Anode Materials and Their Sulphur Poisoning Behaviour Matthias Gerstl[2], Michael Doppler[1], Marco Brandner[3], Martin Bram[4], Jürgen Fleig[1] and Alexander K. Opitz[1]; [1]Electrochemistry, Vienna University of Technology, Wien, Austria; [2]Electrochemistry, Vienna University of Technology, Vienna, Austria; [3]Innovation Services, Plansee SE, Reutte, Austria; [4]Institute of Energy and Climate Research, Forschungszentrum Juelich GmbH, Juelich, Germany.

From a materials science point of view two of the most important issues in the ever advancing development of efficient solid oxide fuel cells (SOFCs) are the optimization of both electrodes. SOFC anodes still rely on nickel yttria stabilized zirconia (YSZ) cermet structures for the fuel oxidation reaction and also, in the case of hydrocarbon fuels, for steam reformation catalysis. However, minute quantities of H_2S in the fuel gas cause a dramatic increase in the anode polarization resistance of Ni/YSZ, which is only partially explained by adsorption of sulphur. Therefore, the quest is on to, on the one hand, fully understand the mechanism behind sulphur poisoning in the classic Ni/YSZ cermet electrode, which might point to ways to mitigate its adverse effects on SOFC performance. On the other hand, alternative materials may also be a way to improve sulphur tolerance and consequently lifespan of an SOFC.

In this contribution we present results of impedance spectroscopy studies on geometrically well-defined model-composite electrodes, which allow us to separate elementary processes such as ionic and electronic conductivity, chemical capacitance as well as the surface reaction resistance. Keeping the general two component system of the Ni/YSZ cermet electrode we replaced the ion conducting YSZ phase by gadolinium doped cerium oxide (GDC) and the electron conducting Ni phase by e.g. donor doped strontium titanate or buried Pt current collectors. These GDC/Pt, STO/GDC and STO/GDC/Pt model-composite electrodes could then be compared to Ni/YSZ and Ni/GDC cermets, which are more common as SOFC anodes.

Finally the effect of sulphur poisoning is evaluated regarding its impact on the surface and bulk defect chemistry in the above mentioned model systems.

A6.49

Electrical Conductivity and Redox Behavior of Donor and Acceptor Co-Substituted $SrTiO_3$ as Fuel Electrode Material Aleksey Yaremchenko, Javier Macias and Jorge Frade; CICECO, Department of Materials and Ceramic Engineering, University of Aveiro, Aveiro, Portugal.

Donor-doped strontium titanate exhibits outstanding redox stability combined with sulfur tolerance and resistance to carbon deposition, and, therefore, is considered as promising ceramic component of composite fuel electrodes for solid oxide fuel/electrolysis cells. However, its electrical conductivity is on the level of 10 S/cm under prospective operation conditions, implying significant current collection limitations. Furthermore, in-situ reduction of electrode layers often requires comparatively long treatments due to nearly frozen defect equilibrium in perovskite lattice of donor-doped $SrTiO_3$ and slow conductivity relaxation at temperatures $\leq$ 1000°C. Although high conductivity can be attained by pre-firing at high temperatures under very reducing conditions, this is probably a metastable state, undergoing long-term degradation in operating conditions. Recent computer calculations predicted that donor- and acceptor-type co-substitutions should induce mixed ionic-electronic conductivity in strontium titanate; this can be expected to facilitate the kinetics of re-equilibration on redox cycling. The present work was focused on the effect of co-substitution in $Sr_{0.85}Pr_{0.15}Ti_{1-x}A_xO_{3\pm d}$ (M = Mg, Al, Ga, Fe,…). The characterization of materials included structural and microstructural studies, electrical conductivity measurements as function of temperature, oxygen partial pressure and pre-treatment conditions, and controlled-atmosphere thermogravimetric analysis. The emphasis was on the level of electrical conductivity and redox behavior, including the relaxation of conductivity and oxygen nonstoichiometry in redox cycling.

A6.50

Chemical Compatibility of Doped Yttrium Chromite and Ceria Composite Anode with YSZ Electrolyte Kang Yan[1], Haruo Kishimoto[1], Katherine D. Bagarinao[1], Katsuhiko Yamaji[1], Teruhisa Horita[1] and Harumi Yokokawa[1, 2]; [1]National Institute of Advanced Industrial Science and Technology, Tsukaba, Japan; [2]the University of Tokyo, Tokyo, Japan.

$Y_{0.8}Ca_{0.2}Cr_{0.8}Co_{0.2}O_3$ (YCCC) oxide is one of potential anode materials for using coal syngas as fuel in SOFC, because it has high electrical conductivity, high redox-stability and good tolerance to S-poisoning. However, similar to the well-known chromite-based materials $La_{0.7}Ca_{0.3}CrO_3$ (LCC), the YCCC has chemical reaction with electrolyte of

Yttrium Stabilized Zirconia (YSZ), which would degrade its anode performance. In this study, by mixing with ceria $Ce_{0.9}Gd_{0.1}O_{1.95}$ (GDC), we find that a certain amount of ceria can suppress the interfacial reaction between YCCC and YSZ. It is explained based on cation diffusion and various reaction activities between the different compounds.

The chemical stability and the anode performance of the YCCC-GDC composite with different YCCC/GDC ratio are investigated. For pure YCCC anode, the YCCC reacts with YSZ and forms $CaZrO_3$ at their interface during the cell fabrication at high temperature in air. On the other hand, for the YCCC-GDC composite anode, the GDC and YCCC mixing particles constitute anode frameworks with a large amount of triple phase boundary (TPB) and show no reaction with YSZ electrolyte. The GDC in this composite not only prevent the interfacial reaction between YCCC and YSZ, but also improves the catalytic activity of anode, and thus leads to large performance enhancement.

A6.51

In Search for Alternative Ceramic Components for SOFC Anodes: $SrVO_3$-$SrTiO_3$ Solid Solutions Javier Macias, Aleksey Yaremchenko and Jorge Frade; Department of Materials and Ceramic Engineering, University of Aveiro, Aveiro, Portugal.

Limitations of conventional Ni-based solid oxide fuel cell (SOFC) cermets anodes, such as microstructural instability, or fast coking and sulfur poisoning in hydrocarbon fuels, motivate the search for alternative anode components, and, in particular, ceramic materials mostly based on perovskite-like phases. Strontium vanadate and strontium titanate were demonstrated to exhibit a good sulfur tolerance and resistivity to carbon deposition. Perovskite phase of strontium vanadate has however a limited stability domain, while donor-doped strontium titanates exhibit high electronic conductivity only when reduced at high temperatures; pre-reduced anode layers may undergo a long-term degradation under operation conditions. The present work focused on $SrVO_3$-$SrTiO_3$ system aiming to find a compromise between high electrical conductivity of vanadate and high stability of titanate lattice.
$SrV_{1-x}Ti_xO_{3\pm d}$ (x = 0-1.0) ceramics were prepared by solid-state synthesis assisted with high-energy milling, and sintered in 10%H_2-N_2 atmosphere. XRD analysis confirmed the formation of single-phase materials with cubic perovskite structure for entire compositional range. The characterization of ceramic materials included structural and microstructural studies, measurements of electrical properties as function of temperature and oxygen partial pressure, controlled-atmosphere thermogravimetry and dilatometry. The emphasis was on the properties relevant for SOFC anode applications including the level of electrical conductivity under operation conditions, thermomechanical compatibility with solid electrolyte materials, and redox behavior on cycling between reducing and inert or oxidizing atmospheres.

A6.52

Electrochemically Modified, Robust Solid Oxide Fuel Cell Anode for Direct-Hydrocarbon Utilization Yoonseok Choi and WooChul Jung; Materials Science and Engineering, Korea Advanced Institute of Science and Technology, Daejeon, Korea (the Republic of).

A main advantage of solid oxide fuel cells (SOFCs) operating at high temperature (>650°C) is their fuel flexibility, specifically the possibility of utilizing methane (natural gas). Unfortunately, however, the state-of-the-art SOFC anode, composed of nickel and an aniodically conducting oxide such as yttria-stabilized zirconia (YSZ), suffers from Ni-catalyzed carbon deposition and resulting degradation of anode performance. Here, we address these issues through the application of a simple, cost-effective ceramic coating method—cathodic electrochemical deposition (CELD). Samaria-doped ceria (SDC) was chosen as a coating material due to its high chemical stability against carbon formation, high electronic and ionic conductivities, and favourable electrocatalytic activity toward fuel oxidation reaction. Nanostructured SDC layers with high surface area were successfully obtained on Ni surfaces. The physical attributes of each coatings were characterized by a diversity of analysis tools—SEM, TEM, XRD, and EDS, ICP-MS and Raman spectroscopy. Significantly enhanced electrode conductance and coking stability were found by electrochemical impedance spectroscopy (EIS) under wet methane fuel (2% H_2O) at 650°C with well-defined Ni patterned YSZ symmetric cells (anode/electrolyte/anode) with the SDC coatings. These results suggest that Ni-surface modification using CELD can be a feasible solution for directly utilizing hydrocarbon fuels in SOFCs.

A6.53

Effect of Fuel Thermal Pretreatment on the Electrochemical Performance of a Direct Lignite Coal Fuel Cell Nikolaos Kaklidis[1], Vasileios Kyriakou[3, 2], George Marnellos[1, 2], Ana Arenillas[4] and Michalis Konsolakis[5]; [1]Department of Mechanical Engineering, University of Western Macedonia, Kozani, Greece; [2]Chemical Process & Energy Resources Institute, Centre for Research & Technology Hellas, Thessaloniki, Greece; [3]Department of Chemical Engineering, Aristotle University of Thessaloniki, Thessaloniki, Greece; [4]Instituto Nacional del Carbon, Oviedo, Spain; [5]School of Production Engineering and Management, Technical University of Crete, Chania, Greece.

Introduction

Coal is considered an abundant and widely distributed natural resource, currently accounting for more than 30% of global energy consumption [1]. Direct Carbon Fuel Cells (DCFC) are electrochemical devices, which can directly convert the chemical energy bound in carbon to electricity at almost 100% theoretical efficiency leading to lower coal consumption and CO_2emissions per produced kW [2].
Recently, it has been found that the chemical and physical properties of carbon fuels can notably affect the electrochemical performance. For instance, volatile matter and structure disorder greatly enhanced the achieved DCFC performance, whereas ash and sulphur contents have a detrimental effect on cell characteristics [1]. In this regard, acid and heat treatment are usually applied to modify the carbon characteristics and in consequence the DCFC performance. Moreover, by following this approach fundamental insights on the carbon properties-performance correlation can be obtained [1, 2].

In the present communication, the effect of fuel heat pretreatment on DCFC characteristics is investigated. Several parameters related to purging gas type (inert He or reactive CO_2) and molten carbonates infusion into the carbon feedstock were also examined. Lignite, a coal of particular importance for many European countries economies, is employed as fuel.

Experimental

The electrochemical measurements were carried out in a cell consisted of an YSZ tube as electrolyte, in the temperature range of 700-800°C at atmospheric pressure. Ag was used as cathode, while the anode was consisted of Co/CeO_2. Lignite was imposed to three different thermal pretreatments under pure He atmosphere (30 cm^3/min): a) 200°C overnight, b) 500°C for 1 h and c) 800°C for 1 h. Then, all lignite samples were tested either as received (DCFC mode) or by ad-mixing them with an eutectic mixture of carbonates (62mol% Li_2CO_3 + 38mol% K_2CO_3) at a lignite to carbonates weight ratio of 4:1 (Hybrid Carbon Fuel Cell, HCFC mode). The AC impedance spectra were acquired under open circuit conditions in the frequency range between 0.1 Hz and 1 MHz with an amplitude of 30 mV RMS.

Results and Discussion

The proximate and ultimate analysis of the as delivered and pretreated lignite samples showed that upon increasing the pretreatment temperature the carbon content is monotonically increased, whereas the volatile matter, H_2O, sulphur and oxygen contents are decreased. These modifications are reflected on the achieved DCFC performance, which is clearly improved upon increasing treatment temperature.

A similar trend was also observed under HCFC mode of operation. In that case, however, a superior electrochemical performance was observed in relation to DCFC mode. When carbonates are infused to lignite feedstock, the power output is enhanced up to 100%, depending on fuel pre-treatment and temperature. AC impedance spectroscopy measurements were also acquired at conditions identical to those employed in fuel cell experiments to interpret the impact of feedstock heat treatment and characteristics on overall cell and electrode resistances and as a consequence on DCFC performance.

Conclusions
The obtained results clearly reveal that lignite thermal treatment significantly modifies fuel physicochemical characteristics, which then is reflected on the DCFC power output. The results are well interpreted on the basis of AC impedance spectroscopy measurements.

References
[1] N. Kaklidis, V. Kyriakou, I. Garagounis, A. Arenillas, J.A. Menendez, G.E. Marnellos, M. Konsolakis, RCS Advances 4 (2014) 18792-18800.
[2] T.M. Gür. Chem. Rev. 113 (2013) 6179–6206.

SESSION A7: SOFC
A: Solid Oxide Fuel Cells and Electrolyzers
Chair: Stephen Skinner
Wednesday Morning, June 17, 2015
Keystone Resorts, Longs Peak

10:30 AM **A7.01
SOFC Cathode Oxygen Reduction Reaction Mechanisms under Real World Conditions Eric D. Wachsman, Y. L. Huang, C. Pellegrinelli, J. A. Taillon and L. G. Salamanca-Riba; University of Maryland Energy Research Center, University of Maryland, College Park, Maryland, United States.

Cathode polarization and its increase with time are widely regarded to be the key issue hindering solid oxide fuel cell (SOFC) commercialization. Numerous investigations of the rate limiting oxygen reduction reaction (ORR) have provided mechanistic insight; however, they have typically been performed at conditions that do not represent real world SOFC cathode conditions, such as lower temperature, oriented thin films (vs. random surface porous microstructures), and pure gas (vs. with H_2O, CO_2, and other ambient contaminants). In order to understand the various mechanistic contributions to cathode polarization and apply this knowledge to development of lower-polarization and higher durability SOFC cathodes, we have embarked on a multi-faceted, multi-disciplinary approach to deconvolute the various contributions to SOFC cathode polarization.

To study the ORR mechanism and the effects of ambient gas composition on ORR, we used in-situ ^{18}O isotope exchange techniques to probe the exchange of H_2O and CO_2 with two of the most common SOFC cathode materials, $(La_{0.8}Sr_{0.2})_{0.95}MnO_{3-x}$ (LSM) and $La_{0.6}Sr_{0.4}Co_{0.2}Fe_{0.8}O_{3-x}$ (LSCF). In these experiments, heavy water, D_2O (with a mass/charge ratio of m/z=20), was used to avoid the overlapping of the H_2O and the $^{18}O_2$ cracking fraction, which both have a peak at m/z=18. A series of temperature programmed isotope exchange measurements were performed to comprehensively study the interaction of H_2O and CO_2 with the cathode surface as a function of temperature, oxygen partial pressure, and contaminant gas concentration. The experimental data are summarized in a Temperature-P_{O2} diagram to visualize the dominant reactions at each temperature and P_{O2} for the two cathode materials.

We also used FIB/SEM to quantify the cathode microstructure in terms of tortuosity and porosity for gas diffusion, solid-phase surface area for gas adsorption/surface diffusion, and triple phase boundaries for the charge transfer reaction and how these evolved with time and contaminant exposure. These results were then combined (and contrasted) with the more conventional electrochemical polarization techniques (impedance spectroscopy and I-V behavior) to try and elucidate each of the mechanisms as a function of cathode composition and microstructure and ambient gas composition. The progress to date on this investigation will be presented.

11:00 AM A7.02
Correlation Between Cation Ordering and Oxygen Vacancies in Layered Double Perovskite Cathodes Carlos Bernuy-Lopez, Mari-Ann Einarsrud and Tor Grande; NTNU, Trondheim, Norway.

Mixed ionic electronic conductors (MIEC) are materials which have the ability to conduct both ionic and electronic charge carriers. This particular property opens up for numerous applications at high and intermediate temperatures (500-800 ºC) such as selective gas separation membranes or electrode materials for solid oxide fuel cells and electrolysers[1,2]. One family of materials that has attracted a lot of attention in recent years is the layered double perovskites with general formula $LnBaM_2O_{5+\delta}$ (*Ln* = La, Pr, Y or Gd; M = Mn, Fe, Co) due to their promising properties as MIEC[3]. The structure of $LnBaM_2O_{5+\delta}$ consists of *Ln*-O and Ba-O layers alternately stacked along the c-axis with oxygen vacancies in the *Ln*-O layer. The oxygen content in these materials can vary significantly ($0 \leq \delta \leq 1$) depending on the nature on the *Ln* cation, synthesis atmosphere and thermal history. At the same time, the cation ordering also seems to be influenced by the same conditions. It is also known that the equivalent family of disordered perovskite materials with the general formula $Ln_{0.5}Ba_{0.5}MO_{3-\delta}$ can also be obtained by a different synthesis path, which normally results in a significant change in their MIEC properties relative to the ordered counterparts. However, the correlation between the cation ordering and oxygen vacancy ordering at the operating temperatures is still unclear. This work focusses on a particular ordered layered double perovskite material, $LaBaCo_2O_{5+\delta}$, and its equivalent disordered form, $La_{0.5}Ba_{0.5}CoO_{3-\delta}$ by *in situ* high temperature X-Ray diffraction and thermogravimetrical analysis in various partial pressures of oxygen in order to correlate the cation ordering with oxygen non-stoichiometry. Likewise, the crystal structure and oxygen non-stoichiometry is correlated to the conductivity of the materials.

References
1. U. Balachandran, B. Ma, P. S. Maiya, R. L. Mieville, J. T. Dusek, J. J. Picciolo, J. Guan, S. E. Dorris and M. Liu, *Solid State Ionics*, **1998**, 108, 363-370.
2. A. Esquirol, N. P. Brandon, J. A. Kilner and M. Mogensen, *Journal of the Electrochemical Society*, **2004**, 151, A1847-A1855.
3. S. Sengodan, S. Choi, A. Jun, T. H. Shin, Y.-W. Ju, H. Y. Jeong, J. Shin, J. T. S. Irvine and G. Kim, *Nature Materials*, **2014**, advance online publication. doi:10.1038/nmat4166.

11:20 AM A7.03
Fabrication and Performance of Stainless Steel-Supported SOFC Kun Joong Kim, Byung Hyun Park, Sun Jae Kim and Gyeong Man Choi; Mat. Sci. & Eng., POSTECH, Pohang, Korea (the Republic of).

Metal-supported solid oxide fuel cells (SOFCs) are expected to provide high mechanical strength and thermal-shock resistance and thus promise stable performance at intermediate temperature. In this study, we have designed and fabricated thin-film SOFCs supported on porous stainless-steel (STS). We used tape-casting to fabricate a thick-film support, and pulsed laser deposition to fabricate the thin-film SOFCs. A composite of nano-porous $(La,Sr)(Ti,Ni)O_3$ conductor and electrolyte is applied as a contact layer between the macro-porous STS and the thin-film SOFCs. Excellent electrochemical performance at or below 550ºC and thermal cycling ability for this SOFCs were shown and will be further discussed.

11:40 AM A7.04
Cobalt-Free Polycrystalline $Ba_{0.95}La_{0.05}FeO_{3-\delta}$ Thin Films as Cathodes for Intermediate-Temperature Solid Oxide Fuel Cells Francesco Ciucci[1, 2], Chi Chen[1] and Dengjie Chen[1];[1]Mechanical and Aerospace Engineering, The Hong Kong University of Science and Technology, Kowloon, Hong Kong; [2]Chemical and Biomolecular Engineering, The Hong Kong University of Science and Technology, Kowloon, Hong Kong.

Solid oxide fuel cells (SOFCs) are devices that can convert chemical energy to electricity directly with advantages are efficient, distributable and environmental-friendly. Here, we fabricate perovskite single crystal thin films as cathodes with the composition of $Ba_{0.95}La_{0.95}FeO_{3-\delta}$ (BLF) by pulsed laser deposition (PLD) on yttria-stabilized zirconia (YSZ) substrates. Sm-doped Ceria (SDC) is deposited between YSZ and perovskite thin films in this study as an interlayer. The phase structure, surface morphology and roughness of the BLF thin films are characterized by X-ray diffraction and atomic force microscopy. X-ray photoelectron spectroscopy is used to analyze the elemental composition and chemical state of the deposited thin film. Electrochemical impedance spectra

measurements obtained from the symmetric cells with the configuration of BLF /SDC/YSZ/SDC/ BLF reveal that polarization resistance of BLF (001) thin films (100 nm) is as low as ~0.1 Ω cm^2 at 700 °C and 0.21 atm oxygen pressure. The polarization resistances of BLF are lower than those of other perovskite electrodes, e.g., $La_{0.6}Sr_{0.4}Co_{0.8}Fe_{0.2}O_{3-\delta}$. Furthermore, our computational results, including density functional theory and molecular dynamics simulations, show that the BLF is characterized by low vacancy formation energy and fast oxygen transport.

[1] D. Chen, C. Chen, F. Dong, Z. Shao, F. Ciucci, J. Power Sources, 250, 188-195 (2014)
[2] C. Chen, D. Chen, Y. Gao, Z. Shao, & F. Ciucci. J. Mater. Chem. A, 2, 14154-14163 (2014)

SESSION A8: SOEC
A: Solid Oxide Fuel Cells and Electrolyzers
Chair: Steven McIntosh
Thursday Morning, June 18, 2015
Keystone Resorts, Longs Peak

10:30 AM **A8.01
Prospects and Challenges of Solid Oxide Electrolysis Peter V. Hendriksen[1], Ming Chen[1], Ragnar Kiebach[1], Xiufu Sun[1], Karsten Agersted[1], Yi-Lin Liu[1], Sebastian Molin[1], Sune D. Ebbesen[1], Christopher Graves[1], Anne Hauch[1], Karen Brodersen[1], Mogens B. Mogensen[1], Johan Hjelm[1], Soren H. Jensen[1], Christodoulos Chatzichristodoulou[1] and Brian V. Mathiesen[2];[1]Department of Energy Conversion and Storage, Technical University of Denmark, Roskilde, Denmark; [2]Department of Development and Planning, Aalborg University, Copenhagen SV, Denmark.

Concerns to reduce future adverse effects on the global climate have led to increased focus on means to reduce anthropogenic CO_2 emission. The amount of electricity generated from renewable and intermittent energy sources (e.g. wind and sun) is consequently likely to increase globally in the coming decades. High temperature electrolysis of CO_2 and/or H_2O using solid oxide electrolysis cells (SOECs) has the potential to become a key technology in enabling reduced emissions by providing an energy efficient way to "store" electricity from periods of surplus production. The energy can, in the form of gaseous or liquid hydrocarbon fuels produced from the electrolysis products, be transferred to the transport sector, where emission reduction is especially difficult.

In this presentation we discuss the prospects of the SOEC technology for enabling larger shares of intermittent electricity production in the energy system and give examples from scenario analyses of its role in a future energy system based on 100 % renewable energy.

Whereas state of the art SOFCs have been shown to be fully reversible, there are important differences between SOFC and SOEC operation in terms of degradation phenomena. Highlights from the technical SOEC R&D at DTU Energy will be presented including a status on achieved cell durability and cell operation under high pressure. Problems in terms of life time limiting degradation phenomena during SOEC operation will be discussed in detail based on own findings and literature. This will cover both microstructural degradation phenomena at electrode and cell level as well as phenomena occurring in stacks, specifically related to the interconnects. It will be illustrated how detailed modeling of the chemical potential profiles over the cells and interconnects can be useful in unravelling which processes contribute to the observed performance degradation during long term operation.

11:00 AM A8.02
Surface and Bulk Properties of Polarized Mixed Conducting LSF Electrodes: An in-situ Study in H_2/H_2O and O_2 by Simultaneous near-Ambient Pressure XPS and Impedance Spectroscopy Alexander K. Opitz[1], Andreas Nenning[1], Sandra Kogler[1], Christoph Rameshan[2], Raffael Rameshan[3, 4], Raoul Blume[4, 5], Michael Haevecker[4, 5], Axel Knop-Gericke[4], Guenther Rupprechter[2], Bernhard Kloetzer[3] and Juergen Fleig[1]; [1]Insititute of Chemical Technologies and Analytics, Vienna University of Technology, Vienna, Austria; [2]Institute of Materials Chemistry, Vienna University of Technology, Vienna, Austria; [3]Institute of Physical Chemistry, University of Innsbruck, Innsbruck, Austria; [4]Department of Inorganic Chemistry, Fritz Haber Institute of the Max Planck Society, Berlin, Germany; [5]Catalysis for Energy, Group E-GKAT, Helmholtz-Zentrum Berlin fuer Materialien und Energie GmbH, Berlin, Germany.

Mixed ionic and electronic conductors (MIECs) find applications in a wide range of oxygen partial pressures and in numerous electrochemical devices. For example, in solid oxide electrolysis cells (SOEC) reduction stable MIECs are an attractive alternative to the presently used Ni/YSZ SOEC cathodes.

In this study the acceptor doped mixed conductor $La_{0.6}Sr_{0.4}FeO_{3-\delta}$ (LSF) was investigated as an SOEC cathode in H_2/H_2O atmosphere and electrochemical properties such as surface exchange resistance are compared to those of LSF in air. Model-type LSF thin film electrodes were prepared on YSZ and the relatively poor electronic conductivity of LSF under reducing conditions was compensated by Pt current collectors beneath the MIEC thin film.

On these model-composite electrodes the relation between surface chemistry and electrochemical surface activity was investigated by means of simultaneous synchrotron-based near-ambient-pressure XPS and impedance spectroscopy. Special focus was laid on the effect of electrochemical polarization on the composition and valence states of near surface cations of the LSF electrodes. Cathodic polarization (i.e. water splitting conditions) caused the evolution of metallic iron on the LSF surface, which was accompanied by a strong decrease of the electrode polarization resistance for the water splitting reaction [1]. This correlation suggests a fundamental difference in the water-splitting mechanism on LSF with and without near-surface metallic iron and may provide new paths in the search for novel mixed conducting SOEC electrode materials. Moreover, the XPS binding energy shift of different cations under electrochemical polarization is discussed in terms of bulk defect chemistry of LSF.
[1] A. K. Opitz et al., Angewandte Chemie International Edition 54 (2015), p.2628–2632.

11:20 AM A8.03
Infiltrated Double Perovskite Electrodes for Proton Conducting Steam Electrolysers Einar Vollestad, Ragnar Strandbakke and Truls Norby; Department of Chemistry, University of Oslo, Oslo, Norway.

The oxygen side electrode remains a major challenge in the development of cost efficient and durable high temperature ceramic proton conducting fuel and electrolyser cells. This is due to the scarce availability of mixed proton electron conductors with high conductivities, high catalytic activity, and chemical stability. Composite electrodes comprising a proton conducting phase and an electronically conducting active electrode component are therefore necessary to increase the active area and the amount of triple phase boundaries
.
In this contribution, we present structures of porous $BaZr_{0.7}Ce_{0.2}Y_{0.1}O_3$ (BZCY72) backbones applied using both spray coating and brush painting, infiltrated with the double perovskite $BaGd_{0.8}La_{0.2}Co_2O_{6-\delta}$ (BGLC) as the active electrode component. The infiltrated structures form a percolating nanoscopic layer of BGLC, finely distributed throughout the electrode structure. The electrodes are tested as oxygen side electrodes by impedance spectroscopy as a function of temperature and pO_2. The electrodes display area specific resistances of ~1 Ωcm^2at 600 °C in wet air. Extracted polarization resistances are fitted to a model resolving partial polarization resistances for protons and oxide ions in a system of multiple charge carriers [1]. From these resistances combined with parameterized morphology of the backbone structure, we can identify how the electrode microstructure influences both ohmic and polarization resistances and thus find various routes for further improvement of the electrode performance.

References:
[1]: R Strandbakke, V Cherepanov, A Zuev, D. S. Tsvetkov, C Argirusis, G Sourkouni, S Prünte, T Norby: Gd- and Pr-based double perovskite cobaltites as oxygen electrodes for proton ceramic fuel cells and electrolyser cells (under publication).

11:40 AM A8.04
Compositional Engineering of Perovskite Oxides for Highly Efficient Oxygen Reduction Reactions Chi Chen[1], Dengjie Chen[1], Zongping Shao[2] and Francesco Ciucci[1]; [1]Mechanical and Aerospace Engineering, Hong Kong University of Science and Technology, Kowloon, Hong Kong; [2]Nanjing Tech University, Nanjing, China.

Mixed conducting perovskite oxides are promising catalysts for high-temperature oxygen reduction reaction. Pristine $SrCoO_{3-\delta}$ is a widely used parent oxide for the development of highly active mixed conductors. Doping a small amount of redox-inactive cation into the B site (Co site) of $SrCoO_{3-\delta}$ has been applied as an effective way to improve physico-chemical properties and electrochemical performance. Most findings however are obtained only from experimental observations and no universal guidelines have been proposed. In this work, combined experimental and theoretical studies are conducted to obtain fundamental understanding of the effect of B-site doping concentration with redox-inactive cation (Sc) on the properties and performance of the perovskite oxides. The phase structure, electronic conductivity, defect chemistry, oxygen reduction kinetics, oxygen ion transport and electrochemical reactivity are experimentally characterized. In-depth analysis of doping level effect is also undertaken by first-principles calculations. Among the compositions, $SrCo_{0.95}Sc_{0.05}O_{3-\delta}$ shows the best oxygen kinetics and corresponds to the minimum fraction of Sc for stabilization of the oxygen-vacancy-disordered structure. The results strongly support that B-site doping of $SrCoO_{3-\delta}$ with a small amount of redox-inactive cation is an effective strategy towards the development of highly active mixed conducting perovskites for efficient solid oxide fuel cells and oxygen transport membranes.

SESSION A9: SOFC—Electrolytes II, Anodes
A: Solid Oxide Fuel Cells and Electrolyzers
Chairs: John Irvine and Manfred Martin
Thursday Afternoon, June 18, 2015
Keystone Resorts, Longs Peak

1:30 PM *A9.01
Oxide Ion Conductivity in Doped $LnBaInO_4$(Ln=La, Nd) Tatsumi Ishihara[1], Yu Yan[2], Takaaki Sakai[2] and Shintaro Ida[2]; [1]International Institute for Carbon Neutral Energy Research, Kyushu University, Fukuoka, Japan; [2]Department of Applied Chemistry, Faculty of Engineering, Kyushu University, Fukuoka, Japan.

Oxide ion conductor is an important material for electrolyte of fuel cell or sensor. At present, Y_2O_3 stabilized ZrO_2 is widely used as oxide ion conductor. However, because of insufficient conductivity, higher operating temperature is required. On the other hand, perovskite oxide is attracting much attention as a new oxide ion conductor. In particular, perovskite with defect oxygen structure like K2NiF4 or double perovskite oxide is highly expected as a new fast oxide ion conductor. However, because of high electronic or hole conduction, there are limited number of oxide showing pure oxide ion conductivity. Recently, it is reported that $NdBaInO_4$ has a unique crystal structure, i.e., perovskite unite is rotated 45 degree and parallel to rock salt unit. Therefore this oxide has straight oxygen diffusion route in K2NiF4 structure and high oxygen diffusivity is expected. In this study, effects of dopant in $NdBaInO_4$ oxide were studied. The electrical conductivity was much increased by doping higher valence cation into In site. Among the examined dopant, it was found that Ti^{4+} is the most effective for increasing electrical conductivity. The highest electrical conductivity was achieved at $NdBaIn_{0.75}Ti_{0.25}O_4$ and the conductivity is achieved to $\log(\sigma/Scm^{-1})$ =-2.5 at 1173 K. P_{O2} dependence of conductivity suggests that hole and electron conductivity was slightly observed in high and low P_{O2} range, respectively, however, conductivity is almost independent of P_{O2} suggesting dominant oxide ion conductivity. In fact, the estimated oxide ion transport number by H_2-O_2 cell is higher than 0.8. Effects of dopant on Nd site and also Ba site will be reported. As a result, this study revealed that doped $NdBaInO_4$ is a new class of oxide ion conductor.

1:50 PM A9.02
Double Perovskite Oxide $Sr_2FeMo_{2/3}Mg_{1/3}O_6$ as Redox Stable Anode Material for Solid Oxide Fuel Cells Zhihong Du, Hailei Zhao, Yang Zhang and Mengya Fang; University of Science and Technology Beijing, Beijing, China.

Double perovskite Sr_2FeMoO_6 shows recently excellent performance as anode material for solid oxide fuel cells (SOFCs), including the required chemical stability, electronic and ionic conductivity, electrocatalytic activity as well as high tolerance to carbon deposition and sulphur poisoning. However, it suffers from decomposition badly in oxidizing atmosphere, thus extra attentions must be paid on cells fabrication, cells start-up and shut-down and the fault conditions. It is very meaningful to explore redox stable anode materials.

In this work, in order to get a redox stable anode material, we substitute the divalent element Mg for Mo to produce a novel double perovskite $Sr_2FeMo_{2/3}Mg_{1/3}O_6$ (SFMM) The detailed structural chemistry of this material is earnestly investigated to unveil the structure-property relationship. High resolution TEM, selected area electron diffraction and high temperature XRD results show that it adopts a B site ordered double perovskite structure with visible antisite defects and suitable thermal expansion coefficient ($16\text{-}17\times10^{-6}$ K^{-1}). The reversible transformation of conduction behavior from *p*-type in air to *n*-type in reducing atmosphere is demonstrated by electrical conductivity tests and first-principles calculation. ECR study reveals the fast oxygen surface exchange kinetic process (rate constants, k = ~1×10^{-5} cm s^{-1}). The LSGM electrolyte (about 300 μm) supported single cell with SFMM as anode and $La_{0.58}Sr_{0.4}Co_{0.2}Fe_{0.8}O_3$ as cathode shows a very promising cell performance. The maximum power density in H_2 reaches 866 and 1044 mW cm^{-2} at 850 and 900 °C, respectively. All these results indicate that $Sr_2FeMo_{2/3}Mg_{1/3}O_6$ is a very promising candidate anode material for SOFCs.

2:10 PM A9.03
Structural and Transport Properties of Doped LAMOX - Electrolytes for IT SOFC Svetlana Pavlova[1], Yuliya Bespalko[1], Vladislav Sadykov[1], Vladimir Pelipenko[1], Nikita Eremeev[1], Tamara Krieger[1], Yurii Chesalov[1], Ekaterina Sadovskaya[1], Artem Ulihin[2], Nikolai Uvarov[2] and Alevtina Smirnova[3]; [1]Boreskov Institute of Catalysis SB RAS, Novosibirsk, Russian Federation; [2]Institute of Solid State Chemistry SB RAS, Novosivirsk, Russian Federation; [3]South Dakota School of Mines and Technology, Rapid City, South Dakota, United States.

Doped $La_{2-x}R_xMo_{2-y}W_yO_9$ (LAMOX) (R= Bi, Gd, Pr, Sm, Nd; x=0-0.5, W=0.5-1) were synthesized via polymerized precursors method or mechanochemical activation. The structural properties of doped LAMOX were studied by thermal analysis, XRD, SEM, IR and Raman spectroscopy. Transport properties were characterized using impedance spectroscopy and isotope temperature–programmed exchange with $C^{18}O_2$ including SSITKA. It has been revealed that doping prevents phase transition from a cubic form of high conductivity to a monoclinic phase of low conductivity at about 580 °C. For all substituted cations in La-position, well-crystalline cubic β-phase stable at low temperatures is formed from polymerized precursors at 700°C calcination except Bi. Single phase of cubic W-doped LAMOX is formed after calcination of MA products at 700-900°C depending on W concentration. High dispersion of doped LAMOX powders obtained via low-temperature synthesis allows the production of ceramics with the density of 92-95% after annealing at 950°C. If the total conductivity of $La_2Mo_2O_9$ shows a sharp decrease at around 570 °C due to phase transition, for all doped LAMOX conductivity changes continuously with temperature rising due to stabilization of cubic phase at low temperature. In the range of 300-480°C, it can be satisfactorily fitted by a conventional Arrhenius-type law with the activation energy (E_a) 1.2-1.5 eV. The conductivity deviation from linearity observed at temperatures higher than 450 °C evidences the transition of conduction mechanism toward an empirical Vogel-Tammann-Fulcher (VTF) regime with E_a=0.045 eV. Comparison of the oxygen self-diffusion coefficients (D_0) obtained from the results of SSITKA and conductivity measurements (at 600 K ~$3*10^{-13}$ cm^2/s and $3*10^{-12}$ cm^2/s, correspondingly) shows, in the first approximation, a reasonable agreement. The lower D_0 of SSITKA could be due to incorporation of carbonate groups at low temperatures into the surface layers of LAMOX thus decreasing oxygen mobility.

Support by EC 7th Framework Program within TheBarCode Project is gratefully acknowledged

2:30 PM A9.04
Ubiquitous Current Constriction Impedance in Oxide Ion Conductors Described by Capacitance Spectroscopy Young-Hun Kim[1], Su-Hyun Moon[1], Dong-Chun Cho[1], Eui-Chol Shin[1], Ji Haeng Yu[3], Jong-Ho Lee[2] and Jong-Sook Lee[1]; [1]Materials Science and Engineering, Chonnam National University, Gwangju, Korea (the Republic of); [2]Korea Institute of Science and Technology, Seoul, Korea (the Republic of); [3]Korea Institute of Energy Research, Daejeon, Korea (the Republic of).

Space charge layers along the grain boundaries where the oxygen vacancy charge carriers are depleted have been considered responsible for the increase in resistance in polycrystalline oxide ion conducting solid electrolytes, representatively, YSZ, LSGM, GDC and also lanthanum silicates in apatite structure. Generally overlapped circular responses have been described by the resistors and constant phase elements connected respectively in parallel. The temperature dependence of AC characteristics of YSZ, LSGM and apatite clearly suggest the current-constriction effects by the grain boundaries, which should be distinguished from the electrode effects, which generally exhibits different activation energy values. Despite the strong frequency dispersion shown in the individual spectra, several characteristic capacitance plateaus are indicated in the series of Bode plots. The overall AC response can be described by Cole-Davidson dielectric functions in parallel to the total sample resistance (including the grain boundary effects). The CD functions represent the respective capacitance magnitudes observed in Bode plots and all the relaxation time constants exhibit the same activation energy as the bulk conduction. The frequency dispersions in the high frequency region are either characteristic of the universal dielectric response in the bulk or represent the particular material system and microstructure for the current-constriction effects. Temperature and frequency dependence of the polycrystalline oxide ion conductors can be thus described by a set of well-defined parameters. The present approach is thus suggested to be by far the most physically based impedance model for the polycrystalline oxide ion conductors with current constriction effects.

2:50 PM A9.05
Factors Impacting Chemical Expansion in Perovskite Oxides Nicola H. Perry[1, 2], Dario Marrocchelli[3], Harry L. Tuller[2, 1] and Sean R. Bishop[2, 1]; [1]I2CNER, Kyushu University, Nishi-ku, Fukuoka, Japan; [2]Materials Science and Engineering, MIT, Cambridge, Massachusetts, United States; [3]Nuclear Science and Engineering, MIT, Cambridge, Massachusetts, United States.

Stoichiometric chemical expansion represents the gradual lattice dilation accompanying small changes in (non-integer) chemical stoichiometry. *In operando* expansion and contraction of mixed ionic and electronic conducting perovskites often arises from a change in their oxygen content and a corresponding change in the sizes of multivalent cations. These chemical strains and the stresses generated are large enough in brittle ceramics to cause mechanical failure of devices such as solid oxide fuel/electrolysis cells. While factors have been identified to tailor chemical expansion in the fluorite structure, less has been known about how to controllably manipulate the chemical expansion coefficients of perovskites.In the present work [1] we investigated the chemical expansion of perovskite oxides at an atomistic level, by density functional theory and molecular dynamics calculations, in order to understand the lattice distortions taking place upon changing the oxygen content and the size of the A-site or B-site cations. Furthermore, we developed an empirical model relating the size of constituent ions, including that of an oxygen vacancy, to the measured or simulated chemical expansion. From these results it appears that the effective size of an oxygen vacancy in perovskite oxides varies considerably, though in most cases it is slightly smaller than or equal in size to an oxygen ion. From our additional experimental measurements of chemical expansion in model gallate and titanate systems [2-4] it is clear that, beyond the effective oxygen vacancy size, many other factors can impact the magnitude of chemical expansion in the more complex perovskite structure, including: charge localization, temperature, and crystal symmetry. Each of these will be discussed as a potential variable to tune in order to control chemical expansion coefficients of perovskites.

[1] D. Marrocchelli*, N.H. Perry* (equal contribution), and S.R. Bishop, "Understanding Chemical Expansion in Perovskite Oxides," (under review at *Phys. Chem. Chem. Phys*.)
[2] N.H. Perry, J.E. Thomas, D. Marrocchelli, S.R. Bishop, and H.L. Tuller, *ECS Trans.* 57 (1) (2013) 1879-1884
[3] N.H. Perry, S.R. Bishop, and H.L. Tuller, *J. Mater. Chem. A* 2 (2014) 18906-18916
[4] N.H. Perry, J.J. Kim, S.R. Bishop, and H.L. Tuller, *J. Mater. Chem. A* 3 (2015) 3602-3611

3:10 PM BREAK

3:30 PM *A9.06
Sintering-Resistant Metal Nanoparticles for High Temperature Electrocatalysis Yoonseok Choi, Siwon Lee and WooChul Jung; DMSE, KAIST, Daejeon, Korea (the Republic of).

Metal nanoparticles are of significant importance for chemical and electrochemical catalysis due to their high surface-to-volume ratio and possible unique catalytic properties. However, the poor thermal stability of nano-sized particles typically limits their use to low temperature conditions (<500C). Furthermore, for electrocatalytic applications they must be placed in simultaneous contact with percolating ionic and electronic current transport pathways. These factors have limited the application of nanoscale metal catalysts (diameter <5 nm) in solid oxide fuel cell (SOFC) electrodes.

Here we address these challenges by stabilizing metal nanoparticles with ultra-low loadings on a scaffold of $Sm_{0.2}Ce_{0.8}O_2$ (SDC) films, where the oxide serves as a support, as a mixed conducting transport layer for fuel electro-oxidation reactions, and as an inherently active partner in catalysis. Despite the nanoscale features, the activity experiences negligible thermal degradation after a long-term annealing (> 100h). These observations may shed new light on achieving high efficiency SOFCs for cost-effective utilization of natural gas in electric power generation.

3:50 PM A9.07
Evaluation of Degradation Behavior of Ni-YSZ Using Electrochemical Capacitance Mirai Takeda[1], Keiji Yashiro[1], Shinichi Hashimoto[2] and Tatsuya Kawada[1]; [1]Graduate School of Environment Studies, Tohoku University , Sendai, Japan; [2]Graduate School of Engineering, Tohoku University , Sendai, Japan.

Long-term durability is the important issue for SOFC development. It is indispensable to understand how microstructure changes during continuous operation. It is widely known that three-phase boundary (TPB) is a main reaction site of Ni-YSZ. The relationship between degradation behavior of Ni-YSZ and TPB is essential. Some researchers have been reported degradation mechanism by FIB-SEM. However, there is no report to generalize degradation behavior of Ni-YSZ quantitatively because it depends on starting materials, preparation method and microstructure. This study aims to establish a simple and real-time analysis method of anode degradation, where electrode capacitance and electrode resistance are analyzed. Electrode resistance and electrode capacitance were obtained by AC impedance measurement. TPB length was obtained from ternarized the cross-section image by FE-SEM.
For the analysis, it is assumed that Ni and YSZ particles are spheres. Then contact area between the particles should be circular shape, where a perimeter of the circle is TPB. Therefore, electrode resistance, R_p, should be inversely proportional to TPB length of Ni-YSZ, $L_{Ni\text{-}YSZ}$, $R_p \propto$. Additionally, electrode capacitance, C_E, is assumed to depend on contact areas of Ni and YSZ. Then $C_E \propto$. In case of 40h-test, the results were well explained by this assumption.

4:10 PM A9.08
Ca_2MnAlO_5 and $La_4Ti_2O_{10}$ Derivatives as Potential SOFC's Anodes Xavier Flandre, Ibtissam Kehal, Christian Eroume, Aurelie Rolle, Edouard Capoen, Axel Loefberg and Rose-Noelle Vannier; Solid State Chemistry, Unit of Catalysis and Solid state Chemistry, Villeneuve d'Ascq, France.

In the frame of Solid Oxide Fuel Cell, one of the bottlenecks is the anode material stability to allow direct methane feeding. In this frame, we considered as potential SOFC's anodes two families of materials, calcium manganites which display the Brownmillerite structure on one hand, and lanthanum titanates with the cuspidine structure on the other hand,. The $Ca_2Mn_{1-x}Al_xO_{5+\delta}$ system was revisited. A $La_4Ti_{2-x}V_xO_{10+\delta}$ solid solution was evidenced for x < 0.3. The samples were prepared by solid route and

characterized by XRD at room temperature and at variable temperature under controlled atmosphere. Their structures were refined using the Rietveld method. The possibility to accommodate an excess of oxygen in the cuspidine structure was confirmed and a possible oxygen diffusion pathway was proposed. To characterize their electrochemical performances, symmetrical cells were first prepared by screen printing composites with gadolinium doped ceria on ceria electrolytes. Once optimized, cells with various electrode thicknesses were characterized by Electrochemical Impedance Spectroscopy (EIS) at variable temperatures under air and hydrogen, using a SOLARTRON 1260 frequency response analyzer, in a frequency range from 0.1 to 1.4 10^6 Hz, applying a 50mV voltage. With Area Specific Resistances (ASR) of 0.04 Ω.cm² at 800°C for $Ca_2Mn_{1,5}Al_{0,5}O_{5+\delta}$ and 0.22 and 0.28 Ω.cm² at 750°C for $La_4Ti_{1,9}V_{0,1}O_{10+\delta}$ and $La_4Ti_{1,8}V_{0,2}O_{10+\delta}$ compounds respectively, first results are promising. However, because of the reducibility of the ceria electrolyte, study with Yttrium stabilized Zirconia (YSZ) as electrolyte is in progress. In parallel, the catalytic activity of these materials for methane reforming and their stability will be studied.

4:30 PM A9.09
Thin Film Carbide Anodes for Solid Oxide Fuel Cells Jun Jiang, Xiaofei Guan and Shriram Ramanathan; School of Engineering and Applied Sciences, Harvard University, Cambridge, Massachusetts, United States.

Conventional Ni-YSZ solid oxide fuel cell anode shows excellent catalytic activity and high conductivity, however suffers severe carbon deposition when interfaced with hydrocarbon fuels and performance degradation due to Ni phase coarsening at high temperatures. Development of new materials or interfaces for direct hydrocarbon oxidation is therefore an important area of study. The surface catalysis resemblance between Pt and WC makes WC a potential anode for SOFCs. We have carried out a systematic study of WC thin film growth by sputtering to understand optimal microstructures for anode components. Deposition conditions such as temperature and ambient play a major role in composition of the carbide and its crystal structure. These in turn have profound impact on performance of solid oxide fuel cells operating in hydrocarbon fuels. In this presentation, we will present results to date on growth of carbides in ultra-thin film form and suspended structures and their high temperature electrochemical characterization in simulated fuel cell conditions.

4:50 PM A9.10
Nanoscaled Ni/YSZ Anodes for Solid Oxide Fuel Cells: Processing and Characterization Dino Klotz[1], Julian T. Szasz[1], Heike Stoermer[2], Dagmar Gerthsen[2] and Ellen Ivers-Tiffee[1];[1]Institute for Applied Materials (IAM-WET), Karlsruhe Institute of Technology (KIT), Karlsruhe, Germany; [2]Laboratorium für Elektronenmikroskopie (LEM), Karlsruhe Institute of Technology (KIT), Karlsruhe, Germany.

Solid oxide fuel cells (SOFC) operated at 600 °C and below require electrodes with outstanding catalytic properties. At the fuel electrode (anode), the hydrogen electrooxidation reaction takes place at the triple phase boundary nickel (catalyst and electronic conductor), yttria-stabilized zirconia (ionic conductor), and pore phase. The microstructure of state-of-the-art SOFC anodes is well engineered, but inherently limits the electrooxidation reaction at ≤ 600°C due to particle and pore sizes in the micrometer scale.

The triple phase boundary length can be significantly enlarged, if a nanometer scaled and well dispersed Ni/YSZ phase can be inserted in the electrochemically active part of the electrolyte/anode interface. In this study, we deposited a 400 nm Ni thin film onto a 9YSZ single crystal electrolyte. By applying a high current density of 2 A/cm² for 10 seconds at 700°C in reverse direction, a porous interlayer emerged at the electrolyte/anode interface consisting of surprisingly small particles. The microstructure and the elemental composition of this interlayer was characterized with nm-resolution by means of transmission electron microscopy and energy dispersive X-ray analysis (TEM-EDXS). Ni particles in the nanometer scale are well embedded in a porous YSZ matrix of the same size, thereby increasing the number of electrochemical active sites (triple phase boundary) significantly. Interestingly, a local demixing of the 9YSZ and Y precipitates in the Ni phase were detected. The underlying reaction mechanism will be explained by thermodynamic considerations.

References:
[1] D. Klotz, B. Butz, A. Leonide, J. Hayd, D. Gerthsen and E. Ivers-Tiffée, J. Electrochem. Soc., 158, B587 (2011).

5:10 PM A9.11
Redox Stability and Electrical Properties of $Sr_{1-x}Y_xV_{1-y}Nb_yO_3$ for Prospective SOFC Anodes Javier Macias, Aleksey Yaremchenko and Jorge Frade; Department of Materials and Ceramic Engineering, University of Aveiro, Aveiro, Portugal.

Perovskite-like $SrVO_{3-d}$ exhibits high electrical conductivity under reducing conditions and good resistance to sulfur poisoning and carbon deposition, and can be considered, therefore, as a promising fuel electrode material for application in solid oxide fuel cells (SOFCs) and reversible solid electrolyte cells. In spite of attractive advantages, the applicability of $SrVO_{3-d}$ is constrained by a limited stability domain of perovskite phase restricted to reducing conditions; oxidation in air results in a transformation into insulating $Sr_2V_2O_7$ accompanied with large dimensional changes. The present work aims at the development of $SrVO_{3-d}$ derivatives with improved redox stability and thermomechanical properties, while retaining sufficient electrical conductivity, through substitutions into strontium and vanadium sublattices.
$Sr_{1-x}Ln_xV_{1-y}Nb_yO_{3-d}$ (Ln = La and Y, x = 0-0.2, y = 0-0.1) ceramics were prepared by solid-state synthesis route assisted with high-energy milling, and sintered at 1500°C in 10%H_2-N_2atmosphere. XRD analysis confirmed the formation of single-phase materials with cubic perovskite structure for all compositions. Co-substitutions with lanthanide and niobium cations were demonstrated to results in a moderate decrease of electrical conductivity, but also to suppress partly the excessive thermochemical expansion characteristic for parent $SrVO_{3-d}$ and to extend the perovskite stability domain towards higher oxygen partial pressures. Although these materials still undergo an oxidative decomposition on heating in air, sluggish kinetics of oxidation under inert gas results in nearly reversible behavior in relatively short-term cycles between reducing and inert atmospheres.

SESSION A10: SOFC—Cathodes IV
A: Solid Oxide Fuel Cells and Electrolyzers
Chair: Werner Sitte
Friday Morning, June 19, 2015
Keystone Resorts, Longs Peak

10:30 AM *A10.01
A Novel R-P Structure Cathode with High Performance for Intermediate Temperature Solid Oxide Fuel Cells Ranran Peng, Zhiquan Wang, Daoming Huan, Wenqiang Yang and Yalin Lu; University of Science and Technology of China, Hefei, China.

Lowering the operating temperature to the intermediate temperature range (500-700 °C) is crucial for the commercial application of SOFCs. Unfortunately, the electrochemical performance of the cells, especially the cathode performance, was degraded dramatically at the lowered operating temperature [1]. To find a proper cathode material with high catalytic activity at intermediate temperature is important to improve the discharging performance of SOFCs. Here, we report a new cathode material $Sr_3Fe_2O_{7-\delta}$ (SFO) with Ruddlesden-Popper structure for IT-SOFCs. The theoretical calculation results based on density functional method (DFT) suggests that oxygen vacancy defects rather than interstitial oxygen defects would like to form in the bulk of SFO oxides. Conductivity relaxation measurements and oxygen permeation measurements suggest that SFO has good oxygen surface exchange coefficient and bulk diffusion coefficient. With SFO as a single phase cathode, the single cell has excellent performance when using SDC as electrolyte. Measured at 700 °C, the peak power density is 890mWcm^{-2}.

References
[1] Brett, D. J.; Atkinson, A.; Brandon, N. P.; Skinner, S. J. Intermediate Temperature Solid Oxide Fuel Cells. Chem. Soc. Rev. 2008, 37, 1568−1578.

Acknowledgement
This work was financially supported by the Natural Science Foundation of China (51472228), the National Basic Research Program of China (973 Program, 2012CB922001 and 2012CB215403), and the Fundamental Research Funds for the Central Universities (WK2060190025).The authors acknowledge the Supercomputing Center of USTC for providing computational resources.

10:50 AM A10.02
Optimization of the Electrochemical Performances of $Ca_3Co_4O_{9+\delta}$ as Air Electrode for Solid Oxide Cell Aurelie Rolle[1], Xavier Flandre[2], Hussein A. Abbas Mohamed[1], Da Huo[2], Giuliano Mignardi[2], Sylvie Daviero-Minaud[2], Edouard Capoen[3], Marie-Helene Chambrier[4], Elisabeth Djurado[5], Amelie Salauen[5], Monica Burriel[5] and Rose-Noelle Vannier[1]; [1]UCCS, ENSCL, Villeneuve d'Ascq, France; [2]UCCS, Université Lille1, Villeneuve d'Ascq, France; [3]UCCS, CNRS, Villeneuve d'Ascq, France; [4]UCCS, Université Jean Perrin, Villeneuve d'Ascq, France; [5]LEPMI, Grenoble-INP - UdS - UJF, Saint Martin d'Hères, France.

With a structure built upon oxygen deficient [$Ca_2CoO_{3-\delta}$] rock salt layers sandwiched in between [CoO_2] layers of CdI_2 type, the well-known thermoelectric misfit compound $Ca_3Co_4O_{9+\delta}$can be viewed as a Mixed Ionic Electronic Conductor. It exhibits high kinetics towards surface oxygen molecule dissociation with a surface exchange coefficient of $1.6.10^{-7}$ cm.s^{-1} measured at 700°C which is in the same order of magnitude that the value reported for La_2NiO_4 (1.310^{-7} cm .s^{-1}) [1]. Since it reacts with yttria stabilized zirconia, this composition was tested as a potential air electrode in symmetrical cell made of a gadolinium doped ceria electrolyte (CGO, $Ce_{0.9}Gd_{0.1}O_{1.95}$). Because of low oxygen diffusion in contrast to high oxygen surface exchange kinetics ($2.7.10^{-10}$ cm^2.s^{-1} at 700°C to be compared to $1.6.10^{-9}$ cm^2.s^{-1} for La_2NiO_4), both pure composition and composite with CGO were studied. When using screen-printing as deposition technique, by optimising both the thickness and composite composition, an optimal Area Specific Resistance (ASR) of 0.5 W.cm^2 was obtained at 700°C. For the pure compound, the Electrostatic Spray Deposition (ESD) led to coral microstructures, with an ASR of 3.32 Ωcm² at 700°C against 4.58 Ωcm² for a screen printed sample. In addition, as shown by the group of Boukamp at University Twente for other cathode materials, the electrochemical performances seemed to be improved when a thin layer of the electrode material was deposited at the interface between the electrolyte and the electrode [2].

References
V. Thoréton, Y. Hu, C. Pirovano, E. Capoen, N. Nuns, A.S. Mamede, G. Dezanneau, C.Y. Yoo, H.J.M. Bouwmeester, R.N. Vannier, *J. Mater. Chem. A*, 2014, 2, p19717.
N. Hildenbrand, B. A. Boukamp ; P. Nammensma; D. H. A. Blank, 2011, *Solid State Ionics*, 192 p 12, N. Hildenbrand, P. Nammensma, D.H.A. Blank, H.J.M. Bouwmeester, B.A. Boukamp, 2013, *J. Power Sources*, 238, p 442.

11:10 AM A10.03
Effect of $La_{0.6}Sr_{0.4}Co_{0.2}Fe_{0.8}O_{3-\delta}$ Microstructure on Oxygen Surface Exchange Kinetics Katherine D. Bagarinao, Haruo Kishimoto, Katsuhiko Yamaji and Teruhisa Horita; National Institute of Advanced Industrial Science and Technology, Tsukuba, Japan.

$La_{0.6}Sr_{0.4}Co_{0.2}Fe_{0.8}O_{3-\delta}$ (LSCF) is a mixed ionic-electronic conducting perovskite (ABO_3) material which has attracted significant research interest in recent years as a cathode for solid oxide fuel cell (SOFC) applications at intermediate temperatures (500–750°C). Fundamental understanding of the oxygen surface exchange kinetics and diffusion in LSCF cathodes is necessary to optimize the cell performance at the required operating temperatures. In this study, we controlled the surface microstructure and crystalline orientation of LSCF films using pulsed laser deposition on yttria-stabilized zirconia (YSZ) single crystal substrates buffered with Gd_2O_3-doped CeO_2 thin films (GDC). Three types of low-index YSZ surfaces were selected, viz., (100), (110), and (111); LSCF films with specific crystalline orientations and distinct surface microstructures were accordingly obtained on these substrates. Moreover, the LSCF microstructure can be further modified by tuning the underlying GDC thin film microstructure through high-temperature annealing prior to LSCF deposition. We employed the $^{18}O/^{16}O$ oxygen isotope exchange technique in conjunction with secondary ion mass spectroscopy (SIMS) depth profile analysis to clarify the effect of the LSCF microstructure on its oxygen surface exchange kinetics. Fitting of the measured ^{18}O fraction to the solution of the diffusion equation yielded significant differences in the oxygen surface exchange coefficient k^* among the LSCF films, with the highest k^*obtained for the LSCF grown on (100)GDC/(100)YSZ. These results suggest dependence of the active surface area on LSCF microstructure as well as crystalline orientation.

11:30 AM A10.04
Oxygen Surface Exchange Kinetics of Praseodymium Nickelates Saim Saher[1], Jean-Marc Bassat[2] and Henny J. Bouwmeester[1]; [1]MESA+ Institute for Nanotechnology, Faculty of Science and Technology, University of Twente, Enschede, Netherlands; [2]Institut de Chimie de la Matière Condensée de Bordeaux (ICMCB-CNRS), Université Bordeaux I, Pessac-Cedex, France.

The oxygen surface exchange kinetics of Ruddlesden-Popper (RP) praseodymium nickelates $(PrO)(PrNiO_3)_n$, with n = 1, 3, and ∞, has been investigated using pulse ^{18}O-^{16}O isotope exchange (PIE). Whilst $PrNiO_3$ ($n = \infty$) adopts an orthorhombic distorted perovskite structure [1], the crystal structure of the RP phases consists of an intergrowth of n consecutive $PrNiO_3$perovskite layers alternating with PrO rock salt layers along the c-direction. In particular $Pr_2NiO_{4+\delta}$ (n = 1) has attracted much interest as a potential cathode material for IT-SOFCs [2]. In the PIE method, an ^{18}O-enriched gas phase pulse is analyzed (by mass spectroscopy) after passage, under isothermal and iso-pO_2 conditions, through a continuous flow packed bed microreactor loaded with the oxide powder [3]. The results confirm that the layered RP phases $Pr_2NiO_{4+\delta}$ (n = 1) and $Pr_4Ni_3O_{10-\delta}$ (n = 3) exhibit significantly higher oxygen surface exchange rates, compared to the parent perovskite phase $PrNiO_3$. Analysis of the distribution of oxygen isotopomers in the effluent pulse suggests dissociative adsorption of oxygen molecules as the rate-determining step for the oxygen surface exchange reaction for all investigated materials.

References:
[1] M. L. Medarde, J. Phys.: Condens. Matter 9 (1997) 1679–1707.
[2] C. Ferchaud, J. C. Grenier, Y. Z. Steenwinkel, M. M.A. van Tuel, F.P.F. van Berkel, J. M. Bassat, J. Power Sources 196 (2011) 1872–1879.
[3] H.J.M. Bouwmeester, C. Song, J. Zhu, J. Yi, M. van Sint Annaland, B.A. Boukamp, Phys. Chem. Chem. Phys. 11 (2009) 9640.

B: Polymer Electrolyte Fuel Cells and Electrolyzers

* Invited Speaker
** Keynote Speaker

SESSION B1: PEMFC/DMFC I
B: Polymer Electrolyte Fuel Cells and Electrolyzers
Chair: Andrew Herring
Tuesday Afternoon, June 16, 2015
Keystone Resorts, Grays Peak III

1:30 PM *B1.01
Nanoscaled Structure of Nafion at Interfaces Joseph Dura[1], Steven DeCaluwe[2] and Paul Kienzle[1]; [1]NCNR, National Institute of Standards and Technology, Gaithersburg, Maryland, United States; [2]Mechanical Engineering, Colorado School of Mines, Golden, Colorado, United States.

Solid state electrochemical devices such as polymer electrolyte fuel cells demand efficiency in both ion transport and catalysis. Both are critically dependent on the nanostructure, in particular the ionic domains. In the most commonly used polymer electrolyte, Nafion, the hydrophilic sulfonic acid group and the water it attracts will phase segregate from the hydrophobic fluorocarbon backbone to form the ionic domains. These facilitate ion transport through reptation of the polymer and ion hopping between the sulfonic acid sites, and thus the morphology significantly affects the ion transport. However the exact morphology of this all important structure, even in bulk materials, is still incompletely understood. Catalysis occurs in the even more complicated three phase region where the catalyst must co-exist with both electron conducting and ion conducting media. Very few studies have attempted to determine the structure of this region. Interfacial regions also play a role in the function of solid additives which are increasingly being explored as means to modify the properties of ionomers to improve the bulk electrolyte characteristics. For example silica particles are added to Nafion to increase water retention especially at high temperatures in fuel cells and to reduce V crossover in flow batteries. In these regions ionomers often are in the form of thin films, applied as binders to coat fuel cell electrode particles with layers that are several nanometers thick. Here, interfacial and confinement effects may alter the morphology or transport properties compared to the more commonly characterized bulk materials.

Neutron reflectometry, NR, studies of thin films can shed light on the morphology of ionomers in these regimes. NR determines a depth profile of the scattering length density (which is determined from composition) with sub-Ångstrom precision in idealized planar interfaces. Because of isotopic contrast variation it is particularly sensitive to certain elements such as H (and thus water) as well as Li, V, and numerous others. Herein, NR has been applied to investigate surface and finite-size effects on the lamellar ordering of water domains in Nafion at interfaces with hydrophilic materials[1-3]. A partial monolayer of sulfonate groups is determined to be bonded to the SiO_2, accompanied by a large excess of water. Moreover, contrast variation was employed to not only determine the phase segregation of water from the polymer, but also to quantify the segregation of the sulfonate groups from the fluorocarbon chains in Nafion. An incomplete remixing of the polymer groups was found to occur after drying the Nafion at 60° C, indicated either limited polymer mobility or retained equilibrium structures at in the Nafion/SiO_2 interface.

1 **Multilamellar Interface Structures in Nafion**, Joseph A. Dura, Vivek S. Murthi, Michael Hartman, Sushil K. Satija, Charles F. Majkrzak, Macromolecules, **42** (13), pp 4769–4774 (June 12 2009) [DOI: 10.1021/ma802823j]

2 **Surface-Induced Nanostructure and Water Transport of Thin Proton-Conducting Polymer Films,** Sangcheol Kim, Joseph A. Dura, Kirt A. Page, Brandon W. Rowe, Kevin G. Yager, Hae-Jeong Lee, and Christopher L. Soles, Macromolecules, **46**, 5630−5637 (2013) [DOI:10.1021/ma400750f]

3 **Phase segregation of sulfonate groups in Nafion interface lamellae, quantified via neutron reflectometry fitting techniques for multi-layered structures,** Steven C. DeCaluwe, Paul A. Kienzle, Pavan Bhargava, Andrew M. Baker, and Joseph A. Dura, Soft Matter **10**, 5763 (2014) [DOI: 10.1039/c4sm00850b]

1:50 PM B1.02
Interplay between Relaxations and Structure in Anion-Exchange Membranes (AEMs) Vito Di Noto[1, 2], Graeme Nawn[1], Keti Vezzu[1, 3], Federico Bertasi[1, 2], Enrico Negro[1, 2], Sandra Lavina[1, 2], Ashley Maes[4], Andrew Herring[4], Sedef Piril Ertem[5] and Bryan Coughlin[5]; [1]Chemical Sciences, University of Padova, Padova, Italy; [2]Consorzio Interuniversitario Nazionale per la Scienza e la Tecnologia dei Materiali, Padova, Italy; [3]Veneto Nanotech S.C.p.a., Padova, Italy; [4]Colorado School of Mines, Golden, Colorado, United States; [5]Department of Polymer Science and Engineering, University of Massachusetts, Amherst, Amherst, Massachusetts, United States.

Recently, a new family of low-temperature FCs has been proposed, mounting OH^--conducting polymer electrolyte membranes. These systems are known as anion-exchange membrane fuel cells (AEMFCs), and show great promise to address successfully crucial issues affecting conventional low-temperature FCs including proton-conducting electrolytes. In particular, the anion-exchange membranes (AEMs) of AEMFCs generate a strongly alkaline environment at the electrodes. Consequently, the efficient operation of AEMFCs does not require electrocatalysts including platinum-group metals (PGMs), which have a very low abundance in Earth's crust and are prone to supply bottlenecks. Furthermore, in AEMFCs the OH^- charge carriers migrate from the cathode to the anode, thus inhibiting fuel crossover. The implementation of efficient AEMFCs requires the development of AEMs: (a) capable of a facile and selective transport of OH^- anions; (b) characterized by good mechanical properties; and (c) showing an acceptable chemical and electrochemical stability. To achieve these objectives it is necessary to obtain a detailed understanding of the complex interplay between the structure and the relaxations of AEMs. The latter membranes are extensively studied by broadband electrical spectroscopy (BES) and thermomechanical methodologies including high-resolution thermogravimetry (HR-TG), modulated differential scanning calorimetry (MDSC) and dynamic mechanical analysis (DMA). The unique synergy of these advanced characterization techniques yields an exhaustive understanding of the various relaxation phenomena taking place in the AEMs. The relaxations play a major role in the mechanism of charge migration, which is elucidated together with its interplay with the chemical features and the hydration degree of the AEMs. The resulting information provides fundamental insights, allowing to improve the synthesis of the materials and to optimize the fabrication process of the AEMs.

2:10 PM B1.03
Anion Exchange Membranes for Fuel Cells and Flow Batteries: Quaternary Ammonium Group Stability and Transport Properties of a Model Membrane Michael G. Marino, Giorgi Titvinidze and Klaus-Dieter Kreuer; Maier, Max Planck Institute for Solid State Research, Stuttgart, Germany.

Anion exchange membranes (AEM) for electrochemical applications require sufficient ionic conductivity and chemical stability. In alkaline fuel cells, AEMs need to be stable in an environment with a high hydroxide concentration. Especially the quaternary ammonium (QA) functional groups are easily attacked by the nucleophilic hydroxide and unfortunately, widely varying and even partially contradicting results in regard to relative and absolute QA stabilities have been published. In order to eliminate the influence of the polymer backbone on the degradation reactions we investigated (26 different) QA groups as simple halide salts in alkaline aqueous solution. This allowed exact control over water content and temperature. Unexpectedly, 6-membered piperidinium based heterocycles proved to be by far the most stable cations.[1]

Furthermore, anion and water transport in a model AEM was investigated and it is demonstrated that hydroxide form AEMs can reach conductivities within a factor of 2 of comparable proton exchange membranes, in accordance with the mobilities of hydroxide and hydronium in water. Lower conductivity is due to carbonate contamination and especially insufficient hydration, which leads to reduced dissociation. This means that sufficient hydration of a hydroxide form AEM is required both for adequate stability and conductivity. Reduced dissociation at low water contents may also explain the SAXS scaling behavior of the investigated AEM. Using conductivity and PFG-NMR measurements it was found that the degree of dissociation in many anionic forms is far from complete, even at high hydration, suggesting the formation of condensates of multiple ions.[2]

[1] M. G. Marino and K. D. Kreuer, Alkaline stability of quaternary ammonium cations for alkaline fuel cell membranes and ionic liquids, ChemSusChem, 8, 513–523, 2015.
[2] M.G. Marino, J.P. Melchior, A. Wohlfarth, and K.D. Kreuer, Hydroxide, halide and water transport in a model anion exchange membrane, J. Mem. Sci., 464, 61–71, 2014.

2:30 PM B1.04
Chemically Stable and Highly Conductive Alkaline Poly(phenylene oxide) Poly(vinyl benzyl trimethyl ammonium) Di-Block Membrane for Fuel Cell Applications Tara P. Pandey, Matthew W. Liberatore and Andrew M. Herring; Chemical and Biological Engineering, Colorado School of Mines, Golden, Colorado, United States.

Polymer membranes, in both acid and basic forms, for fuel cell application have been studied extensively. Due to a low operation temperature, higher cathode reaction kinetics that opens the possibility of using inexpensive metal catalysts, and liquid free electrolytes, anion exchange polymer membrane (AEM) fuel cell offers many advantages over traditional an alkaline fuel cell. A melt pressed Poly(phenylene oxide) poly(venyl benzyl trimethly ammonium) hydroxide membrane was studied as an AEM for fuel cell applications. This work presents the electrochemical properties of the membrane for fuel cell applications.

Environmentally controlled electrochemical impedance spectroscopy measurements were performed as function of temperature and humidity (%RH) under N_2 environment. The membrane ionic conductivities of 0.137 ± 0.015 and 0.024 ± 0.006 S/cm at 95%RH and 40%RH; respectively were observed at 60 ºC in CO_2 free alkaline form. This is the first AEM reported to have a measureable conductivity at as dry as 40%RH. High ionic diffusion, low ionic path tortuosity, and high membrane ionic density led to a high ionic conductivity. However, the ionic conductivity suffered tremendously when the AEM was exposed to ambient air. The membrane showed no chemical degradation as it was evidenced by measurement of OH^- conductivity in controlled environment for a week. Properties of air controlled vs air exposed AEM will be discussed along with the difference in liquid and vapor water uptake behavior of the membrane under similar conditions. A complete set of electrochemical and morphological study of the membrane will be discussed in the presentation.

2:50 PM *B1.05
Thermoreversible Gels – A New Route to Create Blocky Ionomer Membranes via Non-Random Functionalization Samantha Talley, Greg Fahs, Xijing Yuan, Sonya Benson andRobert Moore; Department of Chemistry, Virginia Tech, Blacksburg, Virginia, United States.

Recent findings from the ion-containing polymer membrane community have taught us the importance of controlled sequencing of ionic groups along polymer chains in the development of ordered domains for enhanced transport properties. When compared on an equal ion content basis, a blocked arrangement of ionic groups along polymer chains tends to produce ordered nano-phase-separated domains that are capable of yielding superior transport, solvent swelling, and mechanical properties over that of analogous random ionomers. Inspired by these demonstrated membrane enhancements, we have begun to explore the impact of variable post-polymerization sulfonation reactions on the spatial distribution of functional groups in ionomers. Very recently, we have discovered a non-functionalizing solvent for PEEK that allows for a homogeneous sulfonation reaction. Surprisingly, this new solvent also allows for the formation of a thermo-reversible gel. Following a method we recently developed to sulfonate syndiotactic polystyrene (sPS) in the gel state, we are now able to prepare a blocky form of sulfonated PEEK that has a high degree of sulfonation and a high degree of crystallinity. Membrane properties as a function of sulfonation procedure will be explored.

SESSION B2: Poster Session: PEMFC/DMFC
B: Polymer Electrolyte Fuel Cells and Electrolyzers
Tuesday Afternoon, June 16, 2015
5:20 PM
Keystone Resorts, Red Cloud Peak

B2.01
Synthesis and Characterization of Water Stable, Silicotungstic Acid Functionalized Perfluorocyclobutyl Polymer Electrolyte Andrew R. Motz, Mei-Chen Kuo and Andrew M. Herring; Chemical and Biological Engineering , Colorado School of Mines, Lakewood, Colorado, United States.

Trifluorovinyl aryl ether (TFVE) functionalized silicotungstic acid has been copolymerized with other TFVE monomers, resulting in a water stable, free standing film. Polymerization occurs via thermally induced cyclo-polymerization, forming perfluorocyclobutyl groups. In order for the resulting polymer to be water-stable, a hydrophobic comonomer is used. Perfluorocyclobutyl polymers have been shown to have several properties that are ideal for high temperature fuel cell operation including high T_g, high dielectric constant, and chemical stability. Silicotungstic acid, an inorganic super acid, is able to retain tightly bound water and conduct protons above 100 °C. Both the acid functional group and the backbone of this novel polymer are suitable for high temperature and low humidity proton exchange membrane fuel cell (PEMFC) operation. The disappearance of the IR peak at 1833 cm^{-1} and appearance at 961 cm^{-1} are indicative of depletion TFVE groups and the formation of perfluorocyclobutyl groups, respectively. 19F NMR has also been used to confirm polymerization has occurred, by disappearance of peaks at -120, -127, and -134 ppm, corresponding to the three fluorines of the TFVE group. Preliminary proton conductivity over 0.040 S/cm at 80 °C and 95% RH has been achieved.

B2.02
Synthesis and Properties of Poly(phenylene)-Poly(ether ketone) Block Copolymer Electrolytes (V)-Investigation of Chemical Composition Shogo Nagaya, Masahiro Fujita, Yuko Takeoka and Rikukawa Masahiro; Sophia University, Tokyo, Japan.

Sulfonated aromatic polymers have been widely studied as polymer electrolyte membrane (PEM) materials for fuel cell applications. The mechanical and dimensional stability are insufficient under humidified conditions due to their high ion exchange capacities (*IEC*). It is necessary to achieve both high proton conductivity and low water uptake for sulfonated aromatic polymers. To maintain high proton conductivity without decreasing mechanical properties under humidified conditions, we have focused on block copolymers consisting of hydrophilic and hydrophobic segments, which are expected to form continuous ionic channels by a micro-phase separation. In this study, we synthesized multiblock copolymers consisting of hydrophilic sulfonated poly(4-phenoxybenzoyl-1,4-phenylene) (S-PPBP) and hydrophobic poly(arylene ether ketone) (PAEK), and their mechanical and electrochemical properties were investigated.

The sulfonated monomer, 2,2-dimethylpropyl-4-[4-(2,5-dichlorobenzoyl) phenoxy]benzene- sulfonate (NS-DPBP), and the hydrophobic oligomer, dichloro-terminated poly(arylene ether ether ketone6H) (PAEK6H-Cl), were polymerized via nickel-catalyzed coupling polymerization to obtain the copolymers (S-6H(*n*)*x*:*y*) with varying the composition ratio. The *n* indicates the unit length of hydrophobic oligomer, and the *x*:*y* indicates the unit composition ratio of S-PPBP:PAEK. The weight-average molecular weights of S-6Hs were 75 - 180 kg mol^{-1}.

The *IEC*values of S-6Hs were 1.2 - 2.1 meq g^{-1}. The *IEC* values of S-6H(7)4:1, 3:1, and 2:1 were 2.1, 1.9, and 1.6 meq g^{-1}, respectively, and these block copolymers showed a high proton conductivity of over

10^{-3} S cm^{-1} at 80 ºC and 30%RH. S-6H(7)3:1 and 2:1 membranes showed high mechanical properties and flexibility under humidified conditions. The proton conductivity and mechanical properties of S-6H(10)2:1 and S-6H(18)2:1 were almost the same as those of S-6H(7)2:1. This result suggested that the unit length of hydrophobic oligomer did not affect these properties.

Acknowledgements
This work was financially supported by the New Energy and Industrial Technology Development Organization (NEDO).

B2.03
Activity of Nanographitic Structures toward Oxygen Reactions in the Solid State CsH_2PO_4 Electrochemical System Hadi Tavassol[2, 1] and Sossina M. Haile[2, 1]; [1]Material Science, California Institute of Technology, Pasadena, California, United States; [2]Material Science, Northwestern University, Evanston, Illinois, United States.

We report on the electrochemical activity of nanographites toward oxygen reduction and evolution reactions in the superprotonic CsH_2PO_4 solid acid electrochemical system. Oxygen reduction and evolution are catalytically challenging reactions relevant to the fuel cell and water splitting applications. Because of the strong O=O bond, oxygen reduction is a slow reaction. Heteroatom containing carbon based materials are known to show high activities toward oxygen reduction. However, the possibility of oxygen reactions catalysis on all-carbon catalysts and their reaction mechanism(s) remains poorly understood. Here using well defined nanographitic structures we study oxygen reactions catalysis in the superprotonic CsH_2PO_4 solid acid electrochemical system.

Compared with bulk graphitic structures, because of the presence of open edges in the nano-sized graphite particles, different electronic and possibly catalytic properties are expected for these materials. The size of the nanographites crystallites is determined by Raman spectroscopy. The I_D/I_G ratio provides a measure of nanographite crystallite sizes. Using impedance spectroscopy, the catalytic activity of nanographites is examined under (symmetric) humidified O_2 at ca. 240 °C. The zero bias area specific resistance of the nanographite samples decreases as the crystallite sizes becomes smaller. Scanning electron microscopy images show smaller features in the higher surface area samples with higher I_D/I_G ratio. We will discuss the correlation between catalytic activity of nanographites with the crystallite sizes in well-defined nanographitic structures and explore possible reaction mechanisms.

B2.04
Characterization of PBI Based High Temperature PEMFC Using Methanol Reformed Gas Properties Sung-Kwan Ryu[3], Seung-Gon Kim[1], Minjin Kim[1, 2] and Young-Jun Sohn[1, 2];[1]Korea Institute of Energy Research, Daejeon, Korea (the Republic of); [2]University of Science and Technology, Daejeon, Korea (the Republic of); [3]Chemical Engineering, Yonsei University, Seoul, Korea (the Republic of).

High temperature proton electrolyte membrane fuel cell based on phosphoric acid(PA) doped polybenzimidazole membrane operates elevated temperature above 100 ℃. It is due to many advantages such as kinetics, CO tolerance and simplified system. In general, due to the low transition temperature (TG) of Nafion membrane, thermal and structural degradation occurs rapidly above 100 degrees. Therefore, the durability of the fuel cell are reduced significantly. To resolve this problem, many studies have been conducted high-temperature PEMFC using the phosphoric acid doped polybenzimidazole membrane in recent year. Especially, many research has been carried out to improve the conductivity of the PBI, mechanical stability and rigidity. In this study, we prepared single cell using a commercial PA-PBI membrane. And single cell performance were observed using feed gas such as hydrogen and reformed hydrogen. The effect of oxygen stoichiometry on the single cell performance and the electrochemical properties were investigated by performing cyclic voltammetry (CV) measurements. To observe MEA durability, we performed the single cell long term test (500hrs).

B2.05
Optimization of the Lifetime for Polybenzimidazole Based High Temperature PEM Fuel Cell Stacks Minjin Kim, Young-Jun Shon and Seung-Gon Kim; Fuel Cell Research Center, Korea Institute of Energy Research, Daejeon, Korea (the Republic of).

General stationary fuel cell systems use hydrogen for a fuel which is produced by a hydrocarbon reformer. When use reformed gas to the fuel cell, the water in this gas should be removed using additional devices because the reformed gas included hydrogen contains lots of vapor or liquid water. In this study, we develop a numerical stack degradation model which includes the effect of water in the reformed gas. And then we find out the effect of the water which affects the durability of HT-PEMFCs and conduct an operating optimization for improving the performance. We fulfill simulations according to current density and relative humidity of the reformed gas in order to find out the effect of the water inside HT-PEMFCs stack and analyze these results. From the simulation results, it is show that the obtained performance and durability by the operating optimization are much higher than those by arbitrary conditions. The performance and durability according to current density and relative humidity of the reformed gas are a dominant effect by the temperature of the stack.

B2.06
Application of Block Copolymers Having Aliphatic Side Chains to Cathode Ionomer (II) - Properties Related to Gas Transport Ken Akizuki[2, 3], Atsushi Ohma[3], Toyoaki Matsuura[1], Masahiro Yoshizawa-Fujita[1], Yuko Takeoka[1] and Masahiro Rikukawa[1]; [1]Department of Materials and Life Sciences, Faculty of Science and Technology, Sophia University, Tokyo, Japan;[2]Department of Materials and Life Sciences, Sophia University, Tokyo, Japan; [3]Nissan Research Center, Nissan Motor Co., Ltd., Kanagawa, Japan.

The reduction of oxygen transport resistance in cathode catalyst layer under highly humidified conditions is one of key issues to increase the power density of polymer electrolyte fuel cells in the direction of reducing total amount of Pt used in the system. It has been reported that the molecular structure of ionomer influences on oxygen transport properties in the catalyst layers. However, the direction of molecular structure design of ionomer has not been cleared, especially for polyaromatic electrolytes showing lower gas permeability than that of perfluorinated electrolytes. In this study, sulfonated poly(p-phenylene)-based diblock copolymers having aliphatic side chains (SBuH) were synthesized via catalyst transfer polycondensation in order to increase the gas permeability of polyaromatic electrolytes by introducing aliphatic side chains as the spacer among polymer backbones. The viscoelasticity, gas permeability, and contact angle of SBuH membranes were evaluated in comparison with Nafion® membranes as representative properties related to gas transport properties in the catalyst layers. Membrane electrode assemblies (MEAs) were fabricated by using each electrolyte as the ionomer in the cathode catalyst layer, and their oxygen transport resistances were estimated. SBuH membranes showed a low elastic modulus and equivalent loss modulus to Nafion® membranes, and comparable gas permeability coefficient to Nafion® membrane under highly humidified conditions as well as contact angle. The oxygen transport resistance of SBuH catalyst layer was also equivalent to that of Nafion® catalyast layer at 90%RH. These results suggest that the aliphatic side chains on the aromatic backbone act as a plasticizer and improve the gas permeability for both of membranes and ionomers.

B2.07
Zirconium Phosphate-Grafted-Sulfoanted Polystyrene/Nafion Composite Membranes for Direct Methanol Fuel Cell Kun-lin Liu, Chi-Yang Chao and Cheng-Wei Pai; Materials Science and Engineering, National Taiwan University, Taipei, Taiwan.

Most of the inorganic additives in organic /inorganic hybrid composite proton exchange membranes exhibited low intrinsic proton conductivity and difficulty in forming homogeneous dispersion of nanoparticles within the membrane. In this case, we developed a novel procedure to prepare composite membranes containing the well dispersed Ziconium phosphate (ZrP) nanoplates.

We first prepared nano-composites by ATRP with initiator tailored nanoplates. The initiator we used was decorated with phosphonic acids in-situ reacted with ZrOCl2 and H3PO4 to afford initiator-modified ZrP (ZrC). ATRP was proceeded with styrene monomer followed by post-sulfonation (ZrC-sPS-I); or styrene sulfonate sodium with the following acid treatment (ZrC-sPS-II). The composite membranes were then prepared by blending Nafion® and ZrC1.5-sPS20k (named as NZrC1.5-

sPS20k-I & II).
The initiator and ZrC nanoplates were characterized by NMR, IR, X-ray, XPS, and TEM. X-ray and TEM exhibited ZrC with a layer structure, and the size of ZrC was larger with decreased initiator concentration. The ZrC-sPS-I composites show morphologies in exfoliated layer arrangements while ZrC-sPS-II show an inverse core shell structure. NZrC1.5-sPS20k-I with 2.5wt% loading exhibited the highest selectivity (C/P=6.3) as triple as that of Nafion (2.18). While NZrC1.5-sPS20k-II showed a slightly decreased proton conductivity but more suppressed MeOH capability with similar loading. The proton conducting mechanism is distinct for NZrC1.5-sPS20k-I and NZrC1.5-sPS20k-II due to the different ZrP arrangement and intermolecular interaction of sulfonated groups. The sulfonated nanoplates demonstrate to be a potential MeOH barrier and the nano-composite membranes show higher C/P value and lower swelling ratio than Nafion®.

SESSION B3: PEMFC/DMFC II
B: Polymer Electrolyte Fuel Cells and Electrolyzers
Chair: Thomas Zawodzinski
Wednesday Morning, June 17, 2015
Keystone Resorts, Quandary Peak I/II

10:30 AM **B3.01
Structural Aspects of PFSA Ionomers as Determined by STEM and Simulations Stephen J. Paddison; Chemical & Biomolecular Engineering, University of Tennessee, Knoxville, Tennessee, United States.

The need for next generation polymer electrolyte membrane fuel cells (PEMFCs) has driven considerable research effort into the development of novel membrane materials that are highly proton conducting at low temperatures. Perfluorosulfonic acid (PFSA) ionomers, (the benchmark Nafion™) consist of a hydrophobic poly-tetrafluoroethylene (PTFE) backbone with pendant perfluorinated vinyl ether side chains each terminated with a sulfonic acid group (i.e., $–SO_3H$). The chemistry and molecular structure of the side chains and backbone in PFSAs play a crucial role in determining the hydrated morphology and transport properties especially in the presence of water. Under hydrated conditions, the mesoscale phase separation occurs due to the hydrophobic and hydrophilic segments of the macromolecules. This is mainly due to the aggregation of ionic clusters and the reorganization of the PTFE backbones, which have been investigated by a variety of experimental and modeling approaches
.
We have recently examined the morphology of dry and hydrated perfluorosulfonic acid (PFSA) ionomers at cryo and room temperature using TEM/STEM with EELS capability. Z-contrast imaging was utilized to identify the micro-phase separation of the hydrophilic side chains containing water and the hydrophobic polytetrafluoroethylene (PTFE) backbones. The results compare very favorably with hydrated morphologies obtained through mesoscale dissipative particle dynamics (DPD) simulations. The cryo-STEM images of plunge-frozen samples was also found to agree with morphologies based on SAXS experiments. Chain conformations of the perfluorosulfonic acid (PFSA) ionomers: Nafion™ and Aquivion® were investigated with electron energy-loss spectroscopy (EELS) on a 200 kV transmission electron microscope (TEM) equipped with a monochromator. The results were compared with polytetrafluoroethylene (PTFE) to evaluate the effect of the pendant perfluoroether side chains of the ionomers on the structure of the PTFE backbone. Several unique spectroscopic features corresponding to conformational changes were identified in the low-loss region and the fine structures of the carbon K-edge. Results obtained from high-level density function theory (DFT) based electronic structure calculations confirm the conformational dependence of the EEL spectra of the PFSA ionomers. Comparison with the spectra obtained from the experiments revealed the correlation between the specific side chain chemistry and backbone conformation. This spectroscopic information will allow us to further explore the morphological properties of these materials when combining with additional imaging techniques.

11:00 AM B3.02
Anion Transport in Polymer Electrolytes Andrew Herring, Ashley Maes, Himanshu Sarode, Ye Liu and Tara Pandey; Chemical and Biological Engineering, Colorado School of Mines, Golden, Colorado, United States.

The potential of anion exchange membrane (AEM) fuel cells to provide inexpensive compact power from a wider variety of fuels than is possible with a proton exchange membrane (PEM) fuel cell, has continued to drive the research interest in this area. Alkaline catalysis in fuel cells has been demonstrated with non-precious metal catalysts, and with a variety of fuels beyond H_2 and methanol. Alkaline fuel cells (AFCs), based on aqueous solutions of KOH, have serious drawbacks associated with system complexity and carbonate formation. Anion exchange membrane (AEMs) fuel cells have a number of advantages over both PEM fuel cells and traditional AFCs; however, although anionic conductivity in AEMs can be comparable to PEMs the chemical stability of membrane attached cations in hydroxide is still not always sufficient for practical applications. The real issue is water transport; water is both a product and a reactant in these systems and wet cations are much more stable than dry.

11:20 AM B3.03
Effect of Hydration on Mechanical Properties of Anion Exchange Membranes Benjamin Caire, Melissa Vandiver, Andrew Herring and Matthew W. Liberatore; Chemical and Biological Engineering, Colorado School of Mines, Golden, Colorado, United States.

Anion exchange membranes facilitate ion transport in polymer electrolyte membrane fuel cells. An AEM must have a high ionic conductivity, low gas/fuel crossover, and be chemically and mechanically stable over the lifetime of the fuel cell. While chemical degradation typically dominates membrane failure pathways in a fuel cell, mechanical breakdown due to humidity cycling is a common occurrence. The sorption and desorption of water can cause pin hole cracks which lead to fuel crossover and stack failure. Development of thin polymer films is critical to reduce membrane resistance. As membrane thickness is decreased, maintaining membrane integrity becomes increasingly difficult. A modified Sentmanat Extensional Rheometer (SER) is used to perform tensile-like testing on thin (10-100 micron) membranes at relevant fuel cell conditions using a humidity delivery system developed for the TA Instruments ARES-G2 rheometer to allow for testing at a range of temperatures (30-100°C) and relative humidity conditions (0-95% RH). The new instrumentation and test procedures were benchmarked with Nafion® N115. The humidity oven can be used with all other rheometer accessories, including dynamic mechanical analysis. Water taken up by the polymers at high humidity acts as a plasticizer increasing elasticity of the films. However, previously tested AEMs displayed low elasticity and elongation under dry conditions, which could lead to pinholes and cracks during humidity cycles. A new polyethylene-b-poly(vinylbenzyl trimethylammonium) diblock AEM has been synthesized with improved elongation and elasticity. This polymer can be solution processed into thin (10 micron) films. Extensional tests of the polyethylene diblock were performed under dry and saturated gas conditions. At dry conditions the polyethylene diblock has a good Young's modulus (210 ± 30 MPa), a good elongation to break (150 ± 20 %), and reasonable strength (28 ± 4 MPa). When hydrated, water in the membrane has a plasticizing effect reducing the modulus by 95% and increasing elongation by 47%, but only reducing strength by 29%. While the changes in strength and elongation are considered acceptable, the dramatic reduction in modulus from dry to hydrated states requires improvement and warranted further investigation. Dynamic mechanical analysis was utilized to investigate moduli changes while ramping humidity. The modulus goes through a dramatic reduction when humidity is ramped and shows signs of hysteresis during dehumidification. Continued study will further investigate the effect of hydration on the mechanical performance of the polyethylene diblock and relate this effect to ionic transport through the membrane. Advanced knowledge of AEM mechanical properties will aid in design of robust membranes to improve fuel cell lifetime.

11:40 AM B3.04
Fundamental Understanding of Water Contribution for Ion Mobility in Anion Exchange Membranes Applied in Alkaline Fuel Cells Ye Liu[1], Bingzi Zhang[2], Söenke Seifert[3], Yuan Yang[4], Yushan Yan[2], Matthew Liberatore[1] and Andrew Herring[1]; [1]Chemical Engineering, Colorado School of Mines, Golden, Colorado, United States; [2]Chemical Engineering, University of Delaware, Newark, Delaware, United States; [3]Argonne National Laboratory, Argonne, Illinois, United States; [4]Chemistry, Colorado School of Mines, Golden, Colorado, United States.

Fuel cells are considered as one of the most promising clean energy sources to substitute for traditional non-renewable energy resources in the 21st century. Proton exchange membrane fuel cells (PEMFCs) as a low temperature fuel cell have been fully studied and well developed due to their advantages of high conductivity and fast start-up time. However, high manufacturing cost from using noble metal catalyst (typically platinum) in electrodes largely hampers their commercialization. Nowadays, alkaline fuel cells (AFCs) receive more investigation as one of the most promising fuel cells that probably can outperform all known low temperature fuel cells

When AFCs were first invented, potassium hydroxide solution was used as the electrolyte. However, when the liquid alkaline electrolyte reacted with CO_2 in the air, a carbonate/bicarbonate solid crystal was generated which precipitated onto the electrode, damaging the active layer and reducing fuel cell performance. Therefore, later, solid electrolytes (anion exchange membranes, AEMs) were used instead of original potassium hydroxide liquid electrolyte in AFCs. The application of AEMs today not only keeps the advantage of liquid alkali electrolytes with high active reaction, but also helps to solve the problems of electrolyte leakage and component corrosion.

So far, the primary limitations of AEMs are the relative low conductivity and chemical stability under alkaline operating conditions. AEMs degrade in alkaline condition with the decomposition of cationic groups occurring via S_N2 or Hofmann elimination. In order to rival the chemical stability of traditional quaternized ammonium, researchers develop a series of bulky novel cations. Zhang designed a new diphenyl (3-methyl-4-methoxyphenyl) tertiary sulfonium cationic group. By soaking in 1M KOD solution at 60, the membrane still maintained its hydroxide conductivity after 10 days indicating the methoxyl substituent assists to increase the chemical stability. Additionally, Our previous study on 1,4,5-trimethyl-2-(2,4,6-trimethoxyphenyl) imidazolium functionalized PPO indicated that the modification of imidazolium cation by attaching 2,4,6-trimethoxyphenyl group could help to increase the polymer chemical stability because of both electron donating function as well as steric effect. Hence, in this study, we focus on the phosphonium cation by adding three 2,4,6-trimethoxyphenyl groups, which expects to display a promising improved durability under the alkaline condition.

With improvement of the chemical stability, understanding ion mobility help to provide a context for assessing conductivity behavior, meanwhile, necessary for the design of next generation cation structure. Water molecules play an important role for facilitating anionic groups transfer via Vehicle and Grotthuss mechanisms. Besides, since the volume of tris(2,4,6-trimethoxyphenyl) phosphonium is large, absorption of water would directly affect the morphology of the membrane so that further influence the transport property and conductivity performance. In our study, water uptake and hydration number are measured through dynamic vapor sorption (DVS). Conductivities under different relative humidity are performed by electrochemical impedance spectroscopy (EIS). Water transportation is measured by pulsed field gradient NMR (PFGNMR), meanwhile, anion transportation is calculated via Mitra equation based on conductivity result. Morphologies are obtained from small angle X-ray scattering (SAXS) and atomic force microscopy (AFM). Insights on the correlations between hydration number and conductivity performance is investigated. A new understanding of water/anion transportation is developed.

SESSION B4: PEMFC/DMFC III
B: Polymer Electrolyte Fuel Cells and Electrolyzers
Chair: Vito Di Noto
Thursday Afternoon, June 18, 2015
Keystone Resorts, Grays Peak III

1:30 PM *B4.01
Nano-Structured Aromatic Ionomers for PEMFC Cristina Iojoiu[1, 2], Huu Dat Nguyen[2, 1], Olesia Danyliv[1, 2] and Sandrine Lyonnard[3]; [1]LEPMI, CNRS, Saint Martin d'Hères, France;[2]Grenoble University, Saint Martin D'Hères , France; [3]INAC SPrAM, CEA Grenoble, Grenoble, France.

The proton conducting membrane is a key component in proton exchanges membrane fuel cell (PEMFC). It transports protons from the anode to the cathode where oxygen is reduced to produce water and electricity. To assure high performance PEMFC the polymer exchange membrane (PEM) requires good thermo-mechanical properties, low gas permeability, good dimensional stability and good chemical and electrochemical stability in fuel cell operating conditions. It has been demonstrated that the microstructure of PEMs is crucial for their performance in the operation of fuel cells. Therefore, one key success of PEM is to design membrane with specifically morphology, i.e. with long range continuity of both the conductivity and mechanically robust domains. In this lecture we will briefly report our advances in the synthesis and characterization of membranes based on aromatic block copolymers containing hydrophilic blocks, i.e. polysulfone or polyether functionalised with perfluorosulfonic acid, and hydrophobic blocks i.e. partially fluorinated aromatic polysulfone. The polymer main chain was performed by polycondensation reaction. The perfluorosulfonic acid was grafted onto the polymer or monomer in two steps: bromination and coupling reactions. The super acidity of acidic function combined with a high flexibility of the spacer allows to the sulfonic acid groups to aggregate and form well defined hydrophilic domains. Additionally, the presence of fluorinated aromatic rings in the hydrophobic blocks increases its hydrophobicity that contributes significantly to the nano-phase separation. Copolymers with different lengths of hydrophobic-hydrophilic blocks were synthetized and characterised. Their membranes obtained by casting are compared in term of ionic conductivity, thermal stability, thermo-mechanical properties and fuel cell performances. The membrane nano-structuration was studied by Small Angle Neutron Scattering (SANS) and the impact of the polymer structure and casting processing conditions on the membrane morphology and functional properties are discussed in this work.

1:50 PM B4.02
Nafion/Zirconium Sulfonylphosphonate Composite Membranes for DMFC and PEMFC Kun-lin Liu[1], Chia-Chin Hsu[1], Cheng-Wei Pai[1], Ying-Ling Liu[2] and Chi-Yang Chao[2];[1]Materials Science and Engineering, National Taiwan University, Taipei, Taiwan; [2]Department of Chemical Engineering, National Tsing Hua University, Taipei, Taiwan.

In this work, a series of Nafion/zirconium sulfonylphosphonates(ZrSPP) composite membranes containing controlled loadings of ZrSPP nanoparticles with various sizes and compositions are prepared via a new preparation method by solvent casting from blends of Nafion solution and reaction mixture of as-synthesized ZrSPP. The compositions and sizes of ZrSPP nanoparticles were controlled by systematically changing the reaction parameters of the synthesis of ZrSPP, including solvent, temperature and feed ratio of the reactants. The resulting Nafion/ZrSPP composite membranes exhibited homogeneous distribution of ZrSPP nanoparticles smaller than 20 nm in size, leading to improvements in ion exchange capacity and proton conductivity by 40% at most as compared to the corresponding pristine Nafion recast. Small ZrSPP with high sulfonylphosphonic acid content significantly suppressed the methanol permeativity of the corresponding Nafion/ZrSPP suppression to half of that of pristine Nafion recast, resulting in a 2 fold increase in selectivity. The concurrent enhancements in proton conductivity and in selectivity should facilitate these composite membranes good candidates for PEM in DMFCs. The Nafion/ZrSPP composite membranes also exhibit improved proton conductivity at elevated temperature comparing to the pristine Nafion recast and the enhancement is more provoked at low relative humidity. A proton conductivity of 3 fold increase is observed at 80°C and 60% R.H.

2:10 PM B4.03
Preparation and Properties of DMFC Membranes from Polymer-Brush Nanoparticles Ilya Zharov[1, 2] and Shelley D. Minteer[1, 2]; [1]Chemistry, University of Utah, Salt Lake City, Utah, United States; [2]Materials Science and Engineering, University of Utah, Salt Lake City, Utah, United States.

We will describe a novel approach for the preparation of proton conducting membranes using polymer brush nanoparticles (PBNPs). PBNPs can be assembled into the membranes directly, or the membranes can be prepared by first assembling porous scaffolds from unmodified NPs followed by surface modification with polymer brushes. In both cases, proton-conducting channels are formed in the interstitial spaces between the nanoparticles.

First, proton conducting membranes were prepared using silica nanoparticles (SNPs) surface-grafted with 40-400 nm sulfonated polymer brushes, poly(3-sulfopropylmethacrylate), pSPM, and poly(4-styrenesulfonic acid), pSSA, grown via surface initiated atom transfer radical polymerization (SI-ATRP). The membranes prepared from the NPs carrying longer polymer chains possessed polymer-like characteristics, compared to the stiffer membranes made with shorter polymer brushes. All these membranes showed comparable proton conductivities, with a maximum value of ~0.06 S/cm at 98 °C and 70% R.H.

Second, we prepared proton conducting pore-filled membranes. In this case, nanoporous colloidal crystals were first assembled from unmodified SNPs, followed by filling the pores with pSPM or pSSA brushes covalently attached to the pore surface using SI-ATRP. The membranes could be hydrated almost completely, and did not swell. The proton conductivity was similar for both polymer-filled membranes, with a maximum value of ~0.02 S/cm achieved at 30 °C and 94% R.H. A sigmoidal dependence of the proton conductivity on the amount of sulfonic acid groups was found for pSPM pore-filled membranes. The proton conductivity remained relatively low at low degrees of sulfonation, increased rapidly around 50% sulfonic acid group content, and did not increase significantly after reaching ca. 75% sulfonic acid group content. We found that OCV for MEAs built using these membranes reached its maximum at 65% sulfonic group, and decreases after that. We attribute this effect to the increased methanol cross-over, which was confirmed by methanol uptake measurements for the membranes.

2:30 PM B4.04
Activity Trends and Design Principles for Multi-Transition-Metal (Oxy)hydroxide Oxygen Evolution Catalysts Shannon W. Boettcher; Chemistry, University of Oregon, Eugene, Oregon, United States.

Oxygen evolution reaction (OER) catalysis limits the efficiency of H_2 production through water electrolysis and photoelectrolysis – routes to large-scale energy storage. Despite 50 years of research the factors governing the activity of OER catalysts are not well understood. The paradigm to describe activity trends and predict new catalysts is based on active-site intermediate binding energies. The experimental data that forms the basis for this paradigm and to which theory is compared, however, has been largely collected on poorly defined materials. This led us to question the validity of the established activity trends and their mechanistic interpretation.

We developed a new thin-film approach to studying OER electrocatalysis that minimizes confounding effects due to mass and electron transport through typical thick films or powders of varying porosity. We measure electrical conductivity *in situ* and use surface-analytical tools to clarify how composition and structure evolves during OER. We discovered that oxides convert to oxyhydroxides and incorporate Fe impurities which form the active sites entirely responsible for OER in record-activity Ni-Fe catalysts. We find new activity trends, opposite of the established ones, and propose a new OER model on mixed-metal oxyhydroxides.

(1) Trotochaud, L.; Ranney, J. K.; Williams, K. N.; Boettcher, S. W. *J. Am. Chem. Soc.* **2012**, *134*, 17253.
(2) Trotochaud, L.; Young, S. L.; Ranney, J. K.; Boettcher, S. W. *J. Am. Chem. Soc.* **2014**, *136*, 6744.
(3) Burke, M. S.; Kast, M. G.; Trotochaud, L.; Smith, A.; Boettcher, S. W. *Submitted J. Am. Chem. Soc.* **2015**.

2:50 PM B4.05
Synthesis and Characterization of Pd-Ni-Sn Electrocatalyst for Use in Direct Ethanol Fuel Cells Sompoch Jongsomjit[1], Paweena Prapainainar[2, 3, 4] and Korakot Sombatmankhong[5];[1]Interdisciplinary Graduate Program in Advanced and Sustainable Environmental Engineering (International Program),Faculty of Engineering, Kasetsart University , Ladyao, Jatujak, Thailand; [2]Department of Chemical Engineering, Faculty of Engineering, Kasetsart University, Ladyao, Jatujak, Thailand; [3]National Center of Excellence for Petroleum, Petrochemicals and Advance Material, Kasetsart University, Ladyao, Jatujak, Thailand; [4]Department of Chemistry and NANOTEC Center for Nanoscale Materials Design for Green Nanotechnology, Kasetsart University, Ladyao, Jatujak, Thailand; [5]National Metal and Materials Technology Center, Thanon Phahonyothin, Tambon Khlong Nueng, Amphoe Khlong Luang, Thailand.

One critical challenge to commercialise direct ethanol fuel cells (DEFCs) is catalyst poisoning associated with the strongly adsorbed CO intermediate on catalyst's surface at low temperature. The present work therefore aimed to develop a highly electrochemically active catalyst which is durable to the presence of CO contaminant. Different Pd-Ni-Sn compositions impregnated on carbon black were synthesised by sodium borohydride reduction method which can be classified as mono-, binary- and ternary-catalyst systems at which 20%w Pd/C was utilised as a base catalyst. The addition of 5-20%w Ni and/or 5-20%w Sn metals was found to increase catalytic activity and catalyst stability for ethanol oxidation reaction (EOR). Several diagnostic techniques were employed to assess their suitability for use in DEFCs including X-ray diffraction (XRD), X-ray photoelectron spectroscopy (XPS), transmission electron microscopy (TEM), scanning electron microscopy-energy dispersive spectrometry (SEM-EDX) and electrochemical techniques. The XRD and XPS spectra verified that the existence of Pd, Ni and Sn in the as-prepared catalysts was in the oxidation state of Pd^0 and Pd^{2+}, Ni^{2+} (in form of $Ni(OH)_2$) and Sn^{4+} (in form of SnO_2), respectively, which were known to promote the EOR and CO oxidation. The average particle size was in the range of 5.46-10.56 nm for all samples. By using SEM-EDX, it was found that the actual ratios of metal loadings were relatively similar to the desired compositions and their surface morphology was uniformly distributed. Moreover, electrocatalytic activity towards EOR was evaluated using cyclic voltammetry in 1M ethanol (in 1M KOH). Among various catalytic compositions, 20%w Pd/C containing 10%w Ni and 10%w Sn exhibited excellent catalytic activity and CO tolerance as the maximum current density of 146 mA cm^{-2} for EOR and the highest electrochemical surface area were obtained while lowering the CO-stripping peak potential to -0.525 V (vs Ag/AgCl).

C: Electrodes and Solid Electrolytes for Batteries

* Invited Speaker
** Keynote Speaker

SESSION C1: Rational Design of Battery Materials
C: Electrodes and Solid Electrolytes for Batteries
Chair: Arumugam Manthiram
Monday Morning, June 15, 2015
Keystone Resorts, Shavano Peak

10:30 AM **C1.01
Lithium Sulfur Batteries: Fundamental Understanding and Materials Design Yi Cui; Department of Materials Science and Engineering, Stanford University. Stanford Institute for Materials and Energy Sciences, SLAC National Accelerator Laboratory, Stanford, California, United States.

Lithium-sulfur (Li-S) batteries have high theoretical specific energy (2500Wh/kg) and energy density (2800Wh/L) for portable and stationary energy storage although both lithium metal anodes and sulfur cathodes present many materials challenges for the operation of Li-S batteries. Here I will present the recent understanding of Li-S battery chemistry and a number of innovative materials design concepts to address these challenges. Some highlights include: 1) Understanding LixS speciation and their interaction with solid support, which guides the materials selection 2) Advanced nanomaterials designs addressing the polysulfide dissolution problems 3) Utilizing separators to control polysulfide species and enhance battery safety. 4) Nansoscale interface design to stabilize Li meal anodes for suppressing dendrites and increasing coulombic efficiency.

11:00 AM C1.02
Atomic-Scale Insights into Lithium and Sodium Battery Materials: Intercalation, Diffusion and Surfaces Saiful Islam; Chemistry, University of Bath, Bath, United Kingdom.

Major advances in rechargeable lithium-ion batteries for portable electronics and electric vehicles requires the discovery and development of new materials. In addition, sodium-ion batteries are attracting growing interest for grid-storage applications largely due to the natural abundance of sodium and cost issues. It is clear that a complete understanding of the properties of both Li- and Na-ion battery materials requires fundamental knowledge of their underlying ion transport, intercalation and surface properties on the atomic- and nano-scales. Such detail is often lacking, but is important for developing strategies for optimizing their properties, as well as identifying next-generation materials.

In this context, advanced materials modelling [1] combined with structural and electrochemical techniques are now powerful tools for investigating these properties. This presentation will highlight recent studies [2-5] in this field covering the following main themes:
(i) defect chemistry and ion diffusion in polyanionic cathode materials such as the silicate Li_2FeSiO_4 and hydroxysulfate $LiFeSO_4OH$;
(ii) surface properties of MnO_2 phases related to their potential use as intercalation electrodes or Li-O_2 battery catalysts;
(iii) Na-ion mobility in phosphate-based materials (e.g. layered Na_2FePO_4F) for sodium-ion batteries

The presentation will aim to demonstrate how the strong synergy of computer modelling and experiment has helped us to shed new light on the structure-property relationships of battery materials. In particular, the simulations based on both potentials-based molecular dynamics (MD) and density functional theory (DFT) have unravelled unique mechanistic detail on ion conduction, voltage trends and surface structures with strong links with complementary experimental techniques (e.g. diffraction, electrochemistry).

References
[1] M.S. Islam; C.A.J. Fisher, *Chem. Soc. Rev.*, **43**, 185 (2014);
[2] C. Eames et al, *Chem. Mater*., 26, 3672 (2014).
[3] D.A. Tompsett et al., *J. Amer. Chem. Soc*., 136, 1418 (2014)
[4] C. Eames ; M.S. Islam, *J. Amer. Chem. Soc*., 136, 16270 (2014)
[5] R. Tripathi et al., *Energy Envrion. Sci*., **6**, 2257 (2013).

11:20 AM C1.03
Accelerated Computation Materials Design of Solid-Electrolyte Materials in All-Solid-State Li-Ion Batteries Yifei Mo; Materials Science and Engineering, University of Maryland, College Park, College Park, Maryland, United States.

All-solid-state batteries using solid electrolyte materials provide intrinsic safety and high energy density. A variety of problems of the electrolyte materials and at the electrolyte-electrode interfaces have been limiting the development of all-solid-state batteries. In this talk, I will present our study of developing first principles techniques to design novel solid-state electrolytes. Using the recently discovered Li10GeP2S12 lithium super ionic conductor as an example, I will show first principles calculations for various properties of solid electrolyte materials. I will demonstrate the computational design and prediction of new lithium ion conductor materials Li10SiP2S12 and Li10SnP2S12 that retain the excellent Li+ conductivity of Li10GeP2S12 at a significantly reduced cost. The computationally predicted new compounds have recently been synthesized, and the measured Li+ conductivity and activation energy are in excellent agreement with first principles predictions. In addition, I will present our recent computational study about the solid-solid interfaces in all-solid-state Li-ion batteries. The modeling study reveals the compatibility issues of the electrolyte that lead to the failure of solid electrolyte materials. I will also discuss the first-principles atomistic modeling about the rate limiting factors at the solid interfaces.

11:40 AM C1.04
Fast Design and Optimization of Solid State Electrolytes for Lithium Rechargeable Batteries Guided by the Combination of Bond-Valence Method and Density Functional Theory Ruijuan Xiao, Hong Li and Liquan Chen; Institute of Physics, Chinese Academy of Sciences, Beijing, China.

Solid-state batteries have been proposed as a solution to improve the safety of current lithium rechargeable batteries because of the stability and non-flammability of inorganic solid electrolytes. One of the biggest challenges for solid-state batteries is the development of good solid electrolytes with high ionic conductivities. A simple and available model to study the lithium ionic transport is based on the bond-valence (BV) theory, which is a fast technique and the simulation of diffusion pathways and barriers for one crystal structure can be finished in several minutes by computer, but the accuracy of the calculated energy barriers from this method is limited to the empirical potential energy function. The method with higher level of accuracy is the density functional theory (DFT) calculations based on quantum mechanical modeling. However, they suffer from high computation cost which limits their efficiency on screening of materials based on ionic transport properties. Because of the distinctive features of each method, combination of the above approaches at different stage maybe a more practical scheme to discover solid electrolytes.

The fast BV technique is suitable for high-throughput pre-screening a wide range of compounds since the trend in the ability of ion motion can be drawn from the relative values of the migration energy barriers despite of their less accuracy compared with quantum mechanical simulations. While the time-consuming DFT method can be adopted to do more precise calculations only for those promising candidates assigned by the BV method. For the derivative structures achieved by substitution or doping the existing compounds, the DFT computation is a powerful tool to predict exact structures which are important information for performing BV calculations. Thus, we believe that the reasonable combination of the BV method and DFT calculations is a great help in realizing the fast screening, design and optimization solid state electrolytes for lithium second batteries.

In this work, employing the self-implemented software based on the BV method, we calculate the lithium ion diffusion pathways and barriers for more than 1000 compounds from the structure database. The effectiveness of the BV method is confirmed by comparing part of the results with DFT simulations. Besides screening a wide range of structures, the scheme combining BV and DFT method is also utilized to design and optimize the materials. We take β-Li_3PS_4, a promising electrolyte material identified in newly investigations, as a model system, and the effects of doping at P sites and S sites on the structure and the ionic transport properties are investigated. The lithium ionic migration properties predicted by BV-based method are confirmed by the first-principle molecular dynamics simulations. As a result, an optimization scheme is proposed for this material.

SESSION C2: Poster Session I
C: Electrodes and Solid Electrolytes for Batteries
Monday Afternoon, June 15, 2015
12:00 PM
Keystone Resorts, Red Cloud Peak

C2.01

Fast Li Self-Diffusion in Amorphous Li-Si Electrochemically Prepared from Semiconductor Grade, Monocrystalline Silicon — Insights from Spin-Locking Nuclear Magnetic Relaxometry Andreas Dunst, Michael Sternad, Viktor Epp and Martin Wilkening; Christian-Doppler Laboratory for Lithium Batteries, Institute for Chemistry and Technology of Materials, Graz University of Technology, Graz, Austria.

Silicon is one of the most promising anode materials for lithium-based rechargeable batteries. Provided the volume changes during Li uptake can be brought under control, Li ion diffusivity is expected to crucially determine the performance of such energy storage systems. Therefore, studying diffusion properties in amorphous Li-Si underpins applied research that is being directed towards the development of powerful storage devices. So far, only little information is available on Li self-diffusion in amorphous Si. Here, we used ^{7}Li NMR spectroscopy [1] to precisely quantify microscopic activation energies and Li jump rates in amorphous Li-Si which is primarily formed if monocrystalline Si is lithiated electrochemically. Our results reveal relatively fast Li diffusivity with an average activation energy for long-range ion transport as high as ca. 0.65 eV; jump rates turn out to be in the order of 2.5×10^5 1/s at 246 K, see also ref. [2]. Comparisons with data from laboratory frame NMR relaxometry, which is sensitive to more localized ion hopping, points to complex dynamics that is most likely governed by non-exponential motional correlation functions originating from a large distribution of activation energies. Noteworthy, a second sample, which is a mixture of amorphous Li-Si and metastable, crystalline $Li_{15}Si_4$ that forms at lower discharge potentials, points to slightly enhanced Li diffusivity (0.51 eV). The data obtained might help optimizing Li-based silicon batteries whose performance critically depend on fast Li-ion transport.

Acknowledgement Financial support by the Federal Ministry of Science, Research and
Economy and the National Foundation for Research, Technology and Development is gratefully acknowledged.

References

[1] V. Epp, M. Wilkening, Phys. Rev. B 82 (2010) 020301.
[2] A. Kuhn, P. Sreeraj, R. Pöttgen, H.-D. Wiemhöfer, M. Wilkening, P. Heitjans, J. Am. Chem. Soc. 113 (2011) 11018.

C2.02

Solubility Behavior of Nanograined Li_2MnSiO_4 Cathode Material in Liquid Electrolytes Marcin Molenda, Michal Swietoslawski and Roman Dziembaj; Faculty of Chemistry, Jagiellonian University, Krakow, Poland.

In recent years, polyanionic cathode materials with $(SiO_4)^{4-}$ structural units has received considerable attention because of their high thermal and chemical stability. Selecting appropriate transition metal compound can assure good redox potential and high capacity. Li_2MnSiO_4 is the most promising member of dilithium orthosilicates Li_2MSiO_4 family. Li_2MnSiO_4 combines high thermal stability, highest theoretical capacity 333 mAh/g, low production costs, safety and high working potential. All of aforementioned make Li_2MnSiO_4 an attractive cathode material for new generation Li-ion batteries [1-3]. Unfortunately, like all of the polyanionic cathode materials, lithium silicates are electric insulators showing electrical conductivity at room temperature within the range of 10^{-12}-10^{-15} $S \cdot cm^{-1}$ [3]. Low electrical conductivity of Li_2MSiO_4 can be enhanced in example by carbon coating.

The present work concerns studies on stability of Li_2MnSiO_4 and C/Li_2MnSiO_4 cathode materials towards most popular Li-ion batteries electrolytes. Li_2MnSiO_4 nanopowders were synthesized using sol-gel Pechini method. Calcination procedure of the precursor allows to control product grain size. Samples of different grain sizes were obtained (from 5-10 nm up to 80-100 nm) [4]. Powders were coated with conductive carbon layers (CCLs) using hydrophilic polymer as a source of carbon [5]. C/Li_2MnSiO_4 nanocomposites with various thickness of carbon coating were produced. Obtained cathode materials were studied to define solubility of Li_2MnSiO_4 in liquid electrolytes. The corrosive influence of different electrolyte compositions on Li_2MnSiO_4 material was defined and the optimal thickness and morphology of protective carbon coatings was determined.

[1] M.E. Arroyo-deDompablo et al. Electrochem Commun 8 (2006) 1292
[2] Z.L. Gong et al. J Power Sources 174 (2007) 524
[3] A. Kokalj et al. Chem Mater 19 (2007) 3633
[4] M. Swietoslawski et al. J Power Sources 244 (2013) 510
[5] M. Molenda et al. Solid State Ionics 179 (2008) 197

C2.03

Studies on PVA Based Nanocomposite Polymer Gel Electrolyte Membranes for High Performance Proton Conducting Batteries S. L. Agrawal[1] and Neelesh Rai[2]; [1]Department of Physics, APS University, Rewa , India; [2]Department of Physics, AKS University, Satna, India.

Though, Lithium-ion based batteries have been looked upon as an alternative power source in recent times to meet the ever growing energy demands due to high specific capacity (~1670mAhg^{-1}), specific energy (~2600Whkg^{-1}) and long cycling life, they pore safety concerns and eco-friendly problems. Development of all solid state batteries based on proton conducting gel electrolytes appear a favorable option to counter these problems besides possessing high ionic conductivity, better stability and high electrochemical windows. However, these gel electrolytes too suffer from liquid exudation problem which may lead to internal short circuiting of batteries. Scientists in recent times have tried with success addition of a third component (nano sized filler) in electrolyte matrix to circumvent the problem of liquid oozing. The present work has been aimed to study the role of Multi walled carbon nanotube on the performance of a polymer gel electrolyte films namely, (PVA:NH_4SCN:DMSO system in batteries. Structural and thermal behavior as well as ionic conductivity of the PVA:NH_4SCN:MWNT free standing electrolyte films is being investigated. XRD and SEM result show improvement in amorphous behavior of composite gel electrolytes membranes with increasing concentration of MWNT filler. The DSC behavior of composite system show better thermal response upon dispersal of MWNTs filler in pristine electrolyte. Bulk conductivity of these polymeric composite gel electrolytes enhance by an order of magnitude with appearance of two conductivity maximas in concentration dependence plots. Cyclic voltammetry studies have been conducted in the voltage window of -3 to 3 V at room temperature to ascertain utility of films in battery development.
Keywords: Gel electrolytes, ionic conductivity, X-ray diffraction, Differential scanning calorimetry, Multi walled carbon nanotube and cyclic voltametry.

C2.04

Lithium in Diffusion Measurements on a Garnet-Type Solid Conductor $Li_{6.6}La_3Zr_{1.6}Ta_{0.4}O_{12}$ (LLZO-Ta) by Pulsed-Gradient Spin-Echo NMR Method Kikuko Hayamizu[1], Yasuaki Matsuda[2], Masaki Matsui[2], Yasuo Takeda[2] and Nobuyuki Imanishi[2]; [1]Institute of Applied Physics, University of Tsukuba, Tsukuba, Japan; [2]Department of Chemistry for Materials, Mie-University, Tsu, Mie, Japan.

Garnet-type solid conductors $Li_{7-x}La_3Zr_{2-x}Ta_xO_{12}$ are known to have high ionic conductivity at room temperature. We found that the polycrystalline $Li_{6.6}La_3Zr_{1.6}Ta_{0.4}O_{12}$ (LLZO-Ta) has high ionic conductivity of $3.7 \times 10^{-}$

[4] Scm^{-1} at 25°C. The ^{7}Li NMR spectra of the LLZO-Ta were observed from 30 to 140 °C. The spectra were composed of narrow and broad components and the line width of the narrow component varied from 0.69 (30°C) to 0.32 kHz (150°C). We attempted the lithium ion diffusion measurements by the pulsed-field spin-echo (PGSE) NMR and found that echo signals of the PGSE measurements can be observed above 50°C with reasonable intensity. The lithium diffusion was observed by varying the observation time (Δ) and pulsed-field gradient (PFG) strength (g) between 50 and 140 °C. We found that the lithium diffusion phenomena depend significantly on Δ and g. When Δ became short and g became smaller, the lithium apparent diffusion constant became larger, which were quite different from lithium ion diffusion in liquids. Δ-dependent diffusion phenomena are known as "anomalous diffusion" for neutral particles diffusing in circumstances with internal structures such as zeolites, polymers and so on. We found that the lithium ion migration in the solid conductor showed similar to so-called anomalous diffusion. In this study when Δ became short less than 30 ms, the diffusion plots showed diffractive patterns which were insensitive to temperature. The diffractive diffusion indicates that the lithium ions collide with standing anions and are diffracted in short time period. Since Δ became longer, the g-dependence of the apparent diffusion constant was reduced and approached to an equilibrated value. We obtained the temperature dependence of the lithium diffusion constant with Δ = 100 ms and g = 9.8 Tm^{-1} between 50 and 140 °C and the activation energy was 34 kJ mol^{-1} between 80 and 140 °C.

C2.05

All Solid State Li-Garnet-Based Batteries: From Materials Development to Thin Film Microstructures Jennifer L. Rupp[1], Semih Ayfon[1], Inigo Garbayo[1], Reto Pfenninger[1], Michael Rawlence[2, 1] and Michal Struzik[1]; [1]Electrochemical Materials, ETH Zurich, Zurich, Switzerland; [2]Laboratory for Thin Films and Photovoltaics, EMPA, Dübendorf, Switzerland.

The next generation of energy storage devices relies on a broad and adaptable range of volumetric and gravimetric energies to compete with the challenges in stationary, mobility and portable electronic electricity supply. Here, all solid state batteries based on Li-garnet-based structures are interesting model systems as these allow for complete *solid state* battery types that: i.) can partially use industrial waste heat to increase charging times (increased Li^{+} diffusion) for stationary, ii.) with new high capacity electrode materials which show conventionally a low stability in standard liquid/polymer based Li-batteries, iii.) are easy transferrable to model thin film battery structures for powering of portable electronics on chip.

Firstly, we report on Al:$Li_{7-2x}La_3Zr_2O_{12}$ bulk pellet and thin film processing, their crystallization and ionic transport characteristics. Secondly, from a materials processing perspective we report on a new modified 2-step sol-gel synthesis-combustion method to lower the nano-particle production of the solids to ~ 600°C. Here, we exemplify stable electrolyte compounds based on $Li_{7-3x}(Ga_x)La_3Zr_2O_{12}$. Thirdly, for N-site doping $Li_{7-x}La_3Zr_{2-x}Te_xO_{12}$ with x = 0.25 to 0.35 were prepared by synthesis in solid state, and Te is studied as alternative to Ga and Al stabilizers as battery electrolyte without grain boundary stabilization. Finally, we concluded on the suitability of these new materials for scaling down to thin film microstructures, as potential Li-garnet electrolytes in all solid state batteries for portable electronic applications. First strategies on how to design optimum thin film-microbatteries adaptable to chemo-mechanical variations during operation will be shown. Here, two different model designs are described: (i.) the fabrication of microbattery dot arrays and (ii.) wrapped anode/electrolyte/cathode microstructures with tunable strain.

C2.06

Proof-of-Concept of All-Solid-State Metal-Metal Battery Fuminori Mizuno[1], Ruigang Zhang[1], Timothy S. Arthur[1], Donovan N. Leonard[2], Miaofang Chi[2] and Jeff Sakamoto[3];[1]Materials Research Department, Toyota Research Institute of North America, Ann Arbor, Michigan, United States; [2]Oak Ridge National Laboratory, Oak Ridge, Tennessee, United States;[3]Mechanical Engineering, University of Michigan, Ann Arbor, Michigan, United States.

All-solid-state Li-ion batteries are of considerable interest owing to their high volumetric energy density, durability, and improved safety. All-solid-state batteries are classified into two categories; thin-film batteries using Lithium phosphrous oxynitride (Lipon) solid electrolyte [1], and bulk-scale batteries employing fast Li-ion conducting solid electrolytes such as Li_3PS_4[2,3], $Li_{10}GeP_2S_{12}$ [4] and $Li_7La_3Zr_2O_{12}$ [5,6]. Based on the recent discovery of ceramic Li-ion conducting solid electrolytes, all-solid-state batteries may operate at rates comparable to state-of-the-art liquid electrolyte Li-ion technology. Moreover, to reduce the interfacial resistance, surface modifications, between cathode active material and solid electrolyte, has been demonstrated [7]. However, improving performance, while maintaining adequate rate capability, requires novel strategies to enable facile transport at the solid electrolyte-electrode interface.

Motivated by the previous work, we present a novel all-solid-state battery system, employing metallic electrodes for both the anode and cathode; a metal-metal battery. In this work, dissimilar metal electrodes were enabled by designing a multi-ion conducting membrane. Essentially, the cell emulates a Daniel cell, but instead of using a hybrid liquid-solid electrolyte, a hybrid solid-electrolyte membrane configuration was investigated. Metallic cathodes and anodes were coupled with corresponding solid electrolytes of the same ionic species. Thus, the simultaneous oxidation of one ionic species was coupled to the reduction of a dissimilar ion species during charging and discharging. Prototypical cells demonstrate unprecedented performance exhibiting voltage plateaus of approximately 2 Volts.

In this presentation, we will elucidate the reaction mechanism(s) and other related electrochemical phenomena including the stability and kinetics of the solid electrolyte-metal interfaces..

References

[1] J. B. Bates et al., *J. Power Sources*, **43-44** (1993) 103.
[2] F. Mizuno et al., *Solid State Ion.*, **177** (2006) 2721.
[3] Z. Liu et al., *J. Am. Chem. Soc.*, **135** (2013) 975.
[4] N. Kamaya et al., *Nat. Mater.*, **10** (2011) 682.
[5] R. Murugan et al, *Angewandte Chemie Int. Ed.*, **46** (2007) 7778.
[6] E. Rangasamy et al., *Solid State Ion.*, **206** (2011) 28.
[7] N. Ohta et al., *Adv. Mater.*, **18** (2006) 2226.

C2.07

The $Li_{(m)}$ / Li_3PS_4 Interface for Solid-State Batteries Timothy S. Arthur[1], Ruigang Zhang[1], Regina Garcia[2], Jeff Sakamoto[2] and Fuminori Mizuno[1]; [1]Materials Research, Toyota Research Institute of North America, Ann Arbor, Michigan, United States; [2]University of Michigan, Ann Arbor, Michigan, United States.

All solid-state (AS-S) batteries based on Li-metal can provide many advantages over current Li-ion batteries. The Li metal anode ($Li_{(m)}$) has a high theoretical capacity of 3861 mAh/g and equilibrium potential of -3.045 V vs NHE, providing great potential as a high-energy density cathode for future mobility. To realize a solid-state battery based on $Li_{(m)}$ relies heavily on the Li^{+} diffusion and stability of the solid-state electrolyte. One potential solid-state electrolyte for AS-S batteries is the amorphous Li_3PS_4 (LPS), previously shown to have excellent Li^{+}conductivity and wide electrochemical window. Here, we present our analysis of the stability of the LPS electrolyte against the $Li_{(m)}$ anode for AS-S batteries.

To understand the effect of $Li_{(m)}$ stripping and plating on the interface of LPS and $Li_{(m)}$, we performed asymmetric cell polarizations of a pressed pellets of LPS between two $Li_{(m)}$electrodes. After electrochemical testing, the cells are dismantled and the LPS pellets are analyzed with X-ray photoelectron spectroscopy (XPS), Raman spectroscopy and scanning electron microscopy (SEM). After cycling, the $Li_{(m)}$ / LPS interface shows a visible discoloration from the yellow LPS to red/black. XPS analysis of the discolored regions showed a decomposition of LPS pellet to Li_xS and Li_xP products. SEM analysis shows that the decomposed regions have different morphologies and are sulfur-rich. From this analysis, we will propose a decomposition mechanism and possible solutions to inhibit the

deleterious interfacial reactions for AS-S batteries based on $Li_{(m)}$ and LPS. In conclusion, solid-solid interfaces are crucial to the performance of AS-S batteries, and require in-depth analysis to guide future synthetic strategies. To reach the stringent demands of vehicular applications, post Li-ion battery technologies will play a key role for future, electrified mobility.

C2.08

Li-Ion Conducting Polymer Electrolytes Based on Biopolymer, Agar Agar Selvasekarapandian Subramanian[1], Vinitha Thiyagarajan Upaassana[1], Sindhuja Manohar[1], Monisha Sampath[1] and Arun A[2]; [1]Physics, Materials Research Centre, Coimbatore, India; [2]Chemistry, Government Arts College, Thiruvannamalai, India.

Agarose or commonly known as agar is a popular ingredient for desserts and have recently been explored to develop electrolytes for batteries due to the evident amorphous nature from XRD characteristics. Using solid state organic electrolytes in Li-ion batteries have typically proved to exhibit various advantages like wider voltage range, three times the energy density of traditional batteries, and resistance to heat. Agar electrolytes doped with Lithium salts and dissolved in ionic liquids like 1-ethyl-3-methylimidazolium acetate and trimethyl ethanol ammonium acetate manifests a conductivity of 10^-3 S/cm at 100 °C. With a concentration of 50 wt. % acetic acid, a conductivity of 10^-4 S/cm is observed at 80 °C in proton conducting membranes. Even the addition of nanoparticles like NiO or SiO_2 reveals not much increase, contradicting the otherwise high ionic conductivity in other organic polymer electrolytes. A remarkable shoot in the conductivity of agar agar electrolytes is achieved by addition of plasticizer, Dimethyl Formamide, which increases the dielectric constant and amorphous phase of the electrolyte. AC Impedance characteristics and CV measurements of electrolytes developed using various compositions of agar agar polymer, lithium salts, plasticizer and nanofillers with water as solvent are presented in this paper. Physicochemistry of the resulting electrolytes are observed using XRD, FTIR, and DSC analysis. A conductivity of 10^-2 S/cm at room temperature was observed when DMF was used as plasticizer with 0.6% concentration of $LiClO_4$. And as expected, the addition of DMF in agar agar matrix enhanced salt-solvating power leading to decrease in the glass transition temperature. The effect of nanofillers, with respect to conductivity, with and without the addition of plasticizers is also discussed. XRD results manifests that the amorphous nature of the electrolyte increases as the concentration of $LiClO_4$ increases and the crystalline nature diminishes vastly with addition of DMF. FTIR Spectroscopy, measured for the range, 0 to 4000 cm^{-1}, revealed intensity and frequency change for various electrolytes indicating complex formation. The batteries constructed with agar electrolytes comfortably reach a very high stable voltage. The CV measurements revealed a stable voltage window of -2.5 V to +2.5 V which is a new high ever since the most extensively used Lithium Hexafluorophosphate ($LiPF_6$) electrolytes which has evinced a maximum conductivity closer to 10^-4 S/cm. The other major advantage of using a bio-degradable polymer is minimised pollution due to electronic waste and easier recycling of the batteries. The high conductivity and voltage established promises greener batteries with long life time and reduced battery recharging time.

C2.09

A Comparative Study of Impact in Conductivity of $LiNiPO_4$ on Doping Europium and Samarium in Lithium and Nickel Sites Prepared Using Modified Pechini and Polymeric Precursor Method Selvasekarapandian Subramanian[1, 2], Goutam Anbunathan V N[2], Kalpana M[2], Senthil Kumar P[3], Vinoth Pandi D[4], Sakunthala A[3] and Gunasekaran K[2]; [1]Physics, Materials Research Centre, Coimbatore, India; [2]Department of Nano Science and Technology, Tamilnadu Agricultural University, Coimbatore, India; [3]Department of Physics, Karunya University, Coimbatore, India; [4]Department of Physics, Coimbatore Institute of Technology, Coimbatore, India.

Abstract

Li-ion batteries are extensively used for powering portable electronics devices and the presently used cathode material ($LiCoPO_4$) has a voltage limitation of 3.7 V. Attempts to improve the battery's voltage from 3.7 V to 5.2 V by changing the different cathode materials are being undertaken. $LiNiPO_4$, an olivine structured compound has been studied as it provides high voltage, and is inexpensive, non-toxic, environmentally benign, excellent cycle stability and good thermal stability. However the main complication in using it as cathode material lies in its poor rate capability which is linked to its low electronic and ionic conductivity. Nano structured cathode materials can provide improved energy storage capacity and charge–discharge kinetics, better cyclic stabilities due to high surface area, short shorter diffusion paths and freedom for volume change that is associated with lithium-ion intercalation and discharge.

In this work, we prepared Pure, Europium and Samarium doped in both Lithium and Nickel sites of $LiNiPO_4$ using modified Pechini method and Polymeric Precursor method. Procedure involves mixing and stirring of Lithium nitrate, Nickel (II) nitrate hexahydrate, Ammonium dihydrogen phosphate and Samarium (III) Nitrate hexahydrate / Europium (III) Nitrate hexahydrate in distilled water and later citric acid and ethylene glycol are added in specific molar ratio followed by pyrolysis and calcination whereas in case of Polymeric precursor method all of the above mentioned salts except citric acid and ethylene glycol are added into molar solution of Polyvinyl pyrrolidone (PVP) solution and followed by pyrolysis and calcination. The preliminary analyses such as XRD, EDAX, FTIR and conductivity measurements have been carried out for all the 8 samples and are compared with pure ($LiNiPO_4$) sample of each method. The X-ray diffraction analysis confirms the formation of orthorhombic structure and lattice constants 'a', 'b', and 'c' are calculated for all the samples. The calculated crystallite sizes of the samples are in the range of 65-147 nm and 95-114nm for Pechini and Polymeric method respectively. The EDAX analysis confirms the presence of Ni, Eu, Sm, and P. The FTIR analysis has been made. Room temperature conductivities in S/cm of Pure $LiNiPO_4$, $Li_{0.99}Eu_{0.01}NiPO_4$, $LiNi_{0.99}Eu_{0.01}PO_4$, $Li_{0.99}Sm_{0.01}NiPO_4$ & $LiNi_{0.99}Sm_{0.01}PO_4$ prepared by Pechini and polymer method are 5.8483×10^{-08}, 8.2037×10^{-08}, 1.0521×10^{-07}, 7.9484×10^{-08} & 1.6473×10^{-07} and 6.8414×10^{-08}, 9.1242×10^{-08}, 1.2634×10^{-07}, 8.6410×10^{-08} & 2.4836×10^{-07} respectively. Comparing Modified Pechini method samples, Polymer Precursor method samples shows slightly higher conductivity. Also, Eu and Sm doped in Ni sites shows improved conductivity by an order than sample doped in Li sites in both preparation methods. Dielectric measurements for all the samples have been discussed.

C2.10

Sputter Deposited $Li_7La_3Zr_2O_{12}$ as Electrolyte for Thin Film Cells Sandra Lobe[1], Christian Dellen[1], Hans-Gregor Gehrke[1], Chih-Long Tsai[1], Martin Finsterbusch[1], Sven Uhlenbruck[1] and Olivier Guillon[1, 2]; [1]Institute of Energy and Climate Research (IEK-1) , Forschungszentrum Jülich, Jülich, Germany; [2]Institut für Gesteinshüttenkunde, Rheinisch-Westfälische Technische Hochschule (RWTH) Aachen, Aachen, Germany.

Most commercial state-of-the-art batteries work with a liquid organic electrolyte which might cause safety problems due to an insufficient thermal and electrochemical stability. Replacing the liquid by a solid electrolyte is one approach to overcome these problems. Next to sulfides and phosphates, oxide compounds like the garnet-structured $Li_7La_3Zr_2O_{12}$ (LLZ) are promising materials for solid electrolytes. LLZ exists in two modifications, a tetragonal and a cubic, whereby the cubic high temperature phase shows a higher Li-ion conductivity (about 10^{-4} S/cm). Further advantageous properties of LLZ are its thermal (up to 1050°C) and electrochemical stability (up to 8V) which allows its usage with high-voltage electrodes or in batteries at elevated temperatures. Since the conductivity is two orders of magnitude lower compared to organic electrolytes the overall resistance can be lowered by reduction to a thin electrolyte layer in all-solid-state cells.

R.f. magnetron sputter deposition is one approach to coat large substrate areas with LLZ electrolyte. In order to get crack-free, dense and single phase LLZ thin films, deposition parameters need to be adjusted carefully, which is shown by x-ray diffraction (XRD), secondary ion mass spectroscopy (SIMS) and scanning electron microscopy (SEM). In our study conductivities up to 10^{-6} S/cm are achieved for single phase cubic thin films. Furthermore, LLZ thin films were successfully integrated into all solid state cells, which are also characterized.

C2.11

Evaluation of Mechanical Properties of Li_2S-P_2S_5-LiI Glass Electrolytes for All-Solid-State Lithium Batteries Atsutaka Kato[1], Atsushi Sakuda[2], Akitoshi Hayashi[1] and Masahiro Tatsumisago[1]; [1]Applied Chemistry, Osaka Prefecture University, Sakai, Japan; [2]Research Institute for Ubiquitous Energy Devices, National Institute of Advanced Industrial Science and Technology (AIST), Ikada, Japan.

Sulfide glasses are expected as solid electrolytes for all-solid-state batteries because of high lithium-ion conductivities. Sulfide electrolyte powders pressed at ambient temperature have much lower grain boundary resistance compared to oxide electrolytes. All-solid-state batteries using Li_2S-P_2S_5 solid electrolytes have thus good interfaces between solid electrodes and solid electrolytes because of a favorable formability of sulfide electrolyte. A high capacity of the batteries was retained during charging and discharging for hundreds of cycles [1]. This would be due to the fact that sulfide solid electrolytes maintain electrode/electrolyte contacts against volume change of electrode materials during Li insertion/extraction. Consequently, these facts indicate the superiority of sulfide solid electrolytes in terms of mechanical properties. Recently, our group has succeeded in evaluating the elastic modulus of Li_2S-P_2S_5 sulfide electrolytes [2]. The Young's moduli of Li_2S-P_2S_5 glasses are about 18-25 GPa and these moduli are lower than those of oxide solid electrolytes such as cubic $Li_7La_3Zr_2O_{12}$, which is reported as 149.8±0.4 GPa at a relative density of ~97% [3].

As mentioned above, solid electrolytes with low Young's modulus would be favorable for battery performance. Young's moduli of Li_2S-P_2S_5 glasses are decreased with decreasing Li_2S content. However, Li_2S-P_2S_5 glasses with lower Li_2S content have lower ionic conductivity. It is reported that lithium-ion conductivities of Li_2S-P_2S_5 glasses are increased by adding LiI [4]. Therefore, higher ionic conductivities and lower Young's modulus are expected by adding LiI for Li_2S-P_2S_5 glasses with low Li_2S content. In this study, (100-x)($0.50Li_2S \cdot 0.50P_2S_5$)·xLiI (x=0, 25, 30 mol%) sulfide glass electrolytes were prepared by mechanical milling. Conductivities of the glasses were increased by adding LiI and the conductivity of $70(0.50Li_2S \cdot 0.50P_2S_5) \cdot 30LiI$ glass was 2.2 x 10^{-4} S cm^{-1} at 25 °C. Young's moduli of these glasses were evaluated by ultrasonic wave velocity measurements. The Young's moduli were lower than those of Li_2S-P_2S_5 glasses. All-solid-state Li-In/Li_2S-P_2S_5/Si cells using $70(0.50Li_2S \cdot 0.50P_2S_5) \cdot 30LiI$ glass were fabricated. The cells showed higher initial discharge capacities and better cycle performance than the cells using Li_2S-P_2S_5 glasses.

References
[1]M. Tatsumisago and A. Hayashi, *Funct. Mater. Lett.*, 1 (2008) 31.
[2] A.Sakuda, A.Hayashi, and M. Tatsumisago, *Sci. Rep.*, 3 (2013) 2261.
[3] J.E. Ni, E.D. Case, J.S. Sakamoto, E. Rangasamy, and J.B. Wolfenstine, *J. Mater. Sci.*, 47 (2012) 7978-7985.
[4] R. Mercier, J.P. Malugani, and B. Fahys, G. Robert, *Solid State Ionics*, 5 (1981) 663-666.

C2.12

Aluminum-Doped $Li_7La_3Zr_2O_{12}$ - A Promising Candidate as a Solid Electrolyte for Lithium-Ion Batteries Miriam Botros[1], Ruzica Djenadic[1, 2, 3] and Horst Hahn[1, 2, 3]; [1]Joint Research Laboratory Nanomaterials, Technical University Darmstadtand and Karlsruhe Institute of Technology, Darmstadt, Germany; [2]Institute for Nanotechnology, Karlsruhe Institute of Technology, Eggenstein-Leopoldshafen, Germany; [3]Helmholtz Institute Ulm, Ulm, Germany.

Lithium-ion batteries for transportation and storage of renewable energy require high energy densities, high power density, reduced costs and, most importantly, safety. The use of liquid organic electrolytes that exhibit high vapor pressures and flammability poses a substantial safety issue in particular for large-scale systems. In this study the substitution of liquid organic electrolytes by Aluminum-doped $Li_7La_3Zr_2O_{12}$ is discussed. Its chemical stability against lithium metal allows the use of pure lithium as a negative electrode, enabling high energy densities. In addition to being a lithium-ion conductor, the solid electrolyte acts as a separator between the electrodes.

The synthesis, processing and characterization of $Li_{7-3x}La_3Zr_2Al_xO_{12}$ solid electrolyte ceramics with nano-scaled crystallites are presented. The synthesis was performed using nebulized spray pyrolysis (NSP), an aerosol-based synthesis method that allows a relatively high production rate on a laboratory scale and is scalable for mass production. The powders were annealed to obtain the desired high conducting cubic phase, compacted and sintered using spark plasma sintering (SPS) to dense ceramics (>90% TD). The SPS method is beneficial as it limits the grain growth compared to conventional sintering methods and allows to study influence of grain size on interfacial resistance and overall lithium ion conductivity, as well as the electrochemical performance of the solid electrolyte. The phase composition was determined using X-Ray Diffraction (XRD) while the microstructure was analyzed using scanning electron microscopy (SEM). The lithium-ion conductivity and electrochemical performance of the solid electrolyte were studied in relation to the microstructure.

C2.13

Microstructure-Electrical Property Relationship in Polycrystalline Sodium β"-Alumina by New Impedance Modelling Approach Jee-Hoon Kim[1], Dong-Chun Cho[1], Su-Hyun Moon[1], Eui-Chol Shin[1], Sansudae Lim[2], Sooseok Kim[2], Keedeok Yang[2], Jinhyung Beom[2] and Jong-Sook Lee[1]; [1]Materials Science and Engineering, Chonnam National University, Gwangju, Korea (the Republic of); [2]FineTech Co., Ltd., Daejeon, Korea (the Republic of).

Variations in the processing parameters such as ball milling mediua and amounts of additives lead to diverse microstructural evolution in polycrystalline β"-alumina. In view of the extreme conduction anisotropy in the material, the microstructural feature is expected to strongly affect the electrical performance. Indeed low temperature impedance spectroscopy indicates strongly characteristic AC behavior of different samples. In spite of intensive research in seventies and eighties the AC characteristics of polycrystalline β- or β"-alumina remained to be understood. Strongly overlapped and dispersive responses cannot be satisfactorily described by conventional brick-layer modeling, even with or because of the employment of constant phase elements which adjust the frequency dispersion arbitrarily. The raw AC data in Bode plots and Arrhenius plots as well as in complex plane presentations provides well-defined capacitance components and frequency and temperature dependence, some of which appear universal for the β"-alumina or for solid electrolytes in general, and some of which can be related with the specific microstructural aspects. Havriliak-Negami type dielectric functions connected in parallel can competently describe the behavior. The modeling allows the simulation and examination of the AC behavior as a function of temperature as well as frequencies and the different characteristics of β"-alumina samples can be definitely defined and compared with each other.

C2.14

Non-Stoichiometry of Composites: Thermodynamic Analysis of Dissociative Storage at Interfaces Chia-Chin Chen, Lijun Fu and Joachim Maier; Max Planck Institute for Solid State Research, Stuttgart, Germany.

The interfacial effect on charge transfer has been extensively studied in the field of nano-ionics [1]. In this contribution, we concentrate on mass storage, and present a general thermodynamic model for interfacial non-stoichiometry, including both excess [2] and deficiency. Different from non-stoichiometry in the bulk, interfacial storage can occur in a heterogeneous way: although neither of the constituents may store M alone, M can be dissociatively stored at their junction, with or accommodated in one phase and or in the other, corresponding to excess and deficiency storage, respectively. Both Li and Ag storage in composites ($RbAg_4I_5$:C; LiF:Ni, Li_2O:Ru) are investigated. Under reversible conditions, the experimental results fit the thermodynamic model well.

References:
[1] J. Maier, Nature Mater. 4, 805-815 (2005).
[2] L.J. Fu, C.-C. Chen, D. Samuelis, J. Maier, Phys. Rev. Lett. 112, 208301 (2014)

C2.15

Rechargeable Batteries and Condensed Matter Physics Lin Gu; Institute of Physics, Chinese Academy of Sciences, Beijing, China.

Rechargeable batteries refer to energy-storage device, commonly realized via shuttling ions between electrodes; whereas condensed matter physics emphasizes more on novel quantum phenomena carried by lattice, charge, orbital and spin. Investigations on rechargeable batteries have so far covered mainly upon lattice and charge, with few ambitions on orbital and spin. Here we discuss based on our recent work [1-33] that, as the dimension shrinks to atomic-cluster scale, e.g. polyhedra or medium range ordering, strong correlations among basic coordinates in condensed matter physics may provide extra perspectives for designing next generation batteries.

References:
G. Cui, et al. ***Adv. Mater.*** **2008**, *20*, 3079-3083.
Y. Yu, et al. ***Angew. Chem. Int. Ed.*** **2009**, *48*, 6485-6489. **[*]**
Y. Yu, et al. ***J. Am. Chem. Soc*****.** **2009**, *131*, 15984. **[*]**
Y. Yu, et al. ***Adv. Mater*****.** **2010**, *22*, 2247-2250. **[*]**
C. Li, et al. ***Adv. Mater*****.** **2010**, *22*, 3650-3654. **[*]**
C. Li, et al. ***Adv. Funct. Mater.*** **2011**, *21*, 1391-1397. **[*]**
C. Li, et al. ***ACS Nano*** **2011**, *5*, 2930-2938.
L. Gu, et al. ***J. Am. Chem. Soc*****.** **2011**, *133*, 4661-4663. **[*]**
Y. Yu, et al. ***Adv. Mater*****.** **2011**, *23*, 2443-2447. **[*]**
C. Li, et al. ***Adv. Funct. Mater*****.** **2011**, *21*, 2901-2905.
C. Zhu, et al. ***Angew. Chem. Int. Ed*****.** **2011**, *50*, 6278-6282. **[*]**
X. Lu, et al. ***Energy Environ. Sci*****.** **2011**, *4*, 2638-2644. **[*]**
X. F. Li, et al. ***Adv. Energy Mater*****.** **2012**, *2*, 238-244.
C. L. Li, et al. ***Nano lett*****.** **2012**, *12*, 1241-1246.
C. L. Li, et al.***Adv. Funct. Mater*****.** **2012**, *22*, 1145-1149.
Y. Q. Wang, et al. ***J. Am. Chem. Soc*****.** **2012**, *134*, 7874-7879.
X. Lu, et al. ***Adv. Mater*****.** **2012**, *24*, 3233-3228 **[*]**
S. Xin, et al. ***J. Am. Chem. Soc*****.** **2012**, *134*, 18510-18513.
X. Lu, et al. **Nano Lett. 2012**, *12*, 6192-6197. **[*]**
Y. Yu, et al. ***Adv. Energy Mater*****.** **2013**, *3*, 281-285. **[*]**
Y. Sun, et al. ***Nat. Commun*****.** **2013**, *4*, 1870. **[*]**
C. L. Li, et al. ***J. Am. Chem. Soc*****.** **2013**, *135*, 11425-11428.
R. Wang, et al. ***Adv. Energy Mater*****.** **2013**, *3*, 1358-1367. **[*]**
C. B. Zhu, et al. ***Adv. Funct. Mater*****.** **2014**, *24*, 312-318. **[*]**
X. Q. Yu, et al. ***Adv. Energy Mater*****.** **2014**, *4*, 1300950.
Z. Jian, et al. ***Adv. Funct. Mater*****.** **2014**, *24*, 4265-4272. **[*]**
H. Yu, et al. ***Angew. Chem. Int. Ed.*** **2014**, *53*, 8963-8969. **[*]**
H. Zheng, et al. ***Nano lett*****.** **2014**, *14*, 4245-4249. **[*]**
Y. N. Zhou, et al. ***Nat. Commun*****.** **2014**, *5*, 5381.
D. D. Xiao, et al. ***Adv. Energy Mater.***, **2014**, **DOI**: 10.1002/aenm.201400664. **[*]**
X. Lu, et al. ***J. Am. Chem. Soc***., **2015**, **DOI**: 10.1021/ja5115562. **[*]**
L. Gu, et al. ***Adv. Mater*****.** **2015**, accepted. **[*]**
Y. S. Wang, et al. ***Nat. Commun*****.** **2015**, accepted. **[*]**

C2.16

Diatomaceous Earth and Algae Based Aqueous Binders Make Environmentally Friendly High-Performance Anodes for Lithium-Ion Batteries Muhammad Hasanuzzaman and Fride Vullum-Bruer; Materials Science and Engineering, Norwegian University of Science and Technology, NTNU, Trondheim, Norway.

The high theoretical capacity and low discharge potential of silica (SiO_2) draw major interest these days as a potential replacement of Si-based anodes. The drastic volume expansion of Si anodes during cycling leads to capacity fading and pulverization and thus requires advanced treatment to make it a viable electrode in Li-ion batteries[1-4]. Abundantly available diatomaceous earth was explored as an anode which can substitute the existing graphite based anode, providing better electrochemical performance in terms of capacity, cyclability and stability.
As conventional binders are not compatible with Si or silica-based materials, other types of binders and binder additives were also explored. Naturally grown algae based aqueous binders were used to prepare the electrodes, which is compatible with the diatomaceous earth and gives it increased stability during lithiation and de-lithiation. First cycle specific discharge capacity of these materials was around 600 $mAhg^{-1}$, which is close to twice the value of the existing graphite based anodes. Various amounts of corn starch were also added to provide a conductive coating on the SiO_2 particles. These SiO_2-C composites exhibited even higher capacity and cyclability compared to non-coated silica particles. Upon extended cycling the reversible capacity, for uncoated as well as coated silica, starts to increase from approximately the forth cycle due to chemical reactions causing a Si phase to appear. The porous morphology and natural nano-structure of the diatomaceous earth anode can accommodate the volume expansion and preserve the solid electrolyte interface. The high reversible capacity, good cycle performance and simple processing of these electrodes make the diatomaceous earth a potential environmentally friendly anode material for lithium-ion batteries.

References:
[1]Favors, Z., et al. (2014). Sci. Rep. 4.
[2]Yan, N., et al. (2013). Sci. Rep. **3**.
[3]Liu, X., et al. (2014). Nano Energy 4.
[4]Epur, R., et al. (2012). Materials Science and Engineering: B 177(14).

C2.17

Preparation of Li_2S-$FePS_3$ Composite Positive Electrode Materials and Their Electrochemical Properties Tomonari Takeuchi[1], Hiroyuki Kageyama[1], Masahiro Ogawa[2], Koji Nakanishi[3], Toshiaki Ohta[2], Atsushi Sakuda[1], Hikari Sakaebe[1], Hironori Kobayashi[1] and Zempachi Ogumi[3]; [1]National Institute of Advanced Industrial Science and Technology, Ikeda, Japan; [2]Ritsumeikan University, Kusatsu, Japan; [3]Kyoto University, Kyoto, Japan.

Lithium sulfide (Li_2S) is one of the promising cathode active materials for high energy rechargeable lithium batteries because of its high theoretical capacity (*ca.* 1170 mAh・g^{-1}). However, this material is electronically and ionically resistive, which gives rise to low active material utilization in the cells. Several attempts have been performed to enhance the conductivity of Li_2S, such as forming composites with metals (Li_2S-Fe, Li_2S-Cu) or carbon. Recently, we have tried to prepare Li_2S-FeS_x composite materials and found that the cells showed the discharge capacity of *ca.* 730 mAh・g^{-1} after the pre-cycling treatment. In the present work, we have tried to incorporate phosphorus ions into the Li_2S-FeS_x composites. $FePS_3$ was used as a phosphorus source, and the electrochemical properties of the resulting Li_2S-$FePS_3$ composites were examined and compared with those of Li_2S-FeS_x.

The obtained Li_2S-$FePS_3$ composite sample was black in color, and its XRD pattern showed that it consisted of mainly Li_2S with low crystallinity and small amounts of FeP as impurity. The calculated FeP content estimated by the X-ray Rietveld analyses was *ca.* 8%. The electrochemical tests for the Li_2S-$FePS_3$ sample cells showed that the initial discharge capacity was*ca.* 780 mAh・g^{-1} without any pre-cycling treatments. This makes a clear contrast to the Li_2S-FeS_x sample cells, which showed the initial discharge capacity of *ca.* 330 mAh・g^{-1} and it was enlarged to *ca.* 730 mAh・g^{-1} after the pre-cycling treatment. *Ex-situ* XRD and S K-edge XAFS measurements showed the reversible changes of the peaks ascribed to Li_2S and valence states of S atoms during cycling, respectively, which were similar to those of the Li_2S-FeS_x composites after pre-cycling treatment. The incorporation of phosphorus ions in the Li_2S-FeS_xcomposites was effective for improving the electrochemical reversibility, resulting in the improved cell performances.

C2.18

Highly Conductive Glass-Ceramic Electrolytes for Advanced Lithium Batteries Miriam Kunze, Meike Schneider, Maria-Luisa Reich, Wolfgang Schmidbauer and Andreas Roters; SCHOTT AG, Mainz, Germany.

Lithium-ion conducting glass-ceramics received much interest as materials for solid electrolytes in future battery generations. Glass-ceramic materials can be divided into sulfidic and oxidic systems. The lithium conducting oxidic glass-ceramics with Li(Na)SICon or garnet crystalline structures are promising materials for advanced battery applications due to high conductivities in the range of 10^{-4} to 10^{-3} S/cm. However, LiSICon often includes expensive raw materials like GeO_2 and garnets like $Li_7La_2Zr_3O_{12}$ have a cost intensive production path via sintering, which prevents commercial utilization.

The presented materials are a germanium-free LiSICon glass-ceramic of the Li_2O-Al_2O_3-TiO_2-P_2O_5 (LATP) system and a room temperature stabilized garnet glass-ceramic of the $Li_7La_2Zr_3O_{12}$ (LLZO) system. Both solid ion conductors, LATP and LLZO, are manufactured via melting production routes. The LATP glass-ceramic material was prepared by a classical glass-ceramic process, while the garnet type LLZO glass-ceramics have been produced for the first time by skull melting technology. The resulting materials have high ionic conductivities of $1x10^{-3}$ S/cm and $3x10^{-4}$S/cm at room temperature (c.f. fig. 1), respectively. Furthermore both materials are electrochemically stable between 0 and 6V vs. Lithium metal and are chemically stable in contact with typical battery materials used in LIB or future battery systems. Both materials have the potential to be produced at industrial scale using SCHOTT melting and glass-ceramic technologies providing leading edge materials for battery applications.

C2.19

Investigation of O3-$Na_{0.9}[Ni_{0.45}Ti_{0.55}]O_2$ Using Electroanalytical Techniques and Ex-Situ XRD for Na-Ion Batteries Rengarajan Shanmugam and Wei Lai; CHEMS, Michigan State University, East Lansing, Michigan, United States.

Layered materials possess promising sodium intercalation properties and are widely evaluated as intercalation-type electrodes for Na-ion batteries. Promising candidate materials include $Na_{2/3}Ni_{1/3}Mn_{2/3}O_2$,[1] $Na_xFe_{1/2}Mn_{1/2}O_2$,[2] $Na_{1-x}Ni_{0.5}Mn_{0.5}O_2$[3] etc. O-type materials undergo reversible phase transformations (O3-P3) during sodium intercalation/de-intercalation.[3] These phase transformations contribute to signature patterns in voltage vs. composition curves and slow moving phase boundaries can potentially limit material performance. In this study, we perform experimental characterization to understand phase transformation mechanism in O3-$Na_{0.9}[Ni_{0.45}Ti_{0.55}]O_2$ composition. We also evaluate the rate of interfacial kinetics and diffusional properties using electroanalytical techniques. XRD confirms the formation of pure phase by solid state reaction at 1000 °C. SEM micrographs show ~5-10 µm particles. Galvanostatic study confirms reversible sodium de-intercalation/intercalation and relatively stable capacity value of 75 mAh/g was obtained at the end of 100th cycles (C/2 rate).

Impedance spectroscopy depicts two high frequency arcs and a low frequency arc. The latter is assigned to interfacial resistance and double layer capacitance (C_{dl}). At low charging voltages (up to 4.0 V), the interfacial resistance was found to have a direct correlation with sodium content due to the formation of higher valence nickel ions. However at higher voltages, interfacial resistance becomes inversely correlated to sodium content due to slow interfacial kinetics of the new phases. The formation of monoclinic O3' phase is suggested by diffraction peak splitting at 17°. Further study is targeted towards understanding low sodium content phases and diffusional analysis.

References

1. D. H. Lee, J. Xu, and Y. S. Meng, *Phys. Chem. Chem. Phys.*, **15**, 3304–12 (2013)
2. N. Yabuuchi, M. Kajiyama, J. Iwatate, H. Nishikawa, S. Hitomi, R. Okuyama, R. Usui, Y. Yamada and S. Komaba, *Nature Mater.*, **11**, 512–7 (2012)
3. S. Komaba, N. Yabuuchi, T. Nakayama, A. Ogata, T. Ishikawa and I. Nakai, *Inorg. Chem.*, **51**, 6211-20 (2012)

C2.20

Evidence for a >1 Electron Reaction in Li_2FeSiO_4: An *in situ* Mössbauer Spectroscopy Study Anti Liivat[1], Josh Thomas[1], Jianghuai Guo[2] and Yong Yang[2]; [1]Chemistry, Uppsala University, Uppsala, Sweden; [2]Chemistry, Xiamen University , Xiamen, China.

Reversible cycling of two lithium ions (and two electrons) per transition-metal (TM) ion in a Li-ion battery is seen as a most attractive way to increase the capacity of cathode materials to better match the capacities of today's anode materials – typically, graphite. Such a process is suggestively more likely to occur in poly-anionic cathode materials, since simple TM-oxides tend to be less stable [1]. Low-cost Fe- or Mn-based silicates, such as lithium iron silicate (Li_2FeSiO_4) [2], are ideal candidate host materials in this context, provided they do not suffer from slow kinetics or structural volatility.

Highly reactive nano-composites of Li_2FeSiO_4 and carbon, further enhanced by the presence of a glassy network to facilitate Li-ion conductivity [3], have here been studied to probe the controversy surrounding the Fe^{3+}/Fe^{4+} redox couple, and the possibility of cycling a 2nd Li-ion in the material. To this end, *in situ* Mössbauer spectroscopy has been used to monitor the oxidation state of the Fe-ions in a symmetric $Li_1Fe^{3+}SiO_4$/1MLiPF$_6$ EC:DEC (1:1)/$Li_1Fe^{3+}SiO_4$ cell cycled at RT and at low rate (C/20). Apart from some side-reactions associated with electrolyte decomposition, almost all the Li can be cycled reversibly within the potential window ±2.8V, as evidenced by electrochemical data in combination with *in situ* Mössbauer spectra.

This work has been supported by the Swedish Energy Agency(VINNOVA) and the Swedish Science Research Council (VR).

[1] A.K. Padhi *et al., J. Electrochem. Soc.*, 144, 1609 (1997).
[2] A. Nytén *et al., Electrochem. Commun.*, 7, 156 (2005).
[3] J. Bai *et al., J. Mater. Chem.*, 22, 12128 (2012).

C2.21

Optimization of Ionic Conductivity in Garnet-Type Solid State Electrolytes for Lithium Ion Batteries Sumaletha Narayanan, Xia Tong and Venkataraman Thangadurai; Department of Chemistry, University of Calgary, Calgary, Alberta, Canada.

The lithium ion batteries attain much attention nowadays because of their high energy density. However, there is safety concern associated with the conventional polymer/organic based electrolytes used in current lithium ion batteries. Solid state lithium ion conducting electrolytes are promising candidates to build safer all-solid-state lithium ion batteries. Among different crystal structured materials studied, garnet-type Li metal oxides gained much attention because of their high Li^+ conductivity, lower electronic conductivity and wide potential window. $Li_7La_3Zr_2O_{12}$ family of garnets shows highest conductivity of ~ 10^{-3} Scm^{-1} at ambient condition which is the same conductivity as that of conventional electrolytes. The present study is about optimizing the Li^+ conductivity in $Li_7La_3Zr_2O_{12}$ by varying the dopants and Li content.

C2.22

Electrochemical Properties of All-Solid-State Lithium-Ion Batteries Using Li_2CO_3-Li_3BO_3 Electrolyte Toyoki Okumura, Tomonari Takeuchi, Masahiro Shikano and Hironori Kobayashi; Advanced Battery Research Group, National Institute of Advanced Industrial and Technology (AIST), Ikeda, Japan.

The realization of all-solid-state lithium-ion batteries (ASS-LIBs) consisting of nonflammable oxide-based solid-state electrolytes (O-SSEs) are desired because of their high safety. The high bulk lithium-ion conductive O-SSEs as garnet, perovskite and NASICON-type structures should be sintered at high temperature (over 1000°C) for obtaining favorable contacts with electrodes. However, the reacted products at the interfaces between electrodes and O-SSEs are ones of the general problems for showing the electrochemical activities of ASS-LIBs. Although lithium-ion conductivity of Li_2CO_3 is extremely low (about 10^{-11} S/cm at room temperature), it could be sintered at low temperature less than 700°C. And, it has been reported that the lithium-ion conductivity was enhanced to 10^{-6} S/cm by preparing Li_2CO_3-Li_3BO_3 solid solution. In present study, we investigated the improvement of the lithium-ion conductivity by substituted BO_3^{3-} for CO^{3-}at Li_2CO_3-Li_3BO_3 solid solution., and successfully prepared ASS-LIB by using the Li_2CO_3-Li_3BO_3 solid solution as O-SSE.

C2.23

Spinel-Based Solid Electrolyte for Lithium-Ion Battery Application Ruzica Djenadic[1, 2, 3], Miriam Botros[3], Chritoph Loho[3] and Horst Hahn[2, 3, 1]; [1]Helmholtz Institute Ulm, Ulm, Germany; [2]Institute of Nanotechnology, Karlsruhe Institute of Technology, Eggenstein-Leopoldshafen, Germany; [3]Joint Research Laboratory Nanomaterials – Technical University Darmstadt & Karlsruhe Institute of Technology, Darmstadt, Germany.

Lithium-ion batteries are the fastest growing and widely used type of batteries. Most of today electronic devices use batteries containing liquid electrolyte facing safety issues (e.g. dendrite growth, leakage, and flammability). Therefore, development of a lithium-ion conducting solid electrolyte is a main focus of current battery research which potentially will lead to a safe all-solid-state battery. Additionally to the safety improvement, solid electrolytes offer stability over a broad electrochemical potential as well as a large temperature range. Several solid electrolyte materials with lithium-ion conductivities equal or higher than liquid electrolytes are reported. However, they are not stable over a wide potential range. Recently, an idea of an all-spinel type solid battery where all three battery components (anode, cathode, and electrolyte) have spinel structure was re-introduced. This “lattice matching” concept should provide fast Li-ion diffusion pathways and lower interface resistance. Herein we report a synthesis of Li-doped $MgAl_2O_4$ nanoparticles by nebulized spray pyrolysis, processing into a dense bulk ceramic by spark plasma sintering, and lithium-ion conductivity study by impedance analysis.

C2.24

Transport of Alkali Ions in an Organic Ionic Plastic Crystal Fangfang Chen and Maria Forsyth; Institute for Frontier Materials, Deakin University, Burwood, Victoria, Australia.

Organic ionic plastic crystals (OIPCs) have shown increasing promise in the development of high conductivity solid-state electrolytes for energy storage devices in recent years due to several advantages, such as non-volatile and non-flammable character, good thermal and electrochemical stability, as well as they enable high target ion diffusion. Experimental studies have demonstrated its potential application for all-solid-state room temperature lithium batteries, and the alternative applications in sodium batteries are also under investigation. A more comprehensive understanding of their phase behaviour and conduction mechanisms, especially after doping with target ions, is critical to their applications in this field.

In this simulation work, we demonstrate that the diffusion of an alkali ion (Me = Li or Na) in the solid phase of an OIPC $[P_{1224}][PF_6]$ is accompanied with breaking and reforming of two types of solvation structures, of which the proportions are different between Li- and Na-doped systems. A tetrahedral structure $Me[PF_6]_4$ is prevalent in the Na-doped system, whereas the more percentage of the triangular structure $Me[PF_6]_3$ is found in the Li-doped system. This difference in solvation structure could account for the different transport rates of ions in this solid electrolyte material.

C2.25

Electrochemical Properties and Structural Evaluation of Amorphous MoS_3 Positive Electrode Active Materials in All-Solid-State Lithium Secondary Batteries Takuya Matsuyama[1], Minako Deguchi[1], Akitoshi Hayashi[1], Masahiro Tatsumisago[1], Tomoatsu Ozaki[2] and Shigeo Mori[3]; [1]Department of Applied Chemistry, Osaka Prefecture University, Sakai, Japan; [2]Technology Research Institute of Osaka Prefecture, Izumi, Japan; [3]Department of Materials Science, Osaka Prefecture University, Sakai, Japan.

Improvement of electrode active materials with high capacity and excellent cyclability is needed for realize all-solid-state lithium secondary batteries. Sulfur is an attractive active material for positive electrode because sulfur has a high theoretical capacity. High capacity of the batteries can be achieved by using active materials with a large content of sulfur. Low electronic conductivity is a drawback of sulphur. We thus focus on a transition metal trisulfides such as TiS_3 with high electronic conductivity. Moreover, amorphization of active materials is potentially capable of achieving higher capacity and cyclability because of open and random structure in amorphous materials. Recently, we have found that amorphous TiS_3 prepared by ball milling had better cyclability than crystalline TiS_3 [1, 2]. MoS_3 is also an attractive material for positive electrode with high capacity. Electrode properties of amorphous MoS_3 (*a*-MoS_3) prepared by pyrolysis of $(NH_4)_2MoS_4$ have been investigated in an organic liquid electrolyte [3]. The cell with *a*-MoS_3 electrode showed the reversible capacity of 400 mAh g^{-1}. In this study, structure and electrochemical properties of *a*-MoS_3 in all-solid-state cells were evaluated. -MoS_3 was prepared by mechanical milling of the mixture of molybdenum metal and sulfur. The obtained active materials were applied as a positive electrode to all-solid-state cells with sulfide solid electrolytes. Structures and morphologies of *a*-MoS_3 electrodes before and after charge-discharge tests were analyzed by XRD, XPS, SEM and HR-TEM.
All-solid-state Li-In/Li_2S-P_2S_5/*a*-MoS_3 cells with *a*-MoS_3 electrodes retained discharge capacity of about 670 mAh per gram of *a*-MoS_3 for 60 cycles. Microstructures of *a*-MoS_3 electrodes before and after charge-discharge measurements were analyzed by electron diffraction (ED) and HR-TEM. It was found from the microstructures of *a*-MoS_3 electrodes before charge-discharge measurements nanoscale regions consisting of crystalline MoS_2 were dispersed randomly inside the *a*-MoS_3 ones, although halo rings showing the presence of amorphous regions were observed in ED patterns. In addition, microstructures of *a*-MoS_3 after charge-discharge measurements remained almost intact to those before charge-discharge measurements. These results imply that good cyclability of *a*-MoS_3 electrodes should stem from the stability of *a*-MoS_3 during charge-discharge cycles.

Reference
[1] A. Hayashi, *et al., Chem. Lett.*, **41** (2012) 886.
[2] T. Matsuyama, *et al., J. Solid State Electrochem.*, **17** (2013) 2697.
[3] J. J. Auborn *et al., J. Electrochem. Soc.*, **134** (1987) 580.
Acknowledgment
This research was financially supported by ALCA-SPRING project.

C2.26

Comparing Electrochemical Performance of Silicate Cathodes and Chevrel Phase Mo_6S_8 in the Analogous Rechargeable Mg-Ion Battery System Xinzhi Chen[1], Lu Wang[1], Sidsel M. Hanetho[2], Paul I. Dahl[2] and Fride Vullum-Bruer[1]; [1]Department of Materials Science and Engineering, Norwegian University of Science and Technology, Trondheim, Norway;[2]Department of Sustainable Energy Technology, SINTEF Materials and Chemistry, Trondheim, Norway.

The interest in rechargeable magnesium ion battery technology has grown in recent years due to several challenges related to lithium ion batteries,[1] such as cost, resource availability and safety issues related to risk of thermal runaway. Lithium ion batteries have and are predicted to dominate the portable battery market for a long time due to the superior power density, while rechargeable magnesium batteries may play an important role in stationary energy storage systems and auxiliary power applications where the low cost and high reliability under a wide temperature range are more important than low weight and high power density. One of the main assets of Mg-ion batteries is the ability to transfer two electrons per magnesium ion migration, compared to one for lithium, giving a theoretical specific volumetric capacity of 3833 mAh/cm^3, which is higher than that for lithium (2046 mAh/cm^3). [2]

Investigation of new cathode materials is dependent on breakthroughs in the development of electrolytes. In Mg-ion batteries all phenyl complex (APC) electrolyte solutions[3] are widely used due to simple and commercially available precursors. Polyanion based silicate cathode materials [4] have been reported as promising cathode materials for magnesium rechargeable batteries, while full cell operations with silicate cathodes and APC electrolyte solution have never been demonstrated so far. Thus it is very interesting to investigate the electrochemical performance of the silicate materials in the same battery system as the chevrel phase Mo_6S_8 has been successfully demonstrated.

In this work, nanostructured $MgMSiO_4$ (M = Fe, Mn, and Co) are prepared by a modified sol-gel method and flame spray pyrolysis. Chevrel phase Mo_6S_8 powders are synthesized by a molten salt method. All the cathode materials are investigated electrochemically using magnesium alloys as the anode and APC electrolyte solution.

1. Novák, P., et al., Electrochimica Acta, 1999. **45**(1–2): p. 351-367.
2. Yoo, H.D., et al., Energy & Environmental Science, 2013. **6**(8): p. 2265-2279.
3. Mizrahi, O., et al., Journal of the Electrochemical Society, 2008. **155**(2): p. A103-A109.
4. Muldoon, J., et al., Chemical Reviews, 2014. **114**(23): p. 11683-11720.

C2.27

Computer Aided Design of Polyanionic Electrolytes: A Molecular Dynamic Study Xingyu Chen; Institute of Frontier Materials, Deakin University, Melbourne, Victoria, Australia.

Polyanionic electrolytes have attracted increasing interest in battery applications as they can mitigate the undesirable polarization concentration and improve batteries lifetime by covalently tethering the anions to polymer backbones, only allowing cations to conduct. However, the polyanionic electrolytes typically exhibit low conductivity because cations tend to form ion complexes with the immobilized anions which crosslink polymer segments and reduce their mobility. Recently, Bouchet et al. [1]reported a BAB triblock copolymer electrolyte based on the poly(styrene trifluoromethanesulphonylimide of lithium) P(STFSILi) (B block) and poly(ethylene oxide) PEO (A block) (Fig.1) which has higher conductivity than the PEO directly laden with LiTFSI salt and superior performances in batteries. The use of delocalized–SO2N(−)SO2CF3 anion can weaken the cation-anion interaction and promote the dissociation of cations, thus improving overall conductivity. However, the effect of polymer architecture on the ion transport remains unclear. To provide insights for the design of future polyelectrolytes, in our study we explored the optimal structures of the P(STFSI)-PEO-P(STFSI) copolymer, such as interspacing between anionic groups, by the means of molecular dynamics simulation.

C2.28

Enhancement of Ionic Conductivity of Battery Electrolytes Using Nanoconfined Polymer Electrolyte, Ionic Liquids and Ionic Liquid/ Polymer Electrolyte Blends Indumini Jayasekara and Dale Teeters; Chemistry and Biochemistry, The University of Tulsa, Tulsa, Oklahoma, United States.

Lithium-ion batteries are of great technological interest due to their high energy density. The challenges for further development of lithium rechargeable batteries are safety, mechanical stability, thermal stability and enhanced ionic conductivity. This study involves the use of nanoporous alumina membranes to make composite solid electrolyte systems. These solid composites are comprised of polymer electrolyte, ionic liquids and mixtures of polymer and ionic liquids under nanoconfinement. Non-conducting aluminum membranes, that contain nanopores and nanochannels, can provide mechanical support, promoting dimensional stability during the formation of nanoconfined electrolyte structures. Alumina (AAO) membranes provide the best configuration of channel geometry due to the perpendicular alignment of pores with respect to the surface of the membrane. These nanoconfined electrolytes have ionic conductivity several orders of magnitude higher than non-confined polymer. Ionic liquids have special characteristics such as thermal stability, non-flammability, low melting temperature, high ionic conductivity, low viscosity, non-volatility and low vapor pressure. Under nanoconfined conditions, and when mixed with polymer electrolytes, they have enhanced properties as solid electrolyte systems. Ionic liquids and polymers, complexed with lithium triflate, can be placed inside channels by wetting of the alumina membranes by taking advantage of capillary action to fill the nanochannels. SEM images can be used to confirm the formation of ionic liquid/polymer composite nanostructures. Impedance analysis can be used for conductivity measurements and dielectric measurements. In addition, FTIR, NMR, TGA and heat dependence studies will be done in order to find characteristics and behavior of nanoconfined ionic liquid/polymerbased electrolyte. Overall, these three electrolyte systems, confined in porous membranes, can be used as electrolytes for the fabrication of a “nanobattery” structure with enhanced ionic conductivity, stability and performance.

C2.29

Investigation of the Unique Crystalline Orientation of a Nanostructured Lithium Cobalt Oxide Thin Film Cathodes for Lithium Ion Batteries Mark Poyner and Dale Teeters; Chemistry and Biochemistry, The University of Tulsa, Tulsa, Oklahoma, United States.

Lithium ion batteries have been the preferred power source for numerous electronic devices over the past two decades. However, improvements to lithium ion battery technology is needed to continue to provide a viable power source for the more advanced and demanding electronic devices and technologies. By nanostructuring electrode materials, battery technologies with enhanced performance can be developed. Nanostructuring a common cathode material, $LiCoO_2$, could aid in the development of Li-ion batteries. Sputter coating $LiCoO_2$ onto a nanoporous template can generate a high surface area nanostructured cathode. 300nm of $LiCoO_2$ can be deposited by RF magnetron sputter coating onto a nanoporous Anodized Aluminum Oxide (AAO) membrane with 200nm diameter pores. This deposition process effectively templates the nanoporous nature of the AAO, resulting in a nanoporous $LiCoO_2$ cathode with about six times the surface area compared to a traditional thin film. The preferred (101) and (104) crystalline planes for Li-ion diffusion and ion conduction appear to be present in these nanostructured $LiCoO_2$ cathodes. These planes are not normally the preferred planes for very thin films of $LiCoO_2$, suggesting a unique crystalline orientation of the nanostructured cathode. The structural and electrochemical properties of the uniquely crystalline nanostructured $LiCoO_2$ thin-film cathodes will be investigated by using SEM, XRD, galvanostatic charge-discharge cycling and ac impedance.

C2.30

Electrical Characterization of $Na_3Sc_2(PO_4)_3$:Eu2+ Su-Hyun Moon, Yun-Hwa Kim, Dong-Chun Cho, Eui-Chol Shin, Won-Bin Im and Jong-Sook Lee; School of Materials Science and Engineering, Chonnam National University, Gwangju, Korea (the Republic of).

AC characterization of polycrystalline Eu-doped $Na_3Sc_2(PO_4)_3$ has been performed in the temperature range 225 to -73◦C. Strongly dispersive multiple impedance components can be systematically described by employing Havrilliak-Negami dielectric functions which can be straightforwardly related to the well-defined capacitance components in the raw data, similarly as recently demonstrated for β''-alumina polycrystalline ceramics. Bulk dielectric dispersion and the current constriction impedance at grain boundaries exhibit the temperature dependence directly related to the mobile charge transport in the lattice. Compared to the pristine $Na_3Sc_2(PO_4)_3$ material, Eu-doped $Na_3Sc_2(PO_4)_3$ system does not exhibit an abrupt rhombohedral-monoclinic transition around 64◦C, consistent with the calorimetry measurements. A reproducible hysteresis between 70◦C to ~0◦C was electrically deconvoluted. Monoclinic phase exhibit a well-defined Arrhenius behavior far below the transition temperature of 64◦C. The activation of the conductivity for the Eu-doped samples was found to be 0.44 eV, higher than 0.41 eV for the pristine material.

C2.31

Dispersive Frequency Response in Low Temperature Silver Iodide by Immittance Spectroscopy Su-Hyun Moon, Young-Hun Kim, Dong-Chun Cho, Eui-Chol Shin and Jong-Sook Lee; School of Materials Science and Engineering, Chonnam National University, Gwangju, Korea (the Republic of).

Motivated by the recent work on β″-alumina polycrystalline ceramics, we revisit the the frequency dispersion behavior of AgI. Series of admittance and capacitance Bode plots at different temperatures revealed the presence of well-de ned parallel capacitance effects and power-law frequency dependences. Non-trivial bulk dispersion is thus successfully described by the parallel connected i) high frequency limit capacitance corresponding to the dielectric constant $\epsilon_\infty \cong 6.4$, ii) a dipolar and vibratory contribution represented by a Cold-Davidson model of the dielectric strength of $\Delta\epsilon_D \cong 1{:}4\epsilon_\infty$ with $\gamma_D \cong 0.11$, $\tau_D \cong 0.003$, corresponding to nearly constant loss behavior, iii) a mobile charge contribution $\Delta\epsilon_C \cong 15\epsilon_\infty$ with $\gamma_C \cong 0.388$ and thermally activated $(\tau_C)^{-1}$ and iv) bulk conductance with activation energy of 0.262 eV. Electrode effects are described by an ideal Warburg response and the coefficient activated by 0.165 eV, connected in parallel to the capacitive elements. The model allows a simulation of AC behavior of AgI as a function of temperature as well as frequencies.

C2.32

Novel Copper-Based Layered Oxide Cathode for Room-Temperature Sodium-Ion Batteries Linqin Mu, Yong-Sheng Hu, Shuyin Xu, Yunming Li and Liquan Chen; Chinese Academy of Sciences, Institution Of Physics, Beijing, China.

In the energy storage field, lithium ion batteries have been extensively explored as power sources for various types of important applications, such as portable electric devices and (hybrid) electric vehicles. Due to the low abundance and uneven distribution of lithium resources in the Earth's crust (0.0065%), large-scale applications of lithium ion batteries become questionable, especially if low cost and high efficient recycling technology could not be developed. Alternatively, room-temperature sodium-ion batteries, which were originally investigated in parallel with lithium-ion batteries, have again aroused interest particularly as stationary batteries for large-scale electrical energy storage in the applications of renewable energy and smart grid owing to a large abundance (2.75%) of sodium resources and potentially low cost, for which the demanding on energy densities of the power sources is not so seriously[1].

Searching for suitable electrode materials to satisfy the long-term stability requirement is an important step to realize the sodium-ion batteries. Recently, many layered Na_xMO_2 (M: 3d transition metals) oxides have been proposed as positive electrode materials for sodium-ion batteries. Amongst them, in general, only layered oxides containing Ni or Co transition metal show promising Na storage performance in terms of high storage capacity, high rate capability and long cycling stability. However, Ni and Co are toxic and their oxides are relatively expensive, which would certainly increase the cost of the battery and is unfavorable for large-scale energy storage applications. Herein, we found that Cu^{2+}/Cu^{3+} redox couple in such layered oxides is electrochemically active and highly reversible in sodium-ion batteries[2]. Take P2-$Na_{0.68}Cu_{0.34}Mn_{0.66}O_2$ as the first example, this material shows a reversible capacity of ca. 70 mAh/g with an average storage voltage of 3.8 V vs. Na^+/Na. To the best of our knowledge, this is the first time to realize the reversible change of Cu^{2+}/Cu^{3+} redox couple with high Na storage voltage and small polarization. Copper is harmless, and is already very common in our daily life. In addition, the cost of copper oxide is only half of that of nickel oxide. Based on this important finding, it is possible to use copper to design new layered oxides with similar Na storage performance as that of Ni or Co containing layered oxides. In this presentation, we further demonstrate that Cu and Fe can be incorporated into an O3-type layered oxide to form $Na_{0.9}Cu_{1/4}Fe_{1/4}Mn_{1/4}Ti_{1/4}O_2$, which was prepared by a simple solid-state reaction route[3]. This material delivers a reversible capacity of 94 mAh g^{-1} with average voltage of 3.2 V, corresponding to 0.4 e^- transfer. Other series of O3-type cathodes were also investigated. We believe that the Na storage performance can be further improved in this series of new layered oxides through turning the compositions of $Na_aCu_{1-x-y-z-d}Fe_xMn_yTi_zD_dO_2$ (D: Dopant, e.g., Li, Mg, Al, etc., $0<x<1$, $0<y<1$, $0\leq z<1$, $0\leq d<1$, $0.6<a\leq 1$,) and oxygen stacking ways of O3, P2, P3, O'3, etc.[4]. Furthermore, full cells were assembled using $Na_aCu_{1-x-y-z-d}Fe_xMn_yTi_zD_dO_2$ as cathode and hard carbon[5] as anode and evaluated their performance. This paves the way for the development of cheaper and non-toxic sodium-ion batteries with superior Na storage performance.

Acknowledgement. This work was supported by funding from the NSFC (51222210, 11234013) and the One Hundred Talent Project of the Chinese Academy of Sciences.

References

Pan, H. L.; Hu, Y. S.; Chen, L. Q. *Energy Environ. Sci.* **2013**, *6*, 2338-2360.
Xu, S.Y.; Wu, X.Y.; Li, Y.M.; Hu, Y. -S.; Chen, L.Q. *Chin. Phys. B* **2014**, *23*,118202.
Mu, L. Q.; Hu, Y. -S.; Chen, L.Q. *Chin. Phys. B* **2015**, *3*, 038203.
Hu, Y. -S.; et al. Several Chinese patents have been filed.
Li, Y. M.; Xu, S. Y.; Wu, X. Y.; Yu, J. Z.; Wang, Y. S.; Hu, Y.-S.; Li, H.; Chen, L. Q.; Huang, X. J. *J. Mater. Chem. A* **2015**, *3*, 71-77.

C2.33

The Degradation Mechanism of Nickel-Rich Cathode Active Materials with Vinylene Carbonate in An Electrolyte for Lithium Ion Batteries at Various Temperatures Su Jung Do,Prasanna Kadirvelayutham, Yong Nam Jo, Robert Ilango Pushparaj and Chang Woo Lee; Kyung Hee University, Yongin-si, Korea (the Republic of).

Lithium ion batteries (LIBs) have become a common power source for portable electronic devices due to their high energy density and are also the most prospective energy storage devices for electric vehicles (EVs) and energy storage system (ESS). As the demands for higher capacity of cathode active materials have increased, Ni-rich cathodes have been intensively studied due to their relative low cost and high capacity. The capacity and the thermal stability of Ni-rich cathodes strongly depend on Ni content. Higher Ni content in Ni-rich cathodes is responsible for higher reversible capacity. However, higher Ni content in Ni-rich cathodes leads to lower thermal stabilities. To minimize trade-off relationship between thermal stability and capacity of Ni-rich cathodes, understanding degradation mechanism of Ni-rich cathodes would be importantly required.

In this work, we have analyzed electrochemical and thermal characteristics of $Li[Ni_{0.8}Co_{0.1}Mn_{0.1}]O_2$ (NCM811) and compared it with those of $Li[Ni_{0.5}Co_{0.2}Mn_{0.3}]O_2$ (NCM523) with vinylene carbonate (VC) in an electrolyte at various temperatures. The electrochemical and the thermal characteristics have been intensively studied by electrochemical impedance spectroscopy (EIS) and differential scanning calorimetry (DSC), respectively.

C2.34

Electrochemical Properties of Sn-Co Electrode with Various Kinds of Binder Materials for Sodium Ion Batteries Yuhki Yui, Masahiko Hayashi, Katsuya Hayashi and Jiro Nakamura; NTT, Atsugi, Japan.

Sodium-ion batteries (SIBs) are anticipated as promising alternatives to lithium-ion batteries (LIBs). Tin electrode has attracted much attention for use as a high capacity negative electrode for SIBs [1]. However, capacities fade owing to changes in volume during cycling. Sn-Co was found to be useful for suppressing changes in volume because cobalt does not alloy with sodium and cobalt buffer. We found that Sn-Co electrodes for SIBs show better cycling performance than tin electrodes and improved cycling performance using PAA binders as substitutes for PVdF [2]. In this study, to further improve the cycle performance of Sn-Co electrodes, we investigated their electrochemical properties with various kinds of binder materials was investigated. The expansion and shrinkage of alloy electrodes have a strong correlation with cycle performance. Hence, changes in electrode volume during cycling using in situ light microscopy were observed, and the correlation between the kinds of binder and change in electrode volume was analyzed.

Sn-Co powder (element ratio: Sn:Co=9:1) was obtained from Mitsubishi Materials Corporation. A working electrode was prepared with Sn-Co powder (80 wt%), Ketjen Black EC600JD (10 wt%), and binder (10 wt%,). Polyvinylidene difluoride (PVdF), polyacrylic acid (PAA), sodium polyacrylate (PAANa), carboxymethyl cellulose (CMC), and polyimide (PI) were used as binders. Sodium metal was used for the counter electrodes. As an electrolyte solution, 1 mol/l $NaPF_6$ /EC- DEC (1:1 in volume) was used. The 2032 coin-type cells were assembled in a glove box filled with Ar (O_2 < 0.1 ppm, H_2O < 0.1 ppm). Electrochemical measurements were carried out at a current density of 25 mA/g in the voltage range from 0.01 to 1.5 V at 25°C. Changes in electrode volume during sodium ion insertion/extraction were observed by using in situ light microscopy. The circular cell for in situ light microscopy examination was a stack consisting of a sodium sheet, separator, and a Sn-Co working electrode. Details about the preparation of the in situ light microscopy can be found in Ref. 2.

The discharge capacities of the cells with PVdF, PAANa, or PI as a binder decreased with cycling. On the other hand, the one with PAA or CMC exhibited about 400 mAh/g for more than 10 cycles. These results suggest that the cycle performance of Sn-Co electrodes was affected by the kinds of binders.

To examine the correlation between the binders and electrode expansion rate, we observed cross-sectional views of cells with various kinds of binders using light microscopy during the first cycle. The electrodes can be given a quantitative expansion rating since the thickness of the Sn-Co electrode measured by line analysis can be seen in in situ light microscopy images. With PVdF as binder, it was about 220 % after sodium-ion insertion and remained swollen even after sodium ion extraction. The one with PAANa or PI as binder showed smaller changes in volume after sodium-ion insertion, but it remained swollen after sodium ion extraction, too. On the other hand, the one with PAA or CMC as binder showed slight changes in volume of about 140% after sodium ion insertion, and well shrunk to about 125 %. The changes in volume might have a connection with the adhesion strength and porous structure of the binders. The electrochemical properties of Sn-Co electrodes were improved by employing suitable binders such as PAA or CMC. The expansion and contraction of the electrode was estimated in the line analysis mode.

[1] S. Komaba et al., *J. Electrochem.Commun.*, **21**, 65 (2012).
[2] Y. Yui et al., *J. Electrochem. Soc.*, **162**, A3098 (2015).

Acknowledgement
We are grateful to Mitsubishi Materials Corp. for supplying Sn-Co powders.

C2.35
Synthesis of Chatode Materials $LiFePO_4$ by Hydrothermal and Ultrasonic Method Wagiyo Honggowiranto and Evvy Kartini; Advanced Materials, National Nuclear Energy Agency, Tangerang Selatan, Indonesia.

Cathode materials of $LiFePO_4$ for solid state rechargeable-battery were synthesized by hydrothermal method. The reaction has been carried out by mixture of $FeSO_4.7H_2O$, H_3PO_4, LiOH and ethylene glycol. After vacuum mixing without and with sonication for 30 min, each mixture was put into a closed *teflon*-tube and placed in the stainless steel autoclave, then it was sealed off tightly followed by heating in an electric oven at temperatures of 180°C for 24 hours. The crystal structure and microstructure of the products were characterized by using X-ray diffraction (XRD) and Scanning Electron Microscope (SEM). Performance of battery was tested by using Battery Analyzer BST-8. From the X-ray data, the sample that was prepared by ultrasonic method showed the crystal structure of orthorhombic belongs to the *P m n b* space group with higher intensity peaks. The microstructure was more homogenous with a diameter particles of 0.2 -2.8 µm and a diameter of commercial particles was 0.5-5.6 µm.The highest spesific capacity obtained for sample prepared by the addition of ethylene glycol with sonication was 118.6 $mAhg^{-1}$, while from commercial was 86.5 $mAhg^{-1}$ at 0.1C.

C2.36
Characterization of Structural and Transport Properties of $LiMn_{1.7}Cu_{0.3}O_4$ Lukasz Kondracki, Anna G. Milewska and Janina Molenda; AGH University of Science and Technology, Kraków, Poland.

INTRODUCTION
Undoped lithium manganese spinel $LiMn_2O_4$ does not exhibit promising charge transport properties in room temperature in which Li-ion batteries operate. Substitution with 3d-metal ions, especially Cu can improve transport properties, even in lower temperatures[1].

EXPERIMENTAL
$LiMn_{1.7}Cu_{0.3}O_4$ was obtained using soft chemistry method. Additionaly, $LiMn_2O_4$ was obtained as a reference material using the same method. As the substrates lithium nitrate $LiNO_3$, copper nitrate $Cu(NO_3)_2 \cdot 3H_2O$ and acetates of manganese $Mn(CH_3COO)_2 \cdot 4H_2O$ were used. The substrates were dissolved in deionized, argonated water and small amounts of ammonia was added to the solution until pH=9 was reached. The precipitates were heated in air at 800°C for 6h and quenched.
Studies of crystal structure were performed using Panalytical Empyrean diffractometer in the range of 10-110° with CuKα radiation. Obtained data was refined using Rietveld method, with GSAS/EXPGUI set of software [2,3]. Measurements of electrical conductivity (EC) were carried out by using a four-probe alternative current method. Seebek coefficient was measured by a dynamic method.

RESULTS
Structural studies confirmed that single-phased $LiMn_{1.7}Cu_{0.3}O_4$ was obtained. Copper-substituted material has 2 orders of magnitude higher electrical conductivity than undoped $LiMn_2O_4$. The sign of Seebek coefficient is positive, around 100µV/K, in contrast to undoped material (for $LiMn_2O_4$ -150µV/K around room temperature)

CONCLUSIONS
Improvement in electrical conductivity obtained by substitution with copper indicates on influence of Cu in charge transfer in low temperatures.

ACKNOWLEDGMENT
The project was funded by a grant from Switzerland through the Swiss Contribution to the enlarged European Union, grant no. 080/2010.

REFERENCES
1. J. Molenda, J. Marzec, K. Świerczek, W. Ojczyk, M. Ziemnicki, M. Molenda, M. Drozdek, R. Dziembaj, *Solid State Ionics* 171 (2004) 215–227
2. A.C. Larson, R.B. Von Dreele, *Los Alamos Natl. Lab. Rep. - LAUR* 86-748 (2004)
3. B.H. Toby, *J. Appl. Cryst.* 34 (2001) 210-213

C2.37
Comparative Analysis of Structure-Property Relationship of Nanosilicon Anodes for Lithium-Ion Batteries Diana Golodnitsky, Emanuel Peled, Fernando Patolsky, Kathrin Freedman, Meital Goor, Keren Goldstein, Guy Davidi and Dan Schneier; School of Chemistry, Tel Aviv University, Tel Aviv, Israel.

We report on the synthesis and characterization of anodes based on silicon, silicon-alloy MWCNTs and amorphous silicon nanowires. The synthesis routes include electroless, pyrolysis and CVD methods. The particles and nanowires are characterized by a variety of analytical (ESEM, TEM-EELS, XPS, XRD) and electrochemical methods. On electrochemical testing of Li/Si cells, we achieved 10% irreversible capacity, and a fast charge–discharge rate (2.7C-rate or 20mA/cm^2) for the 3-4 mAh/cm^2 loaded core-shell SiNW anodes. Current efficiency greater than 99.5% was obtained for both nanoparticles and nanowires. Anodes based on Si-alloy MWCNTs and SiNWs were cycled for over 200 cycles, exhibiting stable cycle life and 1000 to 1500mAh/g_{Si} reversible capacity. The effect of the shape and composition of active-material particles, and anode architecture on the electrochemical performance of Li-ion cells will be discussed in details.

Acknowledgments
This work is funded by EU FP7 MARS-EV" Project, and by the Israel Academy of Science

C2.38
A Na^+ Superionic Conductor Based on NASICON and Its Application in All-Solid-State Sodium Batteries Zhizhen Zhang, Kaiqi Xu, Yong-Sheng Hu and Liquan Chen; Institute of Physics Chinese Academy of Sciences, Beijing, China.

All-solid-state batteries have emerged to address the safety problem caused by the liquid electrolytes commonly used in present secondary batteries. Sodium ion batteries are considered to be competitive in large-scale energy storage applications owing to its natural abundance and low cost[1]. Solid electrolyte is the most vital component in developing all-solid-state batteries. Among the possible Na+ ion conductors, NASICON type solid electrolyte ($Na_{1+x}Zr_2Si_xP_{3-x}O_{12}, 0 \leq x \leq 3$) is of great interest because of its excellent ionic conductivity, chemical stability and wide electrochemical window[2,3]. For the x=2 composition, the value reaches a maximum of 10^{-4} $S \cdot cm^{-1}$ order. However, such a value is still unmatched when compared to the conductivity of liquid electrolyte.

Here we report a series of M-doped NASICON electrolytes which are demonstrated to have the highest ionic conductivity of 3 $mS \cdot cm^{-1}$ at 25°C. The super high ionic conductivity was found to be mainly attributed to the significantly higher densification of the pellet by the M substitution. All-solid-state batteries composed of $Na_3V_2(PO_4)_3$ composite cathode, Na anode, and optimized NASICON electrolyte exhibit good performance at 80°C.

References
[1] Pan, H. L., Hu, Y.-S. & Chen, L. Q. Room-temperature stationary sodium-ion batteries for large-scale electric energy storage. *Energy Environ. Sci.* **6,** 2338-2360 (2013).
[2] Hong, H. Y-P. Crystal structures and crystal chemistry in the system $Na_{1+x}Zr_2Si_xP_{3-x}O_{12}$. *Mater. Res. Bull.* **11,** 173-182 (1976)
[3] Goodenough, J. B., Hong, H. Y-P. & Kafalas, J. A. Fast Na^+-ion transport in skeleton structures. *Mater. Res. Bull.* **11,** 203-220 (1976)

C2.39

Impedance Measurement for Ti-Zr-Ni Alloy Electrodes Produced by Mechanical Alloying and Subsequent Annealing Akito Takasaki[1], Youhei Ariga[1], Wojciech Zajac[2] and Konrad Swierczek[2]; [1]Engineering Science and Mechanics, Shibaura Institute of Technology, Tokyo, Japan; [2]Faculty of Energy and Fuels, AGH University of Science and Technology, Krakow, Poland.

Ti-Zr-Ni icosahedral (i) quasicrystal might possess a large number of interstitial sites in the quasilattice compared with those for normal crystal structures [1], implying a possibility as a candidate of the hydrogen storage alloys. We have previously reported that Ti-Zr-Ni i- phase could be produced by mechanical alloying (MA) and subsequent annealing, and that the maximum discharge capacity of the $Ti_{45}Zr_{38}Ni_{17}$ i-phase electrode was 23.9 mAh/g although the theoretical charge capacity estimated from its chemical composition and the maximum H/M (1.9) was 795mAh/g. We have also investigated the effect of substitution of Ti or Zr for Ni and Ti/Zr for Zr/Ti on electrochemical hydrogenation performances. The maximum discharge capacity after these elemental substitution achieved was about 130mAh/g from a $Ti_{49}Zr_{26}Ni_{25}$ i-phase electrode [2]. In this study, we measured the electrochemical impedance by a three-electrode cell at room temperature for several Ti-Zr-Ni alloy electrodes produced by MA and subsequent annealing. The microstructures of the electrodes consisted of i-phase and minor phases, such as a Ti_2Ni type crystal phase, even after the elemental substitution. The impedance was measured by electrochemical impedance spectroscopy (EIS) using a Solartron 1287 Potentiostat/ Galvanostat and a Solartron 1252A frequency response analyzer with a Z-PLOT software. The impedances at 10, 50 and 100% depth of discharge (DOD) were measured. The charge-transfer resistance lowered with increasing the discharge capacity of the electrodes. The impedance for charge-transfer resistance at the electrode surface drastically decreased when Ti or Zr was substituted for Ni ($Ti_{45}Zr_{30}Ni_{25}$, $Ti_{37}Zr_{38}Ni_{25}$). The addition of Pd as the forth element also decreased the impedance.

[1]P.C. Gibbons, and K.F. Kelton: Toward industrial applications. Edited by Z.M. Stadnik, (Physical Properties of Quasicrystals, Springer, Berline, (1999), p.403.
[2]Y. Ariga, A. Takasaki, C. Kuroda, A. Kulka, Journal of Alloys and Compounds 580 (2013), S251.

C2.40

Structural Evaluation of Delithiated $Li_xMn_{1.5}Ni_{0.5-y}Cu_yO_4$ Spinels Lukasz Kondracki, Anna Milewska, Artur Bogacki, Slawomir Lalik and Janina Molenda; AGH University of Science and Technology, Kraków, Poland.

INTRODUCTION

Growing demand on portable electronic devices is the main reason that drives the development of Li-ion batteries. The nickel-doped lithium manganese spinels exhibit a 5V-plateau and therefore they are attractive candidates for high-voltage Li-ion batteries [1]. This work contains studies on crystal structure in the temperature range -250 to 300°C, of $LiMn_2O_4$, $LiNi_{0.5}Mn_{1.5}O_4$, $LiNi_{0.48}Cu_{0.02}Mn_{1.5}O_4$ and $LiNi_{0.45}Cu_{0.05}Mn_{1.5}O_4$ spinels.

EXPERIMENTAL

Materials $LiMn_{1.5}Ni_{0.5-y}Cu_yO_4$ were obtained using sol-gel method. As the substrates lithium nitrate $LiNO_3$, copper nitrate $Cu(NO_3)_2 \cdot 3H_2O$ and acetates of manganese and nickel $Mn(CH_3COO)_2 \cdot 4H_2O$ and $Ni(CH_3COO)_2 \cdot 4H_2O$ were used. Stoichiometric amounts of these sustrates were taken to obtain $LiMn_2O_4$, $LiNi_{0.5}Mn_{1.5}O_4$, $LiNi_{0.48}Cu_{0.02}Mn_{1.5}O_4$ and $LiNi_{0.45}Cu_{0.05}Mn_{1.5}O_4$ [2]. Studies of crystal structure were performed using Panalytical Empyrean diffractometer in the range of 10-110° with CuKα radiation. For the measurements above and below the room temperature an AP HTK 1200 oven and Oxford Cryostat sample stages were used. Obtained results were refined using Rietveld method.

RESULTS

Structural studies carried in the temperature range -250 to 300°C confirmed obtaining single-phased $LiMn_{1.5}Ni_{0.5-y}Cu_yO_4$ materials with Fd-3m space group. However, Undoped $LiMn_2O_4$in room temperature is a two-phased material – a mixture of cubic Fd-3m and orthorhombic Fddd. The amount of orthorhombic phase increases with the decrease of temperature. The temperature does not affect space group in $LiMn_{1.5}Ni_{0.5-y}Cu_yO_4$. Deintercalation of lithium decreases the unit cell parameters for all measured materials.

CONCLUSIONS

Substitution with foreign 3d- ions (Ni,Cu) in manganese sublattice removes the phase transition present in undoped $LiMn_2O_4$.

ACKNOWLEDGMENT

The project was funded by a grant from Switzerland through the Swiss Contribution to the enlarged European Union, grant no. 080/2010.

REFERENCES

1. J. Molenda, M. Ziemnicki, K. Świerczek, J. Marzec, *Defect Diffus Forum* 242-244 (2005) 65-76
2. A. Milewska, Ł. Kondracki, M. Molenda, M. Bakierska, J. Molenda, *Solid State Ionics*, 267 (2014) 27-31

C2.41

Synthesis, Structure and Ionic Conductivities of Novel Li-Ion Conductor $A_3Li_xTa_{6-x}Zr_xSi_4O_{26}$ (A = Ba, Sr) Akihisa Aimi[1], Yoshiyuki Inaguma[1], Miki Kubota[1], Daisuke Mori[1], Tetsuhiro Katsumata[2], Minoru Ikeda[3] and Takahisa Ohno[3, 4]; [1]Chemistry, Gakushuin University, Toshima-ku, Japan; [2]Chemistry, Tokai University, Hiratsuka-shi, Japan; [3]National Institute for Materials Science, Tsukuba-shi, Japan; [4]Global Research Center for Environment and Energy based Nanomaterials Science, Tsukuba-shi, Japan.

Li-ion battery using Li metal anode is expected to possess the high energy density. However, applying Li metal as anode with liquid electrolyte is difficult because dendritic growth of Li metal during discharge-charge cycles leads to explosion hazards. All-solid-state Li-ion battery using ceramic oxide electrolyte is expected to possess high energy density, reliability and safety by preventing dendritic growth of Li metal. On the other hand, there are some difficulties such as high resistivity of electrolyte and the lack in electrochemical stability when oxide solid state electrolytes are applied to all-solid-state batteries. In this study, $A_3Li_xTa_{6-x}Zr_xSi_4O_{26}$ (A = Sr, Ba) as the candidate solid electrolytes stable against Li metal were synthesized by a conventional solid state reaction, and their structure and ionic conductivities were investigated. Both the compounds with A = Sr and Ba crystallize in hexagonal structure with space group*P*-62*m* the same as $A_3Ta_6Si_4O_{26}$ does. The substitution limits for $A_3Li_xTa_{6-x}Zr_xSi_4O_{26}$ (A = Sr, Ba) are up to x = 1.0 and 3.0, respectively. Rietveld and MEM analyses, first principles calculation, and NMR spectroscopy showed that Li ions reside in interstice sites. The sample with A = Ba exhibits higher ionic conductivity (e.g. 6.9×10^{-8} S cm^{-1} at 500 K in x = 1.0) than that with A = Sr (e.g. 3.2×10^{-8} S cm^{-1} at 500 K in x = 1.0). The ionic conductivity was enhanced with an increase of x, i.e. the substitution of Li and Zr. Further enhancement of ionic conductivity was attained by the introduction of deficiency at A site cation, which corresponds to y in $A_{3-y/2}Li_{x+y}Ta_{6-x}Zr_xSi_4O_{26}$. Consequently, $Ba_{2.75}Li_{1.5}Ta_5ZrSi_4O_{26}$ exhibits the highest total ionic conductivity at 500 K of 4×10^{-7} S / cm and the lowest activation energy of 0.72 eV, respectively. The consideration of the size of bottlenecks and first principles calculation showed that Li ions diffuse two dimensionally in A cation (A = Sr, Ba) deficient layer. These results suggest that the ionic conductivity of $A_3Li_xTa_{6-x}Zr_xSi_4O_{26}$ (A = Sr, Ba) could be improved by forming new diffusion path between A cation containing layer and A site deficient layer.

C2.42

Properties of Lithium-Stuffed Garnet-Type Oxide Solid Electrolyte Thick Film Fabricated by Aerosol Deposition Method Ryoji Inada, Takayuki Okada, Keiji Tsuritani, Kota Wagatsuma, Tomohiro Tojo and Yoji Sakurai; Department of Electrical and Electronic Information Engineering, Toyohashi University of Technology, Toyohashi, Japan.

Lithium-stuffed garnet-type oxide solid electrolyte with the formula of $Li_7La_3Zr_2O_{12}$ (LLZ) have been widely studied for the apprication to all-solid-state lithium battery because of their high ionic conductivity above 10^{-4} Scm^{-1} at room temperature, excellent thermal performance and stability against lithium metal anode. Film-shaped solid electrolyte provides both low electrical resistance, downsizing for the devices and increasing volumetric energy density of all-solid-state battery. In this study, we fabricated LLZ thick film by aerosol deposition (AD) method and evaluated their crystallinity, microstructure and ionic conductivity. Cubic LLZ powder with an averaged particle size of 2 υm was used as raw material and splayed directly on a stainless steel or glass substrate for 60 minutes to form LLZ film via room temperature impact consolidation. Although small amount of impurity phases such as $La_2Zr_2O_7$ and Li_2CO_3 was confirmed by XRD measurements, as-deposited LLZ film by AD had cubic-garnet structure on the substrate without any heat treatment. From SEM observation, it was confirmed that fractured LLZ particles with the size of 0.5-1 υm is consisting the film and film thickness is 12 υm. From AC impedance measurements, ionic conductivity of LLZ film by AD was estimated to be 2.4 x 10^{-6} S cm^{-1} at 27ºC, which is nearly two digits lower than sintered LLZ as previously reported. The low conductivity of LLZ film fabricated by AD could be attributed to increased volume ratio between grain and grain-boundaries and presence of impurity phases in the film.

C2.43

Defect Chemistry and Transport in Alkali Superoxides Oliver Gerbig, Rotraut Merkle and Joachim Maier; MPI for Solid State Research, Stuttgart, Germany.

Alkali peroxides and superoxides are possible reaction products in rechargeable alkali metal-oxygen batteries with aprotic electrolytes. Transport in Li_2O_2 was found to proceed via holes (i.e. superoxide ions on peroxide sites) and lithium vacancies [1]. The present work investigates the electrical transport and reaction kinetics of the superoxides of potassium, rubidium and cesium [2] and elucidates the underlying defect chemistry, which - in contrast to oxides - is largely terra incognita so far. The conductivities were obtained from electrochemical impedance spectroscopy and further separated into electronic and ionic contributions by electromotive force measurements and dc stoichiometry polarization with selectively blocking electrodes. The oxygen exchange kinetics was investigated by means of oxygen isotope exchange experiments and analysis of the gas phase composition.

Lithium and sodium peroxide are found to be mixed conductors with alkali ions as main ionic charge carrier and holes (localized on a peroxide site yielding superoxide defects) as main electronic charge carriers. In contrast, in alkali superoxides the electronic carriers are excess electrons (likely localized on a superoxide site yielding peroxide defects). A defect model for alkali superoxides is proposed and the dependences of the defect concentrations on the alkali metal activity and the oxygen partial pressure are derived (Kröger-Vink diagrams). The oxygen exchange surface reaction is found to be much faster than in other large bandgap oxides such as $SrTiO_3$, and in particular for RbO_2 and CsO_2 to proceed without dissociation of the O=O bond.

[1] O. Gerbig, R. Merkle, J. Maier, Adv. Mat. 25 (2013) 3129
[2] O. Gerbig, R. Merkle, J. Maier, submitted

C2.44

Dielectric and Transport Properties Study of Clay Based Solid Polymer Electrolyte Namrata Tripathi[1], Awalendra K. Thakur[3], Archana Shukla[2] and David T. Marx[1]; [1]Physics, Illinois State University, Normal, USA, Normal, Illinois, United States; [2]Physics, Indian Institute of Technology Bombay, Maharastra, Mumbai, India; [3]Physics, Indian Institute of Technology Patna, Bihar, Patna, India.

Solid polymer electrolyte (SPE) is the key component in a solid-state lithium polymer battery. It offers advantage in weight, size, high safety, leak proof and flexibility in the shape of the cell design. However the conductivity of these electrolytes falls short of required standards. The main cause of poor ionic conductivity of SPEs is the ion-pair formation, which reduces the number of mobile charge carriers. Formation of clay based solid polymer electrolyte is considered to be an effective approach where ion pair formation can be minimized due to Coulombic interaction between cations and anions. Using the approach the conductivity of SPE has been improved but it is still insufficient for device applications. The main hurdle in achieving required conductivity is poor understanding of the conduction mechanism in solid polymer electrolyte.
The conductivity of SPE is mostly a function of number of charge carriers and their mobility. To understand the mechanism of ion conduction in SPE it is important to determine the values of n and μ. A number of approaches have been carried out such as neutron scattering, nuclear magnetic resonance (NMR), dielectric spectroscopy and computer simulations to determine transport parameters. Recently a new more direct method, based on impedance spectroscopy is developed to determine transport properties of polymer electrolytes.

In the present work, solid polymer electrolyte films based on Poly (methyl methacrylate) (PMMA) and sodium montmorillonite clay (NaMMT) are prepared by solution-cast technique. The dielectric behavior of the films has been analyzed in terms of frequency response of dielectric permittivity (ε') and dissipation factor (tanδ). Such an analysis has confirmed the presence of electrode polarization effects due to space charge polarization at lower frequency. The appearance of the loss peak in the low frequency region is attributed to the losses due to conduction. The real part of ac conductivity spectra of the materials obeys Jonscher power law at higher frequency whereas dispersion in lower frequency confirms the presence of electrode polarization effect. The transport parameters of prepared samples are calculated using new approach based on impedance spectroscopy. The results suggest a new finding that the higher ionic conductivity of such PNCs at elevated temperature is not only due to increased thermally-activated hopping rates, rather supported by some significant increase in carrier concentration.

C2.45

The Effect of Cathode Microstructure on the Performance of All Solid-State Li Battery Sven Uhlenbruck, Chih-Long Tsai, Christian Dellen, Qianli Ma, Sandra Lobe and Olivier Guillon; Institute of Energy and Climate Research, Forschungszentrum Jülich GmbH, Jülich, Germany.

All solid-state Li batteries based on oxide-class solid electrolyte are considered to be out-standing from the other electrolytes due to their high safety and higher energy density. Among the Li-ion conductive oxides, materials with garnet structure such as Ta-substituted $Li_7La_3Zr_2O_{12}$ (LLZ:Ta) have been attracting most of attention due to their high total Li-ion conductivity, wide electrochemical stability window, stability against metallic Li and easy handling for fabrication (i.e. inertness to oxygen). The use of LLZ as solid electrolyte for solid-state battery had been reported in several papers. However, the reported solid-state batteries were all constructed with a thin film cathode which was made either by physical vapor or sol-gel deposition. The thin film cathodes were usually under or around one micrometer in thickness which made the energy density of these SSBs useful for small scale applications.
Electrolyte supported solid-state batteries using LLZ:Ta with thick cathodes (> 50 micrometers) have been constructed in our laboratory by screen-printing process. A proper sintering process was invested for well bonding the thick cathode layer to the supporting electrolyte. The constructed solid-state Li batteries exhibited good charge-discharge utilization of active material of more than 80% which is equal to a capacity density of more than 1 mAh cm^{-2} at 100 ºC. It also exhibited good cycle ability so that one hundred of cycles were achieved. However, the reduction of high internal resistance of the cell is still the major challenge for further improvement of the battery performance, especially if the application of this all solid state Li battery is toward room temperature. During this presentation, results from material chemical stability, cell morphology, electrochemical performance and the challenges of building up Li battery by using LLZ:Ta will be discussed.

C2.46

Conductivity and Scaling Behavior of Nd^{3+} Ions Containing Lithium Borate Glasses Durgaprasad D. Ramteke[1, 2], Hendrik C. Swart[1] and Rupesh S. Gedam[2]; [1]Department of Physics, University of Free State , Bloemfontein , South Africa; [2]Department of Applied Physics, Visvesvaraya National Institute of Technology, Nagpur, India.

The ability of glasses to form over a wide range of composition with the desired shape, homogeneity and chemical inertness make them suitable candidates as solid electrolytes. These glasses can be synthesized by embedding various ions to increase its ion conductivity. From all the ion conducting glasses lithium borate glasses have fascinated researchers due to the well-known borate anomaly and high electropositive nature of lithium ions. These glasses are also known for their coordination geometry, higher bond strength, high transparency, low melting point and good rare earth ions solubility. Rare earth (RE) element offer unique combination of partially filled *4f* shells and completely filled $5s^2 5p^6$ electron shells. Addition of REs elements in glasses make them feasible to design various electro-optical devices. Despite of their uniqueness, the ion conducting properties of rare earth oxide containing glasses are reported only by a few. Here, we report detail study of lithium borate glasses containing Nd_2O_3 by impedance spectroscopy.

We synthesized the glass series 27.5 Li_2O-(72.5-X) B_2O_3-X Nd_2O_3 with X= 0.5, 1, 1.5 and 2 by a simple melt quench technique. These glasses were analyzed by impedance spectroscopy to study insight of conduction phenomenon. From the conductivity measurements it were observed that, the conductivity of the glasses increased with the increase in temperature. It is also observed that addition of Nd_2O_3 decreases the conductivity of these glasses because Nd^{3+} ions hinders the motion of mobile charge carriers Li^+ ions. To get a better insight of the conduction behavior we further analyzed the modulus and scaling behavior of these glasses. The study elucidated that the conduction phenomenon is compositional dependent rather than temperature. The dielectric constant and dielectric loss decreased with a decrease in temperature. This effect is ascribed to a change in the orientational vibrations. We found good correlation between the electrical, structural and dielectric properties of the glasses.

C2.47

A Battery Made from a Single Material Fudong Han[1], Tao Gao[1], Yujie Zhu[1], Karen J. Gaskell[2] and Chunsheng Wang[1]; [1]Department of Chemical and Biomolecular Engineering, University of Maryland, College Park, Maryland, United States; [2]Department of Chemistry and Biochemistry, University of Maryland, College Park, Maryland, United States.

Bulk-type all-solid-state lithium-ion batteries with nonflammable inorganic solid electrolyte are being considered as the ultimate solution for safe lithium-ion batteries. The current all-solid-state lithium-ion batteries suffer from low power density mainly due to strong kinetic limitation at the electrode/electrolyte interface. Here, we report a novel concept of a single-material all-solid-state lithium-ion battery, wherein a single $Li_{10}GeP_2S_{12}$ serves as an electrolyte, an anode, and a cathode, to eliminate the highly resistive interface between the electrodes and electrolyte. The realization of the single-$Li_{10}GeP_2S_{12}$ battery is based on the fact that the Li-S and Ge-S components in $Li_{10}GeP_2S_{12}$ electrolyte could act as the active centers for lithiation/delithiation as a cathode and an anode, respectively, when electronically-conductive carbon is mixed, while pure $Li_{10}GeP_2S_{12}$ can be used as an electrolyte. Using a single material for a battery can also significantly simplify the fabrication process and reduce the cost. This unique concept of a single-material lithium-ion battery can be extended to other solid-state battery systems, providing a new direction for high-power, high-energy, long-cycling solid-state batteries.

C2.48

High Rate Growth by Pulsed Laser Deposition and Characterization of Epitaxial $LiCoO_2$ Films Kazunori Nishio[1], Tsuyoshi Ohnishi[1, 2, 3], Minoru Osada[3], Narumi Ohta[1, 2], Ken Watanabe[2] and Kazunori Takada[1, 2, 3]; [1]Global Research Center for Environment and Energy based on Nanomaterials Science, National Institute for Materials Science, Tsukuba, Japan;[2]Environment and Energy Materials Division, National Institute for Materials Science, Tsukuba, Japan; [3]International Center for Materials Nanoarchitectronics , National Institute for Materials Science, Tsukuba, Japan.

Thin-film lithium batteries are key components in today's portable electronics and the microdevices such as MEMS and drug delivery systems. One of the objectives in the development of thin film batteries is to increase the areal capacity in order to store a high energy within the limited footprint. A simple way to increase the areal capacity compared to 3D solid-state batteries [1] is increasing the electrode thickness; however, it lowers the rate capability [2]. Because one of the dominant rate-determining factors is the grain boundary resistance, epitaxial film enables us to overcome this trade-off problem by removing such grain boundaries. In this study $LiCoO_2$ was selected as a typical cathode material and synthesized into epitaxial films by pulsed laser deposition (PLD). High laser fluence and repetition rate were employed to achieve high rate growth for the establishing of the recipe of thick-film fabrication. The crystallinity and electrode performance were investigated for the films grown under varied conditions such as oxygen partial pressure (P_{O2}) and substrate temperature (T_{sub}).

[1] P. H. L. Notton *et al*, Adv. Mater. 19 (2007) 4564-4567.
[2] N. J. Dudney *et al*, J. Power Sources 119-121 (2003) 300-304.
[3] K. Nishio *et al*, J. Power Sources 247 (2014) 687-691.

C2.49

Assembly and Electrochemical Properties of $LiFePO_4$/C Pouch Cell Evvy Kartini and Wagiyo Honggowiranto; Science and Technology Center for Advanced Materials, National Nuclear Energy Agency, South Tangerang, Indonesia.

A new pouch cell of Lithium ion rechargeable battery has been assembled at the Integrated Battery Laboratory, National Nuclear Energy Agency (BATAN), Indonesia. The cathode sheet was prepared from double sided coated $LiFePO_4$/C on aluminum foil with the thickness of 180 µm. The anode sheet was prepared from double sided coated artificial graphite on the copper foil with thickness of 197 µm. Both aluminum and copper foils are functioned as positive and negative current collectors, respectively. The cathode and anode sheet was cut using slitting machine with a dimension of 6.7cm x 17.0cm. The composition, crystal structure, morphology and conductivity of coated $LiFePO_4$/C and Graphite was measured by an XRD, SEM and EIS. A separator was put between the cathode and anode sheet to prevent the short circuit. Battery cells are constructed by rolling thin layers of cathode, separator, and anode material to cylindrical shapes by using a winding machine. The cylindrical cell was inserted into aluminum pouch case then sealed at 180°C with one side left open. The positive and negative connectors made from aluminum and nickel tab were welded on the top of aluminum and copper foil, respectively. The pouch cell was put into Glove Box then filled with ~ 2.5 ml liquid electrolyte $LiPF_6$. Liquid electrode makes up the internal space. A vacuum sealing machine was used to seal the rest of pouch case at 180°C. The electrochemical properties of lithium ion battery (pouch cell) were characterized by using a BST8 Battery analyzer. The $LiFePO_4$ exhibited a discharge capacity of 250 mAh, with the specific capacity of 127 mA h g^{-1}. The pouch cell showed good performance after 100 cycles with the efficiency of 99%.

C2.50

Towards Control over Redox Behavior and Ionic Conductivity in $LiTi_2(PO_4)_3$ Fast Lithium-Ion Conductor Wojciech Zajac[1], Mateusz Tarach[1] and Anita Trenczek-Zajac[2]; [1]Faculty of Energy and Fuels, AGH University of Science and Technology, Krakow, Poland; [2]Faculty of Materials Science and Ceramics, AGH University of Science and Technology, Krakow, Poland.

Location of redox couples in transition metal compounds is a key factor determining their application. NASICONs $AM_2(PO_4)_3$ (A = Na, Li; M = Ti, Zr, Hf, Ge, Sn, Fe, ...) form an intriguing group of compounds embracing fast ion conductivity and tunable reduction/oxidation potentials and they are considered as solid electrolytes or electrode materials for lithium cells. The present work focuses on $LiTi_2(PO_4)_3$ member of this family and possibility of modification of its transport and redox properties.
Here we show the effect of doping of $LiTi_2(PO_4)_3$ parent compound with Al, Ga, In, Nb, Sn, Zr at the constant level of 0.15 mol/mol Ti on crystal structure, ionic conductivity, electronic band structure, as well as lithium intercalation and Ti^{4+}/Ti^{3+} redox potential. The interrelations are studied by X-ray diffraction technique, AC impedance spectroscopy, UV-VIS and EPR spectroscopy along with cyclic voltammetry.

Significant correlation between both ionic conductivity and position of Ti^{4+}/Ti^{3+} redox potential and unit cell size is observed, indicating that the size of the Li^+ diffusion paths and Ti-lattice sites are the key factors affecting materials properties. Depending on charge and ionic radius of the dopant they show fairly linear dependence between ionic radius and unit cell volume. In the case of some of the examined dopants (Nb, Sn, In) more complex interaction was observed, since their introduce their own redox activity, enabling further modifications of the material. Additionally, there is a significant impact of dopant type as well as intercalation stage on the position of fundamental absorption edge observed in the UV-VIS reflectance spectra. For selected compositions variation of XRD pattern as a function Ti^{4+}/Ti^{3+} ratio is discussed.

Acknowledgment
This work was funded by National Science Centre Poland under grant no. 2012/05/D/ST5/00472.

C2.51

Advanced Planar Lithium-Sulfur Batteries Based on Solid Ceramic Li-Ion Conducting Separators Feng Zhao and John Bi; Ceramatec, Inc. , Salt Lake City, Utah, United States.

Ceramatec is developing new batteries funded through ARPA-e RANGE program. The new batteries make use of a non-porous, high ion conductivity ceramic membrane employing a lithium-sulfur (Li-S) battery chemistry. Porous separators found in today's batteries contain liquids that negatively impact cycle life. To address this, Ceramatec's battery includes a ceramic membrane to help to hold charge while not in use. This new design would also provide load bearing capability, improved mechanical integrity, and extend battery life. Ceramatec will build and demonstrate its innovative, low-cost, non-porous membrane in a prototype Li-S battery with a smaller size and higher storage capacity than conventional batteries. The project progress will be updated.

C2.52

Development of NaSICON-Type Lithium Ion Conductors Feng Zhao and John Bi; Ceramatec, Inc. , Salt Lake City, Utah, United States.

Lithium ion-conducting solid electrolytes have been extensively investigated for the past century and a number of solid materials, such as Li3N, Li2S-based glass, NaSICON-type oxides and polymer electrolytes have been shown to exhibit good Li-ion conductivity. The NaSICON-type lithium ion conductors are attractive as electrolytes for batteries and electrochemical devices because they exhibit a high conductivity of 8×10-4 S/cm at room temperature and are stable under atmosphere and in water. In the case of the Lil+xAlxTi2-x(PO4)3 (LATP) system, the tetravalent Ti4+ are partially substituted by Al3+. The residual negative charges are neutralized with additional Li+, leading to an increase of Li stoichiometry in Lil+xAlxTi2-x(PO4)3. The substitution of Ti4+ by smaller Al3+ cations also reduces unit cell dimensions of the NaSICON framework and significantly enhances Li+ conductivity by about 3 orders of magnitude. The compound family with general formula Lil+xMxTi2-x(PO4)3 (M=Al, Ga, In, Sc) has been systematically investigated in terms of lithium mobility. We have investigated systematically a novel composite conductors based Li-ion Super Conductors (LiSICON). This conductors exhibited higher conductivity, stability and mechanical strength compared to the pure LiSICON. We will talk about the project progress in our presentation.

C2.53

Preparation of Li_2S–P_2S_5 Solid Electrolytes Using Organic Solvents as Synthetic Media Nguyen H. Phuc, Kei Morikawa, Mitsuhiro Totani, Hiroyuki Muto and Atsunori Matsuda; Electrical and Electronic Information Engineering, Toyohashi University of Technology, Toyohashi, Japan.

The sulfide electrolytes are being prepared in laboratory scale by the conventional planetary ball-milling method or solid state reaction of Li_2S and P_2S_5. The synthesized electrolytes exhibit excellent Li^+ ion conductivity; however, the usage of this method for industrial scale production faces many difficulties, including high energy and time consumption. Recently, the synthetic of sulfide electrolytes in organic solvent media is getting attraction from researchers [1-3]. In this study, we found that the reaction of Li_2S and P_2S_5 can be mediated by dimethyl carbonate, ethyl propionate at room temperature to form precursors of sulfide electrolyte. Upon heating at appropriate temperatures in vacuum, the precursors were decomposed to form amorphous and/or crystalline electrolytes. The solid products of the preparation processes were characterized with Raman spectroscopy, powder X-ray diffraction and AC impedance spectroscopy to determine the structures and ionic conductivities.

Acknowledgement: This study was supported by the Japan Science and Technology Agency, the Advanced Low Carbon Technology (JST-ALCA) (Special Priority Research Areas, All-solid-state battery team).

References:

[1] S. Ito, M. Nakakita, Y. Aihara, T. Uehara, N. Machida, *J Power Sources* **271**, 342 (2014).
[2] Z. Liu, W. Fu, E.A. Payzant, X. Yu, Z. Wu, N.J. Dudney, J. Kiggans, K. Hong, A.J. Rondinone, C. Liang, *J Am Chem Soc* **135**, 975 (2013).
[3] S. Teragawa, K. Aso, K. Tadanaga, A. Hayashi, M. Tatsumisago, *J Power Sources* **248**, 939 (2014).

C2.54

Mechanochemical Preparation of Lithium Sulfide-Lithium Iodide Solid Solutions as Active Materials for All-Solid-State Lithium Secondary Batteries Takashi Hakari, Akitoshi Hayashi and Masahiro Tatsumisago; Department of Applied Chemistry , Osaka Prefecture University, Sakai-shi, Japan.

All-solid-state lithium secondary batteries with inorganic solid electrolyte (SE) have attracted much interest because of their safety. Recently, we reported that all-solid-state cells with composite electrodes prepared by mechanical milling (MM) of mixtures of sulfur (S) or lithium sulfide (Li_2S) active material, acetylene black and Li_2S-P_2S_5 SE showed high reversible capacities with good cyclabilities [1, 2]. However, the capacities per gram of positive electrodes are significantly small because S or Li_2S contents in the electrodes are still small. Maintaining the utilizations of S and Li_2S with increasing their contents is difficult because of the insulating nature of S and Li_2S. In this study, to increase the content of Li_2S active material content in the electrode for all-solid-state cell, the enhancement of Li^+ ion conductivity of the Li_2S active material was done by preparing Li_2S-LiI solid solutions.

Li_2S-LiI solid solutions were prepared by MM of crystalline Li_2S and LiI and then characterized by XRD and ionic conductivity measurements. From XRD patterns of the obtained (100 - x) Li_2S·xLiI (mol%, $0 \leq x \leq 20$), diffraction peaks attributable to LiI dissappeared and those attributable to Li_2S shifted to the lower angle side with increasing the LiI content, suggesting that Li_2S-LiI solid solutions were obtained by MM. The ionic conductivities of Li_2S-LiI solid solutions were increased with an increase in the LiI content. The solid solution at the composition of x = 20 showed the highest ionic conductivity of 2.2×10^{-6} S cm^{-1}, which is two orders of magnitude higher than that of Li_2S. Electrochemical performances of all-solid-state cells with the Li_2S-LiI solid solutions as active materials will be discussed.

References

[1] M. Nagao *et al.*, *Electrochim. Acta*, **56** (2011) 6055.
[2] M. Nagao *et al.*, *J. Mater. Chem.*, **22** (2012) 10015.

Acknowledgement: This research was financially supported by ALCA-SPRING project.

C2.55

A Study on the Effects of Mechanical Alloys as Anodes on Corrosion and Hydrogen Evolution Reaction in Zinc-Air System Yong Nam Jo, Prasanna Kadirvelayutham, Su Jung Do, Subburaj Thiruvengadam and Chang Woo Lee; Kyung Hee University, Yongin-si, Korea (the Republic of).

Zinc-air system has been regarded as an attractive energy device due to its high specific energy, environmental friendliness and economic advantages. The zinc-air system has been classified as a fuel cell or secondary battery, according to its electrical rechargeability. Both systems encounter a common critical problem of corrosion in zinc electrodes. Zinc has a greater negative reduction potential than hydrogen, which evolves hydrogen gas on the zinc particle surface and creates the problem of corrosion. The corrosion of zinc anodes has a severely negative influence on electrochemical performance. In previous, zinc had been added with mercury to suppress the hydrogen evolution brought on by the self-discharge reactions of zinc and by the increase in internal cell impedance. However, the use of mercury has become an environmental issue and the attention has been focused on developing mercury-free system.

In this study, we tried different composition of alloy materials as anodes to suppress the corrosion and hydrogen evolution reaction (HER). So as to study the electrochemical and corrosion behavior of attempted materials, electrochemical storage test, electrochemical impedance spectroscopy and Tafel extrapolation method have been carried out. In addition, the gas evolved from the attempted materials has been measured by a volumetric method.

C2.56

Synthesis and Electrochemical Property of Garnet-Type Lithium-Ion Conductor $Li_{7-x-y}Al_yLa_3Zr_{2-x}Ta_xO_{12}$ Yasuaki Matsuda[1], Yuya Itami[1], Masaki Matsui[1, 2], Yasuo Takeda[1] and Nobuyuki Imanishi[1]; [1]Chemistry, Mie University, Tsu, Japan; [2]PRESTO, Japan Science and Technology Agency, Honcho, Kawaguchi, Japan.

Fast lithium ion conductors are key to the development of next generation energy storage systems such as all-solid-state lithium secondary batteries and lithium-air batteries. Among the electrolyte proposed, garnet-type lithium-ion conductor $Li_{7-x-y}Al_yLa_3Zr_{2-x}Ta_xO_{12}$ is one of the most promised compounds because of high ionic conductivity, chemical and electrochemical stability with the lithium metal. However, the phase formation and ionic conductivity of $Li_{7-x-y}Al_yLa_3Zr_{2-x}Ta_xO_{12}$ is still unclear, because the contamination of Al^{3+} from Al_2O_3 crucible occurs during the synthesis.

We synthesized Al-free $Li_{7-x}La_3Zr_{2-x}Ta_xO_{12}$ by conventional solid state methods using MgO crucible. The tetragonal garnet phase was obtained from $x = 0 – 0.375$ and the cubic phase was obtained for $x = 0.40 – 1.0$ in $Li_{7-x}La_3Zr_{2-x}Ta_xO_{12}$. A linear decrease of *a* and linear increase of *c* were observed from $x = 0$ to 0.375, and then linear decrease of *a* was observed for $x = 0.4 – 1.0$, which is in good agreement with the systematic compositional change of $Li_{7-x}La_3Zr_{2-x}Ta_xO_{12}$. These results suggest that the structural change from the tetragonal to the cubic one is caused by the introduction of the lithium vacancies. The ionic conductivity increased with *x* and the highest ionic conductivity of 3.7×10^{-4} S cm^{-1} at 25°C was obtained for $x = 0.40$, then decreased with increasing *x* in $Li_{7-x}La_3Zr_{2-x}Ta_xO_{12}$.

Then the phase formation and ionic conductivity of $Li_{6.6-z/2}Al_{z/2}La_3Zr_{1.6+z}Ta_{0.4-z}O_{12}$ was investigated focusing on the lithium vacancy content. The cubic garnet phase was obtained for $z = 0 – 0.27$ in $Li_{6.6-z/2}Al_{z/2}La_3Zr_{1.6+z}Ta_{0.4-z}O_{12}$ and the samples with 0.4 mol of lithium vacancies exhibited high ionic conductivity above 5.0×10^{-4} Scm^{-1} at 25°C. These results suggest that control of the lithium vacancy concentration is key to obtain the fast lithium-ion conduction phase of $Li_{7-x-y}Al_yLa_3Zr_{2-x}Ta_xO_{12}$.

C2.57

On V Substitution in Li_2MnSiO_4/C as Potential Positive Electrode for Li-Ion Batteries Nils Wagner, Ann-Mari Svensson and Fride Vullum-Bruer; Material Science and Engineering, Norwegian University of Science and Technology, Trondheim, Norway.

Li-ion technology is superior to other battery concepts with respect to energy density, cycling stability, self-discharge and expected lifetime [1]. Polyanionic compounds have attracted interest since the discovery of $LiFePO_4$ as a safer cathode material in 1997 [2], and of Li_2FeSiO_4 as a new Li-battery cathode material in 2005 [3]. Lithium-transition-metal-silicates are promising candidates as cathode materials, since they allow Li extraction/insertion beyond one Li-ion per formula unit. Additionally, they consist of cheap, environmentally benign and abundant elements [4].

Here we focus on V substitution in Li_2MnSiO_4 (LMS). LMS can theoretically deliver two Li-ions per formula unit since Mn possesses two redox couples (Mn^{3+}/Mn^{2+} and Mn^{4+}/Mn^{3+}) and can thus achieve a high specific capacity of 333 mAh/g. LMS has three shortcomings, namely low ionic and electronic conductivity and amorphization upon Mn oxidation, probably caused by Jahn-Teller distortions [5]. The structural stability might be improved by limiting the delithiation or by incorporating stabilizing dopants. Poor conductivity can be overcome by nano-sizing and conductive coatings. V substitution can deliver more accessible redox couples (V^{3+}/V^{2+}, V^{4+}/V^{3+} and V^{5+}/V^{4+}) [6] and more importantly cause cation vacancy formation if V exists in oxidation state +3 or +5.

Here, synthesis of V substituted LMS was demonstrated by an acidic, PVA-assisted sol-gel method. A conductive carbon coating was created by mixing the precursor with corn-starch. Incorporation of V on either the Mn or the Si site was achieved by varying the stoichiometry and was shown to have a significant impact on phase purity and cycling behavior. Synthesis of completely phase pure lithium transition metal silicates is challenging and for $Li_2Mn_{0.9}V_{0.1}SiO_4$, a clear increase in secondary phases for the nominal composition was observed, while $Li_2MnSi_{0.9}V_{0.1}O_4$ showed an increase in phase purity compared to the pristine sample. The corresponding first discharge capacities at a current density of 10 mA/g were 150 mAh/g for $Li_2MnSi_{0.9}V_{0.1}O_4$ and 110 mAh/g for both $Li_2Mn_{0.9}V_{0.1}SiO_4$ and Li_2MnSiO_4.

[1] Tarascon J. M., Armand M., Nature, 2001, 414, 359-367.
[2] Padhi A. K., Nanjundaswamy K. S., Goodenough J. B., J. Electrochem. Soc, 1997, 144, 1188-1194.
[3] Nyten A., Abouimrane A., Armand M., Gustafsson T., Thomas J. O., Electrochemistry Communications, 2005, 7, 156-160.
[4] Saiful Islam M., Dominko R., Masquelier C., Sirisopanaporn C., Armstrong A. R., Bruce P. G., J. Mater. Chem., 2011, 21, 9811-9818
[5] Muraliganth T., Stroukoff K. R., Manthiram A., Chem.Mater. 2010, 22, 5754–5761.
[6] Li Y., Cheng X., Zhang Y., J. Electrochem. Soc., 2012, 159 (2) A69-A74.

C2.58

Electrical Conductivity Characterization of $LiAlO_2$ Thin Films Prepared by ALD Yang Hu, Amund Ruud, Ville Miikkulainen, Truls Norby, Ola Nilsen and Helmer Fjellvag; Centre for Materials Science and Nanotechnology, Department of Chemistry, University of Oslo, Oslo, Norway.

Atomic Layer Deposition (ALD) allows deposition of highly conformal films on complex and 3-dimensional (3D) structures. Recently, it has been successfully applied to deposit thin films of Li ion conducting materials, opening up new possibilities for the development of 3D all-solid-state Li-ion batteries. The limited capacity per footprint area (μA h cm^{-2}), in regard to the lower Li-ion conductivity in solid-state electrolytes, can be compensated by the enhancement of active electrode area inside the batteries, giving rise to desired power density for Li-ion battery application. The electrical conductivity in such thin films is not yet widely studied, much due to challenges in electrical measurement on films with nano-scale thickness and amorphous structure.

In the present work, the electrical conductivity of $LiAlO_2$ amorphous films deposited by ALD was measured by impedance spectroscopy through both in-plane and cross-plane configurations, using, respectively, an insulating sapphire or conducting Ti substrate. The setup for conductivity measurement on these films was established in combination with suitable effective electrode contacts. Room-temperature conductivities of the $LiAlO_2$ films were readily measured at ambient condition and shown to be in the range of $1–6\times10^{-10}$ S cm^{-1}. Temperature-dependent conductivities were obtained in controlled inert atmosphere from room temperature to around 200 ºC, exhibiting activation energies of 0.7–0.8 eV. The transport properties are discussed in terms of ionic defects and diffusion. Conductivities obtained from different thicknesses and substrates were comparative. This study demonstrates the importance of understanding and correctly interpreting the electrical conductivity in ALD amorphous films, with respect to contributions from electrochemical electrode impedance, parasitic conductance and effects from adsorbed water.

C2.59

Solid Electrolytes for Lithium-Sulfur Batteries Alice Cassel[1, 2, 3], Benoit Fleutot[1, 2, 3], Christine Surcin[1, 2, 3], Virginie Viallet[1, 2, 3] and Mathieu Morcrette[1, 2, 3]; [1]Laboratoire de Réactivité et Chimie des Solides, Amiens, France; [2]Réseau sur le Stockage Electrochimique de l'Energie, Amiens, France; [3]Alistore-ERI, Amiens, France.

Lithium-sulfur system (Li-S) is considered to be one of the most promising solutions to store enough energy for electric vehicles application because of a theoretical energy density of 2245 Wh/kg. However, the lifetime remains limited due to the formation of many polysulfides (noted Li_2S_x $1 \leq x \leq 8$) during the sulfur reduction towards Li_2S which are dissolved in liquid electrolyte and diffuse between both electrodes, leading to a rapid decrease of electrochemical performances.

To reduce this polysulfide shuttle, solid electrolytes were employed as separator in our study. We considered two solid electrolytes as ceramics, $Li_{1,5}Al_{0,5}Ge_{1,5}(PO_4)_3$ (noted LAG) and $Li_{1,2}Zr_{1,9}Ca_{0,1}(PO_4)_3$ (noted LCZP), interesting because of their high ionic conductivity of $2{,}8x10^{-4}$ and $4{,}9x10^{-5}$ S.cm^{-1} at room temperature respectively. Two different shaping methods were used: Spark Plasma Sintering (or SPS) for dense pellets and tape-casting for thin ceramic membranes. The conduction properties as a function of synthesis and set-up parameters will be discussed and the use of these solid electrolytes in Li-S battery will be presented.

In parallel, we studied all-solid-state Li-S batteries in order to bypass the limitations of liquid electrolyte. The solid electrolyte is sandwiched between both positive and negative electrode. The positive electrode is a composite material with active material, solid electrolyte for ionic conduction and additive conductor for electronic conduction and the negative electrode is metallic lithium. In this condition, the solid electrolyte must be stable versus metallic lithium electrode and with the active material inside composite electrode. The two previous ceramics being not stable in contact with metallic lithium, we considered Argyrodite Li_6PS_5Cl as solid electrolyte.

The first assembled Li-S battery based on composite electrode, constituted by sulfur as active material, Argyrodite as solid electrolyte and ketjen black as additive conductor, displays an extra-capacity of 1800 mA.h.g^{-1} during ten cycles at current rate of C/20.

C2.60

Preparation and Properties of Lithium Conducting Membranes from Polymer-Brush Nanoparticles Ilya Zharov[1, 2]; [1]Chemistry, University of Utah, Salt Lake City, Utah, United States; [2]Materials Science and Engineering, University of Utah, Salt Lake City, Utah, United States.

We will describe a novel approach for the preparation of lithium conducting membranes using polymer brush nanoparticles (PBNPs). PBNPs can be assembled into the membranes directly, or the membranes can be prepared by first assembling porous scaffolds from unmodified NPs followed by surface modification with polymer brushes. In both cases, lithium-conducting channels are formed in the interstitial spaces between the nanoparticles.

First, lithium conducting membranes were prepared using 500 nm silica nanoparticles (SNPs) surface-grafted with PEO-containing polymer brushes, poly(ethylene glycol) monomethyl ether methacylate, PEGMA, and with poly(ethyl methacralyte), PEEMA, grown via surface initiated atom transfer radical polymerization (SI-ATRP). The membranes prepared from the NPs carrying longer polymer chains possessed polymer-like characteristics, compared to the stiffer membranes made with shorter polymer brushes. There materials showed high ionic conductivity and unusual conductivity temperature dependence. Specifically, their conductivity was relatively low (~0.8 mS/cm) at 4 °C, increased to ~2.5 mS/cm in the range of 40-80 °C and decreased to ~1.0 mS/cm around 100 °C. We attribute this behavior to the temperature-responsive properties of PEGMA and PEEM brushes.

Second, we prepared lithium conducting pore-filled membranes. In this case, nanoporous colloidal crystals were first assembled from unmodified SNPs, followed by filling the pores with PEGMA brushes covalently attached to the pore surface using SI-ATRP. We used two ethylene glycol monomethyl ether methacylate monomers, containing PEO side chains with 10 and 20 PEO units. The ionic conductivity of both resulting pore-filled membranes was high, and dependent on the molecular weight of the PEO used. The ionic conductivity of the membranes prepared using PEGMA-10 was 1.3 mS/cm, while that prepared using PEGMA-20 was lower, ~0.8 mS/cm, as expected based on Li^+ transport mechanism through solid polymer electrolytes.

We will discuss in detail the preparation and properties of the above membranes, as well as their applications in lithium ion batteries.

C2.61

Separators Based on Novel Triblock Polyelectrolyte for Lithium Battery: Improving Performance and Safety Kun-lin Liu and Chi-Yang Chao; Materials Science and Engineering, National Taiwan University, Taipei, Taiwan.

Solid state separators based on polymer electrolyte and polyelectrolyte exhibiting high ionic conductivity, high lithium transference number and mechanical durability are highly desired for next generation solid state lithium battery pursuing better safety. In this work, we designed and synthesized a series of novel triblock polyelectrolyte (TBPE) polystyrene-*block*-polyisoprene-*block*-poly(sulfonated isoprene) (SII) as well as prepared the corresponding separators. SII, featuring lithium sulfonates highly grafting onto the polymer backbone via flexible spacers in the sulfonated polyisoprene segment (sPI) serving as polyelectrolyte to assist lithium ion transport, were synthesized from anionic polymerization and the following analogous chemistry to allow accurate control on molecular architecture. SII exhibited reasonably good solubility in selected solvent combination, allowing the corresponding separators to be prepared via simple solvent casting with tunable processing parameters. By adjusting the molecular weight of each building segment and the separator preparation condition, the microstructure, the mechanical and the transport properties of the separator can be tailored. Morphologies including cylinders, bicontinuous network and lamellae were observed and the relationship between the morphology and the ionic conductivity were investigated. By increasing the length of the central flexible polyisoprene segment, the mechanical properties and the ionic conductivity of the separator could be improved. Remarkably, the maximum ion conductivity could reach $1.2\ x10^{-4}$ S cm^{-1} at ambient temperature with merely 20 wt% liquid electrolyte uptake, comparable with the separator based on mesoporous PE/PP membrane uptaking over than 200 wt% liquid electrolyte. The lithium transference number was as high as 0.86, demonstrating the single ion conductor characteristic of SII TBPE could effectively promote both ion conductivity and lithium ion transference number.

C2.62

Rechargeable Lithium Semi-Flow Battery Using $Li_7P_3S_{11}$ Rayavarapu Prasada Rao, Jia Ming Yuen and Stefan Adams; Materials Science & Eng., National University of Singapore, Singapore, Singapore.

Rechargeable batteries play a pivotal role in conversion of chemical energy to electrical energy and energy storage. Lithium batteries have been considered as promising power supply for various electric vehicles and grid storage systems. However, presently available lithium-ion technology cannot satisfy the increasing demand for energy density. Among the conceivable high energy systems based on lithium metal anodes, lithium–sulphur (Li–S) batteries appear to be particularly attractive candidates for next-generation high-energy density batteries. However, dissolution of polysulfide in liquid electrolytes, the formation of lithium dendrites are major impediment in realizing the potential of these batteries. To overcome these challenges here we demonstrate the use of fast-ion conducting solids as solid electrolytes in semi-flow Li-S batteries containing catholyte slurries.

Lithium conducting $Li_7P_3S_{11}$ was prepared using ball mill followed by annealing at 330°C. Rietveld refinements of compounds indicated that the product is $Li_7P_3S_{11}$ with space group *P*-1 and lattice parameters of *a*=12.420(3) Å, *b*=6.066(1) Å, *c*= 12.528(3) Å. $Li_7P_3S_{11}$ electrolyte prepared in the way described above exhibits an ionic conductivity of 7.4×10^{-4} S/cm at 30°C. The variation of ionic conductivity of the electrolyte with variation of pressure and temperature will be studied. We investigate the stability of these solid electrolytes in contact with catholytes consisting of polysulfide, Li_2S_8, dissolved in monoglyme. The Li_2S_8/Li_7P3S_{11}/Li semi-flow rechargeable battery exhibits an initial discharge specific capacity of 1450 mAh/g at 1C rate and of 1000 mAh/g after the 10th cycle. Thus with the help of such catholyte-compatible solid electrolyte membranes this rechargeable and easily scalable battery concept can be realized with high energy density and promising capacity retention.

C2.63

$Li_{10}SnP_2S_{12}$, an Electrolyte and Negative Electrode Material for Solid State Li-Ion Batteries? Ilyas Tarhouchi[3, 2], Virginie Viallet[1, 2], Philippe Vinatier[3, 2] and Michel Menetrier[3, 2];[1]LRCS - UMR CNRS 7314, Amiens, France; [2]Réseau sur le Stockage Electrochimique de l'Energie (RS2E), FR CNRS 3459, Amiens, France; [3]ICMCB - CNRS, Pessac, France.

$Li_{10}SnP_2S_{12}$, the tin analogue of the $Li_{10}GeP_2S_{12}$ superionic conductor is characterized and used in room-temperature solid-state cells. Rietveld refinement of capillary powder X-Ray diffractograms confirms that the material provided by NEI Corporation is mainly composed of $Li_{10}SnP_2S_{12}$ with the LGPS-type structure, with 6 weight % of Li_2SnS_3 impurity. ^{31}P MAS NMR detects Li_3PO_4 and Li_3PS_4-type additional impurities and reveals the actual composition of the LGPS-type phase to be $Li_{9.8}Sn_{0.8}P_{2.2}S_{12}$.

Very strong reactivity at low voltage and vs. Li metal is shown by impedance measurements using both Au and Li electrodes, as well as by 3-electrode cyclic voltammetry. Galvanostatic measurements confirm that $Li_{10}SnP_2S_{12}$ reacts with 8 lithium per mole below 0.5 V vs.Li^+/Li, most probably following a conversion/alloying process. Taking advantage of this reactivity, we prove the concept of a $LiCoO_2$/$Li_{10}SnP_2S_{12}$ cell, where the electrolyte also acts as negative electrode at the contact with the negative current collector. 0.5 Li can be deintercalated from $LiCoO_2$, although reversibility appears to be hampered by the conversion/alloying reaction in the solid state, at least with a non-optimized electrode formulation.

C2.64

Preparation and Electrochemical Studies on Fe-Doped $LiVPO_4F$ Cathode M.V. Reddy[1, 2], Rayavarapu Prasada Rao[1], Stefan Adams[1] and B.V.R. Chowdari[2]; [1]Materials Science & Eng., National University of Singapore, Singapore, Singapore; [2]Dep. of Physics, National University of Singapore, Singapore, Singapore.

Framework cathode materials based on the phosphate polyanion building blocks are increasingly regarded as favorable replacements for conventional oxide-based cathode materials in lithium-ion battery applications. The lithium insertion phases $LiFePO_4$ and $Li_3V_2(PO_4)_3$ were the first of such materials identified and characterized. Recently, few groups have described the insertion properties of the $LiVPO_4F$. To understand the effect of replacement of V with Fe, here we prepared Fe-doped $LiVPO_4F$ using carbothermal reduction method. We explored the temperature dependent structure variations and characteristics of Li^+ ion migration pathways in $LiVPO_4F$ and Fe-doped $LiVPO_4F$ using the bond valence (BV) approach and atomistic MD simulations.

Our Rietveld refinements of $LiVPO_4F$ in the temperature range revealed that $LiVPO_4F$ undergoes a second order phase transition at about T = 750 K from a triclinic phase to a monoclinic phase (*C*2/*c*). To emphasize the structural relationship between both phases the triclinic phase is described in the non-standard space group setting *C*-1 as common practice in the literature for transitions of related phases.
MD simulations of a 2048 atom supercell of the *C*-1 unit cell accordingly yield a monoclinic to triclinic phase transition, yet with a slightly lower transition temperature (ca. 700 K). The diffusion coefficient in the monoclinic high temperature phase is highest along channels extending along the z direction (with the lowest $E_A \approx 0.4$ eV), while the perpendicular directions exhibit somehwhat higher activation energies of about 0.75 eV or 0.9 eV and for T= 700 K show about 0.5 or 1 order of magnitude lower conductivity.

Charge–discharge cycling of $LiVPO_4F$ in the voltage range 3.0–4.5 V at a current rate of 15 mA/g (0.12 C) shows a reversible capacity of 130(±3) mAh g^{-1} in the range of 20–200 cycles and thereafter a slow capacity fading between 200 and 360 cycles. Fe-doped $LiVPO_4F$ exhibited a stable discharge capacity of 120 mAh/g at 30 mA/g (0.24 C) current after 45 cycles.

C2.65

Effect of Polysorbate Plasticizer on the Structural and Ion Conduction Properties of the Polyethylene oxide/NH_4PH_6 Solid Polymer Electrolyte Kuldeep Mishra[2], Saurabh S. Pundir[1] and D. K. Rai[1]; [1]Department of Physics & Materials Science & Engineering, Jaypee Institute of Information Technology University, Noida , Noida, India; [2]Department of Physics & Materials Science, Jaypee University, Anoopshahr, Bulandshahr, India.

Effect of polysorbate, as a new plasticizer, on the polyethylene oxide (PEO) – ammonium hexfluorophosphate (NH_4PF_6) polymer electrolyte system has been investigated using different structural and electrochemical techniques. A significant increase in the amorphicity of the solid polymer electrolyte has been observed on the introduction of plasticizer. The room temperature ionic conductivity pattern of the electrolyte system shows a regular pattern of enhancement in the conductivity with the increasing concentration of the plasticizer and jumps from ~ 10^{-7} Scm^{-1} to ~ 10^{-5} Scm^{-1}. The H^+ ion conduction in the electrolyte system has been confirmed by cyclic voltammetric analysis which reflects two distinct cathodic and anodic current peaks corresponding to the H^+ ion transport in the electrolyte. The loss tangent study shows that the plasticization establishes faster ion hopping in the electrolyte system. The frequency dependence of the conductivity has been found to obey the Jonscher's power law and slower backward ion hopping is observed on plasticization. The introduction of the plasticizer has not been found to affect the electrochemical stability window of the polymer electrlyte significantly.

SESSION C3: Solid Electrolyte I
C: Electrodes and Solid Electrolytes for Batteries
Chair: Diana Golodnitsky
Monday Afternoon, June 15, 2015
Keystone Resorts, Shavano Peak

2:30 PM *C3.01
Structure and Dynamics of Lithium Garnet Oxides Studied by Neutron Scattering and Molecular Dynamics Simulation Wei Lai[1], Yuxing Wang[1], Matthew Klenk[1] and Katharine Page[2]; [1]Michigan State University, East Lansing, Michigan, United States; [2]Oak Ridge National Lab, Oak Ridge, Tennessee, United States.

Lithium garnet oxides have become one of the most promising candidates as solid electrolytes for lithium-ion batteries, due to their high lithium ionic conductivity and wide electrochemical window. While most studies have been focused on different doping strategies to increase the conductivity values, mechanistic understanding of structure and dynamics of lithium ions in these complex materials remains limited. In this talk, we will present some of our recent results on two model materials in this garnet family: cubic disordered composition Li5La3Ta2O12 (LLT) and tetragonal ordered composition Li7La3Zr2O12 (LLZ), studied by neutron scattering and molecular dynamics simulation.

In lithium garnet oxides, there are two types of cages, i.e. tetrahedral (Td) and octahedral (Oh), to host lithium ions. These two cages are connected by triangular bottlenecks formed by three oxygen atoms. The application of Rietveld refinement and Reverse Monte Carlo analysis of neutron scattering data and molecular dynamics simulation allows us to study lithium distribution and dynamics within Td cages, Oh cages, and triangular bottlenecks. We found that lithium ions prefer to stay off-center inside both Td and Oh cages, due to the uneven Li-Li interaction of the nearest-neighbor lithium clusters. Our studies support that the lithium conduction path goes through the triangular bottleneck in a 3D continuous network of Td/Oh cages, without a direct Oh to Oh jump. However, the conduction mechanism should not be generalized as they are greatly influenced by the local environments or temperatures. Broadly speaking, lithium atoms hop through the bottleneck with an edge-passing mechanism for low symmetry clusters or at low temperatures, while they proceed with a center-passing mechanism for high symmetry clusters or at higher temperatures. For LLZ, the redistribution of lithium from one Td cage (8a), to another Td cage (16e), through one Oh cage (32g) drives the tetragonal to cubic phase transition.

2:50 PM C3.02
A Full Study of a Garnet Ceramic Electrolyte: From Atomistic Simulation to Actual Application in Rechargeable Lithium-Metal Batteries William Manalastas[1], Randy Jalem[2, 3], Frederic Aguesse[1], Lucienne Buannic[1], Juan Miguel Lopez del Amo[1], Carlos Bernuy-Lopez[1], Gurpreet Singh[1], Ainara Aguadero[4], Anna Llordes[1], Masanobu Nakayama[3] and John Kilner[4,1]; [1]Solid State Electrolytes Group, CIC Energigune, Miñano, Spain; [2]Unit of Element Strategy Initiative for Catalysts and Batteries, Kyoto University, Kyoto, Japan; [3]Department of Materials Science and Engineering, Nagoya Institute of Technology, Nagoya, Japan; [4]Department of Materials, Imperial College, London, United Kingdom.

Li-conducting ceramic membranes have the potential to address many problems faced in Li-ion batteries with the use of flammable organic electrolytes such as thermal runaway, Li-dendrite crossover, anode/cathode system incompatibility and scalability limitations. The key to a successful application of ceramic electrolytes lies in developing a dense material with high ionic conductivity and a broad spectrum of electrochemical stability (0V-5V vs Li). Disordered-lithium garnets such as the cubic-phase nominal $Li_7La_3Zr_2O_{12}$ composition (LLZrO, σ_{Li+} = 0.4 mS.cm^{-1} at 25ºC) are some of the most promising candidates; however further improvement in their ionic conductivity is still required for application.[1]

To this end, we used aliovalent substitutions to modulate the lithium carrier/vacancy populations, stabilize the room-temperature cubic phase and aid powder sintering. Most studies focus on La and Zr site substitutions to promote Li-ion hopping mechanisms, thereby avoiding obstruction of the lithium pathway, under ambient air-processing conditions.[2] In contrast we pursued Li-site substitution by Ga^{3+} substituents. Using ^{71}Ga MAS NMR, we confirmed preferential location of Ga^{3+} in Li-sites, which produces two lithium vacancies per substituent atom, pushes lithium into distorted octahedral sites and promotes disordered lithium. The ramifications from this, in terms of energetics, percolation pathways, and measured conductivities, towards superionic conductivity, are explainable from our molecular dynamics analyses.[3]

Additionally ultrafast ^{1}H and ^{7}Li MAS-NMR revealed increased Li-trapping with progressive proton contamination from atmospheric moisture.[4] The observation of $La_2Zr_2O_7$ pyrochlore formation with aging in ambient atmosphere also supports this finding indicating a slow atmospheric corrosion process. Working from this insight, we observed that the densification and diffusivity of lithium ions can be strongly improved in a dry environment rich in oxygen, under astringent CO_2 and H_2O control (<2 ppm). Room-temperature total conductivities reaching 1.5 mS cm^{-1} (>93% relative densities) corroborate our simulation predictions. The best materials were selected and incorporated in Li-metal battery devices; electrochemical measurements will be reported.

Acknowledgements
W.M., J.K., F.A., L.B. and M.H. would like to thank the Basque Government for the financial support through the ETORTEK (Energigune'13) Strategic Program.

References
[1] R Murugan, V Thangadurai, W Weppner, (2007) *Angew. Chem. Int. Ed.* 46, 7778-7781
[2] V Thangadurai, S Narayanan and D Pinzaru (2014) *Chem Soc Rev* 43, 4714-4727
[3] R Jalem, M Rushton, W Manalastas Jr, M Nakayama, T Kasuga, JA Kilner, and RW Grimes. *Submitted to Chem. Mater.*
[4] C Bernuy-Lopez, W Manalastas Jr., JM Lopez del Amo, A Aguadero, F Aguesse and JA Kilner, (2014) *Chemistry of Materials*, 26 - 12, pp. 3610 - 3617.

3:10 PM C3.03
Revealing Lithium Conduction Pathways in Lithium-Rich Garnets Using Aliovalent Dopants Rowena H. Brugge, Ainara Aguadero and John Kilner; Imperial College London, London, United Kingdom.

Lithium stuffed garnets such as $Li_7La_3Zr_2O_{12}$ (LLZO) show promise as solid state lithium ion conductors for use in high energy density storage applications due to their chemical and thermal stability and electrochemical performance versus current technology electrolytes. Much work has focused on improving the conductivity of these systems by optimizing the lithium content in the cubic garnet phase rather than the less conducting tetragonal polymorph.

Despite extensive studies on these materials, there is uncertainty as to the preferred migration of Li; whether the ions move from one octahedral (Oh) site to another via a neighbouring tetrahedron (Oh-Td-Oh path), or hop directly across Oh sites, bypassing the Td site (Oh-Oh path), is still up for debate.

We seek to confirm the lattice site occupancy of the mobile lithium ions and their associated conduction pathways by varying the lithium-substituted dopant species (Ga, Zn, Ge), thereby blocking Li movement through one of the two paths. The effect of dopant charge and ionic radius on cubic phase stabilization (as a result of Li concentration) and lattice strain is studied.

Moreover, the moisture sensitivity of Li-conductor ceramics has been recently associated with a deterioration of Li transport[1] and density of the material, of great importance in battery applications[2]. In this study, we use an argon-supplied glove box coupled to a furnace for processing and synthesis, preventing proton exchange with Li, thus avoiding the creation of proton charge carriers and improving the densification to above 90% relative density. This is fundamental to analyze the real Li-conduction mechanism and optimize the Li conductivity in garnets. To study the degradation process of lithium displacement by protons in moisture, and the effect of the protons on the ionic conductivity, we conduct isotopic exchange experiments on the samples using H2O and D2O followed by

secondary ion mass spectroscopy. The total conductivity of the samples is found by AC impedance in a range of humidities and temperatures. X-ray diffraction and neutron diffraction are employed to determine the structural features, specifically to localize the dopants, Li and protons and to analyse the conduction pathways as a function of the dopant.
[1] Aguesse, F. et al. (2014) Adv. Mater. Interfaces, 1 (7), 1300143
[2] Bernuy-Lopez, C. et al. (2014) Chem. Mater., 26 (12), 3610-3617

3:30 PM C3.04
Charge Transport Properties in the Li-Garnet $Li_{7-x}La_3Zr_{2-x}Te_xO_{12}$ System Michal Struzik, Reto Pfenninger and Jennifer L. Rupp; Department of Materials, ETH Zurich, Zurich, Switzerland.

All Solid State Lithium Ion Batteries are attractive alternative to capitalize on a wider range of electrode materials when compared to liquid based batteries. I.e. sulfur, lithium and many other electrodes of low stability with liquid based electrolytes may be used in combination with solid state electrolytes. Recently, cubic $Li_7La_3Zr_2O_{12}$ stabilized with Al attracted much attention due to their high ionic conductivity of 2×10^{-4} S·cm^{-1} and possibilities of doping on the -$M_3N_2O_{12}$ garnet framework structure. The high conductive cubic phase may be stabilized by doping on both, M and N sites of the garnet framework structure, thereby tuning the Li-ions concentration and mobility.

Through this work, we report on the N-site doped $Li_{7-x}La_3Zr_{2-x}Te_xO_{12}$ solid solutions for which we dope with tellurium in the range of 0.20 to 0.35 mol%. The particles were prepared by a solid state route. It is shown that doping with tellurium has a positive effect in stabilizing the desired cubic phase; XRD revealed cubic garnet structure in the Ia-3d symmetry group and near order structural oxygen anionic-cationic changes are discussed based on Raman vibrational modes. We report on sintering and employ electrochemical impedance spectroscopy to gain further insights on the role of tellurium doping on the Li-ionic transport via symmetric cells with blocking and reversible electrodes. Finally, we compare here synthesized tellurium-doped Li-garnet structures to the state-of-the-art garnet based electrolytes in the field and implicate their potential for application.

3:50 PM C3.05
Investigating the Effects of Al Doping on the Local and Average Structure of Al-LLZ Using Atomistic Simulations Matthew Klenk and Wei Lai; Chemical Engineering and Material Science, Michigan State University, East Lansing, Michigan, United States.

The ever increasing demand for high performance lithium-ion batteries to be used in safety critical applications such as electric vehicles has driven researchers to find new electrolyte materials which provide increased safety and stability over conventional liquid electrolyte systems. The fast ion conducting lithium garnet oxide family ($Li_{7-x}La_3Zr_{2-x}Ta_xO_{12}$, x=0-2) has been of particular interest as a suitable solid electrolyte to replace liquid systems due to its stability to lithium metal and high ionic conductivity which approaches 10^{-3} Scm^{-1}.

In this study, we performed energy minimization (GULP[1]) and molecular dynamic simulations (DLPOLY_Classic[2]) in order to investigate the role of aluminum in modifying the local arrangement of lithium in $Al_xLi_{7-3x}La_3Zr_2O_{12}$ (Al-LLZ) and inquire how aluminum stabilizes the cubic phase of $Li_7La_3Zr_3O_{12}$ (LLZ). This study expands upon our previous work with the model compositions $Li_5La_3Ta_2O_{12}$[3] (LLT) and LLZ[4] which were successful in replicating pair distribution (PDF), phase transformation, and conductivity values from experimental work.

Lithium has 16 possible local configurations in the garnet structure, but tetragonal LLZ only exhibits four types of lithium arrangements with lithium only on the 8a tetrahedral, 32g octahedral and 16f octahedral sites. Resulting in an ordered structure and cooperative diffusion. However, with sufficient thermal energy lithium will overcome the configurational entropy of LLZ resulting in disorder about lithium sites which in turn drives the phase transformation from tetragonal to cubic LLZ. Our simulations show that aluminum will preferentially occupy lithium tetrahedral sites in Al-LLZ. Aluminum introduces disorder in tetragonal LLZ by forcing lithium to the previously unoccupied 16e tetrahedral sites again leading to cubic LLZ.

References
[1] J.D. Gale; A.L. Rohl. Mol. Simul. 2003, 29, 291-341.
[2] Smith, W.; Forester, T. R. J. Mol. Graphics 1996, 14, 136−141.
[3] Wang; Klenk; Page; Lai. *Chem. Mater.*, **2014**, *26* (19), pp 5613–5624, **DOI:** 10.1021/cm502133c.
[4] Klenk; Lai. Phys. Chem. Chem. Phys.,2015, DOI: 10.1039/c4cp05690f.

4:10 PM C3.06
Influence of La Ordering in $Li_{3x}La_{2/3-x}TiO_3$ Epitaxial Films on Li-Ion Conduction Tsuyoshi Ohnishi, Kazutaka Mitsuishi, Kazunori Nishio and Kazunori Takada; National Institute for Materials Science, Tsukuba, Japan.

In this study, we have prepared epitaxial thin films of $Li_{3x}La_{2/3-x}TiO_3$ by means of pulsed laser deposition in order to investigate the relationship between Li-ion conduction and various types of domain boundaries. We have previously reported growth of epitaxial $Li_{3x}La_{2/3-x}TiO_3$ thin films [1,2] and found planar defects that draw Nazca lines on the film surface [2], although the Li-ion conductivity of those films was as low as the order of 10^{-5} S/cm [1]. A series of films obtained in this study have revealed that the thin film quality and Li-ion conductivity are highly sensitive to growth conditions as well as target composition. Here, we report strategies to increase the conductivity through the improvement of the film quality by careful composition control in the pulsed laser deposition process. The obtained epitaxial thin films are mostly *c*-axis oriented, containing a small amount of *a*-axis domains and anti-phase boundaries. The relationship between the domain boundary structure and Li-ion conductivity suggests that the *a*-axis domains and the anti-phase boundaries included in the films are not predominantly resistive against the ionic conduction [3].

[1] T. Ohnishi and K. Takada, Solid State Ionics **228** (2012) 80-82.
[2] K. Mitsuishi, T. Ohnishi, Y. Tanaka, K. Watanabe, I Sakaguchi, N. Ishida, M. Takeguchi, T. Ohno, D. Fujita, and K. Takada, Appl. Phys. Lett. **101** (2012) 073903.
[3] T. Ohnishi, K. Mitsuishi, K. Nishio, and K. Takada, Chem. Mater. (2015) in press, DOI: 10.1021/cm504033r

4:30 PM C3.07
Lithium Dendrite Growth in Hot Pressed Ta-Substituted $Li_7La_3Zr_2O_{12}$ Chih-Long Tsai[1], Vinodchandran Chandrasekharan Nair[2], Astrid Besmehn[3], Sven Uhlenbruck[1], Hans G. Gehrke[1], Thorsten Reppert[1], Paul Heitjans[2] and Olivier Guillon[1]; [1]Institut fuer Energie- und Klimaforschung: Werkstoffsynthese und Herstellungverfahren (IEK-1) , Forschungszentrum Juelich GmbH, Juelich, Germany; [2]Institut für Physikalische Chemie und Elektrochemie, Leibniz Universität Hannover , Hannover, Germany; [3]ZEA-3, Forschungszentrum Juelich GmbH, Juelich, Germany.

Lithium metal has the lowest native electrochemical potential, -3.4 V vs. H_2, and extremely high specific capacity, 3860 mA h/g, and low density, 0.59 g/cm^3. These properties make it an ideal anode for rechargeable batteries as well as for next generation Li-S and Li-air batteries. However, the use of metallic Li in a rechargeable battery is not succesful until now due to the difficulty of suppressing the growth of Li dendrite. Theoretical calculations suggest the dendrite can be suppressed if the used electrolyte has a shear modulus of more than twice that of the metallic Li, ~10^9 Pa, or a Li-ion transfer number t_{Li+} approaching 1. Therefore, the garnet structured $Li_7La_3Zr_2O_{12}$ (LLZ) solid state Li-ion conductor is an ideal material for preventing dendrite growth because of its unity ionic transfer number, high mechanical strength and chemically stability in contact with metallic Li.

However, Li dendrite formation was reported by Yamamoto et al[1]. from their Al-substituted LLZ and Ta-substituted LLZ with unclear reason. In this research, two samples which are Al contaminated and Al free Ta-substituted LLZ were fabricated by hot pressing. Both samples have relative densities >99% and total conductivities ~1 mS/cm at room temperature. During the dendrite studies, impedance measurements show rapid decrease in total resistances within a couple of hundred seconds which indicates the dendrite can be formed in such a high dense ceramic in a short time. Solid-State NMR shows metallic Li was found inside the dense pellet which was also supported by XPS. The dendrite test results and the possible reasons for the formation of the Li dendrite will be discussed in this presentation.

[1] J. Electrochem. Soc., 161 (2014) A668.

4:50 PM C3.08
Excellent Stability of a Solid Electrolyte upon Li^+/H^+ Exchange: A Discovery Resulting from Successfully Suppressing Electron Beam Damage Cheng Ma[1], Chengdu Liang[1], Jeffrey Sakamoto[2], Karren More[1] and Miaofang Chi[1]; [1]Center for Nanophase Materials Sciences, Oak Ridge National Laboratory, Oak Ridge, Tennessee, United States; [2]Department of Chemical Engineering and Materials Science, Michigan State University, East Lansing, Michigan, United States.

Batteries with aqueous catholyte and Li metal anode have attracted intensive research interests due to their exceptional energy density and high charge/discharge rate. The long-term operation of such batteries requires particular conditions for the solid electrolyte separator between the anode and aqueous solutions. In addition to the compatibility with Li, the separator must be stable over a wide pH range. Unfortunately, no such compound has yet been reported. In this study, the ion exchanging behavior of Li^+ and H^+ in the cubic $Li_7La_3Zr_2O_{12}$ garnet was investigated by combining high resolution Scanning Transmission Electron Microscopy (STEM) and Electron Energy Loss Spectroscopy (EELS). The ion exchange experiments were performed by immersing the TEM specimen in aqueous solutions with different pH values for 15 mins. Our results showed that LLZO experienced a significant while reversible Li^+/H^+exchange. The garnet crystalline framework remained stable even under a high exchange rate of 63.6%. After the protonated specimen was treated with the 2M LiOH solution, the ion exchange was reversed without any structural change. These observations suggest that cubic $Li_7La_3Zr_2O_{12}$ shows an excellent stability in neutral and strong basic solutions and is a promising candidate for the separator in aqueous lithium batteries.

SESSION C4: Interfaces in Batteries
C: Electrodes and Solid Electrolytes for Batteries
Chair: M. Stanley Whittingham
Monday Afternoon, June 15, 2015
Keystone Resorts, Quandary Peak I/II

2:30 PM *C4.01
Predicting Lithium Transport in Solid Electrolyte Interphases Yue Qi; Department of Chemical Engineering and Materials Science, Michigan State University, Lansing, Michigan, United States.

Improving Li transport and preventing electron leakage through the solid electrolyte interphase (SEI) are critical to capacity drop and power loss of Li-ion batteries. A multi-scale modeling approach was developed to predict ionic and electronic transport properties in components of SEI, as a necessary step to understand the functionality of SEI before tailoring its properties. First, dominant Li diffusion carriers and ionic conductivity in idealized SEI components (Li_2CO_3 and LiF) were predicted with density functional theory (DFT) over a broad voltage range of the electrode materials. Meso-scale Li^+ ion diffusion equations were then formulated based on the diffusion mechanisms discovered by DFT and the boundary conditions of isotope exchange experiments in order to make direct comparison with TOF-SIMS measurements. A new mechanism of electron leakage via Li_i^0 interstitials diffusion through SEI was also proposed. The methods employed in this study can be generalized to other ionic conducting materials.

2:50 PM C4.02
Theory of Space Charge Layers in Lithium All-Solid-State Batteries Arnulf Latz[1, 2, 3], Stefanie Braun[1, 2] and Chihiro Yada[4]; [1]German Aerospace center , Stuttgart, Germany;[2]Helmholtz Institute Ulm for Electrochemical Energy Storage, Ulm, Germany; [3]Institute for Electrochemistry, University of Ulm, Ulm, Germany; [4]Toyota Motor Europe NV/SA, Zaventem, Belgium.

One of the most severe problems in Lithium all solid state batteries is the as yet rather limited power density, which is mainly ascribed to a strongly increased interfacial resistance. The cause of this resistance is the formation of space-charge layers near the electrodes, which go along with very high electric fields. Understanding in detail the mechanisms and parameters involved in the space-charge-layer formation will be an important step towards improved solid-state systems with more favourable properties.

In this work, we propose a new mathematical model for ionic transport in a solid electrolyte, which is based on first principles only. We provide analytical and numerical solutions for a solid electrolyte in contact with electrodes and study the parametric dependencies of the cation and potential distributions under the influence of varying electrode potentials. We compare our results both with the predictions of classical Poisson-Nernst-Planck theory and with experimental results [1]. Estimates on the width of the different anodic and cathodic space charge regions are given as well as qualitative predictions on the behaviour of this region under different conditions. Consistent with experiments [2] we find that the space charge regions and thus the distribution of electric fields can be systematically modified by carefully choosing layers of materials with varying dielectric properties. Those modifications can potentially be used to decrease considerably interfacial resistances.

[1] K. Yamamoto, Y. Iriyama, T. Asaka, T. Hirayama, H. Fujita, C. a J. Fisher, et al., Dynamic visualization of the electric potential in an all-solid-state rechargeable lithium battery., Angew. Chem. Int. Ed. Engl. 49 (2010) 4414–7. doi:10.1002/anie.200907319.
[2] C. Yada, A. Ohmori, K. Ide, H. Yamasaki, T. Kato, T. Saito, et al., Dielectric modification of 5V-class cathodes for high-voltage all-solid-state lithium batteries, Adv. Energy Mater. 4 (2014) 1–5. doi:10.1002/aenm.201301416.

3:10 PM C4.03
Negligible "Negative Space-Charge Layer Effects" at LiPON/ $LiCoO_2$ Interfaces of Thin-Film Batteries Taro Hitosugi, Masakazu Haruta, Ryota Shimizu and Susumu Shiraki; Tohoku University, Sendai, Japan.

We report the *surprisingly low electrolyte/electrode interface resistance* of 8.6 Ωcm^2 observed in thin-film batteries.
This value is an order of magnitude smaller than that presented in previous reports on all-solid-state lithium batteries.
The value is also *smaller than that found in a liquid electrolyte based batteries*. The low interface resistance indicates that the negative space-charge layer effects at the $Li_3PO_{4-x}N_x/LiCoO_2$ interface are negligible, and demonstrates that it is possible to fabricate all-solid state batteries with faster charging/discharging properties.

3:30 PM C4.04
Lithium and Hydrogen Storage at Abrupt Junctions Lijun Fu, Chia-Chin Chen and Joachim Maier; Max Planck Institute for Solid State Research, Stuttgart, Germany.

Storage of lithium and hydrogen plays an important role in fuel cells and batteries. Besides searching for optimized storage materials, identifying storage mechanisms is of more fundamental interest and equal significance. In this contribution, we present a novel interfacial lithium and hydrogen storage mode: in a composite of two phases, such as $Ru:Li_2O$, although none of which can store lithium or hydrogen alone, Li or H can be dissociatively stored at interface, with Li^+ or H^+ accommodating at one phase and e^- or H^- (e^-) at another, for lithium and hydrogen storage, respectively[1, 2]. Both the thermodynamic modeling and experiments are applied for investigation. For both storage systems, the extracted parameters from experiments are in good agreement with the thermodynamic model. For lithium interfacial storage, the Nuclear Magnetic Resonance (NMR) and electrochemistry impedance spectra (EIS) results show that the side reactions are not the main contributions of the storage capacity in the interfacial storage voltage regime. For hydrogen interfacial storage, the thermodynamic study favors H^+/H^- over H^+/e^- mechanism.

References:
[1] J. Maier, Angew. Chem. Int. Ed., **52**, 4998 (2013)
[2] L.J. Fu, C.-C. Chen, D. Samuelis, J. Maier, Phys. Rev. Lett. **112**, 208301 (2014)

3:50 PM C4.05
Double Layer Formation and Energy Level Alignment at Li-Ion Electrode-Electrolyte Interfaces: Impact on Charge Transfer and Electrode Potential Rene Hausbrand, Andre Schwoebel, Wolfram Jaegermann, Mathias Fingerle and Ruben Precht; Institute of Materials Science, Darmstadt University of Technology, Darmstadt, Germany.

Electrode-electrolyte interfaces play a key role for the performance and degradation of electrochemical devices such as lithium-ion cells. Differences in ion chemical potential between electrode and electrolyte phase lead to the formation of double layers with impact on electrode potential and charge transfer. For ionic devices parasitic electron transfer results in side reactions and the formation of interlayers, generally adversely affecting cell performance. Key features of electrochemical interfaces are well demonstrated by energy level diagrams allowing conclusions with respect to thermodynamic and kinetic properties [1]. We perform ultra-high vacuum based model experiments on the formation and electronic structure of electrode-electrolyte interfaces [2]. Interfaces are formed stepwise by condensation or deposition of electrolyte phase on thin film electrodes (or vice versa) and analyzed with photoemission after each step in a quasi *in-situ* approach. Previously we reported first results on the interface formation of $LiCoO_2$ with organic solvent (DEC) and solid electrolyte (LiPON). We observed different phenomena such as diffuse double layer (space charge layer) formation in the $LiCoO_2$ and chemically modified electrolyte phases.

In this contribution, we present results on the LiPON-lithium interface [3] as well as additional data on the $LiCoO_2$-LiPON interface. We evaluate the energy level diagram of the full cell and discuss the impact on charge transfer as well as on the origin of the voltage. The results demonstrate the formation of both reaction- and diffuse double layer at the LiPON-lithium interface, contributing to Li-ion charge transfer resistance, and indicate that the ionic contribution to the cell voltage remains low.

[1] R. Hausbrand, Phys Status Solidi A, 211 (2014) p. 2049-2051.
[2] R. Hausbrand, D. Becker, and W. Jaegermann, Prog Solid State Chem (2014) (DOI: 10.1016/j.progsolidstchem.2014.04.010).
[3] A. Schwöbel, R. Hausbrand, and W. Jaegermann, Solid State Ionics (2014).

4:10 PM C4.06
Reduced Grain-Boundary Resistance of Oxide-Type Lithium Ion Conductors by Surface Coating Hirotoshi Yamada[1], Daisuke Tsunoe[2] and Shota Shiraishi[1]; [1]Graduate School of Engineering, Nagasaki University, Nagasaki, Japan; [2]Faculty of Engineering, Nagasaki University, Nagasaki, Japan.

Solid electrolytes have attracted interests not only for their scientific aspects but also for their possible application to all solid state electrochemical devices. Owing to many efforts of researchers to discover ionic conductors, various solid electrolytes have been developed. Among several types of solid electrolytes, lithium-ion conductors are intensively studied to be applied to all solid-state batteries (ASSB). As for oxide-type lithium-ion conductors, overall ionic conductivity is rather low due to large resistance at grain boundaries, even though their bulk conductivity is relatively high. Grain boundary resistance is usually decreased by high-temperature sintering processes, but high temperature processes may cause interphases between solid electrolytes and active materials of all solid-state batteries. In this study, we successfully decreased grain boundary resistance of oxide-type lithium ion conductors without high temperature processes.

Particles of well-known ionic conductors: a NASICON-type $Li_{1.3}Al_{0.3}Ti_{1.7}(PO_4)_3$ (LATP) and a garnet-type Al-doped $Li_7La_3Zr_2O_{12}$ (LLZ) were coated with a poor ionic conductor of Li_2SiO_3 (LSO). Homogeneous LSO layer was successfully prepared without change in the core solid electrolytes (LATP and LLZ) by a sol-gel method, which was confirmed by XRD, FE-SEM, EDS, and TEM. A.c. impedance was conducted for as-pressed pellets of LSO/LATP and LSO/LLZ nanocomosite powder without sintering. It was demonstrated that such surface coating with poor lithium-ion conductor (LSO) is effective to reduced grain-boundary resistance of high lithium-ion conductors (LATP and LLZ) by one order of magnitude. The phenomena may be explained with idea that lithium ions are depleted at solid electrolyte surfaces and the LSO layer suppresses the depletion layer in LATP or LLZ. The results suggest a novel strategy to reduce the grain-boundary resistance of solid electrolytes and to develop oxide-type ASSB.

4:30 PM C4.07
Investigation of Electrode-Electrolyte Interface in Bulk-Type All-Solid-State Lithium Batteries Using $LiCoO_2$ Particles Coated with Sulfide Solid Electrolyte Thin Films Yusuke Ito[1], Atsushi Sakuda[1], Takamasa Ohtomo[2], Akitoshi Hayashi[1] and Masahiro Tatsumisago[1]; [1]Department of Applied Chemistry, Osaka Prefecture University, Sakai, Japan; [2]Battery Research Division, Toyota Motor Corporation, Shizuoka, Japan.

All-solid-state lithium secondary batteries with nonflammable inorganic solid electrolytes have been widely studied as next generation batteries. Especially, bulk-type all-solid-state batteries, which use composite electrodes with a powder mixture of electrode active material and solid electrolyte, are anticipated for large-scale power storage systems such as electric vehicles. Coating solid electrolyte thin films directly on electrode materials is effective for bulk-type batteries with an ideal electrode-electrolyte interface. So far, we have reported to prepare amorphous Li_2S-P_2S_5 and Li_2S-GeS_2 thin films for surface-coating on $LiCoO_2$ particles by pulsed laser deposition (PLD). Highly ion-conductive solid electrolyte thin films are strongly demanded for further improving cell performances. We previously fabricated Li_2S-GeS_2-P_2S_5 thin film with an ionic conductivity of 1.1×10^{-4} S cm^{-1}, and the ionic conductivity was increased to 1.8×10^{-3} S cm^{-1} by a heat-treatment at 200 °C. In this study, we investigated charge-discharge performances and microstructural changes at the electrode-electrolyte interface in order to examine the influence of electrolyte-coating and the heat-treatment for $LiCoO_2$ particles on electrochemical performance of all-solid-state batteries.

The surface of $LiCoO_2$ particles were uniformly covered with Li_2S-GeS_2-P_2S_5 (SE) thin films. The thickness of SE-coating layer was estimated to be about 180 nm, corresponding to the amount of 3 wt% SE in the composite electrode. Bulk-type all-solid-state cells using SE-coated $LiCoO_2$ particles showed a larger capacity of 67 mAh g^{-1} in comparison with that using $LiCoO_2$ without SE-coating. On the other hand, the cell using SE-coated $LiCoO_2$ particles with the heat-treatment showed a larger capacity of 80 mAh g^{-1} and better cycle performance. As a result, the electrode-electrolyte interfacial resistance considerably decreased to 5.8 Ω cm^2. It was confirmed that a favorable interface between $LiCoO_2$ particles and SE-coating layer was retained after cycling tests from microstructural observations of the composite positive electrode using SE-coated $LiCoO_2$ particles with the heat-treatment.

4:50 PM C4.08
Probing Interfaces of Garnet Solid Electrolytes in Lithium Batteries Lei Cheng[1, 2], Guoying Chen[2] and Marca Doeff[2]; [1]Material Science and Engineering, University of California, Berkeley, Berkeley, California, United States; [2]Environmental Energy Technological Division, Lawrence Berkeley National Laboratory, Berkeley, California, United States.

Critical technical barriers for current battery technology involve ensuring safe operation of devices that can deliver both high energy and power densities with sufficiently long cycle lives. “Beyond Lithium-Ion” chemistries utilizing metallic lithium electrodes such as lithium/sulfur and lithium/air systems are promising because they have high theoretical specific energies but are plagued by safety concerns. The tendency for dendritic growth and mossy plating of lithium during prolonged cycling when conventional liquid or polymer electrolytes are used, is a formidable obstacle to their development. Solid ceramic electrolytes have been proposed as a possible solution for lithium metal systems. Cubic garnet phases such as $Li_7La_3Zr_2O_{12}$ (LLZO) are especially interesting because of their high ionic conductivities (>10^{-4} S/cm) and apparent resistance to reduction by metallic lithium [1]. However, it has proven very challenging to process LLZO to simultaneously achieve high ionic conductivity, good chemical stability, and, most importantly, low resistances at solid electrolyte/electrode interfaces.

We have found that formation of very thin layers of Li_2CO_3 on LLZO pellet surfaces due to air exposure [2] is responsible for the high interfacial impedances observed in Li/LLZO/Li cells. The area specific impedance

(ASR) is reduced by an order of magnitude when the Li_2CO_3 layer on the pellet surface is removed. Further insights into the evolution of interfacial local environment and crystal structures upon air exposure have been provided by grazing incidence Zr-K edge extend x-ray absorption fine structure spectroscopy (EXAFS) and x-ray diffraction (XRD). [3] We developed new processes to fabricate dense samples of different thicknesses with various interfacial microstructures; large-grained, small-grained, and hetero-structures [4, 5], thus allowing us to study the effect of microstructure on electrochemical properties of interface. Lower interfacial impedances are associated with smaller grain sizes, resulting in more stable DC cycling at higher critical current densities for Li/LLZO/Li symmetrical cells containing the small-grained materials. By tuning the microstructure and controlling the processing to avoid formation of Li_2CO_3, we have been able to achieve the lowest ASR (37 W-cm^2) ever reported for symmetrical Li/LLZO/Li cells.

1. R. Murugan, V. Thangadurai, and W. Weppner, *Angew. Chem.*, 119, 7925 (2007).
2. L.Cheng, E. J. Crumlin, W.Chen, R. Qiao, H. Hou, S. F. Lux, V. Zorba, R. Russo, R. Kostecki, Z. Liu, K. Persson, W. Yang, J. Cabana, T. Richardson, G. Chen, and M. Doeff, *Phys. Chem. Chem. Phys*., 34, 18294 (2014)
3. L. Cheng, E. J. Crumlin, A. Metha, R. Davis, G. Chen and M. Doeff, in prep
4. L. Cheng, J. Park, H. Hou, V. Zorba, G. Chen, T. J. Richardson, J. Cabana, R.E. Russo, and M. M. Doeff, *J. Mater. Chem. A*, 2, 172 (2014).
5. L. Cheng, W. Chen, M. Kunz, K. Persson, N. Tamura, G. Chen, and M. M. Doeff, *ACS Applied Mater. & Interfaces.*, DOI 10.1021/am508111r

SESSION C5: Metal-Air Batteries
C: Electrodes and Solid Electrolytes for Batteries
Chair: Yue Qi
Tuesday Morning, June 16, 2015
Keystone Resorts, Shavano Peak

10:30 AM **C5.01
Aprotic Sodium (And Li)-Oxygen Batteries Chun Xia, Robert Black, Russel Fernandes, Dipan Kundu, Brian Adams and Linda Nazar; Department of Chemistry, University of Waterloo, Waterloo, Ontario, Canada.

In the search for improved energy storage, rechargeable metal-oxygen batteries are very attractive owing to their reliance on molecular oxygen, which forms oxides on discharge that decompose reversibly on charge. Although much focus has been on aprotic Li-O_2 cells, the aprotic Na-O_2 system is of equal interest because of its better reversibility. This talk will provide an overview of our better understanding of both systems, based on characterization techniques including rotating ring disk electrode studies, surface spectroscopy, operando electrochemical mass spectrometry and ESR. I will present results on novel high surface area and conductive inorganic nanostructures as cathode hosts in A-O_2 cells that lower the charge overpotential as a direct consequence of suppressed cathode corrosion, along with presenting a novel redox mediator with highly favorable features for soluble oxidation catalysis in Li-O_2 cells. In particular, I will discuss the critical role and mechanism of oxygen reduction and oxygen evolution in the Na-O_2 system that is solely responsible for the growth and dissolution of micron-sized cubic NaO_2 crystals and for the reversible cell-capacity. This leads to a holistic, new understanding of the mechanism of Na-O_2 batteries, which further sheds light on Li-O_2 cells.

11:00 AM *C5.02
Hybrid Lithium-Air Batteries: Inexpensive Catalysts and Novel Cell Designs Arumugam Manthiram, Longjun Li and Siyang Liu; Materials Science and Engineering, University of Texas at Austin, Austin, Texas, United States.

Nonaqueous Li-air batteries are hampered by electrolyte decomposition, clogging of the air electrodes by insoluble discharge products, and contaminants in air. These problems could be overcome with hybrid Li-air batteries in which a solid electrolyte separates the lithium-metal anode in an aprotic electrolyte from the air electrode in an aqueous catholyte. However, there are several challeges that need to be overcome with the hybrid Li-air cells, *e.g.*, poor chemical stability and low ionic conductivity of the solid electrolyte and lack of affordable, efficient, durable oxygen reduction reaction (ORR) and oxygen evolution reaction (OER) catalysts. Much effort has been focused on developing bifunctionl catalysts to improve the efficiency and stability of hybrid Li-air batteries in recent years, but the cycle life is still limited. This presentation will focus on advanced cell configurations and development of inexpensive, high-performance catalysts for hybrid lithium-air batteries. Specifically, with a cell configuration in which the ORR and OER catalysts are decoupled, carbon-free oxide catalysts with high surface area such as $NiCo_2O_4$ and Co_3O_4 nanoflakes/nanowires grown onto a nickel foam serve as the OER electrode and hierarchical porous carbons with optimized nitrogen doping loaded onto a hydrophobic carbon-fiber paper serves as the ORR electrode. These cells offer performance superior to that of conventional cell configurations with conventional catalyts such as Pt/C and IrO_2. While the metal-free carbon-based ORR catalysts are cost-effective, the carbon-free OER catalysts eliminate the persistent problem of carbon corrosion at high charge voltages. Also, the synergistic effect between metal oxide and carbon substrate provides an efficient method to further enhance the catalytic activity. Finally, buffer catholytes with moderate pH values that avoid the corrosion of the solid electrolyte in highly alkaline or acidic solutions will also be presented. The ORR and OER catalysts developed also offer promise for other all-aqueous metal-air batteries.

11:20 AM *C5.03
Ionic Transport Issue in Solid Lithium Air Batteries Hao Zheng[1], Dongdong Xiao[2], Jiayue Peng[1], Jie Huang[1], Degang Xie[3], Xin Li[4], Penghan Lu[3], Yuecun Wang[3], Hangyu Xu[1], Xianlong Wei[4], Qing Chen[4], Zhiwei Shan[3], Lin Gu[2] and Hong Li[1]; [1]Renewable Energy Laboratory, Institute of Physics, Chinese Academy of Sciences, Beijing, China; [2]Laboratory for Advanced Materials, Institute of Physics, Beijing, China; [3]State Key Laboratory for Mechanical Behavior of Materials, Xi'an Jiaotong University, Xi'an, China; [4]Key Laboratory for the Physics and Chemistry of Nanodevices, Peking University, Beijing, China.

Rechargeable Li air battery has attracted wide attention due to its high theoretical gravimetric energy density. Operating the batteries in real air is desirable but there are still many challenges to be solved. In all types of Li-air batteries, one of the barriers is high charging overpotential, which is related to the decomposition of Li2O2 and Li2CO3. High charging overpotential leads to low energy efficiency and instability of materials in batteries. Several strategies have been purposed, such as using OER catalysts, introducing redox mediator in nonauqeous system, controlling the size and morphology of the ORR products as well as increasing operating temperature. Decomposing mechanism of solid Li2O2 and Li2CO3 at atomic and molecular level is still not clear. Charge transfer, transport of electrons, transport of lithium ions and oxygen anions, release of O2 and CO2 should be involved. In order to understand the complicated solid OER reaction, in situ SEM and TEM investigations on a Li/Li2O/carbon nanotube battery have been performed. Formation and decomposition of Li2O2 or Li2CO3 under O2 or CO2 atmosphere are recorded. Accordingly, transport behaviors and discharge and charge reaction mechanism in solid lithium air batteries are understood from the results.

11:40 AM C5.04
Inorganic-Organic Composite Membranes for Aqueous Li-Air Batteries Dorsasadat Safanama, Zhen Feng Yow, Hu Yan, Daniel H. Chua and Stefan Adams; Materials Science & Eng., National University of Singapore, Singapore, Singapore.

Novel high efficiency grid-scale high energy density storage systems, such as rechargeable Li-air batteries (LABs), are urgently needed to enable and manage a wide-spread utilization of renewable energy sources. Among these LABs offer the highest gravimetric energy density, but subtypes employing organic electrolytes suffer from limited cyclability and poor energy efficiency due to the high over-potential during charge and discharge. LABs relying on aqueous catholytes promise somewhat lower theoretical capacity but a higher potential to reach the respective theoretical limits in practical devices. In aqueous LABs catholytes with high solubility for the discharge product enhance the cycle efficiency and power performance.

The fast ion-conducting electrolyte membrane is the key component of an aqueous Li-air battery, as it protects the lithium anode from chemical reaction with the catholyte solution. Here, inorganic-organic hybrid membranes based on NASICON-type $Li_{1.5}Al_{0.5}Ge_{1.5}(PO_4)_3$ (LAGP) or doped $Li_{7-x}La_3Zr_{2-y}M_yO_{12}$ (LLZ, M=Ta,Nb) ceramics and PEO:PVDF:$LiBF_4$ with a thickness of ca. 100 µm are designed and tested inside an aqueous LAB. By varying the mass fraction of the ceramic and polymer constituents mechanical properties and ionic conductivity of the membrane were optimized yielding total conductivities of 5×10^{-4} S cm^{-1} for the NASICON-based membranes. For the LLZ-based membranes a proton-for Li exchange leads to substantial structural changes unless the LiOH concentration is sufficiently high. Slight reductions of the Li content in contact with weakly alkaline catholytes stabilize the cubic phase and our molecular dynamics simulations clarify that the Lithium ion mobility is hardly affected by the partial H^+/Li^+ exchange.

The membrane in Li-air cell also has to be stable in contact with the lithium anode. Cyclic voltammetry of the membranes up to 4 V vs. Li/Li^+ shows only two distinct peaks of cathodic deposition and anodic dissolution of the anode, confirming the wide electrochemical window of the membranes. To identify a suitable solid electrolyte:catholye couple, the membranes were immersed in typical aqueous catholytes incl. 5M LiOH , and acidified 10M LiCl monitoring changes in the structure and conductivity. For the latter catholyte geometry and XRD pattern of the membrane are almost identical before and after immersion for 20 days, while the conductivity of the membrane increases with immersion time.

The performance of the membranes is tested in aqueous and hybrid Lithium air batteries using the same range of aqueous catholytes. To enhance charge transfer at the Li/solid electrolyte interface, the anode chamber in hybrid cells is additionally filled with $LiPF_6$ in EC/DMC electrolyte. Oxygen reduction/evolution at the air cathode is catalyzed through finely dispersed Pt on multi-walled carbon nanotube arrays. Cells are tested in the voltage range 2-4.5V under constant current of 20µA at room temperature in ambient air. LABs with capacities of up to 500mAh/g of carbon have been cycled with flat potentials. When each cycle is limited to 40 minutes the hybrid cell with a LAGP-based membrane retains its charge and discharge capacity for 140 cycles with <0.1V polarization between charge/discharge for the first 70 cycles. Thereafter the overpotential of open-air cells employing LiOH increases by Li_2CO_3 deposition as confirmed by ex situ X-ray diffraction. Performance enhancement can thus be expected from extracting CO_2 from the supplied air and by maintaining a temperature gradient between catholyte reservoir and cell. For LABs employing acidified catholytes, the gradually rising Li/solid electrolyte interfacial impedance limits the cycle life, so membrane coatings promise cycle life enhancements.

SESSION C6: Solid Electrolyte II
C: Electrodes and Solid Electrolytes for Batteries
Chair: Yan Yu
Tuesday Afternoon, June 16, 2015
Keystone Resorts, Shavano Peak

1:30 PM *C6.01
Confined-in-Ceramic Solid Polymer Electrolyte for Microbattery Application Diana Golodnitsky[1], Raymond Blanga[1], Yevgeny Rakita[2] and Amir Natan[2]; [1]School of Chemistry, Tel Aviv University, Tel Aviv, Israel; [2]Engineering Department, Tel Aviv University, Tel Aviv, Israel.

Our mobile society relies heavily on portable energy sources, a fact which drives improvements in battery technology. Although lithium-ion batteries offer the highest energy density among present commercial rechargeable batteries, the technology is still evolving and improving. Improvements are particularly important for wireless network systems and implantable devices, which require rechargeable microbatteries with dimensions on the scale of 1–10mm^3, high energy-density storage and high power capability. 3D concentric on-Si-chip architecture developed by our group, enables the fabrication of 10,000-30,000 microbattery units connected in parallel which minimizes the ion-path length between the electrodes and provides high capacity per footprint area. This is achieved by the insertion of thin films of active battery materials in the high-aspect-ratio microchannels of the perforated Si chip, glass or polymer substrate. Special attention is paid to the electrolyte, since it must have fast ionic transport through inherent ion-conducting pathways and electrochemical compatibility with anode and cathode materials.

In this work, we report on recent achievements in the development of thin-film confined-in-ceramic solid polymer electrolytes for application in 3D-battery configurations by electrophoretic deposition (EPD) combined with mechanochemistry. We tested the electrophoretic co-deposition of several types of ceramics and polymers. In order to gain a phenomenological understanding of the EPD process for a system of charged colloidal particles covered with a polyelectrolyte (PE), we developed a model for the electric potential on the basis of the Poisson-Boltzmann (PB) relation. We simulate a set of scenarios in an attempt to present the influence of pH, surface potential, PE density, and PE brush length on the electric-potential and charge-distribution profiles as a function of distance from the solid-surface/brush interface. TGA-IR, XRD, TOFSIMS, ESEM and AC-impedance tests were used for the characterization of the films. We found that the relative content of polymer and ceramics in the film depends on the type of solvent and composition of the suspension. The room-temperature ionic conductivity of confined-in-ceramic solid polymer composites prepared by electrophoretic deposition, followed by impregnation with $Li(CF_3SO_3)_2N$ and LiI salts, was 0.3 and 0.5mS/cm, respectively. The membrane follows the complex 3D contours of the electrodes conformally and provides strong mechanical integrity of the microbattery.

1:50 PM C6.02
Extremely Mobile Ions in Solid Electrolytes as Seen by NMR Martin Wilkening; Institute for Chemistry and Technology of Materials, Graz University of Technology, Graz, Austria.

The thorough characterization of electrochemically stable solid electrolytes is indispensable for the development of safe all-solid-state batteries. Over the last years much progress has been achieved and a number of candidates with extremely good ionic conductivities comparable to those of liquid electrolytes have been presented.
So far, Li ion diffusivities of some of the most promising solid electrolytes have already been characterized by nuclear magnetic resonance (NMR), particularly with the help of spin-lattice relaxation (SLR) techniques being able to probe both long-range and short-range ion dynamics over a dynamic range spanning many orders of magnitude. Since no post-preparation of the powder samples is needed, NMR provides a non-destructive and unmediated access to bulk parameters such as absolute jump rates and activation energies of the underlying elementary hopping processes.

Recent studies took advantage of both ^7Li and ^6Li SLR NMR partly performed down to cryogenic temperatures. For example, Li-bearing sulfides (*e.g.*, $Li_7P_3S_{11}$) and garnet-type oxides represent solid electrolytes with very fast lithium ion movements. Li-argyrodites have attracted special attention [1,2]. In particular, Li^+ diffusivity in argyrodite-type Li_6PS_5Br turned out to be outstanding [1]: well below room temperature (263 K) the diffusion-induced SLR NMR rate peaks reveal jump rates in the order of $10^9\,s^{-1}$ corresponding to diffusion coefficients in the order of $7.6\times10^{-8}\,cm^2\,s^{-1}$. This translates into ion conductivities as high as 10 mS cm^{-1} comparable to liquid-like behaviour. Such values are fully consistent with activation energies of ca. 0.20 eV, see Ref. [1].

[1] V. Epp, Ö. Gün, H.-J. Deiseroth, M. Wilkening, J. Phys. Chem. Lett., 4 (2013) 2118.
[2] V. Epp, Ö. Gün, H.-J. Deiseroth, M. Wilkening, Phys. Chem. Chem. Phys., 15 (2013) 7123.

2:10 PM C6.03
High Ionic Conductivity in the System $Na_{3+x}Sc_2(SiO_4)_x(PO_4)_{3-x}$ Marie Guin[1], Kaustubh Bhat[2], Frank Tietz[1] and Olivier Guillon[1,3]; [1]Forschungszentrum Jülich GmbH, Institute of Energy and Climate Research (IEK-1), Jülich, Germany; [2]Forschungszentrum Jülich GmbH, Peter-Grünberg-Institute (PGI-1), Jülich, Germany; [3]Jülich Aachen Research Alliance, JARA-Energy, Aachen, Germany.

The abundance of sodium and the similarities between lithium and sodium intercalation processes make it an attractive alternative as a charge carrier in alkali ion-batteries. Therefore, interest in high sodium ion-conductive materials is increasing, especially in the widely studied class of NASICON solid electrolytes [1].

A literature survey concluded that the partial substitution of phosphorus with silicon in the NASICON materials of general formula $Na_{1+2w+x-y+z}M^{(II)}_wM^{(III)}_xM^{(V)}_yM^{(IV)}_{2-w-x-y}(SiO_4)_z(PO_4)_{3-z}$ enhances the ionic conductivity [2]. The aim of this work is to elucidate the impact of introducing silicon ions in the highly conductive material $Na_3Sc_2(PO_4)_3$ [3] (σ_{Na}=3.8·10^{-5} S·cm^{-1} at 30 °C) and to obtain an even better ionic conductor suitable as electrolyte in a solid state sodium battery.

Various compositions of the solid solution $Na_{3+x}Sc_2(SiO_4)_x(PO_4)_{3-x}$ with 0.1≤x≤0.8 were synthesized by solid state reaction and crystallographic data were gathered, correlated with results of ionic conductivity measurements and compared simulation models. As a result, one of the 10 best ion-conductive NASICON materials to date was obtained for x=0.4 (σ_{Na}=8.3·10^{-4} S·cm^{-1} at 30 °C).

Furthermore, the ionic conductivity data were correlated with the structural bottleneck along the conduction pathway of the sodium ions and agrees well with the conductivity-structure-relationship established for the series $Na_{1+x+y}Zr_{2-x}Sc_x(SiO_4)_y(PO_4)_{3-y}$ [2,4]. Besides, different ionic pathways of the sodium ions in the structure were studied with density functional theory (DFT) [5] and the nudged elastic band (NEB) method [6] and the resulting activation energies were compared with the experimental values.

[1] H.Y.P. Hong, Mat. Res. Bull. 11 (1976) 173-182
[2] M. Guin, F. Tietz, J.Power Sources 273 (2015) 1056-1064.
[3] J.M. Winaud, A. Rulmont, P. Tarte, J.Mater. Sci. 25 (1990) 4008-4013
[4] M.A. Subramanian, P.R. Rudolf, A. Clearfield, J.Solid State Chem. 60 (1985) 172-181.
[5] P.E. Blöchl, Phys. Rev. B 50 (1994) 17953-17979
[6] G. Henkelman, B.P. Uberuaga, H. Jónsson, J.Chem. Phys. 113 (2000) 9901-9904

2:30 PM C6.04
Very High Li-Ion Conductivity in $Li_{1.5}Al_{0.5}Ti_{1.5}(PO_4)_3$ Prepared by a Novel Sol-Gel Method Qianli Ma[1,2], Chih-Long Tsai[1,2], Qi Xu[1,2], Frank Tietz[1,2] and Olivier Guillon[1,2];[1]Forschungszentrum Jülich, Jülich, Germany; [2]Jülich Aachen Research Alliance, JARA-Energy, Jülich, Germany.

Al-substituted lithium titanium phosphates (LATP) were widely investigated as promising candidates as solid electrolyte in lithium batteries, because of their high ion-conductivity, mechanical strength and chemical stability in ambient atmosphere. Major challenges are faced during the fabrication of LATP materials. Usually expensive devices and complicated methods, like pressure-assisted sintering, have to be used to prepare dense and phase-pure LATP samples. In this study, $Li_{1.5}Al_{0.5}Ti_{1.5}(PO_4)_3$ powders were easily prepared in kg-level and at low cost by a novel sol-gel method with high phase purity, densification activity and conductivity. After sintering at 900 °C, the relative density of $Li_{1.5}Al_{0.5}Ti_{1.5}(PO_4)_3$ samples reached 99%. Because of the thermal expansion anisotropy of the materials, micro-cracks also appeared at the same time. Higher sintering temperatures led to accelerated grain growth and larger cracks. At 25 °C in ambient air the conductivity of $Li_{1.5}Al_{0.5}Ti_{1.5}(PO_4)_3$ is higher than 1 × 10^{-3} S/cm, which is among the highest value of reported data. However, conductivity of the same sample tested in dry Ar is only 5 × 10^{-4} S/cm. Immediately after immersing the sample into water for 2 h, the measured conductivity strongly increased to almost 3 × 10^{-3} S/cm. According to the impedance spectra, the difference mainly results from the grain boundaries. It is assumed that the higher conductivity in moisture-containing conditions arises from proton exchange or formation of conductive Li salts at the grain boundaries. Therefore the true conductivity data of the samples should be tested under dry conditions. The temperature dependence of the conductivity of $Li_{1.5}Al_{0.5}Ti_{1.5}(PO_4)_3$ gives a straight line with the activation energy of 0.34 eV, whereas the measurement in humid atmosphere shows a strongly bent temperature dependence .

2:50 PM C6.05
Structural and Fast-Ion Conduction Properties of Solid Electrolytes within the Li_4SiO_4- Li_3PO_4 System Yue Deng[1], Chris Eames[2], Jean-Noël Chotard[1], Christian Masquelier[1] and Saiful Islam[2]; [1]Laboratoire de Réactivité et Chimie des Solides, Université de Picardie Jules Verne, Amiens, France; [2]Department of Chemistry, University of Bath, Bath, United Kingdom.

The revolution in portable electronic devices has been powered by rechargeable lithium-ion batteries. Batteries with liquid electrolytes, however, have severe safety issues and all-solid-state batteries with inorganic electrolytes may be regarded as a safer long term solution. The search for solid electrolytes that are chemically stable and have a high ionic conductivity is vital for solid-state batteries. Among potential candidates, solid solution compositions between Li_4SiO_4 and Li_3PO_4 exhibit high ionic conductivity (above 10^{-3} S/cm at 573K for $Li_{3.5}Si_{0.5}P_{0.5}O_4$) and large enhancement compared to the two end members.

Here we investigate the structural and lithium-ion transport properties of these materials by combining experimental and computer modeling techniques.

High purity samples have been synthesized and further investigated by various diffraction (single crystal, powder X-ray, powder neutron) techniques. An immiscibility zone has been found for (1-*z*) Li_4SiO_4 – *z* Li_3PO_4 compositions around 0.35 < *z* < 0.45. Lower *z* compositions can be indexed in Li_4SiO_4-like structures while higher *z* compositions are γ–Li_3PO_4 like. The crystal structures of the mixed compositions $Li_{3.5}Si_{0.5}P_{0.5}O_4$ and $Li_{3.25}Si_{0.25}P_{0.75}O_4$ have been determined for the first time, and can be described as isolated SiO_4 and PO_4 tetrahedra with dispersed distributions of lithium ions. Both AC impedance and MD simulated results show three orders of magnitude higher ionic conductivities (10^{-3} S/cm at 573K) in the mixed compositions than those of the end members. The MD simulations reveal 3D Li^+-conduction pathways and a cooperative knock-on type mechanism of interstitial lithium in the mixed compositions, which are not found in the end members.

These insights from a combined structural, conductivity and simulation study are valuable in developing strategies for optimizing novel polyanion-type solid electrolytes.

3:30 PM C6.06
Investigation of Electrolyte-Electrolyte Interface in All-Solid-State Metal-Metal Battery Ruigang Zhang[1], Timothy S. Arthur[1], Donovan N. Leonard[2], Miaofang Chi[2] and Fuminori Mizuno[1]; [1]Toyota Technical Center, Ann Arbor, Michigan, United States; [2]Oak Ridge National Lab, Oak Ridge, Tennessee, United States.

All-solid-state batteries are attracting significant interest for their potential to go beyond state-of-the-art Li-ion battery technology. The solid-state batteries could offer higher energy density, because the solid electrolyte eliminates electrolyte leakage enabling novel configurations such as bipolar stacking leading to less dead space. To enhance the energy density of solid-state batteries, both a high capacity and low working voltage anode must be coupled with a high capacity and high working voltage cathode. A Li metal anode is the ultimate goal, because it has a high theoretical capacity (3861 mAh/g, 2061 mAh/cc) and low working voltage. At the same time, the solid electrolytes are expected to suppress Li dendrite growth, which is familiar with Li anode as well as graphite anode operated severely. On the other hand, the research on cathode materials is still mainly focused on traditional intercalation type materials, such as $LiCoO_2$. Not only limited theoretical capacity of such cathode materials but also poor availability of the materials in bulk scale restrict the further enhancement of solid-state batteries in terms of energy density. We propose a novel solid-state battery system, which is called all-solid-state metal-metal battery. Concretely, Li and Ag metals were used as anode and cathode, respectively. Then, Li-ion conducting and Ag-ion conducting solid electrolytes were inserted separately between Li anode and Ag cathode, forming four solid layers in the solid-state cells. In this presentation, mechanically milled $75Li_2S{\cdot}25P_2S_5$ (mol%, LPS) and $70Ag_2S{\cdot}30P_2S_5$ (mol%, APS) were used as the solid state electrolytes. The prototype cell showed a flat discharge plateau around 2.0 V and was

repeatedly rechargeable with a capacity limitation. However, the discharge-charge performances were gradually deteriorated and finally failed to cycle. In order to clarify the fading mechanism, we focus on the interface between APS and LPS which is very unique in the solid-state cell. The dissimilar interface formed by two different solid electrolytes was intensively characterized by Electrochemical impedance spectroscopy (EIS), X-ray diffraction (XRD), X-ray photoelectron spectroscopy (XPS), Raman spectroscopy, Scanning electron microscopy (SEM) equipped with Energy dispersive X-ray spectroscopy (EDS) and Transmission electron microscopy (TEM) equipped with Electron energy-loss spectroscopy (EELS). From these analyses, we will discuss the charge transfer and ion diffusion/migration at the LPS/APS dissimilar interface. This study will provide a promising route to design new types of solid-state batteries.

3:50 PM C6.07
An All-Solid State NASICON Sodium Battery Operating at 200°C Fabien Lalere[1, 2], Jean-Bernard Leriche[1, 2], Mattieu Courty[1, 2], Sylvain Boulineau[1, 2], Virginie Viallet[1, 2], Christian Masquelier[1, 2] and Vincent Seznec[1, 2]; [1]Laboratoire de Réactivité et Chimie des Solides, Amiens, France; [2]Réseau de Stockage Electrochimique de l'Energie, Amiens, France.

Na-ion batteries have attracted recent interest and start now to be counted as viable alternatives vs. Li-ion technologies for specific applications [1, 2] . Safety issues related to the use of flammable liquid electrolytes remain, especially due to the high reactivity of sodium with moisture and oxygen. All-solid state batteries, which use non-flammable solid electrolytes, are considered as strong candidates for alternative energy storage devices. Following a recent successful approach developed for Li-ion all-solid state batteries [3, 4], we were able to assemble a monolithic all-solid state Na-ion battery using NASICON-based electrodes and electrolyte using the SPS technique. $Na_3V_2(PO_4)_3$ was used as both positive (V^{4+}/V^{3+} couple) and negative (V^{3+}/V^{2+}), $Na_3Zr_2Si_2PO_{12}$ was used as the solid electrolyte. Both compositions present order-disorder phase transitions and ionic conductivities of 1.5 $x10^{-3}$ S/cm and 1.9 $x10^{-4}$ S/cm at 200°C, for $Na_3Zr_2Si_2PO_{12}$ and $Na_3V_2(PO_4)_3$, respectively. Thanks to a new experimental set-up, we report on the electrochemical characteristics of an all-solid state Na-ion battery at temperatures as high as 200°C [5]. The battery operates at 1.8 V with 85% of the theoretical capacity at C/10 rate with good capacity retention, for an overall energy density of 1.87 $x10^{-3}$W.h/cm^2 and a capacity of 1.04 mA.h/cm^2. Recent advances in powder engineering and electrode formulations will be presented.

References
[1] B. E. Ellis et al., *Current opinion in Solid State and Materials Science* 16 (2012) 168–177
[2] V. Palomares et al. *Energy Environ. Sci*., 2012, 5, 5884-5901
[3] A. Aboulaich et al., *Advanced Energy Materials*, 1 (2011) 179-183.
[4] G. Delaizir et al. *Advanced Functional Materials*, 22 (2012) 2140-2147.
[5] F. Lalère et al. *J. Power Sources*, 247 (2014) 975-980.

4:10 PM C6.08
Assessment of Solid Electrolytes for All-Solid-State Lithium Batteries Philipp Braun, Moses Ender, Joerg Illig and Ellen Ivers-Tiffee; Institute for Applied Materials (IAM-WET), Karlsruhe Institute of Technology (KIT), Karlsruhe, Germany.

All-solid-state lithium batteries (SLIBs) are considered as promising next generation energy storage system for electric vehicles [1]. However, as this application needs low internal cell resistance even at high charging/discharging currents, a meaningful selection of materials and material combinations is absolutely essential. Commonly known prerequisites are (i) high ionic conductivity of the solid electrolyte and (ii) low charge transfer resistance at the electrode/electrolyte interface.
This study aims on guidelines for selecting solid electrolytes and their electrode interfaces, and on determining targets for further material development. A newly developed one-dimensional model for SLIBs is presented, based on a design concept with composite electrodes. The expected performance is simulated by linking two phase transmission line models for both composite electrodes [2] with an ohmic resistance for the solid electrolyte. Variations of (i) electrical parameters, i.e. ionic and electronic conductivity, (ii) electrochemical parameters, i.e. charge transfer resistance, and, (iii) microstructure parameters, i.e. phase tortuosity and composite electrode thickness, indicate the most important material and design parameters for high-performance. Performance potential will be presented for various anorganic solid electrolytes, i.e., glassy types (Phosphates, Oxides and Sulfides ($Li_7P_3S_{11}$)) and crystalline types (LISICON, Garnets ($Li_7La_3Zr_2O_{12}$), Perovskites ($Li_{3x}La_{2/3-x}TiO_3$)).

References:
[1] A. L. Robinson and J. Janek, *Solid-state batteries enter EV fray*, MRS Bulletin, 39, pp 1046-1047, **(2014)**
[2] J. Illig et al., *Modelling Graphite Anodes with Serial and Transmission Line Models*, Journal of Power Sources **(2015)**, doi:10.1016/j.jpowsour.2015.02.038.

4:30 PM C6.09
Solid Electrolytes in Batteries Dominik A. Weber[1], Stefan Berendts[2], Joachim Sann[1], Martin Busche[1], Sebastian Wenzel[1] and Juergen Janek[1]; [1]Physikalisch-Chemisches Institut, Justus-Liebig-Universität Gießen, Gießen, Germany; [2]Institut für Chemie, Technische Universität Berlin, Berlin, Germany.

For reasons of ultimate safety and long term stability, the solidification of batteries has recently become a topic of growing interest. Aiming at maximized energy densities, the preparation of thick film solid state batteries with a lithium metal anode is worthwhile, but bears a number of crucial challenges. In this contribution, a critical review on factors determining the performance of thick film SSB and statements on the minimum requirements, these systems have to fulfill, will be given. The discussion will clarify the fact that high conductivity of the solid electrolyte alone will not be the main determinant in the development of large scale solid state batteries. In fact, most state-of-the-art solid electrolytes present serious drawbacks: Li-ion conductivity in garnet-type[1] materials is highly dependent on the microstructure, as will be shown by experiments on charge transport in the materials and charge transfer along the interface between a Li metal electrode and the electrolyte. Interface kinetics will be highlighted in terms of mechanical degradation of the electrode and the formation of constriction resistances. Furthermore, solid electrolytes like "LiPON"[2] and NASICON-type materials are known to be electrochemically unstable in contact with Li metal. The concept of electronically and ionically mixed conducting interphases (MCI)[3] that form at the interface between metal and electrolyte, leading to the degradation of the latter, will be introduced. In addition, a simple approach for the preliminary determination of the likelihood for the degradation of a particular material, based on thermodynamic data, and a concept for its protection will be presented.

[1] Thangadurai, V.; Weppner, W. *J. Am. Ceram. Soc.* 2005, 88, 411.
[2] Schwöbel, A.; Hausbrand, R.; Jaegermann, W. *Solid State Ionics* , 2.
[3] Hartmann, P.; Leichtweiss, T.; Busche, M. R.; Schneider, M.; Reich, M.; Sann, J.; Adelhelm, P.;Janek, J. *J. Phys. Chem. C* , *117*, 21064.

4:50 PM C6.10
Safety Assessment of All-Solid-State Lithium-Ion Polymer Battery Using Forced Destruction System Yo Kobayashi, Kumi Shono, Takeshi Kobayashi and Hajime Miyashiro; Central Research Institute of Electric Power Industry, Tokyo, Japan.

Safety is more important than high energy density in stationary batteries. Safety assessments of lithium-ion cells have been estimated by the judgment of the possibility of explosion and/or ignition of the tested cells. However, existing judgment of the safety is based on the qualitative assessment so that quantitative evaluation approach is required. We developed a forced destruction system in which pressure change in event can quantitatively estimate using a pressure tight housing surrounding the test cell. We report the comparative results of the nail penetration test between conventional lithium-ion cell using organic liquid electrolyte and our developed all-solid-state lithium ion polymer battery. In both systems, we prepared the same active materials ($LiNi_{1/3}Mn_{1/3}Co_{1/3}O_2$ cathode and graphite anode). In the liquid electrolyte system, we used 1M $LiPF_6$ in EC/DMC=1/1 solution. By contrast, in the polymer system, we used polyether-based dry polymer electrolyte provided from DAISO. In the abuse condition of SOC 120% at 343 K, the surface temperature of the liquid electrolyte system (13 Wh) reached 523 K at the rate of 100 K/sec.

The gas evolution in the event was 7 liter. On the other hand, the temperature increase of the polymer system (12 Wh) in the same abuse condition was within 5 K, and no gas evolution was observed. These results suggested that the dry polymer electrolyte played a significant contribution of the improvement of the safety in the condition. We believe that the proposed forced destruction system will provide the important role for the development of various all-solid-state batteries to evaluate the intrinsic safety of the system.

SESSION C7: Characterization of Nanoscale and Local Structures I
C: Electrodes and Solid Electrolytes for Batteries
Chair: Wei Lai
Tuesday Afternoon, June 16, 2015
Keystone Resorts, Quandary Peak I/II

3:30 PM C7.01
Soft X-Ray Absorption Spectroscopy Studies on $LiNi_{0.5}Mn_{1.5}O_4$ Spinel Ruimin Qiao[1], Jung-Hyun Kim[2], Nicholas P. Pieczonka[3], Andrew Wray[4] and Wanli Yang[1]; [1]Advanced Light Source, Lawrence Berkeley National Lab, Berkeley, California, United States; [2]Chemical & Materials Systems Laboratory, General Motors Global R&D Center, Warren, Michigan, United States; [3]Optimal CAE Inc, Plymouth, Michigan, United States; [4]Department of Physics, New York University, New York, New York, United States.

Batteries are powered by the redox reactions of the electrode materials, which typically involve transition metal compounds. Their electrochemical properties are closely related with the half-filled 3*d* states of the transition metal. Soft x-ray absorption spectroscopy is able to directly probe the transition metal 3*d* states. $LiNi_{0.5}Mn_{1.5}O_4$ spinel is a promising candidate as a high voltage electrode in next generation Li-ion batteries for electric vehicle applications due to its high operating voltage of ~4.7 V (vs. Li/Li^+) and high rate performance. Over the last decade, a number of research groups have devoted their resources to understand and optimize the electrochemical properties of the material. Here we performed comprehensive soft x-ray absorption spectroscopy studies on $LiNi_{0.5}Mn_{1.5}O_4$ electrodes at different states of charge. The high resolution spectra demonstrate the transition between Ni^{2+}/Ni^{3+} to Ni^{3+}/Ni^{4+} redox couples at half-charge and provide us the direct evidence on the two single-electron-transfer reactions. An electrochemically inactive Ni^{2+} phase is observed on the electrode surface, which associates with the cycling stability. Moreover, we are able to visualize the energy positions of the empty 3*d* states of Ni^{4+}, Mn^{4+} and the substituted Ti^{4+} in the spinel structures, which regulate the electrochemical reaction of the material.

3:50 PM C7.02
Electronic Origin of the Step-Like Character of the Discharge Curve for Na_xCoO_{2-y} Cathode Janina Molenda; AGH University of Science and Technology, Krakow, Poland.

We focus mostly on first principles calculations of Na_xCoO_{2-y} cathode material emphasizing the interplay between a remarkable effect of oxygen vacancy on DOS and relative occupancy of sodium sites, where electron correlations are described in the framework of the LDA approach. We have used spin-polarized Korringa-Kohn-Rostoker (KKR) [1] method combined with the coherent potential approximation (CPA) [2], which allows to account for chemical disorder (vacancy defects) both on alkaline and O sites. We suppose that the remarkable interplay between the variation of the *z* parameter (O positional parameter in the unit cell) and the strong redistribution of electronic states in the vicinity of the Fermi level (presumably responsible for decrease or increase of the total energy of the system), appears to be a driving force of the observed sharp variation of chemical potential of electrons (E_F) and transport properties. Performed comprehensive studies [3, 4] of the structural, transport and electronic specific heat properties of Na_xCoO_{2-y} cathode material in the characteristic points of the discharge curve i.e. on the pseudo-plateaus and on the potential jumps, show non-monotonous variations of its transport properties (metallic/semiconducting/metallic/semiconducting/metallic) during sodium intercalation, which indicate that the density of states at the Fermi level is anomalously (either finite or vanishing). We concluded that this unusual electronic structure behaviour leads to an abrupt changes in the position of E_F, reaching the oxygen-defect DOS peaks during intercalation and finally resulting in step-like character of the discharge curve of $Na/Na^+/Na_xCoO_{2-y}$ cell.

This work was supported by NCN grant no. NCN 2011/02/A/ST5/00447.

1. S. Bei der Kellen et al., Phys. Rev. B 51 (1995) 9560
2. J. Tobola et al., J. Electron. Mater. 39 (2010) 2064
3. J. Molenda et al., Phys. Chem. Chem. Phys. 16 (2014) 14845
4. J. Molenda et. al., Funct. Mater. Lett. 7 (2014) 1440009

4:10 PM C7.03
In Situ TEM of Lithiation-Induced Displacement Reactions in Individual Copper Sulfide Nanocrystals Matthew McDowell[1] and Yi Cui[2]; [1]Chemistry and Chemical Engineering, California Institute of Technology, Pasadena, California, United States; [2]Materials Science and Engineering, Stanford University, Stanford, California, United States.

The transport of ions within electrode materials often determines the rate capability and reversibility of battery systems; thus, understanding correlated mass transport and phase transformations in novel battery materials is of utmost importance to guide development. Here, in situ transmission electron microscopy (TEM) is employed to observe the reaction of lithium with individual Cu_2S nanocrystals, offering an atomic-scale view of the unique displacement reaction that occurs during the conversion of Cu_2S to Li_2S. The results show that as Li^+ions are inserted into the Cu_2S lattice, highly mobile Cu^+ ions are removed from the crystal and are deposited externally as Cu metal. The transformation is complete when the Cu^+ is completely replaced by Li^+, leaving a Li_2S crystal in contact with a newly grown Cu metal domain. The final Li_2S crystals were observed to have nearly the same size and shape as the original Cu_2S crystals. This is because of the considerable structural similarities between the two phases: the hexagonal close packed (HCP) sulfur sublattice of Cu_2S shifts to a face centered cubic (FCC) sublattice in Li_2S with only small changes (<2%) in spacing between close packed planes. High-resolution imaging of the dynamic reaction process showed that the sublattice shift was induced by the local concentration of Li^+, not by a coordinated shear process. Finally, transformation of interconnected Cu_2S nanocrystal arrays resulted in the striking growth of larger Cu metal dendrites due to diffusion of Cu^+ through connected nanocrystals and the subsequent deposition as Cu metal at a single location. These results, along with comparison to different reaction mechanisms in other metal sulfides (Co_3S_4 and FeS_2), indicate that the extrusion of Cu metal through the displacement reaction mechanism is enabled by the structural similarities between the initial and final phases, as well as by the high mobility of Cu^+ ions within the Cu_2S lattice. Furthermore, the observations show that the final morphology of the reacted material (Li_2S + Cu) is strongly dependent on the initial arrangement of particles, which has significant ramifications for the design of reversible battery electrode architectures featuring metal sulfides.

4:30 PM C7.04
Atomic-Scale Recognition of Structure and Intercalation Mechanism of MoS_2 and Ti_3C_2X Xuefeng Wang, Xi Shen, Yurui Gao, Zhaoxiang Wang, Richeng Yu and Liquan Chen; Institute of Physics, Chinese Academy of Sciences, Beijing, China.

Two-dimensional (2D) materials have been extensively exploited and shown great potential in various applications. Their distinctive electronic and chemical properties are closely related to the structure and intercalation chemistry. Herein, the structure and the intercalation mechanism of MoS_2 and Ti_3C_2X are clarified by aberration-corrected scanning transmission electron microscope (STEM). Both materials show excellent rate performance and long-term cycling stability as anode materials for sodium (Na) ion batteries. Our findings enrich the understanding of the 2D materials and shed light on the future material design and applications.

MoS_2 stands for a typical transition-metal dichalcogenide. The controversial phase transition from semiconductive 2H to metallic 1T phase and the occupancy of the intercalated Na in $MoS_2$are clarified at the atomic scale. Further, a series of other complicated phase transitions along with lattice distortion, structural modulation, and even irreversible

structural decomposition are recognized in MoS_2 depending on the content of Na ion intercalation. It is shown for the first time that x = 1.5 in Na_xMoS_2 is a critical point for the reversibility of the structural evolution. MXenes represent a large family of functionalized 2D transition-metal carbides and carbonitrides. However, most of the understandings on their unique structures and applications are stopped at the theoretical suggestion and lack of experimental support. Herein, the STEM studies show that the surface functional groups (*e.g.* OH-, F-, O-) and the intercalated Na ions prefer to stay on the top sites of the centro-Ti atoms and the C atoms of the Ti_3C_2 monolayer, respectively. Double Na-atomic layers are found within the Ti_3C_2X interlayer upon extensive Na intercalation *via* two-phase transition and solid-solution reactions. In addition, aluminum (Al)-ion intercalation leads to horizontal sliding of the Ti_3C_2X monolayer. Density functional theory (DFT) calculations using the modified modeling help to understand more about their physical and chemical properties.

4:50 PM C7.05
Phase Evolution in Single-Crystalline $LiFePo_4$ in a Micrometer-Sized Battery Followed by *In Situ* Scanning Transmission X-Ray Microscopy Nils Ohmer[1], Bernhard Fenk[1], Dominik Samuelis[1], Chia-Chin Chen[1], Joachim Maier[1], Markus Weigand[2], Eberhard Goering[2] and Gisela Schuetz[2]; [1]Max Planck Institute for Solid State Research, Stuttgart, Germany;[2]Max Planck Institute for Intelligent Systems, Stuttgart, Germany.

$LiFePO_4$ (LFP) is one of the most important and most frequently studied materials for Li-based batteries. Nevertheless, there is still an extensive debate on the mechanism of the phase transformation to $FePO_4$ (FP). On the one hand this is due to the lack of *in situ* observations with appreciable space and time resolution, while on the other hand this is due to the undefined state of the defect chemistry of most of the studied LFP materials. But it is the defect chemistry allowing to draw general conclusions for an overall understanding of the materials behaviour. We use oriented $LiFePO_4$ single crystals, which have previously been carefully characterized and their defect chemistry analyzed, to deposit a solid electrolyte layer (LiF) and a layer of aluminum, functioning as anode material, on top. Using a focused ion beam inside a scanning electron microscope (FIB/SEM) we fabricate out of this layered structure a micrometer-sized all-solid-state thin film battery with attached platinum current collectors. The oriented LFP single crystal cathode has a size of 16 x 1 x 0.2 micrometer (**c** x **b** x **a** direction). Here we present scanning transmission X-ray microscopy (STXM) measurements following in situ the phase evolution within the $LiFePO_4$ single crystal cathode along the (010) orientation during electrochemical lithiation/delithiation with a lateral resolution of 30 nm and with minutes of time resolution [1]. Our results disclose the influence of the defect chemistry, in terms of ionic and electronic conductivities, as well as elastic effects on the (de)lithiation process.

References
1. N. Ohmer et al., Nature Communications 6, 6045 (2015).

5:10 PM C7.06
Investigating Transient and Persistent Chemical Heterogeneity in $Li[Ni_{1/3}Co_{1/3}Mn_{1/3}]O_2$ Secondary Particles Using Transmission X-Ray Microscopy William Gent[1], Yiyang Li[1], Johanna Weker[2], Anna Wise[2], David Mueller[1] and William Chueh[1]; [1]Stanford University, Stanford, California, United States; [2]SLAC National Laboratory, Stanford, California, United States.

Heterogeneities in lithium ion battery electrodes are significant factors affecting battery performance. At high rates of charge and discharge, solid solution electrodes will exhibit a lithium concentration gradient to drive lithium diffusion in the solid, resulting in increased over potential and reduced cycling efficiency. It is typically assumed that this concentration gradient disappears at sufficiently low currents. In this work we investigated the mechanisms of lithium diffusion and relaxation in the $Li[Ni_{1/3}Co_{1/3}Mn_{1/3}]O_2$ (NMC) solid solution electrode using a suite of hard X-ray imaging techniques. Using transmission X-ray microscopy (TXM) at the Ni K edge, we probed the local state-of-charge of the ~10um NMC secondary particles *ex situ* at 30nm resolution. We observed a residual concentration gradient within the particles harvested at intermediate states-of-charge that was present several days after current was stopped and that was independent of charge rate. We have conducted *ex situ* TXM tomography on the secondary particles to gain insight into the relationship between the residual concentration gradient and morphological features. We have also performed *operando* TXM at the Ni K edge to reveal the mechanism of redistribution from the transient lithium concentration gradient during charge to that in the quasi-relaxed state once current is stopped. Being able to understand and control these heterogeneities will allow for the design of more efficient battery electrodes.

SESSION C8: Poster Session II
C: Electrodes and Solid Electrolytes for Batteries
Tuesday Afternoon, June 16, 2015
5:20 PM
Keystone Resorts, Red Cloud Peak

C8.01
Structural and Electronic Properties of Na2MnPO4F as a Cathode Material for Na-Ion Batteries Yin Zheng, Rao Huang, Yuhua Wen and Zizhong Zhu; Xiamen University, Xiamen, China.

Initial research on rechargeable Na-ion batteries could trace back to the later 1970s. In the past decade, there has been a resurgence of research interests in Na-ion battery electrode materials due to their lower cost comparing with Li-ion based ones. Among them, the fluorophosphates group Na_2MPO_4F (M=Mn, Fe, Co, Ni, etc.) has received considerable attentions because of its possibility of utilizing two sodium ions per transition metal ion during charging/discharging process, which could ultimately lead to higher specific capacities and energy densities. Recently, a new type of polyanion-based cathode material for rechargeable Na-ion batteries, based on Na_2MnPO_4F, has been proposed in order to enhance the discharge voltage and the energy density. In our work, the structural and electronic properties of crystalline Na_xMnPO_4F (x=2.0, 1.5, 1.0, 0.0) have been investigated by employing density functional theory (DFT) within the GGA+U framework. Two energetically stable intermediate phases, *i.e.*, $Na_{1.5}MnPO_4F$ and $NaMnPO_4F$ have been discovered. Their electrochemical properties, together with those of fully Na extracted product $MnPO_4F$, have been examined for analysis of the Na-ion intercalation/deintercalation process. Furthermore, the average deintercalation voltages have been calculated. A comparison of the results with available theoretical and experimental results has also been presented.

C8.02
Investigation of Capacity Fading of Li-Rich Layer-Structured Cathode Materials Kuan-Zong Fung[2, 1], Shu-Yi Tsai[1, 2], Chung-Ta Ni[1, 2] and Wei-Zhi Lin[1, 2]; [1]Materials Science and Engineering, National Cheng Kung University, Tainan City, Taiwan; [2]Research Center for Energy Technology and Strategy, National Cheng Kung University, Tainan City, Taiwan.

Li-rich layer-structured cathode materials formulated as xLi_2MnO_3 -(1 x) $LiMO_2$ (M = Mn, Ni, Co, etc.) have received much attention due to their surprisingly high reversible capacity for Li-ion battery applications. For the understanding of these materials, a systematic study on complicated crystal structures and reaction mechanisms during electrochemical charge/discharge cycles is employed.

Although Li-rich layer-structured cathode material show a reversible capacity as high as 250 mAh/g at low rate, its electrochemical properties such as capacity loss at first cycle, rate capability and capacity fading still need to be improved. The TEM structural analysis shows that the evidence of spinel phase after cycling. It is believed that the transition from layered structure to spinel structure may induce a large lattice distortion resulting in lattice breakdown and capacity. In additions, the phase transition is caused by the redox reaction of transition metal ions through charging/discharging tests. Thus, the cycling behavior of Li-rich layer-structured oxides is studied by changing the oxidation state of transition metal ions in the layered structures. XRD, SEM, TEM will be used for characterization of cycled cathode materials.

C8.03

Improvement of Cycling Performance of $LiMn_{1.5}Ni_{0.5}O_4$ Cathodes by Surface Treatment with Trimethyl Phosphite Vapor Ryosuke Okamoto[1], Kazuhiko Okubo[1], Mitsukuni Kondo[2] and Yoshiyuki Abe[1]; [1]Ichikawa Research Laboratories, Sumitomo Metal Mining Co., Ltd., Ichikawa-City, Japan; [2]Battery Research Laboratories, Sumitomo Metal Mining Co., Ltd., Niihama-city, Japan.

Active cathode materials of $LiMn_{1.5}Ni_{0.5}O_4$ (LMN) for high voltage lithium ion batteries were prepared and their surface was treated with trimethyl phosphite (TMP) vapor. Analysis of XPS revealed that the surface of treated LMN powders contained phosphorus. Using the LMN as the cathode and the carbon as the anode, coin-cells were assembled to evaluate the electrochemical properties. The treatment with TMP unaffected initial charge/discharge capacity, while it improved the cycling performance; the discharge capacity retention of the battery using the treated LMN sample showed 10 percent larger than that using the untreated sample after the cycling test for 200 cycles at 60 °C. Analysis of anodes of the batteries after the cycling test showed that the TMP treatment effectively diminished the amount of manganese metal and nickel metal moved from the cathode to the anode during the cycling test. The improvement of the cycling performance by the TMP treatment was due to the decrease in the dissolved metals from the LMN. The phosphorus in the surface of LMN had a role to prevent the metal dissolution into the electrolyte.

C8.04

Synthesis of Nanostructured $Li_3M_2(PO_4)_2F_3$ Glass-Ceramics (M = V, Fe, Ti) Tomasz K. Pietrzak, Przemyslaw P. Michalski, Agata Dorau, Anna Kaleta, Agnieszka Starobrat, Jakub Plachta, Marek Wasiucionek and Jerzy E. Garbarczyk; Physics, Warsaw University of Technology, Warszawa, Poland.

Lithium/sodium transition metal phosphates, including $Li_3V_2(PO_4)_3$ and $Na_3V_2(PO_4)_2F_3$, belong to interesting cathode materials for lithium/sodium ion batteries, mainly due to their high theoretical capacity (~190 mAh/g) and reversibility. In our recent papers we have shown that glassy analogs of some cathode materials exhibit significantly increased electric conductivity when subject to appropriate thermal treatment. This phenomenon was ascribed to the appearance of densely packed nanograins (sub-100 nm).

In this research, we have attempted to synthesize amorphous analogs of $Li_3M_2(PO_4)_2F_3$ (M = V, Fe, Ti), including such compositions as e.g. $Li_3FeV(PO_4)_2F_3$. After pre-heating at 200°C, the initial powders were melted at 1300°C for ca. 30 minutes using a double crucible technique. Then they were poured onto a stainless steel plate and pressed with another plate (melt quenching technique). This simple and time-efficient technology was successful in many compositions, with the exception of those with high Fe content. The structure and electrical and thermal properties of the batches are discussed with respect to transition metal used in composition.

The structure of as-received materials was investigated by X-ray diffractometry (XRD). Thermal events taking place in samples upon heating (e.g. glass transition and crystallization) were observed by differential thermal analysis (DTA) at different heating rates (from 1 to 40°C/min). Activation energies of glass transition and crystallization (in amorphous batches) were calculated using a Kissinger formula.

Electric conductivity was determined by impedance spectroscopy (IS) during heating and subsequent cooling ramps. An irreversible and significant change in the conductivity occurred at temperature range well correlated with that of the crystallization peak observed in DTA traces . The conductivity of best-conducting samples was as high as 10^{-3} S/cm. The grain size in selected samples was determined from SEM micrographs and XRD patterns (Scherrer formula).

C8.05

Lithium/Polymer Electrolyte Interface Stabilization by In Situ and Ex Situ Formation of Protective Surface Layers Nassus Brown and Dale Teeters; Chemistry and Biochemistry, The University of Tulsa, Tulsa, Oklahoma, United States.

Novel methods of stabilizing the interface of PEO polymer electrolytes, using either of two techniques, will be discussed. In one technique, film stabilization agents are “bloomed” to the surface of the electrolyte during film formation. In the second, a “hybrid” polymer electrolyte film was fabricated. This method utilizes a wax additive having a general chemical formula of $H\text{-}(CH_2)_{32}\text{-}(CH_2\text{-}CH_2\text{-}O)_{10}\text{-}H$ that can be positioned at the polymer electrolyte surface. In the blooming process, the hydrocarbon tails of the wax preferentially occupy the polymer surface and align making crystalline regions. AFM studies have shown that the hydrocarbon regions are arranged in “island” configurations with uncovered PEO surrounding the hydrocarbon areas. Long-term stability studies show that this surface, when in contact with lithium metal, stabilizes the lithium/polymer electrolyte interface. The second method of interface stabilization uses a hybrid film fabricated by making a thin layer of the wax materials by solvent casting and then casting a second layer of PEO polymer electrolyte on the wax film. This wax layer adheres to the polymer electrolyte surface, making a stabilized interface. Techniques have been developed to “tailor” the two sides of a polymer electrolyte film so stability for a lithium anode is maximized on one side of the film while at the same time having a different surface structure for the stabilization of the cathode on the opposite side of the film. The addition of wax, by the blooming method or by formation of a hybrid film, increases the apparent bulk ion conduction. The stabilization of the lithium/polymer electrolyte interface and the increase in ionic conduction has been studied by using ac impedance spectroscopy, AFM phase imaging and attenuated total reflection IR (ATR-FTIR) spectroscopy. The mechanism for stabilization and increased ionic conduction will be discussed.

C8.06

Development of Na_3PS_4-Based Sulfide Electrolytes for All-Solid-State Batteries Masahiro Tatsumisago[1] and Akitoshi Hayashi[1, 2]; [1]Department of Applied Chemistry, Osaka Prefecture University, Sakai, Osaka, Japan; [2]ESICB, Kyoto Univ., Kyoto, Japan.

Rechargeable sodium batteries attract much attention because of several advantages of using ubiquitous Na sources and having high energy density. All-solid-state rechargeable batteries with inorganic solid electrolytes have potential merits of high safety and long cycle life. Bulk-type solid-state batteries using electrode and electrolyte particles are suitable for application to large-sized batteries in eco-cars and distributed power sources. Sodium-ion conducting oxide electrolytes such as *b*-alumina and NASICON crystals are known to have high conductivity of over 10^{-3} S cm^{-1} at room temperature in sintered body. However, their conductivity drastically decreased in pelletized specimens prepared by compressing electrolyte powders because tremendous grain-boundary resistance appears for the specimens without heat-treatment. Sulfide solid electrolytes essentially have good formability; for example, grain boundaries in Li_3PS_4 sulfide glass electrolyte almost vanished by cold pressing. However, Na^+ ion conducting sulfide electrolytes with high conductivity have not been reported. Recently, we have prepared the cubic Na_3PS_4 electrolyte by crystallization of the Na_3PS_4 glass, and it showed a conductivity of over 10^{-4} S cm^{-1} at 25°C. All-solid-state Sodium Na-Sn/Na_3PS_4/TiS_x cells fabricated by cold-pressing without high-temperature sintering operated as a secondary battery at 25°C. Enhancement of ionic conductivity of sulfide electrolytes contributes to improving cell performance. Partial substitution of Si for P in cubic Na_3PS_4 increased conductivity up to $7.4\text{x}10^{-4}$ S cm^{-1} and the addition of interstitial Na^+ ions in the Na_3PS_4-Na_4SiS_4 solid solutions brought about high conductivity. In this study, preparation of Na_3PS_4-based sulfide electrolytes with high conductivity by partial elemental substitution will be discussed.

References: A. Hayashi *et al.*, *Nat. Commun.*, 3 (2012) 856; M. Tatsumisago and A. Hayashi, Int. J. Appl. Glass Sci., 5 (2014) 226.

Acknowledgement: a part of this work was performed under a management of ‘Elements Strategy Initiative for Catalysts & Batteries (ESICB)’ supported by MEXT, Japan.

C8.07

Development of Solid Electrolyte Membranes Aude A. Hubaud[1], David Schroeder[2, 1], Brian Ingram[1] and John Vaughey[1]; [1]Argonne National Laboratory, Argonne, Illinois, United States; [2]Northern Illinois University, Dekalb, Illinois, United States.

The recent years have seen the emergence of new solid electrolyte materials that exhibit ionic conductivities comparable to liquid systems used in Li-ion batteries. One of the most studied has been the lithium lanthanum zirconium oxide garnet $Li_7La_3Zr_2O_{12}$ (LLZ). Its high conductivity and its stability against lithium make it a promising electrolyte candidate for lithium metal-based batteries including lithium-sulfur or lithium-oxygen. Depending on the end use, areal capacities requirements range from 2 to 8 mAh/cm^2, which correspond for a solid electrolyte such as LLZ to thickness values from 20 to 60 µm. To achieve those values, our approach is to develop a supported thin film of the solid electrolyte LLZ. A thin robust electrolyte membrane would provide physical strength to the cell as well as the thickness required to achieve energy densities goals.

C8.08

Reactions at Silicon Electrode Surfaces Fulya Dogan[1], Aude Hubaud[1], Zhenzhen Yang[1], Danielle Proffit[1], David Schroeder[2] and Jack Vaughey[1]; [1]Chemical Sciences and Engineering, Argonne National Laboratory, Lemont, Illinois, United States; [2]College of Engineering and Engineering Technology, Northern Illinois University, DeKalb, Illinois, United States.

Knowledge of how silicon interacts with lithium electrochemically is only the first step to solving the problem of making practical silicon anodes for lithium-ion batteries. Incorporating silicon into a real electrode involves not just compensating for its large volume expansion but also understanding how the passivation surface interacts within the battery environment (e.g. first cycle irreversible capacity, cycling efficiency), how it interacts with the current collector during electrode formation (% utilization), and how simple processing changes surface functionality (binder stability and capacity fade). In this work we will be discussing how the reactiivity of silica and lithium silicates at the surface of a LIB silicon electrode affects the electrochemical properties. Using a combination of XPS, ^{29}Si NMR, ^{7}Li NMR, and EIS, we have identified several condensation reactions that occur at the surface of the electrode after first charge that gradually alter the interface with the electrolyte to reduce the ionic conductiity and impede electrode performance. Additionally, EQCM studies of Si and Si/SiO_2 thin film electrodes have been studied to assess the effect of this surface reactivity on the electrolyte and electrolyte additives. Work with fluoroethylene carbonate (FEC) has shown that it forms a denser SEI film at the electrode surface, consistent with the calcualtions of Balbuena, et al., than other common cylic or aliphatic carbonate solvents.

C8.09

Oxygen Nonstoichiometry and Charge Transfer in the Double Perovskites $Gd_{1-x}La_xBaCo_2O_{6-\delta}$ (x=0-1) Dmitry Malyshkin, Dmitry Tsvetkov, Evgeny Sterkhov, Ivan Ivanov and Andrey Zuev; Ural Federal University, Ekaterinburg, Russian Federation.

Mixed ionic- and electronic-conducting perovskite-type oxides are the state-of-the-art materials for HT and IT solid-state electrochemical devices such as solid oxide fuel cells (SOFCs), oxygen membranes and sensors. Many of such materials are cobaltite-based oxides.

Recently, double perovskites $REBaCo_2O_{6-d}$, where RE is a trivalent rare earth and the oxygen content, d, have received a great attention as attractive materials for such applications. Many interesting phenomena, such as giant magnetoresistance, charge ordering, metal-insulator transition have been observed in these compounds. It is generally recognized that defect structure is of key importance for understanding these properties. However, the data on the defect structure and related properties depending on oxygen partial pressure, *pO2*, and temperature are very limited to date.
Crystal structure, oxygen nonstoichiometry, total conductivity and Seebek coefficient of the double perovskites $Gd_{1-x}La_xBaCo_2O_{6-\delta}$ (x=0-1) were studied as functions of oxygen partial pressure $-5 \le \log(pO2/atm) \le 0$ and temperature $800 \le T, °C \le 1050$.

In situ x-ray diffraction study of $Gd_{1-x}La_xBaCo_2O_{6-\delta}$ (x=0-1) crystal structure was carried out. Total conductivity and Seebek coefficient of $Gd_{1-x}La_xBaCo_2O_{6-\delta}$ (x=0-1) were measured simultaneously by means of four-probe dc method. Oxygen nonstoichiometry of the double perovskites $Gd_{1-x}La_xBaCo_2O_{6-\delta}$ (x=0-1) was measured using thermogravimetric technique.

Results obtained are discussed on the basis of the defect structure of the double perovskite $Gd_{1-x}La_xBaCo_2O_{6-\delta}$ (x=0-1).

C8.10

Synthesis and Electrochemical Performance of Carbon-Coated $0.8Li_2MnO_3$-$0.2LiCoO_2$ Cathode Material for Lithium Ion Batteries Zhuang Wang, Zhiyong Yu, Wenji Li, Mengyun Lu and Hanxing Liu; School of Materials Science and Engineering, Wuhan University of Technology, Wuhan, China.

Li-rich layered structure xLi_2MnO_3-$(1-x)LiMO_2$ (M=transition metal, $0 < x < 1$) cathode materials are most promising cathode materials for Li-ion batteries with excellent practical specific discharge capacity (>250 mAh/g). However, the low rate capability hindered their further development. The present work shows the electrochemical performance of lithium rich cathode materials $0.8Li_2MnO_3$-$0.2LiCoO_2$ is improved by low temperature carbon coating technology in air. The synthesis temperature and time as well as carbon content were optimized in this work. X-ray diffraction (XRD) analyses inferred that the crystal structure of layered oxides $0.8Li_2MnO_3$-$0.2LiCoO_2$ was not destroyed during the carbon coating processes. Transmission electron microscope (TEM) images confirmed that carbon was coated on the surface of $0.8Li_2MnO_3$-$0.2LiCoO_2$ particles. Charge and discharge tests showed that the cycle performance and the rate capability of $0.8Li_2MnO_3$-$0.2LiCoO_2$ were improved by carbon coating. The composite with 10 wt% glucose at 400°C for 1 h showed the best electrochemical performance. At the current density of 20, 50, 100mA/g, the initial capacities increased 26, 86, 241.5% than the sample without carbon coating, respectively. The electrochemical impedance spectroscopy (EIS) results manifested that the enhanced electrochemical performance caused by carbon coating was mainly attributed to the decrease of the charge transfer resistance.

C8.11

Advanced, Nanostructured $LiMn_2O_{4-y}S_y$ Cathode Materials Exhibiting an Outstanding Capacity and Rate Capability Marcin Molenda, Monika Bakierska and Roman Dziembaj; Faculty of Chemistry, Jagiellonian University, Krakow, Poland.

The high energy density of lithium-ion battery technology is attracting widespread interest due to the application prospects in electric vehicles (EV), hybrid electric vehicles (HEV) as well as stationary energy storage systems. The $LiMn_2O_4$ spinel is a highly promising candidate to replace layered Co and Ni oxides as cathode material in lithium-ion batteries, owing to high thermal stability, environmental friendliness, natural abundance and low cost. However, the broad application of lithium manganese spinel requires the improvement of structural stability. Near room temperature $LiMn_2O_4$ undergoes a reversible phase transition associated to the Jahn-Teller distortion of Mn^{3+} ions that leads to capacity fading during the electrochemical cycling. One of the strategies to enhance the structural properties of lithium manganese spinel and thus, improve its electrochemical performance is partial substitution of sulphur in the oxygen sublattice.

In the present work, the structure and morphology of $LiMn_2O_{4-y}S_y$ spinel materials were correlated to the electrochemical characterization and discussed in terms of the substitution effect.
Nanostructured $LiMn_2O_{4-y}S_y$ (y = 0 or 0.01) spinel materials were obtained in a modified sol-gel process. The prepared Li-Mn-O-S systems were investigated using X-ray powder diffraction (XRD), elemental analysis (EA), nuclear magnetic resonance spectroscopy (NMR), low temperature N_2 adsorption-desorption measurements (N_2-BET), differential scanning calorimetry (DSC) and electrical conductivity (EC) studies. The electrochemical characteristic of $Li/Li^+/LiMn_2O_{4-y}S_y$ cells was determined by galvanostatic cycling tests (CELL TEST) and electrochemical impedance spectroscopy (EIS) measurements.

The substitution of sulphur into the $LiMn_2O_4$ spinel structure did not decrease the electrical conductivity of the spinel materials and enabled suppression of the adverse phase transition close to room temperature. The electrochemical studies indicated an outstanding capacity and cycling behavior of $LiMn_2O_{3.99}S_{0.01}$ cathode. Such performance is due to the excellent structural stability, favorable morphology and the high crystallinity of the sulphided spinels.

C8.12

Study of the Mechanism of Electrophoretic Deposition of Composite Lithium-Ion-Conducting Membranes Raymond Blanga and Diana Golodnitsky; Chemistry, Tel Aviv University, Biniamina, Israel.

The electrophoretic-deposition (EPD) method was examined to fabricate pristine and composite polymer-ceramic membranes for lithium-ion battery applications. Lithium aluminium oxide, doped garnet and lithium tin phosphorous sulfide were used as ceramic precursors; PEGDME, PEO and PEI were tested as polymer binders. Effect of surface-active additives on zeta-potential and stability of the suspension has been investigated. The relative content of polymer and ceramics in the film was found to strongly depend on the type of solvent (acetone, ethanol, toluene and their mixtures), solid load in the suspension and EPD voltage. Films deposited at 50V are smoother, conformal and more uniform than those prepared at 100, 150 and 200V. The deposition of ceramics predominates that of polymer, leading to increased concentration of ceramics in the film. Characterization of the films has been carried out by MTGA, DSC, XRD, TOFSIMS, ESEM and AC-impedance methods and the data will be discussed in details. The ionic conductivity of hybrid polymer-in-ceramic composites, prepared by electrophoretic deposition, with impregnated $LiTFSI\text{-}PYR_{14}TFSI$ ionic-liquid electrolytes, is 1.5mS/cm at room-temperature, and 8mS/cm at 100°C. The bulk conductivity of solid $LiI:PEO:LiAlO_2$electrolyte is 0.5mS/cm and does not change with temperaure.

C8.13

***Operando* X-Ray Absorption Study on Charge-Discharge Mechanism of Li_2MnO_3 and Li_2RuO_3 Lithium-Rich Cathode** Takanori Kobayashi, Koji Nakanishi, Takuya Mori, Kentaro Yamamoto, Titus Masese, Yuki Orikasa and Yoshiharu Uchimoto; Kyoto University, Kyoto-shi, Japan.

Lithium-rich layered materials such as Li_2MnO_3 and Li_2RuO_3 are promising cathode materials because they exhibit a large theoretical capacity of more than 300 mAh g^{-1}. In the case of Li_2MnO_3, it is presumed that the large discharge capacity is attributed to the activation of Li_2MnO_3 upon initial charging beyond 4.4 V; a process that involves the concomitant removal of lithium and oxygen from the host framework [1]. In the case of Li_2RuO_3, anion-redox process has recently been proposed in addition to the oxidation and reduction of ruthenium during charge-discharge process [2]. Most of the proposed mechanisms in these systems are based on *ex situ* measurements. However, the oxygen evolution or anion-redox reaction is not stable and the material state might be changed during *ex situ* measurements. Therefore, *operando* measurements are necessary to directly capture the electronic and local structural changes during charge-discharge process. In this regard, we have developed an *operando* cell in order to clarify electronic structures using hard and soft XAS measurement.

Li_2RuO_3 is prepared by solid state reaction. The working electrode consisted of a composite mixture Li_2RuO_3, acetylene carbon black and polyvinylidene fluoride (PVdF) binder (80:10:10 (*wt*%)) coated on Al foil. For hard XAS measurement, three electrode cell packed with laminated Al films were prepared. Hard XAS measurements in a transmission mode were performed at BL01B1 of SPring-8. Soft XAS measurements were performed at BL27SU of SPring-8.

During the initial charge reaction, the absorption edge at Ru K-edge shifts towards higher energy from Li_2RuO_3 to $LiRuO_3$, which corresponds to redox reaction of ruthenium. For the further delithiation from $LiRuO_3$, the absorption edge is almost constant, which implies other redox mechanism contributes this range.

[1] M. M. Thackeray et al., *J. Mater. Chem.*, **17**, 3112 (2007).
[2] M. Sathiya et al., *Chem. Mater.*, **25**, 1121 (2013).

C8.14

Phase Transition Mechanism of $LiFePO_4$-$FePO_4$ Using a Thin-Film Model Electrode Takahiro Yoshinari, Kentaro Yamamoto, Eri Kato, Mori Takuya, Titus Masese, Yuki Orikasa and Yoshiharu Uchimoto; Kyoto University, Kyoto, Japan.

$LiFePO_4$ is considered as a high power cathode material for lithium-ion battery. Improvement of rate capability in cathode materials is one of important issues. Under charging and discharging, the material undergoes phase reactions between Li-rich and Li-poor phases[1]. The rate-determining step in the phase transition of Li_xFePO_4 is expected to be the nucleation reaction[2]. Recently, some modifications have been reported to enhance the nucleation reaction[3, 4]. However, the origin of improvement in rate performance is still not understood well. It is difficult to analyze the interfacial reaction using composite electrode due to complex structure of a mixture employing active materials, carbon, and binder. Herein, we apply thin-film model electrode to focus an ideal interface of the cathode material and clarify the reaction kinetics. The nucleation and growth reaction are investigated based on Kolmogorov-Johnson-Mehl-Avrami (KJMA) theory[5]. $LiFePO_4$ thin-film was prepared on a polycrystalline Au substrate by pulsed laser deposition method. The deposition was conducted under Ar atmosphere (0.0001 Pa) at 923K for 30 min. The obtained thin-film was characterized by X-ray diffraction. For the electrochemical analysis, three-electrode cells employing Li metal as a counter and a reference electrode, and 1 M $LiClO_4$ in propylene carbonate liquid electrolyte were prepared.

The obtained Avrami exponent of ca. 1 is indicative of a one-dimensional phase-boundary movement instead of three-dimensional growth like shrinking core model, which is consistent with the previously reported mechanism. We will also discuss the reaction kinetics of $LiFePO_4$ with anion surface modification to enhance rate performance.

[1] A. Padhi *et al*, *J. Electrochem. Soc.*, **144**, 1188 (1997).
[2] C. Delmas *et al*, *Nature Mater.*, **7**, 665 (2008).
[3] P. Kyu-Sung *et al*, *Chem. Mater.*, **24**, 3212 (2012).
[4] J. Hong *et al*, *J. Phys. Chem. C*, **116**, 20787 (2012).
[5] M. Avrami, *J. Chem. Phys.*, **9**, 177 (1941).

C8.15

Molten Salt Method of Preparation and Electrochemical Characterisation of MnO_2 M.V. Reddy, Yun Hong Lee and Stefan Adams; Materials Science & Eng., National University of Singapore, Singapore, Singapore.

Mn-based oxides have various advantages like low cost and low toxicity. They can also be used flexibly as electrode material for Li-ion and air cathode in Li-air batteries. While α-MnO_2 is usually prepared by a hydrothermal method, here we attempted to prepare it by a more easily scalable one pot molten salt method and studied the effect of different polymers like Polyvinylpyrrolidone (PVP), and Polyvinyl Alcohol (PVA). Rod type morphology was noted for the control MnO_2 prepared without the addition of a polymer. X-ray diffraction (XRD) patterns for this sample showed lattice parameters of a = 9.85Å, c = 2.87Å. The BET surface areas are in range, 32 and 15 to 19 m^2/g for bare and polymer assisted MnO_2 compounds. Raman and X-ray photoelectron spectroscopy (XPS) were used to characterise structural effects of the MnO_2 preparation method. Electrochemical properties of the samples prepared with different additives were characterized using galvanostatic cycling (GC) and cyclic voltammetry. Li-cycling studies showed average discharge and charge potentials of 0.47, 1.14 V, respectively vs. Li/Li^+ close to CV redox potentials. Li-intercalation reaction was noted when cycled in the range, 3.0-1.0V vs. Li followed by conversion reaction if the voltage region is extended down to 0.005 V. For the latter case, 1st cycle capacities of 1050, 478 and 548 mAh/g where reached, of which 600, 300 and 400 mAh/g respectively for bare MnO_2, MnO_2-PVP and MnO_2-PVA where retained at the end of the 35th cycle. Preliminary studies on the suitability of MnO_2 prepared in this way for application in air cathodes of Li-air batteries will be discussed.

C8.16

Electrochemical and Magnetic Properties of $LiMn_{1.5}Ni_{0.5}O_4$ Spinel Oxide Reiko Hanafusa, Kazuki Kotani, Kousuke Ishidzu, Yoshihiro Oka and Tatsuya Nakamura; Dept. of Electrical Engineering , University of Hyogo, Himeji, Japan.

Spinel oxide $LiMn_{1.5}Ni_{0.5}O_4$ has received significant attention as high-energy density cathode material, due to its high operating voltage. But this compound is unstable at high temperature and decomposed to other spinel oxide with the less Ni content and NiO rock-salt phase. It may be attributed to a partial reduction of Mn^{4+} in the spinel compound. It results in the difficulty of the large particles with smaller specific surface area. There exists another serious problem in the high-voltage cathode application: the oxidative decomposition of organic electrolyte solution. It is thought to be promoted by direct contact to the charged high-voltage cathode. From this point of view, it is likely that the large particles are suitable for the practical application.

In our research group, several cathode materials have been studied with low-temperature magnetism. The Ni^{2+} incorporation in $LiMn_2O_4$ leads to the magnetic change from antiferromagnetic to ferromagnetic phase. The $LiMn_{1.5}Ni_{0.5}O_4$ compound is a ferromagnetic material with Curie temperature of approximately 130K. In this study, we first studied the low-temperature magnetism of the decomposed spinel oxide. Second, we have prepared the compounds of $LiMn_{1.6}Ni_{0.4}O_2$ which is stable at high temperature. Finally, the low-temperature annealing with Li-acetate and Ni-acetate was carried out to obtain $LiMn_{1.5}Ni_{0.5}O_4$ large particles. The results about the electrochemical property as well as low-temperature magnetic property are presented and discussed.

C8.17

Influence of Synthesis Conditions on Crystal Structure and Electrochemical Properties of Spinel $Li_4Ti_5O_{12}$ Used as Anode Material for Li-Batteries Anna Drobniak, Danuta Olszewska and Wojciech Zajac; AGH University of Science and Technology, Krakow, Poland.

A spinel based on Li4Ti5O12 (LTO) was use as model material for anode of Li-ion batteries for the first time in 1994 year by Ferg et al. [1]. It is capable of reversible incorporation of up to 3 moles of lithium per formula unit, which is coupled with reduction of Ti4+ into Ti3+ with virtually no change of volume. However, efficiency of this process is limited by low lithium-ion and electron transport properties. The lithium titanate spinel exhibit a 1,6V-plateau and therefore they are attractive candidates for high-voltage Li-ion batteries. Materials Li4Ti5O12 were obtained using solid state method. As the substrates lithium carbonate Li2CO3 and titanium oxide TiO2 were used. Stoichiometric amounts of these substrates were mixed, milled and heated in tube furnace, different amount of time and temperature. Milling was doing at a few way and time. Prepared materials Li4Ti5O12, were characterized in terms of phase composition, crystal structure, grain size and surface morphology, as well as ionic and electronic conductivity using. Phase composition and crystal structure parameter were determinated using X-ray Panalytical Empyrean XRD diffractometer in the range of 10-110° with CuKα radiation. Obtained results were analyzed using Rietveld refinement implemented in GSAS computer software. Electrical conductivity measurements were carried out using Impedance Spectroscopy. Moreover, studies were carried out using scanning electron microscope – SEM. Structural studies carried in the room temperature confirmed obtaining single-phased materials with Fd-3m space group. Change a temperature and time conditions was reason difference in size and appearance of grain.

The author wishes to acknowledge the financial support from the Polish Ministry of Science and Higher Education, under project AGH statutory research led by D. Olszewska (task manager).

REFERENCES

[1] E. Ferg, R.J. Gummow, A. de Kock, M.M. Thackeray, *J. Electrochem. Soc.* 141 (11) (1994) L147.

C8.18

$Li_4Ti_5O_{12}$ Doped with Copper as Anode Material for Li-Batteries Anna Drobniak, Danuta Olszewska and Wojciech Zajac; AGH University of Science and Technology, Krakow, Poland.

INTRODUCTION

Lithium-ion batteries (LiBs) possess favorable combination of operational properties and therefore they are considered to be a favorable energy source for portable electronic devices as well as for hybrid and electric vehicles (HEV & EV). A spinel based on $Li_4Ti_5O_{12}$ (LTO) was use as model material for anode of Li-ion batteries for the first time in 1994 year by Ferg et al. [1]. The copper-doped lithium titanate spinels exhibit a 1,6V-plateau and therefore they are attractive candidates for high-voltage Li-ion batteries.

EXPERIMENTAL

Materials $Li_{4-x}Cu_xTi_5O_{12}$ (x=0-0.2) were obtained using solid state method. As the substrates lithium carbonate Li_2CO_3, titanium oxide TiO_2 and copper oxide CuO were used. Stoichiometric amounts of these substrates were taken to obtain and with 5% wt. excess of Li_2CO_3. Prepared materials $Li_4Ti_5O_{12}$ doped with Cu, were characterized in terms of phase composition, crystal structure, grain size and surface morphology, as well as ionic and electronic conductivity. Phase composition and crystal structure parameter were determinated using X-ray Panalytical Empyrean XRD diffractometer in the range of 10-110° with CuKα radiation. Obtained results were analyzed using Rietveld refinement implemented in GSAS computer software. Electrical conductivity measurements were carried out using impedance spectroscopy. Moreover, studies were carried out using scanning electron microscope – SEM.

RESULTS

Structural studies carried in the room temperature confirmed obtaining single-phased materials with Fd-3m space group.

CONCLUSIONS

Substitution with Cu in lithium sublattice reverses the transport properties present in undoped $Li_4Ti_5O_{12}$.

ACKNOWLEDGMENT

The author wishes to acknowledge the financial support from the Polish Ministry of Science and Higher Education, under project AGH statutory research led by D. Olszewska (task manager).

REFERENCES

[1] E. Ferg, R.J. Gummow, A. de Kock, M.M. Thackeray, *J. Electrochem. Soc.* 141 (11) (1994) L147.

C8.19

Acoustic Emission Study of SnO Anode for Lithium-Ion Batteries Naoakai Kuwata[1], Shutaro Kato[1], Junichi Kawamura[1], Kazuhisa Sato[1, 2] and Junichiro Mizusaki[1]; [1]IMRAM, Tohoku University, Sendai, Japan; [2]Graduate School of Engineering, Tohoku University, Sendai, Japan.

Acoustic emission (AE) technique is nondestructive and sensitive method by detecting supersonic elastic waves. This technique is expected as diagnostic tool for lithium-ion batteries by evaluating the AE signals from formation of cracks, gas generation, exfoliation etc. In this study, the degradation mechanism of lithium-ion batteries using SnO thin-film anodes has been investigated by using the AE technique.

SnO is a promising anode material because of its higher capacity (1000 mAh/g) than conventional graphite (372 mAh/g). However, a capacity degradation problem is not resolved, which includes the formation of cracks induced by large volume expansion/contraction during Li intercalation/deintercalation process. In addition, the unstable SEI is formed on the SnO surface by decomposition of solvent in the electrolyte. The SnO thin films were prepared on Cu substrates by pulsed laser deposition using 4th harmonics of Nd:YAG laser, where the substrate was kept at room temperature. Two-electrode stainless-steel cell attached with AE sensor was used for electrochemical measurement. The electrochemical cell of Li/ $LiPF_6$ (EC: DMC)/ SnO was prepared.

A large number of AE signals were detected from the SnO anode. Especially, most of AE signals were detected in the first lithium intercalation/deintercalation process. We found characteristic three regions within the first cycle. In the first region (region I), low frequency (20~100kHz) AE signals are detected, which is probably due to strains by Li_2O generation and volume expansion. In the region II and III, high frequency (200~500kHz) AE signals are detected, which is due to cracks by large volume contraction. The region II and III are corresponding to the two large volume contraction processes of Li-Sn dealloying ($Li_{22}Sn_5 \rightarrow Li_7Sn_2$ and $Li_7Sn_3 \rightarrow LiSn$).

The electrode reactions of lithium-ion battery can be distinguished using frequency analysis of AE signals. Moreover, the structural changes were able to be presumed from AE signals.

C8.20
Lattice Volume Change of $Li[Ni_xCo_yMn_z]O_2$ Cathodes during Charge/Discharge Reaction and Their Cycle Performance Kosuke Ishizu, Yoshihiro Oka and Tatsuya Nakamura; University of Hyogo, Himeji, Japan.

Both high capacity and cycle stability are required for the cathode materials in Li-ion secondary battery. Generally speaking, the unit cell volume of active materials during charge and discharge reaction does not remain unchanged. The volume change may cause the mechanical stress, resulting in some mechanical damages such as micro-cracks in the particle and so on. In this work, we studied cycle performance of $Li[Ni_xCo_yMn_z]O_2$ from the view-point of the lattice volume change during Li-extraction/Li-insertion reactions. $Li[Ni_xCo_yMn_z]O_2$ specimens, presented in the solid solution of $Li[Ni_{0.5}Mn_{0.5}]O_2$-$LiNiO_2$-$LiCoO_2$, were prepared by combining hydroxide co-precipitation method and solid phase reaction. The in-situ X-ray diffraction was taken on the initial cycle (2.5-4.5V and 0.05C) with use of special-designed electrochemical cell. The structural analysis exhibited the single phase reaction and the lattice parameter variation (Δa, Δc and ΔV): the variation of the lattice parameter *a* is mainly attributed to the change of TM ion radius and that *c* is related to Coulomb repulsion between oxygen-ion layers. It was found that the unit cell volume variation increases with the $LiNiO_2$ fraction.

The cycle performances were also evaluated with the charge-discharge cycling. It was seen that the initial discharge capacity increases with $LiNiO_2$ fraction. However, the capacity retention after 100 cycles was improved with a decrease in the $LiNiO_2$ fraction, that is, the cell performance was seriously degraded with the cathode having large ΔV volume variation. Therefore, there exists a trade-off relationship between high capacity and cycling stability. SEM observation was carried out on the cathode extracted from the cycled cell. It indicated the micro-crack formation in the secondary particles, which is thought be one of the reason for the cell performance degradation. From the observation, it was found that the micro-crack growth is dependent on the cathode composition. Detail discussions are presented in the conference.

C8.21
Investigation of All-Solid-State Li-O_2 Batteries Hirokazu Kitaura and Haoshen Zhou; Energy Technology Research Institute, National Institute of Advanced Industrial Science and Technology, Tsukuba, Japan.

The lithium-air batteries have attracted much more attentions because of its high theoretical energy density, which is over 3500 Wh kg^{-1}. However the lithium-air batteries still have a lot of problems and the problem related with the decomposition of organic liquid electrolytes is the most serious and one of the main research topics in the present stage. Thus, we have developed all-solid-state lithium-air batteries using the inorganic solid electrolytes, which are more stable than the liquid electrolytes. The application of the solid electrolytes to the lithium-air batteries can solve not only the decomposition of electrolytes but also the safety problem and some other problems specific to the liquid such as leakage and volatilization.

In this study, an all-solid-state cell consisting of Li anode, $Li_{1+x}Al_yGe_{2-y}(PO_4)_3$ (LAGP) solid electrolyte, and LAGP-carbon nanotube (CNT) composite cathode was operated in the pure oxygen atmosphere (so-called Li-O_2 cell). Fundamental electrochemical performance was examined and electrochemical reaction process was investigated.
The electrochemical performance was investigated by cyclic voltammetry and galvanostatic measurements. The cell showed the discharge potential of 2.4 ~ 2.0 V and charge potential of 3.0 ~ 4.2 V. The cell can be cycled during 10 cycles. The air electrode after discharging and charging was analyzed by using XPS and IR. From these measurements, it was suggested that $Li_2O_2$was produced after discharging and decomposed after charging.

C8.22
Electrochemical Properties of $LiNi_{1/3}Co_{1/3}Mn_{1/3}$ Electrodes Prepared with Water-Based Slurry Dispersed Conducting Additive by Using Plasma Treatment Yoshihiro Oka, Tomoya Sasaki, Hideyoshi Matsumoto and Tatsuya Nakamura; University of Hyogo, Himeji, Japan.

N-methyl-2-pyrrolidone (NMP) has been widely used as solvent of slurry in order to disperse cathode materials such as active material, conducting additive, and binder. However, the NMP have a negative impact on the human body because it is reproductive toxicant. Therefore, it is required to prepare cathode films by using slurry with water solvent. But it is difficult to uniformly disperse the hydrophobic conducting additive in water solvent. Non-homogenous slurry would deteriorate the electronic conduction in the cathode film, resulting in poor electrochemical performances. In this study, the conducting additive was uniformly dispersed in water solvent by using plasma treatment, resulting in the $LiNi_{1/3}Co_{1/3}Mn_{1/3}$ electrodes have smooth surface without serious aggregation. The $LiNi_{1/3}Co_{1/3}Mn_{1/3}$ electrodes prepared using the water-based slurry had superior cycling performance resembling to that by the NMP-based slurry. When used the slurry of the same weight ratio of cathode materials, the rate capability of the $LiNi_{1/3}Co_{1/3}Mn_{1/3}$ electrode prepared using the water-based slurry limited compared to that by the NMP-based slurry. The rate capability of the $LiNi_{1/3}Co_{1/3}Mn_{1/3}$ electrode prepared using the water-based slurry was improved more than that by the NMP-based slurry by adjusting the carboxymethyl cellulose (CMC) amount and the solid content concentration.

C8.23
Fabrication of High-Purity LATP Powders and Ceramic Pellet by a Wet Chemistry Process Xiangwei Wu, Cai Liu, Meifen Wu and Zhaoyin Wen; CAS Key Laboratory of Materials for Energy Conversion, Shanghai Institute of Ceramics, Chinese Academy of Sciences, Shanghai, China.

The market-dominating Organic electrolyte and polymer-based batteries still have the inherent safety concerns dominate the market. To solve the safety problem, batteries with inflammable ceramic electrolytes have been developed and been considered as the ultimate safe batteries. Among the ceramic electrolytes, NaSICON type $Li_{1+x}Al_xTi_{2-x}(PO_4)_3$ (LATP) compounds are regarded as one of the most promising candidates to be used in lithium ion batteries due to its high ionic conductivity, high structural stability and environmental friendliness. In this paper, high-purity LATP powders were successfully synthesized by a water-based sol-gel process at 800°C for 3h with tetrabutyl titanate, ammonium citrate tribasic, lithium nitrate, aluminum nitrate were chosen as the starting materials and deionized water was used as the reaction medium. The process possesses high reproducibility. LATP pellets prepared at 900°C from the high purity powder demonstrated a conductivity as high as 3.03×10^{-4} $S\times cm^{-1}$ at room temperature. The LATP ceramic membrane was successfully applied in a solid state designed lithium battery.

C8.24
Reduced Free-Standing Co_3O_4 Electrode for Li-Oxygen Battery Chen Shen, Zhaoyin Wen, Fan Wang and Xiangwei Wu; CAS Key Laboratory of Materials for Energy Conversion, Shanghai Institute of Ceramics, Chinese Academy of Sciences, Shanghai, China.

The increasing interests in lithium-oxygen (Li-O_2) come from their ultra-high energy density, however, a lot of obstacles have to be overcome to develop a practical Li-O_2 battery, such as low cycle efficiency, capacity fading under high current, poor cycling performance, electrolyte decomposition, and the possible decomposition of carbon material in the cathode. Herein, we report a novel reduced free-standing Co_3O_4 electrode as cathode for Li-O_2 battery.

A facile electro-deposition method was used to synthesize the free-standing Co_3O_4 electrode. XRD result showed that the reduced electrode material maintained the spinel phase Co_3O_4. However, the FTIR spectrum indicated the increase of the absorption peak related to Co^{2+}, and the decrease of the absorption peak corresponding to Co^{3+}. These results prove that the reduction process does reduce partial of the Co^{3+} to Co^{2+} while morphology and phase of the Co_3O_4 product remains unchanged. The reduced Co_3O_4 electrode showed a stable cycle performance for 30 cycles with only a small increase in charge potential. While the unreduced electrode showed an obvious voltage fading during 30 cycles. This result proves the advantage of reduced Co_3O_4 electrode in improving the cycle stability of Li-O_2 battery.

C8.25

Lithium Storage in Tin Oxide@Carbon by Carbonizing Polydopamine Coating Peng Peng, Zhaoyin Wen, Yu Liu and Jun Jin; CAS Key Laboratory of Materials for Energy Conversion, Shanghai Institute of Ceramics, Chinese Academy of Sciences, Shanghai, China.

Due to the generation of inert lithium oxide which acts as a buffering material during the initial lithiation, SnO_2 anode can display weak volumetric effect. And its high specific capacity (783 mAh•g^{-1}) also offers chances to become the favorable candidate. Of particular note is that a nanoparticle-based system is expected to improve the electrochemical performance, but active nanoparticles tend to aggregate during cycling, resulting in the capacity fading. Composite materials have been widely accepted to deal with the problem. In this paper, we reported a core-shell SnO_2@carbon composite prepared by carbonizing polydopamine coating. The polydopamine is beneficial for achieving the core-shell structure, and is deposited on any surface spontaneously and serves as an adhesion layer immobilized to the surface.

TEM measurements showed that ultrafine SnO_2 nanospheres were interconnected to form larger nanoclusters which were wrapped by a thin uniform carbon coating. The internal SnO_2 core was assembled by amount of crystalline SnO_2 nanoparticles with a diameter less than 5nm. The reversible capacity of SnO_2@C composite anode leveled up to about 850 mAh•g^{-1} at 0.1C and 600 mAh•g^{-1} at 1C, while SnO_2 nanoparticle anode was already lower than 600 mAh•g^{-1} even at 0.1C, demonstrating the good protective role of carbon shell. Moreover, the SnO_2@C composite anode established better cycling stability than the SnO_2 nanoparticles.

C8.26

Electrode and Interface Design for Rechargeable Lithium Sulfur Batteries Zhaoyin Wen, Guoqiang Ma, Jun Jin, Xiangwei Wu, Qingsong Wang and Meifen Wu; CAS Key Laboratory of Materials for Energy Conversion, Shanghai Institute of Ceramics, Chinese Academy of Sciences, Shanghai, China.

Lithium sulfur battery is one of the most promising candidates for next generation secondary battery because of its high theoretical energy density, earth-abundant element and low cost. Nevertheless, the low utilization of active-sulfur material, poor cycling performance and low coulombic efficiency of Li-S batteries have significantly hindered their commercialization. Great efforts have been devoted to suppress the dissolution and shuttle effect by designing the morphology of sulfur electrode to capture sulfur and sulfides, or to stop the dissolved sulfides from penetrating to the lithium electrode by densified separators.
We have designed and prepared a variety of composite sulfur cathode based on the electronic and lithium ion matrices of ordered mesoporous carbon sphere, graphene sheet, and hollow PANi sphere, hollow PPy spheres, et al. Preparation of the composites normally included steps to form the matrices and penetration of sulfur into them. Polycrystalline Li_3N with an exceptionally high Li-ion conductivity and the lithium ion conductive $Li_{1.5}Al_{0.5}Ge_{1.5}(PO_4)_3$ (LAGP) membrane were adopted as separators to stop penetration of dissolved lithium sulfides. In addition, PEDOT, tubular PPy, CNT/PPy hybrid were also used as the separators. A hollow PANi sphere based sulfur electrode delivered a reversible capacity of 602 mAh/g after 1000 cycles, the capacity decay during 510-1000 cycles was as low as 0.016% per cycle. A room temperature lithium-sulfur cell using lithium metal, LAGP solid electrolyte as separator eliminated the shuttle effect thoroughly and worked well at the rate as high as 0.5C, showing excellent coulombic efficiency of 100%.
Soft package cells with the highest capacity of 12.9Ah capacity delivered nearly the designed capacity at 0.2C rate and stably ran for several tens of cycles. A 100Wh module demonstrated the energy density of more than 320Wh/kg calculated with the total mass of the whole module and good stability at the initial charge/discharge stage.

C8.27

Rechargeable Na–O_2 Batteries with a Covalently Coupled Three-Dimensional Graphene/ Mn_3O_4 Hybrids as an Oxygen Cathode Catalyst Sanpei Zhang, Zhaoyin Wen and Xiangwei Wu; CAS Key Laboratory of Materials for Energy Conversion, Shanghai Institute of Ceramics, Chinese Academy of Sciences, Shanghai, China.

Recently, sodium-air batteries have attracted great interests due to low cost and natural abundance of sodium (the fourth most abundant element). However, there are a number of problems including limited practical capacity, low round-trip efficiency, bad power characteristic and poor cycle life to limit the practical application of the Na–O_2 batteries. In this work, we utilize the three-dimensional graphene/Mn_3O_4 hybrids material synthesized by a hydrothermal method as a cathode catalyst and explore the ORR and OER electrocatalytic activities in nonaqueous Na–O_2 cells. Scanning electron microscopy (SEM) images clearly reveal the well-defined 3D open pore nature of the GA/Mn_3O_4 product. XRD pattern shows that the attached Mn_3O_4 particles are tetragonal phase. The loading amount of Mn_3O_4 in the hybrids is 63.32%. Under the condition of deep cycling between 1.8 V and 4.0 V, the initial discharge specific capacity is 1044.2 mAh/g. The discharge capacity is about 515 mAh/g even after 10 deep cycles. The charge potential is mostly unchanged throughout the first 15 cycles by limiting the discharge capacity to 500 mAh/g.

C8.28

Defect Interaction and Solid Electrolyte Transition in $K_3H(SeO_4)_2$ Oscar S. Hernandez-Daguer[2, 1], Diego Pena-Lara[3] and Ruben A. Vargas-Zapata[3]; [1]Department of Physics, Universidad del Atlántico, Barranquilla, Colombia; [2]Department of Physics, University of Puerto Rico., Mayaguez, Puerto Rico, United States; [3]Department of Physics, Universidad del Valle, Cali, Colombia.

This paper explores and proposes a structure-conductivity correlation in the $K_3H(SeO_4)_2$ (TKHSe) solid electrolyte. The proposed correlation is derived from interpretations of powder X-ray diffraction (PXRD), differential scanning calorimetry (DSC), thermogravimetric analysis (TGA), mass spectroscopyc coupled to TGA (TG-MS) and impedance spectroscopy (IS) measurements. The thermal transformation which appears around T_p = 388 K is endothermic in addition to showing a slight weight loss. The enthalpy (DH) and weight loss changes on successive heating and cooling runs through T_p decrease slightly, showing evidence that T_p marks the onset of a slow thermal dehydration of TKHSe, probably to $K_2Se_2O_7(s)$+ $2K_2SeO_4(s)$ + H_2O (v) (s=solid phase, v=vapor phase,) The step change in the dc- ionic conductivity of about three orders of magnitude is also reduced slightly on successive heating and cooling runs. Our results then show that the observed DH at T_p is due to a first-order phase transition of the order-disorder type with that occurs simultaneously with a slow dehydration process. Moreover, the observed decrease of the magnitude of conductivity on successive thermal runs is a consequence of decomposition at the surface of the TKHSe grains, but the jump in conductivity is only a consequence of the order-disorder transition in the TKHSe phase that remains inside the grains.

The observed first-order phase transition that leads to the fast-ion conducting phase in TKHSe above T_p is studied by a trial free energy density. By properly adjusting the model parameters, an abrupt change of disordering mobile ion concentration, c, is predicted at a transition temperature, T_p. The temperature dependence of the dc-conductivity, s, is well fitted to the c´(T) equilibrium configuration obtained from the trial free energy function.

C8.29

Synthesis, Structure and Electrochemical Properties of Lithium Solid Electrolyte: The Li-P-S-O System Kota Suzuki[1], Satoshi Hori[1], Masamitsu Sakuma[1], Tetsuya Nakazawa[1], Miki Kubota[2], Masaaki Hirayama[1], Masao Yonemura[2] and Ryoji Kanno[1]; [1]Electronic Chemistry, Tokyo Institute of Technology, Yokohama, Japan; [2]High Energy Accelerator Research Organization, Tokai, Japan.

Lithium ion conductors play a key role to develop all solid-state batteries with larger energy density and higher safety compared to those of conventional battery systems with organic electrolyte. Among the present lithium ion conductors, $Li_{10}GeP_2S_{12}$ (LGPS) is the most promising candidate because of its enormously high ionic conductivity of over 10^{-2} S cm^{-1} at room temperature [1]. In this study, a novel lithium ionic conductor with the LGPS structure was synthesized in the Li-P-S-O system. The new phase with the LGPS type structure was obtained with a certain range of solid solution described as $Li_{3+5x}P_{1-x}S_{4-z}O_z$. This indicates an existence of LGPS family materials in large variety of compositions with anionic and cationic substitution systems. The highest ionic conductivity of 2.02 x 10^{-4} was obtained in this solid solution at room temperature. Lower ionic

conductivity than that of the original LGPS is attributed to its lattice contraction due to the substitution of Ge and S by smaller P and O ions, respectively. Rietveld refinement using synchrotron X-ray diffraction data confirmed that the cation vacancy is formed at the P site and the S is partially substituted by O ions in the crystal structure, which can be described as $(P/\square)(S/O)_4$. The $(P/\square)(S/O)_4$ tetrahedra combines one-dimensional polyhedral chains to each other, which is formed by LiS_6 and PS_4 units along *c* axis. Effects of the P and O substitution on the crystal structure and electrochemical properties were elucidated.

Reference
[1] N. Kamaya, K. Homma, Y. Yamakawa, M. Hirayama, R. Kanno, M. Yonemura, T. Kamiyama, Y. Kato, S. Hama, K. Kawamoto and A. Mitsui, *Nat. Mater.*, 2011, **10**, 682-686.

C8.30

High Sensitivity Detection of Mn Ion Dissolution by *In Situ* 1H MRI Yoshiki Iwai, Masato Ohzu, Naoaki Kuwata and Junichi Kawamura; Institute of Multidisciplinary Research for Advanced Materials, Tohoku University, Sendai, Japan.

Spinel $LiMn_2O_4$ is a promising cathode material for lithium ion battery. however Mn ion dissolution is a problem for the battery life.
We have developed detection technique of Mn ion by 1H MRI (Magnetic Resonance Imaging).
It can detect dissoluted Mn ion from the cathode at ppm-level. With charging and discharging of the battery, relationship between amount of Mn ion dissolution and voltage will be discussed.

C8.31

Li Ion Conductivity in a Cation Deficient Scheelite Ryan D. Bayliss[1], Stuart N. Cook[2] and Jordi Cabana[1]; [1]Department of Chemistry, University of Illinois at Chicago, Chicago, Illinois, United States; [2]Department of Materials Science and Engineering, Massachusetts Institute of Technology, Boston, Massachusetts, United States.

Energy storage with increased density is required for electronic devices, electric vehicles, and smart grids. Current lithium ion battery technology utilizes cathodes with high voltage and high capacity against a carbon anode, shuttling Li ions back and forth on charge and discharge in a non-aqueous electrolyte. No new commercially viable cathodes with greater capacity than those identified by Goodenough and co-workers[1–3] have yet been found, with no significant increase in capacity over the original $LiCoO_2$ layered cathode (~150 mAh/g) composition since 1980. Alternative strategies to increase energy density are under intense investigation throughout the fields of chemistry, materials science and engineering.

From a chemical point of view, increasing the voltage of cathode could potentially increase the energy density of the cathode by 20-50%, though oxygen loss is known with high voltage cathodes on cycling, especially under high rate applications.[4] These high voltage cathodes also have compatibility issues with non-aqueous electrolytes, often forming a non-passivating layer resulting in low coulombic efficiency on cycling.
From an engineering perspective, increasing the energy density at cell level can also be achieved by the use of pure metal anodes, such as Li, however dendritic growth from pure metal anodes is a major safety hazard. No clear understanding of how to inhibit dendrite growth is currently known but it remains an area of important investigation. Interestingly, Li ion conductivity is possible in solid ceramic materials with examples of conductivity as high as some liquid electrolytes (10^{-3} S/cm).[5] Solid state electrolytes could allow the use of Li metal anodes in an all solid state battery for higher energy density cells by blocking the growth of Li dendrites towards the anode. Furthermore, significantly smaller form factor batteries could be constructed providing additional energy density per volume, removing parasitic mass of separators and liquid electrolytes.[6]

Towards this goal we have produced A-site cation deficient scheelite-type oxide phases with analogous substitutions to the Li-ion conducting perovskite $La_{2/3-x}Li_{3x}TiO_3$[7] in an attempt to produce Li ion conductivity in a new structural family of materials. Structural analysis with in-house X-ray diffraction confirms the room temperature structure is a disordered scheelite type oxide, however, the X-rays are very insensitive to the Li sites. Initial electrochemical measurements (AC impedance) show a substantial jump in ionic conductivity at elevated temperatures and high values of alkali ion conductivity are observed in excess of 10^{-3} S/cm. This work has investigated the structure of these materials in more detail, both at room and high temperatures to rationalize this high conductivity in these new compositions of alkali metal substituted cation deficient $La_{2/3-x}A_{3x}MoO_4$ type scheelites.

[1] K. Mizushima, P. C. Jones, P. J. Wiseman, J. B. Goodenough, *Mater. Res. Bull.* **1980**, *15*, 783.
[2] M. Thackeray, W. David, P. G. Bruce, J. B. Goodenough, *Mater. Res. Bull.* **1983**, *18*, 461.
[3] A. Padhi, K. Nanjundaswamy, J. B. Goodenough, *J. Electrochem. Soc.* **1997**, *144*, 1188.
[4] R. A. Huggins, *J. Electrochem. Soc.* **2013**, *160*, A3001.
[5] N. Kamaya, K. Homma, Y. Yamakawa, M. Hirayama, R. Kanno, M. Yonemura, T. Kamiyama, Y. Kato, S. Hama, K. Kawamoto, A. Mitsui, *Nat. Mater.* **2011**, *10*, 682.
[6] J. F. M. Oudenhoven, L. Baggetto, P. H. L. Notten, *Adv. Energy Mater.* **2011**, *1*, 10.
[7] Y. Inaguma, L. Q. Chen, M. Itoh, T. Nakamura, T. Uchida, H. Ikuta, M. Wakihara, *Solid State Commun.* **1993**, *86*, 689.

C8.32

High Volt Stability of Lithium Borate Thin-Film as Solid Electrolyte for All-Solid-State Thin-Film Battery Haruka Itabashi, Naoaki Kuwata and Junichi Kawamura; IMRAM, Tohoku University, Sendai, Japan.

High voltage lithium battery is a promising way to next generation energy sources. By using solid electrolyte instead of conventional liquid electrolyte, one can overcome the degradation of the electrolyte under high voltage operation. Actually, we have demonstrated a 5-V-class thin-film lithium battery (TFB) using a solid electrolyte thin film of Li_3PO_4 [1]. Although, the Li_3PO_4 or related nitrogen doped LIPON is stable to the reduction even by metallic lithium, small decomposition is seen above 4.7V vs. Li/Li^+. [2], which is serious problem for realization of 5-V-class TFB. While searching for the stable solid electrolyte, lithium borate (LBO) based glass film is found a good candidate. Here, we report the preparation and the electrochemical characterization of the lithium borate glass films as well as test thin-film batteries using the same.

The thin-film of the lithium borate glasses were prepared by pulsed laser deposition (PLD) method with ArF excimer laser (193nm) or vacuum thermal evaporation (VTE) method. The electrochemical stability was analyzed by cyclic voltammetry (CV) between -0.1 to 6.5 V. The samples were prepared under different substrate temperatures. The ionic conductivity was measured by impedance spectroscopy at different temperatures.

From cyclic voltammograms of LBO films, no remarkable decomposition peak is observed in the high potential range up to 6.5 V, which suggests that the LBO thin-film has higher electrochemical stability than Li_3PO_4. Ionic conductivity depends on the preparation conditions, whose highest value is 6.4×10^{-7} S/cm at room temperature.

Reference
[1]. Naoaki Kuwata et al., *Solid State Ionics*, 262 (2014) 165
[2]. Naoaki Kuwata et al., *J. Electrochem. Soc.*, 157 (4) (2010) A521.

C8.33

Highly Reversible Capacity at the Surface of a Lithium-Rich Manganese Oxide Li_2MnO_3 Masaaki Hirayama[1], Sou Taminato[1], Kota Suzuki[1], Ryoji Kanno[1] and Masao Yonemura[2];[1]Tokyo Institute of Technology, Yokohama, Japan; [2]KEK, Tokai, Japan.

The crystal structures in the surface region of intercalation electrodes drastically change at the initial reaction processes due to interfacial reactions between the electrodes and organic liquid electrolytes. The surface phase formation could have a large impact on capacity, power, and stability of nanosized electrodes that have high contact area with the electrolytes. Here we will present the intercalation properties and the structure changes of nanosized Li_2MnO_3 with a lithium-rich layered rocksalt structure, investigated using an epitaxial-film model electrode[1]. The Li_2MnO_3 films with different thicknesses of 12.6, 29.8, and 47.8 nm

were synthesized on 30 nm-thick $SrRuO_3$(111)/Nb-doped $SrTiO_3$(111) substrates by pulsed laser deposition. The films generated 00*l* and 0*k*0 XRD peaks along the $SrTiO_3$[111] and [1-10] directions, which confirmed the epitaxial growth of Li_2MnO_3. Lithium and oxygen vacancies in the films were determined by XANES, XPS and neutron reflectivity, which were assigned the chemical composition $Li_{1.90}Mn^{IV}O_{2.95}$. No significant changes in the crystal structure or the composition were observed when varying the film thicknesses. In the first charge curve, the plateau region was observed at 4.6 V, corresponding to structural transformation of Li_2MnO_3 to an electrochemically active phase. All the films exhibited reversible charge/discharge reactions on subsequent cycling. The initial discharge capacities increased with decreasing film thickness from 47.8 nm (120 mAh g^{-1}) through 29.8 nm (194 mAh g^{-1}) to 12.6 nm (279 mAh g^{-1}). Furthermore, the discharge capacity of the 12.6 nm thick film gradually increased with subsequent cycles to reach 318 mAh g^{-1} on the fiftieth cycle. Our results suggest that the surface region of the Li_2MnO_3 electrode is intrinsically active with regard to the electrochemically-induced transformation to a high capacity phase. Detailed reaction mechanism will be discussed with the results of surface XRDs at the initial cycles.

Reference

1. S. Taminato, *et al.*, *Chem. Commun.*, 2015, 51, 1673-1676.

C8.34

Fabrication and Electrochemical Properties of All-Solid-State Batteries with 5V $LiNi_{0.5}Mn_{1.5}O_4$ Cathode and $Li_{10}GeP_2S_{12}$ Solid Electrolyte Gwangseok Oh, Masaaki Hirayama, Ohmin Kwon, Kota Suzuki and Ryoji Kanno; Electronic Chemistry, Tokyo Institute of Technology, Yokohama, Japan.

All-solid-state lithium batteries have attracted increased attention in recent years due to their high safety. Although there have been many studies on all-solid-state batteries comprising 4 V-class cathodes and solid sulfide electrolytes for large-scale systems, there are no reports of a 5 V-class cathode combined with a sulfide electrolyte. In this study, we investigated reversible lithium intercalation from a $LiNi_{0.5}Mn_{1.5}O_4$ cathode through a solid sulfide electrolyte $Li_{10}GeP_2S_{12}$ with a high lithium conductivity of 10^{-2} S/cm [1]. The $LiNi_{0.5}Mn_{1.5}O_4$ surface was modified with $LiNbO_3$ by a sol–gel method to decrease interfacial resistance between the oxide cathode and sulfide electrolyte [2]. $LiNi_{0.5}Mn_{1.5}O_4$ cathode, $Li_{10}GeP_2S_{12}$ solid electrolyte and acetylene black were mixed using a pot mill rotator. The mixture, $Li_{10}GeP_2S_{12}$ solid electrolyte and Li/In alloy were used as positive electrode, solid electrolyte, and negative electrode, respectively. Electrochemical tests were performed between 2.9 and 4.4 V (vs. Li/In) under a current density of 0.05 C. Although no electrochemical activity was observed for the uncoated $LiNi_{0.5}Mn_{1.5}O_4$, 3 wt% $LiNbO_3$-coated $LiNi_{0.5}Mn_{1.5}O_4$ exhibited lithium intercalation activity with a first discharge capacity of 53 mAh/g. A plateau region was observed at approximately 4.0 V, which corresponds to the Ni^{4+}/Ni^{3+} and Ni^{3+}/Ni^{2+} redox reactions due to lithium deintercalation from and intercalation into $LiNi_{0.5}Mn_{1.5}O_4$. An oxygen-deficient $LiNi_{0.5}Mn_{1.5}O_{4-d}$phase prepared by high temperature annealing showed electronic conductivities on the order of 10^{-4} S/cm, which was much higher than that of unannealed $LiNi_{0.5}Mn_{1.5}O_4$ (5.6×10^{-6}S/cm). The $LiNi_{0.5}Mn_{1.5}O_{4-d}$ exhibited a high discharge capacity of 80 mAh g^{-1}. Our results demonstrate the possibility of 5 V-class all-solid-state batteries using the $LiNi_{0.5}Mn_{1.5}O_4$cathode and the $Li_{10}GeP_2S_{12}$ solid electrolyte.

References

[1] N. Kamaya et al., Nat. Mater., **10** (2011) 682.
[2] N. Ohta et al., Adv. Mater., **18** (2006) 2226.

C8.35

Electrochemical Performance of Li_2MnO_3 Cathode Material by Fluorine Substitution Sha Wu, Zhiyong Yu, Hanxing Liu, Wenji Li and Mengyun Lu; School of Materials Science and Engineering, Wuhan University of Technology, Wuhan, China.

Lithium rich cathode materials $Li_2MnO_{3-z}F_z$ (z=0, 0.03, 0.05, 0.10) were successfully synthesized using a facile sol-gel method followed by a fast combustion method and heat treatment. The effects of fluorine content on the structure, morphology, electrochemical properties have been extensively studied. All the prepared samples in this work show no obvious impurity phases. The morphology results indicate that a small quantity of NH_4F could accelerate the growth of primary particle. The specific initial charge/discharge capacities and cycling performance of F-doped samples have obvious improvement than the pristine material. Among the materials prepared in this work, sample z=0.03 exhibits the best electrochemical properties in terms of initial discharge capacity of 240 mAh/g at the current of 5 mA/g and a capacity retention of 79% up to 30 cycles. On the contrary, the pristine material only shows an initial discharge capacity of 174 mAh/g and 58% capacity retention cycling for 30 times. Electrochemical impedance spectroscopy showed that fluorine substitution played an important role of reducing the charge transfer resistance.

C8.36

EELS Investigations of Aging Mechanisms in $LiFePO_4$ Cathodes after Extended Electrochemical Cycling Samartha Channagiri[1], Nicholas Warner[2], Frank Scheltens[1], Marcello Canova[2], Yann Guezennec[2] and David W. McComb[1]; [1]Materials Science and Engineering, The Ohio State University, Columbus, Ohio, United States; [2]Center for Automotive Research, The Ohio State University, Columbus, Ohio, United States.

Lithium iron phosphate ($LiFePO_4$) has considerable potential as a cathode in batteries for automotive applications due to its high rate capability, reasonable energy density and environmentally benign nature. However, performance degradation seen after thousands of cycles at high charging-rates (C-Rates) has been a point of major concern. Studies of the aging mechanism suggest that phases ($LiFePO_4$/$FePO_4$) formed in the cathode during discharge influence the aging profile. Previously, we used electron energy-loss spectroscopy (EELS) to demonstrate the use of Li-K edge for qualitative and quantitative analysis lithium distribution.

In this contribution aged cells were produced for EELS analysis utilizing capacity retention, cycling temperature and battery size factor (B.S.F) as metrics. Electron transparent thin foils were prepared from the cathode materials by FIB milling. We performed EELS in the low energy-loss regime (DE<90eV) on both unaged and aged (aged at B.S.F = 1, T = 35°C up to 90% capacity retention) samples.

Both unaged and aged cells have similar microstructures with a large particle size distribution making it challenging to identify directly structural variations introduced by aging. However, EELS performed in the low loss region exhibit subtle variation in the Li K-edge energy-loss near-edge structure (ELNES). In particular, the intensity and separation of the peaks in ELNES varies within a given sample and between samples. The correlation between EELS and microstructure is providing new insights into the complex aging mechanism in these electrodes that is in part responsible for the capacity loss with extended cycling.

C8.37

Mixed Conduction Transmission Line Impedance Model for Olivine Structured Cathode Material Eui-Chol Shin[1], Jihyeon Gim[1], Jinju Song[1], Sung-Won Kang[1], Docheon Ahn[2], Jaekook Kim[1] and Jong-Sook Lee[1]; [1]Materials Science and Engineering, Chonnam National University, Gwang-Ju, Korea (the Republic of); [2]Pohang Accelerator Laboratory, Pohang, Korea (the Republic of).

The electrical properties of the olivine structured cathode materials $LiFePO_4$/$FePO_4$ and $LiMnPO_4$/$MnPO_4$ are investigated by electrochemical impedance spectroscopy combined with galvanostatic intermittent titration technique. In view of poor electronic conductivity a mixed conduction transmission line model was applied for the diffusion impedance at low frequency range. Electronic and ionic resistance and chemical capacitance as well as solid electrolyte interface and charge transfer impedance were obtained for the single phase region as a function of temperature. One-dimensional and three-dimensional diffusion models are compared. To understand the two-phase plateau regime behavior, one-dimensional diffusion impedance model is modified to simulate the mixed phase situation and the interface mobility. $LiFePO_4$ cathode material prepared by polyol process, solvothermal and solid state reaction are compared. $LiMnPO_4$ prepared with and without carbon additives are compared.

C8.38

In Depth First-Principles Study with Experiment on Origins and Mechanism of Phase Transformation of Mn^{4+}-Related Bulk Li_2MnO_3 Jin-Myoung Lim[1], Duho Kim[1], Young-Geun Lim[2], Min-Sik Park[2], Young-Jun Kim[2], Kyeongjae Cho[3] and Maenghyo Cho[1]; [1]Seoul National University, Seoul, Korea (the Republic of); [2]Korea Electronics Technology Institute, Seongnam, Korea (the Republic of); [3]The University of Texas at Dallas, Richardson, Texas, United States.

Lithium ion batteries have been successfully utilized to portable electronics for several decades, yet there is a big demand for large scale energy storages such as electric vehicles and energy storage systems. The development of new cathode materials with higher capacity than that of currently used layered transition metal oxides ($LiMO_2$, M: transition metal) is highly required. For these reason, the Li-rich oxide consists of Li_2MnO_3 and $LiMO_2$ has been a strong candidate for its high capacity (> 250 mAh g^{-1}), low cost, and eco-friendliness. However, Li-rich oxide has critical drawbacks such as large irreversible capacity and voltage drop caused by undesirable phase transformation involving oxygen evolution during the repeated cycles. This phase transformation is mainly induced by the structural instability from the Mn^{4+}-related Li_2MnO_3 after Li^+ extraction. For overcoming this challenge of Li_2MnO_3, the origins and mechanism of phase transformation of this material are necessary to be figured out. In this study, we mainly focused on the phase changes of bulk Li_2MnO_3 to find out a clue for suppressing this undesirable phase transformation with combined first-principles calculation and experiment. First-principles calculation was not only thermodynamically conducted on bulk atomic models of possible transformed structures configured by experiment, but also kinetically carried out on the predicted directions of Mn atomic motion for phase transformation. On the basis of these theoretical results, electronic structure analyses with crystal field theory were employed to figure out the origins and mechanism of phase transformation. To substantiate the calculation results, *ex-situ* X-ray photoelectron spectroscopy and electrochemical experiments were performed using as-synthesized Li_2MnO_3 structurally confirmed by X-ray diffractometer, field-emission scanning electron microscope, and scanning transmission electron microscope for an agreement with our atomic models for simulation. Eventually, practical approaches to prevent the phase transformation were further suggested based on our findings.

C8.39

The High-Capacity Effect in the All-Glass Composites Conducting Electrons and Silver Ions Wioleta Slubowska, Jan L. Nowinski, Jerzy E. Garbarczyk and Marek Wasiucionek; Faculty of Physics, Warsaw University of Technology, Warsaw, Poland.

The work presents the synergy effect observed in the materials composed of the two types of glasses: an electronic conductor (E) and a superionic conductor of Ag+ ions (I). Such heterogeneous materials could be considered as model systems to study electrical properties of composites with mixed electronic-ionic conductivity, which could be used, for instance, as composite electrodes in modern batteries.
The 30AgI·35Ag2O·35P2O5 (superionic) and 30AgI·35Ag2O·35P2O5 (electronic) glasses were used as the components. They, after preparation were ground and from the resultant powder a fraction containing grains of 40-60 μm in size was extracted for further processing. Then, the components were mixed in selected volume ratios E:I and pressed to from pellets. Both, the starting glasses and the samples after pressing were investigated by x-ray diffraction (XRD) and differential scanning calorimetry (DSC) methods. The investigation showed that applied processing did not cause any crystallization of the components or formation of some new glassy phases. This indicated that the formed composites was composed entirely with the E and I glasses. DC investigations revealed that during electric current passing through a sample a high electric charge was stored. Estimated values of specific volumetric capacity increased with a content of the ionic glass in the composite varying in the range 5 mF/cm3 to 1F/cm3. The AC investigations ruled out that the high-capacity effect was due to some electrode phenomena, instead they pointed out on bulk effects attributing the observed high-capacity to the electronic-ionic interface formed by the contacting grains of the componential glasses.

C8.40

Electrochemical Impedance Spectroscopy of Supercapacitors: Analysis Using Evolutionary Programming Alon Oz, Shany Hershkovitz, Emanuelle Goren, Sioma Baltianski and Yoed Tsur; Technion - Israel Institute of Technology, Haifa, Israel.

Supercapacitors (SCs) are gaining a lot of interest due to their high capacitance, high power density and long cycle-life. Electrochemical impedance spectroscopy (EIS) in a wide range of frequencies is routinely used in SCs research, yet a thorough analysis of the spectra is not usually performed. Here, we show an evolutionary programming based technique that finds an analytical form of the distribution function of relaxation times (DFRT) of the system. The analysis is based on a computer program developed in our research group, Impedance Spectroscopy Genetic Programming (ISGP), which finds the best fitted model to the measured data, while minimizing the chance of over-fitting and other pitfalls of the common methods.

EIS measurements of SCs does not comply with the Kramers-Kronig (KK) criteria, yet following transformation to the complex capacitance plane, C(ω), the data does comply with this very common validation technique. The outcome of our analysis is an analytic function, comprised of known mathematical peaks (e.g. Gaussian, Lorentzian, etc.) that can be assigned to the different processes taking place in the tested sample. The relative area of each peak is its contribution to the capacitance of the cell, which allows us to separate and understand how each process affects the total capacitance. Our obtained models are comprised with two or three peaks, one of which has a relaxation time at the time constant referred to in the literature as the 'dielectric relaxation time characteristic of the whole system' or as the SC's figure of merit.

The impedance data below 1 kHz is usually related to the diffusion process and the EDLC layer accumulation. Several systems that show different diffusion characteristics are reported.

C8.41

Two-Dimensional Imaging of Charge/Discharge by the Bragg Edges Analysis of the Electrode Materials for the Pulsed Neutron-Beam Transmission Spectra of a Li-Ion Battery Koichi Kino[1], Masao Yonemura[2], Yoshihisa Ishikawa[2] and Takashi Kamiyama[2, 3]; [1]Faculty of Engineering, Hokkaido University, Sapporo, Japan; [2]Institute of Materials Structure Science, High Energy Accelerator Research Organization, Tokai, Japan; [3]The Graduate University for Advanced Studies (Sokendai), Tokai, Japan.

The lithium-ion battery (LIB) is desired to improve the charge performance and suppress the deterioration by cycling. It is needed to observe the intercalation and deintercalation of lithium ions to the crystalline electrode materials quantitatively and nondestructively. We have been conducting the experimental study for visualizing the charge and discharge inside commercial LIBs nondestructively using the pulsed-neutron transmission method at the Materials and Life Science Experimental Facility of the Japan Proton Accelerator Research Complex. Neutron beam is superior for nondestructive study by its high penetrability of materials. Furthermore, the lithium ions in the crystalline electrode materials can be analyzed by the neutron's interference with crystals. This interference is seen as Bragg edges on the neutron transmission spectra as a function of the neutron wavelength. We used a commercial 18650-type LIB as an experimental sample. The LIB sample was four charge states: discharged (3.2 V), intermediate of charge (3.7 V), charged (4.2 V), and intermediate of discharge (3.7 V). The μPIC-type two-dimensional neutron detector was set downstream of the LIB sample on the neutron beam line. Bragg edges that are originating from the electrodes, current collectors, and vessel are observed on the transmission spectra and they are assigned by modifying the lattice parameters of the crystals. Two-dimensional distributions of lithium ions are obtained by fitting the Bragg edges of the electrodes by the theoretical function for each area of the LIB sample. In this presentation, we introduce our experimental method and discuss the two-dimensional distributions of charge/discharge by comparing the LIBs of different charge states.

This study was supported by New Energy and Industrial Technology Development Organization (NEDO). This work was carried out as the S-type project of KEK (Proposal No. 2009S10, 2014S10).

C8.42

Alluaudite Sodium Iron Sulfate $Na_{2+2x}Fe_{2-x}(SO_4)_3$ for High Energy Density Sodium-Ion Battery Shin-ichi Nishimura[1, 2], Prabeer Barpanda[3, 1], Gosuke Oyama[1] and Atsuo Yamada[1,2]; [1]Department of Chemical System Engineering, The University of Tokyo, Bunkyo-ku, Japan; [2]ESICB, Kyoto University, Kyoto, Japan; [3]Indian Institute of Science, Bangalore, India.

Energy storage technology is continuously growing along with rapid expansion of its applications. Especially larger and cheaper energy storage technology is a key to realize the smart and green society. An obsolete system, sodium-ion battery (SIB), has come in to the spotlight again, due to high abundance of sodium in the Earth. This technology allow the secondary battery to expand toward larger and broader applications. One of the crucial problem in the SIB is lower voltage than the lithium-ion battery(LIB), because of higher electrodeposition potential of Na than Li. Therefore, high-potential cathode material is required to gain the voltage to comparable level with the LIB.

Fe , the abundunt element in the Earth's crust, is the best candidate as a constituent element of the cathode material for the SIB. Successful design of the Fe-based materials has beem achieved in the LIB, for example $LiFePO_4$, $LiFeSO_4F$, $LiFeBO_3$, Li_2FeSiO_4, etc. Utilizing Fe^{3+}/Fe^{2+} redox and oxyanion XO_4^{n-} (X = B, Si, P, S) facilitate stable electrochemical cycling at feasible potential of around 3 ~ 3.9 V vs. Li/Li^+. According to these knowledge, analogue compounds are expected to work in the SIB system. Indeed, several new active compounds have been discovered (ex. Na_2FePO_4F, $Na_4Fe_3(PO_4)_2(P_2O_7)$, $Na_2FeP_2O_7$, while the best candidates $NaFePO_4$ (maricite) and $NaFeSO_4F$ are not active. Following this pursuit, we have discovered a new active compound $Na_{2+2x}Fe_{2-x}(SO_4)_3$ in the sulfate system Na_2SO_4-$FeSO_4$. This material exhibits reversible electrochemical activity at extremely high reaction potential of 3.8 V vs. Na/Na^+ (4.0 V vs. Li/Li^+), whereas Fe^{3+}/Fe^{2+} redox dominates charge compensation in this materials. This potential is the highest among the Fe-oxyanionic compounds so far. The $Na_{2+2x}Fe_{2-x}(SO_4)_3$ crystallizes in alluaudite structure, which is known as phosphate mineral. Large tunnels in this structure facilitate good sodium Na ionic transport. Detailed structural analysis and crystal chemical evaluations supports this picture. This material will gain the energy density and the power density of the SIB upto comparable level with the LIB.

C8.43

Structure and Electrochemical Performance of $LiCoO_2$ Cathode Materials Xiaoli Xi; Beijing University of Technology, Beijing, China.

The structure of recycled cobalt oxide and its electrochemical performance when deployed in lithium ion batteries have been studied. Both recycled and ore-produced cobalt carbonate crystallized in a monoclinic structure, although the crystallization of the recycled cobalt carbonate was inferior to that of the ore-produced sample. A product calcined at 450 °C in nitrogen for 6 h was found to have a fcc structure of CoO, and its crystallization was superior to that of a product calcined in air. $LiCoO_2$ cathode materials prepared from the recycled and the ore-produced cobalt oxide samples both possessed a layered structure of α-$NaFeO_2$ type, and the difference in their crystallinities was much smaller. The initial discharge capacity of the recycled and the ore-produced $LiCoO_2$ cathodes were measured as 109.4 mA h g^{-1} and 110.3 mA h g^{-1}. The capacity retentions were 86.6% and 86.3%, respectively, after 50 cycles.

C8.44

Origin of High Rate Performance of $LiFePO_4$ Investigated by Time-Resolved X-Ray Diffraction Kazufumi Otani[1], Toshiyuki Munesada[1], Takuya Mori[1], Kentaro Yamamoto[1], Titus N. Masese[1], Yuki Orikasa[1], Koji Ohara[2], Katsutoshi Fukuda[2], Yukinori Koyama[2], Toshiyuki Nohira[3], Rika Hagiwara[4], Zempachi Ogumi[2] and Yoshiharu Uchimoto[1]; [1]Graduate School of Human and Environmental Studies, Kyoto University, Kyoto, Japan; [2]Office of Society-Academia Collaboration for Innovation, Kyoto University, Uji, Japan; [3]Institute of Advanced Energy, Kyoto University, Uji, Japan; [4]Graduate School of Energy Sciences, Kyoto University, Kyoto, Japan.

$LiFePO_4$ is a most promising cathode material for lithium-ion batteries as it exhibits high rate performance. The origin of the high rate performance exemplified in $LiFePO_4$ should provide design principles for further development of high rate cathode materials. Under high rate cycling, we revealed the metastable phase formation of $Li_{0.6}FePO_4$ (L_xFP) which acts as a buffer layer between Li-rich phase (LFP) and Li-poor phase (FP)[1]. However, the detailed reaction between LFP and FP during high rate cycling has not fully been understood due to short lifetime of metastable L_xFP phase.

To investigate the phase transition mechanism, with respect to L_xFP phase, we use two types of approaches. One is cycling conducted at elevated temperatures because L_xFP is thermodynamically stable above 200ºC[2]. The electrolyte used was a binary molten salt electrolyte based on $MN(SO_2CF_3)_2$ (M=Li, Cs). Herein, we demonstrate a two-step (dis)charge potential plateau in $LiFePO_4$ upon cycling at 230ºC. The phase transition behavior is investigated by using electrochemical and spectroscopic techniques.

The other approach is phase transition analysis at low temperature because metastable L_xFP phase might have long lifetime. Depending on operating temperatures, phase transition behavior is varied, which is observed time-resolved X-ray diffraction measurements. We will discuss the phase transition kinetics of $LiFePO_4$ — $FePO_4$ *via* the metastable L_xFP phase.

[1] Y. Orikasa *et al, J. Am. Chem. Soc,* **135**, 5497-5500 (2013).
[2] J. L. Dodd *et al, Electrochem. Solid-State Lett.,* **93**, A151-A155 (2006).

C8.45

A Cation-Selective Separator as the Oxygen-Barrier for Non-Aqueous Metal-Air Batteries Xiaodi Ren[1], Mingzhe Yu[1], Mitchell E. Steindler[2], Qiang Zhao[1] and Yiying Wu[1];[1]Chemistry and Biochemistry, Ohio State University, Columbus, Ohio, United States; [2]Chemical and Biomolecular Engineering, Ohio State University, Columbus, Ohio, United States.

In recent years, metal-air batteries, especially non-aqueous lithium-air batteries, have attracted considerable research attention due to high theoretical specific energy densities (3505 Wh/kg for Li-O_2). Along with Li-air batteries, alternative chemistries featuring the more reversible one-electron transfer O_2/O_2^- redox couple, for example K-air and Na-air batteries, show great promise for realizing low-cost and high-efficient energy storages. However, these alkali metal anodes used in batteries are confronted with stability issues, which could greatly limit the battery life. The highly reductive alkali metals can react not only with organic electrolytes, but also oxygen molecules from crossovers of the cathode. In our previous studies, it has been proved that oxygen crossover could significantly accelerate the decay of the anodes and cause battery failures. We are reporting the design of a composite separator membrane, which is able to selectively conduct metal cations while suppressing oxygen crossover to the anodes. The membrane features low oxygen permeability, high cation conductivity, and moreover can be easily tailored to accommodate the needs in different battery systems. Our results have proved that the battery anode stability can be greatly improved with this protective membrane and the cycle life can be elongated.

C8.46

How to Get a Conversion Reaction Reversible? Lithium Storage in Electroactive Metal Sulphide Nanodots Yan Yu[1, 2], Changbao Zhu[2] and Joachiam Maier[2]; [1]Department of Materials Science and Engineering, University of Science and Technology of China, Hefei, China; [2]Max-Planck-Institute for Solid State Research, Stuttgart, Germany.

Among Lithium storage modes, conversion reactions have attracted great attention as on one hand the theoretical capacity is very high since more than one electrons can be transferred per transition metal ion, while on the other hand the kinetic problems associated with it are extraordinarily severe. Here we present several examples to show how to make the conversion reaction reversible. Our solution is to prepare mechanically isolated but electrochemically well connected nanodots. One of the pertinent examples is nanodots of MoS_2 embedded in thin carbon nanowires, which was successful synthesized through electrospinning. [1] Not only are the storage properties found to be outstanding, i.e. high rate performance and cycling stability for lithium storage, but also the storage behaviour of such nano-dots is highly exciting from a fundamental point of view. Moreover, this concept of extreme reaction confinement can be applied to other conversion electrodes, for example, FeS nanodots in porous graphitic carbon nanowires where excellent lithium storage performance is obtained as well. [2]

Reference:
[1] C. Zhu, X. Mu, P. A. van Aken, Y. Yu and J. Maier, *Angewandte Chemie International Edition*, 2014, **53**, 2152.
[2]C. Zhu, Y.-R. Wen, P. A. van Aken, J. Maier, and Y. Yu, *Advanced Functional Materials, accepted.*

C8.47

Constructing 3D Porous and Carbon-Coated Electrode Materials for High Performances Li-Ion Batteries Yan Yu[1, 2], Jun Liu[2] and Joachiam Maier[2]; [1]Department of Materials Science and Engineering, University of Science and Technology of China, Hefei, China; [2]Max Planck Institute for Solid State Research, Stuttgart, Germany.

The development of high rate Li-ion batteries with improved safety and a long cycle life is essential for most battery applications, in particular for portable devices, Electric vehicles (EVs) and Hybrid Electric Vehicles (HEVs). Although the progress of Li-ion batteries development is substantial, their energy density, cycle life and rate capability remain insufficient. To obtain a further noticeable improvement in Li-ion batteries, it is essential to develop electrode materials with higher reversible capacity and rate capability, as the battery's performance is mainly determined by the anode and cathode. For this purpose, the following two strategies have been successfully developed: a) constructing of 3D porous structures to shorten the Li^+ diffusion length and provide better electrical contacts of the electrode and electrolyte; b) electrical conductive coating of electroactive electrode particles to improve their electrical conductivity and buffer their stress of volume expansion during cycling.
Herein, we summarize our recent progress in the structural design, chemical synthesis, and electrochemical properties of some typical anode and cathode materials (i.e. Ge, Ni-Sn, FeS_2, $Li_4Ti_5O_{12}$) via constructing 3D porous and carbon-coated structures.[1-4] By highly porous microstructure and rational carbon coating design, the Li-ion storage performance of these electrode materials were significantly improved.

References:
1. J. Liu, K. Song, C. Zhu, C. C. Chen, P. A. van Aken, J. Maier and Y. Yu, ACS Nano, 2014, 8, 7051-7059.
2. J. Liu, K. Song, P. A. Van Aken, J. Maier and Y. Yu, Nano Letters, 2014, 14, 2597-2603.
3. J. Liu, Y. Wen, P. A. van Aken, J. Maier and Y. Yu, Nano Letters, 2014, 14, 6387-6392.
4. J. Liu, Y. Wen, Y. Wang, P. A. van Aken, J. Maier and Y. Yu, Advanced Materials, 2014, 26, 6025-6030.

C8.48

Synthesis and Characterization of $Li(Li_yFe_zV_{1-y-z})O_{2-\delta}$ – Anode Material for Li-Ion Batteries Bartlomiej Gedziorowski and Janina Molenda; AGH University of Science and Technology, Krakow, Poland.

Layered $Li_{1+x}V_{1-x}O_2$ is considered as a potential anode material for Li-ion batteries, competitive to commonly used graphite. It exhibits low potential plateau at ~0.1V during lithium intercalation process and volumetric capacity of 1360 mAh/cm^3 – almost twice the capacity of the graphite. In this work an evaluation of crystal structure, transport and electrochemical properties are given for $Li(Li_yFe_zV_{1-y-z})O_{2-\delta}$ materials with y=0, 0.03, 0.07 and z=0, 0.05, 0.1. Materials were synthesized by a high-temperature method with Li_2CO_3, V_2O_3 and Fe_2O_3 taken as substrates. Stoichiometric amount of substrates were ball-milled, pressed into pallets then followed by two steps of annealing: 10h at 800ºC in argon atmosphere and 12h at 1050ºC in mixture 5%At-95%H_2 followed by quenching.
Structural studies were performed in 10-110° range with CuKα radiation using Panalytical Empyrean diffractometer. Oxygen nonstoichiometry was determined by usage of thermogravimetric (TG) method during oxidation on TA Q5000IR apparatus combined with high-temperature structural analysis during oxidation in equivalent conditions. Electrical conductivity was determined using frequency response analyzer Solartron 1260 with dielectric interface Solartron 1296.

Structural analysis shown all obtained materials to be single phased with α-$NaFeO_2$ type structure and R-3m space group. Unit cell parameter *a* is increasing and *c* parameter is decreasing with substitution of vanadium by both lithium and iron. Materials oxygen stoichiometry δ depends on iron content – δ is close to zero when z=0 and it grows to 0,15 for $Li(Li_{0.07}Fe_{0.1}V_{0.83})O_{2-\delta}$. Electrical conductivity shown activated character with values varying from ~10^{-5} Scm^{-1} for $LiVO_2$ to ~10^{-2} Scm^{-1} for $Li(Li_{0.07}Fe_{0.1}V_{0.83})O_{2-\delta}$. Resistivities of materials tend to constant value when frequency of current tends to zero, indicating that measured values of conductivity are equivalent of its electronic component.

This work was supported by NCN grant no. NCN 2011/02/A/ST5/00447.

C8.49

Unusual Surface Redox Behaviors of Li_2MnO_3: First-Principles Prediction and Experimental Validation Duho Kim[1], Jin-Myoung Lim[1], Young-Geun Lim[2], Min-Sik Park[2], Young-Jun Kim[2], Kyeongjae Cho[3] and Maenghyo Cho[1]; [1]School of Mechanical Aerospace Engineering, Seoul National University, Seoul, Korea (the Republic of); [2]Advanced Batteries Research Center, Korea Electronics Technology Institute, Seongnam, Korea (the Republic of); [3]Department of Materials Science and Engineering, University of Texas at Dallas, Dallas, Texas, United States.

Within Li-rich compounds such as $xLi_2MnO_3 \cdot (1-x)LiMO_2$ (M = Ni, Co, Mn), Li_2MnO_3 plays an essential role in increasing the reversible capacity, and it independently possesses a high theoretical capacity of 460 $mAhg^{-1}$ (if all the lithium is utilized) in lithium ion batteries (LIBs). Although Li_2MnO_3 is not active below 4.5 V (*vs.* Li/Li^+), Li^+ can be extracted from the host structure beyond 4.5 V. During the initial de-lithiation process, however, Li_2MnO_3 is known to transform into a layered $LiMnO_2$ structure, and subsequent cycling induces a gradual phase transformation to a spinel structure ($LiMn_2O_4$). Considering the fact that the electrochemical reaction of Li_2MnO_3 may be initiated from the surface and interfaces between different phases.

Herein, we establish a fundamental understanding of the origin of the phase transformations at the surface of Li_2MnO_3 along with Li^+ extraction through a first-principles study with a reliable surface model combined with a proper experimental validation. For a more realistic environment, a surface model with a semi-infinite bulk below the Li_2MnO_3 surface is proposed. The theoretical and experimental findings suggest that Li_2MnO_3 has unusual redox activities. From a thermodynamic viewpoint, the surface Li^+ can be extracted at a lower redox potential (< 4.5 V vs. Li/Li^+), which is dominant along with the Li^+ transport direction. The Mn near the surface of the Li^+ channel orientation can be oxidized in advance of Mn in the bulk because the surface Mn involves more electrons at higher energy states (e_g bands) by comparison with the Mn^{4+}. Through the Mn migration barriers, the phase transformation of a spinel ($LiMn_2O_4$) is initiated from the surface and would propagate to the bulk. The presented observations provide new insight into the origin of the phase transformation of Li_2MnO_3 that will impact the general approach for investigating various cathode materials for LIB applications.

C8.50

Ultrasonic-Assisted Synthesis of Nanostructured Transition Metal Oxides as Cathode Materials for Mg-Ion Batteries Lu Wang[1], Xinzhi Chen[1], Sidsel M. Hanetho[2] and Fride Vullum-Bruer[1]; [1]Department of Materials Science and Engineering, Norwegian University of Science and Technology, Trondheim, Norway; [2]SINTEF Materials and Chemistry, Trondheim, Norway.

Mg-ion batteries have been regarded as the most promising alternative to Li-ion batteries, due to chemical stability and its high natural abundance in the earth's crust (13.9% as compared to $7*10^{-4}$ % for Li).[1] However, strong interactions between the divalent Mg^{2+} ions and the host matrix during insertion/extraction causes slow solid-state diffusion. This gives rise to poor charge and discharge capacities as well as large differences between charge and discharge potentials. Thus the electrode is far away from its equilibrium potential, leading to high kinetic limitations.[1,2] Developing new and improved cathode materials with higher ionic conductivities is therefore a key issue in order to provide viable solutions for Mg-ion batteries.

Here, we report a facile direct synthesis of spinel structure nanoparticles (Mn_3O_4 and Fe_3O_4) and olivine structure nanoparticles ($MgMnSiO_4$ and $MgFeSiO_4$) via an ultrasonic process, without any additional surfactant or template. The structures of these nanoparticles are confirmed by X-ray diffraction. The studies of Mg-ion battery performances were carried out

in a standard coin cell with the synthesized materials as cathode, magnesium alloys as anode, glass fiber as separator and $(PhMgCl)_2$-$AlCl_3$/THF as electrolyte. The electrochemical performance was evaluated by cyclic voltammetry (CV), electrochemical impedance spectroscopy (EIS) and galvanostatic charge–discharge techniques within the voltage ranging from 0.5 to 2.1 V.

[1] E. Levi, Y .Gofer, and D. Aurbach, *Chem. Mater.*, 2010, **22**, 860-868.
[2] D. Aurbach, Z. Lu, A. Schechter, Y. Gofer, H. Gizbar, R. Turgeman, Y. Cohen, M. oshkovich and E. Levi, *Nature*, 2000, **407**, 724-727.

C8.51

Synthesis and Electrochemical Performance of $Li_4Ti_5O_{12}$ Modified with Carbon Nanotubes Yingbin Lin and Zhigao Huang; Physics and Energy College, Fujian Normal University, Fuzhou City, China.

A hole-rich $Li_4Ti_5O_{12}$ was synthesized by spray drying using carbon nanotubes as additives in precursor solution. The structure, morphology, and texture of the as-prepared composites were characterized with XRD, Raman, BET and SEM techniques. The electrochemical properties of the as-prepared composites were investigated systematically by charge/discharge testing, cyclic voltammograms and AC impedance spectroscopy, respectively. In comparison with the pristine $Li_4Ti_5O_{12}$, $Li_4Ti_5O_{12}$ modified with carbon nanotubes exhibits superior electrochemical performance, especially at high rates. The obtained excellent electrochemical performances might be attributed to the hole-rich structure induced by carbon nanotubes, which could not only efficiently avoid aggregation of nanoparticles during the cacination process and correspondingly enlarge electrode-electrolyte contact area, but also offer channels for infiltration of liquid electrolyte during electrochemical cycling.

C8.52

Structural, Electrical and Electrochemical Properties of the $Na_{2/3}Ni_{1/3}Mn_{2/3-x}Ti_xO_{2-\delta}$ ($0 \le x \le 1/3$) Cathode Materials Anna G. Milewska and Janina Molenda; AGH Academy of Science and Technology, Krakow, Poland.

Results

In this work we present the results of structural, electrical and electrochemical studies of mixed sodium oxides $Na_{2/3}Ni_{1/3}Mn_{2/3-x}Ti_xO_{2-\delta}$ (x=1/10, 1/5, 1/4 and 1/3) as cathode materials for Na-ion batteries. All the samples show P2-type layered structure doped with the impurity NiO phase (samples with x =1/10 and 1/5 contain also additional phase isostructural with $NaTiO_2$). When x in $Na_{2/3}Ni_{1/3}Mn_{2/3-x}Ti_xO_2$ change from 0 to 1/3 *a* parameter linearly increases from 2.885 to 2.925Å and the *c* parameter initial decreases from 11,163Å for x=0 to 11,151Å for x=0.1 and then slightly increases. The thermally activated character of electrical conductivity for all samples is detected. The activation energy of the electrical conductivity is in the range of 0.33 - 0.53 eV. The measured electrical conductivity is low and for $Na_{2/3}Ni_{1/3}Mn_{2/3}O_2$ is equal at about 10^{-7} S/cm at RT. Titanium addition worsens the electrical conductivity of the $Na_{2/3}Ni_{1/3}Mn_{2/3-x}Ti_xO_2$ compounds. Changes of the electrical conductivity measured vs. x at RT correspond with changes of the *c* lattice parameter. We expect that in the temperature over 70°C oxygen nonstoichiometry provides to the modification of the electrical properties of the analysed $Na_{2/3}Ni_{1/3}Mn_{2/3-x}Ti_xO_{2-\delta}$ compounds. Charge-discharge curves measured for $Na/Na^+/Na_{2/3}Ni_{1/3}Mn_{2/3}O_2$ cell exhibits three plateau. H. Yoshida et al. [1] suggests that these phenomena might be related with Na/vacancy ordering, electronic/magnetic ordering and/or phase transition. Titanium substitution suppress these phenomena.

Acknowledgements

The project was funded by a grant from Switzerland through the Swiss Contribution to the enlarged European Union, grant no. 080/2010.

Literature

H. Yoshida, N. Yabuuchi, K. Kubota, I. Ikeuchi, A. Garsuch, M. Schults-Dobrick and S. Komaba, Chem. Commun., 50 (2014) 3677.

C8.53

Dynamics Study of Lithium Ion Diffusion in Super Lithium Ion Conductors, $Li_{10}GeP_2S_{12}$ (LGPS) Masao Yonemura[1], Takashi Kamiyama[1, 2], Ohmin Kwon[3], Satoshi Hori[3], Masaaki Hirayama[3], Ryoji Kanno[3], Kazuhiro Mori[4], Kaoru Shibata[5], Takeshi Yamada[6] and Yukinobu Kawakita[5]; [1]Institute of Materials Structure Science (IMSS), High Energy Accelerator Research Organization (KEK), Tokai, Japan; [2]The Graduate University for Advanced Studies (Sokendai), Tokai, Japan; [3]Department of Electronic Chemistry, Interdisciplinary Graduate School of Science and Engineering, Tokyo Institute of Technology, Yokohama, Japan; [4]Research Reactor Institute, Kyoto University, Kumatori, Japan; [5]Materials and Life Science Division, J-PARC Center, JAEA, Tokai, Japan; [6]Neutron R&D Division, CROSS-Tokai, Tokai, Japan.

Fast ionic conduction in solid electrolytes plays a key role in feasibility of the all-solid-state battery system. Among the lithium ion conductors, the $Li_{10}GeP_2S_{12}$ (LGPS) system shows the conductivity comparable to organic liquid electrolytes. The recent study focused on the synthesis of solid solutions of this material, which might introduce either lithium vacancy or interstitial lithium ions and might affect its ionic conductivity and electrochemical stability. The solid solution was synthesized in the $Li_{4-x}A^{4+}_{1-x}B^{5+}_xS_4$ system and its structure and electrical properties were examined. The crystal structures of the solid solution were studied using neutron diffraction technique. The conduction mechanism was estimated using Maximum Entropy Method (MEM) based on the structure information. This result indicates the lithium conduction pathway is one-dimensional pathway along c axis. However, to understand lithium ionic conductivity in more details, the study of lithium diffusive behaviors is necessary. The dynamics of lithium ion diffusions can be obtained by the Quasielastic Neutron Scattering (QENS) because the quasielastic scattering spectrum is a broadening of elastic peak caused by the diffusion of atoms or ions within a material. When ions cause diffusion motions on a fixed sublattice, the quasielastic scattering spectra can exhibit a *Q*-dependence, which provides information on the dynamical structure of the ions diffusion. The QENS measurements were performed using the high-resolution Si crystal analyzer TOF type near-backscattering spectrometer, DNA, at MLF/J-PARC, Tokai, Ibaraki, Japan, at the energy resolution of 3.6 μeV. From QENS measurements, the dynamics of lithium-ions including the self-diffusion coefficient, jump distance and number density of conduction lithium ions in LGPS system were determined. In this presentation, the mechanism of lithium ion diffusion in LGPS system will be discussed.

Acknowledgement

This work was carried out as the Project research on structure and dynamics of protonic, superionic and amorphous functional Materials using DNA.

C8.54

Lithium Superionic Conductors with $Li_{10}GeP_2S_{12}$-type Structure in the $Li_4MS_4 – Li_3PS_4$ System (M = Si, Ge, Sn): Synthesis, Conduction Mechanism and Phase Relationships Satoshi Hori[1], Ohmin Kwon[1], Kota Suzuki[1], Masaaki Hirayama[1], Masao Yonemura[2], Takashi Kamiyama[2, 3] and Ryoji Kanno[1]; [1]Electrochemistry, Tokyo Institute of Technology, Yokohama, Japan; [2]High Energy Accelerator Research Organization, Institute of Materials Structure Science, Ibaraki, Japan; [3]The Graduate University for Advanced Studies (Sokendai), Ibaraki, Japan.

New lithium superionic conductors promise the potential to replace organic liquid electrolytes and thereby improve the safety of next-generation high-energy batteries. $Li_{10}GeP_2S_{12}$ (LGPS) exhibits an extremely high bulk conductivity of over 10^{-2} Scm^{-1} at room temperature, and is a potential electrolyte candidate for an all-solid-state battery. In order to obtain fundamental information on ionic conductivity, phases and structures, and thereby explore the material diversity of LGPS based electrolytes, the present study focused on the pseudo binary system $Li_4MS_4 – Li_3PS_4$ (M = Si, Ge and Sn). The powdered samples synthesized with the formula $[(1-k)\ Li_4MS_4 + k\ Li_3PS_4]$ were characterized by thermal analysis, diffraction techniques and conductivity measurement. A phase diagram was constructed for the $Li_4GeS_4 – Li_3PS_4$ system and thus the phase formation areas were clarified for the compounds appearing in this

system; Li_4GeS_4, α-/ β-/ γ-Li_3PS_4, and LGPS. The LGPS-phase was found to melt incongruently around 650 °C, transforming into Li_4GeS_4- and liquid- phases, and show the solid-solution range at room temperature from $k = 0.50$ ($Li_{10.5}Ge_{1.5}P_{1.5}S_{12}$) to $k = 0.67$ ($Li_{10}GeP_2S_{12}$) in [(1-k) Li_4GeS_4 + k Li_3PS_4]. The ionic conductivity of the Ge system varied with compositions, reaching the highest value of 1.42×10^{-2} Scm^{-1} (27 °C) at $k = 0.55$. The structural analysis using neutron diffraction data in conjunction with maximum entropy method clarified the lithium distribution, which is closely related to the ionic conduction mechanism. The lithium distribution and lattice size changed depending on the cation *M*, which affects the solid-solution range (Si: $0.525 \leq k \leq 0.60$ and Sn: $0.67 \leq k \leq 0.75$) and the maximum ionic conductivity (Si: 6.7×10^{-3} Scm^{-1} and Sn: 5.0×10^{-3} Scm^{-1}). The relationships between ionic conductivity, phases and structures will be discussed.

C8.55

Effect of Zn-Doping on Densification of $Li_7La_3Zr_2O_{12}$ Emil Hanc, Wojciech Zajac, Angelika Orzeszek and Janina Molenda; Faculty of Energy and Fuels, AGH University of Science and Technology, Cracow, Poland.

One of the basic requirements of the materials for Li-ion batteries is the safety of their use. Recently, due to chemical instability and flammability of liquid organic electrolytes, lithium conducting ceramic oxides attract much attention as electrolytes for Li-cells. Garnet-structured materials from $Li_7La_3Zr_2O_{12}$-group (LLZO) seems to be especially attractive, what is caused by their extraordinary wide electrochemical window ranging up to 10 volts and high ionic conductivity. The standard synthesis process of LLZO is 2-step high-temperature solid state method. The temperature as high as 1200°C is required to obtain dense pellets of LLZO. However, annealing in as high temperature leads to intensified evaporation of Li_2O, what causes difficulty in controlling the stoichiometry of material. Effect of improvement of sinterability by addition of zinc oxide was observed in perovskite-type proton conductors by Babilo and Haile [1]. Similar effect should be observed in garnet structure Li-ion electrolytes.
All samples were prepared by high temperature solid state synthesis. Crystal structure of the obtained materials was investigated at ambient and high temperature using X-ray diffraction (XRD) method. Crystal structure parameters were determined using the Rietveld method with GSAS/ EXPGUI software package. Electrical conductivity was measured in the range 25 - 700°C by means of impedance spectroscopy. Sinterability of materials was investigated using dilatometric method.
The large effect of the Zn addition on the sinterability of LLZO-garnet was observable. The possibility of obtaining dense LLZO-sinters during one-step synthesis was confirmed. The optimal amount of the Zinc additive was defined as 0.1 mol per mol of LLZO. Zn-doped materials exhibit higher ionic conductivity. Electronic conductivity was determined as 10^{-9} S/cm.

[1] Babilo P. Haile S, J. Am. Ceram. Soc., 88 [9] 2362–2368 (2005)

C8.56

Evolution of Microstructure and Its Relation to Ionic Conductivity in $Li_{1+x}Al_xTi_{2-x}(PO_4)_3$ Thomas Hupfer[1], Claudia Bucharsky[1], Günter Schell[1], Anatoliy Senyshyn[2], Mykhailo Monchak[2, 3] and Michael J. Hoffmann[1]; [1]IAM-KWT, KIT, Karlsruhe, Germany; [2]FRM II, SPODI, TU Munich, Garching, Germany; [3]IAM-ESS, KIT, Karlsruhe, Germany.

Solid State Electrolytes are supposed to be key enabling components for the development of the next generation lithium ion batteries. One of the promising materials for Li-ion conduction is $Li_{1+x}Al_xTi_{2-x}(PO_4)_3$ (LATP) due to its high ionic conductivity and stability against water, allowing water based production processes. Much effort is made to understand the influence of crystallographic structure and secondary phases on the ionic conductivity, but little is known about the influence of microstructure. This work aims to provide further information about microstructural properties of LATP, including the influence of heat treatment and grain growth as well as the local distribution of secondary phases. Analytics are done by SEM, EDX and EBSD. It turns out that the limitation for Li^+ conductivity can most likely be found in the combination of grain growth with highly anisotropic thermal expansion. Ionic conductivity reaching up to 1E-3 S/ cm can be achieved by optimized thermal treatment using a conventional air furnace.

C8.57

New Intercalation Cathodes for Calcium Ion Batteries Danielle Proffit[1], Albert Lipson[1], Baofei Pan[1], Brian Ingram[1], Miao Liu[2], Anubhav Jain[2], Kristin Persson[2] and Jack Vaughey[1];[1]Chemical Sciences and Engineering, Joint Center for Energy Storage Research, Argonne National Laboratory, Lemont, Illinois, United States; [2]Electrochemical Technologies Group, Joint Center for Energy Storage Research, Lawrence Berkeley National Laboratory, Berkeley, California, United States.

The increasing demand for energy and sustainability has pushed the search for battery technologies beyond that offered by lithium-based materials. Particularly, predictions of higher energy density from multivalent systems, which can theoretically transfer two or more electrons per ion, have increased interest in the development of calcium and magnesium batteries, which require the development of new electroactive materials . Several technical challenges for these post-Li ion battery chemistries exist, one of which is the transport of the ion through the solid intercalation host. In the case of multivalent ions, the increased valence of the ion is expected to slow the kinetics of diffusion and may limit the choice of electrode material. We will present recent research on potential intercalation cathodes for calcium ions that have shown promise. For example, the potential for layered oxides such as Ca_xCoO_2 to intercalate Ca will be compared to the monovalent sodium and lithium analogs. In particular, it will be noted that the design rules for calcium transport do not necessarily correspond well to sodium, lithium, or magnesium transport. Finally, the promise of calcium ion batteries will be discussed.

C8.58

Mixed Glass Former Effect in $50Li_2O$-$50[xNb_2O_5$-$(1-x)P_2O_5]$ Glasses Prashant Dabas and K. Hariharan; Physics, Indian Institute of Technology Madras, Chennai, India.

Binary lithium phosphate glasses are ionic conductors; however, their hygroscopic nature and low ionic conductivity has limited their use in solid state ionic devices. Adding a suitable second glass former is expected to not only improve their stability but also the conduction characteristics of these glasses. In this regard, glasses in the series mol% $50Li_2O$-$50[xNb_2O_5$-$(1-x)P_2O_5]$, x=0 to 0.8 are investigated with Nb_2O_5 as the second glass former. Glasses up to x=0.6 were prepared by the conventional quenching method while the x=0.7 and 0.8 glasses were prepared using a home-built twin-roller rapid quenching setup. The glass modifier (Li_2O) content is kept fixed at 50 mol% while P_2O_5 is sequentially replaced by Nb_2O_5. The conductivity (σ) of a sample depends on the concentration (n) and mobility (μ) of the charge carriers by the relation, $\sigma = nq\mu$, where q is the charge on the carriers. In the above samples, the charge carrier concentration is fixed (mol% 50). Therefore, the structural changes dictate the mobility of the lithium ions. Variation of the following physical quantities with composition are investigated; i) glass transition temperature, ii) dissolution rate, iii) density, iv) Vickers hardness, v) structure, vi) ionic conductivity, vii) activation energy for lithium ion conduction, viii) fragility index, and ix) crystallization behavior. Addition of just 5 mol% (x=0.1) Nb_2O_5 renders the glass non-hygroscopic. The glass x=0.4 depicted a maximum conductivity of 2.0×10^{-6} Scm^{-1} (403 K) with a corresponding minima in the activation energy for lithium ion motion. The competitive network formation of PO_4 tetrahedra and NbO_6 octahedra in the glass matrix influences the lithium ion motion leading to the “mixed glass former effect”. The variation in ionic conductivity and activation energy for lithium ion motion in the glasses are discussed considering the Raman spectra in light of “Anderson-Stuart Model”.

C8.59

Tin Networked Electrode Providing Enhanced Volumetric Capacity and Pressureless Operation for All-Solid-State Li-Ion Batteries Justin M. Whiteley[1], Ji Woo Kim[1], Chan Soon Kang[2], Jong Soo Cho[1], Kyu Hwan Oh[2] and Se-Hee Lee[1]; [1]Mechanical Engineering, University of Colorado, Boulder, Boulder, Colorado, United States; [2]Materials Science and Engineering, Seoul National University, Seoul, Korea (the Republic of).

Pure tin (Sn) metal nano-powder is investigated as a high capacity negative electrode for rechargeable all-solid-state Li-ion batteries. Sn is used to form a fully dense network intertwining with solid electrolyte negating necessary conductive additive. Galvanostatic cycling of the Sn composite electrode delivers a reversible capacity 800 mAh g^{-1} of Sn with a constant coulombic efficiency over 99.2%. We report on the effect of pressure and rate upon the delithiation mechanics, drawing correlations between Sn volume increase factors and stress accumulation over the course of Sn-Li phase transformations. Due to the fabricated electrode microstructure, we are able to operate the cell at ambient pressure conditions – the next step toward commercialization of the solid-state battery. We believe that this initial work provides new opportunities to study the electrochemical expansion of Sn with the inclusion of rigid electrolyte particles.

C8.60

Synthesis and Electrochemical Properties of SiO_x/C Amorphous Composite as Anode Material for Lithium Ion Batteries Pengpeng Lv, Hailei Zhao, Chunhui Gao and Zhaolin Li; University of Science and Technology Beijing, Beijing, China.

Silicon oxycarbide (Si-O-C) glass-like material has been extensively investigated for potential high-performance anode material since it was first reported by J. Dahn in 1994. The Si-O-C glass-like materials usually include Si-O-C glass as a major phase, which consists of tetrahedral units of ($SiO_{4-n}C_n$) (where $0 \le n \le 4$), and free carbon as a second phase. Due to the disordered Si-O-C networks, this material can offer high specific capacity and good cycling stability. The choice of polymeric precursor containing Si-C bonds is crucial to the preparation of the Si-O-C glass material. However, the existence of Si-C bonds in the Si-O-C phase restricts in a certain degree the electrochemical activity of silicon because of the irreversible formation of inactive SiC_4 units during lithiation process. In this work, SiO_x-C dual-phase glass without Si-C bonds was synthesized via a sol-gel and pyrolysis route with a low-cost siloxane (tetraethoxysilane, TEOS) as silicon source. The synthesized SiO_x-C dual-phase glass, which consists of well-dispersed amorphous SiO_x and free carbon phases at nanoscale, exhibits high specific reversible capacity, good rate capability and stable cycling performance. The preparation process of SiO_x-C dual-phase glass is facile, low-cost and productive. NMR examination shows that there are different units of $Si(O_4)$, $Si(SiO_3)$, $Si(Si_2O_2)$ and $Si(Si_4)$ existing in SiO_x-C dual-phase glass. No SiC_4 building unit (SiC phase) is observed, revealing the absence of Si-C bonds in the SiO_x-C dual-phase glass. The synthesized SiO_x-C dual-phase glass demonstrates a high reversible capacity and an excellent cyclic performance. The reversible capacity remains at 840 $mAhg^{-1}$ till 100 cycles without any tendency of degradation. The synthesized SiO_x-C dual-phase glass is a promising anode material for lithium ion batteries.

C8.61

Impedance Investigation of the Processes on SiC/Li^+-Electrolyte Interface Ekaterina Antonova[2], Elizaveta Evschik[1], Alexey Levchenko[1], Viktor Berestenko[1] and Yury Dobrovolsky[1];[1]IPCP RAS, Chernogolovka, Russian Federation; [2]IHTE UB RAS, Ekaterinburg, Russian Federation.

Lithium-ion batteries are one of the most promising rechargeable energy sources. In all commercialized lithium-ion batteries negative electrode is produced from carbon materials. Modern lithium-ion batteries have specific energy 150–200 W*h/kg. These values probably are possible limit in utilization of current materials. Thus, a search of the new electrode materials with higher capacity is one of the main problems in a battery development. Systems based on silicon carbides are promising materials for anodes in lithium-ion batteries. Theoretical capacity values of these anodes can reach 2500 mA*h/g [1].

The aim of the present research was a characterization of electrode processes on SiC/Li^+-electrolyte interface depending on synthesis conditions for SiC.

SiC powders were synthesized by plasma-chemical method. In the present work two types of SiC samples obtained in argon- and hydrogen-containing atmospheres were studied. Electrical measurements were carried out using an electrochemical impedance spectroscopy in a three-contact cells. Li was taken as the material for counter and reference electrodes. $LiPF_6$ in ethylenecarbonate : diethylcarbonate : dimethylcarbonate mixture in ratio 1:1:1 (Merck) was used as an electrolyte.

From the obtained results it follows that charge curves for both type of samples have a similar view: a potential sharply decreases from initial value of 2,7 – 2,9 V to 1,25-1,3 V and then decreases smoothly with several bends. The type of a carrier gas used in the SiC synthesizing has a significant influence on a view of impedance spectra. For a sample synthesized in argon both high frequency and low frequency components of hodographs have significantly smaller resistance values than for SiC synthesized in hydrogen. Nevertheless all spectra may be interpreted within one equivalent circuit.

Studies have shown that during the process of equilibrium establishing on the interface SiC/Li^+-electrolyte impedance hodographs changes. The high frequency semicircle increases and inductive-like feature appears. It may be associated with the formation of the solid electrolyte interphase at the boundary.

During the charging process a size of high frequency part of the spectra increases. This effect may be a consequence of increasing thickness of solid electrolyte interphase on the SiC surface during the lithium intercalation. At the same time low frequency part of impedance spectra decreases. It may be probably caused by increasing reversibility of lithium transfer processes at the electrode / electrolyte interface.

Acknowledgements
This work was partly supported by the Russian Foundation for Basic Research, project No. 14-33-50939.

References

1. Bup Ju Jeon, Joong Kee Lee. Electrochemical characteristics of nc-Si/SiC composite for anode electrode of lithium ion batteries // Journal of Alloys and Compounds. 2014. N.590, P.254–259.

C8.62

Synthesis and Na^+ Conduction Properties of Rare Earth-Free NASICON-Type Solid Electrolyte Toshinori Okura[1], Naoya Yoshida[1] and Kimihiro Yamashita[2]; [1]Kogakuin University, Hachioji, Japan; [2]Tokyo Medical and Dental University, Chiyoda, Japan.

Glass-ceramics of the phosphorus containing $Na_5RSi_4O_{12}$ (N5)-type (R=rare earth) Na^+-superionic conductors have been developed by crystallization of glasses with the composition $Na_{3+3x-y}R_{1-x}P_ySi_{3-y}O_9$ (Narpsio). These materials are comparable to the conventional ceramic Na^+-conductors such as NASICON, β- and β”-aluminas (e. g., $NaAl_{11}O_{17}$ and $NaAl_5O_8$). Our phosphorus containing compositions have been confirmed superior to the mother composition of N5, especially in the production of the single-phase glass-ceramics. The R elements also have been expected to have a significant effect on the crystallization of glasses, as well as on the conduction properties. To date, polycrystalline N5-type Narpsio has been obtained with Sc, Y, Gd or Sm as the R element. It is currently assumed from the analogy with N5 that all the R ions can be octahedrally coordinated with the non-bridging oxide ions of the (SiO_4, PO_4)-tetrahedra of the 12-membered rings. Our main work has recently been focused on the synthesis of various glass-ceramics with N5 single-phase. In the present study, we tried to synthesize them without R elements, but with Fe of high abundance and low costs, by melt quenching and glass-crystallization method. The glass-ceramics of the boron-containing N5-type Na^+-superionic conductors from the glasses with the composition $Na_{5+x}FeB_xSi_{4-x}O_{12}$ were successfully produced. Ionic conductivities of sintered disks were measured by the AC two-probe

method with Au-sputtered blocking electrodes with a LF impedance analyzer. The temperature dependence of the conductivity was measured at several temperatures ranging from room temperature to 350°C. The ionic conductivity and the activation energy of the glass-ceramic $Na_{5.2}FeB_{0.2}Si_{3.8}O_{12}$ (x=0.2) were 3.05×10^{-3} at 300°C and 48.5 kJ/mol, respectively.

C8.63

Interfacial Modification of All-Oxide-Solid-State Battery with Low Surface Energy Solid Electrolyte Shogo Komagata, Shingo Ohta and Takahiko Asaoka; Toyota Central R&D Labs. Inc., Nagakute, Japan.

Recently lithium-ion batteries are widely used as power sources of cell phones, laptop PCs, EVs and so on. However, safety issue of these batteries becomes big problem, due to their high energy density and using combustible organic electrolytes. Substitution of an organic electrolyte to a stable oxide lithium ionic conductor is one candidate to solve this problem. Until now our group has developed the garnet type lithium ionic conductor $Li_{6.75}La_3Zr_{1.75}Nb_{0.25}O_{12}$ (LLZN) and has demonstrated the battery operation by intervention of a low melting point solid electrolyte between the LLZN and an active material [1, 2]. The solid electrolyte having low melting point acts an important role as adhesion bond to form solid-solid interface whose character often controls solid battery performance. One of a guide to fabricate electrochemically good solid-solid interface is to choose an electrolyte that shows low surface energy between both the other electrolyte and an active material. One candidate who has low surface energy to both LLZN electrolyte and $LiCoO_2$ active material is Li_2CO_3 based material. Li_2CO_3 is easily produced and densely coats at surface both of them. It certainly indicates that the surface energy between Li_2CO_3 and LLZN or $LiCoO_2$ is low.

In order to confirm the impact of surface energy to electrochemical interface, fabrication of Li / LLZN / $LiCoO_2$+Li_2CO_3-Li_3BO_3 (LBCO) cell is done. LBCO is chosen because its high ionic conductivity among Li_2CO_3 based materials. [3] The cell shows the capacity of 108mAh/g-$LiCoO_2$ (94% of high availability) and no significant capacity deterioration in primary charge and discharge cycles. Also charge transfer resistance of the cell becomes 97 Ωcm^2, which is half of what our group reported previously [2]. The result shows that electrochemically good solid-solid interface is fabricated by using LBCO solid electrolyte.

Reference
[1] S. Ohta et al., J. Power Sources, 196 (2011) 3342
[2] S. Ohta et al., J. Power Sources, 238 (2013) 53
[3] R. Shanon, Electrochimica Acta, 22 (1977) 783

C8.64

Fluoride-Phosphates as Positive Electrode Materials for Metal-Ion Batteries Nellie Khasanova, Stanislav Fedotov, Oleg Drozhzhin and Evgeny Antipov; Chemistry Department, Lomonosov Moscow State University, Moscow, Russian Federation.

Among the energy storage technologies, rechargeable battery technology is one of the most promising means of storing electricity on a large-scale due to its flexibility and high energy conversion efficiency. The success of metal-ion batteries for large scale applications such as electric vehicles and stationary energy storage devices relies heavily on the development of new cathode materials with high power and energy density along with long cycle life. In the search for high-energy cathode materials for metal-ion batteries we have explored the A_2MPO_4F (A=Li, Na; M=Co, Mn, Fe) fluoride-phosphates with 3D and layered structures. The fluoride-phosphates were prepared through different synthetic routes (solid-state reactions, cryochemistry, ion-exchange) depending on the chemistry of transition metal. Combination of synchrotron X-ray/neutron diffraction and NMR spectroscopy were applied to present a thorough structural characterization; electrochemical activity of fluoride-phosphate materials was tested in Li- and Na-cells. Electrochemical measurements revealed that lithium de/intercalation in 3D-Li_2MPO_4F system occurs in the solid solution regime with average discharge voltages ranging from 3.4 V (vs. Li/Li^+) for Li_2FePO_4F to 4.8 V for the Co-counterpart; and the redox potential might be tuned by appropriate substitution on the transition metal site. Electrochemical properties of 3D fluoride-phosphate family will be compared with those of layered compounds; and impact of structure peculiarities (dimensionality, conjugation of transition metal octahedra) will be discussed.

C8.65

Evaluations of Iron Based Cathode Materials for Li-Ion Batteries--Case of $LiFe_{1-y}M_yPO_4$, Nanometric $LiFePO_4$ and $LiFeO_2$ Andrzej J. Kulka, Wojciech Zajac, Konrad Swierczek, Katarzyna Walczak and Janina Molenda; AGH-University of Science and Technology, Cracow, Poland.

Iron based cathode materials for Li-ion batteries are especially interesting in terms of their non-toxicity and low fabrication costs. In past decade, $LiFePO_4$ and $LiFeO_2$ have attracted considerable research attention. Here we present systematic study of doping effect of 3d transition metal ions (Co, Mn) on structural and electrochemical properties of $LiFe_{1-y}M_yPO_4$, as well as evaluation of electrochemical properties of nanometric $LiFePO_4$ and $LiFeO_2$/Mo glassy phase composite.

We performed electrical conductivity and Seebeck coefficient measurements of $LiFe_{1-y}M_yPO_4$ cathode materials. Additionally, by means of in-situ XRD studies and OCV measurements of $Li/Li^+/Li_xFe_{1-y}M_yPO_4$ cells we investigated lithium deintercalation/intercalation process into iron-site doped phosphoolivines and nanometric $LiFePO_4$. We found that nanosized $LiFePO_4$operates broadly via single-phase lithium deintercalation/intercalation reactions under charge/discharge process. Electrical conductivity of $LiFe_{0.75}Co_{0.25}PO_4$ is higher than undoped $LiFePO_4$ and results in diffusional mechanism of lithium intercalation/deintercalation. Simultaneous doping of Mn and Co in $LiFe_{1-w-y}Co_wMn_yPO_4$ leads to lower electrical conductivity than pristine $LiFePO_4$ and two phase lithium deintercalation/intercalation mechanism. Additionally, HT-XRD measurements of deintercalated $Li_xFe_{1-w-y}Co_wMn_yPO_4$ revealed that at temperatures above 250°C homogenization of two phases occurs which can be attributed to increase of the electrical conductivity.

$LiFeO_2$ possesses high theoretical capacity but is regarded as metastable upon lithium deintercalation/intercalation process. We present data regarding electrochemical properties of $LiFeO_2$/Mo glassy phase composite obtained by simple high-temperature method which show remarkably high and stable discharge capacity during charge/discharge process. It was found that Mo-glassy phases stabilize crystal structure of $LiFeO_2$ which is present after 60 charge/discharge cycles. In-situ XRD measurements were employed in order to investigate the evolution of crystal structure of $LiFeO_2$ during first and forth charge/discharge process. Our result indicate possibility of stabilization of $LiFeO_2$ metastable phase during lithium intercalation/deintercalation process by introduction Mo-glassy phases. Work was supported by the Polish-Swiss Research Programme under grant no. 080/2010 LiBeV.

C8.66

Effect of Glass Additives on Relative Density and Li-Ion Conductivity of $Li_{7-x}La_3Zr_{2-x}Nb_xO_{12}$ Solid Electrolyte Nataly C. Rosero Navarro, Taira Yamashita, Akira Miura, Mikio Higuchi and Kiyoharu Tadanaga; Hokkaido University, Sapporo, Japan.

$Li_7La_3Zr_2O_{12}$ (LLZO) solid electrolyte presents a high chemical stability against Li metal and a rather high Li^+ conductivity ($3x10^{-4}$ S/cm). Efforts to increase the Li ion conductivity of pristine LLZO garnet and/or reduce the sintering temperature (Ts <1200 ºC) have been reported by different authors. The partial substitution of similar or larger ionic radii elements (Ge, Ta, Y and Nb) helps to increase the total Li-ion conductivity reaching maximum around $8x10^{-4}$ S/cm at 25 ºC. However, dense ceramic material sintered at lower temperatures only has been achieved by the use of sintering additives. Li-ion conductivity using Li_3BO_3 as additive (Ts: 800 – 900 ºC) in the order of 10^{-4} S/cm has been reported [1-2]. The next challenge is to obtain an adequate performance in the interface electrolyte/cathode. Here, the effect of glass additives on the performance of Lithium garnet-type oxides $Li_{7-x}La_3Zr_{2-x}Nb_xO_{12}$ (LLZNbO, x=0-1) solid electrolyte is studied. Glass additives: LiO_2-B_2O_3-SiO_2 (Li-B-Si) and BaO-B_2O_3-SiO_2 (Ba-B-Si) were used. The maximum density of composites with additives sintered at 900 ºC achieves 86%. In the composites sintered with Ba-B-Si glass, the presence of $La_2Zr_2O_7$ was detected at concentration higher of 4 wt%, while single cubic phase was obtained for the composites sintered with Li-B-Si glass. The ion conductivity attained was $8x10^{-5}$ S/cm at 30 ºC using 4 wt% of Li-B-Si glass at 900 ºC. Interface between solid electrolyte composite and $LiCoO_2$ cathode is also studied by SEM and

EIS, which should have an important contribution to further applications of the solid electrolyte to all-solid-state battery.

References
1. K. Tadanaga, R. Takano, T. Ichinose, S. Mori, A. Hayashi and M. Tatsumisago, Electrochemistry Communications, 33, 51 (2013).
2. S. Ohta, J. Seki, Y. Yagi, Y. Kihira, T. Tani and T. Asaoka, Journal of Power Sources, 265, 40 (2014).

C8.67

Sodium Ion Conducting Ceramics with $Na_5YSi_4O_{12}$-Type Structure Synthesized by a Polymerized Complex Method Naohiro Horiuchi[1], Kaede Ryu[2], Naoya Yoshida[2], Toshinori Okura[2] and Kimihiro Yamashita[1]; [1]Institute of Biomaterial & Bioengineering, Tokyo Medical and Dental University, Tokyo, Japan; [2]Kogakuin University, Hachioji-shi, Japan.

Sodium ion conducting ceramics with $Na_5YSi_4O_{12}$-type (N5-type) structure which has the composition formula $Na_{5+3x-y}Y_{1-x}P_ySi_{4-y}O_{12}$ were synthesized by a polymerized complex method. The SiO_4-tetrahedra were substituted by the PO_4-tetrahedra, and the charge compensation was achieved by substitution of Y^{3+} for Na^+. In this study, the synthesis was started from sodium silicate water solution. Citric acid and ethylene glycol were used as complexation/polymerization agents. X-ray powder diffraction confirmed that the sintered pellets had single phase with N5-type structure. The ionic conductivity of ceramic pellet with $x = 0.20$, $y = 0.27$ sintered at 1373 K reaches about 4.3×10^{-2} S/cm at 573 K. This value is comparable to that of glass–ceramics (our previous report: Solid State Ionics, 262, 604–608, 2014)In this study, we also tried to synthesize Ca doped pellets ($Na_{5+3x-y-2z}Ca_zY_{1-x}P_ySi_{4-y}O_{12}$) with N5-type structure. The influence of Ca on the phase stability of N5-type structure also discussed in this presentation.

C8.68

Development of Salty-Gel Electrolytes Composed of Metal Salt and Small Amount of Organic Solvent as a New Concept for Organic Solid Electrolytes Makoto Moriya[1, 2, 3], Shohei Nabeno[3], Yutaro Hanawa[3], Wataru Sakamoto[3] and Toshinobu Yogo[3]; [1]Graduate School of Science, Shizuoka University, Shizuoka, Japan; [2]JST PRESTO, Kawaguchi, Japan; [3]EcoTopia Science Institution, Nagoya University, Nagoya, Japan.

We herein report the synthesis of new solid electrolytes consisting of lithium, sodium, or magnesium salt with small amount of organic solvent that we have named salty-gel electrolytes. The salty-gel electrolytes are a mixture of the metal salt and a molecular crystal with low melting point, which is yielded by the coordination of organic solvent to metal ion. Since the salty-gel electrolytes exhibit solid-liquid coexistence state composed of metal salt as a solid matrix and melt of the molecular crystal, these electrolytes show high ionic conductivity at ambient temperature in the solid state as a result of fast ion diffusion through the liquid content. For example, a salty-gel electrolyte, which is an equimolar mixture of a novel molecular crystal, [Na{$N(SO_2CF_3)_2$}(CH_3CN)], and Na{$N(SO_2CF_3)_2$} (NaTFSA), shows solid-state ionic conductivity of approximately 10^{-3} S cm^{-1} at room temperature. We also report the fabrication of rechargeable batteries by using the obtained salty-gel electrolytes.

C8.69

Investigation of Negative Electrode for All-Solid-State Lithium Ion Battery using Garnet-Type Oxide Electrolyte Tetsuro Kobayashi, Shingo Ohta and Takahiko Asaoka; Toyota Central R&D Labs.,Inc., Nagakute, Japan.

All-solid-state batteries using nonflammable solid electrolytes have attracted much attention as a next-generation battery having both safety and high energy density. We are conducting research on an all-solid-state lithium ion battery with a garnet-type oxide $Li_{7-x}La_3Zr_{2-x}Nb_xO_{12}$ (LLZONb) as the electrolyte. In our previous works, we have used $LiCoO_2$ as a positive electrode and Li metal as a negative electrode for the battery. However, the other electrode materials for this all-solid-state battery are also strongly required in order to improve the battery performance further. In this work, we have focused on an InSb alloy which has been reported that its volume change during charge-discharging is small. Firstly, In, Sb metals and an InSb alloy were deposited respectively on a Cu foil by a pulse laser deposition (PLD) method, and then the changes in volume of these metals and the alloy during charge-discharging were measured in cells using an organic liquid electrolyte and Li metal as a counter electrode. The volume change of the InSb alloy was smaller than those of In and Sb metals. Next, an all-solid-state battery was fabricated by depositing an InSb alloy on the sintered pellet of a garnet-type oxide LLZONb by a PLD method and contacting a Li metal foil on the opposite side of the pellet as a counter electrode. This all-solid-state battery was able to be charged and discharged well at room temperature with an average voltage of 0.93 V and a capacity of 3500 mAh/cm^3-InSb.

C8.70

Low Temperature Synthesis of Yb Doped $SrCeO_3$ Electrolyte Thin Film for Hydrogen Separation Yang Lei, Chao Zhang, Di He, Shuai Li, Xiaopeng Liu and Lijun Jiang; Department of Energy Materials and Technology, General Research Institute for Non-Ferrous Metals, Beijing, China.

High temperature proton conducting electrolytes have attracted wide attentions due to their applications in hydrogen sensors, permeable membranes for hydrogen separation, and solid oxide fuel cells (SOFCs) etc. Among the various proton conducting electrolytes, $SrCeO_3$ is a promising electrolyte material because of its high proton conductivity. However, the traditional solid state reaction in the $SrCeO_3$ preparation suffers from drawbacks such as high heat-treatment temperature and impurities introduced during repeated ball milling.

In this work, Yb doped SrCeO3 (SCYb) powders were synthesized by a gel combustion method with the citric acid and NH_4NO_3, which combined gel process and combustion process. The effect of ratio of citric acid to metal cations (C/M), oxidizer and calcination temperature on the properties of powders was investigated in detail. The powder was characterized by TGA, XRD and SEM. The mechanism of combustion reaction was studied by the thermodynamic calculation. The experimental results indicated that the relative amount of SCYb in the powder increased as the C/M ratio increased. The relative amount of $SrCeO_3$ of the as-ignited powder was 95.2 wt% with the C/M ratio of 3. Thermodynamic calculation showed that the adiabatic flame temperature of the combustion was 1903.1 °C, which favored the formation of $SrCeO_3$. Furthermore, the pure perovskite phase powder with agglomerated microstructure and average grain size of 2 mm was obtained after calcination at 1200 °C for 5 h.
Through this work, it is demonstrated that the SCYb powders we prepared by a gel combustion method can be applied as a high performance electrolyte material in the hydrogen separation device.

C8.71

Improved of Electrochemical Performances of Manganese-Substituted $Na_{0.7}Co_{1-y}Mn_yO_2$ - Cathode Material for Rechargeable Sodium-Ion Batteries Dominika Baster, Filip Hartman, Lukasz Kondracki, Andrzej Kulka, Wojciech Zajac and Janina Molenda; AGH University of Science and Technology, Krakow, Poland.

Sodium-ion batteries were proposed as a low cost alternative to Li-ion batteries, and rapid progress has been made in developing high capacity cathode materials. It has become clear that the Na analogues of the successful layered $LiMO_2$ electrodes behave very differently from their Li equivalents. For example, $LiCoO_2$ has excellent operating voltage in wide range of lithium content with high discharge capacity, but Na_xCoO_{2-y} exhibits unusual step-like shape of a voltage curve, with several characteristic voltage pseudo-plateaus. In order to improve electrochemical properties of Na_xCoO_{2-y} manganese substitution in cobalt sublattice is proposed.

This work presents a high-temperature method of synthesis $Na_xCo_{1-y}Mn_yO_2$ - new cathode materials for Na-ion batteries. The crystal structure and mechanism of charge transport in $Na_{0.7}Co_{1-y}Mn_yO_2$ is discussed. The obtained materials were applied as cathodes in $Na/Na^+/Na_xCo_{1-y}Mn_yO_2$ -type cells. Specific capacity, reversibility and stability during charge-discharge cycles were evaluated to characterize electrochemical properties of the cells. The highest discharge capacity of examined cells is observed for $Na_{0.7}Co_{0.7}Mn_{0.3}O_2$ (104 mAh·g^{-1}) with voltage in the range 2.5-3.4 V delivering energy density over 300 mWh·g^{-1}. In order to

understand details of mechanism of electrode reaction impedance spectra measurements were performed on cathode material in which sodium content was changed by electrochemical titration in the wide range of compositions. $Na_{0.7}Co_{0.7}Mn_{0.3}O_2$ showed stability in contact with electrolyte (1M solution of $NaClO_4$ in propylene carbonate) in temperature range from -30 °C to 150 °C and proved to be a safe and reliable candidate cathode material for Na-ion batteries. Thermal stability were investigated using low and high temperature XRD measurements in wide range of temperature (13-1073 K).

The project was funded by the National Science Centre Poland (NCN) on the basis of the decision number DEC-2011/02/A/ST5/00447.

C8.72

Earth-Abundant Cathode Materials for Sodium-Ion Batteries P2-$Na_{2/3}Fe_{1-y}Mn_yO_2$ Dominika Baster, Piotr Trzaska and Janina Molenda; AGH University of Science and Technology, Krakow, Poland.

Nowadays, further development of rechargeable batteries is focused on the discovery of new, high-performance and low-cost electrode materials. Recently, sodium-ion batteries have attracted much attention due to their many advantages, such as high abundance of sodium in the Earth's crust, its low cost and suitable redox potential (only 0.3 V above that of lithium). Among possible electrode materials for Na-ion batteries, layered compounds Na_xMO_2 (M = 3*d* transition metal element) have attracted much interest since the 1980s. However, layered oxides mostly based on expensive and toxic transition metals such as Co and Ni. Therefore, the major challenge in advancing Na-ion batteries technology lies in finding suitable cathode material based on abundant, low-cost, safety and environmental benign elements such as manganese and iron.

This work presents synthesis method of P2-$Na_{2/3}Fe_{1/2}Mn_{1/2}O_2$ by a solid-state reaction with Na_2CO_3 (POCH, 99.8%), Fe_2O_3 (POCH, 99%), $MnCO_3$ (Chempur, > 99.9%) used as substrates. XRD measurements with Rietveld analysis confirmed the presence of a single phase with *P6$_3$/mmc* symmetry. The lattice parameters for the obtained material were found to be equal to: a = 0.29223(9) nm and c = 1.12582(8) nm. The powder was then applied as cathode materials in Na/Na^+/$Na_xMn_{1/2}Fe_{1/2}O_2$-type cells. Specific capacity, reversibility and stability during charge-discharge cycles were evaluated to characterize electrochemical properties of the cells. Recorded discharge capacity of examined cells is equal ~140 $mAh \cdot g^{-1}$. The shapes of the discharge curves together with the mechanism of electrode reaction during sodium intercalation/deintercalation are discussed. Measurements of thermal and chemical stability of cathode material with organic electrolyte confirm safety for using in Na-ion batteries. In order to explain mechanism of charge transport temperature dependence of electrical conductivity and Seebeck coefficient were examined.

The project was funded by the National Science Centre Poland (NCN) on the basis of the decision number DEC-2011/02/A/ST5/00447.

C8.73

Low Temperature Conductivity Response in Polymer Blend Electrolyte Avirup Das[2], A K. Thakur[1] and K Kumar[2]; [1]Physics, Indian Institute of Technology Patna, Patna, India;[2]Physics, Indian Institute of Technology Kharagpur, Kharagpur, India.

Portable power systems endowed with high energy density is a mandatory requirement to cater the need of ever expanding consumer electronics market. Devices workable over wide temperature limits ranging from sub-ambient (<0^0C) to super-ambient (>30^0C) temperature are the most sought after. K. Tikonov *et.al* [1] has demonstrated that Li ion battery can be operated over temperature limits~± 80^0C whereas the consumer electronics operates in between 60^0C to -20^0C. The low temperature performance of different Li ion cells [2] like Panasonic, AT & T and Moli shows a drastic degradation of performance at sub-ambient temperature (~ - 40^0C) in sharp contrast to ambient temperature performance. According to literature reports, the origin of failure of Li ion battery at low temperatures arise due to; (a) the "electrolyte property" [3], (b) enhanced interfacial resistance at sub-ambient temperatures [2]. To overcome the problems, different approaches such as introducing new carbonate based solvent mixture or replacing the existing Li based salt by efficient alternatives are under investigation [4].

In the present work, we have attempted to explore such an alternative using blend based polymer-salt over wide ranging Li-salt composition. It has already been observed previously that PEO-PDMS (30wt %) blended matrix complexed with LiI has successfully enhanced the conductivity of the PEO-LiI system [5]. So, in a blend polymer matrix, the physical property of the individual polymer hosts (e.g. flexibility of polymer chain, glass transition - T_g ~ -65^0C for PEO and T_g ~ -127^0C for PDMS etc.) can produce a combined effect making the blend host compatible at lower temperatures. Literature indicates ambient temperature(~30^0C) conductivity of PEO-$LiCF_3SO_3$ based systems varies from 10^{-6} Scm^{-1} to 10^{-8} Scm^{-1} whereas inclusion of carbonate based solvent increases the ambient temperature conductivity as high as ~10^{-4} Scm^{-1}. We, therefore, extended this work over sub-ambient temperature (<0^0C) limit.

We report optimization of ionic conductivity in a PEO–PDMS blend complexed with $LiCF_3SO_3$. The blend formation and ionic interaction between the cation and polymer blend has been confirmed by Raman analysis results. The cation coordination site is in the PEO–PDMS blend. X-ray diffraction (XRD) and scanning electron microscopy (SEM) has been analyzed to examine structural and surface property. Thermal stability has been investigated using DSC techniques. An optimum conductivity of 1×10^{-6} S cm^{-1} has been obtained for Ö/Li ~15 after investigating the polymer salt samples within ±30 °C range. Further, this optimized conductivity reduced up to two orders at 0 °C and it remains unchanged at −10 °C. The free standing blend polymer electrolyte shows a predominantly ionic (t_{ion} ~98 %) conduction with voltage stability upto 2.3V. Further investigations to enhance the conductivity in the sub-ambient range are going on in the laboratory.

Reference:

1. K. Tikonov, V. R. Koch www.covalentassociates.com
2. G. Nagasubhramanian J. of applied electrochemistry 31 (2001) 99-104
3. M.e. Smart', B.V. Ratnakumar, and L. D. Whitcanack AIAA.
4. S.S. Zhang, K. Xu, T.R. J. Electrochimica Acta 49 (2004) 1057–1061
5. Lee JY, Bhattacharya B, Kim DW, Park JK J Phys Chem C 112, (2008). 12576–12582

C8.74

Supercapacitor Response of Tin Sulfide Electrodes Pradip Leuaa, Ajay D. Thakur and Awalendra K. Thakur; Physics, IIT Patna, Patna, India.

High energy density portable power sources such as rechargeable batteries, supercapacitors etc. have become indispensable ingredient of the rapidly changing face of the consumer electronics and our heavy dependence on them. It is well understood that electrodes as component play a crucial role in determining the performance of portable power devices. So, the search of low cost, high capacity, non-toxic and stable electrode materials has always been a challenging task.

Many alternatives including carbon allotropes, metal oxides, Sn based combinations like SnO_2, SnSe etc. have been extensively studied as anode materials for LIBs and symmetric electrodes for supercapacitor design. However, it has been noted that lithium diffusion into these materials creates a large volume expansion and performance degrades over time due to loss of contact with the current collector. Instead, tin sulfide (SnS) is an interesting anode material for lithium ion battery (LIB) and may also be a suitable electrode for supercapacitor applications because of its high theoretical capacity, synthesis out of inexpensive earth abundant elements and role of sulfur as a buffer layer imparting increased cycling performance.

In this work, we report a hierarchically nano-structured SnS endowed with desirable features such as; pure phase, high surface area, shortened lithium ion diffusion pathways and increased electrode-electrolyte interface properties. Its properties as a supercapacitor electrode have been investigated using a 3-electrode cell configuration in aqueous 1 M KOH, 1 M KCL and 1 M H_2SO_4 solutions. The chemical and electrochemical stability of SnS nanocrystals was observed robust over 1000 cycles. Coulombic efficiency has been observed to be ~100 % and specific capacitance remained stable over 1000 cycles. Further studies are going on.

C8.75
Spinel $LiCrTiO_4$ as a LIB Anode : A Density Functional Theory Approach Biswajit Mondal and Awalendra K. Thakur; Physics, IIT Patna, Patna, India.

Spinel structures (e.g.; AB_2O_4) have received great attention as future generation electrode materials for Li ion battery (LIB) applications. As far as anode for LIB design is concerned, graphite is the only material commercialised successfully till date. However, it has inherent problems related to Li plating, durability and costly processing. This has necessitated the quest for future generation anode materials having ideal properties like high capacities, good electronic conductivity, acceptable Li-intercalation-deintercalation into or out of the lattice without destroying crystal structure, minimal strain and eco-friendly attributes etc.

Since beginning of research in the area of LIB electrodes, transition metal oxides and chalcogenides etc. have been explored extensively as electrodes for LIBs applications. Recently, oxide of titanium and oxide of silicon have received more attention, the typical examples being Li_2FeSiO_4, $LiM_xMn_{2-x}O_4$. On the other hand, for anode applications, $Li(Li_{1/3}Ti_{5/3})O_4$(abbreviated as $Li_4Ti_5O_{12}$) is reported to be more promising than their conventional counterparts. However, it has poor Li^+ diffusion coefficient and poor electronic conductivity in spite of being found suitable otherwise. So, search for an appropriate anode material is still on.

In this work, we report the results of our first principle density functional theory (DFT) analysis on structural, electronic and electrochemical property of $LiCrTiO_4$ system full potential augmented plane wave approach. The results are encouraging and have provided further insight to explore experiments to realise improvements in electrode performance.

SESSION C9: Characterization of Nanoscale and Local Structures II
C: Electrodes and Solid Electrolytes for Batteries
Chair: Miran Gaberscek
Wednesday Morning, June 17, 2015
Keystone Resorts, Shavano Peak

10:30 AM C9.01
A Simple *In Situ* Approach to Study the Solid Electrolyte / Lithium Interphase by Photoelectron Spectroscopy Thomas Leichtweiss, Sebastian Wenzel, Dominik Krueger, Achim Kronenberger, Joachim Sann and Juergen Janek; Institute of Physical Chemistry, Justus-Liebig-University Giessen, Giessen, Germany.

Solid-state batteries (SSB) promise long cycle life and inherent safety as no liquid components are being used. In order to achieve high energy densities lithium metal is the desired anode material. Therefore, (electro-) chemical stability of the solid electrolyte in contact with metallic lithium is crucial for the operation and performance of SSB.[1] In principle, three types of interface formation between lithium metal anodes and solid electrolytes are possible: In the first case, the solid electrolyte is stable in contact with lithium and a sharp *two-dimensional interface* is formed. In contrast, both materials can form a *three-dimensional interphase* due to a chemical reaction. Depending on the electric properties of the reaction products one can distinguish between two kinds of such interphases: First, due to a high partial electronic and ionic conductivity of the formed products the interphase may steadily grow “into” the solid electrolyte thereby altering the properties of the bulk material. The formation of such a mixed conducting interphase (MCI) will eventually allow electron current through the electrolyte and lead to a self-discharge or even destruction of the battery. In contrast, a stable interphase may form if the reaction products are electronically non-conductive. This layer would be comparable to the anode SEI as known for current-generation lithium ion batteries comprising aprotic liquid electrolytes.

Such buried interfaces (or interphases) are generally difficult to investigate by spectroscopic techniques like photoelectron spectroscopy (XPS). We report on a strikingly simple “bottom-up” approach for the lithiation of solid electrolytes in a standard lab-scale photoelectron spectrometer by ion beam sputtering using the built-in argon sputter gun. Reactions during the formation of interphases can be observed *in-situ* by XPS. As a proof-of-concept, we demonstrate the interphase formation on lithium phosphorous oxide nitride (“LiPON”), which is known to react with lithium metal[2].

The developed setup is not limited to battery materials and allows the sequential deposition of ultra-thin metal films on any kind of sample thereby facilitating the *in-situ* chemical analysis by XPS during the formation of various interfaces and/or interphases.

(1) Hartmann, P.; Leichtweiss, T.; Busche, M. R.; Schneider, M.; Reich, M.; Sann, J.; Adelhelm, P.; Janek, J. *J. Phys. Chem. C* 2013, *117*, 21064.
(2) Schwöbel, A.; Hausbrand, R.; Jaegermann, W. *Solid State Ionics* 2014, 2.

10:50 AM C9.02
***Operando* SAXS/WAXS Measurements of Amorphous and Nano-Crystalline Anodes for Na-Ion Batteries** Sabrina Sartori; Department of Physics, University of Oslo, Oslo, Norway.

Understanding the physical and chemical principles behind the nano-sizing on the performances of electrodes is a key issue for developing efficient and competitive batteries.
Structural characterisation of the electrodes are often done *ex situ*, opening single-use, disposable, coin cells. Recent publications, however, indicates that new information can be obtained by performing *in situ* measurements. We present a series of innovative *operando in-situ* SAXS/WAXS studies of amorphous and/or nano-crystalline materials as anodes for Na-ion batteries.

An in house electrochemical cell developed by our team has been designed for simultaneous *operando* SAXS and WAXS acquisition on DUBBLE BM26, at ESRF (Grenoble), while performing sodiation/desodiation cycles.
These measurements gave us new insights on the structural evolution of the electrodes, and contributed to reveal important factors critical to improve their electrochemical performance.

This work is a collaboration between the team at the University of Oslo (Sartori, Mauro Povia, Jonas Sottmann, Serena Margadonna, and the beamline scientist at ESRF Giuseppe Portale).

11:10 AM C9.03
***In Situ* Raman Spectroscopy of Thin-Film Battery $Li/Li_3PO_4/LiMn_2O_4$ Using a Transparent Electrode** Naoakai Kuwata[1], Tatsunori Okawa[1], Yasutaka Matsuda[1], Osamu Kamishima[2]and Junichi Kawamura[1]; [1]IMRAM, Tohoku University, Sendai, Japan; [2]Faculty of Science and Engineering, Setsunan University, Neyagawa, Japan.

A spinel-type lithium manganese oxide, $LiMn_2O_4$, is well-known cathode material for thin-film batteries. The thin-film lithium batteries using $LiMn_2O_4$ cathode and Li anode was operated at 3.9 to 4.1 V. The spinel-type lithium manganese oxide shows high operating voltage by replacing the Mn to Co, which enable a 5-V-class solid-state battery [1].

Structural changes of $LiMn_2O_4$ in the thin-film battery was studied by *in situ* Raman spectroscopy. The thin-film batteries $Li/Li_3PO_4/LiMn_2O_4$ were prepared by pulsed laser deposition and thermal evaporation technique. *In situ* micro Raman spectroscopy was measured using a vacuum-tight cell with optical glass window. The excitation laser was 532 nm semiconductor laser.

Since the Li metal layer reflects the excitation laser, the Raman spectra of $LiMn_2O_4$ was measured in the side of Li from the surface (upper) side of thin-film batteries. As a results of measurement from the surface side, structural change of $LiMn_2O_4$ has been confirmed. However, a deviation was found between the electrochemical reactions and the structural change observed by Raman spectroscopy.

In order to observe just below the Li metal layer, we attempted the reverse side *in situ* Raman measurements using a tin-doped indium oxide (ITO) transparent current collector. As a result, the electrochemical reactions and the structural change in the Raman spectra were occurred almost same

time. Reversible change of $Li_xMn_2O_4$ was clearly observed in both the Raman spectra and electrochemistry. Two phase reaction of $LiMn_2O_4$ was also observed in the solid-state battery similar to the liquid batteries. Moreover, form the deviation of electrochemical reaction and structural change, the chemical diffusion coefficient of $LiMn_2O_4$ can be roughly estimated. *In situ* Raman spectroscopy has been confirmed to be an excellent tool for examining the intercalation reactions of the solid-state battery.

[1] Naoaki Kuwata, Shota Kudo, Yasutaka Matsuda, Junichi Kawamura, *Solid State Ionics*, **262**, (2014) 165.

11:30 AM C9.04
Pore Collapse and Regrowth in Silicon Electrodes for Rechargeable Batteries Steven C. DeCaluwe[2, 1, 4], Bal-Mukund Dar[3], Joseph A. Dura[2] and Howard Wang[3, 4, 5]; [1]NIST Center for Neutron Research, Gaithersburg, Maryland, United States; [2]Mechanical Engineering, Colorado School of Mines, Golden, Colorado, United States; [3]Institute for Materials Research and Dept. of Mechanical Engineering, State University of New York, Binghamton, New York, United States; [4]Materials Science and Engineering, University of Maryland, College Park, Maryland, United States; [5]Material Measurement Laboratory, National Institute of Standards and Technology, Gaithersburg, Maryland, United States.

Numerous strategies have been attempted to improve the durability of Si anodes for high-capacity rechargeable Li-ion batteries, including thin-film anodes and protective coatings. However, efforts have yet to identify a mechanically robust anode design that maintains a stable capacity. Part of the difficulty is due to a paucity of *in situ* techniques to observe definitively how proposed modifications impact the correlation between structure, mechanical properties, and function in Si anodes.

This presentation reports the structural and composition changes of an 11 nm thick amorphous Si thin film anode, capped with a 4 nm thick alumina film, measured *in operando* by neutron reflectivity (NR) and electrochemical impedance spectroscopy in a lithium half-cell. NR data are analyzed to quantify the Si layer thickness and composition at various states of charge over six cycles. The Si anode expands and contracts during cycling, while maintaining its integrity and low interfacial roughness (<1.6 nm). The apparently non-linear expansion of the Si film versus lithium content agrees with previous findings. However, a proposed pore collapse and regrowth (PCRG) mechanism establishes that solid domain expansion in the porous film is consistent with linear expansion vs. Li content at a rate of 8.48 cm^3/mol-Li, similar to bulk Si. In the PCRG model, during lithiation the solid Li_xSi expands both isotropically, to fill the pores, and anisotropically to expand the film. Porosity is reversibly reestablished at 5-28% upon delithiation. Data also show that the alumina protective on the Si film functions as an effective artificial solid electrolyte interphase.

SESSION C10: Fundamentals of LIB Electrodes I
C: Electrodes and Solid Electrolytes for Batteries
Chair: William Chueh
Thursday Morning, June 18, 2015
Keystone Resorts, Shavano Peak

10:30 AM **C10.01
The Ultimate Limits of Intercalation Reactions for Battery Electrodes Stanley Whittingham; NECCES, SUNY, Binghamton, New York, United States.

Today's Li-ion cells achieve around 200 Wh/kg and 600 Wh/liter. In principle it shuld be possible to achieve 350 Wh/kg and well-over 1 kWh/liter in single cells. Substituting the carbon anode might increase the volumetric energy to 900 Wh/liter. However, to substantially increase the energy storage it will be necessary either to **close the gap** between the theoretical and achievable capacities of the layered oxides or to have more than one electron involved per redox center. Both of these options will require (a) electrolytes with higher voltage capabilities than those available today and (b) thicker electrodes (=higher ionic mobility) so as to reduce the quantity of inactive coponents. The former layered oxide approach will require understanding why more than 0.7 Li cannot be cycled in $LiMO_2$ without capacity degradation. The latter 2e approach might be achieved by using magnesium as the anode. An alternative, maybe more pragmatic approach, is to intercalate two lithium ions into the host lattice. In this latter approach the present commercial anode and electrolyte can be used. The cathode options will be discussed with an emphasis on vanadyl phosphate, which exists in a number of polymorphs and where the compounds $LiVOPO_4$ and Li_2VOPO_4 are known but not yet well understood. This research is supported by the DOE-EFRC-NECCES at Binghamton under award DE-SC0012583.

11:00 AM *C10.02
Parameters Influencing Reversible Intercalation of Cations in Spinel Oxides Jordi Cabana; Chemistry, University of Illinois at Chicago, Chicago, Illinois, United States.

Since the discovery by Thackeray and co-workers of their ability to reversibly intercalate Li, spinel oxides have become a canonical electrode material in battery technologies. Phases with this structure typically present very stable cycle life in the bulk and fast kinetics. In Li-ion batteries, the best performance is obtained with significant amounts of Mn in the structure. While full intercalation from M_2O_4 (M=Mn, Ni, Co...) to $Li_2M_2O_4$ is possible, it is also poorly reversible. As a result, practical applications limit the utilization to processes between M_2O_4 and LiM_2O_4. In other words, this material highlights the barrier of two electron reactivity that is pervasive in battery electrodes based on intercalation reactions.

In this talk, we will overview the understanding of electrochemical function of spinel oxides that we have collected over recent years. We will discuss our efforts to understand the kinetic limitations of the M_2O_4-Li-Mn_2O_4-$Li_2M_2O_4$ (M=Mn, Ni) transitions in light of composition-structure-properties relationships. We will describe strategies to visualize these transitions in order to pinpoint chemical and mechanical ineffiencies. Finally, we will introduce evidence that this family of oxides is also capable of reversibly intercalate multivalent ions such as Mg^{2+}, and discuss avenues to optimize properties.

11:20 AM C10.03
Revealing the Origins of Lithiation Heterogeneities in $LiFePO_4$ Using Nanoscale Chemical Imaging Yiyang Li[1], William E. Gent[1], Jongwoo Lim[1], Johanna Nelson Weker[2], Norman Jin[1], Sophie Meyer[1], Daniel A. Cogswell[3], Tolek Tyliszczak[4] and William C. Chueh[1]; [1]Stanford University, Stanford, California, United States; [2]SLAC National Accelerator Center, Menlo Park, California, United States; [3]Samsung Advanced Institute of Technology-America, Cambridge, Massachusetts, United States; [4]Berkeley National Laboratory, Berkeley, California, United States.

Lithiation heterogeneities are significant drivers of degradation and failure in Li-ion batteries. We use $LiFePO_4$, a phase-separating positive electrode, as a model system to investigate the origins of lithiation heterogeneities at the single particle and porous electrode length scales. Two particle morphologies were investigated: ellipsoidal and platelet. In ellipsoidal-shaped $LiFePO_4$ particles, we first analyze the extent of heterogeneity as a function of the cycling rate using *ex situ* single-particle X-ray spectro-microscopy. We observe that the electrochemical current in a porous electrode is highly heterogeneous at low cycling rates and more homogeneous at higher rates. We confirm these findings using *operando* X-ray microscopy, which images the migration of Li in a battery as it cycles in an organic liquid electrolyte. This rate-dependent heterogeneity behavior arises from a competition between the thermodynamic transformation barrier in phase-separating materials and the kinetics of inserting and removing Li from a particle. Next, we use the *operando* imaging platform to track lithiation in platelet particles. Contrary to the ellipsoidal particles, lithiation in the platelet particles is significantly more homogeneous, with nearly all particles concurrently intercalating. We propose that the dichotomy in the lithiation pathway of the two morphologies result from their different surface reactivities. These insights can be used to control heterogeneity and the cycle life in phase-separating battery electrodes.

11:40 AM C10.04
Computational Identification and Experimental Realisation of Lithium Vacancy Introduction into the Olivine $LiMgPO_4$ Leopoldo Enciso-Maldonado[1], Matthew S. Dyer[1], Michael D. Jones[1], Ming Li[1], Michael J. Pitcher[1], Mona K. Omir[1], John B. Claridge[1], Frederic Blanc[1, 2] and Matthew J. Rosseinsky[1]; [1]Department of Chemistry, University of Liverpool, Liverpool, United Kingdom; [2]Stephenson Institute for Renewable Energy, University of Liverpool, Liverpool, United Kingdom.

Calculation of the energetics of aliovalent substitution into the olivine $LiMgPO_4$ suggests that replacement of Mg^{2+} by In^{3+} is the most effective way to introduce lithium vacancies and thus generate lithium ion conductivity. Experimental synthesis accesses materials with up to 17% Li vacancy content. An order of magnitude increase in the high temperature hopping rates probed by ^7Li nuclear magnetic resonance (NMR) spin lattice relaxation, and over two orders of magnitude increase in the room temperature Li^+ ion conductivity measured by ac impedance spectroscopy (ACIS) is observed on introduction of In^{3+} ions and Li vacancies. NMR spectroscopy and calculations reveal that the energy barrier to site-to-site hopping is 0.3 eV – 0.5 eV, comparable with best-in-class non-oxide systems such as argyrodite, but NMR derived hopping rates, and impedance spectroscopy shows that longer range transport is less facile with activation energies in the range of 0.7 – 1 eV and room temperature bulk lithium conductivities in the range of $\sim 5 \times 10^{-12}$, $\sim 4 \times 10^{-10}$ $S.cm^{-1}$ and $\sim 2 \times 10^{-9}$ $S.cm^{-1}$ for $LiMgPO_4$, the 10 % and 17 % In doped $LiMgPO_4$, respectively. Calculations suggest that this is because the Li vacancies are strongly bound to the In^{3+} dopants, suggesting that high lithium mobilities in oxides are accessible but high conductivities require strategies to separate defect from dopant.[1]

[1] Enciso-Maldonado, L. *et al. Chem. Mater.* **2015**, DOI: 10.1021/cm504518q

SESSION C11: Beyond Lithium
C: Electrodes and Solid Electrolytes for Batteries
Chair: Scott Barnett
Thursday Afternoon, June 18, 2015
Keystone Resorts, Shavano Peak

1:30 PM *C11.01
Room-Temperature Sodium-Ion Batteries: Improving the Rate Capability Using Porous Carbon Networks Yan Yu, Joachiam Maier and Changbao Zhu; Max Planck Institute for Solid State Research, Stuttgart, Germany.

Na-ion batteries (NIBs) have attracted rapidly increasing attention because sodium is abundant resources, low cost. However, the development of NIBs is greatly hampered due to the lack of appropriate active materials for both cathodes and anodes, because of the large radius of Na^+. NASICON-type $Na_3V_2(PO_4)_3$ has recently been investigated as a promising cathode material for NIBs. While it is difficult to reach high rate performance of $Na_3V_2(PO_4)_3$ cathode due to the poor electronic conductivity of phosphates. For anode materials, MoS_2 has shown promising electrochemical performance. The electrochemical performance of MoS_2 depends on the size of MoS_2 and the species of carbon in the composites.

Here, we reported electrode materials for NIBs based on porous carbon with excellent rate performance: (1) Carbon-coated nanosized $Na_3V_2(PO_4)_3$ embedded in the porous carbon matrix (denoted as CC-NVP@PC); (2) Single-layered Ultrasmall Nanoplates of MoS_2 Embedded in Carbon Nanowires.

The CC-NVP@PC was synthesized using a facile soft-chemistry based method with post heat-treatment. It delivers high rate performance (44 $mAhg^{-1}$ at 200C).[1] This ultrahigh rate performance is comparable to that of supercapacitor, but with much higher energy density.

The single-layered MoS_2 nanoplates embedded in carbon nanowires were prepared by pyrolysis of $(NH_4)_2MoS_4$/PVP nanofibers through electrospinning process. It displays rate capacity of around 436, 331, 224, 155, 75 mAh/g at current densities of 5, 10, 20, 30, 50 A/g, respectively.[2]

The outstanding electrochemical performance of electrode materials with porous carbon network for NIBs is attributed to the special structure design, which confined a variety of advantages: hierarchical porous channels facilitating fast ions and electrons transport, carbon coated structure resulting in low resistances, good mechanical properties leading to the excellent morphology stability.

[1] C. Zhu, K. Song, P. A. van Aken, J. Maier, Y. Yu, *Nano Lett.*, 2014, **14**(4), 2175–2180 .
[2] C. Zhu, X. K. Mu, P. A. van Aken, Y. Yu, and J. Maier. *Angew. Chem. Int. Ed.*, 2014,**53**(8), 2152–2156.

1:50 PM C11.02
Recent Progress for Room-Temperature Stationary Sodium-Ion Batteries Yong-Sheng Hu; Key Laboratory for Renewable Energy, Institute of Physics, Chinese Academy of Sciences, Beijing, China.

With the tremendous development of renewable energies such as solar and wind powers, the smooth integration of their energies into the grid, thus improving the grid reliability and utilization, critically needs large-scale energy storage systems with long-life, high efficiency, high safety and low cost. Among the various energy storage technologies, electrochemical approach represents one of the most promising means to store the electricity in large-scale because of the flexibility, high energy conversion efficiency and simple maintenance. Due to the highest energy density among practical rechargeable batteries, lithium-ion batteries have been widely used in the portable electronic devices and would undoubtedly be the best choice for the electric vehicles. However, the rarity and non-uniform distribution of lithium in the Earth's crust may limit their large-scale application in renewable energy. In this regard, room-temperature sodium-ion batteries with lower energy density compared with lithium-ion batteries have been reconsidered particularly for such large-scale applications, where cycle life and cost are more essential factors than energy density owing to the abundant sodium resources and potentially low cost as well as similar "rocking-chair" sodium storage mechanism as lithium [1].

In this contribution, I will present some promising cathode and anode materials including Na3V2(PO4)3/C [2-4], Li3[LiTi5]O12 [5-7], zero-strain P2-Na0.66[Li0.22Ti0.78]O2 [8], Na2C8H4O4 [9], Na2Ti3O7 [10] and hard carbon sphere (HCS) [11] as well as a new electrolyte system for room-temperature stationary sodium-ion batteries. In particular, I will emphasize our recent work on a series of air-stable layered metal oxide cathodes with the building block of Cu instead of Co/Ni in the transition metal layer which exhibit superior Na storage performance [12-14]. The full cells based on our developed cathode and anode materials will also be demonstrated.

Acknowledgement. This work was supported by funding from the NSFC (51222210, 11234013) and the One Hundred Talent Project of the Chinese Academy of Sciences.

References
[1] H. L. Pan, Y.-S. Hu, L. Q. Chen, *Energy Environ. Sci.*, **2013**, 6, 2338-2360. (an invited review article)
[2] Z. L. Jian, L. Zhao, H. L. Pan, Y.-S. Hu, H. Li, W. Chen, L. Q. Chen, *Electrochem. Commun.*, **2012**, 14, 86-89.
[3] Z. L. Jian, W. Z. Han, X. Lu, H. X. Yang, Y.-S. Hu, J. Zhou, Z. B. Zhou, J. Q. Li, W. Chen, D. F. Chen, L. Q. Chen, *Adv. Energy Mater.*, **2013**, 3, 156-160.
[4] Z. L. Jian, C. C. Yuan, W. Z. Han, X. Lu, L. Gu, X. K. Xi, Y.-S. Hu, H. Li, W. Chen, D. F. Chen, Y. Ikuhara, L. Q. Chen, *Adv. Funct. Mater.* 2014, 24, 4265-4272.
[5] L. Zhao, H. L. Pan, Y.-S. Hu, H. Li, L. Q. Chen, *Chin. Phys. B*, 2012, 21, 028201.
[6] Y. Sun, L. Zhao, H. L. Pan, X. Lu, L. Gu, Y.-S. Hu, H. Li, M. Armand, Y. Ikuhara, L. Q. Chen, X. J. Huang, *Nature Communications*, **2013**, 4, 1870.

[7] X. Q. Yu, H. L. Pan, W. Wan, C. Ma, J. M. Bai, Q. P. Meng, S. N. Ehrlich, Y.-S. Hu, X.-Q. Yang, *Nano Lett.*, **2013**, 13, 4721-4727.
[8] Y. S. Wang, X. Q. Yu, S. Y. Xu, J. M. Bai, R. J. Xiao, Y.-S. Hu, H. Li, X.-Q. Yang, L. Q. Chen, X. J. Huang, *Nature Communications*, **2013**, 4, 2365.
[9] L. Zhao, J. M. Zhao, Y.-S. Hu, H. Li, Z. B. Zhou, M. Armand, L. Q. Chen, *Adv. Energy Mater.*, **2012**, 2, 962-965.
[10] H. L. Pan, X. Lu, X. Q. Yu, Y.-S. Hu, H, Li, X.-Q. Yang, L. Q. Chen, *Adv. Energy Mater.*, **2013**, 3, 1186-1194.
[11] Li, Y. M.; Xu, S. Y.; Wu, X. Y.; Yu, J. Z.; Wang, Y. S.; Hu, Y.-S.; Li, H.; Chen, L. Q.; Huang, X. J. *J. Mater. Chem. A*, **2015**, *3*, 71-77.
[12] Xu, S.Y.; Wu, X.Y.; Li, Y.M.; Hu, Y. -S.; Chen, L.Q. *Chin. Phys. B* **2014**, *23*,118202.
[13] Mu, L. Q.; Hu, Y. -S.; Chen, L.Q. *Chin. Phys. B* **2015**, *3*, 038203.
[14] Hu, Y. -S.; et al. Several Chinese patents have been filed.

2:10 PM C11.03
Structural Study of $Na_{2/3}[Ni_{1/3}Ti_{2/3}]O_2$ Using Neutron Diffraction and Atomistic Simulations for Na-Ion Batteries Rengarajan Shanmugam and Wei Lai; CHEMS, Michigan State University, East Lansing, Michigan, United States.

Investigation of electrode materials for Na-ion batteries has become an active area of research in the pursuit to develop low-cost energy storage technologies. Layered oxide materials such as P2-$Na_{2/3}Ni_{1/3}Mn_{2/3}O_2$,[1] P2-$Na_{0.7}CoO_2$,[2] etc. have been studied as intercalation electrodes. We evaluated the electrochemistry of P2-$Na_{2/3}[Ni_{1/3}Ti_{2/3}]O_2$ as 'bi-functional' electrode.[3]

We make use of neutron diffraction experiments and atomistic simulations to evaluate the structural properties of this ternary oxide material. Neutron diffraction was performed at beamline 11A of POWGEN diffractometer facility at Spallation Neutron Source (SNS) of Oak Ridge National Lab (ORNL). The average structural information was obtained using Rietveld refinement (GSAS). The 194 space group Bragg reflections matched the experimental pattern. The '2b' sodium sites were found to have a lower occupancy than '2c' sites due to their unfavorable repulsive interaction with transition metal atoms. Sodium thermal ellipsoids were found to be fairly oblong along the 'ab' plane whereas oxygen was found to be fairly spherical (isotropic).

The energetics of disordered structures was evaluated with the energy minimization algorithm implemented in GULP code. The large energy landscape was explored by studying 2000 randomized 3x2x1 supercells. The interatomic pair potentials were represented by Buckingham and Morse-based models. Disordered structures with equal atomic distribution were found to be energetically favored. The simulated density maps are consistent with the experiments. There is no intermixing of transition metal atoms in the sodium layers suggesting high diffusional energy barriers and favoring unhindered sodium diffusion. We found evidence of stacking faults due to displacive offsetting of oxygen atoms.

References
1. D. H. Lee, J. Xu, and Y. S. Meng, *Phys. Chem. Chem. Phys.*, **15**, 3304–12 (2013)
2. R. Berthelot, D. Carlier and C. Delmas, *Nature Mater.*, **10**, 74–80 (2011)
3. R. Shanmugam, R. and W. Lai, *ECS Electrochem. Lett.*, **3**, A23–A25 (2014)

2:30 PM C11.04
Electrochemical Properties for MXene $Ti_3C_2T_x$ as Negative Electrode in a Non-Aqueous Sodium-Ion Electrolyte Satoshi Kajiyama, Hiroki Iinuma, Masashi Okubo and Atsuo Yamada; Department of Chemical System Engineering, School of Engineering, The University of Tokyo, Tokyo, Japan.

Electrochemical energy storage with high energy density at high rates has attracted increasing attention because of the demands for their widespread use in smart grid. Sodium-ion batteries are regarded as potential alternatives to the state-of-the-art lithium-ion batteries because sodium is an abundant and low-cost-available resource. However, the present set of the negative electrode for the sodium-ion batteries cannot satisfy all the requirements for sodium-ion batteries.

Recently, Gogotsi *et al.* have reported the synthesis of a family of MXene nanosheets ($M_{n+1}X_nT_x$; M = Ti, Cr, V, etc., X = C, N, n = 1–3, T = surface functional groups) by chemical extraction of A layers from MAX phases ($M_{n+1}AX_n$; A = Al, Si, P *etc.*).[1] Importantly, MXenes exhibit a pseudocapacitic behavior in aqueous and nonaqueous electrolytes[1-3]. In this presentation, we report MXene $Ti_3C_2T_x$ (n = 2) as anode materials for sodium-ion batteries. The charge-discharge experiments reveal that the $Ti_3C_2T_x$ electrode delivers a specific capacity over 100 mAh/g at the average potential of 0.9 V vs. Na/Na^+. Ex-situ X-ray diffraction and transmission electron microscopy show that upon initial Na-ion insertion the interlayer spacing of $Ti_3C_2T_x$ expands from 9.7 Å to 12.5 Å whereas the interlayer spacing does not change on the subsequent charge/discharge. On the basis of energy-dispersive X-ray results, residual Na ions serve as a pillar to maintain the expanded interlayer distance. The present study promises that the MXene negative electrodes are potential candidates to realize advanced sodium-ion batteries.

(1) M. R. Lukatskaya, *et al.* and Y. Gogotsi, *Science 341*, 1502 (2013).
(2) M. Ghidiu, *et al*. & Y. Gogotsi, *Nature 516*, 78-81(**2014**).
(3) X. Wang, S. Kajiyama, *et al.* and A. Yamada, *Nat. Commun.* (2015) *in press*.

2:50 PM C11.05
Amorphous Cathodes for Magnesium Batteries Timothy S. Arthur, Keiko Kato, Fuminori Mizuno and Jason Germain; Materials Research, Toyota Research Institute of North America, Ann Arbor, Michigan, United States.

To exceed the demands of current hybrid, plug-in hybrid and electric vehicles, new battery systems with high energy density are required. Magnesium (Mg) is an attractive alternative to current lithium-ion technologies because of the transfer of 2 electrons per magnesium-ion, higher volumetric capacity of magnesium metal compared to lithium metal (3833 mAh/cm^3 Mg vs 2061 mAh/cm^3 Li), and greater natural abundance. However, to realize complete magnesium batteries, cathodes capable of reversible Mg^{2+} reactions are required.

Recently, we proposed α-MnO_2 as a viable candidate for Mg batteries because of a large initial discharge capacity of 280 mAh/g. However, the capacity faded to 70 mAh/g by the 10thcycle, and a deep mechanistic investigation was required to determine the source of the capacity fade. We observed that instead of following the typical insertion reaction as with Li^+ to produce $LiMnO_2$, magnesiation occurs through a conversion pathway to form an amorphous (Mg, Mn)O product. Through various transmission electron microscopy techniques and soft X-ray absorption spectroscopy, we determined that magnesiation is partially reversible through the amorphous layer of the cathode. From these results, we were encouraged to pursue amorphous materials as an avenue for magnesium battery cathodes.

The V_2O_5-P_2O_5 amorphous glass system has previously been shown to have good cycling and rate capabilities for lithium batteries. Encouragingly, sputtered- and nanocrystalline-V_2O_5 has recently been highlighted as a promising cathode for magnesium batteries; however, there are no reports on the insertion of Mg^{2+} into amorphous-V_2O_5. In our presentation, we will show a the electrochemically reversible magnesiation of amorphous V_2O_5-P_2O_5 cathodes for magnesium batteries, which approaches a maximum current density at a 75:25 V_2O_5:P_2O_5 ratio. Additionally, we will present a thorough analyis, including X-ray photoelectron spectroscopy; soft X-ray absorption spectroscopy and ^{31}P solid-state nuclear magnetic resonance spectroscopy, to identify the electrochemical activity for the amorphous cathodes. Importantly, we have propose the formation of a meta-stable phase which gives the amorphous V_2O_5-P_2O_5system improved electrochemical properties over the bulk, crystalline-V_2O_5. Mg batteries have great potential as a post Li-ion technology, but finding a viable cathode material is vital to realizing a practical system. The V_2O_5-P_2O_5 system shows excellent potential as a cathode material, and provides us with an alternative, promising path for a complete magnesium battery.

3:30 PM C11.06

Magnesium Ion Intercalation into a Spinel like λ-Manganese Oxide Ryan D. Bayliss[1], Chunjoong Kim[1], Tanghong Yi[1], Abdullah Adil[1], Patrick J. Phillips[2], Baris Key[3], Young-Sang Yu[4], Tiffany L. Kinnibrugh[5], Karena W. Chapman[5], Peter J. Chupas[5], Robert K. Klie[2] and Jordi Cabana[1]; [1]Department of Chemistry, University of Illinois at Chicago, Chicago, Illinois, United States; [2]Department of Physics, University of Illinois at Chicago, Chicago, Illinois, United States; [3]Chemical Sciences and Engineering Division, Argonne National Laboratory, Argonne, Illinois, United States; [4]Advanced Light Source, Lawrence Berkeley National Laboratory, Berkeley, California, United States; [5]Advanced Photon Source, Argonne National Laboratory, Argonne, Illinois, United States.

Multivalent ion battery chemistries are an attractive candidate for higher energy density storage than current Li-ion battery technology, which while closely resembling systems using Li-ion, can store more charge per mole of intercalated species. The double charge present on Mg creates the opportunity for less dramatic structural rearrangements in the host materials, and hence the possibility of enhanced structural stability on cycling. There is only one proven working positive electrode material, the Chevrel phase, for Mg ion batteries which unfortunately operates at a relatively low working voltage window. [1, 2] Most previous studies of multivalent ion intercalation electrochemistry in oxide compounds have provided little information on the reaction mechanisms leading to the electrochemical data. Often the evidence provided is determined by the existence of an electrochemical capacity, which whilst promising does not actually directly evidence Mg intercalation. In this work, by using combinatorial characterization tools, reversible (Mg) intercalation into a spinel-type structure has been confirmed. Tetragonal $MgMn_2O_4$ is achieved by the intercalation of Mg into the cubic spinel structure, λ-MnO_2, and reversibly oxidized back to the cubic spinel structure by deintercalation of Mg. The experimental observations by XRD, XAS, STEM-EDX, and NMR, all verify that the intercalation reaction occurred successfully. These results are exciting on many fronts. Finally, the first steps in microstructural optimisation have been investigated to produce nano sized particles, therefore reducing diffusion distances for the Mg ion to travel in the crystalline phase. Intersting additional complex structural behavior in the nanosized system has been probed by X-ray PDF studies.

[1] D. Aurbach, Z. Lu, A. Schechter, Y. Gofer, H. Gizbar, R. Turgeman, Y. Cohen, M. Moshkovich, and E. Levi, *Nature*, **407** (6805), 724-727 (2000)
[2] H. D. Yoo, I. Shterenberg, Y. Gofer, G. Gershinsky, N. Pour, and D. Aurbach, *Energ Environ Sci*, **6** (8), 2265-2279 (2013)

3:50 PM C11.07

Rechargeable Magnesium Battery Using Polyanion Compounds Cathode and Triglyme Electrolyte Yuki Orikasa, Titus Masese, Yukinori Koyama, Takuya Mori, Masashi Hattori, Kentaro Yamamoto, Cedric Tassel, Yoji Kobayashi, Takeshi Abe, Hiroshi Kageyama and Yoshiharu Uchimoto; Kyoto University, Kyoto, Japan.

Magnesium rechargeable batteries are one of interesting candidate for next generation battery system. However, the energy density remained rather constrained by the cathode material, and the narrow potential window, corrosion, and safety problems posed by the electrolyte have hampered the commercial realization of these batteries. Even though extensive research has been performed[1], the cathode materials await breakthroughs for the development of practically usable rechargeable magnesium batteries. In this study, we address the problems plagued by the cathode materials by using concept of ion-exchanged polyanion cathode, $MgFeSiO_4$ and demonstrate a rechargeable magnesium battery using this high energy density cathode material[2].

The preparation of $MgFeSiO_4$ involves, two electrochemical processes, namely, $2Li^+$ extraction from Li_2FeSiO_4 followed by Mg^{2+} insertion. The charge-discharge profiles in a magnesium battery cell of the electrochemically prepared $MgFeSiO_4$ are shown in Fig. 1. The application of ion-exchanged $MgFeSiO_4$ polyanion compounds as magnesium rechargeable battery cathode materials enables a capacity of more than 300 $mAh \cdot g^{-1}$ at an average potential of 2.4 V *vs*. Mg^{2+}/Mg, with good retention upon cycling. The electronic and crystal structure changes upon charging and discharging process, which demonstrates the (de) insertion of magnesium in the host structure.

We propose a novel magnesium battery system where ion-exchanged $MgFeSiO_4$ and Mg metal are used as the cathode and anode, respectively, and $Mg(TFSI)_2$–triglyme as the electrolyte. These materials would be highly beneficial for increasing the energy density of the electrode materials in magnesium batteries without imposing significant constraints on available resources.

[1] H. D. Yoo, D. Aurbach *et al., Energy Environ. Sci.*, **6**, 2265 (2013).
[2] Y. Orikasa, Y. Uchimoto *et al., Sci. Rep.*, **4,** 5622(2014).

4:10 PM C11.08

Reversible Intercalation of Multivalent Ions into Nanostrctured Vanadium Oxide Cathodes Premkumar Senguttuvan and Christopher S Johnson; Chemical Sciences and Engineering, Argonne National Laboratory, Argonne, Illinois, United States.

To address our ever increasing energy storage demand, battery science has taken new dimensions to explore its spaces beyond lithium ion technology. The concept of multivalent ion intercalation ideally aims to store multivalent cations in the place of lithium ions inside host material to double or triple energy density of cathodes.[1] However, development of such technology is severely plagued by electrode and electrolyte materials development. Many of cathode materials investigated so far, including oxides, sulfides and polyanionic compounds, showed no or limited amount of intercalation owing to slow solid-state diffusion of multivalent cations inside host lattice. On the other hand, Chevrel phases exhibited reversible magnesium ion intercalation which could be attributed to soft-chemical bonding of Mg^{2+} ions with sulfide host lattice.[2] In order to improve multivalent ion intercalation, strategies including nano-sizing and incorporation of water or solvent molecules in host materials were attempted and reported to be successful.[3, 4] In this context, here we report a simply way to synthesize nanostrucutred vanadium oxide host material that contains water molecules and its multivalent ion intercalation properties. This talk will mainly focus on role of water molecules on multivalent ion diffusion and its compatibility with various electrolytes.

References

(1) Muldoon, J.; Bucur, C. B.; Gregory, T. *Chem. Rev.* **2014**, *114*, 11683.
(2) Aurbach, D.; Lu, Z.; Schechter, A.; Gofer, Y.; Gizbar, H.; Turgeman, R.; Cohen, Y.; Moshkovich, M.; Levi, E. *Nature* **2000**, *407*, 724.
(3) Novák, P.; Scheifele, W.; Joho, F.; Haas, O. *J. Electrochem. Soc.* **1995**, *142*, 2544.
(4) Novák, P.; Scheifele, W.; Haas, O. *J. Power Sources* **1995**, *54*, 479.

4:30 PM C11.09

Data-Driven Models of Ion Conduction for Rapid Screening of New Generation Conductors Using Statistical Methods Austin Sendek[1], Qian Yang[3], Yi Cui[2] and Evan Reed[2]; [1]Applied Physics, Stanford University, Stanford, California, United States; [2]Materials Science, Stanford University, Stanford, California, United States; [3]Institute for Computational and Mathematical Engineering, Stanford University, Stanford, California, United States.

Leveraging the new paradigm of data-driven materials science, we develop a model for ion conduction that illuminates the structure-property relationship for ionic conductivity while also enabling rapid predictions of conductivity in thousands of candidate next generation materials. Although the volume of known Mg-, Na-, and K-containing materials numbers into the tens of thousands, only a small subset of these materials has reported ionic conductivity values. Individually testing the conductivity of each of these untested materials is intractable, even with the fastest electronic structure codes available. We circumvent this restriction with our data-driven approach, in which we aggregate the wealth of experimental data on lithium ion conductors in the literature, use physical intuition to generate a set of microscopic descriptors, utilize statistical learning strategies to uncover trends buried deep in the data, and then apply these trends to candidate next generation conductors. We use these descriptors to develop a computationally efficient, predictive model capable of screening over 10,000 candidate Mg-, Na-, and K-ion conductors in the Materials Project database, effectively doing in hours what would take decades by ab initio simulation or experiments. We develop a confidence metric for each prediction and also compile bandgap, stability, and raw materials cost data for each candidate material. Through this screening we identify a number of promising, untested candidate structures for further study.

SESSION C12: Fundamentals of LIB Electrodes II
C: Electrodes and Solid Electrolytes for Batteries
Chair: Jordi Cabana
Friday Morning, June 19, 2015
Keystone Resorts, Shavano Peak

10:30 AM **C12.01
Powerful Electrical Model Explaining the Operation of Insertion Batteries Miran Gaberscek; National Institute of Chemistry, Ljubljana, Slovenia.

Typical lithium battery electrode contains enormous number of active particles (up to 10^{14} per 1 cm^2 of metallic substrate) and at least 3 or 4 other phases (binders, coatings, conductive additive, electrolyte) that provide its proper functioning. The mass and charge transport in such a system is inherently complex. The use of conventional transport models has partly improved our understanding of core mechanism taking place in insertion electrodes. However, many unusual findings or rarely reported phenomena are still not understood, such as: i) the non-linear characteristic of current voltage curves; ii) the so-called memory effect, iii) the apparent enhancement of kinetics when nanomaterials are decorated with glassy surface films, iv) the variable slope of the Warburg diffusional feature during charge and discharge etc.

We here present a conceptually new and quite general electrical model that can give coherent answers to most of the peculiar phenomena mentioned above. The model is focused on description of long relaxation times, that is, low frequency phenomena in terms of impedance spectroscopy picture. Among others, the model contains two unconventional elements: a switch and a variable resistor. Despite its simplicity the model is able to describe most of the known first-order phenomena occurring in insertion batteries. The model also predicts a couple of hitherto unknown insertion battery features such as the existence of clear correlation between impedance and galvanostatic measurements or a surprising phenomenon termed the dual nature of insertion battery non-linearity. The model is extensively verified using specially designed electrochemical experiments.

11:00 AM C12.02
Layered Cathode Materials Prepared by Spray Pyrolysis for High-Energy Lithium-Ion Batteries Feng Lin[1], Yuyi Li[1], Dennis Nordlund[2], Tsu-Chien Weng[2], Huolin Xin[3], Yijin Liu[2]and Marca Doeff[1]; [1]Lawrence Berkeley National Lab, Berkeley, California, United States; [2]SLAC, Menlo Park, California, United States; [3]BNL, Upton, New York, United States.

Stoichiometric layered lithium transition metal oxides ($LiNi_{1-x-y}Mn_xCo_yO_2$) represent a family of cathode materials suitable for high-energy lithium ion batteries. However, their structural instability (e.g., surface reconstruction from the layered structure to a rock-salt/spinel mixed structure) when charged to high voltages impedes efforts to improve their energy densities. Here, we report on a study of $LiNi_{1-x-y}Mn_xCo_yO_2$ materials prepared by a spray pyrolysis technique to provide improved cycling performance.

The as-prepared $LiNi_{1-x-y}Mn_xCo_yO_2$ materials assemble into spherical structures that consist of nanosized primary particles. Revealed by transmission electron microscopy, these primary particles are “fused” together to form atomically disordered interfaces that may allow for lithium and electron diffusion. $LiNi_{1-x-y}Mn_xCo_yO_2$ materials with different ratios of transition metals were synthesized, *i.e.*, $LiNi_{1/3}Mn_{1/3}Co_{1/3}O_2$, $LiNi_{0.4}Mn_{0.4}Co_{0.2}O_2$, $LiNi_{0.5}Mn_{0.3}Co_{0.2}O_2$, $LiNi_{0.6}Mn_{0.2}Co_{0.2}O_2$, most of which show improved electrochemical performance (*i.e.*, discharge capacity, capacity retention) compared to the counterparts synthesized by the conventional co-precipitation method, although different thermal treatment protocols are needed after the spray pyrolysis process. Surface reconstruction was quantified by soft X-ray absorption spectroscopy to investigate the surface phase transition of the $LiNi_{1-x-y}Mn_xCo_yO_2$ materials after electrochemical cycling, and it is found that the materials prepared by spray pyrolysis have thinner surface passivation layers (a rock-salt/spinel mixed structure), which accounts for better capacity retention. This study suggests that morphological engineering by spray pyrolysis may offer an efficient pathway towards stable high-energy layered cathode materials.

11:20 AM C12.03
Stabilizing the Structure of Li-Rich Oxide Cathode Materials Zhaoxiang Wang[1], Yurui Gao[1], Xin Feng[1], Jun Ma[1], Yong-ning Zhou[2], Lin Gu[1], Qingyu Kong[3], Xiao-qing Yang[2] and Liquan Chen[1]; [1]Institute of Physics, Chinese Academy of Sciences, Beijing, China; [2]Brookhaven National Laboratory, Upton, New York, United States; [3]Argonne National Laboratory, Argonne, California, United States.

Lithium-rich manganese-based oxide ($xLi_2MnO_3\times(1-x)LiMO_2$ or $Li_{1+x}M_{1-x}O_2$, M = Ni, Co, Mn, etc) are regarded as one of the most important candidate cathode materials for high energy-density lithium ion batteries. In these oxides, the Li_2MnO_3 phase acts as a Li-ion reservoir and structure stabilizer when the cell is charged over 4.5 V vs. Li^+/Li. However, it seems that most of the drawbacks of the Li-rich Mn-based cathode materials are related to the structural instability of Li_2MnO_3. Therefore, in order to improve the electrochemical performances of the Li-rich oxides, the structure of Li_2MnO_3 or its replacer has to be enhanced. This report is to introduce our recent findings and proposals on stabilizing the structure and improving the performance of the Li-rich cathode materials.

Our first-principles calculations indicate that the oxygen vacancy triggers the migration of the Mn ions and distortion of the MnO_6 octahedra in Li_2MnO_3. With the help of lithium vacancies, the Mn migration is promoted. Therefore, metal atoms or anions that can former stronger O-M or M^+-A^- bonds are required to substitute for Mn or O and to suppress Mn migration and O_2 evolution.

Among a number of candidate substituent atoms such as Ti, V, Cr, Fe, Co, Ni, Zr and Nb, first-principles calculations show that Nb is the best substituent for Mn in Li_2MnO_3 because it can narrow the band gap, donate extra electrons to O, suppress the oxidation of O upon Li removal and bind O tightly. All the other elements can only have one or two of its benefits. Electrochemical evaluations indicate that phase-pure $Li_{1.95}Mn_{0.95}Nb_{0.05}O_3$ indeed has superior behaviors over Li_2MnO_3. Alkali substitution for Li ions in the Li-rich oxides leads to lowered capacity. However, we found that it is possible to dope Ti in the Li-layer of Li_2MnO_3. $Li_{1.2-x}Ti_xMn_{0.54}Co_{0.13}Ni_{0.13}O_2$shows a slower drop of discharge potential during long-term cycling and much improved cycling and rate performances as well as increased capacity. XRD analysis confirms the position of the doped Ti atoms in the material. First-principles calculations further support that aliovalent Ti doping in the Li-layer can promote Li diffusion and suppress Mn migration though Ti doping will introduce O vacancies.

Oxygen vacancy is generated in Li_2MnO_3-based Li-rich oxide cathode materials because O^{2-} is the only electron donator to compensate for the charges upon Li removal. We propose to replace Li_2MnO_3 with Li_2MoO_3 for constructing novel Li-rich oxide cathode materials. Extensive physical and electrochemical studies indicate that the easy and reversible Mo^{4+} to Mo^{6+}oxidation can compensate for the charges. Although Mo migration is not completely inhibited, its migration is found partially reversible. In addition, no O^{2-} oxidation is observed upon to 4.8 V. Supporting results are obtained in Mo-substituted Li_2MnO_3 experimentally and by DFT calculations. Therefore, it is feasible to replace Li_2MnO_3 with Li_2MoO_3 in constructing novel Li-rich oxide cathode materials with enhanced structural and long-term cycling stability.

11:40 AM C12.04

Integrated Nano-Domains of Disordered and Ordered Spinel Phases in $LiNi_{0.5}Mn_{1.5}O_4$ for Li-Ion Batteries

Jung-Hyun Kim[1], Ashfia Huq[2], Craig A. Bridges[2], Miaofang Chi[2], Nicholas P. Pieczonka[3], Arumugam Manthiram[4] and Bob R. Powell[1]; [1]Chemical and Materials Systems Laboratory, General Motors R&D Center, Warren, Michigan, United States; [2]Oak Ridge National Laboratory, Oak Ridge , Tennessee, United States; [3]Optimal CAE., Plymouth, Michigan, United States; [4]Materials Science and Engineering Program, The University of Texas at Austin, Austin, Texas, United States.

The $LiMn_{1.5}Ni_{0.5}O_4$ (LNMO) spinel has attracted great interest as a promising cathode material for Li-ion batteries due to its high $Ni^{2+/4+}$ redox potential (c.a. ~ 4.7 V vs. Li) and rapid Li-ion transport through 3-dimensional (D) pathways in its spinel lattice compared with that of 2-D layered oxides or 1-D olivine materials. The LNMO crystallizes into two different symmetries depending on the occurrence of disordering/ordering of Ni^{2+} and Mn^{4+} in the lattice. Ordering between Ni and Mn (1:3 ratio) lowers the symmetry from $Fd\bar{3}m$ (disorder) to $P4_332$ (order), which strongly affects the electrochemical properties of the LNMO spinel. [1] However, it has been recently pointed out that LNMO may contain a significant amount of short-range Ni/Mn ordering rather than purely ordered or disordered phases. It was further suggested that the short-range ordering strongly depends on the cooling-rate after sintering at 900 °C, because it determines the amount of oxygen uptake by the LNMO.[2]

Firstly, our presentation contains a discussion of the presence of integrated nano-domains of disordered and ordered spinel phases in LNMO. The long- and short-range ordering behavior of Ni and Mn were analyzed by combining neutron powder diffraction and X-ray powder diffraction (XRD).[3] Further, TEM analysis of thin-sliced specimens allowed the direct observation of local distributions of ordered and disordered phase from surface to bulk. The powder diffraction techniques allowed us to quantify the degree of ordering and the size of ordered domains in LNMO as functions of annealing time at 700°C. The results show that the fraction of ordered phase rapidly increases during the first 6 h of annealing at 700 °C and accompanied by decreasing amounts of secondary phases. Annealing longer than 6 h led to the enlargement of the ordered domains along with a slower increase in the fraction of ordered phase (domain growth). The increase in the degree of ordering increases the open circuit voltage (OCV) and the initial capacity but reduces cycle life and rate capability. The LNMO delivered optimal battery performance (capacity, cycle life, and rate capability) after annealing at 700 °C for 2 h. The partially ordered sample thus obtained showed the respective advantages from both disordered and ordered spinels: better spinel-phase purity (thus, higher initial capacity) from the ordering and better cycle life and rate capability from the disordering.

Secondly, we will present the effects of elemental substitutions on the short-range ordering behavior of Ni and Mn in LNMO. Although the elemental substituted-LNMO do not have long-range Ni/Mn ordering, neutron powder diffraction analysis provides evidence of short-range ordering. For example, Shin et al. [4] reported nanometer-size ordered domains in the LiNi0.5−xMxMn1.5O4 (M = Cr, Fe, and Ga), as evidenced by broad reflections associated which was attributed to Ni/Mn ordering. The electrochemical properties of elemental substituted-LNMO were nevertheless greatly affected by short-range ordering of Ni/Mn. Since the elemental substituted-LNMO spinel is a relatively promising new material, its electrochemical performance needs to be optimized by tuning chemical compositions and synthesis parameters. Therefore, we will also discuss what influence these factors have on crystal structure, phase purity, and electrochemical performance.

References

[1] J.-H. Kim, S.-T. Myung, C.S. Yoon, S.G. Kang, and Y.-K. Sun, *Chem. Mater.*, 16, 906 (2004).
[2] J. Zheng, J. Xiao, X. Yu, L. Kovarik, M. Gu, F. Omenya, X.-Q. Yang, J. Liu, G. L. Graff, M. S. Whittingham, J.-G. Zhang, *Phys. Chem. Chem. Phys.*, 14, 13515 (2012).
[3] J.-H. Kim, A. Hug, M. Chi, N. P. W. Pieczonka, E. Lee, C. A. Bridges, M. M. Tessema, A. Manthiram, K. A. Persson, B. R. Powell, *Chem. Mater.*, 26, 4377 (2014).
[4] D. W. Shin, C. A. Bridges, A. Huq, M. P. Paranthaman, A. Manthiram, *Chem. Mater.*, 24, 3720 (2012).

D: Fundamentals of Transport and Reactivity and Nanoionics

* Invited Speaker
** Keynote Speaker

SESSION D1: Fundamentals of Transport and Reactivity and Nanoionics I
D: Fundamentals of Transport and Reactivity and Nanoionics
Chair: Joachim Maier
Monday Morning, June 15, 2015
Keystone Resorts, Grays Peak I/II

10:30 AM **D1.01
Oxygen Nonstoichiometry in Thin Films and Nanoparticles: Measurement, Control and Implications for Energy and Memory Related Devices Harry L. Tuller; Department of Materials Science and Engineering, MIT, Cambridge, Massachusetts, United States.

Oxides are playing an increasing critical role as functional components in the fields of energy conversion/storage, microelectronics, displays, sensors/actuators and catalysis. In turn, their electrical (ionic & electronic), optical, magnetic and catalytic properties depend sensitively on their oxygen nonstoichiometry, often frozen in during processing, and rarely well defined. This is particularly true for thin films, where conventional methods, appropriate to bulk materials, do not apply. In this presentation, we review in-situ optical, electrochemical and dilatometric methods, developed or refined in our laboratory, to monitor, analyze and control the nonstoichiometry, defect equilbria, transport and optical properties of oxide thin films and nano-sized particles. Examples will include materials of interest as electrodes in fuel cells and photoelectrochemical cells, oxidation catalysts and magnetic memory devices.

11:00 AM D1.02
Investigating Thin YSZ Perovskite Films Using Analytical Electron Microscopy Melissa Neish[2], Frank Scheltens[1], Robert E. Williams[1], Leslie J. Allen[2] and David W. McComb[1];[1]Materials Science and Engineering, The Ohio State University, Columbus, Ohio, United States; [2]School of Physics, University of Melbourne, Melbourne, Victoria, Australia.

There have been numerous reports in the literature of significantly enhanced ionic conductivity in multilayer heterostructures formed from ionic conductors and insulators. There have also been a number of reports suggesting that these enhancements are due to electronic rather than ionic conductivity. Many reports have focused on epitaxial heterostructures between strontium titanate (STO) and yttria-stabilised zirconia (YSZ). Those advocating that the enhanced conductivity is electronic rather than ionic have often suggested that acceptor dopants in the STO layers dominate over the ionic conductivity in the YSZ layer. Others have puzzled to understand how the lattice mismatch (>7%) between STO and YSZ is accommodated. It has been suggested by some groups that a highly disordered region is present at the interface resulting in high local concentration of oxygen vacancies. It has been generally accepted that the YSZ layer adopts the normal fluorite structure. In this contribution we will present compelling evidence from scanning transmission electron microscopy (STEM) and energy-dispersive x-ray spectroscopy (EDS) analysis that the YSZ thin film in the STO-YSZ-STO heterostructure can adopt the perovskite rather than the fluorite structure. Atomic scale compositional fluctuations in STEM-EDS analysis will be critically analysed in the context of the limits of spatial resolution. We will discuss the thermodynamic stability of this perovskite thin film and consider the structure-property relationship that might lead to the observed conductivity measurements.

11:20 AM D1.03
Cation Surface Segregation and Composition Depth Profile Variations in Thin Films Of SOFC Cathode Materials Analysed by Low Energy Ion Scattering Jose Santiso[1], Helena Tellez-Lozano[2], Araceli Gutierrez-Llorente[3], James Zapata[1], Roberto Moreno[1], Jaume Roqueta[1], Nuria Bagues[1], Anna Magraso[1], Jose M. Caicedo[1], John Druce[2], John A. Kilner[2] and Tatsumi Ishihara[2]; [1]ICN2 Institut Catala de Nanociencia i Nanotecnologia, Barcelona, Spain; [2]Hydrogen Production, I2CNER, International Institute for Carbon Neutral Energy Research, Fukuoka, Japan; [3]Universidad Rey Juan Carlos, Madrid, Spain.

Surface activity for the oxygen reduction reaction in oxide SOFC cathode materials with perovskite structure is expected to be very dependent on the chemical composition of the outermost atomic layer where presumably oxygen adsorption and dissociation takes place. In polycrystalline cathode materials many factors such as surface roughness, crystallite size and orientation as well the presence of grain boundaries, make very difficult the exploration of the intrinsic phenomena taking place at the material surface during oxygen reduction. Therefore, in many occasions flat epitaxial films grown by vapour deposition techniques have been considered as an ideal platform for fundamental studies of surface reactivity. Low Energy Ion Spectroscopy (LEIS) is one of the few techniques capable of analysing the chemical composition of one single atomic layer at the surface, which in combination with a low energy ion sputtering enables high resolution depth profiling.

In this study we have analysed by LEIS the surface chemical termination as well as the composition depth profile in the near-surface region of high crystal quality epitaxial films of different perovskite oxide cathode materials, like $Ba_{0.5}Sr_{0.5}Co_{0.8}Fe_{0.2}O_{3-d}$, $GdBaCo_2O_{5.5+d}$ and La_2NiO_{4+d}. The analyses showed in all cases A-site terminated surface. Despite the high crystal quality shown by HRXRD analysis all as deposited films presented inhomogeneities of the A-site or B-site occupancies along the film growth direction in the first few nanometres depth profile. This suggests that surface segregation processes are already activated during thin film growth at deposition temperatures of about 700-800°C. Post deposition annealing at temperatures as low as 500°C (well below the deposition temperatures) in 200 mbar O_2 induced further changes in the composition profile of the outermost surface even after a short time annealing of only 15 min. These changes point to a metastable condition of the outer and sub-surface film regions as well as non-negligible kinetics for A or B cation migration at the nanoscale. The driving forces underlying this phenomenon are discussed in view of the results.

11:40 AM D1.04
The Influence of Water on the Ionic Conductivity in Ordered Mesoporous YSZ Thin Films Matthias T. Elm[1, 2], Jonas D. Hofmann[1], Christian Suchomski[1, 3], Juergen Janek[1] and Torsten Brezesinski[3]; [1]Institute of Physical Chemistry, Justus-Liebig University Giessen, Giessen, Germany; [2]Institute of Experimental Physics I, Justus-Liebig University Giessen, Giessen, Germany; [3]Institute of Nanotechnology, Karlsruhe Institute of Technology, Eggenstein-Leopoldshafen, Germany.

Mesoporous materials are characterized by a regular structure of pores with diameters ranging between 2 and 50 nm. Due to this highly ordered architecture these materials can be considered as a close-packed and interconnected 3D arrangement of nanocrystallites with high surface to volume ratio – making them an ideal model system to study the effect of surface states on point defects and point defect mobility. Here we present the investigation of mesostructured 8 mol% yttria-stabilized zirconia (YSZ) thin films, which were produced by solution-phase coassembly of chloride and nitrate salt precursors with an amphiphilic diblock copolymer using an evaporation-induced self-assembly process (EISA) process. After calcination and an annealing step at 600 °C the characterization of the obtained thin oxide films by high-resolution transmission electron microscopy (HR-TEM), wide-angle X-ray diffraction (WAXD), secondary-ion mass spectroscopy (SIMS) and Raman spectroscopy confirmed a high quality 3D network of pores averaging 24 nm in diameter surrounded by a crystalline wall structure with 7 to 9 nm grains. The electrical properties of the mesoporous thin films were investigated under ambient and dry atmosphere using impedance spectroscopy in a

temperature range between 200°C to 600°C. The mesoporous YSZ films show a constant ionic conductivity (comparable to bulk YSZ) upon variation of the oxygen partial pressure between 1 and 10^{-5} bar. While in ambient atmosphere (wet air) the thermally activated ionic transport can be described well by a single activation energy, measurements in dry atmosphere show a higher conductivity and have to be described by two different activation energies at low and high temperatures. The observed differences are explained by the annihilation of oxygen vacancies due to adsorbed water molecules and hydration of the surface, thus demonstrating the large influence of surface effects on the transport properties in mesoporous materials quantitatively.

SESSION D2: Poster Session: Fundamentals of Transport and Reactivity and Nanoionics I
D: Fundamentals of Transport and Reactivity and Nanoionics
Monday Afternoon, June 15, 2015
12:00 PM
Keystone Resorts, Red Cloud Peak

D2.01
***In Situ* Optical Absorption Studies of Defect Equilibria and Kinetics: Application to Sr(Ti,Fe)$O_{3-\alpha}$ Thin Films** Nicola H. Perry[1, 2], Jaejin Kim[2] and Harry L. Tuller[2, 1]; [1]I2CNER, Kyushu University, Nishi-ku, Fukuoka, Japan; [2]Materials Science and Engineering, MIT, Cambridge, Massachusetts, United States.

Rapid surface oxygen exchange kinetics are desired for high temperature sensors, gas separation membranes, and solid oxide fuel/electrolysis cell electrodes. Unambiguous characterization of new materials' native exchange kinetics under operating conditions benefits from the use of dense thin films having controlled surface area, thickness, and triple phase boundary length, *in situ* / *in operando* measurements, and the absence of potentially catalytic current collectors. Recently our group demonstrated a new technique for *in situ*, contact-less interrogation of both thin film defect equilibria and surface exchange kinetics, using optical absorption relaxation verified by simultaneous ac-impedance measurements, on the model system Pr-doped CeO_2 [1].

In the present work, the optical absorption relaxation technique is extended to the study of defect equilibria and surface oxygen exchange kinetics of mixed conducting $SrTi_{1-x}Fe_xO_{3-\alpha}$ ($0.05 \leq x \leq 0.5$) thin films deposited by pulsed laser deposition. Absorption corresponding to the presence of Fe^{4+} was monitored to evaluate defect concentrations and surface exchange kinetics over a range of oxygen activities, temperatures, and aging times. Steady-state concentrations were compared to those predicted by the bulk defect model [2], and surface exchange coefficients were compared to those measured by other techniques, e.g., impedance spectroscopy. Rapid, precise, and reversible electrochemical control of oxygen activity in the films over a wide range was demonstrated. Broader applicability, requirements, and limitations of the technique will be discussed.

[1] Jaejin Kim *et al. Chem. Mater.* 26, 1374 (2014)
[2] Melanie Kuhn *et al. Chem. Mater.* 25, 2970 (2013)

D2.02
Millimeter Wave Spectroscopy and Molecular Dynamics Simulation of Ionic Liquids Teruyoshi Awano[1], Arimitsu Shikoda[1] and Toshiharu Takahashi[2]; [1]Tohoku Gakuin University , Tagajo, Japan; [2]Research Reactor Institute, Kyoto University, Kumatori, Japan.

We have observed millimeter wave absorption bands around 6 and 8 cm^{-1} in AgI-superionic conductive glasses. These bands were also observed in CuI-superionic ones. These bands seems to be due to collective motion of conductive ions, although how conduction ions move in correlation is not clear. Ionic liquid is molten salt at room temperature. It is interesting to compare ionic motion in ionic liquids with those in superionic conductor.

Ionic liqids N,N-Diethyl-N-methyl-N-(2-methoxyethl) ammonium tetrafluoroborate ([DEME][BF_4]) and N,N-Diethyl-N-methyl-N-(2-methoxyethl)ammonium bis(trifluoromethanesulfonyl)imide ([DEME][TFSI]) (Kanto Chem. co., inc.) were spread into filter paper. Transmission spectra of single and double papers with ionic liquids were measured at room temperature and low temperatures. Absorption spectra were obtained by subtraction of them.

Two absorption bands were observed around 6 and 8 cm^{-1}, which are almost coincident with those in AgI-superionic conductive glasses. These bands have almost equal peak positions and intensities in both ionic liquids. This means that these absorption bands are due to cation motion, which are common in these liquids. However, temperature dependence of these bands are different between these ionic liquids. This difference seems to be due to the difference of their phase transition temperatures and solid states.

D2.03
Structural vs. Intrinsic Carriers: Contrasting Effects of Cation Disorder on Ionic Conductivity in Pyrochlores Romain Perriot and Blas P. Uberuaga; Materials Science and Technology Division, Los Alamos National Laboratory, Los Alamos, New Mexico, United States.

We use molecular dynamics to independently investigate the role of cation disorder and chemistry on oxygen diffusion in $Gd_2Zr_2O_7$ (GZO) and $Gd_2Ti_2O_7$ (GTO) pyrochlores, a class of complex oxides which contain a structural oxygen vacancy relative to the fluorite structure. The introduction of disorder, in the form of A_B or B_A antisites (A=Gd, B=Zr,Ti), has contrasting effects depending on the chemistry, enhancing the diffusivity by up to four orders of magnitude in GZO, while enabling diffusion to occur in GTO, for which diffusion was not observed in the ordered case. The disorder results in both an increase in the concentration of mobile structural carriers and their mobility.

The disorder also generally enhances the diffusivity in materials containing intrinsic defects, such as additional oxygen vacancies or interstitials. However, in low concentration, cation antisites can act as traps for the vacancies and interstitials, resulting in a lowering of the conductivity, and causing a non-monotonic behavior of the diffusivity with disorder.

Together, these results indicate that oxygen diffusion in pyrochlores is a function of both the pyrochlore chemistry and the level of disorder. Further, intrinsic defects only make a sizeable contribution for very special cases. These results provide new insight into the relationship between structural carriers and mass transport in complex oxides.

D2.04
Intrinsic Material Properties Dictating the Formation Energetics of Oxygen Vacancies in Wide Gap Oxides Ann Deml[1, 2], Aaron Holder[2], Ryan O'Hayre[1], Charles Musgrave[3] and Vladan Stevanovic[1, 2]; [1]Colorado School of Mines, Golden, Colorado, United States; [2]National Renewable Energy Laboratory, Golden, Colorado, United States; [3]University of Colorado Boulder, Boulder, Colorado, United States.

Oxygen vacancies in metal oxides are extensively utilized to enable vital material functionalities. While methods to predict defect formation energies have seen significant advancement, understanding of the intrinsic material properties that govern defect energetics is lagging. We used first principles calculations to study the connection between intrinsic material properties and the energy to form a single, charge neutral oxygen vacancy (*Ev*). We investigated 45 different binary and ternary oxides and found that a simple model which combines (*i*) the oxide enthalpy of formation, (*ii*) the mid-gap energy relative to the O-2p band center, and (*iii*) atomic electronegativities reproduces calculated *Ev* values within ~0.2 eV. This result provides both valuable insights into the key properties influencing oxygen vacancy formation energetics as well as a direct and simple method to predict *Ev*. We subsequently predicted the *Ev* values of ~1800 additional oxide materials and validated the predictive nature of our approach against direct defect calculations for a subset of 18 randomly selected materials.

D2.05

***Ab Initio* Studies on Bismuth Oxide Based Solid Electrolytes** Marcin Krynski[1], Franciszek Krok[1], Isaac Abrahams[2], Wojeciech Wrobel[1], Jozef Dygas[1] and Piotr Spiewak[3]; [1]Physics, Warsaw University of Technology, Warszawa, Poland; [2]Centre for Materials Research, School of Biological and Chemical Sciences, Queen Mary, London, United Kingdom; [3]Materials Engineering, Warsaw University of Technology, Warszawa, Poland.

In this study electrical properties of the fluorite-like type-II Bi_3NbO_7 have been investigated by means of *ab initio* simulations. For this purpose, a series of molecular dynamic simulations within density functional theory (DFT) were carried out for a range of elevated temperatures from 1223K to 1373K. Structural studies of Bi_3NbO_7 reveal high structural disorder, therefore to model it, five parallel runs over 60ps, with different initial anion and cation distributions were performed in a 2x2x2 super-cell (88 atoms in total). Lattice parameters and initial atom positions were obtained from X-ray and neutron diffraction.

Results of DFT molecular dynamics simulations were analysed in order to examine the oxide ion positions in respect to the bismuth and niobium cations. The preferred six-folded coordination of niobium cations was observed, that is in agreement with structural studies. This results in high concentration of oxide ion vacancies around Nb^{5+} cations (on average two vacancies per niobium cation) and consequently in a very low content of vacancies in bismuth rich areas. Oxide ion trajectories were examined in order to describe rotational movement of oxide ions around niobium cations. In contrast the translational movements of O^{2-} in the bismuth rich areas are observed. Differences between bismuth and niobium surrounding is reflected also in the residence times and will be used to explain the overall poor ionic conductivity of δ-Bi_3NbO_7.

The electron structure of δ-Bi_3NbO_7 was studied by analysing the electron charge density function. Results prove the existence of stereochemically active electron lone pair of bismuth $6s^2$orbital. The cation-anion bonding type was also studied and confirmed the semi-covalent nature of Bi-O bonds and ionic nature of Nb-O bonds.
Results of DFT studies for Bi_3NbO_7 will be compared to the results of similar study of δ-Bi_3YO_6 , where a trapping mechanism of oxide ions in yttrium rich compartments was described.

D2.06

Role of Oxide Ion Transport on Promoting Iron Oxide Redox Reaction with Oxide Ion Conductors as Supports for Energy Storage and Conversion Fumihiko Kosaka[1], Hiroyuki Hatano[2], Yoshito Oshima[1] and Junichiro Otomo[1]; [1]The University of Tokyo, Kashiwa City, Japan; [2]Chuo University, Bunkyo-Ku, Japan.

Redox reaction of metal oxides (MO) such as iron oxide is one of candidates for energy conversion and storage. In chemical looping systems, fuels are converted to chemical and thermal energies[1]. Electrical power is stored as metal (M) in a power storage system integrated with reversible fuel cells[2]. $(2n+m)MO+C_nH_{2m} \rightarrow (2n+m)M+nCO_2+mH_2O$ $M+1/2O_2 \rightarrow MO$ $M+H_2O \rightleftarrows MO+H_2$ It has been reported that pure and mixed conductors such as yttlia stabilized zirconia (YSZ) and iron doped calcium titanate (CTFO) promote the reduction reaction of iron oxide and nickel oxide[3,4]. Understanding of oxide ion transport at around the interface between iron oxide and oxide ion conducting supports is important for designing highly reactive material and long term stability. In this study, we investigated the effect of pure and mixed conductors on the redox reaction of iron oxide and discussed the role of oxide ion and electronic conductivity on the reaction enhancement. Fe_2O_3 in H_2 or wet CH_4 atmosphere with oxide ion conductors such as YSZ, gadolinia-doped ceria (GDC) and CTFO showed higher reduction rate in comparison with that with Al_2O_3support. We discussed the enhancing effect with model analysis of oxide ion transport in iron oxide and support composite particle using finite element method. The result suggests that oxide ion transport at the interface enhances the total reduction rate of iron oxide. In addition, it was found that the oxide ion conductors promoted the oxidation reaction of metal iron by H_2O. These results contribute to downsizing the reactors of the reduction and oxidation processes.

Reference
[1] J. Adanez *et al*., *Prog. Energy Combust. Sci.*, **38** (2012) 215.
[2] N. Xu *et al*., *Energy Env. Sci.*, **4** (2011) 4942.
[3] J. Otomo *et al*., *Fuel*, **104** (2013) 691.
[4] S. Isogai *et al*., *Chem. Lett.*, **42** (2013) 143.

D2.07

Ionic and Electronic Energy Level Diagrams for the CaF_2/BaF_2 Heterojunction Giuliano Gregori and Joachim Maier; Max Planck Institute for Solid State Research, Stuttgart, Germany.

In recent years, ionic redistribution phenomena at heterojunctions proved to be of utmost importance. A well-understood system is based on CaF_2/BaF_2 heterostructures, whose conductivity is governed by an redistribution [1]. Referring to a previous thorough analysis [2], we give a thermodynamically precise account by evaluating the individual standard chemical potentials of the carriers as true materials parameter.
The quantitative results can be most vividly represented by the construction of an ionic level picture [3] analogous to the electronic level diagrams. The consideration of the combination of both diagrams [4] allows for a generalized thermodynamic picture of the CaF_2/BaF_2 heterocontact.

The electrical potential jump between the two outermost heterolayers shows to be significant for the total electrical potential drop in this system.

References

[1] N. Sata, K. Eberman, K. Eberl, and J. Maier, Nature 408, 946–949 (2000).
[2] X. X. Guo and J. Maier, Adv. Funct. Mater. 19(1), 96–101 (2009).
[3] J. Jamnik, J. Maier, and S. Pejovnik, Solid State Ionics 75, 51–58 (1995).
[4] J. Maier, Physical Chemistry of Ionic Materials. Ions and Electrons in Solids, John Wiley & Sons, Ltd, Chichester, West Sussex/UK, 2004.

D2.08

Glass Formation and Fast Ag Ion Conduction in the System Ag_2Se-Ga_2Se_3-$GeSe_2$ Maxwell A. Marple[1], Derrick Kaseman[1], Bruce Aitken[2], Sangtae Kim[1] and Sabyasachi Sen[1];[1]Chemical Engineering and Materials Science, University of California Davis, Davis, California, United States; [2]Corning Inc, Corning, New York, United States.

Ag-chalcogenide glasses are potential candidate materials for solid electrolyte and ionic switch applications where the high mobility of Ag ions gives rise to large ionic conductivity. Although significant work has been done on Ag-Ge-Se glasses to develop fast ion conducting glasses, compositions with high Ag content and correspondingly high conductivity are also unstable towards phase separation and eventual deterioration with thermal cycling. We have synthesized glasses in the stochiometric Ag_2Se-Ga_2Se_3-$GeSe_2$ ternary system with improved stability against phase separation and remarkably large electrical conductivity on the order of ~10^{-4} $ohm^{-1}cm^{-1}$ at ambient temperature. ^{109}Ag NMR spectroscopy studies indicate that the conductivity is ionic and results from fast Ag ion dynamics. Compositional evolution of the structure of these glasses has been studied using Raman and ^{71}Ga and ^{77}Se NMR spectroscopy. These results will be discussed and related back to the trends observed in conductivity.

D2.09

Fast-Ion Conductor Design for Grid-Scale Batteries Stefan Adams, Haomin Chen, Lee L. Wong and Rayavarapu Prasada Rao; Materials Science & Eng., National University of Singapore, Singapore, Singapore.

Revolutionary high performance energy storage systems are urgently needed to manage power grids based on non-dispatchable renewable sources. For such large-scale energy storage systems low materials and processing costs become key performance indicators along with minimal operational costs, enhanced cycle-life, and higher capacity. Electrochemically stable fast sodium, lithium and magnesium-ion conductors (FIC) gradually gain a wider range of applications beyond their traditional application in solid-state-batteries as FICs as key components in the most promising large-scale battery concepts (metal-air, metal-

sulphur, alkali-redox flow, etc.). This makes identifying and realizing such FICs crucial to enable the storage concepts both technically and commercially. Fast-ion conductivity of mixed conductors is moreover a decisive parameter for the power performance of most battery electrode materials.

Exploiting our bond valence site energy approach for the modeling of ion transport pathways as well as for empirical molecular dynamics simulations, we have screened a wide range of Li, Na and Mg compounds for their suitability as ionic conductors factoring in also economical constraints. For the case of Na-based large-scale batteries the aim of translating cost advantages of sodium into competitive large-scale systems e.g. requires a consistent restriction to low-cost earth-abundant elements restricting materials design options. A range of recently proposed low cost sodium cathode materials will be discussed from the point of view of alkali ion mobility and hence power performance in the ideal crystal structure and more realistic local structure models, comparing predictions from our ab initio and empirical bond valence studies.

The decisive role of disorder in the immobile substructure for a robust high power performance will also be demonstrated for a range of known and novel alkali sulfide solid electrolytes, and complemented by explorations on how to enhance the stability of FIC sulfides against hydration (a major cost factor limiting their industrial application). Finally, low cost preparation and application of selected FICs in several large-scale battery designs will be exemplified.

D2.10

Grain Boundaries Across Length Scales; Correlating Orientation Imaging and Nanospectroscopy William J. Bowman[1], Amith Darbal[2], Madeleine Kelly[3], Gregory S. Rohrer[3], Cruz A. Hernandez[1], Kimberly McGuinness[1] and Peter A. Crozier[1]; [1]Materials Science and Engineering, Arizona State University, Tempe, Arizona, United States; [2]AppFive LLC, Tempe, Arizona, United States; [3]Materials Research Science and Engineering Center, Carnegie Mellon University, Pittsburgh, Pennsylvania, United States.

Grain boundaries' significant variety makes them difficult to characterize and optimize. Statistical methods coupled with SEM orientation imaging via electron back scatter diffraction (EBSD)—which typically samples >50,000 boundaries, are powerful techniques for quantifying microscopic grain boundary parameters such as the crystallographic plane distribution and misorientation texture [1]. Conversely, TEM and scanning-TEM (STEM) atomic resolution imaging and spectroscopies have proven invaluable in elucidating nanoscale boundary properties including local atomic structure and elemental composition [2]. However, correlating such micro- and nano-scale observations has been challenging due to the difficulty of unambiguously determining the statistical relevance of grain boundaries observed in the TEM.

Recently-commercialized precession nanobeam diffraction (PND) instrumentation and techniques have made possible routine orientation imaging in the TEM [3]. This mesoscale technique facilitates the location and identification of statistically relevant grain boundaries in a TEM specimen that can then be targeted for in-depth analysis via high resolution imaging and/or nanospectroscopy. This capability bridges the gap between microscopic SEM measurements and nanoscopic and STEM characterizations to offer a more complete and contiguous understanding of grain boundary properties across a considerable range of length scales. Here, we employ a suite of techniques including SEM EBSD, TEM PND and aberration-corrected STEM (AC-STEM) spectroscopies to correlate grain boundary data acquired across micron, meso and nanometer length scales from ceria-based conductors We present results of stereological analyses characterizing microscopic parameters derived from SEM EBSD data such as plane distribution and misorientation texture. These parameters are related to TEM orientation imaging data, and we present electron and x-ray nanospectroscopic data acquired from the same boundaries using an AC-STEM.

1. L. Helmick et al. *Int. J. Appl. Ceram. Technol*., **8** [5] 1218-1228 (2011)
2. W.J. Bowman et al. *Solid State Ionics*, **272** 9-17 (2015)
3. A.D. Darbal et al. *Microsc. Microanal*., **19**, 111-119 (2013)

D2.11

Determining the Effect of Gas Phase Concentration Polarization on Porous Thick Film Oxygen Surface Exchange Coefficients Determined via the Curvature Relaxation Technique Yuxi Ma and Jason D. Nicholas; Chemical Engineering and Material Science, Michigan State University, East Lansing, Michigan, United States.

The Curvature Relaxation (KR) technique is a new, *in situ*, electrode-free method used to measure the chemical oxygen surface exchange coefficient (k_{chem}) of dense thin film or porous thick film samples [1-2]. The KR technique determines k_{chem} by fitting a solution of Fick's 2nd Law to the curvature response of mechano-chemically active film | inert substrate bilayers reacting to sudden oxygen partial pressure changes. The objective of the present work was to quantify the k_{chem} errors caused by gas-phase concentration polarization in porous thick film samples. To achieve this, porous $La_{0.6}Sr_{0.4}FeO_{3-\delta}$ (LSF64) thick films with variable porosity, gas-phase tortuosity, and film thickness were evaluated using the KR technique. These porous LSF64 thick films were prepared by 1) air-brushing colloidal LSF64 suspensions onto pre-annealed $(Y_2O_3)_{0.13}(ZrO)_{0.87}$ substrates and 2) heating the bilayers to 1050°C to partially sinter the LSF64 films. The samples were then cooled to 500°C and KR tested down to ~275°C in 25°C increments. KR measurements were performed by switching the atmosphere from either air to a 50% air-50% N_2 mixture, or from a 21% O_2-79% He mixture to a 50% (21% O_2,79% He)-50% N_2 mixture. Use of these gas mixtures assured that O_2 gas-phase diffusivity could be varied while the oxygen partial pressure differences driving oxygen surface exchange were kept constant. After KR measurements, the porosity, gas-phase tortuosity and film thickness were measured using 3D Focused Ion Beam Scanning Electron Microscopy microstructural reconstructions. The results show that care must be taken to limit gas-phase concentration polarization when conducting porous thick film KR measurements.

Reference

[1] Yang Q, Nicholas J D. "*Porous Thick Film Lanthanum Strontium Ferrite Stress and Oxygen Surface Exchange Bilayer Curvature Relaxation Measurements*" J. Electrochem. Soc., 2014, 161(11): F3025-F3031.

[2] Yang Q, Burye T E, Lunt R R, et al. "*In situ Oxygen Surface Exchange Coefficient Measurements on Lanthanum Strontium Ferrite Thin Films via the Curvature Relaxation Method*" Solid State Ionics, 2013, 249: 123-128.

D2.12

The Direct Measurement of Ionic Piezoresistance Stuart N. Cook, Jae Jin Kim and Harry L. Tuller; Massachusetts Institute of Technology, Cambridge, Massachusetts, United States.

Ionic conductivity in the solid state must be significantly enhanced in order to facilitate future advancements in a range of technologies including oxygen permeation membranes, sensors, batteries and fuel cells. In many cases, the traditional approach of chemical and structural optimization have only led to incremental increases in conductivity. To overcome these limitations, alternative routes to fast ion conduction have been explored, including the engineering of nano- and heterostructures. Recent publications in this field of nanoionics have reported up to 8 orders of magnitude enhancement in oxide ionic conductivity by the latter route. The origin of this effect, and even the accuracy of its measurement, however, remain under debate.
Three principle arguments have been proposed to explain the observed phenomena, including formation of space charge regions altering defect concentrations, relaxation of interfacial misfit by the formation of dislocation networks presenting alternative diffusion pathways and interfacial misfit-induced strain altering the ionic migration barrier. The latter arguably presents the greatest scope for ionic conductivity maximization. In all measurements reported thus far, this strain state parameter has been manipulated by changing the interfacial lattice misfit by replacing either the secondary material in the multi-layered heterostructure or the substrate on which the film is grown. This technique is, however, accompanied by many potential sources of error arising from inter-sample variability, including reducibility, impurity content, film growth quality, film thickness, dislocation density, and the sharpness of interfaces
.

In this study, we describe a method for directly measuring the effect of strain on ionic conduction in ceramics, a phenomenon we refer to as ionic piezoresistance, by mechanically varying the strain state using a novel mechanical-electrical testing rig. This allows us to avoid the limitations discussed above and directly establish piezoresistive coefficients for ionic conduction in all crystallographic orientations for the first time. Preliminary results are presented for fluorite-structured oxides and discussed in light of earlier published models.

D2.13

Statistical Methods for Solid State Electrochemistry with Applications to Impedance Spectroscopy and Conductivity Relaxation Francesco Ciucci[1, 2]; [1]Mechanical and Aerospace Engineering, The Hong Kong University of Science and Technology, Kowloon, Hong Kong; [2]Chemical and Biomolecular Engineering, The Hong Kong University of Science and Technology, Kowloon, Hong Kong.

Mathematical models are ubiquitous in science and engineering and are used to interpret and predict the outcome of experiments and the behavior of devices or systems. Models with varying degree of complexity are found in the study of electro active materials and they have been used to explain the nature of electrochemical reactions both at kinetic and the quantum level, to determine defect chemistry and transport properties, to establish the processes that are rate limiting and to gain insight on reactions occurring at the nanoscale [1]. In this work, a statistical link between experimental date obtained widely used in solid state electrochemistry, such as Electrochemical impedance spectroscopy (EIS), Electrical Conductivity Relaxation (ECR) and Isotope Exchange Depth Profiling (IEDP), and mathematical model is made in order to increase the quality of the estimated parameters via Optimal Experimental Design (OED).

The link between errors in the measurements and errors of the parameter set that constitute the underlying model are clarified analytically. Then, within the optimal experimental design setting, the controllable experimental variables are optimized so that the confidence on the parameters estimated parameters during the experiment are reduced. Subsequently synthetic experiments are performed to check the quality of the analytical estimators of the parameters errors. Concurrent minimization of the experimental time and of the quality of the parameters estimates is also considered and the result of this optimization procedure is the determination of experimental configurations that can improve the quality of the estimated parameters (up 90% relative error reduction) and drastically reduce (up 80%) the experimental time [2-3] leading to non-traditional sampled frequencies. Finally, guidelines for EIS [2-3], IEDP [4] and ECR [5] optimization are provided in a unified setting and the test results are compared to novel Bayesian analysis methods [6]. A freely available Matlab code is also introduced [7].

References

[1] A. Kumar, F. Ciucci, A.N. Morozovska, S. Jesse and S. Kalinin, Nat. Chem., 3, 707-713 (2011)
[2] F. Ciucci, T. Carraro, W.C. Chueh, and W. Lai, Electrochim. Acta, 56, 5416 (2011)
[3] F. Ciucci. Electrochimica Acta. 87, 532–545 (2013)
[4] F. Ciucci. Solid State Ionics 232, 97–105 (2013)
[5] F. Ciucci. Solid State Ionics 239, 28–40 (2013)
[6] F. Ciucci, C. Chen. Submitted
[7] F. Ciucci http://sites.google/ecrtools & http://sites.google/drttools

D2.14

Kinetic Unmixing and Decomposition in Ternary Oxides under Electric Field Jakyu Chun[1], Manfred Martin[2] and Han-Ill Yoo[1]; [1]Department of Materials Science and Engineering, Seoul National University, Seoul, Korea (the Republic of); [2]Institute of Physical Chemistry, RWTH Aachen University, Aachen, Germany.

A general expectation is that in a uniform oxygen activity atmosphere, cation electrotransport induces a ternary or higher oxide, e.g., $AB_{1+\xi}O_{3+\delta}$, to kinetically unmix unless the electrochemical mobilities of, i.e. $A^{2+}$and B^{4+} cations are identically equal, and eventually to decompose into the component oxides AO and BO_2 once the extent of unmixing exceeds the stability range of its nonmolecularity ξ. It has, however, earlier been reported [Yoo et al., *Appl. Phys. Lett.*, 2008, **92**, 252103] that even a massive cation electrotransport induces $BaTiO_3$ to neither unmix nor decompose even at a voltage far exceeding the so-called decomposition voltage U_d, a measure of the standard formation free energy of the oxide ($|\Delta G_f^o|=nFU_d$). Here, we report that as expected, $NiTiO_3$ unmixes at any voltage and even decomposes if the voltage applied exceeds seemingly a threshold value larger than U_d. We demonstrate experimentally that the electrochemical mobilities of Ni^{2+} and Ti^{4+} should be necessarily unequal for unmixing. Also, we show theoretically that equal cation mobilities appear to be a sufficiency for $BaTiO_3$only for a thermodynamic reason.

D2.15 Moved to C11.09

D2.16

Influence of Space-Charge on the Surface Defect Chemistry of $BaZrO_3$ Jonathan M. Polfus[1], Tor S. Bjørheim[2], Mehdi Pishahang[1], Truls Norby[2] and Rune Bredesen[1]; [1]Materials and Chemistry, SINTEF, Oslo, Norway; [2]Department of Chemistry, University of Oslo, Oslo, Norway.

The high resistance for proton conduction across grain boundaries in $BaZrO_3$ has been ascribed to the formation of space-charge regions due to a positively charged grain boundary core [1-4]. In the present contribution, first-principles calculations are utilized to elucidate the complete defect equilibria of the *surface* of proton conducting $BaZrO_3$, encompassing the outer and inner surface, bulk and the surrounding atmosphere. Defect calculations are performed for the $BaZrO_3$ (001) surface with focus on protons, oxygen vacancies and Y-acceptor dopants as well as adsorbed hydroxyl and oxygen species on the surface. Methodological approaches for treating charged defects in periodic surface cells within density functional theory calculations are also presented. The defect calculations are implemented with thermodynamic models to describe the equilibrium space-charge of the surface as function of thermodynamic variables such as temperature and water vapour pressure.

It is found that protons exhibit a particularly strong tendency to segregate to the surface. While the concentration of negatively charged hydroxide species on the outer surface can be quite high, they do not fully charge compensate the protons, yielding a net positive charge of the surface. The resulting space-charge potential can be significant, i.e., in the order 1 V. The results are compared with experimental and theoretical results from grain boundaries and heterointerfaces in $BaZrO_3$ and $BaCeO_3$ ceramics, and the potential influence of surface space-charge on surface exchange kinetics is discussed.

Acknowledgement
Financial support from the Research Council of Norway, project Nanomat/228355 “Functional oxides for clean energy technologies: fuel cells, gas separation membranes and electrolysers” (FOXCET) conducted by SINTEF Materials and Chemistry, University of Oslo, and NTNU, is gratefully acknowledged.

[1] C. Kjølseth, H. Fjeld, Ø. Prytz, P.I. Dahl, C. Estournès, R. Haugsrud, T. Norby, Solid State Ionics 181 (2010) 268.
[2] R. De Souza, Z. a. Munir, S. Kim, M. Martin, Solid State Ionics 196 (2011) 1.
[3] J.M. Polfus, K. Toyoura, F. Oba, I. Tanaka, R. Haugsrud, Phys. Chem. Chem. Phys. 14 (2012) 12339.
[4] A. Lindman, E.E. Helgee, G. Wahnström, Solid State Ionics (2013).

D2.17

A Novel Oxygen Pressure Relaxation Technique and Isotope Exchange on $SmBaCo_2O_{6-\delta}$ Vadim Eremin[1], Maxim Ananyev[1, 2] and Edhem Kurumchin[1]; [1]Laboratory of the Electrochemical Materials Science, Institute of High Temperature Electrochemistry, UB RAS, Yekaterinburg, Russia, Yekaterinburg, Russian Federation; [2]Institute of Chemical Technology, Ural Federal University, Yekaterinburg, Russian Federation.

The oxides with double perovskite structure $LnBaCo_2O_{6-\delta}$ where Ln – rare earth metal are promising materials for cathodes in IT-SOFC.
A novel pressure relaxation technique has been developed in this study for the oxygen chemical surface exchange and chemical diffusion coefficients measurement. The idea of this method is very simple. A sample is equilibrated with the gas phase at proper temperature and oxygen pressure. After the equilibration the oxygen pressure is dropped up or down depending on the type of a step (oxidative or reductive). The oxygen

pressure in closed gas circuit of a constant volume is monitored in time until the equilibration state has been reached. In the case of oxidative step the sample after drop-wise pressure change starts taking up oxygen from the gas circuit. The time dependence of the oxygen pressure is used for the equilibration rate and chemical oxygen diffusion coefficient calculations. In order to understand the mechanism of the oxygen pressure relaxation process the isotope exchange experiments under equilibrium and non-equilibrium conditions have been done. The tracer oxygen exchange rate, the tracer diffusion coefficient and the rates of three types of oxygen exchange has been calculated at the same ranges of temperature and oxygen pressure (T = 600–800 °C and $Po_2 = 10^{-3}$–10^{-1} atm) as is the case of the pressure relaxation technique. It was found that the equilibration rate is almost two orders of magnitude higher than the interphase exchange rate. Taking into account the thermodynamic enhancement factor gives a good agreement in diffusion coefficients whereas it is not valid for the exchange rates. The possible oxygen exchange mechanisms for the oxygen pressure relaxation and the equilibrium oxygen isotope exchange experiment are discussed.

D2.18

Giant Electrostriction in Doped Bi_2O_3 Ceramics Nimrod Yavo[1], Alaric Smith[2], Roman Korobko[1], Peter R. Slater[2] and Igor Lubomirsky[1]; [1]Materials and Interfaces, Weizmann Institute of Science, Rehovot, Israel; [2]School of Chemistry, University of Birmingham, Birmingham, United Kingdom.

Electrostriction is a property of a material to develop strain proportional to the applied electric field. It is described by a fourth rank tensor, M_{ikjl}, (m^2/V^2). According to common wisdom, the higher the dielectric constant, ε, the larger is the electrostriction coefficient, M. For ceramics with ε<100, M is usually within the range of 10^{-21}-10^{-22} m^2/V^2 . The best commercial electrostrictor, (1-x)[$Pb(Mg_{1/3}Nb_{2/3})O_3$]-x[$PbTiO_3$](PMN-PT), have ε=10,000-20,000 and exhibit M=10^{-16}-$10^{-15}m^2/V^2$. This corresponds to the polarization strain coefficient, $Q_{PMN\text{-}PT}=M/[\varepsilon_0(\varepsilon\text{-}1)]^2$ <0.1 m^4/C^2. The largest Q ever reported is for Mg-doped alumina with M<10^{-21} m^2/V^2, Mg-doped alumina $Q_{alumina}$=1.58.

We have recently reported that thin films of Gd-doped ceria ($Ce_{1-x}Gd_xO_{2-x/2}$) exhibit M=10^{-16}-$10^{-17}m^2/V^2$ though their dielectric constant is ε<30, corresponding to Q>300 m^4/C^2. This discrepancy indicates that in Gd-doped ceria, a previously unknown mechanism of electrostriction is at work.

To test the generality of these findings, we have investigated electrostriction in bulk ceramics of Bi_2O_3 doped with Nb and Y. These ceramics, similar to Gd-doped ceria, have a fluorite crystal structure, large concentration of oxygen vacancies and dielectric constant ε≈25-40. We have found that these ceramics exhibit electrostriction coefficient (0.5-1.2)·$10^{-17}m^2/V^2$, which increases with the concentration of vacant oxygen sites (14%-21.5%, Figure 1). These M values correspond to a Q-coefficient within the range of 40-270.

Our findings suggest that the large electrostriction effect is an inherent property of fluorite-structured oxides with a large concentration of oxygen vacancies.

D2.19

A Molecular Dynamics Study of Oxygen Ion Diffusion in A-Site Ordered Perovskite $PrBaCo_2O_{5.5}$: Data Mining the Oxygen Trajectories Chi Chen and Francesco Ciucci; Mechanical and Aerospace Engineering, Hong Kong University of Science and Technology, Kowloon, Hong Kong.

Molecular dynamics (MD) simulations have been widely used to study oxygen ion diffusion in crystals. In the data analysis, one typically calculates the mean squared displacements to obtain the self-diffusion coefficients. Further information extraction for each individual atom poses significant challenges due to the lack of general methods. In this work, oxygen ion diffusion in A-site ordered perovskite $PrBaCo_2O_{5.5}$ is studied using MD simulations and the oxygen migration is analyzed by k-means clustering, a machine learning algorithm. The clustering analysis allows the tracking of each individual oxygen jump along with its corresponding location, i.e., oxygen site in BaO, $PrO_{0.5}$ and CoO_2 layers. Therefore it increases the understanding into the factors influencing oxygen diffusion. For example, it is found that the oxygen occupation fraction in the $PrO_{0.5}$ layers increases with temperature, while in the CoO_2layers it decreases with temperature. Additionally, the activation enthalpies of oxygen jumps from CoO_2 to CoO_2, CoO_2 to $PrO_{0.5}$ and $PrO_{0.5}$ to CoO_2 are 0.22 eV, 0.54 eV and 0.34 eV respectively, exhibiting anisotropic characteristics. Furthermore, the dwell times of oxygen atoms suggest that they are highly mobile in $PrO_{0.5}$ layers. Combining the analysis of activation enthalpies and dwell times, it is suggested that the oxygen transport is fast within the CoO_2 layers while the $PrO_{0.5}$ layers work as oxygen vacancy reservoirs.

D2.20

A Novel Model for Gas Phase Analysis of Oxygen Isotope Exchange in Ceramic Materials with Different Diffusion Pathways Lev Putilov[1] and Maxim Ananyev[1, 2]; [1]Laboratory of the Electrochemical Materials Science, Institute of High Temperature Electrochemistry, Ural Branch of Russian Academy of Sciences, Yekaterinburg, Russian Federation; [2]Institute of Chemical Technology, Ural Federal University, Yekaterinburg, Russian Federation.

The isotope exchange method provides essential information about the oxygen surface exchange kinetics and diffusion in solid oxide materials. The isotope exchange depth profiling (IEDP) technique is commonly used for study of oxygen diffusivity in solid oxide materials. The tracer profile can give information about the oxygen bulk diffusion and in some cases about the grain boundaries diffusion.
In the case of oxygen isotope exchange with gas phase analysis (GPA) the time dependence of the tracer concentration in the gas phase is determined by not only the oxygen surface exchange kinetics but also different diffusion pathways in dense ceramic oxide materials. Unfortunately, the model with fast grain boundary diffusion with constant surface concentration of tracer developed by Whipple (1954) for IEDP does not suit for GPA due to more complicated boundary conditions.
Several models are used for processing of GPA results. Models developed by Haul et al. (1962) and Klier et al. (1966) allows the determination of the diffusion coefficient in bulk regardless of the inner structure of ceramic material. The two-layer model developed by Ezin et al. (1996) includes two series layers with different diffusion coefficients. All these models for GPA can not be correctly used for data treatment in the case of ceramic materials with two parallel diffusion pathways with different diffusivities, for example in grains and along grain boundaries.

In this study a novel phenomenological model for GPA isotope exchange in ceramics with two different diffusive pathways is developed assuming time dependent surface concentration boundary condition. The model is implemented for the experimental data treatment using lanthanum-strontium manganite as an example. Both diffusion coefficients in grains and along grain boundaries can be evaluated using the proposed model. The model can also be implemented to IEDP data processing with time dependent surface concentration boundary condition.

D2.21

DFT and Hybrid Calculations on the Stability of Shear Planes and Point Defects in WO_3 Marit N. Getz, Tor S. Bjorheim and Truls Norby; Department of Chemistry, University of Oslo, Oslo, Norway.

WO_3 has attracted renewed interest in the recent decade and finds potential application in electrochromics [1], photocatalysis [2], thermoelectrics [3] and nanoelectronics [4]. Still, many aspects related to whether and how defects affect its functional properties are poorly understood. Experimentally, defect formation in WO_3 has been suggested to proceed via planar defects called crystallographic shear (CS), giving rise to a wide range of non-stoichiometric WO_{3-x} [5]. Previous computational studies on defects in WO_3 have, however, only included point defects. The CS-structures have earlier been treated as separate materials, with computational studies focusing on electronic properties [6]. In this contribution, we explore the defect structure of WO_3 computationally, with focus on its tendency for CS-plane and oxygen vacancy formation upon reduction, and how this affects the stability of other point defects.

DFT calculations within VASP, using GGA and hybrid functionals, have been employed to determine point defect and planar defect formation in WO_3. The calculations show that the band structure of the CS-structure $W_{10}O_{29}$ is closely related to that of the parent WO_3, except for additional

defect levels with conduction band character in some directions of the Brillouin zone. Band projected charge densities indicate that these levels reflect states with more localized character along the shear planes due to reduction of W^{6+}. The thermodynamic stability of the CS-planes in $W_{10}O_{29}$ and $W_{25}O_{73}$ are compared with reduction of WO_3 by oxygen vacancy formation, and the tendency for CS plane formation at finite temperatures is discussed. In addition, we determine the atomistic arrangement and thermodynamic stability of protonic defects in both WO_3 and the CS-structures in order to evaluate how the CS-structures affect the proton uptake under various atmospheric conditions.

D2.22
Lithium Ion Mobility in Sulphonate-Based Ionomer Systems Containing Quaternary Ammonium Co-Cations Yogita Oza, Luke A. O'Dell and Maria Forsyth; Institute for Frontier Materials, Deakin University ARC Centre of Excellence for Electromaterials Science (ACES), Victoria, New South Wales, Australia.

The use of solid polymer electrolytes instead of traditional liquid electrolytes provides significant advantages for battery technologies. However several decades of research has not yet identified a polymer with sufficient ionic conductivity around room temperature, and this remains an obstacle for polymer electrolytes due to the strong coupling of ion motion with the polymer segmental dynamics. Decoupling the ionic conductivity from the segmental dynamics might open a way to the design of polymers with high ionic conductivity below their glass transition temperature[1]. Our recent work involves the design of ionomers in which the ion dynamics are decoupled from the T_g of the polymer in an attempt to develop a family of fast ion conducting polymers for application in secondary lithium and sodium ion batteries[2]. In this contribution, we have characterized the Li^+ decoupling behavior in ionomer systems based on poly(2-acrylamido-2-methyl-1-propanesulfonic acid) (PAMPS) containing mixtures of Li^+ and quaternary ammonium cations.

These PAMPS systems were studied by NMR, DSC and impedance spectroscopy. The results shows that the incorporation of 90 mol% of the ionic liquid cation methyl triethyl ammonium (N_{1222}) reduces T_g and enhances the conductivity, which reaches 10^{-4} Scm^{-1} at higher temperatures. ^{7}Li NMR spectroscopy shows decoupling of the lithium-ion dynamics from the polymer dynamics, implying increased Li ion dissociation from sulphonate anion. In the case of an ether-functionalised ammonium cation, lower observed conductivity despite a significantly lower T_g (60 °C), was possibly due to associations between the Li^+ and the ether group on the ammonium cation, or between the latter cations and the sulphonate anions.

Reference:
[1]Y. Wang, A.L. Agapov, F. Fan, K. Hong, X. Yu, J. Mays and A.P. Sokolov, Phys. Rev. Lett. 2012,108, 088303
[2] S.A. Mohd. Noor, D.Gunzelmann, D.R. MacFarlane, M. Forsyth, J. Mater. Chem. A. 2014, 2, 365.

SESSION D3: Fundamentals of Transport and Reactivity and Nanoionics II
D: Fundamentals of Transport and Reactivity and Nanoionics
Chair: Hans-Dieter Wiemhoefer
Monday Afternoon, June 15, 2015
Keystone Resorts, Grays Peak I/II

2:30 PM *D3.01
Low-Temperature Alpha Silver Iodide Confined in Glass: Structure and Dynamics Klaus Funke[1], Radha Banhatti[1], Pawel Grabowski[2], Jan Nowinski[2], Wojtek Wrobel[2], Robert Dinnebier[3] and Oxana Magdysyuk[3]; [1]Institute of Physical Chemistry, University of Muenster, Muenster, Germany; [2]Faculty of Physics, Warsaw University of Technology, Warsaw, Poland; [3]Max Planck Institut für Festkörperforschung, Stuttgart, Germany.

In 1937, Wilhelm Jost speculated about the possible positions and dynamics of the silver ions in the high-temperature phase of silver iodide, α-AgI, that one would encounter, if it could be cooled far below its regular 147 °C α-β phase transition. Would a (continuous) 'liquid-solid transition' occur in the silver sublattice and would the 'liquid-like' dynamics of the mobile silver ions change into a 'solid-like' hopping motion? We are now, for the first time, able to answer Jost's questions, both of them in the affirmative. In our samples, globules of crystalline α-AgI were contained in a powdered glass of composition $0.78\ AgI \cdot 0.165\ Ag_2O \cdot 0.055\ B_2O_3$, prepared from the melt by roller quenching and subsequent grinding in liquid nitrogen. In a Rietveld refinement of x-ray diffraction data taken at 100 K, the silver ions were found to be localized within the tetrahedral voids provided by the α-AgI anion structure. The change from the high-temperature 'liquid-like' dynamics of the silver ions into a 'solid-like' hopping motion could be verified by considering spectra of the ionic conductivity. With decreasing temperature, the spectra do indeed develop the characteristic frequency dependence which is a hallmark of ionic hopping.

2:50 PM D3.02
Frequency - Dependent Conductivity and Anomalous Diffusion in Ag β-alumina Osamu Kamishima[1], Junichi Kawamura[2] and Yoshiki Iwai[2]; [1]Faculty of Science and Engineering, Setsunan University, Neyagawa, Japan; [2]Institute of Multidisciplinary Research for Advanced Materials, Tohoku University, Sendai, Japan.

Ionic conductivity of a single crystal of Ag β-alumina has been measured as a function of frequency between 1 Hz and 1M Hz and of temperature between approximately 100 K and room temperature. The conductivity spectra $\sigma(\omega)$ were found to have the small power-law dependence $\sigma(\omega) \propto \omega^{n}$ with frequency exponent $n = 0.11 \sim 0.15$. The frequency dependence of ionic conductivity does not follow a well known Drude-type for free charges or Debye-type for dipole moments; instead, it is well expressed by power-law functions. The power-law dependence conductivity $\sigma(\omega) \propto \omega^{n}$ has been widely observed for disordered materials with frequency exponent $n = 0.6$ approximately. Ag β-alumina is a two-dimensional superionic conductor. Its*two* - dimensionality of the geometrical disorder will give rise to a different power-law dependence from $n = 0.6$. The fractal theory for the random walk in disordered systems was helpful us to understand the small power-law dependence with spatial and temporal physical meanings. We suggested that a "scale-invariance" would hold true behind the super ionic conduction in the self-similarity point of view.

3:10 PM D3.03
Investigation of the Effect of Pressure and the Concentration of Charge Carriers on the Ionic Transport in Sodium Scandium Phosphate $Na_3Sc_2(PO_4)_3$ Kaustubh Bhat[1], Marie Guin[2], Stefan Bluegel[1] and Hans Lustfeld[1]; [1]Peter Grünberg Institute (PGI-1)/Institute for Advanced Simulation (IAS-1), Forschungszentrum Jülich GmbH, Jülich, Germany; [2]Institute of Energy and Climate Research (IEK-1), Forschungszentrum Jülich GmbH, Jülich, Germany.

Sodium ionic conductors are receiving renewed attention as their lower cost and abundant availability offers significant advantages over Li-ion batteries for large scale energy storage systems. The class of NASICON [1,2] materials has shown excellent ionic conductivity, which correlates with the size of a certain area in the crystal which is a bottleneck for Na-ion transport [3].

We investigate the pathways available for Na-ion conduction in Sodium Scandium Phosphate ($Na_3Sc_2(PO_4)_3$) [4] and calculate the energy barriers for ionic transport using Density Functional Theory (DFT) and the Nudged Elastic Band (NEB) Method [5,6].

The effect of positive and negative external pressure on the $Na_3Sc_2(PO_4)_3$ crystal is investigated [7]. The change in volume changes the area of the bottleneck mentioned above, allowing us to study its influence on the energy barrier.

The substitution of pentavalent phosphorus by tetravalent silicon leads to change in (a) bottleneck area and (b) the number of sodium charge carriers. We separate (a), which has been modeled with the pressure change above, from (b) by inducing artificial background charge in the crystallographic unit cell and repeating the DFT+NEB calculations. We then validate these findings experimentally with the solid solution $Na_{3+x}Sc_2(SiO_4)_x(PO_4)_{3-x}$.

Thus we can establish the effect of cell volume and the charge carrier concentration independent of one another, giving us a profound insight into the nature of ionic transport in such materials and the strategies for minimising the energy barrier.

References:
1. H.Y.P. Hong, MRB 11 (1976) 173-182
2. H.Y.P. Hong, J.B. Goodenough, J.A. Kafalas, MRB 11 (1976) 203-220
3. M. Guin, F. Tietz, J.Power Sources 273 (2015) 1056-1064.
4. J.M. Winaud, A. Rulmont, P. Tarte, J.Mater. Sci. 25 (1990) 4008-4013
5. P.E. Blöchl, PRB 50 (1994) 17953-17979
6. G. Henkelman, B.P. Uberuaga, H. Jónsson, J.Chem. Phys. 113 (2000) 9901-9904
7. J.A. Hirschfeld, H. Lustfeld, PRB 84, 224308.

3:30 PM D3.04
Electronic Transport of Metal Oxide Single Crystals for Solar Water Splitting: Bismuth Vanadate and Iron Oxide Alexander J. Rettie[1], William Chemelewski[2], Jeffrey Lindemuth[3], John McCloy[4], Luke Marshall[5], David Eisenberg[6], Jianshi Zhou[2], David Emin[7] and Buddie Mullins[1, 4, 8]; [1]Chemical Engineering, University of Texas at Austin, Austin, Texas, United States; [2]Materials Science and Engineering, University of Texas at Austin, Austin, Texas, United States; [3]LakeShore Cryotronics, Westerville, Ohio, United States; [4]Materials Science and Engineering, Washington State University, Pullman, Washington, United States; [5]Chemical Engineering, Northeastern University, Boston, Massachusetts, United States; [6]Van't Hoff Institute for Molecular Sciences, University of Amsterdam, Amsterdam, Netherlands; [7]Physics and Astronomy, University of New Mexico, Albuquerque, New Mexico, United States;[8]Chemistry, University of Texas at Austin, Austin, Texas, United States.

Bismuth vanadate ($BiVO_4$, BVO) has emerged as a champion photoanode material for water splitting, but fundamental studies of this material are lacking. Electronic transport studies are especially uncommon, likely due to difficulties in synthesizing high quality samples and measuring high resistivity, low mobility materials. Recently, we reported the synthesis of both undoped and tungsten doped BVO single crystals using the floating zone technique. We showed that electrons in this material move via thermally activated small polaron hopping transport between 250 and 400 K, and that the AC Hall mobility is low at room temperature: ~0.2 $cm^2 V^{-1} s^{-1}$. Unlike conventional, wide-band semiconductors, in small-polaron conductors the Hall and drift mobility may be vastly different. To determine a true drift mobility, the conductivity, Seebeck coefficient and AC Hall effect were measured in these crystals as functions of temperature and orientation. Additionally we synthesized single crystals of titanium doped iron oxide - another high performance photoanode whose electrons form small polarons - by chemical vapor transport for similar measurements. Comparison with small-polaron theory will yield information about the energy barriers, hopping regime (adiabatic or non-adiabatic), hop geometry and any anisotropy. The goal of our work is to gain insight into the nature of small polarons in these materials around room temperature. We hope our approach will be applicable to elucidating transport in many low-mobility metal oxides.

3:50 PM D3.05
Redox Reactions and Transport at Room Temperature in Nanoionic Systems Based on Macroscopic Insulators Ilia Valov; Electronic Materials, Research Centre Juelich, Juelich, Germany.

The ability to control the redox behavior and transport properties at the atomic scale is of primary interest for a wide range of fields, including energy conversion, nanoelectronics and information technology, and nanoionics. A significant progress is achieved in the recent years on revealing microscopic details on redox processes and transport of mass and charge in nanoscaled or in generally nano-constrained systems. However, one aspect that is still insufficiently considered is the electrochemical electrode reactions and ion transport kinetics in nanoionic solid systems at room temperature.

In this contribution, we present experimental results and discuss on the charge transfer processes and ion transport in nano-scaled thin films of thickness between 5 nm and 30 nm at room temperature using macroscopic insulators e.g. SiO_2 and Ta_2O_5 as ion transporting solid (solid electrolyte). We show that the structure and reactivity of the interfaces are of crucial importance for reproducible and reliable experiments. We demonstrate that both potentiodynamic and steady state measurements can be used to determine reaction kinetics parameters [1-3]. The influence of the counter charge/electrode reaction[4] and its influence on the overall cell behavior will be emphasized as well as the role of the electro catalytic activity of the counter electrode[5].
We show that electrode processes are occurring even in/within macroscopic insulators involving dissolution of not only electrochemically active metals such as Ag,Cu and Ni but also inert metals as Pt.

Our results highlight the electrochemical systems in a qualitatively different way, showing that at the nano-scale insulators can turn in electrolytes and inert metals can undergo electrode reactions[6].

References:
[1] S. Tappertzhofen, H. Mündelein, I. Valov, R. Waser, Nanoscale 4 (2012) 3040.
[2] I. Valov, E. Linn, S. Tappertzhofen, S. Schmelzer, J. van den Hurk, F. Lentz, R. Waser, Nature Communications 4 (2013) 1771.
[3] S. Tappertzhofen, S. Menzel, I. Valov, R. Waser, Appl. Phys. Lett. 99 (2011) 203103.
[4] S. Tappertzhofen, I. Valov, T. Tsuruoka, T. Hasegawa, R. Waser, M. Aono, ACS Nano 7 (2013) 6396.
[5] S. Tappertzhofen, R. Waser, I. Valov, ChemElectroChem 1 (2014) 1287.
[6] Y. Yang, P. Gao, L. Li, X. Pan, S. Tappertzhofen, S. Choi, R. Waser, I. Valov, W. D. Lu, Nat. Commun. 5 (2014) 4232.

4:10 PM D3.06
Atomistic Mechanism of Lithiation of Nanomaterials as Li-Ion Battery Anodes Studied by *In Situ* TEM Xuedong Bai; Institute of Physics, Chinese Academy of Sciences, Beijing, China.

In-situ transmission electron microscopy (TEM) method is powerful in a way that it can directly correlate the atomic-scale structure with physical and chemical properties. In this presentation, we will report the atomistic mechanism of lithiation of nanomaterials as potential lithium ion battery anodes studied by in-situ TEM method. We recently studied the dynamic electrochemical lithiation process of MoS_2 nanosheets. It is found that MoS_2 undergoes a trigonal prismatic (2H)-octahedral (1T) phase transition upon lithium intercalation. A systematical study has been performed on the structural properties of MoS_2 nanosheets during the lithiation process, which can be correlated with the ex-situ performance of MoS_2 coin-type cells. And the studies on the dynamic lithiation processes of the coated SnO_2 nanowires and silicon nanowires will be also included in this talk. The in-situ characterization at atomic scale provides a fundamental understanding of the lithium ion storage mechanism.

4:30 PM D3.07
The Effects of Lattice Strain and Cationic Disorder on the Li-Ion Diffusion in $LiFePO_4$ Cristina Tealdi[1, 2] and Piercarlo Mustarelli[1, 2]; [1]Department of Chemistry, University of Pavia , Pavia, Italy; [2]UdR Pavia, INSTM, Pavia, Italy.

Since phospho-olivines have been suggested as potential cathode materials for rechargeable Li-ion batteries, $LiFePO_4$ has been considered a key material in the field of chemical energy storage. It is characterized by good thermal stability, high voltage versus the Li^+/Li couple and a large theoretical gravimetric capacity. However, the intrinsic low electronic and ionic conductivities restrict its practical application.
The crystal structure of $LiFePO_4$ is usually described in the orthorhombic space group P*nma*. In this structure, Fe and P atoms generate a polyhedral arrangement that leaves open channels running along the *b* axis, where Li ions are located in octahedral coordination. It is generally acknowledged that the [0 1 0] direction is the preferential direction for Li ion migration in the $LiFePO_4$ system; ionic conductivity along this direction is impeded by the presence of anti-site defects, i.e. the exchange of Li and Fe in their respective sites.

In this study, two classes of atomistic modelling methods are used, namely static lattice (energy minimization) and molecular dynamics. Different sets of simulations are performed on the perfect structure as well as on partially delithiated systems. Particular attention is paid to the effect of the

application of lattice strain and the presence of anti-site defects on the mechanism and dimensionality of Li transport in the system.
The results of this study show that, under specific circumstances, Li–Fe antisites defects may act as centres for inter-channel crossing so that their presence promotes migration along other directions, hence removing at least part of the anisotropy of lithium mobility that is characteristic of olivine-type iron phosphate. On the other hand, lattice strain affects the defect chemistry of $LiFePO_4$ and it is proved to be an effective way to modulate the activation energy for Li-ion transport within the system.

4:50 PM D3.08
Elucidating Li Ion Dynamics and Diffusion Pathways in Li_2SnO_3 – A Comparative ^{6,7}Li NMR Study Julia Langer[1, 2], Patrick Bottke[1, 2] and Martin Wilkening[1, 2, 3]; [1]Institute for Chemistry and Technology of Materials, Graz University of Technology, Graz, Austria; [2]DFG Research Unit 1277, Graz University of Technology, Graz, Austria; [3]Graz University of Technology, Christian Doppler Laboratory for Lithium Batteries, Graz, Austria.

A comprehensive understanding of ion dynamics in solids plays a crucial role in many fields of today's materials research. In particular, the investigation of Li ion transport properties attracts great scientific interest since it is highly relevant for the development of new energy storage systems. Solid-state nuclear magnetic resonance (NMR) provides the necessary means to collect information ion hopping processes on different time and length scales from an atomic-scale point of view.
Here, polycrystalline Li_2SnO_3 served as a model substance to quantitatively study Li ion diffusion via ^{7}Li spin-lattice relaxation (SLR) NMR and spin-alignment echo (SAE) NMR. As conventional SLR NMR is per se sensitive to rather fast Li exchange processes, NMR measurements in the rotating frame of reference take advantage of locking frequencies in the kilohertz range that enabled us to probe Li ion dynamics on a much broader length scale. Both SLR techniques point to rather slow Li ion mobility in Li_2SnO_3. Therefore, ion transport in Li_2SnO_3 is perfectly suited to be studied by SAE NMR that is sensitive to extremely slow Li diffusion. Temperature-dependent echo decay rates directly reflecting Li jumps between the three available Li sites in the oxide, reveal Arrhenius behavior over several decades; the corresponding activation energy (0.4 eV) is in good agreement with that obtained by SLR measurements in the rotating frame of reference.
Finally, in combination with 1D and 2D ^{6}Li exchange NMR experiments, we were able to obtain a detailed picture of ion dynamics and, in particular, preferred diffusion pathways in Li_2SnO_3.

5:10 PM D3.09
Lithium Segregation Induces Localized Order-Disorder Transitions Amorphous TiO_2 Nanoparticles Subramanian Sankaranarayanan[1, 2]; [1]Center for Nanoscale Materials, Argonne National Laboratory, Argonne, Illinois, United States; [2]Computation Institute, University of Chicago, Chicago, Illinois, United States.

Development of efficient energy storage technologies remains one of the major challenges. By manipulating materials chemistry, considerable advances have been made in energy storage systems based on rechargeable Li ion batteries (LIBs). Today, however, we have reached the performance limits of standard electrode materials, and further improvements are crucial. An exciting new direction is to use nanomaterials and nanoscale architectures for LIB applications. Nanomaterials provide better accommodation of strain upon Li insertion and removal, thus improving cycle life. The higher electrode/electrolyte contact area and short lengths for both electronic and ionic transport can yield higher charge/discharge rates. However, understanding of atomistic details regarding nanoscale effects on dynamics of Li-ion transport, and the accompanying structural changes in nanostructured electrodes, has not reached the level of bulk materials. Development of such understanding could accelerate the development of nanostructured electrodes.

We present a molecular dynamics simulation study to elucidate the Li segregation and transport characteristics in amorphous TiO_2 nanoparticles (NPs) used as electrode material in battery applications. We observe a strong intraparticle segregation of Li, and the degree of segregation is found to correlate with Li concentration. With increasing Li concentration, Li diffusivity and segregation are enhanced, and this behavior is tied to the structural response of the NPs with increasing lithiation. The atoms in the amorphous NPs undergo rearrangement in the regions of high Li concentration, introducing new pathways for Li transport and segregation. These localized atomic rearrangements, in turn, induce preferential crystallization near the surfaces of the NPs. Such rich, dynamical responses are not expected for crystalline NPs, where the presence of well-defined lattice sites leads to limited segregation and transport at high Li concentrations. The preferential crystallization in the near-surface region in amorphous NPs may offer enhanced stability and fast Li transport for Li-ion battery applications, in addition to having potentially useful properties for other materials science applications.

SESSION D4: Fundamentals of Transport and Reactivity and Nanoionics III
D: Fundamentals of Transport and Reactivity and Nanoionics
Chair: John Irvine
Tuesday Morning, June 16, 2015
Keystone Resorts, Grays Peak I/II

10:30 AM **D4.01
Cathode Materials for Proton Conducting SOFC: Bulk Defect Chemistry and Mechanism of Oxygen Reduction Reaction Rotraut Merkle, Daniel Poetzsch and Joachim Maier; MPI for Solid State Research, Stuttgart, Germany.

Owing to the higher ionic conductivity of the electrolyte, solid oxide fuel cells based on proton conducting oxides have a great potential for lowering the operation temperature. To achieve good performance, cathode materials with mixed protonic and electronic conductivity are required. Since the frequently used perovskites also contain oxygen vacancies, a situation with three carriers is met, in which proton uptake can proceed by hydration or hydrogenation.[1] This scenario is investigated for $Ba_{0.5}Sr_{0.5}Fe_{0.8}Zn_{0.2}O_{3-d}$ (BSFZ) by thermogravimetry under different pO_2 and pH_2O, and complemented by numerical simulations. While the proton concentration in BSFZ in the range of 0.1-1 mol% at 350-600 °C [2] is lower than in $Ba(Zr,Ce,Y)O_{3-x}$ electrolytes, the resulting proton conductivity is expected to suffice for oxygen reduction on the whole cathode surface ("bulk path"). This is confirmed by the diameter dependence of the surface reaction resistance on dense BSFZ microelectrodes on $Ba(Zr,Y)O_{3-x}$.[3]
The presence of protons does not only lead to a more complex bulk defect chemistry, but also opens additional pathways for the oxygen reduction reaction: (i) to reduce O_2 to water, oxygen incorporation into the electrode materials is not necessarily required (nevertheless, oxygen vacancies may be important catalytic centers), (ii) protonated intermediate species may appear, with different concentrations and reaction barriers compared to the proton-free case. Rate equations for these scenarios are derived, and compared to the measured pO_2 and pH_2O dependencies for BSFZ on $Ba(Zr,Y)O_{3-x}$.

While this presentation is focussed on BSFZ, the conclusions are relevant for the whole class of proton/hole mixed conducting perovskites. Since a comparably low proton conductivity suffices for the "bulk path" of oxygen reduction, a significant bulk path contribution may be anticipated for many mixed conducting perovskites on proton conducting electrolytes.

[1] D. Poetzsch, R. Merkle, J. Maier, Adv. Funct. Mat (2015) doi:10.1002/adfm.201402212
[2] D. Poetzsch, R Merkle, J. Maier, PCCP 16(2014) 16446; Farad. Discuss. (2015) submitted
[3] D. Poetzsch, R. Merkle, J. Maier, in preparation

11:00 AM D4.02
Oxygen Exchange and Transport in Mixed Conducting Dual Phase Composites John Druce[1], Helena Tellez[1], Tatsumi Ishihara[1] and John A. Kilner[1, 2]; [1]I2CNER, Kyushu University, Fukuoka, Japan; [2]Department of Materials, Imperial College London, London, United Kingdom.

Dual phase ceramic composites find use in many applications, including as electrodes in solid oxide electrochemical cells and as dense membranes for oxygen separation. The most typical dual phase ceramic composite consists of a fluorite structured oxide ion conductor such as $Ce_{1-x}Gd_xO_{2-x/2}$ (CGO) with a perovskite-structured material to provide electronic conductivity, such as $La_{1-x}Sr_xCo_{1-y}Fe_yO_{3-\delta}$ (LSCF).

One concern is that the constituent phases often inter-react at the elevated temperatures required for sintering. In the $Zr_{1-x}Y_xO_{2-x/2}$-$La_{1-x}Sr_xMnO_{3-\delta}$ system, this inter-reaction typically results in secondary phases such as $La_2Zr_2O_7$. Although secondary phases are not typically observed in the CGO-LSCF system, it is widely believed that cation inter-diffusion occurs between the two phases. The effect of such cation inter-diffusion on the transport properties, such as oxygen surface exchange, in the composites is not yet known.

In this work, we apply a combination of ^{18}O exchange, ToF-SIMS and surface compositional analysis by low energy ion scattering (LEIS) spectroscopy to address the oxygen transport properties of CGO-LSCF composites. High lateral resolution SIMS analysis allows us to investigate the distribution of the ^{18}O tracer on a microscopic level.

At lower temperatures (500 °C), the surface ^{18}O isotopic fraction is slightly higher in the LSCF than in the CGO, suggesting that exchange takes place on the LSCF, and is transferred relatively quickly to the CGO. Strikingly, at higher temperature (700 °C), the CGO is brighter in ^{18}O, suggesting that it is more active than the LSCF for oxygen exchange.

We discuss the apparent enhancement of surface exchange on CGO considering changes in surface composition observed through LEIS studies. As well as a catalytic spillover mechanism, we find evidence that the surfaces of CGO grains in the composite are cleaner, and do not show the typical segregated impurities which are thought to block oxygen exchange in single phase CGO.

11:20 AM D4.03
A Concept of Three Exchange Types in Oxygen Isotope Exchange Kinetic Analysis for Solid Oxide Materials Maxim Ananyev[1, 2]; [1]Laboratory of the Electrochemical Materials Science, Institute of High Temperature Electrochemistry, Ural Branch of Russian Academy of Sciences, Yekaterinburg, Russian Federation; [2]Institute of Chemical Technology, Ural Federal University, Yekaterinburg, Russian Federation.

Oxygen isotope exchange methods are commonly used in solid state chemistry for analysis of the oxygen isotope exchange kinetics. Oxygen surface exchange kinetics includes a number of stages which can be characterized not only by the integral parameter like the surface exchange coefficient. Using methods of the isotope exchange with the gas phase analysis the surface exchange kinetics can be characterized in details by several steps and the rates of these steps can be calculated
.
The mechanism of the oxygen isotope surface exchange can be considered using the three exchange type concept developed by Muzykantov and Boreskov et al. According to the concept the oxygen surface exchange kinetics is described by the rates of three exchange types: r_0, r_1 and r_2, where subscripts corresponds to the amount of atoms from the solid surface participating in the elementary act. Such consideration does not mean an appropriate oxygen exchange mechanism. Three exchange types show only statistical redistribution the oxygen ^{18}O isotope between three types of oxygen molecules ($^{18}O_2$, $^{18}O^{16}O$, $^{16}O_2$) and the solid surface oxygen.

It this study it was shown that any oxygen exchange mechanism with appropriate list of elementary stages can be described using the three exchange type concept. The rates of the elementary stages are expressed through r_0, r_1 and r_2. A set of elementary acts depends on types of surface species, a number of phases on a solid surface etc. Several cases of different rate-determining elementary stages have been considered in this paper: dissociative adsorption mechanism including two-step models developed by Den Otter et al. (2001), mechanism with two-atomic species on a solid surface, mechanism for composite materials and electrode-electrolyte system. All cases are illustrated by the experimental data analysis.

11:40 AM D4.04
First Principles Calculations of Formation and Migration of Oxygen Vacancies in the Bulk and on Surface of Complex Perovskites for Solid Oxide Fuel Cell Cathodes Eugene Kotomin[1], Yuri Mastrikov[2], Rotraut Merkle[1], Maija Kuklja[3] and Joachim Maier[1]; [1]Dept.Phys.Chem., Max-Planck-Institute FKF, Stuttgart, Germany; [2]Institute for Solid State Physics, Riga, Latvia; [3]University of Maryland, College Park , Maryland, United States.

ABO_3-type perovskite solid solutions with a large oxygen deficiency exhibit a perceptible ionic conductivity, leading to their use as electrolytes ($(La,Sr)(Ga,Mg)O_{3-d}$ or materials for oxygen permeation membranes and solid oxide fuel cell cathodes ($(La,Sr,Ba)(Mn,Fe,Co)O_{3-d}$) [1,2]. The oxygen migration occurs by the vacancy mechanism with the migration through “critical triangle” of one *B* site cation and two *A* cations as the bottleneck [3]. As it is established now, the formation and migration energies of oxygen vacancies are two major factors determining oxygen reduction rate.

Based on first principles DFT calculations for supercells containing 40 up to 320 atoms, we analyze these two quantities for the bulk and surface for a series of complex $(La,Sr)(Co,Fe)O_{3-d}$(LSCF) perovskites [4]. The atomic relaxation, charge redistribution and energies of the transition states for oxygen ion migration are obtained and differences with $Ba_{1-x}Sr_xCo_{1-y}Fe_yO_{3-d}$(BSCF) perovskites [2,3] (which exhibit considerably lower migration barriers) are discussed in detail.

[1]. E.A. Kotomin, R. Merkle, Yu.A. Mastrikov, M.M. Kuklja, and J. Maier. Chapter 6 in a book: *Computational Approaches to Energy Materials* (eds. A.Walsch, A.Sokol, C.R.A. Catlow, Wiley), 2013, p. 149-186.
[2] M. Kuklja, E. Kotomin, R. Merkle, Yu. Mastrikov, J. Maier, PCCP **15**, 5443 (2013).
[3] R. Merkle, Yu.A. Mastrikov, E.A. Kotomin, M.M. Kuklja, J. Maier. J Electrochem. Soc. **159**, B 219 (2012).
[4] Yu.A. Mastrikov, R. Merkle, E.A. Kotomin, M.M. Kuklja, J. Maier, Phys. Chem. Chem. Phys. **15,** 911 (2013)

SESSION D5: Fundamentals of Transport and Reactivity and Nanoionics IV
D: Fundamentals of Transport and Reactivity and Nanoionics
Chairs: Rotraut Merkle and Truls Norby
Tuesday Afternoon, June 16, 2015
Keystone Resorts, Grays Peak I/II

1:30 PM *D5.01
An Extended Analysis of Dopant Strategies to Control Mixed Ion and Electron Transport in Ceria Based Oxide Solutions Jens-Peter Eufinger[2], Maximilian Daniels[1], Stefan Berendts[3], Kerstin Neuhaus[1], Sebastian Eickholt[1], Gregor Ulbrich[3], Aditya Maheshwari[1], Annika Buchheit[1], Juergen Janek[2], Martin Lerch[3] and Hans D. Wiemhoefer[1]; [1]Institute of Inorganic and Analytical Chemistry, Univ. Münster, Münster, Germany; [2]Physikalisch-Chemisches Institut, Univ. Giessen, Giessen, Germany; [3]Institute of Chemistry, Techn. Univ. Berlin, Berlin, Germany.

A systematic experimental study of a variety of dopant effects has been carried out on ceria based oxides covering a) the differences between doped single crystalline and polycrystalline materials, b) a wide temperature range between room temperature and 800 °C, and c) a detailed measurement of electron and ion transport properties such as partial conductivities, chemical diffusion coefficients, and transference numbers. Acceptors such as Y, Gd, Ba, Sr, Zn, donors such as Ta, Nb, W, Sb, isovalent dopants like Zr, Ti, and variable valence dopants like Pr have been investigated.

Detailed point defect models and free energy schemes for ionic as well as electronic defects are discussed to explain the results and used to predict favorable strategies how to enhance oxygen storage properties, catalytic and electrochemical activity towards surface redox processes, oxygen permeation, and even controllable optical properties in the UV as well as in the FIR. Furthermore, examples are shown and interpreted regarding non-equilibrium effects during voltage induced polarization at blocking contacts. e.g. local conductivity switching.

Mixed oxygen ion and electron conduction can be easily demonstrated in doped and undoped ceria at temperatures down to room temperature. Such results offer a good explanation for the already known good catalytic efficiency of ceria nanoparticles and films at low temperatures.

1:50 PM D5.02
Room Temperature Polarization Phenomena in Doped Ceria Kerstin Neuhaus[1], Gregor Ulbrich[2], Martin Lerch[2] and Hans-Dieter Wiemhöfer[1]; [1]Institute for Inorganic and Analytical Chemistry, University of Münster, Münster, Germany; [2]Institut für Chemie, Technische Universität Berlin, Berlin, Germany.

Introduction
Pure and doped ceria is a material which gains more and more interest for low-temperature applications, e.g. as catalyst material or for pharmaceutical purposes [1,2]. While for standard operating temperatures in the range of 400-1200 °C the defect chemistry of these materials is well established, experimental data and theoretical background at room temperature are scarce. [3,4]. By executing a combined polarization/ Kelvin probe force microscopy (KPFM) mapping experiment in air at room temperature [5], the time-dependent reaction of ceria to reduction and oxidation by bias application can be made visible. Further, the reaction to polarization and time dependent fading of the effect of the single crystals is compared to polycrystalline samples. The effect of dopant concentration as well as the impact of grain boundaries on the polarization and fading behavior can thus be studied with high local resolution.

Experiments and Results
Single crystals of 10 mol% Gd3+-doped and 20 mol% Y3+-doped ceria which were obtained by the skull melting method as well as ceramic samples with the composition Ce0.8Gd0.2-xPrxO2-δ (x=0.2, 0.09, and 0.01) were investigated. The samples were polarized using an AFM tip as working electrode and a large silver paste (back or ring) contact as counter electrode (see Fig. 1, left). Due to the difference in size, most of the voltage drop occurs in the region near the AFM tip. After the end of polarization experiment, the surface potential is mapped with time. Polarization leads to the development of circular effects with an increased or decreased potential, depending on the applied bias. For single and polycrystalline materials strongly differing relaxation times (see Fig. 1, right) were found.

Fig. 1: Left: Polarization/KPFM measurement setup. Right: Time-dependent relaxation behavior of the surface potential for Ce0.8Pr0.2O2-δ (ceramic pellet) and Ce0.8Y0.2O2-δ (single crystal) after end of polarization experiment.

Size, surface potential variation, and fading behavior of the introduced effect were also differing for positive and negative applied biases as well as for different application times and also for varying acceptor dopant concentrations. The effect was not found for donor-doped materials. The measured data will be discussed in terms of a defect model.

Acknowledgements
The authors want to thank the Deutsche Forschungsgemeinschaft for funding within the collaborative project grants# WI 952/9-1 and LE781/14-1.

Literature
[1] Trovarelli, Catal. Rev. 1996, 38, 439. [2] Tarnuzzer et al., S. Nano Lett. 2005, 5, 2573. [3] Sasaki, Maier, J. Appl. Phys. 86 (1999) 5422. [4] Sasaki, Maier, J. Appl. Phys. 86 (1999) 5434. [5] Lee et al. Nanotechnology 20 (2009) 1. 03006009001200-2-

2:10 PM *D5.03
Microscopic Origin of Electrostriction in Gd-Doped Ceria and Prospects for Practical Applications in MEMS Roman Korobko[1], Eran Mishuk[1], Nimrod Yavo[1], Alyssa Lerner[2], Yuanyuan Li[2], Wachtel Wachtel[1], Anatoly Frenkel[2] and Igor Lubomirsky[1]; [1]Materials and Interfaces, Weizmann Institute of Science, Rehovot, Israel; [2]Physics Department, Yeshiva University, New York, New York, United States.

We have been studying the mechanism of electrostriction in oxygen deficient and Gd-doped ceria thin films from the fundamental physics point of view while also considering prospects for its practical applications. The magnitude of the electrostriction stress (γ) and strain (M) coefficients of supported Gd-doped ceria films exhibit complex behavior as a function of Gd content. With 5 mol% Gd, both the electrostrictive strain and stress coefficients are maximum: γ= 380 kPa/(kV/cm)^2 and M=130×10^{-18} ; the pseudo-piezoelectric strain coefficient is ~300 pm/V with DC field strength 20 kV/cm. Upon increase of the Gd content to 20 mol%, the electrostriction strain coefficient decreases by a factor of ~14. Increase of the Gd content from 20 mol% to 33 mol% increases the electrostriction stress coefficient by ~1.7. Given that the dielectric constant (ε) of Gd-doped ceria is < 30, the values of the polarization electrostriction coefficient Q are orders of magnitude larger (e.g., $Q_{5\%}$>2000 m^4/C^2,$Q_{20\%}$=157 m^4/C^2) than the values measured for commonly used electrostrictors based on $Pb(Mg_{1/3},Nb_{2/3})O_3$–$PbTiO_3$ (PMN-PT). For these materials, ε ~ 20,000 and Q < 0.1 m^4/C^2. Another striking difference between Gd-doped ceria and PMN-PT is that a thin film of PMN-PT elongates parallel to the applied electric field, while a textured Gd-doped ceria film contracts.

In situ differential EXAFS and XANES measurements show that the large electrostrictive stress generation can be associated with the presence of a few percent of unusually short Ce-O chemical bonds in the vicinity of oxygen vacancies. These chemical bonds increase in length under an external electric field, while the degree of order of the environment of the Ce cation also increases. The rest of the lattice does not appear to participate in the stress generation and remains as a passive spectator. Such unusual properties certainly point to a heretofore unrecognized mechanism of electrostriction.

One of the major practical advantages of Gd-doped ceria as an electromechanically active material is that it is completely compatible with Si-microfabrication. Using only Si-compatible processes, we have fabricated large area (4 mm^2) self-supported films (300-500 nm) of 10 mol% Gd-doped ceria ($M_{10\%}$=2.5×10^{-17} m^2/V^2) with top and bottom Al contacts. We have also developed a process to control buckling type and mode in the self-supported structures. Using a proximity sensor, we have determined that application of an alternating electric field produces electromechanical response at double the frequency, which is typical for electrostriction. The amplitude of the film displacement (a few μm) is linearly proportional to the square of the amplitude of the applied electric field until at least 150 kV/cm. This implies that saturation would occur at still larger field. Vertical displacement persists with increasing frequency until at least 1 MHz. Application of 7.5V@ 50 kHz (150 kV/cm) for a period of 17 hrs (~3×10^9 cycles) does not cause detectable film degradation or fatigue. On the basis of measurements made till now, Gd-doped ceria can be viewed as a very promising material for electromechanical applications in MEMS, in particular for actuators, mechanical switches and tunable capacitors.

2:30 PM D5.04
An *In Situ* Optical Spectroscopic Study of Thermodynamics and Redox Kinetics of $Ce_{0.08}Y_{0.2}Zr_{0.72}O_{2-\delta}$ Jianmin Shi[1], Martin Lerch[2], Jueürgen Janek[3] and Klaus D. Becker[1];[1]Technische Universität Braunschweig, Braunschweig, Germany; [2]Technische Universität Berlin, Berlin, Germany; [3]Justus Liebig University Giessen, Giessen, Germany.

Oxides of the fluorite structure are of importance for energy conversion and storage devices. For example, ceria-based oxides are promising solid electrolytes for SOFC operating at intermediate temperatures and catalysts for fuel production. The performance of these devices is largely influenced by the defect chemistry, reactivity and related kinetic processes occurring in the materials at operating conditions. To understand the atomic mechanism of materials degradation and transport processes in these materials, we have developed in-situ optical spectroscopy to study the defect chemistry and diffusion in oxides at elevated temperatures under various atmospheres. In this contribution, we will present an optical in-situ study of defects equilibrium and redox kinetics of Ce-containing yttria stabilized zirconia, $Ce_{0.08}Y_{0.2}Zr_{0.72}O_{2-\delta}$. The optical absorption of defects in equilibrium can be described in terms of a defect model involving oxygen vacancies and electrons. Chemical diffusion coefficients obtained from modelling redox processes upon rapid changes in oxygen activity will be discussed by considering defect interactions and their effects on ionic diffusion.

2:50 PM *D5.05

Effect of Chemomechanical Coupling on Defect Equilibrium and Transport in Solid State Ionic Devices Tatsuya Kawada, Yuta Kimura, Yuki Gonoi, Keiji Yashiro, Shin-ichi Hashimoto and Koji Amezawa; Tohoku University, Sendai, Japan.

Since solid state electrochemical systems consist of multilayers of solids, the materials are subjcect to mechanical stresses under operation due to thermal expansion mismatch. Chemical expansion or chemical-potential-driven mass transport may also cause the development of mechanical stress and strain in the device, and vice versa, the local mechanical stress can affect the defect equilibrium and mass tranport in and at the boundary of the materials. The magnitude of the effect of mechanical stress on oxygen nonstoichiometry of several perovskite type oxides were investigated by a potentiometric technique, which utilizes an oxide ionic conductor as the local oxygen potential sensor and as the indentor at the same time. Upon application of the compressive stress, the oxygen potential in the sample around the probe (or indentor) first shifted in the negative direction, and then gradually came back to the original value. It was explained by a transient shift of oxygen vacancy concentration, which comes from the thermodynamic shift of the equilibrium shift achieved through oxygen vacancy diffusion. The magnitude of the change in vacancy concentration was not very high under a stress developed under a practical use of a solid electrochemical devices.

On the other hand, a large change in defect equilibrium is sometimes observed in a material when it is deposited as a film deposited by pulsed laser deposition. Also, transport properties are discussed to have large effects of mechanical stress. Several related phenomena reported so far will be reviewed and discussed.

3:30 PM *D5.06

Electro-Chemo-Mechanics in Solid State Materials: Let`s Design the Structural-Defect Twists Jennifer L. Rupp; Electrochemical Materials, ETH Zurich, Zurich, Switzerland.

The next generation energy conversion and storage, information memories and new neuromorphic computer logic concepts rely largely on solving fundamental questions of mass and charge transport of oxygen ionic or Li-defects in materials and their structures. Here, understanding the defect kinetics in the solid state material building blocks and their interfaces with respect to lattice and interfacial strains are the prerequisite to design new material properties beyond classic doping. Through this presentation basic theory and model experiments for solid state electro-chemo-mechanics and lattice strain modulations is being discussed as a new route for tuning material and properties in ionic conducting oxide film structures up to new device prototypes. We will discuss basic fundamentals of oxygen ionic transport under strain and exemplify the impact on novel electrochemical devices. Firstly, we will show the use electro-chemo-mechanics on doped ceria free-standing oxygen ionic membranes and how to combine near-order measurements and non-contact optical 3D profiling measurements to describe and compute strain patterns on these membranes. This knowledge is used to evaluate new design routes to tune the strain state of the free-standing membranes and to influence the conductivity of the electrolyte for potential energy applications.[1,2] Secondly, we research interfacial strain as a new tool for resistive switching memories. Interfacial strain is applied through lattice mismatch using the model systems $Gd_{0.1}Ce_{0.9}O_{2-\delta}/Er_2O_3$ and $Gd_{0.1}Ce_{0.9}O_{2-\delta}/Sm_2O_3$ for compressive strain and tensile strain, respectively. This concept is being integrated in electrochemical micro-dot devices and has been applied to control properties of resistive switches, like R_{on}/R_{off} ratio.[3-5] Thirdly, we focus on the use of electro-chemo-mechanics for the fabrication of optimized all solid state microbatteries based on Li-conducting garnet electrolytes. Wrapped cathode/electrolyte/anode trilayers with tunable strain will be shown as a model system for studying the electro-chemo-mechanic interactions during battery operation.

[1)] Twisting Electro-Chemo-Mechanics to Control Oxygen Ionic Transport in Solid State Energy Conversion Membranes
Y. Shi, A.H. Bork, S. Schweiger, M. Struzik and J.L.M. Rupp
in review (2014)

[2)] Scalable oxygen-ion transport kinetics in metal-oxide films: Impact of thermally induced lattice compaction in acceptor doped ceria films
J.L.M. Rupp, E. Fabbri, D. Marrocchelli, J.-W. Han, D. Chen, E. Traversa, H.L. Tuller and B. Yildiz
Advanced Functional Materials, 24, 11, 1562 (2014)

[3)] A Micro-Dot Multilayer Oxide Device: Let's Tune the Strain-Ionic Transport Interaction
S. Schweiger, M. Kubicek, F. Messerschmitt, C. Murer and J.L.M. Rupp
ACS Nano, 8, 5, 5032 (2014)

[4)] Memristor Kinetics and Diffusion Characteristics for Mixed Anionic-Electronic $SrTiO_{3-\delta}$: The Memristor-based Cottrell Analysis Connecting Material to Device Performance
F. Messerschmitt, M. Kubicek, S. Schweiger and J.L.M. Rupp
Advanced Functional Materials, 24, 47, 7448 (2014)

[5)] Patent Application PCT/EP2014/001020: "Strained Multilayer Resistive-switching Memory Elements" (2013)
J.L.M. Rupp, S. Schweiger, F. Messerschmitt
Spark award winner: most inventive and economically important patent of the year at ETH Zurich

3:50 PM D5.07

Engineering Mixed Ionic Electronic Conduction in $La_{0.8}Sr_{0.2}MnO_{3+\delta}$ Nanostructures through Fast Grain Boundary Oxygen Diffusivity Aruppukottai Muruga Saranya[1], Dolors Pla[1], Alex Morata[1], Andrea Cavallaro[2], Jesus Canales-Vazquez[3], John A Kilner[2], Monica Burriel[1, 2] and Albert Tarancon[1]; [1]Catalonia Institute for Energy Research (IREC), Barcelona, Spain; [2]Imperial College London, London, United Kingdom; [3]Universidad Castilla la Mancha, Albacete, Spain.

The simultaneous conduction of ions and electrons constitutes the working principle of a wide variety of devices such as batteries, fuel cells and electrolyzers, and electrochromic displays. Since mixed ionic-electronic conductors (MIECs) are key functional materials in all these solid state devices, novel approaches to improve their ionic/electronic transport properties have attracted increasing attention in recent years. However, the enhancement of the mass transport properties at the nanoscale has been often found difficult to implement in nanostructures.
$La_{0.8}Sr_{0.2}MnO_{3+d}$ (LSM) was selected for this study since it is considered a cornerstone material in a wide variety of electrochemical and electronic devices. In order to study the dominating transport properties in nanostructured LSM, films with a high density of grain boundaries were prepared by Pulsed Laser Deposition (PLD). The oxygen mass transport properties of the prepared heterostructure were evaluated by performing ^{18}O isotope exchange experiments at different temperatures followed by depth profiling analysis by Secondary Ion Mass Spectroscopy (IEDP-SIMS). Finite Element Analysis (FEM) was carried out to simulate the concentration profiles obtained by IEDP-SIMS, revealing a remarkable enhancement for the oxide-ion mass transport properties along grain boundaries. The functionality of these vertically nanostructured thin films was also investigated in conventional electrochemical cells.
In this communication we present the fabrication of an artificial mixed ionic electronic conducting oxide by grain boundary engineering thin films of LSM. While in bulk form LSM is essentially a pure electronic conductor with a very low concentration of oxygen vacancies, this compound was converted into an excellent mixed ionic electronic conductor by creating a nanostructure with high density of grain boundaries. Our results lead to fundamental insights into oxygen diffusion along grain boundaries and to the application of these engineered nanomaterials in new advanced solid state ionics devices such as micro-solid oxide fuel cells or resistive switching memories.

4:10 PM D5.08

Oxidation Kinetics of Thin Metal Films & Diffusion in NiO Yeliz Unutulmazsoy, Rotraut Merkle, Joachim Maier and Jochen Mannhart; Max Planck Institute for Solid State Research, Stuttgart, Germany.

The growth of oxide layers on metals is determined by formation and migration of point defects in the forming oxide layer and thus is an issue of fundamental importance. So far, mainly oxidation kinetics of thick metal films, crystals and bulk samples were investigated in the literature. The main interest is to understand the processes that determine the oxide growth rate and attempts to increase the reaction rate for potential applications. During the oxidation of metal films in a tube furnace, the resistance changes were measured by electrical impedance spectroscopy. Oxide growth follows the parabolic rate law of oxidation for Cr, Al, Ti, V, Zn, Ni and Co film samples with a thickness typically ranging from 10-150 nm. Thus the rate determining process of the oxidation of these metal films is chemical diffusion through the oxide layer according to the

Wagner theory. NiO is chosen for a thorough understanding of oxidation kinetics and diffusion. Ni diffusion in NiO is mainly controlled by singly and doubly ionized Ni vacancies. Thus, donor doping of NiO is expected to increase the reaction rate by increasing the Ni-vacancy concentration. However, the oxidation rate of undoped Ni and Cr-doped Ni films with different concentrations of Cr showed no significant change in the rate. Since it is difficult to modify the grain size and to obtain a homogenous dopant distribution in the growing oxide films, the transport properties of undoped and donor doped NiO ceramics by conductivity relaxation measurements are studied as ceramic samples. Conductivity (σ) and chemical diffusion coefficient (D^{δ}) values are obtained as a function of p_{O2} and temperature which depend in a nontrivial way on Cr content, grain size and thermal history of the samples. The comparison of σ and D^{δ} values of as-prepared (hot-pressed at 1100 °C) and annealed samples (8h at 1500 °C) shows that the Cr dopants seem to be electrochemically inactive for the as-prepared and active for annealed ceramics.

4:30 PM D5.09

H^- Ionic Conduction in Alkaline Hydrides John T. Irvine[1], George Carins[1], Maarten Verbaeken[1] and Martin Owen Jones[2]; [1]School of Chemistry, University of St Andrews, St Andrews, United Kingdom; [2]STFC, Didcot, United Kingdom.

Hydride materials have received much interest over the last years for their potential to store hydrogen in the solid state. Because much of the research is aimed at hydrogen storage for onboard applications, such as low temperature fuel cells for the automotive industry, scientists have focused on finding lightweight materials for optimum gravimetric hydrogen densities. Although the heavy alkaline earth hydrides are of limited interest for their hydrogen storage potential, due to low gravimetric densities, their ionic nature may prove useful in new electrochemical applications, especially as an ionically conducting electrolyte material. Here we show that barium hydride shows fast pure ionic transport of hydride ions (H^-) in the high temperature, high symmetry phase. Although some conductivity studies have been reported on related materials previously, the nature of the charge carriers has not been determined. I

In this study BaH_2 is shown to give rise to hydride ion conductivity of 0.2 S/cm at 630ºC. This is an order of magnitude larger than that of state-of-the-art proton conducting perovskites or oxide ion conductors at this temperature. In situ neutron diffraction has been utilised to follow isotopic exchange with simultaneous ionic conducivity measurements being performed. This demonstrates a clear isotope effect, consistent with hydride ion conduction. This is confirmed by isotope concentration cell EMF measurements. Hydride conduction is also demonstrated in CaH_2 in these experiments. These results suggest that the alkaline earth hydrides form an important new family of materials, with potential use in a number of applications, such as separation membranes, electrochemical reactors, etc.

4:50 PM D5.10

Modeling a Surface-Mediated Spinodal in Doped Mixed Conducting Perovskites David S. Mebane; Mechanical and Aerospace Engineering, West Virginia University, Morgantown, West Virginia, United States.

The segregation of dopant cations at the surface of perovskite mixed ionic-electronic conductors strongly influences the electrocatalytic properties of the material. As dopant concentrations are typically quite high, the usual Poisson-Boltzmann approach to the modeling of the surface and near-surface defect structure is not appropriate, as multiple experimental results revealing segregation layer thicknesses nanometers in size (whereas the Debye length is less than a nanometer) confirm. A better approach for the concentrated case is a phase-field approach. This presentation will introduce a Cahn-Hilliard model for the segregation of A-site dopants to the surface of mixed conducting perovskites. The model admits a surface-mediated spinodal decomposition: a first-order phase transition in which dopant cations segregate to the surface in high concentrations. Initial model results suggest that such a transition must be considered in light of the surface dopant cation concentrations seen in experiments.

SESSION D6: Poster Session: Fundamentals of Transport and Reactivity and Nanoionics II
D: Fundamentals of Transport and Reactivity and Nanoionics
Tuesday Afternoon, June 16, 2015
5:20 PM
Keystone Resorts, Red Cloud Peak

D6.01

The Role of Ceria in Electro-Reduction of Nitrogen Oxide Based on Solid State Cell Reactor at Intermediate-Temperature Wenyi Tan[1, 2], Fei Chen[1], Lei Gong[1], Yunfei Bu[2], Yang Song[2] and Qin Zhong[2]; [1]Nanjing Institute of Technology, Nanjing, China; [2]School of Chemical Engineering, Nanjing University of Science & Technology, Nanjing, China.

Electrochemical reduction of nitrogen oxides in solid state cell reactor (SSCR) was conducted at intermediate-temperature (400-600ºC) on four various cathodes, including three different amount of ceria-containing $(La_{0.85}Sr_{0.15})_{0.9}MnO_3$ (LSM) composites and one ceria-free LSM. Performances of NO electrochemical reduction, i.e., NO conversion and current / voltage produced were evaluated. Higher NO conversion is achieved at 550ºC with closed circuit at a fixed voltage of 0.3V. Ceria-containing cathodes advantage NO conversion and thus higher current density at 0.3V is obtained when compared with ceria-free cathodes. When the composite cathode for LSM-GDC22 was typically applied, total NO conversion (the sum of electrochemical conversion and non-electrochemical conversion) at closed circuit state at 550oC is almost 60%. And the corresponding current density at 0.3V reaches 17 mA cm^{-2}. The effect of the ceria content on the NO electrochemical reduction was investigated in the presence of oxygen, too. The role of ceria in the electrochemical reduction was characterized by means of electrochemical impedance spectra and in-situ infrared spectroscopy.

D6.02

Li-Ion Dynamics Along the Inner Surfaces of Layer-Structured 2H-Li_xNbS_2 Bernhard Stanje[1], Viktor Epp[1], Suliman Nakhal[2], Martin Lerch[2] and Martin Wilkening[1]; [1]Institute for Chemistry and Technology of Materials, Technical University of Graz, Graz, Austria; [2]Institut für Chemie, Technische Universität Berlin, Berlin, Germany.

Layer-structured materials such as graphite (LiC_y) or $Li_x(Co,Ni,Mn)O_2$ are important electrode materials in current battery research that still relies on insertion materials. This is due to their excellent ability to reversibly accommodate small alkali ions such as Li^+ and Na^+. Despite of these applications behind, microscopic information on Li ion self-diffusion in transition metal sulfides are relatively rare. Here, we used ^{7}Li nuclear magnetic resonance (NMR) spectroscopy to study translational Li ion diffusion in the model system hexagonal (2H) Li_xNbS_2 (x = 0.3, 0.7 and 1) by means of variable-temperature NMR relaxometry. ^{7}Li spin-lattice relaxation rates and ^{7}Li NMR spectra were used to determine Li jump rates and activation barriers as a function of Li content. Hereby, NMR spin-lattice relaxation rates recorded with the spin-lock technique offered the possibility to study Li ion dynamics on both the short-range and long-range length scale. Dynamic parameters, such as jump rates and activation barriers, could be extracted from complete diffusion-induced rate peaks, which are obtained when the relaxation rate is plotted *vs* reciprocal temperature. The peak maximum of the three samples studied shifts towards higher temperatures with increasing Li content x in 2H-Li_xNbS_2 revealing a decrease of Li diffusivity with increasing x. Information on the dimensionality of the diffusion process was experimentally obtained by *frequency dependent* R_ρ measurements carried out at T = 444 K, that is in the high-temperature regime of the rate peaks. A slight, but measurable frequency-dependence within this limit is found for all samples; it is in agreement with predictions from relaxation models developed to approximate low-dimensional (2D) jump diffusion; thus, Li diffusivity within the van der Waals gap governs the NMR rates recorded.

D6.03

Catalytic Activity and Oxygen Storage Properties of Doped $Ba_{1-x}Sr_xY_{1-y}Ln_yMn_2O_{5+\delta}$ (Ln - lanthanides) for Application in Three-Way Catalytic Converters Alicja Klimkowicz[2,1], Konrad Swierczek[2], Tomasz Rzasa[2], Akito Takasaki[1] and Bogdan Dabrowski[3]; [1]Department of Engineering Science and Mechanics, Shibaura Institute of Technology, Tokyo, Japan;[2]Faculty of Energy and Fuels, AGH University of Science and Technology, Krakow, Poland; [3]Department of Physics, Northern Illinois University, DeKalb, Illinois, United States.

Recently, numerous new materials with higher reversible oxygen storage capacity (OSC) and faster reduction/oxidation kinetics have been studied for possible application as support catalyst in three-way catalytic converters (TWC), as well as for other applications, where precise control and possibility of fast changes of the oxygen partial pressure are required [1, 2]. New materials, belonging to group of cation-ordered perovskite-type oxides, with $Ba_{1-x}Sr_xY_{1-y}Ln_yMn_2O_{5+\delta}$ (Ln - lanthanides) general formula are of interest, as their application in TWCs should allow for a decrease of the catalyst mass, amount of utilized rare earth elements and precious metals, and therefore, should bring substantial decrease of production costs.

We report on crystal structure and its evolution on temperature of reduced and oxidized $Ba_{1-x}Sr_xY_{1-y}Ln_yMn_2O_{5+\delta}$, changes of valence state of manganese cations, reversible OSC, heat effect, kinetics of reduction/oxidation processes, and correlation of all these properties with catalytic ability for CO, NO_x and CH_x conversion. It was documented that much faster oxidation speed of $Ba_{1-x}Sr_xY_{1-y}Ln_yMn_2O_5$ (compared to reduction) originates from a large heat effect (~200 kJ·mol^{-1}), which causes local over-heating of material, speeding up bulk diffusion. Additionally, it was found possible to enhance OSC of the samples by partial substitution of Ba by Sr, but small range of solid solution formation is the limiting factor. It was established that catalytic ability for conversion of CO, NO_x and CH_x of the $Ba_{1-x}Sr_xY_{1-y}Ln_yMn_2O_{5+\delta}$ correlates well with OSC and kinetics of reduction process. It can be stated that the conducted research allows for selection of the best candidate material, which should be suitable for commercial application.

The project was funded by the National Science Centre Poland (NCN) on the basis of the decision number DEC-2011/01/B/ST8/04046.

[1] T. Motohashi, et al., J. Phys. Chem. C, doi:10.1021/jp511648b
[2] A. Klimkowicz, et al., Mater. Res. Bull. 65 (2015) 116-122

D6.04

Electrical Conductivity, Oxygen Diffusion Coefficient and Surface Exchange Coefficient of $La_4Co_3O_{10}$ by Electrical Conductivity Relaxation Technique Yoshinobu Adachi, Naoyuki Hatada and Tetsuya Uda; Materials Science and Engineering, Kyoto University, Kyoto, Japan.

$LaCoO_3$ is a cathode material of solid oxide fuel cells (SOFC), owing to its mixed electronic and oxide ion conductivity. Since $La_4Co_3O_{10}$ has a similar layered perovskite-related structure, it may also exhibit mixed conductivity. However, its electrical conductivity and charge carriers have not been studied yet. In this study, the electrical conductivity of $La_4Co_3O_{10}$ was measured, and its oxygen diffusion coefficient (D_{chem}) and surface exchange coefficient (k) were evaluated by electrical conductivity relaxation technique. $La_4Co_3O_{10}$ was synthesized by solid state reaction method. The relative densities of sintered bodies were 92-94%. Several sintered bodies also contained a small amount of La_2CoO_4. After the surfaces of the sintered bodies were mirror-polished, their electrical conductivities were measured by four-probe dc technique.

The electrical conductivity of $La_4Co_3O_{10}$ increased with temperature at 500-800 °C in O_2/Ar gas mixtures, and reached ~210 S cm^{-1} at 800 °C and an oxygen partial pressure (p_{O2}) of 1 atm. The apparent activation energy of charge transport was 0.14 eV. The electrical conductivity also increased with p_{O2}, suggesting change in oxygen non-stoichiometry. At 500-700 °C, the conductivity relaxation profiles of the two samples having different thickness (200 μm and 600 μm) were acquired, by switching p_{O2} from 0.2 to 1 atm. Assuming the surface reaction was the rate determining step (rds), the fitting results of k was consistent between two samples. However, when oxygen diffusion was assumed to be rds, derived D_{chem} values were different by 2.5-10 times. Thus, they should be incorrect. These results indicate that surface reaction was a main limiting step at 500-700 °C. The k value was 3.3×10^{-5}-2.0×10^{-4} cm s^{-1} at 500-700 °C. For obtaining the precise value of D_{chem}, samples having lager thickness and/or specific surface area are needed. The results with these samples will be presented at the meeting.

D6.05

Influence of Cation Nonstoichiometry to Oxygen Nonstoichiometry in Mixed Ionic and Electronic Conducting Perovskite Oxides Yusuke Okamoto[1], Akihide Kuwabara[2], Takashi Nakamura[3], Tatsuya Kawada[1] and Koji Amezawa[3]; [1]Graduate Study of Environmental Studies, Tohoku University, Sendai, Japan; [2]Japan Fine Ceramics Center, Atsuta, Japan; [3]IMRAM, Tohoku University, Sendai, Japan.

In complex oxides containing a number of cation species, state of the oxides cannot be defined only by controlling temperature and oxygen partial pressure, since more than one degree of freedom remain. This suggests that even if the material seems to be in a single phase, the cation composition can differ and its properties such as oxygen nonstoichiometry and electronic structures change consequently. In this work, we study the influences of cation nonstoichiometry in complex oxides on the oxygen nonstoichiometry, the electronic and the crystal structure. Perovskite-type $SrFeO_{3-d}$ was selected as a model complex oxide. The perovskite with different cation ratio (A/B = 0.9~1.1) were synthesized. By XRD measurements, the main phase was confirmed as a perovskite structure for all the compositions, while $Sr_AFe_BO_{3-d}$ with 1 mol% and 3 mol% or more excess amount of A-site and B-site showed a very few amount of impurity phases respectively. Oxygen nonstoichiometry $Sr_AFe_BO_{3-d}$ with cation composition of A/B = 0.97 and 1.03 was measured. Although small amounts of impurity phases were observed, we investigated these materials. This is because the state of the main phase can be defined according to the phase rule and oxygen nonstoichiometry in impurity phases could be negligible. Measurements were performed at 873-1073 K using high temperature gravimetry in higher pO_2 and coulometric titration in lower pO_2. The oxygen nonstoichiometry of the Sr-excess sample is similar to that of Mizusaki *et al.* reported as a result of "stoichiometric" $SrFeO_{3-d}$. On the other hand, the sample with the excess amount of Fe showed relatively less oxygen compared to one with the excess amount of Sr and reported "stoichiometric". These results indicate that the oxygen nonstoichiometry of $SrFeO_{3-d}$ can be influenced significantly by a small change in the cation composition.

D6.06

Structure, Transport and Stability of Layered Ruddlesden-Popper $La_{n+1}Ni_nO_{3n+1}$ (n = 1, 2 and 3) Epitaxial Films Kuan-Ting Wu[1, 2], Monica Burriel[5, 2], Fan Yang[3], David McComb[3], John Kilner[2, 4] and Stephen Skinner[2]; [1]Department of Applied Chemistry, Kyushu University, Fukuoka, Japan; [2]Department of Materials, Imperial College London, London, United Kingdom; [3]Department of Materials Science and Engineering, Ohio State University, Columbus, Ohio, United States; [4]International Institute for Carbon-Neutral Energy Research (wpi-I2CNER), Fukuoka, Japan; [5]Laboratoire des Matériaux et du Génie Physique (LMGP), Grenoble, France.

Layered Ruddlesden-Popper (RP) $La_{n+1}Ni_nO_{3n+1}$ (n = 1, 2 and 3) phases have recently attracted attention as potential cathode candidates for intermediate temperature solid oxide fuel cells (IT-SOFC). Previous research has reported that a very high ionic conductivity (σ_i = ~10^{-2} Scm^{-1}) is obtained for $La_2NiO_{4-\delta}$ but performance is limited by its electronic conductivity (σ_e = 10-100 Scm^{-1}). $La_3Ni_2O_{7-\delta}$ (n = 2) and $La_4Ni_3O_{10-\delta}$ (n = 3) are expected to possess good stability, and superior electronic conductivity. [1] Thus these higher order compounds may be more suitable for IT-SOFCs.

A series of c-axis oriented $La_{n+1}Ni_nO_{3n+1}$ (n = 1, 2 and 3) epitaxial films have been deposited on NGO (110) and reported in the previous work. [2] In this work, structure, transport, stability properties of these materials will be further investigated. These investigations will aid in the understanding of the relationship of these properties.

The film quality and compositions were confirmed by high-resolution XRD, atomic force microscopy, energy dispersive X-ray spectroscopy and high-resolution transmission electron microscopy. High-temperature total planar electrical conductivity measurements were addressed by four-point van der Pauw method, while oxygen transport measurements were conducted by the isotope exchange depth profile method. The electrical conductivity results reveal that a larger conductivity along the a-b plane than the randomly oriented polycrystalline bulk samples, and a systematic enhancement of electrical conductivity when the "n" value increases, showing a promising conductivity value of ~700-1000 Scm^{-1} in the intermediate temperature region (500-700°C) for n = 2 and 3 films. The findings indicate a strong structural relationship for the electrical conductivity behavior of the RP films. Good stability of the n = 2 and 3 films are also demonstrated in the study.

References
[1] G. Amow, I. J. Davidson, S. J. Skinner, *Solid State Ionics* **2006**, 177, 1205.
[2] K.-T. Wu, Y.-A. Soh, S. J. Skinner, *Mater. Res. Bull.* **2013**, 48, 3783.

D6.07

Low Temperature Protonic Transport in Nanocrystalline Porous Oxides Sindre O. Stub[1], Per M. Rorvik[2], Reidar Haugsrud[1] and Truls Norby[1]; [1]Centre for Materials Science and Nanotechnology, Department of Chemistry, University of Oslo, Oslo, Norway; [2]Sector for Sustainable Energy Technology, SINTEF Materials and Chemistry, Oslo, Norway.

High protonic conductivity has been reported for nanocrystalline porous oxides, e.g. YSZ and mesoporous silica, under humid conditions at temperatures below 150°C [1-3]. Many aspects of this phenomenon have only been described in qualitative terms. In this contribution we present a mathematical model based on surface chemistry that accounts for the effects of water vapour on the low temperature conductivity behaviour of such porous oxides. The model is applied to conductivity data of samples of YSZ with varying porosity and grain size.

YSZ with 8 mol% Y_2O_3 was prepared through a solid state route and grain size and microstructure was characterized by XRD, BET and SEM. The conductivity was investigated with impedance spectroscopy in dry and wet oxygen below 450°C.

By comparing results from impedance spectroscopy with theoretical behaviour, we find that the protonic conduction takes place in both the chemisorbed and physisorbed layers of water below 450°C. At intermediate temperatures (300-150°C) proton conduction in the chemisorbed layer appears to occur via the Grotthuss mechanism. Below 150°C the protonic conduction in the physisorbed water layers dominates, and the conductivity increases as a result of increasing relative humidity with decreasing temperature. The surface is covered by the first complete physisorbed layer, on top of the chemisorbed layer at around 50°C. Multilayers are formed by lowering the temperature further. In accordance with the liquid-like state of the water layers, protonic mobility appears to exhibit a very low activation energy.

Authors acknowledge funding by the Research Council of Norway (NaProCs, #216039/E20).

1. Gregori, G., et al., Advanced Functional Materials, 2013. 23: 5861-5867.
2. Avila-Paredes, H.J., et al., Journal of Materials Chemistry, 2010. 20(5): 990-994.
3. Fujita, S., et al., Chemistry of Materials, 2013. 25(9): 1584-1591.

D6.08

The Influence of Aging and Humidity on Transport Properties of Ceria Thin Films at Low Temperatures Matthias Kleine-Boymann, Matthias Elm, Raika W. Oppermann and Juergen Janek; Institute of Physical Chemistry, Justus-Liebig University, Giessen, Germany.

Cerium-based oxides are frequently studied as a model system for the class of mix ionic/electronic conductors with fluorite structure. High surface area nanocrystalline CeO_{2-x} and its solid solutions with other oxides are an exceptional material for oxygen storage and catalysis of redox reactions. The oxygen exchange kinetic correlates with the electrical properties, which are affected by the microstructure in nanocrystalline CeO_{2-x} thin films. At elevated temperatures, the microstructure might undergo changes during long-term electrochemical impedance spectroscopy (EIS) measurements, due to crystallite growth or aging effects, which may significantly change the electrical properties. At low temperatures enhanced proton conductivity in nanostructured ceria was reported, but its origin is still controversially discussed.
Using EIS, we investigated the transport properties of nominally undoped CeO_2 thin films prepared by PLD and contacted with interdigital platinum electrodes between 30 °C and 550 °C –under varying humidity. Previous studies rarely differentiated between measurements under dry or wet atmosphere, and thus, we carried out conductivity measurements as a function of $p(H_2O)$ for a wide humidity range. Our results show that the conductivity is only influenced by humidity at low temperatures around 30°C. This enhancement is ascribed to water absorbing at the surface. Furthermore, even after careful pretreatment at temperatures higher than the maximum temperature during the conductivity measurements, significant changes of the conductivity between different measurement sequences can occur, which we attribute to morphological changes of the sample and the electrodes. In order to study these phenomena in more detail, nominally undoped CeO_{2-x} thin films were investigated using XRD, SEM, and EBSD. Depending on the thermal treatment, grains reveal a significant growth with grain sizes from 10 nm up to several microns in the temperature range between 500 - 1500°C. Especially for nanocrystalline thin films, these ripening processes have to be carefully considered for the interpretation of conductivity measurements.

D6.09

Correlation between Mobile Oxygen Ion Distances and Characteristic Length Scales for $La_{2-x}Er_xMo_2O_9$ Type Oxide Ion Conductor Tanmoy Paul and Aswini Ghosh; Solid State Physics, Indian Association for the Cultivation of Science, Kolkata, India.

The Composition dependence of oxide ion conductivity is determined for $La_{2-x}Er_xMo_2O_9$ by analyzing complex impedance data. Ac conductivity spectra show frequency independent behavior at low frequencies and at high frequencies show dispersion. The dispersive behavior at high frequencies indiactes the non-random hopping of oxygen ions. We have found the time-dependent mean-square displacement ($\sqrt{\langle R^2(t)\rangle}$) by analyzing the electrical data. A crossover from sub-diffusive to diffusive ion dynamics is observed at a characteristic time $t = t_p$ and in terms of spatial displacement is denoted as $\sqrt{\langle R^2(t_p)\rangle}$. It has been observed that $\sqrt{\langle R^2(t_p)\rangle}$ shows opposite behavior as that obtained for the ionic conductivity suggesting the interaction distance for forward-backward motion is not sufficient to explain the mechanism for ion conduction. We have estimated the values of static dielectric constant (ε_s) and high frequency dielectric constant (ε_∞) by analyzing the real part of dielectric spectra ($\varepsilon'(\omega)$) using Cole-Cole model. The spatial extent of the sub-diffusive motion ($\sqrt{\langle R'^2(\infty)\rangle}$) for all the compositions is also estimated from the $\varepsilon'(\omega)$ spectra. This is in favor with localized hop of mobile oxygens. The room temperature Rietveld refinement of X-ray patterns for all the samples confirms the cubic structure with space group $P2_13$. The composition dependence of mobile oxygen ion-ion (O2-O3) distances obtained after Rietveld refinement exhibits similar behavior as that obtained by $\sqrt{\langle R'^2(\infty)\rangle}$. The electron density contour plot confirms that the ion migration is favorable along (110) plane indicating localized the traps at the O2 and O3 sites. The overall analysis shows that the interionic coulomb interactions of mobile oxygen ions are responsible on the ion dynamics.

D6.10

Tuning the Defect Structure of $La_{0.5}Sr_{0.5}Co_{0.5}Mn_{0.5}O_{3-\delta}$ for Optimized Redox Behavior under Polarisation Conditions Celeste A. van den Bosch, George F. Harrington, Stephen J. Skinner and Ainara Aguadero; Department of Materials, Imperial College London, London, United Kingdom.

It is imperative to improve energy storage for renewable energy sources to become viable alternatives. Currently oxygen evolution and oxygen reduction are two key electrochemical reactions which limit the efficiency of energy storage devices. Hence, improving these reactions would greatly benefit the development of a renewable energy economy.

It has previously been demonstrated that the perovskite $La_{0.5}Sr_{0.5}Co_{0.5}Mn_{0.5}O_{3-\delta}$ (LSCM) can reversibly accommodate both a fully oxidised phase ($\delta = 0$) and reduced phase ($\delta = 0.62$), making this the most hypo-stoichiometric simple perovskite reported to date.[1] The oxygen vacancies introduced as a result of the variable stoichiometry as well as the potential range of transition metal oxidation states make LSCM an ideal candidate to investigate as a redox mediator for oxygen reduction and evolution reactions.

The ability to tune and control the defect structure of this system will allow optimisation of the electrochemical behaviour. With this is mind, LSCM thin films of 20 – 75 nm thick have been prepared by pulsed laser deposition with initial x-ray diffraction results indicating a change in lattice structure depending on the substrate the films are deposited on, likely due to strain effects [2].

Since surface characteristics are fundamental factors that govern the activity of these materials, further characterisation of the films included low energy ion scattering (LEIS) to consider segregation effects [3], atomic force microscopy and x-ray photoelectron spectroscopy to determine changes in transition metal oxidation state. The redox activity of LSCM under different polarisation conditions has been investigated with isotopic labelling through secondary ion mass spectroscopy [4].

A systematic study of the $La_{0.5}Sr_{0.5}Co_{0.5}Mn_{0.5}O_{3-\delta}$ thin films has shown that the cell parameters of LSCM can be controlled by growing thin films on different substrates. The LEIS measurement revealed that the induced strain may be affecting the surface termination which is expected to be instrumental in optimising the electrochemical behaviour of the perovskite.

[1] A. Aguadero, et. al., Angew. Chem. Int. Ed. Engl., 2011, 50, 6557–61.
[2] M. Kubicek, et. al., ACS Nano, 2013, 7, 3276–86.
[3] J. Druce, et. al., Solid State Ionics, 2014, 262, 893–896.
[4] J. A. Kilner, et. al., J. Solid State Electrochem., 2011, 15, 861–876.

D6.11

Defect Chemistry and Diffusion in $Cu_2ZnSnSe_4$ and Cu_2ZnSnS_4 Thin Films Steven Harvey, Glenn Teeter and Ingrid Repins; National Renewable Energy Laboratory, Golden, Colorado, United States.

Thin-film $Cu_2ZnSn(S,Se)_4$ (CZTSSe) is a promising absorber material for low-cost photovoltaic applications capable of terawatt-level per year production due to the relative abundance of all the component elements when compared to other thin-film photovoltaic applications. The highest-reported cell efficiency to date is over 12.5% [1]. We will discuss several novel methods that were developed to extract the activation energy of diffusion for both cations and anions in CZTSSe materials.

Diffusion of Se through the CZTSe layer results in conversion of the Mo back-contact layer to $MoSe_2$, increasing the sheet resistance of the film stack. An activation energy of 0.5 eV has been measured for Se diffusion in CZTSe by monitoring the rate of $MoSe_2$ formation as a function of annealing temperature. Our data suggest that the chalcogen diffusion in polycrystalline CZTSe materials is dominated by grain-boundary diffusion. The partial-pressure-dependent data also suggest that chalcogen vacancies are not the defect-controlling grain-boundary diffusion in these materials [2].

Cation diffusion in CZTS was investigated via *in situ* electrical measurements during film growth by elemental co-evaporation at elevated temperatures. In these experiments, CZTS sheet resistance was monitored during film growth, and transients in the resistance were observed when film growth was temporarily arrested. We interpret these transients as arising from re-equilibration of cation species associated with variations in chemical potential during the growth process. By monitoring the equilibration times of the resistivity at various processing temperatures, we have extracted an activation energy for cation diffusion of 2.0 eV. For both techniques, we will discuss fundamental connections between the results and the overall defect chemistry within CZTS and CZTSe.

[1] W. Wang, M.T. Winkler, O. Gunawan, T. Gokmen, T.K. Todorov, Y. Zhu, and D.B. Mitzi, Advanced Energy Materials 4(7)1301465 (2014). DOI: 10.1002/aenm.201301465
[2] S.P. Harvey, I. Repins, and G. Teeter, Defect chemistry and chalcogen diffusion in thin-film $Cu_2ZnSnSe_4$ materials, Journal of Applied Physics, Jan 2015 (accepted manuscript JR14-8925), DOI: 10.1063/1.4907951.

D6.12

Ionic Conductivity Modification in Nanoscale Proton-Conducting Oxide Heterostructures Prepared by Pulsed Laser Deposition Stefan B. Nikodemski[1], Daniel Clark[1], Jianhua Tong[1], Ryan O'Hayre[1], Philip Parilla[2], David Ginley[2] and Joseph Berry[2]; [1]Metallurgical and Materials Engineering, Colorado School of Mines, Golden, Colorado, United States; [2]National Renewable Energy Laboratory, Golden, Colorado, United States.

Planar multilayer stacks and interpenetrating nanoparticle composites based on combinations of proton-conducting ceramics (e.g. $BaCe_{0.6}Zr_{0.3}Y_{0.1}O_{2.95}$, BCZY) with other oxides (e.g. $SrTiO_3$, STO) as well as H_2 permeable metals (e.g. Pd) were fabricated by using the pulsed laser deposition (PLD) technique and the conductivities for these well-defined heterostructures were measured via electrochemical impedance spectroscopy (EIS). Pure PLD-deposited BCZY thin films showed better conductivity than pellets of the same composition, which is likely a result of fewer grain boundaries due to film texturing from single crystal substrates. Both metal/oxide (Pd/BCZY) and oxide/oxide (STO/BCZY) heterostructures were prepared after extensive optimization of the PLD deposition conditions. The deposition of oxide/oxide heterostructures was optimal at intermediate temperatures (sufficient to promote crystallization but low enough to limit layer inter-diffusion) especially in the case of ultrathin film superlattices. The conductivity of the BCZY/STO multilayer structure was measured to be lower than the BCZY and STO controls in both UHP Ar and in 5%H_2. EIS results for the multilayer structure deliberately prepared at higher temperatures to induce inter-diffusion also showed lower total conductivity than their individual counterparts despite the anticipated contribution of additional electronic carriers from a doping effect. EIS analysis concluded that Pd/BCZY nanocomposites also have a lower conductivity than the pure BCZY film, which is consistent with some previous reports of nanocomposites. The sharp decrease in the proton conductivity can be ascribed to positive space charge layer repulsion surrounding metallic particles in a ceramic matrix. We are currently investigating this possibility as well as the prospect of a contamination phase from the PLD process. In this regard, atom probe topography (APT) was employed to probe the Pd/BCZY interface to look for non-conducting undesirable phases.

D6.13

Investigating the Origins of Modified Transport Properties of YSZ in Confined Systems George Harrington[1, 2, 3], Andrea Cavallaro[3], Tobias M. Huber[1, 2], Harry L. Tuller [2, 4], Bilge Yildiz[5, 2], Kazunari Sasaki[6, 1], David W. McComb[7, 3], Stephen J. Skinner[3] and John A. Kilner[3]; [1]Next-Generation Fuel Cell Research Centre, Kyushu University, Fukuoka, Japan;[2]Department of Materials, Massachusetts Institute of Technology, Cambridge, Massachusetts, United States; [3]Department of Materials, Imperial College London, London, United Kingdom;[4]International Institute for Carbon Neutral Energy Research, Kyushu University, Fukuoka, Japan; [5]Lab. for Electrochemical Interfaces, Massachusetts Institute of Technology, Cambridge, Massachusetts, United States; [6]Department of Mechanical Engineering, Kyushu University, Fukuoka, Japan; [7]Department of Materials Science and Engineering, The Ohio State University, Columbus, Ohio, United States.

Chemo-mechanical engineering has huge potential for ionic transport in solid systems. This approach may be particularly rewarding when combined with the ability to tune conduction mechanisms on the nanoscale (nano-ionics) to produce unprecedented material properties. To this end, yttria-stabilised zirconia (YSZ) has been intensively investigated both experimentally [1] and computationally [2]. Studies of YSZ in confined systems have led to reports of both extreme enhancements [3] and modest reductions [4] in the transport properties. Lattice strain, either at an interface or surrounding a dislocation core has repeatedly been attributed to higher conductivity, but firm evidence of these effects remains neither conclusive nor reproducible. In this study we have investigated the effects of both residual and interfacial lattice strain as well as that caused by dislocations.

We have grown highly textured 8 mol.% YSZ films by pulsed laser deposition (PLD), on to MgO, sapphire, LAO, and NGO substrates, corresponding to a range of lattice mismatches from 4.5% tensile to 18% compressive. From x-ray diffraction (XRD) measurements we observe dramatic changes in the lattice parameters corresponding to strains of up to 2.5% over that of bulk sintered powders. Combining electrochemical impedance spectroscopy (EIS) and isotope exchange tracer diffusion (IETD), we can unambiguously and accurately assess the oxygen ion conductivity in the films. Surprisingly we find the ionic transport to be independent of the lattice parameter despite such a large modulation in the strain in the films. Detailed analysis of the microstructure by high-resolution transmission electron microscopy (HR-TEM) reveals that the transport is most likely dominated by grain boundary conduction, and instead thickness sensitive changes in the films conductivity can be attributed to a heterogeneous distribution of grain sizes. In addition we find no enhancement in the films due to the high density of misfit dislocations at the interfaces. We have employed high resolution scanning transmission electron microscopy (HR-STEM) and energy-dispersive X-ray spectroscopy (EDX) mapping to evaluate their chemical and structural properties. Finally the implications for chemo-mechanical engineering in confined systems will be discussed.

References

[1] Korte, C., et al., Physical Chemistry Chemical Physics, 2014. **16**(44): p. 24575-24591.
[2] Yildiz, B., MRS Bulletin, 2014. 39(02): p. 147-156.
[3] Sillassen, M., et al., Advanced Functional Materials, 2010. 20(13): p. 2071-2076.
[4] Gerstl, M., et al., Physical Chemistry Chemical Physics, 2013. 15: p. 1097 - 1107.

D6.14

Understanding Proton Conductivity within Porous Organic Cage Networks Scott Lewis, Ming Liu, Linjiang Chen, Iain Aldous, Marc Little, Samantha Chong, Laurence Hardwick and Andrew I. Cooper; Chemistry, University of Liverpool, Liverpool, United Kingdom.

Organic molecular cage salts containing protonated secondary amine groups show promise as proton conducting electrolytes due to their high water uptake, intrinsic porosity and appreciable ionic conductivity. Herein we report the proton conductivity of reduced amine cage salts with conductivities in the range 10^{-3}-10^{-2} S cm^{-1}, at temperatures up to 80°C. These cages are formed from reversible imine bond formation and packing of discrete, rigid cage molecules results in a defined microporous structure [1, 2]. Proton conductivity was investigated using the 2-probe AC method of impedance spectroscopy under varying humidity and temperature for various cage systems. The determined activation energies of ca. 0.3 eV indicate a mixed Grotthuss and vehicular method of proton transport and suggest high intrinsic proton transport for some cage materials. Proton transference number was measured to be 0.71 via chronoamperometry using an H-cell containing equimolar concentrations of acidic and basic media, indicated that the counter ion was not the major charge carrying species. Comprehensive simulation studies and structural characterisation using powder XRD, solid state NMR and water uptake measurements suggests that water molecules form clusters within the voids of the charged cage cations and as a result, become polarised which facilitates proton transport. Both molecular dynamic simulation and transference number studies suggest that the anionic moieties investigated (for example Cl^- and SO_4^{2-}) are too large to be mobile and remain fixed around each cage cation.

1. Hasell, T. *et al.* Triply interlocked covalent organic cages. *Nat. Chem.* **2,** 750–5 (2010).
2. Tozawa, T. *et al.* Porous organic cages. *Nat. Mater.* **8,** 973–8 (2009).

D6.15

Highly-Conductive Nanomaterials Based on Li_2O–FeO–V_2O_5–P_2O_5 Glasses Tomasz K. Pietrzak, Jerzy E. Garbarczyk, Marek Wasiucionek, Jan L. Nowinski and Przemyslaw P. Michalski; Physics, Warsaw University of Technology, Warszawa, Poland.

Many potential cathode materials for lithium and sodium ion batteries have poor electric conductivity. This deficiency has usually been circumvented by addition of various forms of carbon. It is however possible to increase the conductivity to the acceptable level without use of any carbon additive – e.g. by thermal nanocrystallization of glassy analogs of selected cathode materials.

In this research, we have synthesized glasses of the Li_2O–FeO–V_2O_5–P_2O_5 system, with the formula $LiFe_{1-5x/2}V_xPO_4$ ($0.08 \leq x \leq 0.20$), corresponding to $LiFePO_4$ with a small fraction of iron replaced by vanadium. It was found out that thermal treatment of these glasses up to temperature between 460 to 500°C (optimized for each composition separately) led to: i) a giant and irreversible increase in conductivity at room temperature by a factor of up to 10^9 and ii) a change in the microstructure from purely amorphous to nanocrystalline (for samples with lower vanadium contents) or polycrystalline (for a sample with higher vanadium content).
STEM and HRTEM microscopy studies showed that in the materials with lower vanadium content (exhibiting electric conductivity (at RT) of up to 10^{-2} S/cm) the heat treatment had led to a formation of very small (ca 10 nm) crystallites densely distributed inside the glassy matrices. The observed correlation between the improvement of the electrical properties and a change of microstructure induced by heat-treatment was attributed to a substantial role of the interfacial regions in the electrical conduction. These strongly disordered regions contain an increased concentration of transition metal aliovalent ions, which can provide multiple channels for electronic hopping between: Fe^{2+} and Fe^{3+}, V^{4+} and V^{5+}, or V^{3+} and V^{4+} centers.

Diffractometry (XRD) and differential thermal analysis (DTA) were performed to provide with supplementary information. This work has been financed by National Science Centre: project OPUS–4 no. DEC–2012/07/B/ST5/03184 (2013–2016).

D6.16

The Mixed Alkali Effect in $(Li_{1-x}A_x)_2Si_2O_5$ (A = K, Rb) Glasses Melissa Novy, Sabyasachi Sen and Sangtae Kim; Materials Science and Engineering, UC Davis, Davis, California, United States.

In mixed-alkali oxide glasses, evidence suggests that each type of alkali ion is associated with characteristic charge compensating sites that form a pathway for ionic migration through the matrix. More energy is required for an ion of one type to move into a site associated with a different ion, as the site must relax to accommodate the mismatched ion. An example is the mixed alkali effect, which refers to the minimum in dc conductivity observed in glasses containing an approximately equal ratio of two different alkali ions compared to glasses with just one type of alkali ion. The minimum becomes more pronounced with decreasing temperature and increasing site mismatch between ions. The ac conductivity of these glasses displays a power law frequency dependence, where the exponent $n < 1$ has been related to the dimensionality of the conducting pathways. In this study, the frequency- and temperature-dependent ionic conductivity of annealed $(Li_{1-x}K_x)_2Si_2O_5$ and $(Li_{1-x}Rb_x)_2Si_2O_5$ glasses was measured using impedance spectroscopy in the frequency range of 0.1 - 10^7 Hz at different temperatures (100 - 300°C). The dc conductivity decreases by three orders of magnitude in the $(Li_{0.5}K_{0.5})_2Si_2O_5$ glass and the value of *n* decreases from about 0.7 in the single-alkali glasses to 0.6. Consistent with the above interpretation of *n*, we believe that the decrease to a dimensionality of about 2.5 in the mixed alkali compositions was a result of blocking of the conducting pathways of Li by charge compensating sites of K or Rb, and vice versa. The deeper minima in dc conductivity and values of *n* in the Li-Rb system compared to the Li-K system were attributed to the larger site mismatch between Li and Rb.

D6.17

Reduction of the Grain Boundary Resistance in Yttria Stabilized Zirconia Thin Films: Incorporation of Mg^{2+} from the Substrate Edmund M. Mills[1], Matthias Kleine-Boymann[2], Juergen Janek[2], Hao Yang[1], Nigel Browning[3], Yayoi Takamura[1] and Sangtae Kim[1]; [1]CHMS, UC Davis, Davis, California, United States; [2]Institute of Physical Chemistry, Justus-Liebig University Geissen, Geissen, Germany; [3]Pacific Northwest National Laboratory, Richland, Washington, United States.

To improve the performance of SOFCs, electrolyte materials with higher ionic conductivity must be developed. The enhancements obtained by doping known electrolytes have reached their upper limit, so in recent years research has turned to the use of interfaces to enhance ionic conductivity. Interfaces, including grain boundaries, those in composite materials, and thin film hetero-interfaces, have different structural, chemical, and electrical environments than a material's bulk, leading to differences in conductivity—the ionic conductivity of electrolyte thin films may be enhanced by multiple orders of magnitude. However, the influences of structural, chemical, and electrical factors on the ionic conductivity have not been fully untangled. We have deposited nano-crystalline thin films of yttria-stabilized zirconia on MgO substrates using pulsed laser deposition, and characterized them with impedance spectroscopy, X-ray diffraction, high-resolution transmission electron microscopy, and secondary-ion mass spectrometry. We demonstrate the presence of a highly conductive layer near film-substrate interface. This enhancement is linked to diffusion of Mg^{2+} from the substrate into the YSZ film's grain boundaries, reducing their resistance and increasing the measured conductivity. This work presents an example of the complex interactions of different interfaces and their effect on ionic conductivity, something necessary to consider in the design of materials and devices with enhanced ionic conductivity through the incorporation of interfaces.

D6.18

Ionic Conductivity of β-eucryptite Doped with Mg Yachao Chen and Ivar E. Reimanis; Colorado School of Mines, Golden, Colorado, United States.

Lithium aluminum silicates such as β-eucryptite ($LiAlSiO_4$) are well-suited for thermal shock resistant structures, precision optics platforms, and various other applications where low or negative coefficient of thermal expansion (CTE) is required. Particularly, β-eucryptite has potential use in many of these applications because it exhibits an average negative CTE. When β-eucryptite is doped with small amounts of Zn (as low as 0.1 molar percent), the CTE increases significantly, and the tendency of microcracking decreases greatly compared with pure β-eucryptite. The present study explores the reasons Zn influences the CTE so dramatically and also extends the work to Mg doped β-eucryptite. In-situ high temperature X-ray diffraction tests are performed on pure and Mg doped β-eucryptite synthesized from chemical precursors. And the temperature dependence of ionic conductivity of β-eucryptite is measured for doped and un-doped samples to explain Mg occupation in the structure.

D6.19

Analysis of Grain Boundary Conductivity of Ionic Oxides at Elevated Temperature: Doped CeO_2 and Bi_2O_3 – a Case Study NoWoo Kwak and WooChul Jung; Material Science & Engineering, Korea Advanced Institute of Science and Technology (KAIST), Daejeon, Korea (the Republic of).

Doped CeO_2 and Bi_2O_3 have gained a lot of attention as a solid electrolyte material for intermediate-temperature solid oxide fuel cells (IT-SOFCs) due to their superior oxygen ion conductivity at relatively reduced temperature (500 – 700°C). Typical solid electrolytes are largely polycrystalline, and it is common for grain boundaries to block the motion of the mobile oxygen vacancies as they migrate from one grain to the next. Accordingly, it is of significance to precisely measure the grain boundary conductivities of fast ion conducting oxides, particularly at temperature of relevance (500 – 700°C). AC impedance spectroscopy (ACIS) is a useful tool to deconvolute the contributions of bulk (grain interior) and grain boundary on the total ionic conductivity by examining the electrical response function in the frequency domain, since each of them typically has different characteristic frequencies. However, the corresponding frequencies of bulk and grain boundary responses in doped CeO_2 and Bi_2O_3 generally increase with temperature, often going beyond the instrument frequency limit, when a typical symmetric sample with metallic electrode on both sides of a polycrystalline oxide pellet is used. Therefore, it is difficult to measure the grain boundary conductivity at elevated temperature (> 400°C).

To address these issues, we perform a quantitative analysis of transport properties of thin films as a function of a choice of substrates and a film thickness. In order to precisely extract the grain boundary contribution out of the total conductivity at the elevated temperature, both epitaxial and polycrystalline thin films of doped CeO_2 and Bi_2O_3 are grown via pulsed layer deposition. Electrical conductivities were investigated by ACIS under controlled temperature and pO_2. Under a basis of space charge theory, the impact of grain boundary and substrate on the ionic transport properties of those ionic oxides will be discussed.

D6.20

Interfacial Ionic Conductivity in Epitaxial $Y_2Zr_2O_7$ Thin Films Elisa Gilardi[1], Giuliano Gregori[1], Yi Wang[2], Wilfried Sigle[2], Peter A. van Aken[2] and Joachim Maier[1]; [1]Physical Chemistry of Solids, Max Planck Institute for Solid State Research, Stuttgart, Germany; [2]Stuttgart Center for Electron Microscopy, Max Planck Institute for Intelligent System, Stuttgart, Germany.

Thin films of mixed and ionic conducting oxides have attracted much interest because (i) they can be used in micro solid oxide fuel cells (SOFC) and (ii) they are excellent model systems to study effects not easily accessible in ceramics (e.g. strain or space charge).
Here, we investigate defective fluorites with the chemical formula $A_2B_2O_7$, which have been already considered as possible electrolyte in SOFC because of their ionic conductivity and high chemical stability.
Specifically, thin films of the model system $Y_2Zr_2O_7$ grown on different substrates (Al_2O_3 and MgO) by pulsed laser deposition have been characterized by impedance spectroscopy together with XRD, pole figures and AFM. A careful characterization of the film/substrate interface has been carried out by high-resolution scanning transmission electron microscopy (STEM), energy dispersive x-ray (EDX) and electron energy loss spectroscopy (EELS). Remarkably, films grown on different substrates and thus having different microstructures exhibit very similar electrical properties (ionic conductivity owing to oxygen vacancies migration), indicating that grain boundaries only slightly affect the electrical transport properties.

Moreover, epitaxial thin films with different thicknesses grown on MgO (110), measured between 400°C and 700°C, exhibit significant film/substrate interface effects resulting in an enhanced ionic conductivity near the interface. Quite interestingly, high resolution STEM analysis reveals a high density of misfit dislocations at the interface, which are required to release the compressive strain deriving from the large lattice mismatch (-23%) between the film and the substrate. Moreover, the STEM analysis indicated that the density of misfit dislocations is decreased when the film is exposed to high temperature for an extended period of time. The role of the microstructure, particularly of the dislocations, local cationic intermixing, strain and space charge effects on the enhanced ionic transport at the interface is discussed. We also present results on PLD grown $Y_2Zr_2O_7$/8YSZ heterostructures.

D6.21

Nanocomposite Ceramics Based on $Ce_{0.9}Gd_{0.1}O_{1.95}$ and MgO Jens Zosel[1], Vladimir Vashook[1], Evgeni Sperling[2], Kristina Ahlborn[1], Frank Gerlach[1], Wolfgang Fichtner[1], Matthias Schelter[1], Ulrich Guth[1, 2] and Michael Mertig[1]; [1]Kurt-Schwabe-Institut für Mess- und Sensortechnik e.V. Meinsberg, Waldheim, Germany; [2]Chemistry, Dresden University of Technology, Dresden, Germany.

Introduction
Grain boundaries of single-phase solid electrolyte ceramics are usually less conductive in comparison with grain volumes (bulk). Another situation can appear in composite materials consisting of solid electrolytes (SE) and dielectric phases (insulators, Ins). The SE/Ins grain boundaries can exhibit higher conductivities compared to the bulk of the solid

electrolyte grains in composites where the epitaxial connecting zone between SE and Ins is characterized with certain structures containing irregularities and additional defects [1]. In this study nanocomposite powders based on MgO nanopowder as the insulator phase and $Ce_{0.9}Gd_{0.1}O_{1.95}$ (GDC) nanopowders as the solid electrolyte phase have been prepared and investigated with respect to microstructure and electrical conductivity.

Experimental
GDC nanopowders have been synthesized by a glycine-citrate–nitrate auto-combustion method as described in [2]. Three different methods were used to mix the synthesized GDC nanopowders with MgO nanopowder based on milling, ultrasonic mixing and direct composite formation during modified autocombustion process. The composites were characterized by SEM, XRD and TEM and pressed then into rectangular bars and investigated by electrochemical impedance spectroscopy in atmospheres with different oxygen partial pressures.

Results and Discussion
The most homogeneous and dispersive distribution of nanocomposite powders was achieved by adding $Mg(NO_3)_2$ directly to the auto combustion process. The SEM results proof that this nanocomposite exhibits a minimum size of the Mg-containing grains (100-300 nm) and the most disperse distribution of components. TEM-images reveal that the thickness of the interphase layers of composites ranges between 2.5-7.5 nm.
The conductivity curves show that between the GDC and MgO phases a specific grain boundary layer with enhanced conductivity is formed by using the synthesis method described above, which might correspond to double peaks found in the XRD patterns of that material.
The results indicate possibilities to form highly conductive grain boundaries in CeO_2-based SE/Ins composites also by classical synthesis routes which can result in total conductivities that are significantly higher than that of single phase SE, if the grain boundaries form a network.

Conclusions
Apparently, a grain boundaries network between a solid electrolyte (GDC in this work) and an insulator (MgO) can be formed at nanometer scale by well-established autocombustion synthesis route if the GDC/MgO ratio and mixing homogeneity of the composite powders are optimized. This network enables significantly higher grain boundary conductivities than the single phase materials.

References
[1] H. Mehrer, Springer Series in Solid-State Sciences, Vol. 155 (2007) XIX, 654
[2] S. Banerjee et al., Adv. Funct. Mater. 2007, 17, 2847–2854

D6.22
Reduction Stages of Ni-doped Polycrystalline YSZ Amy Morrissey[1], James R. O'Brien[2], Jianhua Tong[1] and Ivar E. Reimanis[1]; [1]Colorado School of Mines, Golden, Colorado, United States; [2]Off Grid Research, San Diego, California, United States.

A small amount of Ni-dopant below the solid solution limit (< 2 molar percent) in yttria-stabilized zirconia (YSZ) aids densification by lowering the sintering temperature and time. In hydrogen environments, the Ni^{2+} ions can reduce to metallic Ni^0 particles on surfaces, grain boundaries, and in grain interiors. The present work examines the stages of reduction and the relative importance of surfaces and grain boundaries in dictating the resulting microstructure. A chemical synthesis technique was used to prepare high purity 0.5 molar percent Ni-doped 10YSZ pellets. A dedicated furnace was fabricated to control temperature, oxygen partial pressure, and relative humidity during reduction. The extent of reaction was measured optically and with SQUID magnetometry. The DC magnetic susceptibility quantifies the amount of Ni^{2+} reduced to metallic Ni^0 and the AC magnetic susceptibility quantifies various metallic Ni^0particles sizes. Microstructural characterization of as-sintered pellets using transmission electron microscopy and atom probe tomography show Ni^{2+} ions are randomly distributed in the microstructure before reduction. Upon reduction, the reaction occurs in three stages: 1) up to 10 h, surface reduction ocurrs, leading to coarse 200-400 nm metallic Ni^0 particles in pores, 2) up to 50 h, fine 5-10 nm metallic Ni^0 particles form along grain boundaries and coarsen, and 3) for longer times, internal reduction leads to the formation of very fine Ni^0 in the grain interiors. Redox studies revealed that the microstructure development during reduction is irreversible. A model is developed to describe the stages of reduction in polycrystalline materials.

D6.23
Electrical and Oxide Ionic Conductivity in Metal Disparsed Pr_2NiO_4-Based Oxides Junji Hyodo[1, 2], Shintaro Ida[1, 2] and Tatsumi Ishihara[1, 2]; [1]Applied Chemistry, Kyushu University, Fukuoka, Japan; [2]International Institute for Carbon Neutral Energy Research (I2CNER), Fukuoka, Japan.

Nano size effects on ionic conductors are focused, recently. Most reports on strain effects are on the effect of bi-axial strain in epitaxial thin film. This bi-axial strain makes it difficult to understand the effect of strain because strain relaxes out-of-plane direction. Further, the detail analyses for thin film, such as oxygen non-stoichiometry, are also difficult. Therefore, we tried to induce the strain into bulk materials by dispersing the metal particles, which could induce the strain around the metal particles due to the different thermal expansion properties. In this study, the electrical conductivity and oxide ionic conductivity in strained $Pr_2Ni_{0.71}Cu_{0.24}Ga_{0.05}O_{4+\delta}$(PNCG) with metal particle was measured. In addition, detail analysis on oxygen non-stoichiometry and lattice defect were also performed. XRD results indicated that tensile strain was induced into PNCG by dispersing Au metal particles. Observed conductivity improved with dispersing Au particles. In addition, oxygen partial pressure dependency decreased. To explain the reason for this phenomenon, oxygen non-stoichiometry was measured. The oxygen content increases with dispersing Au. To compensate the increased oxygen content, electron holes is introduced into PNCG resulting in the increased conductivity. Furthermore, P_{O2} dependency of oxygen non-stoichiometry also decreased. This suggests that introduced strain changes the oxygen nonstoichiometry. TEM observation suggests that larger strain is induced around dispersed Au particle. Local structure of oxygen around Au particle was studied with EELS spectra around Au particle. It was found that oxygen local structure was changed around Au particle and so strain induced by difference in thermal expansion induced change in interstitial oxygen amount resulting in the large change in electrical conductivity. Further detail study on oxygen exchange with tracer oxygen was studied with SIMS and it was found that diffusivity of oxygen was varied with dispersion of Au.

D6.24
Encroachment of Titanium Oxide on Ni Surface for Ni/TiO_2 under Reducing Atmosphere Fangfang Wang[1, 2], Haruo Kishimoto[1, 2], Katherine D. Bagarinao [1, 2], Katsuhiko Yamaji[1, 2], Teruhisa Horita[1, 2] and Harumi Yokokawa[3]; [1]National Institute of Advanced Industrial Science and Technology, Tsukuba, Japan; [2]CREST, JST, Kawaguchi, Japan; [3]The University of Tokyo, Tokyo, Japan.

Migration of the reduced metal oxide onto metal surface (Pt, Ni) has been reported for several decades, which is called as strong metal-support interaction (SMSI). However, this phenomenon usually occurs for the nanometer size noble metal particle supported on transition metal oxide. Transmission electron microscopy (TEM) result shows that just nanometer level reduced metal oxide layer is observed on the metal surface. Here, TiO_2 is one of typical oxide substrates to evaluate the SMSI effect. In our previous result, we firstly observed the titanium oxide encroachment on the Ni film with micrometer size supported on TiO_2 when the carbon deposition experimental was performed. In this work, Ni film with micrometer size was deposited on TiO_2 and these Ni/TiO_2 samples were annealed under different conditions. We investigated the effect of the annealing temperature and the oxygen partial pressure on the titanium oxide encroachment on Ni film and tried to find the suitable annealing condition to cause this behavior. Our results suggest that this titanium oxide encroachment on Ni film can occur even the micrometer size Ni film is used.

D6.25
Ionic Transport Properties of $NdBaInO_4$ Stephen Skinner, Yuning Zhou and Manyu Chen; Imperial College London, London, United Kingdom.

$NdBaInO_4$ has recently been identifed as a potential oxide ion conducting electrolyte [1] consisting of a layered crystal structure with InO_6 octahedra separated by (Nd,Ba)O units. DFT calcualtions combined with crystallographic measurements confirmed that this is a layered perovskite structure, rather than, as stoichiometry might suggest, a K_2NiF_4 structure. From these studies an ionic conduction pathway was visualised and consisted of pathways in the A-O layers between the InO6 octahedra. These phases were demonstrated to have total conductivity of 10^{-3} Scm^{-1} 1000ºC of which there was found to be a significant ionic component. In the pO_2 window of 10^{-20} - 10^{-6} atm an ionic domain was reported. These conductivity data were obtained from impedance measurements, with no direct measurement of the oxide ion transport. Additionally the scope to enhance the conductivity through substitution has not been explored, nor the suppression of the electronic components. In this presentation we will provide isotopic exchange data for the parent $NdBaInO_4$ phase over a range of temperatures, confirming the ionic transport of this material, and provide further data on the solubility limits of both A and B site dopants, and their effect on the total and ionic conductivity of this family of oxides.

[1] K. Fujii et al, Chem. Mater., 26 2488 2014

D6.26
Oxygen Transport Properties of Ca/W-Substituted Lanthanum Nickelate Peter V. Hendriksen and Simona Ovtar; Department of Energy Conversion and Storage, Technical University of Denmark, Roskilde, Denmark.

Lanthanum nickelates (LNO) are mixed oxygen-ionic and electronic conductors (MIECs) and candidate materials for the cathode of solid oxide fuel cells operating at intermediate temperature (IT-SOFC) and for oxygen permeation membranes. The advantage of LNO compared to the well-known $La_{1-x}Sr_xMnO_{3-d}$ is the thermal stability and the comparable thermal expansion coefficient to the mostly used electrolytes. La_2NiO_4 has a K_2NiF_4-type crystal structure, with the perovskite-like layers separated by rock-salt La_2O_2 layers. In contrast to perovskite MIECs the LNO has oxygen excess with oxygen anions in interstitial positions in the La_2O_2 layers of the structure which are charge compensated by p-type electronic charge carriers. Doping with the alkaline-earth cations decreases oxygen excess and ionic conductivity but increases the electronic conductivity.

Powders of lanthanum nickelates partially substituted with Ca on A side and/or W on B side were prepared by combustion synthesis. The gel was dried and fired at 300°C, and subsequently calcined at different temperature to achieve a single phase material. The calcined powders were pressed in rectangular bar shape and sintered at 1300°C for 10 h. The dense bars were ground and polished to certain size and used for the electrical conductivity measurements. Crystal structure of powders as well as bars were analyzed by x-ray diffraction and the microstructure of polished surface was investigated by scanning electron microscope. The oxygen transport properties of the samples were studied by electrical conductivity relaxation (ECR), which is a well-established method to determine the oxygen transport properties of MIECs; oxygen surface exchange coefficient (k_{ex}) and the chemical diffusion coefficient (D_{chem}). The conductivity of Ca and/or W substituted LNO is thermally activated and activation energies from 4 - 16 kJ/mol were measured for different substitutions. The highest conductivity of 68 S/cm at 500°C was measured for $La_{1.4}Ca_{0.6}Ni_{0.9}W_{0.1}O_{4+d}$.The total conductivity is decreasing with the pO_2, indicating that LNO is a p-type electronic conductor. However, the pO_2dependence of the conductivity for the Ca and Ca-W substituted LNO is very low. While, for the W substituted LNO ($La_2Ni_{0.9}W_{0.1}O_{4+d}$) much stronger dependence was observed and the oxygen transport properties were determined. At 500 °C and for pO_2 change from 0.2 to 0.1 bar the k_{ex} is $5x10^{-3}$ cm/s and D_{chem} is $5x10^{-3}$ cm^2/s, which is several times higher than observed for LNO doped with aluminum [1]. The electrical properties and strategies to achieve fast oxygen transport in substituted LNO as well as possible applications of the materials will be discussed.
[1] S.-Y. Jeon, J. Alloy. Comp. 589 (2014) 572

D6.27
Characterization of Solid Lithium Ceramic and Glass-Ceramic Nano-Thin Film Electrolytes Prepared by RF Magnetron Sputtering Erik Burton and Dale Teeters; Chemistry and Biochemistry, University of Tulsa, Tulsa, Oklahoma, United States.

All solid state lithium ion batteries are of great technological interest because of manufacturing and safety advantages. Solid materials with high electrochemical stability and high ionic conduction are needed for use as electrolyte materials. Fabrication of batteries with low internal resistance results in enhanced performance. Five ceramic and glass-ceramic materials ($Li_5La_3Ta_2O_{12}$, $Li_{0.33}La_{0.55}TiO_3$, $Li_{1.5}Al_{0.5}Ge_{1.5}P_3O_{12}$, $Li_{1.3}Al_{0.3}Ti_{1.7}P_3O_{12}$, and $Li_7La_3Zr_2O_{12}$), which have recently been shown in literature to have potential for solid electrolytes, have been studied. RF magnetron sputtering was used to form nanoscale thin layers of the electrolyte materials. These layers are similar to those that would be used in thin film, solid state batteries. AC impedance spectroscopy has been used to characterize these materials for their ionic conductivity. General morphology and the grain boundary structure of the bulk material and the surface have been analyzed using X-ray diffraction, atomic force microscopy and scanning electron microscopy. The effect of annealing on ion conduction was also investigated. These data will then be used to explain the differences in conductivities for the electrolytes. The potential for use in commercial battery systems will be evaluated and discussed.

D6.28
Characterisation of Electrochemical Transport Parameters in Multi-Ion Systems Truls Norby, Ragnar Strandbakke, Anna Evans and Shay A. Robinson; Department of Chemistry, University of Oslo, Oslo, Norway.

Solid and liquid electrolytes necessarily contain at least two types of ions (cations and anions) which generally respond simultaneously and indistinguishably in electrochemical driving forces. Hence, a molten Li salt (e.g. the carbonate or hydroxide) can well work in for instance fuel cells by transport of Li ions even if the electrodes at first sight seem irreversible with respect to Li redox chemistry. And cations move slowly but steadily in solid oxygen transport membranes, slowly degrading or decomposing the material.

However, with significant concentrations and conductivity of foreign ions, the situation becomes considerably more complex. Examples that we will discuss comprise protons in oxides and hydroxide or oxide ions in molten carbonates. Electronic conduction adds to the multitude. Some combinations of foreign and native ion and/or electron transport can be utilized in applications, but the scientific determination of transport becomes challenging. This is further troubled by the electrode or surface kinetics limitations of the individual ionic pathways. We will discuss approaches to determination of partial ionic volume conductivities by EMF-type transport number measurements and to characterization of electrodes using impedance spectroscopy in such cases.

D6.29
Dependence of Surface Defect Chemistry on Sr Concentration in $La_{1-x}Sr_xFeO_{3-\delta}$ Zixuan Guan; Applied Physics, Stanford University, Stanford, California, United States.

$La_{1-x}Sr_xFeO_{3-\delta}$ is employed as the air electrode in solid oxide fuel cells and electrolyzers, and is a model mixed ionic and electronic conductor. At elevated temperatures, subsurface Sr atoms tend to precipitate out as SrO_x phase, causing a decrease in the oxygen exchange rates[1]. Presently, the nature of surface Sr precipitates and subsurface Sr segregation remains elusive. We employed ambient pressure X-ray absorption and photoelectron spectroscopy to study the surface oxygen exchange present under conditions approaching that for solid-oxide fuel cells. Atomically-flat $La_{0.6}Sr_{0.4}FeO_{3-\delta}$ and $La_{0.8}Sr_{0.2}FeO_{3-\delta}$ on $SrTiO_3$(100) were fabricated by pulsed-laser deposition. We characterized the unoccupied electronic states of oxygen and iron characters[2], as well as the occupied valence band states. Additionally, we quantified the Sr species on the surface using core-level photoelectron spectroscopy. All measurements are sensitive to the first nanometer of the surface. By comparing thin films of different Sr doping level, we establish a surface defect chemical model. The equilibration of Sr species on the surface with bulk Sr vacancy and oxygen vacancy contributes to the redox reaction and affects the concentration of all ionic and electronic defects. Our result highlights the significance of Sr

on the surface defect chemistry in $La_{1-x}Sr_xFeO_{3-\delta}$, which likely extend to other transition-metal perovskite oxides as well.

Reference:
[1] Cai Z, Kubicek M, Fleig J, et al. Chemical Heterogeneities on $La_{0.6}Sr_{0.4}CoO_{3-\delta}$ Thin Films□ Correlations to Cathode Surface Activity and Stability. *Chemistry of Materials*, 2012, 24(6): 1116-1127.
[2] Mueller D N, Machala M L, Bluhm H, et al. Redox activity of surface oxygen anions in oxygen-deficient perovskite oxides during electrochemical reactions. *Nature communications*, 2015, 6.

D6.30

Glass Transition in Superprotonic Phase of Inorganic Solid Acid Haruyuki Takahashi, Yoshitaka Suzuki and Takashi Sakuma; Graduate School of Science and Engineering, Ibaraki University, Hitachi, Japan.

The structure and the dynamics in the superprotonic phase of the inorganic solid acid $Cs_2(HSO_4)(H_2PO_4)$ have been investigated. The $Cs_2(HSO_4)(H_2PO_4)$ shows the superprotonic conduction same as the CsH_2PO_4 at the transition to the cubic phase. The characteristic feature of the $Cs_2(HSO_4)(H_2PO_4)$ is that the high temperature superprotonic phase readily exists as a metastable state at room temperature. So the $Cs_2(HSO_4)(H_2PO_4)$ is considered to be a model material for investigating the superprotonic conduction mechanism in the inorganic solid acids. We have examined the XRD patterns, the thermal anomaly and the proton conductivity for the superprotonic phase of the $Cs_2(HSO_4)(H_2PO_4)$ in wide temperature range in order to elucidate the nature of the superprotonic conduction of the inorganic solid acids. New structure model for the cubic lattice of the superprotonic phase has been proposed. We have found that the superprotonic phase of the $Cs_2(HSO_4)(H_2PO_4)$ has a glass transition at 220K on the basis of the temperature dependence of the lattice constant, the thermal anomaly and the heating rate dependence of the transition temperature. Therefore it is considered that the superprotonic phase of the $Cs_2(HSO_4)(H_2PO_4)$ is a glassy crystal. The proton conductivity seems to obey the Arrhenius equation above room temperature, on the other hand, the conductivity decreases steeply like the Vogel-Tammann-Fulcher equation toward the glass transition temperature. It is clear that the observed conductivity reflects the proton conduction mechanism in the superprotonic phase. The proton motion freezes accompanied by the extinction of the reorientation of SO_4 and PO_4 tetrahedra at the glass transition. It is supposed that the transition from the normal crystal to the glassy crystal is essential for the superprotonic behavior in the inorganic solid acids.

D6.31

Unraveling the Origin of Surface Capacitance in Mixed Ion Electron Conducting Oxides Chirranjeevi Balaji Gopal, Albert Z. Feng and William Chueh; Materials Science and Engineering, Stanford University, Menlo Park, California, United States.

The fundamental thermodynamic property that underpins the application of mixed ion electron conducting (MIEC) oxides in electrochemical energy conversion devices is the oxygen nonstoichiometry variation with temperature and oxygen partial pressure. The nonstoichiometry of thin film MIECs cannot be determined by conventional thermogravimetric and coulometric titration methods due to their small mass. It can be, however, determined by AC impedance spectroscopy (ACIS) by measuring the chemical capacitance. This technique has been shown to be successful for the case of undoped and Sm, Pr doped ceria. In undoped ceria, the chemical capacitance scales with the volume of the thin film, as would be expected. However, in the case of doped ceria, there is an additional contribution which scales with the surface area, labelled as “surface capacitance”. The origin of this surface capacitance is not yet clear.

In this study, we aim to understand the origins of surface capacitance and its relationship to surface defect chemistry in undoped and doped ceria. While bulk defect chemistry of both systems are well established, their surface defect chemistry have only recently been studied and found to differ markedly from the bulk. Using ACIS to obtain the capacitance and ambient pressure X-ray photoelectron spectroscopy to quantify the surface and bulk concentrations of small polarons and oxygen vacancies, we demonstrate that the surface capacitance arises from variation of surface oxygen nonstoichiometry with oxygen chemical potential, i.e., from surface chemical capacitance.

D6.32

Disorder and Ionic Transport in Pyrochlore/Defect Fluorite Oxides Cortney Kreller[1], James Valdez[2], Terry Holesinger[1], Yongqiang Wang[2] and Blas Uberuaga[2]; [1]Materials Physics and Applications, Los Alamos National Laboratory, Los Alamos, New Mexico, United States; [2]Materials Science in Radiation and Dynamics Extremes, Los Alamos National Laboratory, Los Alamos, New Mexico, United States.

Numerous avenues are currently being explored to enhance ionic conductivity in solid oxide materials including dopants, nano-structuring, and strain engineering. Their effect on material properties, specifically mobile carrier concentration and mobility, needs to be understood and ultimately exploited to develop advanced functional materials. In this work, we seek to explore the relationship between intrinsic disorder and oxygen ion conduction. The pyrochlore compounds, $A_2B_2O_7$, consist of both ordered cation and anion sublattices. The introduction of anti-site disorder, where the A and B cations switch positions, is accompanied by increasing disorder on the anion sublattice, and complete randomization of the A- and B-site cations results in the defect fluorite phase. Several workers have previously studied the influence of structural disorder on ionic conductivity by introducing disorder through dopants, temperature or pressure. In the present work, we are using irradiation as a tool to introduce, and control the extent of, structural disorder in pyrochlore oxides. We have chosen to investigate the end members of the $Gd_2(Zr_xTi_{1-x})_2O_7$ system as $Gd_2Zr_2O_7$ is an intrinsic fast-ion conductor that is also very rad tolerant whereas $Gd_2Ti_2O_7$ is a comparatively poor ionic conductor that is much more susceptible to amorphization under irradiation than the zirconates. Electrochemical Impedance spectroscopy is used to measure the conductivity of materials with varying degrees of structural disorder in order to better understand how the underlying transport mechanisms depend on crystalline disorder.

D6.33

Correlating Conductivity and Composition of $Ca_xCe_{1-x}O_{2-\delta}$ Grain Boundaries via Aberration-Corrected Transmission Electron Microscopy William J. Bowman, Kimberly McGuinness, Cruz A. Hernandez and Peter A. Crozier; Materials Science and Engineering, Arizona State University, Tempe, Arizona, United States.

High grain boundary resistivity relative to grain interiors is believed to result from an intrinsic space charge potential barrier emanating from boundary cores several nanometers into grains, creating regions of charge carrier depletion [1,2]. The barrier’s magnitude, and thus the width of the space charge zone are thought to be closely related to the atomic structure and elemental composition within nanometers of the boundary core. However, it is well known that there is significant diversity in the interfacial atomic structure of grain boundaries in a given material, and recent electron-energy loss spectroscopy (EELS) in an aberration-corrected scanning transmission electron microscope (AC-STEM) by our group suggest that there is also considerable variation in boundary core composition. Here, we employ AC-STEM imaging and nanospectroscopy to quantify elemental composition of boundaries in a series of Ca-doped cerias, and correlate findings with grain interior and boundary electrical conductivity determined via AC impedance spectroscopy.

Atomic resolution STEM images were correlated with core-loss EELS to characterize electronic structure and to quantify local composition of grain boundaries. Bulk polycrystalline samples were fabricated from which electrical conductivity data and TEM specimens could be extracted. EELS acquired at boundary cores indicated that Ca concentration was typically greater than twice that of the grain interior. 2D elemental maps derived from EELS spectrum images illustrate very variability in ionic concentration in the vicinity of boundaries. The Ce-$M_{4,5}$ EELS fine structure signal varied within several nanometers of boundary cores, indicating reduction of Ce^{4+} to Ce^{3+}. The O-K fine structure also contained features indicative of the presence of oxygen vacancies in and around boundary cores. Electronic structure data, quantification of ion concentrations, and correlation with boundary electrical conductivity will be discussed.

1. X. Guo et al. *Electrochem. Soc.*, **148** (3) E121-E126 (2001)
2. W.J. Bowman et al. *Solid State Ionics*, **272** 9-17 (2015)

D6.34
Dynamic Pulse Isotopic Exchange for Assessing Oxygen Transport Kinetics Prasna S. Ray, Brian Ray, Guangru Zhang, Evangelos I. Papaioannou and Ian S. Metcalfe; Chemical Engineering and Advanced Materials, Newcastle University, Newcastle-upon-Tyne, United Kingdom.

The efficiency of systems employing solid oxide conductors, for example in oxygen storage capacity materials in chemical looping for hydrogen production or solid oxide fuel cell components, will depend on the kinetics of oxygen transport. Transport kinetics can be assessed by using isotopically-labelled oxygen. Isotopic exchange depth profiling determines the surface exchange coefficient and bulk tracer diffusion coefficient[1]; however, the technique is not in-situ because it requires quenching samples from elevated temperatures and destroys the sample during secondary ion mass spectroscopy. An alternative is pulse isotopic exchange (PIE) which determines the rate of surface exchange from pulsing $^{18}O_2$ into a $^{16}O_2$ gas-stream with which the cathode material is in equilibrium[2]. The rate of surface exchange is extracted from the distribution of gas-phase oxygen isotopologues and can further be dissociated into the rates of surface processes of adsorption and incorporation into the bulk. However, the prior PIE experiments reported in the literature do not evaluate the kinetics of bulk processes, nor investigate kinetics under dynamic conditions. In this study, oxygen-conducting powders in a fixed-bed reactor were pre-reduced to a known oxygen partial pressure at elevated temperatures, thereby creating a non-equilibrium between the materials and gas-phase oxygen. The oxidation states of the powders were varied by exposing the reduced powders to fixed quantities of $^{16}O_2$ before pulsing $^{18}O_2$. The $^{18}O^{16}O$ distribution was found to vary with the oxidation state of the solid oxide. By modelling the transport of oxygen species from the gas-phase, across the solid surface and into the bulk, the shape of the $^{18}O^{16}O$ distribution can yield a complete spectrum of kinetic information. Hence a dynamic PIE technique has been developed here to evaluate oxygen transport kinetics in-situ under non-equilibrium conditions allowing thorough, but rapid, material performance studies.

1. De Souza, R.A. and J.A. Kilner, Oxygen transport in $La_{1-x}Sr_xMn_{1-y}Co_yO_{3\pm\delta}$ perovskites: Part I. Oxygen tracer diffusion. Solid State Ionics, 1998. 106(3–4): p. 175-187.
2. Bouwmeester, H.J.M., et al., A novel pulse isotopic exchange technique for rapid determination of the oxygen surface exchange rate of oxide ion conductors. Physical Chemistry Chemical Physics, 2009. 11(42): p. 9640-9643.

SESSION D7: Fundamentals of Transport and Reactivity and Nanoionics V
D: Fundamentals of Transport and Reactivity and Nanoionics
Chair: Jennifer Rupp
Thursday Morning, June 18, 2015
Keystone Resorts, Grays Peak I/II

10:30 AM **D7.01
Oxygen Thermotransport in Mixed Conductor Oxides Han-Ill Yoo; Materials Science and Engineering, Seoul National University, Seoul, Korea (the Republic of).

Thermotransport-induced unmixing, or Soret effect, of mixed ionic electronic conductor compounds, that seems to have long been forgotten, is now attracting new attention, as the devices thereof, e.g., memristors, atomic switches, thermoelectrics, and gas permeation membranes, grow smaller or thinner with their driving forces, whether electrical, chemical or thermal, ever increasing. Particularly in the oxide-based devices, thermotransport of component oxygen is often of interest because all the defect-structure-sensitive properties of the oxide are normally governed by the nonstoichiometry δ.

According to irreversible thermodynamics, the direction and extent of thermotransport of mobile O in a mixed conductor oxide, e.g., $La_2NiO_{4+\delta}$, is completely governed by the sign and magnitude, respectively, of its reduced heat-of-transport q_O^*. Experimental measurement of q_O^*, however, is by no means trivial and hence, numerical data are extremely scarce for oxides in particular. Even the qualitative prediction of δ-redistribution under a temperature gradient, thus, remains far beyond reach.

We have recently developed a very simple electrochemical method to measure q_O^* by using zirconia-based Galvanic cells, and successfully applied it to the system of $La_2NiO_{4+\delta}$ which is known to be hyperstoichiometric across its entire stability range. It is found, to one's surprise, that q_O^* even changes its sign against oxygen activity depending on temperatures. We will review the irreversible thermodynamic formulation of thermotransport, and report on the measurement principle and the results on $La_2NiO_{4+\delta}$ together with their connotations.

11:00 AM D7.02
Reduction of the Grain Boundary Resistance in Yttria Stabilized Zirconia Thin Films: Incorporation of Mg^{2+} from the Substrate Edmund M. Mills[1], Matthias Kleine-Boymann[2], Juergen Janek[2], Hao Yang[1], Nigel Browning[3], Yayoi Takamura[1] and Sangtae Kim[1]; [1]CHMS, UC Davis, Davis, California, United States; [2]Institute of Physical Chemistry, Justus-Liebig University Geissen, Geissen, Germany; [3]Pacific Northwest National Laboratory, Richland, Washington, United States.

To improve the performance of SOFCs, electrolyte materials with higher ionic conductivity must be developed. The enhancements obtained by doping known electrolytes have reached their upper limit, so in recent years research has turned to the use of interfaces to enhance ionic conductivity. Interfaces, including grain boundaries, those in composite materials, and thin film hetero-interfaces, have different structural, chemical, and electrical environments than a material's bulk, leading to differences in conductivity—the ionic conductivity of electrolyte thin films may be enhanced by multiple orders of magnitude. However, the influences of structural, chemical, and electrical factors on the ionic conductivity have not been fully untangled. We have deposited nano-crystalline thin films of yttria-stabilized zirconia on MgO substrates using pulsed laser deposition, and characterized them with impedance spectroscopy, X-ray diffraction, high-resolution transmission electron microscopy, and secondary-ion mass spectrometry. We demonstrate the presence of a highly conductive layer near film-substrate interface. This enhancement is linked to diffusion of Mg2+ from the substrate into the YSZ film's grain boundaries, reducing their resistance and increasing the measured conductivity. This work presents an example of the complex interactions of different interfaces and their effect on ionic conductivity, something necessary to consider in the design of materials and devices with enhanced ionic conductivity through the incorporation of interfaces. I

11:20 AM D7.03
Determination of Transport Coefficients *D* and *K* in Materials Having Mixed Ionic-Electronic Conductivity Kun Zheng[1], Konrad Swierczek[1], Alicja Klimkowicz[1, 2] and Grzegorz Brus[1]; [1]Faculty of Energy and Fuels, AGH University of Science and Technology, Kraków, Poland; [2]Department of Engineering Science and Mechanics, Shibaura Institute of Technology, Tokyo, Japan.

Determination of chemical diffusion coefficient *D* and surface exchange reaction coefficient *K* is essential for numerous systems, which properties are controlled by transport of mobile ions. Commonly, so called relaxation techniques are employed for determination of the coefficients. In the measurements, for instance for oxide materials, mass or electrical conductivity changes are recorded during immediate changes of the oxygen partial pressure at elevated temperatures [1-3]. Theoretical basis for these methods relies on a solution combining first and second Fick's law and flux density of the species at the surface boundary, through which motion of the ions occurs [2]. Depending on a geometry (3-dimensional, disc-like, etc.), the respective solutions are different, however, for simultaneous determination of both coefficients $0.03 \le L = l_i \cdot K/D \le 30$ inequalities have to be satisfied, where *L* - dimensionless parameter, l_i - distance of diffusion along considered direction [3]. Consequently, depending on the intrinsic values of *D* and *K*, as well as for particular conditions of the experiment it may be or may not be possible to determine both, *D* and *K*.

In this study, we show application of mass and electrical conductivity relaxation techniques for determination of *D* and *K* in materials having mixed ionic-electronic conductivity, for the particular case of highly-conducting $LnBa_{1-x}Sr_xCo_{2-y}Fe_yO_{6-\delta}$ (Ln - selected lanthanides) and $Ba_{1-x}Ln_x(Zr,In,Sn)O_{3-\delta}$ proton-conducting oxides. Additionally, we discuss

possibility of determination of *D* and *K* on a basis of mass relaxation measurements of powders having various grain size distribution.
The project was funded by the National Science Centre Poland (NCN) on the basis of the decision number DEC-2012/05/E/ST5/03772.

Reference
[1] W. Preis, et al. Solid State Ionics 175 (2004) 393
[2] J. Crank, The Mathematics of Diffusion, 2nd Ed. Oxford University Press, New York, 1975
[3] M.W. den Otter, et al. J. Electrochem. Soc. 148 (2001) J1

11:40 AM D7.04
Oxide-Ion Conduction with Strong Correlation in Apatite-Type Lanthanum Silicate Kazuaki Toyoura[1], Kouta Imaizumi[1], Atsutomo Nakamura[1] and Katsuyuki Matsunaga[1, 2];[1]Nagoya University, Nagoya, Japan; [2]Japan Fine Ceramics Center, Nagoya, Japan.

Lanthanum silicate with the apatite-type structure, $La_{9.33+0.67x}(SiO_4)_6O_{2+x}$ ($0 \leq x \leq 1$), exhibits high oxide-ion conductivity at intermediate temperatures, which is, therefore, expected as a future electrolyte lowering the operating temperature of SOFCs. In the present study, the fast oxide-ion conduction mechanism has theoretically been investigated in a first-principles manner on the basis of the nudged elastic band (NEB) method and the kinetic Monte Carlo (KMC) method, to provide a novel atomic-scale picture of the oxide-ion conduction with strong correlation.

According to the previous literature, the oxide-ion conductivity is enhanced with increasing the composition *x* due to the formation of interstitial oxide ions. The interstitial oxide ions are reported to be located at the periphery of the O4 columns along the *c* axis and to migrate fast within the single columns by a cooperative interstitialcy mechanism, so-called “push-pull mechanism”. The push-pull mechanism is actually fast also as the result of our NEB calculations, whose calculated potential barrier is less than 0.01 eV in $La_{10}(SiO_4)_6O_3$. However, the subsequent KMC simulations found that the oxide-ion migration by the push-pull mechanism is frequently blocked by adjacent interstitial oxide ions in the one-dimensional O4 columns, resulting in lower conductivity than expected from the low potential barrier.

Instead, the getting-out mechanism from the O4 columns with a potential barrier of 0.58 eV is crucial in the long-range oxide-ion conduction, which temporarily transfers a part of interstitial oxide ions out of the columns to relax the blocking effect. The oxide-ion conduction perpendicular to the *c* axis is also made possible by the getting-out mechanism, which results in the comparable activation energies of the oxide-ion conductivities along the *c* axis and in the *ab* plane.

SESSION D8: Fundamentals of Transport and Reactivity and Nanoionics VI
D: Fundamentals of Transport and Reactivity and Nanoionics
Chairs: Roger De Souza and Han-Ill Yoo
Thursday Afternoon, June 18, 2015
Keystone Resorts, Grays Peak I/II

1:30 PM *D8.01
The Transport Properties of Dislocations in the Perovskite-Oxide SrTiO Roger A. De Souza; Institute of Physical Chemistry, RWTH Aachen University, Aachen, Germany.

The one-dimensional lattice defects known as dislocations are widely believed to provide short-circuit paths for diffusion in crystalline materials. In this contribution I will present recent work that we have been doing on characterizing and understanding mass transport processes along dislocations in the perovskite-type oxide $SrTiO_3$. I will focus on experimental studies of oxygen diffusion along the periodic array of dislocations that constitutes a low-angle tilt grain boundary. Isotope penetration profiles obtained by Secondary Ion Mass Spectrometry (SIMS) indicated no evidence of fast diffusion along the dislocation array. I will also present complementary results obtained from atomic-level studies of point-defect processes by means of static lattice and molecular dynamics simulations. Combining all results and literature reports, I will present a comprehensive and consistent picture of the transport properties of dislocations in $SrTiO_3$. Finally I will describe the consequences for memresistive devices.

1:50 PM D8.02
Driving Forces Related to Acceptor-Oxygen Vacancy Defect Complex Formation in Perovskite Oxides Russell Maier; NIST, Gaithersburg, Maryland, United States.

Defect complexes consisting of acceptor impurities and nearest neighbor oxygen vacancies often constitute a significant concentration of defect species in the $SrTiO_3$ perovskite lattice at room temperature. These oppositely charged point defects form dipoles that have also been documented in the ferroelectric phases of $BaTiO_3$. The impact of these defect dipoles on the dielectric properties of perovskite oxides is not clear. Acceptor-oxygen vacancy defect dipoles have been proposed to be responsible for aging in ferroelectric materials, and it has been suggested that defect complex formation has a significant effect on the mobility of oxygen vacancies. As a result, effective characterization of these defect centers is critical to establishing a connection between their formation and their effect on ionic tranport in perovskite materials. Electron paramagnetic resonance (EPR) studies have shown that these defect complexes are clearly identifiable in the paraelectric $SrTiO_3$ lattice; however, data will be presented on single crystals with the conclusion that these defect complexes do not form in large concentrations in $BaTiO_3$.

Because defect dipoles appear to form in high concentrations in the iron doped $SrTiO_3$ system in contrast to the lack of evidence of similar complex formation in the room temperature phase of $BaTiO_3$, it is concluded that there is large discrepancy in the driving force for defect dipole formation between these two similar oxide lattices. Work will be presented on EPR investigations of acceptor doped solid solutions of polycrystalline $SrTiO_3$, $BaTiO_3$, and similar perovskite oxides. These studies are desinged to identify defect complexes in samples containing a range of dopant concentrations and dielectric permittivities in order to help construct a more rigorous model to describe the energetics of defect dipole formation in the perovskite lattice. These experimental results will be applied to a working theory of defect complex formation controlled by a Debye-Hückel screening potential in an oxygen vacancy potential energy landscape.

2:10 PM D8.03
Conductivity Relaxation Experiments on Donor Doped Barium Titanate Ceramics: Effect of Microstructure Wolfgang Preis and Werner Sitte; Chair of Physical Chemistry, Montanuniversitaet Leoben, Leoben, Austria.

The electrical properties of functional electroceramic materials, such as $BaTiO_3$ – based PTC (positive temperature coefficient) resistors, are strongly affected by re-oxidation processes during annealing at certain well-defined temperatures and oxygen partial pressures as well as the cooling period after sintering at high temperatures. Fast diffusion of oxygen along grain boundaries plays a key role for the re-oxidation kinetics of these interfacially controlled materials. Conductivity relaxation experiments are a powerful technique for the investigation of diffusion processes in electroceramics.

It is the aim of this contribution to present finite element simulations for conductivity relaxation processes in polycrystalline materials. The finite element calculations are based on a square grain model which is suitable for modeling fast interfacial diffusion. The grain boundaries consist of a thin slab (0.5 nm thickness), representing the core, and a region adjacent to the grain boundary slabs which corresponds to blocking space charge layers for the transport of electronic charge carriers. Interestingly, in the case of extremely fast grain boundary diffusion the relaxation curves for mass transport deviate significantly from the conductivity relaxation curves, if the electronic charge carriers are blocked by the grain boundaries. In the case of negligible grain boundary resistivities, the relaxation curves for mass transport and dc conduction coincide perfectly.

The present modeling approach is applied to interpret conductivity relaxation experiments on n-type $BaTiO_3$ ceramics, where diffusion processes are governed by extremely fast diffusion along the grain boundaries. At temperatures around 1200°C the grain boundary resistivities can certainly be neglected, resulting in conductivity relaxation curves which enable the determination of the chemical diffusion coefficient of the bulk. However, at 900°C highly resistive space charge layers as well as conductive core regions have to be taken into account. A detailed interpretation of conductivity relaxation curves for both oxidation and reduction steps will be provided.

2:30 PM D8.04
Oxygen Diffusion/Exchange Processes in Two-Dimensional $Ln_2NiO_{4+\delta}$ (Ln=La, Pr, and Nd) Single Crystals: IEDP/LEIS Measurements Jean-Marc Bassat[2], Helena Tellez[1], Monica Burriel[3], Remi Castaing[2, 3], W. Paulus[4], P. Veber[2], Tatsumi Ishihara[1] and John Kilner[1, 3]; [1]Hydrogen Production Division, International Institute for Carbon-Neutral Energy Research, Fukuoka, Japan; [2]Institut de Chimie de la Matière Condensée de Bordeaux, Pessac, France; [3]Department of Materials, Imperial College London, London, United Kingdom; [4]Institut Charles Gerhardt, Montpellier, France.

Ln_2NiO_{4+d} nickelates, with Ln = La, Nd or Pr, are promising materials for the next generation of intermediate temperature solid-oxide fuel cell (SOFC) cathodes (500 < T (°C) < 700) or air electrodes for high temperature electrolysis (EHT) devices. They possess reasonable electronic conductivity together with good catalytic, electrochemical and thermo-mechanical properties. Unlike the most studied perovskite-type oxides, where the oxygen exchange and diffusion occurs via a 3D network of oxygen vacancies, oxygen transport in these materials involves three types of oxygen ions in a 2D structure. In order to understand the fundamental aspects of the oxygen diffusion and surface exchange phenomena in these Mixed Ionic Electronic Conducting (MIEC) materials, we have combined two kinds of measurements on orientated single crystals:

The Isotopic Exchange Depth Profiling (IEDP) method to determine the temperature dependence of the oxygen diffusion D* and surface exchange coefficients k* for the different crystallographic orientations and rare-earth cations (Ln=La, Nd, Pr). A large anisotropy was evidenced for both coefficients, being the highest values along the so-called “ab-blocks” including apical and interstitial oxygen, in comparison to the perpendicular direction (c-axis). Moreover, the activation energy E_a of the oxygen diffusion along the ab-block depends on Ln, being the E_a value the lowest for Ln=Pr, as has been previously evidenced using electrochemical measurements (polarization resistance values).

LEIS measurements of the outermost surface composition on the main crystallographic faces of the single crystals in order to determine the possible surface reconstruction during the high temperature treatments and the correlation between the catalytic activity of the materials and their surface composition. For the two main orientations ((010) and (001) faces in La_2NiO_{4+d}, no Ni was detected at the first atomic layer, indicating that both surfaces are La-O terminated.

2:50 PM D8.05
Influence of Dislocations on Electrical and Chemical Properties in Metal Oxides Lixin Sun[1], Dario Marrocchelli[1] and Bilge Yildiz[1, 2]; [1]Department of Nuclear Science and Engineering, Massachusetts Institute of Technology, Cambridge, Massachusetts, United States; [2]Department of Material Science and Engineering, Massachusetts Institute of Technology, Cambridge, Massachusetts, United States.

Strained oxide thin films are of interest for accelerating oxide ion conduction in electrochemical devices. While the effect of elastic strain has been uncovered theoretically, the effect of dislocations on the diffusion kinetics in such strained oxides remained largely unexplored to date. High density of dislocations can be found in metal oxide nanostructures upon elastic strain relaxation. For example, misfit dislocations form at the interfaces of metal oxide thin films due to the lattice mismatch between two different structures. Dislocations can modify the local electrical and chemical properties in an oxide by altering the defect chemistry and the electronic structure. The under-coordination environment at the dislocation core and the extended strain field of the dislocation may affect the stability and kinetics of electronic and ionic defects that dominate the electron/ionic conductivity and surface reactions, which are crucial for performance in solid oxide fuel cells.

Our recent atomistic simulations show that an ½<110>{100} edge dislocation in 4-12% reduced or doped CeO_2 (doped with Gd, Y and Sc) slows down the oxide ion conductivity. This finding is contrary to the well-known fast diffusion of atoms along the dislocations in metals, and should be considered when quantitatively interpreting the experimental results. The reason for this behavior is the segregation of charged defects at equilibrium. Dopants larger than the host cation enrich at the tensile strain field around the dislocation, while a depletion zone of dopant cations is formed at the compressive strain field because of elastic energy minimization. The oxygen vacancies follow the same redistribution profile as the dopants due to the electro-static interaction between the dopant cations and the oxygen vacancies. The associative interactions among the point defects in the enrichment zone and the lack of oxygen vacancies in the depletion zone slow down oxide ion transport.

This work demonstrates that dislocations can significantly alter the distribution and mobility of charged defects in metal oxides. Our work is ongoing in modulating these defects at the dislocation by selective and local doping.

3:30 PM *D8.06
Space Charge Layers and Their Role in Properties of Interfaces in Solid State Ionics Truls Norby; Department of Chemistry, University of Oslo, Oslo, Norway.

It is well established that the core of clean grain boundaries in many solid electrolytes attract preferred defects for strain relief and thereby become charged. This is accompanied by space charge layers (SCLs) of the same (but decaying) electrical potential and a net charge of opposite sign. The potential enhances or suppresses the concentrations of point defects in the SCLs, depending on the sign of their effective charge, which can dramatically change the electrical properties. The behaviour can be modelled by minimizing the energy of the entire grain boundary region, i.e., equalization of the electrochemical potential across the same region for all species. Inputs from DFT calculations of defect energies and certain materials constants and assumptions allow us to solve the system mathematically and thermodynamically and to reproduce experimental observations reasonably well. We will use proton and oxide ion conducting Y-substituted $BaZrO_3$ (BZY) as example.

Charged interfaces will also exist for electrodes and surfaces, hence also space charge layers. It is however not common to use similar approaches as for grain boundaries in rationalizing electrode impedances and slow surface kinetics. The space charge layers here may contribute with bulk-like resistances due to the depletion of carriers in a subsurface layer, but also by interacting with the thermodynamics of species adsorbed on surfaces, and through the kinetics of reactions where the reactant and product are in the SCL. We will in this contribution discuss these possibilities in order to encourage the development of suitable new models for interpretation of measured data.

3:50 PM D8.07
Defect Chemistry of CeO_2 Surfaces from First Principles and Space Charge Theory Tor S. Bjorheim[1], Eugene Kotomin[2] and Joachim Maier[2]; [1]FASE, Department of Chemistry, University of Oslo, Oslo, Norway; [2]Max Planck Institute for Solid State Research, Stuttgart, Germany.

Ceria (CeO_2) is a technologically important oxide, with numerous potential applications. It is a promising oxygen incorporation material, and exhibits remarkable catalytic properties towards hydrocarbon and CO oxidation, and water splitting reactions. Further, acceptor doped ceria exhibits significant oxide ion conductivity and is of interest as electrolyte for SOFCs. [1]Nano-crystalline ceria in addition displays significant proton conduction down to room temperature,[2] suggested to be due to surface, or sub-surface proton transport. These functional properties in many cases originate from the rich surface, or interface, defect chemistry of ceria, and corresponding space charge layers.[3, 4,5]

In this contribution, we explore the defect chemistry of ceria surfaces from first principles calculations and space charge theory. Plane-wave based DFT calculations are used to determine bulk and surface defect formation energetics, while combination with space charge theory allows us to numerically evaluate space charge potential and defect concentration profiles, and the surface defect chemistry.

Charged oxygen vacancies and protons exhibit highly favorable surface segregation energies, and tend to accumulate on ceria surfaces. Although these defects are partly charge-compensated by oxide and hydroxide add-ions, and Ce^{3+} at the surface, the surface is positively charged and charge-compensated by a negative space charge region, at least at high temperatures. Under humid conditions at lower temperatures, the surfaces are saturated by protonic species, forming water layers. We finally discuss the effect of saturation of the surface by $H_2O(l)$ on the charge of the surface and the space charge regions.

1. H. L. Tuller and A. S. Nowick, J. Electrochem. Soc., 1975, **122**, 255-259.
2. E. Ruiz-Trejo and J. Kilner, J. Appl. Electrochem., 2009, **39**, 523-528.
3. Z. A. Feng *et al.*, Nat Commun, 2014, **5**, 4374
4. G. Gregori *et al.*, Adv. Funct. Mater., 2013, **23**, 5861-5867.
5. M. Shirpour *et al.*, 2011, PCCP **13**, 937.

4:10 PM D8.08
On Determining the Built-In Potential at Grain Boundaries in Ion-Conducting Oxides Sangtae Kim[1], Seong K. Kim[1], Sergey Khodorov[2] and Igor Lubomirsky[2]; [1]University of California, Davis, Davis, California, United States; [2]Weizmann Institute of Science, Rehovot, Israel.

Electrical properties of polycrystalline ceramics are often defined by the grain boundaries. The difference in conductivity between the grain interior and the grain boundary can be substantial particularly in ion-conducting ceramics, reaching several orders of magnitude. Their reliable interpretation is however being greatly sought after because the Schottky barrier-type formalism, currently in exclusive use, may be inadequate for describing ionic current. Recently we have demonstrated that I–V characteristics of grain boundaries in prominent solid electrolytes that conducts either oxygen ions or protons can be accurately described using a simple linear diffusion formalism (I-V model). The prime parameter that controls current flow across the grain boundaries is namely built-in electrical potential. The potential barrier is formed at the grain boundary as a result of the ion depletion in the space charge zones and is responsible for the high grain boundary resistance. The height of the barrier has been determined exclusively by the ratio of an effective resistivity of a single grain boundary to that of grain interior at a given temperature. The assumption made for such determination is that the grain boundary resistance is attributed solely to the depletion of charge carriers in the space charge zone. However voltage drop across a grain boundary may result from combination of various causes. Hence, the barrier height determined from the ratio can be overestimated for a grain boundary with multiple origins of its resistance as is often the case in reality. In this contribution, we demonstrate that the potential barrier height in an ionic conductor can be determined accurately using the *I-V* model even when both potential barrier and current constriction are responsible for the resistance. We estimate the partial contribution of the potential barrier to the grain boundary resistance.

4:30 PM D8.09
Solid Oxide-Molten Carbonate Nanocomposite Fuel Cells II: Surface Charge Effects Mehmet Ali Gulgun[1, 2], Yelda Yorulmaz[1], Hazal Batili[1], Cinar Oncel[1], Shalima Shawuti[3] and Miran Ceh[4]; [1]FENS, Sabanci University, Istanbul, Turkey; [2]Nanotechnology Application Center, Sabanci University, Istanbul, Turkey; [3]Physics Dept, Istanbul University, Istanbul, Turkey;[4]Department for Nanostructured Materials, Josef Stefan Institute, Ljubljana, Slovenia.

Particle size effects on the ionic conductivity in solid oxide-molten carbonate nano-composites fuel cells were investigated as a function of temperature. A threshold type behavior was confirmed as function of solid oxide particle loading. Nano-composites have a lower activation energy the carbonate matrix phase. The difference in activation energies were corresponding to the dissociation energy of the carbonate. Solid oxide particles do not only make up the backbone for the composite but also provide a surface for the dissociation of the molecules of the amorphous carbonate matrix phase. The “freed” carbonate ions appear to be responsible for the enhanced ionic conductivity of the composite.
The role of the surfaces on the dissociation of the sodium carbonate molecules were studied in composites made with various solid oxide particles with different iso-electric points. Impedance measurements indicated that not only the surface charges but also electronic structure/conductivity of the particles affect the conductivity of the nano-composite. Analytical electron microscopy studies were utilized to visualize the oxide surface charge-amorphous matrix interactions in the composites.

4:50 PM D8.10
Accurate Measurement of Fast Grain Boundary Ionic Diffusion by ToF-SIMS Depth Profiling with Selective Attenuation of Specific Secondary Ions (SASI) Helena Tellez[1], John Druce[1], Tatsumi Ishihara[1, 2] and John Kilner[3, 1]; [1]Hydrogen Production Division, International Institute for Carbon-Neutral Energy Research, Fukuoka, Japan; [2]Department of Applied Chemistry, Kyushu University, Fukuoka, Japan; [3]Department of Materials, Imperial College London, London, United Kingdom.

A very efficient strategy to enhance the overall oxygen exchange and diffusion kinetics might be via microstructure engineering in order to optimize the grain boundary (GB) density in mixed ionic-electronic conductors (MIECs), especially for those materials showing slow bulk ionic diffusion kinetics, such as $La_{0.8}Sr_{0.2}MnO_{3+\delta}$.[1] In order to characterize the ionic transport properties through the grain boundaries, ^{18}O tracer diffusion measurements using Time-of-Flight Secondary Ion Mass Spectrometry (ToF-SIMS) on thin films with a controlled grain size provide a good estimation of the GB diffusion properties[2]. On the other hand, the high GB density in these films might also facilitate the segregation of impurities and constituent cations towards the surface, inducing compositional changes and blocking in-grain bulk exchange and diffusion pathways by precipitation of secondary phases on the surface. A direct measurement of the GB diffusion properties and the intrinsic bulk properties in MIECs can be performed on ceramic pellets, provided the grain size is large enough as to allow the discrimination of the parallel oxygen diffusion pathways at the exchange conditions and the diffusion takes place under a mixed control (*i.e.* Harrison type B diffusion). In this case, the main experimental limitation comes from the poor signal statistics in the diffusion “tails” when using conventional strategies to avoid dead-time effects in ToF-SIMS. In this work, we use “Selective Attenuation of Secondary Ions” (SASI) ToF-SIMS depth profiling to improve the accuracy and precision in the determination of the GB transport properties in Sr-doped polycrystalline ceramics.[3] Furthermore, the SASI approach allows the simultaneous detection of other low yield species, such as cation oxides or impurities, providing additional information about compositional changes or surface blocking that might have a drastic impact on the ionic transport properties.
1. R. A. De Souza *et al.*, *Mater Lett* **2000**, 43, 43.
2. E. Navickas *et al.*, *Phys Chem Chem Phys* **2015**.
3. H. Téllez *et al.*, *Anal Chem* **2015**. doi: 10.1021/ac504409x.

SESSION D9: Fundamentals of Transport and Reactivity and Nanoionics VII
D: Fundamentals of Transport and Reactivity and Nanoionics
Chair: Igor Lubomirsky
Friday Morning, June 19, 2015
Keystone Resorts, Grays Peak I/II

10:40 AM **D9.01
Molecular Insights Into Structure and Dynamics of Organic Ionic Plastic Crystal Electrolytes Maria Forsyth[1, 2]; [1]Institute for Frontier Materials, Deakin University, Burwood, Victoria, Australia; [2]ARC Center of Excellence for Electromaterials Science, Burwood , Victoria, Australia.

The application of organic ionic plastic crystals (OIPCs) as a new class of solid electrolyte for energy generation and storage devices such as solar cells, fuel cells, lithium batteries[1], and, more recently, sodium batteries[2], is attracting increasing attention. Achieving sufficient target ion transport through the material is key to each of these applications and requires fundamental understanding of the structure and dynamics in these complex solids. Typically, an OIPC has several solid-solid phase transitions evident from the thermal analysis traces. These may be either distinctly different crystal structures or order-disorder transitions that may arise from rotator phases. Doping, or mixing, of a second component such as a lithium or sodium salt can often lead to distinctly new compounds with unique

crystal structures and dynamics[2-4]. We have used a combination of characterisation tools including multinuclear NMR spectroscopy, XRD, vibrational spectroscopy as well as conductivity, to characterise and understand these novel materials. Recently, Molecular Dynamics simulations have provided further insight into the mechanism of the transport properties[5,6]. The efficient use of these materials in lithium metal batteries has been recently demonstrated[7] This paper will discuss these new insights and demonstrate the favourable properties that can be present in these solid electrolyte materials.

1. Pringle, J.M., Howlett, P.C., MacFarlane, D.R., Forsyth, M., Journal of Materials Chemistry 20 (2010) no.11, 2056-2062
2. M. Forsyth, T. Chimdi, A. Seeber, D. Gunzelmann, P.C. Howlett, Journal of Materials Chemistry A, 2 (2014) 3993-4003
3. T Chimdi, D Gunzelmann, J Vongsvivut, M Forsyth., Solid State Ionics 272 (2015), 74-83
4. N. Iranipour, D. Gunzelmann, A. Seeber, J. Vongsvivut, C. Doherty, F. Ponzio, L. A. O'Dell, A. F. Hollenkamp, M. Forsyth, P. C. Howlett, Journal of Materials Chemistry A 2015, **DOI:**10.1039/C4TA07155G
5. H. Zhu, F. Chen, L. Jin, L.A. O'Dell, M. Forsyth, ChemPhysChem, 15 (2014) 3720-3724.
6. F. Chen, S. W. de Leeuw, M. Forsyth, The Journal of Physical Chemistry Letters 2013, 4 (23), 4085-4089.
7. L. Jin, P.C. Howlett, J.M. Pringle, J. Janikowski, M. Armand, D.R. MacFarlane, M. Forsyth, 7 (2014) 3352-3361

11:10 AM *D9.02

Structure and Lithium Ion Dynamics of the Tetragonal LGPS-Type Superionic Conductors $Li_{11-x}M_{2-x}P_{1+x}S_{12}$ with M = Si, Ge, Sn Alexander Kuhn[1], Sascha Harm[1, 2] and Bettina V. Lotsch[1, 2]; [1]Chemistry , Max Planck Institute for Solid State Research, Stuttgart, Germany; [2]Chemistry, University of Munich (LMU), Munich, Germany.

The prospect of high energy densities along with safe handling has intensified research into new solid Lithium electrolytes for next-generation all-solid-state battery systems. While thin-film battery concepts allow for the use of high voltage electrodes such as Lithium metal and show enhanced cycle stability and shelf life, the solid electrolytes currently employed suffer from moderate ionic conductivity and high interfacial resistance. Therefore, the development of fast ($\sigma > 10^{-4}$ S/cm at RT) solid Li electrolytes which are mechanically robust and stable against Lithium is currently the key bottleneck for the deployment of thin film solid-state batteries in practical applications. In 2011, the new solid electrolyte $Li_{10}GeP_2S_{12}$ (LGPS), a metastable tetragonal thiophosphate occurring in the system $xLi_4GeS_4 : yLi_3PS_4$, was reported, exhibiting a record Li ion diffusivity of 12 mS/cm and a wide electrochemical window of up to 4 V vs. Li/Li^+, thus reinvigorating the quest for high-performance solid electrolytes with relevance for practical applications [1].
Here, we report on the synthesis of a new solid solution member of tetragonal LGPS - Li_7GePS_8 - as well as the Sn and Si analogues of LGPS, which are exclusively based on abundant elements [2,3,4]. The LGPS crystal structure and Li ion dynamics were studied using multiple complementary techniques, including single crystal X-ray diffraction, electron diffraction, impedance spectroscopy, ^{7}Li PFG NMR, ^{7}Li NMR relaxometry, and ^{31}P MAS NMR. The exceptionally high ionic conductivity of LGPS-type electrolytes of $\approx 10^{-2}$ S/cm is traced back to nearly isotropic Li hopping processes in the crystalline lattice with $E_A \approx$ 0.20 eV. We observe a clear correlation between the diffusivity and the unit cell volumes of the LGPS-type electrolytes. The Si analogue, $Li_{11}Si_2PS_{12}$, exhibits a higher room temperature Li ion diffusivity and lower activation energy than the present record holder $Li_{10}GeP_2S_{12}$, thus setting a new benchmark in the realm of ultrafast solid electrolytes [3].

[1] a) N. Kayama, K. Homma, Y. Yamakawa, R. Kanno, M. Yonemura, T. Kamiyama, Y. Kato, S. Hama, K. Kawamoto and A. Mitsui, *Nat. Mater.*, 2011, 10, 682; b) A. Kuhn, J. Köhler and B. V. Lotsch, *Phys. Chem. Chem. Phys*., 2013, 15, 11620.
[2] A. Kuhn, V. Duppel and B. V. Lotsch, *Energy Environ. Sci.*, 2013, 6, 3548.
[3] A. Kuhn, O. Gerbig, C. Zhu, F. Falkenberg, J. Maier and B. V. Lotsch, *Phys. Chem. Chem. Phys.* 2014, 16, 14669.
[4] P. Bron, S. Johansson, K. Zick, J. Schmedt a. d. Guenne, S. Dehnen and B. Roling, *J. Am. Chem. Soc.* 2013, 135, 15694.

11:30 AM D9.03

Correlation Between the Electronic Structure and the Interstitial Oxygen Formation in Layered Perovskite Oxides Takashi Nakamura[1], Yihan Ling[1], Ryo Oike[1], Yusuke Tamenori[2]and Koji Amezawa[1]; [1]IMRAM, Tohoku University, Sendai, Japan; [2]JASRI, Sayo-gun, Japan.

La_2NiO_4-based oxides are promising materials for SOFC cathodes and oxygen permeation membranes because of excellent electrochemical properties, such as mixed ionic and electronic conduction, oxygen storage, and catalytic activity. These properties arise from the interstitial oxygen. Therefore, understandings of the mechanism of the interstitial oxygen formation are important to design and control the performance and the reliability of the above electrochemical devices.

The purpose of this study is to understand the correlation between the electronic structure and the interstitial oxygen formation in layered perovskite oxides. For this purpose, $La_2(Ni_{0.9}M_{0.1})_{4+\delta}$ (M = Fe, Co, Cu) were synthesized by a solid state reaction method. The concentrations of interstitial oxygen in the oxides were evaluated by high temperature gravimetry and coulometric titration. The electronic structures were studied by soft X-ray absorption spectroscopic measurements at BL27SU, SPring-8. $La_2(Ni_{0.9}Fe_{0.1})O_{4+\delta}$ and $La_2(Ni_{0.9}Fe_{0.1})O_{4+\delta}$ showed higher interstitial oxygen concentration than non-doped $La_2NiO_{4+\delta}$, while $La_2(Ni_{0.9}Cu_{0.1})O_{4+\delta}$ showed lower concentration. At 1073 K in 1 bar of O_2, d in $La_2(Ni_{0.9}Fe_{0.1})O_{4+\delta}$, $La_2(Ni_{0.9}Fe_{0.1})O_{4+\delta}$, $La_2NiO_{4+\delta}$, and $La_2(Ni_{0.9}Cu_{0.1})O_{4+\delta}$ were about 0.15, 0.14, 0.098 and 0.071, respectively. There results indicate Fe- and Co-doped samples are more preferable to the interstitial oxygen formation than non-doped $La_2NiO_{4+\delta}$.

By the interstitial oxygen formation, the change of XAS spectra at Fe, Co and Cu *L*-edges was negligibly small. This suggests the redox of 3d transition metals does not contribute to the interstitial oxygen formation. The change of the XAFS spectra at O *K*-edge was much larger than that at Ni *L*-edge, indicating strong contribution of O2*p* band to the interstitial oxygen formation. The detailed comparison of the electronic structure will be shown in the presentation.

11:50 AM D9.04

Vacancy Engineering for New Compounds and Low Temperature Oxide Ion Conduction Yaoqing Zhang; Tokyo Institute of Technology, Yokohama, Japan.

Aurivillius phases of the general formula $Bi_2A_{n-1}B_nO_{3n+3}$, where *A* is an electropositive atom, *B* site accepts the early transition metal and *n* is the number of perovskite blocks, are particularly interesting from the point view of fast ionic conduction.[1,2] A notable example is the high temperature phase of $Bi_4V_2O_{11}$ whose oxide ion conductivity has been observed in the range of 0.1-1 S/cm between 870 and 1100 K with an extremely low activation energy (0.17 eV).[3,4] Such an exceptionally high O^{2-} mobility is believed to be facilitated by the presence of a large number of intrinsic and disordered oxygen vacancies in the vanadium oxide layer which is sandwiched between the rock-salt $[Bi_2O_2]^{2+}$ layers to form the host lattice. This conducting phase, however, does not survive the reduced temperatures as these oxygen vacancies would readily become ordered to enable less conducting polymorphs. To stabilize such a high temperature structure to ambient conditions, the traditional approach proves effective by means of foreign cation substitution at either Bi or V site, but suffers from the low doping level. Here in this work by looking into the defect chemistry, it was found that merely introducing some vacancies into the system would realize quenchable high temperature Aurivillius-type $Bi_{4-x}V_2O_{11-y}$ phase that exhibits good conductivity of around 10^{-5} S/cm at 200 °C. Interestingly, the fundamental $[Bi_2O_2]$ layer allows strong deficiency and plays a role not revealed in prior studies.

E: Transparent Conducting Oxides

* Invited Speaker
** Keynote Speaker

SESSION E1: TCO I—Defects, Materials
E: Transparent Conducting Oxides
Chair: David Paine
Monday Morning, June 15, 2015
Keystone Resorts, Quandary Peak I/II

10:30 AM **E1.01
Defect Theory for Transparent Conducting Oxides Stephan Lany; National Renewable Energy Laboratory, Golden, Colorado, United States.

Electronic structure theory has played an important role in explaining the phenomenology of semiconductors in terms of microscopic models, e.g., for doping, defects, interfaces, or alloy compositions. Increasingly, it becomes instrumental for the design and discovery of novel materials, either via high throughput computational screening of a pool of candidate materials, or by the targeted design and optimization of materials. The availability of quasi-particle energy calculations in the GW approximation allows now for a fairly robust band gap prediction, which is important for an accurate prediction of defect and surface/interface properties combination with density functional theory (DFT) supercell calculations. As an example, ZnO has attracted high interest as a prototypical wide gap semiconductor and transparent conducting oxide (TCO), and served as a test bed for defect theory. The predicted low formation energies of compensating Zn vacancies, however, are seemingly conflicting with the high carrier densities achievable in doped ZnO based TCO. This finding spurred an in-situ annealing study where the formation of these compensating defects comes close to thermodynamic equilibrium, allowing for a direct comparison with the carrier densities predicted from the theory. Surprisingly, these experiments showed a non-monotonic temperature dependence of the conductivity with a minimum around 500°C and with good agreement with the equilibrium theory at higher temperatures. These results established that the high conductivities achievable in ZnO originate from non-equilibrium effects during thin film deposition [1]. The dopant-defect interactions were studied in more detail in Ga-doped ZnMgO alloys, which led to the finding that careful annealing could be used to pair the positively charged dopants with negatively charged defects, thereby reducing the ionized defect scattering and increasing the mobility while the carrier concentration remains practically constant [2].

In SnO_2, the group V dopants are considered as a viable alternative to fluorine doping. However, the group V elements (P, As, Sb, Bi) are multivalent and can assume both a +V and +III oxidation state, which implies an ambipolar doping character and the possibility to act as both electron donors and as compensating acceptors. The electrical activity of these dopants is determined by the energy difference between the conduction band minimum and the transition level between the two oxidation states. For the accurate prediction of this energy difference, we employed an approach that combines HSE06 hybrid functional calculations with GW quasi-particle energy calculations for both the band-edge energies and the defect state [3]. We find that Bi shows a clear deep-level behavior with Fermi level pinning inside the band gap, thereby preventing doping and leading to insulating behavior. As is a borderline case, and only P and Sb act as electron-donors without being affected by multivalency.

[1] A. Zakutayev *et al.*, Appl. Phys. Lett. **103**, 232106 (2013).
[2] Y. Ke, *et al.*, Adv. Funct. Mater. **24**, 2875 (2014).
[3] H. Peng, J.D. Perkins, S. Lany, Chem. Mater. **26**, 4876 (2014).

11:00 AM E1.02
Tuning Charge Collection Efficiency at the Transparent Conductive Electrode in Polymer Photovoltaics with Solution-Processed LiF Cleva W. Ow-Yang[1, 2], Hasan Kurt[1], Junjun Jia[3] and Yuzo Shigesato[3]; [1]Materials Science and NanoEngineering, Sabanci University, Istanbul, Turkey; [2]Nanotechnology Research and Application Center, Sabanci University, Istanbul, Turkey; [3]Graduate School of Science and Engineering, Aoyama Gakuin University, Sagamihara/Kanagawa, Japan.

While the design of new materials and device architectures will lead to enhanced organic electronic device performance, the interfaces arising from adjacent layers offer an additional degree of engineering optimization. We present a study in which the charge collection of tin-doped indium oxide (ITO) is enhanced by a nanostructured layer of solution-processed lithium fluoride (sol-LiF) nanoparticles in a bulk heterojunction of polymer, poly(3-hexylthiophene), and metallofullerene ($P3HT:PC_{60}BM$) photovoltaic cell. The sol-LiF nanoparticles were synthesized using micelle nanoreactors, which yielded size-monodisperse colloids and enabled control over the surface coverage, when deposited onto ITO electrodes. Surface coverages investigated ranged from 2% up to 13.2%. The surface work function of the nanostructured ITO films increased linearly with surface coverage from 4.88 to 5.30 eV, as measured by photoelectron spectroscopy. Electron energy loss spectroscopy analysis of a cross-section in an aberration-corrected scanning transmission electron microscope verified that some of the nanoparticles were LiF, while others were LiO_xF_y. When the ITO electrodes modified by sol-LiF were incorporated into polymer solar cells of the architecture ITO/sol-LiF/PEDOT:PSS/P3HT:PCBM/thermal-LiF/Al, a maximum power conversion efficiency (PCE) was recorded for a device with an ITO anode modified by 5.3% of sol-LiF coverage, which corresponded to a measured work function of 5.07 eV. *In-situ* impedance spectroscopy analysis of the devices under operation revealed a correlation between the average charge carrier lifetime under illumination and PCE. The improvement in short circuit current density by 87% and PCE by 74.3% suggests that the sol-LiF interlayer density enabled work function tuning of the ITO anode to better match the highest occupied molecular orbital level of PEDOT:PSS. The resulting improved energy level alignment would have facilitated hole-charge collection, which was further substantiated by a 6-fold increase in carrier lifetime.

11:20 AM E1.03
Tuning of Electrical and Optical Properties of Polycrystalline TiO_2-Based Transparent Conducting Films Piero Mazzolini[1, 2], Giuliano Gregori[3], Valeria Russo[1], Daniel Chrastina[4], Rafael O. Ferragut[4], Carlo S. Casari[1, 2] and Andrea Li Bassi[1, 2]; [1]Energy, Politecnico di Milano, Milano, Italy; [2]CNST @PoliMI, Istituto Italiano di Tecnologia, Milano, Italy; [3]Physical Chemistry of Solids, Max Planck Institute for Solid State Research, Stuttgart, Germany; [4]L-NESS, physics department, Politecnico di Milano, Como, Italy.

In this work we show and discuss the possibility of tuning electrical and optical properties of Ta-doped TiO_2 (TaTO) thin films by exploring the effect of different synthesis and post-deposition annealing conditions. The interest in TiO_2-based Transparent Conducting Oxides (TCO) is related to the peculiar properties of TiO_2, such as its high chemical stability in reducing atmosphere. Moreover, the usual employment of TiO_2 as a blocking layer and photoanode in dye sensitized/perovskite solar cells, offers the possibility of implementing TiO_2-based TCOs for tuning material interfaces properties in real devices.

Amorphous TaTO films were deposited at room temperature on soda lime glass substrates via Pulsed Laser Deposition. The deposition was followed by thermal annealing to obtain single phase polycrystalline anatase. Undoped TiO_2 was deposited for comparison.

The best functional properties (resistivity $5.7x10^{-4}$ Ωcm for 150 nm thick TaTO film, mean transmittance in visible range exceeding 80%) were obtained when depositing with an oxygen pressure of 1.25 Pa followed by vacuum annealing at 550°C (ramp 10°C/min, 1 hour dwell, $p < 4\times10^{-5}$ Pa). Notably, we demonstrate here also the possibility to crystallize the films exploiting an ultra-fast thermal treatment at 460°C (ramp 300°C/min) by monitoring the crystallization threshold of the films via in-situ electrical

measurements. This process not only reduces the total time (nearly 8 minutes vs. almost 3 hours for a conventional heating cycle at 550°C) necessary to obtain high quality polycrystalline films, but gives also the possibility to uncouple the electrical properties from the influence of the atmosphere during fast crystallization. Remarkably, fast crystallization in N_2 (20-40 ppm of oxygen) yields virtually the same conductivity of a conventional annealing carried out in vacuum (for doped and undoped TiO_2). Complementary analyses were performed (XRD, Raman, Positron Annihilation Spectroscopy), with the aim of addressing the role of microstructure and defect chemistry.

11:40 AM E1.04
Indium-Zinc-Oxide TFTs Using *In Situ* Converted Al_2O_3/HfO_2 Gate Stack Yang Song[1], Stylianos Siontas[2], Alexander Zaslavsky[1, 2], David Paine[2] and Alexander Katsman[3]; [1]Physics, Brown University, Providence, Rhode Island, United States; [2]School of Engineering, Brown University, Providence, Rhode Island, United States; [3]Dept. of Materials Science and Engineering, Technion, Haifa, Israel.

Recently, oxide semiconductors have displaced a-Si as dominant materials for high-performance thin film transistors (TFTs). An important issue in oxide semiconductors in TFTs is the fabrication of a high-k dielectric gate stack with low leakage and good interface properties. Here we report a novel dielectric gate stack on high-mobility In-Zn-O (IZO) TFT channels by using an *in-situ* metal oxidation process.

Our top-gated IZO TFTs feature a thin 3 nm Al layer between the 10 nm thick IZO channel and 24 nm HfO_2 gate insulator. Anneals at 300 °C were used to convert Al *in-situ* into Al_2O_3, resulting in a passivated Al_2O_3/HfO_2 gate stack.

When the gate capacitance C_G-V_G of large TFTs (gate length L_G = 50 µm) is measured as a function of anneal time, the C_G-V_G loops show little hysteresis, with interface trapped charge density estimated at ~4×10^12 cm^{-2}. Transfer characteristics of 8-hour-annealed TFTs show excellent on/off ratio ~10^7, $|V_T|$ < 0.2 V, and high saturation mobility μ_S ~ 115 $cm^2/V{\cdot}s$ in large L_G = 50 µm TFTs.

In order to understand the effects of annealing on interface quality and carrier mobility, we have performed Hall effect measurements on ungated Van der Pauw samples fabricated analogously to the TFTs. Our preliminary data of low-field Hall mobility and sheet channel density *n* of annealed IZO channels as a function of measurement *T* in the 50–300 K range show: first, longer anneal time yields higher *n*, indicating that the reaction between Al and IZO injects more oxygen vacancies into the IZO channel; and second, the Hall mobility shows thermally-activated behavior under 100 K, whereas above 100 K the negative dependence of mobility on temperature is consistent with degenerate ionized impurity scattering. Additional measurements on gated Van der Pauw samples will be performed to quantify the influence of surface scattering.

SESSION E2: Poster Session
E: Transparent Conducting Oxides
Monday Afternoon, June 15, 2015
12:00 PM
Keystone Resorts, Red Cloud Peak

E2.01
Textured Transparent Conductive Oxide Electrode having Bilayer Structure of ITiO/GAZO Prepared by D.C. Magnetron Sputtering Yoshiyuki Abe and Kazuhide Hayashi; Ichikawa Research Laboratories, Sumitomo Metal Mining Co., Ltd., Ichikawa-city, Japan.

We have developed a new textured transparent conducting oxide (TCO) electrode having a bilayer structure of an indium oxide film doped with titanium (ITiO) and a zinc oxide film doped with gallium and aluminum (GAZO). Both of the films were prepared by the conventional d.c. magnetron sputtering method. The film of ITiO deposited on a glass substrate had characteristics of the high conductivity and the high transmittance in the visible region and the near-infrared region. The film of GAZO deposited on the ITiO film had the textured surface generating large haze of the TCO electrode. The haze of the TCO electrode depended on the deposition condition of the ITiO film; the ITiO film deposited without heating the substrate followed by heating at 350 °C (ITiO-1) was effective to promote the formation of the surface texture of GAZO leading to increase in the diffuse transmittance as compared with the ITiO film deposited with heating the substrate at 350 °C (ITiO-2). X-ray diffraction analysis with two-dimensional detector revealed that the ITiO-1 film had the crystal orientations of the film thickness direction and in-plane direction and that the GAZO film on the ITiO-1 film had strong c-axis orientation of the film thickness direction which was not shown in the GAZO film on the ITiO-2 film. The textured TCO electrode on glass substrate (glass/ITiO-1/GAZO) showed the low resistivity of 15 ohm/sq, the high total transmittance of 76 % in the wavelength of 400 – 1200 nm and the large haze value of 29 %. It may be candidate to replace the fluorine-doped tin oxide (FTO) films fabricated by CVD methods as front electrodes of thin-film-type solar cells.

E2.02
Effect of Different Size Silver Nano Particles on Frequency and Temperature Dependent Parameters of Discotic Liquid Crystals for Solar Cell Applications Avneesh Mishra; Centre of Material Sciences, University of Allahabad, Allahabad, India.

Avneesh Mishra, Sandeep Kumar and Ravindra Dhar

E2.03
On the Application of ZnO Varistor Material in Piezotronics Till Froemling[1], Raschid Baraki[1], Nikola Novak[1], Michael Hofstaetter[2], Peter Supancic[2] and Juergen Roedel[1]; [1]Materials Science, Technische Universtät Darmstadt, Darmstadt, Germany; [2]ISFK, Montanuniversität Leoben, Leoben, Germany.

In recent years, the modification of electrical properties of Schottky-barriers in piezoelectric semiconductors via mechanical strain has gained a lot of attention. This research field, termed piezotronics, has been shown to have huge potential for applications like gated field effect transistors and sensors [1]. Zinc oxide nano-wires that allow extensive deformation were the focus of many investigations of metal-semiconductor Schottky-barriers. Polycrystalline ZnO is well known for varistor applications. In this case, the potential barriers at grain boundaries inhibit electrical transport until breakdown at high voltages. Therefore, ZnO is often used for surge protection or for voltage regulation. The piezoelectric contribution to varistor properties has so far only been discussed with respect to the decrease of the onset of the non-linear current-voltage relationship and increase of leakage current due to possible potential barrier lowering. Hence, it is considered an unwanted effect in varistor applications.

In this work, the possibility of using varistor materials for piezotronic applications (e.g. as pressure sensor) will be discussed. Our investigations show a large impact of mechanical stress on the linear leakage current in ZnO varistor samples [2]. Extensive conductivity changes could be induced in this low voltage region via application of uniaxial pressure. Hence, very high possible Gauge factors (figure of merit for the use in strain/stress sensors) around 800 can be obtained. Commercial sensors can reach only a factor of 200 so far. Temperature dependent measurements show a highly complex behavior of the material with application of uniaxial pressure. This will be discussed with respect to potential barrier modification at the grain boundaries and the dominant conduction pathways in the material.

[1] Z.L. Wang, Nano Today, (2010), **5**, 540-552
[2] R. Baraki, N. Novak, T. Frömling, T. Granzow, J. Rödel, Appl. Phys. Lett., (2014), **105**, 111604

E2.04
Atomic Layer Deposition of Nanoscale Seed Layers for Enhanced Performance of Transparent Conducting Oxide Thin Films on Glass Stefan B. Nikodemski[1], Ryan O'Hayre[1], Arrelaine Dameron[2], David Ginley[2], John Perkins[2] and Joseph Berry[2]; [1]Metallurgical and Materials Engineering, Colorado School of Mines, Golden, Colorado, United States; [2]National Renewable Energy Laboratory, Golden, Colorado, United States.

Transparent conducting niobium doped TiO_2 films were deposited on amorphous substrates (glass) by sputtering. The deposition conditions to produce crystalline anatase films were first optimized and indicated that the substrate temperature and oxygen pressure are important parameters to produce the desired phase and high conductivity. To generate the anatase phase, films must be deposited in a high oxygen pressure environment with subsequent annealing/crystallization done in a reducing atmosphere (typically vacuum). The conductivity of these doped TiO_2films were improved through the use of nanoscale seed layers deposited by atomic layer deposition (ALD). The bottom seed layer appears to behave as a nucleation center during crystallization to produce films with larger crystal domains at lower temperatures. A variety of ALD growth conditions including precursor chemistry, seed layer thickness, and temperature were examined. Design of experiments was subsequently used to identify the key parameters to produce the highest performing thin films. Results mapping out this complex deposition parameter space and the consequences to the obtained electrical transport properties will be presented along with an observed order of magnitude enhancement in the Nb-TiO_2 films using a nucleation/seed layer approach. Raman spectroscopy, X-ray diffraction, and transmission measurements used to assess the role of the seed layer in determining the performance of the oxide thin films will also be presented.

SESSION E3: TCO 2—Materials, Processing, and Structures
E: Transparent Conducting Oxides
Chair: David Ginley
Tuesday Morning, June 16, 2015
Keystone Resorts, Quandary Peak I/II

10:30 AM **E3.01
Material Design of Novel Transparent Oxide Conductors/ Semiconductors Hideo Hosono; Tokyo Institute of Technology, Yokohama, Japan.

Transparent conducting oxides (TCO) and semiconducting oxides (TOS) are primarily made from a combination of In_2O_3, SnO_2, ZnO, Ga_2O_3, and CdO.[1)] We have concentrated on exploration of novel type TCO/TOS materials beyond these traditional materials. In this talk, I would like to talk about recent progress of our research along this direction. Concrete materials are as bellows:

A First GeO_2-based TCO: $SrGeO_3$ with cubic perovskite structure[2)]
This is a fist GeO2-based TCO material and is realized by utilizing unique electronic structure of cubic perovskite, superdegeracy.

B Amorphous electride semiconductors:[3)]
Electride is a crystal in which electrons serve as anions. Electron-doped $12CaO{\cdot}7Al_2O_3$ (C12A7:e) is the first RT-stable electride. We found amorphous C12A7:e shows semiconducting properties with a low work function of 3.0eV and chemical inertness. This material works as an electron-injection material for OLEDs.[4)]

C. D2-dimensional electrides:[5)]
We reported Ca_2N is a 2D-electride in which anionic electrons populate in between cationic layers $[Ca_2N]^+$. The mobility of this material is very high irrespective of high electron concentration. This feature comes from electron-electron interaction dominates the electron transport. Thus, 2D-electride may be regarded as bulk crystal of 2-dimensional degenerate gas (2DEG). Although Ca2N is not a transparent, this material concept will be useful for designing new TCMs.

D. Band lineup[6)]
P/N orientation and carrier dupability including SrGeO3 andC12A7 are comprehensively understood from the band lineup constructed for various materials.

[1)] Ginley, Hosono and Paine(Edited), Handbook of Transparent Conductors, Springer, 2010, [2)] Nat. Commun., 2, 470 (2011). [3)]Science, 333, 71 (2011)., [4)]IDW'14 Technical Digest, [5)] Nature, 494, 336 (2013), [6)] (Review) Jpn. J. Appl. Phys. 52 090001(2013).

11:00 AM E3.02
Effect of Phase Transition on Electronic Defects of Ni-Co Oxide and Its Application on Optoelectronics Shu-Yi Tsai[3, 1], Kuan-Zong Fung[1, 3], H.-Y. Bor[2] and C.-N. Wei[2]; [1]Materials Science and Engineering, National Cheng Kung University, Tainan City, Taiwan; [2]Chung-Shan Institute of Science and Technology(CSIST), Taoyuan County, Taiwan; [3]Research Center for Energy Technology and Strategy, National Cheng Kung University, Tainan City, Taiwan.

Transition metal oxides, nickel and cobalt oxides tend to crystallize in a rock salt structure at high temperatures. Due to the variation in oxidation states, the crystal structures of Ni/Co oxides will gradually change to a spinel structure, especially when the annealing temperatures is below 500℃.

The Ni/Co oxide spinel tends to adopt the inverse-spinel arrangement with the tetrahedral sites completely occupied by Co^{+3} since the ionic radius of Ni^{+2} is much larger than that of Co^{+3}.

NiCo2O4 spinel has been used as a bifunctional catalyst for oxygen evolution and reduction reaction as electrode in both inorganic and organic electrosyntheses. Recently, $NiCo_2O_4$ spinel was found to be an infrared transparent conducting material with potential for optoelectronic applications. By using rf magnetron sputtering technique, a $NiCo_2O_4$ solid film was deposited on a glass substrate from a sintered oxide target with the same composition. With annealing at adequate temperature, a thin film of nickel-cobalt oxides showing spinel structure was obtained. The electrical property of spinel film was measured using 4-probe technique. A resistivity as low as 10^{-2}~10^{-1} ohm/cm was obtained. The optical property of this spinel was also measured as a function of thickness/deposition time in the wavelength range of infrared radiation.

11:20 AM E3.03
Effect of Precursor Solvent on the Nature of Spin Coated 1at%Ga-ZnO Transparent Conducting Films Amit K. Srivastava and Jitendra Kumar; Materials Science, I I T Kanpur, Kanpur, India.

In pursuit of developing transparent conducting oxide (TCO) for replacement of indium-tin- oxide (ITO) in solar cells and photovoltaic devices, an attempt has been made to study the effect of three precursor solvents on the nature of 1at% gallium containing ZnO spin coated thin films. The solutions of zinc acetate and gallium nitrate precursors prepared in each methanol, ethanol, and 2-methoxyethanol are used to deposit thin films by spin coating on quartz substrates which, in turn, annealed purposely in vacuum at 500 °C for 1h to create oxygen vacancies.
All the films are characterized with regard to morphology, structure, crystallographic orientation, optical absorption, and electrical properties. They are shown to exhibit wurtzite-type hexagonal structure, optical transmittance of 70-100%, and sheet resistance in the range of $5.16x10^2$-$1.11x10^3$ Ω/ Sq depending upon the solvent. On the basis of factors like toxicity, sol stability and resulting properties, ethanol is suggested as the most appropriate solvent to yield quality TCO thin films of 1at% Ga- ZnO with (0001) preferred orientation, 75-96% transmittance in the wavelength range 400-900 nm, electrical resistivity of ~ $3x10^{-2}$ Ω-cm, and carrier mobility of ~ 24 $cm^2V^{-1}s^{-1}$ for solar cell, photovoltaic, flat panel display, and touch screen monitor applications. Also, a novel way is demonstrated for further reduction of the electrical resistivity by about an order with introduction of extra zinc species during the solution preparation stage itself.

11:40 AM E3.04

Transparent and Conductive Coatings with Nanoparticulate Magnetic Additives Gesa Beck[1], Stephan Barcikowski[2], Bilal Goekce[2], Maja Jelic[1] and Martin Kirsch[3]; [1]Physics, Chair of Resource Strategies, Augsburg, Germany; [2]Technical Chemistry I , University of Duisburg-Essen and Center for Nanointegration Duisburg-Essen (CENIDE) , Essen, Germany; [3]Fa. Kirsch Kunststofftechnik GmbH, Ebersbach, Germany.

Indium-Tin-Oxide (ITO) coatings are todays most important transparent and electrical conducting coatings, but indium is an especially rare and resource critical element. Therefore, there are research activities to find substitutions for ITO. A new promising approach is shown here: The preparation of transparent and electrical conducting coatings on a plastic varnish base with ferromagnetic nano-additives. For this purpose, the nano-additives were dispersed into a transparent varnish and the obtained dispersions were coated onto transparent plastic substrates. During hardening of the dispersion the magnetic nano-additives were aligned into lines by a magnetic field. Accordingly, the formed coatings have electrical pathways along the lines and areas of high transparency between the lines. The electrical conductivity is correspondingly anisotropic and it depends on the alignment of the nano-additives as well as on the thickness of an oxide and/or solvent shell around the nano-additives. The transparency also depends on the alignment and here especially on the thickness, the distance and the number of the formed lines. The quality of the alignment in turn, depends on the magnetic properties and on the size of the particles. We used commercial plastic varnishes [which form electrically isolating ($\geq 10^{-12}$ S/m) and transparent (about 90 %) coatings] and () different magnetic additives such as Co-, $CoPt_3$-, and Fe@Au-nanoparticles as well as Co- and CoNi-nanowires. With Fe@Au-nanoparticles coatings with even discharging conductivities (10^{-5} S/m - 10^{-6} S/m) and good transparencies (about 70 %) could be prepared. The coatings with the other nano-additives have antistatic electrical conductivities (10^{-9} S/m - 10^{-7} S/m) and transparencies up to 80 %. Furthermore, in addition to the magnetic nano-additives, transparent Al_2O_3-particles and carbon-nanotubes (CNTs) were added to the varnish. The coatings with the additional transparent particles show more transparency, but less electrical conductivity. The coatings with CNTs and magnetic nanoparticles have a higher conductivity than coatings with only the magnetic nanoparticles, but with much less transparency. Moreover, ionic liquids as dispersing agents increase the electrical conductivity of the coatings and the stability of the used dispersion.

F/H: Solid State Photoelectrochemistry/High Temperature Routes to Solar Fuels

* Invited Speaker
** Keynote Speaker

SESSION F/H1: Solid State Photoelectrochemistry/High Temperature Routes to Solar Fuels I
F/H: Solid State Photoelectrochemistry/High Temperature Routes to Solar Fuels
Chair: Tim Davenport
Monday Morning, June 15, 2015
Keystone Resorts, Grays Peak III

10:30 AM **F/H1.01
Concentrating Solar Thermochemical Fuels: Key Materials Issues for Commercial Viability and Scalability Ellen B. Stechel[1] and James E. Miller[2]; [1]LightWorks, Arizona State University, Tempe, Arizona, United States; [2]Sandia National Laboratories, Albuquerque, New Mexico, United States.

Sunshine to Petrol was a multidisciplinary effort organized at Sandia National Laboratories that progressed down a technical path for systems (sunlight to liquid hydrocarbons), reactors (CR5, packed bed particles), and materials (redox active ceria and more recently perovskite metal oxides). The objective is to synthesize liquid hydrocarbon fuels from concentrated sunlight, waste carbon dioxide, and brackish water motivated to address the dual challenges posed by the strategic and economic importance of petroleum and the increasing concentration of atmospheric carbon dioxide. In this presentation, we will talk about a number of comparative metrics of significance and concern to accelerating a transition to a low carbon sustainable transportation future. We present a general examination of resource and economic considerations and conclude that solar-to-fuel ef ficiency is a key metric that drives not only the potential impact (scalability) of a technology for storing (contemporary) sunlight and sequestering carbon above ground as energy dense fuels, but also the economics. Given the importance of high efficiency, we will present some key considerations and approaches to achieving the required high efficiency with an emphasis on material properties and requirements.

11:00 AM F/H1.02
Discovery of Novel Perovskites for Solar Thermochemical Water Splitting from High-Throughput First-Principles Calculations Antoine A. Emery and Chris Wolverton; Materials Science and Engineering, Northwestern University, Evanston, Illinois, United States.

The use of hydrogen as fuel is a promising solution to reduce the amount of greenhouse gases emitted into the atmosphere. Among the several possible routes of synthesis, thermochemical water splitting (TWS) cycles is a promising method for large scale production of hydrogen. The choice of metal oxide used in a TWS cycle is critical since it governs the rate and efficiency of the gas splitting process. In this work, we present a high-throughput density functional theory (HT-DFT) study of ABO_3 perovskite compounds to screen for thermodynamically favorable two-step thermochemical water splitting materials. We demonstrate the use of two screens, based on thermodynamic stability and oxygen vacancy formation energy, on 5,329 different compositions to predict 104 stable potential candidate materials for water splitting applications. Several of these compounds have not been experimentally explored yet and present promising avenues for further research. Additionally, our results show that several considerations such as the oxidation state and atomic sizes of the constituent elements influence the performance of TWS materials. Finally, the large dataset of compounds and stability in our possession allowed us to revisit the structural maps for perovskites. This study shows the benefit of using first-principles calculations to efficiently screen an exhaustively large number of compounds at once. It provides a baseline for further studies involving more detailed exploration of a restricted number of those compounds.

11:20 AM *F/H1.03
Fuel Production from Concentrated Solar Radiation Christian Sattler and Martin Roeb; Solar Chemical Engineering, German Aerospace Center - DLR, Cologne, Germany.

Concentrated solar radiation is an option to produce fuels in large quantities by thermochemical reactions based on the splitting of water or CO_2. To achieve the possible very high theoretical efficiency of the processes presently under development a special focus has to be put on how to couple the concentrated radiation to the chemical reactions. The talk will cover options how to design solar concentrators and receiver reactors for different chemical reactions at differnt temperature levels. On the example of the solid metaloxide thermochemical cycles a roadmap to an industrial plant will be discussed starting with the present state of the art and evaluating the gaps that have to be closed to prepare the technology firstly for a further scale-up and secondly for being economically competitive.

11:40 AM F/H1.04
Decisive Thermodynamic Factor of Perovskite Catalysts for Thermochemical Water Splitting Yoshihiro Yamazaki[1, 2], Chih-Kai Yang[3] and Sossina M. Haile[3]; [1]Inamori Frontier Research Center, Kyushu University, Fukuoka, Japan; [2]Japan Science and Technology Agency, Kawaguchi, Japan; [3]California Institute of Technology, Pasadena, California, United States.

Two-step thermochemical water splitting is a unique way to produce hydrogen in use of water dissociation. At a higher temperature, oxygen would be released from the oxide while making oxygen vacancies in the oxide. Exposed to vapor at a reduced temperature, the oxide will be reoxidized with water where the oxide absorbs oxygen from water molecules while releasing hydrogen to the atmosphere. Utilization of partial redox in nonstoichiometric oxides speeds up the reaction rate, which makes it possible to determine the solar-fuel conversion efficiency. Here we chose strontium-doped lanthanum manganite perovskite as a catalyst for thermochemical water splitting. We measured oxygen and hydrogen yields in the two-step thermochemical cycle between 800 and 1400 C. Both oxygen and hydrogen yields increase with increasing strontium substitution in the perovskite, which quantitatively agrees with what thermodynamics suggests. The peak value of hydrogen kinetics decreases with increasing the strontium content. The slow kinetics at higher strontium content is due to lower driving force of water dissociation.

SESSION F/H2: Poster Session: Solid State Photelectrochemistry/ High Temperature Routes to Solar Fuels
F/H: Solid State Photoelectrochemistry/High Temperature Routes to Solar Fuels
Monday Afternoon, June 15, 2015
12:00 PM
Keystone Resorts, Red Cloud Peak

F/H2.01
Material Design Criteria for Solar-to-Fuel Perovskites: Lower Temperature-Operation Range with Strontium and Cobalt Doped Lanthanum Chromates Alexander H. Bork, Markus Kubicek, Michal Struzik and Jennifer Rupp; Materials - Electrochemical Materials, ETH Zürich, Zürich, Switzerland.

Two-step thermochemical fuel production is an attractive renewable energy technology utilizing solar power to convert water and carbon dioxide into synthetic fuels. Ceria typically cycled at temperatures as high as 1000-1500 ˚C received most attention due to a high theoretical efficiency. Despite the promise, increasing the efficiency is impaired, since extrinsic doping of the fluorite structure of ceria has limited effect on the

oxygen release and storage capacity. Here, perovskites with the general formula ABO_3 are a promising alternative material class to increase efficiency, owing to wide possibilities of doping both the A- and the B-site cation. In this work we apply new thermodynamic design criteria for doping solar-to-fuel perovskites. With this approach, we exploit the significant variations in the non-stoichiometry and thermodynamic properties obtained by doping. We demonstrate the generality of the material criteria by a systematic experimental study of the splitting capabilities of Co- and Sr-doped lanthanum chromates. Indeed, for $La_{0.6}Sr_{0.4}Cr_{0.8}Co_{0.2}O_{3-\delta}$, similar fuel yield as for ceria were obtained but for a 300°C lower temperature in the reduction step. Raman spectroscopy and in-situ XRD proved the absence of carbonates and structural stability of all compositions, which is crucial for cyclability and long term performance. The newly suggested perovskite compound can be operated as a lower temperature solar-to-fuel reactor material to minimize heat loss and ultimately lower the cost of solar synthesized fuel.

F/H2.02

Thermodynamics of Praseodymium-Doped Ceria for Thermochemical Water Splitting Timothy C. Davenport[1], Webster Guan[1] and Sossina M. Haile[2]; [1]California Institute of Technology, Pasadena, California, United States; [2]Northwestern University, Evanston, Illinois, United States.

Two-step thermochemical water splitting has become a promising route to generate hydrogen from water with solar energy. One particularly attractive approach uses ceria as the reactive medium due to its rapid reaction kinetics, encompassing both high surface reaction rates and rapid bulk diffusion. However, due to the high enthalpy associated with ceria reduction, very high temperatures (1500 °C) are required to reduce ceria sufficiently for water splitting. Thus, introduction of redox-active dopants with a lower enthalpy of reduction has been a strategy that has been pursued for improving hydrogen yields with lower reduction temperatures. In this contribution, we will present a thermodynamic characterization of ceria materials doped with the redox-active dopant praseodymium ($Ce_{1-x}Pr_xO_2$, x = 0.05 – 0.6) by thermogravimetric analysis and consider the implications for thermochemical water splitting.

F/H2.03

Investigation on Nonstoichiometric Perovskite Oxides of $Sr_{1-x}La_xMn_{1-y}Al_yO_{3-\delta}$ for Solar Thermochemical Hydrogen Production Debora Barcellos[1], Jianhua Tong[1], Michael Sanders[1], Anthony McDaniel[2] and Ryan O'Hayre[1]; [1]Metallurgical & Materials Engineering, Colorado School of Mines, Golden, Colorado, United States; [2]Sandia National Laboratories, Livermore, California, United States.

Solar thermochemical (STC) fuels production is seeing increased scientific interest because of its high theoretical efficiency (~60%). The nonstoichiometric perovskite oxides of $Sr_{1-x}La_xMn_{1-y}Al_yO_{3-\delta}$ (SLMA) were discovered in our recent work (*Energy & Environmental Science, 2013, 6 (8), 2424-2428*) to be excellent STC materials for both water splitting and carbon dioxide decomposition, and demonstrated a hydrogen yield of 9 times higher than ceria, the state-of-the-art STC material. However the kinetics of the water splitting (reoxidation) step is much slower for SLMA than that for ceria. Furthermore, even small changes in SLMA stoichiometry are thought to significantly alter the reoxidation kinetics. Because Mn-containing materials frequently suffer from Mn-loss during calcination at high temperatures (e.g. 1300ºC), we adopt a modified polymeric gelation synthesis method and calcination profile for the synthesis of SLMA, which allows precise control of the SLMA stoichiometry. Based on this process, rectangular bars of stoichiometric SLMA and Mn-deficient SLMA were fabricated for conductivity measurement. Steady-state and transient conductivities versus temperature, oxygen partial pressure, and water vapor pressure were measured by a four-probe DC method and used for deriving the diffusivities of oxygen vacancy and electron hole and the surface reaction constant. These measurements are used to provide insights into the reoxidation mechanism in SLMA, which involves the combination of surface reaction ($H_2O + V_O^{\circ\circ} = O_O^x + 2h^\circ + H_2$) and bulk internal oxidation (ambipolar diffusion of oxygen vacancies and electron holes from the surface to the bulk).

F/H2.04

Polarization Enhanced Transport of Hot Carriers in Liquid/InGaN Semiconductor Junctions Blair C. Connelly, Anand V. Sampath, Ryan W. Enck, Chad S. Gallinat, Stephen B. Kelley, Nathaniel T. Woodward, Grace D. Metcalfe, David R. Baker, Cynthia A. Lundgren, Hongen Shen, Meredith L. Reed and Michael Wraback; US Army Research Laboratory, Adelphi, Maryland, United States.

Solar water splitting efficiency is reduced by the kinetic limitations of hydrogen/oxygen evolution reactions at doped semiconductor surfaces that generally requires an overpotential to drive the reaction that results in a lower efficiency than theoretically predicted. Conversely, polarization charges present at the heterointerfaces of *c*-plane, wurtzite nitride heterostructures can be engineered to extend the depletion width to match the absorption layer thickness while creating strong electric fields associated with a large internal potential to drive electrons to the semiconductor/liquid junction for a more efficient reaction. InGaN is ideally suited as an absorber of solar radiation as its bandgap can be tuned between 365 nm and 2 μm, which spans the solar spectrum. We propose the use of the InGaN/*p*-GaN material system for the production of efficient and unassisted solar water-splitting cells. This is made possible by the transport of hot, energetic electrons to the InGaN-liquid junction in polarization-engineered InGaN heterostructures. Time-domain THz measurements are used to demonstrate the ability of InGaN on GaN to drive electrons to the semiconductor surface, showing that the acceleration of optically-generated electrons is toward the InGaN surface due to an internal electric field that is primarily associated with piezoelectric polarization charges at the heterointerface. Time-resolved electro-absorption measurements of carrier velocities in InGaN/GaN heterostructures indicate velocity overshoot, which demonstrates the ability to provide hot electrons to overcome the reaction overpotential at the semiconductor/liquid junction. The ability to drive energetic electrons to the semiconductor/liquid interface indicates that this system is capable of an unassisted reaction. Furthermore, initial results have demonstrated that GaN is corrosion resistant to oxidation reactions up to 2.5 V vs. Ag/AgCl in low pH electrolytes. InGaN/GaN strucutres would therefore provide a stable substrate, indicating that InGaN/GaN heterostructures will withstand the harsh environment in electrolyte solutions.

F/H2.05

Electrocatalyst-Semiconductor Interfaces in Water Splitting Photoelectrodes Shannon W. Boettcher; Chemistry, University of Oregon, Eugene, Oregon, United States.

High-efficiency photoelectrochemical water-splitting devices require integrating electrocatalysts (ECs) onto light-absorbing semiconductors (SCs), but the energetics and charge transfer processes at SC|EC interfaces are poorly understood. In order to understand ECs on photoanodes, we fabricate model EC-coated single-crystal TiO_2 electrodes and directly probe SC|EC interfaces *in situ* using a new dual-electrode photoelectrochemistry technique to independently monitor and control the potential/current at both the SC and the EC.[1] We discover that redox-active ion-permeable ECs such as $Ni(OH)_2$/NiOOH yield "adaptive" SC|EC junctions where the effective Schottky barrier height changes *in situ* with the oxidation level of the EC. In contrast, dense, ion-impermeable IrO_x ECs yield constant-barrier-height "buried" junctions. Conversion of dense, thermally deposited NiO_x on TiO_2 into ion-permeable $Ni(OH)_2$/NiOOH correlated with increased apparent photovoltage and fill-factor. A new theory of adaptive EC|SC junctions is proposed and applied via numerical simulation to understand this behavior.[2] The theory can also be used to understand catalyst-modified hydrogen-evolving photocathodes as well as catalyst-modified visible-light-absorbing oxides such as $BiVO_4$, and experiments are underway to directly test the predictions. These results provide new insight into the dynamic behavior of SC|EC interfaces that help guide the design of efficient SC|EC devices. They also illustrate a new class of adaptive semiconductor junctions.

(1) Lin, F.; Boettcher, S. W. Adaptive semiconductor-electrocatalyst junctions in water splitting photoanodes. *Nature. Mater.* **2014**, *13*, 81-86.
(2) Mills, T. J.; Lin, F.; Boettcher, S. W. Theory and simulations of electrocatalyst-coated semiconductor electrodes for solar water splitting. *Phys. Rev. Lett.* **2014**, *112*, 148304.

F/H2.06

Photoelectrochemical Water Splitting Promoted with a Disordered Surface Layer Created by Electrochemical Reduction Pengli Yan[1, 2], Yang Gan[1] and Can Li[2]; [1]Harbin Institute of Technology, Harbin, China; [2]Dalian Institute of Chemical Physics, Chinese Academy of Sciences, Dalian, China.

The recent discovery of colored TiO_2 indicated that the disordered surface layer over the TiO_2 particles/photoelectrodes is beneficial for higher photocatalytic performance; however, the role of the disordered surface TiO_2 layer is not well understood. Here, we report an electrochemical strategy for tuning the surface structure of TiO_2 nanorod arrays (NRAs) and try to understand the role of the disordered surface TiO_2 layer. Photoelectrodes of TiO_2 NRAs with a disordered shell were prepared by an electrochemical reduction method. The photocurrent of the NRAs with a disordered shell can reach as high as ~1.18 mA/cm^2 at 1.23 V, which is 2.2 times of that of the pristine TiO_2 NRAs. Our results show that the surface disordered layer not only improves the bulk charge separation but also suppresses the charge recombination at the electrode/electrolyte interface, acting as an efficient water oxidation co-catalyst of photoelectrochemical cell for solar water splitting.

Keywords: TiO_2 Nanorod arrays; surface disorder layer; electrochemical reduction; water splitting; charge injection efficiency

F/H2.07

Comprehensive Photoelectric Characterization of Dye-Sensitized Solar Cells Dang-Thanh Nguyen[1], Seok-Jae Kim[3], Eui-Chol Shin[1], Soon-Hyung Kang[2], Eun-Mi Han[3] and Jong-Sook Lee[1]; [1]School of Materials Science and Engineering, Chonnam National University, Gwangju, Korea (the Republic of); [2]Department of Chemistry Education, Chonnam National University, Gwangju, Korea (the Republic of); [3]School of Applied Chemical Engineering, Chonnam National University, Gwangju, Korea (the Republic of).

In spite of the worldwide extensive research efforts for the developments of solar cells (Thin films solar cells, DSSCs, OPV cells…) in-depth electrical characterization using impedance spectroscopy appears to be limited to a very few research groups. In this work, we perform a comprehensive photoelectric characterization of dye-sensitized solar cells (DSSCs) constituted of a nanostructured TiO2 semiconductor on a transparent conducting oxide (TCO), a photoactive dye material (N719 dye), and Pt counter electrode. Not only I-V characterization, impedance spectra are taken at different potentials over a wide frequency range in dark and under different illumination condition. I-V measurements provide the typical cell properties as the short-circuit current, open-circuit voltage, fill factor and conversion efficiency. The general impedance model for DSSC developed by Bisquert group provides more detailed information on the cell performance in view of the materials and processing. The electron kinetics parameters such as recombination lifetime, diffusivity, diffusion length by impedance analysis are favorably compared with those by light-modulated methods (IMVS/IMPS). The difference in the cell performance of many laboratory prepared cells will be in-depth understood.

F/H2.08

Impedance Spectroscopy of Various ZnO Photoelectrodes Prepared by Solution Method Dang-Thanh Nguyen, Dong-Chun Cho, Eui-Chol Shin and Jong-Sook Lee; School of Materials Science and Engineering, Chonnam National University, Gwangju, Korea (the Republic of).

ZnO films on ITO substrates grown in the nitrate solution at 90ºC upon the seed layer prepared by bias-assisted deposition and thermal annealing at 500ºC were investigated as photoanodes for the water splitting. By controlling the voltage level and the solution concentration, different morphologies of the nanorod films can be prepared. Lower seed deposition voltage of 1.2 V and lower concentration of 0.1 M led to the formation of the dense film of 1 μm thickness of well-aligned nanorods, which exhibited I-V curve of an ideal Schottky barrier. The higher concentration of 0.5 M resulted in the inhomogeneous coverage of the substrate. The higher deposition voltage of 2.5 V and higher concentration of 0.5 M resulted in the skeleton structure which developed into the brush-like morphology upon secondary growth. The combination of high voltage (2.5 V) and low concentration (0.1 M) resulted in randomly grown nanorods film of ca 3 μm thickness exhibited high photocurrents but also substantial leakage. With increased seed deposition time from 5 min to 10 min the best photoelectrochemical performance was obtained which can be attributed to the sufficient coverage of ITO substrate during the seed deposition. Besides standard photoelectrochemical characterization of photocurrents and IPCE and in-depth electrochemical impedance spectroscopy was performed as a function of potential not only in the anodic region but also in the cathodic range. Deconvolution of the frequency-independent Schottky capacitance parameter is attempted for the anodic behavior, while the electron kinetic parameters of ZnO can be derived by the transmission line model analysis in the cathodic regime. A comprehensive modeling to bridge two regimes is under development. The parametric analysis will provide the relation between morphology and performance of various ZnO electrodes.

F/H2.09

Transport Properties of the Heterojunction Formed between a Fe/Y-Codoped $BaZrO_3$ Mixed Conductor and a Ti-Doped Fe_2O_3 Light Absorber for an Elevated-Temperature Solid-State Photoelectrochemical Cell Madhur Boloor, Xiaofei Ye, Liming Zhang, Nicholas A. Melosh and William C. Chueh; Materials Science and Engineering, Stanford University, Fremont, California, United States.

The majority of photoelectrochemical cells used for solar water splitting operate at room temperature with a liquid electrolyte, and are limited by kinetics and thermodynamic losses at heterojunction and electrolyte interfaces. It has been recently determined via a detailed-balance calculation that the migration to a solid-state heterojunction device operating at elevated temperature could lead to solar-to-hydrogen efficiencies as high as 17% at 450^{0}C for a semiconductor with a 2.0eV bandgap and a 0.3 eV band offset [1]. In this work, we experimentally examine the transport properties and band alignment for a thin film heterojunction interface between a Ti-doped Fe_2O_3 light absorber and a Fe/Y-codoped $BaZrO_3$ (Fe-BYZ) mixed ionic and electronic conductor to determine its viability to be used in a solid-state PEC.

We show the protonic and electronic conductivities for the Fe-BYZ thin film as the Fe-doping was increased incrementally to 50% while the Y-doping remained constant at 20%. For hydrated films, the conductivity showed a weak dependence on the varying partial pressure of oxygen as the conductivity was dominated by protonic transport. This value of protonic conductivity did not vary significantly with Fe-codoping, whereas the electronic conductivity increased with Fe, as consistent with recent reports by Kim et al [2]. Increasing the Fe-codoping was additionally shown to significantly decrease the valence band offset between the Fe-BYZ and the Ti- Fe_2O_3 from 1.6 to -0.1 eV.

[1] X. Ye, *et al*. *Phys. Chem. Chem. Phys*., 2013, **15**, 15459-15469
[2] D. Kim et al. ECS Trans., 2012, 45 (1) 161-170

F/H2.10

Polarity and Doping Effects on the Photoelectrochemial Performance of ZnO Single Crystalline Anode by In-Depth Impedance Spectroscopy Eui-Chol Shin[1], Dang-Thanh Nguyen[1], Joachim Maier[2] and Jong-Sook Lee[1]; [1]Materials Science and Engineering, Chonnam National University, Gwang-Ju, Korea (the Republic of); [2]Max Planck Institute for Solid State Research, Stuttgart, Germany.

The ZnO C-plane bulk photoanodes with diffusion-bonded ohmic Pt back contacts were prepared by splitting C-plane bicrystals with different crystallographic polarity and dopants of Mn and Co. As well as the standard photoelectrochemical characterization of j-V behavior and IPCE, the semiconductor-electrolyte interface was characterized by electrochemical impedance spectroscopy (EIS) as a function of potentials not only in the anodic region but also in the cathodic range. Deconvolution of the frequency-independent Schottky capacitance parameter is attempted for the anodic behavior, while the electron kinetic parameters of ZnO can be derived by the transmission line model analysis in the cathodic regime. A comprehensive modeling to bridge two regimes is under development. The parametric analysis will provide a fundamental understanding of the photoelectrochemical properties of ZnO material. Polarity-engineered ZnO materials can be a promising candidate for the high performance photoanodes.

F/H2.11

Impedance Spectroscopy on Fe_2O_3 Films Prepared by Anodization for Photoelectrochemical Applications Eui-Chol Shin[1], Dong-Chun Cho[1], Dang-Thanh Nguyen[1], Soon-Hyung Kang[2], Hui-Kyung Park[1], Jaeyeong Heo[1] and Jong-Sook Lee[1]; [1]Materials Science and Engineering, Chonnam National University, Gwang-Ju, Korea (the Republic of); [2]Chemistry Education, Chonnam National University, Gwang-ju, Korea (the Republic of).

Hematite is a promising photoelectrode material because of its significant light absorption, chemical stability in aqueous environments, plentiful supply and relatively low cost. Poor electronic conductivity, carrier trapping and phonon coupling, and high surface overpotentials are limiting its performance as a water-oxidizing photoanode. Nanostructuring is one of the strategies to improve the performance. As in the case of Ti and Al, nanotubular oxides can be prepared by anodization of Fe foils. Different nanostructure of iron oxides was prepared by changing the anodizing bias and temperature. At same temperature, the higher bias led to the larger size of tubular holes. Anodization at higher temperature resulted in aggregates of the separated nanotubes, the size of which depends on the anodization voltage. Annealing at 500°C, however, made the anodized films and as-received Fe foils almost indistinguishable, without any indication of the tubular morphology. The photoelectrochemical performance indicated some correlation with the anodization process. As annealing destroyed the anodized structures, stabilization by Al_2O_3 coating by the atomic layer deposition (ALD) was attempted. To obtain frequency-independent Mott-Schottky analysis, capacitance spectroscopy using Havriliak-Negami models were employed for the impedance spectra measured at different potentials and near flatband potential and breakdown regions were separated from the reverse biased semiconductor-electrolyte junction consistent with I-V characteristics. Cathodic characteristics are related with the electron kinetic parameters of Fe_2O_3 by diffusion-recombination impedance model.

F/H2.12

Cation-Control of Aggregation in the Conjugated Polyelectrolyte TFB Meilin Li and Stefan Adams; Materials Science & Eng., National University of Singapore, Singapore, Singapore.

TFB (poly(9,9'-di-n-octylfluorene-alt-N-(4-butylphenyl)-diphenylamine)) is a conjugated polyelectrolyte with two alkyl side chains per monomer that are terminated by sulfonic acid groups wherein the protons can be exchanged by various monovalent cations. The combination of optoelectronic/redox properties of the conjugated backbone, ionic contributions to charge transport, solvatochromism, enhanced solubility and processability due to the ionic side groups led to significant technical interest for hole transport in organic solar cells or LEDs.

However, the charge transport properties of TFB and related amphiphilic ionomers are strongly affected by the formation of ionic aggregates. Obviously the strength of the cation sulfonate interaction and hence the choice of the cation can be employed to control the tendency for aggregation and thereby the optoelectronic properties of TFB. To overcome the limited insight so far available on the atomic level structure of cation-exchanged TFB phases, we applied systematic Molecular Dynamics (MD) simulations combining TFB with a wide range of monovalent cations of different coordination strengths (Li^+, Na^+, K^+, Rb^+, Cs^+, NMe_4^+ and $P(ph)4^+$). In all cases a complete ion exchange is assumed, so that the number of cations of the respective type equals the number of (fully deprotonated) sulfonate groups. The resulting MD trajectories for each cation-TFB polyelectrolyte are analysed with respect to the influence of the cation type on the ionic aggregation and related structural features that may affect the conduction mechanism. As a key tool we employed the analysis of Radial Distribution Function (RDF), Running Coordination Number (RCN) of cations and sulfonate groups as well a statistical evaluation of the forming ion clusters and the intramolecular as well as intermolecular order parameters of the polymer chains. These simulations reveal how the coordination strength of the chosen cation controls the size and extent of cation-cation as well as cation-anion clustering in TFB. MD simulations thus provide a novel insight into cation aggregation and its influence on the optoelectronic properties of TFB.

SESSION F/H3: Solid State Photoelectrochemistry/High Temperature Routes to Solar Fuels II
F/H: Solid State Photoelectrochemistry/High Temperature Routes to Solar Fuels
Chairs: Shannon Boettcher and Tim Davenport
Monday Afternoon, June 15, 2015
Keystone Resorts, Grays Peak III

2:30 PM *F/H3.01

Characterization of La-Mn Perovskites and Doped Ceria for Thermochemical H_2O and CO_2 Splitting Applications Jonathan Scheffe[1], Thomas Cooper[2], Michael Takacs[2] and Aldo Steinfeld[2]; [1]Mechanical and Aerospace Engineering, University of Florida, Gainesville, Florida, United States; [2]Department of Mechanical and Process Engineering, ETH Zurich, Zurich, Switzerland.

Doped La-Mn perovskite oxides and doped ceria are both considered promising reaction intermediates for solar thermochemical production of fuels through H_2O and CO_2 splitting. Current state of the art materials, such as pure ceria, are stable at elevated temperatures and display rapid kinetics, but suffer from relatively low nonstoichiometries. This necessarily places a moderately low upper limit on the efficiency of a ceria based thermochemical cycle unless operating under extreme conditions (high T, low p_{O2}). From a thermodynamic point of view, a more ideal oxide would have a lower reduction enthalpy than ceria, resulting in lower operating temperatures, and a higher reduction entropy, resulting in a smaller temperature difference between reduction and oxidation steps. Both of these effects would have a direct impact on process efficiencies and operating constraints, as temperatures approaching the stability limit of metallic components rather than refractory ceramics may be achievable. In this talk we will discuss recent experimental results for La-Mn perovskites doped with Ca^{2+} and Sr^{2+} on the A-site and Al^{3+} on the B site, and Zr^{4+} doped ceria, in the context of their thermodynamic impact on two step thermochemical cycles. Previously identified $La_{0.6}Sr_{0.4}Mn_{0.6}Al_{0.4}O_3$ (LSMA) and the newer $a_{0.6}Ca_{0.4}Mn_{0.6}Al_{0.4}O_3$ (LCMA) boast a four- to nine-fold improvement in the reduction extent compared to the state-of-the-art material CeO_2 in the temperature range T_{red}= 1200 to 1400 °C. The increase in reduction extent when doping ceria with Zr^{4+} was not as dramatic but increases substantially with increasing Zr^{4+} concentration. In both cases, the increase in reduction extent was attributed to significantly lower reduction enthalpies; however, reduction entropies were negatively affected, resulting in larger temperature swings between reduction and oxidation steps. Nevertheless, we show that process efficiencies may be increased substantially compared to pure ceria using select perovskite materials and present a pathway for further increasing the efficiency and practicability of solar thermochemical cycles through material design.

2:50 PM F/H3.02

Perovskites from Earth-Abundant Elements for Thermochemical Energy Storage Rounak Kharait[1], Luca Imponenti[1], Michael Sanders[2], Jianhua Tong[2], Ryan O'Hayre[2] and Gregory S. Jackson[1]; [1]Mechanical Engineering, Colorado School of Mines, Golden, Colorado, United States; [2]George S. Ansell Dept. of Metallurgical and Materials Engineering, Colorado School of Mines, Golden, Colorado, United States.

To explore the feasibility of perovskites derived from earth-abundant elements, our team has explored doped calcium manganites for thermochemical energy storage (TCES). Perovskites of the form $CaM_xMn_{1-x}O_{3-\delta}$ (where M is earth-abundant cation dopant) have been studied for their potential in concentrated solar power plants wherein particles are reduced in N_2 (with O_2partial pressures, $P_{O2} \approx 10^{-4}$ bar) at temperatures T_h = 900 °C or higher in a solid-particle central solar receiver. Energy stored in the particles both chemically and sensibly can be released to a power-cycle working fluid as needed by reoxidation and cooling in a fluidized bed oxidation reactor / heat exchanger. This study presents thermogravimetric measurements and differential scanning calorimetry to test $CaM_xMn_{1-x}O_{3-\delta}$ where M=Fe or Cr with values of $x \leq 0.1$ for the potential of these earth-abundant perovskite compositions for TCES over 600 kJ/kg with T_h at or above 900 °C and $P_{O2} \approx 10^{-4}$ bar and cold storage at T_c = 500 °C and $P_{O2} \approx 0.21$ bar.

The thermodynamic tests are complemented by kinetic measurements in a packed bed reactor in which rates of O_2 release and uptake are measured

for particles (250-400 μm in diameter) as a function of temperature and P_{O2}. Measurements indicate that the most favorable TCES capacities with cyclic stability are obtained for $CaCr_xMn_{1-x}O_{3-\delta}$ and $CaFe_xMn_{1-x}O_{3-\delta}$ with the lowest values of x that stabilize the perovskite structure during high-temperature reduction. For these compositions, the extent of reduction (i.e., δ) significantly increases with T_h from 900 to 1000 °C with total TCES capacity approaching 850 kJ/kg at 1000 °C with more than half the TCES in chemical energy. Kinetic measurements show that reoxidation is much more rapid than high-temperature reduction, thereby implying the challenge to find compositions with optimal reduction kinetics for integration into concentrated solar particle receivers.

3:10 PM **F/H3.03
Engineering Materials and Interfaces for Efficient and Stable Photocatalytic Water Splitting Jinhui Yang, Jason K. Cooper, Francesca M. Toma and Ian D. Sharp; Lawrence Berkeley National Laboratory, Berkeley, California, United States.

Photoelectrochemical conversion of solar energy to chemical fuel relies on the availability of semiconductors that are stable under aqueous conditions, possess bandgaps suitable for harvesting light from the sun, and can be integrated with active catalysts. Regardless of the desired reduction product, water oxidation is necessary to provide an abundant source of protons and electrons for fuel formation. However, semiconductor (photo)corrosion under oxidizing conditions has limited the application of materials like Si, which are characterized by rapid performance degradation and instability. Indeed, a recent life-cycle net energy analysis revealed that a lifetime of 10 years for a system providing 10% solar-to-hydrogen conversion efficiency is required to achieve a reasonable energy return on energy invested [1]. Significant research advancements will be required before long-term stable devices with suitable efficiencies are reached. Here, we provide an overview of different approaches to achieving durable semiconductor photoanodes and highlight two specific examples of how catalyst integration can be used to improve chemical stability.

In the first example, we show that plasma-assisted atomic layer deposition (PE-ALD) of cobalt oxide onto silicon enables efficient and sustained photoelectrochemical water splitting under alkaline conditions [2]. While ALD has recently emerged as a powerful tool for protection of photoelectrodes from corrosion, the composition and structure of deposited materials often differ significantly from those synthesized by other methods. We find that low temperature PE-ALD provides access to nanocrystalline, yet conformal, layers that are characterized by higher concentrations of active sites. Engineering the catalyst and the semiconductor/catalyst interface at the nanoscale is essential for simultaneously achieving efficient charge extraction and chemical stability. This work offers insight into the role of structural disorder and nanocrystallinity on catalytic activity and provides a path to higher performance photoelectrodes for solar fuels systems.

In the second example, semiconductors that possess an increased native stability are investigated. These semiconductors are often polycrystalline thin film metal oxides possessing lateral inhomogeneities, poorly understood interactions with the electrolyte environment, and relatively unknown optoelectronic properties. One such material is bismuth vanadate ($BiVO_4$), an ~2.5 eV bandgap n-type semiconductor. We have utilized a suite of spectroscopic and microscopic methods to probe local compositional non-uniformities, understand the role of catalyst integration on (photo)chemical stability, and determine electronic structure and photocarrier dynamics that govern charge extraction efficiency [3,4]. These measurements provide valuable insight into basic properties – often defined by local nonuniformities – that affect the ultimate performance of functional photoanodes. The examples presented here highlight that, although few materials are inherently stable under conditions required for photocatalytic water splitting, catalyst integration and interface engineering allow control over semiconductor/electrolyte interactions and provide a viable approach to sustained operation in harsh environments.

[1] R. Sathre, *et al., Energy Environ. Sci.* **2014**, *7*, 3264.
[2] J. Yang, *et al., J. Am. Chem. Soc.*, **2014**, *136*, 6191.
[3] J. Cooper, *et al., Chem. Mater.*, **2014**, *26*, 5365.
[4] J. Cooper, *et al., J. Phys. Chem. C*, **2015**, *119*, 2969.

3:40 PM **F/H3.04
Excited State Dynamics in Oxynitride Nanocrystals and Implications for Solar Fuel Generation Gordana Dukovic; Chemistry and Biochemistry, University of Colorado Boulder, Boulder, Colorado, United States.

Zinc-gallium oxynitride ($(Ga_{1-x}Zn_x)(N_{1-x}O_x)$) exhibits visible absorption with a band gap that depends on composition (i.e., the value of *x*) and has been demonstrated to split water under visible irradiation when functionalized with a proton reduction catalyst. The origin of visible absorption in this solid solution material is not well understood. Furthermore, the excited state relaxation dynamics in this material have not been elucidated. Carrier lifetime is a critical parameter for performance in photochemical and photoelectrochemical devices because it determines carrier diffusion length and thus the ability to extract the photoexcited carriers before they decay.

We have previously reported a synthesis of single-crystalline nanoparticles of $(Ga_{1-x}Zn_x)(N_{1-x}O_x)$. By targeting a nanocrystalline form of this material, we were able to decrease the synthesis temperature, compared to the bulk material, and obtain a broad range of compositions with the value of *x* ranging from 0.06 to 0.98. The absorption onset depends strongly on the value of *x* and can be as low as 2.2. eV. Transient absorption measurements show that $(Ga_{1-x}Zn_x)(N_{1-x}O_x)$ have very long excited state lifetimes. For x=0.73, the lifetime of the transient bleach in the visible is on the order of microseconds, suggesting excited state properties that are favorable for applications in solar photochemistry. In addition to excited state dynamics, the insights into the origin of visible absorption in $(Ga_{1-x}Zn_x)(N_{1-x}O_x)$ obtained from transient absorption spectroscopy will be discussed.

4:10 PM **F/H3.05
Charge Carrier Transport and Catalysis on Solution-Processed Photoelectrodes for Solar Water Splitting Kevin Sivula; Laboratory for Molecular Engineering of Optoelectronic Nanomaterials, Institute of Chemical Science and Engineering, École Polytechnique Fédérale de Lausanne, Lausanne, Switzerland.

The conversion of solar energy directly into chemical fuels is a promising technology for a sustainable energy future and can be accomplished with a photoelectrochemical (PEC) device. The economic viability of PEC hydrogen production via water splitting is limited by the cost of the device and its performance compared to traditional PV+electrolysis. While inexpensive photoelectrode fabrication techniques (e.g. solution-based processing) are economically suitable for a PEC cell, the resulting quality of the photoactive semiconducting layers in the device often leads to limitations in charge transport and charge transfer to the electrolyte (i.e. catalysis for the oxidation and reduction reactions). In this presentation an introduction to PEC fuel production is given along with its economic feasibility. Promising systems using inexpensive materials (e.g. Fe_2O_3, $BiVO_4$, Cu_2O, $CuFeO_2$, WSe_2) and fabrication techniques are discussed along with strategies to overcome limitations of charge transfer and charge transport in functional electrodes. In particular, the feasibility of a $BiVO_4$/Cu_2O photoanode/photocathode tandem cell for overall unassisted solar water splitting is evaluated. Using state-of-the-art photoelectrodes current-matching conditions for the tandem cell are identified by altering the photoanode active layer thickness. By further employing water oxidation and reduction catalysts (Co-Pi and RuO_x, respectively) together with an operating point analysis an unassisted solar photocurrent density on the order of 1 mA cm^{-2} is demonstrated and routes for improvement are identified. Fundamental challenges to the stable operation of high performance tandem cells are finally discussed.

4:40 PM F/H3.06
Enhanced Photoactivity in Mo:$BiVO_4$ by Thermally Activating Small Polaron Hopping Liming Zhang, Xiaofei Ye, Madhur Boloor, Andrey Poletayev, Nicholas Melosh and William Chueh; Materials Science & Engineering, Stanford University, Stanford, California, United States.

The extremely low carrier mobility in small-polaron semiconductors, such as $BiVO_4$, limits their photoactivity when being used as light absorbers in photoelectrochemical (PEC) devices. By increasing the temperature, the carrier mobility can be enhanced exponentially, providing an efficient strategy to improve the collection of minority carriers in the diffusion region. Although the photovoltage of semiconductor decreases with temperature, its decrease can be mitigated by the cathodic shift of the thermodynamic potential and the decrease of the kinetic overpotential at the semiconductor/electrolyte interface. Here we explored the effect of elevated temperatures on the PEC properties of Mo-doped bismuth vanadate (Mo:$BiVO_4$) photoanode in buffered neutral aqueous electrolyte. By elevating the temperature from 9°C to 42°C, the saturation current density increased by 52%, from 2.1 to 3.2 mA/cm^2. The photocurrent increases dramatically compared to the photovoltage degradation, which drops by a rate of 2.1 mV/K. The stability evaluation indicates that CoPi/Mo:$BiVO_4$ has an extended durability up to 30 h and the degradation rate does not depend on the temperature under the conditions examined. Our results highlight the significant benefit of thermally activating carrier transport in polaronic light absorbers, which is not observed in band conductors with delocalized charge carriers, such as Si. We expect that our observation is general and will be applicable to other localized electron semiconductors.

5:00 PM F/H3.07
Mixed Conductivity as the Origin of Capacitive and Hysteretic Anomalies in Organo-Lead Halide Perovskites Giuliano Gregori[1], Tae-Youl Yang[1], Norman Pellet[2], Michael Graetzel[2] and Joachim Maier[1]; [1]Max Planck Institute for Solid State Research, Stuttgart, Germany; [2]Swiss Federal Institute of Technology, Lausanne, Switzerland.

The recent employment of organo-lead iodide perovskites in photoelectrochemical cells has considerably increased the conversion efficiency of such devices compared to the conventional dye-sensitized solar cells. Interestingly, such a beneficial effect is accompanied by some intriguing anomalies that are currently matter of intense debates: High apparent dielectric constant at low frequencies and pronounced hysteresis during voltage-current sweeps. Typically, in the existing literature, such phenomena are explained in terms of ferroelectricity or trapping/detrapping at grain boundaries.
In this study, we focus our attention on the electrical transport properties of organo-lead iodide perovskite and measure both ion – due mostly to iodine migration – and electron conductivities. From dc polarization experiments performed with blocking electrodes, we determine the chemical diffusion coefficient of iodine and follow the kinetics of stoichiometric changes. Notably, the ionic conduction is very substantial and under dark conditions it even surpasses the electronic one.
Such a mixed conducting nature of these compounds naturally explains the phenomena mentioned above. Specifically, if the organo-lead iodide perovskite is sandwiched between neighboring phases that block the ions – as in photoelectrochemical applications – and is charged with a dc current, a stoichiometric polarization occurs resulting in a high apparent dielectric constant at low frequencies. The same stoichiometric polarization is also responsible of the pronounced hysteretic behavior during i-V sweeps. In addition to the experiments, we also verify these effects by mimicking the observed electrical behavior using a relevant equivalent circuit.

G: Switching and Sensing Phenomena

* Invited Speaker
** Keynote Speaker

SESSION G1: Switching and Sensing Phenomena I
G: Switching and Sensing Phenomena
Chairs: Jennifer Rupp and Shu Yamaguchi
Tuesday Morning, June 16, 2015
Keystone Resorts, Grays Peak III

10:30 AM **G1.01
Bulk Mixed Ion Electron Conduction in Highly Disordered Oxides Causes Memristive Behavior Manfred Martin[1, 2]; [1]Institute of Physical Chemistry, RWTH Aachen University, Aachen, Germany; [2]Department of Materials Science and Engineering, Seoul National University, Seoul, Korea (the Republic of).

In thin films of mixed ionic electronic conductors sandwiched by two ion-blocking electrodes, the homogeneous migration of ions and their polarization will modify the electronic carrier distribution across the conductor, thereby enabling homogeneous resistive switching. Here we report non-filamentary memristive switching based on the bulk oxide ion conductivity of amorphous, highly non-stoichiometric gallium oxide, GaO_x (x~1.1) [1]. We directly observe reversible enrichment and depletion of oxygen ions at the blocking electrodes responding to the bias polarity by using photoemission and transmission electron microscopies, proving that oxygen ion mobility causes memristive behaviour. The shape of the hysteresis I-V curves is tunable by the bias history, as found in the mathematically derived memristor model. This dynamical behaviour can be attributed to the coupled ion drift and diffusion motion and the oxygen concentration profile acting as a state function of the memristic device.

1. Y. Aoki, C. Wiemann, V. Feyer, H.-S. Kim, C. M. Schneider, H.-I. Yoo, M. Martin, *Nat. Commun*. 5:3473 doi: 10.1038/ncomms4473 (2014)

11:00 AM *G1.02
Dislocations in $SrTiO_3$: Easy to Reduce but not so Fast for Oxygen Transport Dario Marrocchelli, Lixin Sun and Bilge Yildiz; Nuclear Science & Engineering, Massachusetts Institute of technology, Cambridge, Massachusetts, United States.

Resistive switching is the ability of a material to have at least two resistive states that can be switched upon application of an electrical bias. This property can be used to produce memories (dubbed ReRAM) with highly desired properties, such as high density, low cost, fast write and read access, low energy operation and long life-times. However, the origins of resistive switching in some materials, especially valence change materials (usually metal oxides) are still widely debated. Indeed, while there is overwhelming evidence that dislocations (or other extended defects) play an important role in resistive switching, a clear quantitative mechanism describing the role of dislocations in this process is missing.

In this work, we take $SrTiO_3$ as a model perovskite and assess the impact of dislocations on redistribution and migration of oxygen vacancies by atomistic simulations. We find that, in the dilute limit, oxygen vacancy formation energy in $SrTiO_3$ is lower at sites close to the dislocation core, by as much as 2 eV compared to that in the bulk. Oxide-ion diffusion was studied for a low vacancy concentration regime (ppm level) and a high vacancy concentration regime (up to 2.5%). In both cases, no evidence of pipe-diffusion, i.e. significantly enhanced mobility of oxide ions, was found as determined from the calculated migration barriers, contrary to the well-known pipe diffusion of atoms in metals. However, in the low vacancy concentration regime, the vacancy accumulation at the dislocation core gives rise to a higher diffusion coefficient, even though the oxide-ion mobility itself is lower than that in the bulk. The observed lower oxygen vacancy formation energy at the dislocation core provides a quantitative and direct explanation for the electronic conductivity of dislocations in $SrTiO_3$, thus providing a microscopic picture of the atomistic factors responsible for resistive switching at dislocations.

11:20 AM G1.03
Electroforming in Valence Change Memories Based on Mixed Ionic Electronic Conductors Dima Kalaev[1], Eilam Yalon[2] and Ilan Riess[1]; [1]Physics, Israel Institute of Technology, Haifa, Israel; [2]Microelectronics Research Center, Technion – Israel Institute of Technology, Haifa, Israel.

There are many reports on resistive switching phenomena in thin films of metal oxides placed in between two electrodes, induced by an applied voltage. This effect can be exploited to design new types of electronic (memristive) devices, in particular nonvolatile memory. Similar resistive switching effects occur in diversity of oxides under different conditions. This implies that there is a common physical basis which leads to resistive switching in a large class of devices. In most of the cases the resistive switching process can be divided into two steps. First, a relatively slow, order of microseconds, initial preconditioning of the device, called by the most authors - the electroforming step. The second step is a very fast reversible resistive switching. In order to understand the nature of the second step, we should first explain the electroforming one, which, in general, can be different in underlying physical mechanism from the fast resistive switching step.

We argue that electroforming can be explained in a wide range of the materials by taking into account the ionic motion of defects, which in metal oxides can be oxygen vacancies. The oxide is assumed to be a mixed-ionic-electronic-conductor, able to change its electronic properties by changing the distribution of the mobile ionic defects and their valence state under an applied driving force of the relevant electrochemical potential.

In the frame of our one dimensional model we explain several experimental observations in the $Electrode_1|Oxide|Electrode_2$ devices [1]. In particular we show that the direction of propagation of electroforming active zone e.g. the filament (represented by a high concentration of ionic defects) depends not only on the polarity of the applied voltage but also on the type of the device's electrodes e.g. their reactivity and permeability for oxygen exchange with the ambient. The model also predicts existence of nano thin gap of low conductivity near one of the electrodes. Predictions of the theory were demonstrated experimentally by Yalon E. et al. in resistive switching devices based on HfO_2, by using a bipolar transistor as a probing electrode on one side [2].

To model the transport in a nano scale devices, we use the high driving force nonlinear current density equations for both the ionic and electronic defects [3]. The nonlinearity leads to an exponential decrease in time of the electroforming with the applied voltage and thus the endurance of the electroforming step, when no voltage is applied.

[1] D. Kalaev, E. Yalon and I. Riess, *On the direction of the conductive filament growth during electroforming*, Solid State Ionics, 2014, Submitted.
[2] E. Yalon, A. Gavrilov, S. Cohen, D. Mistele, B. Meyler, J. Salzman, and D. Ritter, *Resistive Switching in HfO_2 probed by a Metal Insulator Semiconductor Bipolar Transistor*, IEEE Electron Device Lett., 33, no. 1, 2012, 11
[3] I. Riess, D. Kalaev, J. Maier, *Currents under high driving forces*, Solid State Ionics, 251, 2013, 2.

11:40 AM G1.04
Field-Enhanced Bulk Conductivity and Resistive-Switching in Ca-Doped $BiFeO_3$ Ceramics Nahum Maso[1, 2] and Anthony R. West[2]; [1]Chemistry, University of Oslo, Oslo, Norway;[2]Materials Science and Engineering, University of Sheffield, Sheffield, United Kingdom.

The bulk conductivity at room temperature of Ca-doped $BiFeO_3$ ceramics is p-type and increases reversibly by up to 3 orders of magnitude under the influence of a small *dc* bias voltage in the range 33 to 200 Vcm^{-1}. The effect occurs in both grain and grain boundary regions, is isotropic and does not involve creation of filamentary conduction pathways. It is proposed that, by means of capacitive charging and internal ionisation processes under the action of a *dc* bias, hole creation leads to a more conductive excited state. This gradually returns to the ground state when the *dc* bias is removed and the holes recombine with electrons trapped at the sample surface. The holes are believed to be created on oxygen, as O^- ions. We thank the EPSRC for financial support.

SESSION G2: Switching and Sensing Phenomena II
G: Switching and Sensing Phenomena
Chairs: Jennifer Rupp and Shu Yamaguchi
Tuesday Afternoon, June 16, 2015
Keystone Resorts, Grays Peak III

3:30 PM *G2.01
Various Functional Nano-Ionic Devices Achieved by Controlling Hetero-Interface Characteristics using Local Ion Migration Kazuya Terabe, Takashi Tsuchiya and Masakazu Aono; MANA, National Institute for Materials Science, Tsukuba, Japan.

The fine processing scale for conventional semiconductor devices will reach the atomic scale in near future. It is evident that not only the limits to conventional fine processing technology but also the physical operating limits of semiconductor devices are being reached. One possible way to overcome these technological and physical limits is to achieve breakthroughs in device materials and device-operation principle using nanotechnology. A promising type of such nano-devices is the nano-ionic device, which is operated by controlling the local ion migration and electrochemical reaction instead of electron and hole migration. The nano-ionic device can be expected high performance and novel functionality which are not obtained by the conventional semiconductor device. In this presentation, we will introduce ways to control the local ion migration and electrochemical reaction at hetero-interfaces. Furthermore, the unique physical and chemical phenomena and functions caused by these controlling in order to fabricate novel nano- ionic devices are demonstrated.

We have fabricated two-/three-terminal nano-ionic devices with simple stacked layers, such as metal oxide or graphene oxide/ionic conductor layers, in which the ion (H^+, O^{2-} or Li^+) migration and redox reaction can be occurred by applying bias voltage. By tunning Schottkey-like barrier, electric double layer and electrochemical reaction using the ion migration and electrochemical reaction at various hetero-interfaces, useful electrical and optical functions, such as rectification, resistive switching, photoluminescence, superconductivity and so on, are obtained in these devices [1-4].

[1] R. Yang, K. Terabe, et.al., ACS NANO, **6**, 9515 (2012).
[2] T. Tsuchiya, K. Terabe, et.al, Applied Physics Letters., **103**, 073110 (2013).
[3] T. Tsuchiya, K. Terabe, et. al, Advanced Materials, **26**, 1087 (2014).
[4] T. Tsuchiya, K. Terabe, et. al, ACS NANO online publication, Jan. (2015)

3:50 PM *G2.02
Ionic Switching Devices: Operation Principle and Application in Computing Daniele Ielmini; Politecnico di Milano, Milano, Italy.

Resistive (or memristive) switching devices based on ionic migration are attracting a huge deal of interest as next generation memory and computing devices. Ionic switching relies on defect migration induced by the local field and temperature, causing the formation and dissolution of filaments with size as small as only few atoms. This makes ionic switching device concepts potentially scalable to few nm technologies, which cannot be matched by conventional silicon-based technology.

This talk will review the switching mechanisms for filament disruption (reset) and reconnection (set) in ionic switching devices for electrolytes based on chalcogenide (e.g., Ag:GeS2) and oxides (e.g., HfOx). The modeling of switching will be reviewed, showing that switching models today can predict not only the device characteristics in AC and DC conditions, but also noise and switching statistics affecting the reliability of practical memory devices. The role of local mechanical stress in controlling the filament stability will be discussed. Then, novel applications in computing enabled by ionic switching devices will be reviewed, including random number generation (RNG), neuromorphic circuits based on spike-timing dependent plasticity (STPD) and logic gates. The main challenges for a future application space of ionic switching logic will be finally identified and discussed.

4:10 PM *G2.03
$La_{0.8}Sr_{0.2}(Mn,Co)O_3$ Perovskite Oxides as Resistive Switches: Influence of B-Site Substitution on the Resistive Switching Properties Monica Burriel[1, 2], Rafael Schmitt [3], Aruppukottai Muruga Saranya[2], Alex Morata[2], Aitor Hornes[2], Sebastian Schweiger[3], Michel Bourdard[1], Jennifer L. M. Rupp[3] and Albert Tarancon[2]; [1] Laboratoire des Matériaux et du Génie Physique (LMGP), Grenoble, France; [2]Catalonia Institute for Energy Research-IREC, Barcelona, Spain; [3]ETH Zurich, Zurich, Switzerland.

Recently, Resistive Random Access Memories (ReRAM) constructed from oxide thin films have generated significant interest both in industry and in the scientific community for their use as non-volatile memories beyond classic transistors [1,2]. ReRAMs are considered one of the most promising emerging non-volatile memories due to their high speed, high density, great scalability and low power consumption. These devices can store and process information and offer several key performance characteristics that exceed conventional integrated circuit technology. However, the current lack of understanding of the underlying device mechanisms constitutes a significant barrier to their widespread application. Particular attention is drawn into the use of perovskite oxides, materials for which the resistive switching and physical property of memristance may originate from valence changes under the high local electric field strength operation (> 10 MV/m) of the switch.

In this work $La_{0.8}Sr_{0.2}Mn_{1-x}Co_xO_{3\pm\delta}$ perovskite thin films have been fabricated by combinatorial Pulsed Laser Deposition (PLD) on silicon nitride-passivated Si chips. Platinum was used both as top and bottom electrodes. To evaluate the switching performance of the series, a complete set of electrical characterization measurements was performed by I-V cyclic voltammetry for 3 different compositions (x=0, 0.25 and 0.5). For each composition a set of systematic measurements was carried out in which the influence of different voltage ranges, different sweep rates and the influence of electroforming were assessed. The reproducibility of the measurements has also been evaluated by a number of repeated cycles and by repeating the measurements on different contacts.

While the undoped films presented a small hysteresis, those with a 50% Co substitution showed the largest memristive response. The evolution of the memristance as a function of Co substitution will be discussed taking into account near order structural changes, electronic changes and variation in the oxygen transport in the films.

References:
[1] Messerschmitt et al., Advanced Functional Materials, 2014, 24, 47, 7448
[2] Waser et al., Advanced Materials, 2009, 21, 25-26, 2632

4:30 PM G2.04
STM Investigations of Resistive Switching on Binary Metal Oxides and Chalcogenides Anja Wedig[1], Marco Moors[1], Tsuyoshi Hasegawa[2], Masakazu Aono[2], Rainer Waser[1, 3] and Ilia Valov[1, 3]; [1]Electronic Materials, Juelich Research Center, Juelich, Germany; [2]International Center for Materials Nanoarchitectonics, National Institute for Materials Science, Tsukuba, Japan; [3]Institute for Materials in Electrical Engineering II, RWTH Aachen University, Aachen, Germany.

In redox-based resistive random-access memory (ReRAM) devices, a resistance switching can occur due to the formation/dissolution of electron-conducting filaments within an insulator or electrolyte matrix. To investigate the microscopic composition of the filament and the kinetics of filament formation, techniques with high spatial resolution such as local-conduction atomic force microscopy (LC-AFM) and scanning tunneling microscopy (STM) exhibit great potential. In contrast to LC-AFM, STM offers advantages such as the absence of a mechanical contact between the sample surface and the scanning probe as well as a particularly high resolution due to the small probe diameter. Nevertheless, STM studies of resistive switching have so far been mainly devoted to materials with mixed ionic-electronic conductivity (e.g., Cu_2S[1] and Ag_2S[2]) or pure electronic conductors (Nb-doped $SrTiO_3$[3]).

We demonstrated the extension of these investigations to the macroscopic ion conductor $RbAg_4I_5$ doped with a small amount of an electron donor[4]. By STM, it was possible to obtain important information regarding the kinetics of gap-type atomic switching. In particular, the formation of a critical Ag nucleus on the sample surface was found to determine the overall rate of the switching. The STM investigations were then extended to other electronic oxides and chalcogenides used in electrochemical metallization memories as well as valence change memories. By using different modes of STM (scanning/stationary probe), it was possible to switch the sample surface locally, and important insight was gained into the transport and reaction processes involved in the switching. Furthermore, it was possible to test out the limits of miniaturization of the switching processes.

[1] A. Nayak et al., Nanotechnology 22, 235201 (2011).
[2] A. Nayak et al., J. Phys. Chem. Lett. 1, 604 (2010).
[3] Y. L. Chen et al., J. Appl. Phys. 112, 023703 (2012).
[4] I. Valov et al., Nat. Mater. 11, 530 (2012).

4:50 PM G2.05
Strained Heterolayers as Resistive Switching Oxide: Materials and Devices Sebastian Schweiger, Reto Pfenninger and Jennifer L. Rupp; Materials, ETH Zurich, Zurich, Switzerland.

Redox-based resistive memories are a promising alternative to current memories and logics.[1] Resistive switches are usually composed of a single metal oxide film, e.g. $SrTiO_3$, TiO_2, CeO_2, sandwiched between two metal electrodes. Despite proof-of-concepts new materials and concepts to alter carrier contributions at high field strength require attention. New concepts beyond classic doping of oxides are discussed to control device properties like retention, R_{on}/R_{off} ratios and power consumption. In this work, lattice strain engineering is being discussed as a new route for tuning material and device properties in metal oxide films for resistive switching through the manipulation of mass and charge transport. Lattice strain engineering using heterostructures is a versatile concept and for potential energy applications but so far no real micro-devices have been demonstrated. The concept of strain at internal interfaces in heterostructures can be used to tune material properties, like conductivity, far beyond the change accessible by doping. The benefits of strain manipulation is the biggest at low temperature, this makes it particularly interesting for resistive switching memories. A novel microfabrication strategy was developed and applied to contact the in-plane nanoscopic interfaces of the strained heterostructures. It is imperative to establish a fabrication route that allows placing the electrodes at close distances to operate switches at >> 10E6 V/m while accessing all the interfaces. The material systems $Gd_{0.1}Ce_{0.9}O_{2-x}/Er_2O_3$ and $Gd_{0.1}Ce_{0.9}O_{2-x}/Sm_2O_3$ were investigated to address different strain states ranging from tensile to compressive in-plane strain. The magnitude of strain was changed by changing the number of interfaces from 1 to 60 while keeping the device at constant thickness.[2] The near-order ionic transport interaction is supported by near order Raman spectroscopy measurements which are introduced as new measurement technique to investigate and describe the strain state with high spatial resolution. A strain activated volume tensor model was applied to describe the changes in migration energy. Electrical measurements revealed that highly strained samples show stable hysteretic IV-profiles. Excitingly, it can be shown that interfacial strain can be used to actively tune the R_{on}/R_{off} ratio for oxide based heterolayer resistive switches.

References:
[1] Messerschmitt et al., Advanced Functional Materials, 2014, 24, 47, 7448
[2] Schweiger et al., *ACS Nano*, 2014, 8 ,5, pp 5032–5048

5:10 PM G2.06
Sensing Nitrogen Oxides and Ammonia with Porous Electrolyte Devices Fernando Garzon[1], Eric Brosha[2], Cortney Kreller[2] and Rangachary (Mukund) Mukundan[2]; [1]Chemical and Biological Engineering, University of New Mexico, Albuquerque, New Mexico, United States; [2]Materials Physics and Applications, Los Alamos National Laboratory, Los Alamos, New Mexico, United States.

Minimization of harmful emissions from combustion processes often requires sensitive and accurate chemical measurements of the effuent gases. Solid state sensors provide useful feedback information for optimization of the combustion process and catalytic aftertreatment systems under varying load/process conditions. Zirconium oxide solid electrolyte sensors have provided reliable measurements of fuel/air stoichimetry for many years and more recently, nitrogen oxide production. Ammonia and urea injection bases selective catalytic reduction systems have greatly reduced NO_x emissions from powerplants and internal combustion engines. The measurement of nitrogen oxides in the presence of ammonia or the reverse, however is problemmatic; with serious cross interferences commonly ocurring between the species. We have developed a new class of durable sensors based on dense catalytic electrodes and porous solid electrolytes to meet these challenges. The sensors are fabricated using ceramic tape casting and thick film electrode deposition. The solid electrolyte sensors can successfully measure PPM levels of NO_x and ammonia in real engine exhaust gas environments for extended time periods.

5:30 PM G2.07
Single Crystalline $SrTiO_3$ as a Memristive Model System: Roles of Oxygen Vacancies and Schottky Barrier, and Neural Function Mimicking Xin Guo; Materials Science and Engineering, Huazhong University of Science and Technology, Wuhan, China.

In various perovskite materials, the phenomenon of resistive switching has been extensively observed. Among the perovskites, $SrTiO_3$ (STO) of the entire doping spectrum, i.e. from acceptor- to donor-doped STO, has been extensively investigated, since the works on STO help understanding the switching behavior of all perovskite materials. Different mechanisms have been proposed to explain the switching behavior of STO. The works on acceptor-doped STO emphasize the property change in the crystal bulk, in which oxygen vacancies play a key role: either the fast transport of oxygen vacancies along dislocations or the formation of oxygen-vacancy array under high electrical stress is suggested to be responsible for the switching. A Schottky barrier is formed at the metallic electrode/STO contact; therefore, the role of the Schottky barrier is emphasized for donor-doped STO: the change in Schottky barrier height under voltages of different polarities is responsible for different resistance states.

Single crystalline STO is used as a model system to evaluate the roles of oxygen vacancies and the Schottky barrier. The advantages of single crystalline STO are: (1) STO, including its oxygen vacancies and Schottky barrier, has been thoroughly investigated, the knowledge obtained from these works is very helpful to the understanding of the switching mechanism, and (2) unlike thin films, a single crystal has good homogeneity in properties. We clearly demonstrated that oxygen vacancy drift from the anode to the cathode and a significantly increased overall concentration of oxygen vacancies in the crystal bulk are the most prominent process of electroforming of acceptor-doped STO. While for donor-doped STO, we established an unambiguous relation between the resistance state and the Schottky barrier height.

More importantly, we successfully mimicked the basic neural functions, for example, learning, forgetting and rehearsal processes, by the Ni/Nb:STO Schottky junction.

SESSION G3: Poster Session
G: Switching and Sensing Phenomena
Tuesday Afternoon, June 16, 2015
5:20 PM
Keystone Resorts, Red Cloud Peak

G3.01

Resistive Switching in $SrRuO_3$ Probed by Scanning Tunneling Microscopy Kiran K. Adepalli[1,2], Marco Moors[3], Qiyang Lu[1], Rainer Waser[3], Harry Tuller[1], Ilia Valov[3] and Bilge Yildiz[2]; [1]Materials Science and Engineering, Massachusetts Institute of Technology, Cambridge, Massachusetts, United States; [2]Nuclear Science and Engineering, Massachusetts Institute of Technology, Cambridge, Massachusetts, United States; [3]Peter Grünberg Institute, Forschungszentrum Jülich, Jülich , Germany.

Resistive switching random access memory (Re-RAM) or memristive devices are being considered as the next generation information storage technology. Relative to the current state-of-the-art flash devices, Re-RAM devices promise lower power consumption, high scalability, simpler architecture, faster switching times (under sub-nanoseconds) and longer data retention. While there has been considerable progress in recent years in revealing details of the microscopic mechanism of resistive switching by several *ex situ* and *in situ* techniques such as c-AFM, STM and HRTEM, an incomplete picture remains regarding the ability to describe a fully quantitative predictive physical model. The fundamental questions relating to the switching mechanism of these devices that need addressing include the effects of strong electric fields on defect creation and transport, and on the electronic structure. In this work, we induced and characterized localized electronic switching in electronic oxide under the electric field of a scanning tunneling microscope tip, operating in non-contact mode. In this manner, switching can be studied at the local level, without necessitating a top electrode that limits access to the functional oxide in conventional memristor device structures. Furthermore, scanning tunneling microscopy in spectroscopy mode provides electronic structure information, allowing for characterization of the electronic switching process in situ, in a localized manner, and in a single experiment, without necessitating the removal of the metal electrode for spectroscopic characterization ex situ. The work highlights the use of tunneling microscope for characterizing resistive memory material surfaces under applied electric fields and variable oxygen partial pressure.

G3.02

Topotactic Phase Transition in $SrCoO_x$ Controlled by Electrochemical Potential Qiyang Lu[1] and Bilge Yildiz[1,2]; [1]Department of Materials Science and Engineering, Massachusetts Institute of Technology, Cambridge, Massachusetts, United States; [2]Department of Nuclear Science and Engineering, Massachusetts Institute of Technology, Cambridge, Massachusetts, United States.

Topotactic phase transition of functional oxides induced by oxygen non-stoichiometry change has attracted great interest for applications which require fast oxygen transport and exchange. These phase transitions do not merely change the lattice structure of oxides, but also more importantly, can largely alter multiple important physical and chemical properties. These properties include electrical conductivity, oxygen diffusivity and oxygen reduction/evolution reactivity, which are of pivotal importance for electrocatalytic applications, such as solid oxide fuel cell cathodes. Here we demonstrate a simple but and unique means to trigger phase transitions, by precisely controlling oxygen non-stoichiometry in a functional oxide as previously demonstrated by Chen et al[1]. We use electrochemical potential to induce phase transition in strontium cobaltites ($SrCoO_x$, denoted as SCO) between Brownmillerite phase $SrCoO_{2.5}$ and perovskite phase $SrCoO_{3-\delta}$. *In situ* X-ray diffraction (*in situ* XRD) was performed on the electrochemical cell of $SrCoO_{2.5}$/YSZ electrolyte/Ag at 500°C in air. An external electrical bias up to 200mV was applied across the SCO and YSZ interface in order to change the effective pO_2 in SCO to trigger the phase transition. The evolution of *in situ* XRD patterns with increasing applied bias showed that the phase transition from Brownmillerite phase to perovskite phase can be triggered at a bias as low as 30mV. Also, the polarization curves (current-time) showed a clear kink when phase transition was induced, which suggests the rate of oxygen incorporation is distinct for the two phases. This result proves the concept of using electrical bias to control the phase and lattice structure of functional oxides. We are currently working on reducing the phase transformation temperature and mapping out the temperature-dependent bias needed for the transformation. Applying electrochemical bias and changing oxygen non-stoichiometry, enables fast and easily-accessible switching between different phases as well as access to distinct physical and chemical properties. Therefore, this work provides a new pathway of tailoring functional oxides properties by applying electrical bias.

1. Chen, D. & Tuller, H. L. Voltage-Controlled Nonstoichiometry in Oxide Thin Films: $Pr_{0.1}Ce_{0.9}O_{2-\delta}$ Case Study. *Adv. Funct. Mater.* 24, 7638–7644 (2014).

G3.03

Atomistic Modelling of the Formation of Conducting Filaments in Resistive RAM Cells David Z. Gao, Samuel R. Bradley, Manveer Munde and Alexander L. Shluger; Physics and Astronomy, University College London, London, United Kingdom.

Hafnia (HfO_2) and amorphous silicon dioxide (a-SiO_2) are currently being explored as the insulating oxide layer in metal-insulator-metal resistive RAM (ReRAM) cells. The prevailing theory of the switching processes in these cells involves the formation of a conductive filament comprised of sub-stoichiometric oxide. However, the atomistic mechanisms behind these processes are not yet well understood.

In this work we used density functional theory (DFT) to study the initial stages of conductive filament formation in bulk HfO_2 and a-SiO_2. We modeled the interactions between oxygen vacancies in HfO_2 and found that neutral oxygen di-vacancies and tri-vacancies are thermodynamically stable. We also modeled the formation of oxygen Frenkel defect pairs and found that the nearest neighbour and more distant oxygen vacancies and interstitial ions are stabilized against recombination by electron injection into the system. In this situation, a neutral oxygen vacancy and a charged O^{2-}interstitial ion are formed. The barrier for forming this defect pair is subsequently lowered through the injection of more electrons and the formation of a negatively charged oxygen vacancy. Finally, we extended our study to a-SiO_2, where di-vacancies were also found to be thermodynamically stable and the injection of electrons similarly lowered the barriers for vacancy-interstitial oxygen ion pair formation. Combining these findings we have developed a model for the initial stages of formation of conducting filaments, which includes oxygen vacancy production initiated by negatively charged, pre-existing oxygen vacancies, and the subsequent fast diffusion of oxygen interstitials [1].

[1] D. Z. Gao et al. (submitted)

G3.04

Controllable Resistive ON- and OFF-States by Two Switching Mechanisms in Epitaxial Strontium Titanate-Based Resistive Switches Markus Kubicek, Rafael Schmitt, Felix Messerschmitt and Jennifer Rupp; Department of Materials, ETH Zurich, Zurich, Switzerland.

Resistive switching oxides are a class of non-volatile memories with the potential to improve today's transistor-based information technology. Their typical hysteretic current-voltage profiles allow addressing a high and a low resistance state within ns and at a low switching energy. In this study $SrTiO_{3-\delta}$, a material with well-known defect chemistry was chosen as active oxide material. Despite several reports in literature, the exact defect related switching mechanisms and electric field inflicted changes thereof remain elusive. To elucidate defect dynamics, we prepare model device structures for which the oxide is a 5 nm thin $SrTiO_3$ epitaxial PLD film without grain boundaries grown on (100) $LaAlO_3$ single crystals. Using epitaxial $LaNiO_3$bottom- and Pt top-electrodes, we observe bipolar resistive switching and pinched hystereses in I-V profiles for electric field strengths < $4 \cdot 10^8$V/m and R_{off}/R_{on} ratios of 10-200. Excitingly, two competing switching mechanisms were observed at a bias threshold of ±3V ($6 \cdot 10^8$V/m) that lead to changes in switching direction (clockwise vs. counter-clockwise), kinetics and number of I-V crossovers. By impedance spectroscopy, TEM, and AFM, more details on the two switching processes were accessible: One process is filament-based whereas the second one relies on altering charge carrier concentrations. High stability of both processes allows for control of R_{on}/R_{off} resistance magnitudes and ratios for individual switches, being an exciting new possibility to tune memory device functionality.

G3.05

Enhanced Stability of Ag-SbTe Chalcogenide Solid Electrolyte by Nitrogen Doping Young Sam Park[2] and Seung-Yun Lee[1]; [1]Department of Applied Materials Engineering, Hanbat National University, Daejeon, Korea (the Republic of); [2]ETRI, Daejeon, Korea (the Republic of).

Chalcogenide has been considered one of the most important amorphous semiconductors in the fields of solid-state electronics and photovoltaics. Among the chalcogenide compounds, SbTe has gained much attention due to its switching characteristic required for non-volatile memory applications, as well as its benificial effect on performance improvement in CdTe solar cells. Metal-diffused SbTe solid electrolyte exhibits reversible resistive switching, and it is generally believed that the switching behavior originates from the electrochemical formation of conducting filaments related to metal ions. The stability of the SbTe solid electrolyte under repetitive switching is a crucial factor that must be addressed to commercialize SbTe based devices. As a practical method for stability improvement of the solid electrolyte, nitrogen doping is presented in this work. Multilayer structures of Ag/SbTe/TiW were fabricated to determine the resistive switching characteristics of the SbTe solid electrolyte. Nitrogen was incorporated into the SbTe layer by sputtering in argon and nitrogen atmosphere. Although any specific heat treatment was not carried out for Ag diffusion, it was observed that Ag atoms diffused to form the Ag-SbTe solid electrolyte. The resistance of the multilayer structure reversibly changed between on- and off-state resistances, depending on the magnitude of the voltage applied through the top and bottom electrodes. Compared to pure Ag-SbTe, the nitrogen-doped solid electrolyte showed more stable endurance up to 10^4 repetitive switching cycles. Microstructural observation revealed that this enhanced stability results from retarded Ag diffusion in the presence of nitrogen.

G3.06

YSZ-based NO_2 Sensor Utilizing Hierarchical In_2O_3 Electrode Fangmeng Liu[1, 2], Yehui Guan[1, 2], Ruize Sun[1, 2], Xishuang Liang[1, 2], Peng Sun[1, 2], Yuan Gao[1, 2] and Geyu Lu[1, 2];[1]College of Electronic Science and Engineering, Jilin University, Changchun, China; [2]State Key Laboratory on Integrated Optoelectronics, Jilin University, Changchun, China.

Nitrogen dioxide (NO_2), as one of harmful pollutants, causes a wide variety of adverse health and environmental impacts. Up to now, to accurately monitor NO_2, single and complex oxides (perovskite and spinel type oxides) have been investigated as the sensing electrodes of the YSZ-based NO_2 sensors. In this work, the NO_2 sensor using YSZ as electrolyte and hierarchical In_2O_3 as sensing electrode (SE) was fabricated. The present study mainly focused on the effect of In_2O_3 morphology on NO_2 sensing performances. The result showed that the diffraction peaks agreed well with the data of JCPDS# 06-0416 regarding In_2O_3 oxide. Additionally, the NO_2 sensing performances of the sensor using typical In_2O_3–SE were given. The 90% response and recovery times of the sensor to 100 ppm NO_2 were approximately 20 and 30 s, respectively. The response of the sensor to 100 ppm NO_2 was still as large as 114 mV at 700°C. The ΔV was almost linearly dependent on the logarithm of NO_2 concentration at 700°C. The slope of the dependence is 70 mV/decade. Given these excellent sensing performances, the sensor has potential application value in the detection of NO_2 gas.

G3.07

Mixed Potential Type Acetone Sensor Using Stabilized Zirconia And $M_3V_2O_8$ (M: Zn, Co, Ni and Mg) Sensing Electrode Fangmeng Liu [1, 2], Yehui Guan[1, 2], Ruize Sun[1, 2], Xishuang Liang [1, 2], Peng Sun[1, 2], Fengmin Liu [1, 2] and Geyu Lu[1, 2]; [1]College of Electronic Science and Engineering, Jilin University, Changchun, China; [2]State Key Laboratory on Integrated Optoelectronics, Jilin University, Changchun, China.

Acetone is a volatile chemical reagent and extensively used in chemical industry. However, inhalation of acetone will cause headache, fatigue and even harmfulness to nerve system. Besides, it is well known that acetone has been classified as an important breath biomarker for noninvasive diagnosis of human type-1 diabetes. Therefore, it is necessary to develop the smart sensing device that can precisely monitor the acetone concentration for health and safety. In this work, a kind of solid electrolyte type acetone sensors based on stabilized zirconia plate and $M_3V_2O_8$ (M= Zn, Co, Ni and Mg)sensing electrodes have been fabricated and tested. As a result,the sensor attached with $Zn_3V_2O_8$ exhibited the largest value among four kinds of tested oxides. Thus, the detailed sensing properties of the sensor using $Zn_3V_2O_8$ as sensing electrode were further examined. The ΔV was almost proportional to the logarithm of acetone concentration, and the sensitivity (slope) for the sensor was -56mV/decade at 700 °C. Additionally, the speedy response and recovery characteristics are obtained. The 90% response and recovery times of the sensor to 100 ppm acetone were approximately 28 and 40 s, respectively. Given these excellent sensing characteristics,such sensor can accurately monitor acetone.

G3.08

Electrolyte Related Parameters of Coulometric Solid State Devices Jens Zosel, Matthias Schelter, Vladimir Vashook, Ulrich Guth and Michael Mertig; Kurt-Schwabe-Institut für Mess- und Sensortechnik e.V. Meinsberg, Waldheim, Germany.

Introduction

Coulometric solid electrolyte sensors and measuring systems grow in importance for a variety of applications [1]. One of their main advantages concerns their relatively precise function based on Faraday´s law enabling calibration free performance over long time spans. Using these devices for the measurement of very small amounts of analytes, deviations from the Faraday´s law become visible [2]. The present paper gives an overview on these sources of error and discusses possibilities of their diminishment.

Experiments

Tubular solid electrolyte sensors based on zirconia stabilized with yttria (YSZ) were prepared with electrode materials Pt and different ABO_3-perovskites doped at A- and B-sites. Operated as flow-through devices, the sensors were investigated with respect to their zero currents, based on hole and electron conductivity in a wide potential range. Additionally, their oxygen storage behavior was characterized at oxygen partial pressures between $p(O)_2 = 4.2*10^{-17}$... $2.5*10^{-3}$ Pa. Selected sensor probes were investigated as devices for measuring of oxygen and water exchange in solid and gaseous materials.

Results and Discussion

An YSZ based coulometric sensor with a tubular flow through cell (inner diameter 4 mm, outer diameter 6 mm, length 60 mm), was purged with ultraclean nitrogen to measure the partial conductivities of electrons and defect-electrons in a wide potential range. These conductivities are mainly responsible for the steady-state deviations from the Faraday´s law. Especially the electron-related partial conductivity was found to be significantly lower than that published in [3]. Non-steady state deviations occur if the electrode potential has to be changed during measurement. The current response during a step like change of electrode potential of 50 mV in both directions exhibits a peak like curve. According to [4] most of the charge covered by the pulse is represented by oxygen incorporated into or extracted from the sensor according to the step direction. The all-temperature minima of the charge at -450 mV within the potential range -300 ... -1050 mV as well as the different time constants in the current recovery curve indicate that different storage processes have to be taken into account [5]. In contrast to the pulse related non faradaic charge the peak current depends solely on temperature and pulse potential difference.

Conclusions

Solid electrolyte flow-through devices were investigated with respect to their errors when operated as coulometric sensors. The measurements show that in stationary and transient conditions deviations from the faradayic conversion occur which can, however, be quantified precisely.

References

[1] V. Vashook, J. Zosel, U. Guth, J Solid State Electrochem **16** (2012) 3401.
[2] J. Maier, Festkörper - Fehler und Funktion, B. G.Teubner, Leipzig, 2000.
[3] J.-H. Park, N. Blumenthal, J. Electrochem. Soc. 136 (1989) 2867.
[4] Hartung, Z. phys. Chemie, Leipzig 254 (1973) 5/6, 393-410
[5] S. B. Adler, Chem. Rev. 2004, 104, 4791-4843.

G3.09

Enhanced Ambient-Dependent Photoresponse of $LaAlO_3$/$SrTiO_3$ Heterointerface via Catalytic Pd Nanoparticles Haeri Kim[1, 2], Ngai Yui Chan[3], Ji-yan Dai[3] and Dongwook Kim[1];[1]Physics, Ewha Womans University, Lexington, Kentucky, United States; [2]Clean Energy Research Center, Korea Institute of Science and Technology (KIST), Seoul, Korea (the Republic of); [3]The Hong Kong Polytechnic University, Hong Kong, Hong Kong.

Pd nanoparticle (NP) coated $LaAlO_3$/$SrTiO_3$ (LAO/STO) heterointerface exhibits significantly enhanced ambient-dependent UV photoresponse than a sample without the NPs. We performed Kelvin probe force microscopy and transport measurements simultaneously while varying the ambient gas (N_2, H_2/N_2, and O_2) and illuminating with UV light (wavelength: 365 nm), which revealed close relationships between the surface work function (*W*) and conductance (*G*) of the samples. Quantitative analyses suggest that a surface adsorption/desorption-mediated reaction and redox, resulting in a band-alignment modification and charge-transfer, could explain the gas- and photo-induced conductance modulation at the LAO/STO interface. Such surface-and-interface coupling enhanced by catalytic Pd NPs is a unique feature, quite distinct from conventional semiconductor hetero-junctions, which enables the significant conductance tunability at ultrathin oxide heterointerfaces by external stimuli.

G3.10

Hybrid Organic-Inorganic Perovksite Thin Films for Nonvolatile Memory and Broadband Photodetector Koo Tak Hong[1], Jaeho Choi[1], Ki Chang Kwon[1], Sunghak Park[1], Sooyoung Kim[2], Ki Tae Nam[1] and Ho Won Jang[1]; [1]Materials Science & Engineering, Seoul National University, Seoul, Korea (the Republic of); [2]School of Chemical Engineering and Materials Science, Chung-Ang University, Seoul, Korea (the Republic of).

Hybrid organic-inorganic perovskite have attracted huge attentions as solar sensitizer for next-generation solar cells due to its high charge carrier mobilities, high photoconversion efficiencies, low cost, and solution synthesis process. Among the Hybrid organic-inorganic perovskite materials, methyl ammonium lead iodide($(CH_3NH_3)PbI_3$) is a strong candidate for high efficient solar sensitizer. Futhermore, with controlling and tailoring the structure of $(CH_3NH_3)PbI_3$, $(CH_3NH_3)PbI_3$ can be applicable in various applications.

In this study, we report that various characteristics of $(CH_3NH_3)PbI_3$ to make use of non-volatile memory and broadband photodetectors. With highly uniform $(CH_3NH_3)PbI_3$ thin films including precise thicknesses and reproducible crystallinity, we could fabricate devices are diverse structures by spin coating. Our experimental results reveal that I-V characteristics of $(CH_3NH_3)PbI_3$ thin films are insulating in low voltage bias, but the thin films become conducting in high voltage bias. From these electrical properties (I-V), it is possible to analyze conduction mechanism in $(CH_3NH_3)PbI_3$ thin films. We reveal that the conduction mechanism by the change of metals for electrodes with conductive atomic force microscopy. Also, it is suggested that interplay between Schottky emission and Ohmic conduction are a key for unveiling conduction mechanism.

Furethermore, $(CH_3NH_3)PbI_3$ thin films show excellent performance as a broadband photodetector with fast response and recovery. $(CH_3NH_3)PbI_3$ broadband photodetector reponse to a broadband wavelength from the ultraviolet and to visible light region. With controlling the thickness of $(CH_3NH_3)PbI_3$ thin films, the response ratio of $(CH_3NH_3)PbI_3$ broadband phodetector increases to 10^3. From the results, $(CH_3NH_3)PbI_3$ has the strong potential for application to various field and multifunctional devices.

I: Ion Transport in Hybrid Organic-Inorganic Solids

* Invited Speaker
** Keynote Speaker

SESSION I1: Poster Session
I: Ion Transport in Hybrid Organic-Inorganic Solids
Tuesday Afternoon, June 16, 2015
5:20 PM
Keystone Resorts, Red Cloud Peak

I1.01
Hydration and Proton Transfer in DNA-M (M=H, Li, Na) Saki Ito, Hitoki Semizo and Yasumitsu Matsuo; Department of Science and Engineering, Setsunan University, Osaka, Japan.

Most of tissue-derived biomaterials have ion permeability and become superior ion transfer materials. Therefore, a lot of tissue-derived biomaterials act as proton conductor and can be applied as a new fuel cell electrolyte. In the present work, we have prepared water insolubility DNA, DNA-Na and DNA-Li fibers and their films, and investigated the relation between the orientation of DNA molecule and proton transfer.
DNA solutions derived from the testis of the salmons were used in the present work. DNA-Na specimens were prepared from DNA using ethanol precipitation with sodium acetate by in order to bond a Na ion to phosphate group of DNA. DNA-Li specimens were prepared by ethanol precipitation using lithium chloride. In DNA-Li, Li ion is bonded with phosphate group. Water insolubility DNA specimens were grown by irradiating ultraviolet rays of 16mW/cm^2 at 254nm for 24 hours.
It was found that DNA-Na shows proton conductivity in the humidified condition. The proton conductivity strongly depend on the orientation of DNA molecule, and proton conductivity parallel to DNA-Na fiber direction is higher than that normal to DNA fiber. From these results, it is deduced that there is strong anisotropy in the formation of water bridge which yields proton transfer. In addition, by the bond between PO_4 of DNA side chain and Na (or Li), proton conductivity in DNA increases. These results indicate that the existence of Na and Li facilitates proton conductivity in DNA.

I1.02
Synthesis and Characterization of Bis (acetylacetonato κ-O, O') [zinc (II)/cobalt (II)] Hybrid Organic-Inorganic Complexes as Solid Metal Organic Precursor Reza Rooydell,Matin Roshanzamir Modaberi, Sanjaya Brahma and Chuan-Pu Liu; MSE Material and Science Engineering, National Cheng Kong University, Tainan, Taiwan.

Synthesis of hybrid organic-inorganic materials has been a subject of intensive research [1,2] New bimetallic as precursor compounds of bis (acetylacetonato) [Zn/Co], synthesized. This complex prepared by reactions of Zn (NO3)2.6H2O and Co(NO3)2.6H2O with acetylacetonate (acac) in water. The crystallizes complex in the monoclinic system, space group P1 21/c1. The cell dimensions are a = 10.789(4) Å, b = 5.355(2) Å, c = 11.058(5) Å, α = 90°, β = 105.683(8)°, γ = 90°and Volume is 615.0(4) Å3 . Besides this method, X-ray diffraction (XRD), X-ray photoelectron spectroscopy (XPS), energy-dispersive X-ray spectroscopy (EDX), Infrared spectroscopy (IR), and Mass Spectroscopy (MS) and TEM also confirm this structure. The C10 H18 Co0.40O6 Zn0.60 compound is a metal-organic precursor (MO). This complex prepared from safe and short reaction time. With control of amount of Zn/Co and optimization the amount of Zn/Co initiators, pH and temperature, bimetal complex prepared in high yield. Fig 1 shows (a), XRD spectrum and (b) chemical structure complex.

References
1]Y. Chujo KONA (2007) 255-260 (b) Z. Zeng, D. Matuschek, A. Studer, C. Schwickert, R. Pöttgenc H. Eckert Dalton Trans., 2013 , 42, 8585
2] M. Baibarac, I. Baltog, I. Smaranda, M. Scocioreanu, S. Lefrant, J. Mol. Struct. 985 (2011) 211

I1.03
Nanocomposite Polymer Electrolyte Membranes Based on PVA-PVP Blend Polymer: An Evidence of Ion Diffusion through Open and Closed Polymer Network Govind K. Prajapati[1], Prem N. Gupta[2] and Ravindra Dhar[1]; [1]Center of Material Sciences, Institute of Interdisciplinary Center, University of Allahabad, Allahabad, India; [2]Department of Physics, Faculty of Science, Banaras Hindu University, Varanasi, Varanasi, India.

Nanocomposite membranes composed of PVA-PVP blend and phosphoric acid dispersed with fumed silica nanoparticles are prepared by cost effective solution cast technique. The prepared membranes were characterized by XRD, SEM, DSC, FTIR and broadband dielectric impedance spectroscopy. The X-ray diffraction study confirms that electrolyte films have predominantly amorphous morphology. The FTIR peak at 3400 cm^{-1} in presence of PVP in PVA/H_3PO_4-SiO_2 composite demonstrates the grafting between two polymers. The presence of open ionic channels and variation in morphology for different wt% of SiO_2 was confirmed by SEM. A single melting and glass transition temperature observed in DSC shows the miscibility of blend polymers. The analysis of impedance spectroscopy represented by semicircle pattern is driven by conduction mechanism and correlated with electrical conductivity. The enhanced AC conductivity is directly proportional to frequency which allows the ion diffusion through hopping mechanism assisted with polymer chains. The complex-dielectric function spectra of these membranes have dispersion at high frequencies due to polymer chain segmental dynamics, whereas the electrode polarization phenomenon dominates in low frequency region. Results reveal that the complex-dielectric spectroscopy is an effective tool for studying DC ionic conductivity and their nano-dynamics in complex electrolytes. The maximum dc conductivity ~ 1.2x10^{-5}Scm^{-1} (1.5 wt% silica) has been evaluated from Arrhenius plot. It is observed that at high silica content, mobility is an important parameter for variation in ionic conductivity. It can be suggested that at lower silica content, the available charge carriers' forms an open silica network through which charge carries can easily hop from one site to other, however, they form a closed polymer network at higher silica content which reduces the ionic mobility and thereby conductivity. The evaluated results of structural, morphological and electrical properties of present nanocomposite membranes make the present research applicable for all-solid-state electrochemical devices.

SESSION I2: Ion Transport in Hybrid Perovskites
I: Ion Transport in Hybrid Organic-Inorganic Solids
Chair: Hemamala Karunadasa
Wednesday Morning, June 17, 2015
Keystone Resorts, Grays Peak I/II

10:30 AM **I2.01
Electromigration of Ions in Hybrid Perovskites for Switchable Photovoltaic, Memristors and Synapses Jinsong Huang; Department of Mechanical and Materials Engineering, University of Nebraska, Lincoln, Lincoln, Nebraska, United States.

Understanding of the origin of ions electromigration in hybrid perovskite materials not only helps explore the origin of the notorious photocurrent hysteresis in the orgonatrihalide perovskite (OTP) solar cells, but also helps understand the long term stability of OTP solar cells. We will report giant switchable OTP photovoltaic devices with vertical and lateral cell configurations induced by the electromigration of ions in the OTP materials. The photocurrent direction can be switched repeatedly by applying a small electric field of <1 V/μm. The switchable photocurrent, generally observed in devices based on ferroelectric materials, reached 20.1 mA/ cm2 under one sun illumination in OTP devices with a vertical architecture, which is four orders of magnitude larger than that measured in other ferroelectric photovoltaic devices. The lateral OTP devices can output a large open circuit voltage over 70 V with excellent connection in series without losing the photocurrent output. This field-switchable photovoltaic effect can be explained by the formation of reversible p–i–n structures induced by ion drift in the perovskite layer. The contribution of ion transportation to the total electric current in hybrid perovskite devices will be discussed. We will also discuss our recent study in identifying what is moving in OTP materials under electric field, and describe the potential application as memristors and synapses.

11:00 AM I2.02
Photo-Induced Instability in Mixed Halide Perovskite Absorbers Daniel Slotcavage[1], Eric Hoke[1], Emma Dohner[2], Andrea Bowring[1], Hemamala Karunadasa[2] and Michael McGehee[1];[1]Materials Science & Engineering, Stanford University, Stanford, California, United States; [2]Chemistry, Stanford University, Stanford, California, United States.

Metal-organic trihalide perovskites have received significant attention in recent years due to their exceptional photovoltaic properties. In particular, $(CH_3NH_3)PbI_3$ has shown power conversion efficiencies exceeding 18%. One particularly useful property of $(CH_3NH_3)PbI_3$ is that its bandgap can be increased by replacing I with Br. Perovskites of the form $(CH_3NH_3)Pb(Br_xI_{1-x})_3$ offer bandgaps ranging from 1.6eV ($(CH_3NH_3)PbI_3$) to 2.3eV ($(CH_3NH_3)PbBr_3$), making them attractive for use in tandem solar cells with 1.1eV bottom cells such as Si or CIGS. However, when incorporated into solar cells, the mixed I/Br perovskites do not yield the expected higher open circuit voltages corresponding to their higher bandgaps. We performed in-situ XRD coupled with photoluminescence and absorption spectroscopy to investigate why higher open circuit voltages have not been achieved and discovered a reversible, light-induced phase segregation. In-situ XRD of mixed I/Br perovskite thin films revealed that photoexcitation causes a structural transformation, forming distinct I-rich and Br-rich perovskite phases. Photoluminescence spectra showed that a new, lower energy peak formed at 1.68eV over the course of one minute when exposed to one-sun light intensity. Absorption spectra of light-soaked films confirmed the formation of a phase that absorbed at lower energy. We imaged these phases using photoluminescence and cathodoluminescence hyperspectral mapping. The phase segregation was reversible; when left in the dark for several minutes, the original (pre-light soaking) XRD, photoluminescence, and absorption spectra were attained. We propose that photoexcitation promotes halogen segregation into a lower bandgap I-rich phase and a higher bandgap Br-rich phase and that the former acts as a luminescent trap. The formation of this lower energy trap state may limit open circuit voltages in mixed halide solar cells, and the migration of halogen ions may have serious implications for the long-term stability of metal-organic trihalide optoelectronic devices.

11:20 AM I2.03
Ionic Conductivity in 3-D Organic-Inorganic Mixed Halide Perovskites Abraham Saldivar Valdes and Hemamala Karunadasa; Chemistry, Stanford University, Stanford, California, United States.

My work focuses on ion migration in lead-halide based 3-D organic-inorganic perovskites; semiconductors relevant to photovoltaic and optoelectronic applications. Previous work by our group has reported changes in the structure and optical properties of mixed-halide 3-D organic-inorganic perovskites upon white light irradiation, which we postulate occurs through halide ion migration and segregation. [1] I have demonstrated ion migration in these materials by incorporating perovskite thin films into solid-state electrochemical cells, and will present data for perovskites with a range of halide and counterion compositions in order to shed light on the conduction mechanism. Halide conduction and defects are emerging as fundamental properties of perovskite semiconductors, akin to oxide ion conductivity in transition metal oxide perovskites. This could have serious implications for the stability and reliability of perovskites in photovoltaics, and contribute to the oft-mentioned sensitivity of perovskite solar cell efficiency to processing conditions. I will conclude by elaborating on possible avenues to minimize the instability of these materials to irradiation.

1. E.T. Hoke, et al. Chem. Sci., 2015, 6, 613–617

11:40 AM I2.04
Uniform Perovskite Layers for Low Hysteresis Planar Heterojunction Solar Cells Yanbo Li[1, 2], Ian D. Sharp[2] and Francesca Maria Toma[1, 2]; [1]Lawrence Berkeley National Lab, Berkeley, California, United States; [2]Joint Center for Artificial Photosynthesis, Berkeley, California, United States.

A new method for achieving high efficiency planar organometal hybrid perovskite photovoltaics, based on a low pressure, reduced temperature vapor annealing is demonstrated.[1]Heterojunction devices based on $CH_3NH_3PbI_{3-x}Cl_x$ perovskite exhibit a top power conversion efficiency (PCE) of 16.8%, reduced *J–V* hysteresis, and highly repeatable performance without need for a mesoporous or nanocrystalline metal oxide layer. X-ray diffraction, valence band spectroscopy, and transient absorption measurements of these thin films reveal that structural modifications induced by chlorine dominate over chemical and electronic doping effects, without affecting the Fermi level or photocarrier lifetime in the material. X-ray diffraction of $CH_3NH_3PbI_{3-x}Cl_x$ and $CH_3NH_3PbI_3$ films provides evidence for the highly crystalline nature of our samples. However, Rietveld refinement reveals significantly reduced texture in $CH_3NH_3PbI_{3-x}Cl_x$ films compared to $CH_3NH_3PbI_3$ films synthesized under identical conditions. This finding supports that thin film crystallographic texture is important, indicating a change in growth orientation with Cl incorporation, which shows the highest efficiency
.
In addition, we demonstrate that large hysteresis is not an inherent feature of planar heterojunctions, and that efficient charge extraction can be achieved with uniform halide perovskite materials with desired composition. Several possible causes of hysteretic behavior have been proposed, with ionic mobility in this material one of the leading candidates. The influence of different halide composition ($CH_3NH_3PbI_3$, $CH_3NH_3PbI_{3-x}Cl_x$, $CH_3NH_3PbI_{3-x}Br_x$) and the role of structure, as well as the possibility of ionic mobility, of the perovskite films on efficiency and hysteresis of photovoltaic devices are also investigated.
1 Y. Li, J. K. Cooper, R. Buonsanti, C. Giannini, Y. Liu, F. M. Toma, and I. D. Sharp, *J. Phys. Chem. Lett*. **2015**, 6, 493-499

SESSION I3: Ion Transport in Organic-Inorganic Hybrid Solids
I: Ion Transport in Hybrid Organic-Inorganic Solids
Chair: Abraham Saldivar Valdes
Friday Morning, June 19, 2015
Keystone Resorts, Grays Peak III

10:30 AM **I3.01
Discovery of Molecular Disorders in Coordination Frameworks for Solid State Ionics Satoshi Horike; Kyoto University, Kyoto, Japan.

Disorder of molecules and their ions in crystalline solids plays a crucial role for ionic functions. We have focused on a variety of disordering in inorganic/organic hybrid crystals including metal organic frameworks (MOFs).[1] In terms of proton conductivity, proton carriers such as imidazole and phosphate can be involved in the coordination bond-based frameworks (coordination frameworks) with highly disordered fashion,[2] and it results over 10^{-2} S cm^{-1} of conductivity at above 100 degC under water-free condition. Control of disorder of metal ions and ligands in coordination frameworks provides not only fast ion conduction, but gives plastic crystal behavior and reversible crystalline-amorphous transformation which relates to ion conduction switching and anisotropic ion transportation.[3]

[1] S. Horike, D. Umeyama, S. Kitagawa, *Acc. Chem. Res.*, **2013**, 46, 2376–2384.
[2] S. Horike, D. Umeyama, S. Kitagawa, et al. *J. Am. Chem. Soc.* **2012**, 134, 9852–9855.
[3] D. Umeyama, S. Horike, S. Kitagawa, et al. *J. Am. Chem. Soc.* **2015**, 137, 864–870.

10:55 AM **I3.02
Designing Proton Conducting MOFs George Shimizu; Chemistry, University of Calgary, Calgary, Alberta, Canada.

Metal organic frameworks (MOFs) or porous coordination polymers (PCPs) represent a tunable molecular scaffolding that can be adjusted for a breadth of applications. This presentation will concern our efforts towards tailoring MOFs towards making new proton conductors. In contrast to the macromolecular approaches typically employed towards these electrolytes, we have used a MOF strategy to generate crystalline networks with acidic pores. These MOFs present options to address higher temperature conduction,[1] conduction over 10^{-2} Scm^{-1},[2] and water stability.[3] The emphasis in the talk will concern routes to designing these systems and improving both conduction and water stability.

1. J. A. Hurd et al. *Nature Chem*. **2009**, *1*, 705.
2. S. Kim et al., *J. Am. Chem. Soc*. **2013**, *135*, 963.
3. J. M. Taylor et al., *J. Am. Chem. Soc*. **2013**, *135*, 1193.

11:20 AM I3.03
Effect of Ionic Liquid 1-Butyl-3-Methylimidazolium Methylsulfate on (Polyethylene Oxide, PEO + Sodium Methyl Sulfate Salt, Nams) Polymer Electrolyte Membrane Rajendra K. Singh; Physics, Banaras Hindu University, Varanasi, India.

Polymer electrolyte membranes based on polymer PEO, ionic liquid BMIMS and salt sodium methyl sulfate, NaMS {PEO+x wt.% BMIMMS for x =0 and 20 and (PEO+10 wt.% of NaMS)+x wt.% BMIMMS)} are prepared by solution cast technique. Prepared membranes are characterized by various techniques like TGA/DTGA, DSC, XRD, SEM, ac impedance spectroscopy and cyclic voltametery (CV). The synthesized polymer electrolyte membranes are free-standing and flexible with good mechanical stability. From FTIR spectroscopic studies, it is observed that the ether oxygen group of the PEO backbone complexes with the cation of the Na-salt / or IL. SEM, XRD and DSC studies show that the crystallinity of the polymer electrolyte membranes decreases on increasing the concentration of IL due to the plasticization effect of IL. The polymer electrolyte membrane containing 60 wt.% BMIMMS provides maximum ionic conductivity of ~1.05×10^{-4} S cm^{-1} at room temperature. This composition of polymer electrolyte shows highest electrochemical potential window of order of ~4.8 V.

11:40 AM I3.04
On the Origin and Underappreciated Effects of Ion Doping in Silica Xiaohui Song and Hongyu Chen; Chemistry and Biological Chemistry, Nanyang Technological University, Singapore, Singapore.

We argue for a paradigm shift in viewing silica nanomaterials. Silica is an old material with useful applications. It is a covalent network solid well known of its insolubility in water. In contrast to the silica materials underwent molten conditions (sand, glass, etc.), those synthesized by solution methods have drastically different properties, in terms of the microporosity, the incorporated impurities, and the solubility in neutral aqueous solutions. Here, we investigate the fundamental reasons for the hollowing of silica nanoparticles upon etching. We realize that, during the synthesis, silica precursors are essentially crosslinked polyelectrolytes, which can take in lots of counter ions and should be highly swollen by the polar solvents. Most importantly, their solubility should depend on the size/length of the poly(silicic acid), the concentration of the counter ions, and the solvent polarity. Thus, the “silica” that nucleates out at the different stages of synthesis should have different degrees of ion doping, which explains the unusual solubility of the Stöber silica, its microporosity, and the selective hollowing of the nanoparticles. The embedded ions in silica are confirmed by elemental analysis (CHNS) and ICP-MS. With this knowledge and the shift from the conventional views, we design different quality of silica by modulating the solvent ratio, acidity, and salt concentration, creating new toolboxes for future applications.

J: Permeation Membranes

* Invited Speaker
** Keynote Speaker

SESSION J1: Poster Session I
J: Permeation Membranes
Monday Afternoon, June 15, 2015
12:00 PM
Keystone Resorts, Red Cloud Peak

J1.01
Hydrogen Membranes Based on Group-IV Metal Nitrides Yoshitaka Aoki[1, 2], Chiharu Kura[1], Etsushi Tsuji[1] and Hiroki Habazaki[1]; [1]Faculty of Engineering, Hokkaido University, Sapporo, Japan; [2]JST-PRESTO, Kawaguchi, Japan.

Hydrogen is an ideal fuel resource, because it can be generated by water electrolysis by using renewable electricity from solar, window and water power generation. However, the difficulties in storage and transportation of hydrogen hinder its application for commercial fuels. Therefore, various kinds of hydrogen-containing compounds, such as alcohol, organic hydrides, borohydrides and ammonia have been investigated as a 'hydrogen carrier'. Among them, ammonia has attracted considerable interest as a carbon-free fuel source for fuel cells due to the low cost, ease in liquefaction and transportation at ambient temperatures, and high volumetric energy density. Hydrogen permeation membranes are the key components to separate pure hydrogen in ammonia fuel reforming process. Group 5 metals (ex. Nb, Ta) have higher hydrogen permeability and are used as hydrogen separation membranes, however, they are severely corroded by NH_3 even at room temperature. Hence, it is the motivation to develop the hydrogen permeation membranes which can work under NH_3 atmosphere. Nitrides of group 4 metals (ex. ZrN, HfN, TiN) are known to be tolerant in ammonium atmosphere and have a hydrogen adsorption ability. In this work, we demonstrate the hydrogen permeability of MN_x (M=Ti, Zr) by fabricating the self-standing membrane on a porous oxide substrate. The relationship between hydrogen permeability and nitrogen nonstoichiometry of MN_x thin films was investigated. Highly-crystalline, nonstoichiometric MN_x films (x = 1.02 -0.62) were successfully fabricated by reactive RF sputtering processes with adjusting the nitrogen partial pressure and the substrate temperature. Hydrogen permeability test was performed in the temperature range of 300 to 500°C by fabricating sub-1 mm-thick MN_x membranes on γ-Al_2O_3 / α-Al_2O_3 porous substrates.

J1.02
Synthesis and Characterization of Chitosan/Sulfonated Poly(terephthalate) Polyelectrolyte Complexes and Study of Its Effects on Water Vapor Flux in Commercial Polycarbonate Membranes Rayane d. Vale; Chemistry, Universidade Federal de São Carlos, São Carlos, Brazil.

Polyelectrolyte complexes (PECs) are defined as materials formed by combining oppositely charged polyelectrolytes together via ionic interaction. PECs have some unique physical properties such as non-solubility in common organic solvents, no glass transitions, high surface hydrophilicity,tunable surface charge, and stable structures. These properties make PEC membranes ideal candidates for pervaporation, nanofiltration and próton exchange membranes.

The systematic analysis of how the internal structure of the PEC and the subsequent membrane formation can affect water transport capacity and thus rejection to ionic solutes is a scientific opportunity to be exploited. Based on this context, a new type of PEC based on chitosan (CS) and sulfonated poly(terephthalate) (SPET) were synthesized in two different media, buffer solution and salt solution acidified with acetic acid. Fourier transform infrared spectroscopy, thermal gravity analysis, X-ray diffraction and zeta potencial were used to characterize the chemical structure, thermal stability, crystallinity and particle charge, respectively. Solutions of PEC were spread via casting in commercial polycarbonate membranes. These membranes have been characterized using Scanning Electron Microscopy and water vapor flux.

FT-IR results indicated that the SPET have been dissociated into SO_3^- groups that complex with protonated amino groups of CS through electrostatic interaction to form the polyelectrolyte complex. TGA curves were quite different to each other, indicating that thermal stability of PECs are influenced by the media. From the results of zeta potential it was found that the surfaces of CS-SPET nanoparticles have positive charges of about 25–44 mV. DRX indicated the semi-crystalline structure of CS and the amorphous structure of SPET, PECs also presented amorphous structure. The deposition of the PEC on the membranes was confirmed by SEM and the increase of water vapor flux of membranes indicated that the presence of the complex significantly alter the hydrophilic profile of the polycarbonate matrix.

J1.03
The Effect of Compatibilizer in sPEEK/PVdF/UAN Composite Membrane for Vanadium Redox Flow Battery Seon G. Rho[1] and Ho Y. Jung[2]; [1]School of Applied Chemical Engineering, Chonnam National University, Gwangju, Korea (the Republic of); [2]Department of Environment & Energy Engineering, Chonnam National University, Gwangju, Korea (the Republic of).

For Vanadium Redox Flow Battery (VRFB), the compatibilizer, urethane acrylate non-ionomer (UAN), is introduced to sulfonated poly(ether ether ketone) (sPEEK) / poly (vinylidene fluoride) (PVdF) to improve their interfacial stability between different domains. The composite membrane based on sPEEK/PVdF/UAN is characterized by the water uptake, the proton conductivity and SEM (scanning electron microscopy). UAN, the compabilizer, improves the interfacial stability between sPEEK and PVdF domains, and the proton conductivity due to the interconnected morphology of hydrophilic domains in sPEEK polymer. It leads good cell performance at the initial stage of the unit cell operation, and good cycle performance due to the suppressed permeation of vanadium ion and high proton conductivity. Therefore, the composite membrane based on sPEEK/PVdF/UAN can be the candidate for the application of the vanadium redox flow battery.

[Acknowledgement]
This research was supported by Korea Electric Power Corporation Research Institute through Korea Electrical Engineering & Science Research Institute (grant number : R14XA02-29).

J1.04
Nickel Nanocatalyst Exsolution on Modified $La_{0.75}Sr_{0.25}Cr_{0.5}Mn_{0.5}O_3$ and $La_{0.75}Sr_{0.25}Cr_{0.5}Fe_{0.5}O_3$ Perovskites for the Fuel Oxidation Layer of Oxygen Transport Membranes Despoina Papargyriou and John T. Irvine; School of Chemistry, University of St Andrews, St Andrews, United Kingdom.

Oxygen Transport Membranes (OTMs) offer a promising technology for directly supplying oxygen to a fuel gas for the purpose of generating syngas or heat. In this project, the OTM is based upon an inactive support that sequentially has a fuel oxidation layer, a dense layer and a reduction layer, which are a combination of perovskites and fluorites. In order to improve the fuel oxidation layer's performance, the incorporation of a catalyst in the perovskite lattice is necessary. As the fuel oxidation layer is deeply buried in the structure the traditional method of direct impregnation of a solution containing desired cations would be difficult, not to mention wasteful, costly and time consuming. The in situ nanocatalyst exsolution appears to be the best approach to solve this problem. Redox exsolution tends to grow pinned metal nanoparticles on the reduced oxide surface offering excellent possible catalytic properties and the possibility to regenerate the nanostructure via a redox cycle.

In the present study, $La_{0.75}Sr_{0.25}Cr_{0.5}Mn_{0.5}O_3$ (LSCM) and $La_{0.75}Sr_{0.25}Cr_{0.5}Fe_{0.5}O_3$ (LSCF) perovskites with partial substitution of Mn and Fe by 5 mol% of Ni were synthesized and characterized. X-ray diffraction was used to study the phase formation in different temperatures and it evidenced that single phase compounds were obtained at 1300°C. LSCM exhibits a rhombohedral structure and LSCF an orthorhombic structure. Both materials retain their structures, after doping the B site with

Ni, with small changes on the unit cell parameters. Thermal analysis under reducing conditions was used to investigate the reducibility of these perovskites up to 900ºC, which appears to be enhanced by doping with Ni. The formation of Ni nanoparticles (30-50nm) on the LSCM-Ni and LSCF-Ni grains was observed by scanning electron microscopy, after reducing the samples in 5%H_2/Ar at 900ºC, indicating possible enhanced catalytic activity and potential benefits for the development of the OTMs.

J1.05

Surface Characterization of Dual-Phase Oxygen Transport Membrane by Low Energy Ion Scattering (LEIS) Chi Ho Wong, Stephen Skinner and John Kilner; Materials, Imperial College London, London, United Kingdom.

Introduction

Oxygen transport membranes offer a viable alternative to current reaction processes that are environmentally and/or economically costly. To optimize the rate of oxygen flux through the membrane, it is necessary to ascertain the amount of each phase present on the surface. In combination with oxygen tracer experiments [1,2], surface incorporation and bulk migration of oxygen can be better understood.
Low Energy Ion Scattering (LEIS) allows a semi-quantitative analysis of the elemental composition of the outermost atomic surface layer [3]. Surface analyses were performed on fully-dense dual-phase scandia stabilized zirconia (50vol%) / lanthanum chromite based perovskite (50vol%) (ScSZ/LSCr) ceramic composites.

Experimental

Powders of ScSZ and LSCr obtained from industrial sources were mixed in the specified ratio, ball milled in ethanol and sintered in air at 1450ºC for 6 hours producing dense pellets. Surface analysis was performed using an IONTOF LEIS system (He^+ primary ion beam, 3 keV).

Results and Discussion

The LEIS spectrum of a ScSZ/LSCr membrane, Figure 1, shows the presence of all major elements in the dual-phase membrane within instrument detection limits [3]. A strong signal was observed at higher energies (~2500 eV), possibly due to Sr segregation. Separate analysis by LEIS of each of the individual phases of the membrane shows significant impurity segregation on the surface of ScSZ, resulting in the complete absence of the bulk elements. It is reasoned that the presence of impurities on ScSZ, possibly Na or Si, is a contributor to low oxygen incorporation in this phase. In contrast, the surface of LSCr was nearly devoid of impurities, and all major elements were present.

Conclusions

LEIS was performed on a dual-phase oxygen transport membrane to determine the elemental composition of the outermost surface atomic layer for comparison with oxygen transport measurements. All major elements were present on the surface within detection limits.

Acknowledgements

We express our gratitude to Praxair Inc. for the supply of powder samples and funding.

References

[1] J. A. Kilner et al., *J Solid State Electrochem*, **15** (2011) 861-876
[2] H. Tellez et. al, *Applied Physics Letters*, **101** 151602 (2012) 1-4
[3] H. H. Brongersma et. al., *Surface Science Reports*, **62** (2007), 63-107

J1.06

A and B Site Co-Doped Lanthanum Chromite Perovskite – Doped Zirconia Fluorite Composites for Oxygen Transport Membrane Systems Sapna Gupta[1, 2] and Prabhakar Singh[1, 2]; [1]Materials Science and Engineering, University of Connecticut, Storrs, Connecticut, United States; [2]Center for Clean Energy Engineering, University of Connecticut, Storrs, Connecticut, United States.

Oxygen transport membrane (OTM) technology is currently being investigated for efficient and clean power generation from coal and natural gas as well as liquid fuel production. This study investigates chemical and structural stability of strontium doped lanthanum chromite based perovskite ($(La_{0.8}Sr_{0.2})_{0.95}Cr_{1-y}B_yO_3$ - LSCrB) and stabilized zirconia composites as they can provide combination of redox stability, thermal expansion match with adjacent materials, and high electronic and ionic conductivity resulting in higher oxygen flux required for OTM system. Crystal structure, electrical conductivity, thermal expansion and electrochemical performance of the composites have been evaluated in oxidizing and reducing atmospheres in the temperature range of 30-1200°C. Role of Cr: B' ratio (7:3, 8:2, 9:1) and oxygen partial pressure (PO_2) are investigated on the stability of the composites using high temperature X-ray diffraction (HT-XRD), scanning and transmission electron microscopy (SEM and TEM) and electrochemical impedance spectroscopy. Mechanistic understanding and the role of Cr: B ratio and PO_2 on the properties and interfacial stability will be provided. Electrochemical performance degradation and the interaction between the perovskite and fluorite will be presented.

J1.07

Influence of the Oxygen Partial Pressure on the Oxygen Diffusion and Surface Exchange Coefficients in Mixed Conductors Jean-Marc Bassat; ICMCB-CNRS, Pessac , France.

Mixed ionic and electronic conductor materials (MIEC) are of great interest with respect to the development of Catalytic Membrane Reactor (CMR) as well as oxygen separation (semi-permeation) devices. High electronic and ionic conductivity values, as well as good kinetics in their oxygen surface exchanges are required. The oxygen diffusion (related to the oxygen conductivity) and/or surface exchange, characterized by the D and k coefficients, respectively, could be the limiting parameters with respect to the electrochemical performances of the systems. D and k can be determined 1) using the so-called IEDP (Isotopic Exchange Depth Profile) method coupled with SIMS recording on dense pellets, 2) designing a specific apparatus to measure at the same time the oxygen semi-permeation flux and the activity gradient at both membrane surfaces. The oxygen partial pressure at the surface of the studied material can be highly different on both faces of the pellet especially in the case of semi-permeation devices, where the pO_2 ratio between the oxygen-rich and the oxygen-lean is about 10^5-10^6. As a consequence, it is of high importance to include pO_2 as another experimental parameter, with the aim to clearly identify the rate determining steps.

Two different MIEC materials have been here studied, the first one with an oxygen deficient perovskite structure, the second one with a Ruddlesden-Popper (n=1) network including additional oxygen. From the two different kinds of measurements, the D and k coefficients were independently determined, as a function of temperature and oxygen partial pressure, then compared. We have demonstrated that the pO_2 in the surrounding gas atmosphere has a large impact on the surface exchange coefficients values of these mixed conductors.
A preliminary discussion for the suitable description of oxygen surface exchanges in the mixed conductors will be given.

J1.08

Scaling of Oxygen Transport Membranes Marie-Laure Fontaine[1], Christelle Denonville[1], Adam Stevenson[2], Christian His[2], Emmanuel Mercier[2], Caroline Tardivat[2], Xing Wen[1], Jonathan Polfus[1], Ove Paulsen[1], Paul Inge Dahl[1], Partow Henriksen[1] and Rune Bredesen[1]; [1]Materials and Chemistry, SINTEF, Oslo, Norway; [2]Saint Gobaine CREE, Cavaillon, France.

Oxy-combustion is a promising option for implementing cost-efficient carbon capture and sequestration (CCS) in future coal-fired power plants. The use of oxygen transport membranes (OTM) for oxygen production has the potential to significantly reduce efficiency losses associated with CO_2 capture and to improve the overall process economy. Benefits and challenges related to the scaling up and integration of OTM technology in power generation are currently investigated in a European project called "Highly Efficient Tubular Membranes for Oxy-Combustion" (HETMOC, FP7 Energy, 2009-2016). The project addresses critical technical challenges underpinning OTM technology from developmental processes to pilot scale component fabrication, materials production, assembly and testing in real conditions. Module design, construction and integration of balance-of-plant technologies at both laboratory and demonstration scales have been investigated with regards to optimization of the 100 TPD oxygen separation. The project embodies a multinational consortium from industry and research centres: Department of Energy Conversion and

Storage at the Technical University of Denmark (coordinator; DK), Forschungszentrum Julich GmbH (D), Fraunhofer IKTS (D), VITO (B), SINTEF (N), Air Liquide (Fr), Saint-Gobain CREE (Fr) and INABENSA (ESP). eliable and scalable fabrication processes are required for the cost effective production of highly efficient asymmetric membrane architectures consisting of thin (10-50 µm), dense films deposited on porous supports. This provides a balance between the competing requirements of high flux and mechanical robustness. Both reliability and scalability of manufacturing routes have been demonstrated through technology transfer of production technology from 0.2m – 0.4m long membranes at SINTEF to 0.7m long membranes for large production capacity at Saint Gobain CREE. A two-step transfer process has been carried out with progressive scale-up of both membrane length and production yield. In this presentation, we show that the membranes currently produced at SINTEF and Saint-Gobain CREE exhibit similar characteristics, indicating successful transfer of technology.

J1.09

Freeze-Casting Technique for the Manufacture of Hierarchical Porous Planar and Tubular Support for Gas Separation Ceramic Membranes Cyril Gaudillere, Julio Garcia-Fayos, Jose M. Serra and Sonia Escolastico; ITQ (UPV-CSIC), Valencia, Spain.

Asymmetric ceramic membrane manufacture remains today challenging and a good control of support porosity is crucial for membrane performances. The most conventional and easy route to elaborate porous support is to sinter at high temperature a mixture of ceramic powder with a pore former like starch or graphite. The resulting porosity is randomly organized, its size depends on the initial pore former particle size and the associated pressure drop through it is high and results in gas diffusion limitations. A very interesting route used recently for bone substitution and named *freeze-casting* seems to be promising for the elaboration of hierarchical and vertically-oriented porous support for asymmetric membrane[1]. It consists of freezing a liquid ceramic suspension, followed by the sublimation of the solvent under both low temperature and pressure and the final sintering of the ceramic particles for consolidation. The obtained structure is porous with oriented channels corresponding to the replica of the solvent crystals along the propagation direction of the solid-liquid interface. Modifying the powder characteristics, the freezing conditions or the slurry formulation, the porosity of the sample can be tailored for the targeted requirements.

Here, we present the fabrication and the characterization of freeze-cast porous support by using prototypical ionic conductor ceramic materials like $Ba_{0.5}Sr_{0.5}Co_{0.8}Fe_{0.2}O_{3-\delta}$ (BSCF), $Ce_{0.8}Gd_{0.2}O_{2-\delta}$ (CGO), Y_2O_3 doped ZrO_2 (YSZ) and $La_{0.6}Sr_{0.4}Co_{0.2}Fe_{0.8}O_{3-\delta}$ (LSCF) and its further implementation in both planar and tubular asymmetric membrane for gas separation applications.

The porous support elaboration process and the related microscopic study of the porosity will be firstly detailed. Emphasize on the versatility of the technique will be done. A full gas permeance study through porous freeze-cast support will show that the highly organized pore structure allows the gaseous transport resistance to be minimized with very low pressure drop in comparison with conventional porous support. Secondly, full asymmetric ceramic membranes in both configurations were manufactured, assessed for gas separation application and revealed unprecedented oxygen permeation values. A systematic comparison of permeation results for both configuration and with the state-of-the-art asymmetric membrane from literature will be detailed.

[1] S. Deville, E. Saiz, R.K. Nalla, A.P. Tomsia, Science, 311 (2006) 515-518.

J1.10

Cation-Site Determination in $(Ba_{0.5}Sr_{0.5})(Co_{0.8}Fe_{0.2})O_{3-d}$ by Exploiting Channelling Effects in Transmission Electron Microscopy Matthias Meffert, Heike Stoermer and Dagmar Gerthsen; Laboratory for Electron Microscopy (LEM), Karlsruhe Institute of Technology (KIT), Karlsruhe, Germany.

The anomalous X-ray emission in samples caused by fast electrons propagating close to a zone-axis orientation or parallel to crystallographic planes (channelling) can be exploited to gain quantitative information about the position of specific elements in the unit cell. The technique, known under the acronym ALCHEMI ("atom location by channelling enhanced microanalysis"), has been known for quite some time and is frequently used in analytical transmission electron microscopes equipped with energy dispersive X-ray and/or electron energy loss spectrometer. There are many variants of the ALCHEMI technique which have been refined over the years to correct for several errors like the delocalization of the X-ray emission event.

In this study we used a theoretical approach where we compared orientation-dependant inelastic ionization cross-sections of cations of interest from first principle calculations with the experimentally determined X-ray intensities. This approach was applied for the cubic perovskite phase of $(Ba_{0.5}Sr_{0.5})(Co_{0.8}Fe_{0.2})O_{3-d}$ where different cations like Sc and Y were partially substituted (up to 10 at%) for the B-site elements Co and Fe. Since channelling effects strongly depend on the speed of the electrons and local sample thickness the impact of both parameters was investigated. The local sample thickness was measured using convergent beam electron diffraction. Our channelling experiments demonstrate that a significant fraction of Y-cations occupy A-sites (25 % of 10 at%) although B-site substitution was targeted. In contrast, Sc was not detected on A-sites. Mixed occupation of Y on A- and B-sites can be rationalized in terms of the large ionic radius of Y compared to the B-site elements whereas the ionic radius of Sc is quite similar to that of Fe and Co.

SESSION J2: Poster Session II
J: Permeation Membranes
Tuesday Afternoon, June 16, 2015
5:20 PM
Keystone Resorts, Red Cloud Peak

J2.01

Oxygen Permeation Characteristics of Strontium Cobaltite Membranes Shivendra K. Jaiswal[2] and Jitendra Kumar[1]; [1]Materials Science, I I T Kanpur, Kanpur, India; [2]Physics, NIT Patna, Patna, India.

ABO_3 perovskite-type cubic compounds have generated immense interest in recent past due to their potential application in variety of devices which operate at elevated temperatures and require high oxygen flux, e.g., inorganic membrane, gas sensor, oxygen pumps, solid oxide fuel cells, catalyst for oxidative coupling of methane, etc. The present paper concerns with the development of strontium cobaltite ($SrCoO_3$) solid membranes displaying stability and excellent oxygen permeability. The initial compound is synthesized by a simple sol-gel route taking $Sr(NO_3)_2$ and $Co(NO_3)_2.6H_2O$ as precursors with ethanol and water as solvents. The process involves oxalate formation, drying at 150°C for 24h, and decomposition in air at 800 - 1000°C for 10h. The product is ground, sieved and pressed in a die to obtain dense membranes (diameter 10 mm, thickness 1-2 mm) for studying their phase stability, air separation ability, oxygen permeation and electrical conductivity. The product at room temperature corresponds to a rhombohedral phase (matching well with the composition $Sr_6Co_5O_{15}$, lattice parameters 'a' = 6.869 Å, β = 87.543°, Z = 1, and space group R32) with ~7 wt% of spinel cubic Co_3O_4 (a = 8.0862 Å) as a secondary phase. But, they depict a single and stable pervoskite- type cubic phase with an enlarged lattice parameter at elevated temperatures. They serve as air separator and show oxygen permeation flux of J_{O2} = 3.0 ml/cm^2.min at 1000 °C with activation energy of ~ 68 kJ/mol. Further, a small polaron conduction mechanism is operative for carrying the electrons (released following oxygen desorption) from the back side of the membrane to the front for participating in the reaction $O_2 + 4\ e \rightarrow 2O^{2-}$ there. The cubic phase is responsible for high J_{O2} and remains intact at elevated temperatures for extended period with random distribution of oxygen vacancies.

J2.02

Investigation of Ceramic Composite Membranes for Hydrogen Gas Separation Jason Fish[1, 2], Sandrine Ricote[3], Ryan O'Hayre[1] and Nikolaos Bonanos[2]; [1]Metallurgical and Materials Engineering, Colorado School of Mines, Golden, Colorado, United States; [2]Energy Conversion and Storage, Technical University of Denmark, Roskilde, Denmark; [3]Mechanical Engineering, Colorado School of Mines, Golden, Colorado, United States.

The electrical properties and hydrogen flux behavior of an all-ceramic protonic/electronic composite material are evaluated as a function of composite phase volume ratio. The composite consists of the protonic conductor Y-substituted $BaCeO_3/BaZrO_3$ solid solution (BCZY) and the electronic conductor Nb-substituted $SrTiO_3$ (STN) and has been prepared by spark plasma sintering to achieve membrane-quality samples. Total conductivities of 0.01–0.06 S cm^{-1} are measured in moist H_2/inert gas from 600–800 °C for 50 volume % STN. With increasing STN content (60 and 70 volume %), total conductivity increases by 5–10 times, but displays a semiconductor-type dependence, even at 70 %. The conductivity is modeled with a modified effective medium approach, incorporating a term for the heterojunctions between the two phases. Hydrogen fluxes of 0.004–0.008 μmol cm^{-2} s^{-1} (0.005–0.01 mL cm^{-2} min^{-1}) are obtained for a 50 % STN sample (1 mm thick) at 600–800 °C using dry argon as a sweep gas (measured by gas chromatography). A nearly five-fold increase to a maximum of 0.026 μmol cm^{-2} s^{-1}(0.039 mL cm^{-2} min^{-1}) is observed over the same temperature range upon adding palladium layers as catalysts to a 50 % STN sample. Hydrogen flux is not observed for membranes composed of 60 and 70 % STN. Overall, there remain significant challenges for this material as a membrane and further investigation is needed, e.g., in a thin-film configuration.

J2.03

Hydrogen Permeability of TiN_x Thin Films Prepared by RF Reactive Sputtering Chiharu Kura[1], Yoshitaka Aoki[1, 2], Etsushi Tsuji[1, 2] and Hiroki Habazaki[1, 2]; [1]Graduate School of Chemical Sciences and Engineering, Hokkaido University, Sapporo, Japan; [2]Graduate School of Engineering, Hokkaido University, Sapporo, Japan.

Hydrogen is an ideal fuel resource, because it can be generated by water electrolysis by using renewable electricity from solar, window and water power generation. However, the difficulties in storage and transportation of hydrogen hinder its application for commercial fuels. Therefore, various kinds of hydrogen-containing compounds, such as alcohol, organic hydrides, borohydrides and ammonia have been investigated as a 'hydrogen carrier'. Among them, ammonia has attracted considerable interest as a carbon-free fuel source for fuel cells due to the low cost, ease in liquefaction and transportation at ambient temperatures, and high volumetric energy density. Hydrogen permeation membranes are the key components to separate pure hydrogen in ammonia fuel reforming process. Group 5 metals (ex. Nb, Ta) have higher hydrogen permeability and are used as hydrogen separation membranes, however, they are severely corroded by NH_3 even at room temperature. Hence, it is the motivation to develop the hydrogen permeation membranes which can work under NH_3 atmosphere. Nitride of group 4 metals nitride (ex. HfN, TiN) are known to be tolerant in ammonium atmosphere and have a hydrogen adsorption ability. In this work, we demonstrate the hydrogen permeability of TiN_x by fabricating the self-standing membrane on a porous oxide substrate. The relationship between hydrogen permeability and nitrogen nonstoichiometry of TiN_x thin films was investigated.

Highly-crystalline, nonstoichiometric TiN_x films (x = 1.02 -0.62) were successfully fabricated by reactive RF sputtering processes with adjusting the nitrogen partial pressure and the substrate temperature. Hydrogen permeability test was performed in the temperature range of 300 to 500 °C by fabricating 600 nm-thick TiN_x membranes on γ-Al_2O_3 / α-Al_2O_3 porous substrates. TiN_x membranes revealed the selective permeation of hydrogen: hydrogen permeation rates exhibit Arrhenius-type temperature dependence and these are at least one order of magnitude higher than the rates of nitrogen leakage.

J2.04

Influence of Crystal Orientation on the Deuterium Permeation of Cr_2O_3 Coatings Deposited by MOCVD Di He, Shuai Li, Xiaopeng Liu, Yang Lei, Chao Zhang, Shumao Wang and Lijun Jiang; Department of Energy Materials and Technology, General Research Institute for Nonferrous Metals, Beijing, China.

Cr_2O_3 film is an efficient hydrogen permeation barrier for structural material which could be applied in areas such as hydrogen storage devices, vacuum solar receivers and fusion reactors. A corundum structure Cr_2O_3 film which is beneficial to a high performance film could be easily prepared at 500°C by metal organic chemical vapour deposition (MOCVD). Furthermore, it was found that film with different crystal orientation could be obtained by varied composition of the carrier gas when prepared Cr_2O_3 film on 316L stainless steel by MOCVD. However, a very limit number of investigations on the relationship between the deuterium permeation performance and the crystal orientation of the Cr_2O_3 film have been reported. In this study, Cr_2O_3films with (110) preferred orientation and random orientation were prepared by MOCVD on 316L. Then the hydrogen permeation inhibition performance of films were investigated by deuterium permeation experiment. The microstructure and phase structure were characterized by scanning electron microscope (SEM) and X-ray diffraction (XRD), respectively. The permeability of the Cr_2O_3 film with preferred orientation was $P=4.58\times10^{-6}exp(-112688/RT)$ mol•m^{-1}•s^{-1}•$Pa^{0.5}$ while the random orientation film was $P=1.20\times10^{-5}exp(-102057/RT)$ mol•m^{-1}•s^{-1}•$Pa^{0.5}$. The PRF of the preferred orientation Cr_2O_3 film was 38.2, 21.1 and 13.1 at 600°C, 650°C and 700°C, respectively, while the random orientation film was only 2.6, 1.9 and 1.5, 10 times lower than the former one. It is suggested that the crystalline grain of the preferred orientation coating was regularly arranged, so the structure of the coating was compact. Whereas the random orientation coating possesses a crystalline grain of messy arrangement, defects like through-hole were easily generated in the coating resulted in a serious decline of the hydrogen permeation performance.

J2.05

The Composite Membrane Based on Sulfonated Graphene Oxide/ Sulfonated Poly(Ether Ether Ketone) for Unitized Regenerative Fuel Cells Seon G. Rho[1] and Ho Y. Jung[2];[1]School of Applied Chemical Engineering, Chonnam National University, Gwangju, Korea (the Republic of); [2]Department of Environment & Energy Engineering, Chonnam National University, Gwangju, Korea (the Republic of).

Composite membranes based on sulfonated graphene oxide (sGO) / sulfonated poly(ether ether ketone) (sPEEK) were prepared for the unitized regenerative fuel cells (URFCs). For high performance of URFC, the proton conductivity and the permeability are important. In this study, poly(ether ether ketone) polymer was sulfonated to introduce the ionic conduction site for high proton conductivity. The sulfonation of poly(ether ether ketone) increased the number of sulfonic acid functional groups (SO_3H) in the membrane, which increased the ionic conductivity of composite membrane. The gas permeability of composite membrane decreased due to the incorporation of sGO particles as barriers. Therefore, it was found that the composite membrane based on sGO/sPEEK exhibited high selectivity (conducvity/permeability) and can be useful for URFCs.

[Acknowledgement]
This work was supported by the Energy Efficiency & Resources Core Technology Program of the Korea Institute of Energy Technology Evaluation and Planning(KETEP) granted financial resource from the Ministry of Trade, Industry & Energy, Republic of Korea (No. 20142010102930)

J2.06

The Application of 3D Imaging Techniques, Simulation and Diffusion Experiments to Explore Transport Properties in Porous OTM Support Materials Bernhard Tjaden[1], Zac Dehaney-Steven[2], Philip Withers[3], Robert Bradley[3], Jonathan Lane[4], Dan J. Brett[1] and Paul R. Shearing[1]; [1]Chemical Engineering, UCL, London, United Kingdom; [2]School of Chemistry, University of St Andrews, St Andrews, United Kingdom; [3]School of Materials, The University of Manchester, Manchester, United Kingdom; [4]Praxair, Inc, Tonawanda, New York, United States.

Microstructural parameters play an important role in characterising, comparing and evaluating porous materials. Among such parameters, tortuosity, porosity and average pore size diameter are crucial for describing gaseous diffusion mechanisms in electrochemical devices. However, unlike the latter two parameters, tortuosity cannot be measured directly which is why different methods have been developed for this purpose. These methods differ considerably from each other in terms of calculation approach and consulted underlying data.

Here, we utilise tomography techniques, simulation and diffusion cell experiments to calculate tortuosity of a porous support layer of an oxygen transport membrane. The results are then compared and the suitability of

these approaches in estimating diffusive mass transport of gases through porous membranes is assessed.

For diffusion cell experiments, planar porous support samples are fabricated and the diffusive fluxes of a selection of binary gas mixtures across the membrane are measured through gas chromatography. Tortuosity is then extracted by applying equimolar and equimass diffusion models.

In addition, image analysis and simulation are carried out across X-ray nano computed tomography and FIB-SEM tomography sample reconstructions: image analysis applies a fast marching computation technique using MATLab while the simulation in StarCCM+ models the effective transport parameters of the porous phase.

We conclude, that image and simulation based methodologies arrive at lower tortuosity values in comparison to diffusion cell experiments; the difference, depending on the calculation method, can be larger than a factor of two. The difference may stem from Knudsen diffusion effects which currently are not accounted for in the image based modelling technique. Secondly, tortuosity values extracted via diffusion cell experiments are a function of gas mixture and microstructural characteristics rather than a constant value as suggested by the former two approaches. Consequently, care must be taken in applying purely continuum interpretations of diffusion in these complex porous media.

J2.07

LSCr-ScSZ Composites as Dense Separation Layers in Oxygen Transport Membranes Zonghao Shen, Stephen J. Skinner and John A. Kilner; Materials, Imperial College London, London, United Kingdom.

Introduction

Ceramic membranes are being developed for diverse applications allowing significant improvement in industrial processes[1-3]. Oxygen Transport Membranes (OTM) for the generation of syngas and heat is one of the applications and has attracted considerable interest[4]. In the OTM, the Mixed Ionic-Electronic Conducting (MIEC) dense ceramic separation layer is an important component and in this work the dense layer consists of 50 vol% lanthanum chromite based perovskite (LSCr) and 50 vol% scandia stabilized zirconia (ScSZ). Whilst the OTM can function effectively with these materials, the detailed mechanism by which the dense layer transports oxygen is unclear. Thus, in this work, the fundamental transport properties of the dense composite layers are investigated.

Experimental

LSCr and ScSZ powders were provided by Praxair Inc, USA. The dual phase materials were sintered into dense pellets at 1450°C for 6 hours. The crystalline structure, microstructure and density after sintering were characterised.

The total electrical conductivity was measured by the 4-point DC method up to 1000°C in a static air atmosphere. The experimental technique used to determine the oxygen transport kinetics was Isotopic Exchange Depth Profiling (IEDP) performed using Secondary Ion Mass Spectrometry (SIMS)[5].

Results and discussion

The X-ray diffraction (XRD) patterns indicated there were no impurity phases present, within the limits of the measurement technique. The composition of the dual phase materials was verified by Rietveld analysis and the microstructure was characterised by SEM.

The total conductivity of the composites increases linearly at elevated temperature and the conductivity at 1000°C (1.46 Scm^{-1}) is one order of magnitude lower than the LSCr single phase (16.19 Scm^{-1}). From the Arrhenius plot the activation energy of both the dual-phase (0.22 eV) and the LSCr single phase (0.21 eV) materials were obtained. Based on the results, LSCr makes the predominant contribution to the total conductivity of the dual-phase and the incorporation of the pure ionic conductor ScSZ appears to simply dilute the electrical conductivity provided by the perovskite phase.

For the diffusion studies, the ''effective'' or ''macroscopic'' diffusion data (at 900°C, $D^*= 5.4x10^{-8}$ $cm^2 \cdot s^{-1}$ and $k=2.5x10^{-7}$ $cm \cdot s^{-1}$) were obtained based on the assumption that the sample is a single phase rather than a dual-phase material. Depth profiles in individual grains of the two phases were also performed and indicated that in the surface exchange step the active phase is LSCr while in the bulk the ScSZ phase dominates the diffusion process.

Conclusion

The LSCr/ScSZ dual phase composites were characterised by a combination of techniques. The electrical conductivity and diffusion results will help to determine how the oxygen transport takes place in these composites and aid in the development of optimised ceramic materials.

Acknowledgement

This work is a part of a collaborative project supported by Praxair Inc, USA.

References

[1] P. N. Dyer et al., *Solid State Ionics,* 134 (2000) 21-33.
[2] A. Thursfield et al., *Energy & Environmental Science,* 5 (2012) 7421-7459.
[3] H. A. Meinema et al., *High-Performance ceramics,* 54 (2005) 86-91.
[4] B. A. van Hassel, *Solid State Ionics*, 174 (2004) 253-260.
[5] J. A. Kilner et al., *Journal of Solid State Electrochemistry*, 15 (2011) 861-876.

J2.08

Rapid Oxygen Transport Membrane Evaluation at St Andrews Zac Dehaney-Steven, Despoina Papargyriou and John Irvine; School of Chemistry, University of St Andrews, St Andrews, United Kingdom.

Oxygen Transport Membranes (OTM) show promise as a replacement for cryogenic oxygen separation as an integral part of oxyfuel combustion for CCS, production of synfuels and lab-scale gaseous oxygen production. The causes and mechanisms for degradation of oxygen transport in these systems are not fully understood, and there is potential to improve oxygen flux. Real-world systems are large and tubular, making evaluation of new materials expensive and difficult. Small planar cells suit this role better, being quicker and easier to fabricate, seal and test.

In the present study, membranes comprised of a mix of strontium doped lanthanum chromite based perovskite (LSCr) and scandia stabilized zirconia (ScSZ) have been fabricated, with exchange layers deposited by screen printing. Membranes were characterized both before and after testing using SEM and EDX.

The methods used in this study focused on variation of dense layer thickness and the addition of exchange layers. Data on membranes 1 mm thick show that the activation energy is 0.66 eV corresponding to ScSZ, indicating that the limitation is in the ionically conductive phase. An exchange layer of $La_{0.75}Sr_{0.25}Cr_{0.5}Mn_{0.5}O_3$ (LSCrM) is used on the fuel side to improve flux, and has been found to cause a performance improvement versus an equivalent cell with no exchange layer, from 0.013 to 0.024 ml cm-2 min-1 at 700C. The catalytic properties of nickel have been exploited to improve flux further, using LSCrM or $La_{0.75}Sr_{0.25}Cr_{0.5}Fe_{0.5}O_3$ (LSCrF) with Mn or Fe partially substituted with Ni. Heating of the material in a reducing environment induces the migration of Ni0 to the surface as nanoparticles. Comparison of the Ni-doped materials with their undoped equivalents shows that the Ni is catalytically active, with performance approximately doubling between LSCrM and LSCrM-Ni. Also discussed will be the effect of concentration polarization on the attainable flux of thin membranes, and Arrhenius plots will be provided showing the correlation between bulk diffusion, surface exchange and membrane thickness for different oxidation electrodes.

J2.09

Dual Phase Composite Materials as Oxygen Suppliers under Harsh CO_2 and SO_2-Containing Environments Julio Garcia-Fayos[1], Maria Balaguer[1, 2] and Jose M. Serra[1]; [1]ITQ (UPV-CSIC), Valencia, Spain; [2]IEK-1, Forschungszentrum Jülich, Jülich, Germany.

World energy demand is expected to increase within the next years, being satisfied mainly by burning fossil fuels. Therefore, oxyfuel technology is presented as a feasible solution for minimizing the resulting CO_2 emissions. Oxygen Transport Membranes as oxygen suppliers on oxyfuel-based power plants are being considered recently as alternative to cryogenic distillation of air, due mainly to their high oxygen yields with infinite selectivity, on-site cost-effective production and high thermal integration in the process. Nevertheless, critical issues as loss of performance and material instability under oxyfuel environments still remain to be solved. Dual-phase composite materials comprising two different crystalline materials is a very interesting option for obtaining membranes with enough mixed conductivity and stability under these conditions.

Dual-phase membranes based on $NiFe_2O_4$ – $Ce_{0.8}Tb_{0.2}O_{2-d}$ composition were prepared by Pechini method. An evaluation of $Ce_{0.8}Tb_{0.2}O_{2-d}$ content and its relation with oxygen permeation was performed, determining that fluorite phase content improves $J(O_2)$. An oxygen flux of 0.25 (ml·min^{-1}·cm^{-2})·mm at 1000 ºC was obtained for a monolithic membrane with 40% NFO – 60% CTO formula. Aiming to validate composite materials for their use in oxyfuel applications, a study reproducing typical process harsh conditions was performed on a 50% NFO – 50% CTO membrane. CO_2 content as well as SO_2 presence on sweep gas stream were evaluated in terms of oxygen permeation. Oxygen fluxes of 0.13 and 0.09 ml·min^{-1}·cm^{-2} at 850 ºC were obtained for a 0.59 mm thick membrane under CO_2 and 250 ppm SO_2 in CO_2 sweep conditions, respectively. Long-term periods under CO_2 and SO_2-containing atmospheres also showed good results for the considered membrane. Finally, XRD, BSD-SEM and EDS measurements on the spent membrane confirmed material stability when exposed to oxyfuel environments. Results establish composite materials based on $NiFe_2O_4$ – $Ce_{0.8}Tb_{0.2}O_{2-d}$ system as very promising materials for their implementation as oxygen suppliers in oxyfuel power plants.

J2.10

Oxygen Transport in $(Ba_{0.5}Sr_{0.5})(Co_{0.8}Fe_{0.2})_{1-x}Y_xO_{3-\delta}$ (x = 0.01…0.1) Determined by ECR Measurements Lana-Simone Unger, Christian Niedrig, Wolfgang Menesklou, Stefan Wagner and Ellen Ivers-Tiffee; Institute for Applied Materials (IAM-WET), Karlsruhe Institute of Technology (KIT) , Karlsruhe, Germany.

Mixed ionic-electronic conducting (MIEC) oxides are important materials for a variety of high-temperature applications, such as gas sensors, solid oxide fuel cell (SOFC) cathodes or oxygen-permeation membranes. Within a promising class of perovskite solid solutions, $(Ba_{0.5}Sr_{0.5})(Co_{0.8}Fe_{0.2})O_{3-\delta}$ (BSCF) exhibits outstanding oxygen transport properties. One major disadvantage of BSCF is, however, its phase instability in an intermediate-temperature range (< 840 °C) [1-6]. By doping, e.g., with yttrium, phase stabilization of cubic BSCF becomes feasible [7].

The surface exchange coefficient k^δ and the chemical diffusion coefficient D^δ are the electrochemical parameters determining the kinetics of oxygen transport. By performing electrical conductivity σ relaxation (ECR) measurements on dense ceramic bulk samples with a well-defined geometry, both k^δ and D^δ can be determined [8] as a function of temperature (700…900 °C) and oxygen partial pressure pO_2 (10^{-5}…1 bar). Experiments were performed in a closed tubular zirconia “oxygen pump” [9] where pO_2 can be adjusted and precisely monitored continuously down to 10^{-18} bar. The numerical analysis tool (using MATLAB) identifies a confidence region for a set of possible k^δ and D^δ values.

In this study the kinetic parameters k^δ and D^δ of Y-doped BSCF have been evaluated in order to get information about the influence of the dopant Y on the oxygen transport in BSCF.

References:

[1] S. Švarcová et al., *Solid State Ionics* **178**, 1787 (2008).
[2] M. Arnold et al., *Chem. Mater.* **20**, 5851 (2008).
[3] K. Efimov et al., *Chem. Mater.* **22**, 5866 (2010).
[4] D.N. Mueller et al., *Phys. Chem. Chem. Phys.* **12**, 10320 (2010).
[5] C. Niedrig et al., *Solid State Ionics* **197**, 25 (2011).
[6] P. Müller et al., *Chem. Mater.* **25**, 564 (2013).
[7] P. Haworth et al., *Sep. Purif. Tech.* **81**, 88 (2011).
[8] M. W. den Otter et al., *J. Electrochem. Soc.* **148**, J1 (2001).
[9] C. Niedrig et al., *J. Electrochem. Soc.* **160**, F135 (2013).

J2.11

Chemical State and Electrical Conducting Property of $Ba_{2-x}La_xFe_2O_{5+\delta}$ Tsubasa Sato[1], Takashi Okiba[1], Katsumi Shozugawa[2], Motoyuki Matsuo[2], Fumito Fujishiro[3], Eiki Niwa[1] and Takuya Hashimoto[3]; [1]College of Humanities and Sciences, Nihon University, Setagaya-ku, Japan; [2]College of Arts and Sciences, The University of Tokyo, Meguro-ku, Japan; [3]Kochi University, Faculty of Science, Akebono-cho, Japan.

Electric conductivity of $Ba_2Fe_2O_{5+\delta}$ drastically increases approximately at 900 ºC under 10^{-4} bar of oxygen by the phase transition from monoclinic to cubic. Since the phase transition involves variation of ordered arrangement of oxide ion vacancy to disordered one, high temperature cubic phase of $Ba_2Fe_2O_{5+\delta}$ is expected as new material with high oxide ion and electrical conductivity. For practical application, decrease of the phase transition temperature is required. Since discrete increase of oxygen content is observed at the phase transition, it is probable that partial substitution of La^{3+} for Ba^{2+} decreases the phase transition temperature. In this study, crystal structure, electrical conducting property, oxygen nonstoichiometry and chemical state of $Ba_{2-x}La_xFe_2O_{5+\delta}$ have been analyzed using X-ray diffraction at various temperatures, electrical conduction measurements, iodometry and Mössbauer spectroscopy.

With variation of La content, three phases were observed in $Ba_{2-x}La_xFe_2O_{5+\delta}$. The specimens with $0.00 \leq x \leq 0.05$ have monoclinic structure and oxygen content less than 5.00 at room temperature. They show the structural phase transition from monoclinic to cubic above 800 ºC accompanied with discrete increase of electrical conductivity. Mössbauer spectroscopy indicated coexistence of antiferromagnetic and paramagnetic Fe. For the specimens with $0.10 \leq x \leq 0.20$, monoclinic structure at room temperature is maintained: however, oxygen content exceeds 5.00. The high electrical conductivity from 200 ºC to 1000 ºC with and semi-metallic temperature dependence was observed. Only antiferromagnetic Fe was observed and paramagnetic Fe disappeared in Mössbauer spectra of these specimens. Discrete decrease of oxygen content was observed between x=0.20 and x=0.25, indicating existence of phase boundary. The specimens with $x \geq 0.25$ show cubic symmetry at room temperature, high electrical conductivity semi-metallic behavior with and antiferromagnetic Mössbauer spectra, suggesting that the specimens with $x \geq 0.25$ have potential as new mixed conductor.

J2.12

Study of Y-doped $(Ba_{0.5}Sr_{0.5})(Co_{0.8}Fe_{0.2})O_{3-d}$ by Analytical Transmission Electron Microscopy Matthias Meffert[1], Lana S. Unger[2], Heike Stoermer[1], Christian Niedrig[2], Stefan F. Wagner[2], Ellen Ivers-Tiffee[2] and Dagmar Gerthsen[1]; [1]Laboratory for Electron Microscopy (LEM), Karlsruhe Institute of Technology (KIT), Karlsruhe, Germany; [2]Institute of Materials for Electrical and Electronic Engineering (IWE), Karlsruhe Institute of Technology (KIT), Karlsruhe, Germany.

The cubic phase of the mixed ionic and electronic conducting perovskite $(Ba_{0.5}Sr_{0.5})(Co_{0.8}Fe_{0.2})O_{3-d}$ (BSCF) has been identified as promising membrane material due to its high O_2permeability. However, the formation of several non-cubic phases at temperatures below 840 °C limits the performance especially during prolonged operation. Since the divalent nature of Co plays a key role in the degradation process B-site doping with monovalent Y^{3+} promises higher chemical stability. In this study substitution of the B-site by up to 10 at% Y combined with various temperature treatments was investigated by means of transmission electron microscopy to elucidate the impact on the phase stability. For low dopant concentrations (1…3 at% Y) most secondary phases were suppressed. Only a small volume fraction of the hexagonal phase was detected along grain boundaries. A complete suppression of the hexagonal phase was achieved for highly doped (10 at%) BSCF at a temperature of 800 °C. The oxidation state of the multivalent cations was determined by electron energy loss spectroscopy to gain further insights into the stabilization behaviour of Y. An average Co-valence state of +2.2 was measured for both doped and undoped BSCF suggesting a compensation of the charge imbalance by the reduction of oxygen vacancy concentration. Since most of the secondary phases exhibit less B-site space the large ion radius of Y successfully counteracts a phase transformation. Even though a sole B-site occupation is assumed it has never been experimentally checked. Hence, the lattice site of the Y-cations was analysed by the atom location channeling enhanced microanalysis technique showing indeed a mixed

A/B-site occupation for Y. Furthermore, the chemical composition was analysed by energy dispersive X-ray spectroscopy to correlate the mixed occupation with the measured stoichiometry which yields a noticable deviation compared to undoped BSCF.

J2.13

Oxygen Non-Stoichiometry and Thermo-Chemical Expansion of Ba0.5Sr0.5Co0.8Fe0.2O3-δ Studied by High Temperature X-Ray Diffraction and Thermogravimetry Mtabazi G. Sahini[1], Julian R. Tolchard[2], Kjell Wiik[1] and Tor Grande[1]; [1]Materials Science and Engineering, Norwegian University of Science and Technology (NTNU), Trondheim, Norway; [2]SINTEF Materialer og kjemi, Trondheim, Norway.

Mixed ionic and electronic conducting $Ba_{0.5}Sr_{0.5}Co_{0.8}Fe_{0.2}O_{3-\delta}$ (BSCF) has a cubic perovskite structure with general formula $ABO_{3-\delta}$. BSCF was derived by partial substitution of Sr with Ba from cubic perovskite $SrCo_{0.8}Fe_{0.2}O_{3-\delta}$ (SCF) possessing excellent oxygen flux but low stability. Owing to the increased stability of BSCF relative to SCF the latter has been considered as one of the promising materials for application as oxygen separation membranes and as cathode for solid oxide fuel cells. Despite the excellent oxygen transport properties of BSCF, it has been revealed that cubic BSCF is metastable below 900ºC and transform into a hexagonal phase, and the phase transformation arise a concern regarding the long term stability. We have investigated the stability of BSCF with regard to chemical and thermal expansion as well as formation of the hexagonal phase by using *in situ* high temperature X – ray diffraction and thermo-gravimetric analysis from ambient to 1000 ºC in air, pure oxygen and nitrogen atmospheres. The BSCF powder, heat treated at 1000 ºC and quenched to ambient prior to the analysis, was shown to oxidize in oxidizing atmosphere before thermal reduction took place. With decreasing partial pressure of oxygen the initial oxidation was suppressed and only reduction and loss of oxygen were observed. The thermal expansion of BSCF was determined from the X-ray diffraction data, demonstrating that the thermal expansion of BSCF depends on the atmosphere. Chemical expansion of BSCF was also estimated based on the diffraction data and thermo-gravimetrical analysis. A hexagonal polymorph BSCF, coexisting with the cubic polymorph, was observed to form above 600 ºC during heating. The formation of the hexagonal polymorph was driven by oxidation, and the unit cell of cubic BSCF was shown to decrease with increasing amount of hexagonal BSCF formed. The hexagonal BSCF polymorph disappeared upon further heating, accompanied with an expansion of the unit cell of the cubic BSCF.

References

Svarcová S., Wiik K., Tolchard J., Bouwmeester H.J.M., Grande T. *Solid State Ionics* (2008), **178**, 1787–1791

Arnold M., Gesing T.M., Martynczuk J., and Feldhoff A., *Chem. Mater.* (2008), ***20***, 5851–5858

Yaremchenko A.A., Mikhalev S.M., Kravchenko E.S., Frade J.R., Journal of the European Ceramic Society (2014), **34**, 703–715.

M.G. Sahini, J.R. Tolchard, K. Wiik and T. Grande, *High temperature X-ray diffraction and thermo-gravimetrical analysis of the cubic perovskite* $Ba_{0.5}Sr_{0.5}Co_{0.8}Fe_{0.2}O_{3-\delta}$ *in different atmospheres,* submitted.

SESSION J3: Permeation Membranes I
J: Permeation Membranes
Chairs: Jonathan Lane and Martin Sogaard
Wednesday Morning, June 17, 2015
Keystone Resorts, Grays Peak III

10:30 AM **J3.01

Advances in ITM Technology for Oxygen and Syngas Production Michael F. Carolan[1], Lori L. Anderson[1], Phillip A. Armstrong[1], Robert R. Broekhuis[1], Charles M. Woods[1], Mark Hutcheon[1], Charles A. Lewinsohn[2], Jack Chen[2] and Dale Taylor[2]; [1]Air Products and Chemicals, Inc., Allentown, Pennsylvania, United States; [2]Ceramatec, Inc. , Salt Lake City, Utah, United States.

Since the late 1980's, Air Products has been developing ceramic, mixed-conducting Ion Transport Membranes (ITM) for oxygen and synthesis gas production. With other industrial and academic partners, and through collaboration with the U.S. Department of Energy, Air Products has progressed ITM technology to be a cost-effective method of industrial gas production. Two ITM technologies are in development. ITM Oxygen membranes have the potential to integrate well with advanced power generation processes, as well as traditional energy intensive industrial processes requiring oxygen. ITM Syngas membranes have the potential to dramatically lower the cost of syngas production. This paper will summarize the state of development of both technologies.

In the ITM Oxygen program, a number of important technical and project milestones were achieved in the past year. Most notably, construction was completed on the 100 TPD Intermediate-scale Test Unit (ISTU), followed by commissioning and operation of the unit. Ceramatec manufactured an inventory of modules for the first phases of ISTU testing. The ISTU features many of the equipment designs that will be used at commercial scale. Data from the ISTU will support the design of commercial-scale systems. In addition to the ISTU, a commercial-scale ceramic membrane manufacturing facility, the CerFab, was commissioned. In parallel to these efforts, long-term testing of smaller scale module exceeded 13000 hrs, demonstrating the robustness of the technology. Potential future development steps toward a large-scale Demonstration facility will be reviewed.

In the ITM Syngas program, next-generation membrane designs have been produced by Ceramatec and tested at Air Products. These membranes include features to increase oxygen flux and improve reliability. Paths to scale-up up the ITM Syngas technology will be presented.

This abstract was written with support of the U.S. Department of Energy under Contracts No. DE-FC26-98FT40343 and DE-FE0012065.

11:00 AM J3.02

Lattice Structure and Oxygen Permeability of In-Doped $BaFeO_{3-\delta}$ Perovskite-Type Oxides Yao Lu[1], Hailei Zhao[1], Xing Cheng[1], Kun Zheng[2] and Konrad Swierczek[2]; [1]University of Science and Technology Beijing, Beijing, China; [2]AGH University of Science and Technology, Krakow, Poland.

Mixed ionic-electronic conduction (MIEC) oxides have been extensively studied because of their potential applications in oxygen separation technology, solid oxide fuel cells and chemical process for conversion of hydrocarbons to syngas. Among these MIECs, perovskite-type $BaFeO_{3-\delta}$ oxide has attracted much attention owing to its potentially high oxygen permeability and structural stability. While the small B-site cation (Fe) cannot form sufficiently big BO_6 octahedra to accommodate big A-site (Ba) cation, the perovskite would take hexagonal structure with oxygen vacancy ordering, which will unfortunately cause the attenuation of MIEC properties. With inducing of more than 10 at.% of In substituting for Fe ions, the cubic perovskite structure can be successfully stabilized to room temperature. Thermal reducibility and thermal expansion coefficient are effectively reduced by indium doping, owing to the less changes of concentration of oxygen vacancies in these compounds upon heating. However, more In-doping decreases the electrical conductivity and oxygen permeability. When using He/Air as sweep/feed gas, the $BaFe_{0.9}In_{0.1}O_{3-\delta}$ dense membrane with 1.0 mm thickness delivers a high oxygen permeation flux of 1.11 mL cm^{-2} min^{-1} at 950 °C. It is also found that for membranes thinner than 0.8 mm, the oxygen flux is no longer limited by the bulk diffusion, while the oxygen surface exchange process becomes the dominant factor. Rietveld refinement and first principle calculation were performed to get an insight into the In influence on lattice structure, oxygen migration energy and electron conduction behaviour of $BaFe_{1-x}In_xO_{3-\delta}$.

11:20 AM *J3.03

Influence of Yttrium Doping on $Ba_{0.5}Sr_{0.5}Co_{0.8}Fe_{0.2}O_{3-\delta}$ Lana-Simone Unger[1], Stefan Baumann[2], Christian Niedrig[1], Wolfgang Menesklou[1], Stefan Wagner[1], Wilhelm A. Meulenberg[2]and Ellen Ivers-Tiffee[1]; [1]Institute for Applied Materials (IAM-WET), Karlsruhe Institute of Technology (KIT), Karlsruhe, Germany; [2]Institute of Energy and Climate Research IEK-1 Materials Synthesis and Processing, Forschungszentrum Jülich GmbH, Jülich, Germany.

The state-of-the-art perovskite solid solution $Ba_{0.5}Sr_{0.5}Co_{0.8}Fe_{0.2}O_{3-\delta}$ (BSCF) possesses formerly unobtainable oxygen transport properties [e.g., 1,2] in its cubic phase while being chemically stable even at very low oxygen partial pressures [e.g., 3]. This has made BSCF a very promising candidate for high-temperature oxygen-transport membranes (OTMs) [e.g., 4]. However, cubic BSCF exhibits a limited long-term phase stability at $T \leq 840$ °C [5], forming secondary phases that result in a degradation of its oxygen permeability. Previous reports in literature suggest the possibility of stabilizing the cubic phase by, e.g., yttrium doping [6].
This study focuses on a systematic analysis of the influence of B-site Y doping on (i) oxygen permeation and (ii) the electrical properties of the BSCF matrix. Single-phase BSCF powders doped with 1…10 at-% Y on the B-site were prepared by mixed-oxide route. It could be shown by coulometric titration that the introduction of Y does not affect the excellent low-pO_2stability of BSCF (stable down to ~ 10^{-12} bar O_2 at 900 °C). Dense ceramic pellets were electrically characterized at temperatures between 700…900 °C and at oxygen partial pressures of 10^{-5}…1 bar.

The conductivity degradation for pure BSCF at 800 °C (~ 3 % after 800 h) could be completely suppressed by addition of ≥ 3 % B-site Y. Oxygen-permeation experiments were carried out between 650…1000 °C. In long-term (up to 1600 h) measurements at 800 °C the stabilizing influence of yttrium doping on BSCF could be proven; low Y doping levels (1…3 at-%) even led to a slight increase in oxygen flux. These findings corroborate recent results from microstructural analyses [7] where the partial substitution of divalent Co by monovalent Y could be shown to inhibit a phase transformation of cubic BSCF, thus charting a path forward toward a stable long-term operation of BSCF OTMs.

References:
[1] Z. P. Shao et al., *J. Membrane Sci.* **172**, 177 (2000).
[2] S. Baumann et al., *J. Membrane Sci.* **377**, 198 (2011).
[3] C. Niedrig et al., *J. Electrochem. Soc.* **160**, F135 (2013).
[4] J. Sunarso et al., *J. Membrane Sci.* **320**, 13 (2008).
[5] C. Niedrig et al., *Solid State Ionics* **197**, 25 (2011).
[6] P. Haworth et al., *Sep. Purif. Tech.* **81**, 88 (2011).
[7] M. Meffert et al., manuscript in preparation.

11:40 AM J3.04

Stability and Oxygen Permeability of Sol-Gel Derived $SrCo_{0.8}Fe_{0.2}O_{3-\delta}$ Based Compound Membranes Vijay K. Kashyap and Jitendra Kumar; Materials Science, I I T Kanpur, Kanpur, India.

$SrCo_{0.8}Fe_{0.2}O_{3-\delta}$ (SCFO) and $SrCo_{0.8}Fe_{0.2-y}Zr_yO_{3-\delta}$ (y = 0.05) (SCFZO) dense membranes (dia ~ 10 mm, thickness 1 – 1.5 mm) have been prepared by compacting sol-gel derived oxide powders and characterized with regard to their formation, phase stability at elevated temperatures, electrical conductivity and oxygen permeation behavior. X-ray diffraction confirms the presence of a perovskite-type cubic phase above 800°C and x-ray photoelectron spectroscopy reveals the existence of both 4+ and 3+ oxidation states for cobalt and iron with O_2^{2-}, O_2^- and O^- species. The electrical conductivity (σ) increases invariably up to a characteristic temperature due to rise in mobility and then decreases slowly following pronounced scattering of carriers, released with oxygen desorption. The partial replacement of iron by zirconium in $SrCo_{0.8}Fe_{0.2}O_{3-\delta}$ causes increase in number of cobalt and iron species with oxidation state (4+). This leads to rise in oxygen content and, in turn, reduction in electron concentration and electrical conductivity as well. Although the SCFO membrane of 1mm thickness exhibits oxygen permeation flux (Jo_2) of 1.8 x 10^{-6} mol cm^{-2} s^{-1} at 1000°C yet displays inadequate long term stability. However, zirconium insertion not only increases the Jo_2 by ~ 40% but also improves the stability significantly, i.e., steady oxygen permeation sustains for 120 h at least at 900°C. The results indicate that zirconium presence is vital in determining the stability of SCFZO. With high structural stability and excellent oxygen permeation properties in the temperature range 800 – 1000°C, SCFZO membrane can be a potential candidate for oxygen separation from air.

SESSION J4: Permeation Membranes II
J: Permeation Membranes
Chairs: Henny Bouwmeester and Robert Kee
Thursday Morning, June 18, 2015
Keystone Resorts, Grays Peak III

10:30 AM **J4.01

Dual Phase Membranes for Oxygen Separation Martin Sogaard, Jonas Gurauskis, Andreas Kaiser, Peter V. Hendriksen and Wolff-Ragnar Kiebach; Department of Energy Conversion and Storage, Technical University of Denmark, Roskilde, Denmark.

The use and benefits of Oxygen Transport Membranes (OTMs) in different applications will be described as will the challenges in developing the technology. The benefits of a close thermal and chemical integration of the OTMs with the process to which the oxygen is supplied will be highlighted. An OTM material should ideally have high ionic and electronic conductivity as well as good chemical stability under both oxidizing and reducing conditions. Gd-doped ceria (CGO) possess many of these properties except electronic conductivity under oxidizing conditions. Strategies for increasing the electronic conductivity will be discussed including *i*) co-doping CGO with cobalt and praseodymium, and *ii*) preparing composite membranes of CGO and a good electronic conductor. Particularly the strategy of preparing dual phase membranes seems promising, and several different candidate composites were investigated. Membranes including $La_{0.6}Sr_{0.4}FeO_{3-\delta}$ (LSF) and CGO was selected for further studies. Electrical conductivity relaxation has been used to study the effect on the chemical diffusion and surface transport properties of composites of CGO and LSF under both oxidizing and reducing conditions. At 600°C it has been found that the chemical diffusion coefficient is enhanced relative to that of the LSF due to the good ionic conductivity of CGO, however, it is also found that the surface exchange reaction is strongly enhanced at particularly lower temperatures. Both planar and tubular thin film membranes of LSF-CGO have been prepared. The planar membrane was prepared using phase inversion tape casting resulting in a support structure with a highly oriented porous structure. The tubular LSF/CGO-membranes were prepared on a low cost porous support of magnesium oxide. Both the planar and tubular membrane demonstrate high oxygen fluxes >10 Nml min^{-1} cm^{-2} at 850°C when subjected to air on one side and strongly reducing conditions on the other side (CO, H2).

11:00 AM J4.02

Phase Inversion Tape Casting and Oxygen Permeation Properties of $Zr_{0.84}Y_{0.16}O_{1.92}$-$La_{0.8}Sr_{0.2}Cr_{0.5}Fe_{0.5}O_{3-\delta}$ Dual-Phase Composite Membranes with Asymmetric Structure Yu Zhang, Ronghua Yuan, Jianfeng Gao and Chusheng Chen; University of Science and Technology of China, Hefei, China.

$Zr_{0.84}Y_{0.16}O_{1.92}$(YSZ)-$La_{0.8}Sr_{0.2}Cr_{0.5}Fe_{0.5}O_{3-\delta}$ (LSCrF) dual-phase composite membrane was prepared by the phase-inversion tape casting/sintering technique. The membrane possessed an asymmetric two-layered structure: a dense layer of thickness 25 μm providing the oxygen separation function, and a finger-like porous layer of thickness 1mm acting as a mechanical support to the functional layer. To promote the surface oxygen exchange, the dense side of the membrane was coated with a porous YSZ-LSCrF layer while the porous side (support side) was impregnated with $Sm_{0.2}Ce_{0.8}O_2$ nano-particles. The oxygen permeation flux through the membrane was measured by feeding air on the dense side and sweeping the porous support side with helium or CO. The membrane was found to exhibit desired oxygen permeability at elevated temperatures. At 900 °C, an appreciable oxygen permeation flux of 0.106 $ml \cdot cm^{-2} \cdot min^{-1}$(STP) was obtained under the air/helium gradient, and a much larger one of 2.48 $ml \cdot cm^{-2} \cdot min^{-1}$(STP) under the air/CO gradient. The oxygen permeation flux increased with temperature. The activation energy associated with the

oxygen permeation was determined to be 142.8 kJ·mol^{-1} for air/helium gradient, and 46.7 kJ·mol^{-1} for air/CO gradient. By comparing the oxygen permeability of membranes with various thickness of the dense layer, it was revealed that the oxygen permeation process through the membrane is jointly controlled by the transport of oxide ions in the bulk of the dense layer and the surface oxygen exchange. By comparing the oxygen permeability of the membranes with various surface composition and morphology, it was further revealed that the surface oxygen exchange kinetics is more sluggish at the dense side (air side) than that at the support side (permeate side). Since the YSZ-LSCF planar membrane exhibits desired oxygen permeability and satisfactory mechanical and chemical stability under stringent conditions, it holds promise for oxygen separation and fuel processing applications.

11:20 AM J4.03
Microstructural Influence on Oxygen Transport of $Ce_{0.8}Gd_{0.2}O_{2-\delta}$ - $FeCo_2O_4$ Dual Phase Membrane Madhumidha Ramasamy[1], Stefan Baumann[1], Falk Schulze-Kueppers[1], Maria Balaguer[1], Wilhelm A. Meulenberg[1], Justinas Palisaitis[2], Joachim Mayer[2], Ramesh Bhave[3], Daejin Kim[3] and Martin Bram[1]; [1]Institute of Energy and Climate Research, Forschungszentrum Juelich GmbH, Juelich, Germany; [2]Ernst Ruska-Centre (ER-C) for Microscopy and Spectroscopy with Electrons, Juelich, Germany; [3]Chemical Sciences Division, Oak Ridge National Laboratory, Oak Ridge, Tennessee, United States.

Mixed conducting membranes are an important area of research with respect to oxyfuel process, a promising concept of carbon capture and storage technology (CCS). Major setback with single phase mixed ionic electronic conducting membranes is their long term stability at high temperatures in aggressive atmospheres. Dual phase membranes, in which oxygen ion vacancies and electron holes are transported in separate phases resulting in an effective MIEC, excel overcoming this setback. In this work, one such robust candidate is CGO-FCO (60 vol% $Ce_{0.8}Gd_{0.2}O_{2-\delta}$ - 40 vol % $FeCo_2O_4$) identified to provide good oxygen permeation flux with substantial stability in harsh atmosphere. CGO-FCO composite synthesized by one pot method, was made into dense gas tight pellets by sintering at 1200°C. XRD and SEM microstructure analysis indicate the presence of a third phase, orthorhombic perovskite in the sintered composite. In addition TEM analysis showed oxygen deficient grain boundary phase formed by Fe and Co cations segregation from spinel phase, when in contact with CGO and/ or perovskite phases. This grain boundary phase may boost the electronic conductivity of the composite. The volume ratio of the CGO, FCO phases as low as 90:10 showed reasonable oxygen flux indicating the existence of sufficient percolating network of an electronic conducting phase. Surface exchange limitation of the membrane was addressed by porous layer coating over the composite on both sides and hence its impact on the permeation rate was identified to be significant. The oxygen permeation flux of CGO-FCO screen printed with a porous layer of 20 µm thick $La_{0.6}Sr_{0.4}Co_{0.2}Fe_{0.8}O_{3-\delta}$ (LSCF) is 0.11 mL cm^{-2} min^{-1} at 850°C with argon and air as sweep and feed gas at the feed rate of 50 mL min^{-1} and 250 mL min^{-1}.

11:40 AM J4.04
Dramatically Enhanced Oxygen Permeation Fluxes in Fluorite-Rich Dual-Phase Membrane by Surface Modification Jong Hoon Joo, Kyong Sik Yun, Chung-Yul Yoo and Ji Haeng Yu; Korea Institute of Energy Research, Daejeon, Korea (the Republic of).

Dual-phase ceramic membranes with very high oxygen flux have been designed by taking into account the volume fraction of the fluorite phase, membrane thickness, and surface modification. The oxygen flux of Gd-doped ceria (GDC)–perovskite dual-phase membranes has been systematically investigated as a function of membrane thickness and volume fraction of the fluorite phase with or without surface modification. The percolation threshold of the composites for electronic conduction has been determined by general effective-medium theory. The oxygen flux of uncoated fluorite phase-rich membrane exhibits a low oxygen flux under an air/He gradient, indicating that the permeation is controlled by only the surface-exchange kinetics of GDC. However, with modification of the surface on both sides, the flux of the membrane was surprisingly improved by about three orders of magnitude compared with that of the membrane with non-modified surfaces. This observation implies that the formation of an electronic short circuit at the fluorite surface as a result of surface modification on both sides played a decisive role in the dramatic improvement in oxygen permeation flux. This significant enhancement of the oxygen fluxes is of particular importance as dual-phase membranes are the most studied class of the chemical and mechanical stable membrane. This encouraging result indicates that the fluorite-dominant dual-phase membrane is a promising candidate for next-generation oxygen-permeable membranes.

SESSION J5: Permeation Membranes III
J: Permeation Membranes
Chairs: Truls Norby and Jose Serra
Thursday Afternoon, June 18, 2015
Keystone Resorts, Grays Peak III

3:30 PM *J5.01
Ceramic Permeation Membranes and Membrane Reactors Ian S. Metcalfe; Chemical Engineering, Newcastle University, Newcastle upon Tyne, United Kingdom.

Membranes and membrane reactors are of great interest in the chemical industries because they offer the possibility of improved yields and more compact plant. Clearly the availability of membrane systems having suitable performance at an acceptable cost is an important consideration. Organic membranes can be difficult to use at high temperatures, while porous inorganic membranes tend to have problems associated with selectivity. In this talk we will focus on the use of inorganic, dense, ion-conducting membranes. Such membranes can be highly selective. We will explore their use in new membrane-based chemical process applications. Mixed ionic and electronic (MIEC) conducting metal oxides can be employed as oxygen permeable membranes (in the case of coupled oxygen ion and electron transport) or hydrogen permeable membranes (in the case of coupled proton and electron transport). Dual ion conducting membranes are defined as membranes in which there are two ionic charge carriers. Such membranes may be single phase or dual phase. If a porous oxide ion conductor is infiltrated with a molten carbonate salt a dual phase dual ion conducting membrane is formed. Carbon dioxide permeation is due to the counter diffusion of carbonate ions and oxygen ions. Such a membrane has previously been investigated by Lin et al (1) and Lackner et al (2). Alternatively molten carbonate infiltration into a porous host phase that is an electronic conductor results in a dual phase mixed ionic and electronic membrane (also previously investigated by Lin et al (3)).
The talk will also focus on the application of such membranes in chemical processes. For example, under an oxygen chemical potential difference an oxygen permeable ceramic membrane can supply pure oxygen to a hydrocarbon for e.g. partial oxidation. This permits the use of air as the oxidant and can lead to more intensified, efficient hydrocarbon processing. Other novel processes involving hydrogen production, internal reforming within a solid oxide fuel cell and carbon dioxide capture. Different modes of membrane operation (counter current versus co-current) will be reviewed and their advantages compared and contrasted. Membrane process options will be presented and discussed. The state-of-the-art for different membrane classes will be reviewed. Finally, targets for future membrane performance will be discussed and set.
Parallels will also be drawn with chemical looping processes in which an oxygen carrier undergoes periodic redox reactions leading to reaction and separation. We will show that any chemical looping process has a membrane analogue and vice versa.

References
1. B. Lu, Y. S. Lin, *J. Membr. Sci.,* **444**, 402 (2013).
2. J. L. Wade, C. Lee, A. C. West, K. S. Lackner, *J. Membr. Sci.,* **369**, 20 (2011).
3. S. J. Chung *et al.*, *Ind. Eng. Chem. Res.,* **44**, 7999 (2005).

3:50 PM J5.02
Defect Chemistry and Oxygen Transport Properties of Bi-Sr-Fe-Based Perovskite-Type Oxides Doohyun Baek, Itaru Oikawa, Atsunori Kamegawa and Hitoshi Takamura; Department of Materials Science, Tohoku University, Sendai, Japan.

Mixed ionic and electronic conductors (MIECs) are considered promising materials not only for use as cathodes for SOFCs but also as oxygen permeable membranes (OPMs). The superior electrochemical performance of the Co-based mixed conductors with perovskite-type structure such as LSCF and BSCF makes them strong candidates for use as SOFC cathodes and OPMs. However, the Co-based perovskite-type oxides have two drawbacks; one is their high thermal expansion coefficient, and the other is their low chemical stability. To overcome the drawbacks, Co-free mixed conductors are highly demanded. In this study, Bi-Sr-Fe-based perovskite-type oxides, $Bi_{1-x}Sr_xFeO_{3-\delta}$ (BSF), is focused on as a Co-free MIEC. Based on the oxygen nonstoichiometry and electrical conductivity of BSF as functions of temperature and pO_2, ionic compensation, *i.e.* the formation of oxygen vacancies, seems to be dominant in BSF regardless of the acceptor content, temperature and pO_2; however, La doping on Bi site promotes electronic compensation even with the same Sr and Fe contents. $Bi_{0.5}Sr_{0.5}FeO_{3-\delta}$ (BSF55) was thermodynamically stable down to 10^{-12} to 10^{-16} bar at 750 and 650 ºC, which appears to be a wide pO_2 range enough to use as an SOFC cathode and OPM for pure oxygen production. To take advantage of its mixed conductivity, a 12 μm-thich BSF dense thin film was successfully fabricated on a porous BSF substrate. By applying a porous surface modification layer, the 12 μm-thick BSF dense thin film showed a high oxygen flux density of above 1 sccm/cm^2 at 800 ºC among Co-free MIECs.

4:10 PM J5.03
Low Metal Content Silver/Doped Ceria Composites for Oxygen Separation and Methane Partial Oxidation Enrique Ruiz-Trejo[1], Paul Boldrin[1], Jawwad Darr[2], Alan Atkinson[3] and Nigel P. Brandon[1]; [1]Earth Science and Engineering, Imperial College London, London, United Kingdom; [2]Chemistry, University College London, London, United Kingdom; [3]Materials, Imperial College London, London, United Kingdom.

Gadolinia-doped ceria (CGO) exhibits high oxygen ion conductivity and is catalytically active for reforming; silver is an excellent catalyst for the reduction of oxygen and its addition to CGO increases the oxygen surface exchange coefficient by orders of magnitude.
The composite membranes were fabricated by first coating ultrafine nanoparticles (< 5 nm) of CGO with silver using Tollens' reagent. The compressed powders were then sintered at a temperature low enough to minimize silver losses but high enough to sinter the CGO. This unique combination led to dense (>95%) and electronically percolating composites (σ = 100 Scm^{-1}) with low content of silver (<10 vol %). The samples were characterised by conductivity measurements, SEM and XRD.

The oxygen permeation through a 1 mm thick membrane from air to argon as sweep gas, was estimated to be 0.02 mL cm^{-2} min^{-1} (NTP) at 700 °C, while using a CH_4-containing atmosphere on the low oxygen activity side, the permeation rate was greater than 0.18 mL cm^{-2} min^{-1} (NTP). At 700 °C, high selectivity for CO (>90%) was observed and good methane conversion was measured (approximately 21%) despite the simplicity of the reactor and the thickness of the membrane. The samples operated under CH_4 for at least 48 h below 700 °C without being mechanically compromised, however if operated at 800 °C, silver exuded to the surface as a consequence of the heat released during methane oxidation. Due to the stability of CGO in carbon atmospheres, the Ag/CGO composites are expected to function well in these reducing atmospheres and under large transmembrane p_{O2} differences.

4:30 PM J5.04
Characterization of Dual Phase $BaCe_{1-x}Eu_xO_{3-\delta}$:$Ce_{1-y}Y_yO_{2-\delta}$ (x=0-0.2; y=0-0.2) Ceramic Composite for Membrane Application in H_2-Separation Maria Balaguer[1], Mariya E. Ivanova[1], Sonia Escolastico[2], Justinas Palisaitis[3], Yoo Jung Sohn[1], Jose M. Serra[2], Wilhelm A. Meulenberg[1], Olivier Guillon[1] and Joachim Mayer[3]; [1]Institute for Energy and Climate Research Materials Synthesis and Processing (IEK-1), Forschungszentrum Jülich GmbH, Jülich, Germany; [2]Instituto de Tecnologia Quimica , Valencia, Spain; [3]Ernst Ruska Center, Jülich, Germany.

High performance ceramic membranes for *in situ* separation of hydrogen require materials combining high mixed protonic and electronic conductivity, redox catalytic properties and chemical compatibility with water and carbon dioxide at high temperatures and pressures, which are present in the sweeping flow. This is a challenging task, since an increase in proton conductivity comes along with a drop in stability and viceversa. By combining a predominant protonic conductor with an electronically conductive phase into a dual-phase material, the ambipolar conductivity can be increased effectively, although the high temperature reactivity between phases in contact must be avoided.

The present work shows the hydrogen permeation study of a composite membrane made of nominal $BaCe_{0.8}Eu_{0.2}O_{3-\delta}$ (BCEO) and $Ce_{0.8}Y_{0.2}O_{2-\delta}$ (CYO) single phase materials. These two crystalline phases synthesized via the conventional solid-state route at 1400 °C form a cer-cer composite in a 50/50 volume ratio. Dense membranes were prepared by calcining uniaxially pressed pellets at 1600 °C. Although both perovskite and fluorite phases are well distinguished, Rietveld refinement on XRD and TEM analysis reveal the migration of Eu to the ceria phase. DC conductivity has been measured in dry and wet H_2, and D_2 atmospheres (where H_2 and D_2 were 5% in He (95%), and pH_2O and pD_2O correspond to 0.025 atm). The results suggest that electrons and/or oxygen ions are the predominant charge carriers in the studied temperature range. Hydrogen permeation rate higher than 0.6 ml·cm^{-2}·min^{-1} was achieved at 700 °C, when 50% H_2 in He was used as feed gas and humidified Ar for sweeping (pH_2O=0.042 atm). This value approaches the target of 1 ml·cm^{-2}·min^{-1} for proton conducting ceramics. By adding 15 vol% CO_2 in the feeding stream, chemical stability was demonstrated at 700 °C. The updated conclusions about the effective H_2 conducting phase will be presented.

4:50 PM J5.05
Hydrogen Permeation through CO_2-Stable Dual Phase Ceramic Membranes Sonia Escolastico, Cecilia Solis and Jose M. Serra; Instituto de Tecnología Química (UPV-CSIC), Valencia, Spain.

Mixed electronic-protonic conductors can be apply for the separation of hydrogen at high temperature in processes as integrated gasification combined cycle (IGCC) and catalytic membrane reactors. These materials need to fulfill two properties in order to apply them in the abovementioned applications: important mixed electronic-protonic conduction at high temperatures under hydrogen-containing atmospheres and enough stability under atmospheres containing CO_2, H_2O and H_2S. Lanthanum tungstate, $La_{5.5}WO_{11.25-\delta}$ (LWO), presents both properties; however the lack of electronic transport presented by LWO below 800 ºC produces relatively low hydrogen fluxes. On the other hand, $La_{0.87}Sr_{0.13}CrO_3$ (LSC) shows high mixed ionic (protonic)-electronic conductivity in reducing atmospheres and sufficient stability, but it is difficult to get fully dense membranes of this material.

This work presents the preparation, primary characterization, hydrogen permeation and stability study of $La_{5.5}WO_{11.25-\delta}$/$La_{0.87}Sr_{0.13}CrO_3$ (LWO/LSC) composites.

The mixture of LWO and LSC phases in different composites allows to improve the LSC sintering behavior and to obtain compounds with high total conductivity, higher than that shown for LWO and LSC separately. In fact, the mixture of these two ion conducting phases led to non-linear synergetic effects, i.e. unexpected enhancement of the total conductivity and well-balanced ambipolar conductivity, resulting in appealing H_2 permeation fluxes through robust ceramic membranes. The influence on

the H_2 permeation of the composite composition, the humidification of gas streams, temperature and the use of different catalytic coatings (screen-printed and sputtered) on the membrane surface is evaluated. The nature of the transport mechanism is investigated by permeation studies using deuterium tracers.

Finally, it is remarkable that the hydrogen flows for a 370 μm thick 50%-LWO/LSC membrane (0.15 $mL \cdot min^{-1} \cdot cm^{-2}$ at 700 ºC) are the highest values reported nowadays for bulk mixed protonic electronic membranes in addition to its stability under CO_2 containing atmospheres.

5:10 PM J5.06
Chemical Stability of Cercer H_2 Membranes in the Lanthanum Tungstate–Lanthanum Chromite System Jonathan M. Polfus, Zuoan Li, Martin F. Sunding, Wen Xing, Marie-Laure Fontaine, Partow P. Henriksen and Rune Bredesen; Materials and Chemistry, SINTEF, Oslo, Norway.

Cercer H_2 membranes of the two mixed ionic-electronic conductors $La_{28-x}W_{4+x}O_{54+3x/2-\delta}$ and $La_{0.87}Sr_{0.13}CrO_{3-\delta}$ have recently been shown to be chemically and thermo-mechanically compatible and exhibit state-of-the-art H_2 permeabilities [1-2]. The apparent hydrogen permeability, with contribution from both H_2 permeation and water splitting on the sweep side, has however been found to degrade at higher temperature and reducing atmospheres. In the present contribution, we have investigated the degradation phenomena by long-term flux measurements up to 1500 hours at 1000 °C in 50% H_2 in N_2/He feed and wet Ar sweep. The flux degradation seems to follow a two-stage kinetic process, and degrades from 2.8×10^{-2} to 4.7×10^{-3} mL min^{-1} cm^{-2} over the course of 1500 hours for a 1.8 mm thick membrane. Post-characterization of the membranes is performed by means of XRD, TEM and SEM, in order to elucidate structural, microstructural and chemical changes in the cercer materials. Segregation of La_2O_3 and metallic tungsten was observed, and in this respect, several compositions of the $La_{28-x}W_{4+x}O_{54+3x/2-\delta}$ material with varying La/W ratio (x) were investigated; La_2O_3 segregatoin is reduced with increasing x but degradation is still apparent, indicating a complex degradation process. Further stability assessment is performed by flux measurements in CO_2 containing atmospheres

The flux and post-characterization results are discussed in terms of the inherent structural disorder in $La_{28-x}W_{4+x}O_{54+3x/2-\delta}$ and formation of secondary phases. As such, changes in the transport properties of the cercer membrane may be ascribed to each materials contribution to ionic and electronic conductivity and ambipolar transport.

Acknowledgement
This publication has been produced with support from the BIGCCS Centre, performed under the Norwegian research program Centres for Environment-friendly Energy Research (FME). The authors acknowledge the following partners for their contributions: Gassco, Shell, Statoil, TOTAL, GDF SUEZ and the Research Council of Norway (193816/S60).

[1] S. Escolastico, S. Cecilia, C. Kjølseth, J.M. Serra, Energy Environ. Sci. 7 (2014) 3736.
[2] J.M. Polfus, W. Xing, M. Fontaine, C. Denonville, P.P. Henriksen, R. Bredesen, J. Memb. Sci. 479 (2015) 39.

K: Proton-Conducting Oxides

* Invited Speaker
** Keynote Speaker

SESSION K1: Poster Session I
K: Proton-Conducting Oxides
Monday Afternoon, June 15, 2015
12:00 PM
Keystone Resorts, Red Cloud Peak

K1.01
Defect Chemistry of $LaCrO_3$ from First Principles Calculations Sarmad W. Saeed, Tor S. Bjorheim, Reidar Haugsrud and Truls Norby; Department of Chemistry, University of Oslo, Oslo, Norway.

Acceptor doped lanthanum chromite (LCO) is a thermally stable, p-type conducting perovskite oxide which finds usage as interconnectors for SOFC, electrodes for MHD generators, and heating elements. Defect chemical-wise, LCO is reported to be dominated by electron holes ($h^\bullet$) under oxidizing conditions and oxygen vacancies ($v_O^{\bullet\bullet}$), and/or protons ($OH_O^\bullet$) under reducing conditions, and it has been proposed as a hydrogen transport membrane [1-2]. However, some aspects related to the defect properties of LCO are still unknown, especially under conditions where protons come into play.

To the best of our knowledge this is the first computational study on defect chemistry of LCO, in which we use first principles calculations applying two levels of theory, PBE+U and the HSE hybrid exchange-correlation functionals. We focus on the atomistic and thermodynamic behavior of electron holes, oxygen vacancies and protons. Our calculations confirm earlier assumptions that electron holes are localized at the Cr-ions ($Cr_{Cr}^\bullet$) in the form of small polarons, corresponding to oxidation of chromium. Further, we focus on the thermodynamics of the two competing hydration reactions: $H_2O(g)+v_O^{\bullet\bullet}+O_O^x=2OH_O^\bullet$ (1) $H_2O(g)+2h^\bullet+2O_O^x=2OH_O^\bullet+1/2O_2(g)$ (2) For the hydration of oxygen vacancies, reaction (1), the calculations reveal a standard enthalpy of -80 kJ/mol, in reasonable agreement with the experimentally deduced value of -70 kJ/mol [2]. The calculations indicate that reaction (2) plays a major role under oxidizing conditions, where electron holes are dominating. Based on the deduced defect thermodynamics, we explore the relative dominance of $h^\bullet$, $v_O^{\bullet\bullet}$ and $OH_O^\bullet$ at finite temperatures as a function of atmospheric conditions through thermodynamic modelling. The results are combined with surface calculations on LCO to get insight to the bulk and surface defect chemistry of importance for surface kinetics of membranes.

1. B.K. Flandermeyer, et al., J. Am. Ceram. Soc. 67(3), 195 (1984)
2. Y. Larring, et al., Membranes 2012, 2, 665-686.

K1.02
Investigation of Sinterability of $BaCe_{0.9}Y_{0.1}O_{3-\delta}$ at Several Schedules Profiles Huyra E. Araujo[3, 2] and Dulcina M. Souza[1, 3]; [1]Materials Engineering Department, Federal University of Sao Carlos, Sao Carlos, Brazil; [2]Federal Institute of Education, Science and Technology, Piracicaba, Brazil; [3]PPGCEM-UFSCar, Sao Carlos, Brazil.

The development of SOFC's for operating at intermediate temperature (500~600ºC) is the major challenge to practical application of this device and the decrease of operation temperature depends on the increase of electrical conductivity of electrolyte. Aiming to decrease the cell operating temperature, the substitution of YSZ by more conductive and stable materials is an actual possibility for solving the problem. Proton-conducting ceramics have attracted interest as alternative to solid electrolyte. Y-doped BaCeO3 has drawn attention as a candidate to electrolyte proton-conductor. Several studies have investigated the correlation between ceramic processing and properties of these materials, however the understanding of sintering mechanism and remains unclear. This work has investigated the sintering development of $BaCe_{0,9}Y_{0,1}O_{3-\delta}$ at several schedules of sintering. The ceramic powders were prepared by citrate process and mixed oxide process aiming to compare the sintering behavior of two different powder systems. On the citrate process, the precursor powder was calcined two times at 1100ºC for 10h whilst $BaCO_3$,CeO_2 and Y_2O_3 powders were mixed at stoichiometric ratio and calcined at 1100°C for 10h on mixed oxide process. The final powders were isostatic pressed at 200 MPa and sintered at several schedules from 1250°C~1550°C with *Fast Heating(~1500*ºC/min) *and Conventional Schedule(~13*ºC/min) at several dwell times. The calcined powders were characterized by X -Ray Diffraction and an orthorhombic perovskite crystalline phase was found in both powders systems. The sintering development was analyzed by measurement of linear shrinkage and density of pellets. Both powders has showed highest densification at 1550°C for 10h and a decrease on densification to lower temperatures whereas the powder from citrate process shows higher densification than mixed oxide process in all conditions. Furthermore, the *Fast Heating* schedule was more effective to citrate process with pellets achieving high densification with lower dwell time, 01h instead 10h at *Conventional Schedule*. This behavior may be associated to higher diffusion coefficients and fine -grained powders and can lead to decrease of dwell time and avoiding barium losses at the sintering.

K1.03
Lattice Expansion upon Hydration of Doped Barium Cerate/ Zirconate (BZY/BCZY) Proton Conducting Ceramics as Measured by High Temperature X-Ray Diffraction (HTXRD) Grant A. Hudish[1], Sandrine Ricote[2], Anthony Manerbino[1], W. G. Coors[1] and Neal P. Sullivan[2]; [1]R&D, CoorsTek, Golden, Colorado, United States; [2]Department of Mechanical Engineering, Colorado School of Mines, Golden, Colorado, United States.

Solid solutions of barium cerate and barium zirconate doped with yttrium ($BaCe_xZr_{1-x-y}Y_yO_{3-\delta}$) are currently promising candidates for industrial proton-conducting ceramic membranes. However, in the presence of moisture/steam these materials incorporate protonic defects ($OH_o^\cdot$) causing a chemical lattice expansion, in addition to any temperature induced thermal expansion. This lattice expansion manifests as an internal strain at the component level causing mechanical failure. For successful component design and manufacture this issue must be understood and contro lled. To investigate this behavior, high temperature XRD was performed on two compounds, $BaCe_{0.2}Zr_{0.7}Y_{0.1}O_{3-\delta}$ (BCZY27) and $BaZ_{0.9}Y_{0.1}O_{3-\delta}$ (BZY10). The lattice parameter of BCZY27 and BZY10 was measured from 1000°C to room temperature (RT) in 4% H_2 forming gas (balance Ar) with 0, 1, and 3% H_2O contents. Samples were dehydrated at 1200°C then hydrated in-situ. The maximum lattice expansion due to hydration of BCZY27 was measured to be nearly 2.5 times greater than BZY10 (0.005 vs. 0.0019Å, respectively). Additionally, this maximum expansion occurred between 400 and 600°C for BCZY27, but was much less pronounced peaking at 550°C for BZY10. Further experiments comparing pre hydrating samples and the use of bulk discs are also underway to further explore the hydration and accompanying expansion of these materials.

K1.04
Proton Dissolution in $BaZr_{1-x}Y_xO_{3-\delta}$ Genki Imai[1], Takashi Nakamura[2] and Koji Amezawa[2]; [1]Graduate School of Engineering, Tohoku University, Sendai, Japan; [2]Institute of Multidisciplinary Research for Advanced Materials, Tohoku University, Sendai, Japan.

Among candidate electrolytes for proton ceramic fuel cells, $BaZr_{1-x}Y_xO_{3-\delta}$ attracts attentions because of its high chemical stability and high proton conductivity. The proton conductivity in $BaZr_{1-x}Y_xO_{3-\delta}$ depends on the concentration and the mobility of proton. Therefore, it is important to understand the proton dissolution process of this material for developing better electrolytes based on $BaZr_{1-x}Y_xO_{3-\delta}$. Kreuer[1] and Schober *et al.*[2] investigated the proton concentration to discuss the proton dissolution process. In their interpretation, the standard formation enthalpy for the proton dissolution is assumed constant at a constant temperature. On the other hand, Sasaki *et al.* suggested the standard formation enthalpy depends on not only temperature but also proton concentration[3]. In this study, the proton concentration of $BaZr_{1-x}Y_xO_{3-\delta}$ (x = 0.05, 0.1, 0.2) was investigated by high accuracy thermogravimetry as functions of temperature and $P(H_2O)$ and thermodynamic properties for the proton dissolution were elucidated.

The standard free energy change for the proton dissolution was expressed by, $\Delta G° = \Delta H° - T\Delta S° = -RT\ln([OH^{\bullet}_{O}]^2 / P(H_2O)[V^{\bullet\bullet}_{O}][O^{\times}_{O}]) - RT\ln(\gamma_{OH^{\bullet}_{O}}{}^2 / \gamma_{V^{\bullet\bullet}_{O}}\gamma_{O^{\times}_{O}})$ (1) where $\gamma_{OH^{\bullet}_{O}}$, $\gamma_{V^{\bullet\bullet}_{O}}$ and $\gamma_{O^{\times}_{O}}$ are the activity coefficients of the defects. From the evaluated proton concentration, we found the activity coefficients of the defects in $BaZr_{1-x}Y_xO_{3-\delta}$ is not equal to 1 but depends on the proton concentration, meaning the standard formation enthalpy for the proton dissolution depends on the proton concentration. A similar dependence of the thermodynamic properties on defect concentration was often reported for oxygen vacancies in perovskite-type oxides[4]. Considering this, in the presentation, thermodynamic discussion will be made in a similar way as for the formation of oxygen vacancies.

(1) K. D. Kreuer, *Solid State Ionics*, **125**, 285-302 (1999), (2) T. Schober, *et al*., *Solid State Ionics*, **127**, 351-360 (2000), (3) I. Sasaki, *et al*., *Spring Meeting of Jpn. Soc. Met*. (2009), (4) J. Mizusaki, *et al*., *Solid State Ionics*, **12**, 119-124 (1984)

K1.05

Incorporation and Dissociation Behavior of Protons in $BaZrO_3$-Based Perovskite-Type Proton Conductors Tomohiro Ishiyama[1, 3], Haruo Kishimoto[1, 3], Katherine D. Bagarinao[1, 3], Katsuhiko Yamaji[1, 3], Toshiaki Yamaguchi[2, 3] and Yoshinobu Fujishiro[2, 3]; [1]Energy Technology Research Institute, National Institute of Advanced Industrial Science and Technology, Tsukuba, Japan; [2]Advanced Manufacturing Research Institute, National Institute of Advanced Industrial Science and Technology, Nagoya, Japan; [3]CREST, Japan Science and Technology Agency (JST), Saitama, Japan.

Acceptor-doped perovskite-type proton conductors incorporate protons as hydroxyl ions at oxygen vacancies and exhibit proton conductive properties. These oxides are known to exhibit complicated electrical conductive properties depending on temperature or atmosphere. This characteristic is related to the amount of dissolved proton and defect equilibrium in oxide. In-situ investigation of protons in the oxide is important to obtain new insights about the defect chemistry of these materials. Recently, our studies have shown that dissolved protons can be studied via in-situ diffuse reflectance infrared fourier transform spectroscopy (DRIFTs). In our previous study, we observed a dependence of the amount of dissolved protons in $BaZr_{0.1}Ce_{0.7}Y_{0.1}Yb_{0.1}O_{3-\delta}$ on temperature and atmosphere. Moreover, the dominant charge carrier gradually changed from protons to either oxygen ion or electron hole, in 1%H_2 or air, respectively, accompanied with a corresponding decrease in amount of dissolved protons. However, the correlation between the type of dominant carrier and the state of dissolved protons has not been clearly observed. The dominant carrier which is determined by defect equilibrium in oxide is dependent on governing reactions which determine how protons leave the oxide. In this study, the dissociation behavior of protons in $BaZr_{0.8}Y_{0.2}O_{3-\delta}$ were investigated via combination of in-situ DRIFTs and thermal desorption gas analysis in vacuum conditions at 30~800°C. Results show a significant correlation between proton incorporation state and dissociation behavior. Protons which were considered to have dissolved in the vicinity of dopant ions were easily removed and dissociated as water, whereas those which dissolved in vicinity of host ions were retained even at high temperatures and eventually dissociated as hydrogen. In our presentation, the dissociation behavior of D_2O saturated sample and correlation between conductivity and proton dissolution state will be discussed as well.

This research is partially supported by CREST program of the Japan Science and Technology Agency.

K1.06

First Principles Calculations of Carrier Trapping in Proton Conductive Acceptor-Doped $BaZrO_3$ Akihide Kuwabara, Craig A. Fisher and Hiroki Moriwake; Japan Fine Ceramics Center, Nagoya, Japan.

Acceptor-doped $BaZrO_3$ shows high proton conductivity under wet atmosphere conditions and is a promising material used for a proton conductive electrolyte. Similar to other kinds of ionic conductors, however, carrier trapping by dopant occurs and suppresses conductivity of the acceptor-doped $BaZrO_3$ [1]. The carrier trapping is an unavoidable phenomenon for ionic conductors because formation of charge carriers for ionic conduction is attributed to dopants with opposite charge states to the carriers. We have to understand and to control the carrier trapping behavior to optimize properties of ionic conductors. In this work, we calculate association energies between acceptors and protons in $BaZrO_3$ using first principles calculations. Several types of cations, Sc, In, Lu, Y, Er, Gd and Eu, are adopted as acceptors for comparison. Total energy calculations were performed using the VASP code. At first, a unit cell of $BaZrO_3$ was fully optimized, and then supercells of 5 × 5 × 5 unit cells containing 625 atoms was constructed for calculations of defective systems. Distances between a dopant and a proton are systematically changed and dependence of associatioin energy on the distance is investigated.

From the series of our calculations, it is revealed that dopants can be categorized into two types. In the cases of dopants with smaller ionic size such as Sc, In and Lu, protons prefer to be located at the first nearest neighbor from the dopants. Cations with larger ionic size like Y, Er, Gd and Eu capture protons at the next nearest neighbor sites.

[1] Y. Yamazaki, F. Blanc, Y. Okuyama, L. Buannic, J. C. Lucio-Vega, C. P. Grey, S. M. Haile, *Nature Mater.*, **12** (2013) 647-651.

K1.07

Densification and Microstructural Evolution in NiO-Added $BaZr_{0.8}Y_{0.2}O_{3-\delta}$ Ceramics Young-Woo Ryu, Joon-Hyung Lee, Young-Woo Heo and Jeong-Joo Kim; School of Materials Science & Engineering, Kyungpook National University, Daegu, Korea (the Republic of).

Because of the high protonic conductivity and excellent chemical stability, Y-doped $BaZrO_3$ (BZY) has been received increasing attention among various electrolyte materials. However, the refractory nature of BZY leads to significant challenges to its implementation in fuel cells and other devices. The poor sinterability of the Y-doped $BaZrO_3$ requires extreme sintering conditions, such as high temperature over 1600°C and long sintering times over 24 h. In order to alleviate the extreme sintering conditions, transition metal oxides, such as ZnO, CuO, NiO, were introduced. These sintering aids were found as effective sintering additives for lowered sintering temperatures and homogeneous microstructures in BZY. Particularly, a tentative mechanism for the sintering behaviour with NiO additive was suggested.

In this study, the effect of NiO addition on densification and microstructural evolution of BZY was carefully examined. It was found that most of the added NiO was squeezed out and covered the surface of the sample. However, in the case when the samples were covered with atmosphere powders, which are frequently used to minimize the evaporation of Ba, the outmost NiO layer was not observed due to the reaction with the atmosphere powders. X-ray diffraction, SEM and STEM analysis were conducted for the understanding the evolution.

K1.08

Dopant Concentration Dependence of Electrical Transport in Y-Doped $BaZrO_3$ Shogo Miyoshi, Ayano Ebara and Shu Yamaguchi; Department of Materials Engineering, The University of Tokyo, Tokyo, Japan.

Acceptor-doped $BaZrO_3$ has attracted much attention due to its high protonic conductivity as well as good chemical stability. On the other hand, the mechanism governing the proton solubility and transport has not been fully understood, which leaves further investigation necessary for optimization of $BaZrO_3$-based materials.

Recently, it has been suggested that protons in Y-doped $BaZrO_3$ (BZY) are trapped within YO_6 octahedra, which requires some activation energy for protons' escaping from that [1]. It has also been reported for BZY that the oxygen sites favorable to protons may extend to the second nearest neighbor of Y [2]. Such a strong interaction between dopants and the accompanying carriers can lead to a non-linear dependence of macroscopic conductivity on dopant concentration as has been observed for hole conduction in $BaZr_{1-x}Fe_xO_3$ [3]. In this study, the authors investigate the protonic conductivity of BZY as a function of dopant concentration focusing on possible percolation behavior at a low doping level.

Dense specimens of $BaZr_{1-x/100}Y_{x/100}O_3$ (BZYx, x=1, 2, 4, 8) have been prepared, and subjected to two terminal AC impedance measurements. The bulk protonic conductivity has been well evaluated below 400C from the highest frequency part, which is confirmed by H/D isotope effect. For this

temperature range, the apparent activation energy of the bulk conductivity is around 0.44 eV irrespective of composition. On the other hand, the isotherms of the bulk conductivity show a non-linear increase against Y concentration, especially around *x*=4. Assuming that the proton concentration of each composition reaches the saturation for the given Y concentration, the results indicates that the macroscopic proton diffusivity increases with Y concentration. This behavior will be discussed in terms of interaction between the dopant and protons as well as possible occurrence of percolation.

[1] Y. Yamazaki et al., *Nature Mater.* 12 (2013) 647.
[2] F. Blanc et al., *J. Phys. Chem. Lett.* 5 (2014) 2431.
[3] D. Kim et al., *Solid State Ionics* 262 (2014) 875.

K1.09

Proton Trapping: A Key to Control Proton Transport in Oxides Yoshihiro Yamazaki[1, 4], Yuji Okuyama[2], Jason Potticary[3], Kentaro Yamamoto[1] and Sossina M. Haile[3]; [1]Inamori Frontier Research Center, Kyushu University, Fukuoka, Japan; [2]Miyazaki University, Miyazaki, Japan; [3]California Institute of Technology, Pasadena, Colorado, United States; [4]Japan Science and Technology Agency, Kawaguchi, Japan.

Proton trapping is a phenomenon in which proton occupying oxygen site near dopant is more bound to that free from the trap. Such energy landscape might limit proton transport in proton-conducting oxides. We experimentally showed that there are indeed two types of protons, trapped and trap-free protons, in 20 at% yttrium-doped barium zirconate based on AC impedance spectroscopy, thermogravimetry, and nuclear magnetic resonance [1]. We expand this effort to barium zirconates doped with Lu, Er, and Gd which are larger or smaller than yttrium. Atomistic simulation predicts that the association energy varies with ionic radius. To determine proton diffusivities in 20 at% Lu, Er, Y, and Gd-doped barium zirconates, we utilized AC impedance spectroscopy and thermogravimetry. The proton diffusivities show downward curved Arrhenius plots for all cases, which is a clear indication of proton trapping in the oxides. The association energies extracted from the curvature are -28, -29 and -44 kJ/mol for Lu, Y, and Gd-doped, respectively. The values of association energies are quantitatively in good agreement with those from atomistic simulation.

[1] Yamazaki et al., Nature Materials 12 (2013) 647.

K1.10

The Effect of Yttrium Source on the Microstructure and Hygroscopic Behavior of $BaCe_{0.8}Y_{0.2}O_{3-\delta}$ Using ZnO as Sintering Aid Elcio L. Pires; Materials Engineering, Federal University of São Carlos, São Carlos, Brazil.

Yttrium-doped barium cerate (BCY) is a well-known proton-conducting oxide with perovskite structure which has been extensively studied along the last 30 years mainly for uses such as solid electrolyte in SOFCs. In this work the influence of two different sources of Yttrium on the BCY microstructure was investigated. Two samples with similar composition $BaCe_{0.8}Y_{0.2}O_{3-\delta}$ + 1 wt% ZnO were obtained via the Solid-State Reactive Sintering method, developed by researchers from the Colorado School of Mines. The use of small amounts of ZnO as sintering aid is an efficient way to increase the BCY sinterability without compromising its proton conductivity. Stoichiometric amounts of comercial $BaCO_3$, CeO_2, ZnO and Y_2O_3(YO-sample) or $Y(NO_3)_3 \cdot 6H_2O$ (YN-sample) were all dispersed in isopropanol in a jar together with 1 wt% of PVB. The slurries were ball milled for about 60 h and then dried and sieved with a 300 µm mesh. The powders were pressed into pellets isostatically at 200 MPa and sintered at different temperatures ranging from 1000 to 1500 °C for 12 h, using a heating rate of 2 °C/min. Both samples presented the highest densification at 1100 °C (YN-sample = 5.92 ± 0.03 g/cm^3 and YO-sample = 6.03 ± 0.03 g/cm^3). The fracture surface and the polished cross section of 1.28 mm thickness sintered pellets were analyzed by SEM. Both samples presented a visually distinguishable core region with smaller grain size and a shell region with larger ones. Z-contrast images and EDS maps also showed grains with different Y and Zn content. Comparing both samples sintered at 1100 °C, the YN-sample presented larger grain size and more homogenous Y and Zn distribution than the YO-sample; however it was visually observed that the YN-sample presented a hygroscopic behavior starting to degrade after two weeks exposed to the environment, while the YO-sample stayed unchanged.

K1.11

Y-doped $BaZrO_3$ Thin Films for Water Electrolysis at Intermediate Temperatures Deposited by Aerosol Assisted Chemical Vapor Deposition Alexander Benes[2], Oliver Clemens[2,1], Wolfram Jaegermann[3] and Horst Hahn[2, 1]; [1]Institute for Nanotechnology, Karlsruhe Institute of Technology (KIT), Karlsruhe, Germany; [2]Joint Research Laboratory Nanomaterials, Technical University of Darmstadt and Karlsruhe Institute of Technology (KIT), Darmstadt, Germany; [3]Surface Science Group, Technical University of Darmstadt, Darmstadt, Germany.

A current major challenge is the development of sustainable and clean energy sources as well as the storage of the produced energy. Solid oxide fuel cells (SOFC) are considered to be a promising technology for power generation due to their high efficiencies and fuel flexibility. If an SOFC is run in reverse mode it is called solid oxide electrolysis cell (SOEC) and hydrogen is produced. In this way energy can be converted from electrical to chemical energy and thus be stored efficiently. Y-doped $BaZrO_3$ (BZY) has found increased use as a proton conducting electrolyte in SOFCs since it offers advantages in terms of high bulk conductivity at lowered temperatures (350 °C – 600 °C) and since it shows good chemical stability, especially towards CO_2.
To reduce the ohmic resistance and thereby enable the lowering of the operating temperature, thin films of BZY (0 mol%, 10 mol% and 20 mol% of Y) have been deposited by aerosol assisted chemical vapor deposition at ambient atmosphere. By varying the process parameters several structural and microstructural aspects such as density, film thickness and crystallinity as well as phase and defect arrangement have been optimized. The films were deposited on different substrates and characterized by X-ray photoelectron spectroscopy (XPS) and X-ray diffraction (XRD) to confirm stoichiometry and phase purity respectively. In addition electrochemical impedance measurements were carried out to investigate the influence of doping and film thickness on the materials' conductivity.

K1.12

Investigation of $Ba_{1-x}Gd_{0.8}La_{0.2+x}Co_2O_{6-\delta}$ (X = 0 - 0.5) as Oxygen Electrode Material for Proton Conducting Fuel Cells and Electrolyzer Cells Ragnar Strandbakke, Einar Vollestad and Truls Norby; Department of Chemistry, University of Oslo, Oslo, Norway.

Double perovskite $BaGd_{0.8}La_{0.2}Co_2O_{6-\delta}$ (BGLC) is a promising oxygen side electrode material for proton conducting fuel cells (PCFCs) and electrolyzer cells (PCECs) with measured apparent polarization resistance of 0.05 Ωcm^2 at 650 °C on proton conducting $BaZr_{0.7}Ce_{0.2}Y_{0.1}O_3$. BGLC is potentially a new mixed proton / electron hole conducting MIEC material, and significant hydration is confirmed by thermogravimetric measurements at 300-400 °C, yielding a hydration enthalpy of around -50 kJ mol^{-1} [1]. The $BaRECo_2O_{6-\delta}$ materials class generally display layered structures, with alternating Ba and rare earth (RE) layers along the crystal cell *c*-axis and with oxygen vacancies ordered along the *b*-axis in the RE layers [2]. In a proton conducting cell, the oxygen electrode will benefit from mixed protonic / electronic conductivity, and oxide ion conductivity is thus in principle of less importance.
Electrolyzer operation requires materials stability at high steam pressures, catalytic activity towards water dissociation, high electrical conductivity and preferably a considerable proton transport. Substituting some of the A′-site Ba with La will give higher overall A-site valence, and thus lower δ, and by substituting some La for Ba, the layered ordering will be disrupted, possibly also with respect to the oxygen sublattice. In this study, hydration properties, chemical stability, electrical conductivity and electrode performance is investigated for five compositions of perovskite $Ba_{1-x}Gd_{0.8}La_{0.2+x}Co_2O_{6-\delta}$ (X = 0 - 0.5) by use of thermogravimetry, x-ray diffraction, four point DC measurements and electrochemical impedance spectroscopy. The results show that while BGLC hydrates with ~1.1 and ~0.5 % protons per mole BGLC at 300 °C for X = 0 and 0.5, respectively, the former decomposes and the latter is stable in 1.5 bars of steam at 700 °C.

References:
[1]: R Strandbakke, V Cherepanov, A Zuev, D. S. Tsvetkov, C Argirusis, G Sourkouni, S Prünte, T Norby (to be published).
[2]: A. Maignan, C. Martin, D. Pelloquin, N. Nguyen, B. Raveau, *Journal of Solid State Chemistry* 142 (1999) (2) 247.

K1.13

Channel-Level Modeling of Protonic Ceramic Fuel Cells and Model Calibration Kevin J. Albrecht[1], Chuancheng Duan[2], Robert J. Braun[1] and Ryan P. O'Hayre[2]; [1]Mechanical Engineering, Colorado School of Mines, Golden, Colorado, United States; [2]Materials Science, Colorado School of Mines, Golden, Colorado, United States.

Protonic ceramics fuel cells (PCFC) have emerged as a promising candidate for distributed power generation. The cells offer the potential for reduced temperature operation and implement manufacturing techniques which reduce costs when compared to their oxygen ion conducting counterparts. The development of a protonic ceramic fuel cell computational modeling tool is imperative to the design and implementation of systems. A framework is presented for a predictive channel-level PCFC model capturing the mixed conducting nature of the protonic ceramic materials. The model employs a 1-D channel-level modeling strategy where fuel depletion and flow configuration effects are resolved and coupled to a semi-empirical electrochemical model. Modeling results calibrated against experimental data of a state-of-the-art PCFC composition are presented.

The low temperature nature and hydrogen removal from the anode channel present a unique condition where a thermodynamic analysis is presented for operating regimes where solid carbon formation is not thermodynamically favorable. Simulation results are presented for the operation of the cell in the required regime. Model predicted distributions of gas phase species, temperature, and local current density are resolved. The model predicted cell performance when operating on a humidified methane fuel source (S/C = 2.4) at 500ºC and 80% utilization indicates a power density greater than 0.100W/cm^2 is attainable at an average current density of 0.15A/cm^2. The model presented is capable of being incorporated into a system-level model to predict LHV electrical and combine efficiencies.

K1.14

Defect Entropies of $BaZrO_3$ from First Principles Phonon Calculations Tor S. Bjorheim[1], Eugene Kotomin[2] and Joachim Maier[2]; [1]FASE, Department of Chemistry, University of Oslo, Oslo, Norway; [2]Max Planck Institute for Solid State Research, Stuttgart, Germany.

The high temperature proton conductor Y-doped $BaZrO_3$ is a promising candidate material for electrolytes in proton conducting intermediate temperature SOFCs. Y-doped $BaZrO_3$ hydrates by replacement of $v_O^{\bullet\bullet}$ by $OH_O^{\bullet}$ as the dominating positive charge-compensating defect.
While the effect of dopant type on the corresponding $\Delta_{Hydr}H$ usually is rationalized by more basic oxygen ions close to the dopant [1], $\Delta_{Hydr}S$ is, however, poorly understood [2], as it contains vibrational contributions from both $v_O^{\bullet\bullet}$ and $OH_O^{\bullet}$, and $H_2O(g)$. In this paper, we determine the phonon contribution to the formation entropy of $v_O^{\bullet\bullet}$ and $OH_O^{\bullet}$ in bulk $BaZrO_3$and at the (100) surface, and thus to its hydration and surface segregation thermodynamics, from first principles calculations.

First principles calculations were performed using DFT at the GGA level using the plane-wave based VASP code. Phonon properties were evaluated within the quasi-harmonic approximation using finite atomic displacements, allowing determination of the defect formation entropies.

There is a notable negative contribution from phonons to the formation entropy of $v_O^{\bullet\bullet}$ which stems from large local lattice relaxations and unit cell contraction upon and $v_O^{\bullet\bullet}$ formation. Neglect of the phonon contributions therefore leads to a significant error in the free energy of formation $v_O^{\bullet\bullet}$, which is as large as 110 kJ/mol at 1000 K. The contribution from phonons to the entropy of $OH_O^{\bullet}$ is significantly smaller than for $v_O^{\bullet\bullet}$. Hence, the largest contributions to $\Delta_{Hydr}S$ come from loss of $H_2O(g)$ and filling of $v_O^{\bullet\bullet}$ by oxygen ions.

Further, the phonon contribution to the formation energy of $v_O^{\bullet\bullet}$ at the (100) surface is notably smaller than in bulk, and the vacancy displays a positive surface *segregation* entropy. Hence, phonons affect the relative stability of $v_O^{\bullet\bullet}$ and $OH_O^{\bullet}$ at the surface compared to in the bulk oxide, which has implications for the surface defect structure, and thus the surface space-charge potential arising from accumulation of $v_O^{\bullet\bullet}$ and $OH_O^{\bullet}$ at the surface.

Refences

[1] Kreuer et al., Solid State Ionics, 2001, 145, 295
[2] Norby et al. Dalton Trans. 2004, 3012-3018

K1.15

Effect of Al_2O_3 and Y_2O_3 Addition on Proton Conductivity of Electrochemically Proton Injected Phosphate Glasses Takuya Yamaguchi[1], Kanji Sakuragi[1], Takahisa Omata[1], Tomohiro Ishiyama[2], Junji Nishii[3], Toshiharu Yamashita[4], Hiroshi Kawazoe[4], Naoaki Kuwata[5] and Junichi Kawamura[5]; [1]Graduate School of Engineering, Osaka University, Suita, Japan;[2]National Institute of Advanced Industrial Science and Technology (AIST), Tsukuba, Japan; [3]Research Institute for Electronic Science, Hokkaido University, Sapporo, Japan; [4]Kawazoe Frontier Technologies Corp., Yokohama, Japan; [5]Tohoku University, Sendai, Japan.

We recently developed a new proton-carrier injection technique that is an electrochemical substitution of alkali ions in phosphate glasses with protons (alkali proton substitution; APS) and obtained a pure proton-conducting phosphate glass by application of APS to $35NaO_{1/2}$-$1WO_3$-$8NbO_{5/2}$-$5LaO_{3/2}$-$51PO_{5/2}$ glass (1W-glass). The proton conductivity of the glass after APS was 4×10^{-4} Scm^{-1} at 250 °C, and the glass softened and deformed at >250 °C. Because the proton conductivity of the glass is expected to be $>1\times10^{-2}$ Scm^{-1} at >370 °C based on its Arrhenius plot, the 1W-glass after APS will be applicable as a solid electrolyte to the ITFCs when its thermal stability is improved.

In the present study, we improved the thermal stability of the 1W-glass by addition of M_2O_3 (Al_2O_3 and/or Y_2O_3) and studied its proton conductivity. By addition of M_2O_3, the glass became stable at >300 °C; however, the proton conductivity decreased 1~2 orders of magnitude. Because the concentrations of proton-carriers in M_2O_3 added 1W-glasses injected by APS were similar to that of 1W-glass without M_2O_3 addition, the reduction of proton conductivity is attributable to the reduction of the proton mobility. The Raman and ^{31}P MAS-NMR spectra showed that the glasses consist of chained phosphate ions of $(PO_3^-)_n$; the glasses involve Q^2 and Q^1 units that are the PO_4 units existing in inner and terminal of chained $(PO_3^-)_n$ ions, respectively. M_2O_3 addition induces the fragmentation of $(PO_3^-)_n$ ions and increases the concentration of the terminal Q^1 unit. According to the previous study, the protons tightly bond to oxygen atoms in Q^1 units rather than in Q^2 units. Consequently, we conclude that the reduction of the proton mobility is caused by the increase of protons that bond to oxygen atoms in Q^2units because of the fragmentation of chained $(PO_3^-)_n$ ions induced by M_2O_3 addition.

K1.16

Hydrogen Induced Rupture of Si-O Bonds in Amorphous Silicon Dioxide Al-Moatasem El-Sayed[1, 2], Matthew Watkins[1, 2], Tibor Grasser[3], Valery Afanas'ev[4] and Alexander Shluger[1,2]; [1]Department of Physics and Astronomy, University College London, London, United Kingdom; [2]London Centre for Nanotechnology, London, United Kingdom; [3]Institute for Microelectronics, Technische Universitat Wien, Vienna, Austria; [4]Department of Physics, University of Leuven, Leuven, Belgium.

The interaction of hydrogen with amorphous silicon dioxide (a-SiO_2) is important for many applications due to its widespread use in optical and electronic device fabrication processes. Hydrogen, in its more prevalent forms (H_2 and water), is known to induce hydrolytic weakening of quartz and tectosilicate minerals [1], as well as being involved in degradation phenomena in optical fibers [2] and SiO_2-insulated electronic devices. However, the involvement of atomic hydrogen in silica network degradation mechanisms is still poorly understood.

Using *ab initio* modeling, we show that the interaction of atomic hydrogen with strained Si–O bonds in a defect-free a-SiO_2 network results in the formation of a new defect structure consisting of a 3-coordinated Si atom facing a hydroxyl group which we refer to as the hydroxyl E′ center [3]. To study the distribution of defect properties, 116 configurations of the defect were calculated. We find that this defect is preferentially generated at bridging O sites where the oxygen forms a statistically long Si –O bond. In order to understand the origins of this defect, the kinetics of formation have been calculated. The energy barriers to form this defect from

interstitial H atoms range between 0.5 and 1.3 eV. We find that this defect can trap a hole and release a proton which can diffuse through the a-SiO_2 network with a barrier of 0.8 eV. This discovery of unexpected reactivity of atomic hydrogen may have significant implications for our understanding of processes in silica glass and nano-scaled silica, e.g., in porous low-permittivity insulators, and strained variants of a-SiO_2.

[1] B.E. Hobbs, "Point defects in minerals," (American Geophysical Union, 1985) pp. 151-169
[2] D. L. Griscom, Nucl. Instr. Methods B **46**, 12 (1990)
[3] A-M. El-Sayed, M. B. Watkins, T. Grasser, V. V. Afanas'ev, A. L. Shluger, Phys. Rev. Lett., *Accepted* (2015)

K1.17
Defect Associations as a Potential Cause for Limiting Proton Concentrations in Acceptor Doped Oxides Andreas Loken, Tor S. Bjorheim and Reidar Haugsrud; Department of Chemistry, University of Oslo, Oslo, Norway.

In the present contribution we aim to show that defect associations may be the origin for lower proton saturation levels. The proton concentrations in acceptor doped oxides can often be significantly lower than the theoretical limit given by the acceptor concentration i.e. $[OH_O^{\bullet}{}_{measured}] < [Acc'_{nominal}]$. Several causes for these limits have been suggested but a full understanding is still lacking. Low dopant solubilities can be disregarded as these are in principle easy to distinguish due to the formation of secondary phases. Lowering of the effective acceptor level due to BaO (g) evaporation is another potential cause [1, 2]. However, this explanation cannot account for proton concentration limits experienced in material systems with non-volatile cations such as acceptor doped $SrZrO_3$ and $LaYbO_3$ [3, 4].

To illustrate the effects of defect associations on the proton saturation levels and how these vary depending on dopant type, we have studied $BaCe_{0.9}X_{0.1}O_{3-\delta}$ (X = Sc, Y, In, Gd and Er) by means of thermogravimetric (TG) and computational techniques (DFT, VASP, GGA-PBE). DFT calculations demonstrate that concentration limits can stem from associated complexes of acceptors and positively charged defects. Complexes of two acceptors and one oxygen vacancy, $(X_{Ce}v_OX_{Ce})^X$, will only hydrate to form a single proton, $(X_{Ce}OH_OX_{Ce})'$, as the formation of the second proton in the complex, $(X_{Ce}OH_OX_{Ce}OH_O)^X$, is energetically unfavourable. This effectively lowers the total proton concentration that can be achieved. The binding energies of the associated complexes were also consistent with the proton concentration limits determined experimentally by TG measurements.

[1] D. Shima, S.M. Haile, *Solid State Ionics* **97** (1997) (1–4) 443.
[2] K.D. Kreuer, *Annu. Rev. Mater. Res.* **33** (2003) 333.
[3] F. Krug, T. Schober, *Journal of the American Ceramic Society* **80** (1997) (3) 794.
[4] Y. Okuyama, T. Kozai, T. Sakai, M. Matsuka, H. Matsumoto, *Electrochimica Acta* **95** (2013) (0) 54.

SESSION K2: Protonic Oxides I
K: Proton-Conducting Oxides
Chairs: Truls Norby and Yoshihiro Yamazaki
Tuesday Afternoon, June 16, 2015
Keystone Resorts, Longs Peak

1:30 PM **K2.01
Protonic Conduction in Perovskites: NMR and DFT Studies of Yttrium-Doped $BaZrO_3$ and Related Perovskites Luke Sperrin[1], Riza Dervisoglu[1], Lucienne Buannic[1], Frederic Blanc[2] and Clare Grey[1]; [1]Department of Chemistry, University of Cambridge, Cambridge, United Kingdom; [2]Department of Chemistry, University of Liverpool, Liverpool, United Kingdom.

Hydrated yttrium-doped $BaZrO_3$ is one of the most promising proton-conducting solid-state electrolytes for use in intermediate temperature fuel cells. Fundamental to improving the property of this material, and proton conductors in general, involves an understanding of the local environments for protons within the structure and their relationship with the conduction mechanisms. In particular, in structures where the incorporation of protons occurs because of an extrinsic defect or substituted ion (in this case Y^{3+}), proton trapping nearby the defect can result in an increase in the activation barrier for diffusion.[1] Structural analysis of the protonic defects is not straightforward when using conventional diffraction techniques. By contrast, multinuclear solid-state NMR spectroscopy (often in combination with double resonance NMR techniques and DFT calculations) provides a method with which to directly probe the local structure. This talk will describe a joint multinuclear NMR spectroscopy and DFT (total energy and GIPAW NMR calculations) study of dehydrated and hydrated $BaY_xZr_{1-x}O_{3-x/2-y}(OH)_{2y}$. Samples were studied by ^{17}O and ^{89}Y NMR spectroscopy as a function of composition (x = 0.1, 0.3, 0.5), to determine the location of the vacancies in the dry samples, relative to the Y substituent. ^{17}O NMR reveals the presence of two chemically distinct oxygen sites that are labeled Zr-O-Y and Zr-O-Zr. Two ^{89}Y resonances are observed which are assigned to 5- and 6-coordinated yttrium sites: YO_5 and YO_6. Total energy calculations show that the oxygen vacancies are preferentially located within the 1st or 2nd yttrium coordination shell. The vacancy – cation ordering is, however, strongly dependent on the Y – Y separation: there is a strong energetic preference for oxygen vacancies (V_O) to locate between two nearby Y ions and form a Y–V_O–Y environment. The hydrated samples were then investigated, the results from the DFT GIPAW chemical shift calculations being used to correlate ^1H chemical shift with local environment and the nature of H-bonding. ^1H-^{89}Y CP and HETCOR MAS spectra of $BaY_xZr_{1-x}O_{3-x/2-y}(OH)_{2y}$ as a function of composition (x = 0.1, 0.3, 0.5) were performed allowing sites on both the A and B sites of the perovskite to be resolved and the spatial proximity between H and Y local environments to be explored. The results for Y-substitution are compared with those for other substituents such as Sc.

[1]"Proton trapping in yttrium-doped barium zirconate", Y. Yamazaki, F. Blanc, Y. Okuyama, L. Buannic, J.C. Lucio-Vega, C.P. Grey, and S.M. Haile, *Nat. Mat.*, **12**, 647 – 651 (2013).

2:00 PM K2.02
Local Structural Analysis of Sc-Doped $BaZrO_3$ Using Electric-Field Gradient at Sc Site Itaru Oikawa and Hitoshi Takamura; Department of Materials Science, Tohoku University, Sendai, Japan.

Perovskite-type oxides doped with rare-earth elements have widely been investigated as a candidate electrolyte for intermediate temperature SOFCs. It is known that amounts of protons varied not only with the dopant concentration but also cations of the host perovskite-type oxides. Since protons are introduced by a reaction of oxygen vacancies and water vapor, our previous study suggests that the local structure in the vicinity of the vacancies seems to affects the concentration of protons; however, it has not been understood well. This study is aimed to clarify the local structure around an acceptor using electric-field gradient (EFG) at its site. EFG at a nucleus site can be obtained both theoretically and experimentally by first-principles calculation and NMR spectroscopy. In this study the local structure of 5-coordination in Sc-doped $BaZrO_3$ is investigated by means of EFG at Sc site. First-principles calculation based on density functional theory was carried out by introducing one or two Sc and one oxygen vacancy in eight unit cells of cubic perovskite-type structure. The structure was optimized to minimize force among each atoms. Before the structural optimization, calculated EFG at Sc expressed in the form of quadrupole coupling constant, a NMR parameter proportional to the strength of EFG, was 60 MHz which is approximately twice as large as the value determined from ^{45}Sc NMR. Meanwhile the EFG value after structural optimization decreased to 40 MHz and approached to the experimental value. The atomic displacement due to the optimization was less than 5% of the Sc-O bond length. This result indicates that EFG at Sc site is quite sensitive characteristics toward slight change in local structure of picometer-scale and has potential to clarify the difference in the local structure around oxygen vacancy with respect to cations of the host perovskite-type lattice.

2:20 PM *K2.03
Variation of Kinetic Parameters, Chemical Diffusivity and Surface Exchange Coefficient of $Ba(Zr_{0.84}Y_{0.15}Cu_{0.01})O_{3-\delta}$ during the Conductivity Relaxation Experiments Jong-Ho Lee, Sung Min Choi, Moon-Bong Choi, Jongsup Hong, Hyoungchul Kim, Kyung Joong Yoon, Ji-Won Son and Byung-Kook Kim; High-Temperature Energy Materials Research Center, Korea Institute of Science and Technology, Seoul, Korea (the Republic of).

The hydration/dehydration kinetics of a proton conducting oxide, $Ba(Zr_{0.84}Y_{0.15}Cu_{0.01})O_{3-\delta}$ were investigated via conductivity relaxation method upon a sudden change of water vapor pressure ($-4.40 \leq \log(P(H_2O)) \leq -1.79$ range) with fixed oxygen partial pressure ($P(O_2)=0.21$). The conductivity relaxation during the hydration/dehydration process shows typical two-fold non-monotonic behavior that can be explained by the decoupled chemical diffusion of H and O. However we found some significant variation of relaxation behavior with respect to elapsed experimental time, thereby the estimated chemical diffusivity and surface exchange coefficient are not constant anymore even under same $P(H_2O)$ and $P(O_2)$ condition. In this study, we investigated these strange behaviors of kinetic parameters during the conductivity relaxation experiment and attempted to analyze the cause for these unusual behaviors using thorough compositional and microstructural examination.

2:40 PM K2.04
The Influence of Dopant Levels on the Hydration Properties of SZCY and BZCY Proton Conducting Ceramics for Hydrogen Production Kwati Leonard[1], Yuji Okuyama[4], Young-Sung Lee[1] and Hiroshige Matsumoto[1, 2, 3]; [1]International Institute for Carbon-Neutral Energy Research (I2CNER-WPI), Kyushu University, Fukuoka, Japan; [2]INAMORI Frontier Research Center (IFRC), Kyushu University, Fukuoka , Japan; [3]Next Generation Fuel cell Research Center (NEXT-FC), Kyushu University, Fukuoka, Japan; [4] Organization for the Promotion of Tenure Track, University of Miyazaki, Miyazaki, Japan.

Ionic conductivity is an important transport process for all electrochemical energy conversion and storage devices and very relevant for a sustainable energy economy. In the present work Yttria-doped strontium zirconate partially substitted with ceria $SrZr_{0.5}Ce_{0.4}Y_{0.1}O_{3-\alpha}$ (SZCY541) have been studied as a potential proton conducting electrolyte for intermediate temperature steam electrolysis. The effects of Ba substitution for Sr on the lattice structure, proton content, electrical properties, hydration behavior, as well as chemical stability are investigated. Proton content was examined by tailoring dopant concentration to improve the proton conductivity. Thermo-gravimetric analyses revealed a similar proton concentration in both SZCY541 and $SrZr_{0.44}Ce_{0.35}Y_{0.2}O_{3-\alpha}$ (SZCY542) with a constant Zr/Ce fraction of 5:4. Both samples showed almost comparable proton conductivities in both wet hydrogen and oxygen atmosphere. Whereas $BaZr_{0.44}Ce_{0.35}Y_{0.2}O_{3-\alpha}$ (BZCY542) showed a higher proton mobility than $BaZr_{0.5}Ce_{0.4}Y_{0.1}O_{3-\alpha}$ (BZCY541) and retained the highest proton conductivity of 1.44×10^{-2} Scm^{-1} in wet 1 % H_2 at 600 °C as well as excellent chemical stability under 80 % steam for 200 hours. These results suggest Ba and Sr at A-site have different effects on hydration and proton mobility. This paper discusses these aspects based on experimental results as well as steam electrolysis using SZCY-541 and BZCY542 as electrolytes.

Acknowledgement
This work was supported by Council for Science, Technology and Innovation (CSTI), Cross-ministerial Strategic Innovation Promotion Program (SIP), "energy carrier"(Funding agency: JST) and by World Premium International Research Center Initiative (WPI), MEXT Japan.

SESSION K3: Poster Session II
K: Proton-Conducting Oxides
Tuesday Afternoon, June 16, 2015
5:20 PM
Keystone Resorts, Red Cloud Peak

K3.01
Effect of Ba Nonstoichiometry in $Ba_x(Zr_{0.8}Y_{0.2})O_{3-\delta}$ on Population of 5-Coordinated Y Joon-Hyung Lee[1], Young-Woo Heo[1], Jeong-Joo Kim[1], Zhehong Gan[2] and Oc Hee Han[3];[1]School of Materials Science & Engineering, Kyungpook National University, Daegu, Korea (the Republic of); [2]National High Magnetic Field Laboratory, Tallahassee, Florida, United States; [3]Korea Basic Science Institute, Western Seoul Center, Seoul, Korea (the Republic of).

The local environments of Y in the Y-substituted $BaZrO_3$ of the starting compositions of $Ba_x(Zr_{0.8}Y_{0.2})O_{3-\delta}$ (x = 0.97, 1.0, 1.03, and 1.06) were analyzed by ^{89}Y magic angle spinning NMR spectroscopy. The result showed a strong population dependence of 5-coordinated Y^{3+} ions mostly at the B site on the Ba contents. The enhancement of Ba contents by 9 at% (from 0.97 to 1.06 in the starting Ba contents) in a nominal composition increased the amount of 5-coordinated Y^{3+} ions from 35%± 7% to 49%± 5%, suggesting the importance of maximizing the Ba contents to populate more oxygen vacancies which is related to the concentration of protons incorporated during the hydration process. The wide variation in the lattice parameter of yttrium-substituted $BaZrO_3$ perovskite materials in previous reports was reinterpreted with the variation in the Ba contents resulting from the evaporation of BaO during the sintering processes. Y^{3+} ions were confirmed to replace mainly the Zr^{4+} ions, as expected, and a tendency of oxygen vacancy clustering near the Y^{3+} ions was discussed.

K3.02
Studies of Y-Doped Ba (Ce, Zr) O_3 for Electrochemical Promotion Applications Efstratios Stavrakakis and Danai Poulidi; Chemistry and Chemical Engineering, Queen's University Belfast, Belfast, United Kingdom.

Yttrium doped-Barium Cerate (BCY) is one of the exceptional mixed ion-electron conductors that present both proton and oxygen ion conductivity depending on the operating temperature. Following the formula: $BaCe_{1-x}Y_xO_{3-\delta}$, x amount of Y^{3+} substitutes Ce^{4+} in $BaCeO_3$, creating δ oxygen vacancies which correspond to x/2 values [1]. Despite its multiple conducting behaviour and its high proton conductivity, the disadvantage of BCY is the chemical instability in CO_2 atmospheres [2]. This can be restricted by further substitution of Ce^{4+} with Zr^{4+}although the material (BCZY) will be slightly less proton conductive (BCZY) [3].
In the present study, BCY samples for Y-doping level of 5-20% were synthesised via an aqueous sol-gel method in order to be used as the solid electrolyte-catalyst support in electrochemically promoted catalytic reactions. Structural analysis by XRD showed that the samples presented a sufficiently pure phase. Dynamic thermogravimetric analysis (TGA) of water incorporation on the BCY powder was carried out in order to test the proton conductivity of the material. TGA results showed that the dopant concentration is strongly related to the hydration capacity. The maximum water uptake (0.4% wt at 300°C) was recorded for the highest Y-doped barium cerate and 71% of the oxygen vacancies were filled. For dopant levels 10-15%, water absorption took place in higher temperatures but water loss was accompanied by oxygen loss resulting in a sharp overall weight decrease after 900°C.

Further experiments will be conducted in order synthesise a material that combines high proton conductivity and chemical stability being suitable for applications as electrochemical promotion of CO_2 hydrogenation.

[1] K. Li, Ceramic membranes for separation and reaction. Hoboken, N.J., Chichester: Wiley, 2007
[2] S.M. Haile, G. Staneff and K.H. Ryu, Journal of Materials Science 36 (2001), 1149-1160.
[3] S. Barison, M. Battagliarin, T. Cavallin, L. Doubova, M. Fabrizio, C. Mortalo, S. Boldrini, L. Malavasi and R. Gerbasi, Journal of Materials Chemistry, 18 (2008), 5120-5128

K3.03

Moving Boundary Diffusion Mechanism for Non-Monotonic Conductivity Relaxation of Proton Conducting Perovskites Gye-Rok Kim[1], Hyun-Ho Seo[1], Jung-Mo Jo[1], Eui-Chol Shin[1], Ji Haeng Yu[2] and Jong-Sook Lee[1]; [1]Materials Science and Engineering, Chonnam National University, Gwangju, Korea (the Republic of); [2]Korea Institute of Energy Research, Daejeon, Korea (the Republic of).

A high temperature van der Pauw method using a bulk disk sample was successfully applied to monitor non-monotonic conductivity relaxation upon water in-/ex-corporation of a protonic ceramic conductor, barium zirconates doped with 20 m/o yttrium (BZY20). Application of four electrodes along the entire lateral thickness of the disk sample and the averaging of the reciprocal and reversed polarity measurements allow a reliable estimation of the conductivity effects described by one-dimensional diffusion processes. The faster hydrogenation process was found slightly more strongly activated than the slower oxygenation process and dehydrogenation kinetics upon water excorporation was slower than the hydrogenation. The observation can be explained by the moving boundary diffusion problem as previously directly evidenced by optical spectroscopy where the hydrogenation relaxations are controlled by the development of the hydration fronts over the fraction of the sample thickness from the surface up to the the maximum hydrogenation, while the (re)oxidation appear to be involved with the diffusion process over the entire sample thickness. The mechanism is shown to be general for all protonic ceramic conductors exhibiting non-monotonic conductivity relaxations. For the zirconate-cerate solid solution system, the activation energies decreases with increasing cerate composition and slightly lower than those for oxidation/reduction in the respective system. The activation energy values for chemical diffusivities represent essentially hole trapping effects.

K3.04

The Influence of NiO Sintering Additive on the Stability and Conductivity of $BaCe_{0.9-x}Zr_xY_{0.1}O_{3-d}$ Proton-Conducting Ceramics Sandrine Ricote[1], Anthony Manerbino[2], David Martinefski[2], W. Grover Coors[2] and Neal P. Sullivan[1]; [1]Department of Mechanical Engineering, Colorado School Of Mines, Golden, Colorado, United States; [2]CoorsTek Inc., Golden, Colorado, United States.

It is well established that NiO can be used as a sintering additive to prepare highly dense $BaCe_{0.9-x}Zr_xY_{0.1}O_{3-d}$ (BCZY) proton-conductors. Without the NiO addition, long dwell times at temperatures above 1700 °C are required; this results in detrimental barium evaporation, and costly manufacturing. BCZY powder can be prepared by solid-state reaction and subsequently sintered with the addition of NiO as a sintering aid (SSR-Ni). Alternatively, NiO may be added directly to the unreacted precursor oxides in a single-step process known as 'solid-state reactive sintering' (SSRS). Pellets of the raw precursors are sintered only once at 1550 °C for only six hours, combining phase formation and body densification. While the SSR-Ni and SSRS specimens exhibit similar conductivity in moist reducing atmosphere at 600 °C, the grain-boundary contribution to the total conductivity for the SSR-Ni specimen becomes significantly larger than that of the SSRS specimen at lower temperatures. At 200 °C, the grain-boundary resistance for the SSR-Ni specimen is twelve-times larger than for the SSRS specimen, highlighting the advantage of SSRS. Intra-granular fractures are observed for BCZY after SSRS; in contrast, the materials fracture at the grain boundaries after annealing in reducing atmosphere. It is hypothesized that Ni forms an amorphous oxide phase at the grain boundaries during SSRS. In reducing atmosphere, this phase transforms into Ni metallic, confirmed by the presence of Ni nanoparticles decorating grain boundaries. This residual Ni causes degradation of the specimens used for conductivity tests, particularly when switching repetitively between oxidizing and reducing atmospheres. The re-oxidation and reduction of the Ni at the grain boundaries leads to the failure of the specimen.

In this study, we present both the degradation mechanism, and the new manufacturing process we have developed to maintain the desirable large-grain microstructure obtained with SSRS without the ensuing mechanical instability.

K3.05

Development of Cu-Based Anodes for BZCY72 Proton Ceramic Membrane Reactors Shay A. Robinson[1], Christian Kjoølseth[2], W. Grover Coors[2] and Truls Norby[1]; [1]Chemistry, University of Oslo, Oslo, Norway; [2]Protia AS, Oslo, Norway.

$BaZr_{0.7}Ce_{0.2}Y_{0.1}O_{3-\delta}$ (BZCY72) electrolyte membranes are stable in carbon-containing atmospheres; however, development of suitable electrodes remains a major technological challenge. BZCY72 and copper resist carbon deposition, though the kinetic behavior of the copper-BZCY metal-electrolyte interface isn't well known. This work describes the development of Cu-based electrodes for operation in carbonaceous atmospheres.

Utilizing impedance spectroscopy, point-contact electrodes were used to characterize the hydrogen oxidation kinetics of the copper-BZCY interface. Point-contact architecture alleviates complexities of composite electrodes, reducing the size of the triple-phase boundary (TPB). A reaction mechanism is proposed based on measurements taken ranging 325 – 625 °C with variable H_2 and H_2O pressures. Impedance spectra revealed the total polarization resistance is dominated by low-frequency components attributed to surface diffusion.

To reduce the area-specific resistance (ASR) associated with diffusion processes and increase the number of TPB sites, a micro-porous backbone was fabricated, extending the copper-BZCY72 metal-electrolyte interface. This was infiltrated with solutions of copper nitrate to deposit an electronically conductive phase, and cerium nitrate to deposit an electro-catalytically active phase. The percolated Cu network exhibits in-plane point-to-point room-temperature resistance of order 0.01 Ω. Due to coarsening of Cu-based networks at 500 °C, cobalt was electro-deposited as a textural promoter to prevent Cu particle growth. The resulting electrode morphology has electronic and electro-catalytically active phases, supported by an ionic phase. Electrochemical characteristics of these novel electrodes were measured using impedance spectroscopy. Results show the extended TPB of this multi-phase electrode is effective at reducing ASR associated with surface diffusion. When the temperature is increased above 700 °C, a slight coarsening of the percolated network is observed. This remains a challenge if these electrodes are to be utilized for industrial processes; preventing this effect is a topic of continued research.

The authors acknowledge support from the Research Council of Norway (NANO2021, RoMA, project number 219194).

K3.06

Hydrogen Permeation Degradation due to Yttrium Migration in Dense $BaCe_{0.8}Y_{0.2}O_{3-\delta}$-$Ce_{0.8}Y_{0.2}O_{2-\delta}$ Composite-Ceramic Membranes Wade A. Rosensteel, Sandrine Ricote and Neal P. Sullivan; Mechanical Engineering - Colorado Fuel Cell Center, Colorado School of Mines, Golden, Colorado, United States.

This report seeks to explain the degradation in hydrogen permeation rates through dense composite-ceramic membranes used in hydrogen separations. The membranes are a $BaCe_{0.8}Y_{0.2}O_{3-\delta}$ – $Ce_{0.8}Y_{0.2}O_{2-\delta}$ (BCY-YDC) composite; BCY serves as a proton conductor, and YDC serves as an electronic conductor. With this materials set, hydrogen gas dissociates into protons and electrons which then conduct through the membrane and recombine as hydrogen gas on the opposite side. Membranes are fabricated by solid-state reactive sintering with 1 wt.-% NiO and standard ceramic processing methods. The membranes are hermetically sealed into a ceramic manifolding assembly, and fed hydrogen and helium (for leak detection) to the permeant (feed) side. Argon is fed to the permeate (sweep) side of the membrane, and the permeate exhaust composition is monitored using a gas chromatograph, allowing the hydrogen permeation rate to be quantified.

While modest hydrogen fluxes of 0.075 $mL_{STP}cm^{-2}$ min^{-1} ($5.6\square10^{-4}$ mol m^{-2} s^{-1}) are observed at 900 °C with a hydrogen partial pressure gradient of 0.5 atm through a 1.44 mm thick membrane, permeation rates rapidly decline over the course of a few days in this operating condition. When the hydrogen partial pressure gradient is decreased to 0.1 atm, no degradation is observed over the course of five days. In both cases, X-ray diffraction patterns of the membranes after testing do not reveal the formation of an undesired phase; however, scanning electron micrographs of the permeant

side of the membranes tested in either condition exhibit morphological changes near the surface. Energy dispersive X-ray spectroscopy of grains near the surface indicate the formation of yttrium-rich YDC grains, "sponge-like" yttrium-deficient YDC grains, and yttrium-deficient BCY grains. Performance degradation may be attributed to the formation of this observed layer of yttrium-deficient BCY grains near the surface, which impede proton transport.

K3.07

Correlation between Structural and Transport Properties of Proton-Conducting $Ba_{1-x}Ln_x(Zr,In,Sn)O_{3-\delta}$ (Ln - lanthanides) Oxide Konrad Swierczek[1], Xin Liu[2], Alicja Klimkowicz[1, 3], Wojciech Zajac[1] and Bogdan Dabrowski[4]; [1]Faculty of Energy and Fuels, AGH University of Science and Technology, Kraków, Poland; [2]School of Materials Science and Engineering, University of Science and Technology Beijing , Beijing, China; [3]Department of Engineering Science and Mechanics, Shibaura Institute of Technology, Tokyo, Japan;[4]Department of Physics, Northern Illinois University, DeKalb , Illinois, United States.

Proton conducting ceramic materials seem to be an interesting alternative electrolytes for Solid Oxide Fuel Cells operating at lowered temperatures [1]. Among candidate materials, B-site substituted $AB_{1-x}Ln_xO_{3-\delta/2}$ (A: Sr, Ba; B: Zr, Ce, Sn) perovskite-type oxides are of interest, with Ln^{3+} cations (Y^{3+}, lanthanides) being introduced in order to induce an appearance of the oxygen nonstoichiometry δ. Also, In^{3+}-containing materials are studied, which originate from $Ba_2In_2O_5$ brownmillerite. While modification of the B-site is commonly conducted in these materials, introduction of +3 cations at the A-site is less studied.
In this work A-site substituted $Ba_{1-x}Ln_x(Zr,In,Sn)O_{3-\delta}$ (Ln: selected, large lanthanides) oxides were analyzed in terms of elaboration of materials having high protonic conductivity. The performed systematic research was based on the structural considerations, taking into account chemical composition, and therefore ionic radii of the elements, resulting Goldschmidt's tolerance factor *t*, electronegativity of the elements, as well as the expected oxygen nonstoichiometry δ. Also, In and Sn influence on sinterability of the materials was considered.
Structural studies of $Ba_{1-x}Ln_x(Zr,In,Sn)O_{3-\delta}$ were performed at room and high temperatures, and the data were analyzed using Rietveld method. Kinetics of hydration and dehydration of the materials were measured on thermobalance in dry, H_2O- and D_2O-containing artificial air. Electrical conductivity of the compounds was measured on dense sinters by electrochemical impedance technique. The measurements were conducted in dry, H_2O- and D_2O-containing artificial air, in order to establish the isotope effect [2] and proton transference number. The obtained results suggest possibility of further optimization of protonic conductivity in the studied system.

The project was funded by the National Science Centre Poland (NCN) on the basis of the decision number DEC-2012/05/E/ST5/03772.

[1] N. Ito, M. Iijima, K. Kimura, S. Iguchi, J. Power Sources 152 (2005) 200
[2] A.S. Nowick, A.V. Vaysleyb, Solid State Ionics 97 (1997) 17

K3.08

Studies of Chemical Stability of Dense $BaCe_{0.6-x}Zr_{0.2}Y_{0.2}M_xO_{3-\delta}$ (M-transition metal) Protonic Conductors Mateusz Tarach, T. Jerominek, M. Szymula and Wojciech Zajac; AGH University of Science and Technology, Faculty of Energy and Fuels, Department of Hydrogen Energy, Krakow, Poland.

Introduction:
Proton conducting ceramics have unique electrochemical properties that make them suitable materials for a number of applications including protonic ceramic fuel cells, hydrogen sensors and steam electrolysers. However, extreme synthesis conditions such as high temperatures and long sintering times of barium zirconates and cerates as representatives, result in significant challenges to their further implementation.
Aim of this work is investigation of the sinterability, crystal structure, chemical stability and transport properties of selected barium cerates as a function of grain size and content of sintering additives.

Experiments:
Four different transition metal oxides (NiO, ZnO, CoO, CuO) were used as sintering aids during synthesis of $BaCe_{0.6}Zr_{0.2}Y_{0.2}O_{3-\delta}$ (BCZY) perovskite-structure proton conductor. The compound was obtained simultaneously by high-temperature solid-state reaction and soft chemistry techniques, including sol-gel, reverse micelles and co-precipitating methods. Phase composition, crystal structure and thermal stability studies were performed using X-ray powder diffraction. Microstructure was investigated by scanning electron microscopy. AC impedance spectra were measured to determine transport properties. Sintering of pressed powders was studied with linear dilatometry. Final density of the sinters was measured by Archimedes' method.

Results and Discussion:
Single-phase perovskite-structure materials were obtained in all of the synthesis routes. Examined additives facilitated formation of the BCZY solid solution at lower temperatures as compared with the unmodified system. Furthermore, significant effect of reduced particle size on lowering sintering temperature was also recorded.

Conclusions:
The observed correlation between concentration of sintering additives, grain size and sintering temperature of BCZY enables fabrication of fully dense sinters with high ionic conductivity and good stability against steam and CO_2 atmosphere under working conditions. However, the mechanism underlying enhanced sintering in this system still needs to be further clarified.

Acknowledgments:
This work was supported by the Polish Ministry of Science and Higher Education research grant 'Diamentowy Grant' No. D12013 003243.

K3.09

Enhanced Chemical Stability and Sinterability of Refined Proton-Conducting Perovskite: Case Study of $BaCe_{0.5}Zr_{0.3}Y_{0.2}O_{3-\delta}$ Ji Haeng Yu[1], Muhammad Hakim[2], Chung-Yul Yoo[1]and Jong Hoon Joo[1]; [1]Advanced Materials and Devices Lab., Korea Institute of Energy Research, Daejeon, Korea (the Republic of); [2]Advanced Energy Technology, University of Science and Technology, Daejeon, Korea (the Republic of).

Improving the chemical stability and sinterability of proton-conducting perovskites has been a challenge for the development of durable electrochemical devices. In this study, we demonstrate that residual barium compounds after incomplete solid state reaction cause the chemical instability and poor sinterability of $BaCe_{0.5}Zr_{0.3}Y_{0.2}O_{3-\delta}$ (BCZY). As-calcined BCZY requires both a high sintering temperature (1470°C) and controlled atmosphere (O_2 purging) to obtain dense, crack-free ceramic specimens, but shows continuous degradation of electrical conductivity in the presence of trace amounts of CO_2. The excess barium component, identified as mostly $Ba(OH)_2$ by X-ray photoelectron spectroscopy, can be removed by rinsing the as-calcined powder with distilled water. Thermogravimetric analysis reveals that this refining process to remove $Ba(OH)_2$ residues enhances the durability of BCZY in a CO_2-containing atmosphere. From the refined BCZY, a dense, durable proton-conducting ceramic can be prepared by sintering at the relatively low temperature of 1360°C. The effects of BCZY refinement on cell stability under operational fuel cell conditions are also investigated. For this purpose, anode-supported cells, comprised of a nickel oxide (NiO)-BCZY anode, a BCZY electrolyte, and a BCZY-$La_{0.6}Sr_{0.4}Co_{0.2}Fe_{0.8}O_{3-\delta}$ composite cathode are successfully prepared with refined or as-calcined BCZY powder. The long-term fuel cell performance is evaluated under a potentiostatic measurement at 600 °C. The cell with the refined BCZY electrolyte shows a modest power density of 47 mW cm^{-2} at a 600 °C operating temperature over 480 h without any significant performance loss, whereas the cell with the as-calcined BCZY electrolyte displays a rapid degradation of cell performance over 110 h. A post-testing analysis of the cell with the refined BCZY does not reveal any evidence of delamination resulting from electrolyte surface decomposition. These results demonstrate that the refinement process significantly enhances the chemical stability of BZCZY-based proton conducting fuel cells, which produce a high content of water vapor on the cathode side.

K3.10

Effect of Titanium Doping on Structural Stability and Electrical Properties of Proton-Conducting Solid Electrolyte $BaCe_{0.8}Sm_{0.2}O_{3-\delta}$ Hailei Zhao, Chunyang Yang, Zhihong Du, Yongna Shen and Chunli Yan; University of Science and Technology Beijing, Beijing, China.

Rare metal-doped perovskite $BaCeO_3$ exhibits high proton conductivity in hydrogen and water vapor containing atmosphere at intermediate temperatures and it is regarded as one of the most promising candidate materials as electrolyte in solid oxide fuel cells. Our previous work has reported that the electrical conductivity of 20 mol% Sm doped $BaCeO_3$ could reach 0.017 S cm^{-1} at 600 °C in moist 5% H_2/Ar atmosphere. However, $BaCeO_3$-based materials suffer from poor chemical and structural stability in CO_2 and water containing atmosphere due to the formation of barium carbonate and hydroxides.

In this work, in order to improve the chemical and structural stability of $BaCe_{0.8}Sm_{0.2}O_{3-\delta}$, the B-site Ce is partially replaced by Ti with high electronegativity to form a novel perovskite material $BaCe_{0.8-x}Ti_xSm_{0.2}O_{3-\delta}$. With increasing content of Ti, both chemical and structural stability of the samples in CO_2 and water containing atmospheres remarkably increase. However, Ti-doping decreases the proton conductivity of $BaCe_{0.8-x}Ti_xSm_{0.2}O_{3-\delta}$ samples, which may be attributed to the difficult hydration of the materials caused by Ti doping. The electrical conductivity of $BaCe_{0.75}Ti_{0.05}Sm_{0.2}O_{3-\delta}$ reaches 0.0103 S cm^{-1} in wet 5% H_2/Ar ($p(H_2O)$ = 0.074 atm) at 650 °C. Considering the good chemical and structural stability in $CO_2$and water containing atmospheres and the high electrical conductivity, $BaCe_{0.75}Ti_{0.05}Sm_{0.2}O_{3-\delta}$ is a promising electrolyte for intermediate temperature solid oxide fuel cells.

K3.11

Up-Scaling of Metallic Nanoparticle Production by Electrical Discharge for Use in Catalytic Membrane Reactor Christelle Denonville[1], Jicheng Feng[2], Marie-Laure Fontaine[1], Harald Fjeld[3], Amin A. Azar[1] and Andreas Schmidt-Ott[2]; [1]SINTEF Materials and Chemistry, Oslo, Norway; [2]Delft University of Technology, Delft, Netherlands; [3]PROTIA AS, Oslo, Norway.

For large scale applications such as catalytic membrane reactors, hybrid membranes or solid oxide fuel cells, environmentally friendly production of (electro)-catalysts is essential. In the present work, we describe the scaling process for the fabrication of metallic nanoparticles by means of electrical discharge (both spark and arc). The variety of metallic nanoparticles (materials, size distribution or composition), which can be produced by simply changing electrodes materials and gas composition shows the flexibility of the process, while the absence of harmful chemical and costly precursor is an asset towards an environmentally friendly process.

Depending on the targeted application, the nanoparticles can be produced by arc discharge with a large production rate and a particle size distribution ranging from 15 to 200 nm, whereas spark discharge provides a narrower particle size distribution and mean particle size of 5nm. The nanoparticles can be selected by size or charge, directly deposited from the aerosol phase or collected and dispersed in appropriate solvents.

Here we describe a method to simultaneously produce and deposit nickel nanoparticles on a ceramic membrane with both spark and arc discharge. The membrane is a ceramic composite of acceptor doped $LaCrO_3$ and $La_xW_yO_z$ designed as a thin film tubular membrane for hydrogen transport (HTM) to be used in steam methane reforming.

The research leading to these results has received funding from the European Union's Seventh Framework Program under Grant Agreement No. 280765 (BUONAPART-E).

K3.12

Proton Conductors Based on Lanthanum Scandate for an Electrolyte of Intermediate Temperature Operating SOFCs Takuya Yamane[1], Fumitada Iguchi[1], Hisahi Kato[2], Takahiro Ouchi[2], Makoto Shimizu[1] and Hiroo Yugami[1]; [1]Graduate School of Engineering, Tohoku University, Sendai, Japan; [2]Tohoku Electric Power Co., Inc., Sendai, Japan.

Proton conductors which shows high proton conductivity and suitable for film deposition by pulsed laser deposition method were developed based on lanthanum scandate, and anode-supported type cells were fabricated and tested.

Sr-doped $LaScO_3$ (LSSc) shows high proton conductivity equivalent to Y-doped $BaCeO_3$ (BCY), and its chemical stability is not as poor as BCY is. Therefore, proton conductors based on this material will be promising candidate for an electrolyte of intermediate temperature SOFCs, which operating at the temperature range of 700-500 °C. However, electrical performances of cells based on them were not well studied.

We adopted PLD method to fabricate thin films of LSSc. But, during PLD process, much debris was scattered from ablated LSSc surface. To prevent short circuits and gas leakage, LSSc was developed to be Co and Sr co-doped $LaScO_3$ (LSScCo), which prevent scattering of debris and PLD process was improved to eliminate debris mechanically.

As a result, we successfully fabricated anode-supported cells which configuration was Pt or LSFC | LSScCo | Ni-YSZ or Ni-BZY. These cells could be operated during 800 to 600 oC with sufficient high OCV over 0.9 V, and maximum power density was ca. 20 $mWcm^{-2}$.

K3.13

Ni - $BaCe_{0.89}Gd_{0.1}Cu_{0.01}O_3$ as Perspective Anode Material for Proton-Conducting SOFC Denis Osinkin[1], Nina Bogdanovich[1], Elena Pikalova[1, 2] and Dimitry Bronin[1, 2]; [1]Laboratory of SOFC, Institution of High Temperature Electrochemistry, Yekaterinburg, Russian Federation; [2]Ural Federal University, Yekaterinburg, Russian Federation.

Solid oxide fuel cells with proton-conducting electrolytes are promising sources of electricity. In such SOFCs, in contrast to the cells with oxygen-conducting electrolyte, water is released at the cathode rather than the anode that prevents a dilution of the fuel, increasing the cell efficiency. In this work, the anodes based on the promising proton-conducting material $BaCe_{0.89}Gd_{0.1}Cu_{0.01}O_3$ (BCGCu) were investigated.

The BCGCu electrolyte powder was synthesized via a two-step ceramic method from CeO_2 (99.99 %), Gd_2O_3 (99.9996 %) and $BaCO_3$ (99.99 %) with addition of CuO (10.3 m^2/g). The initial components were mixed and synthesized at 1100 °C, 2 h. Intermediate product after milling, drying and pressing into the disk under the pressure 150 MPa was sintered at 1400 °C, 5 h. XRD revealed the formation of a single-phase solid solution of orthorhombic perovskite type with lattice parameters a = 8.7912 Å, b = 6.2523 Å and a = 6.218 Å. The relative density of the sintered samples was 94-96% of the calculated crystallographic density (6.34 g/cm^3).

The anode slurries were prepared by mixing the powdered electrolyte and NiO in weight ratio 44/56. The electrode layers were placed symmetrically onto dense BCGCu substrate and sintered at 1400 ºC. The estimated thickness of electrode was about 20-30 µm. The measurement of electrochemical activity was performed by the method of impedance spectroscopy in temperature range of 600-900 ºC.

Electrodes under investigation showed a high electrochemical activity (the polarization resistance was equal to 1 Ω cm^2) at 600 °C. The energy of activation of the polarization conductivity was 0.55 eV. Infiltration with cerium nitrate (up to the 15% of electrode weight) ensured a decrease in polarization resistance approximately two times without noticeable changing of the electrode process energetic.

K3.15

Development of Anode-Supported Electrochemical Cell Based on Proton-Conductive $Ba(CeZr)O_3$ Electrolyte Toshiaki Yamaguchi, Hiroyuki Shimiada, Haruo Kishimoto and Yoshinobu Fujishiro; National Institute of Advanced Industrial Science and Technology, Nagoya, Japan.

Solid oxide fuel cells (SOFCs) have attracted much attention as a highly efficient and low-pollution power generation system. The introduction of a proton conductor as the electrolyte material, instead of conventional oxide ionic conductors such as a stabilized zirconia, is expected to improve the fuel cell performance due to some reasons: (1) Water is produced at the cathode side during fuel cell operation; therefore, the H_2 concentration at the anode side must be kept constant, regardless of the fuel utilization. (2)

The charge carrier, H^+, has the smallest ionic radius, and thus the activation energy is small. As a result, the power generation performance can be improved over a wide range of the operating temperature.
Among several proton conducting materials, a barium zirconate-cerate co-doped with Y and Yb: $Ba(CeZr)O_3$ was reported to exhibit high conductivity below 750 °C and high chemical stability even under CO_2 and H_2O atmospheres [1]. Therefore, when this proton conducting ceramic is used as an electrolyte material, H_2 can be produced at the fuel electrode by application of a direct current to the cell. Despite the significant efforts and the potential of wide range of applications, these proton conducting materials still require improved sinterability to achieve performance by reducing the grain boundary resistance.
In this work, $Ba(CeZr)O_3$ (BCZ) was selected as a proton conducting material to fabricate anode-supported electrochemical cell for SOFC/SOEC applications. In this study, the sinterability and electrical properties of anode-supported BCZ cell were investigated. Dense electrolyte layer was formed on Ni-BCZ porous support by co-sintering technique at around 1300ºC. The formation of a solid solution between NiO and BCZ electrolyte layer was confirmed for 3~5 wt% NiO due to the lack of NiO segregation and the lattice parameter increased until saturation. The cell can be operated in a wide temperature range from 200ºC to 550ºC, and the maximum power density of the cell was about 0.5W/cm² at 550ºC.

K3.14
Electrical Properties of Nonstoichiometric $Ba_xZr_{0.85}Y_{0.15}O_{2.925}$ Ceramics Prepared by Solid State Reactive Sintering Nahum Maso[1], Jonathan . Polfus[2], Marie-Laure Fontaine[2] and Truls E. Norby[1]; [1]Chemistry, University of Oslo, Oslo, Norway; [2]SINTEF Materials and Chemistry, Oslo, Norway.

Yttrium-doped barium zirconate, $BaZr_{1-x}Y_xO_{3-x/2}$, shows high-temperature proton conductivity in water-vapor containing atmospheres. It has high chemical and mechanical stability, which allows application in fuel cells, gas sensors, and membrane technology. However, to obtain dense ceramics by solid state reaction and conventional sintering, high sintering temperatures (~1700 °C) are required which leads to barium loss during sintering.

Recently, the solid state reactive sintering method has been applied to fabricate dense $BaZr_{1-x}Y_xO_{3-x/2}$ ceramics at relatively low sintering temperatures, e.g. 1500 °C, using NiO as sintering aid. However, it is observed experimentally (but rarely commented in the literature) that, during sintering, barium (and nickel) loss also occurs by solid state reactive sintering.

Here we report the effect of barium deficiency/excess on the electrical properties of $Ba_xZr_{0.85}Y_{0.15}O_{2.925}$ ($0.94 \leq x \leq 1.06$) ceramics prepared by solid state reactive sintering using 1 wt% NiO as sintering aid. Furthermore, the solubility of Ni in the perovskite structure and its influence on the stability of Ba vacancies is elucidated by density functional theory calculations.

We thank the Research Council of Norway (RCN) for financial support through Nano2021 program (BioPCFC, 219731).

K3.16
Transport Kinetics of the Mixed Conductor Lanthanum Tungstate Andreas Falkenstein[1, 2] and Manfred Martin[1, 2]; [1]Institute of Physical Chemistry I, RWTH Aachen University, Aachen, Germany; [2]JARA-ENERGY, Aachen, Germany.

The electrical conductivity relaxation method is widely used for determining the transport kinetics upon oxidation/reduction of mixed ionic-electronic conductive oxides. This technique has been modified to perform relaxation experiments upon de-/hydration on materials with high electronic conductivity. Separate kinetics for oxygen and proton diffusion have been found in perovskite type oxides, showing twofolded non-monotonic relaxation patterns as a superposition of two relaxation curves[1;2]. Also, the surface reaction constants show different behaviors for proton incorporation and oxygen incorporation[3].

In this study, the electrical conductivity relaxation of the fluorite type protonic conductor lanthanum tungstate (LaWO54) has been investigated. It shows twofold relaxation kinetics, and two individual chemical diffusion coefficients and surface reaction constants can be attributed to the incorporation and diffusion of protons and oxygen. Since electronic and protonic contributions to the change in conductivity upon de-/hydration of lanthanum tungstate are in the same order of magnitude, a detailed derivation of the amplitude factors of each partial curve is necessary. Furthermore, the existence of structural and thermal vacancies in lanthanum tungstate‘s anion sublattice[4] has been considered in the derivation. The kinetic transport parameters of lanthanum tungstate are investigated in dependency of the partial pressures of oxygen and water as well as of the temperature. Twofolded monotonic and non-monotonic, and, under specific conditions, singlefolded relaxation curves are observed and their characteristics are explained.

[1] H.-I. Yoo, J.-K. Kim, C.-E. Lee, *J. Electrochem. Soc.* **2009**, *156*, B66-B73.
[2] H.-I. Yoo, C.-E. Lee, *Solid State Ionics* **2009**, *180*, 326-337.
[3] D.-K. Lim, T.-R. Lee, B. Singh, J.-Y. Park, S.-J. Song, *J. Electrochem. Soc.* **2014**, *161*, F710-F716.
[4] S. Erdal, L.-E. Kalland, R. Hancke, J. Polfus, R. Haugsrud, T. Norby, A. Magrasó, *Int. J. Hydr. Energy* **2012**, *37*, 8051-8055

K3.17
Surface Segregation in Sr Doped $LaNbO_4$: Implications for Proton Transport Cheng Li and Stephen J. Skinner; Department of Materials, Imperial College London, London, United Kingdom.

Introduction
Acceptor doped $LaNbO_4$ has been proposed as a novel proton conductor, due to its excellent chemical stability in environments containing acidic gas such as CO_2. However, in contrast to the well-established bulk transportation mechanism [1], the surface chemistry of this material, which plays a key part in the proton incorporation process, is not yet known. It is well documented in the literature that the surface composition of MIEC and oxygen ion conductors can differ significantly from the bulk [2]. To our knowledge, no previous work, experimental or simulation, has ever probed the surface chemistry of acceptor doped $LaNbO_4$.

The Low Energy Ion Scattering (LEIS) technique is extremely sensitive to the outmost atomic layer of the surface and in the present work, we have applied this powerful tool to study the surface of 1 at% Sr doped $LaNbO_4$, and their evolution as a function of processing and anneal conditions.

Experimental
The 1at% Sr doped LaNbO4 was prepared by conventional solid state reactions. Single phase was confirmed by XRD and electron probe microanalysis (EPMA). For the LEIS analysis, the pellets were ground, finely polished and annealed at temperature varying from 600 °C to 1000 °C for 10 hours. The surface was successively cleaned in acetone ethanol and finally in de-ionised water prior LEIS experiment.

Results and Discussion
The LEIS spectrum of the outmost atomic layer indicates that the La/Nb ratio of the 600 °C annealed sample is very similar to that of the $LaNbO_4$ reference, no Sr peak was observed within the detection limit. Depth profile of the sample (not shown) revealed that the surface composition is almost identical to that of the bulk.
A shoulder at lower energy was observed in the 800 °C annealed sample which might result from a slight enrichment of Sr on the surface. Such a feature is clearly detected for the 1000 °C annealed sample: the Nb signal on the surface is much weaker and a strong Sr segregation on the outmost layer was observed. Depth profile of the same sample suggests that the segregation layer is about 10 nm thick.
Sr segregation was also observed on the unpolished, as-sintered sample. Interestingly, the intensity of the Sr peak is weaker comparing with the 1000°C annealed one, although the sintering temperature is 1400 °C. This result suggests that the surface chemistry is very sensitive to the processing routine. It is worth emphasizing that the bulk contains only 1 at % of Sr on the A site, Sr segregation on the surface would thus result in a significant reduction in Sr content and thus oxygen vacancy in the bulk, which might affect the proton conduction process.

Conclusions
Dopant segregation was observed on the outmost layer of the Sr doped LaNbO4 after annealing at temperatures above 800 °C. The effect of the segregation on proton transport and surface exchange is to be investigated.

References
1. Haugsrud, R. & Norby, T. *Nat. Mater.* **5,** 193–196 (2006). 2. Téllez, H *et al. Int. J. Hydrogen Energy* **35,** 20856-20863 (2014)

K3.18
Impedance Spectroscopy on Proton Conducting Oxides $La_{1-x}A_xNbO_4$ (x=Sr,Ca) Su-Hyun Moon, Dieu Nguyen, Dong-Chun Cho, Young-Hun Kim, Eui-Chol Shin, John G. Fisher and Jong-Sook Lee; School of Materials Science and Engineering, Chonnam National University, Gwangju, Korea (the Republic of).

Alkaline earth-doped lanthanum niobates $La_{1-x}A_xNbO_4$ (A=Sr,Ca) are candidates for thermally stable high temperature proton conductors. Substantial proton conductivity is indicated at temperatures as high as 800C. However, the AC characteristics is rather non-trivial, which may be related to the co-presence of the mixed oxide-ion and electron conduction, grain boundary impedance, and the phase transition to monoclinic and tetragonal. Therefore, instead of the deconvoluted bulk or total sample conductivity, mono-frequency AC conductivity has been also reported. Non-trivial AC characteristics are clearly indicated at lower temperatures. The high frequency bulk conductivity exhibits frequency dispersion close to $\omega^{1/3}$. On the other hand, the huge impedance triggered below the transition temperature, often attributed to the grain boundary, shows the exceptionally ideal RC behavior. There appears to exist an intermediate component between very dispersive bulk and very ideal grain boundary response. The bulk frequency dispersion in niobates is definitely different from the universally observed $\omega^{2/3}$behavior. Recently suggested Cole-Davidson (CD) dielectric function model for the bulk dispersion due to mobile charge carriers can be however similarly applied. The intermediate frequency component can be also described by another CD dielectric function without an explicit resistance components and attributed to the current-constriction impedance closely correlated with high frequency bulk conductivity in the humidity dependence. On the other hand, the huge RC response does not show a systematic behavior with humidity. The response is thus attributed to a Schottky depletion layer generated at the electrolyte and electrode interface. The effects of different alkaline earth dopants and preparation methods on the impedance parameters are discussed.

K3.19
Cation Diffusion in Proton Conducting Lanthanum Tungstate Einar Vollestad and Reidar Haugsrud; Department of Chemistry, University of Oslo, Oslo, Norway.

The proton and mixed proton electron conducting lanthanum tungstate, $La_{27}W_5O_{55.5}$ (LWO), has been subject of many studies elucidating its transport properties, defect chemistry and chemical stability. Under operation as a proton transport membrane for fuel and electrolyser cells or in hydrogen separation, the material is exposed to elevated temperatures and gradients in chemical potential, which – in most cases – result in a driving force for cation migration. Little data is available for LWO on cation diffusion related degradation such as kinetic demixing or decomposition, and morphological instabilities which is essential to lifetime evaluations.

In this contribution, bulk and grain boundary interdiffusion and chemical tracer diffusion in LWO are studied using Electron Probe Micro Analysis and Time-of-Flight Secondary Ion Mass Spectroscopy, respectively. The bulk diffusivities of La^{3+} and W^{6+} are almost identical between 1000 and 1350 °C, despite their large difference in ionic radius and valence state. Since 1/5 of the W atoms reside on La2 sites in the LWO structure, we suggest that both cations migrate via vacancies on the lanthanum sublattice. Enhanced migration along the grain boundaries was evident for La diffusion only. This is discussed in light of space charge theory; a positively charged grain boundary core yields enhanced concentration of cation vacancies and depletion of hexavalent W^{6+} on La2 sites.
Cation diffusion in LWO is faster than in the robust oxygen deficient fluorite YSZ, but significantly slower than for many state-of-the-art oxygen transport membranes. Enhanced diffusion of lanthanum along the grain boundaries may lead to kinetic demixing or decomposition, but steady-state demixing will not be reached before 20 years. However, performance degradation may also occur during the transient towards steady-state, and detailed studies on long term degradation are called for to further clarify the stability of LWO under large chemical potential gradients.

K3.20
Thermodynamics and Stoichiometry Relaxation Kinetics in Materials with Three Carriers: Analytic Relations and Numerical Simulations Daniel Poetzsch, Rotraut Merkle and Joachim Maier; MPI for Solid State Research, Stuttgart, Germany.

Materials with more than two mobile carriers are of interest e.g. as cathode materials for proton-conducting solid oxide fuel cells, which mostly come from the family of hole/oxygen vacancy/proton mixed conducting perovskites. Already the incorporation of protons into such mixed-conducting oxides is complex, as it can occur by acid-base reaction (hydration of oxygen vacancies) as well as by redox reaction (proton uptake at expense of holes, hydrogenation). Depending on conditions, one-fold or two-fold relaxation after pH_2O steps is found experimentally. [1-3]

The diffusion processes are described with a model taking all three carriers into account. It is shown that for a complete description of the system, a set of four diffusion coefficients is required, comprising direct as well as "indirect" terms. The complex non-monotonic kinetic behavior can arise already at small driving forces. This is related to the fact that in a three carrier system the electroneutrality condition - comprising three mobile defects - does not lead to a simple coupling between the carrier fluxes (in contrast to the two carrier systems, where electroneutrality results in a direct relation between both carrier fluxes by simple prefactors). Numerical simulations for a wide range of materials (different defect concentrations and diffusivity ratios) are discussed.[4]

[1] J. H. Yu, J. S. Lee, J. Maier, Angew. Chem. Int. Ed. 46 (2007) 8992.
[2] H. I. Yoo, J. Y. Yoon, J. S. Ha, C. E. Lee, Phys. Chem. Chem. Phys. 10 (2008) 974.
[3] E. Kim, H. I. Yoo, Solid State Ionics 252 (2013) 132.
[4] D. Poetzsch, R. Merkle, J. Maier, Adv. Funct. Mat. (2015) doi:10.1002/adfm.201402212

K3.21
Nanoscale Stabilization of Scheelite-Type Structure in $La_{0.99}Ca_{0.01}NbO_4$ Thin Films Cristina Tealdi[1, 2], Eliana Quartarone[1, 2], Piercarlo Mustarelli[1, 2] and Lorenzo Malavasi[1, 2];[1]Department of Chemistry, University of Pavia , Pavia, Italy; [2]UdR Pavia, INSTM, Pavia, Italy.

Proton conduction in oxides at elevated temperatures is a relatively rare phenomenon which may be exploited in electrochemical devices for the separation or oxidation of hydrogen.
Among proton conducting materials, the acceptor-doped rare-earth ortho-niobates and tantalates of general formula $RE(Ta,Nb)O_4$ (RE=rare earth) represent a good compromise between transport properties and material chemical stability. At present, the highest ionic conductivity coupled to the highest proton mobility has been observed for 1% Ca-doped $LaNbO_4$. Such materials crystallize in the monoclinic fergusonite-type structure at low temperatures and in the highly conductive tetragonal scheelite-type structure at high temperatures. Stabilization of the scheelite-type phase at room temperature would be beneficial to technological applications, especially in thin film samples.
In this study, thin film deposition of $La_{0.99}Ca_{0.01}NbO_4$ was performed at room temperature by means of radio frequency (RF) magnetron sputtering on SiO_2 substrates, starting from $La_{0.99}Ca_{0.01}NbO_4$ powders synthesized by solid-state reaction. Different post-deposition thermal treatments were carried out on the deposited films in the range 700-1200°C. Characterization techniques were X-ray diffraction and Atomic Force Microscopy.

The starting $La_{0.99}Ca_{0.01}NbO_4$ powders showed the usual monoclinic crystal structure at room temperature. The as-deposited films were amorphous and the subsequent thermal treatments iallowed to obtain crystalline samples with different structural properties, as revealed by X-ray diffraction. In particular, a modulation of the crystal phase from tetragonal to monoclinic

as a function of the annealing temperature was obtained, with the tetragonal phase retained at room temperature. Results were analysed in view of the morphological characteristics of the samples as determined by AFM, revealing a modulation of the particle size in the range 25 nm – 1 μm. Such a stabilization is most probably related to the inversion in the polymorphs stability due to the nanostructured nature of the thin films.

K3.22
Modeling of Defect Segregation and Space-Charge Formation in Proton-Conducting Oxides Edit E. Helgee, Anders Lindman and Goeran Wahnstroem; Applied Physics, Chalmers University of Technology, Gothenburg, Sweden.

Acceptor-doped barium zirconate ($BaZrO_3$) shows considerable potential as an electrolyte material for intermediate temperature solid oxide fuel cells due to its high bulk proton conductivity and chemical stability. However, in polycrystalline materials the grain boundaries (GBs) display high proton resistivity, severely limiting the overall proton transport in the material. The low GB conductivity has been thought to be due to an intrinsic mechanism, the space charge effect.

Using density functional theory (DFT) proton and oxygen vacancy segregation have been investigated for an extensive set of tilt GBs. Both defect species are found to segregate to the GB core, with typical segregation energies of -1.5 eV and -1.0 eV for oxygen vacancies and protons, respectively. A layer-by-layer space charge model (E. E. Helgee, A. Lindman, G. Wahnström, Fuel Cells, **13**, 19 (2013)) is employed to determine the potential barrier and core charge resulting from defect segregation. Below 900 K and at wet conditions potential barrier heights around 0.6V are obtained, which is consistent with experimental results. We have also investigated dopant segregation and its effect on the potential barrier. We find that if low-energy sites in the core are saturated with positive defects, an increase in the dopant concentration does lower the potential barrier. However, if the low-energy sites are not saturated an increased dopant concentration in the core could also lead to an increase in the concentration of positive defects and the core concentration is instead limited by the electrostatic potential.

To conclude, segregation of oxygen vacancies and protons plays an important role in the formation of space charge potentials at the grain boundary interface. Additionally, our results show that protons may be the main source to the space-charge potentials under conditions relevant for fuel cell applications.

SESSION K4: Protonic Oxides II
K: Proton-Conducting Oxides
Chairs: Marie-Laure Fontaine and Jose Serra
Thursday Morning, June 18, 2015
Keystone Resorts, Quandary Peak I/II

10:30 AM **K4.01
Development of Proton Conducting Electrolyser Cells Marie-Laure Fontaine, Jonathan Polfus, Wen Xing, Rune Bredesen and Christelle Denonville; Materials and Chemistry, SINTEF, Oslo, Norway.

High-temperature electrolysers (HTEs) produce hydrogen efficiently utilizing steam and electricity from renewable sources such as solar and geothermal or from nuclear reactors. During operation of traditional solid oxide electrolyser cells (SOECs), hydrogen is generated on the steam side, with reduced efficiency. In contrast, a proton-conducting ceramic electrolyser cell (PCEC) removes hydrogen from the steam side and can directly pressurize dry hydrogen. In addition, delamination of electrodes due to generation of oxygen bubbles in SOECs is alleviated in PCECs. In this work, we present current activities related to the processing and characterization of tubular cells using proton-conducting electrolytes based on state-of-the-art yttrium-doped barium zirconate cerates (BCZY). Both solid state reactive sintering and a polymeric route are studied using in situ and ex situ high resolution characterization techniques combined with computational modelling to identify sintering mechanisms and define critical processing parameters, such as precursor types, sintering atmosphere, and sintering additives.

From this study, a protocol is selected for manufacturing of tubular, NiO-based electrode-supported half cells with BCZY electrolytes. Development of the steam-oxygen electrode is currently in progress and will be discussed in this presentation. Results from electrochemical characterization of the produced cells will also be presented.

11:00 AM K4.02
Exploring BCZY Proton-Conducting Ceramics for Use in Electrolysis Michael Dippon[3], Sean Babiniec[1], Hanping Ding[1], Sandrine Ricote[1] and Neal P. Sullivan[2]; [1]Mechanical Engineering, Colorado School of Mines, Golden, Colorado, United States; [3]Institute of Materials for Electrical and Electronic Engineering, Karlsruhe Institute of Technology, Karlsruhe, Germany.

This work focuses on the formation of undesirable electronic-leakage currents in proton-conducting ceramic membranes used in H_2O-electrolysis applications. Recent work has shown lower efficiencies in protonic ceramics when operated in electrolysis mode, demonstrating electrolytic hydrogen flux that is much lower than the calculated hydrogen faradaic flux. The missing hydrogen flux is not compensated by oxygen ions, leaving electronic leakage as the feasible compensating current. Curiously, these same materials show little electronic leakage in fuel-cell operation. In this work, we show that through careful selection of ceramic-membrane composition, the electronic leakage can be greatly reduced across the operating range.

For this study, three different $BaCe_xZr_{0.9-x}Y_{0.1}O_{3-d}$ (BCZY) membranes were compared, x = 0, 0.1, and 0.2 (BZY10, BCZY18, and BCZY27, respectively). All membranes were ~ 25 μm thick, and were supported on a porous composite ceramic-metallic fuel electrode comprised of BCZY27 and nickel. The air electrode was a ~ 20-μm-thick porous gold. All devices were fabricated using solid-state reactive sintering, a lower-cost fabrication method.

These devices were tested over a wide range of temperatures and electrode gas compositions. While significant electronic leakage is observed in the BCZY27 material under electrolysis operation, minimal leakage is observed in BCZY18 and BZY10. Additionally, the ceria-containing materials demonstrated improved sintering characteristics in comparison to the BZY10 material. Based on this study, $BaCe_{0.1}Zr_{0.8}Y_{0.1}O_{3-d}$ is the preferred barium-cerate-zirconate composition for electrolysis applications.

11:20 AM K4.03
CsH_2PO_4-Based Fuel Cells and Electrolyzers Laura Navarrete and Jose M. Serra; ITQ (UPV-CSIC), Valencia, Spain.

CsH_2PO_4 has emerged as the new generation of electrolytes to work at low temperature (200- 300 ºC). CsH_2PO_4 transforms to a cubic phase showing a superprotonic conductivity when the temperature is increased above 230 ºC. The low operation temperature of this material allows the possibility to use cheap materials for the stack construction, reducing the cost of the device. The synthesis method avoids thermal treatments and long periods of calcination for the single phase manufacture, reducing the production costs. Electrodes should favor the oxidation and recombination of hydrogen in the anode and cathode respectively.

In the present work different symmetrical cells have been measured in order to check the influence of pH_2O and operation temperature. When the temperature is higher than 240 ºC, there is not a significant change in the electrolyte conductivity (0.015 $S \cdot cm^2$ at 240 ºC and 0.037 $S \cdot cm^2$ at 250 ºC). More important is the water partial pressure influence in the electrolyte conductivity changing from $3.96 \cdot 10^{-4}$ $S \cdot cm^2$ at 0.025 atm to 0.015 $S \cdot cm^2$ at 0.3 atm of water. Carbon Gas Diffusion Layer (GDL) has been employed as electrode and different catalysts have been introduced to improve the hydrogen reaction. Some of the materials infiltrated in the Carbon GDL, are Cu, Zn and Pt. The infiltration of the different catalyst has been checked by means of FESEM images, showing nanoparticles around 40 nm. The electrolyte conductivity has been recorded by means of Electrochemical Impedance Spectroscopy (EIS) obtaining values of 0.04 $S \cdot cm^2$ in fuel cell mode. The influence of hydrogen partial pressure and oxygen has been tested as well. Finally, the influence of the pressure in the

system was studied. The fuel cell power density increased six times changing the pressure from atmospheric to 4.5 bar absolute pressure. The electrolysis mode was also evaluated using MS and GC analysis.

11:40 AM K4.04

Electrochemical Synthesis of Ammonia under Atmospheric Pressure Using a $BaCe_{0.2}Zr_{0.7}Y_{0.1}O_{2.9}$ Electrolyte Michael Stoukides[1, 2], Eirini Vasileiou[1, 2], Vasileios Kyriakou[1, 2], Ioannis Garagounis[1, 2], Anastasios Vourros[1, 2], Anthony Manerbino[3] and Grover Coors[3]; [1]Chemical Engineering, Aristotle University of Thessaloniki, Thessaloniki, Greece; [2]Chemical Process and Energy Resources Institute, Centre for Research and Technology Hellas, Thessaloniki, Greece; [3]CoorsTekInc, Golden, Colorado, United States.

Introduction

The industrial process of ammonia synthesis is considered as the most important invention in the 20th century and plays a central role in the worldwide economy. Its primary use is for the fertilizer industry and the production of ammonia is estimated at about 140 million tons per year. Moreover, it has been proposed for energy storage in combination with renewable power sources [1]. Today, the "Haber-Bosch" process is the main method of ammonia production worldwide, using temperatures in therange of 400 – 500 °C and pressures of about 120 atm, at which the equilibrium conversion is of the order of 15% [2]. In 1998, the solid – state electrochemical synthesis of ammonia (SSAS) has been proposed and it shows many advantages such as a) there is no thermodynamic limit in the conversion to ammonia, b) it is environmentally friendly and c) it consumes less energy [3]. In the present work both catalytic and electrocatalytic studies have been conducted in a Ni-$BaCe_{0.2}Zr_{0.7}Y_{0.1}O_{2.9}$ (BCZY27) double chamber proton conducting cell.

Experimental

Catalytic (open-circuit) and electrocatalytic (closed-circuit) experiments took place using various catalyst-electrodes. The electrocatalytic experiments were carried out in a double chamber cell-reactor. The $BaCe_{0.2}Zr_{0.7}Y_{0.1}O_{2.9}$ perovskite (BCZY27) was used as proton conductor [4]. The cathodic electrode (ammonia synthesis catalyst) was a cermet of the form 60% NiO - 40% BCZY27. Ammonia was analyzed by an online analyzer with the use of Cavity Ringdown Spectroscopy.

Results and Discussion

In order to evaluate the electrocatalytic results, the rate of ammonia synthesison the Ni-BCZY27 catalyst were compared to those obtained with industrial catalysts. The effect of temperature and reactant gas composition on the reaction rate was tested at 300 - 750 °C, with the H_2/N_2 ratio varying from 0.1 to 9.0. In the electrocatalytic studies, the effect of imposed voltage was also studied. Experiments were conducted at temperatures between 450 and 750 °C, with a stoichiometric H_2/N_2 ratio and atmospheric total pressure (Figure 1). An increase of up to 15% on the rate of ammonia formation was observed (620 °C).

Acknowledgements

We gratefully acknowledge financial support of this research by the European Union and the General Secretariat of Research and Technology of Greece (Program ARISTEIA, Project Number 1089) and IKY fellowships of excellence for postgraduate studies in Greece - Siemens Program.

References

[1] Amar, I. A., Lan R., Petit C. T. G. and Tao S. *Journal of Solid State Electrochemistry* 15 (2011) 1845.
[2] Appl M. "Ammonia" in Ullmann's Encyclopedia of Industrial Chemistry, Wiley-VCH, Weinheim, 2006.
[3] Garagounis, I., Kyriakou, V., Skodra, A., Vasileiou, E., Stoukides, M. *Frontiers in Energy Research*, 2 (2014) 1-10.
[4] Robinson S., Manerbino A., Coors W.G. *Journal of Membrane Science*, 446 (2013) 99-105.

SESSION K5: Protonic Oxides III
K: Proton-Conducting Oxides
Chairs: Tor Grande, Jong-Ho Lee, Anna Magraso and Hiroshige Matsumoto
Thursday Afternoon, June 18, 2015
Keystone Resorts, Quandary Peak I/II

1:30 PM K5.01

Preparation and Electrochemical Characterization of Yttrium-Doped Barium Zirconate Thin Films by Chemical Solution Deposition Hanlin Xie, Mridula Biswas, Yong Li and Pei-Chen Su; School of Mechanical and Aerospace Engineering, Nanyang Technological University, Singapore, Singapore.

Proton-conducting oxides, such as acceptor-doped perovskites, are promising electrolyte candidates for low temperature solid oxide fuel cells operating below 600 °C. In particular, Y-doped $BaZrO_3$ (BZY) has attracted special attention due to its high bulk proton conductivity and excellent chemical stability. To improve the fuel cell performance, BZY electrolyte thin film was desirable to reduce the ohmic resistance. In this work, we employed chemical solution deposition (CSD) method to prepare $BaZr_{0.8}Y_{0.2}O_{3-d}$ (BZY20) thin film due to its advantages of cost effectiveness, scalability and low processing temperature. The conduction properties of the BZY thin film were studied at temperature range from 300 to 600 °C.

The BZY solution was chemically based on barium acetate, zirconium acetate, and yttrium nitrate. The BZY thin film was prepared by spin coating the solution on Si_3N_4 passivated Si wafer in multiple layers, followed by low temperature sintering at 800 °C. The obtained BZY thin film had a sub-micrometer thickness with smooth surface and dense structure

.

For the conductivity measurements, a planar cell geometry with dense platinum electrodes was used. Impedance measurements were carried out in various atmospheres in order to study the different conduction mechanisms. The conductivity value of the BZY thin film was almost one order of magnitude higher than BZY sintered pellet conductivity. The results indicate the BZY thin film prepared by CSD route is possible to work as promising electrolyte at low temperature regime.

1:50 PM K5.02

A Novel High-Performance Triple Conducting Oxide Cathode for Protonic Ceramic Fuel Cell Jianhua Tong, Meng Shang, Chuancheng Duan, David Shnaider and Ryan O'Hayre; MME, Colorado School of Mines, Golden, Colorado, United States.

The solid state reactive sintering technique enables the cost-effective fabrication of thin, dense, and highly proton conductive electrolyte membranes for protonic ceramic fuel cells (PCFCs). This approach opens the door at least in terms of the electrolyte performance, for PCFC operation at 300-600°C. However, at these temperatures the sluggish oxygen reduction reaction (ORR) at the conventional MIEC cathodes generally leads to unacceptably poor PCFC performance. The overall oxygen reduction reaction (ORR) at the cathode of a PCFC, as described by the global reaction $2OH_O^{\cdot}+1/2O+2e'=H_2O+2O_O^X$, is very different from the overall ORR at the cathode of a SOFC, as described by $V_O^{\cdot\cdot}+1/2O_2+2e'=O_O^X$. Because the ORR process at a PCFC cathode involves the combination of protons, electrons/electron holes, and oxygen ions in the solid phases, porous cathodes with triple conducting properties (electronic, oxygen ion, and proton conductivity) could provide unique catalytic advantages . In our recent work, we successfully developed a new triple conducting (proton, electron hole, and oxygen ion) oxide based on $BaCo_{0.4}Fe_{0.4}Zr_{0.1}Y_{0.1}O_{3-\delta}$ ($BCFZY_{0.1}$). The polarization resistance of this cathode material was measured to be less than 0.5 Ω cm² with gold as the current collector at 500 °C in wet air in symmetric cell testing. A single cell constructed from the $BCFZY_{0.1}$ cathode with a $BaCe_{0.7}Zr_{0.1}Y_{0.1}Yb_{0.1}O_{3-\delta}$ (BCZYYb) electrolyte and BCZYYb-Ni anode demonstrated a power density of 450 mW/cm² at 500 °C.

2:10 PM K5.03
All-Oxide Composite Cathode Materials Prepared by *In Situ* Oxidation Driven Decomposition Tor Grande, Mari-Ann Einarsrud and Guttorm Syvertsen-Wiig; Materials Science and Engineering, Norwegian University of Science and Technology, Trondheim, Norway.

A novel synthesis route to all-oxide composite cathode materials by *in-situ* oxidation driven decomposition was developed as an alternative to conventional mechanical mixing of oxide powders. Materials with nominal composition $La_{0.8}Sr_{0.2}Nb_{0.4}M_{0.6}O_3$ (M = Fe, Mn, Co, Ni) were synthesised by a modified Pechini route. The phase composition of the materials was designed by controlling the oxidation state of the transition metal M during synthesis and thermal treatment. The evolution of the phase composition of the materials was investigated by a number of techniques as function of thermal treatments in different atmospheres. All materials were nano-crystalline after calcination at ~400 °C in air. The materials with Fe or Mn were single phase perovskites after annealing in 5 % H_2 at 650 °C, while the two other materials contained several phases due to reduction of Co and Ni to the metallic state. Oxidation of all four materials took place at 200–350 °C and due to the lack of cation mobility, coarsening and grain growth of the phases formed were suppressed below 850 °C. The single phase materials with Fe and Mn were sintered by hot pressing, and the formation of a composite consisting of $LaNbO_4$ and $La_{0.67}Sr_{0.33}MnO_3$ or $La_{0.67}Sr_{0.33}FeO_3$ was successfully obtained by successive oxidation. Formation of $La_{1-x}Sr_xNb_{1/3-y}Co_{2/3+y}O_3$ or $La_{1-x}Sr_xNb_{1/3-y}Ni_{2/3+y}O_3$, coexisting with a minor amount of $La_{3-x}Sr_xNbO_{7-x}$ was confirmed in the two other materials after oxidation. The present findings demonstrate that all-oxide composite cathode materials can be prepared at low or intermediate temperatures by this method.

2:30 PM K5.04
Catalytic Properties of Proton Conducting Oxides in Cermet Electrodes and as Ceramic Supports for Dehydrogenation Catalysts Hyun H. Shin and Steven McIntosh; Chemical Engineering, Lehigh University, Bethlehem, Pennsylvania, United States.

The ionic transport properties of proton conducting oxides are currently quite well understood, with a number of ongoing efforts to improve conductivity through new material development. Less attention has been paid to the role of these materials in fuel cell electrodes or for other catalytic applications. Here we examine two reactions utilizing pure and doped barium cerates and barium zirconates. In the first case, we deploy a pulsed hydrogen/deuterium exchange technique to probe the mechanism of proton incorporation on SOFC cermet electrodes. We find that the proton incorporation rates are primarily dictated by the rates of hydrogen dissociation on the metallic components of the cermets.

Following this we examined the role of a barium cerates and barium zirconates as support materials for Cr for ethane dehydrogenation reactions. When compared to traditional oxide support materials, the proton conductors lead to a significant increase in reaction rate and suppression of deleterious carbon deposition. All of these results are supported by analysis of both reaction rates and surface composition.

2:50 PM K5.05
Chemical Stability and Membrane-Catalyst Compatibility of Selected Proton Conducting Materials Potentially Applicable in Hydrogen Membrane Reactors Mariya E. Ivanova[1], Desiree van Holt[1, 2], Emanuel Forster[3], Maria Balaguer[1], Wendelin Deibert[1], Wilhelm A. Meulenberg[1], Michael Mueller[3] and Olivier Guillon[1]; [1]Institute for Energy and Climate Research Materials Synthesis and Processing (IEK-1), Forschungszentrum Jülich GmbH, Jülich, Germany; [2] Institute of Energy and Climate Research Fundamental Electrochemistry (IEK-9), Forschungszentrum Jülich GmbH, Jülich, Germany; [3]Institute for Energy and Climate Research (IEK) IEK-2: Material Structure and Properties, Forschungszentrum Jülich GmbH, Jülich, Germany.

The harsh conditions encountered in catalytic H_2-membrane reactors include CO, CO_2, SO_x, SH_2, H_2O, different levels of ash and high temperatures (above 600 °C). Therefore, they require hydrogen conducting materials which in addition to high separation rates remain stable under the relevant operating conditions. The same is true for the substrate material, which in some cases differs from membrane material. Moreover, membrane material must be chemically compatible with the reaction catalysts.

In this work, $BaZr_{0.8}Y_{0.15}Mn_{0.05}O_{3-\delta}$ (BZYM), $BaCe_{0,5}Zr_{0,4}Y_{0,1}O_{3-d}$ (BCZY), $BaCe_{0,2}Zr_{0,7}Yb_{0,1}O_{3-d}$ (BCZYb), $BaCe_{0,2}Zr_{0,7}Yb_{0,08}Ni_{0,02}O_{3-d}$ (BCZYbNi) and $La_{5,5}WO_{12-d}$ (LaWO) were investigated in terms of their stability as proton conducting membrane materials potentially suitable for application in membrane reactors at elevated temperatures (above 600 °C). On the other hand, the stability of MgO as an inert and cost-effective support for manufacturing of asymmetric LaWO membranes was investigated as well. These membrane materials were therefore synthesized via the solid-state reaction, while the substrate-related powder was used as delivered. Bulk samples were shaped and sintered and substantially exposed to coal-gasification-related conditions, i.e. syngas atmosphere (15 vol.% H_2, 34 vol.% CO and 51 vol.% H_2O) and a retentate flow (90 vol.% CO_2, 9.9 vol.% H_2O and 0.1 vol.% H_2) at 600, 700, 800 and 900 °C for 72 h. After the exposures, it could be concluded on the stability of these materials based on the phase purity and microstructural investigations done on reference and exposed samples. In addition, the chemical compatibility of selected proton conducting membrane materials with CO-shift-catalysts (100Fe, 86Fe14Cr, 86Fe10Cr4Cu) was studied under operation conditions (see above) and potential membrane-catalysts systems were identified.

3:30 PM K5.06
Y-doped Barium Zirconate prepared by Flame Spray Synthesis as Electrolyte for Intermediate Temperature Proton Conducting Fuel Cells Francesco Bozza and Thomas Graule; Laboratory for High Performance Ceramics, EMPA, Dübendorf, Switzerland.

$BaZr_{0.8}Y_{0.2}O_{3-\delta}$ nanoprecursors were prepared by Flame Spray Synthesis (FSS) technique. The nanoprecursors, composed of a perovskite phase, barium nitrate and doped Zirconia, could form the pure perovskite phase after calcination at 1200°C. The sintering behavior, microstructure and electrical properties after sintering at 1600 °C were analyzed for both nanoprecursors and pure phase powder. The nanoprecursors derived BZY20 showed enhanced grain growth and an enhanced total conductivity of 7.7×10^{-3} S/cm at 450°C.

The effect of Ni doping on the sintering and electronic behavior of the BZY20 nanoprecursors was also investigated. Microstructures and electrical properties of 1% and 2% mol. Ni doped BZY20 were analyzed after sintering at 1400°C and 1500°C.

Finally, the effects of Ni interdiffusion during co-sintering, on the sintering and electrical behaviour of a BZY20 film supported on a Ni containing anode was investigated.

3:50 PM K5.07
Size and Shape of Oxygen Vacancies and Protons in Acceptor-Doped Barium Zirconate Erik Jedvik, Anders Lindman and Goeran Wahnstroem; Applied Physics, Chalmers University of Technology, Göteborg, Sweden.

Acceptor-doped barium zirconate ($BaZrO_3$) is experimentally found to exhibit high proton conductivity and is considered to be one of the more promising candidates for an efficient electrolyte material for intermediate temperature solid oxide fuels cells. However, stoichiometric fluctuations in the material may introduce significant mechanical stresses and it becomes important to understand the defect-induced strain, the chemical expansion.

When the system is hydrated a +2 charged oxygen vacancy is filled and two proton interstitials are created, forming hydroxide ions and causing a chemical expansion. This defect induced chemical expansion is investigated using density-functional theory (DFT) calculations. The two defect species, the vacancy and the proton interstitial are considered both as free defects and in association with the dopants Y, In, Sc and Ga. The defect induced strain tensor is introduced, which provides a natural generalisation of the ordinary chemical expansion to three dimensions and to anisotropic distortions.

We find that both a vacancy and a proton cause anisotropic distortions of the ideal crystal and a net contraction of the lattice, indicating that both the vacancy and the hydroxide ion are smaller than the oxygen ion. The contraction is considerably larger for the vacancy and the net effect in hydration is an expansion. This is consistent with the experimental findings. The effect of the dopants on the chemical expansion in hydration is found to be quite small, even if it is assumed that both the vacancy and the proton are fully associated with a dopant atom in the lattice.

[1] D. Marrocchelli, S. R. Bishop, H. L. Tuller, B. Yildiz, Adv. Funct. Mater. **22**, 1958 (2012).
[2] K.D. Kreuer, Ann. Rev. Mater. Res. **33**, 333 (2003)

4:10 PM K5.08
Proper Theoretical Description of Oxidation of Acceptor-Doped Perovskites Anders Lindman, Paul Erhart and Göran Wahnström; Applied Physics, Chalmers University of Technology, Gothenburg, Sweden.

Acceptor-doped ABO_3-type perovskites is a class of materials that has been shown to display significant proton, oxide ion, electronic and hole conductivity, both as pure and mixed conductors, which make them ideal as electrolyte and electrode materials in solid oxide fuel cells. The acceptor-doping forms oxygen vacancies, which are a necessity for oxide ion conduction, while protons are incorporated into the material at the expense of these vacancies by equilibration with atmospheric water. Similarly, holes are incorporated by the oxidation of oxygen vacancies when the material is in contact with atmospheric oxygen. In order to predict the conductive nature of these materials it is important to have a proper description of the defect chemistry.

Electronic structure methods like density functional theory (DFT) have become a powerful tool to elucidate the defect properties and complement nowadays more traditional experimental investigations. However, the presence of the combination of various charge carriers, such as protons, oxide ions (oxygen vacancies), holes and electrons put challenges on the theoretical treatment. The standard approach using DFT and the generalized gradient approximation (GGA) with the PBE functional is found to be insufficient for the oxidation reaction. Here we present results based on the G_0W_0 method, a many-body perturbation approach, which in a systematic way improve on DFT results. We also compare with results using a hybrid functional (PBE0). Hybrids improve substantially on GGAs in many aspects, but the dependence on adjustable parameters remains a concern.

We have investigated the hydration and oxidation behavior of acceptor-doped $BaZrO_3$. We find that all three approximations give a reasonable description for the hydration reaction. For the oxidation reaction the results differ qualitatively with an exothermic reaction with PBE while endothermic with PBE0 and G_0W_0. The latter behavior is more consistent with experimental data of charge carrier concentrations, oxidation enthalpies and conductivities.

4:30 PM K5.09
Understanding Blocking Grain Boundaries within Proton Conducting Ceramics Using Atom Probe Tomography Daniel Clark[1], Dave Diercks[1], Huayang Zhu[2], Robert Kee[2], Sandrine Ricote[2], Brian Gorman[1] and Ryan O'Hayre[1]; [1]Metallurgical and Materials Engineering, Colorado School of Mines, Golden, Colorado, United States; [2]Mechanical Engineering, Colorado School of Mines, Golden, Colorado, United States.

Proton conducting ceramics have applications in a variety of electrochemical energy conversion devices including fuel cells, electrolysis, membrane reactors, etc. In many proton conducting ceramics, interfaces often dominate bulk proton conductivity behavior and are not well understood. For example, grain boundaries are often 10-50X more resistive to proton flow than the grain interiors in the prototypical proton conducting perovskite $BaZr_{0.9}Y_{0.1}O_{3-\delta}$ (BZY10). Atom probe tomography (APT) is a technique that controllably evaporates ion species off a small tip and can rebuild the volume in 3-dimensions. Because APT allows for sub-nanometer spatial resolution and parts-per-million chemical resolution, it is a powerful tool for understanding the limiting interfacial chemistry within proton conducting ceramics and gives insights that no other characterization technique can give (e.g. oxygen non-stoichiometry at grain boundaries). In addition to quantifying interfacial chemistry, the technique can be taken a step further to map charge density and potential, thereby providing a new way to measure grain-boundary space-charge regions. Using this approach, the effect of different sintering techniques on grain boundary chemistry and charge density/potential can be explored. These studies provide insight into the origins of these proton-limiting grain boundaries and provide guidance on potential strategies to reduce their impact.

4:50 PM K5.10
On the Impact of Strain on the Proton Conductivity of Barium Zirconate Thin Films Anna Magraso[1, 3], Jonathan Polfus[2] and Jose Santiso[1]; [1]ICN2, Bellaterra, Spain; [2]SINTEF, Oslo, Norway; [3]Dep. Chemistry, University of Oslo, Oslo, Norway.

Y-doped BaZrO3 (BZY) is one of most studied proton conducting oxides for use as electrolyte in proton conducting solid oxide fuel cell devices, since it is chemically stable and exhibits a high grain interior conductivity. In this contribution, we report recent developments on the fabrication and characterization of epitaxial thin films of BZY by pulsed laser deposition (PLD) on standard single crystal substrates. The proton conductivity of the films depending on deposition conditions are presented. Atomistic Density Functional Theory (DFT) calculations are performed in order to elucidate interfacial effects on the conducting properties of BaZrO3. The effect of strain is of particular interest, and the migration path and energy barrier for protonic defects is investigated by the nudged elastic band approach.

SESSION K6: Protonic Oxides V
K: Proton-Conducting Oxides
Chairs: Tor Bjorheim and Jong-Sook Lee
Friday Morning, June 19, 2015
Keystone Resorts, Quandary Peak I/II

10:30 AM *K6.01
Hydride Conduction in Oxyhydrides Genki Kobayashi[1, 2]; [1]Research Center of Integrative Molecular Systems, Institute for Molecular Science, Okazaki, Japan; [2]Precursory Research for Embryonic Science and Technology, Japan Science and Technology Agency, Kawaguchi, Japan.

Hydrogen-containing oxides play an important role in electrochemical devices such as fuel cells, because the hydrogen that is present in the oxide lattice is stable both in ambient air and at high temperatures. Indeed, proton conduction in some perovskite oxides is well known. In contrast, hydrogen can also accept one electron to form hydride (H^-). However, H^- is not widely recognized as a mobile ion, and evidence of pure H^- conduction in oxides has not been reported to date, even though H^- has ionic radii suitable for fast ion conduction and a strong reducing property (E_0 = -2.25 V vs. SHE), and is thus attractive for storage/conversion devices with high-energy density. In the present study, we succeeded in synthesizing a novel oxyhydride that hydride ions coexist with oxide ions in a crystal lattice. This material, $La_{2-x-y}Sr_{x+y}LiH_{1-x+y}O_{3-y}$, has wide compositional range made possible by O^{2-}/H^- sharing anion, and shows a H^-conductivity of 0.2 mS·cm^{-1} at 573 K. The pure H^- conduction properties of the oxyhydride were clarified by electrochemical impedance spectroscopy (EIS), first principles calculations, and galvanostatic discharge reactions of all-solid-state electrochemical cells, using the oxyhydrides as the solid electrolyte.

[Reference]
G. Kobayashi and R. Kanno *et al.*, (submitted).

10:50 AM K6.02
Development of Hydrogen Sensor Using Proton Conductor with Redox Protonation Yuji Okuyama[1], Shinya Nagamine[2], Akira Nakajima[3], Fusako Takahashi[4], Koji Kimata[4], Tomoko Oshima[4], Go Sakai[5] and Naoki Matsunaga[5]; [1]Organaization for Promotion of Tenure Track, University of Miyazaki, Miyazaki, Japan; [2]Department of Applied Chemistry, Faculty of Engineering, University of Miyazaki, Miyazaki, Japan; [3]Frontier Science Research Center, University of Miyazaki, Miyazaki, Japan; [4]Functional

Materials R&D Center, TYK Corp., Tajimi, Japan; [5]Department of Environmental Robotics, Faculty of Engineering, University of Miyazaki, Miyazaki, Japan.

ABO_3 perovskite-type oxide show protonic conduction. The oxide ion vacancies are formed in crystal when the *B* site is substituted for the low valence cation. Then, the uptake of water takes place at the formed oxide ion vacancy. On the other hand, transition metal ion doped perovskite oxide take in proton from hydrogen by reduction of transition metal. If transition metal ion doped perovskite oxide show the proton conduction under reducing atmosphere and the hole conduction under air, hydrogen sensor that required no reference gas due to a known hydrogen concentration can be developed. When the hole transport number is unity at reference electrode of galvanic-cell, the electric potential can be decided without depending on an hydrogen concentration. On the other hand, the electrical potential of working electrode depends on the hydrogen concentration because electrolytes on the working electrode show the proton conduction.

In this study, electrochemical properties of Mn doped $CaZrO_3$ were examined for development of hydrogen sensor. ESR spectra were observed for sample annealed in hydrogen, and annealed in oxygen, which can be corrected to the presence of Mn^{2+}. The intensity of spectra of the sample annealed in hydrogen was larger than that of the sample annealed in oxygen. Moreover, IR spectra were observed at 3300 cm^{-1} which can be attributed to O-H vibration. The absorptivity shows the same tendency of the ESR spectra intensity. These result suggested that Mn doped $CaZrO_3$ take in proton from hydrogen by reduction of Mn.
From the electromotive force of the gas concentration cell, it was found that Mn doped $CaZrO_3$ show proton conduction under the reducing atmosphere and hole conduction under the oxidizing atmosphere. The emf of sensor was found to dependent only the hydrogen potential of the working electrode when air was used as the reference gas.

11:10 AM K6.03
Impact of the Electrochemical Proton-Carrier Injection on the Structure of $NaO_{1/2}$-WO_3-$NbO_{5/2}$-$LaO_{3/2}$-$PO_{5/2}$ Glass Takahisa Omata[1], Tomohiro Ishiyama[2], Junji Nishii[3], Toshiharu Yamashita[4], Hiroshi Kawazoe[4], Naoaki Kuwata[5] and Junichi Kawamura[5]; [1]Graduate School of Engineering, Osaka University, Suita, Japan; [2]National Institute of Advanced Industrial Science and Technology (AIST), Tsukuba, Japan; [3]Research Institute for Electronic Science, Hokkaido University, Sapporo, Japan; [4]Kawazoe Frontier Technologies Corp., Yokohama, Japan; [5]Tohoku University, Sendai, Japan.

The material stably containing proton-carriers with a high concentration is strongly requested in order to materialize the intermediate temperature fuel cells. Recently, we developed a new proton-carrier injection technique that is composed of the electrochemical substitution of alkali ions in phosphate glasses with protons (Alkali-proton substitution; APS) at 200-500 °C [1]. By using this technique, the theoretical limit of the proton concentration corresponds to the sodium concentration of the starting glass; it is expected to be up to ~1×10^{22} cm^{-3}. We successfully injected proton-carriers into phosphate glasses with a concentration higher than 4×10^{21} cm^{-3}.
We fabricated a pure proton conductor for the starting glass with a composition of $35NaO_{1/2}$–$1WO_3$–$8NbO_{5/2}$–$5LaO_{3/2}$–$51PO_{5/2}$ glass [2].
In this presentation, we describe that structural change of the $35NaO_{1/2}$-$1WO_3$-$8NbO_{5/2}$-$5LaO_{3/2}$-$51PO_{5/2}$ glass before and after APS was studied by means of Raman and ^{31}P MAS-NMR spectroscopies. The APS induced fragmentation of the phosphate chains, i.e., the average length of the phosphate chain reduced n=8.6 to 3.7 in $(PO_3^-)_n(P_2O_7^{4-})$ during APS, despite the total number of modifier cations of sodium and lanthanum ions and protons did not change before and after APS. The fragmentation of the phosphate chain was introduced by that some of the non-bridging oxygens in the NbO_6 and WO_6 octahedra before APS changed to bridging oxygens of the M-O-P bonds that was formed during APS. This structural change introduced by the APS is arising from the preferential formation of P-OH bonds than M-OH bonds. Based on these observations, it was shown that the APS is not simple substitution of sodium ions with protons but is accompanied with the structural relaxation to stabilize the protons introduced by APS.

References
[1] T. Ishiyama, et al., J. Electrochem. Soc. 160 (2013) E146.
[2] T. Ishiyama, et al., J. Mater. Chem. A 2 (2014) 3940.

11:30 AM K6.04
Surface-Proton Conductivity of Titanium Phosphate Nanoparticles in Water Hiroshige Matsumoto, Osamu Fujiwara, Kwati Leonard and Young-Sung Lee; International Institute for Carbon-Neutral Energy, Kyushu University, Fukuoka, Japan.

Proton conductivity of Ti-P-O complex oxide nanoparticles in water has been investigated, assuming the use as an electrolyte material for water electrolysis. Most of the solid ion conductor is crystalline and ionic defects works as charge carriers, so that relatively high temperature is necessary for the ionic conduction. Surface of the solid can work another type of the ion conduction field and nanoparticles equipped with large surface area can be ion conduction media, with examples of ceria nanoparticles and acid-modified metal oxides. In this work proton incorporated on the surface of Ti-P oxide nanoparticles in the form of hydroxyl group is assumed as a charge carrier and its conductivity with a help of liquid water is considered.
The Ti-P oxide particles were prepared via a wet chemical method using titanium alkoxide and phosphoric acid. Resulting precipitates are washed dried and compacted in a disk or bar shape and electrical conductivity in water was measured. Dissolution of phosphoric acid into water was evaluated by measuring the pH. The conductivity and the dissolution tendency depends largely on the heat treatment and the ratip of Ti/P. Infrared absorption measurement reveals the P=O double bond and Ti-O-P bond, with existence of OH group part of which can be assumed to work as a source of protonic charge carrier.

L: Plenary

SESSION L1: Plenary I
Chair: Joachim Maier
Monday Morning, June 15, 2015
Keystone Resorts, Shavano Peak

Shu Yamaguchi

9:25 AM L1.01
Bulk and Surface Oxide Protonics for Energy Conversion Devices: Role of Percolation and Grotthus Mechanism in Oxide Protonics Shu Yamaguchi; Department of Materials Engineering School of Engineering, The University of Tokyo, Tokyo, Japan.

Bulk and surface proton activity of oxide materials is discussed based on both theoretical approach (DFT calculation, *ab initio* MD simulation) and experimental ones (PES/XAS measurements using synchrotron radiation and electrochemical measurements). The materials we have been interested are the oxide materials that can conduct protons and holes, termed as oxide protonics in bulk state and along surface region. Recent progress on electrochemical transport and its future applications are summarized.

Our curiosity on bulk oxide protonics materials typically with perovskite structure lies in heavily non-linear conductivity behavior against dopant concentration. The recent study has revealed the occurrence of bond percolation conductivity, which has scarcely been considered in ionic conductors. It is natural, if one realize that the systems are perovskite oxides heavily doped with acceptor dopants on B-site, that network of octahedral conduction shells with dopant/matrix cations and localize (or trapped) carrier on oxide ions are connected due to high dopant concentration far from impurity semiconductor situations. Further details of site preference can explain the origin of such peculiar behavior of carriers due to strong lattice/proton interaction by local distortion.

On the other hand, the surface oxide protonics, defined as proton activity originated from high mobility at the surface and its applications, has been receiving increasing attentions as a playground of proton for proton-addition/subtraction reactions of adsorbed gaseous species in material/energy conversion devices. The classical topics of oxide surface hydration are now analyzed with the MD simulation to understand proton dynamics and acid/base chemistry on surface, in order to discuss why such proton activities are available on wide range of basicity of oxides' surface. Finally, our dream to develop novel functionalities of surface oxide protonics is introduced as future applications like catalyst for thermal/electrochemical CO_2 conversion into fuels, photo-catalyst, and so on.

SESSION L2: Plenary II
Chair: Harry Tuller
Tuesday Morning, June 16, 2015
Keystone Resorts, Shavano Peak

Sossina M. Haile

9:25 AM L2.01
Insights into Proton Transport in Superprotonic Solid Acids Sossina M. Haile; Department of Materials Science and Engineering, Northwestern University, Evanston , Illinois, United States.

Superprotonic solid acid electrolytes, materials with chemical and physical properties intermediate between conventional acids (*e.g.*, H_3PO_4) and conventional salts (*e.g.*, Cs_3PO_4) have emerged as attractive candidates for fuel cell and other electrochemical applications. Key characteristics of these materials are tetrahedral oxyanion groups linked by hydrogen bonds, and a polymorphic structural transition to a disordered state at moderate temperatures. Rapid oxyanion reorientation and dynamic disorder of the hydrogen bond network facilitate high proton conductivity in the high temperature phase. Materials exhibiting a superprotonic transition include $CsHSO_4$, $Cs_3H(SeO_4)_2$, CsH_2PO_4, and $Cs_2(HSO_4)(H_2PO_4)$. Here we review the present state of understanding of proton transport mechanisms and the factors governing the transition behavior as gathered from macroscale measurements of conductivity and thermal properties and from atomistic level studies using nuclear magnetic resonance spectroscopy and quasielastic neutron scattering.

SESSION L3: Plenary III
Chair: Klaus Funke
Wednesday Morning, June 17, 2015
Keystone Resorts, Shavano Peak

Juergen Janek

9:25 AM L3.01
Electrode Kinetics in the Solid State Juergen Janek; Institute of Physical Chemistry, Justus-Liebig University, Giessen, Germany.

The kinetics of electrode interfaces often plays the most critical role for the behavior of any electrochemical device. Therefore, electrode kinetics has necessarily been in the focus of solid state ionics since its very beginning. But while theoretical concepts for the description of electrodes and their kinetics are well developed in the liquid state, the description and understanding of electrodes on solid electrolytes appears to be less developed. Obviously the fact that solid electrolytes are intrinsically more diverse than liquid electrolytes (the "solvent + conducting salt" concept cannot systematically be applied to the solid state) complicates the development of a coherent description. The partial electronic conductivity of solid electrolytes and mechanical strain effects may add further complications.

After a brief introduction, considering the differences between electrodes in the liquid and the solid state (with a short view into electrodes in the plasma phase) and trying to categorize different electrode situations, the lecture will focus on the current state of understanding of a few typical electrode systems: (a) Parent metal/electrolyte interfaces (like e.g. Li/LiSICon electrodes) form conceptionally the most simple electrode system as two-phase boundaries, and metal dissolution and deposition are important reactions in electrochemical cells employing parent metal electrodes. But despite early attempts, the kinetics of parent metal electrodes is still poorly understood. Current research for reversible and stable lithium metal electrodes in all-solid-state batteries exemplifies our current understanding. (b) Gas electrodes – often requiring the description as three-phase boundaries – play perhaps the most intensively studied group of electrodes on solid electrolytes. Oxygen electrodes for solid oxide fuel cells are particularly well studied, but still offer new insights – not at least due to the diversity of oxide-based electrode materials and their complex surface chemistry. One fascinating phenomena which always has been closely linked to the kinetics of oxygen electrodes is the NEMCA effect, and new findings on the mechanism of the NEMCA effect will be presented. (c) Finally, less typical but highly interesting electrode interfaces will be addressed – highlighting directions for future research.

SESSION L4: Plenary IV
Chair: Maria Forsyth
Thursday Morning, June 18, 2015
Keystone Resorts, Shavano Peak

Joachim Heberle

9:25 AM L4.01
On the Mechanism of Cation Translocation across Channelrhodopsin Joachim Heberle; Experimental Molecular Biophysics, Freie Universität Berlin, Berlin, Germany.

The discovery of the light-gated ion channel channelrhodopsin (ChR) set the stage for the novel field of optogenetics where cellular processes are controlled by light (1). Channelrhodopsin has revolutionized neurophysiological experimentation where neurons are controlled with optogenetics for fast, specific excitation or inhibition within systems as complex as freely moving mammals.

Despite the fact that the crystallographic structure of a ChR chimeric construct was solved (Fig. 1), the underlying molecular mechanism of light-induced cation permeation remains largely elusive. We have traced the structural changes of ChR2 by time-resolved IR spectroscopy, complemented by electrophysiological measurements (3-6). The vibrational changes were resolved across the entire chemical time range (10^{-14}-10^{1} s) including the open states of the channel. Analysis of the amide I vibrations suggests a transient increase in hydration of transmembrane a-helices with $t_{1/2}$ = 60 ms which tally the onset of cation permeation. To address structural changes of the channel, ChR2 was subjected to pulsed electron double resonance (pELDOR) spectroscopy (7). Comparison of spin-spin distances in the dark state and after illumination reflect conformational changes in the conductive state involving helices B and F.

Structural changes in proteins are related to proton transfer reactions. Transient protonation and deprotonation of specific amino acid side chains were monitored. It is demonstrated that reprotonation of aspartic acid 156 is rate-limiting to the closure of the cation channel.

Based on the opportunity to trigger ion gating by light, we believe that ChR will become a model system for detailed biophysical studies on the mechanism of ion channels with utmost temporal resolution and spatial sensitivity.

References:
Fenno, L., Yizhar, O., Deisseroth, K., Annu. Rev. Neurosci. 34 (2011), 389-412
Kato, H.E., Zhang, F., et al., Nature 482 (2012), 369-374
Lórenz-Fonfría, V.A., Resler, et al., Proc. Natl. Acad. Sci. USA 110 (2013), E1273-E1281
Neumann-Verhoefen MK, Neumann K, et al., J. Am. Chem. Soc. 135 (2013), 6968-6976
Lorenz-Fonfria, V A, Heberle, J., Biochim. Biophys. Acta 1837 (2014), 626-642
Lórenz-Fonfría, V.A., Schultz, B.J., Resler, T., Schlesinger, R., Bamann, C., Bamberg, E., Heberle, J., J. Am. Chem. Soc. 137 (2015), 1850−1861
Krause N, Engelhard C, et al., FEBS Lett. 587 (2013), 3309-3313

SESSION L5: Special Plenary
Chair: M. Stanley Whittingham
Friday Morning, June 19, 2015
Keystone Resorts, Shavano Peak

John Goodenough

9:25 AM L5.01
Alternative Strategies for Electrical Energy Storage John Goodenough; University of Texas at Austin, Austin, Texas, United States.

A sustainable energy supply for a variable demand requires a transition to energy sources other than fossil fuels. This transition requires storage of electrical energy generated by wind, solar, and nuclear energy; these sources are either variable or constant, so we need to be able to store the electrical energy they generate. Energy is most economically stored as chemical energy and electrical energy can be converted efficiently to chemical energy as a CO_2-neutral fuel or in a rechargeable battery. The electrolysis of water below 150°C to obtain H_2 is an attractive option, and the gaseous H_2 generated would be, preferably, catalytically reacted with CO_2 to form a liquid alcohol.

Rechargeable batteries can power a hand-held device, an electric vehicle EV, or provide stationary storage. The Li-ion battery has already transformed society by powering hand-held devices; this application does not compete with fossil fuels. However, Li is too costly to be used in batteries that compete with fossil fuels. Batteries that power EVs must operate safely under potentially abusive conditions and over a wide temperature range and yet use sodium as the anode and provide a low-cost volume energy density and a long cycle and calendar life. Stationary storage of electrical energy also needs to be safe and low-cost; the environmental and energy-density requirements are replaced by an emphasis on cycle and calendar life. Strategies for these different approaches will be discussed and compared.

AUTHOR INDEX

This index indicates the paper number for authors and sessions chairs. Bold lettered paper numbers indicate those being presented by the author, and non-bolded paper numbers indicate associate author status. The ** (asterisk) indicates keynote speaker and * (asterisk) indicates an invited speaker. The following typical examples show the code system

B	Topic (see page 1 for topic listing)
B2	Session Chair for Session (Topic B, Session 2)
B2.01	Author of Paper Number (Topic B, Session 2, First Paper)

NOTES